Exploring Transition Metals (Co, Cu, Rh & Ir) for the Construction of C–C and C–Heteroatom Bonds *via* C–H Activation Strategy: Expeditious Synthesis of Densely Functionalized Heterocyclic Architectures

THESIS SUBMITTED TO JADAVPUR UNIVERSITY
FOR THE DEGREE OF
DOCTOR OF PHILOSOPHY (SCIENCE)

2022

By

Writhabrata Sarkar

ORGANIC AND MEDICINAL CHEMISTRY DIVISION
CSIR-INDIAN INSTITUTE OF CHEMICAL BIOLOGY
4, RAJA S. C. MULLICK ROAD, JADAVPUR
KOLKATA-700 032, INDIA

Dedicated to...

Maa and Baba

सी.एस.आई.आर–भारतीय रासायनिक जीवविज्ञान संस्थान
वैज्ञानिक तथा औद्योगिक अनुसंधान परिषद की एक इकाई
विज्ञान एवं प्रौद्योगिकी मंत्रालय के अधीन, एक स्वायत्त निकाय, भारत सरकार
4, राजा एस. सी. मल्लिक रोड, यादवपुर, कोलकाता - 700 032

CSIR - INDIAN INSTITUTE OF CHEMICAL BIOLOGY

A Unit of Council of Scientific & Industrial Research
An Autonomous Body, under Ministry of Science & Technology, Government of India
4, Raja S. C. Mullick Road, Jadavpur, Kolkata-700 032

Dr. Indu Bhusan Deb
Principal Scientist, Associate Professor (AcSIR)
Organic and Medicinal Chemistry Division
CSIR-Indian Institute of Chemical Biology
4, Raja S.C. Mullick Road, Jadavpur
Kolkata-700 032

CERTIFICATE FROM THE SUPERVISOR

This is to certify that the thesis entitled **"Exploring Transition Metals (Co, Cu, Rh & Ir) for the Construction of C–C and C–Heteroatom Bonds *via* C–H Activation Strategy: Expeditious Synthesis of Densely Functionalized Heterocyclic Architectures"** submitted by Sri **Writhabrata Sarkar** who got his name registered on **04.09.2018** for the award of **Ph.D. (Science)** degree (Index No.: **139/18/Chem./26**) of **Jadavpur University**, is absolutely based upon his own work under the supervision of **Dr. Indu Bhusan Deb** and that neither this thesis nor any part of it has been submitted for either any degree/diploma or any other academic award anywhere before.

Indu Bhusan Deb.
(Dr. Indu Bhusan Deb)
25.03.2022
Signature of the Supervisor
& Date with Official Seal

Dr. Indu Bhusan Deb, PhD.
Principal Scientist & Associate Professor (AcSIR)
Organic & Medicinal Chemistry Division
C.S.I.R-Indian Institute of Chemical Biology
Government of India
4, Raja S. C. Mullick Road, Kolkata-700 032, India

CONTENTS

Acknowledgement i-iii

List of Abbreviations v-ix

Synopsis xi-xxi

Chapter 1: Introduction || Part-I

A Brief Overview of Cobalt and Copper-Catalyzed C–H Activation

1.1. A Brief History of Transition Metal-Catalyzed Cross-Coupling Reactions 3-6

1.2. Introduction to Transition Metal-Catalyzed C–H Activation 6-9

1.3. Mechanisms of C–H Activation 9-13

1.4. Kinetic Isotope Effect (KIE) Studies 13-15

1.5. Historical Background of C–H Activation 15-16

1.6. Modern Era of C–H Activation Leading to C–H Functionalization 16-20

1.7. First-Row Transition Metal-Catalyzed C–H Activation 20

1.8. Cobalt-Catalyzed C–H Activation 20-43

1.8.1. C–H Activation Using Well-Defined Cobalt Complexes 21-22

1.8.2. Low-Valent Cobalt-Catalyzed C–H Activation 23-25

1.8.3. High-Valent Cobalt-Catalyzed C–H Activation 25-32

1.8.4. Oxidative C–H Activation Using Simple Cobalt Salts 32-43

1.9. Copper-Catalyzed C–H Activation 43-70

1.9.1. C–C Bond Formation 46-53

1.9.2. C–N Bond Formation 54-58

1.9.3. C–O Bond Formation 58-61

1.9.4. C–S and C–Se Bond Formation 61-62

1.9.5. C–P Bond Formation 62-63

1.9.6. C–Z (Z = F, Cl, Br, I) Bond Formation 63-65

1.9.7. Tandem C–H Activation/Annulation 65-68

1.9.8. Electrochemical C–H Functionalization 68-69

1.9.9. Mechanistic Aspects of Copper-Catalyzed/-Mediated C–H Activation 69-70

1.10. References 71-88

Chapter 2: Cobalt || Acetoxylation

Cobalt-Catalyzed Directed sp^2 C–H Acetoxylation of Arenes Employing $Mn(OAc)_3 \cdot 2H_2O$ As Acetoxy Source

2.1. Introduction 91-97

2.1.1. Relevance of Acetoxy Functional Group Containing Compounds 91-92

2.1.2. Strategies For Transition Metal-Catalyzed C–O Bond Formation 92-94

2.1.3. 8-Aminoquinoline Directing Group in C–H Activation 94-95

2.1.4. Cobalt-Catalyzed C–H Functionalization 95-97

2.2. Objective 97

2.3. Results and Discussion 98-110

2.3.1. Optimization Studies 98-100

2.3.2. Scope of the Reaction 100-104

2.3.3. Gram-Scale Reaction and Synthetic Transformation of the Product 104-105

2.3.4. Mechanistic Experiments and Plausible Mechanism 105-110

2.4. Summary 111

2.5. Experimental Section 111-133

2.5.1. General Information 111

2.5.2. General Procedure for the Preparation of Starting Materials 112-113

2.5.3. General Procedure for Acetoxylation 113-114

2.5.4. Characterization Data for the Acetoxylated Products 114-130

2.5.5. Synthetic Transformation of the Acetoxylated Product **2a** 130

2.5.6. Mechanistic Experiments 131-133

2.6. ^{1}H and ^{13}C NMR Spectra of Representative Compounds 134-154

2.7. References 155-159

Chapter 3: Copper || Thiolation

Copper-Mediated Direct and Selective C–H Thiolation of Quinazolinones

3.1. Introduction 163-168

3.1.1. Relevance of Quinazolinones and Sulfur based Compounds 163-164

3.1.2. Strategies for Thioquinazolinone Synthesis 164-165

3.1.3. Transition Metal-Catalyzed/-Mediated C–S Bond Formation 165-167

3.1.4. Quinazolinones in C–H Activation 167-168

3.2. Objective 168-169

3.3. Results and Discussion 169-176

3.3.1. Optimization Studies 169-170

3.3.2. Scope of the Reaction 170-174

3.3.3. Gram-Scale Reaction 174-175

3.3.4. Control Experiment and Radical Scavenging Experiments 175-176

3.3.5. Plausible Mechanism 176

3.4. Summary 177

3.5. Experimental Section 177-193

3.5.1. General Information 177

3.5.2. General Procedure for the Preparation of Starting Materials 177-178

3.5.3. General Procedure for Thiolation 178-179

3.5.4. Characterization Data for the Unknown Substrates and Sulfenylated Products 179-192

3.5.5. Radical Scavenging Experiments 193

3.6. ^{1}H and ^{13}C NMR Spectra of Representative Compounds 194-213

3.7. References 214-216

Chapter 4: Copper || Silylation

Copper-Catalyzed Direct sp^2 C–H Silylation of Arylamides Using Disilanes

4.1. Introduction 219-224

4.1.1. Relevance of Silyl Functional Group Containing Compounds 219

4.1.2. Strategies For Transition Metal-Catalyzed C–Si Bond Formation 220-222

4.1.3. 8-Aminoquinoline Directing Group in C–H Activation 222-224
4.2. Objective 224
4.3. Results and Discussion 225-237
4.3.1. Optimization Studies 225-227
4.3.2. Scope of the Reaction 227-232
4.3.3. Gram-Scale Reaction 232
4.3.4. Mechanistic Experiments and Plausible Mechanism 232-237
4.4. Summary 237
4.5. Experimental Section 238-261
4.5.1. General Information 238
4.5.2. General Procedure for the Preparation of Starting Materials 238
4.5.3. General Procedure for Silylation 239-240
4.5.4. Characterization Data for the Silylated Products 240-260
4.5.5. Mechanistic Experiments 260-261
4.6. ^{1}H and ^{13}C NMR Spectra of Representative Compounds 262-280
4.7. References 281-284

Chapter 5: Introduction || Part-II

A Brief Overview of Rhodium and Iridium-Catalyzed C–H Activation

5.1. Transition Metal-Catalyzed C–H Activation/Functionalization 287
5.2. Rhodium-Catalyzed C–H Activation 287-321
5.2.1. C–C Bond Formation 289-296
5.2.2. C–X Bond Formation 296-302
- C–N bond formation 296-298
- C–O bond formation 298-299
- C–S and C–Se bond formation 299-300
- C–Z (Z = Cl, Br, I) bond formation 300-301
- Other C–X bond formation 301-302

5.2.3. C–H Annulation Reaction 302-321
- Redox-active/Oxidative annulation 304-311
- Redox-neutral annulation 312-317
- Photochemical and Electrochemical annulation 317-318

➢ Enantioselective annulation 318-321
5.3. Iridium-Catalyzed C–H Activation 321-334
5.3.1. C–C Bond Formation 323-327
5.3.2. C–X Bond Formation 327-331
5.3.3. C–H Annulation Reaction 331-333
5.3.4. Electrochemical C–H Activation 334
5.4. References 335-349

Chapter 6: Rhodium || Spirocyclization

Regio- and Diastereoselective [3+2]-Spiroannulation of Benzoxazines with Chalcones: A Rh(III)-Catalyzed Redox-Neutral Approach to α-Aroyl Spiro-Indanamines

6.1. Introduction 353-360
6.1.1. Relevance of Benzoxazine and Indane/Indene Frameworks 353-355
6.1.2. Strategies For Transition Metal-Catalyzed [3+2]-Annulation 355-357
6.1.3. Benzoxazines and Chalcones in C–H Activation 358-360
6.2. Objective 360-361
6.3. Results and Discussion 361-393
6.3.1. Optimization Studies 361-363
6.3.2. Scope of the Reaction 364-370
6.3.3. Gram-Scale Reaction 371
6.3.4. Interchange of the Diastereomers 371-372
6.3.5. Determination of the Relative Stereochemistry of the Spirocyclized Products 372-385
6.3.6. Mechanistic Experiments and Plausible Mechanism 385-393
6.4. Summary 394
6.5. Experimental Section 394-433
6.5.1. General Information 394
6.5.2. General Procedure for the Preparation of Starting Materials 394-395
6.5.3. General Procedure for Spirocyclization 395-397
6.5.4. Characterization Data for the Spirocyclized Products 398-425
6.5.5. General Procedure for the Interchange of the Diastereomers 425-427

6.5.6. Mechanistic Experiments 428-433

6.6. ^{1}H and ^{13}C NMR Spectra of Representative Compounds 434-467

6.7. References 468-472

Chapter 7: Iridium || Arylation

Iridium-Catalyzed Direct C–H Arylation of Cyclic *N*-Sulfonyl Ketimines with Arylsiloxanes at Ambient Temperature

7.1. Introduction 475-482

7.1.1. Relevance of Biaryls and *N*-Sulfonyl Ketimines and Benzosultams 475-476

7.1.2. Strategies For Transition Metal-Catalyzed C–H Arylation 476-480

7.1.3. Cyclic *N*-Sulfonyl Ketimines as Directing Group in C–H Activation 480-482

7.2. Objective 482-483

7.3. Results and Discussion 483-497

7.3.1. Optimization Studies 483-485

7.3.2. Scope of the Reaction 485-492

7.3.3. Gram-Scale Reaction and Synthetic Transformation of the Product 492-493

7.3.4. Mechanistic Experiments and Plausible Mechanism 493-497

7.4. Summary 497-498

7.5. Experimental Section 498-521

7.5.1. General Information 498

7.5.2. General Procedure for the Preparation of Starting Materials 498-499

7.5.3. General Procedure for Arylation 499-500

7.5.4. Characterization Data for the Arylated Products 501-518

7.5.5. Synthetic Transformation of the Arylated Product **3aa** 518-519

7.5.6. Mechanistic Experiments 520-521

7.6. ^{1}H and ^{13}C NMR Spectra of Representative Compounds 522-545

7.7. References 546-550

List of Publications 551-552

Acknowledgement

First and foremost, I would like to express my deepest gratitude to my supervisor, Dr. Indu Bhusan Deb for his constant guidance and encouragement throughout my doctoral studies without which this thesis work would not have been possible. His zeal and unrelenting support have always pushed me to work hard and strive for excellence in my research career and beyond. His mentorship skills have helped me to build up my personality and scientific temperament and also taught me how to be street-smart. He has always encouraged us to develop an independent and self-reliant scientific mindset. I am indebted to him for enlightening my global perspective of scientific and professional view.

I would like to thank my research advisory committee (RAC) members: Prof. Swapan Kumar Bhattacharya, Head of the Department of Chemistry, Jadavpur University and Prof. Sanjay Bhar, Jadavpur University for assessing my research work and providing their scientific insights, suggestions and encouragement. I am thankful to the present director of our institute Dr. Arun Bandyopadhyay, CSIR-Indian Institute of Chemical Biology (CSIR-IICB) for offering the research support. I gratefully acknowledge the head of our Organic and Medicinal Chemistry Division, Dr. Parasuraman Jaisankar for providing all the research support needed in the chemistry department. I would like to express my sincere gratitude to my MSc project supervisor Prof. Rina Ghosh, Jadavpur University for her excellent guidance and giving me the first-hand experience of a research lab, which highly motivated me to pursue my career in scientific research.

Throughout the journey of my academic career, I am highly blessed to have come across some of the finest teachers and mentors who have been instrumental in building up my character and shaping my academic career. I would like to thank all the faculty members of CSIR-IICB and Jadavpur University for teaching us important courses during my Ph.D. coursework and giving us an insight to the scientific knowledge required in doctoral studies. Especially, I would like to acknowledge Dr. Ramalingam Natarajan for teaching us how to solve X-ray crystal data. I am thankful to Dr. Basudeb Achari for his valuable suggestions. I would like to take this opportunity to specially thank my teachers from Jadavpur University who have showered their love and knowledge during my graduation and post-graduation days. Their constant guidance and nurturing of our minds always motivated us to believe in ourselves and strive forward to achieve our goal. Jadavpur University truly shaped me as a person to be kind, strong and independent. I would like to express my sincere gratitude to my schools B.D.Memorial Institute

(now B.D.M. International), Kolkata and DAV Public School, Bankura, West Bengal and all their teachers who gave me important basic lessons and taught with love and affection starting from my childhood days and made me ready to enter into the bigger academic world. Also, I would like to thank all my private tutors Hirak Sir, Sisir Sir, Late Shib Sir, Subho Da, Chittaranjan Sir who taught me during my school and university days and helped me in getting a stronghold of my knowledge in various subjects. Special thanks go to my Chemistry tutor Sisir Sir whose way of teaching made me fall in love for the subject and highly motivated me to take up Chemistry as my honours subject for my graduation.

I am indebted to my institute CSIR-Indian Institute of Chemical Biology (CSIR-IICB) for providing me with the platform to work on. A very special gratitude goes to Council of Scientific and Industrial Research (CSIR), India for providing me the financial support during my Ph.D. tenure. I am grateful to the following scientific technical staffs: Dr. Tapas Sarkar (NMR operator, retired), Dr. E. Padmanabhan (NMR operator), Mr. Sandip Kundu (NMR and SCXRD operator), Mr. Gautam Karmakar (NMR operator), Mr. Shahfiaz Khan (NMR operator), Mr. Diptendu Bhattacharyya (ESI MS operator), Mr. Soumik Laha (ESI MS operator), Mr. Santu Paul (LTQ-Orbitrap MS operator), Mr. Sandip Chowdhury (EI MS operator), and the Central instrumentation Facility (CIF) for their help in providing us with experimental data on a daily basis. I would also like to thank all the administrative and other staffs associated with the institute who have been very generous to extend their help always.

It is my pleasure to express my sincere thanks to all my past and present labmates Aniket da, Arup, Shantonu, Siddhartha, Koushik, Imtiaj, Sudip, Tripta, Anupama, Mahesh, Saidalvi, Upasana, Arindam da, Aiswarya, Sudha for their companionship and support. Since the last five years, I have thoroughly enjoyed sharing workspace with them and helping each other out in day-to-day lab work. The lab parties and trips were fun. It has been a wonderful experience. I thank them for being there. I would also like to thank Gautam da for lab management and Sandipan da for helping me in solving X-ray crystal data whenever needed.

I would like to take this opportunity to express my wholehearted gratitude and love to all my school and university friends who form an integral part of my life. Shubham, Sagnik, Koushik, Pranoy, Ranit, Saptarshi, Sandipan, Amlan have been amazing friends starting from my school days. We have always met and shared a laugh whenever we got time, especially during the Durga puja days. They have been compassionate and supportive throughout. When I stepped into the university, I met some of the most talented and warm-hearted friends, seniors and

juniors. Shantanu, Anas, Subarna, Deblina, Late Rajdeep, Kaustuv, Supriyo, Biswajit, Rapti, Souradeep, Asim, Arka, Trisha, Tanmay, Debayan, Soumya have always inspired me in one way or another in all aspects of life. Espescially, Anas, Shantanu, Subarna, Deblina have always had my back and instilled a sense of confidence in me whenever I felt down. I have thoroughly enjoyed all our trips and gatherings and spending time with all of them has been a bliss. I have also been lucky to come across some of the best seniors Baitan da, Manamohan da, Aritra da who have always stepped up in lending a helping hand whenever I needed them, and some of the most affectionate juniors Anwesha and Soumyadip who are amazing souls full of optimism and enthusiasm. I also extend my sincere thanks to Anas and Late Rajdeep who have been amazing roommates with whom I have shared some of the most precious moments during this time. I sadly lost my friend Rajdeep who was like a brother to me and I pray his soul rests in peace. I am thankful to all of them for staying beside me through thick and thin.

Finally, I cannot put into words my love and deepest gratitude for my parents, my father Mr. Satyabrata Sarkar and my lovely mother Mrs. Ila Sarkar. Without their blessings and sacrifice I would not be able to reach where I am. They have brought me up in the best possible way to help me become a good person at the first place. My father has always encouraged me and taught me to work hard and stay level-headed whatever be the situation in my life. My mother has taught me to be kind and helpful and stay disciplined in my life. I am fortunate to share my happiness with them and all my achievements belong to them. I also thank my relatives for their love and unconditional support.

Throughout this wonderful journey, I have come across innumerable brilliant and caring people who have impacted my life greatly. It would have been impossible without all of them. Therefore, it is my great pleasure to conclude this roller-coaster of an expedition by expressing my sincere gratitude to all of them.

(Writhabrata Sarkar)

March, 2022
Organic and Medicinal Chemistry Division
CSIR-Indian Institute of Chemical Biology
Kolkata-700032

List of Abbreviations

Ac	Acetyl
Ac_2O	Acetic anhydride
AcOH	Acetic acid
Ad	Adamantyl
AIBN	Azobisisobutyronitrile
Am	Amyl
AMLA	Ambiphilic metal ligand activation
AQ	Aminoquinoline or 8-aminoquinoline
aq	aqueous
Ar	Aryl
BHT	Butylated hydroxytoluene
BIES	Base-assisted internal electrophilic substitution
BINAP	2,2′-bis(diphenylphosphino)-1,1′-binaphthyl
BIPHEMP	2,2′-bis(diphenylphosphino)-6,6′-dimethyl-1,1′-biphenyl
BM	Bond metathesis
Boc	*Tert*-butyloxycarbonyl
BQ	1,4-benzoquinone
calcd	calculated
CAM	Complex assisted metathesis
Cbz	Carboxybenzyl
CCDC	Cambridge crystallographic data centre
CDC	Cross-dehydrogenative coupling
CDI	1,1′-carbonyldiimidazole
CETP	Cholesteryl ester transfer protein
CFL	Compact fluorescent lamp
CGRP	Calcitonin gene-related peptide
CIF	Crystallographic information file
CMD	Concerted metalation-deprotonation
cod	1,5-cyclooctadiene
COSY	Correlation spectroscopy
COX	Cyclooxygenase

Cp	Cyclopentadienyl
Cp*	Pentamethylcyclopentadiene
Cp^x	Chiral cyclopentadienyl
Cy	Cyclohexyl
cym	cymene
Cys	Cysteine
DABCO	1,4-diazabicyclo[2.2.2]octane
DBU	1,5-diazabicyclo[5.4.0]undec-5-ene
DCE	1,2-dichloroethane
DCM	Dichloromethane
DDQ	2,3-dichloro-5,6-dicyano-1,4-benzoquinone
DEAD	Diethyl azodicarboxylate
DEPT	Distortionless enhancement by polarization transfer
DFT	Density functional theory
DG	Directing group
DHB	2,5-Dihydroxybenzoic acid
DIAD	Diisopropyl azodicarboxylate
DIPEA	*N*,*N*-diisopropylethylamine
DMA	*N*,*N*-dimethylacetamide
DMAP	4-(dimethylamino)pyridine
DMF	*N*,*N*-dimethylformamide
DMPU	*N*,*N*-dimethylpropyleneurea
DMSO	Dimethyl sulfoxide
DPEPhos	(Oxydi-2,1-phenylene)bis(diphenylphosphine)
dr	diastereomeric ratio
DTBP	Di-*tert*-butyl peroxide
dtbpy	4,4′-di(*tert*-butyl)-2,2′-bipyridyl
ee	enantiomeric excess
EI	Electron ionization
er	enantiomeric ratio
ESI	Electrospray ionization
equiv	equivalent(s)
F	Faraday or Farad

FID	Flame ionization detector
GC	Gas chromatography
GF	Graphite felt
Gly	Glycine
HCV	Hepatitis C virus
HFIP	1,1,1,3,3,3-hexafluoroisopropanol
HIV	Human immunodeficiency virus
HMBC	Heteronuclear multiple bond coherence
HMDS	Hexamethyldisilane
HMQC	Heteronuclear multiple quantum coherence
HPLC	High performance liquid chromatography
HRMS	High resolution mass spectrometry
HSQC	Heteronuclear single quantum coherence
Hz	Hertz
ICy	1,3-Dicyclohexylimidazolium
IES	Internal electrophilic substitution
IMes	1,3-Dimesitylimidazolium
IPr	1,3-Bis(2,6-diisopropylphenyl)imidazolium
iPr or i-Pr or ^{i}Pr	isopropyl
IR	Infrared
J	Coupling constant
KIE	Kinetic isotope effect
LC	Liquid chromatography
LED	Light emitting diode
mA	milliampere
m-CPBA	*m*-Chloroperoxybenzoic acid
Mes	Mesityl
MHP	*N*-2-pyridylhydrazide
mp	melting point
MPAA	Mono protected amino acid
MPS	*N*-methylphenyl sulfoximine
MPyS	*S*-methyl-*S*-2-pyridyl-sulfoximine
MS	Mass spectrometry or molecular sieves

Ms	Mesyl
MW	Microwave
NBP	*N*-bromophthalimide
nBu or n-Bu or ^{n}Bu	n-butyl
NCTS	*N*-cyano-*N*-phenyl-*p*-toluenesulphonamide
nd	not detected
NHC	*N*-heterocyclic carbene
NIS	*N*-iodosuccinimide
NMO	*N*-methylmorpholine-*N*-oxide
NMP	*N*-methyl-2-pyrrolidone
NMR	Nuclear magnetic resonance
NOESY	Nuclear overhauser effect spectroscopy
nr	no reaction
Ns	Nosyl
NSAID	Nonsteroidal anti-inflammatory drug
OA	Oxidative addition or oxalamide
O. S.	Oxidation state
Oxa	2-aminophenyl oxazoline
PA	Picolinamide or 2-picolinamide
PEG	Polyethylene glycol
PFT	Protein farsenyl transferase
PIDA	Phenyliodonium diacetate
PIP	2-pyridylisopropylamine
Piv	Pivalic or pivaloyl
Ph	Phenyl
Phe	Phenylalanine
PP	2-Aminophenyl-1*H*-pyrazole
Py	Pyridyl
Pym	Pyrimidyl
PyO	Pyridine-*N*-oxide
PyPhos	2-(2-(Diphenylphosphino)ethyl)pyridine
Q	Quadrapole or quinoline
rds	rate determining step

rt	room temperature
RVC	Reticulated vitreous carbon
SC	Single crystal
S_EAr	Electrophilic aromatic substitution
SET	Single electron transfer
SIMes	1,3-Bis(2,4,6-trimethylphenyl)imidazolinium
TBAB	Tetrabutylammonium bromide
TBAI	Tetrabutylammonium iodide
TBHP	*tert*-butyl hydroperoxide
tBu or t-Bu or ^{t}Bu	*tert*-butyl
Tces	Trichloroethoxysulfonyl
TCP	1,2,3-Trichloropropane
TEMPO	(2,2,6,6-tetramethylpiperdin-1-yl)oxyl
TFA	Trifluoroacetic acid
TFE	2,2,2-trifluoroethanol
THF	Tetrahydrofuran
TIPS	Triisopropylsilyl
TIPS-EBX	1-[(Triisopropylsilyl)ethynyl]1,2-benziodoxol-3(1*H*)-one
TLC	Thin layer chromatography
TM	Transition metal
TMAO	Trimethylamine *N*-oxide
TMEDA	Tetramethylethylenediamine
TMS	Tetramethylsilane or trimethylsilyl
$TMSCF_3$	Trifluoromethyltrimethylsilane
TMSCN	Trimethylsilyl cyanide
TOAB	Tetraoctylammonium bromide
Tof	Time of flight
TosMIC	*p*-Tosylmethyl isocyanide
TPBP	*tert*-butyl peroxybenzoate
TS	Transition state
Ts	Tosyl
TsOH	*p*-Toluenesulfonic acid
XRD	X-ray diffraction

Synopsis

The thesis entitled "***Exploring Transition Metals (Co, Cu, Rh & Ir) for the Construction of C–C and C–Heteroatom Bonds via C–H Activation Strategy: Expeditious Synthesis of Densely Functionalized Heterocyclic Architectures***" has been divided into seven chapters based on the results obtained by the experiments conducted during the period of research. **Chapters 1** and **5** are introductory chapters on transition metal-catalyzed C–H activation. The rest of the five **Chapters** (**2**, **3**, **4**, **6**, **7**) emphasize on the formation of C–C and C–Het bonds employing Co, Cu, Rh and Ir-catalyzed C–H activation.

In **Chapter 1** and **Chapter 5**, a general overview of transition metal-catalyzed C–H activation is given with a detailed sketch of cobalt (Co), copper (Cu), rhodium (Rh) and iridium (Ir)-catalyzed C–H activation. **Chapter 1** gives an outline of the origin of the C–H activation field and the brief history associated with it, the swift transition from traditional approaches, the challenges associated with it, its classifications and synthetic applications. Thereafter, emphasis is given on the earth-abundant first-row transition metals, Co and Cu-catalyzed C–H activation reactions. The other half of the story is covered in **Chapter 5**, which provides a thorough understanding of the second-row and third-row transition metal, Rh and Ir-catalyzed C–H activation reactions respectively. Combining both these chapters, the various modes of C–H activation, the concept of the undirected and directing group assisted C–H activation, the classification of C–H activation reactions based on the nature of substrates, the various types of bond forming reactions via C–H activation strategy, the importance of kinetic isotopic effect and other mechanistic studies to rationalize the mechanism of a reaction, are all discussed in detail. Asymmetric C–H activation, which has transformed this field to a whole new level for the efficient synthesis of chiral architectures in an atom and step-economic manner has also been exemplified. New-edge photochemical and electrochemical C–H activation reactions are also briefly discussed.

In **Chapter 2**, a cobalt-catalyzed *ortho* sp^2 C–H acetoxylation of benzamides is described using $Mn(OAc)_3.2H_2O$ as an unprecedented acetoxy source with the aid of a bidentate 8-aminoquinoline directing group. The beauty of this methodology lies in the role played by manganese(III) acetate which serves both as an oxidant and also as the acetoxylating reagent, which was not known in C–H functionalization chemistry. A brief account of the importance of the acetoxy (–OAc) group has been provided because of its ubiquitousness in various pro-

drugs, natural products, and medicinal chemistry.[1] One of the prime examples of it is the biologically active aspirin molecule which plays a pivotal role in daily human life, which further underlines the importance of this work. A thorough literature survey showed that second-row transition metals like Ru, Rh, and especially Pd have been well explored in C–H acetoxylation chemistry.[2] But, these noble metal catalysts suffer from the drawbacks of low earth abundance, expensive nature and bio-incompatibility. Later on, to overcome these, sporadic examples of earth-abundant Cu-mediated direct C–H acetoxylation reactions came up and opened the door for the first-row base metal catalysts to be explored for this purpose.[3] In this context, a series of commonly used acetoxy sources has been studied and reviewed. Cobalt is a cheap and earth-abundant 3d transition metal which is known to have excellent catalytic properties in C–H activation chemistry,[4] more prominent with bidentate directing groups. So, we envisioned that this metal carries the potential for catalyzing direct C–H acetoxylation reaction in aromatic systems with the aid of 8-aminoquinoline bidentate auxiliary.

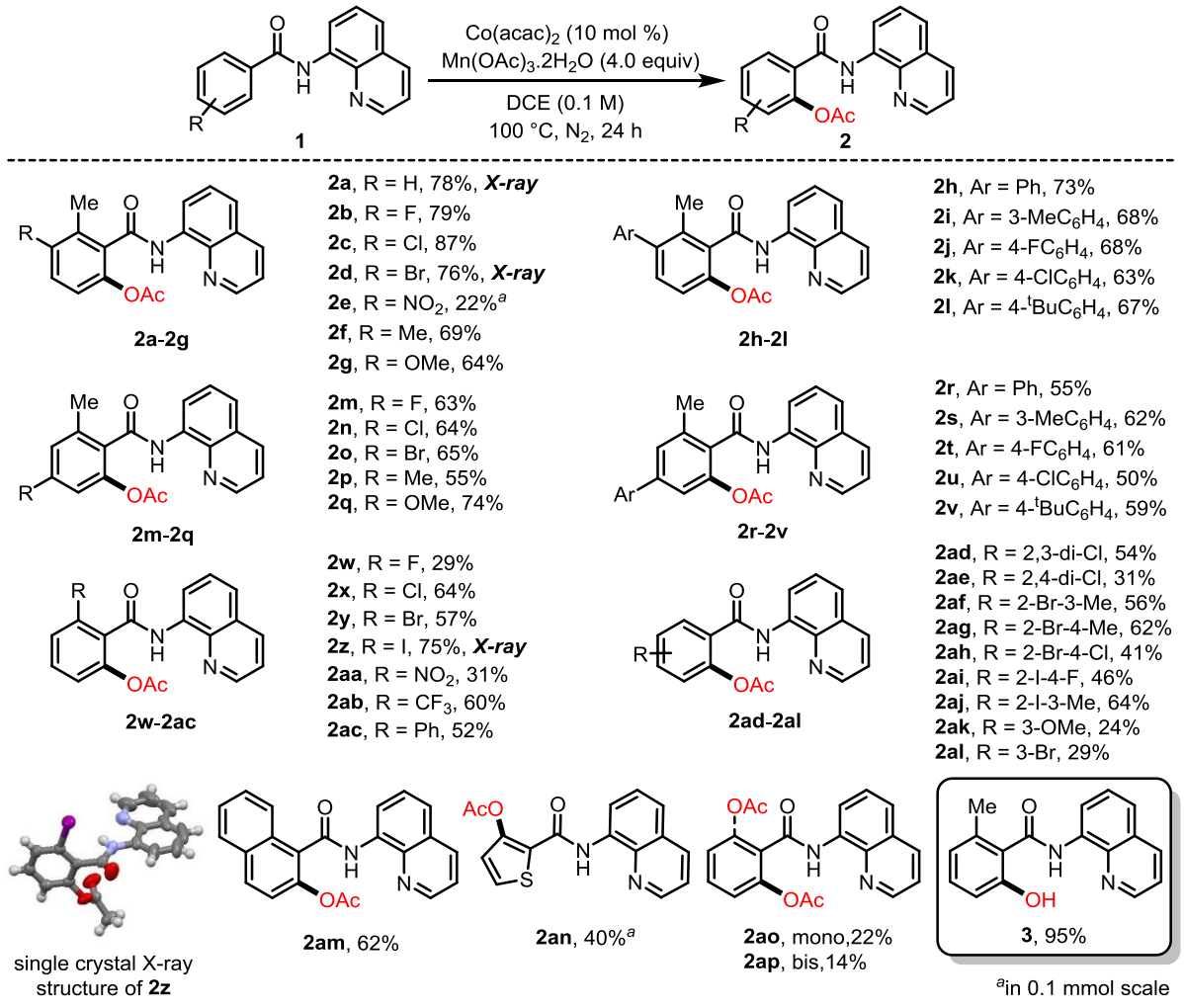

Scheme 1. Cobalt-catalyzed *ortho* sp^2 C–H acetoxylation of arylamides.

Thorough optimization studies led to $Co(acac)_2$ as the optimal catalyst for the reaction with a super-stoichiometric amount of $Mn(OAc)_3.2H_2O$ in DCE solvent, giving access to a wide range of acetoxylated benzamides in good to excellent yields. The substrate scope was quite broad and the functional group tolerance was also fair throughout (Scheme 1). But, *ortho* unsubstituted benzamides produced diminished yields of mono acetoxylated products and the formation of the bis acetoxylated product was observed in case of the parent substrate. On a higher note, the reaction was found to be scalable on a gram scale and the acetoxylated product could be successfully hydrolysed to the *ortho* hydroxy benzamide product under suitable conditions, showcasing the synthetic utility of the methodology. Next, a series of mechanistic experiments like the H/D exchange experiment, kinetic isotope experiments, understanding the effect of substituents on the reaction, and synthesis of one of the key possible intermediates of the reaction which could catalyze the reaction, were performed and are discussed. Gaining knowledge from these experiments, a plausible catalytic cycle for this reaction has been proposed.

In **Chapter 3**, a copper-mediated direct and selective thiolation of quinazolinones is demonstrated for the synthesis of pharmaceutically relevant thioquinazolinones. Quinazolinones are one of the privileged scaffolds in organic chemistry due to its presence in varieties of medicinally important molecules and drugs. Similarly, thio-tethered quinazolinones are found in many drugs and also known to exhibit anti-cancer, anti-platelet, and anti-inflammatory activities making their synthesis of utmost importance.[5] To achieve this feat, we wanted to harness the power of directing group assisted transition metal-catalyzed direct C–H functionalization strategy. An extensive literature search showed that direct C–H sulfenylation reactions were well established using both 4d and 5d transition metals like Pd, Rh, Ru as well as 3d transition metals like Cu, Co, Ni.[6] Also, quinazolinone substrates have been employed as a directing group in C–H activation chemistry and only a few examples exist where their direct functionalization was achieved.[7] With our aim of developing a sustainable method for the synthesis of thioquinazolinones, we set out to explore the power of cheap and abundant copper salts for this purpose, and thereby reported a copper-promoted thiolation of relatively less explored quinazolinones with the assistance of monodentate pyridine or pyrimidine directing group using readily available diaryl disulfides.

Optimization studies led to the fact that $Cu(OAc)_2$ salt in a stoichiometric amount in combination with a stoichiometric amount of *p*-benzoquinone additive in DCE solvent is the

ideal combination for realizing the desired thiolation reaction. Attempts toward the development of its catalytic version remained unsuccessful which is the only drawback of this methodology. The reaction failed to deliver the product in high yield with catalytic amounts of $Cu(OAc)_2$ and oxidant combination. Employing the optimized condition, a series of substrates furnished the desired thiolated products in moderate to excellent yields (Scheme 2). Gratifyingly, the method was not only limited to quinazolinones, but could also be extended to pyrimidinones expanding the scope of the reaction. Control experiment signified the importance of the pyridine/pyrimidine directing group, and radical scavenging experiments suggested that a radical mechanism might be involved in the reaction course based on which a plausible mechanism has been proposed.

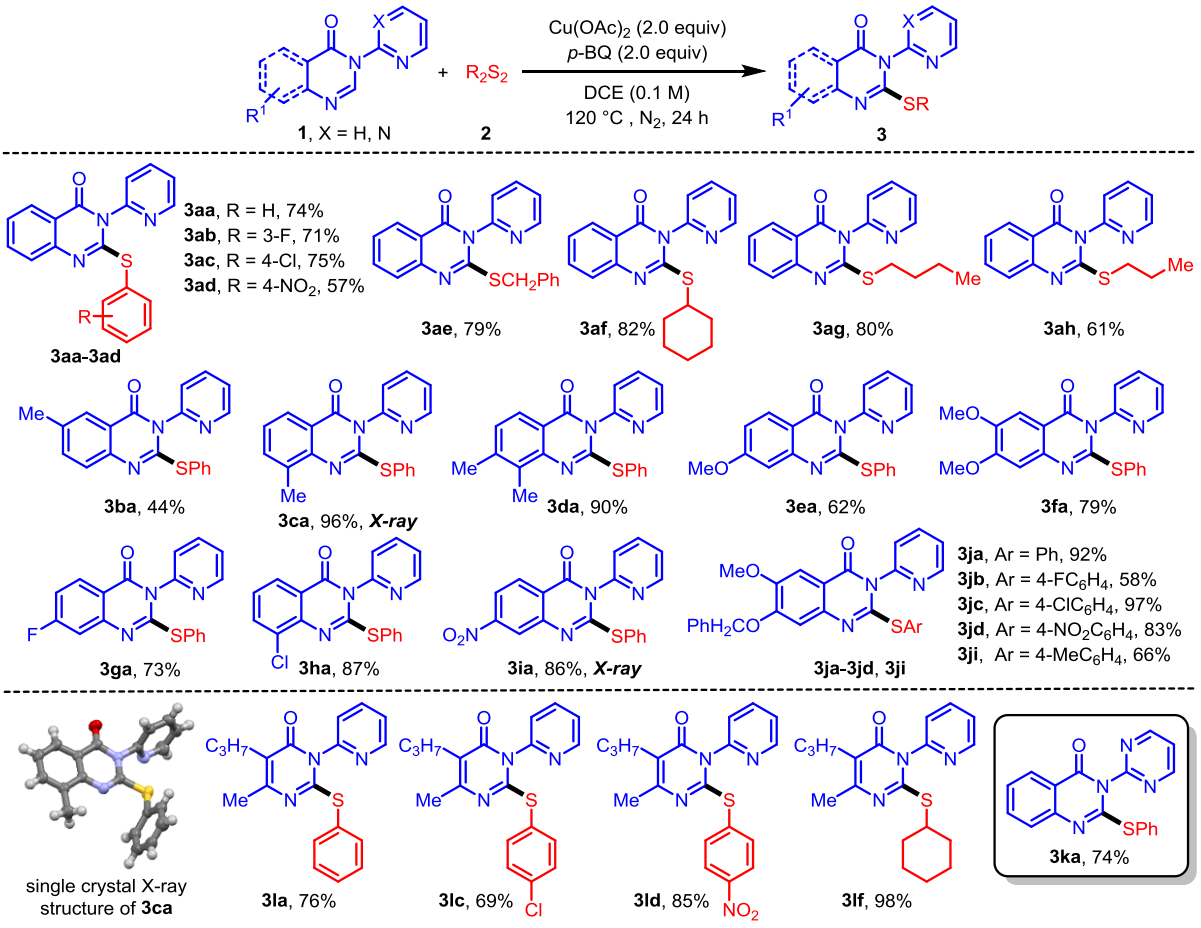

Scheme 2. Copper-mediated direct C–H thiolation of quinazolinones and pyrimidinones.

Chapter 4 discusses about an 8-aminoquinoline directed copper-catalyzed intermolecular C–H silylation of benzamides using easily accessible disilanes to afford an array of organosilane products. Organosilicons remain an indispensable source for the synthesis of large variety of compounds due to the nature of the C–Si bond. Owing to its physical, chemical, and bioactive

properties, these compounds have found regular use in the fields of synthetic organic chemistry, polymer chemistry, material sciences, and in pharmaceutical industry.[8] In this context, their synthesis has become a foremost necessity in organic chemistry and evidently gained lots of interest from different research groups all over the world. Among them, transition metal-catalyzed direct C–H silylation has become the breakthrough strategy over the past years.

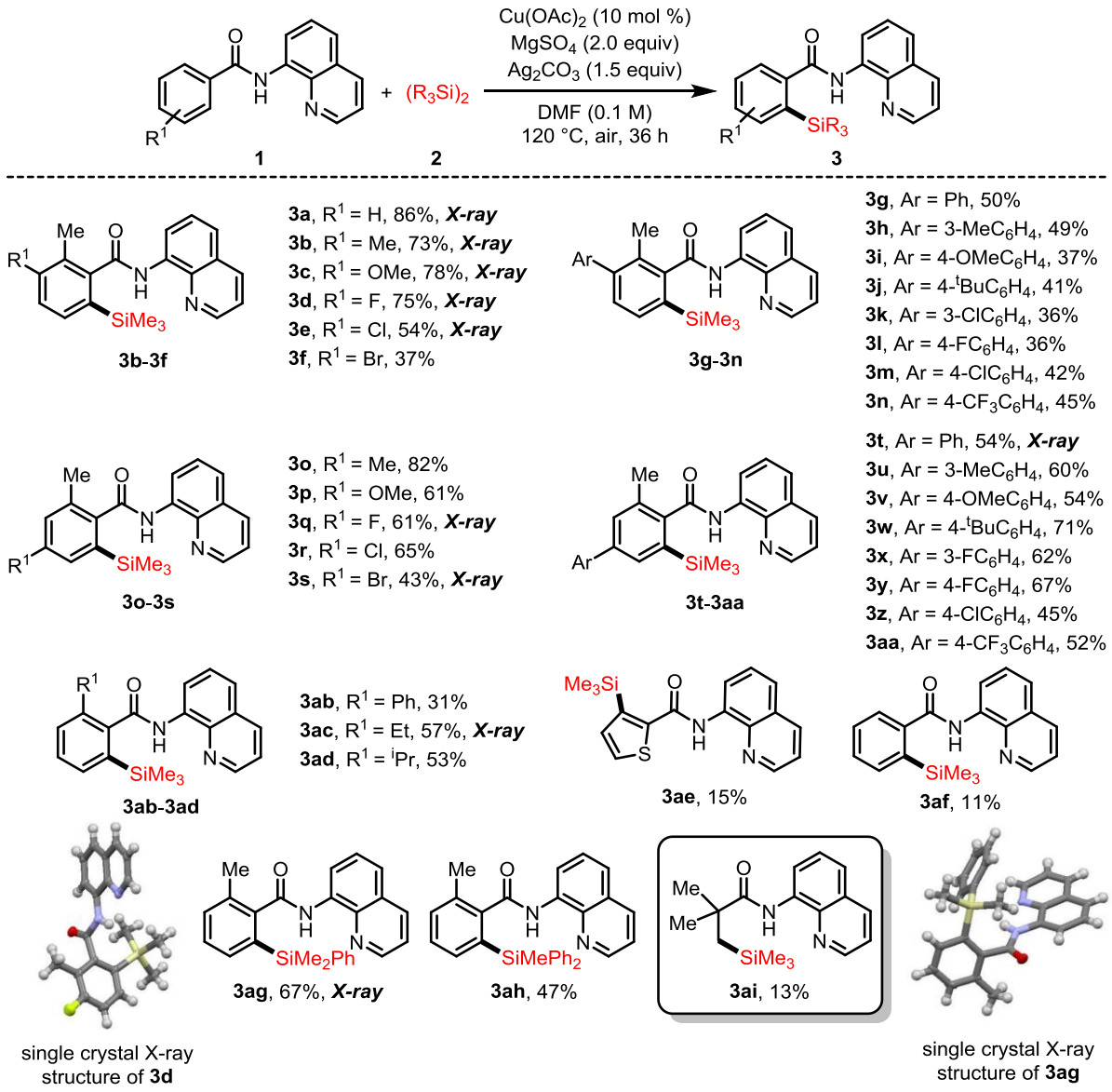

Scheme 3. Copper-catalyzed *ortho* sp^2 C–H silylation of arylamides.

An extensive review has been conducted which indicates that transition metals like Pd, Ru, Rh, Ir, Sc, Pt all have participated in both C(sp^2)–H and C(sp^3)–H silylation reactions.[9] Among them, in recent years, Pd is a well explored transition metal for bidentate DG assisted C–H silylation at *ortho*/*meta*/*para* positions, while earth-abundant first-row transition metal such as

copper was not explored for this purpose to the best of our knowledge. From the literature search, it was observed that 3d transition metals like Cu, Co, Ni, Fe work well with bidentate systems for direct C–H functionalization reactions.[10] In this regard, we aimed to develop a direct silylation strategy employing copper catalysis which would overcome the limitations of low earth-abundance, high cost, bio-incompatibility suffered by the previously employed transition metal catalysts. In this chapter, we have elaborated the findings of a copper-catalyzed approach for *ortho* selective silylation of arylamides with the aid of 8-AQ bidentate chelation using inexpensive disilanes as organosilicon source giving direct access to structural C–Si bonds without the need of an inert atmosphere.

Extensive optimization led us to conclude that, employing $Cu(OAc)_2$ catalyst successfully catalyzes the reaction in the presence of $MgSO_4$ additive and Ag_2CO_3 oxidant in DMF solvent under air atmosphere to produce the desired silylated benzamides in moderate to good yields. The scope of the reaction was found to be quite broad and tolerated a wide range of substituents at various positions of the amides (Scheme 3). Also, $C(sp^3)$–H silylation occurred but in poor yield, and bulky silanes were found to be relatively successful. But one of the drawbacks of this reaction was the drastic decrease in the yield of the reaction in case of *ortho* unsubstituted benzamides. The method was scalable and operationally simple. Few mechanistic studies were conducted which shed light to the reaction mechanism and based on these studies a plausible mechanism has been proposed.

Chapters 2-4 demonstrate the C–H functionalization methodologies developed employing Co and Cu catalysis. **Chapters 6** and **7** elucidate the development of methodologies catalyzed by heavier noble transition metals like Rh (second-row) and Ir (third-row) respectively.

Chapter 6 reveals a rhodium-catalyzed regio- and diastereoselective [3+2]-spiroannulation of benzoxazines with chalcones via a redox-neutral C–H activation/annulation cascade providing access to α-aroyl spiro-indanamines. Both the benzoxazine derivatives and α,β-unsaturated carbonyl compounds like chalcones are pharmaceutically and synthetically important moieties with a plethora of biological activities and synthetic applications.[11] On the other side, indane and indene scaffolds and their multiple analogues are found to be present in many natural products and constitute a series of therapeutically and medicinally relevant molecules.[12] We hypothesized a one-pot methodology which might give rise to poly-substituted spiro-indanyl amine fragments containing 2,3-dihydro-1,4-benzoxazine core clubbing benzoxazines and chalcones. This can be achieved taking advantage of the robust unactivated cyclic iminyl

functional group of benzoxazine as a chelating entity and the activated double bond of chalcone as a suitable coupling fragment. Although there are quite a number of reports on the synthesis of (spiro)indanyl/indenyl frameworks coupling imines and various unsaturated coupling partners employing tandem C–H activation/annulation strategy, but most of them are limited to the use of activated imines as directing groups.[13] Unactivated cyclic ketimines like benzoxazines have been recently used in [3+2]-spiroannulation reactions, whereas the use of chalcones in C–H activation has been largely limited to as 1,4-addition partners.[14] From a thorough literature study, we thought of harnessing the power of rhodium catalysis for developing a process for such annulation reaction and simultaneous generation of more than one stereogenic center which is particularly rare.

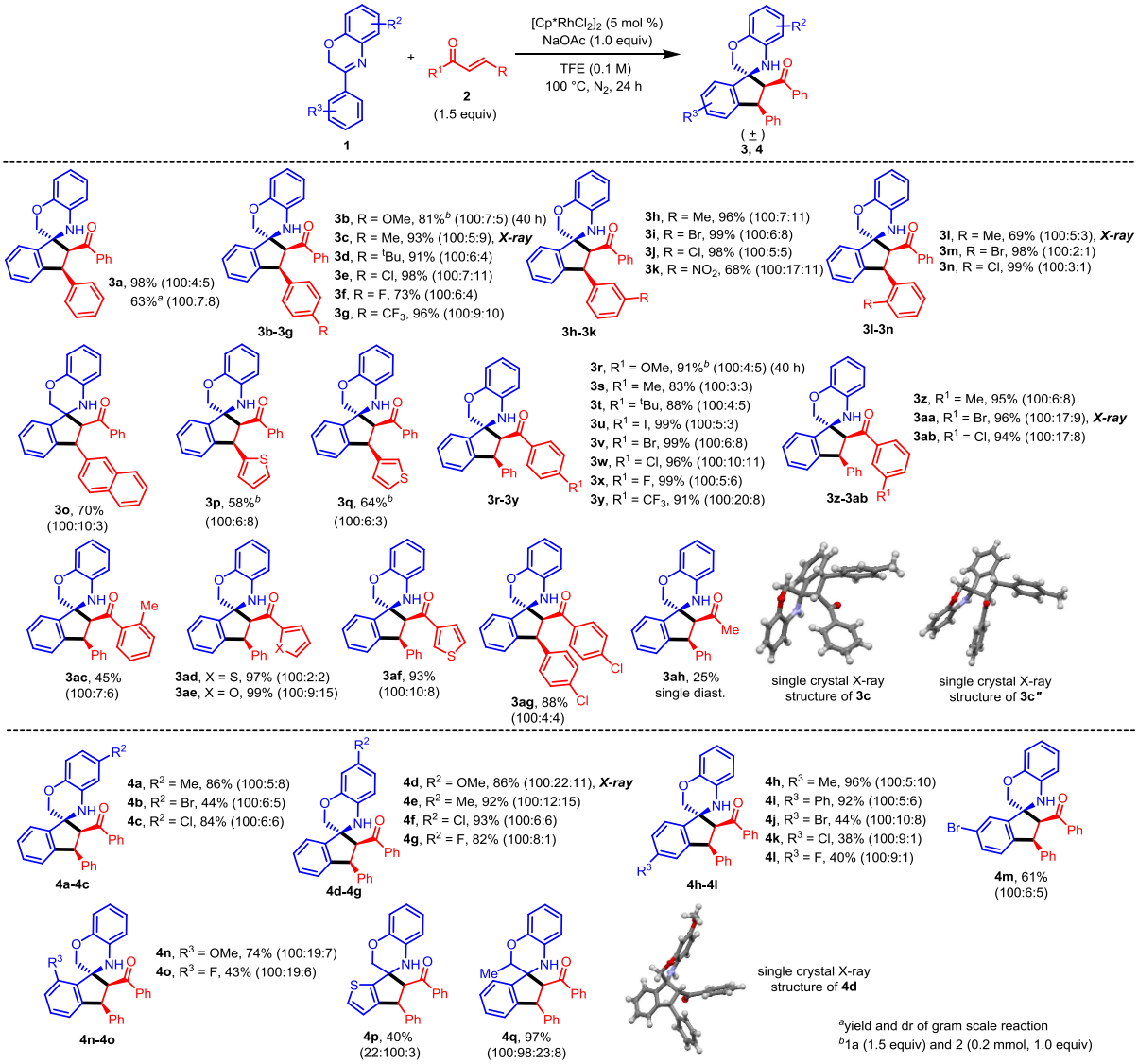

Scheme 4. Rhodium-catalyzed diastereoselective spirocyclization between benzoxazines and chalcones.

Rigorous screening of different catalytic conditions led to the use of $[Cp^*RhCl_2]_2$ as catalyst and NaOAc as an additive in TFE solvent delivering the desired spiroannulated products in good to excellent yields with high diastereoselectivity. All kinds of substitutions both on the chalcones and benzoxazines were found to be compatible under the reaction conditions and showed excellent reactivity. The major diastereomers could be easily obtained by the crystallization of the mixture of diastereomers displaying a broad scope for the reaction (Scheme 4). The major diastereomer could also be easily converted into the minor diastereomers under appropriate conditions. The structure and relative stereochemistry of the isomers was established by 2D NMR studies and single crystal X-ray data analysis. The reaction was scalable implying the practicability of the methodology. A series of mechanistic investigations were executed including the synthesis and application of rhodacycle complexes that helped us in proposing a plausible pathway for the reaction.

In **Chapter 7**, an iridium-catalyzed *ortho* selective C–H arylation of cyclic *N*-sulfonyl ketimines using environmentally benign arylsiloxanes has been delineated. The reaction occurs in short time under ambient temperature providing access to a wide range of pharmaceutically relevant novel biaryl compounds which are found to be substructures of many biologically active scaffolds. Biaryl motifs are extremely important scaffolds in modern organic synthesis from the viewpoints of biological activity, physical property, presence in agrochemicals and natural products, and also from synthetic aspects.[15] Various traditional cross-coupling methods are the most practised strategies for the synthesis of the same which lack utility in terms of atom and step economy as well as require extensive prefunctionalization.[16] Biaryl formation via C–H activation is well documented using diverse arylating reagents out of which arylsiloxanes are one of the cheapest and easily available environmentally friendly alternatives, which have been relatively less explored employing different transition metal catalysts.[17]

Cyclic *N*-sulfonyl ketimines belong to a class of bioactive compounds and are also essential precursors to the synthesis of medicinally important scaffold, benzosultams, which also possess a wide range of biological activities like anti-HIV, anti-diabetic, etc.[18] We envisioned that a hybrid molecule consisting of a biaryl system containing sulfonyl ketimines might manifest unique features and postulated that it can be achieved via direct arylation of inert aryl C–H bonds by exploiting the directing property of cyclic *N*-sulfonyl ketimines. However, the chelating ability of its imine functional group is less explored on account of its weak coordination nature due to the presence of adjacent electron-withdrawing sulfonyl group, and

apparently only a few literature precedents of its application in direct C–H functionalization are available which are discussed in details.[19] Among the established arylation protocols using arylsiloxanes as arylating agents, they suffer from various limitations like high temperature, longer reaction times, among others, except for an iridium-catalyzed arylation methodology which could be achieved at room temperature. Therefore, we hypothesized that we could implement iridium catalysis successfully in our venture.

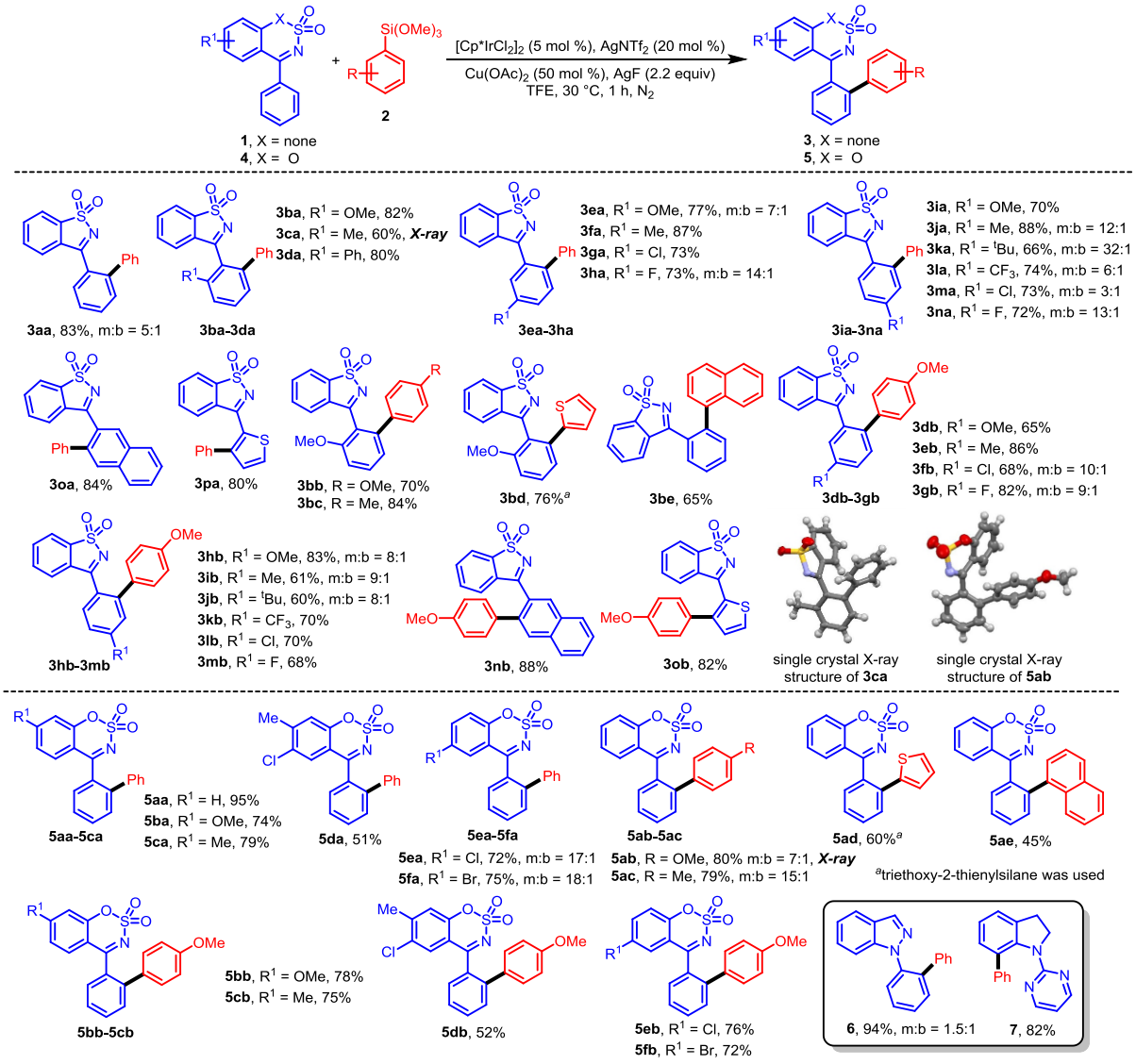

Scheme 5. Iridium-catalyzed direct C–H arylation of *N*-sulfonyl ketimines with arylsiloxanes.

Thorough optimization led us to the optimal conditions employing $[Cp^*IrCl_2]_2$ as catalyst, $AgNTf_2$ as halide scavenger, $Cu(OAc)_2$ as co-oxidant and AgF as the oxidant as well as fluoride source in TFE solvent at ambient temperature for 1 h, which efficiently performed the *ortho* arylation of cyclic *N*-sulfonyl ketimines using arylsiloxanes as the arylating partner. The

reaction exhibited a wide substrate scope with both five-membered as well as relatively less explored six-membered cyclic ketimines yielding arylated products in good yields accompanying high mono selectivity (Scheme 5). The reaction showed gram scale adaptability and the parent arylated product was also easily epoxidized to construct a fused oxaziridine system, features which displayed the generality of this methodology. Few mechanistic experiments like H/D exchange experiment and kinetic isotope effect experiments were conducted which are discussed in details. Based on their observations, a probable catalytic cycle for the reaction has been proposed.

References

1. (a) Nichols, D. E.; Frescas, S. *Synthesis* **1999**, *1999*, 935. (b) Rais, R.; Vávra, J.; Tichý, T.; Dash, R. P.; Gadiano, A. J.; Tenora, L.; Monincová, L.; Bařinka, C.; Alt, J.; Zimmermann, S. C.; Slusher, C. E.; Wu, Y.; Wozniak, K.; Majer, P.; Tsukamoto, T.; Slusher, B. S. *J. Med. Chem.* **2017**, *60*, 7799-7809.
2. (a) Dick, A. R.; Hull, K. L.; Sanford, M. S. *J. Am. Chem. Soc.* **2004**, *126*, 2300. (b) Yu, W.; Chen, J.; Gao, K.; Liu, Z.; Zhang, Y. *Org. Lett.* **2014**, *16*, 4870. (c) Okada, T.; Nobushige, K.; Satoh, T.; Miura, M. *Org. Lett.* **2016**, *18*, 1150.
3. Chen, X.; Hao, X.-S.; Goodhue, C. E.; Yu, J.-Q. *J. Am. Chem. Soc.* **2006**, *128*, 6790.
4. Moselage, M.; Li, J.; Ackermann, L. *ACS Catal.* **2016**, *6*, 498.
5. (a) Gupta, C. M.; Bhaduri, A. P.; Khanna, N. M. *J. Med. Chem.* **1968**, *11*, 392. (b) Converso, A.; Hartingh, T.; Garbaccio, R. M.; Tasber, E.; Rickert, K.; Fraley, M. E.; Yan, Y.; Kreatsoulas, C.; Stirdivant, S.; Drakas, B.; Walsh, E. S.; Hamilton, K.; Buser, C. A.; Mao, X.; Abrams, M. T.; Beck, S. C.; Tao, W.; Lobell, R.; Sepp-Lorenzino, L.; Zugay-Murphy, J.; Sardana, V.; Munshi, S. K.; Jezequel-Sur, S. M.; Zuck, P. D.; Hartman, G. D. *Bioorg. Med. Chem. Lett.* **2009**, *19*, 1240.
6. Iwasaki, M.; Nishihara, Y. *Dalton Trans.* **2016**, *45*, 15278-15284.
7. (a) Feng, Y.; Tian, N.; Li, Y.; Jia, C.; Li, X.; Wang, L.; Cui, X. *Org. Lett.* **2017**, *19*, 1658. (b) Das, D.; Biswas, A.; Karmakar, U.; Chand, S.; Samanta, R. *J. Org. Chem.* **2016**, *81*, 842.
8. Mortensen, M.; Husmann, R.; Veri, E.; Bolm, C. *Chem. Soc. Rev.* **2009**, *38*, 1002.
9. (a) Fumitoshi, K.; Kimitaka, I.; Mitsutaka, M.; Naoto, C.; Shinji, M. *Chem. Lett.* **2001**, *30*, 422. (b) Sakakura, T.; Tokunaga, Y.; Sodeyama, T.; Tanaka, M. *Chem. Lett.* **1987**, *16*, 2375. (c) Ishiyama, T.; Sato, K.; Nishio, Y.; Miyaura, N. *Angew. Chem. Int. Ed.* **2003**, *42*, 5346. (d) Oyamada, J.; Nishiura, M.; Hou, Z. *Angew. Chem. Int. Ed.* **2011**, *50*, 10720.

(e) Uchimaru, Y.; El Sayed, A. M. M.; Tanaka, M. *Organometallics* **1993**, *12*, 2065. (f) Kanyiva, K. S.; Kuninobu, Y.; Kanai, M. *Org. Lett.* **2014**, *16*, 1968.

10. (a) Gandeepan, P.; Müller, T.; Zell, D.; Cera, G.; Warratz, S.; Ackermann, L. *Chem. Rev.* **2019**, *119*, 2192. (b) Rej, S.; Ano, Y.; Chatani, N. *Chem. Rev.* **2020**, *120*, 1788.
11. (a) Ilaš, J.; Jakopin, Ž.; Borštnar, T.; Stegnar, M.; Kikelj, D. *J. Med. Chem.* **2008**, *51*, 5617. (b) Singh, P.; Anand, A.; Kumar, V. *Eur. J. Med. Chem.* **2014**, *85*, 758.
12. Gardelli, C.; Wada, H.; Ray, A.; Caffrey, M.; Llinas, A.; Shamovsky, I.; Tholander, J.; Larsson, J.; Sivars, U.; Hultin, L.; Andersson, U.; Sanganee, H. J.; Stenvall, K.; Leidvik, B.; Gedda, K.; Jinton, L.; Rydén Landergren, M.; Karabelas, K. *J. Med. Chem.* **2018**, *61*, 5974.
13. (a) Kuninobu, Y.; Kawata, A.; Takai, K. *J. Am. Chem. Soc.* **2005**, *127*, 13498. (b) Fukutani, T.; Umeda, N.; Hirano, K.; Satoh, T.; Miura, M. *Chem. Commun.* **2009**, 5141. (c) Zhao, P.; Wang, F.; Han, K.; Li, X. *Org. Lett.* **2012**, *14*, 5506. (d) Li, S.-S.; Wu, L.; Qin, L.; Zhu, Y.-Q.; Su, F.; Xu, Y.-J.; Dong, L. *Org. Lett.* **2016**, *18*, 4214. (e) Liu, H.; Li, J.; Xiong, M.; Jiang, J.; Wang, J. *J. Org. Chem.* **2016**, *81*, 6093. (f) Liu, W.; Zell, D.; John, M.; Ackermann, L. *Angew. Chem. Int. Ed.* **2015**, *54*, 4092.
14. Zhu, C.; Luan, J.; Fang, J.; Zhao, X.; Wu, X.; Li, Y.; Luo, Y. *Org. Lett.* **2018**, *20*, 5960.
15. (a) Horton, D. A.; Bourne, G. T.; Smythe, M. L. *Chem. Rev.* **2003**, *103*, 893. (b) McGlacken, G. P.; Bateman, L. M. *Chem. Soc. Rev.* **2009**, *38*, 2447.
16. Hassan, J.; Sévignon, M.; Gozzi, C.; Schulz, E.; Lemaire, M. *Chem. Rev.* **2002**, *102*, 1359.
17. (a) Yang, S.; Li, B.; Wan, X.; Shi, Z. *J. Am. Chem. Soc.* **2007**, *129*, 6066. (b) Senthilkumar, N.; Parthasarathy, K.; Gandeepan, P.; Cheng, C.-H. *Chem. Asian J.* **2013**, *8*, 2175. (c) Nareddy, P.; Jordan, F.; Szostak, M. *Chem. Sci.* **2017**, *8*, 3204. (d) Hachiya, H.; Hirano, K.; Satoh, T.; Miura, M. *Angew. Chem. Int. Ed.* **2010**, *49*, 2202. (e) Bu, Q.; Gońka, E.; Kuciński, K.; Ackermann, L. *Chem. Eur. J.* **2019**, *25*, 2213. (f) Shin, K.; Park, Y.; Baik, M.-H.; Chang, S. *Nat. Chem.* **2018**, *10*, 218.
18. (a) Hendricks, R. T.; Spencer, S. R.; Blake, J. F.; Fell, J. B.; Fischer, J. P.; Stengel, P. J.; Leveque, V. J. P.; LePogam, S.; Rajyaguru, S.; Najera, I.; Josey, J. A.; Swallow, S. *Bioorganic & Medicinal Chemistry Letters* **2009**, *19*, 410. (b) Elsayed, M. S. A.; El-Araby, M. E.; Serya, R. A. T.; El-Khatib, A. H.; Linscheid, M. W.; Abouzid, K. A. M. *Eur. J. Med. Chem.* **2013**, *61*, 122.
19. Nishimura, T.; Ebe, Y.; Hayashi, T. *J. Am. Chem. Soc.* **2013**, *135*, 2092.

Chapter 1: Introduction || Part-I

A Brief Overview of Cobalt and Copper-Catalyzed C–H Activation

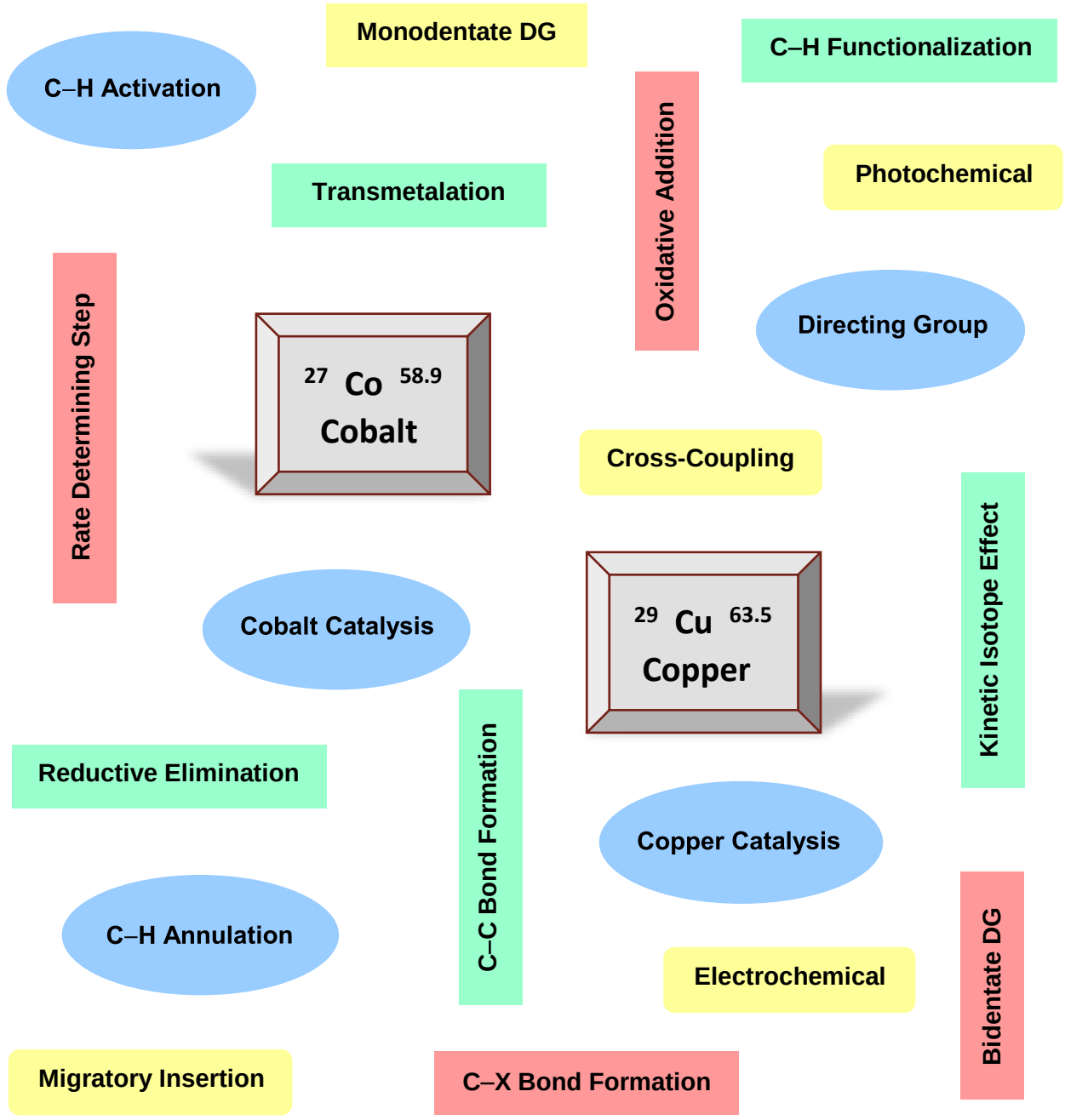

1.1. A Brief History of Transition Metal-Catalyzed Cross-Coupling Reactions

The basic notion of synthetic organic chemistry is the transformation of one functional group to another bringing structural modifications in a molecule. In this realm, transition metal-catalyzed cross-coupling is one of the pioneering discoveries in organic chemistry research area. The development of metal-catalyzed/-mediated cross-coupling reactions can be traced back to 1869 when Glaser reported a copper-promoted homocoupling of metallic acetylides to produce diphenylacetylenes.[1] This seminal work on C(sp)–C(sp) bond formation was followed by another pioneering work in 1901 by Ullmann where he described a C(sp^2)–C(sp^2) homocoupling of halonitrobenzenes using super-stoichiometric amount of copper source.[2,3] This report gave a fundamental understanding that carbon atoms bearing halogen atoms undergo self-coupling. This conclusion gave a breakthrough in the field of metal-catalyzed cross-coupling chemistry which was concurrently further developed by Wurtz-Fittig[4] (organosodium) and Turner[5] (organomagnesium/Grignard reagent). Despite these remarkable achievements, these methods were limited due to the use of (super)stoichiometric amounts of metal salts and issues of selectivity, various side reactions, and also limited to homo-coupled products. This was overcome by the discoveries of Meerwin[6] (1939) and Kharasch[7] (1941) who made the scientific community realize that C–C bond formations employing transition metal is indeed possible in a catalytic fashion. Although it was a huge progress in this field, but still they suffered from drawbacks like functional group compatibility, limited substrate scope, issues of selectivity and varying ratios of homo-coupling to cross-coupling products, thus awaiting further developments. Next, came the solution of the selectivity issues when Cadiot and Chodkiewicz[8] (1955) reported the C(sp)–C(sp) cross-coupling between alkynes and bromoalkynes, followed by the C(sp)–C(sp^2) cross-coupling between aryl/vinyl halides with alkynes developed by Castro and Stephens[9] (1963) using copper salts, furnishing excellent yields of cross-coupled products. Although some drawbacks arose in these methods like the requirement of elevated temperatures and poor solubilities of copper(I) phenylacetylide in case of Castro-Stephens method, these remarkable findings created a fertile ground and paved the way for the organic chemistry research fraternity to nurture and move in a systematic empirical manner to discover further developments in selective cross-coupling chemistry using transition metal catalysis for the next 50 years.

Entered the "jack of all trades", palladium, the revolutionary transition metal in this arena. Hafner's observations of the conversion of ethylene to acetaldehyde in presence of Pd,

popularly known as Wacker's process,[10] and Tsuji's findings in 1965 that carbon nucleophiles undergo reaction with Pd π-allyls,[11] inspired a generation of chemists to utilize palladium as a potent transition metal in cross-coupling chemistry (Scheme 1.1.1). Almost immediately, in parallel Mizoroki[12] (1971) and Heck[13] (1972) independently made the unique discoveries that aryl/benzyl/styryl halides could undergo cross-coupling reactions with alkenes under Pd(II) catalysis, which later came to be known as the famed Mizoroki-Heck reaction. Alongside them, in the same year, Corriu[14] and Kumada[15] independently reported nickel-catalyzed cross-coupling reactions of aryl/alkenyl halides with Grignard reagents, which overcame the shortcomings of the Kharasch coupling reaction. Over the next few years, the scope of palladium catalysis skyrocketed reaching new heights in cross-coupling chemistry. In came the Sonogashira reaction in 1975 employing a Pd-Cu co-catalytic system for the coupling of aryl/vinyl halides with acetylenes under exceedingly mild conditions.[16] At the same time, Murahashi recognized the potential of Pd in Corriu-Kumada reaction and successfully implemented organomagnesium (Grignard) and organolithium reagents as coupling partners, thus improving a lot of factors from the previous Ni-catalyzed process.[17]

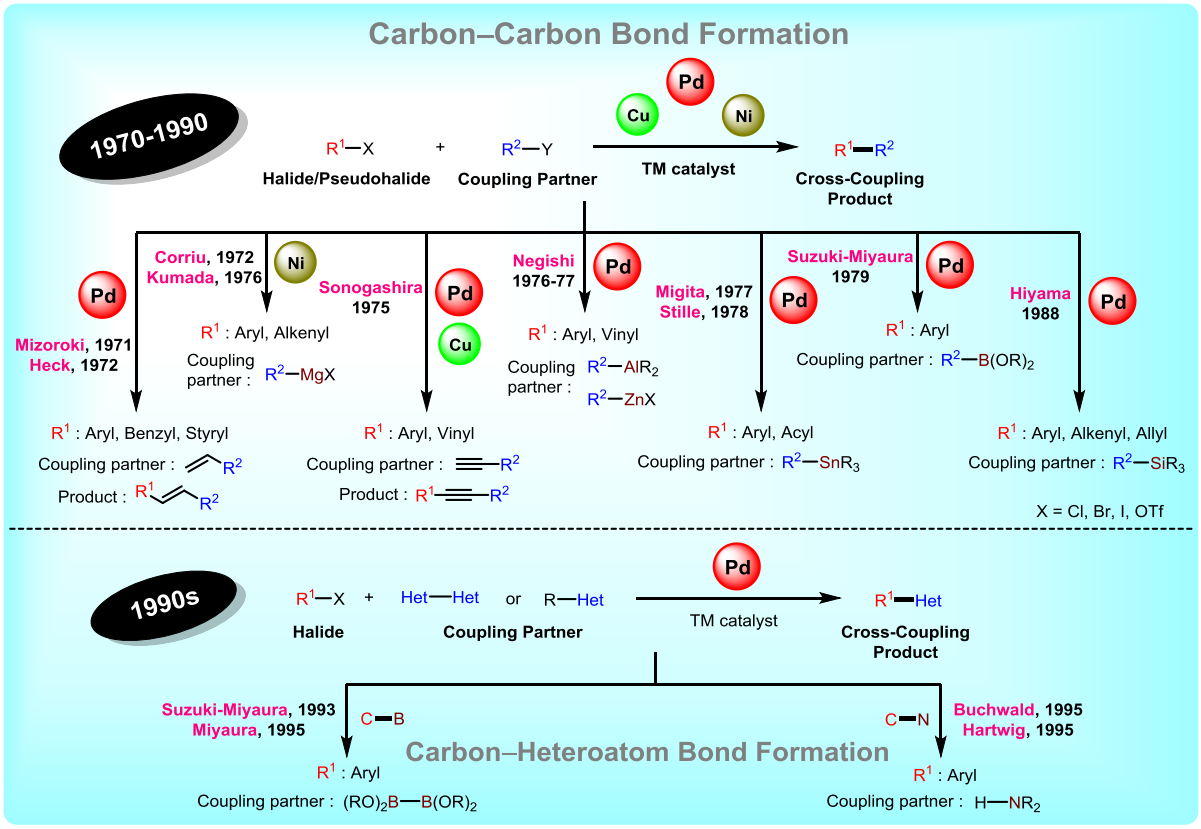

Scheme 1.1.1. Timeline of the developments of transition metal-catalyzed cross-coupling reactions.

These seminal works were followed by another wave of pioneering discoveries where the type of organometallic partners was explored. First, Negishi disclosed the successful implementation of organoaluminium (1976) and organozinc reagents (1977) in cross-coupling reactions, thus providing concrete evidence of the use of other capable organometallic species apart from the lithium and magnesium reagents used till then.[18] The range of partners was further extended shortly to organostannanes, initially by Migita[19] (1977), and then by Stille and Milstein (1978).[20] In 1979, another groundbreaking work was demonstrated by Suzuki where he employed easy-to-handle, air and moisture stable organoboron coupling partners under base-assisted mild Pd-catalyzed coupling reactions with aryl halides.[21] This reaction eventually became a cornerstone in this field with wide industrial applications. The nature of the transmetalation partner was extended again to a more environmentally safe and friendly option to organosilicon reagents by Hiyama in 1988.[22] Hiyama coupling disclosed the cross-coupling of aryl halides and triflates with organosilanes under Pd as well as Ni catalysis in combination with a fluoride source activator. The general mechanistic pathway for these transition metal catalyzed cross-coupling reactions is depicted in Scheme 1.1.2.

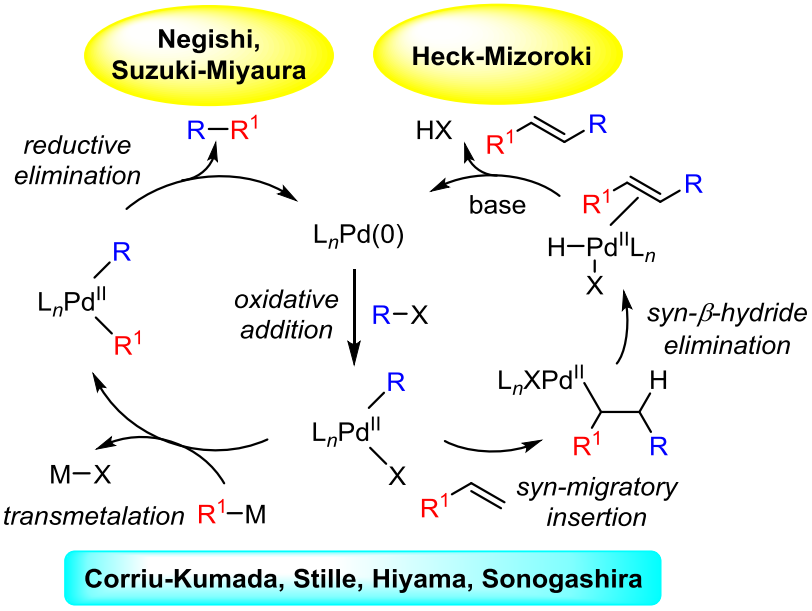

Scheme 1.1.2. General catalytic cycle of cross-coupling reactions.

Up until this point, the evolution of cross-coupling chemistry was limited to C–C bond formations, which was next expanded to C–X (X = heteroatom) bond formations using non-carbon-based nucleophiles, thus adding a new dimension to the palladium-catalyzed cross-coupling processes. In this context, Miyaura and Suzuki (1993, 1995) independently disclosed the formation of C–B bonds using boron esters as suitable coupling partners,[23] followed by the

developments of Buchwald and Hartwig (1995) for C–N cross-coupling reactions under palladium catalysis,[24] and was further extended to C–O, C–S, C–P bonds by various research groups using different transition metals, namely Pd, Ni and Cu (Scheme 1.1.1).[25] To improve on these seminal works on transition metal-catalyzed cross-coupling reactions and make it more general with wider applications in the synthesis of biologically relevant molecules, particularly in a large scale, for the next few years several groups worked on the modifications of previous reaction conditions. This was done in the form of ligand additions and other manipulations,[26] and also by exploring pseudohalides in place of aryl halide partners.[27] Another important discovery, now popularly known as Trost-Tsuji allylation, slightly different from the conventional cross-coupling reactions, was given by Tsuji[11a] (1965) followed by Trost in 1973.[28] They achieved allylic substitutions employing π-allyl palladium complexes.

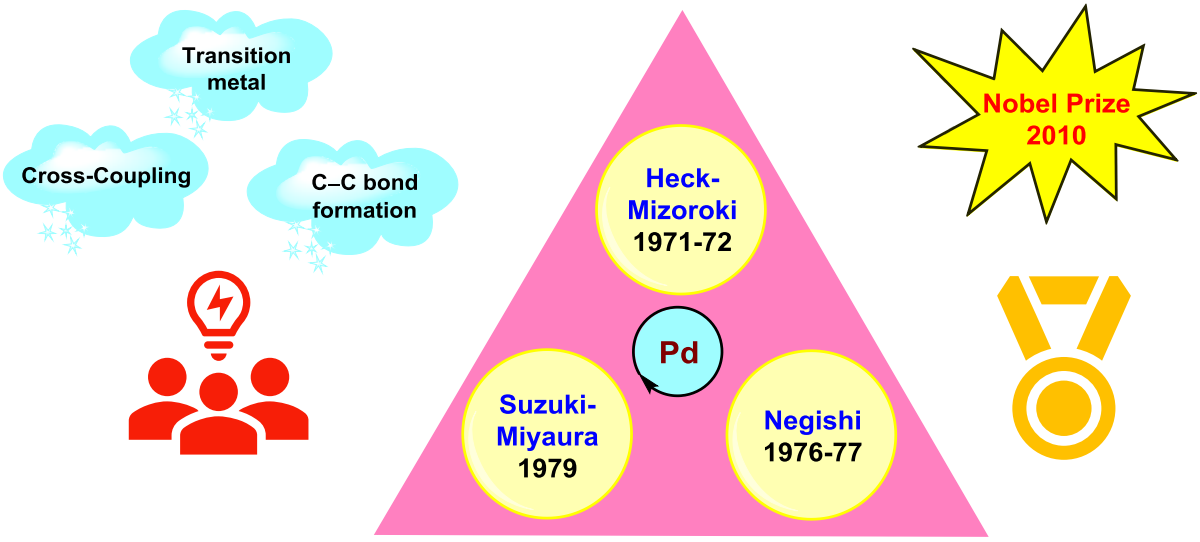

Figure 1.1.1. Nobel-prize winning triad of Heck, Negishi and Suzuki reactions.

All these milestone achievements were fittingly awarded with the 2010 Nobel Prize to Profs. R. F. Heck, E. Negishi, and A. Suzuki (Figure 1.1.1)[29] "for palladium-catalyzed cross couplings in organic synthesis", which further highlighted and strengthened the importance of fundamental research and practical applications of synthetic organic chemistry.

1.2. Introduction to Transition Metal-Catalyzed C–H Activation

Transition metal-catalyzed cross-coupling chemistry, therefore, marked the dawn for modern organic synthesis and became the benchmark process for the generation of carbon–carbon and carbon–heteroatom bonds.[30] Despite all the significant advantages provided by this powerful strategy in terms of vast efficiency, incredible selectivity, and others, it still has its drawbacks

and faces several roadblocks in its applications in synthetic organic chemistry. The primary drawback is the requirement of pre-functionalized starting materials and stoichiometric amounts of organometallic reagents which release toxic halide and metal waste upon reaction, thus making these methods less desirable from the viewpoints of atom and step economy as well as environmental sustainability. It is a dream of organic chemists to develop coupling reactions without the need for pre-functionalization. Therefore, direct activation and functionalization of C–H bonds is highly desirable in synthetic organic chemistry to overcome these challenges (Scheme 1.2.1) which would be the "ideal" synthesis. This chemistry has skyrocketed breaking barriers day in day out for the past two to three decades providing the shortest possible routes to achieve the synthesis of targeted molecules.

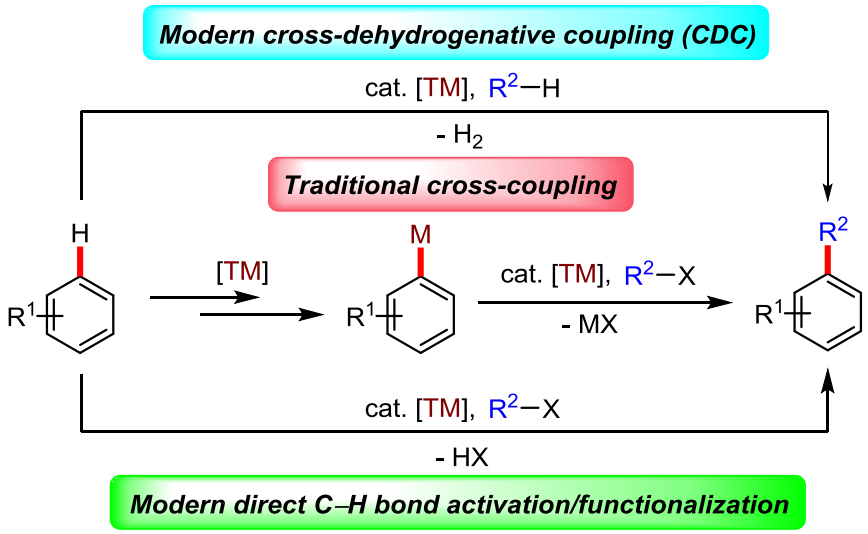

Scheme 1.2.1. Traditional versus Modern C–H functionalization methods.

The ubiquitous nature of C–H bonds in chemical feedstocks makes it a desirable but rarely thought of reactive handle (which has changed in the last two decades) for this purpose. It has even been labelled as the "un-functional" group because of its inherent stability.[31] The omnipresence of C–H bonds in organic molecules reflects the "invisible" character of it and thus the selective functionalization of C–H bonds could be most powerful and broadly applicable method to synthesize organic molecules ranging from the smallest to the most complex natural or unnatural products. But not everything is as easy as said. There are major challenges in the field of C–H activation. First is the high bond dissociation energy (BDE) and pK_a value of a C–H bond which is the reason behind its relatively unreactive nature and robustness.[32] The BDEs and acidities of common C–H bonds are provided in Figure 1.2.1.[33]

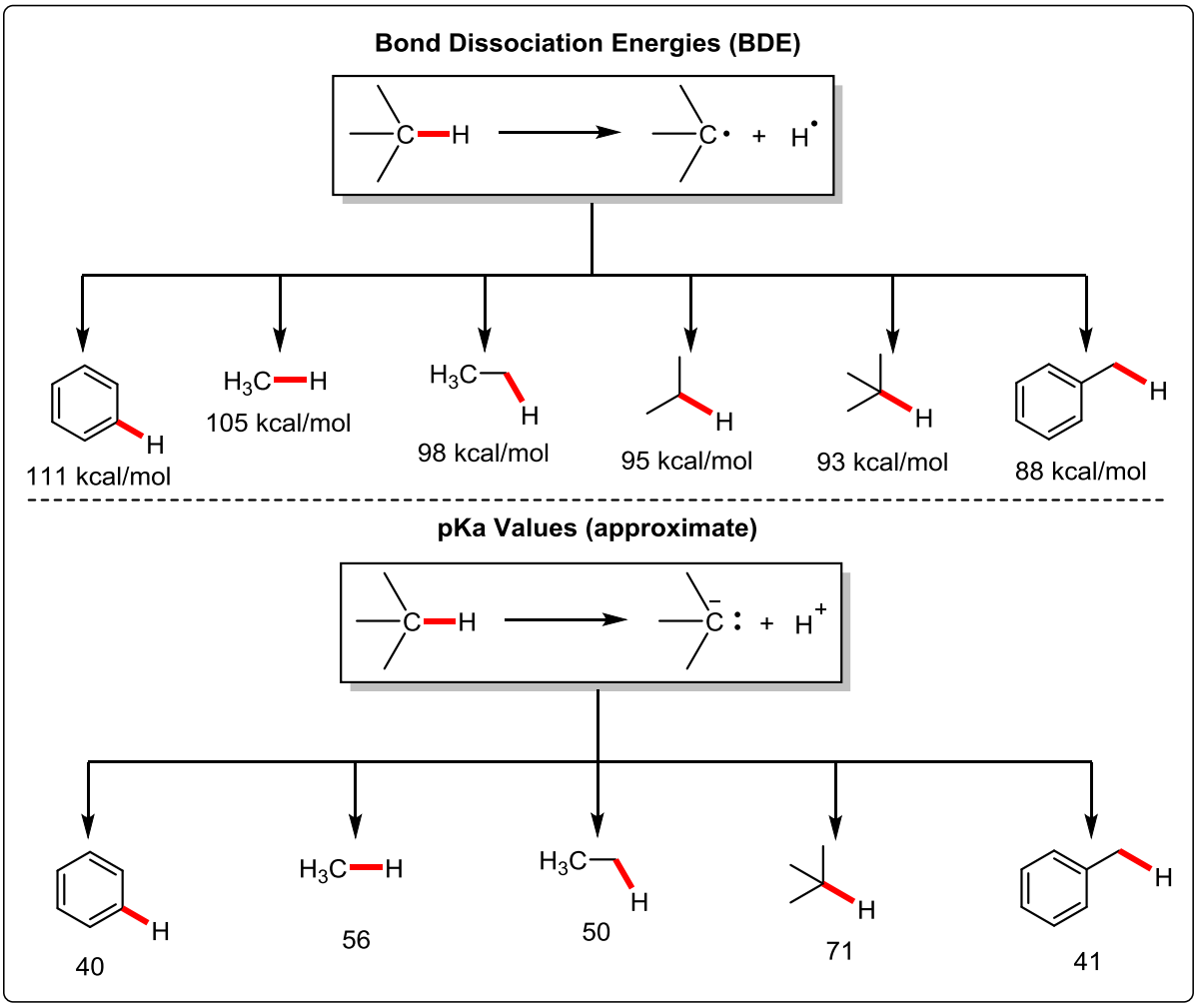

Figure 1.2.1. BDE and pK_a values of various types C–H bonds.

As a result, the direct functionalization of C–H bonds is thermodynamically unfavourable (but not impossible!!). The second issue is the easy availability of C–H bonds, which also becomes the downfall for its usage. A wide variety of C–H bonds constituting different reactivities are present in organic molecules, and thus, many mechanistic pathways exist for an overall C–H functionalization process (Figure 1.2.2). How does one functionalize a particular and selective C–H bond? Apart from the inertness and regioselectivity problems, other issues which pop up include chemo and stereoselectivity, functional group tolerance and others. Key features to overcome these challenges include the appropriate choice of transition metal catalyst and catalyst design, and development of suitable reaction conditions which is the key to exert control on both the selectivity and activity. Also, suitable choice of substrates including the assistance of directing groups (DGs) is important to functionalize a particular C–H bond.

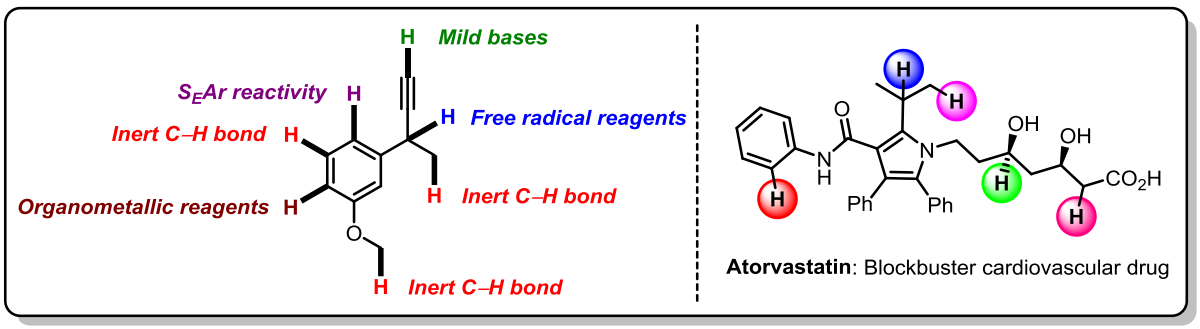

Figure 1.2.2. Nature and reactivity of various C–H bonds present in an organic molecule.

1.3. Mechanisms of C–H Activation

The cleavage of C–H bond is the key step for any C–H functionalization reaction. There exist a primary difference between a "C–H activation" and "C–H functionalization" process (Scheme 1.3.1).[34] A C–H activation reaction involves the transformation of a C–H bond to a C–M bond, where M is a transition metal, which is more easily functionalized to a C–X bond (X = carbon or heteroatom). On the other hand, C–H functionalization is a more general term devoid of a proper definition which involves the transformation of a C–H bond to a C–X bond in any manner. Therefore, a C–H activation followed by a reaction from C–M bond to C–X bond is indeed an overall C–H functionalization reaction, but the other way round may not always be true. So, the mechanism for C–H bond cleavage has been studied in detail and the different modes of action for its cleavage has been identified.[35] Since C–H activation occurs after attaching with a metal center, here the discussion has been mainly restricted to the type of reactions which involve bond formation between the metal and carbon atom of the C–H bond for further functionalization.

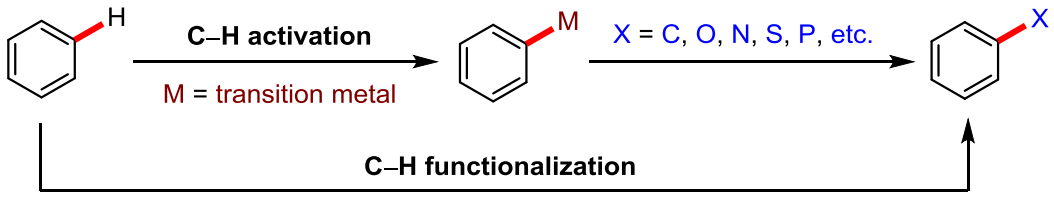

Scheme 1.3.1. Schematic representation of "C–H activation" and "C–H functionalization".

Sanford classified two different mechanistic pathways for C–H functionalizations, namely, "inner-sphere" and "outer-sphere",[35b] also labelled as "organometallic" and "coordination" respectively by Crabtree.[34] They differ in the manner in which C–H bonds to be activated interact with the metal catalyst. Inner-sphere mechanism involves the insertion of the metal

into a C–H bond to form a discrete C–M bond followed by *in situ* functionalization by either an external reagent or at the metal center. Outer-sphere mechanism proceeds via a reaction between the substrate C–H bond and the actively coordinated ligand associated with the metal, and not with the metal itself. Later, a broader and detailed classification of the different modes of C–H activation reactions was provided by Labinger and Bercaw (Scheme 1.3.2).[35a] They categorized the C–H activation modes into five categories- (i) Oxidative addition (OA), (ii) Sigma bond metathesis (σBM), (iii) Electrophilic activation, (iv) Metalloradical activation, and (v) 1,2-addition. Of these, the first three are quite common, while the rest two are rarely seen.

(i) Oxidative addition

Oxidative addition pathway is common for electron-rich, low-valent late transition metal centers like Re, Fe, Ru, Os, Rh, Ir, Pt. Here, a strong synergistic coordination of the σ-C–H bond occurs to the coordinatively unsaturated reactive species [LnM^x] with the concomitant d_π-back donation to the σ^*-C–H orbital resulting in the lowering of the bond order, and hence a homolytic C–H bond cleavage occurs with the increase in oxidation state (O. S.) of the metal by two units (Scheme 1.3.2a). It features the formation of an agostic metal–hydrocarbon complex, followed by oxidative addition via a three-membered cyclic transition state (TS).

(ii) Sigma bond metathesis

This mode of reaction is characteristic for early transition metals with d^0 electronic configuration, i.e., electron-deficient metals in higher oxidation states. Mainly group III metals of the periodic table (scandium, lanthanides and actinides) and some group IV and V metals are known to undergo this mechanism. Here, the bond breaking and formation occurs via a four-membered metalacyclic TS in a concerted fashion without any alternation in the O. S. of the metal center (Scheme 1.3.2b).

(iii) Electrophilic activation

Electrophilic activation or electrophilic aromatic substitution is common for electrophilic metal centers, i.e., cationic complexes of late transition metals in higher oxidation states (eg. Pd^{2+}, Pt^{2+}/Pt^{4+}, Hg^{2+}, Tl^{3+}). First, the electrophilic metal center which acts as a Lewis acid adds to the arene to form a Wheland intermediate enhancing the acidity of the vicinal C(aryl)–H bond which is then lost as a proton and re-aromatization occurs (Scheme 1.3.2c).

(iv) Metalloradical activation

Transition metal complexes that exist in monomer-dimer equilibrium, predominantly rhodium and ruthenium, can reversibly activate and break alkane C–H bonds. They exhibit this mechanism where the two fragments of the C–H bonds are attached to two separate halves of the metal complex (Scheme 1.3.2d). This pathway is relatively rare.

(v) 1,2-addition

This type of mechanism involves early and middle transition metals, where an alkane C–H bond adds to a metal-nonmetal double bond (Scheme 1.3.2e). Although alkane additions to M=N and M=C double bonds are known, but the scope and potential of this type of functionalization still remain unclear and is again a rare phenomenon.

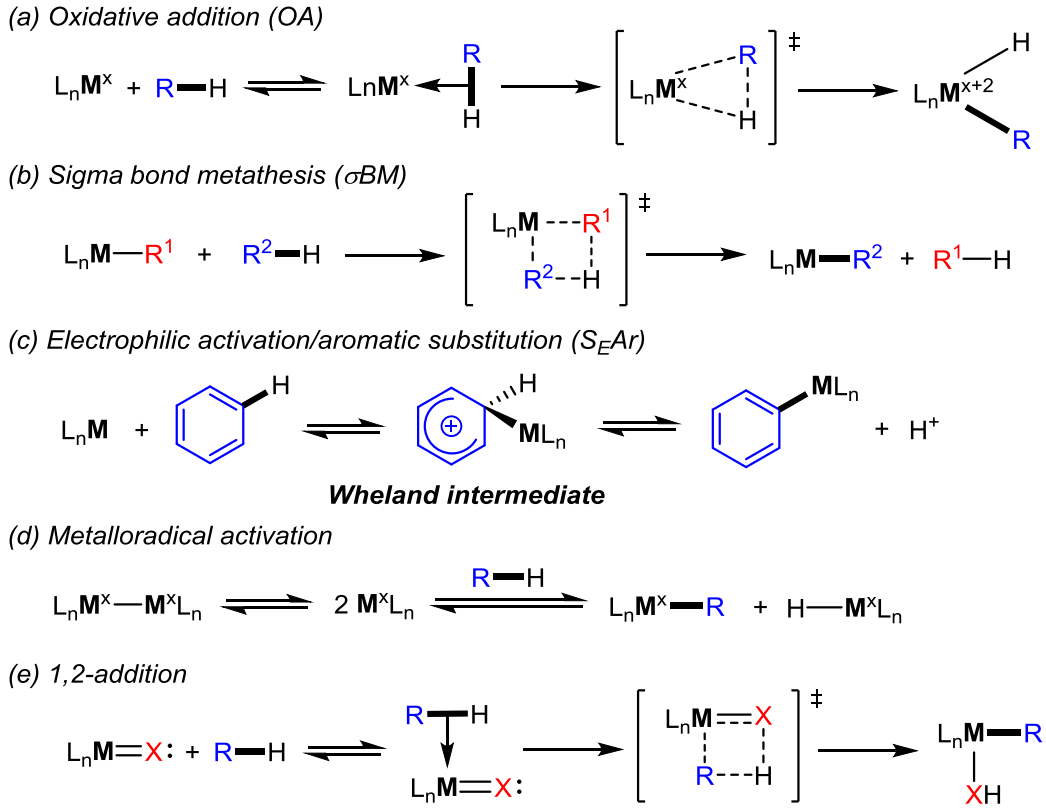

Scheme 1.3.2. Different modes of C–H activation mechanisms under transition metal catalysis.

Apart from the traditional modes of C–H activation mentioned above, recent mechanistic studies with detailed experimental and computational analysis have shown the emergence of other modes of action, namely electrophilic, ambiphilic, and nucleophilic C–H bond activation, which are mechanistically different from the above.[36] These type of mechanisms take place when a base or an acid is used as an external additive which substantially accelerates the C–H

activation process. To mechanistically differentiate, they have been classified as- (i) Internal Electrophilic Substitution (IES), (ii) Concerted metalation-deprotonation (CMD), (iii) Ambiphilic metal-ligand activation (AMLA). (iv) Base-assisted internal electrophilic substitution (BIES).

(i) Internal electrophilic substitution

In this mechanism, the electrophilic metal attached to a coordinating ligand (X = O) activates the C–H bond and generates a positively charged hydrogen. This proton is abstracted by the coordinating lone pair of the M–X bond intramolecularly via a highly strained, high energy four-membered cyclic TS (Figure 1.3.1a).[37]

(ii) Concerted metalation-deprotonation

This mechanistic pathway is mainly applicable for electron-deficient substrates. On using a carboxylate ligand, base-assisted C–H activation can occur via a six-membered cyclic TS in which the ligand on the metal deprotonates the C–H bond with the simultaneous formation of the M–C bond through an inner-sphere mechanism (Figure 1.3.1b).[38] Here, the interaction of the metal and ligand associated with it, particularly, carboxylate type of bases is important for C–H activation to occur. This is common for transition metals with high oxidation states.

(iii) Ambiphilic metal ligand activation

This mode of reaction is similar to CMD process. Heteroatom co-ligands or carboxylate bases in association with electron-deficient late transition metals exhibit this type of mechanism, where C–H activation occurs through a simultaneous ambiphilic activation by lewis acid metal centers and an intramolecular base via a six-membered cyclic TS (Figure 1.3.1c).[39] The primary difference of this mechanism from σBM is the availability of a lone pair on the associated ligand in case of AMLA.

(iv) Base-assisted internal electrophilic substitution

Similar to CMD process but mechanistically slightly different, this pathway also follows an inner-sphere mechanism and takes place in the presence of a carboxylate base and is generally performed in presence of cationic transition metal catalysts. This case is considered as an internal electrophilic metalation since here metalation occurs via a six-membered cyclic TS, initiated by the electrophilic carbon atom instead of the carboxylate (Figure 1.3.1d).[40] Distinguishable feature from CMD is that electron-rich substrates react faster in several

transformations compared to electron-withdrawing ones in this mode. In few cases, base-assisted deprotonation can also lead to C–H activation via outer-sphere mechanism. Stronger bases lead to easier deprotonations, thereby emphasizing the importance of the strength of the base used in this case (Figure 1.3.1e).[40]

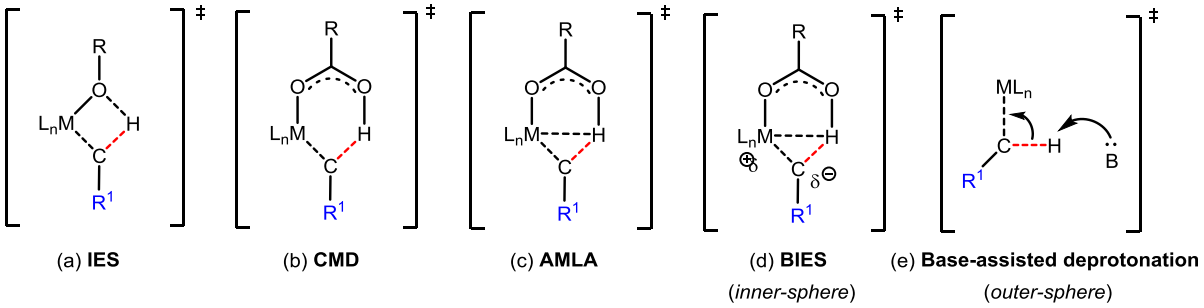

Figure 1.3.1. Proposed transition states of base-assisted C–H activation methods.

1.4. Kinetic Isotope Effect (KIE) Studies

Kinetic isotope effect measurement is one of the most powerful techniques to study reaction mechanisms which gives valuable information about the bonds cleaved and formed at various stages of a reaction and also about the properties of the transition state. This technique goes hand in hand with C–H bond functionalization reactions which involve the breaking of C–H bonds, since KIE experiments measure the differences in the rate for a reaction between a C–H bond and isotopic C–D bond. Also, C–H bonds are not polar enough to undergo exchange in the reaction medium and hence deuterium incorporation is not possible in substrates without the catalyst or an external reagent. Two terms, "rate determining step" (rds) (also referred to as "rate limiting step" or "turnover limiting step") and "product determining step" need to be defined and understood before moving onto KIE discussions. The first term is associated with the overall rate of the reaction, whereas the latter (also referred to as "selectivity determining step") symbolizes the irreversible step controlling which of the two (or more) possible products is formed in a multiple competing pathway reaction. Three very common types of KIE experiments discussed below are generally conducted for a C–H functionalization reaction, where the rate constants are mainly measured by NMR, GC, IR spectroscopy techniques (Scheme 1.4.1).[41]

In the first type, two reactions are carried out in two separate reaction vessels, one containing the substrate carrying a C–H bond and the other bearing a C–D bond (Scheme 1.4.1a). The KIE value is determined from the relative ratio of the rate constants (k_H/k_D). This technique is

the most accurate of the three and gives conclusive information on the involvement of the C–H bond cleavage in the rds of the reaction.

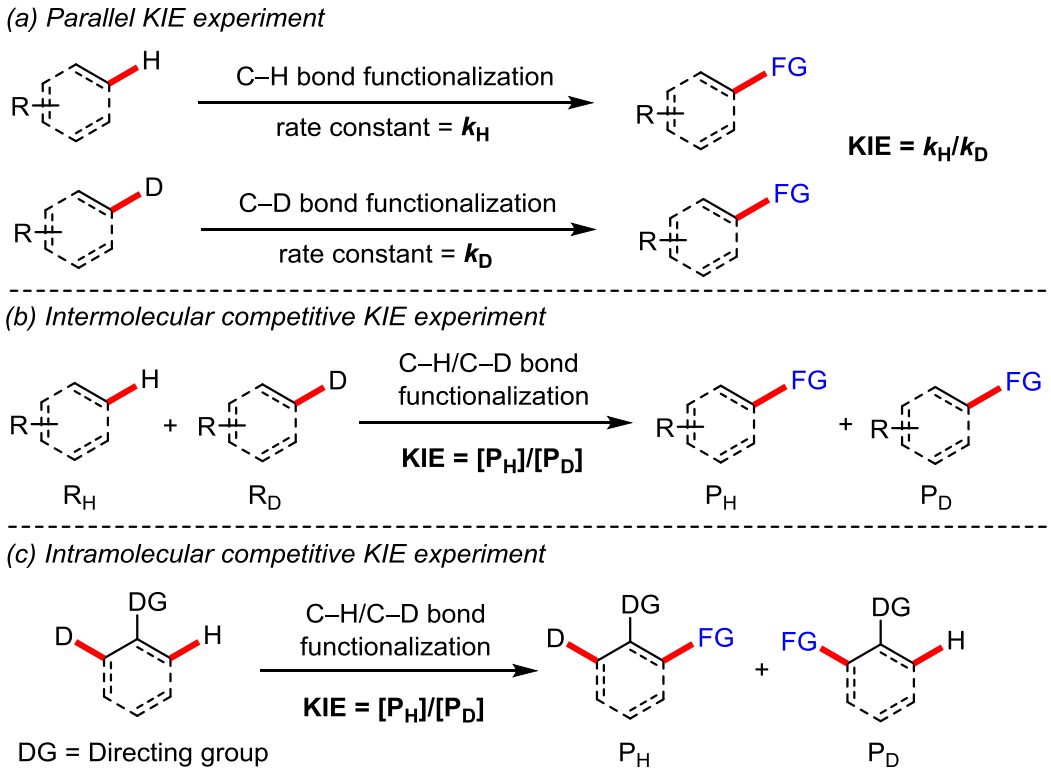

Scheme 1.4.1. Types of kinetic isotope effect experiments.

The second type involve the same two substrates which are made to compete with each other in the same reaction flask with limiting amount of the second reaction partner (Scheme 1.4.1b). In this technique, the KIE value is measured from the relative amounts of the product formed by the activation of the C–H bond versus the C–D bond (P_H/P_D), or the relative amounts of the recovered starting materials after the reaction. However, there exists a major difference in the conclusion from this experiment with that of the first type, which is, in this case, the absence of any KIE rules out the possibility of the involvement of the C–H bond in the rds of the reaction, but its presence does not necessarily ensure that the C–H cleavage occurs in the rds. This method gives the experimental outcome of whether the C–H bond cleavage is involved in the "product determining step" of the reaction or not.

The third type of KIE experiment is just the intramolecular version of the second type, which provides a competition between the functionalization of the C–H bond and C–D bond in the same substrate (Scheme 1.4.1c). Both are conceptually similar and the KIE values provide similar experimental conclusions. However, the application of this method is somewhat

restricted due to the synthetic constraints and the availability of two chemically identical C–H bonds in a substrate.

1.5. Historical Background of C–H Activation

The first taste of homogenous catalysis in C–H activation and functionalization dates back to Fenton's classic 1894 paper of iron-catalyzed oxidation of tartaric acid, which presented the oxidation of hydrocarbons by highly reactive and non-selective hydroxyl radical generated from H_2O_2 in presence of iron.[42] The first seminal work on stoichiometric C–H activation can be dated back to 1963, when Kleiman and Dubeck disclosed the metalation of azobenzene with Cp_2Ni, which arguably represents the first example of chelation assisted C–H activation to form an organometallic compound (Scheme 1.5.1a).[43] Around the same time, Chatt and Davidson, in 1965, reported the first example of unactivated C–H bond activation employing electron-rich, zero-valent diphosphine ligand attached ruthenium complex, which on reaction with naphthalene generates a Ru-hydride complex in an oxidative addition fashion (Scheme 1.5.1b).[44]

Following this elegant study, during the early 1970s, Shilov's C–H activation chemistry of saturated hydrocarbons using Pt(II) salts came up which was believed to proceed via oxidative addition mode.[45] The addition of stoichiometric Pt(IV) salts to a Pt(II) solution of an alkane gave the oxidized species, alkyl chloride or alkyl alcohol in presence of H_2O, products which were distinct from those out of radical halogenation of alkanes (Scheme 1.5.1c). The increase in reactivity from tertiary to primary C–H bonds suggested the C–H activation step to occur via an oxidative addition pathway, although Crabtree and Siegbahn suggested a sigma bond metathesis mechanism for the same.[46] Metalation of arene C–H bonds can undergo via two distinct mechanisms- oxidative addition and electrophilic activation. In the second type, a M–C bond is formed with the release of a proton, as a result, the presence of a base promotes and accelerates these transformations. Davidson and Triggs, in 1968,[47] observed this kind of mechanism in the palladation of benzene, which was later coined the term "concerted metalation-deprotonation" (CMD) by Fagnou.[38,48] Later, other authors used the terms "internal electrophilic substitution" (IES)[37] and "ambiphilic metal ligand activation" (AMLA)[39] for similar cases as discussed in section 1.3. Base-assisted C–H activation/functionalization using Pd-based catalysts has seen a vast number of examples,[49] and is still growing at astounding rates employing other late transition metals like Rh[50] and Ir.[51]

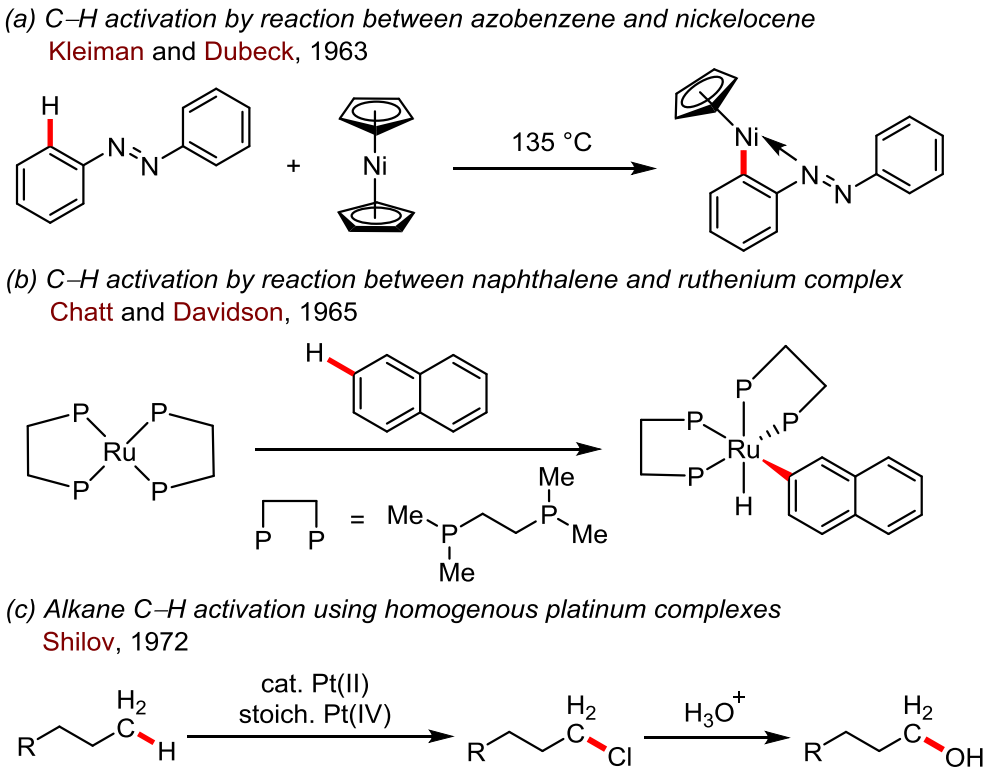

Scheme 1.5.1. Early seminal works on stoichiometric and catalytic C–H activation.

1.6. Modern Era of C–H Activation Leading to C–H Functionalization

The previous section showcased that activation of inert C–H bonds of alkanes or arenes is indeed possible using transition metal catalysts through different mechanisms depending upon the reaction conditions. In order to make the C–H activation strategy a synthetically useful tool in organic chemistry, these elementary steps and initial catalytic processes discussed above need to be applied for C–H functionalizations, *viz.* C–C or C–X (X = heteroatoms like O, N, S, P, B, Si, halides, etc.) bond formations, which are the fundamental transformations in synthetic organic chemistry. These C–H transformations involving transition metals become more preferable in a catalytic fashion rather than a stoichiometric usage of the metal.

The pioneering work which laid the foundation for further advances and achievements in this research area was disclosed by Murahashi in 1955, when he reported the first example of catalytic C–H activation/functionalization for the formation of C–C bond.[52] He showed that carbonylation of Schiff bases with carbon monoxide was catalyzed using low-valent $Co_2(CO)_8$ to synthesize isoindolinones (Scheme 1.6.1).

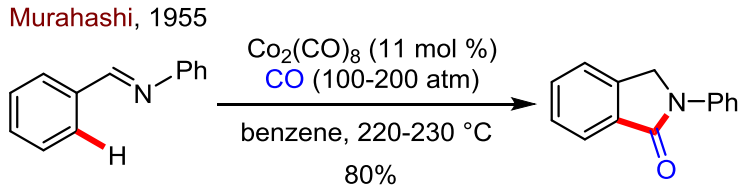

Scheme 1.6.1. Cobalt-catalyzed C–H carbonylation of aromatic imines.

After a long gap, in 1967, Fujiwara and Moritani developed a Pd(II)-catalyzed arylation of olefins to produce 1,2-diarylethylene compounds, i.e., stilbene derivatives by direct substitution of the hydrogen of the aromatic compound with the olefin (Scheme 1.6.2).[53]

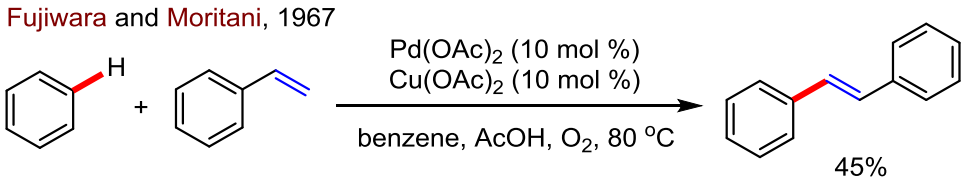

Scheme 1.6.2. Palladium-catalyzed C–H olefination of arenes.

As discussed in Section 1.2, which gave an insight into the challenges faced by the C–H activation technique, one of the primary barriers to overcome was the site-selective functionalization of a particular C–H bond in a molecule comprising several C–H bonds and functional groups. One of the ways to solve this issue is the employment of molecules containing C–H bonds of varying reactivity. This strategy, called "innate C–H functionalization" often falls under the category of "cross-dehydrogenative coupling" (CDC), and has been widely applied over the years for the functionalization of heterocycles.[54] However, this mode of activation is not the topic of discussion in this thesis. A more fascinating aspect is the challenge of solving a more strenuous problem which is the selective functionalization of simple arene systems, like benzene derivatives, where there lies hardly any discrepancy in the behaviour of the reactivities of different C–H bonds and also regioselectivity issues exist. The most successful approach which provides a proper solution to this problem is the concept of directing group (DG) assisted C–H activation and functionalization which is the main theme of detailed discussion in this thesis.

A directing group is a type of ligand (commonly possessing heteroatoms like N, O, S, etc.) present in an organic molecule which is capable of chelating with the metal and selectively guides it to a proximal C–H bond to activate it (positional selectivity), thereby increasing the concentration of the metal center at the site of interest leading to higher reactivity and

regioselectivity.[55] This strategy is often called "guided" or "directed" C–H bond functionalization. In 1993, the revolutionary work of Murai and Chatani published in *Nature* paved the way and opened a new frontier of research for synthetic organic chemists to nurture and explore the potential of C–H bond functionalization.[56] They disclosed the use of ketone as a potent directing group for the *ortho* selective alkylation of aromatic ketones with alkenes under ruthenium catalysis (Scheme 1.6.3). In the reaction, coordination of the ketone functional group to the ruthenium center leads to a key five-membered ruthenacycle intermediate which is proposed to form via oxidative addition of the C–H bond to Ru(0). The reaction did not take place on an arene when the ketone functional group was absent.

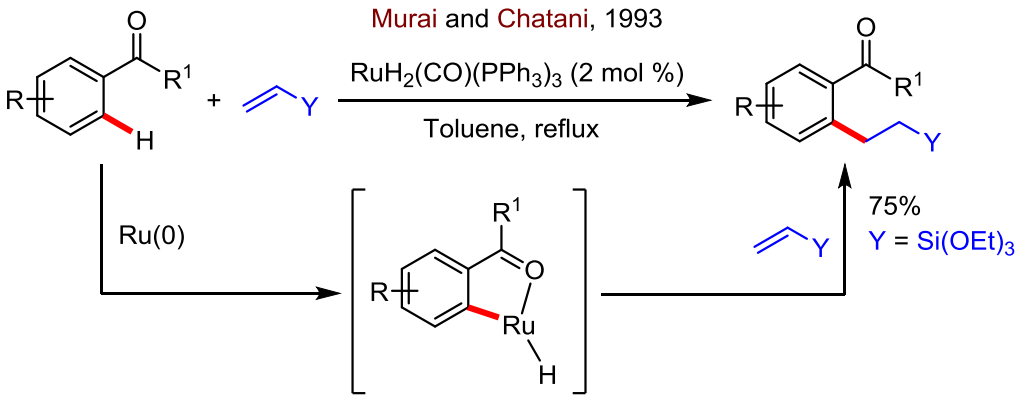

Scheme 1.6.3. Ruthenium-catalyzed *ortho* C–H alkylation of aromatic ketones with alkenes.

Since the seminal work of Murai and Chatani, several research groups have worked on this field for the construction of C–C and C–X (X = heteroatom) bonds via functionalization of both sp^2 and sp^3 C–H bonds, thus making it an extremely active and flourishing research area over the past two decades. These C–H functionalization methodologies have not only been limited to *ortho* C–H bonds, but has been expertly extended to *meta* as well as *para* selective C–H activation protocols as depicted in Scheme 1.6.4.[57] Although the σ-chelating directing groups provide ordered *ortho* selectivity through the formation of conformationally rigid six- or seven-membered cyclic pre-transition state, the need for selective functionalization of distal *meta* and *para* C–H bonds is also highly sought after, since they involve the formation of a macrocyclic geometrically constrained metalacyclic transition state which makes it more challenging. In this regard, the pioneering works of Yu,[58] who developed a removable "U-shaped" template embedded with a DG for *meta* C–H alkenylation, and a "D-shaped" template for *para* C–H olefination and acetoxylation designed by Maiti,[59] opened the door for them and

other research groups to further explore transition metal-catalyzed remote/distal C–H functionalization employing elegantly designed directing templates and new catalytic systems.

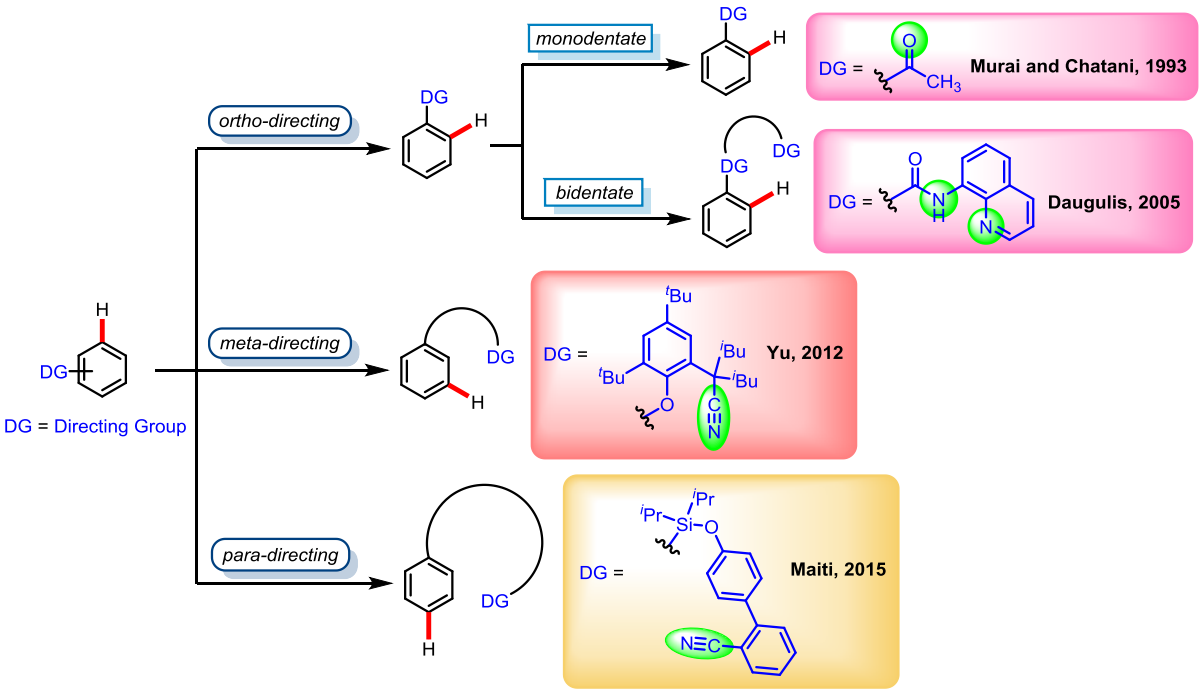

Scheme 1.6.4. Types of C–H activation strategies using directing group assistance.

The focus of this thesis is the *ortho* selective C–H functionalization which has been the basis for C–H activation technique over the years. Murai and Chatani showed the scientific community of the use of monodentate directing group (one chelating ligand), whereas Daugulis, in 2005,[60] provided a huge breakthrough in this field by introducing bidentate directing groups (two chelating ligands) in the form of *N*,*N*-bidentate 8-aminoquinoline and picolinamide DGs for the selective functionalization of unactivated *ortho* C–H bonds. This opened new horizons in the field of C–H activation, as bidentate chelating ligands could effectively stabilize several metal intermediates enabling the functionalization of C–H bonds with a wide array of suitable coupling partners.[57f]

Now, to talk about the type of transition metal catalysts used for C–H activation, it is evident from the above literature background that the most widely used metals for this purpose are 4d and 5d transition metals like Pd, Ru, and Rh, and 3d transition metal like Cu. Apart from them, other metals, *viz*. Ir, Pt, Re, Ag, Au, Mn, Fe, Co, Ni, etc. have also been employed. Catalyst choice, design, and development is one of the key features of C–H activation strategy, since formation of the metalacyclic intermediate is the prime requirement for functionalization of C–H bonds. So, the selective functionalization of unactivated C–H bonds requires a

culmination of various factors moving in the right direction, most important of which are the use of suitable directing group tethered substrate and the correct choice and design of a metal catalyst. This thesis work is primarily based on these two aspects.

1.7. First-Row Transition Metal-Catalyzed C–H Activation

It is evident from the above literature studies that late and noble transition metals, *viz*. second-row and third-row transition metals play a key role in the activation of inert C–H bonds in the usual scenario. Although they provide increased reactivity and productivity, these precious late transition metals fail to check on various boxes because they suffer from low earth abundancy, high cost, toxic nature, etc. thereby restricting their use in the eyes of the scientific community. Given the earth-abundant, cost-effective, and sustainable nature of first-row transition metals, 3d transition metal-catalyzed C–H activation provides a significantly much improved environmentally benign and economically attractive alternative gaining tremendous popularity over the years. In recent years, several reports on C–H functionalization reactions have come up applying metals such as Co,[61] Cu,[62] Ni,[63] Fe,[64] and Mn[65]. The natural earth abundance of the commonly used transition metals in C–H activation reactions is provided in Table 1.7.1.

Transition metal	Mn	Fe	**Co**	Ni	**Cu**	Pd	Ru	**Rh**	**Ir**
Abundance (ppm)	1,100	63,000	**30**	90	**68**	0.0063	0.001	**<0.001**	**<0.001**

Table 1.7.1. Relative earth abundance of selected transition metals.

In spite of the greater earth abundancy, low cost, and unique reactivities of 3d transition metals like cobalt and copper and their growing potential in direct C–H bond functionalization reactions, these base metals have been relatively underutilized in this area compared to the 4d and 5d analogues (rhodium and iridium in particular).

1.8. Cobalt-Catalyzed C–H Activation

Cobalt is an earth-abundant and relatively less toxic 3d transition element. It has played a central role in significant achievements in organic transformations over the years, and the mild and cost-effective nature of this base metal has triggered the C–H activation community towards its application in important transformations. Historically, the application of cobalt catalysis in C–C bond formation can be traced back to the pioneering work of Kharasch and

Fields in 1941, where they described the coupling of organic halides with Grignard reagents.[7a] Subsequently, the following 80 years of research has turned cobalt into one of the most promising metals in homogenous catalysis with important applications in, hydroformylation reaction,[66] cycloaddition reaction,[67] the Bönnemann pyridine synthesis,[68] the Nicholas reaction,[69] the Pauson-Khand reaction,[70] the Jacobsen kinetic resolution of epoxides,[71] and also cross-coupling reaction.[72]

Cobalt has completely different electronic properties than those of its 4d and 5d transition metal counterparts. The reduced electronegativity among other factors renders to more nucleophilic organometallic cobalt intermediates, which thereby allow unprecedented reaction pathways in C–H activation reactions with enhanced positional and chemo selectivities. Inspite of the rich advances in cobalt-catalyzed organic transformations, C–H functionalization reactions under cobalt catalysis has been rather limited. Infact, cobalt was the first metal to be used in the pioneering work of Murahashi[52] as discussed previously, which arguably represents one of the earliest examples of chelation-assisted C–H functionalization reactions (Scheme 1.6.1). Since then, there has been remarkable progress in the usage of cobalt complexes in C–H functionalization reactions, although the volume of examples is comparatively less. In this regard, cobalt-catalyzed C–H activation reactions can be broadly classified into four categories- (i) using well-defined cobalt complexes, (ii) low-valent cobalt catalysis, (iii) high-valent cobalt catalysis, (iv) oxidative C–H functionalizations using simple cobalt salts. The field of cobalt-catalyzed C–H activation has been extensively covered in excellent reviews by Ackermann,[61,73] Yoshikai,[74] Chatani,[75] Niu and Song,[76] Yoshino and Matsunaga,[77] Whiteoak,[78] Ribas,[79] Yu,[80] Cheng,[81] and Grigorjeva.[82] These reviews provide a detailed account of the developments in this field, of which only selected examples is discussed below to highlight the potential of cobalt catalysis.

1.8.1. C–H Activation Using Well-Defined Cobalt Complexes

In 1993, Klein and co-workers reported the first example of stoichiometric C–H bond cleavage of azobenzene system using a low-valent Co(I) complex $Co(Me)(PMe_3)_4$.[83] Lewis base coordination with the concomitant loss of one PMe_3 ligand followed by oxidative addition of Co(I) into the aromatic C–H bond and subsequent reductive elimination of methane leads to the formation of the cyclometalated species (Scheme 1.8.1.1a). The cyclometalation reaction was not only limited to the formation of five-membered rings, but could also be extended to larger six-membered rings and less favourable smaller four-membered rings.

(a) Stoichiometric cyclometalation with low-valent Co(I)-complex

Klein, 1993

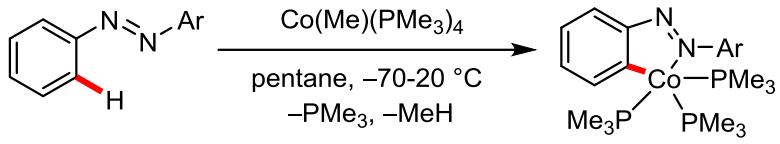

(b) Co(I)-catalyzed ortho alkenylation of azobenzenes

Kisch, 1994

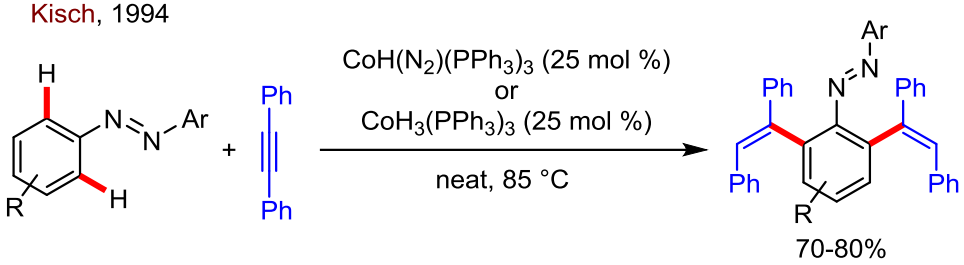

(c) Co(I)-catalyzed hydroacylation of benzaldehydes with olefins

Brookhart, 1997

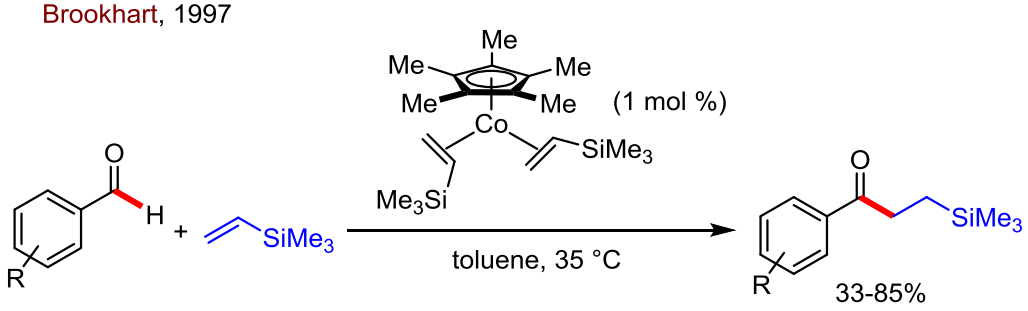

Scheme 1.8.1.1. Early examples of C–H functionalization using well-defined Co(I)-complexes.

Around the same time, in 1994, Kisch delineated *ortho* alkenylation of aromatic azo systems with internal alkynes furnishing trans-addition products in good yields using a Co(I) catalyst $CoH(N_2)(PPh_3)_3$ or $CoH_3(PPh_3)_3$ (Scheme 1.8.1.1b).[84] Here, the sequence of events include a loss of either N_2 or H_2, followed by coordination and oxidative addition steps to give the Co(III) catalytic species. Then, alkyne insertion occurs in one of the Co–H bonds and subsequent reductive elimination gives the desired product and regenerates the active Co(I) species. Depending upon the substitution pattern of the aromatic rings, 2,3-dihydrocinnolines were formed as products under similar catalytic conditions.

In 1997, Brookhart established another key observation by achieving hydroacylation reaction of olefins catalyzed by Cp*Co(I) complex under low catalytic loadings and mild reaction conditions (Scheme 1.8.1.1c).[85] The same group also demonstrated the sp^3 C–H activation of vinyl(dimethyl)silylamines,[86] and C–H activation of simple benzene system employing low-valent Cp*Co(I) catalysis.[87]

1.8.2. Low-Valent Cobalt-Catalyzed C–H Activation

Low-valent cobalt catalysis can be attributed to the reactions where the active catalyst corresponds to Co(0) or Co(I) species. The early work of Kisch which demonstrated the potential of low-valent cobalt complexes in C–H activation, inspired Yoshikai group to study and nurture this area of research and opened a new horizon in this field. In 2010, they developed a new *in situ* generated low-valent cobalt system to catalyze chelation-assisted direct hydroarylation of alkynes by coupling aryl pyridines with alkynes in *syn* fashion affording two-fold *syn* alkenylated products. This was achieved using a ternary catalytic system comprising of a cobalt salt precatalyst ($CoBr_2$), ligand ($PMePh_2$), and stoichiometric amounts of Grignard reagent (MeMgCl) as reducing agent (Scheme 1.8.2.1).[88]

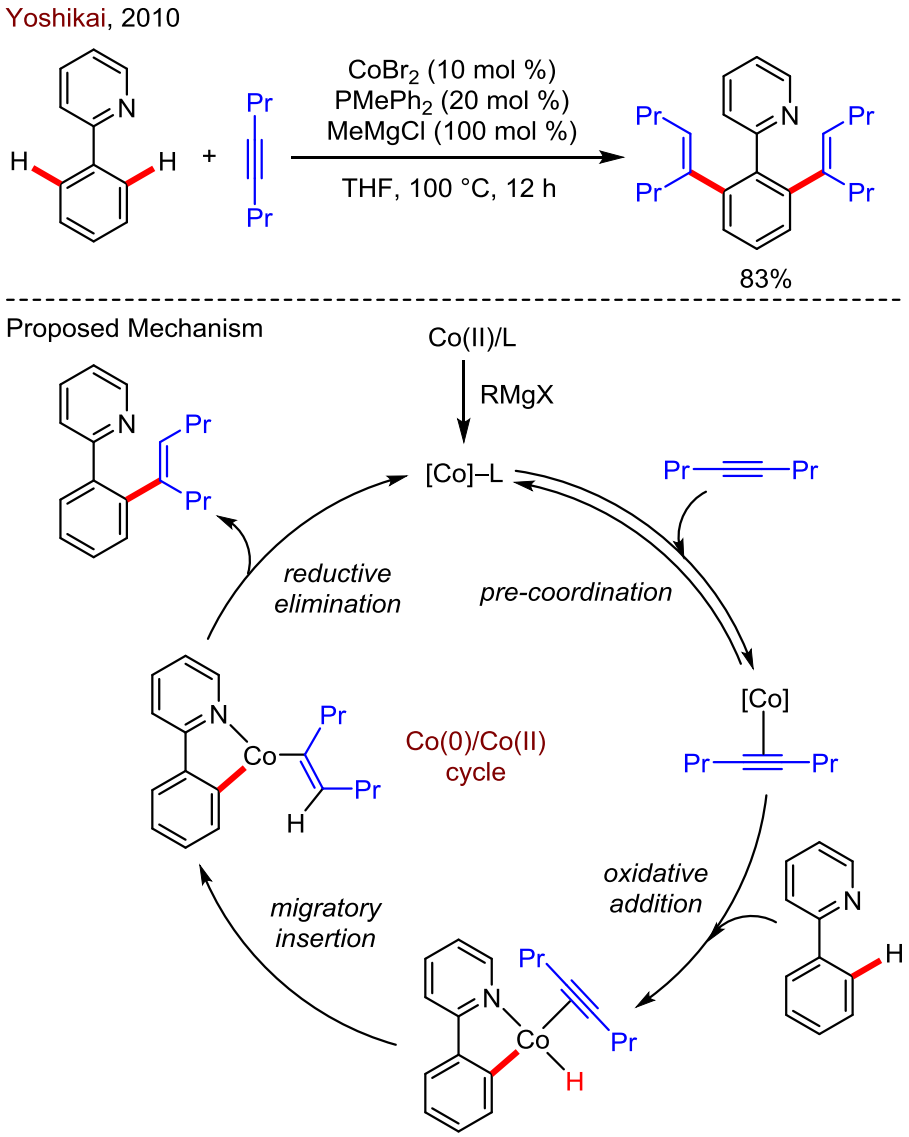

Scheme 1.8.2.1. Hydroarylation of alkynes with 2-arylpyridines.

Mechanistically, the Co(II) species is reduced by the Grignard reagent to a low-valent Co species (most probably a C(0) species) which is stabilized by the phosphine ligand. This Co(0) or Co(I) species is the active catalytic species which then participates in oxidative addition into the aromatic C–H bond to form an aryl-Co(II)-hydride intermediate species. The migratory insertion of alkyne occurs into the Co–H bond, followed by reductive elimination to furnish the cross-coupled product and regenerate the initial cobalt species.

Based on this initial breakthrough, the scope of hydroarylation reactions of alkynes was further extended by Yoshikai and co-workers to other aromatic substrates like ketimines,[89] aldimines,[90] indoles and benzimidazoles.[91] To diversify, hydroarylation reactions could also be successfully performed on heterocycles like (benz)oxazoles and thiazoles.[92] Replacing arenes with alkenes, heteroannulation reaction was possible via vinylic C–H activation/hydroarylation.[93]

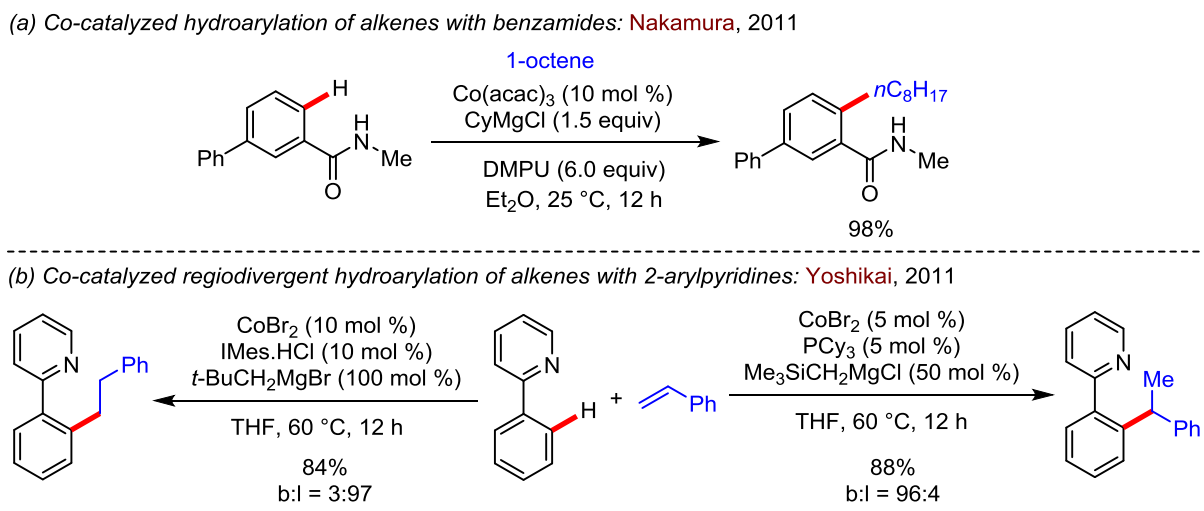

Scheme 1.8.2.2. Hydroarylation of alkenes with benzamides and 2-arylpyridines.

Moving forward, hydroarylation of more challenging alkenes could also be achieved under low-valent cobalt catalysis. Nakamura *et al.* established regioselective linear alkylation of benzamides on coupling with unactivated alkenes (Scheme 1.8.2.2a).[94] On the other hand, Yoshikai group achieved hydroarylation reactions of styrenes with 2-phenylpyridines leading to either linear or branched alkylated products depending upon the choice of ligands and Grignard reagents used, where a $CoBr_2/PCy_3/Me_3SiCH_2MgCl$ combination gave the branched product with high selectivity, and a $CoBr_2$/IMes.HCl/*t*-$BuCH_2MgBr$ combination afforded the linear product with a near complete reversal of regioselectivity (Scheme 1.8.2.2b).[95] The two insertion pathways compete with each other and the regioselectivity is governed by the reductive elimination step. In some cases, the electronic nature of the substrate became a

dominant factor over the ligand control which influenced the formation of the major product. They further extended this strategy to obtain branch selective hydroarylations of alkenes with aromatic aldimines and ketimines.[96] However, some optimizations in terms of the type of ligands or Grignard reagents used is required for each particular substrate to get effective yields and selectivity.

These observations emphasized the importance of ligands used in low-valent cobalt-catalyzed C–H activation since the substitution patterns and small changes in the ligand can massively affect the reactivity in most cases. The *N*-heterocyclic carbene (NHC) or phosphine ligands provide kinetic stabilization of the organometallic intermediates through a bulky substitution pattern, hence generating a significant ligand rate acceleration of the reaction. A list of commonly employed ligands is provided in Figure 1.8.2.1.

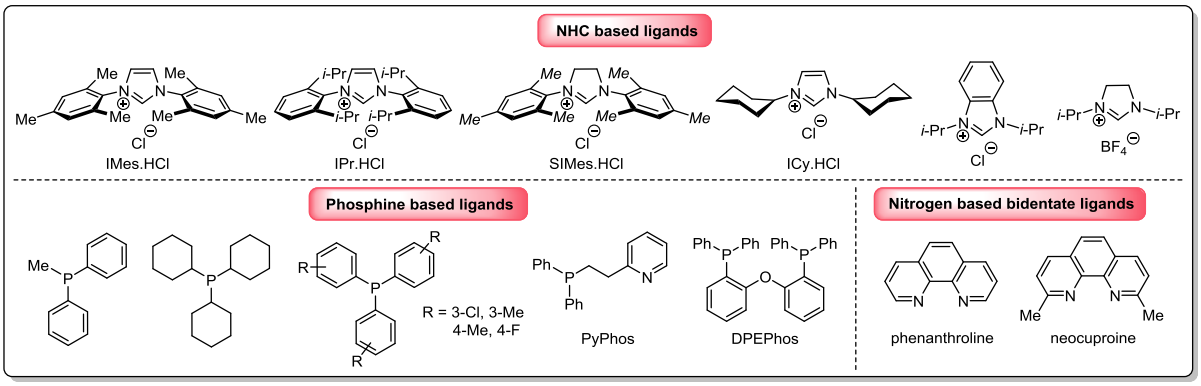

Figure 1.8.2.1. Commonly used (pre)ligands in low-valent Co-catalyzed C–H activation.

These notable results initiated a plethora of other important developments in low-valent cobalt-catalyzed C–H functionalizations, *viz*. direct alkylation and arylation, direct alkenylation, hydroacylation, intramolecular versions of hydroarylation and hydroacylation reaction, enantioselective hydroarylation and hydroacylation, migratory arylzincation of alkynes, namely by Ackermann, Yoshikai, and Nakamura groups, among others.[61,73-74,97] Reminiscent of the early work of Klein, another interesting discovery by Petit showed the application of well-defined low-valent Co(0) complex $Co(PMe_3)_4$ as a potent catalyst in C–H functionalization reactions without the need for any stoichiometric Grignard reagents.[98]

1.8.3. High-Valent Cobalt-Catalyzed C–H Activation

Despite the tremendous progress in low-valent cobalt catalysis, it still had its own merits and demerits. The experimentally tedious nature, tricky handling of sensitive catalysts and reagents, and the involvement of stoichiometric amounts of Grignard reagents which diminished the

overall atom economy and lead to some functional group intolerance, somewhat limited the application of this strategy in general. Therefore, the need for an air-stable, easy-to-handle, and robust cobalt catalyst grew over the years.

Early reports on high valent cobalt-mediated C–H activation could be traced back to 1986, when Broderick and Legg synthesized an organometallic Co(III)-alkyl species using a tetradentate macrocyclic ligand which stabilized the Co(III) center (Scheme 1.8.3.1a).[99] The authors proposed an intramolecular sp^3 C–H activation *via* agostic interaction between the insitu generated oxidized Co(III) coordination complex and the C–H bond to be activated, favoured by the presence of strong field ligands like SO_3^{2-}, CN^-, NH_3. This example provided the first evidence of C–H activation by electrophilic attack of Co(III), proved by the isolation of the Co(III)–C containing organometallic complex.

After a prolonged gap, Avilés reported a Co(III)-mediated C–H activation of azobenzenes employing a CpCo(III) complex [$CpCo(PPh_3)I_2$] to successfully isolate the cyclometalated product (Scheme 1.8.3.1b).[100] These seminal works showed the ready formation of stable alkyl/aryl-Co(III) metalacycles under ambient conditions highlighting the potential of high-valent cobalt catalysis in C–H activation. Also, the early works of Brookhart on the use of Cp*Co(I) complexes demonstrated the power of Cp* ligands in C–H functionalization.

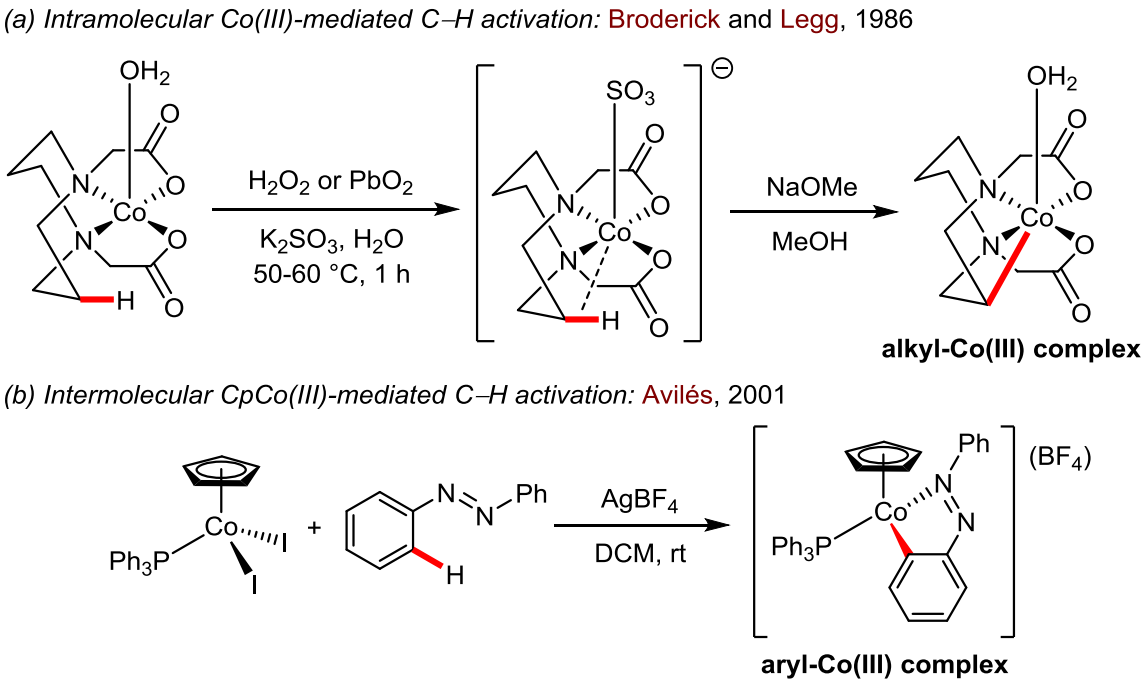

Scheme 1.8.3.1. Early examples of stoichiometric high-valent Co(III)-mediated C–H activation.

However, catalytic C–H functionalization reactions using high-valent Co(III) species were not realized until 2013, when Matsunaga and Kanai group gave a remarkable breakthrough in this field by reporting a Cp*Co(III)-catalyzed hydroarylation of polar electrophiles like imines and α,β-unsaturated carbonyl compounds with 2-arylpyridines (Scheme 1.8.3.2).[101] They used bench-stable $[Cp^*Co(C_6H_6)](PF_6)_2$ as the catalyst for this transformation.

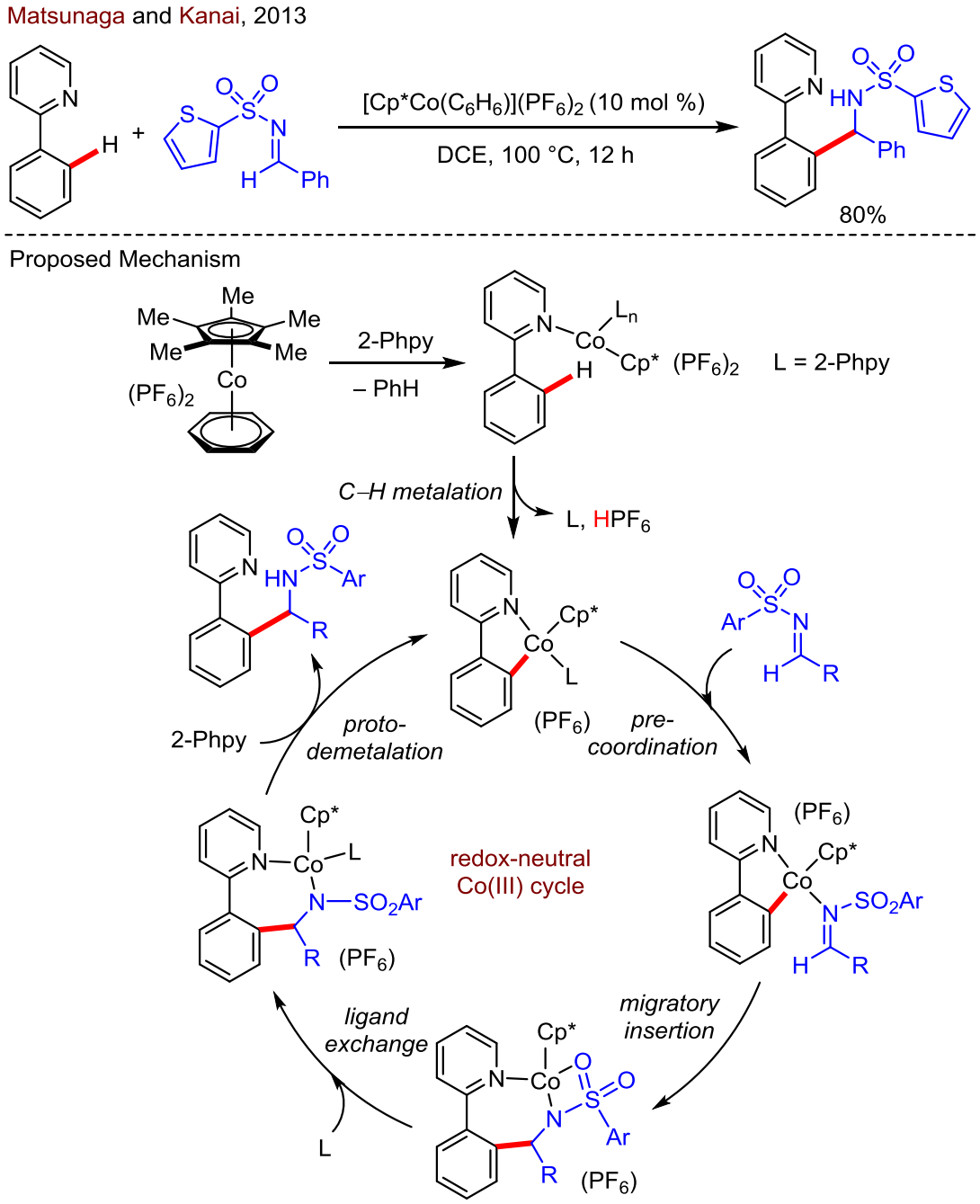

Scheme 1.8.3.2. Cp*Co(III)-catalyzed hydroarytion of imines with 2-phenylpyrdines.

Mechanistically, the authors proposed an initial coordination of the substrate with Cp*Co(III) catalyst through *N*-atom of the pyridyl DG. Then, C–H activation occurs through an

electrophilic aromatic substitution or CMD mechanism to generate the five-membered cyclometalated intermediate. Following this, the imine/Michael acceptor coordinates and subsequent migratory insertion of the double bond occurs across the Co–C bond to give another unstable seven-membered metalacyclic intermediate. Finally, this species undergoes proto-demetalation to furnish the desired addition product and regenerate the active Cp*Co(III) species in coordination with another molecule of 2-phenylpyridine. The reaction does not require any external oxidant, inferring the reaction to undergo via a redox-neutral pathway. The same catalyst in combination with KOAc additive was used by them for the addition of imines to *N*-pyrimidylindoles.[102] The enhanced reactivity on using an acetate source, in this case, could be explained by a carboxylate-assisted C–H activation mechanism.

Following their pioneering work, several groups employed these type of half-sandwich Cp*-based Co(III) catalytic systems in elegant C–H activation/functionalization reactions, which are analogous to the already established Cp*Rh(III)-catalyzed C–H functionalizations.[50a,103] A variety of robust and stable Cp*-derived Co(III) complexes have been synthesized and used as fruitful catalysts in C–H functionalization reactions as shown in Figure 1.8.3.1.

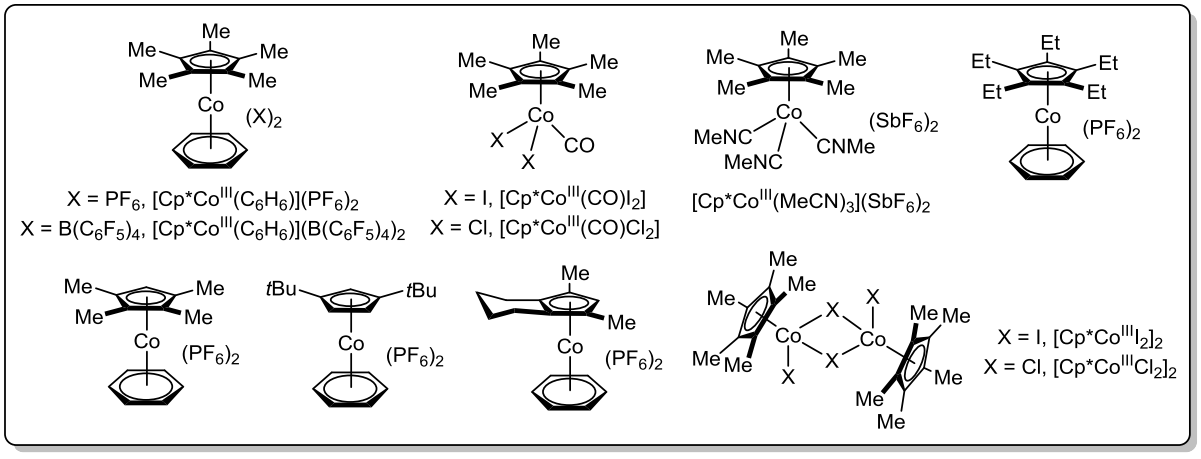

Figure 1.8.3.1. Representative examples of high-valent Cp*-based Co(III) complexes.

Hydroarylation reactions were further extended to alkynes under Cp*Co catalysis.[104] The same group disclosed that a C2-selective indole alkenylation/annulation reaction takes place when *N*-carbamoyl indoles are coupled with alkynes using Cp*Co(III) catalyst and catalytic amounts of KOAc (Scheme 1.8.3.3a).[104a] The nature of DG present influences the formation of product heavily, because, when *N*,*N*-dimethylaminocarbamoyl group is used, proto-demetalation occurs to give the alkenylated product, whereas when a better leaving group in the form of morpholino carbamoyl group is used, intramolecular nucleophilic attack occurs and annulation

takes place leading to one-pot synthesis of pyrroloindolones. Maji *et al.* devised a cobalt(III)-catalyzed *syn*-selective hydroarylation reaction of internal alkynes with *N*-tert-butyl amides to generate mono- and bis-alkenylated benzamides selectively (Scheme 1.8.3.3b).[104b] Highly conjugated system could be constructed via a one-pot four-fold C–H hydroarylation process. Very recently, in 2021, Sahoo and co-workers utilized alkynes in an unconventional one-pot domino double annulation with aryl thioamides employing cobalt(III) catalysis (Scheme 1.8.3.3c).[105] The reaction uncovered the competence of *N*-masked methyl phenyl sulfoximine (MPS) directing group, and established the preferred coordination of *S*-center over the *N*-center of the thioamides to the Co catalyst which in turn regulates the formation of four bonds in one operation. Also, Maji and Ravikumar groups further delineated strategies for Cp*Co(III)-catalyzed diverse C–C bond forming reactions utilizing weakly coordinating DGs.[106] Among these, Ravikumar *et al.* showcased the unique reactivity of alkynes in a Cp*Co-catalyzed weak chelation assisted regioselective C(4)–H functionalization of 3-pivaloyl indoles for the construction of α-hydroxy ketones and α,β-unsaturated ketones (Scheme 1.8.3.3d).[106g] Mechanistic studies confirmed the role of TFE as the source of water in this reaction.

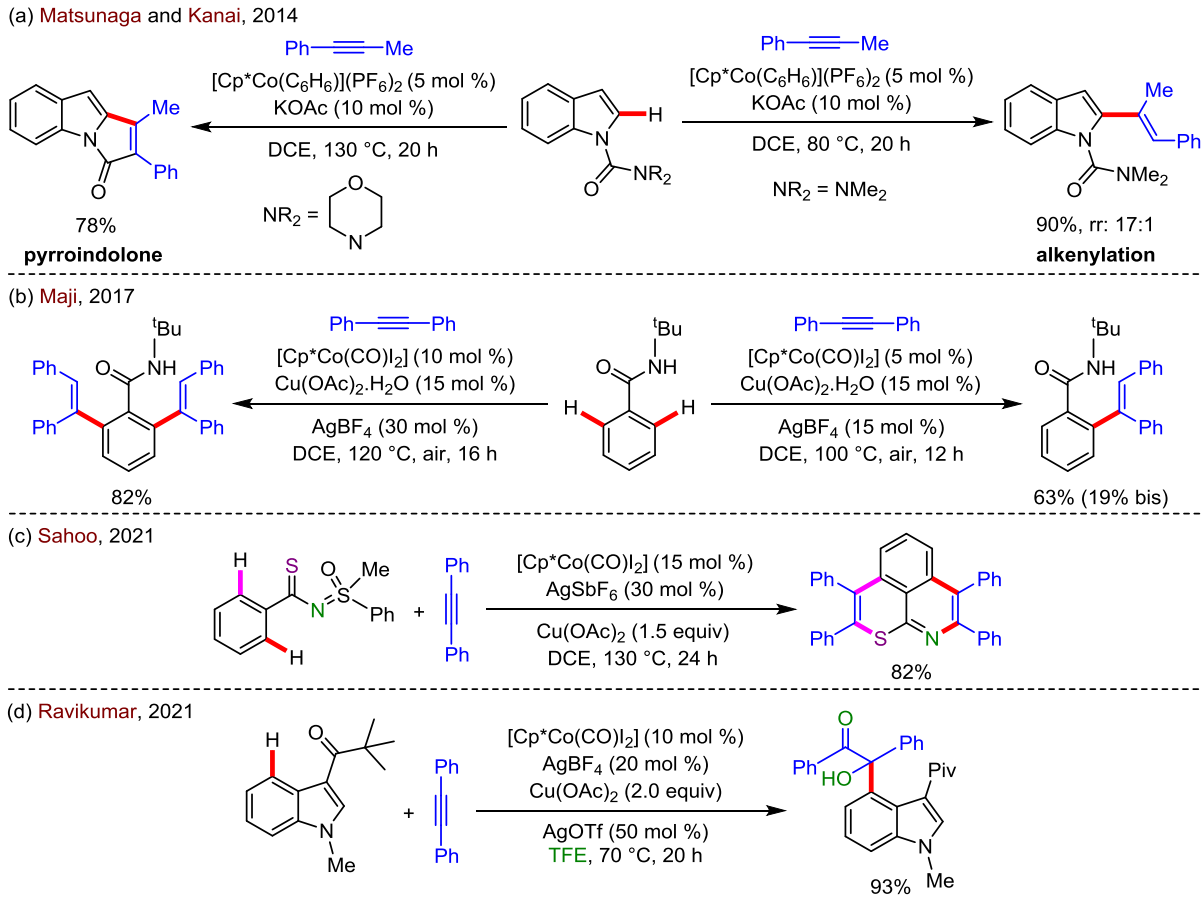

Scheme 1.8.3.3. Cp*Co(III)-catalyzed C–H functionalization reactions with alkynes.

In 2015, Ellman and co-workers showed that apart from the commonly used multiple bonds, simple carbonyls like aldehydes can be used as suitable addition partners for the first time under Co(III) catalysis. They developed a methodology for the one-step convergent synthesis of important heterocycles, namely, indazoles and furans, starting from azobenzenes and α,β-unsaturated oximes respectively (Scheme 1.8.3.4).[107] Sub-stoichiometric amounts of cheap and readily available AcOH additive was required for this reaction.

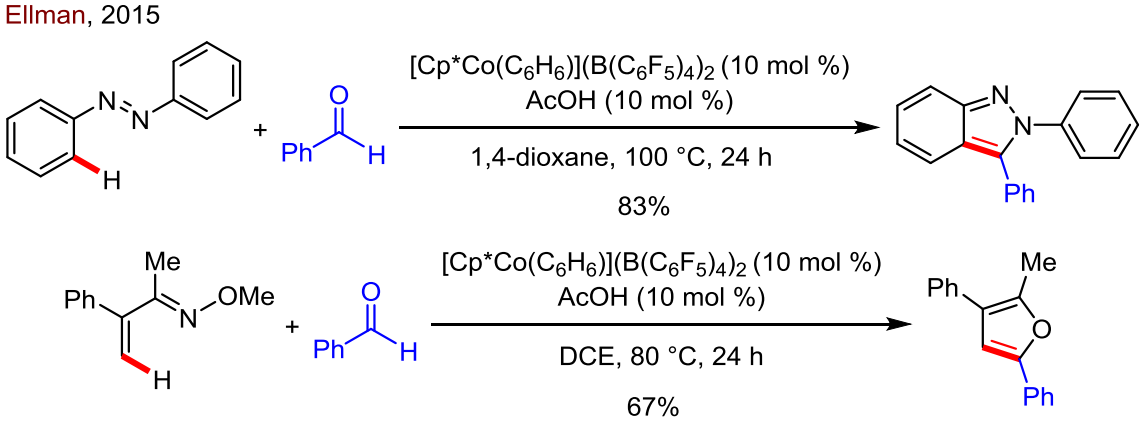

Scheme 1.8.3.4. Cp*Co(III)-catalyzed synthesis of indazoles and furans.

The synthetic utility of high-valent Co(III) catalysis was extended to C–X bond formation reactions also. In 2014, Matsunaga and Kanai reported direct and selective amidation of pyrimidyl-substituted indoles with sulfonyl azides using a catalytic system of [Cp*Co(CO)I_2], $AgSbF_6$, and KOAc (Scheme 1.8.3.5a).[108] Jiao and Ackermann groups independently, and Chang *et al.* further described amidation methodologies using more user friendly amidating reagents like dioxazolones and acetoxycarbamates respectively under cobalt catalysis.[109]

Pseudohalogenation like cyanation of (hetero)arenes employing Cp*Co(III) catalysis was first disclosed by Ackermann group (Scheme 1.8.3.5b), followed shortly by Glorius and co-workers using easy-to-handle cyanating reagent *N*-cyano-*N*-phenyl-*p*-toluenesulfonamide (NCTS).[110] Later, Chang *et al*. applied *N*-cyanosuccinimides as easily accessible and bench-stable electrophilic cyanating agents.[111] C–H halogenations of a wide range of arenes and also olefins were performed by Glorius group using *N*-iodosuccinimides (NIS) and *N*-bromophthalimides (NBP) for iodination and bromination respectively under Co(III) catalysis (Scheme 1.8.3.5c).[110b] Here, PivOH proved to be the beneficial additive over an acetate source which is used in most transformations. The acid additive is thought to be involved in activating the halogenating agent by increasing its electrophilicity, or generating a more reactive cobalt catalytic species with a vacant site for coordination.

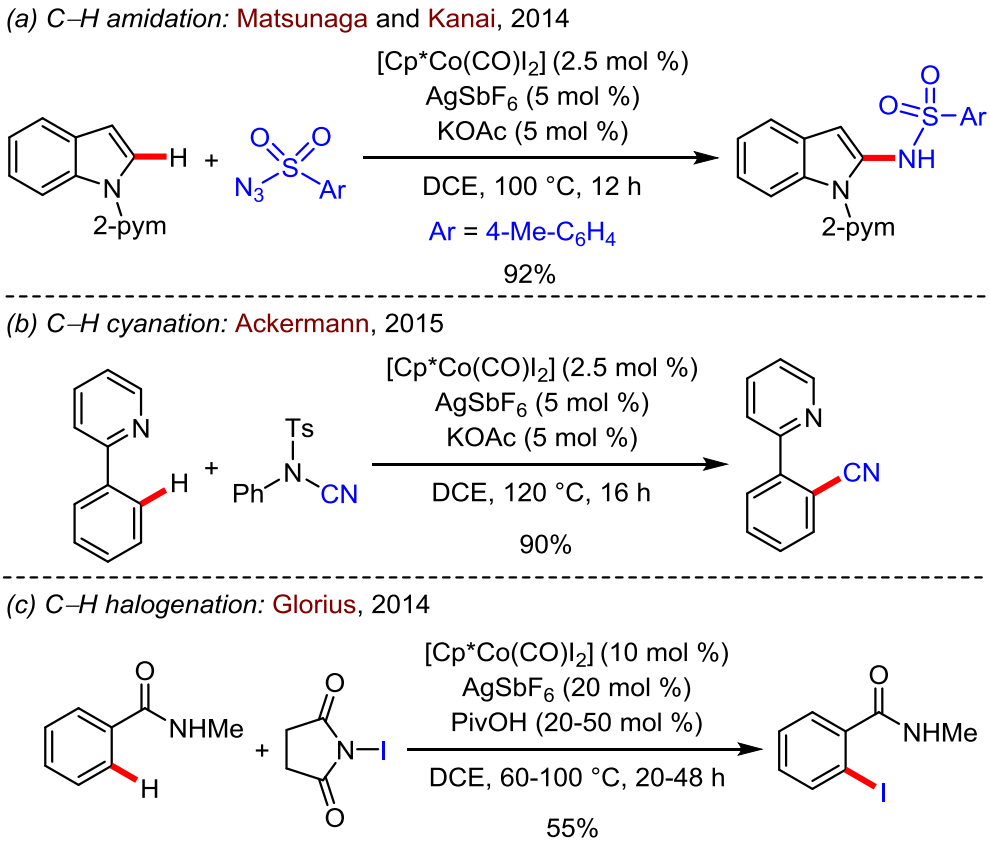

Scheme 1.8.3.5. Cp*Co(III)-catalyzed C–X bond formations.

C(sp^3)–H functionalization under high-valent cobalt(III) catalysis has also been achieved efficiently.[112] For the first time, Sundararaju *et al.* described the use of Cp*Co(III) catalyst in regio- and stereo-controlled synthesis of tri-substituted olefins via sp^3 C–H alkenylation of 8-methylquinolines with alkynes (Scheme 1.8.3.6a).[112a]

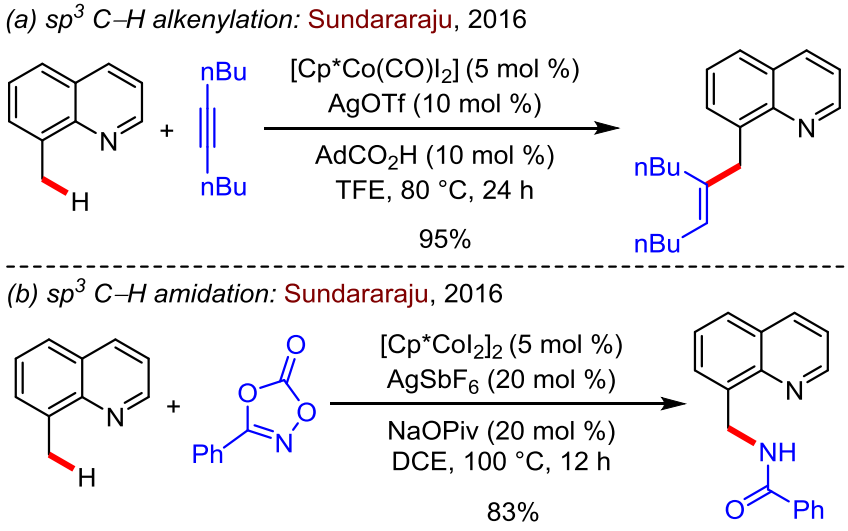

Scheme 1.8.3.6. Cp*Co(III)-catalyzed C(sp^3)–H functionalizations.

From DFT studies and other experimental results, they suggested an external base-assisted concerted metalation-deprotonation pathway for the initial cyclometalation step of the reaction. Subsequently, they delineated a cobalt-catalyzed amidation reaction of the same substrates using aryl/alkyl oxazolones as amidating agent without employing any external oxidant (Scheme 1.8.3.6b).[112b]

It is observed from the above reports that, the mechanistic pathway of high-valent Co(III)-catalyzed C–H activation reactions differ strongly from the low-valent Co(0)/Co(I)-catalyzed C–H activation. Co(III) catalysis follow an electrophilic pathway, either via CMD or through BIES mechanisms, where the hydrogen atom is removed as a proton. On the contrary, cobalt-hydride intermediates are typically involved in low-valent cobalt chemistry, where C–H bond is typically cleaved by an oxidative addition pathway. Apart from these selected notable contributions, Cp*Co(III)-catalyzed C–H activation/functionalization reactions have immensely developed over the years, including enantioselective versions, mostly involving redox-neutral transformations,[73,77,79,82,113] and sporadic examples of oxidative C–H transformations.[114]

1.8.4. Oxidative C–H Activation Using Simple Cobalt Salts

While high-valent cobalt(III) catalysis took off from the reports of Matsunaga and Kanai, around the same time, in 2014, Daugulis group reported a seminal work on a different route of high-valent Co(III)-catalyzed C–H activation using monoanionic bidentate 8-aminoquinoline (8-AQ) and picolinamide (PA) directing groups. The 8-AQ directing group was popularized by the same group back in 2005, in a Pd-catalyzed direct arylation reaction of sp^3 and sp^2 C–H bonds.[60] Since then, this versatile DG has been used as a substrate under Pd, Ru, Fe, Cu, and Ni catalysis among others,[57p,r] and it was further extended to Co catalysis given the ability of high-valent Co(III) complexes to participate in C–H functionalization reactions. They disclosed an oxidative C–H/N–H activation of benzamides followed by alkenylation/annulation with both internal as well as terminal alkynes using simple and readily available air-stable Co(II) salts as (pre)catalyst (Scheme 1.8.4.1).[115] Since it is a known fact that substrates bearing a bidentate chelating group stabilize transition metals in higher oxidation states through a tridentate dianionic pincer type complexation, the authors proposed the formation of a reactive cyclometalated Co(III) intermediate. This cyclometalated intermediate undergoes migratory insertion with the alkyne partner to form another seven-membered metalacyclic intermediate. Finally, reductive elimination delivers the annulated

product and Co(I) species is generated, which is again reoxidized to Co(II) species by the external oxidant and continues the catalytic cycle.

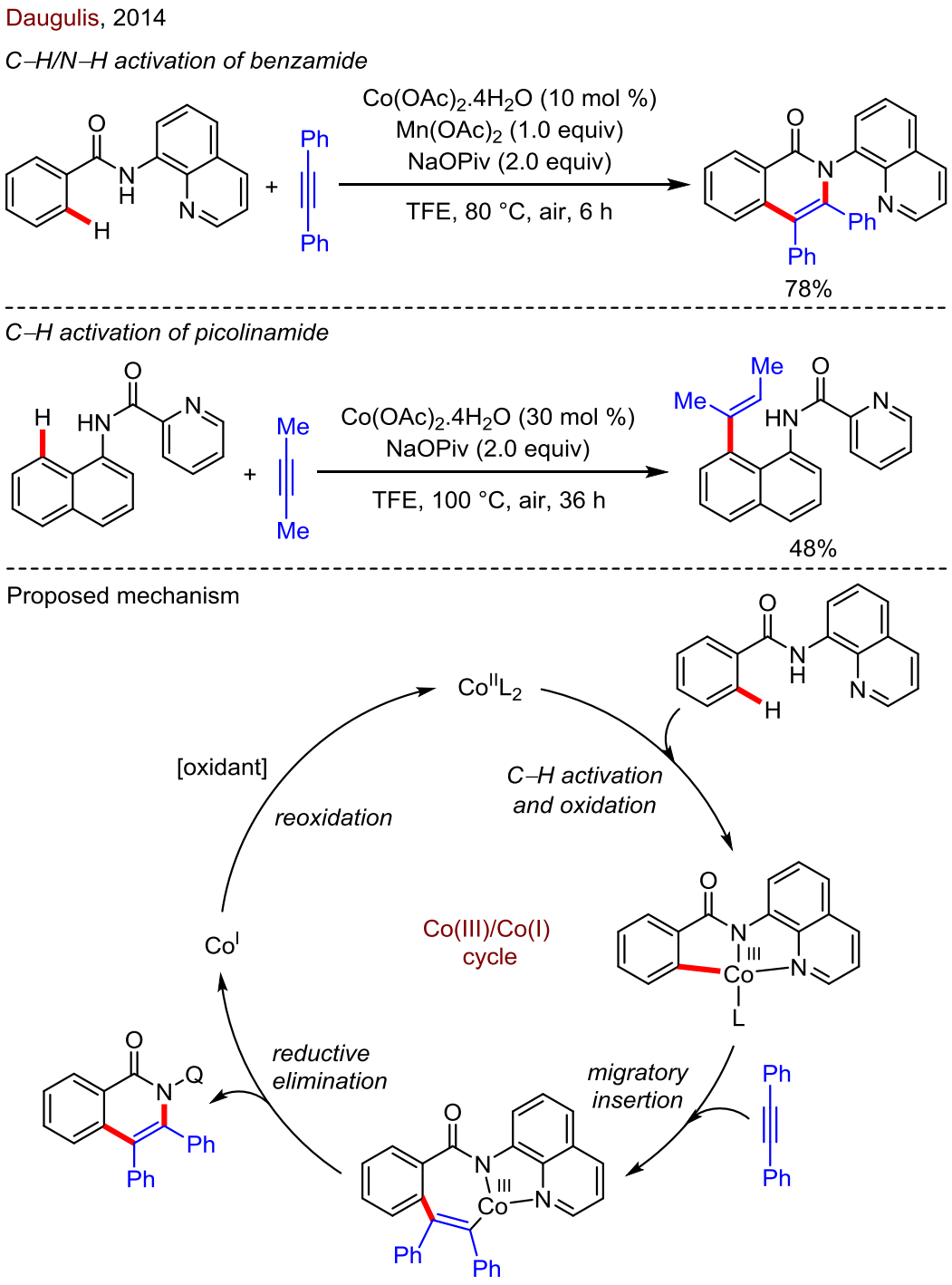

Scheme 1.8.4.1. Cobalt-catalyzed oxidative alkyne annulation of benzamides.

Over the next seven years, cobalt-catalyzed C–H activation/functionalization through bidentate chelation assistance has massively developed. A wide range of *N*,*N*-based bidentate DGs like 8-aminoquinoline (AQ), 2-picolinamide (PA), 2-pyridylisopropylamine (PIP), *N*-2-

pyridylhydrazide (MHP), and *N*,*O*-based bidentate pyridine-*N*-oxide (PyO), 2-aminophenyl oxazoline (Oxa), among others, commonly attached to an amide group or an arene ring have proved to be the most prominent DGs in both C(sp^2)–H and C(sp^3)–H bond functionalization reactions using simple Co(II) or Co(III) salts as catalysts (Figure 1.8.4.1).

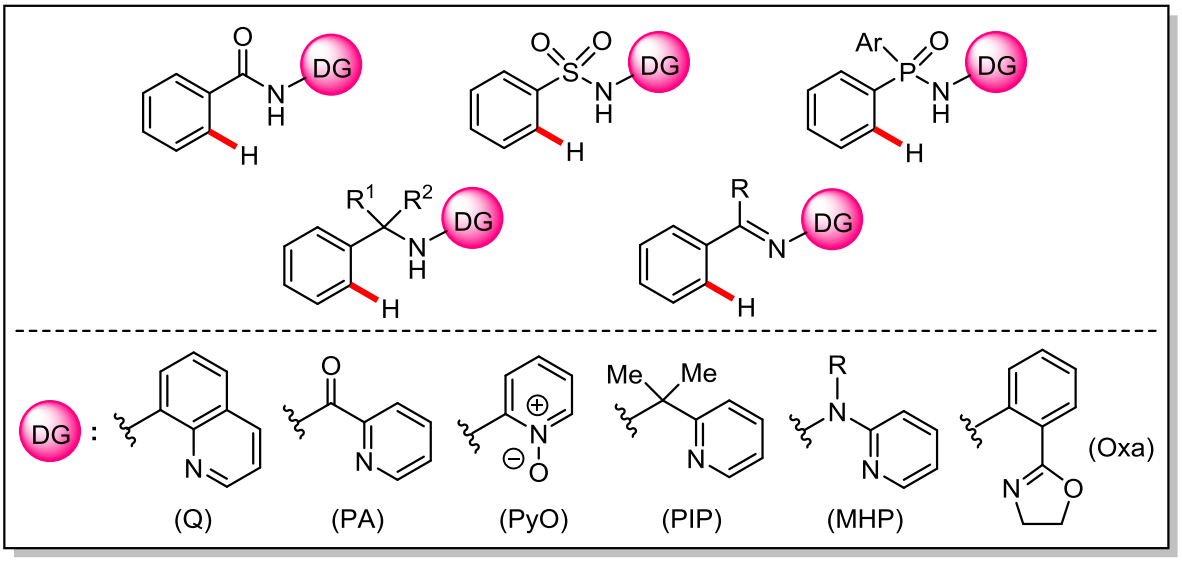

Figure 1.8.4.1. Commonly used bidentate directing groups for cobalt catalysis.

Following the pioneering work of Daugulis, several other elegant reports on C–H/N–H annulation have surfaced leading to a vast array of biologically and pharmaceutically important heterocycles using the strategy of oxidative Co-catalyzed C–H activation. A plethora of suitable unsaturated coupling partners have been explored for this purpose, *viz*. alkynes and dialkynes, alkenes, allenes, maleimides, isocyanates, carbon monoxide or other "CO" sources, and others.[57f,p,r,82] Selected examples are shown in Scheme 1.8.4.2 and discussed accordingly.

In 2016, Ackermann *et al*. devised a methodology for the synthesis of isoquinolones by alkyne annulations with benzamides bearing a PyO bidentate DG employing cobalt-catalyzed oxidase C–H functionalization with molecular oxygen as the sole oxidant (Scheme 1.8.4.2a).[116] Apart from carboxamides, Daugulis and co-workers also employed phosphonic amides in alkyne annulation (Scheme 1.8.4.2b).[117] Efficient synthesis of sultam motifs was disclosed independently by Sundararaju (Scheme 1.8.4.2c) and Ribas under cobalt catalysis.[118] C–H/N–H alkyne annulation was further extended to the application of other DGs like the *N*-2-pyridylhydrazide group by Zhai[119] (Scheme 1.8.4.2d), and picolinamide auxiliary as a traceless DG by Cui[120] group (Scheme 1.8.4.2e) for the synthesis of isoquinolones and isoquinolines respectively. Instead of simple alkynes, Nicholls *et al*. demonstrated the use of

dialkynes in annulation reactions to synthesize a variety of alkynylated isoquinolones (Scheme 1.8.4.2f).[121] Niu and Song developed a methodology employing terminal alkynes furnishing isoindolinones (Scheme 1.8.4.2g),[122] followed by another report on the application of alkynyl carboxylic acids in decarboxylative alkyne annulation which delivered isoquinolones or isoindolinones under switchable reaction conditions (Scheme 1.8.4.2h).[123]

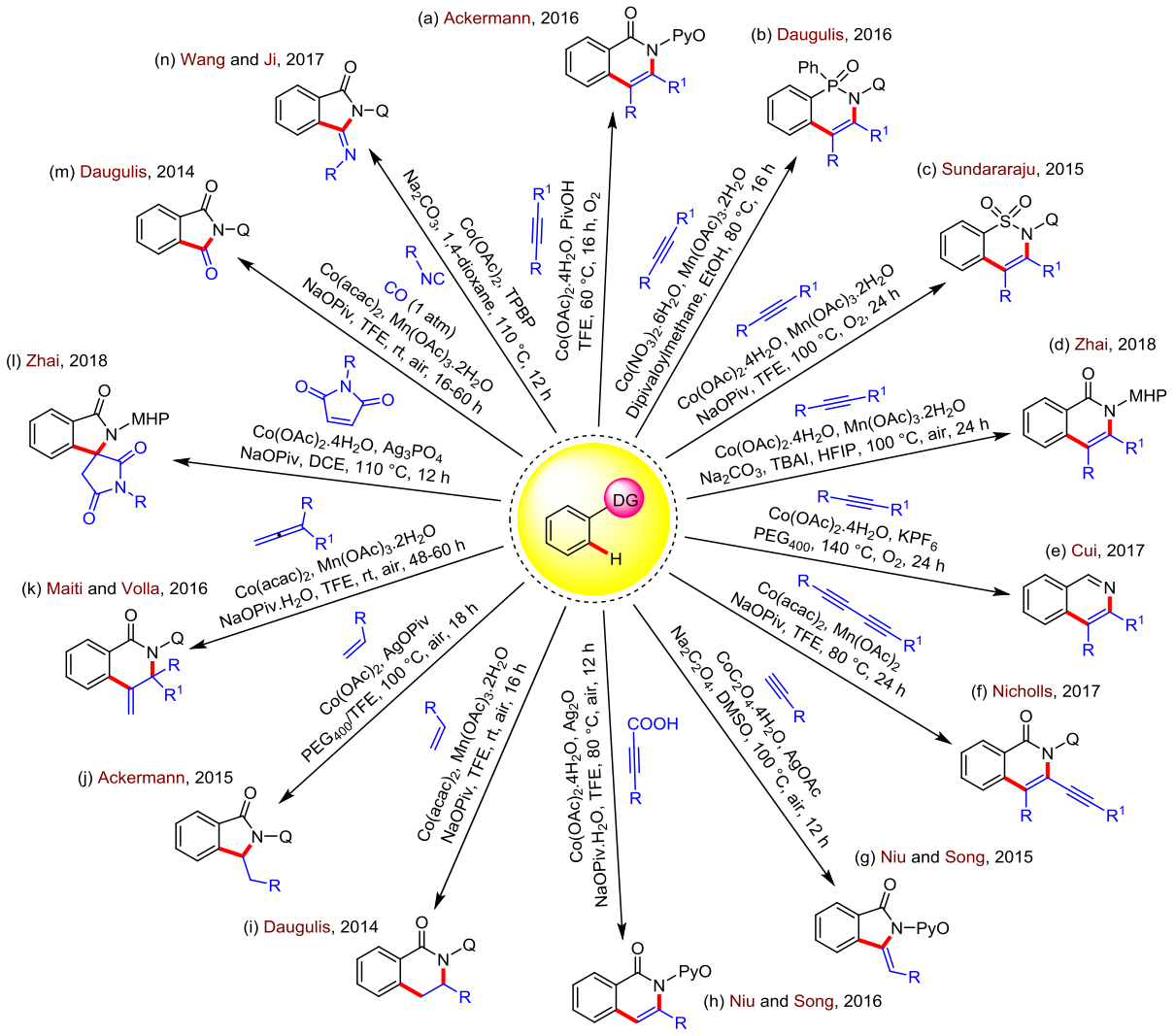

Scheme 1.8.4.2. Representative examples of Co-catalyzed oxidative C–H/X–H annulation.

Moving to alkenes as coupling partners, important contributions by Daugulis and Ackermann groups showed the efficient synthesis of tetrahydroisquinolones and isoindolinones under Co-catalyzed oxidative C–H/N–H annulation reaction conditions (Scheme 1.8.4.2i, 1.8.4.2j).[124] Besides alkynes and alkenes, allenes were also termed as reactive coupling partners under similar conditions by Maiti and Volla for the synthesis of pharmaceutically relevant heterocyclic scaffolds (Scheme 1.8.4.2k).[125] Also, other unsaturated coupling partners like maleimides, carbon monoxide (for carbonylation), and isocyanates were elegantly employed

for annulation reactions under cobalt catalysis in order to synthesize of diverse heterocyclic compounds by the groups of Zhai, Daugulis, and Wang and Ji respectively (Scheme 1.8.4.2l-1.8.4.2n).[126]

In 2018, Daugulis *et al.* accomplished a cobalt-catalyzed oxidative C–H/O–H annulation reaction with simple carboxylic acids which itself act as a directing group. The reaction undergoes in presence of cobalt(II) hexafluoroacetylacetonate catalyst, $(TMS)_2NH$ as base, $Ce(SO_4)_2$ as cooxidant, and O_2 oxidant in TFE solvent. Alkynes, styrenes, 1,3-dienes all are successfully coupled giving cyclic products in good yields (Scheme 1.8.4.3).[127]

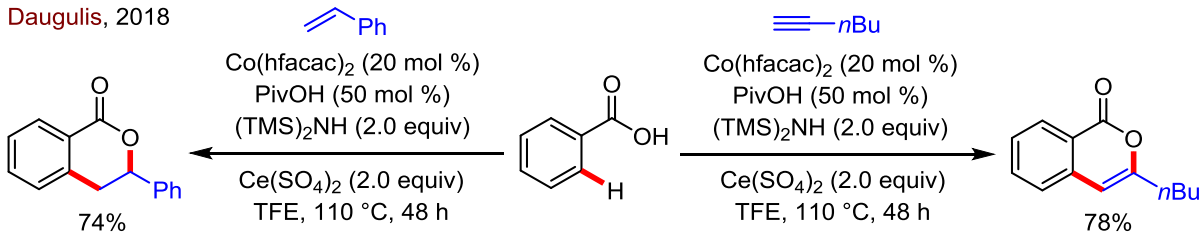

Scheme 1.8.4.3. Cobalt-catalyzed oxidative C–H/O–H annulation of benzoic acids.

The potential of cobalt catalysis in sp^3 C–H functionalization/annulation was harnessed by Ge *et al.* in 2015, when they reported a site-selective dehydrogenative cyclization (or intramolecular amidation) of aliphatic amides using the help of bidentate 8-AQ auxiliary to generate small ring lactams (Scheme 1.8.4.4a).[128]

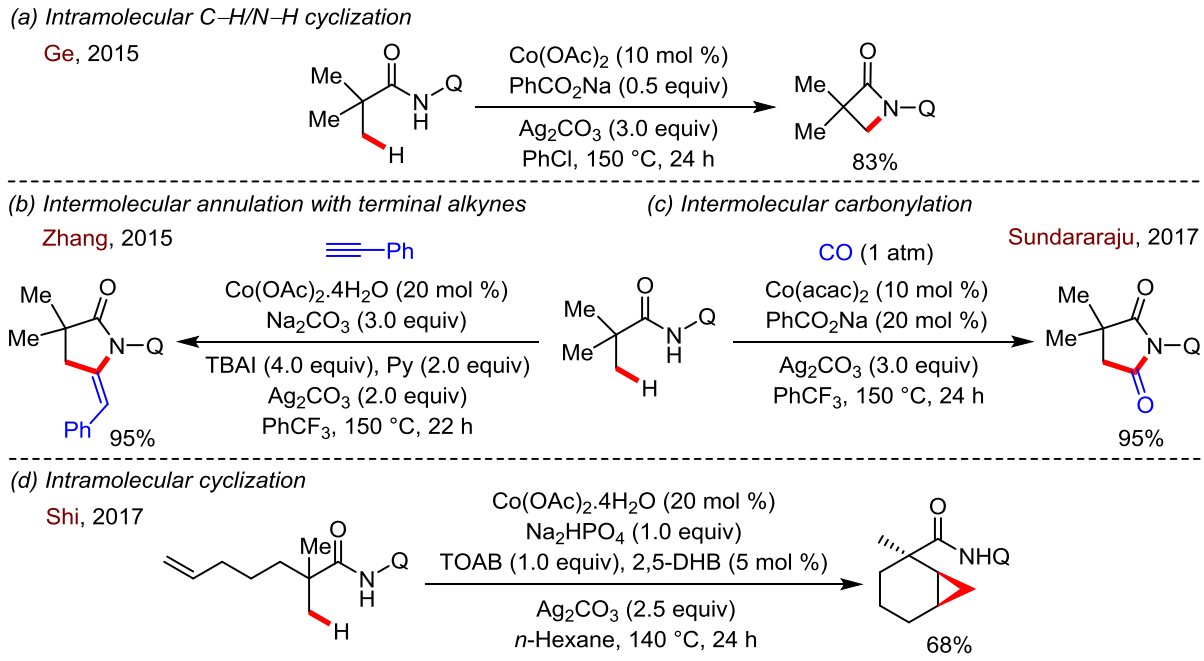

Scheme 1.8.4.4. Bidentate chelation assisted C(sp^3)–H annulation under cobalt catalysis.

Following this, terminal alkynes and aliphatic amides were coupled intermolecularly to synthesize pyrrolidinones by Zhang group (Scheme 1.8.4.4b).[129] Intermolecular carbonylation was also disclosed independently by the groups of Sundararaju, Gaunt, and Lei using CO as a C1-source (Scheme 1.8.4.4c).[130] Also, in 2017, Shi and co-workers delineated the synthesis of cyclopropane frameworks through a triple sp^3 C–H activation strategy (Scheme 1.8.4.4d).[131]

Beside annulation reactions, other forms of cobalt-catalyzed C–C bond formation reactions are also explored (Scheme 1.8.4.5). In 2016, Balaraman and co-workers reported the first example of a bis-alkynylation strategy of 8-aminoquinoline tethered benzamides with (triisopropylsilyl)ethynyl bromides under oxidative cobalt-catalyzed conditions (Scheme 1.8.4.5a).[132] Later, Gao and You group achieved the sp^2 C–H alkynylation by C–H/C–H oxidative cross-coupling between acrylamides and triisopropylsilyl acetylenes (Scheme 1.8.4.5b).[133] Chatani *et al.* disclosed the allylation of arylamides with unactivated aliphatic alkenes in excellent yields and high *E*-selectivities (Scheme 1.8.4.5c).[134] Maiti and co-workers developed methods for unique allylic selectivity via Co-catalyzed dehydrogenative Heck-type reactions using terminal alkenes and internal olefins using the help of different DG assistance (Scheme 1.8.4.5d, 1.8.4.5e).[135] C–H alkylation of carboxamides was also explored by the groups of Li and Lu, and Xu (Scheme 1.8.4.5f-1.8.4.5h).[136]

In 2016, You *et al.* described the first cobalt-catalyzed oxidative cross-coupling of (hetero)arenes with heteroarenes which underwent a single electron transfer (SET) reaction mechanism pathway rather than the conventional oxidative C–H/C–H cross-coupling mechanistic pathway (Scheme 1.8.4.5i).[137] Biaryl synthesis is one of the important applications of C–H activation owing to its presence in a vast number of biologically active scaffolds. Daugulis *et al.* first reported the dimerization of quinoline benzamides under cobalt promoted conditions by two-fold C–H activation (Scheme 1.8.4.5j).[138] Then, the groups of Tan and Ackermann disclosed methods for arylation of benzamides using aryl boronic acids and aryl siloxanes as potent arylating reagents respectively (Scheme 1.8.4.5k, 1.8.4.5m).[139] In 2016, Niu and Song group devised a protocol for the cross-coupling of benzamides and 2-arylpyridines to generate novel bifunctionalized biaryls applying a mixed directing group strategy (Scheme 1.8.4.5l).[140] Here, SET (8-AQ directed) and CMD (pyridine directed) processes take place parallelly to achieve the desired results. Recently, they reported a three-component coupling of benzamides, diazo compounds, and *tert*-butyl hydroperoxide to construct one-pot C–C and

C–O bonds employing cobalt-catalyzed C–H activation (Scheme 1.8.4.5n).[141] Here, TBHP act as a radical initiator, coupling partner, as well as an oxidant in the reaction.

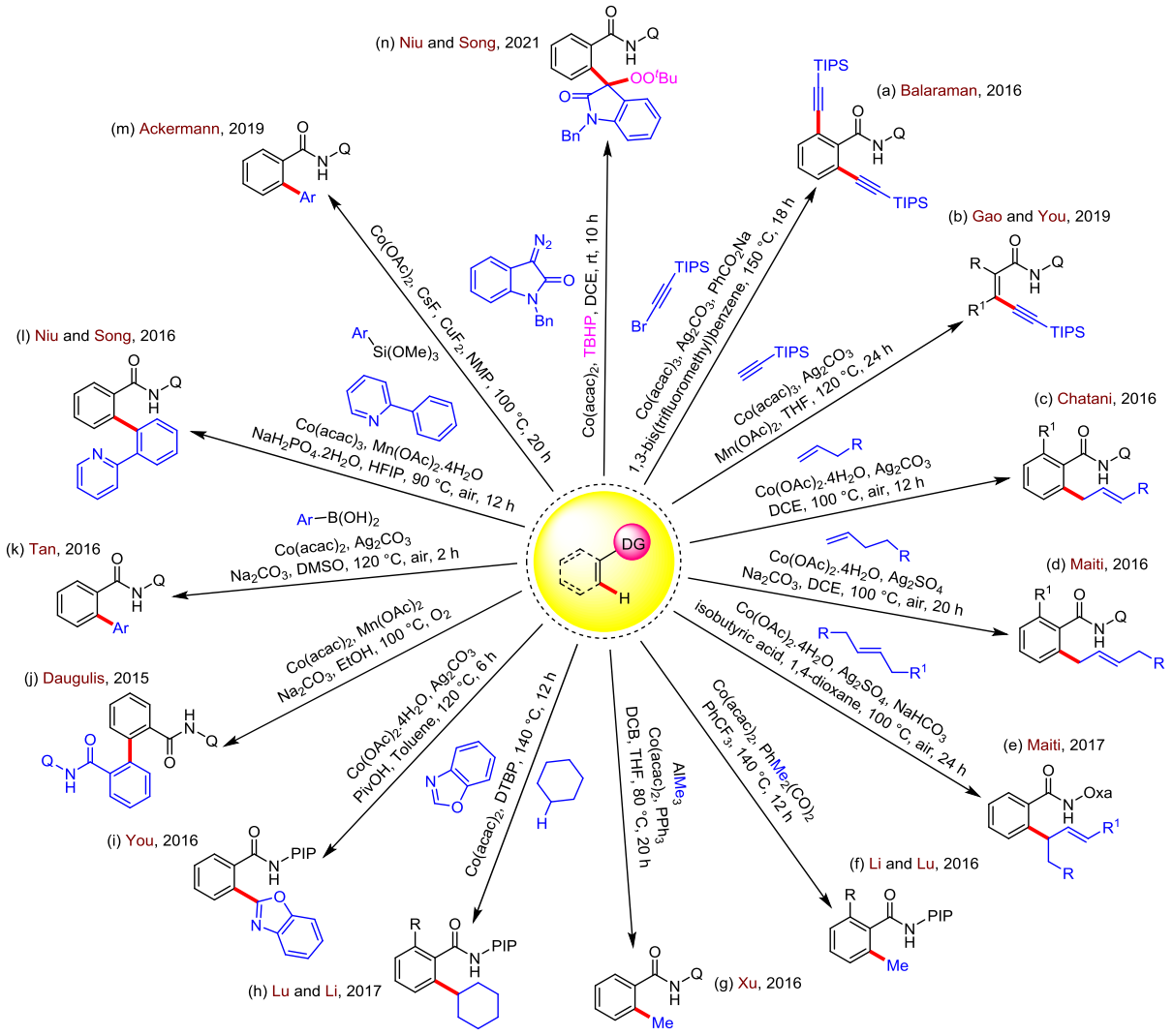

Scheme 1.8.4.5. Representative examples of Co-catalyzed C–C bond formation.

Apart from C–C bond formations, step-economical C–X (X = heteroatom) bond formations have also been realized using the bidentate directing group assisted oxidative cobalt catalysis. Several reports on the formation of C–O, C–N, C–I, C–S bonds have been disclosed over the years, of which some selected examples are shown and discussed below (Scheme 1.8.4.6). Early reports on a SET-type C–O bond formation in presence of Co(III) salts dates back to the seminal work of Kochi in 1973.[142] However, C–H activation strategy was realized in 2015, when Niu and Song reported the first cobalt-catalyzed alkoxylation reaction of aromatic as well as olefinic carboxamides assisted by PyO directing group with simple alcohols as partners, which was also extended to 8-AQ tethered benzamides in a similar fashion by Huang *et al.*

(Scheme 1.8.4.6a, 1.8.4.6b).[143] C–O bond formations were further explored in the form of coupling with carboxylic acids for direct acyloxylation of aryl or alkenyl amides, featuring bidentate chelation independently by the groups of Zeng, Chatani, and Zhang (Scheme 1.8.4.6c-1.8.4.6e).[144] In the meantime, direct acetoxylation of arylamides under cobalt catalysis was also developed which is a part of this thesis work and is discussed in Chapter 2 in detail.

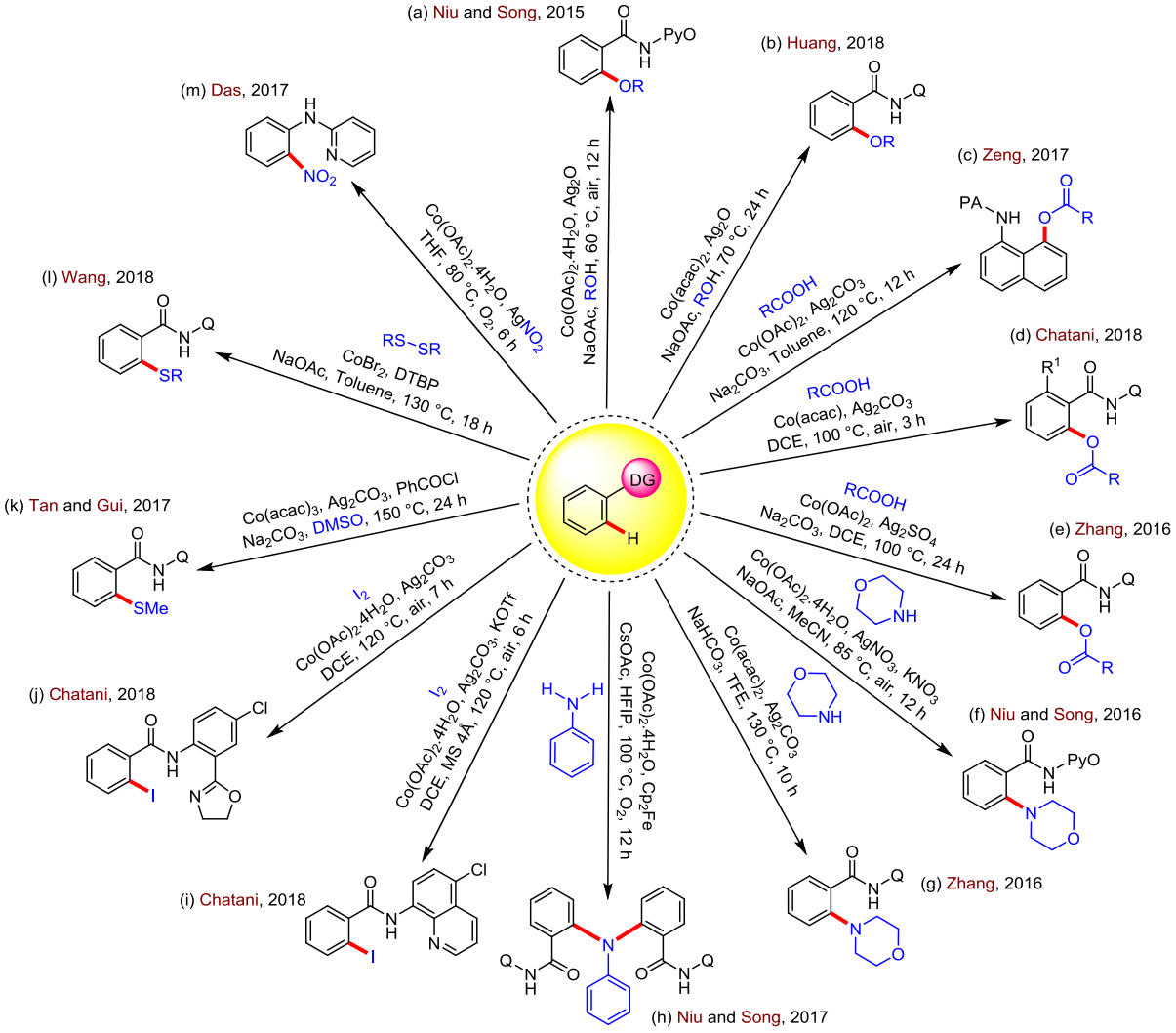

Scheme 1.8.4.6. Selected examples of Co-catalyzed C–X bond formation.

C–N bond forming transformations were displayed independently by Niu and Song, and Zhang groups for the direct amination of arenes with secondary alkylamines (Scheme 1.8.4.6f, 1.8.4.6g).[145] Niu and Song followed it up with another report for the synthesis of sterically congested triarylamines through two-fold C–H/N–H cross-coupling of arenes and anilines (Scheme 1.8.4.6h).[146] C–H halogenation of aromatic amides was accomplished by Chatani and co-workers using appropriately modified directing groups with molecular iodine as iodinating reagent (Scheme 1.8.4.6i, 1.8.4.6j).[147] Oxidative Co-catalyzed chalcogenation reactions were

reported by Tan and Gui, and Wang using DMSO and disulfides as the source of S-containing groups (Scheme 1.8.4.6k, 1.8.4.6l).[148] C–H nitration of aromatic C(sp^2)–H bonds was delineated by Das *et al.* with the help of bidentate chelation using $AgNO_2$ as both the nitro source and oxidant (Scheme 1.8.4.6m).[149]

The mechanism of these reactions is represented by the example of acyloxylation reaction of aromatic amides with carboxylic acids by Chatani group in Scheme 1.8.4.7.[144b] According to the authors, first, Co(II) species undergoes bidentate chelation with the *N*,*N*-coordinating centers of the 8-aminoquinoline directing group, which is then oxidized by Ag(I) salt to generate the Co(III) species. Next, C–H cleavage occurs to form a cobaltacycle intermediate through a CMD process, which undergoes ligand exchange with the carboxylic acid partner giving another Co(III) species. Finally, reductive elimination results in the formation of the desired product and Co(II) is regenerated on oxidation by Ag(I).

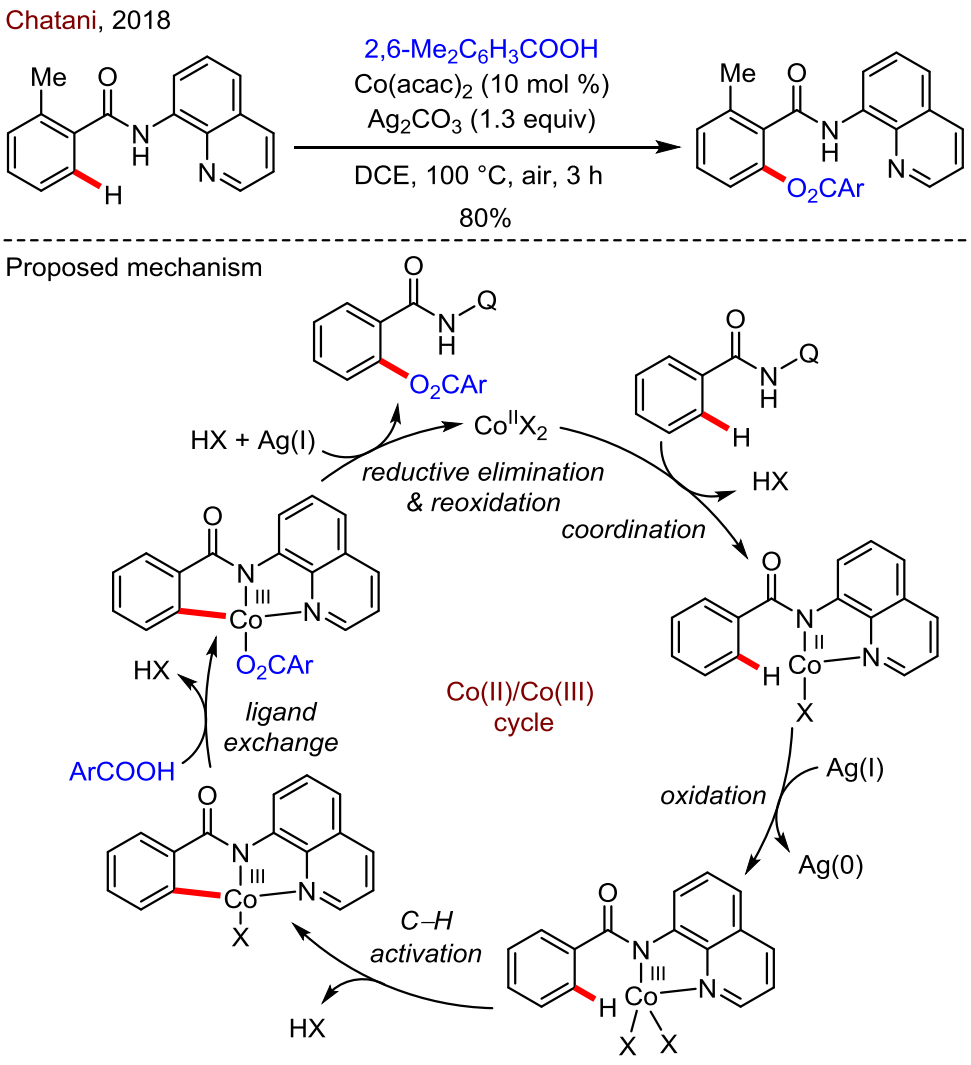

Scheme 1.8.4.7. Co(II)-catalyzed acyloxylation of benzamides and its plausible mechanism.

Although the initial findings of Daugulis[115] had indicated the formation of high-valent cyclometalated Co(III) species through bidentate chelation, the certainty in its formation in oxidative cobalt-catalyzed C–H activation/functionalization reactions was first provided by the reports of Maiti[135a] and later independently by Ribas,[150] when they successfully isolated and characterized organometallic Co–C bond containing Co(III) complexes by X-ray crystallography studies. Based on these results, similar cyclometalated cobalt(III) complexes have been reported by other groups.[144c,146,147b,151] Moreover, these complexes could also act as potential catalysts for the desired C–H functionalization reactions under their standard conditions.

Despite the huge progress in bidentate chelation assisted cobalt-catalyzed C–H functionalization reactions, it requires the prior installation and final removal of the directing group (if possible) after the desired reaction for an effective transformation, which presents itself as one of the setbacks of this strategy. However, throughout the years it has been observed that the directing groups can be efficiently detached under appropriate conditions.

The oxidative Co-catalyzed C–H activation/functionalization is not only limited to the bidentate chelating groups. Although less common, but few examples of the monodentate directing group assisted C–H activation reactions employing cobalt catalysis have also appeared for the formation of C–C and C–X bonds (Scheme 1.8.4.8).[152] In 2017, Niu and Song reported the first Co(II)-catalyzed oxidative arylation of indoles and arenes with arylboronic acids aided by a monodentate pyrimidine or pyridine DG (Scheme 1.8.4.8a).[152a] The pyrimidine DG was further used for C7-arylation of indolines using boronic acids, and C_2-arylation of indoles using arylsiloxanes by the groups of Punniyamurthi[152b] and Loh[152c] respectively (Scheme 1.8.4.8b, 1.8.4.8c). Cai *et al*. described a strategy for direct and regioselective C–H methylation and acetoxylation reaction of anilides using peroxides and acetic acid as corresponding methylating and acetoxylating reagents respectively (Scheme 1.8.4.8d).[152d] They also devised a C–H halogenation (Cl/Br/I) reaction of anilides using *N*-halosuccinimides as halogen source (Scheme 1.8.4.8e).[152e] Recently, Cao and co-workers reported an efficient methodology for the acetoxylation of phenols for the synthesis of functionalized pyrocatechol derivatives with the help of a monodentate pyridine auxiliary (Scheme 1.8.4.8f).[152f] The reaction used $Co(acac)_2$ as the catalyst, PIDA as the acetoxy source, O_2 as a green oxidant, and did not require any other external additive.

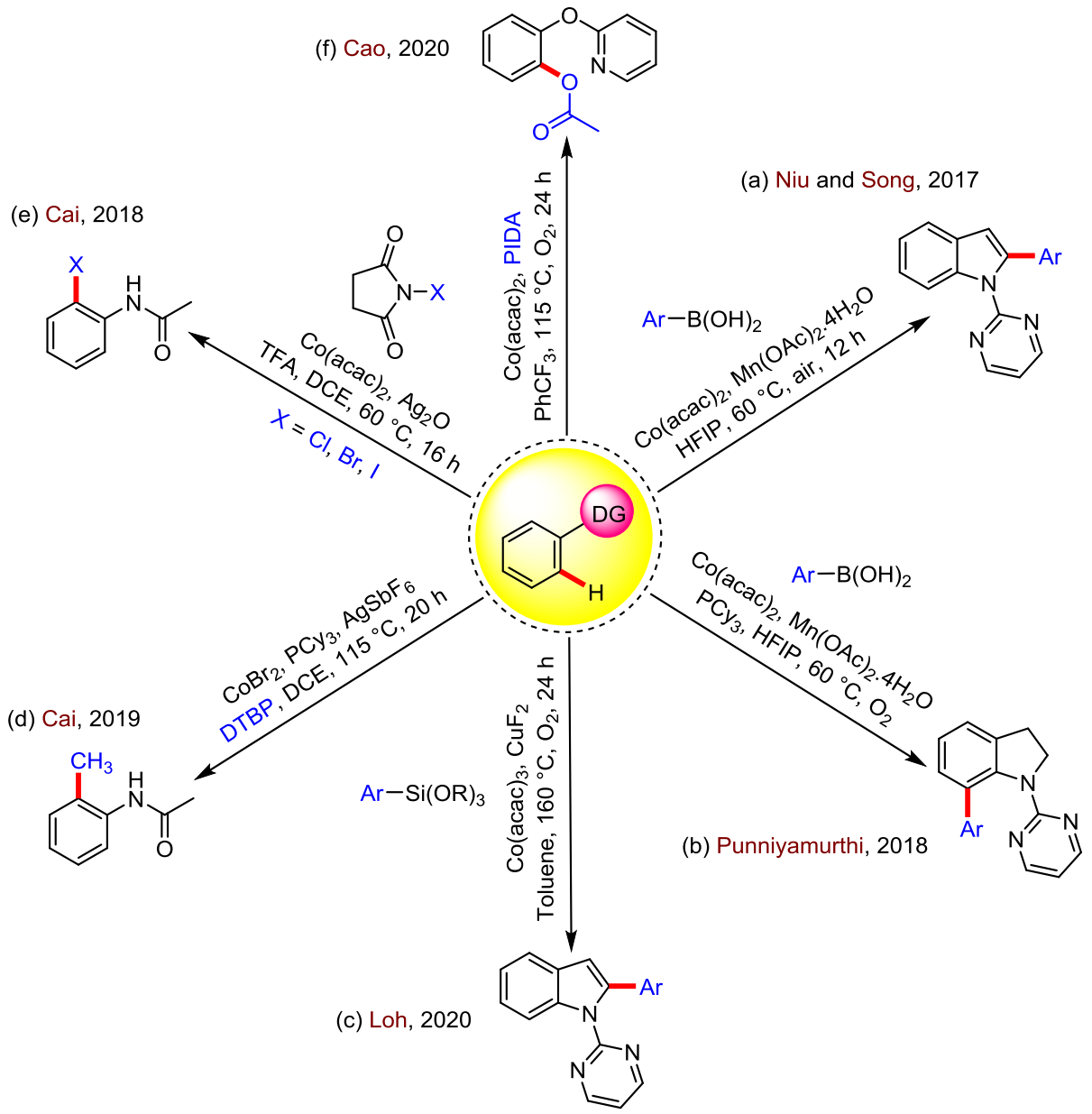

Scheme 1.8.4.8. Monodentate DG aided C–C and C–X bond formations under cobalt catalysis.

It is an evident fact that in most cases stoichiometric amounts of external silver or manganese based oxidants are required for oxidative cobalt-catalyzed C–H activation reactions. So, a greener approach was called for to replace the role of these toxic chemicals with sustainable and environmentally benign techniques. In 2018, Sundararaju and Rueping reported the first C–H/N–H annulation of 8-AQ attached benzamides with alkynes merging cobalt catalysis and photoredox catalysis under mild reaction conditions (Scheme 1.8.4.9).[153] Here, visible light-activated photocatalyst act as an electron-transfer reagent and O_2 as a terminal oxidant. The scope of this technique was further expanded to other C–H functionalization reactions by different groups.[154]

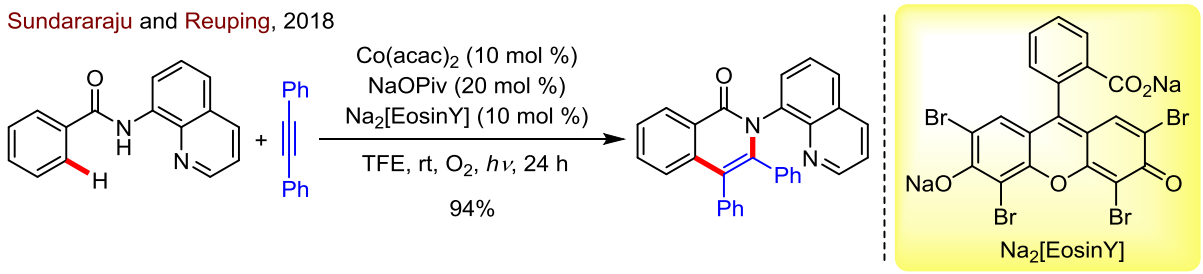

Scheme 1.8.4.9. C–H/N–H annulation with alkynes under cobalt/photoredox catalysis.

Another approach which has risen recently is the cobalt-catalyzed electrochemical C–H functionalization which uses electrical energy as a green oxidant. In this vein, Ackermann group, in 2017, reported the first electrochemical Co-catalyzed C–H oxygenation of arenes and alkenes bearing a PyO bidentate DG under mild conditions (Scheme 1.8.4.10).[155] The reaction setup contains an RVC anode and a Pt cathode as the electrode combination. Since then, steady progress has been achieved in this field by various research groups.[82,156]

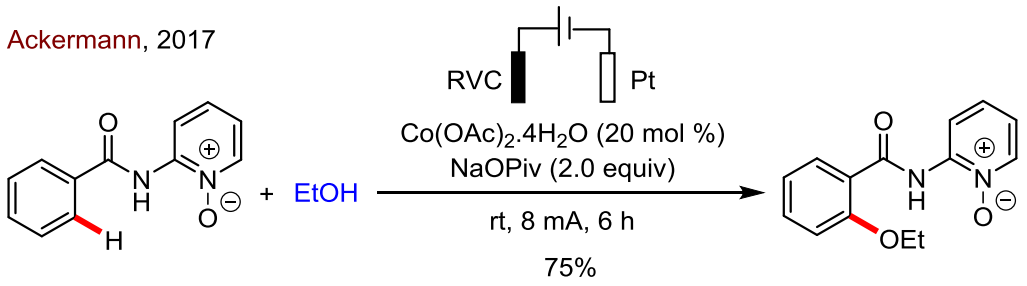

Scheme 1.8.4.10. Cobaltelectro-catalyzed C–H alkoxylation of amides.

1.9. Copper-Catalyzed C–H Activation

Since the landmark discoveries of Ullmann and Goldberg,[2,157] later elegantly modified by Chan, Evans and Lam independently,[158] copper salts as a catalyst have been extensively used for a plethora of C–C and C–X (X = heteroatoms, like N, O, S, Se, P, Cl/Br/I, etc.) bond forming reactions. After the dynasty created by palladium in cross-coupling and C–H activation chemistry, the scientific community searched for an earth-abundant, cost-effective, and less toxic first-row transition metal for this purpose, where copper presented itself as an effective alternative. The Cu salts possess reactivity in a strikingly similar fashion to Pd, also having unique chemo and regioselectivity. Copper complexes can exhibit oxidation states ranging from 0 to +3, making them viable catalysts for new bond forming reactions through both radical pathways initiated by SET mechanism and organometallic copper intermediates. These varied oxidation states allow it to act through one-electron or two-electron processes.

Like other first-row transition metals, Cu metal is cheap, environmentally friendly, and has high abundancy on the earth's crust (Table 1.7.1). Hence, it has grabbed the attention of research groups all over the world for its application in various type of reactions, *viz*. cross-coupling, oxidation, addition, radical, and C–H functionalization reactions for the construction of C–C and C–X bonds.[30g,62,73,159] Among them, copper-promoted and copper-catalyzed C–H activation/functionalization have tremendously grown over the past decade and half which is thoroughly discussed in this section.

Early developed methods relied on the functionalization of activated aromatic C(sp^2)–H bonds adjacent to heteroatoms or benzylic C(sp^3)–H bonds. But with time more focus was given on the functionalization of unactivated C–H bonds under copper catalysis. To achieve this target by overcoming the hurdle of regioselectivity, directing groups were introduced in C–H activation reactions as discussed earlier. As an early example, Reinaud and co-workers reported chelation assisted *ortho* sp^2 C–H hydroxylation of benzoic acid derivatives under copper-mediated conditions (Scheme 1.9.1).[160] They found that on using Cu(0) salt and trimethylamine *N*-oxide (TMAO) oxidant under O_2 atmosphere, Cu(0) is oxidized to Cu(II) which promotes the hydroxylation reaction with TMAO. This example represented the first instance of directing group aided C–H functionalization under copper-mediated conditions. But it was not until the report of Yu that the concept of DG assisted C–H functionalization using Cu salts started developing. The mechanisms of these reactions can be predominantly divided into two categories- (i) initiation by SET from the substrate to the Cu(II) species, resembling organometallic C–H oxidation reactions, (ii) involve the formation of organocopper(II) or organocopper(III) intermediates through Cu(II)-mediated C–H activation.

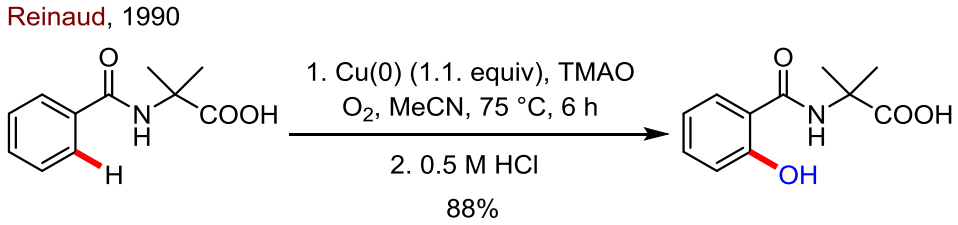

Scheme 1.9.1. Copper-mediated chelation directed C–H hydroxylation of benzamides.

In 2006, Yu group disclosed the pioneering work on monodentate pyridyl-directed Cu-mediated direct C–H functionalization reactions of 2-arylpyridines (Scheme 1.9.2a).[161] Independently, Chatani *et al.* reported *ortho* amination of the same DG attached substrates using anilines under copper-promoted conditions (Scheme 1.9.2b).[162] Also, the development

of 8-aminoquinoline auxiliary by Daugulis and co-workers[60] led to the use of these type of bidentate directing groups in copper-mediated C–H functionalization reactions as well.

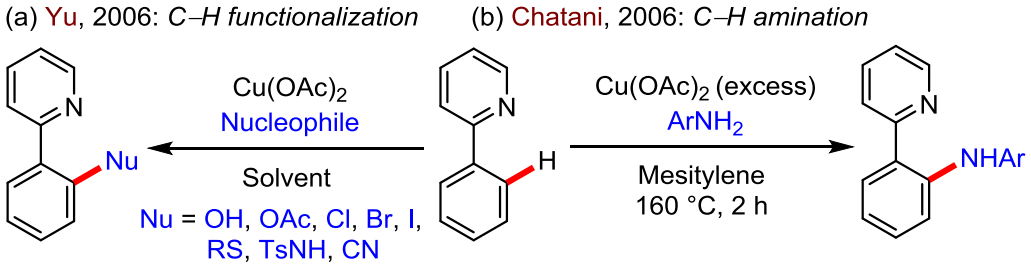

Scheme 1.9.2. Early examples of copper-mediated DG assisted C–H functionalization.

Inspired by these elegant studies, Cu-mediated (both stoichiometric as well as catalytic) chelation assisted C–H activation/functionalization reactions have gained significant attention over the years exemplified by the vast number of reports in this area.[57d,i,r,163] This is the main theme of discussion in this section of the chapter, which is divided into sub-sections broadly categorized by the type of bonds formed, *viz.* C–C, C–N, C–O, C–S and C–Se, C–P, C–Z (Z = F/Cl/Br/I), tandem C–H activation/annulation, and electrochemical C–H activation, using the help of either monodentate or bidentate directing groups.

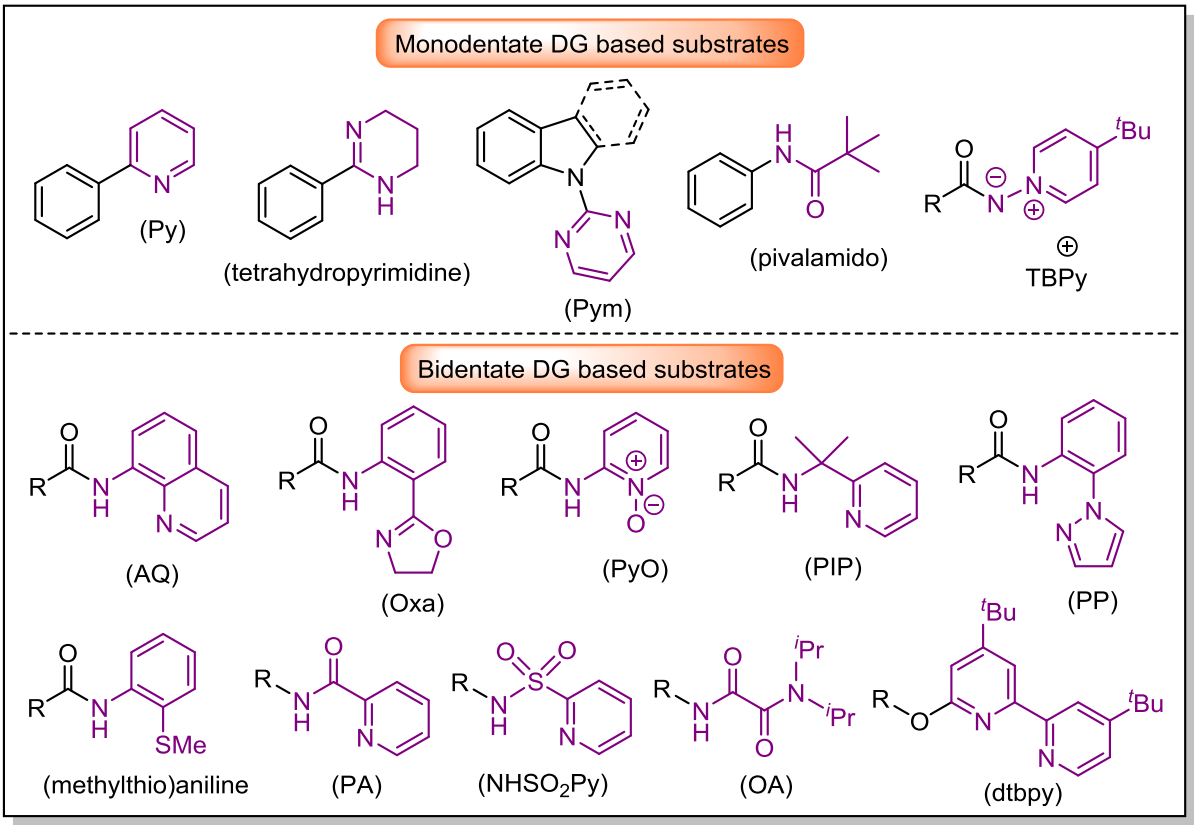

Figure 1.9.1. Commonly used mono and bidentate directing groups in copper catalysis.

A brief account on the mechanistic aspects of copper-catalyzed C–H activation is also provided. Some of the commonly used mono and bidentate directing group attached substrates in these reactions are depicted in Figure 1.9.1.

1.9.1. C–C Bond Formation

C–C bond forming reactions are indispensable in synthetic organic chemistry. In this context, efforts have been made in the development of copper-mediated or copper-catalyzed C–C bond formations via C–H activation pathway. Among them, the synthesis of biaryls is an important part on account of their presence in a vast number of biologically active molecules, pharmaceutically relevant compounds, and their applications in material chemistry.

The first report in this regard came in 2009, when Yu *et al.* disclosed the dimerization of 2-phenylpyridine derivatives under Cu(II)/I_2-mediated conditions (Scheme 1.9.1.1a).[164] The reaction takes place via a double C–H activation/dehydrogenative homocoupling pathway. The authors proposed a SET/electrophilic metalation process for the iodination step, followed by Ullmann type coupling of this intermediate to furnish the biaryl product. Later, Miura group reported a regioselective homocoupling of thiophenes and indoles under Cu-mediated conditions.[165] But the substrate scope was limited and the yields were also on the lesser side. This dehydrogenative homocoupling strategy of indoles was again later employed by Ding and Jiao for the synthesis of 2,2′-bisindoles under modified copper-mediated conditions (Scheme 1.9.1.1b).[166] The cross-coupling with other arylation partners was first demonstrated by Miura group for the biaryl coupling of arylazines and azoles (Scheme 1.9.1.1c).[167] The heteroarylation reaction of C(sp^2)–H bonds occurred in presence of excess amounts of $Cu(OAc)_2$ in combination with PivOH additive to increase the reaction efficiency. 1,3-azoles were again employed by them as effective coupling partners for Cu-mediated cross-coupling with indole and 2-pyridone systems by two-fold C–H cleavage/dehydrogenative heteroarylation sequence (Scheme 1.9.1.1d, 1.9.1.1e).[168] All these reports involved the use of monodentate pyridyl or pyrimidyl directing groups which could not be removed finally in some of the cases.

To overcome this issue, bidentate directing groups were employed for heteroarylation techniques which could be easily installed and cleaved under appropriate conditions. Miura *et al.* developed a copper-mediated C–H/C–H cross-coupling of benzoic acid derivatives with 1,3-azoles with the help of 8-aminoquinoline auxiliary (Scheme 1.9.1.1f).[169] The use of bidentate system also widened the scope of both non-acidic arenes and azoles in the reaction.

Picolinamide DG has also been employed for the successful heteroarylation of naphthylamines under nearly identical conditions (Scheme 1.9.1.1g).[170] The first Cu-catalyzed direct arylation of aromatic amides was accomplished by Dai and Yu group using organoboron reagents (Scheme 1.9.1.1h).[171] This transformation was achieved with the aid of a readily removable oxazoline based bidentate DG. Mechanistically, the transmetalation step in the catalytic cycle provides evidence for the formation of an aryl cupperate intermediate, although the involvement of Cu(III) species remain to be elucidated. Tan and co-workers achieved arylation of 8-AQ assisted benzamides with arylboronic acids under copper-mediated conditions (Scheme 1.9.1.1k).[172] The *ortho* C–H cleavage step was found to be involved in the rds according to deuterium-labelling experiments.

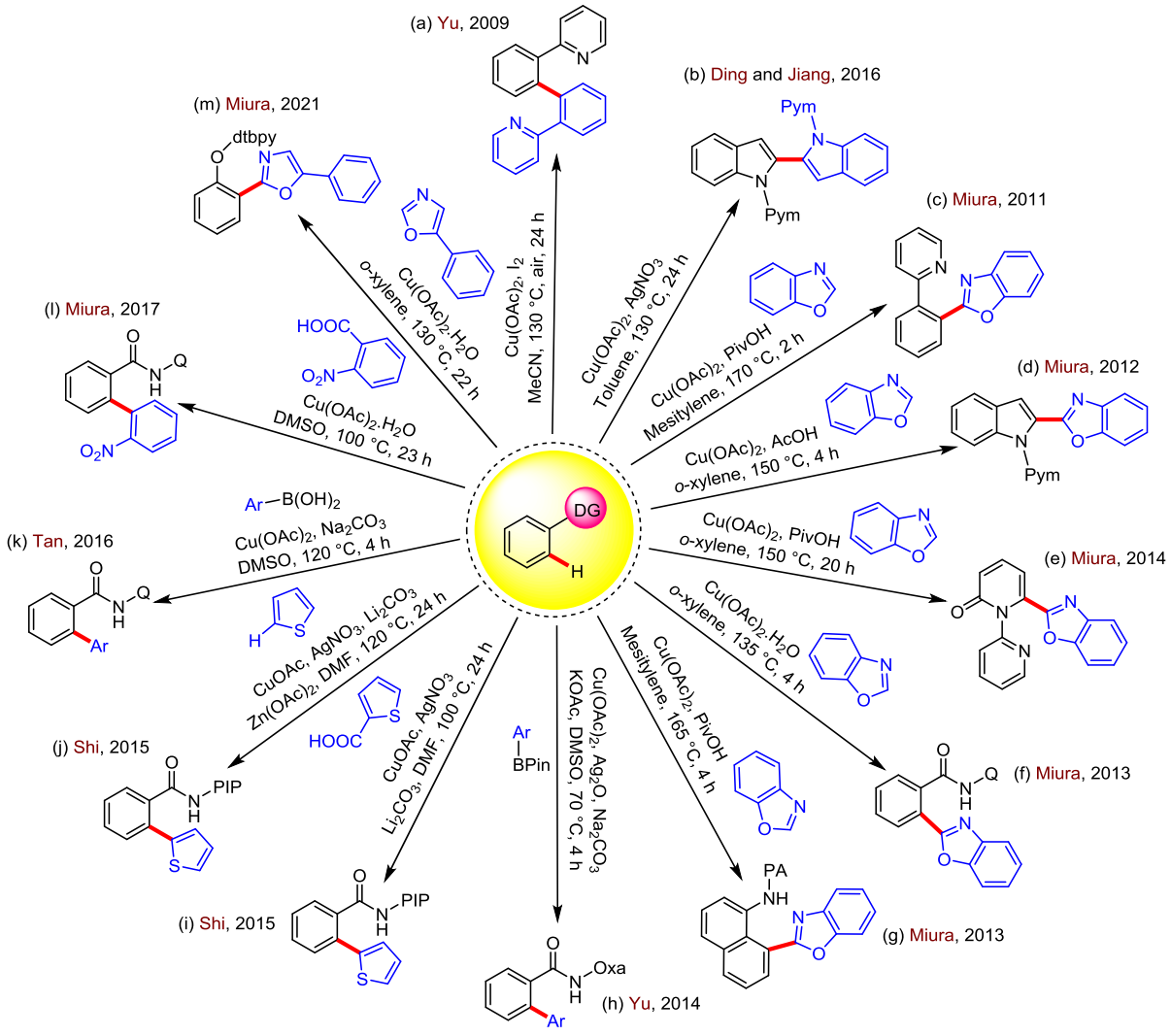

Scheme 1.9.1.1. Selected examples of Cu-mediated C–H (hetero)arylation.

In 2015, Shi group devised a strategy for decarboxylative arylation of PIP-directed benzamides with 2-thiophene carboxylic acids (Scheme 1.9.1.1i).[173] The authors proposed a proto-

decarboxylative/dehydrogenative arylation sequence rather than a direct decarboxylative arylation reaction under a Cu(I)/Ag(I) bimetallic system. Subsequently, they performed the same reaction engaging simple thiophenes as aryl source under slightly adjusted reaction conditions (Scheme 1.9.1.1j).[174] In 2017, Miura and co-workers disclosed a protocol for the decarboxylative coupling of benzamides with *o*-nitrobenzoic acids to synthesize biaryl motifs in good yields (Scheme 1.9.1.1l).[175] Alternatively, under slightly modified conditions, phenanthridinone derivatives were obtained via a decarboxylative C–H arylation/cyclization sequence. Recently, they delineated a Cu-mediated C–H/C–H biaryl coupling of phenols with azoles using a readily prepared, easily attachable/detachable, and recyclable 4,4′-di(*tert*-butyl)-2,2′-bipyridine (dtbpy) bidentate auxiliary (Scheme 1.9.1.1m).[176] The transformation provided phenol-azole heterobiaryls which are of great importance in material chemistry and the pharmaceutical industry.

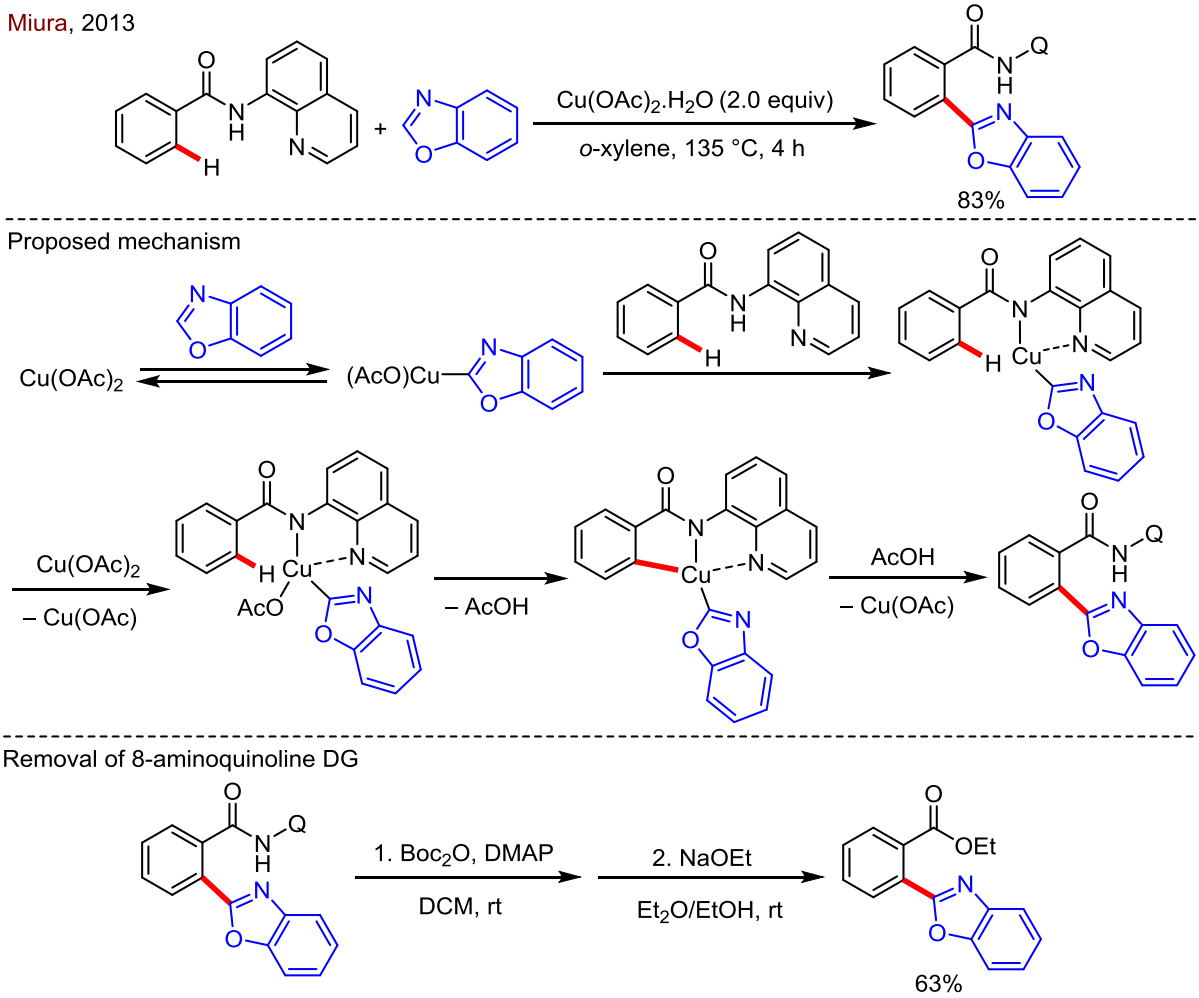

Scheme 1.9.1.2. Copper-mediated C–H heteroarylation of benzoic acids with azoles.

The mechanism of the (hetero)arylation reactions is represented by the example of copper-mediated biaryl coupling of benzamides with azoles, reported by Miura group, in Scheme 1.9.1.2.[169] Based on deuterium-labelling experiments, it was suggested that the C–H cleavage of benzoxazole occurs reversibly, but that of benzamide takes place in an irreversible fashion. Firstly, an initial ligand assisted cupration of the relatively acidic C–H of benzoxazole occurs to form an azolyl copper intermediate. Subsequent ligand exchange occurs with the benzamide to provide a *N*,*N*-bis-chelated complex. This undergoes oxidation in presence of stoichiometric amounts of $Cu(OAc)_2$ to generate a Cu(III) species, followed by C–H activation to generate an arylCu(III) intermediate. Finally, reductive elimination affords the desired heterobiaryl product. The bidentate 8-AQ directing group could be easily removed after the desired reaction. First, Boc-protection of the secondary amide was performed, which on subjection to ethanolysis under NaOEt in Et_2O/EtOH conditions produced the corresponding heterobiaryl ethyl ester in an overall good yield.

In 2016, Shi and co-workers reported the first CuO-catalyzed direct and site-selective C6-arylation of indoles with diaryliodonium triflate salts with the aid of a weakly directing removable N–P(O)^{t}Bu$_2$ (TBPO) chelating group (Scheme 1.9.1.3).[177] The use of sterically hindered DG guided the coupling reaction to occur at the distant C6-position overriding the *ortho* directing effects as well electronic biases at the indole C2, C3, and C7 positions.

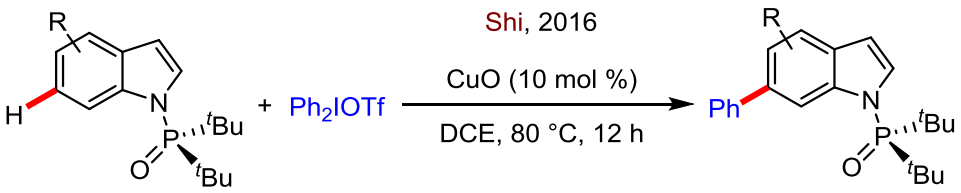

Scheme 1.9.1.3. Copper-catalyzed C–H arylation of indoles.

Aliphatic C–H arylation was first achieved by Ge *et al*. in 2015, when they reported a copper-mediated cross-dehydrogenative coupling of sp^3 C–H containing amides bearing an 8-AQ auxiliary with sp^2 C–H containing polyfluoroarenes (Scheme 1.9.1.4a).[178] The reaction was restricted to α-methyl groups over α-methylene and β- or γ-methyl group, and was also limited to substrates bearing α-tertiary C-center since β-sp^3 carbons turned out to be unsuccessful. You group devised an oxidative cross-coupling strategy of sp^3 C–H bonds with azole sp^2 C–H bonds under Cu-mediated as well as Ni-catalyzed conditions (Scheme 1.9.1.4b).[179] Here, a wide variety of azoles underwent the reaction successfully. PyO and 8-AQ bidentate DGs turned out

to be the effective chelating ligands for the copper-promoted and nickel catalytic conditions respectively.

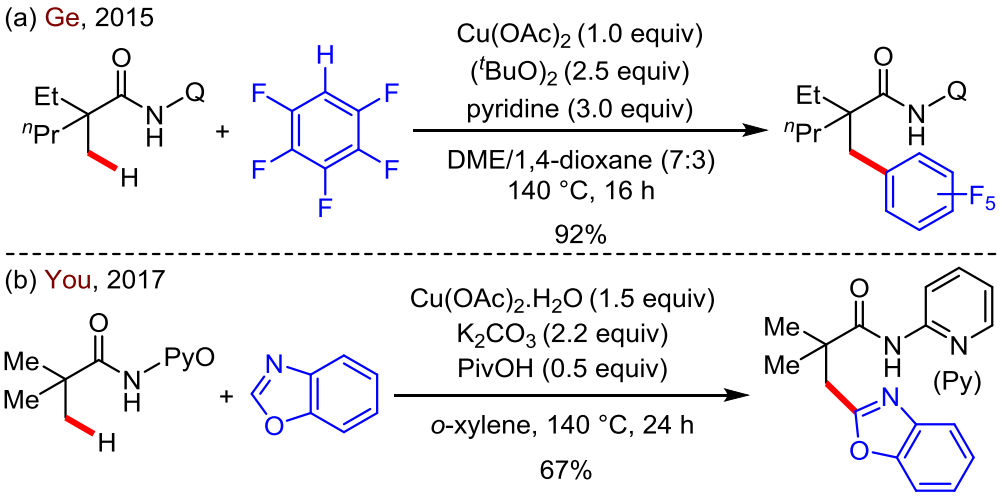

Scheme 1.9.1.4. Copper-promoted sp^3 C–H (hetero)arylation reactions.

Other types of C–C bond formation reactions accomplished under DG assisted Cu-mediated as well as Cu-catalytic conditions include direct cyanation,[180] trifluoromethylation,[181] alkynylation,[182] alkenylation,[183] and alkylation[184] reactions. Among them, cyanation reactions for the synthesis of aryl nitriles has been well explored since the pioneering work of Yu, where, among various C–H functionalization reactions, *ortho* C–H cyanation of 2-phenyl pyridines was achieved using TMSCN and $MeNO_2$ as nitrile sources under different conditions.[161] Monodentate DG attached substrates, in particular 2-phenylpyridine and 1-(pyrimidin-2-yl)-1*H*-indole have attracted most of the attention for direct cyanation protocols using a variety of cyanide anion surrogates. In 2012, Wang group used benzyl nitrile as a safe and operationally benign "CN" source to perform an aerobic oxidative Cu-mediated cyanation of 2-arylpyridines (Scheme 1.9.1.5a).[180a] Chang and co-workers developed a strategy for direct and selective cyanation of 2-phenylpyridines and indoles using NH_4I/DMF as a combined source of cyano unit (Scheme 1.9.1.5b).[180b] The reaction was proposed to occur via a two-step sequence involving electrophilic iodination followed by cyanation.

Han group reported a pyridyl directed arene C–H cyanation reaction employing azobisisobutyronitrile (AIBN) as a free radical cyano source (Scheme 1.9.1.5c).[180c] Shen *et al.* disclosed a protocol for the cyanation of arene units using inert acetonitrile as cyanide source under copper catalytic conditions (Scheme 1.9.1.5d).[180d] Here, disilanes play the role of a Lewis acid which enhances the reaction rate and promotes the C–CN cleavage of acetonitrile. Zhu

group independently reported a C2-selective cyanation of indoles using acetonitrile as a non-metallic cyanating reagent (Scheme 1.9.1.5e).[180e] In 2014, Jiao and co-workers developed a methodology for Cu-mediated direct cyanation of 2-phenylpyridines employing DMF as both the solvent and reagent for the reaction by providing both the C and N units of the "CN" group generated (Scheme 1.9.1.5f).[180f] Bidentate DGs have also been studied for copper-mediated C–H cyanation reactions. In 2017, the groups Chu and Sun reported a Cu-catalyzed sp^2 C–H cyanation of picolinamide DG assisted naphthalene derivatives using benzoyl nitrile as cyano group source (Scheme 1.9.1.5g).[180g] Next year, Shen *et al.* described a 2-(methythio)aniline DG assisted copper-mediated cyanation of arylamides using cheap acetonitrile as a green "CN" source (Scheme 1.9.1.5h).[180h]

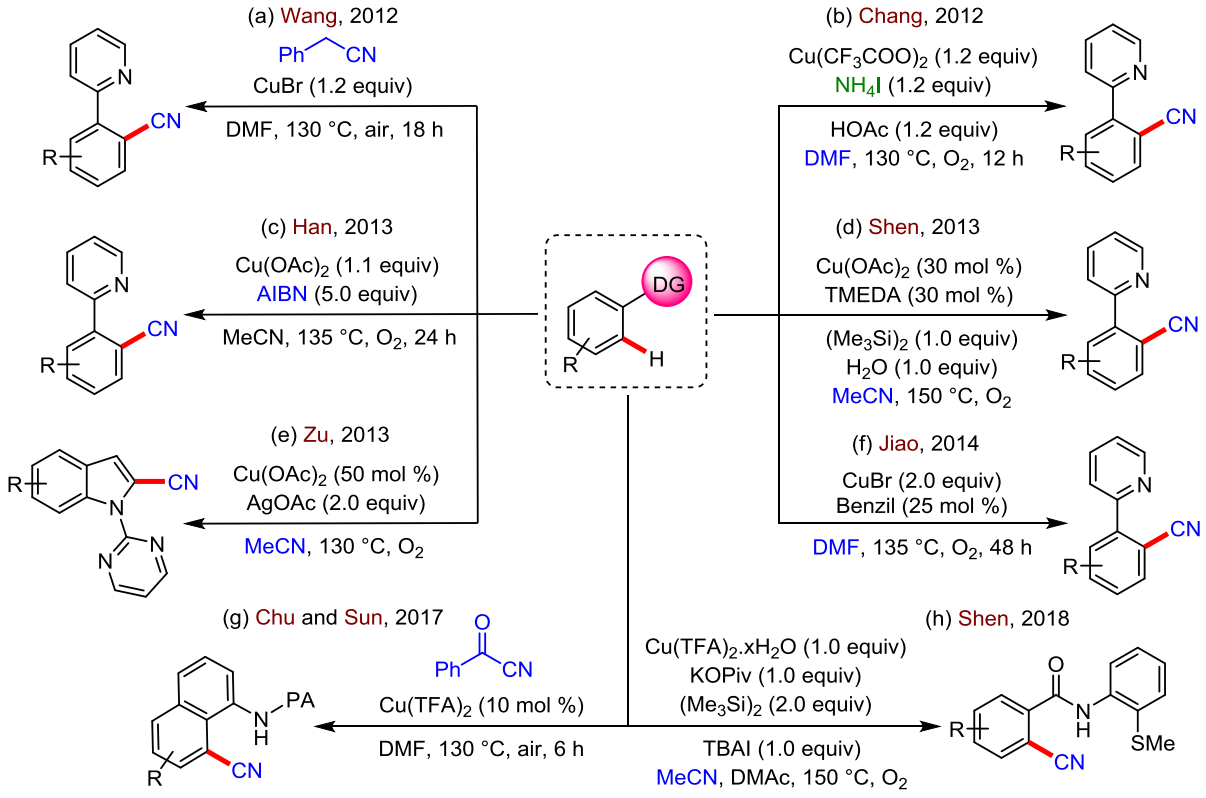

Scheme 1.9.1.5. Copper-mediated C–H cyanation reactions.

Copper-catalyzed direct C–H trifluoromethylation of (hetero)arenes with the help of a monodentate pivalamido DG was first realized by the group of Chen and Xi using Togni reagent as the CF_3 source (Scheme 1.9.1.6a).[181a] In 2014, Yu and Dai group reported an exceedingly fast Cu-mediated *ortho* trifluoromethylation reaction of benzamides with $TMSCF_3$ assisted by a bidentate oxazoline DG (Scheme 1.9.1.6b).[181b] Tan *et al.* further employed 8-AQ bidentate auxiliary for mono selective *ortho* trifluoromethylation of aromatic amides under

copper-promoted conditions (Scheme 1.9.1.6c).[181c] The reaction requires H_2O as an additive to achieve high yields.

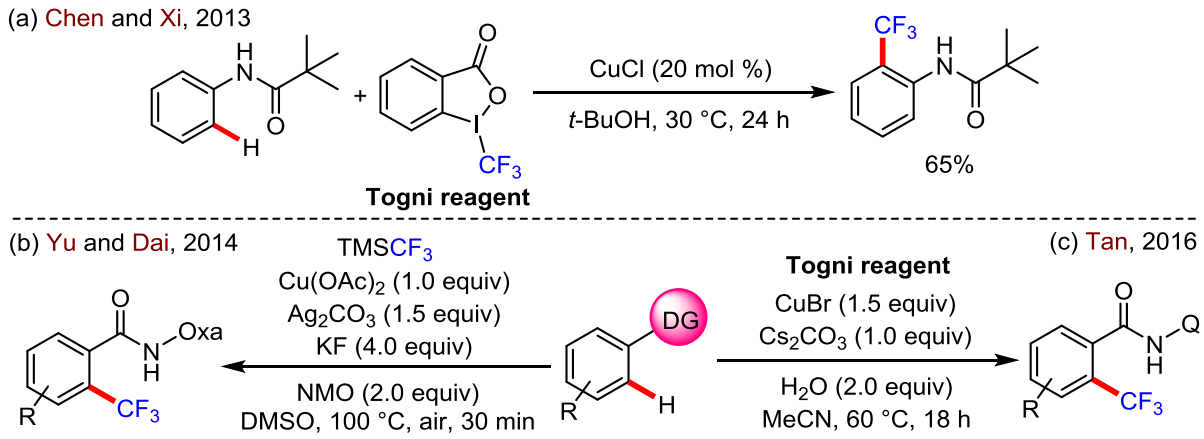

Scheme 1.9.1.6. Copper-mediated C–H trifluoromethylation reactions.

Aryl alkyne synthesis under Cu-mediated conditions was first accomplished by the group of Yu and Dai for direct alkynylation of arenes and heteroarenes using terminal alkynes under mild conditions (Scheme 1.9.1.7a).[182a] A wide array of oxazoline directed arenes and alkynes were found compatible for the reaction, thus providing an alternative pathway to the traditional Sonogashira coupling. Shi and co-workers independently developed a $Cu(OAc)_2$-catalyzed alkynylation of benzamides bearing a PIP bidentate chelating group using bulky TIPS group enabled terminal alkynes (Scheme 1.9.1.7b).[182b] Ag_2CO_3 oxidant and Et_3N base were the other effective ingredients of the reaction. The authors proposed the involvement of a Cu-mediated basic-ligand-enabled CMD pathway rather than a S_EAr pathway for the alkynylation reaction.

C–H alkenylation under copper-catalyzed conditions was first reported by Wang and Yu in 2020. They demonstrated a direct alkenylation reaction of benzoic and acrylic acid derivatives with a wide variety of acyclic as well as cyclic vinyl boronates to furnish a series of alkenes and dialkenes (Scheme 1.9.1.7c).[183] A Cu-mediated decarboxylative C–H alkylation protocol of 8-AQ directed benzamides with potassium malonate esters was established by Miura *et al.* (Scheme 1.9.1.7d).[184a] Guan and Bi group disclosed a strategy for the synthesis alkyl olefin products with excellent regio- and stereoselectivity via a copper-catalyzed intermolecular Heck-type reaction of 8-AQ attached olefinic amides and alkyl halides (Scheme 1.9.1.7e).[184b] The reaction tolerated 1°, 2°, and 3° alkyl bromides and various unactivated alkenes. DFT calculations suggested a radical pathway for the reaction involving a DMSO-assisted concerted HBr elimination event of a conformationally strained Cu(III) cyclic transition state.

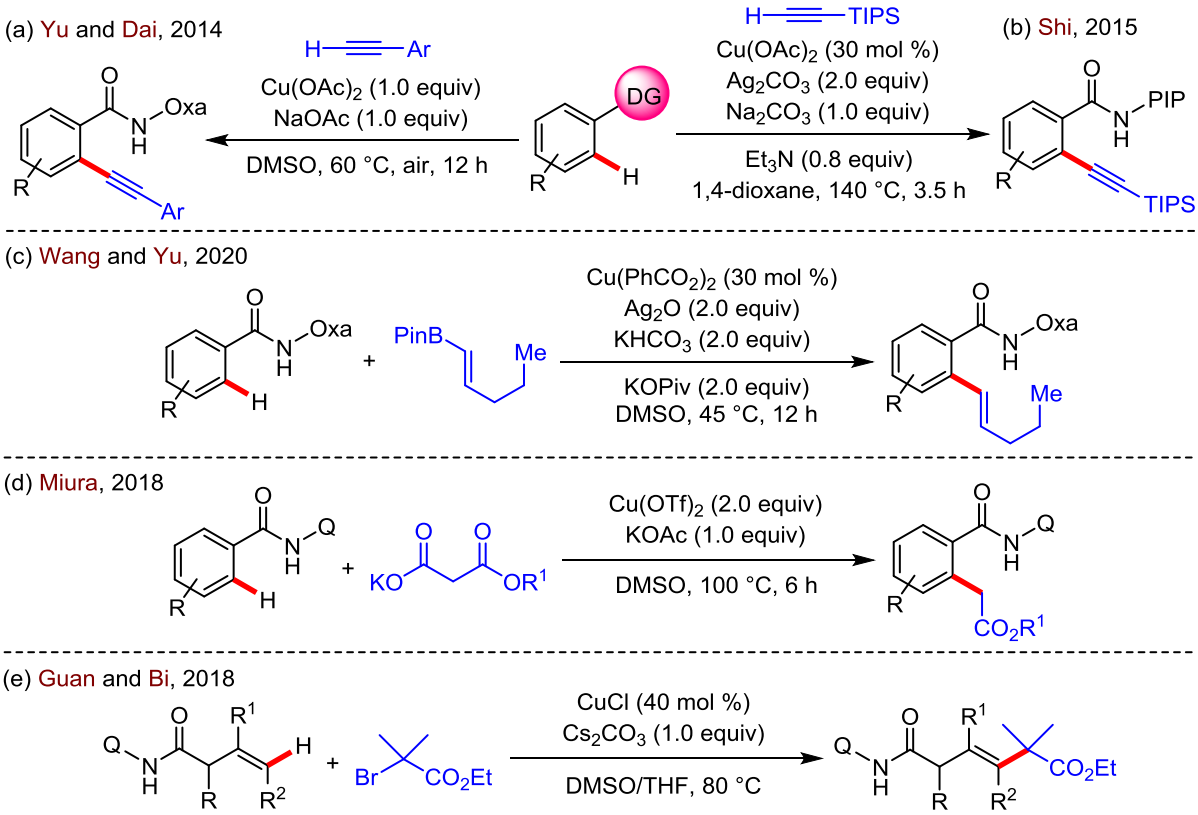

Scheme 1.9.1.7. C–H alkynylation, alkenylation, and alkylation under Cu catalysis.

Despite the advantages of using DGs, it has its drawbacks of pre-installation and post-removal which makes it slightly less desirable. In this regard, Wang and co-workers employed simple phenols devoid of any attached DG in a copper-catalyzed *ortho* aminomethylation reaction with potassium aminomethyltrifluoroborates affording C(sp^2)–C(sp^3) cross-coupling products (Scheme 1.9.1.8a).[185] The reaction was proposed to go via a SET mechanism and represented a rare example of highly selective functionalization of free phenols. In 2020, Zhang and Liu group described a methodology for *ortho* selective alkylation of unprotected phenols and naphthols with α-aryl-α-diazoacetates (Scheme 1.9.1.8b).[186] The reaction went under mild conditions and required only catalytic amounts of $CuCl_2$ without the need for any external additive.

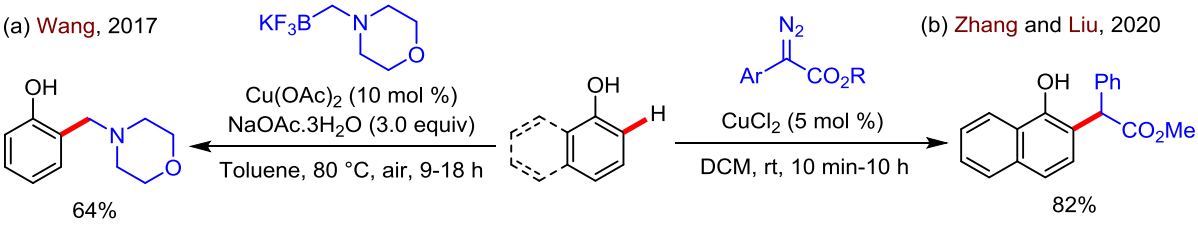

Scheme 1.9.1.8. Cu-catalyzed C–H alkylation of phenols and naphthols.

1.9.2. C–N Bond Formation

Since the seminal work of Yu and Chatani on copper-mediated amination of 2-phenylpyridines (Scheme 1.9.2),[161-162] a plethora of useful methodologies on Cu-promoted and Cu-catalyzed DG assisted C–N bond formation via C–H activation strategy have been developed.

In 2013, Daugulis *et al.* realized a copper-catalyzed direct *ortho* amination reaction of arenes bearing bidentate 8-AQ as well as picolinamide auxiliary (Scheme 1.9.2.1a).[187] Various functional group containing secondary amines were well compatible under the reaction conditions composed of $Cu(OAc)_2$ as catalyst, Ag_2CO_3 as co-catalyst, and NMO as oxidant. Primary amines also underwent the reaction but with less yields. The removable nature of the DG allows for the straightforward synthesis of *ortho* aminobenzoic acid derivatives. Following this, taking the help of diverse DGs, Chen, Carretero, Jana, Dai, and Wu groups, among others devised efficient copper-mediated sp^2 C–H amination protocols with similar secondary amines.[188] These secondary amines have also been applied in intermolecular amination of inert sp^3 C–H bonds with the assistance of 8-AQ auxiliary by the groups of Qin and Yang (Scheme 1.9.2.1b).[189] Rao group used electrophilic *O*-benzoyl hydroxylamines in a similar Cu-catalyzed C–H amination reaction of benzamides.[190]

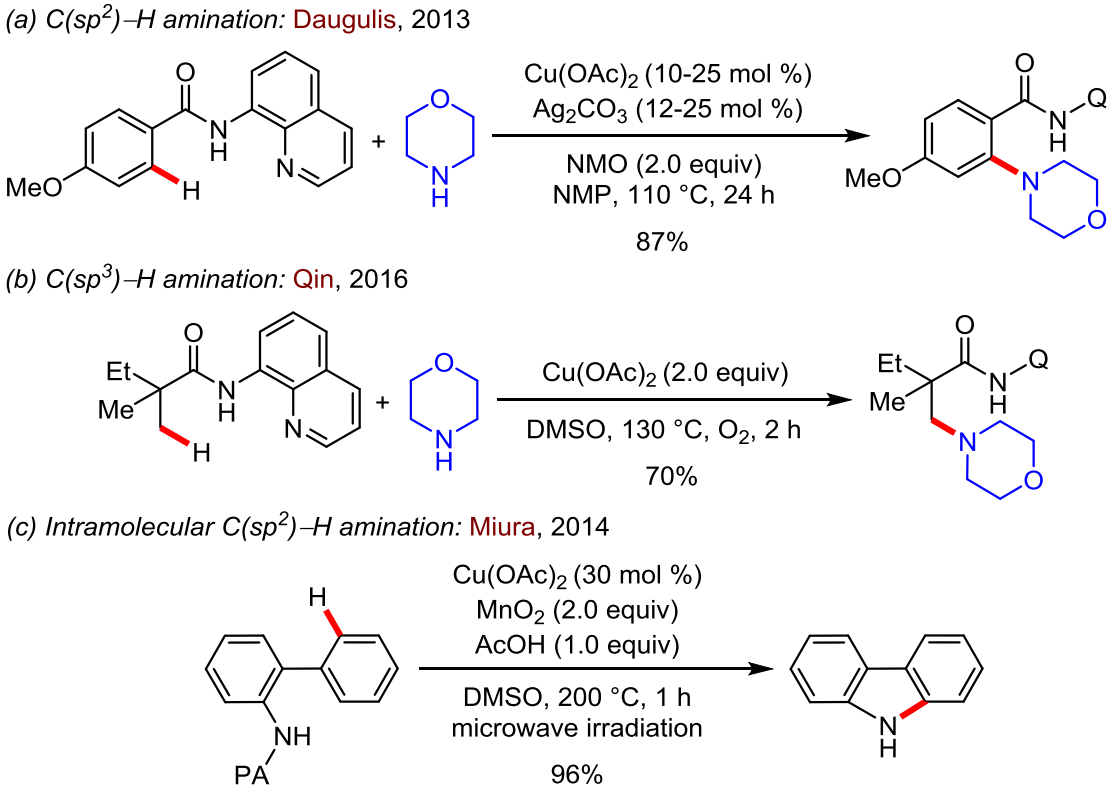

Scheme 1.9.2.1. Representative examples of Cu-mediated C–H amination.

C(sp^2)–H amination of arenes with aromatic systems like anilines and azaheterocycles, *viz.* indoles, pyrroles, pyrazoles, carbazoles, azaindoles etc. was reported by various groups employing copper-mediated conditions.[191] Zhu, Bolm, and Yu groups developed methodologies for the direct conversion of aromatic C–H to C–NH_2 bonds.[192] Zhu employed $TMSN_3$ as nitrogen source for the facile generation of *N*-heterocycle-substituted primary anilines;[192a] Bolm and co-workers used readily accessible dibenzothiophene sulfoximines as NH_3 surrogate for oxidative amination of aromatic amides;[192b] oximes were used as amino donors by Yu for Cu(I)-mediated direct amination of amides to produce primary anilines.[192c] In 2019, Miura group reported a bidentate phenanthroline based DG assisted *ortho* amination of phenol derivatives under copper catalysis.[193] Diarylamines were used in this reaction for the synthesis of *o*-aminophenols. Various diarylamines have also been used in Cu-catalyzed *ortho* C–H diarylamination of indoles, indolines, anilines, *N*-aryl-7-azaindoles to furnish triarylamines.[194] Very recently, Dai *et al.* devised copper-mediated *ortho* amination of anilines using oxalamide (OA) directing group and DMF as amine source.[195] Various heterocycles were well compatible under the reaction condition which was proposed to undergo via a radical pathway from mechanistic investigations. Bolm and Baidya groups described methodologies for the preparation of *N*-arylated sulfoximines via C–H/N–H cross-dehydrogenative coupling of sulfoximines with 2-arylpyridines and 8-AQ derived benzamides respectively.[196] Miura group reported the synthesis of carbazoles via intramolecular C–H amination of 2-aminobiphenyls using $Cu(OAc)_2$ as catalyst and MnO_2 as terminal oxidant under microwave irradiation conditions (Scheme 1.9.2.1c).[197] Similarly, a methodology for the generation of indoline analogues was accomplished by the same group under Cu-mediated conditions.[198] Bidentate picolinamide DG was employed to deliver the desired products in both cases.

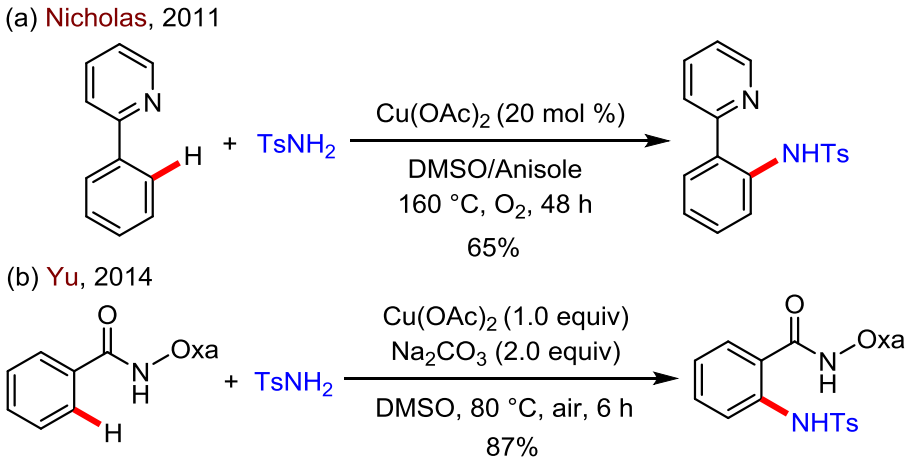

Scheme 1.9.2.2. Representative examples of Cu-mediated C–H amidation.

Moving forward, various groups have reported efficient methodologies for copper-mediated or copper-catalyzed C–H amidation of monodentate as well as bidentate DG tethered substrates (Scheme 1.9.2.2).[199] 2-arylpyridines and *N*-pyrimidyl indolines were successfully amidated with a wide range of amidating reagents, *viz.* carboxamides, sulfonamides, alkylamides, phthalimides, azides, and potassium cyanate.[199a-c,199e-g,199i] On the other hand, oxazoline and aminoquinoline based bidentate DG containing arylamides underwent amidation reactions with sulfonamides and acyl azides respectively.[199d,h]

The first chelation-assisted intramolecular amidation of unactivated sp^3 C–H bonds under Cu-catalyzed oxidative conditions was reported by Kuninobu and Kanai group (Scheme 1.9.2.3).[200]

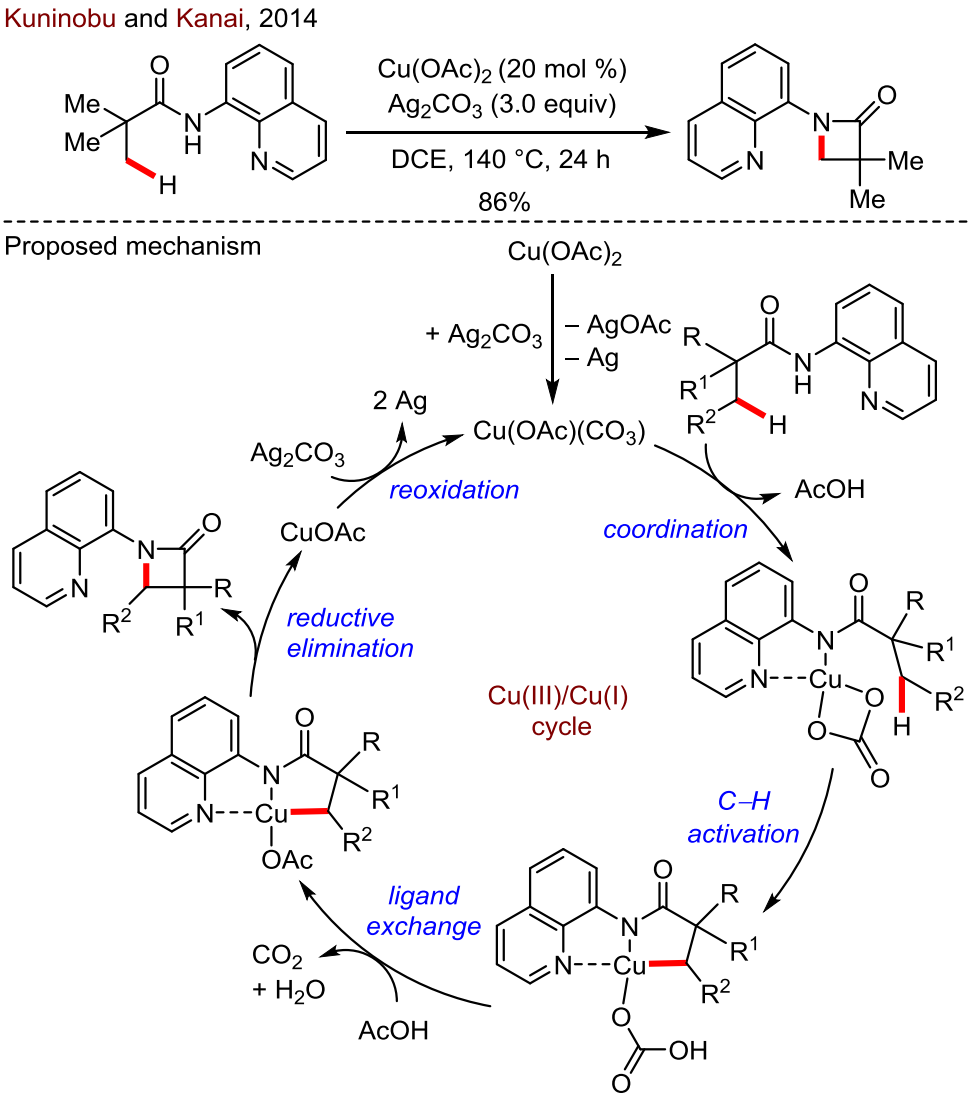

Scheme 1.9.2.3. Copper-catalyzed intramolecular sp^3 C–H amidation.

The reaction proceeded in presence of $Cu(OAc)_2$ catalyst and Ag_2CO_3 oxidant to give access to a vast array of biologically important β-lactam derivatives from 8-aminoquinoline DG

containing benzoic acid derivatives. 2-indolinone scaffolds could also be synthesized by sp^2 C–H amidation on slight tuning of the reaction conditions.

Mechanistically, the authors proposed that initial oxidation of $Cu(OAc)_2$ by Ag_2CO_3 generates the active $Cu(OAc)(CO_3)$ species which undergoes chelation with the *N*,*N*-bidentate system to generate a copper amide intermediate. Next, C–H activation occurs via CMD mechanism providing the metalacyclic intermediate. This *in situ* generated Cu(III) species reacts with AcOH to give another Cu(III) organometallic intermediate by the elimination of H_2O and CO_2. Finally, reductive elimination takes place to give the β-lactam product and CuOAc species which is again oxidized by Ag_2CO_3 to regenerate the $Cu(OAc)(CO_3)$ species and continue the catalytic cycle. Almost at the same time, Ge *et al.* demonstrated the same transformation under copper catalytic conditions using benzoquinone (BQ) as oxidant.[201] Following year, You group reported a more sustainable and economical approach to diverse β-lactams by a similar intramolecular dehydrogenative sp^3 C–H amidation using molecular oxygen as the sole oxidant.[202]

The synthesis of organic azides is important in organic synthesis since it behaves as building blocks or as "masked amines". In this regard, copper-catalyzed C–H azidation reaction has also been developed.[203] Jiao and Hao groups utilized the *ortho* directing effect of the primary amine group for the regioselective *ortho* azidation of anilines under mild conditions using azidotrimethylsilane ($TMSN_3$) (Scheme 1.9.2.4a) and azido-benziodoxolone as azide source respectively.[203a,b] Narula and co-workers reported aromatic C–H azidation of 2-phenylpyridines using benzotriazole sulphonyl azide as a safe and stable azidating agent.[203c]

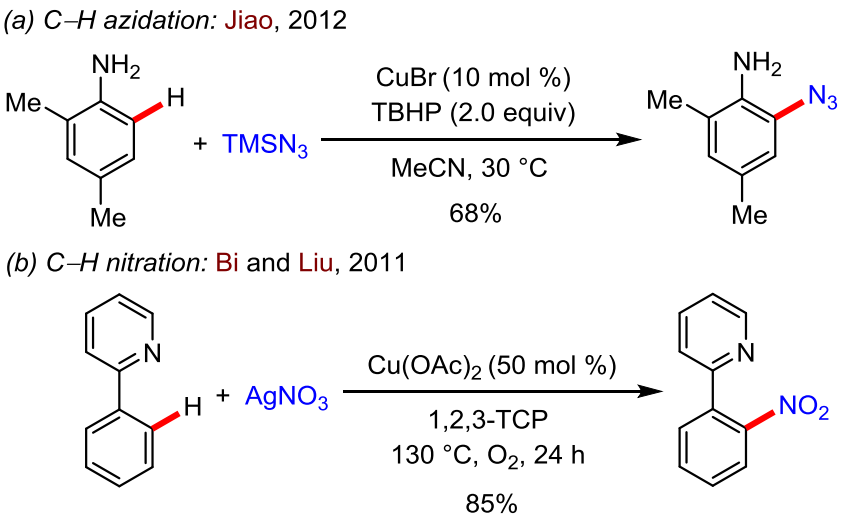

Scheme 1.9.2.4. Example of C–H azidation and nitration reactions under Cu catalysis.

Copper-mediated C–H nitration reactions has seen progress over the years.[204] In 2011, the group of Bi and Liu group described a novel Cu-mediated *ortho* C–H nitration of 2-arylpyridines using $AgNO_3$ as nitrating agent (Scheme 1.9.2.4b).[204a] The groups of Gooβen and Tan developed methods for the direct nitration of benzoic acid derivatives with the aid of bidentate 8-AQ auxiliary.[204b,c] They used $AgNO_2$ and $NaNO_2$ as sources of nitro group respectively. In 2018, Sun *et al.* achieved the nitration of aryl ureas with $Fe(NO_3)_3.9H_2O$ as the nitrating reagent under copper catalytic conditions.[204d]

1.9.3. C–O Bond Formation

Inspired by the pioneering work of Yu on copper-catalyzed *ortho* acetoxylation of 2-arylpyridines (Scheme 1.9.2),[161] C–O bond forming reactions under Cu-mediated or Cu-catalyzed conditions have been thoroughly examined by various research groups. Both monodentate and bidentate directing groups were explored for this purpose. First, oxygenation reactions assisted by monodentate DGs under copper catalysis are discussed (Scheme 1.9.3.1). In 2009, Fujii and Ohno showcased the efficiency of tetrahydropyrimidine as an efficient DG for Cu-mediated oxidative sp^2 C–H *ortho* hydroxylation of arenes, followed by cyclization with triphosgene (Scheme 1.9.3.1a).[205] Cheng group described copper-catalyzed *ortho* acyloxylation of 2-arylpyridines employing anhydrides and acyl chlorides as potent coupling partners (Scheme 1.9.3.1b).[206]

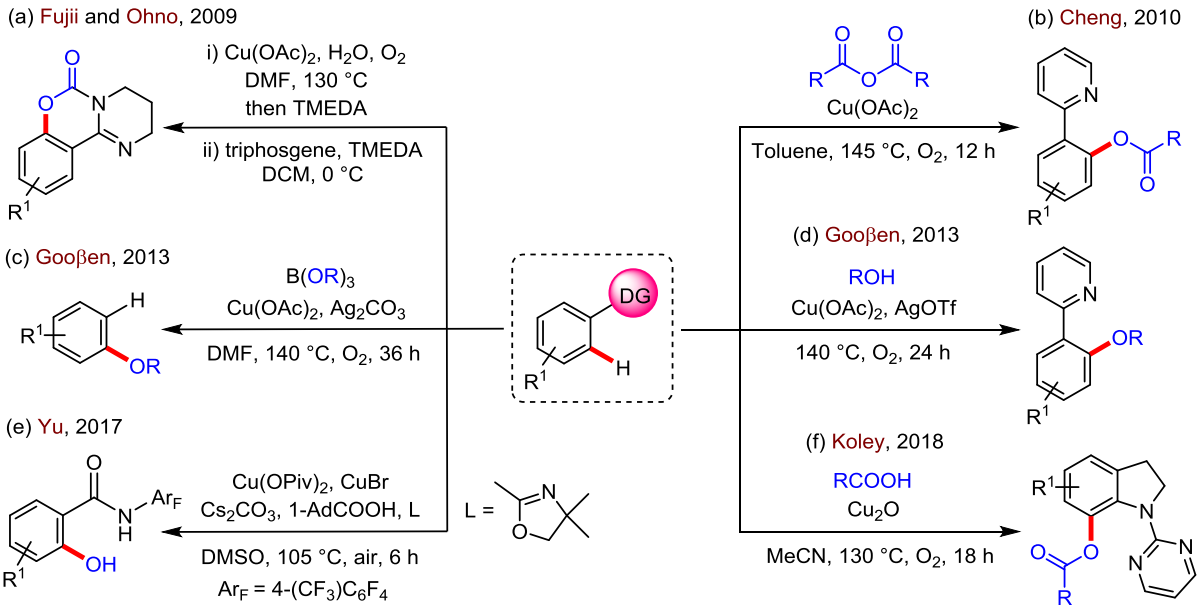

Scheme 1.9.3.1. Selected examples of monodentate DG assisted C–O bond formation under copper catalysis.

In 2013, Gooβen *et al.* used a simple carboxylate functional group as a traceless DG for *ortho* alkoxylation of benzoates with $B(OR)_3$ with concomitant decarboxylation under copper catalysis to furnish a wide range of aromatic ethers (Scheme 1.9.3.1c).[207] They again devised a strategy for regiospecific dehydrogenative cross-coupling of 2-arylpyridines with alcohols using a bimetallic copper/silver catalytic system (Scheme 1.9.3.1d).[208] Shen and co-workers reported a similar transformation using an improved catalytic system under aerobic conditions.[209] Yu group devised a strategy for copper-promoted C–H hydroxylation of monodentate weakly coordinating amides assisted by an external oxazoline ligand (Scheme 1.9.3.1e).[210] In 2018, Koley *et al.* demonstrated a Cu-catalyzed regioselective C7-acyloxylation of indolines with a variety of aryl and alkyl carboxylic acids using O_2 as the sole oxidant (Scheme 1.9.3.1f).[211]

Bidentate chelation has been the more common route to Cu-mediated C–O bond forming reactions (Scheme 1.9.3.2). In 2013, Stahl and co-workers provided a report on the detailed mechanistic study of a copper-mediated oxygenation reaction of benzamides (Scheme 1.9.3.2a).[212] The authors gave clear evidence for the involvement of a base assisted C–H activation/functionalization for the 8-AQ directed methoxylation reaction.

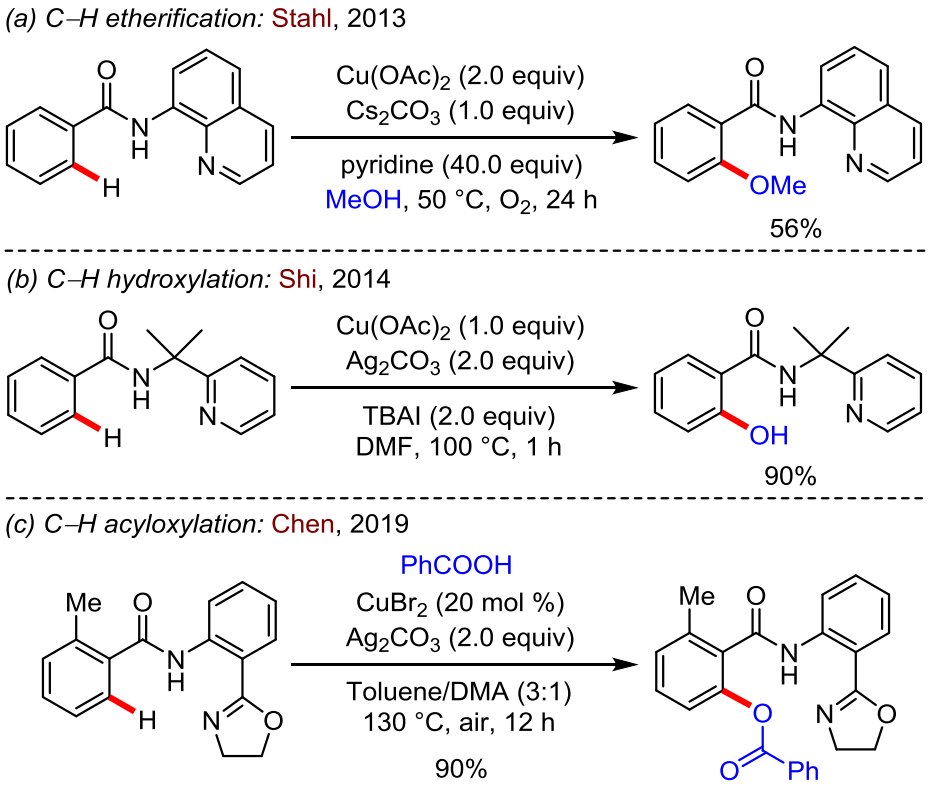

Scheme 1.9.3.2. Examples of Cu-mediated bidentate DG assisted C–O bond formation.

Etherification reactions were further developed by the groups of Daugulis, Shi, Niu and Song, and Punniyamurthi under copper catalysis with the aid of diverse *N*,*N*- or *N*,*O*-based bidentate coordinating groups.[213] In 2014, Shi *et al*. reported an efficient Cu-mediated C(sp^2)–H hydroxylation of PIP directing group tethered (hetero)arenes (Scheme 1.9.3.2b).[214] Yu and Jana groups further devised copper-mediated direct C–H hydroxylation of arenes using oxazoline and 8-AQ bidentate auxiliaries respectively.[215] Direct C–H acyloxylation of arylamides with aromatic, olefinic, and aliphatic acids employing copper catalysis has been accomplished by the groups of Shi, Zhang, and Chen (Scheme 1.9.3.2c).[216]

In the context of intramolecular C–O bond formation, in 2008, Nagasawa group first disclosed a method for the synthesis of 2-arylbenzoxazoles via a copper-catalyzed intramolecular oxidative C–O coupling reaction (Scheme 1.9.3.3).[217] Following this, Zhu *et al*. developed two protocols of intramolecular cycloetherification reaction for the synthesis of dibenzofurans from *ortho* arylphenols using copper salts.[218] In 2013, Martin and Grevorgyan group independently reported Cu-catalyzed intramolecular esterification reactions by applying carboxylic acids in remote C–H oxygenation reactions.[219]

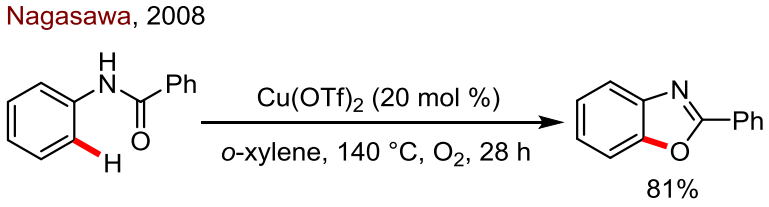

Scheme 1.9.3.3. Cu-catalyzed intramolecular C–O bond formation to give 2-arylbenzoxazoles.

In 2014, Kanai and Ge groups independently reported the first copper-promoted sp^3 C–H acetoxylation of aliphatic amides assisted by 8-AQ directing group (Scheme 1.9.3.4).[220] Direct sp^3 C–H acyloxylation reaction with a variety of acids was developed by Zhang and co-workers using a Cu(II)/TBAB catalytic system.[221]

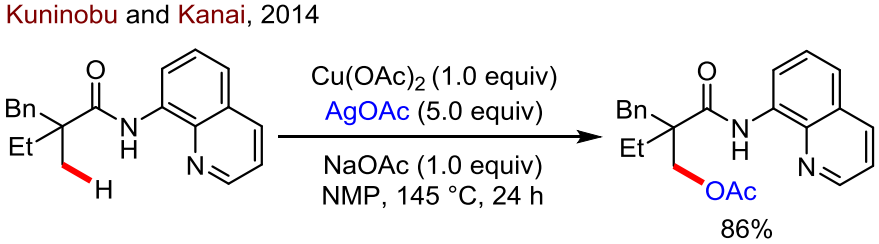

Scheme 1.9.3.4. Copper-mediated sp^3 C–H acetoxylation.

In 2017, Zhang *et al.* devised a methodology for the etherification of β-C(sp^3)–H bonds with organosilanes under Cu-mediated conditions.[222] The authors proposed that the reaction occurs via a tandem C–H oxidation/arylation or vinylation pathway. Isotope labelling studies revealed that $Cu(OAc)_2$ serves as the source of oxygen in the aryloxylated or vinyloxylated products. In 2015, Baran group disclosed a site-specific, rapid, high yielding, and scalable steroidal C12-oxidation protocol utilizing the help of an imine directing group.[223]

1.9.4. C–S and C–Se Bond Formation

Ever since the report of Yu group describing Cu-mediated thioetherification of 2-phenylpyridines,[161] several research groups have developed efficient methodologies for DG assisted copper-mediated or copper-catalyzed C–S and C–Se bond formation (Scheme 1.9.4.1). In 2010, Qing *et al.* reported an unprecedented Cu-mediated sp^2 C–H methylthiolation of 2-arylpyridines employing DMSO as the methylthiolation reagent (Scheme 1.9.4.1a).[224] Jain group further developed the identical transformation under $Cu(OAc)_2$/DMSO-promoted conditions.[225] In 2012, Daugulis and co-workers reported the first copper-mediated AQ directed β-sp^2 C–H sulfenylation of benzoic acid derivatives using disulfide reagents acting as both the source of thiolating agent and oxidant (Scheme 1.9.4.1b).[226]

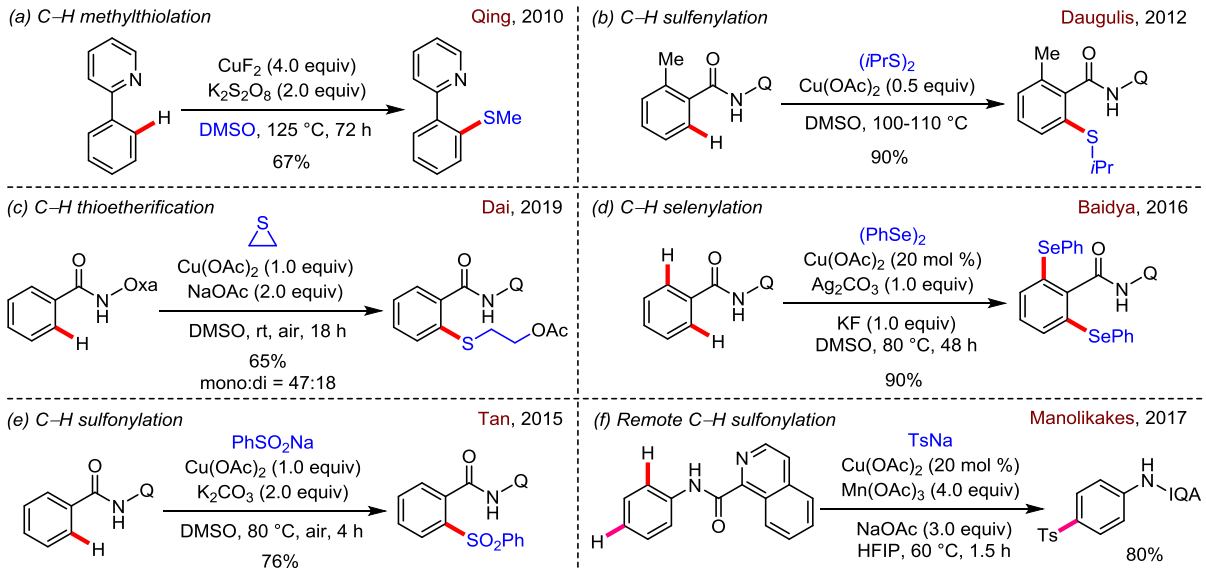

Scheme 1.9.4.1. Selected examples of Cu-mediated C–S and C–Se bond formation.

In 2019, Dai *et al.* reported a Cu-mediated C–H thioetherification of bidentate oxazoline DG based aromatic amides with ethylene sulfides at room temperature (Scheme 1.9.4.1c).[227] The method allows the preparation of aryl trifluorothioethers using appropriate

bis(trifluoromethyl)disulfides. DMSO was chosen as the solvent of choice because of its ability to oxidize thiols to disulfides, thereby *in situ* regenerating $(RS)_2$ from RSH. Also, γ-sp^2 C–H bonds of benzylamine derivatives were successfully sufenylated under similar conditions with the help of bidentate picolinamide auxiliary. Since then, the groups of Liu, Kambe, Jiang and Liu, and Shi have demonstrated effective sp^2 C–H thiolation reactions with disulfides assisted by diverse mono and bidentate DGs.[228] In 2016, Baidya and co-workers delineated a Cu-catalyzed arylselenylation protocol of (hetero)arenes using readily available diaryl diselenides (Scheme 1.9.4.1d).[229] Ackermann, Lu, Miura, Daugulis, and Koley groups further employed both disulfides and diselenides in C–H chalcogenation of arenes assisted by different mono and bidentate chelating groups.[230] In between, a copper-promoted direct C–H thiolation of quinazolinones was developed, which is discussed in detail in Chapter 3 as a part of this thesis work.

Copper-mediated direct *ortho* C–H sulfonylation of benzoic acid derivatives using sodium sulfinates was first reported by Tan group (Scheme 1.9.4.1e).[231] The reaction proceeds with good functional group tolerance and excellent regioselectivity for the synthesis of aryl sulfones. Almost immediately, Shi *et al*. reported a similar sulfonylation reaction using a catalytic amount of $Cu(OAc)_2$ and stoichiometric Ag_2CO_3 oxidant.[232] Song group, in successive years, demonstrated methodologies for copper-mediated direct sulfonylation of benzamides and indolines using *p*-Tosylmethyl isocyanide (TosMIC) and sulfonyl chlorides as sulfonyl group sources respectively.[233] Remote C–H sulfonylation reactions could also be achieved under copper catalysis. In early 2017, Manolikakes and co-workers reported a $Cu(OAc)_2$-catalyzed *para* selective sulfonylation reaction of anilines bearing 1-isoquinoline carboxamide (IQA) directing group with sulfinic acid salts (Scheme 1.9.4.1f).[234] The system overrides the usual *ortho* selectivity of the DG assisted C–H functionalization reactions and occurs exclusively at the *para* position of anilines. Further, Lu and Wu groups devised Cu-catalyzed remote C–H sulfonylation strategies using different sulfonyl group sources.[235] The reactions are proposed to go via a SET pathway.

1.9.5. C–P Bond Formation

Directing group assisted phosphorylation of sp^2 C–H bonds under copper catalysis was first achieved by Cheng and Yu group (Scheme 1.9.5.1).[236] They reported a highly regioselective *ortho* phosphorylation reaction of 8-AQ directed (hetero)arylamides with H-phosphonates

under mild conditions. Inexpensive $Cu(OAc)_2$ was used as catalyst for the reaction which showed good functional group tolerance and furnished mono selective products.

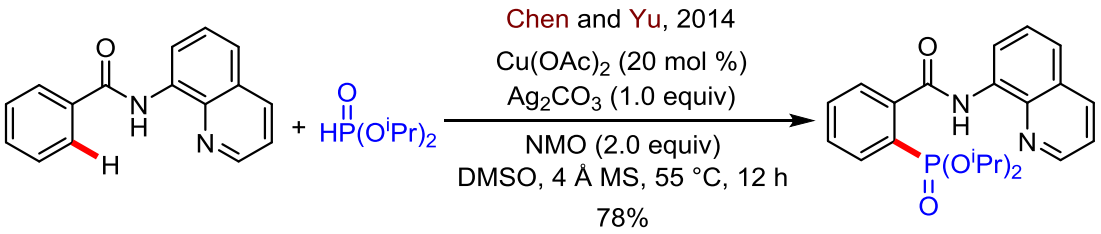

Scheme 1.9.5.1. Copper-catalyzed phosphorylation of benzamides.

1.9.6. C–Z (Z = F, Cl, Br, I) Bond Formation

The synthesis of organohalides is an important organic transformation since they are frequently used as precursors for the synthesis of a plethora of bioactive compounds, natural products, agrochemicals and functional materials. In this vein, several groups have devoted their research in developing copper-mediated or copper-catalyzed C–H halogenation reactions.[237]

The early work of Yu[161] on Cu-catalyzed halogenation of 2-arylpyridines using $Cl_2CHCHCl_2$/$Br_2CHCHBr_2$ solvent for chlorination and bromination, and molecular iodine in $Cl_2CHCHCl_2$ solvent for iodination paved way for the development of other C–H halogenation reactions using different halide sources (Scheme 1.9.6.1). Among monodentate DG assisted C–H halogenation reactions, 2-phenylpyridines are mostly explored.[206b,238] In 2011, Chen and co-workers reported Cu-catalyzed C–H chlorination of 2-arylpyridines using acyl chlorides (Scheme 1.9.6.1a).[206b] During the same time, Shen *et al*. discovered lithium halides as cheap and easy-to-handle halogen sources for *ortho* halogenation of 2-phenylpyridines.[238a] However, toxic CrO_3 was used as a terminal oxidant for this reaction. In 2013, they improved their strategy by performing the same transformation under copper-catalyzed aerobic conditions.[238b] Following year, Han group devised a copper-mediated direct halogenation protocol of 2-arylpyridines using acyl hypohalites as halide source generated *in situ* from readily available carboxylic acids and *N*-halosuccinimides (NXS; X = Cl, Br).[238c] In 2015, Jiang *et al*. accomplished Cu-mediated C2-selective chlorination of indoles with $CuCl_2$ using a removable pyrimidyl directing group.[239] Rameshraju and co-workers employed isothiocyanates as efficient directing groups for *ortho* halogenation of arenes to give 2-halo aromatic isothiocyanates using CuX_2 (X = Cl, Br) salts as halogen source.[240]

Moving onto C–H halogenation reactions employing bidentate chelation, in 2013, Daugulis group developed a method for copper-catalyzed *ortho* selective direct fluorination of 8-AQ directed amides and PA directed benzylamine derivatives using CuI as catalyst and AgF as a nucleophilic fluoride source (Scheme 1.9.6.1b).[241] The authors achieved mono or bis fluorinated compounds selectively by simple tuning of the reaction conditions. In the same year, Carretero and co-workers used *N*-(2-pyridyl)sulfonyl auxiliary for Cu-catalyzed *ortho* selective sp^2 C–H halogenation of anilines.[242] A CuX_2-NXS (X = Cl, Br) system was used for this transformation under aerobic conditions. Further, Shi *et al*. reported an *ortho* halogenation of PIP directing group aided benzoic acid derivatives with NXS (X = Cl, Br, I) under copper-catalyzed conditions.[243] 2-Aminophenyl-*1H*-pyrazole (PP) was discovered as an efficient and removable DG for a copper-mediated oxidative *ortho* C–H chlorination of aromatic amides by Li group using trichloroacetamide as a new chlorine group source.[244]

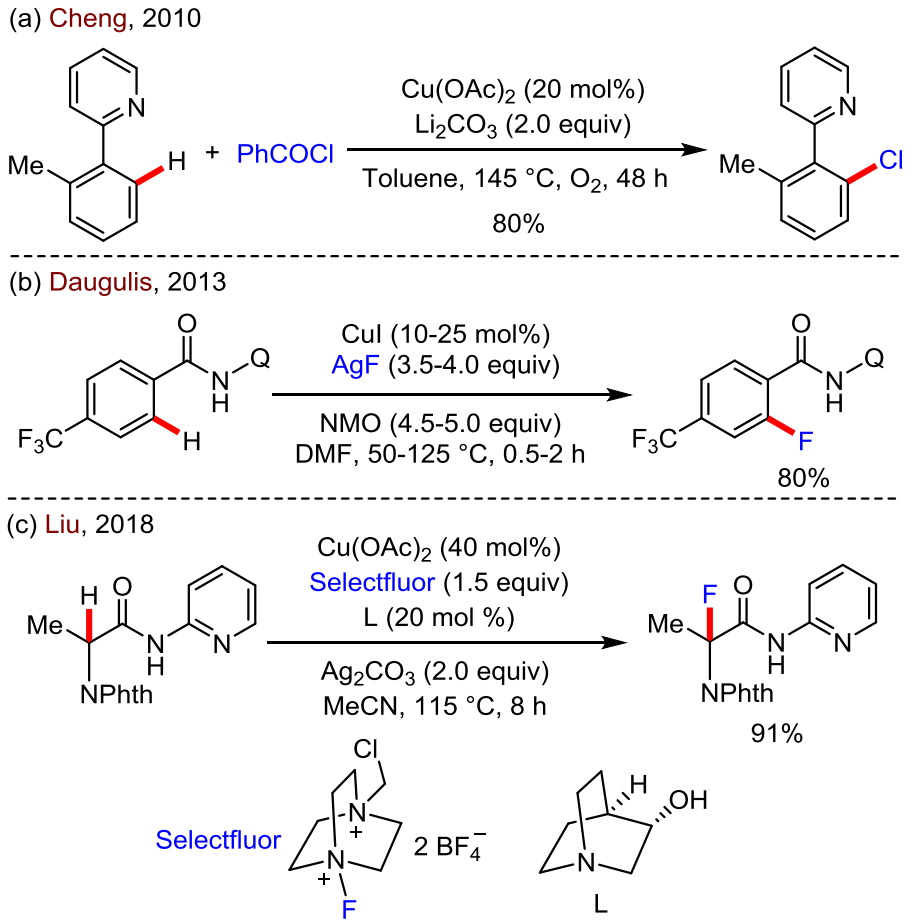

Scheme 1.9.6.1. Representative examples of Cu-catalyzed halogenation.

The first sp^3 C–H halogenation employing copper catalysis was achieved by Liu and co-workers.[245] They demonstrated an auxiliary assisted Cu-catalyzed direct α-sp^3 C–H

fluorination methodology for the synthesis of quaternary α-fluorinated α-amino acid derivatives using Selectfluor as fluorinating agent (Scheme 1.9.6.1c). Mechanistic experiments revealed the occurrence of Cu(II) catalytic SET oxidative addition pathway, in which the formation of a key fluoride coupled Cu(II) charge transfer complex is involved.

In the context of C–X bond formation employing copper catalysis, a direct sp^2 C–H silylation of amides using copper-catalyzed conditions has been developed recently which is a part of this thesis work and is discussed in detail in Chapter 4.

1.9.7. Tandem C–H Activation/Annulation

Intermolecular C–H activation/cyclization strategy in a cascade manner opens the scope to generate multiple bonds in a single step and thereby construct complex (spiro)cyclic molecules. In this realm, copper catalysis has also been nurtured for the synthesis of *N*-containing heterocycles employing bidentate chelation assistance.

In 2014, You group revealed a Cu-mediated tandem oxidative $C(sp^2)$–H/C(sp)–H alkynylation/annulation of 8-AQ tethered arylamides with terminal alkynes (Scheme 1.9.7.1a).[246] In this reaction, $Cu(OAc)_2$ acted both as the promoter and terminal oxidant. The authors found that the *ortho* alkynylated benzamide underwent intramolecular cyclization to provide the corresponding annulated product in presence of either $Cu(OAc)_2$ or CuOAc, indicating a domino process featuring oxidative alkynylation/intramolecular annulation sequence under standard conditions. Shortly after, Huang and Yu reported the same dehydrogenative annulation under aerobic copper catalysis (Scheme 1.9.7.1b).[247] Terminal alkynes were also used by Li *et al*. for tandem alkynylation/annulation with PP-directed benzamides under copper-mediated conditions to furnish arylmethylene isoindolinones (Scheme 1.9.7.1c).[248] In 2014, Liu and co-workers used ethyl cyanoacetate in a $C(sp^2)$–H/$C(sp^3)$–H coupling with benzoic acid derivatives with simultaneous C–N bond formation to produce isoquinolinone scaffolds (Scheme 1.9.7.1d).[249] Yu group demonstrated an oxidative coupling of oxazoline directed amides with malonates under copper-mediated conditions (Scheme 1.9.7.1e).[250] In 2015, Miura group described a Cu-mediated oxidative coupling of benzamides with maleimides (Scheme 1.9.7.1f).[251] The authors proposed an initial C–H alkenylation reaction with the maleimide followed by intramolecular aza-Michael type addition pathway for the synthesis of isoindolone incorporated spirosuccinimides. They also developed a [4+1] cycloaddition reaction of 8-AQ directing group attached (hetero)aromatic amides with isonitriles under copper catalytic conditions (Scheme 1.9.7.1g).[252]

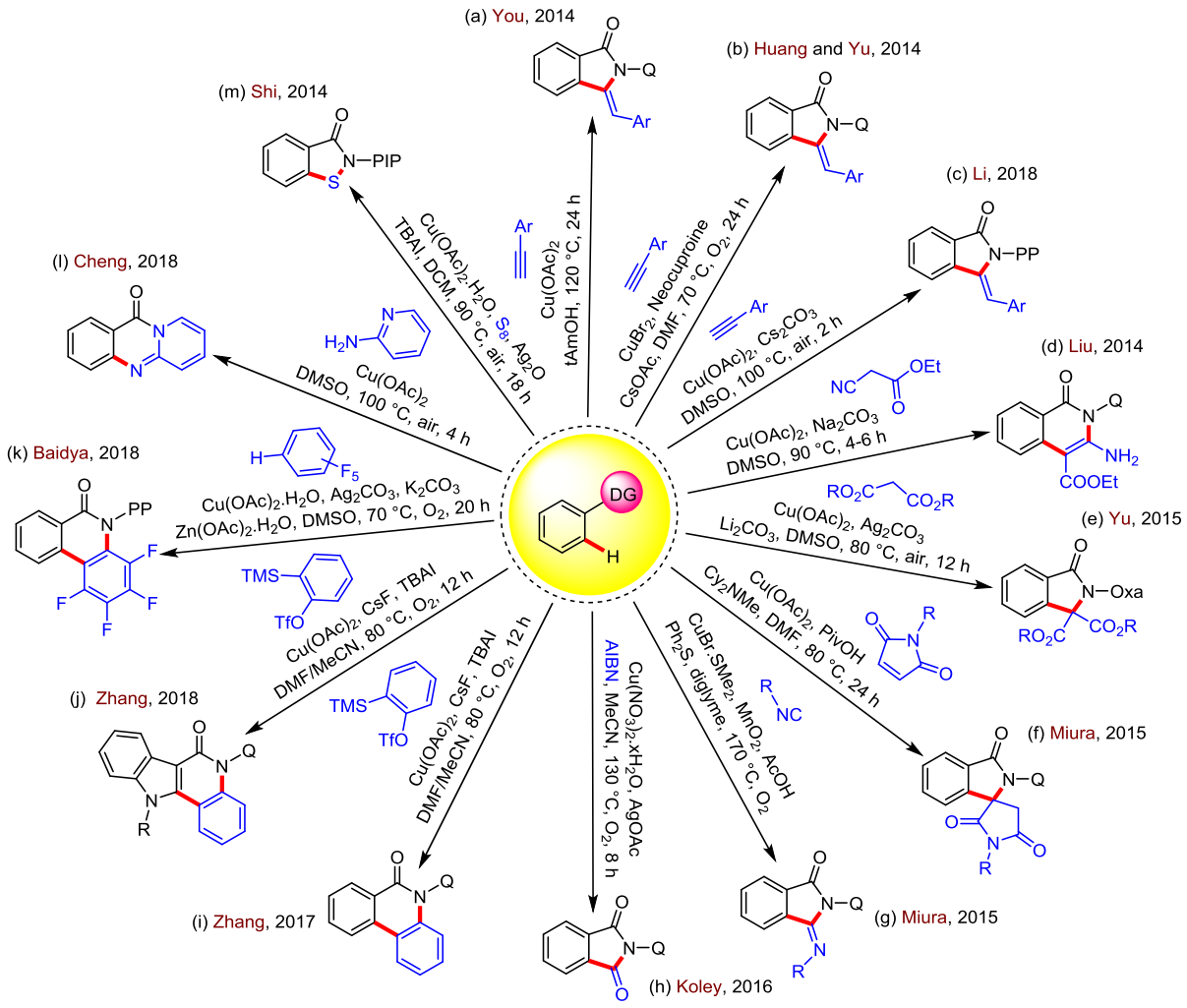

Scheme 1.9.7.1. Representative examples of copper-mediated/-catalyzed annulation reaction.

Following year, Koley and co-workers designed a Cu(II)-catalyzed regioselective carbonylative cyclization of benzamides using AIBN as a traceless cyanating agent (Scheme 1.9.7.1h).[253] The reaction was proposed to proceed via cyanation followed by hydrolysis to yield the carbonylated products. Zhang *et al*. described strategies for cascade C–H/N–H annulation of benzamides and indole carboxamides with arynes to furnish tricyclic phenanthridinones and tetracyclic indoloquinoline scaffolds respectively using inexpensive copper salts (Scheme 1.9.7.1i, 1.9.7.1j).[254] Baidya group synthesized polyfluorinated phenanthridiones by Cu-promoted cross-dehydrogenative annulation of (hetero)aryl amides with readily available polyfluoro(hetero)arenes in high yields (Scheme 1.9.7.1k).[255] Alkenyl amides were also successful under the present protocol. Chen *et al*. reported a copper-mediated tandem C–H amination/annulation reaction between removable 8-AQ attached benzamides and 2-aminopyridines for the synthesis pyrido-fused quinazolinone derivatives (Scheme 1.9.7.1l).[256] In between, Shi and co-workers delineated a Cu-mediated C–S/N–S annulation of

PIP-directed amides with elemental sulfur as the sulfur group source to give access to a series of biologically relevant benzoisothiazolones (Scheme 1.9.7.1m).[257]

Apart from sp^2 C–H annulation, sp^3 C–H activation/annulation reactions have also been achieved under copper catalysis (Scheme 1.9.7.2).[258] In early 2016, Zhang group described a Cu-catalyzed oxidative alkynylation/annulation of sp^3 C–H bonds of 8-AQ bearing aliphatic amides with alkynyl carboxylic acids via decarboxylation (Scheme 1.9.7.2a).[258a] High selectivity for β-methyl groups over methylene groups was observed leading to diverse pyrrolidones. In the same year, Ge *et al*. reported a copper-promoted site-selective carbonylation of both sp^3 C–H and sp^2 C–H bonds of amides with nitromethane as a novel carbonyl source (Scheme 1.9.7.2b).[258b] Mechanistic investigations suggested a reversible sp^3 C–H bond cleavage whereas an irreversible sp^2 C–H bond cleavage, but not the rate-determining step of the reaction, and they proposed an initial dehydrogenative coupling of the substrate with nitromethane followed by a Nef type reaction to give the carbonylation product.

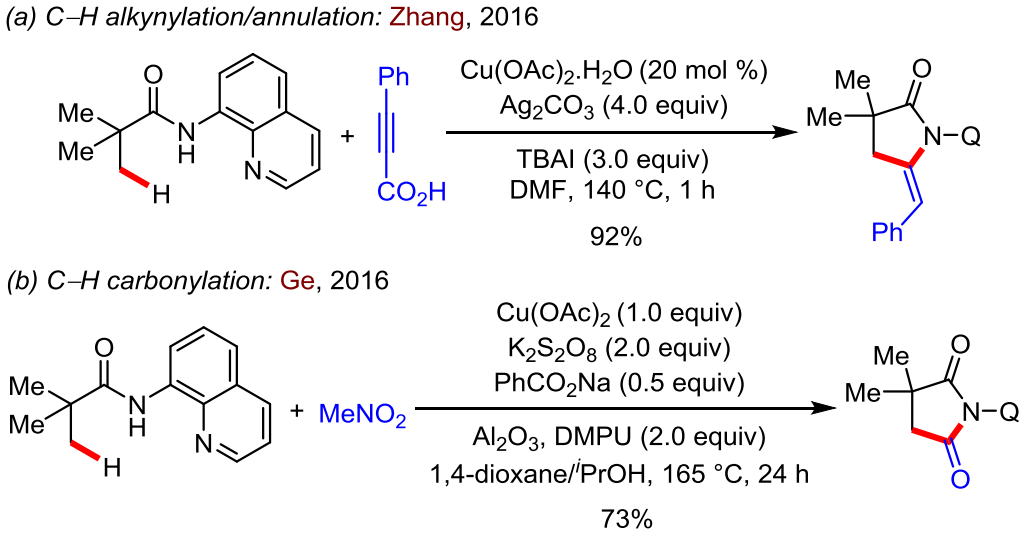

Scheme 1.9.7.2. Copper-mediated sp^3 C–H annulation reactions.

In 2020, Whiteoak and co-workers demonstrated an intramolecular variant of C–H activation/annulation employing copper catalysis giving rise to structurally complex fused dihydrobenzofuran-isoquinolone motifs from 8-AQ directing group attached benzamide derivatives tethered with an alkyne moiety (Scheme 1.9.7.3).[259] This protocol showed the first copper-catalyzed migratory insertion of alkynes to benzamides bearing a bidentate auxiliary, and why the intermolecular variant is not operative, supported by DFT studies.

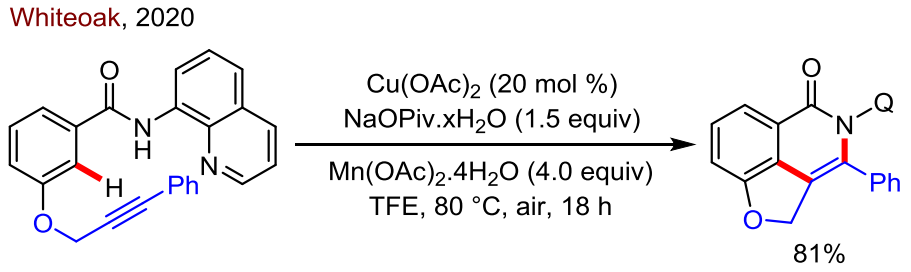

Scheme 1.9.7.3. Copper-catalyzed intramolecular C–H annulation.

1.9.8. Electrochemical C–H Activation

In recent years, transition metal-catalyzed electrochemical C–H activation has seen a sharp rise since it uses renewable electrical energy avoiding the use of exogenous stoichiometric chemical oxidants needed in conventional methods, thus making it a sustainable, environmentally benign, and economically resourceful technique to form diverse C–C and C–Het bonds.[156b] Along this line, copper-catalyzed electrochemical C–H activation/functionalization was first disclosed by Mei and co-workers in 2018, when they reported a Cu-catalyzed C–H amination protocol of electron-rich anilides with secondary amines at room temperature using electricity as a terminal oxidant in undivided electrochemical cells (Scheme 1.9.8.1a).[260] The reaction uses *n*-Bu_4NI as a redox mediator and was proposed to occur via a SET mechanism involving the formation of a high-valent Cu(III) species.

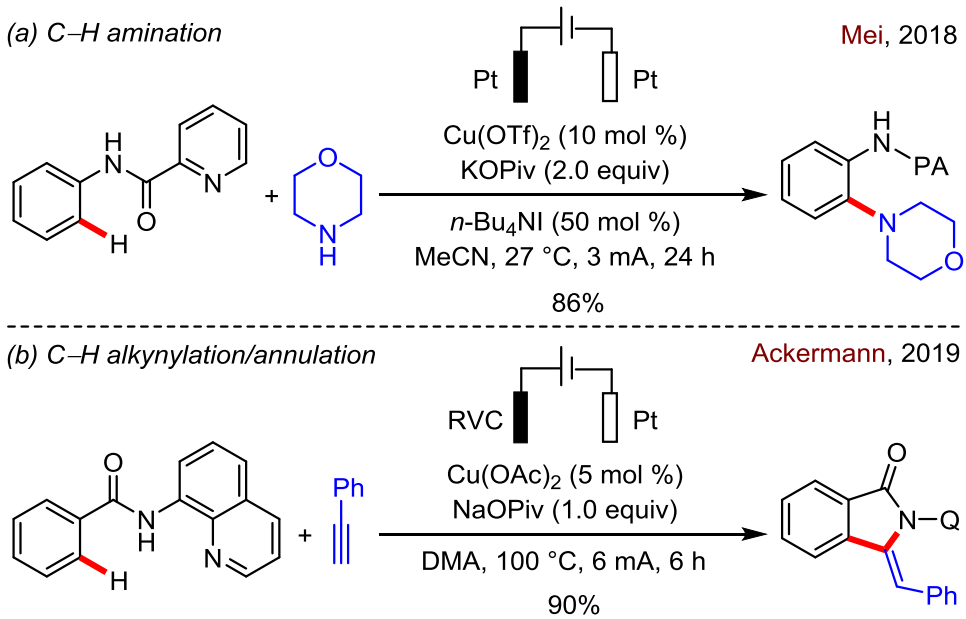

Scheme 1.9.8.1. Copper-catalyzed electrochemical C–H functionalizations.

Following year, Nicholls *et al*. reported another electro-oxidative C–H amination of aromatic amides with the liberation of H_2 as the sole byproduct.[261] Shortly after, Ackermann group demonstrated a cupraelectro-catalyzed oxidative cascade alkynylation/annulation of both electron-rich and electron-deficient benzamides with terminal alkynes to deliver isoindolones (Scheme 1.9.8.1b).[262] Under the standard reaction conditions, alkynyl carboxylic acids also underwent the reaction to give the same cyclized products through decarboxylation.

1.9.9. Mechanistic Aspects of Copper-Catalyzed/-Mediated C–H Activation

Owing to the versatility in the accessible oxidation states (0, +1, +2, +3) of copper metal in a C–H activation/functionalization reaction, this allows the Cu complexes to act in contrasting manners depending on the type of substrates and coupling partners used and also on the reaction conditions, thus creating issues to have a full mechanistic understanding of the reactions. The Cu complexes can act as- (i) a one-electron redox catalyst which promotes radical reactions through SET mechanism, and (ii) a two-electron redox catalyst promoting organometallic pathways consisting of a high-valent Cu(III) intermediate. As a result, Cu-mediated or Cu-catalyzed C–H functionalization reactions can proceed via Cu(I)/Cu(III), Cu(0)/Cu(II), Cu(I)/Cu(II) catalytic pathways.[159j,212,263]

Copper-catalyzed C–H functionalization reactions going through the different type of mechanisms is depicted in Scheme 1.9.9.1. Yu and co-workers proposed their Cu(II)-catalyzed C–H functionalization reactions using O_2 as an oxidant to occur via a SET mechanism (Cu(I)/Cu(II) cycle) (Scheme 1.9.9.1a).[161] Stahl *et al*. observed that different products were formed on Cu(II)-mediated oxidation of *N*-(8-quinolyl)benzamides depending upon the reaction conditions due to the involvement of divergent mechanisms, thereby showcasing the complexities associated with understanding mechanisms of Cu-catalyzed C–H functionalization processes (Scheme 1.9.9.1b).[212] From extensive experimental and computational studies, they understood that, under basic conditions, directed *ortho* C–H methoxylation or chlorination of benzamides occurs via an organometallic pathway (Cu(I)/Cu(III) cycle), whereas, under acidic conditions, non-directed chlorination of the quinoline group takes place via a SET pathway (Cu(I)/Cu(II)).

Wang and Zhang group provided a detailed mechanistic study on Cu(II)-catalyzed oxidative cross-coupling of azacalix[1]arene[3]pyridine and boronic acid, proposing a Cu(II)/Cu(III) catalytic cycle for the reaction (Scheme 1.9.9.1c).[264] The authors suggested that the boronic

acids react with energetically favourable arylcopper(II) species rather than arylcopper(III) species. Also, seminal works by the groups of Stahl, Wang, and Ribas have given a thorough understanding on the involvement of structurally well-defined arylcopper(III) intermediates in organometallic copper-catalyzed C–H functionalization reactions.[265]

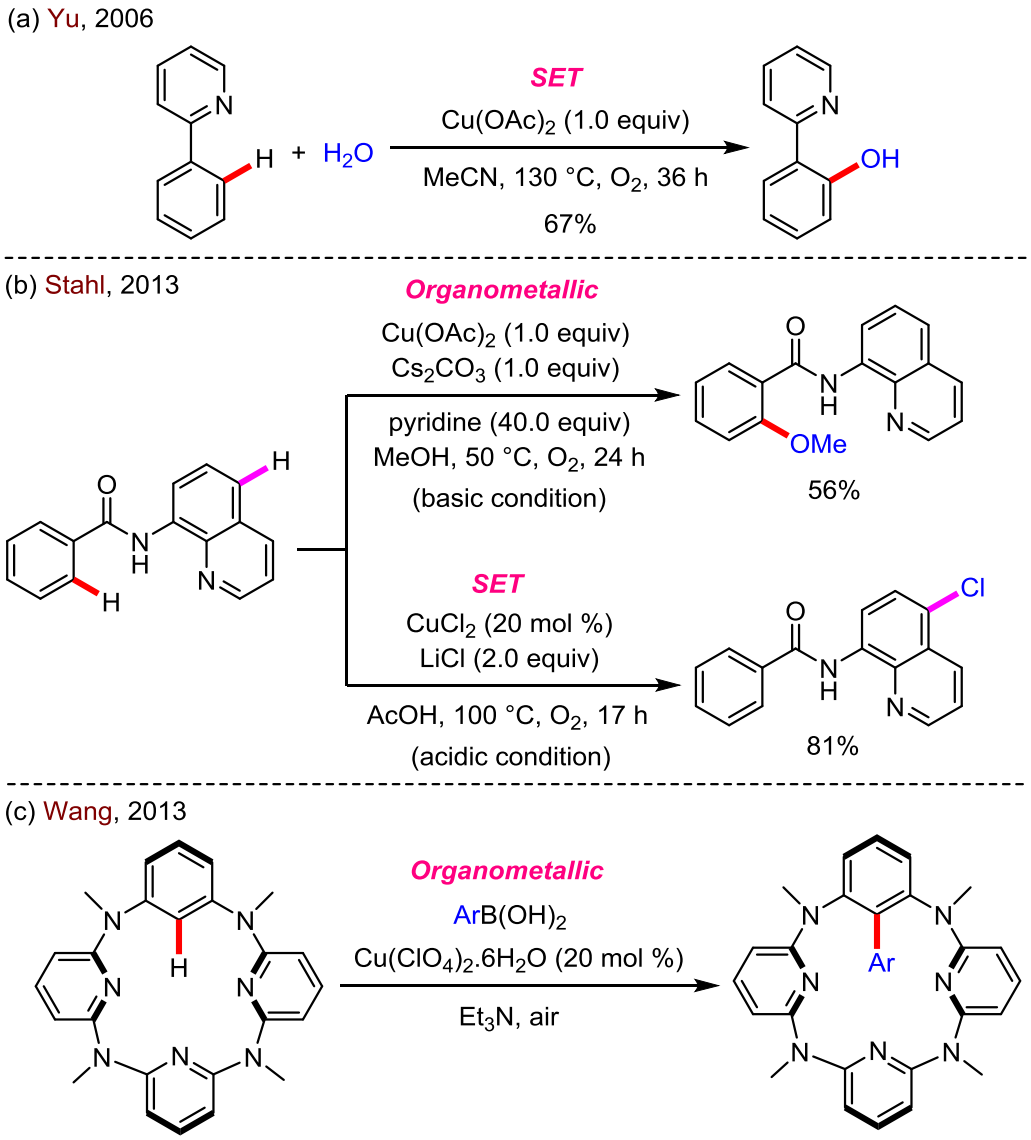

Scheme 1.9.9.1. Selected examples of different mechanisms involved in Cu(II)-catalyzed/-mediated C–H functionalization.

1.10. References

1. (a) Glaser, C. *Ber. Dtsch. Chem. Ges.* **1869**, *2*, 422. (b) Glaser, C. *Ann. Chem. Pharm.* **1870**, *154*, 137.
2. Ullmann, F.; Bielecki, J. *Ber. Dtsch. Chem. Ges.* **1901**, *34*, 2174.
3. For reviews, see: (a) Fanta, P. E. *Chem. Rev.* **1964**, *64*, 613. (b) Hassan, J.; Sévignon, M.; Gozzi, C.; Schulz, E.; Lemaire, M. *Chem. Rev.* **2002**, *102*, 1359.
4. (a) Wurtz, A. *Ann. Chem. Pharm.* **1855**, *96*, 364. (b) Wurtz, A. *Ann. Chim. Phys.* **1855**, *44*, 275. (c) Fittig, R. *Justus Liebigs Ann. Chem.* **1862**, *121*, 361.
5. Bennett, G. M.; Turner, E. E. *J. Chem. Soc. Trans.* **1914**, *105*, 1057.
6. Meerwein, H.; Büchner, E.; van Emster, K. *J. Prakt. Chem.* **1939**, *152*, 237.
7. (a) Kharasch, M. S.; Fields, E. K. *J. Am. Chem. Soc.* **1941**, *63*, 2316. (b) Kharasch, M. S.; Fuchs, C. F. *J. Am. Chem. Soc.* **1943**, *65*, 504.
8. (a) Cadiot, P.; Chodkiewicz, W. *C. R. Hebd. Seances Acad. Sci.* **1955**, *241*, 1055. (b) Chodkiewicz, W. *Ann. Chim. Paris* **1957**, *2*, 819.
9. Stephens, R. D.; Castro, C. E. *J. Org. Chem.* **1963**, *28*, 3313.
10. Smidt, J.; Hafner, W.; Jira, R.; Sedlmeier, J.; Sieber, R.; Rüttinger, R.; Kojer, H. J. A. C. *Angew. Chem.* **1959**, *71*, 176.
11. (a) Tsuji, J.; Takahashi, H.; Morikawa, M. *Tetrahedron Lett.* **1965**, *6*, 4387. (b) Tsuji, J. *Pure Appl. Chem.* **1999**, *71*, 1539.
12. (a) Mizoroki, T.; Mori, K.; Ozaki, A. *Bull. Chem. Soc. Jpn.* **1971**, *44*, 581. (b) Mori, K.; Mizoroki, T.; Ozaki, A. *Bull. Chem. Soc. Jpn.* **1973**, *46*, 1505.
13. (a) Heck, R. F.; Nolley, J. P. *J. Org. Chem.* **1972**, *37*, 2320. (b) Dieck, H. A.; Heck, R. F. *J. Am. Chem. Soc.* **1974**, *96*, 1133.
14. Corriu, R. J. P.; Masse, J. P. *J. Chem. Soc. Chem. Commun.* **1972**, 144a.
15. (a) Tamao, K.; Sumitani, K.; Kumada, M. *J. Am. Chem. Soc.* **1972**, *94*, 4374. (b) Kohei, T.; Koji, S.; Yoshihisa, K.; Michio, Z.; Akira, F.; Shun-ichi, K.; Isao, N.; Akio, M.; Makoto, K. *Bull. Chem. Soc. Jpn.* **1976**, *49*, 1958.
16. Sonogashira, K.; Tohda, Y.; Hagihara, N. *Tetrahedron Lett.* **1975**, *16*, 4467.
17. (a) Yamamura, M.; Moritani, I.; Murahashi, S.-I. *J. Organomet. Chem.* **1975**, *91*, C39. (b) Murahashi, S.; Yamamura, M.; Yanagisawa, K.; Mita, N.; Kondo, K. *J. Org. Chem.* **1979**, *44*, 2408.

18. (a) Negishi, E.; Baba, S. *J. Chem. Soc. Chem. Commun.* **1976**, 596b. (b) King, A. O.; Okukado, N.; Negishi, E. *J. Chem. Soc. Chem. Commun.* **1977**, 683. (c) Negishi, E.; King, A. O.; Okukado, N. *J. Org. Chem.* **1977**, *42*, 1821.
19. (a) Kosugi, M.; Sasazawa, K.; Shimizu, Y.; Migita, T. *Chem. Lett.* **1977**, *6*, 301. (b) Kosugi, M.; Shimizu, Y.; Migita, T. *Chem. Lett.* **1977**, *6*, 1423.
20. (a) Milstein, D.; Stille, J. K. *J. Am. Chem. Soc.* **1978**, *100*, 3636. (b) Stille, J. K. *Angew. Chem. Int. Ed.* **1986**, *25*, 508.
21. (a) Miyaura, N.; Suzuki, A. *J. Chem. Soc. Chem. Commun.* **1979**, 866. (b) Miyaura, N.; Yamada, K.; Suzuki, A. *Tetrahedron Lett.* **1979**, *20*, 3437.
22. (a) Hatanaka, Y.; Hiyama, T. *J. Org. Chem.* **1988**, *53*, 918. (b) Hiyama, T. *J. Organomet. Chem.* **2002**, *653*, 58.
23. (a) Ishiyama, T.; Matsuda, N.; Miyaura, N.; Suzuki, A. *J. Am. Chem. Soc.* **1993**, *115*, 11018. (b) Ishiyama, T.; Murata, M.; Miyaura, N. *J. Org. Chem.* **1995**, *60*, 7508.
24. (a) Guram, A. S.; Rennels, R. A.; Buchwald, S. L. *Angew. Chem. Int. Ed.* **1995**, *34*, 1348. (b) Louie, J.; Hartwig, J. F. *Tetrahedron Lett.* **1995**, *36*, 3609.
25. For selected reviews, see: (a) Kondo, T.; Mitsudo, T.-a. *Chem. Rev.* **2000**, *100*, 3205. (b) Tsuji, J. *Reactions of Organic Halides and Pseudohalides.* Transition Metal Reagents and Catalysts: Innovations in Organic Synthesis. Wiley: New York, **2000**, 27. (c) Qiao, J. X.; Lam, P. Y. S. *Synthesis* **2011**, *2011*, 829. (d) Rosen, B. M.; Quasdorf, K. W.; Wilson, D. A.; Zhang, N.; Resmerita, A.-M.; Garg, N. K.; Percec, V. *Chem. Rev.* **2011**, *111*, 1346. (e) Beletskaya, I. P.; Ananikov, V. P. *Chem. Rev.* **2011**, *111*, 1596.
26. For selected reviews and examples, see: (a) Littke, A. F.; Fu, G. C. *Angew. Chem. Int. Ed.* **2002**, *41*, 4176. (b) Christmann, U.; Vilar, R. *Angew. Chem. Int. Ed.* **2005**, *44*, 366. (c) Marion, N.; Nolan, S. P. *Acc. Chem. Res.* **2008**, *41*, 1440. (d) Martin, R.; Buchwald, S. L. *Acc. Chem. Res.* **2008**, *41*, 1461. (e) Fu, G. C. *Acc. Chem. Res.* **2008**, *41*, 1555.
27. For selected reviews and examples, see: **Pd catalysis**: (a) Roglans, A.; Pla-Quintana, A.; Moreno-Mañas, M. *Chem. Rev.* **2006**, *106*, 4622. (b) Scott, W. J.; Crisp, G. T.; Stille, J. K. *J. Am. Chem. Soc.* **1984**, *106*, 4630. (c) Kang, S.-K.; Lee, H.-W.; Jang, S.-B.; Ho, P.-S. *J. Org. Chem.* **1996**, *61*, 4720. (d) Nguyen, H. N.; Huang, X.; Buchwald, S. L. *J. Am. Chem. Soc.* **2003**, *125*, 11818. (e) Fors, B. P.; Watson, D. A.; Biscoe, M. R.; Buchwald, S. L. *J. Am. Chem. Soc.* **2008**, *130*, 13552. **Ni catalysis:** (f) Yu, D.-G.; Li, B.-J.; Shi, Z.-J. *Acc. Chem. Res.* **2010**, *43*, 1486. (g) Terao, J.; Watanabe, H.; Ikumi, A.; Kuniyasu, H.; Kambe, N. *J. Am. Chem. Soc.* **2002**, *124*, 4222.
28. Trost, B. M.; Fullerton, T. J. *J. Am. Chem. Soc.* **1973**, *95*, 292.

29. "The Nobel Prize in Chemistry 2010-Press Release". NobelPrize.org. Nobel Prize Outreach AB 2021. Thu. 16 Sep 2021. https://www.nobelprize.org/prizes/chemistry/2010/press-release/
30. For selected reviews, see: **Pd catalysis:** (a) Nicolaou, K. C.; Bulger, P. G.; Sarlah, D. *Angew. Chem. Int. Ed.* **2005**, *44*, 4442. (b) Johansson Seechurn, C. C. C.; Kitching, M. O.; Colacot, T. J.; Snieckus, V. *Angew. Chem. Int. Ed.* **2012**, *51*, 5062. (c) Li, H.; Johansson Seechurn, C. C. C.; Colacot, T. J. *ACS Catal.* **2012**, *2*, 1147. (d) Ruiz-Castillo, P.; Buchwald, S. L. *Chem. Rev.* **2016**, *116*, 12564. (e) Biffis, A.; Centomo, P.; Del Zotto, A.; Zecca, M. *Chem. Rev.* **2018**, *118*, 2249. **Ni catalysis:** (f) Yamaguchi, J.; Muto, K.; Itami, K. *Eur. J. Org. Chem.* **2013**, *2013*, 19. **Cu catalysis:** (g) Evano, G.; Blanchard, N.; Toumi, M. *Chem. Rev.* **2008**, *108*, 3054. **Fe catalysis:** (h) Mako, T. L.; Byers, J. A. *Inorg. Chem. Front.* **2016**, *3*, 766.
31. Goldman, A. S.; Goldberg, K. I. *Activation and Functionalization of C—H Bonds*. ACS Symposium Series, American Chemical Society, **2004**, *885*, 1.
32. Arndtsen, B. A.; Bergman, R. G.; Mobley, T. A.; Peterson, T. H. *Acc. Chem. Res.* **1995**, *28*, 154.
33. Anslyn, E. V.; Dougherty, D. A. *Modern Physical Organic Chemistry*. University Science Books: Sausalito, CA, **2006**.
34. Crabtree, R. H. *J. Chem. Soc., Dalton Trans.* **2001**, 2437.
35. (a) Labinger, J. A.; Bercaw, J. E. *Nature* **2002**, *417*, 507. (b) Dick, A. R.; Sanford, M. S. *Tetrahedron* **2006**, *62*, 2439. (c) Balcells, D.; Clot, E.; Eisenstein, O. *Chem. Rev.* **2010**, *110*, 749. (d) Ackermann, L. *Chem. Rev.* **2011**, *111*, 1315. (e) Gallego, D.; Baquero, E. A. *Open Chem.* **2018**, *16*, 1001. (f) Altus, K. M.; Love, J. A. *Commun. Chem.* **2021**, *4*, 173.
36. Ess, D. H.; Goddard, W. A.; Periana, R. A. *Organometallics* **2010**, *29*, 6459.
37. Oxgaard, J.; Tenn, W. J.; Nielsen, R. J.; Periana, R. A.; Goddard, W. A. *Organometallics* **2007**, *26*, 1565.
38. David, L.; Keith, F. *Chem. Lett.* **2010**, *39*, 1118.
39. (a) Boutadla, Y.; Davies, D. L.; Macgregor, S. A.; Poblador-Bahamonde, A. I. *Dalton Trans.* **2009**, 5820. (b) Boutadla, Y.; Davies, D. L.; Macgregor, S. A.; Poblador-Bahamonde, A. I. *Dalton Trans.* **2009**, 5887.
40. Shan, C.; Zhu, L.; Qu, L.-B.; Bai, R.; Lan, Y. *Chem. Soc. Rev.* **2018**, *47*, 7552.
41. Simmons, E. M.; Hartwig, J. F. *Angew. Chem. Int. Ed.* **2012**, *51*, 3066.
42. Fenton, H. J. H. *J. Chem. Soc. Trans.* **1894**, *65*, 899.

43. Kleiman, J. P.; Dubeck, M. *J. Am. Chem. Soc.* **1963**, *85*, 1544.
44. Chatt, J.; Davidson, J. M. *J. Chem. Soc.* **1965**, 843.
45. (a) Shilov, A. E.; Shteinman, A. A. *Coord. Chem. Rev.* **1977**, *24*, 97. (b) Shilov, A. E.; Shul'pin, G. B. *Chem. Rev.* **1997**, *97*, 2879.
46. Siegbahn, P. E. M.; Crabtree, R. H. *J. Am. Chem. Soc.* **1996**, *118*, 4442.
47. Davidson, J. M.; Triggs, C. *J. Chem. Soc. A* **1968**, 1324.
48. (a) Gorelsky, S. I.; Lapointe, D.; Fagnou, K. *J. Am. Chem. Soc.* **2008**, *130*, 10848. (b) Lapointe, D.; Markiewicz, T.; Whipp, C. J.; Toderian, A.; Fagnou, K. *J. Org. Chem.* **2011**, *76*, 749.
49. Chen, X.; Engle, K. M.; Wang, D.-H.; Yu, J.-Q. *Angew. Chem. Int. Ed.* **2009**, *48*, 5094.
50. (a) Colby, D. A.; Bergman, R. G.; Ellman, J. A. *Chem. Rev.* **2010**, *110*, 624. (b) Kuhl, N.; Schröder, N.; Glorius, F. *Adv. Syn. Catal.* **2014**, *356*, 1443.
51. (a) Larsen, M. A.; Hartwig, J. F. *J. Am. Chem. Soc.* **2014**, *136*, 4287. (b) Hartwig, J. F. *J. Am. Chem. Soc.* **2016**, *138*, 2.
52. Murahashi, S. *J. Am. Chem. Soc.* **1955**, *77*, 6403.
53. (a) Moritani, I.; Fujiwara, Y. *Tet. Lett.* **1967**, *8*, 1119. (b) Fujiwara, Y.; Moritani, I.; Danno, S.; Asano, R.; Teranishi, S. *J. Am. Chem. Soc.* **1969**, *91*, 7166.
54. (a) Cho, S. H.; Kim, J. Y.; Kwak, J.; Chang, S. *Chem. Soc. Rev.* **2011**, *40*, 5068. (b) Bugaut, X.; Glorius, F. *Angew. Chem. Int. Ed.* **2011**, *50*, 7479.
55. Ryabov, A. D. *Chem. Rev.* **1990**, *90*, 403.
56. Murai, S.; Kakiuchi, F.; Sekine, S.; Tanaka, Y.; Kamatani, A.; Sonoda, M.; Chatani, N. *Nature* **1993**, *366*, 529.
57. For representative reviews on DG assisted C–H functionalization, see: (a) Lyons, T. W.; Sanford, M. S. *Chem. Rev.* **2010**, *110*, 1147. (b) Rouquet, G.; Chatani, N. *Angew. Chem. Int. Ed.* **2013**, *52*, 11726. (c) Zhang, F.; Spring, D. R. *Chem. Soc. Rev.* **2014**, *43*, 6906. (d) Zhang, M.; Zhang, Y.; Jie, X.; Zhao, H.; Li, G.; Su, W. *Org. Chem. Front.* **2014**, *1*, 843. (e) Chen, Z.; Wang, B.; Zhang, J.; Yu, W.; Liu, Z.; Zhang, Y. *Org. Chem. Front.* **2015**, *2*, 1107. (f) Daugulis, O.; Roane, J.; Tran, L. D. *Acc. Chem. Res.* **2015**, *48*, 1053. (g) Yang, J. *Org. Biomol. Chem.* **2015**, *13*, 1930. (h) Zhu, R.-Y.; Farmer, M. E.; Chen, Y.-Q.; Yu, J.-Q. *Angew. Chem. Int. Ed.* **2016**, *55*, 10578. (i) Liu, J.; Chen, G.; Tan, Z. *Adv. Syn. Catal.* **2016**, *358*, 1174. (j) Pichette Drapeau, M.; Gooßen, L. J. *Chem. Eur. J.* **2016**, *22*, 18654. (k) Ma, W.; Gandeepan, P.; Li, J.; Ackermann, L. *Org. Chem. Front.* **2017**, *4*, 1435. (l) Font, M.; Quibell, J. M.; Perry, G. J. P.; Larrosa, I. *Chem. Commun.*

2017, *53*, 5584. (m) Hummel, J. R.; Boerth, J. A.; Ellman, J. A. *Chem. Rev.* **2017**, *117*, 9163. (n) Zhao, Q.; Poisson, T.; Pannecoucke, X.; Besset, T. *Synthesis* **2017**, *49*, 4808. (o) Saint-Denis, T. G.; Zhu, R.-Y.; Chen, G.; Wu, Q.-F.; Yu, J.-Q. *Science* **2018**, *359*, 359. (p) Sambiagio, C.; Schönbauer, D.; Blieck, R.; Dao-Huy, T.; Pototschnig, G.; Schaaf, P.; Wiesinger, T.; Zia, M. F.; Wencel-Delord, J.; Besset, T.; Maes, B. U. W.; Schnürch, M. *Chem. Soc. Rev.* **2018**, *47*, 6603. (q) Dey, A.; Sinha, S. K.; Achar, T. K.; Maiti, D. *Angew. Chem. Int. Ed.* **2019**, *58*, 10820. (r) Rej, S.; Ano, Y.; Chatani, N. *Chem. Rev.* **2020**, *120*, 1788. (s) Murali, K.; Machado, L. A.; Carvalho, R. L.; Pedrosa, L. F.; Mukherjee, R.; Da Silva Júnior, E. N.; Maiti, D. *Chem. Eur. J.* **2021**, *27*, 12453. (t) Goswami, N.; Bhattacharya, T.; Maiti, D. *Nat. Rev. Chem.* **2021**, *5*, 646.

58. Leow, D.; Li, G.; Mei, T.-S.; Yu, J.-Q. *Nature* **2012**, *486*, 518.
59. Bag, S.; Patra, T.; Modak, A.; Deb, A.; Maity, S.; Dutta, U.; Dey, A.; Kancherla, R.; Maji, A.; Hazra, A.; Bera, M.; Maiti, D. *J. Am. Chem. Soc.* **2015**, *137*, 11888.
60. Zaitsev, V. G.; Shabashov, D.; Daugulis, O. *J. Am. Chem. Soc.* **2005**, *127*, 13154.
61. Moselage, M.; Li, J.; Ackermann, L. *ACS Catal.* **2016**, *6*, 498.
62. Guo, X.-X.; Gu, D.-W.; Wu, Z.; Zhang, W. *Chem. Rev.* **2015**, *115*, 1622.
63. Yamaguchi, J.; Muto, K.; Itami, K. *Top. Curr. Chem.* **2016**, *374*, 55.
64. Shang, R.; Ilies, L.; Nakamura, E. *Chem. Rev.* **2017**, *117*, 9086.
65. Liu, W.; Ackermann, L. *ACS Catal.* **2016**, *6*, 3743.
66. Hebrard, F.; Kalck, P. *Chem. Rev.* **2009**, *109*, 4272.
67. Gandeepan, P.; Cheng, C.-H. *Acc. Chem. Res.* **2015**, *48*, 1194.
68. Bönnemann, H. *Angew. Chem. Int. Ed.* **1978**, *17*, 505.
69. Nicholas, K. M. *Acc. Chem. Res.* **1987**, *20*, 207.
70. (a) Khand, I. U.; Knox, G. R.; Pauson, P. L.; Watts, W. E. *J. Chem. Soc., Perkin Trans. 1* **1973**, 975. (b) Khand, I. U.; Knox, G. R.; Pauson, P. L.; Watts, W. E.; Foreman, M. I. *J. Chem. Soc., Perkin Trans. 1* **1973**, 977.
71. Tokunaga, M.; Larrow, J. F.; Kakiuchi, F.; Jacobsen, E. N. *Science* **1997**, *277*, 936.
72. Cahiez, G.; Moyeux, A. *Chem. Rev.* **2010**, *110*, 1435.
73. Gandeepan, P.; Müller, T.; Zell, D.; Cera, G.; Warratz, S.; Ackermann, L. *Chem. Rev.* **2019**, *119*, 2192.
74. Gao, K.; Yoshikai, N. *Acc. Chem. Res.* **2014**, *47*, 1208.
75. Kommagalla, Y.; Chatani, N. *Coord. Chem. Rev.* **2017**, *350*, 117.
76. Wei, D.; Zhu, X.; Niu, J.-L.; Song, M.-P. *ChemCatChem* **2016**, *8*, 1242.
77. Yoshino, T.; Matsunaga, S. *Adv. Syn. Catal.* **2017**, *359*, 1245.

78. Chirila, P. G.; Whiteoak, C. J. *Dalton Trans.* **2017**, *46*, 9721.
79. Planas, O.; Chirila, P. G.; Whiteoak, C. J.; Ribas, X. *Adv. Organomet. Chem.* **2018**, *69*, 209.
80. Wang, S.; Chen, S.-Y.; Yu, X.-Q. *Chem. Commun.* **2017**, *53*, 3165.
81. Prakash, S.; Kuppusamy, R.; Cheng, C.-H. *ChemCatChem* **2018**, *10*, 683.
82. Lukasevics, L.; Cizikovs, A.; Grigorjeva, L. *Chem. Commun.* **2021**, *57*, 10827.
83. Klein, H.-F.; Helwig, M.; Koch, U.; Flörke, U.; Haupt, H.-J. J. Z. f. N. B. *Naturforsch. B* **1993**, *48*, 778.
84. Halbritter, G.; Knoch, F.; Wolski, A.; Kisch, H. *Angew. Chem. Int. Ed.* **1994**, *33*, 1603.
85. (a) Lenges, C. P.; Brookhart, M. *J. Am. Chem. Soc.* **1997**, *119*, 3165. (b) Lenges, C. P.; White, P. S.; Brookhart, M. *J. Am. Chem. Soc.* **1998**, *120*, 6965.
86. Bolig, A. D.; Brookhart, M. *J. Am. Chem. Soc.* **2007**, *129*, 14544.
87. Lenges, C. P.; Brookhart, M.; Grant, B. E. *J. Organomet. Chem.* **1997**, *528*, 199.
88. Gao, K.; Lee, P.-S.; Fujita, T.; Yoshikai, N. *J. Am. Chem. Soc.* **2010**, *132*, 12249.
89. Lee, P.-S.; Fujita, T.; Yoshikai, N. *J. Am. Chem. Soc.* **2011**, *133*, 17283.
90. Yamakawa, T.; Yoshikai, N. *Tetrahedron* **2013**, *69*, 4459.
91. Ding, Z.; Yoshikai, N. *Angew. Chem. Int. Ed.* **2012**, *51*, 4698.
92. (a) Ding, Z.; Yoshikai, N. *Org. Lett.* **2010**, *12*, 4180. (b) Ding, Z.; Yoshikai, N. *Synthesis* **2011**, *2011*, 2561.
93. Yamakawa, T.; Yoshikai, N. *Org. Lett.* **2013**, *15*, 196.
94. Ilies, L.; Chen, Q.; Zeng, X.; Nakamura, E. *J. Am. Chem. Soc.* **2011**, *133*, 5221.
95. Gao, K.; Yoshikai, N. *J. Am. Chem. Soc.* **2011**, *133*, 400.
96. (a) Lee, P.-S.; Yoshikai, N. *Angew. Chem. Int. Ed.* **2013**, *52*, 1240. (b) Dong, J.; Lee, P.-S.; Yoshikai, N. *Chem. Lett.* **2013**, *42*, 1140.
97. (a) Hapke, M.; Hilt, G. *Cobalt Catalysis in Organic Synthesis: Methods and Reactions*. Wiley-VCH: Weinheim, Germany, **2020**, 89. (b) Yoshikai, N. *Bull. Chem. Soc. Jpn.* **2014**, *87*, 843. (c) Ackermann, L. *J. Org. Chem.* **2014**, *79*, 8948.
98. (a) Fallon, B. J.; Derat, E.; Amatore, M.; Aubert, C.; Chemla, F.; Ferreira, F.; Perez-Luna, A.; Petit, M. *J. Am. Chem. Soc.* **2015**, *137*, 2448. (b) Fallon, B. J.; Garsi, J.-B.; Derat, E.; Amatore, M.; Aubert, C.; Petit, M. *ACS Catal.* **2015**, *5*, 7493. (c) Fallon, B. J.; Derat, E.; Amatore, M.; Aubert, C.; Chemla, F.; Ferreira, F.; Perez-Luna, A.; Petit, M. *Org. Lett.* **2016**, *18*, 2292.

99. (a) Broderick, W. E.; Kanamori, K.; Willett, R. D.; Legg, J. I. *Inorg. Chem.* **1991**, *30*, 3875. (b) Kanamori, K.; Broderick, W. E.; Jordan, R. F.; Willett, R. D.; Legg, J. I. *J. Am. Chem. Soc.* **1986**, *108*, 7122.
100. Avilés, T.; Dinis, A.; Calhorda, M. J.; Pinto, P.; Félix, V.; Drew, M. G. B. *J. Organomet. Chem.* **2001**, *625*, 186.
101. Yoshino, T.; Ikemoto, H.; Matsunaga, S.; Kanai, M. *Angew. Chem. Int. Ed.* **2013**, *52*, 2207.
102. Yoshino, T.; Ikemoto, H.; Matsunaga, S.; Kanai, M. *Chem. Eur. J.* **2013**, *19*, 9142.
103. (a) Satoh, T.; Miura, M. *Chem. Eur. J.* **2010**, *16*, 11212. (b) Song, G.; Wang, F.; Li, X. *Chem. Soc. Rev.* **2012**, *41*, 3651.
104. For selected examples, see: (a) Ikemoto, H.; Yoshino, T.; Sakata, K.; Matsunaga, S.; Kanai, M. *J. Am. Chem. Soc.* **2014**, *136*, 5424. (b) Bera, S. S.; Debbarma, S.; Ghosh, A. K.; Chand, S.; Maji, M. S. *J. Org. Chem.* **2017**, *82*, 420.
105. Shankar, M.; Saha, A.; Sau, S.; Ghosh, A.; Gandon, V.; Sahoo, A. K. *Chem. Sci.* **2021**, *12*, 6393.
106. (a) Sk, M. R.; Bera, S. S.; Maji, M. S. *Org. Lett.* **2018**, *20*, 134. (b) Sk, M. R.; Bera, S. S.; Maji, M. S. *Adv. Syn. Catal.* **2019**, *361*, 585. (c) Banjare, S. K.; Chebolu, R.; Ravikumar, P. C. *Org. Lett.* **2019**, *21*, 4049. (d) Banjare, S. K.; Nanda, T.; Ravikumar, P. C. *Org. Lett.* **2019**, *21*, 8138. (e) Sk, M. R.; Maji, M. S. *Org. Chem. Front.* **2020**, *7*, 19. (f) Banjare, S. K.; Biswal, P.; Ravikumar, P. C. *J. Org. Chem.* **2020**, *85*, 5330. (g) Banjare, S. K.; Nanda, T.; Pati, B. V.; Adhikari, G. K. D.; Dutta, J.; Ravikumar, P. C. *ACS Catal.* **2021**, *11*, 11579-11587.
107. Hummel, J. R.; Ellman, J. A. *J. Am. Chem. Soc.* **2015**, *137*, 490.
108. Sun, B.; Yoshino, T.; Matsunaga, S.; Kanai, M. *Adv. Syn. Catal.* **2014**, *356*, 1491.
109. (a) Liang, Y.; Liang, Y.-F.; Tang, C.; Yuan, Y.; Jiao, N. *Chem. Eur. J.* **2015**, *21*, 16395. (b) Patel, P.; Chang, S. *ACS Catal.* **2015**, *5*, 853. (c) Mei, R.; Loup, J.; Ackermann, L. *ACS Catal.* **2016**, *6*, 793.
110. (a) Li, J.; Ackermann, L. *Angew. Chem. Int. Ed.* **2015**, *54*, 3635. (b) Yu, D.-G.; Gensch, T.; de Azambuja, F.; Vásquez-Céspedes, S.; Glorius, F. *J. Am. Chem. Soc.* **2014**, *136*, 17722.
111. Pawar, A. B.; Chang, S. *Org. Lett.* **2015**, *17*, 660.
112. For selected examples, see: (a) Sen, M.; Emayavaramban, B.; Barsu, N.; Premkumar, J. R.; Sundararaju, B. *ACS Catal.* **2016**, *6*, 2792. (b) Barsu, N.; Rahman, M. A.; Sen, M.; Sundararaju, B. *Chem. Eur. J.* **2016**, *22*, 9135. (c) Tan, P. W.; Mak, A. M.; Sullivan, M.

B.; Dixon, D. J.; Seayad, J. *Angew. Chem. Int. Ed.* **2017**, *56*, 16550. (d) Kumar, R.; Kumar, R.; Chandra, D.; Sharma, U. *J. Org. Chem.* **2019**, *84*, 1542. (e) Tan, H.; Khan, R.; Xu, D.; Zhou, Y.; Zhang, X.; Shi, G.; Fan, B. *Chem. Commun.* **2020**, *56*, 12570.

113. (a) Yoshino, T.; Matsunaga, S. *Adv. Organomet. Chem.* **2017**, *68*, 197. (b) Yoshino, T.; Matsunaga, S. *Synlett* **2019**, *30*, 1384.
114. Mei, R.; Dhawa, U.; Samanta, R. C.; Ma, W.; Wencel-Delord, J.; Ackermann, L. *ChemSusChem* **2020**, *13*, 3306.
115. Grigorjeva, L.; Daugulis, O. *Angew. Chem. Int. Ed.* **2014**, *53*, 10209.
116. Mei, R.; Wang, H.; Warratz, S.; Macgregor, S. A.; Ackermann, L. *Chem. Eur. J.* **2016**, *22*, 6759.
117. Nguyen, T. T.; Grigorjeva, L.; Daugulis, O. *ACS Catal.* **2016**, *6*, 551.
118. (a) Kalsi, D.; Sundararaju, B. *Org. Lett.* **2015**, *17*, 6118. (b) Planas, O.; Whiteoak, C. J.; Company, A.; Ribas, X. *Adv. Syn. Catal.* **2015**, *357*, 4003.
119. Zhai, S.; Qiu, S.; Chen, X.; Wu, J.; Zhao, H.; Tao, C.; Li, Y.; Cheng, B.; Wang, H.; Zhai, H. *Chem. Commun.* **2018**, *54*, 98.
120. Kuai, C.; Wang, L.; Li, B.; Yang, Z.; Cui, X. *Org. Lett.* **2017**, *19*, 2102.
121. Kathiravan, S.; Nicholls, I. A. *Org. Lett.* **2017**, *19*, 4758.
122. Zhang, L.-B.; Hao, X.-Q.; Liu, Z.-J.; Zheng, X.-X.; Zhang, S.-K.; Niu, J.-L.; Song, M.-P. *Angew. Chem. Int. Ed.* **2015**, *54*, 10012.
123. Hao, X.-Q.; Du, C.; Zhu, X.; Li, P.-X.; Zhang, J.-H.; Niu, J.-L.; Song, M.-P. *Org. Lett.* **2016**, *18*, 3610.
124. (a) Grigorjeva, L.; Daugulis, O. *Org. Lett.* **2014**, *16*, 4688. (b) Ma, W.; Ackermann, L. *ACS Catal.* **2015**, *5*, 2822.
125. Thrimurtulu, N.; Dey, A.; Maiti, D.; Volla, C. M. R. *Angew. Chem. Int. Ed.* **2016**, *55*, 12361.
126. (a) Zhao, H.; Shao, X.; Wang, T.; Zhai, S.; Qiu, S.; Tao, C.; Wang, H.; Zhai, H. *Chem. Commun.* **2018**, *54*, 4927. (b) Grigorjeva, L.; Daugulis, O. *Org. Lett.* **2014**, *16*, 4684. (c) Gu, Z.-Y.; Liu, C.-G.; Wang, S.-Y.; Ji, S.-J. *J. Org. Chem.* **2017**, *82*, 2223.
127. Nguyen, T. T.; Grigorjeva, L.; Daugulis, O. *Angew. Chem. Int. Ed.* **2018**, *57*, 1688.
128. Wu, X.; Yang, K.; Zhao, Y.; Sun, H.; Li, G.; Ge, H. *Nat. Commun.* **2015**, *6*, 6462.
129. Zhang, J.; Chen, H.; Lin, C.; Liu, Z.; Wang, C.; Zhang, Y. *J. Am. Chem. Soc.* **2015**, *137*, 1299.

130. (a) Barsu, N.; Bolli, S. K.; Sundararaju, B. *Chem. Sci.* **2017**, *8*, 2431. (b) Williamson, P.; Galván, A.; Gaunt, M. J. *Chem. Sci.* **2017**, *8*, 2588. (c) Zeng, L.; Tang, S.; Wang, D.; Deng, Y.; Chen, J.-L.; Lee, J.-F.; Lei, A. *Org. Lett.* **2017**, *19*, 2170.
131. Zhang, Z.-Z.; Han, Y.-Q.; Zhan, B.-B.; Wang, S.; Shi, B.-F. *Angew. Chem. Int. Ed.* **2017**, *56*, 13145.
132. Landge, V. G.; Jaiswal, G.; Balaraman, E. *Org. Lett.* **2016**, *18*, 812.
133. Zhao, T.; Qin, D.; Han, W.; Yang, S.; Feng, B.; Gao, G.; You, J. *Chem. Commun.* **2019**, *55*, 6118.
134. Yamaguchi, T.; Kommagalla, Y.; Aihara, Y.; Chatani, N. *Chem. Commun.* **2016**, *52*, 10129.
135. (a) Maity, S.; Kancherla, R.; Dhawa, U.; Hoque, E.; Pimparkar, S.; Maiti, D. *ACS Catal.* **2016**, *6*, 5493. (b) Maity, S.; Dolui, P.; Kancherla, R.; Maiti, D. *Chem. Sci.* **2017**, *8*, 5181.
136. (a) Li, Q.; Li, Y.; Hu, W.; Hu, R.; Li, G.; Lu, H. *Chem. Eur. J.* **2016**, *22*, 12286. (b) Wang, H.; Zhang, S.; Wang, Z.; He, M.; Xu, K. *Org. Lett.* **2016**, *18*, 5628. (c) Li, Q.; Hu, W.; Hu, R.; Lu, H.; Li, G. *Org. Lett.* **2017**, *19*, 4676.
137. Tan, G.; He, S.; Huang, X.; Liao, X.; Cheng, Y.; You, J. *Angew. Chem. Int. Ed.* **2016**, *55*, 10414.
138. Grigorjeva, L.; Daugulis, O. *Org. Lett.* **2015**, *17*, 1204.
139. (a) Hu, L.; Gui, Q.; Chen, X.; Tan, Z.; Zhu, G. *Org. Biomol. Chem.* **2016**, *14*, 11070. (b) Bu, Q.; Gońka, E.; Kuciński, K.; Ackermann, L. *Chem. Eur. J.* **2019**, *25*, 2213.
140. Du, C.; Li, P.-X.; Zhu, X.; Suo, J.-F.; Niu, J.-L.; Song, M.-P. *Angew. Chem. Int. Ed.* **2016**, *55*, 13571.
141. Li, M.-H.; Si, X.-J.; Zhang, H.; Yang, D.; Niu, J.-L.; Song, M.-P. *Org. Lett.* **2021**, *23*, 914.
142. (a) Kochi, J. K.; Tang, R. T.; Bernath, T. *J. Am. Chem. Soc.* **1973**, *95*, 7114. (b) Tang, R.; Kochi, J. K. *J. Inorg. Nucl. Chem.* **1973**, *35*, 3845.
143. (a) Zhang, L.-B.; Hao, X.-Q.; Zhang, S.-K.; Liu, Z.-J.; Zheng, X.-X.; Gong, J.-F.; Niu, J.-L.; Song, M.-P. *Angew. Chem. Int. Ed.* **2015**, *54*, 272. (b) Liu, S.-K.; Cui, X.-F.; Liu, X.-X.; Ma, H.-J.; Wei, D.-D.; Luo, X.-L.; Huang, G.-S. *ChemistrySelect* **2018**, *3*, 3989.
144. (a) Lan, J.; Xie, H.; Lu, X.; Deng, Y.; Jiang, H.; Zeng, W. *Org. Lett.* **2017**, *19*, 4279. (b) Ueno, R.; Natsui, S.; Chatani, N. *Org. Lett.* **2018**, *20*, 1062. (c) Lin, C.; Chen, Z.; Liu, Z.; Zhang, Y. *Adv. Syn. Catal.* **2018**, *360*, 519.

145. (a) Zhang, L.-B.; Zhang, S.-K.; Wei, D.; Zhu, X.; Hao, X.-Q.; Su, J.-H.; Niu, J.-L.; Song, M.-P. *Org. Lett.* **2016**, *18*, 1318. (b) Yan, Q.; Xiao, T.; Liu, Z.; Zhang, Y. *Adv. Syn. Catal.* **2016**, *358*, 2707.
146. Du, C.; Li, P.-X.; Zhu, X.; Han, J.-N.; Niu, J.-L.; Song, M.-P. *ACS Catal.* **2017**, *7*, 2810.
147. (a) Kommagalla, Y.; Yamazaki, K.; Yamaguchi, T.; Chatani, N. *Chem. Commun.* **2018**, *54*, 1359. (b) Kommagalla, Y.; Chatani, N. *Org. Lett.* **2019**, *21*, 5971.
148. (a) Hu, L.; Chen, X.; Yu, L.; Yu, Y.; Tan, Z.; Zhu, G.; Gui, Q. *Org. Chem. Front.* **2018**, *5*, 216. (b) Li, M.; Wang, J. J. *Org. Lett.* **2018**, *20*, 6490.
149. Nageswar Rao, D.; Rasheed, S.; Raina, G.; Ahmed, Q. N.; Jaladanki, C. K.; Bharatam, P. V.; Das, P. *J. Org. Chem.* **2017**, *82*, 7234.
150. Planas, O.; Whiteoak, C. J.; Martin-Diaconescu, V.; Gamba, I.; Luis, J. M.; Parella, T.; Company, A.; Ribas, X. *J. Am. Chem. Soc.* **2016**, *138*, 14388.
151. Lukasevics, L.; Cizikovs, A.; Grigorjeva, L. *Org. Lett.* **2021**, *23*, 2748.
152. (a) Zhu, X.; Su, J.-H.; Du, C.; Wang, Z.-L.; Ren, C.-J.; Niu, J.-L.; Song, M.-P. *Org. Lett.* **2017**, *19*, 596. (b) De, P. B.; Pradhan, S.; Banerjee, S.; Punniyamurthy, T. *Chem. Commun.* **2018**, *54*, 2494. (c) Lu, M.-Z.; Ding, X.; Shao, C.; Hu, Z.; Luo, H.; Zhi, S.; Hu, H.; Kan, Y.; Loh, T.-P. *Org. Lett.* **2020**, *22*, 2663. (d) Li, Z.-l.; Wu, P.-Y.; Cai, C. *Org. Chem. Front.* **2019**, *6*, 2043. (e) Li, Z.-l.; Sun, K.-k.; Cai, C. *Org. Biomol. Chem.* **2018**, *16*, 5433. (f) Gou, Q.; Tan, X.; Zhang, M.; Ran, M.; Yuan, T.; He, S.; Zhou, L.; Cao, T.; Luo, F. *Org. Lett.* **2020**, *22*, 1966.
153. Kalsi, D.; Dutta, S.; Barsu, N.; Rueping, M.; Sundararaju, B. *ACS Catal.* **2018**, *8*, 8115.
154. (a) Kalsi, D.; Barsu, N.; Chakrabarti, S.; Dahiya, P.; Rueping, M.; Sundararaju, B. *Chem. Commun.* **2019**, *55*, 11626. (b) Sen, C.; Sarvaiya, B.; Sarkar, S.; Ghosh, S. C. *J. Org. Chem.* **2020**, *85*, 15287. (c) Li, T.; Li, J.; Zhu, Z.; Chen, Y.; Li, X.; Yang, Q.; Xia, J.; Zhang, W.; Zhang, C.; Pan, W.; Wu, S. *Org. Chem. Front.* **2021**, *8*, 928.
155. Sauermann, N.; Meyer, T. H.; Tian, C.; Ackermann, L. *J. Am. Chem. Soc.* **2017**, *139*, 18452.
156. (a) Sauermann, N.; Meyer, T. H.; Ackermann, L. *Chem. Eur. J.* **2018**, *24*, 16209. (b) Dhawa, U.; Kaplaneris, N.; Ackermann, L. *Org. Chem. Front.* **2021**, *8*, 4886.
157. (a) Ullmann, F. *Ber. Dtsch. Chem. Ges.* **1903**, *36*, 2382. (b) Ullmann, F. *Ber. Dtsch. Chem. Ges.* **1904**, *37*, 853. (c) Ullmann, F.; Sponagel, P. *Ber. Dtsch. Chem. Ges.* **1905**, *38*, 2211. (d) Goldberg, I. *Ber. Dtsch. Chem. Ges.* **1906**, *39*, 1691.
158. (a) Chan, D. M. T.; Monaco, K. L.; Wang, R.-P.; Winters, M. P. *Tetrahedron Lett.* **1998**, *39*, 2933. (b) Evans, D. A.; Katz, J. L.; West, T. R. *Tetrahedron Lett.* **1998**, *39*, 2937. (c)

Lam, P. Y. S.; Clark, C. G.; Saubern, S.; Adams, J.; Winters, M. P.; Chan, D. M. T.; Combs, A. *Tetrahedron Lett.* **1998**, *39*, 2941.

159. For selected reviews, see: (a) Ley, S. V.; Thomas, A. W. *Angew. Chem. Int. Ed.* **2003**, *42*, 5400. (b) Ma, D.; Cai, Q. *Acc. Chem. Res.* **2008**, *41*, 1450. (c) Reymond, S.; Cossy, J. *Chem. Rev.* **2008**, *108*, 5359. (d) Alexakis, A.; Bäckvall, J. E.; Krause, N.; Pàmies, O.; Diéguez, M. *Chem. Rev.* **2008**, *108*, 2796. (e) Monnier, F.; Taillefer, M. *Angew. Chem. Int. Ed.* **2009**, *48*, 6954. (f) Daugulis, O.; Do, H.-Q.; Shabashov, D. *Acc. Chem. Res.* **2009**, *42*, 1074. (g) Jerphagnon, T.; Pizzuti, M. G.; Minnaard, A. J.; Feringa, B. L. *Chem. Soc. Rev.* **2009**, *38*, 1039. (h) Zhang, M. *Appl. Organomet. Chem.* **2010**, *24*, 269. (i) Surry, D. S.; Buchwald, S. L. *Chem. Sci.* **2010**, *1*, 13. (j) Wendlandt, A. E.; Suess, A. M.; Stahl, S. S. *Angew. Chem. Int. Ed.* **2011**, *50*, 11062. (k) Hirano, K.; Miura, M. *Chem. Commun.* **2012**, *48*, 10704. (l) Zhang, C.; Tang, C.; Jiao, N. *Chem. Soc. Rev.* **2012**, *41*, 3464. (m) Shi, Z.; Zhang, C.; Tang, C.; Jiao, N. *Chem. Soc. Rev.* **2012**, *41*, 3381. (n) Yoshikai, N.; Nakamura, E. *Chem. Rev.* **2012**, *112*, 2339. (o) Allen, S. E.; Walvoord, R. R.; Padilla-Salinas, R.; Kozlowski, M. C. *Chem. Rev.* **2013**, *113*, 6234. (p) Sambiagio, C.; Marsden, S. P.; Blacker, A. J.; McGowan, P. C. *Chem. Soc. Rev.* **2014**, *43*, 3525. (q) Ryland, B. L.; Stahl, S. S. *Angew. Chem. Int. Ed.* **2014**, *53*, 8824. (r) McCann, S. D.; Stahl, S. S. *Acc. Chem. Res.* **2015**, *48*, 1756. (s) Liang, Y.; Liang, Y.-F.; Jiao, N. *Org. Chem. Front.* **2015**, *2*, 403. (t) Cai, X.-h.; Xie, B. *Synthesis* **2015**, *47*, 737. (u) Miao, J.; Ge, H. *Eur. J. Org. Chem.* **2015**, *2015*, 7859. (v) Zhu, X.; Chiba, S. *Chem. Soc. Rev.* **2016**, *45*, 4504. (w) Pirnot, M. T.; Wang, Y.-M.; Buchwald, S. L. *Angew. Chem. Int. Ed.* **2016**, *55*, 48. (x) Maaliki, C.; Thiery, E.; Thibonnet, J. *Eur. J. Org. Chem.* **2017**, *2017*, 209.
160. Reinaud, O.; Capdevielle, P.; Maumy, M. *Synthesis* **1990**, *1990*, 612.
161. Chen, X.; Hao, X.-S.; Goodhue, C. E.; Yu, J.-Q. *J. Am. Chem. Soc.* **2006**, *128*, 6790.
162. Takeshi, U.; Shinya, I.; Naoto, C. *Chem. Lett.* **2006**, *35*, 842.
163. (a) Rao, W.-H.; Shi, B.-F. *Org. Chem. Front.* **2016**, *3*, 1028. (b) Shang, M.; Sun, S.-Z.; Wang, H.-L.; Wang, M.-M.; Dai, H.-X. *Synthesis* **2016**, *48*, 4381. (c) Li, Z.-K.; Jia, X.-S.; Yin, L. *Synthesis* **2018**, *50*, 4165.
164. Chen, X.; Dobereiner, G.; Hao, X.-S.; Giri, R.; Maugel, N.; Yu, J.-Q. *Tetrahedron* **2009**, *65*, 3085.
165. Odani, R.; Nishino, M.; Hirano, K. *Heterocycles* **2014**, *88*, 595.
166. Le, J.; Gao, Y.; Ding, Y.; Jiang, C. *Tetrahedron Lett.* **2016**, *57*, 1728.

167. Kitahara, M.; Umeda, N.; Hirano, K.; Satoh, T.; Miura, M. *J. Am. Chem. Soc.* **2011**, *133*, 2160.
168. (a) Nishino, M.; Hirano, K.; Satoh, T.; Miura, M. *Angew. Chem. Int. Ed.* **2012**, *51*, 6993. (b) Odani, R.; Hirano, K.; Satoh, T.; Miura, M. *Angew. Chem. Int. Ed.* **2014**, *53*, 10784.
169. Nishino, M.; Hirano, K.; Satoh, T.; Miura, M. *Angew. Chem. Int. Ed.* **2013**, *52*, 4457.
170. Odani, R.; Hirano, K.; Satoh, T.; Miura, M. *J. Org. Chem.* **2013**, *78*, 11045.
171. Shang, M.; Sun, S.-Z.; Dai, H.-X.; Yu, J.-Q. *Org. Lett.* **2014**, *16*, 5666.
172. Gui, Q.; Chen, X.; Hu, L.; Wang, D.; Liu, J.; Tan, Z. *Adv. Syn. Catal.* **2016**, *358*, 509.
173. Zhao, S.; Liu, Y.-J.; Yan, S.-Y.; Chen, F.-J.; Zhang, Z.-Z.; Shi, B.-F. *Org. Lett.* **2015**, *17*, 3338.
174. Zhao, S.; Yuan, J.; Li, Y.-C.; Shi, B.-F. *Chem. Commun.* **2015**, *51*, 12823.
175. Takamatsu, K.; Hirano, K.; Miura, M. *Angew. Chem. Int. Ed.* **2017**, *56*, 5353.
176. Kajiwara, R.; Xu, S.; Hirano, K.; Miura, M. *Org. Lett.* **2021**, *23*, 5405.
177. Yang, Y.; Li, R.; Zhao, Y.; Zhao, D.; Shi, Z. *J. Am. Chem. Soc.* **2016**, *138*, 8734.
178. Wu, X.; Zhao, Y.; Ge, H. *Chem. Sci.* **2015**, *6*, 5978.
179. Tan, G.; Zhang, L.; Liao, X.; Shi, Y.; Wu, Y.; Yang, Y.; You, J. *Org. Lett.* **2017**, *19*, 4830.
180. (a) Jin, J.; Wen, Q.; Lu, P.; Wang, Y. *Chem. Commun.* **2012**, *48*, 9933. (b) Kim, J.; Kim, H.; Chang, S. *Org. Lett.* **2012**, *14*, 3924. (c) Xu, H.; Liu, P.-T.; Li, Y.-H.; Han, F.-S. *Org. Lett.* **2013**, *15*, 3354. (d) Kou, X.; Zhao, M.; Qiao, X.; Zhu, Y.; Tong, X.; Shen, Z. *Chem. Eur. J.* **2013**, *19*, 16880. (e) Pan, C.; Jin, H.; Xu, P.; Liu, X.; Cheng, Y.; Zhu, C. *J. Org. Chem.* **2013**, *78*, 9494. (f) Yan, Y.; Yuan, Y.; Jiao, N. *Org. Chem. Front.* **2014**, *1*, 1176. (g) Song, H.; Liu, X.; Wang, C.; Qiao, J.; Chu, W.; Sun, Z. *Asian J. Org. Chem.* **2017**, *6*, 1693. (h) Yu, Z.; Zhang, S.; Shen, Z. *Chin. J. Chem.* **2018**, *36*, 1139.
181. (a) Cai, S.; Chen, C.; Sun, Z.; Xi, C. *Chem. Commun.* **2013**, *49*, 4552. (b) Shang, M.; Sun, S.-Z.; Wang, H.-L.; Laforteza, B. N.; Dai, H.-X.; Yu, J.-Q. *Angew. Chem. Int. Ed.* **2014**, *53*, 10439. (c) Hu, L.; Chen, X.; Gui, Q.; Tan, Z.; Zhu, G. *Chem. Commun.* **2016**, *52*, 6845.
182. (a) Shang, M.; Wang, H.-L.; Sun, S.-Z.; Dai, H.-X.; Yu, J.-Q. *J. Am. Chem. Soc.* **2014**, *136*, 11590. (b) Liu, Y.-J.; Liu, Y.-H.; Yin, X.-S.; Gu, W.-J.; Shi, B.-F. *Chem. Eur. J.* **2015**, *21*, 205.
183. Li, J.-J.; Wang, C.-G.; Yu, J.-F.; Wang, P.; Yu, J.-Q. *Org. Lett.* **2020**, *22*, 4692.

184. (a) Takamatsu, K.; Hirano, K.; Miura, M. *Chem. Lett.* **2018**, *47*, 450. (b) Tang, C.; Zhang, R.; Zhu, B.; Fu, J.; Deng, Y.; Tian, L.; Guan, W.; Bi, X. *J. Am. Chem. Soc.* **2018**, *140*, 16929.

185. Dai, J.-L.; Shao, N.-Q.; Zhang, J.; Jia, R.-P.; Wang, D.-H. *J. Am. Chem. Soc.* **2017**, *139*, 12390.

186. Ma, B.; Tang, Z.; Zhang, J.; Liu, L. *Chem. Commun.* **2020**, *56*, 9485.

187. Tran, L. D.; Roane, J.; Daugulis, O. *Angew. Chem. Int. Ed.* **2013**, *52*, 6043.

188. (a) Li, Q.; Zhang, S.-Y.; He, G.; Ai, Z.; Nack, W. A.; Chen, G. *Org. Lett.* **2014**, *16*, 1764. (b) Martínez, Á. M.; Rodríguez, N.; Arrayás, R. G.; Carretero, J. C. *Chem. Commun.* **2014**, *50*, 2801. (c) Begam, H. M.; Choudhury, R.; Behera, A.; Jana, R. *Org. Lett.* **2019**, *21*, 4651. (d) Wu, P.; Huang, W.; Cheng, T.-J.; Lin, H.-X.; Xu, H.; Dai, H.-X. *Org. Lett.* **2020**, *22*, 5051. (e) Zu, C.; Zhang, T.; Yang, F.; Wu, Y.; Wu, Y. *J. Org. Chem.* **2020**, *85*, 12777. (f) Li, Q.; Huang, J.; Chen, G.; Wang, S.-B. *Org. Biomol. Chem.* **2020**, *18*, 4802. (g) Singh, H.; Sen, C.; Suresh, E.; Panda, A. B.; Ghosh, S. C. *J. Org. Chem.* **2021**, *86*, 3261. (h) Jia, Z.-S.; Yue, Q.; Li, Y.; Xu, X.-T.; Zhang, K.; Shi, B.-F. *Beilstein J. Org. Chem.* **2021**, *17*, 2488.

189. (a) Gou, Q.; Yang, Y.-W.; Liu, Z.-N.; Qin, J. *Chem. Eur. J.* **2016**, *22*, 16057. (b) Wang, C.; Yang, Y. *Tetrahedron Lett.* **2017**, *58*, 935.

190. Rao, W.-H.; Li, Q.; Jiang, L.-L.; Deng, X.-W.; Xu, P.; Chen, F.-Y.; Li, M.; Zou, G.-D. *J. Org. Chem.* **2021**, *86*, 10580.

191. (a) Roane, J.; Daugulis, O. *J. Am. Chem. Soc.* **2016**, *138*, 4601. (b) Sadhu, P.; Punniyamurthy, T. *Chem. Commun.* **2016**, *52*, 2803. (c) Singh, B. K.; Polley, A.; Jana, R. *J. Org. Chem.* **2016**, *81*, 4295. (d) Pradhan, S.; De, P. B.; Punniyamurthy, T. *J. Org. Chem.* **2017**, *82*, 4883. (e) Yu, J.-F.; Li, J.-J.; Wang, P.; Yu, J.-Q. *Angew. Chem. Int. Ed.* **2019**, *58*, 18141. (f) Kwak, S. H.; Daugulis, O. *J. Org. Chem.* **2019**, *84*, 13022. (g) Sun, S.-Z.; Shang, M.; Xu, H.; Cheng, T.-J.; Li, M.-H.; Dai, H.-X. *Chem. Commun.* **2020**, *56*, 1444.

192. (a) Peng, J.; Chen, M.; Xie, Z.; Luo, S.; Zhu, Q. *Org. Chem. Front.* **2014**, *1*, 777. (b) Li, Z.; Yu, H.; Bolm, C. *Angew. Chem. Int. Ed.* **2017**, *56*, 9532. (c) Xu, L.-L.; Wang, X.; Ma, B.; Yin, M.-X.; Lin, H.-X.; Dai, H.-X.; Yu, J.-Q. *Chem. Sci.* **2018**, *9*, 5160.

193. Takamatsu, K.; Hayashi, Y.; Kawauchi, S.; Hirano, K.; Miura, M. *ACS Catal.* **2019**, *9*, 5336.

194. Kumar, M.; Sharma, R.; Raziullah; Khan, A. A.; Ahmad, A.; Dutta, H. S.; Koley, D. *Org. Lett.* **2020**, *22*, 2152.

195. Cheng, T.-J.; Chen, J.-J.; Wu, P.; Xu, H.; Dai, H.-X. *Org. Lett.* **2021**, *23*, 8505.
196. (a) Wang, L.; Priebbenow, D. L.; Dong, W.; Bolm, C. *Org. Lett.* **2014**, *16*, 2661. (b) Grandhi, G. S.; Dana, S.; Mandal, A.; Baidya, M. *Org. Lett.* **2020**, *22*, 2606.
197. Takamatsu, K.; Hirano, K.; Satoh, T.; Miura, M. *Org. Lett.* **2014**, *16*, 2892.
198. Takamatsu, K.; Hirano, K.; Satoh, T.; Miura, M. *J. Org. Chem.* **2015**, *80*, 3242.
199. (a) Shuai, Q.; Deng, G.; Chua, Z.; Bohle, D. S.; Li, C.-J. *Adv. Syn. Catal.* **2010**, *352*, 632. (b) John, A.; Nicholas, K. M. *J. Org. Chem.* **2011**, *76*, 4158. (c) Xu, H.; Qiao, X.; Yang, S.; Shen, Z. *J. Org. Chem.* **2014**, *79*, 4414. (d) Shang, M.; Sun, S.-Z.; Dai, H.-X.; Yu, J.-Q. *J. Am. Chem. Soc.* **2014**, *136*, 3354. (e) Peng, J.; Xie, Z.; Chen, M.; Wang, J.; Zhu, Q. *Org. Lett.* **2014**, *16*, 4702. (f) Li, G.; Jia, C.; Chen, Q.; Sun, K.; Zhao, F.; Wu, H.; Wang, Z.; Lv, Y.; Chen, X. *Adv. Syn. Catal.* **2015**, *357*, 1311. (g) Kianmehr, E.; Amiri Lomedasht, Y.; Faghih, N.; Khan, K. M. *J. Org. Chem.* **2016**, *81*, 6087. (h) Ghosh, T.; Maity, P.; Ranu, B. C. *J. Org. Chem.* **2018**, *83*, 11758. (i) Kumar, M.; Raziullah; Khan, A. A.; Ahmad, A.; Dutta, H. S.; Kant, R.; Koley, D. *J. Org. Chem.* **2019**, *84*, 13624.
200. Wang, Z.; Ni, J.; Kuninobu, Y.; Kanai, M. *Angew. Chem. Int. Ed.* **2014**, *53*, 3496.
201. Wu, X.; Zhao, Y.; Zhang, G.; Ge, H. *Angew. Chem. Int. Ed.* **2014**, *53*, 3706.
202. Wang, C.; Yang, Y.; Qin, D.; He, Z.; You, J. *J. Org. Chem.* **2015**, *80*, 8424.
203. (a) Tang, C.; Jiao, N. *J. Am. Chem. Soc.* **2012**, *134*, 18924. (b) Fan, Y.; Wan, W.; Ma, G.; Gao, W.; Jiang, H.; Zhu, S.; Hao, J. *Chem. Commun.* **2014**, *50*, 5733. (c) Azad, C. S.; Narula, A. K. *RSC Adv.* **2015**, *5*, 100223.
204. (a) Zhang, L.; Liu, Z.; Li, H.; Fang, G.; Barry, B.-D.; Belay, T. A.; Bi, X.; Liu, Q. *Org. Lett.* **2011**, *13*, 6536. (b) Katayev, D.; Pfister, K. F.; Wendling, T.; Gooßen, L. J. *Chem. Eur. J.* **2014**, *20*, 9902. (c) Liu, J.; Zhuang, S.; Gui, Q.; Chen, X.; Yang, Z.; Tan, Z. *Adv. Syn. Catal.* **2015**, *357*, 732. (d) Wang, C.-M.; Tang, K.-X.; Gao, T.-H.; Chen, L.; Sun, L.-P. *J. Org. Chem.* **2018**, *83*, 8315.
205. Mizuhara, T.; Inuki, S.; Oishi, S.; Fujii, N.; Ohno, H. *Chem. Commun.* **2009**, 3413.
206. (a) Wang, W.; Luo, F.; Zhang, S.; Cheng, J. *J. Org. Chem.* **2010**, *75*, 2415. (b) Wang, W.; Pan, C.; Chen, F.; Cheng, J. *Chem. Commun.* **2011**, *47*, 3978.
207. Bhadra, S.; Dzik, W. I.; Gooßen, L. J. *Angew. Chem. Int. Ed.* **2013**, *52*, 2959.
208. Bhadra, S.; Matheis, C.; Katayev, D.; Gooßen, L. J. *Angew. Chem. Int. Ed.* **2013**, *52*, 9279.
209. Lu, W.; Xu, H.; Shen, Z. *Org. Biomol. Chem.* **2017**, *15*, 1261.
210. Shang, M.; Shao, Q.; Sun, S.-Z.; Chen, Y.-Q.; Xu, H.; Dai, H.-X.; Yu, J.-Q. *Chem. Sci.* **2017**, *8*, 1469.

211. Ahmad, A.; Dutta, H. S.; Khan, B.; Kant, R.; Koley, D. *Adv. Syn. Catal.* **2018**, *360*, 1644.
212. Suess, A. M.; Ertem, M. Z.; Cramer, C. J.; Stahl, S. S. *J. Am. Chem. Soc.* **2013**, *135*, 9797.
213. (a) Roane, J.; Daugulis, O. *Org. Lett.* **2013**, *15*, 5842. (b) Hao, X.-Q.; Chen, L.-J.; Ren, B.; Li, L.-Y.; Yang, X.-Y.; Gong, J.-F.; Niu, J.-L.; Song, M.-P. *Org. Lett.* **2014**, *16*, 1104. (c) Zhang, L.-B.; Hao, X.-Q.; Zhang, S.-K.; Liu, K.; Ren, B.; Gong, J.-F.; Niu, J.-L.; Song, M.-P. *J. Org. Chem.* **2014**, *79*, 10399. (d) Yin, X.-S.; Li, Y.-C.; Yuan, J.; Gu, W.-J.; Shi, B.-F. *Org. Chem. Front.* **2015**, *2*, 119. (e) Roy, S.; Pradhan, S.; Punniyamurthy, T. *Chem. Commun.* **2018**, *54*, 3899.
214. Li, X.; Liu, Y.-H.; Gu, W.-J.; Li, B.; Chen, F.-J.; Shi, B.-F. *Org. Lett.* **2014**, *16*, 3904.
215. (a) Sun, S.-Z.; Shang, M.; Wang, H.-L.; Lin, H.-X.; Dai, H.-X.; Yu, J.-Q. *J. Org. Chem.* **2015**, *80*, 8843. (b) Singh, B. K.; Jana, R. *J. Org. Chem.* **2016**, *81*, 831. (c) Shang, M.; Wang, M.-M.; Saint-Denis, T. G.; Li, M.-H.; Dai, H.-X.; Yu, J.-Q. *Angew. Chem. Int. Ed.* **2017**, *56*, 5317.
216. (a) Zhao, S.; Chen, F.-J.; Liu, B.; Shi, B.-F. *Sci. China: Chem.* **2015**, *58*, 1302. (b) Wang, F.; Hu, Q.; Shu, C.; Lin, Z.; Min, D.; Shi, T.; Zhang, W. *Org. Lett.* **2017**, *19*, 3636. (c) Li, G.-J.; Pan, Y.-L.; Liu, Y.-L.; Xu, H.-F.; Chen, J.-Z. *Org. Lett.* **2019**, *21*, 1740.
217. Ueda, S.; Nagasawa, H. *Angew. Chem. Int. Ed.* **2008**, *47*, 6411.
218. (a) Zhao, J.; Wang, Y.; He, Y.; Liu, L.; Zhu, Q. *Org. Lett.* **2012**, *14*, 1078. (b) Zhao, J.; Zhang, Q.; Liu, L.; He, Y.; Li, J.; Li, J.; Zhu, Q. *Org. Lett.* **2012**, *14*, 5362.
219. (a) Gallardo-Donaire, J.; Martin, R. *J. Am. Chem. Soc.* **2013**, *135*, 9350. (b) Wang, Y.; Gulevich, A. V.; Gevorgyan, V. *Chem. Eur. J.* **2013**, *19*, 15836.
220. (a) Wang, Z.; Kuninobu, Y.; Kanai, M. *Org. Lett.* **2014**, *16*, 4790. (b) Wu, X.; Zhao, Y.; Ge, H. *Chem. Asian J.* **2014**, *9*, 2736.
221. Wang, F.; Li, X.; Li, Z.; Zhou, S.; Zhang, W. *ACS Omega* **2019**, *4*, 331.
222. Zhang, J.; Chen, H.; Wang, B.; Liu, Z.; Zhang, Y. *Org. Lett.* **2015**, *17*, 2768.
223. See, Y. Y.; Herrmann, A. T.; Aihara, Y.; Baran, P. S. *J. Am. Chem. Soc.* **2015**, *137*, 13776.
224. Chu, L.; Yue, X.; Qing, F.-L. *Org. Lett.* **2010**, *12*, 1644.
225. Sharma, P.; Rohilla, S.; Jain, N. *J. Org. Chem.* **2015**, *80*, 4116.
226. Tran, L. D.; Popov, I.; Daugulis, O. *J. Am. Chem. Soc.* **2012**, *134*, 18237.
227. Wang, X.; Yi, X.; Xu, H.; Dai, H.-X. *Org. Lett.* **2019**, *21*, 5981.
228. (a) Yan, X.-B.; Gao, P.; Yang, H.-B.; Li, Y.-X.; Liu, X.-Y.; Liang, Y.-M. *Tetrahedron* **2014**, *70*, 8730. (b) Zhu, L.; Cao, X.; Qiu, R.; Iwasaki, T.; Reddy, V. P.; Xu, X.; Yin, S.-

F.; Kambe, N. *RSC Adv.* **2015**, *5*, 39358. (c) Peng, P.; Wang, J.; Li, C.; Zhu, W.; Jiang, H.; Liu, H. *RSC Adv.* **2016**, *6*, 57441. (d) Li, Y.; Liu, Y.-J.; Shi, B.-F. *Adv. Syn. Catal.* **2017**, *359*, 4117.

229. Mandal, A.; Sahoo, H.; Baidya, M. *Org. Lett.* **2016**, *18*, 3202.
230. (a) Gandeepan, P.; Koeller, J.; Ackermann, L. *ACS Catal.* **2017**, *7*, 1030. (b) Xiong, Y.-S.; Yu, Y.; Weng, J.; Lu, G. *Org. Chem. Front.* **2018**, *5*, 982. (c) Kajiwara, R.; Takamatsu, K.; Hirano, K.; Miura, M. *Org. Lett.* **2020**, *22*, 5915. (d) Nguyen, H.; Daugulis, O. *J. Org. Chem.* **2020**, *85*, 13069. (e) Kumar, M.; Raziullah; Ahmad, A.; Dutta, H. S.; Khan, A. A.; Rastogi, A.; Kant, R.; Koley, D. *J. Org. Chem.* **2021**, *86*, 15185.
231. Liu, J.; Yu, L.; Zhuang, S.; Gui, Q.; Chen, X.; Wang, W.; Tan, Z. *Chem. Commun.* **2015**, *51*, 6418.
232. Rao, W.-H.; Shi, B.-F. *Org. Lett.* **2015**, *17*, 2784.
233. (a) Fan, C.-L.; Zhang, L.-B.; Liu, J.; Hao, X.-Q.; Niu, J.-L.; Song, M.-P. *Org. Chem. Front.* **2019**, *6*, 2215. (b) Zhi, C.; Wang, Q.; Liu, S.; Xue, Y.; Shi, L.; Zhu, X.; Hao, X.-Q.; Song, M.-P. *J. Org. Chem.* **2020**, *85*, 1022.
234. Liang, S.; Bolte, M.; Manolikakes, G. *Chem. Eur. J.* **2017**, *23*, 96.
235. (a) Li, J.-M.; Wang, Y.-H.; Yu, Y.; Wu, R.-B.; Weng, J.; Lu, G. *ACS Catal.* **2017**, *7*, 2661. (b) Xia, H.; An, Y.; Zeng, X.; Wu, J. *Org. Chem. Front.* **2018**, *5*, 366.
236. Wang, S.; Guo, R.; Wang, G.; Chen, S.-Y.; Yu, X.-Q. *Chem. Commun.* **2014**, *50*, 12718.
237. Hao, W.; Liu, Y. *Beilstein J. Org. Chem.* **2015**, *11*, 2132.
238. (a) Lu, Y.; Wang, R.; Qiao, X.; Shen, Z. *Synlett* **2011**, *2011*, 1038. (b) Mo, S.; Zhu, Y.; Shen, Z. *Org. Biomol. Chem.* **2013**, *11*, 2756. (c) Du, Z.-J.; Gao, L.-X.; Lin, Y.-J.; Han, F.-S. *ChemCatChem* **2014**, *6*, 123.
239. Zhao, J.; Cheng, X.; Le, J.; Yang, W.; Xue, F.; Zhang, X.; Jiang, C. *Org. Biomol. Chem.* **2015**, *13*, 9000.
240. Mandapati, U.; Pinapati, S.; Tamminana, R.; Rameshraju, R. *Catal. Lett.* **2018**, *148*, 418.
241. Truong, T.; Klimovica, K.; Daugulis, O. *J. Am. Chem. Soc.* **2013**, *135*, 9342.
242. Urones, B.; Martínez, Á. M.; Rodríguez, N.; Arrayás, R. G.; Carretero, J. C. *Chem. Commun.* **2013**, *49*, 11044.
243. Li, B.; Liu, B.; Shi, B.-F. *Chem. Commun.* **2015**, *51*, 5093.
244. Lee, W.-C. C.; Tehrani, A.; Li, J. J. *Synthesis* **2017**, *49*, 2865.
245. Wei, Q.; Ma, Y.; Li, L.; Liu, Q.; Liu, Z.; Liu, G. *Org. Lett.* **2018**, *20*, 7100.
246. Dong, J.; Wang, F.; You, J. *Org. Lett.* **2014**, *16*, 2884.
247. Zhang, Y.; Wang, Q.; Yu, H.; Huang, Y. *Org. Biomol. Chem.* **2014**, *12*, 8844.

248. Lee, W.-C. C.; Wang, W.; Li, J. J. *J. Org. Chem.* **2018**, *83*, 2382.
249. Zhu, W.; Zhang, D.; Yang, N.; Liu, H. *Chem. Commun.* **2014**, *50*, 10634.
250. Wang, H.-L.; Shang, M.; Sun, S.-Z.; Zhou, Z.-L.; Laforteza, B. N.; Dai, H.-X.; Yu, J.-Q. *Org. Lett.* **2015**, *17*, 1228.
251. Miura, W.; Hirano, K.; Miura, M. *Org. Lett.* **2015**, *17*, 4034.
252. Takamatsu, K.; Hirano, K.; Miura, M. *Org. Lett.* **2015**, *17*, 4066.
253. Khan, B.; Khan, A. A.; Kant, R.; Koley, D. *Adv. Syn. Catal.* **2016**, *358*, 3753.
254. (a) Zhang, T.-Y.; Lin, J.-B.; Li, Q.-Z.; Kang, J.-C.; Pan, J.-L.; Hou, S.-H.; Chen, C.; Zhang, S.-Y. *Org. Lett.* **2017**, *19*, 1764. (b) Zhang, T.-Y.; Liu, C.; Chen, C.; Liu, J.-X.; Xiang, H.-Y.; Jiang, W.; Ding, T.-M.; Zhang, S.-Y. *Org. Lett.* **2018**, *20*, 220.
255. Mandal, A.; Selvakumar, J.; Dana, S.; Mukherjee, U.; Baidya, M. *Chem. Eur. J.* **2018**, *24*, 3448.
256. Liu, J.; Zou, J.; Yao, J.; Chen, G. *Adv. Syn. Catal.* **2018**, *360*, 659.
257. Chen, F.-J.; Liao, G.; Li, X.; Wu, J.; Shi, B.-F. *Org. Lett.* **2014**, *16*, 5644.
258. (a) Zhang, J.; Li, D.; Chen, H.; Wang, B.; Liu, Z.; Zhang, Y. *Adv. Syn. Catal.* **2016**, *358*, 792. (b) Wu, X.; Miao, J.; Li, Y.; Li, G.; Ge, H. *Chem. Sci.* **2016**, *7*, 5260.
259. Wootton, T. L.; Porter, J. A.; Grewal, K. S.; Chirila, P. G.; Forbes, S.; Coles, S. J.; Horton, P. N.; Hamilton, A.; Whiteoak, C. J. *Org. Chem. Front.* **2020**, *7*, 1235.
260. Yang, Q.-L.; Wang, X.-Y.; Lu, J.-Y.; Zhang, L.-P.; Fang, P.; Mei, T.-S. *J. Am. Chem. Soc.* **2018**, *140*, 11487.
261. Kathiravan, S.; Suriyanarayanan, S.; Nicholls, I. A. *Org. Lett.* **2019**, *21*, 1968.
262. Tian, C.; Dhawa, U.; Scheremetjew, A.; Ackermann, L. *ACS Catal.* **2019**, *9*, 7690.
263. (a) Hamada, T.; Ye, X.; Stahl, S. S. *J. Am. Chem. Soc.* **2008**, *130*, 833. (b) Monguchi, D.; Fujiwara, T.; Furukawa, H.; Mori, A. *Org. Lett.* **2009**, *11*, 1607. (c) Chen, B.; Hou, X.-L.; Li, Y.-X.; Wu, Y.-D. *J. Am. Chem. Soc.* **2011**, *133*, 7668. (d) Banerjee, A.; Santra, S. K.; Rout, S. K.; Patel, B. K. *Tetrahedron* **2013**, *69*, 9096. (e) Xu, L.-P.; Haines, B. E.; Ajitha, M. J.; Yu, J.-Q.; Musaev, D. G. *ACS Catal.* **2021**, *11*, 12620.
264. Zhang, Q.; Liu, Y.; Wang, T.; Zhang, X.; Long, C.; Wu, Y.-D.; Wang, M.-X. *J. Am. Chem. Soc.* **2018**, *140*, 5579.
265. For selected reviews and examples, see: (a) Casitas, A.; Ribas, X. *Chem. Sci.* **2013**, *4*, 2301. (b) Huffman, L. M.; Stahl, S. S. *J. Am. Chem. Soc.* **2008**, *130*, 9196. (c) Yao, B.; Wang, D.-X.; Huang, Z.-T.; Wang, M.-X. *Chem. Commun.* **2009**, 2899. (d) King, A. E.; Huffman, L. M.; Casitas, A.; Costas, M.; Ribas, X.; Stahl, S. S. *J. Am. Chem. Soc.* **2010**, *132*, 12068. (e) Huffman, L. M.; Casitas, A.; Font, M.; Canta, M.; Costas, M.; Ribas, X.;

Stahl, S. S. *Chem. Eur. J.* **2011**, *17*, 10643. (f) Wang, Z.-L.; Zhao, L.; Wang, M.-X. *Org. Lett.* **2012**, *14*, 1472. (g) Zhang, H.; Yao, B.; Zhao, L.; Wang, D.-X.; Xu, B.-Q.; Wang, M.-X. *J. Am. Chem. Soc.* **2014**, *136*, 6326.

Chapter 2: Cobalt || Acetoxylation

Cobalt-Catalyzed Directed sp^2 C–H Acetoxylation of Arenes Employing $Mn(OAc)_3{\cdot}2H_2O$ As Acetoxy Source

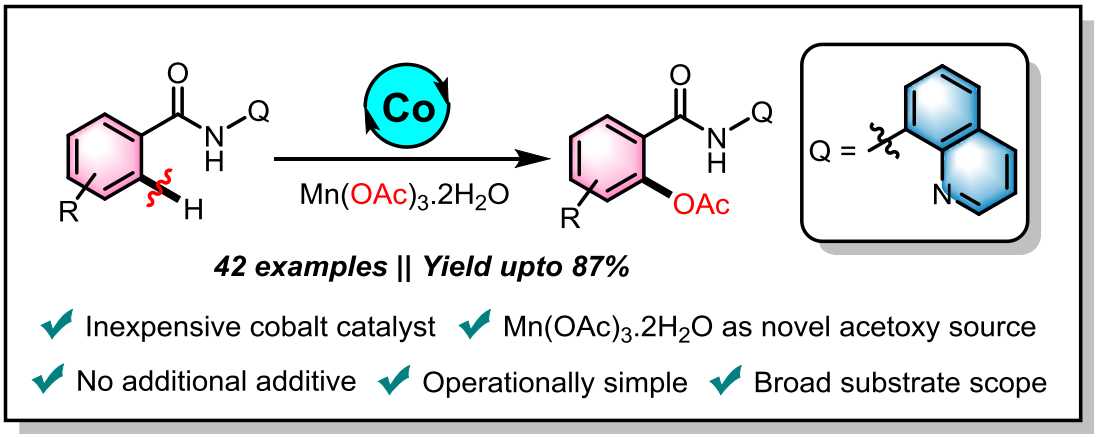

2.1. Introduction

2.1.1. Relevance of Acetoxy Functional Group Containing Compounds

The acetoxy functional group has an ability to impart polar nature to a molecule making it a good functional group modifier. It can be used as an alcohol or phenol group and also possess a unique H-bond donor-acceptor capacity. Aspirin, the acetylated form of salicylic acid, acts as an anti-inflammatory, analgesic, and antipyretic drug making it the most widely used medicine of all time, especially in persons above the age of 50. It along with other non-steroidal anti-inflammatory drugs (NSAIDs) are used in treating fever, inflammation, swelling and pain.[1] Besides, it also reduces the risks of heart attack, stroke, blood clot, and cancer. The acetoxy group binds with the serine residue of the COX-II enzyme which is responsible for the formation of prostaglandins that cause all these health complications. Acetoxy functional group containing Diltiazem is a calcium-chain blocker medicine used to reduce high blood pressure and treat heart diseases.[2]

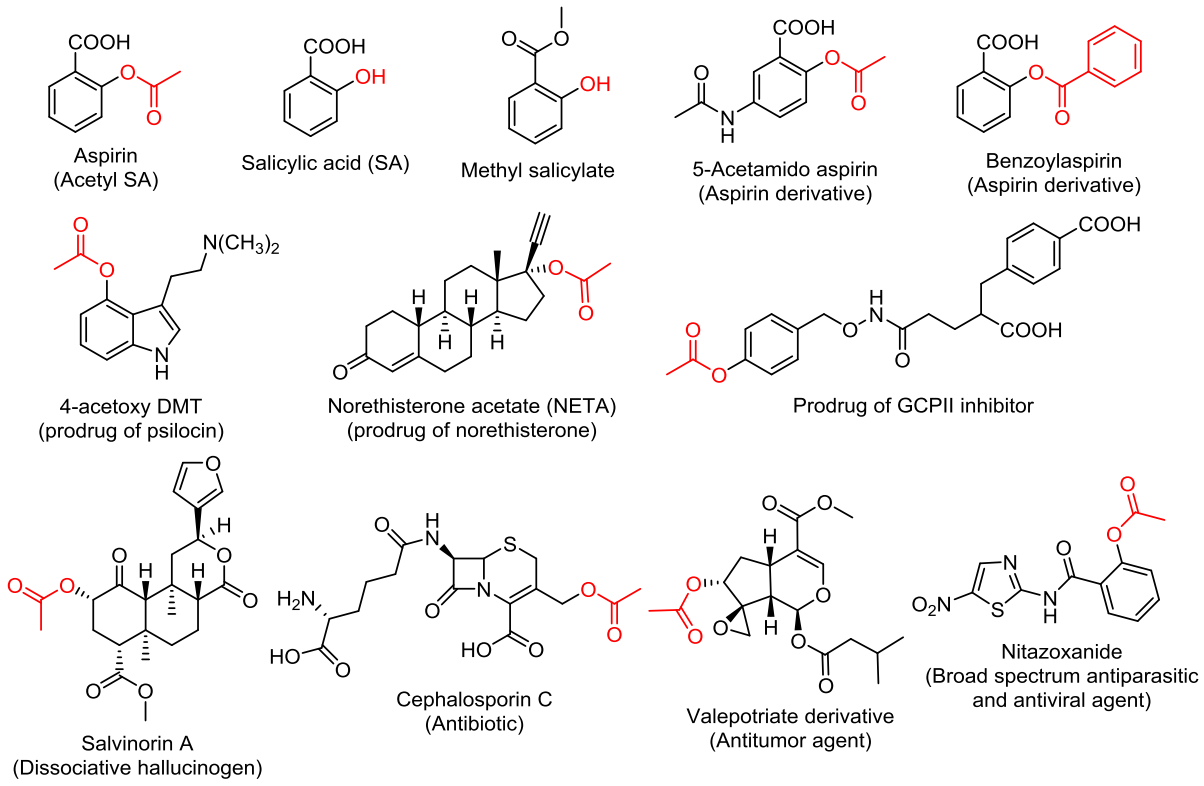

Figure 2.1.1.1. Representative examples of biologically relevant acetoxy compounds.

Salicylic acid (SA), methyl salicylate, Aspirin (Acetyl SA), and other salicylic acid derivatives are also ubiquitous in a plethora of prodrugs, marketed drugs, antimicrobial agents, herbicidal materials and natural products.[3] For example, acetoxy group containing prodrugs like PAB-based prodrug, 4-acetoxy DMT (*O*-acetyl prodrug of psilocin), Cephalosporins (antibacterial

agent), Salvinorin A (psychotopic), Pancuronium (muscle relaxant), Nitazoxanide (antiviral and anticancer), Norethisterone acetate (birth control), and many others have tremendous importance in the pharmaceutical industry and exhibit key biological activities (Figure 2.1.1.1).

2.1.2. Strategies For Transition Metal-Catalyzed C–O Bond Formation

These findings showcasing the immense importance of the acetoxy functional group have led to the development of several methodologies to introduce this functionality in different organic frameworks. C–O bonds are among the most ubiquitous connections in nature. It can be introduced in a molecule by simple oxidation of C–H bonds, however, this method carries major problems like over-oxidation, use of harsh conditions, etc. Apart from the traditional ways to introduce a C–O bond in a molecule, newer methods seeking regiospecific introduction this group in organic molecules therefore continue to be of huge interest. In this regard, the past two decades has seen transition metal-catalyzed/-mediated C–H activation technique imposing itself as one of the leading frontrunners in developing methodologies to form C–O bonds. Metal-based protocols utilizing a suitable directing group (DG) have been extensively sought-after and hence emerged as highly beneficial propositions for direct and regioselective acetoxylation,[4] acyloxylation/aroyloxylation,[5] hydroxylation,[6] and alkoxylation/aryloxylation[7] of inert C–H bonds in a step and atom-economic manner.

Among these C–H oxygenation reactions, some of the direct acetoxylation reactions are represented in Scheme 2.1.2.1. Previous reports show that C–H acetoxylation reactions catalyzed by second-row transition metal catalysts are very much well established, mostly with Pd,[8] and also a few examples with Ru[9] and Rh.[10] In 2004, Sanford group developed for the first time, a highly regio- and chemoselective Pd(II)-catalyzed direct acetoxylation as well as other oxidative functionalization reactions of both sp^2 and sp^3 C–H bonds (Scheme 2.1.2.1a).[8a] Hypervalent iodine reagent, (Diacetoxyiodo)benzene, also known as PIDA was used as an acetoxy source as well as an oxidant. They further demonstrated methodologies for palladium-catalyzed acetoxylation reaction of C(sp^2)–H and C(sp^3)–H bonds of oximes using either PIDA as a stoichiometric oxidant and acetoxy source or peroxide based oxidants in combination with AcOH as the source of acetoxy group.[8b,d,g] Yu *et al*. employed peroxide MeCOOO^{t}Bu to oxidize unactivated aliphatic C–H bonds in a Pd-catalyzed oxazoline directed acetoxylation reaction along with acetic anhydride as the promoter (Scheme 2.1.2.1b).[8c] Wang and co-workers reported an amide-directed $Pd(OAc)_2$-catalyzed *ortho* C–H acetoxylation of anilides with AcOH as an acetate source and $K_2S_2O_8$ as oxidant (Scheme 2.1.2.1c).[8e] Liang group

developed a highly regioselective arene C–H acetoxylation protocol using picolinamide (PA) and 8-aminoquinoline (8-AQ) bidentate directing groups under palladium catalysis using a PIDA and AcOH/Ac_2O system (Scheme 2.1.2.1d).[8f]

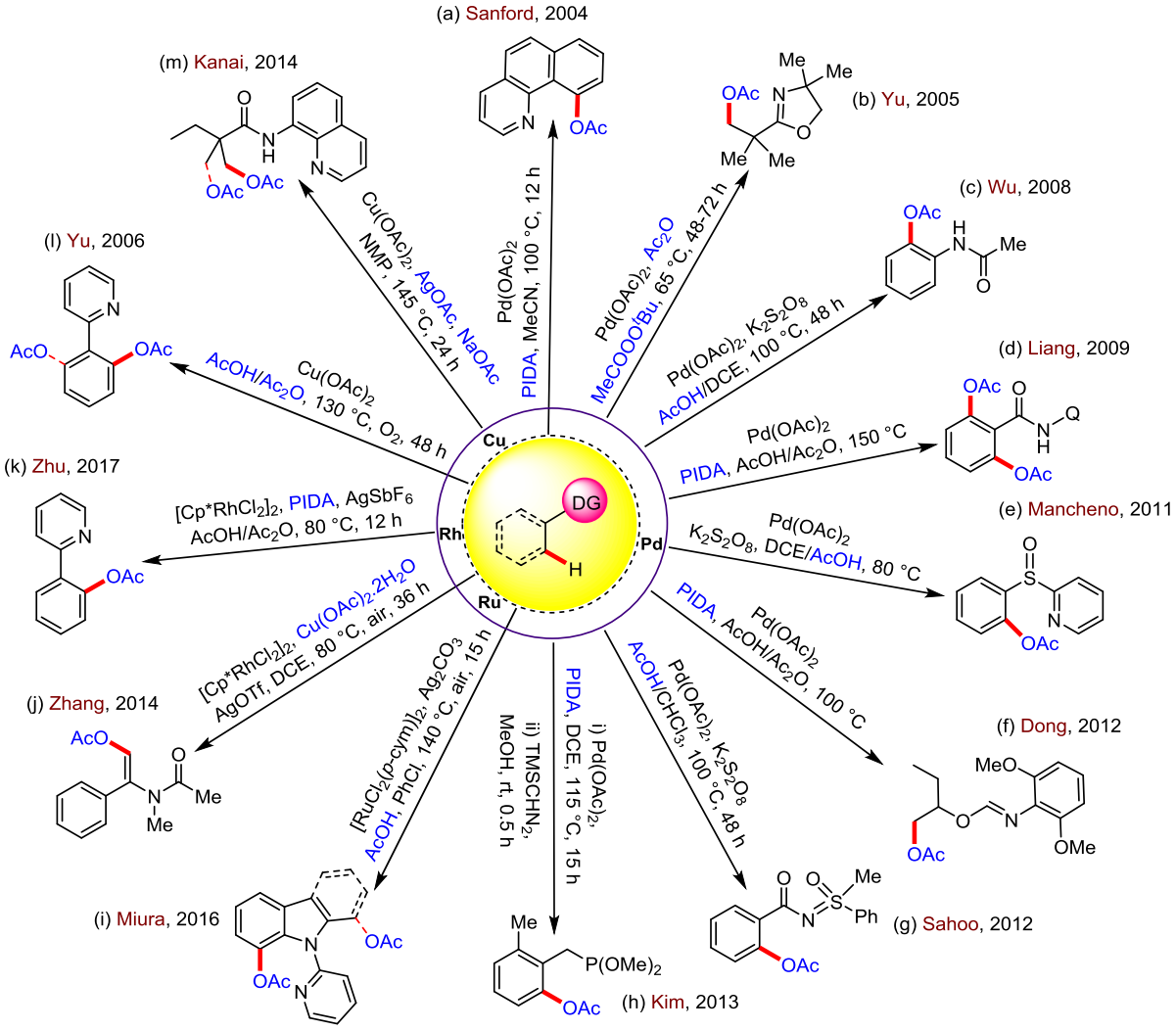

Scheme 2.1.2.1. Representative examples of direct C–H acetoxylation.

In 2011, Mancheño *et al*. designed modifiable sulfur tethers as productive chelating entities for palladium-catalyzed acetoxylation reaction of arenes bearing 2-pyridyl sulfones and sulfoxides (Scheme 2.1.2.1e).[8i] Following year, Dong and co-workers described a novel approach for the synthesis of chemically differentiated 1,2-diols via exo DG-assisted Pd-catalyzed *β*-sp^3 C–H acetoxylation employing PIDA as the acetoxy source (Scheme 2.1.2.1f).[8j] Here, oxime was used both as the DG and alcohol surrogate. Concurrently, Sahoo group reported the use of a new *S*-methyl-*S*-2-pyridyl-sulfoximine (MPyS) removable DG in a Pd-catalyzed acetoxylation of aromatic amides using AcOH as the acetoxylating agent (Scheme 2.1.2.1g).[8k] In 2013, Kim *et al*. elegantly demonstrated the use of organophosphates as efficient DGs for a palladium-

catalyzed *ortho*-acetoxylation reaction of benzyl phosphonic and aryl phosphoric monoacids (Scheme 2.1.2.1h).[8m] Besides these selected examples, several other groups have also contributed in this field.[8h,l,8n-p]

Although palladium-catalyzed C–H acetoxylation is a well-explored area of research, other transition metals have been less studied in comparison. Ruthenium catalysis was exemplified by Miura group in 2016, when they reported a regioselective acetoxylation reaction of *N*-pyridyl carbazoles and indoles with AcOH acetoxy source and Ag_2CO_3 oxidant (Scheme 2.1.2.1i).[9] Zhang and co-workers delineated the first amide-directed rhodium-catalyzed acetoxylation of vinylic sp^2 C–H bonds using silver additive and super-stoichiometric amount of copper acetate as the acetoxy source as well as the oxidant (Scheme 2.1.2.1j).[10a] Zhou reported Rh(III)-catalyzed acetoxylation of directing group-assisted arenes using PIDA as both acetate source and oxidant and AcOH as solvent at elevated temperatures (Scheme 2.1.2.1k).[10b] Around the same time, Deb *et al*. devised a protocol for Rh(III)-catalyzed acetoxylation of azaindole and indoline systems with PIDA under ambient reaction conditions.[10c]

But a major drawback associated with these noble metals is their expensive and toxic nature and low earth abundance. So, newer methodologies involving first-row transition metals were very much welcome. In this vein, only a handful of stoichiometric or sub-stoichiometric copper-promoted C–H acetoxylation methods have come up.[11] In 2006, Yu and co-workers devised the first cost-effective Cu-mediated direct C–H acetoxylation of 2-phenylpyridines using AcOH/Ac_2O combination as acetoxylating reagent and molecular oxygen playing the role of an oxidant (Scheme 2.1.2.1l).[11a] After a prolonged gap, in 2014, Kanai and Ge groups independently developed sp^3 C–H acetoxylation methodologies using 8-aminoquinoline bidentate chelation assistance under copper-promoted conditions (Scheme 2.1.2.1m).[11b,c]

2.1.3. 8-Aminoquinoline Directing Group in C–H Activation

Representing one of the many pioneering research works in the field of C–H bond activation, Daugulis, in 2005, first introduced the use 8-aminoquinoline (8-AQ) auxiliary which can serve as an efficient bidentate directing group for regioselective C–H functionalization. They reported a 8-AQ directed Pd(II)-catalyzed regioselective C–H arylation of aliphatic as well as aromatic amides using aryl iodides as an arylating agent.[12] Encouraged by this advancement, they alongwith several other groups then devised newer methodologies for diverse C–H functionalization reactions using different transition metals like Pd, Rh, Ru, Cu, Fe, Co, Ni,

etc. with the help of this versatile DG.[7f,8f,11b,c,13] The removable nature of the DG also becomes advantageous and allows the synthesis of diversely functionalized acid derivatives.

2.1.4. Cobalt-Catalyzed C–H Functionalization

Very recently, cobalt catalysts in different oxidation states have been utilized for several transformations in synthetic organic chemistry employing C–H activation strategy.[14] Low-valent cobalt catalysis (Co(0)/Co(I))[15] initiated by the seminal works of Yoshikai, and high-valent Co(III) catalysis[16] pioneered by Kanai, have inspired different research groups to design various C–H functionalization methodologies utilizing these fields. The significant drawbacks associated with these methods include the use of highly reactive Grignard reagents (in case of low-valent chemistry) or expensive Cp* ligands (in case of high-valent chemistry).

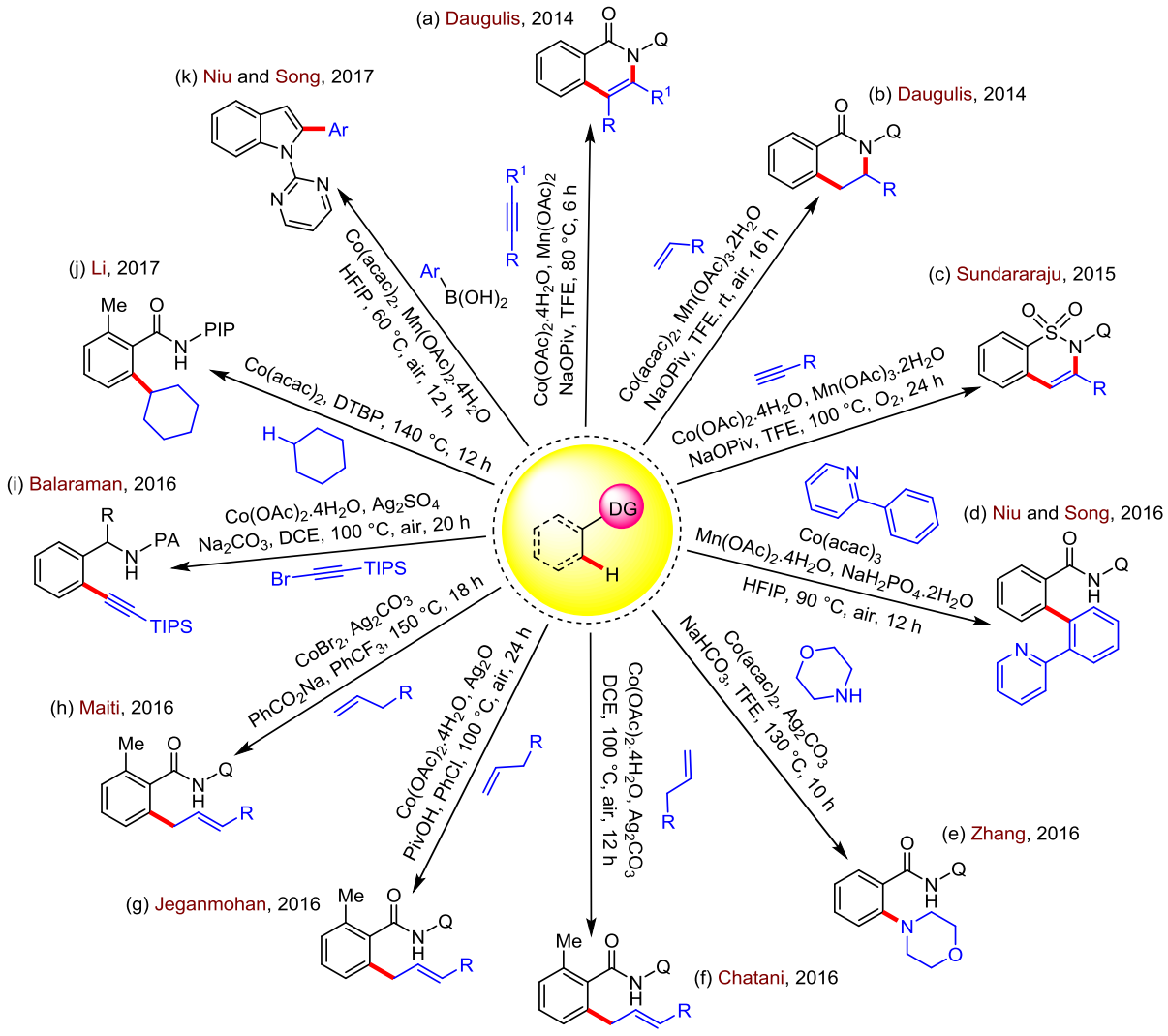

Scheme 2.1.4.1. Representative examples of Co-catalyzed direct C–H functionalization.

As a major development, in 2004, Daugulis *et al*. exemplified the use of easily affordable cobalt(II) salt as a catalyst for C–H alkenylation/annulation of 8-aminoquinoline auxiliary-assisted arylamides with alkynes (Scheme 2.1.4.1a).[13l] Since then, many groups have actively participated in developing efficient C–H functionalization reactions using simple cobalt salts (Scheme 2.1.4.1b-2.1.4.1k).[13n,17] They designed a similar protocol for Co-catalyzed alkylation/annulation of aromatic as well as olefinic amides with alkenes (Scheme 2.1.4.1b).[17a] Next year, Sundararaju and co-workers reported a C–H/N–H annulation reaction of sulfonamides with both internal as well as terminal alkynes under cobalt catalysis (Scheme 2.1.4.1c).[17b] Song and co-workers devised a [Co(acac)$_3$]-catalyzed oxidative C–H/C–H arylation between benzamides and arylpyridines to afford novel bifunctionalized biaryls applying a mixed directing group strategy (Scheme 2.1.4.1d).[17c] Zhang *et al*. developed a Co-catalyzed amination reaction of 8-AQ assisted arenes with secondary alkylamines (Scheme 2.1.4.1e).[17d] In 2016, Chatani, Jeganmohan, and Maiti groups independently delineated strategies for cobalt-catalyzed allylation reaction of 8-aminoquinoline DG-tethered aromatic amides with unactivated alkenes (Scheme 2.1.4.1f-2.1.4.1h).[13n,17e,f] Balaraman and co-workers reported a Co-catalyzed direct C–H alkynylation reaction of benzylamines attached to picolinamide bidentate chelating group (Scheme 2.1.4.1i).[17g] Li *et al*. employed cobalt catalysis to perform an oxidative cross-dehydrogenative coupling of unactivated sp^2 C–H bonds of PIP-directed arenes with sp^3 C–H bonds of alkanes, toluene derivatives, ethers and thioethers (Scheme 2.1.4.1j).[17h] In 2017, for the first time, Niu and Song group revealed the use of monodentate pyridine/pyrimidine DG in a Co(II)-catalyzed direct and selective C2-arylation of indoles with boronic acids as aryl partner (Scheme 2.1.4.1k).[17i]

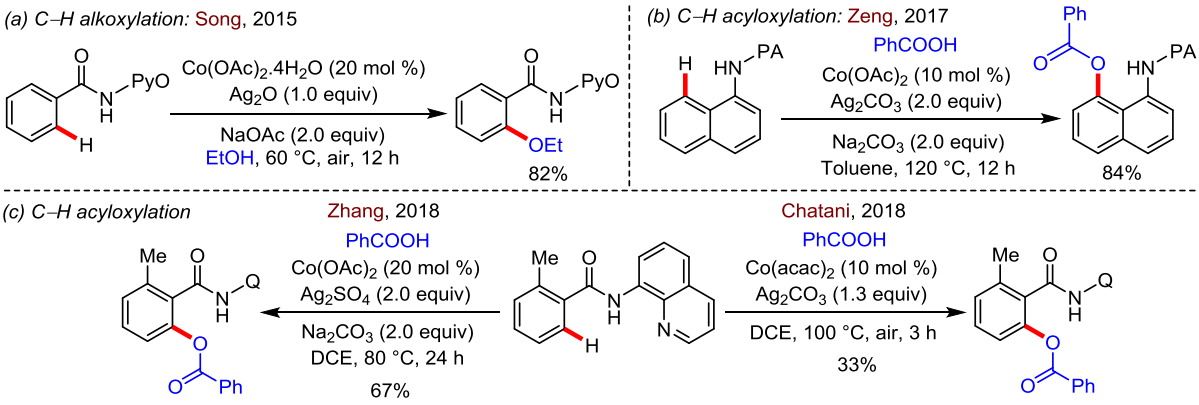

Scheme 2.1.4.2. Cobalt-catalyzed direct C–O bond formation reactions.

Most of the groundbreaking works in this field consist of various C–C and C–X (X = heteroatom) bond forming reactions, where only very few reports on direct C–O bond

formation employing cobalt catalysis were present (Scheme 2.1.4.2).[7i,18] In 2015, Song and co-workers reported a Co-catalyzed C–H alkoxylation of aromatic and olefinic carboxamides with a wide array of alcohols (Scheme 2.1.4.2a).[7i] Zeng *et al.* devised a C–H oxygenation reaction of PA directed arenes with aryl or aliphatic carboxylic acids under cobalt catalysis (Scheme 2.1.4.2b).[18a] In 2018, during our ongoing work and manuscript preparation, Zhang and Chatani groups independently developed cobalt-catalyzed acyloxylation reactions of amides with aromatic as well as aliphatic carboxylic acids with the help of bidentate 8-AQ directing group (Scheme 2.1.4.2c).[18b,c]

2.2. Objective

Directing group-assisted direct and regioselective acetoxylation reactions via transition metal-catalyzed C–H activation have emerged as powerful propositions in recent times. However, there are still a few drawbacks that need to be addressed. Most of these methods rely on Pd, Ru, Rh catalysis which are expensive in nature and also suffer from issues like bio-incompatibility and low earth abundance. A handful of stoichiometric or substoichiometric copper-mediated acetoxylation reactions have also been reported in the literature, but still an efficient catalytic method relying on the earth-abundant and cost-effective first-row transition metal catalysts in place of commonly used second-row ones continues to be highly solicited in organic synthesis. Although cobalt salts have been very recently used as an inexpensive and efficient 3d transition metal catalyst for C–H acyloxylation reaction, direct acetoxylation still remains unaccomplished. On the other hand, remarkable progress has been made exploiting both metallic and non-metallic acetoxy sources such as $Cu(OAc)_2$, AgOAc, AcOH, $PhI(OAc)_2$, etc. However, there remain a need for developing complementary methods using a new, cheap, benign source of acetoxy functional group. Taking inspiration from the pioneering works depicted above and to harness the potential of cobalt catalysis for this objective, we therefore explored a Co-catalyzed *ortho* C–H acetoxylation of 8-aminoquinoline tethered aromatic amides under operationally simple conditions, employing $Mn(OAc)_3.2H_2O$ an unprecedented acetoxy source and also as an oxidant (Scheme 2.2.1).

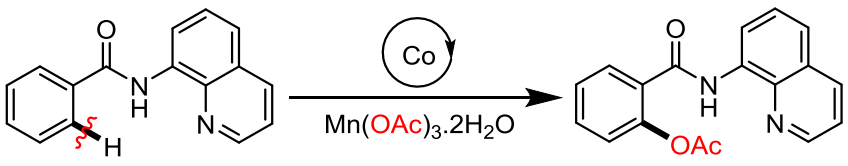

Scheme 2.2.1. Objective of this work: cobalt-catalyzed sp^2 C–H acetoxylation of benzamides.

2.3. Results and Discussion

2.3.1. Optimization Studies

We initiated our study by taking 2-methyl-*N*-(quinolin-8-yl)benzamide (**1a**) as the representative substrate for our methodology (Table 2.3.1.1). We hypothesized $Mn(OAc)_3.2H_2O$ to serve both as oxidant and acetoxy source in our reaction. To our elation, the desired product 3-methyl-2-(quinolin-8-ylcarbamoyl)phenyl acetate (**2a**) was formed in 60% yield in the presence of 10 mol % of $Co(acac)_2$ catalyst and 2.0 equiv of $Mn(OAc)_3.2H_2O$ in MeCN solvent at 85 ℃ for 24 h under N_2 atmosphere (Table 2.3.1.1, entry 1). First, various cobalt catalysts were tested (Table 2.3.1.1, entries 2-6), but all of them gave decreased yields, thus making $Co(acac)_2$ the best catalyst for the reaction. Next, we turned our attention to standardise the best solvent for the reaction. We screened various polar as well as apolar solvents such as DCE, TFE, HFIP, Toluene, 1,4-dioxane (Table 2.3.1.1, entries 7-11) and ended up with DCE was our solvent of choice (Table 2.3.1.1, entry 7). Then, we moved onto see the effect of bases on the reaction, like Na_2CO_3, $NaHCO_3$, NaOPiv, NaOAc, K_2CO_3 (Table 2.3.1.1, entries 12-16), but none of them proved beneficial in improving the yield in a substantial manner.

Now, to amplify the efficacy of the reaction we increased the loading of $Mn(OAc)_3.2H_2O$. It was observed that an increased loading of 4.0 equiv of $Mn(OAc)_3.2H_2O$ led to an elevated yield of 71% (Table 2.3.1.1, entry 17). But further increase to 5.0 equiv had a detrimental effect on the yield of the product (Table 2.3.1.1, entry 18). Again, we tried the reaction under higher temperatures to see the effect of temperature on the reaction. It was observed that on increasing the reaction temperature to 100 ℃, a further improvement in the yield occurred upto 84% (Table 2.3.1.1, entry 19), which finally became the optimized condition for our reaction. More higher temperatures led to diminished yields (Table 2.3.1.1, entry 20). A shorter reaction time of 18 h produced **2a** in lesser yield of 74% (Table 2.3.1.1, entry 20). Replacing the oxidant cum acetoxy source with other common ones such as $Mn(OAc)_2$ and $Cu(OAc)_2$ did not produce the acetoxylated product, whereas AgOAc and PIDA furnished the product in lower yields (Table 2.3.1.1, entries 22-25). So, $Mn(OAc)_3.2H_2O$ was continued as the choice of oxidant and "OAc" source. The use of other common additives, *viz*. AcOH and Ac_2O which act as common acetoxylating agents were also not beneficial (Table 2.3.1.1, entries 26-27). We also wanted to check the effect of commonly used ligands (1,10 phen, PPh_3) if they were advantageous for the current protocol, but no improvements in the yield was observed, showing that ligands played no role in this reaction (Table 2.3.1.1, entries 28-29).

Table 2.3.1.1. Optimization of reaction conditions[a]

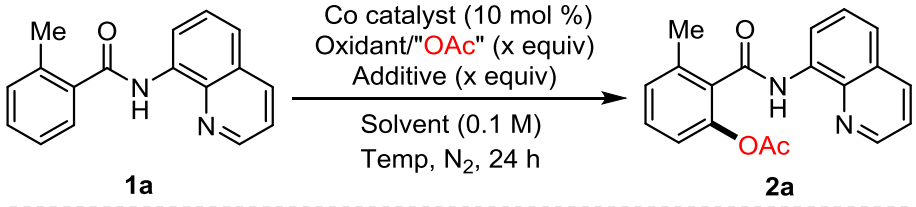

1a **2a**

Entry	Co catalyst (10 mol %)	Oxidant/ "OAc" (x equiv)	Additive (x equiv)	Solvent (0.1 M)	Temp (°C)	Yield of **2a**[b] (%)
1	$Co(acac)_2$	$Mn(OAc)_3.2H_2O$ (2.0)	-	MeCN	85	60
2	$Co(OAc)_2$	$Mn(OAc)_3.2H_2O$ (2.0)	-	MeCN	85	16
3	$Co(OAc)_2.4H_2O$	$Mn(OAc)_3.2H_2O$ (2.0)	-	MeCN	85	13
4	$Co(C_2O_4).2H_2O$	$Mn(OAc)_3.2H_2O$ (2.0)	-	MeCN	85	10
5	$CoBr_2$	$Mn(OAc)_3.2H_2O$ (2.0)	-	MeCN	85	nr
6	$Co(acac)_3$	$Mn(OAc)_3.2H_2O$ (2.0)	-	MeCN	85	13
7	$Co(acac)_2$	$Mn(OAc)_3.2H_2O$ (2.0)	-	DCE	85	64
8	$Co(acac)_2$	$Mn(OAc)_3.2H_2O$ (2.0)	-	TFE	85	17
9	$Co(acac)_2$	$Mn(OAc)_3.2H_2O$ (2.0)	-	HFIP	85	nr
10	$Co(acac)_2$	$Mn(OAc)_3.2H_2O$ (2.0)	-	Toluene	85	60
11	$Co(acac)_2$	$Mn(OAc)_3.2H_2O$ (2.0)	-	1,4-dioxane	85	53
12	$Co(acac)_2$	$Mn(OAc)_3.2H_2O$ (2.0)	Na_2CO_3 (2.0)	DCE	85	57
13	$Co(acac)_2$	$Mn(OAc)_3.2H_2O$ (2.0)	$NaHCO_3$ (2.0)	DCE	85	66
14	$Co(acac)_2$	$Mn(OAc)_3.2H_2O$ (2.0)	NaOAc (2.0)	DCE	85	34
15	$Co(acac)_2$	$Mn(OAc)_3.2H_2O$ (2.0)	K_2CO_3 (2.0)	DCE	85	8
16	$Co(acac)_2$	$Mn(OAc)_3.2H_2O$ (2.0)	NaOPiv (2.0)	DCE	85	37
17	$Co(acac)_2$	$Mn(OAc)_3.2H_2O$ (4.0)	-	DCE	85	71
18	$Co(acac)_2$	$Mn(OAc)_3.2H_2O$ (5.0)	-	DCE	85	66
19	**$Co(acac)_2$**	**$Mn(OAc)_3.2H_2O$ (4.0)**	**-**	**DCE**	**100**	**84 (78)[c]**
20	$Co(acac)_2$	$Mn(OAc)_3.2H_2O$ (4.0)	-	DCE	110	61
21[d]	$Co(acac)_2$	$Mn(OAc)_3.2H_2O$ (4.0)	-	DCE	100	74
22	$Co(acac)_2$	$Mn(OAc)_2$ (4.0)	-	DCE	100	nr
23	$Co(acac)_2$	$Cu(OAc)_2$ (4.0)	-	DCE	100	nr
24	$Co(acac)_2$	AgOAc (4.0)	-	DCE	100	32
25	$Co(acac)_2$	$PhI(OAc)_2$ (4.0)	-	DCE	100	25
26	$Co(acac)_2$	$Mn(OAc)_3.2H_2O$ (4.0)	Ac_2O (10.0)	DCE	100	51
27	$Co(acac)_2$	$Mn(OAc)_3.2H_2O$ (4.0)	AcOH (16.0)	DCE	100	71
28	$Co(acac)_2$	$Mn(OAc)_3.2H_2O$ (4.0)	PPh_3 (0.2)	DCE	100	70
29	$Co(acac)_2$	$Mn(OAc)_3.2H_2O$ (4.0)	1,10-phen (0.1)	DCE	100	69
30[e]	$Co(acac)_2$	$Mn(OAc)_3.2H_2O$ (4.0)	-	DCE	100	69
31[f]	$Co(acac)_2$	$Mn(OAc)_3.2H_2O$ (4.0)	-	DCE	100	80
32	-	$Mn(OAc)_3.2H_2O$ (4.0)	-	DCE	100	nr
33	$Co(acac)_2$	-	-	DCE	100	nr

[a]Reaction conditions: Unless otherwise mentioned, substrate **1a** (0.1 mmol, 1.0 equiv), Co catalyst (10 mol %), Oxidant/"OAc" (x equiv), Additive (x equiv), Solvent (1.0 mL, 0.1 M), Temp (°C), under N_2 for 24 h. [b]Isolated yield. [c]Yield for 0.2 mmol scale. [d]reaction run for 18 h. [e]$Co(acac)_2$ (5 mol %). [f]reaction was performed under air. nr: no reaction.

When $Co(acac)_2$ was used in 5 mol % amount, the yield of **2a** lowered to 69% (Table 2.3.1.1, entry 30). On performing the reaction under air atmosphere instead of inert conditions, slight decrease in the yield was noted (Table 2.3.1.1, entry 31). Control experiments proved the essentiality of the cobalt catalyst and $Mn(OAc)_3.2H_2O$ for the acetoxylation reaction, since in their absence no product formation occurred (Table 2.3.1.1, entries 32-33).

2.3.2. Scope of the Reaction

A series of benzamides (**1**) were prepared depicted in Table 2.3.2.1 following the literature procedure, discussed in the experimental section.

Table 2.3.2.1. List of aromatic amide substrates prepared

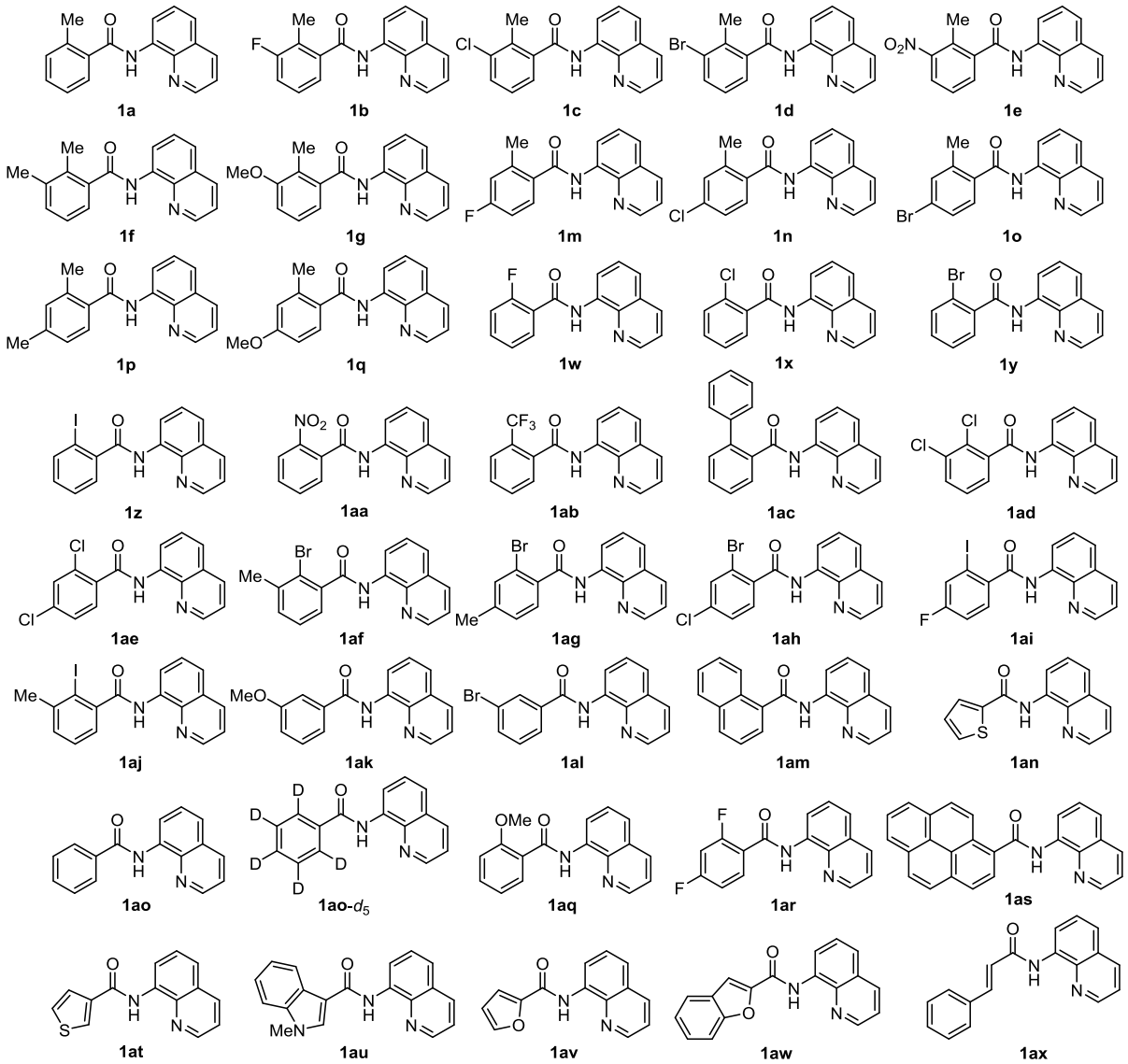

Some substrates (**1h-1l**, **1r-1v**) were prepared by Suzuki cross-coupling method depicted in Table 2.3.2.2, following the literature procedure, discussed in the experimental section.

Table 2.3.2.2. List of aryl-substituted aromatic amide substrates prepared

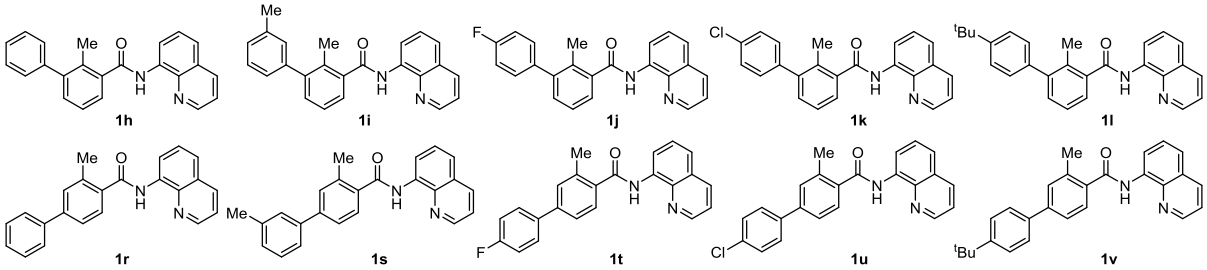

After the preparation of the substituted benzamides (**1**), they were subjected to acetoxylation under the optimized condition to evaluate the scope of the reaction (Table 2.3.2.3). The results showed that in general, the reactivity of substrates *meta*-substituted with electron-donating or electron-withdrawing groups was marginally higher than those of *para*-substituted ones. Electron-withdrawing halogen functional groups like fluoro, chloro or bromo in 3-substituted amides of *o*-toluic acid gave the desired products **2b**-**2d** in good to excellent yields (76–87%). However, the substrate bearing nitro group at the same position (**1e**) underwent moderate conversion (**2e**, 22%). On the other hand, electron-donating groups such as methyl, methoxy at this position gave a satisfactory yield (up to 69%) of desired products **2f**-**2g**. We also explored various aryl substituted benzamides carrying either electron-donating or withdrawing substituents (**1h**-**1l**), giving moderate to good yields. Examining the reactivity of different substituents at the *para* position of amide featuring electron-withdrawing groups (**1m**-**1o**) as well as electron-donating groups (**1p**-**1q**), the yields continued to be satisfactory (55-74%). Different aryl group tethered amides at this position bearing both electron-rich (Ph, Me, ^{t}Bu) and electron-poor functional groups (F, Cl) showed moderate to good conversion (**2r**-**2v**) (up to 62% yield).

Now, apart from methyl group at the *ortho* position of the benzamide, we also screened the presence of other diverse functional groups like fluoro, chloro, bromo, iodo, nitro, trifluoromethyl and phenyl (**1w**-**1ac**). Gratifyingly, they delivered the desired products (**2w**-**2ac**) in moderate to good yields, where stronger electron-withdrawing groups such as fluoro and nitro gave lower yields of 29% and 31% respectively. Next, we moved onto various di-substituted amides **1ad**-**1aj** containing divergent functional groups like F, Cl, Br, I in different combinations, which also furnished the corresponding products **2ad**-**2aj** in moderate yields (up to 64%). Only *meta*-decorated amides featuring methoxy group (**1ak**) and bromo group (**1al**) afforded the mono-acetoxylated products **2ak** and **2al** regioselectively in comparatively inferior yields of 24% and 29% respectively. This showed that *ortho* substitution was necessary

for better conversion probably because of the better chelation of the bidentate 8-aminoquinoline auxiliary with the metal catalyst, and also the rising possibility of bis-acetoxylation in cases without *ortho* substitution.

Table 2.3.2.3. Scope of acetoxylation of arylamides[a]

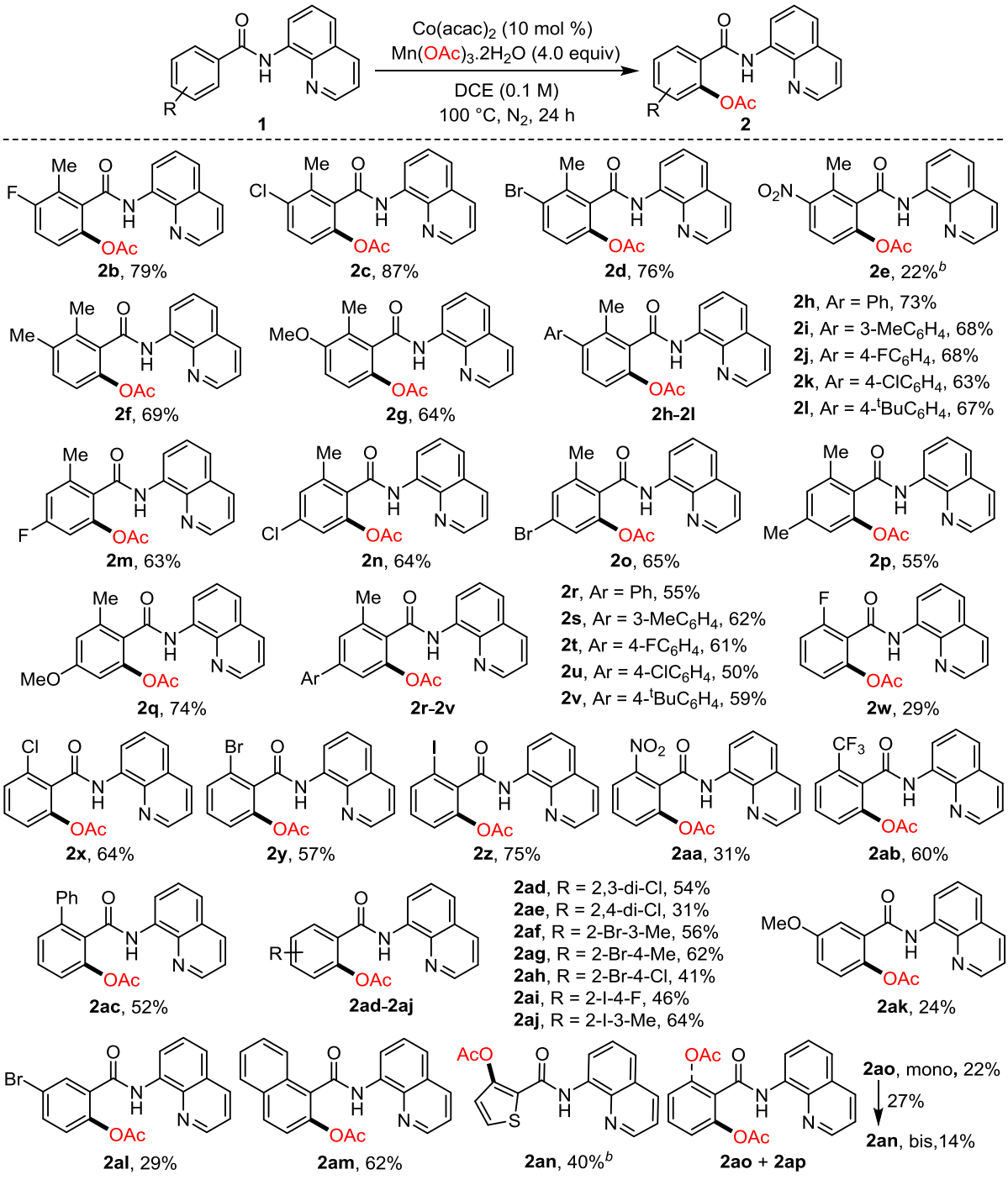

[a]Reaction conditions: Unless otherwise mentioned, **1** (0.2 mmol, 1.0 equiv), $Co(acac)_2$ (10 mol %), $Mn(OAc)_3.2H_2O$ **(**4.0 equiv**)** in DCE (2.0 mL) at 100 °C for 24 h under nitrogen. [b]0.1 mmol scale.

The naphthyl substrate **1am** successfully reacted to deliver the acetoxylated product **2am** in 62% yield. Interestingly, the current protocol also tolerated the heterocyclic thiophene carboxamide **1an** and produced the desired product **2an** in 40% yield. However, the unsubstituted benzamide **1ao** produced both mono- and bis-acetoxylated products, **2ao** and **2ap**, in 22% and 14% yields respectively. Attempts to improve the yield of **2ap** failed by increasing the loading of $Mn(OAc)_3.2H_2O$ and also running the reaction for more time. To our curiosity, when the *ortho*-substituted *O*-acetyl product **2ao** was tried as a substrate under the standard condition, bis-acetoxy product **2ap** was obtained in a low yield of 27%.

All the acetoxylated products (**2**) were duly characterised by ^1H, ^{13}C NMR and HRMS. Single-crystal X-ray analysis of **2a, 2d** and **2z** further confirmed their structures (Figure 2.3.2.1).

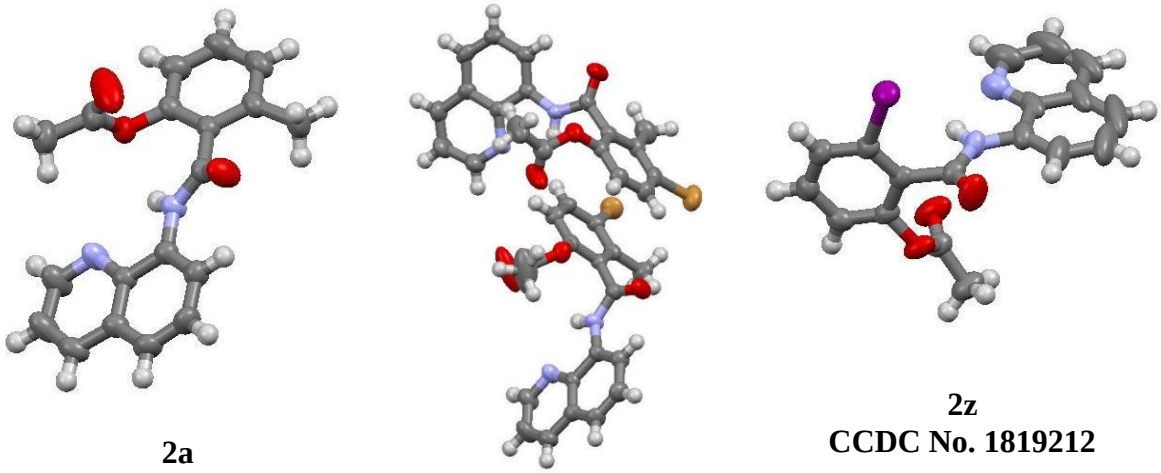

2a
CCDC No. 1819213

2d
CCDC No. 1819214

2z
CCDC No. 1819212

Figure 2.3.2.1. X-ray crystal structures of **2a, 2d** and **2z** (ellipsoid contour at 50% probability level).

The substrates which failed to deliver the desired product or displayed very trace amount of conversion are shown in Figure 2.3.2.2. Strong electron-donating *ortho* methoxy (**1aq**) and electron-withdrawing 2,4-di-fluoro (**1ar**) gave trace amount of their corresponding acetoxylated products probably due to electronic reasons. Bulky pyrene carboxamide (**1as**) did not furnish its desired product maybe due to steric reasons. Other heterocyclic variants (**1at-1aw**) could not be acetoxylated under the present catalytic condition probably because of electronic reasons. Another sp^2 variety of the amide substrate (**1ax**) was also checked under the standard condition but did not furnish any acetoxylated product, again maybe due to electronic as well as coordination issues.

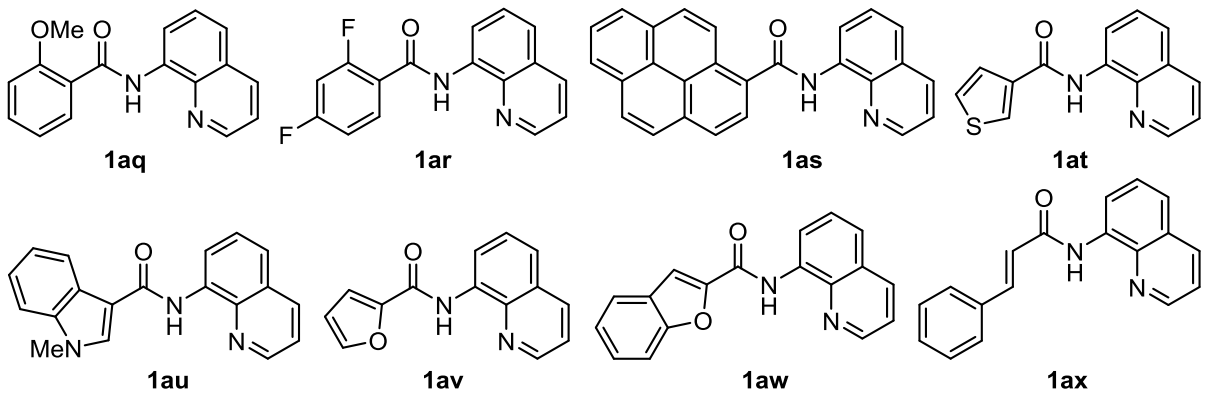

Figure 2.3.2.2. List of failed substrates.

Also, we tried the present acetoxylation reaction on various commonly used bidentate DG attached substrates (**I-V**) in the field of C–H activation. But either they did not participate or showed poor conversion under the optimized condition (Figure 2.3.2.3). Substrate **VI** did not undergo the reaction, thus emphasizing the fact of bidentate coordination taking place between the substrate and cobalt catalyst before the occurrence of the C–H activation reaction.

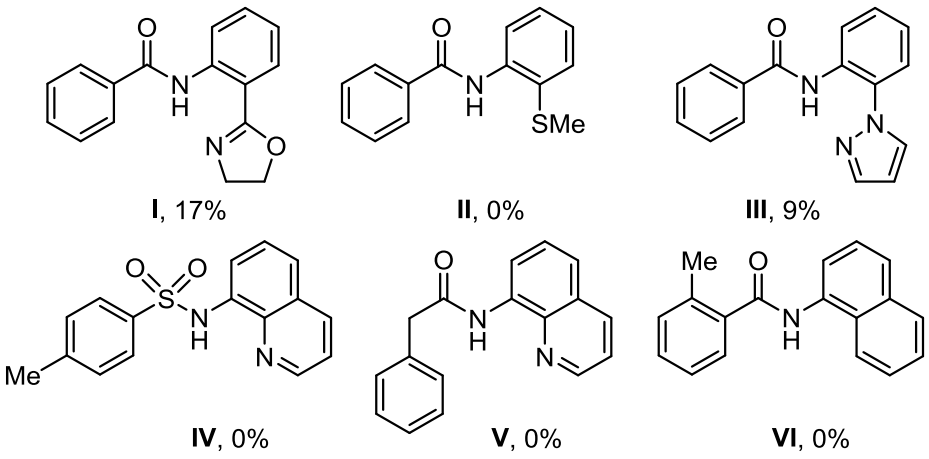

Figure 2.3.2.3. List of unsuccessful bidentate DG attached substrates.

2.3.3. Gram-Scale Reaction and Synthetic Transformation of the Product

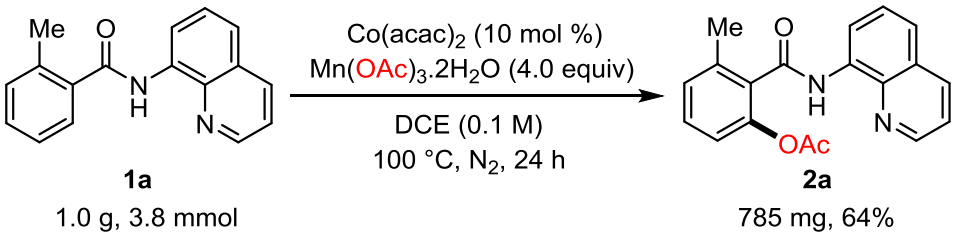

Scheme 2.3.3.1. Gram-scale reaction.

To illustrate the generality and applicability of our methodology, we conducted a scale-up experiment using 1.0 g of the substrate **1a** and obtained the acetoxylated product **2a** in 64% isolated yield (0.785 g) (Scheme 2.3.3.1).

In order to explore the synthetic utility of the acetoxy group, **2a** was successfully hydrolysed in presence of KOH in methanol to obtain the hydroxylated product **3** in an excellent yield of 95% (Scheme 2.3.3.2). This provided an alternative way to get access to *ortho* hydroxylated benzamides.

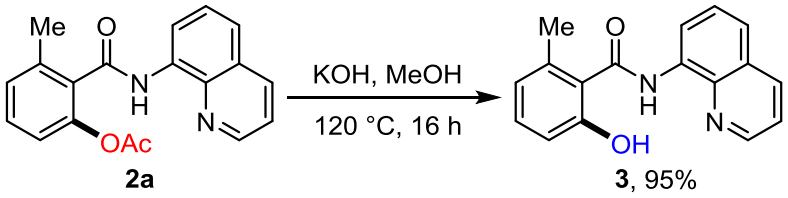

Scheme 2.3.3.2. Hydrolysis of the acetoxylated product.

2.3.4. Mechanistic Experiments and Plausible Mechanism

To have a thorough understanding of the mechanism of the present acetoxylation reaction, a series of kinetic experiments were performed.

When **1ao** was subjected to the standard conditions in presence of $Mn(OAc)_3.2H_2O$ for shorter reaction time and quenched with excess CD_3OD, deuterium-proton exchange was observed in the recovered starting material as well as in the mono-OAc product (Scheme 2.3.4.1a). ^1H NMR studies showed 24% D-incorporation in case of **1ao**-d_n and 32% in case of **2ao**-d_n (Figure 2.3.4.1 and 2.3.4.2). The result illustrated the reversible nature C–H bond cleavage step.

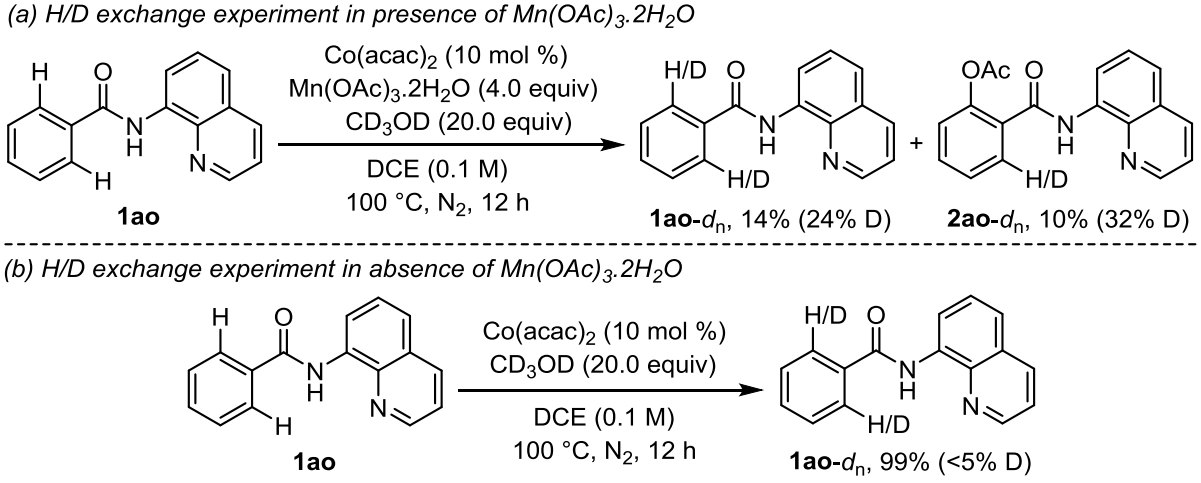

Scheme 2.3.4.1. H/D exchange experiments with excess CD_3OD.

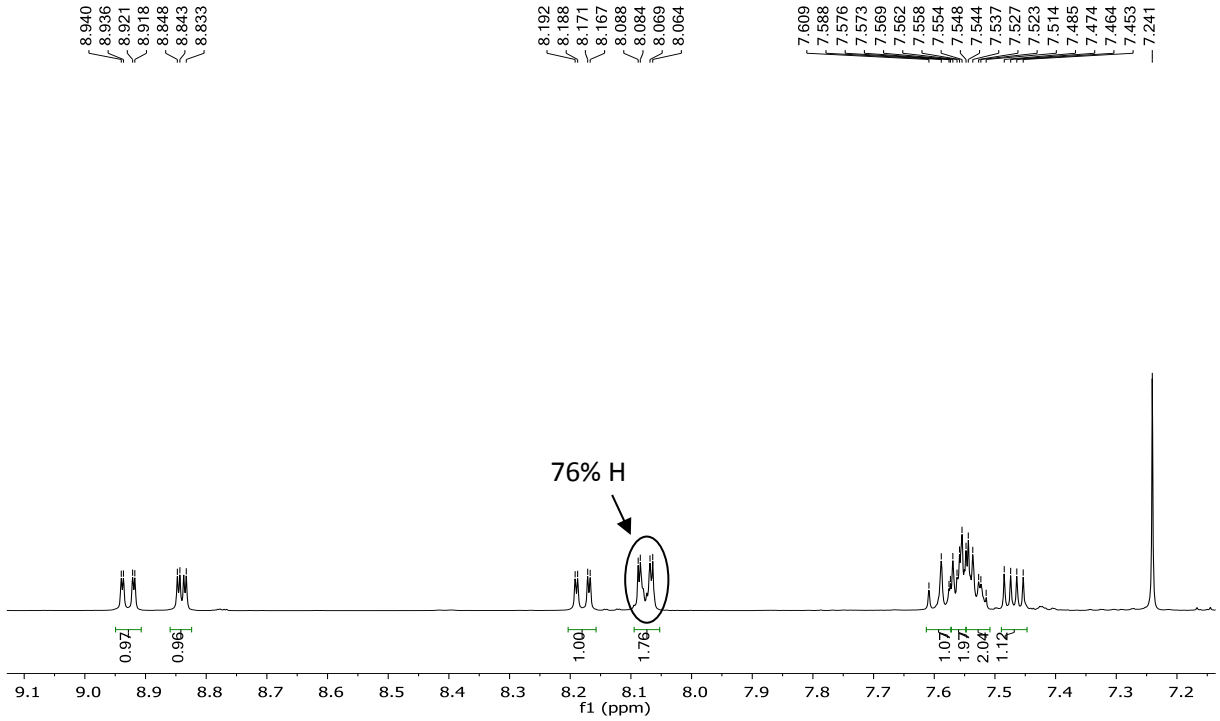

Figure 2.3.4.1. ^{1}H NMR spectrum of **1ao**-d_n after H/D exchange experiment in presence of $Mn(OAc)_3.2H_2O$.

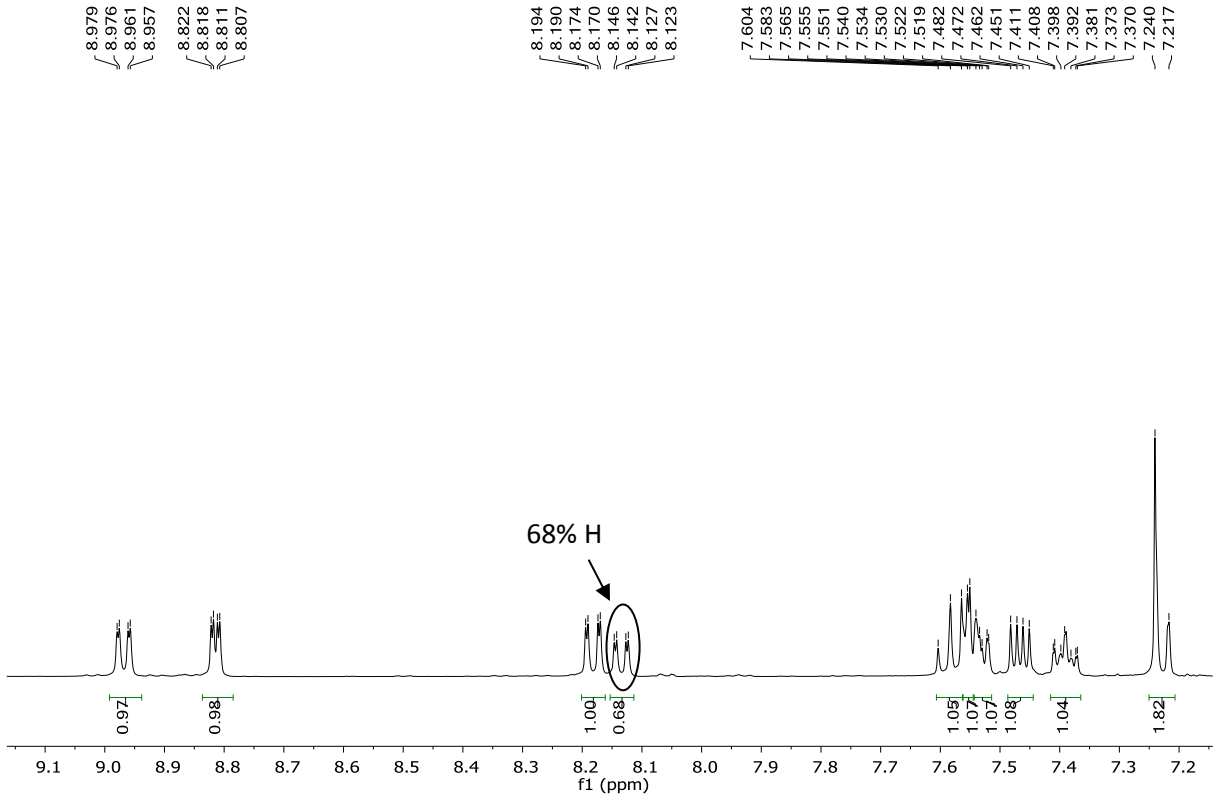

Figure 2.3.4.2. ^{1}H NMR spectrum of **2ao**-d_n after H/D exchange experiment in presence of $Mn(OAc)_3.2H_2O$.

On the contrary, when **1ao** was subjected to the standard conditions in absence of $Mn(OAc)_3.2H_2O$ for shorter reaction time and quenched with excess CD_3OD, no H/D exchange was observed in the recovered starting material (Scheme 2.3.4.1b). The deuterium incorporation (<5%) was determined by ^1H NMR spectroscopy (Figure 2.3.4.3). This result proved that an initial oxidation of Co(II) to Co(III) takes place in presence of $Mn(OAc)_3.2H_2O$, formation of which is essential for the C–H bond activation to occur.

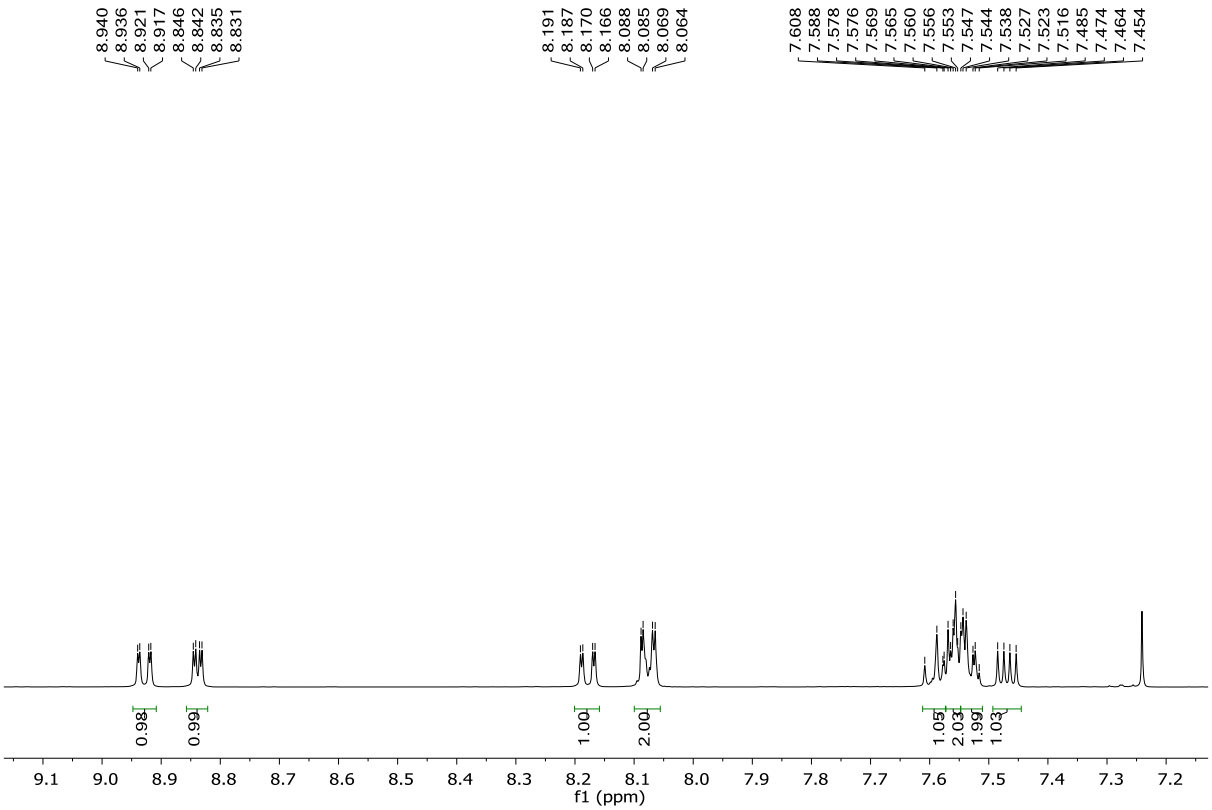

Figure 2.3.4.3. ^1H NMR spectrum of **1ao**-d_n after H/D exchange experiment in absence of $Mn(OAc)_3.2H_2O$.

A set of parallel reactions between **1ao** and **1ao**-d_5 were performed separately under the standard condition for shorter reaction time (Scheme 2.3.4.2) and the ratio of **2ao** and **2ao**-d_4 was determined by ^1H NMR spectroscopy (Figure 2.3.4.4).

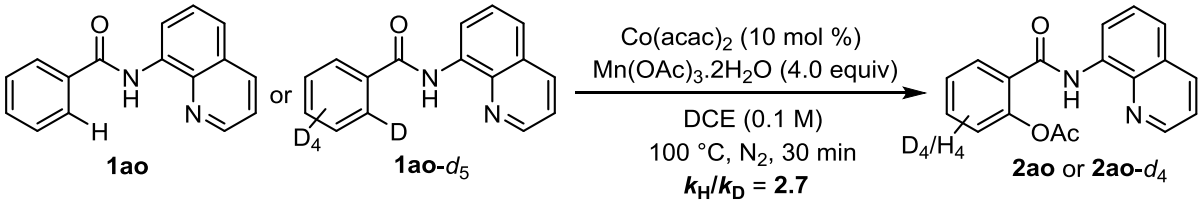

Scheme 2.3.4.2. Parallel experiment between **1ao** and **1ao**-d_5.

Primary kinetic isotopic effect (KIE) was found to be k_H/k_D = (0.73/0.27) = 2.7.

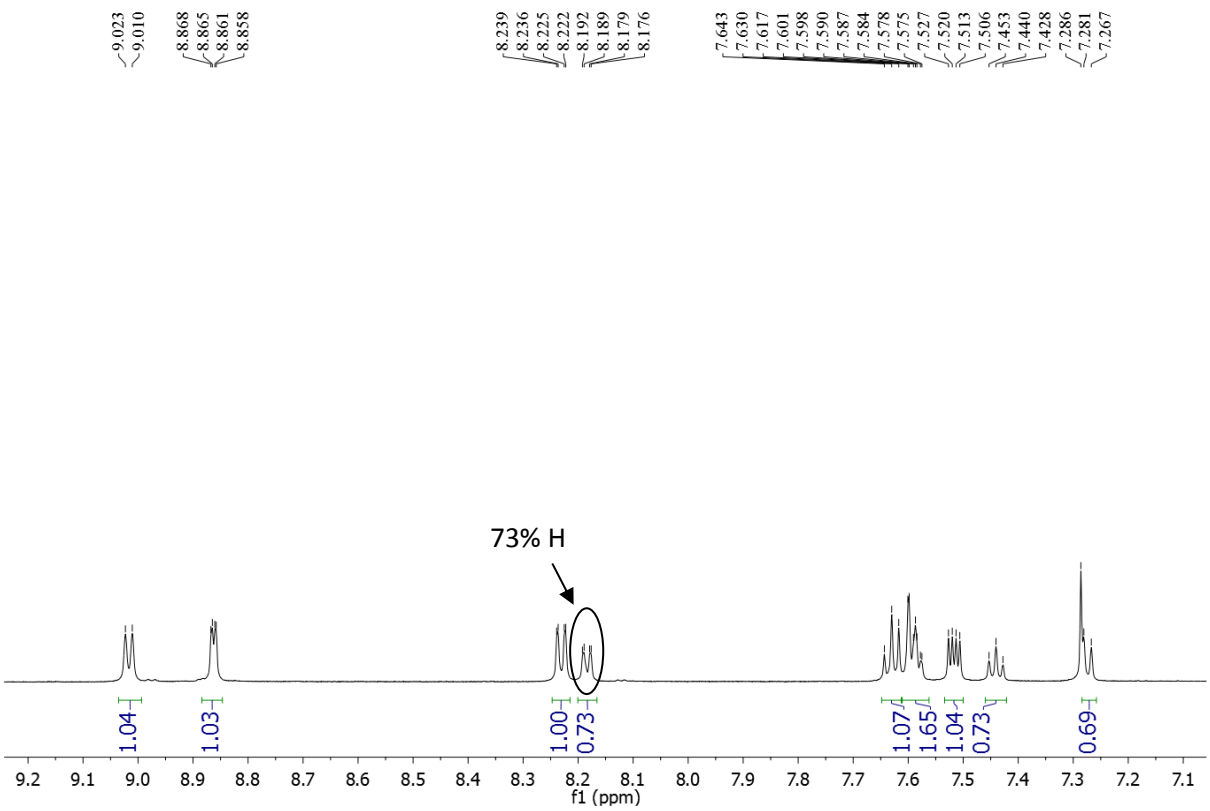

Figure 2.3.4.4. ^{1}H NMR spectrum for parallel experiment between **1ao** and **1ao**-d_5.

A mixture of **1ao** and **1ao**-d_5 was subjected to standard condition in the same reaction vessel for shorter reaction time (Scheme 2.3.4.3) and the ratio of **2ao** and **2ao**-d_4 was determined by ^{1}H NMR spectroscopy (Figure 2.3.4.5).

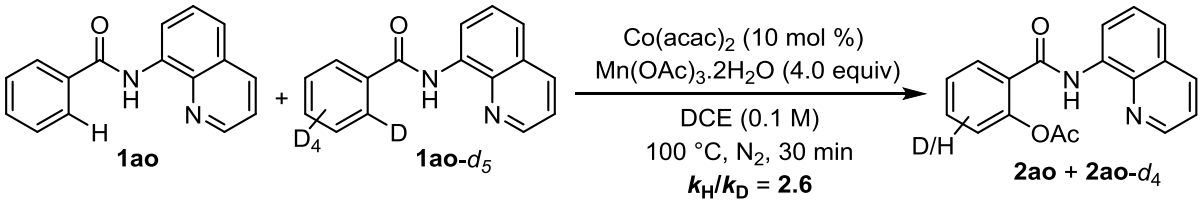

Scheme 2.3.4.4. Competitive experiment between **1ao** and **1ao**-d_5.

Primary kinetic isotopic effect (KIE) was found to be k_H/k_D = (0.72/0.28) = 2.6.

Kinetic isotope effect (KIE) values of 2.7 and 2.6 in the intermolecular parallel and competitive experiments respectively between **1ao** and **1ao**-d_5 implied that the *ortho* C−H bond cleavage of the benzamide may be involved in the turn over limiting step of the mechanism.

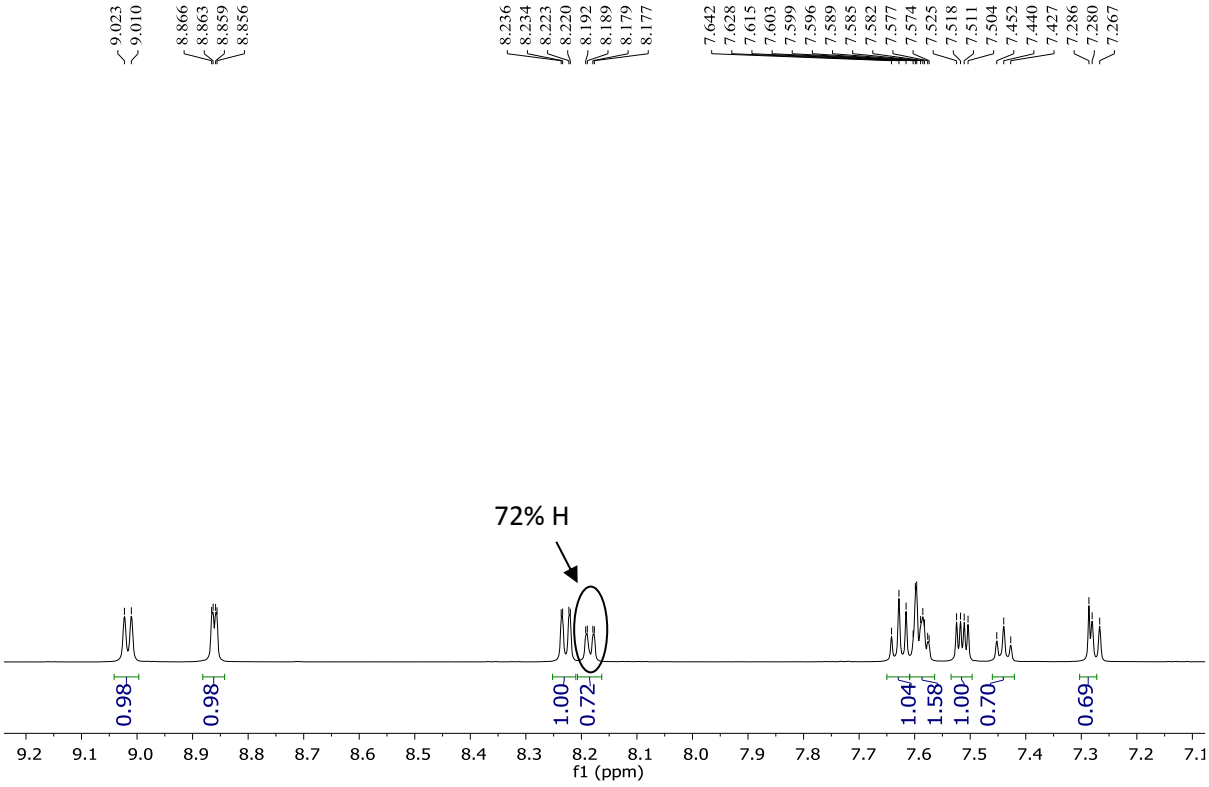

Figure 2.3.4.5. ^{1}H NMR spectrum for competitive experiment between **1ao** and **1ao**-d_5.

When a mixture of electron-donating group containing substrate **1q** and electron-withdrawing group containing substrate **1n** (1:1 ratio) was reacted under the standard condition for shorter reaction time, the corresponding acetoxylated products **2q** and **2n** were isolated in 36% and 35% yields respectively. This result suggested the absence of any significant substituent effect in the competitive experiment of the substrates (Scheme 2.3.4.5).

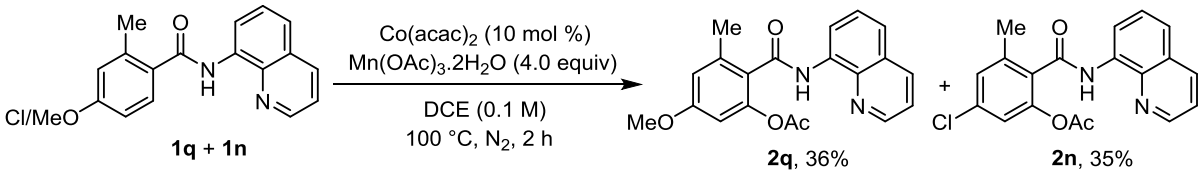

Scheme 2.3.4.5. Competitive experiment between **1q** and **1n**.

We prepared the complex **C$_1$** from a stoichiometric reaction between substrate **1a** and $Co(acac)_2$ following literature procedure discussed in the experimental section. When we performed the acetoxylation reaction treating **C$_1$** as the catalyst under standard conditions, the desired product **2a** was obtained in 80% yield (Scheme 2.3.4.6), comparable to that achieved using $Co(acac)_2$, indicating that the complex is capable of acting as a catalyst for the current protocol and may serve as one of the possible intermediates in the reaction mechanism.

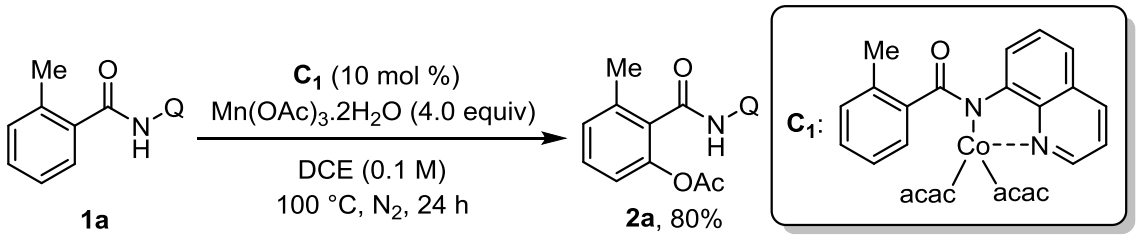

Scheme 2.3.4.6. Acetoxylation reaction with complex **C₁** as catalyst.

On the basis of the above mechanistic studies and previous reports,[18b,c,19] a plausible reaction pathway is proposed as depicted in Scheme 2.3.4.7. Initially, Co(II) species undergoes coordination with the *N*,*N*-bidentate 8-aminoquinoline directing group of substrate **1a** to give intermediate **A**, which is oxidized by $Mn(OAc)_3.2H_2O$ to the Co(III) species (intermediate **B**). A concerted metalation-deprotonation process takes place for the *ortho* C(sp^2)–H activation step affording a bis-chelated metallacyclic complex **C**, which then undergoes reductive elimination to yield the corresponding acetoxylated product **2a** and generates the Co(I) species. Finally, reoxidation of Co(I) to Co(II) by $Mn(OAc)_3.2H_2O$, which acts as both the acetoxy source and terminal oxidant, then continues the catalytic cycle.

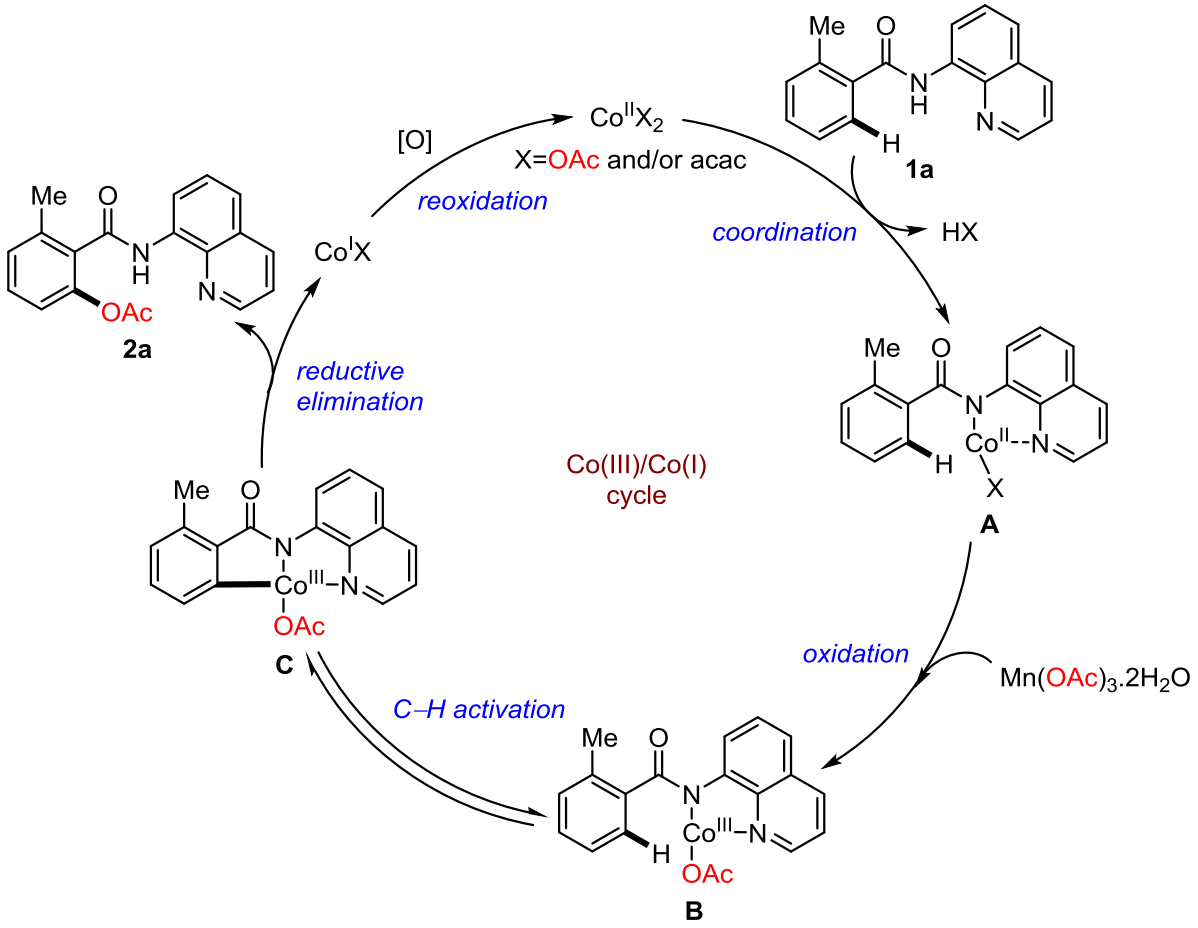

Scheme 2.3.4.7. Plausible reaction mechanism.

2.4. Summary

In summary, we have developed an 8-aminoquinoline directing group assisted cobalt-catalyzed *ortho* C(sp^2)–H acetoxylation of unactivated arenes. This reaction protocol is appealing due to the use of inexpensive cobalt catalyst, employment of simple reaction conditions, absence of any external additive and unravels a novel acetoxy source in $Mn(OAc)_3.2H_2O$. The methodology features a broad scope of substrates and tolerates a wide range of functional groups, and the usefulness of the method has been verified by synthesizing diversely functionalized molecules. This method is scalable also, which was supported by conducting a gram scale experiment and the synthetic utility of the acetoxy group was further illustrated by performing a chemical transformation to the hydroxyl group by simple hydrolysis. A series of kinetic experiments were performed in order to understand the mechanism of the reaction. It was concluded that a reversible cleavage of the C−H bond may be involved in the reaction and the *ortho* C−H cleavage step may be the rate limiting step of the reaction.

2.5. Experimental Section

2.5.1. General Information

All reactions were carried out in oven-dried reaction vessels under nitrogen atmosphere unless otherwise mentioned. TLC analysis was performed on Merck 60 F_{254} silica gel TLC plates. Column chromatography was done using 230−400 mesh silica gel by applying pressure through an air pump. ^1H and ^{13}C NMR spectra were recorded on 300, 400 and 600 MHz spectrometers and are reported as chemical shifts (δ) in parts per million (ppm), and multiplicities are abbreviated as s = singlet, d = doublet, t = triplet, q = quartet, m = multiplet, comp = complex, app = apparent. Internal standards or residual solvent signals were used as reference. HRMS (m/z) was recorded using ESI (Q-Tof and Orbitrap, positive ion) and EI (magnetic sector, positive ion) mode. Melting points were determined in a capillary melting point apparatus and are uncorrected. Single crystal X-ray diffraction data were collected on Bruker APEX II diffractometer with a graphite monochromator using Mo Kα radiation and Bruker D8 Venture with a microfocus optics using Cu Kα radiation.

The CIF files were submitted to CCDC (1819212-1819214) and can be obtained at https://summary.ccdc.cam.ac.uk/structure-summary-form.

2.5.2. General Procedure for the Preparation of Starting Materials

All the benzamides (**1**) were prepared following literature method. Different commercially available benzoic acids were converted to their corresponding acid chlorides which were coupled with 8-aminoquinoline to get the desired benzamides (Scheme 2.5.2.1).[13g,l,n] To a solution of the benzoic acids (1.1 equiv), DMF (3-5 drops) and DCM under N_2 atmosphere, was added oxalyl chloride (1.2 equiv) dropwise under ice-cold condition. The ice bath was removed and the reaction mixture was stirred at room temperature for 5 h. Another solution of 8-aminoquinoline (1.0 equiv), Et_3N (1.5 equiv), DMAP (0.2 equiv) in DCM was stirred at room temperature under N_2 atmosphere and then allowed to cool to 0 ℃. To this solution, the acid chlorides in DCM was added dropwise under ice-cold condition, the ice bath was removed and the reaction mixture was stirred overnight at room temperature. After completion of the reaction, the reaction mixture was quenched with water and extracted with DCM (3 times). The combined organic layers were washed with brine, the organic phase was separated and dried over anhydrous Na_2SO_4, filtered and concentrated under vacuo. The crude reaction mixture was directly purified by column chromatography on silica gel using petroleum ether/ethyl acetate as eluent to give the desired amides.

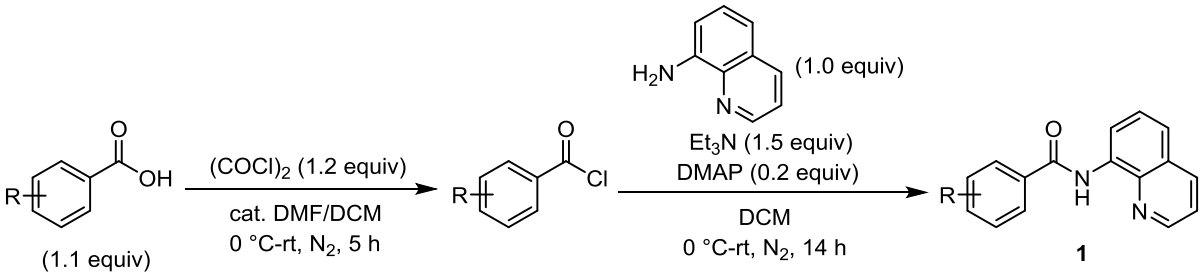

Scheme 2.5.2.1. Preparation of *N*-(quinolin-8-yl)benzamides via acid-amine coupling.

Some substrates (**1h-1l**, **1r-1v**) were prepared following Suzuki cross-coupling method by taking suitable bromo-benzamides (**1d** and **1o**) and arylboronic acids (Scheme 2.5.2.2).[20] A solution of bromo-benzamide (1.0 equiv), arylboronic acid (1.3 equiv), $Pd(OAc)_2$ (3.6 mol %), dppf (3.6 mol %), and Cs_2CO_3 (2.0 equiv) in 1,4-dioxane/H_2O (3:1) was heated to 60 ℃ for 24 h under N_2 atmosphere. After completion of the reaction, the reaction mixture was allowed to cool to room temperature, diluted with EtOAc, filtered through a short celite bed, and concentrated under vacuo. The crude reaction mixture was directly purified by column chromatography on silica gel using petroleum ether/ethyl acetate as eluent to give the desired aryl-substituted amides.

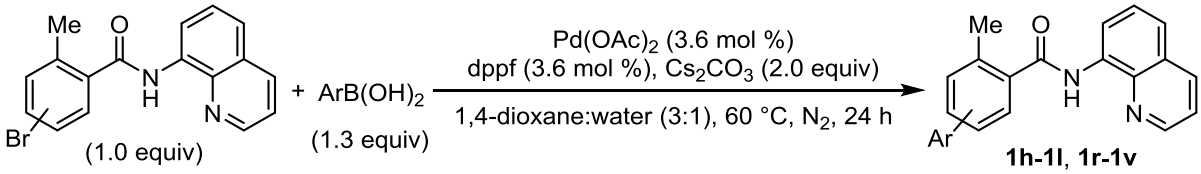

Scheme 2.5.2.2. Preparation of aryl-substituted quinoline benzamides.

2.5.3. General Procedure for Acetoxylation

(0.2 mmol scale):

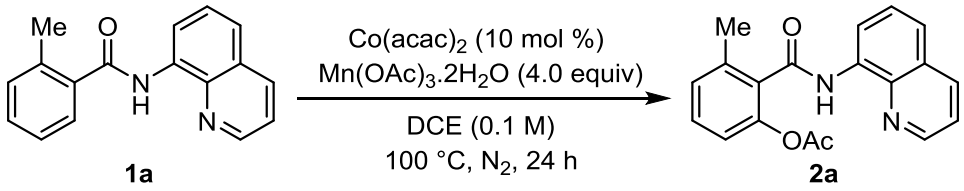

In an oven-dried 10 mL Schlenk tube, 2-methyl-*N*-(quinolin-8-yl)benzamide **1a** (52.5 mg, 0.2 mmol, 1.0 equiv), $Co(acac)_2$ (5.1 mg, 0.02 mmol, 0.1 equiv) and $Mn(OAc)_3.2H_2O$ (214.5 mg, 0.8 mmol, 4.0 equiv) were taken and the reaction mixture was degassed and backfilled with nitrogen. Under nitrogen, 2.0 mL (0.1 M) of anhydrous DCE was added. Then it was degassed and backfilled with nitrogen (3 times). The tube was closed with a teflon-lined cap and kept on stirring in an oil bath. The bath temperature was slowly increased to 100 ^oC. After 24 h, the reaction was stopped and cooled to room temperature. The reaction mixture was filtered through a short pad of celite and concentrated under vacuo. The crude reaction mixture was directly purified by column chromatography on silica gel using petroleum ether/ethyl acetate as eluent to obtain 3-methyl-2-(quinolin-8-ylcarbamoyl)phenyl acetate **2a** (49.7 mg, 78% yield).

(gram-scale):

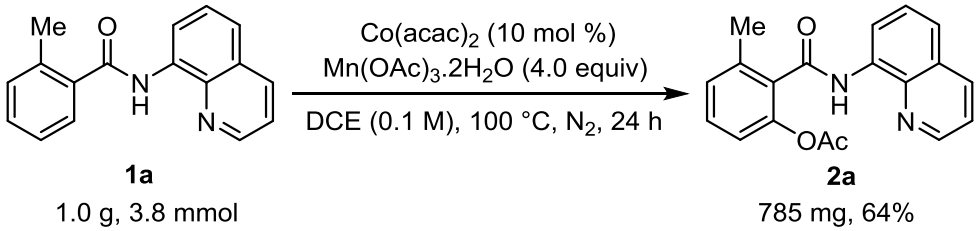

To an oven-dried 100 mL round bottom flask equipped with a reflux condenser, 2-methyl-*N*-(quinolin-8-yl)benzamide **1a** (1.0 g, 3.8 mmol, 1.0 equiv), $Co(acac)_2$ (98.0 mg, 0.38 mmol, 0.1 equiv) and $Mn(OAc)_3.2H_2O$ (4.09 g, 15.2 mmol, 4.0 equiv) were added. Next it was degassed

and backfilled with nitrogen. Under nitrogen, 38 mL (0.1 M) of anhydrous DCE was added. Then it was degassed and backfilled with nitrogen (3 times). The reaction mixture was kept on stirring in an oil bath. The bath temperature was slowly increased to 100 °C. After 24 h, the reaction was stopped and cooled to room temperature. The reaction mixture was filtered through a short pad of celite and concentrated under vacuo. The crude reaction mixture was directly purified by column chromatography on silica gel using petroleum ether/ethyl acetate as eluent to give 3-methyl-2-(quinolin-8-ylcarbamoyl)phenyl acetate **2a** (0.785 g, 64% yield).

2.5.4. Characterization Data for the Acetoxylated Products

3-methyl-2-(quinolin-8-ylcarbamoyl)phenyl acetate (2a):[8f]

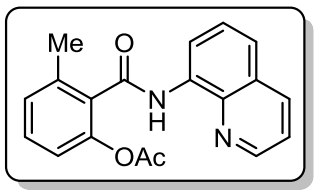

Yield 78% (49.7 mg); colorless solid; **R_f** 0.20 (pet ether/ethyl acetate = 4:1); **eluent composition** petroleum ether/ethyl acetate = 9:1; **mp** 81-83 °C (crystallization from $CHCl_3$ and hexane); **^{1}H NMR** (300 MHz, $CDCl_3$) δ 2.10 (s, 3H), 2.50 (s, 3H), 7.05 (app d, *J* = 8.1 Hz, 1H), 7.19 (app d, *J* = 7.5 Hz, 1H), 7.38 (app t, *J* = 7.8 Hz, 1H), 7.46 (dd, *J* = 8.1 Hz, 4.2 Hz , 1H), 7.55-7.63 (comp, 2H), 8.18 (dd, *J* = 8.4 Hz, 1.8 Hz, 1H), 8.78 (dd, *J* = 4.2 Hz, 1.8 Hz, 1H), 8.94 (dd, *J* = 6.6 Hz, 2.4 Hz, 1H), 10.03 (br s, 1H); **^{13}C NMR** (75 MHz, $CDCl_3$) δ 19.6, 20.8, 116.9, 120.3, 121.7, 122.1, 127.4, 128.0, 128.2, 130.1, 130.7, 134.2, 136.3, 137.6, 138.4, 147.4, 148.4, 164.8, 169.6; **HRMS** (EI, m/z) calcd for $C_{19}H_{16}N_2O_3$ [M^+] 320.1161, found 320.1159.

Crystal data and structure refinement for 2a, CCDC No. 1819213

Empirical formula	$C_{19}H_{16}N_2O_3$
Formula weight	320.34
Temperature/K	296.15
Crystal system	orthorhombic
Space group	Pbca
a/Å	7.803(2)
b/Å	17.668(5)
c/Å	22.978(7)
α/°	90
β/°	90
γ/°	90
Volume/Å^3	3167.8(16)
Z	8
ρ_{calc}g/cm^3	1.343
μ/mm^{-1}	0.092
F(000)	1344.0
Crystal size/mm^3	0.72 × 0.71 × 0.08

Radiation	Mo Kα (λ = 0.71073)
2Θ range for data collection/°	4.94 to 53.78
Index ranges	$-9 \leq h \leq 9$, $-22 \leq k \leq 21$, $-29 \leq l \leq 28$
Reflections collected	43220
Independent reflections	3390 [R_{int} = 0.0586, R_{sigma} = 0.0266]
Data/restraints/parameters	3390/0/220
Goodness-of-fit on F^2	1.033
Final R indexes [I>=2σ (I)]	R_1 = 0.0499, wR_2 = 0.1282
Final R indexes [all data]	R_1 = 0.0765, wR_2 = 0.1436
Largest diff. peak/hole / e $Å^{-3}$	0.16/-0.22

4-fluoro-3-methyl-2-(quinolin-8-ylcarbamoyl)phenyl acetate (2b):

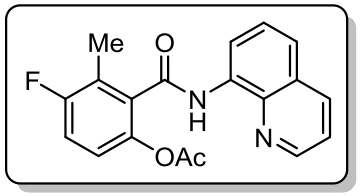

Yield 79% (53.2 mg); colorless solid; **R_f** 0.19 (pet ether/ethyl acetate = 4:1); **eluent composition** petroleum ether/ethyl acetate = 9:1; **mp** 128-130 °C; **^{1}H NMR** (300 MHz, $CDCl_3$) δ 2.09 (s, 3H), 2.39 (d, *J* = 2.1 Hz, 3H), 7.03 (dd, *J* = 9.0 Hz, 4.2 Hz, 1H), 7.14 (app t, *J* = 9.0 Hz, 1H), 7.47 (dd, *J* = 8.4 Hz, 4.2 Hz, 1H), 7.57-7.64 (comp, 2H), 8.19 (dd, *J* = 8.4 Hz, 1.8 Hz, 1H), 8.79 (dd, *J* = 4.2 Hz, 1.5 Hz, 1H), 8.91 (dd, *J* = 5.7 Hz, 3.3 Hz, 1H), 10.03 (br s, 1H); **^{13}C NMR** (150 MHz, $CDCl_3$) δ 12.0 (d, *J* = 4.5 Hz), 20.8, 116.8 (d, $^2J_{F-C}$ = 25.5 Hz), 116.9, 121.6 (d, $^3J_{F-C}$ = 7.5 Hz), 121.9, 122.4, 124.5 (d, $^2J_{F-C}$ = 19.5 Hz), 127.3, 128.0, 132.3 (d, $^3J_{F-C}$ = 4.5 Hz), 134.0, 136.4, 138.4, 143.1 (d, $^4J_{F-C}$ = 3.0 Hz), 148.5, 158.8 (d, $^1J_{F-C}$ = 243.0 Hz), 163.5 (d, *J* = 1.5 Hz), 169.6; **HRMS** (ESI, m/z) calcd for $C_{19}H_{15}FN_2O_3$ $[M + H]^+$ 339.1145, found 339.1153.

4-chloro-3-methyl-2-(quinolin-8-ylcarbamoyl)phenyl acetate (2c):

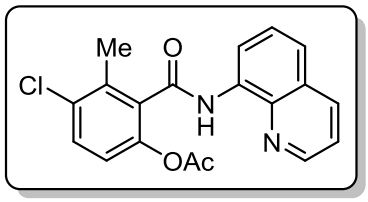

Yield 87% (61.7 mg); colorless solid; **R_f** 0.23 (pet ether/ethyl acetate = 4:1); **eluent composition** petroleum ether/ethyl acetate = 9:1; **mp** 102-104 °C; **^{1}H NMR** (300 MHz, $CDCl_3$) δ 2.09 (s, 3H), 2.48 (s, 3H), 7.04 (d, *J* = 8.7 Hz, 1H), 7.46 (d, *J* = 8.5 Hz, 1H), 7.47 (d, *J* = 8.5 Hz, 1H), 7.57-7.64 (comp, 2H), 8.19 (dd, *J* = 8.4 Hz, 1.8 Hz, 1H), 8.78 (dd, *J* = 4.2 Hz, 0.9 Hz, 1H), 8.91 (dd, *J* = 5.7 Hz, 3.6 Hz, 1H), 9.99 (br s, 1H); **^{13}C NMR** (75 MHz, $CDCl_3$) δ 17.4, 20.7, 116.9, 121.6, 121.8, 122.4, 127.2, 127.9, 130.6, 132.4, 132.5, 133.9, 135.1, 136.2, 138.4, 145.8, 148.5, 163.9, 169.3; **HRMS** (ESI, m/z) calcd for $C_{19}H_{15}ClN_2O_3$ $[M + Na]^+$ 377.0669, found 377.0663.

4-bromo-3-methyl-2-(quinolin-8-ylcarbamoyl)phenyl acetate (2d):

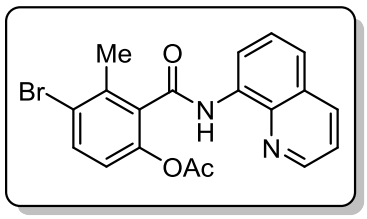

Yield 76% (60.3 mg); colorless solid; $\mathbf{R_f}$ 0.25 (pet ether/ethyl acetate = 4:1); **eluent composition** petroleum ether/ethyl acetate = 9:1; **mp** 116-118 ^{o}C (crystallization from EtOAc and hexane); **^{1}H NMR** (300 MHz, $CDCl_3$) δ 2.09 (s, 3H), 2.51 (s, 3H), 6.97 (d, *J* = 8.7 Hz, 1H), 7.47 (dd, *J* = 8.4 Hz, 4.2 Hz, 1H), 7.58-7.61 (comp, 2H), 7.66 (d, *J* = 8.7 Hz, 1H), 8.19 (dd, *J* = 8.4 Hz, 1.8 Hz, 1H), 8.78 (dd, *J* = 4.2 Hz, 1.5 Hz, 1H), 8.91 (dd, *J* = 5.7 Hz, 3.6 Hz, 1H), 9.98 (br s, 1H); **^{13}C NMR** (75 MHz, $CDCl_3$) δ 20.6, 20.8, 117.1, 122.0, 122.1, 122.5, 123.0, 127.4, 128.1, 132.6, 134.0, 134.1, 136.4, 137.0, 138.5, 146.6, 148.6, 164.1, 169.3; **HRMS** (ESI, m/z) calcd for $C_{19}H_{15}BrN_2O_3$ $[M + H]^+$ 399.0344, found 399.0350.

Crystal data and structure refinement for 2d, CCDC No. 1819214

Empirical formula	$C_{38}H_{30}Br_2N_4O_6$
Formula weight	798.48
Temperature/K	296.15
Crystal system	monoclinic
Space group	$P2_1/n$
a/Å	7.942(4)
b/Å	24.554(12)
c/Å	18.346(9)
α/°	90
β/°	100.729(7)
γ/°	90
Volume/Å^3	3515(3)
Z	4
ρ_{calc}g/cm^3	1.509
μ/mm^{-1}	2.359
F(000)	1616.0
Crystal size/mm^3	0.65 × 0.105 × 0.075
Radiation	Mo Kα (λ = 0.71073)
2Θ range for data collection/°	4.814 to 54.2
Index ranges	$-9 \le h \le 9$, $-31 \le k \le 31$, $-22 \le l \le 23$
Reflections collected	40301
Independent reflections	7561 [R_{int} = 0.0913, R_{sigma} = 0.0848]
Data/restraints/parameters	7561/0/455
Goodness-of-fit on F^2	1.020
Final R indexes [I>=2σ (I)]	R_1 = 0.0681, wR_2 = 0.1690
Final R indexes [all data]	R_1 = 0.1589, wR_2 = 0.2165
Largest diff. peak/hole / e Å^{-3}	1.15/-0.98

3-methyl-4-nitro-2-(quinolin-8-ylcarbamoyl)phenyl acetate (2e):

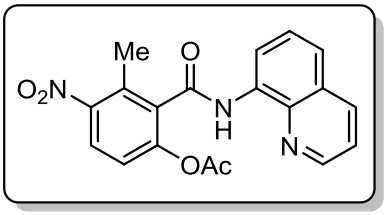

Yield 22% (7.9 mg); colorless solid; **R_f** 0.22 (pet ether/ethyl acetate = 4:1); **eluent composition** petroleum ether/ethyl acetate = 9:1; **mp** 146-148 °C; **^{1}H NMR** (300 MHz, $CDCl_3$) δ 2.13 (s, 3H), 2.65 (s, 3H), 7.28 (d, *J* = 8.4 Hz, 1H), 7.49 (dd, *J* = 8.4 Hz, 4.2 Hz, 1H), 7.62 (app d, *J* = 4.5 Hz, 2H), 8.04 (app d, *J* = 8.7 Hz, 1H), 8.21 (app d, *J* = 8.1 Hz, 1H), 8.79 (app d, *J* = 4.2 Hz, 1H), 8.90 (app t, *J* = 4.8 Hz, 1H), 10.04 (br s, 1H); **^{13}C NMR** (150 MHz, $CDCl_3$) δ 16.9, 20.8, 117.1, 121.6, 122.0, 122.8, 126.5, 127.3, 128.0, 133.2, 133.4, 133.7, 136.4, 138.4, 147.8, 148.7, 150.3, 162.8, 168.7; **HRMS** (ESI, m/z) calcd for $C_{19}H_{15}N_3O_5$ $[M + H]^+$ 366.1090, found 366.1096.

3,4-dimethyl-2-(quinolin-8-ylcarbamoyl)phenyl acetate (2f):

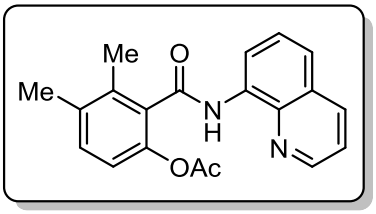

Yield 69% (46.4 mg); colorless solid; **R_f** 0.19 (pet ether/ethyl acetate = 4:1); **eluent composition** petroleum ether/ethyl acetate = 9:1; **mp** 140-142 °C; **^{1}H NMR** (300 MHz, $CDCl_3$) δ 2.08 (s, 3H), 2.32 (s, 3H), 2.36 (s, 3H), 6.96 (d, *J* = 8.4 Hz, 1H), 7.26 (d, *J* = 8.4 Hz, 1H), 7.45 (dd, *J* = 8.1 Hz, 4.2 Hz, 1H), 7.55-7.63 (comp, 2H), 8.18 (dd, *J* = 8.4 Hz, 1.8 Hz, 1H), 8.77 (dd, *J* = 4.2 Hz, 1.8 Hz, 1H), 8.95 (dd, *J* = 6.6 Hz, 2.4 Hz, 1H), 9.98 (br s, 1H); **^{13}C NMR** (75 MHz, $CDCl_3$) δ 16.9, 19.9, 20.9, 116.9, 120.0, 121.8, 122.2, 127.4, 128.1, 131.2, 131.4, 134.4, 135.4, 135.4, 136.4, 138.6, 145.5, 148.5, 165.6, 169.9; **HRMS** (ESI, m/z) calcd for $C_{20}H_{18}N_2O_3$ $[M + H]^+$ 335.1396, found 335.1395.

4-methoxy-3-methyl-2-(quinolin-8-ylcarbamoyl)phenyl acetate (2g):

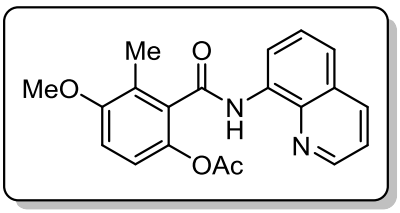

Yield 64% (44.8 mg); colorless solid; **R_f** 0.18 (pet ether/ethyl acetate = 4:1); **eluent composition** petroleum ether/ethyl acetate = 9:1; **mp** 136-138 °C; **^{1}H NMR** (300 MHz, $CDCl_3$) δ 2.08 (s, 3H), 2.32 (s, 3H), 3.87 (s, 3H), 6.92 (d, *J* = 8.7 Hz, 1H), 7.02 (d, *J* = 9.0 Hz, 1H), 7.45 (dd, *J* = 8.1 Hz, 4.2 Hz, 1H), 7.55-7.62 (comp, 2H), 8.17 (dd, *J* = 8.1 Hz, 1.5 Hz, 1H), 8.77 (dd, *J* = 4.2 Hz, 1.8 Hz, 1H), 8.93 (dd, *J* = 6.6 Hz, 2.4 Hz, 1H), 9.98 (br s, 1H); **^{13}C NMR** (150 MHz, $CDCl_3$) δ 13.2, 20.8, 56.0, 111.4, 116.8, 120.6, 121.8, 122.1, 125.7, 127.3, 128.0, 131.9, 134.3, 136.2, 138.5, 140.4, 148.4, 155.7, 164.8, 170.1; **HRMS** (ESI, m/z) calcd for $C_{20}H_{18}N_2O_4$ $[M + H]^+$ 351.1345, found 351.1351.

2-methyl-3-(quinolin-8-ylcarbamoyl)-[1,1'-biphenyl]-4-yl acetate (2h):

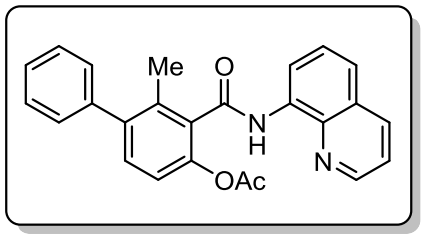

Yield 73% (57.7 mg); colorless oil; **R_f** 0.23 (pet ether/ethyl acetate = 4:1); **eluent composition** petroleum ether/ethyl acetate = 9:1; **^{1}H NMR** (300 MHz, $CDCl_3$) δ 2.11 (s, 3H), 2.34 (s, 3H), 7.12 (d, *J* = 8.4 Hz, 1H), 7.32-7.37 (comp, 3H), 7.39-7.49 (comp, 4H), 7.57-7.61 (comp, 2H), 8.19 (dd, *J* = 8.4 Hz, 1.8 Hz, 1H), 8.80 (dd, *J* = 4.2 Hz, 1.8 Hz, 1H), 8.95 (dd, *J* = 6.3 Hz, 2.1 Hz, 1H), 10.05 (br s, 1H); **^{13}C NMR** (150 MHz, $CDCl_3$) δ 17.7, 20.8, 116.8, 120.1, 121.7, 122.2, 127.2, 127.3, 127.9, 128.2, 129.3, 131.4, 131.6, 134.2, 134.6, 136.2, 138.4, 140.7, 140.8, 146.4, 148.4, 165.2, 169.7; **HRMS** (ESI, m/z) calcd for $C_{25}H_{20}N_2O_3$ $[M + H]^+$ 397.1552, found 397.1562.

2,3'-dimethyl-3-(quinolin-8-ylcarbamoyl)-[1,1'-biphenyl]-4-yl acetate (2i):

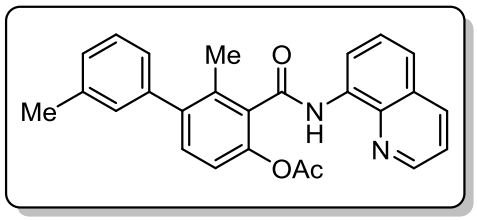

Yield 68% (55.4 mg); colorless solid; **R_f** 0.24 (pet ether/ethyl acetate = 4:1); **eluent composition** petroleum ether/ethyl acetate = 9:1; **mp** 136-138 ^{o}C; **^{1}H NMR** (300 MHz, $CDCl_3$) δ 2.11 (s, 3H), 2.34 (s, 3H), 2.41 (s, 3H), 7.09-7.20 (comp, 4H), 7.30-7.35 (comp, 2H), 7.47 (dd, *J* = 8.4 Hz, 4.2 Hz, 1H),7.58-7.64 (comp, 2H), 8.19 (app d, *J* = 7.5 Hz, 1H), 8.81 (app d, *J* = 4.2 Hz, 1H), 8.96 (dd, *J* = 6.6 Hz, 2.4 Hz, 1H), 10.05 (br s, 1H); **^{13}C NMR** (75 MHz, $CDCl_3$) δ 17.7, 20.8, 21.5, 116.9, 120.0, 121.8, 122.2, 126.4, 127.3, 127.9, 128.0, 128.1, 130.0, 131.4, 131.6, 134.3, 134.6, 136.3, 137.9, 138.5, 140.7, 141.0, 146.4, 148.5, 165.3, 169.7; **HRMS** (ESI, m/z) calcd for $C_{26}H_{22}N_2O_3$ $[M + H]^+$ 411.1709, found 411.1721.

4'-fluoro-2-methyl-3-(quinolin-8-ylcarbamoyl)-[1,1'-biphenyl]-4-yl acetate (2j):

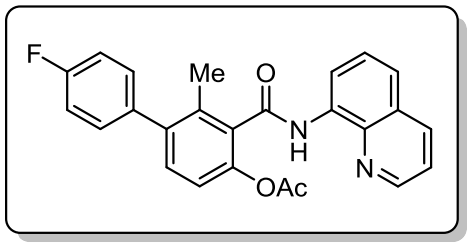

Yield 68% (56.0 mg); colorless solid; **R_f** 0.21 (pet ether/ethyl acetate = 4:1); **eluent composition** petroleum ether/ethyl acetate = 9:1; **mp** 117-119 ^{o}C; **^{1}H NMR** (300 MHz, $CDCl_3$) δ 2.11 (s, 3H), 2.32 (s, 3H), 7.10-7.15 (comp, 3H), 7.27-7.33 (comp, 3H), 7.47 (dd, *J* = 8.1 Hz, 4.2 Hz, 1H), 7.58-7.64 (comp, 2H), 8.19 (dd, *J* = 8.4 Hz, 1.8 Hz, 1H), 8.80 (dd, *J* = 4.2 Hz, 1.8 Hz, 1H), 8.95 (dd, *J* = 6.3 Hz, 2.7 Hz, 1H), 10.04 (br s, 1H); **^{13}C NMR** (75 MHz, $CDCl_3$) δ 17.7, 20.8, 115.2 (d, $^2J_{F\text{-}C}$ = 21.0 Hz), 116.9, 120.2, 121.8, 122.3, 127.3, 128.0, 130.9 (d, $^3J_{F\text{-}C}$ = 8.25 Hz), 131.5, 131.6, 134.2, 134.7, 136.3, 136.6 (d, $^4J_{F\text{-}C}$ = 4.5 Hz), 138.4, 139.8,

146.6, 148.5, 162.1 (d, $^{1}J_{F\text{-}C}$ = 244.5 Hz), 165.2, 169.7; **HRMS** (ESI, m/z) calcd for $C_{25}H_{19}FN_2O_3$ [M + H]$^+$ 415.1458, found 415.1464.

4'-chloro-2-methyl-3-(quinolin-8-ylcarbamoyl)-[1,1'-biphenyl]-4-yl acetate (2k):

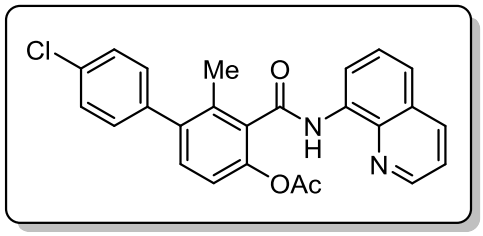

Yield 70% (60.7 mg); colorless solid; **R$_f$** 0.22 (pet ether/ethyl acetate = 4:1); **eluent composition** petroleum ether/ethyl acetate = 9:1; **mp** 92-94 ^{o}C; **^{1}H NMR** (600 MHz, $CDCl_3$) δ 2.14 (s, 3H), 2.35 (s, 3H), 7.14 (d, *J* = 4.2 Hz, 1H), 7.30 (app d, *J* = 4.2 Hz, 2H), 7.34 (d, *J* = 4.2 Hz, 1H), 7.44 (app d, *J* = 4.2 Hz, 2H), 7.49 (dd, *J* = 3.9 Hz, 2.1 Hz, 1H), 7.60-7.65 (comp, 2 H), 8.22 (dd, *J* = 3.9 Hz, 0.6 Hz, 1H), 8.82 (dd, *J* = 2.1 Hz, 0.9 Hz, 1H), 8.97 (dd, *J* = 3.6 Hz, 1.2 Hz, 1H), 10.08 (br s, 1H); **^{13}C NMR** (150 MHz, $CDCl_3$) δ 17.8, 20.8, 117.0, 120.3, 121.8, 122.3, 127.4, 128.0, 128.5, 130.7, 131.5, 131.6, 133.4, 134.2, 134.6, 136.4, 138.4, 139.1, 139.6, 146.7, 148.5, 165.1, 169.7; **HRMS** (ESI, m/z) calcd for $C_{25}H_{29}ClN_2O_3$ [M + H]$^+$ 431.1162, found 431.1165.

4'-(tert-butyl)-2-methyl-3-(quinolin-8-ylcarbamoyl)-[1,1'-biphenyl]-4-yl acetate (2l):

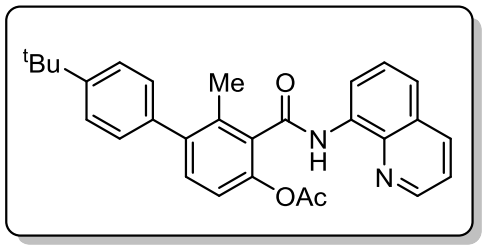

Yield 67% (60.6 mg); colorless solid; **R$_f$** 0.24 (pet ether/ethyl acetate = 4:1); **eluent composition** petroleum ether/ethyl acetate = 9:1; **mp** 142-144 ^{o}C; **^{1}H NMR** (300 MHz, $CDCl_3$) δ 1.37 (s, 9H), 2.11 (s, 3H), 2.36 (s, 3H), 7.10 (d, *J* = 8.4 Hz, 1H), 7.26-7.30 (comp, 2H), 7.35 (d, *J*= 8.4 Hz, 1H), 7.43-7.49 (comp, 3H), 7.56-7.61 (comp, 2H), 8.19 (dd, *J* = 8.4 Hz, 1.8 Hz, 1H), 8.80 (dd, *J* = 4.2 Hz, 1.8 Hz, 1H), 8.96 (dd, *J* = 6.6 Hz, 2.4 Hz, 1H), 10.05 (br s, 1H); **^{13}C NMR** (75 MHz, $CDCl_3$) δ 17.8, 20.8, 31.4, 34.5, 116.8, 120.0, 121.7, 122.1, 125.1, 127.3, 127.9, 129.0, 131.4, 131.7, 134.2, 134.6, 136.2, 137.7, 138.4, 140.8, 146.3, 148.4, 150.0, 165.3, 169.7; **HRMS** (ESI, m/z) calcd for $C_{29}H_{28}N_2O_3$ [M + H]$^+$ 453.2178, found 453.2180.

5-fluoro-3-methyl-2-(quinolin-8-ylcarbamoyl)phenyl acetate (2m):

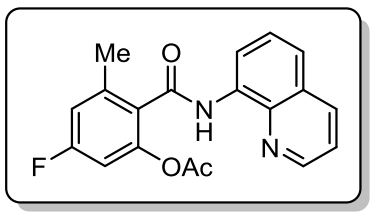

Yield 63% (42.8 mg); colorless solid; **R$_f$** 0.22 (pet ether/ethyl acetate = 4:1); **eluent composition** petroleum ether/ethyl acetate = 9:1; **mp** 116-118 ^{o}C; **^{1}H NMR** (300 MHz, $CDCl_3$) δ 2.10 (s, 3H), 2.50 (s, 3H), 6.83 (dd, *J* = 9.0 Hz, 2.4 Hz, 1H), 6.92 (dd, *J* = 9.3 Hz, 2.4 Hz, 1H), 7.47 (dd, *J* = 8.4 Hz, 4.2 Hz, 1H), 7.56-7.63 (comp, 2H),

8.19 (dd, *J* = 8.4 Hz, 1.8 Hz, 1H), 8.79 (dd, *J* = 4.2 Hz, 1.8 Hz, 1H), 8.91 (dd, *J* = 6.0 Hz, 2.7 Hz, 1H), 10.01 (br s, 1H); **^{13}C NMR** (150 MHz, $CDCl_3$) δ 19.9, 20.8, 108.3 (d, $^2J_{F-C}$ = 24.0 Hz), 115.3 (d, $^2J_{F-C}$ = 21.0 Hz), 116.8, 121.8, 122.3, 127.0 (d, $^4J_{F-C}$ = 4.5 Hz), 127.4, 128.0, 134.2, 136.4, 138.4, 139.8 (d, $^3J_{F-C}$ = 9.0 Hz), 148.5, 148.5 (d, $^3J_{F-C}$ = 10.5 Hz), 162.6 (d, $^1J_{F-C}$ = 249.0 Hz), 164.1, 169.1; **HRMS** (ESI, m/z) calcd for $C_{19}H_{15}FN_2O_3$ $[M + H]^+$ 339.1145, found 339.1141.

5-chloro-3-methyl-2-(quinolin-8-ylcarbamoyl)phenyl acetate (2n):

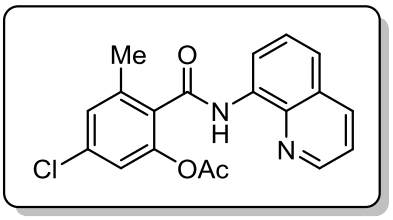

Yield 64% (45.2 mg); colorless solid; **R$_f$** 0.24 (pet ether/ethyl acetate = 4:1); **eluent composition** petroleum ether/ethyl acetate = 9:1; **mp** 90-92 ^{o}C; **^{1}H NMR** (300 MHz, $CDCl_3$) δ 2.10 (s, 3H), 2.47 (s, 3H), 7.10 (d, *J* = 1.8 Hz, 1H), 7.19 (d, *J* = 1.8 Hz, 1H), 7.46 (dd, *J* = 8.4 Hz, 4.2 Hz, 1H), 7.58-7.63 (comp, 2H), 8.18 (dd, *J* = 8.4 Hz, 1.8 Hz, 1H), 8.79 (dd, *J* = 4.2 Hz, 1.5 Hz, 1H), 8.90 (dd, *J* = 5.7 Hz, 3.0 Hz, 1H), 10.02 (br s, 1H); **^{13}C NMR** (75 MHz, $CDCl_3$) δ 19.7, 20.8, 117.0, 121.0, 121.9, 122.4, 127.4, 128.1, 128.5, 129.3, 134.2, 135.4, 136.5, 138.5, 139.2, 148.0, 148.6, 164.0, 169.2; **HRMS** (ESI, m/z) calcd for $C_{19}H_{15}ClN_2O_3$ $[M + Na]^+$ 377.0669, found 377.0668.

5-bromo-3-methyl-2-(quinolin-8-ylcarbamoyl)phenyl acetate (2o):

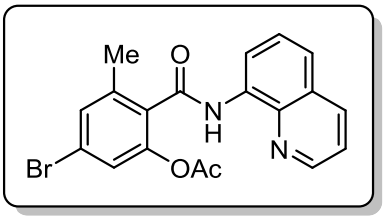

Yield 65% (51.6 mg); colorless solid; **R$_f$** 0.27 (pet ether/ethyl acetate = 4:1); **eluent composition** petroleum ether/ethyl acetate = 9:1; **mp** 102-104 ^{o}C; **^{1}H NMR** (300 MHz, $CDCl_3$) δ 2.10 (s, 3H), 2.47 (s, 3H), 7.25 (app s, 1H), 7.36 (d, *J* = 1.8 Hz, 1H), 7.47 (dd, *J* = 8.4 Hz, 4.2 Hz, 1H), 7.56-7.63 (comp, 2H), 8.19 (dd, *J* = 8.4 Hz, 1.5 Hz, 1H), 8.79 (dd, *J* = 4.2 Hz, 1.8 Hz, 1H), 8.90 (dd, *J* = 5.7 Hz, 3.3 Hz, 1H), 10.01 (br s, 1H); **^{13}C NMR** (75 MHz, $CDCl_3$) δ 19.5, 20.7, 116.8, 121.8, 122.3, 123.2, 123.7, 127.3, 127.9, 129.7, 131.2, 134.0, 136.3, 138.4, 139.2, 147.8, 148.5, 163.9, 169.1; **HRMS** (ESI, m/z) calcd for $C_{19}H_{15}BrN_2O_3$ $[M + H]^+$ 399.0344, found 399.0346.

3,5-dimethyl-2-(quinolin-8-ylcarbamoyl)phenyl acetate (2p):

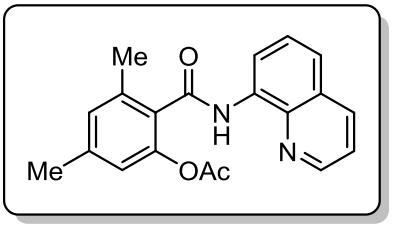

Yield 55% (36.6 mg); colorless solid; **R$_f$** 0.21 (pet ether/ethyl acetate = 4:1); **eluent composition** petroleum ether/ethyl acetate = 9:1; **mp** 107-108 ^{o}C; **^{1}H NMR** (300 MHz, $CDCl_3$) δ 2.09 (s, 3H), 2.38 (s, 3H), 2.46 (s, 3H), 6.86 (app s, 1H), 7.00 (app s, 1H), 7.45 (dd, *J* = 8.1 Hz, 4.2 Hz, 1H), 7.54-7.62 (comp, 2H), 8.17 (dd, *J* = 8.4 Hz,

1.8 Hz, 1H), 8.78 (dd, *J* = 4.2 Hz, 1.8 Hz, 1H), 8.93 (dd, *J* = 6.6 Hz, 2.4 Hz, 1H), 10.02 (br s, 1H); **^{13}C NMR** (75 MHz, $CDCl_3$) δ 19.7, 20.9, 21.4, 116.9, 120.9, 121.8, 122.1, 127.5, 128.0, 128.1, 129.2, 134.5, 136.4, 137.5, 138.6, 140.7, 147.6, 148.5, 165.1, 169.8; **HRMS** (ESI, m/z) calcd for $C_{20}H_{18}N_2O_3$ $[M + H]^+$ 335.1396, found 335.1396.

5-methoxy-3-methyl-2-(quinolin-8-ylcarbamoyl)phenylacetate (2q):

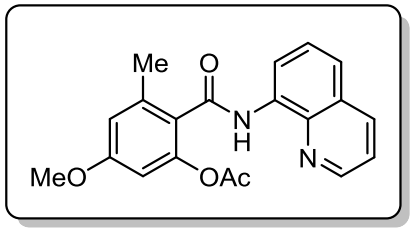

Yield 74% (52.0 mg); colorless solid; **R_f** 0.22 (pet ether/ethyl acetate = 4:1); **eluent composition** petroleum ether/ethyl acetate = 9:1; **mp** 89-91 °C; **^{1}H NMR** (300 MHz, $CDCl_3$) δ 2.09 (s, 3H), 2.49 (s, 3H), 3.83 (s, 3H), 6.58 (d, *J* = 2.4 Hz, 1 H), 6.72 (d, *J* = 2.4 Hz, 1H), 7.45 (dd, *J* = 8.1 Hz, 4.2 Hz, 1H), 7.53-7.62 (comp, 2H), 8.17 (dd, *J* = 8.1 Hz, 1.8 Hz, 1H), 8.78 (dd, *J* = 4.2 Hz, 1.8 Hz, 1H), 8.92 (dd, *J* = 6.9 Hz, 2.1 Hz, 1H), 10.03 (br s, 1H); **^{13}C NMR** (150 MHz, $CDCl_3$) δ 20.2, 20.9, 55.5, 105.9, 114.3, 116.7, 121.7, 121.9, 123.3, 127.4, 128.0, 134.5, 136.3, 138.5, 139.1, 148.4, 148.8, 160.6, 164.8, 169.5; **HRMS** (ESI, m/z) calcd for $C_{20}H_{18}N_2O_4$ $[M + H]^+$ 351.1345, found 351.1350.

5-methyl-4-(quinolin-8-ylcarbamoyl)-[1,1'-biphenyl]-3-yl acetate (2r):

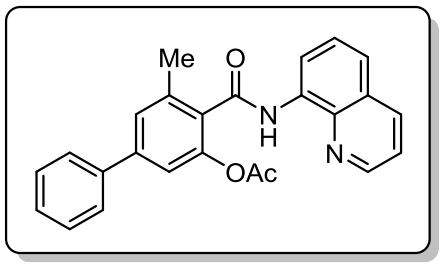

Yield 55% (43.6 mg); colorless solid; **R_f** 0.23 (pet ether/ethyl acetate = 4:1); **eluent composition** petroleum ether/ethyl acetate = 9:1; **mp** 112-114 °C; **^{1}H NMR** (300 MHz, $CDCl_3$) δ 2.13 (s, 3H), 2.57 (s, 3H), 7.27 (d, *J* = 1.3 Hz, 1H), 7.36-7.42 (comp, 2H), 7.44 (d, *J* = 1.3 Hz, 1H), 7.46-7.49 (comp, 2H), 7.56-7.64 (comp, 4H), 8.19 (dd, *J* = 8.4 Hz, 1.8 Hz, 1H), 8.80 (dd, *J* = 4.2 Hz, 1.8 Hz, 1H), 8.96 (dd, *J* = 6.6 Hz, 2.1 Hz, 1H), 10.10 (br s, 1H); **^{13}C NMR** (150 MHz, $CDCl_3$) δ 19.9, 20.9, 116.8, 119.1, 121.8, 122.1, 127.1, 127.3, 127.4, 128.0, 128.0, 128.9, 129.3, 134.3, 136.3, 138.0, 138.5, 139.6, 143.4, 147.9, 148.5, 164.7, 169.6; **HRMS** (ESI, m/z) calcd for $C_{25}H_{20}N_2O_3$ $[M + H]^+$ 397.1552, found 397.1563.

3',5-dimethyl-4-(quinolin-8-ylcarbamoyl)-[1,1'-biphenyl]-3-yl acetate (2s):

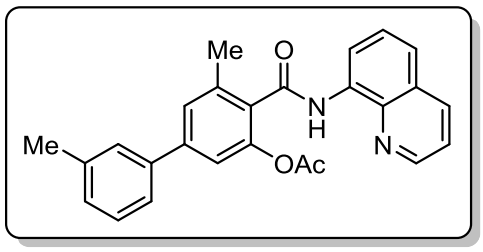

Yield 62% (50.2 mg); colorless solid; **R_f** 0.24 (pet ether/ethyl acetate = 4:1); **eluent composition** petroleum ether/ethyl acetate = 9:1; **mp** 120-122 °C; **^{1}H NMR** (300 MHz, $CDCl_3$) δ 2.13 (s, 3H), 2.44 (s, 3H), 2.57 (s, 3H), 7.21 (app d, *J* = 7.2 Hz, 1H), 7.26 (app s, 1H), 7.35 (app t, *J* = 7.8 Hz, 1H), 7.40-7.42 (comp, 3H), 7.46 (dd, *J* = 8.1 Hz, 4.2 Hz, 1H),7.56-7.64 (comp, 2H), 8.19 (dd, *J* = 8.4 Hz, 1.8 Hz, 1H), 8.80 (dd, *J* = 4.2 Hz, 1.8 Hz, 1H),

8.96 (dd, *J* = 6.6 Hz, 2.4 Hz, 1H), 10.09 (br s, 1H); **^{13}C NMR** (150 MHz, $CDCl_3$) δ 19.9, 20.9, 21.6, 116.8, 119.1, 121.8, 122.1, 124.4, 127.1, 128.0 (x 2), 128.8 (x 2), 129.2, 134.3, 136.3, 138.0, 138.5, 138.5, 139.6, 143.6, 147.9, 148.5, 164.8, 169.7; **HRMS** (ESI, m/z) calcd for $C_{26}H_{22}N_2O_3$ $[M + H]^+$ 411.1709, found 411.1717.

4'-fluoro-5-methyl-4-(quinolin-8-ylcarbamoyl)-[1,1'-biphenyl]-3-yl acetate (2t):

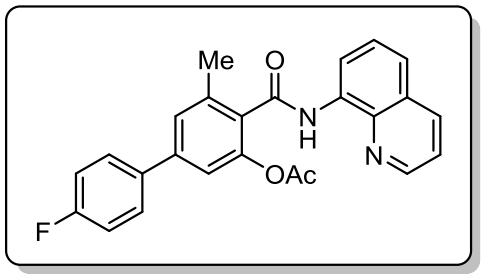

Yield 61% (50.4 mg); colorless solid; **R_f** 0.22 (pet ether/ethyl acetate = 4:1); **eluent composition** petroleum ether/ethyl acetate = 9:1; **mp** 119-121 °C; **^{1}H NMR** (300 MHz, $CDCl_3$) δ 2.13 (s, 3H), 2.56 (s, 3H), 7.12-7.18 (comp, 2H), 7.22 (app d, *J* = 1.8 Hz, 1H), 7.36 (app s, 1H), 7.46 (dd, *J* = 8.1 Hz, 4.2 Hz, 1H), 7.53-7.64 (comp, 4H), 8.19 (dd, *J* = 8.4 Hz, 1.8 Hz, 1H), 8.79 (dd, *J* = 4.2 Hz, 1.5 Hz, 1H), 8.95 (dd, *J* = 6.6 Hz, 2.4 Hz, 1H), 10.08 (br s, 1H); **^{13}C NMR** (75 MHz, $CDCl_3$) δ 19.8, 20.8, 115.7 (d, $^2J_{F-C}$ = 21.0 Hz) , 116.8, 118.9, 121.7, 122.1, 126.8, 127.3, 127.9, 128.8 (d, $^3J_{F-C}$ = 8.25 Hz), 129.2, 134.2, 135.6 (d, $^4J_{F-C}$ = 4.5 Hz), 136.2, 138.1, 138.4, 142.3, 147.8, 148.4, 162.8 (d, $^1J_{F-C}$ = 246.75 Hz), 164.6, 169.5; **HRMS** (ESI, m/z) calcd for $C_{25}H_{19}FN_2O_3$ $[M + H]^+$ 415.1458, found 415.1472.

4'-chloro-5-methyl-4-(quinolin-8-ylcarbamoyl)-[1,1'-biphenyl]-3-yl acetate (2u):

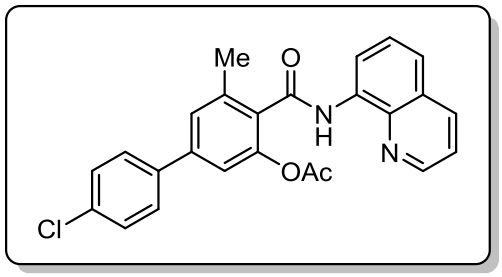

Yield 50% (42.8 mg); colorless solid; **R_f** 0.25 (pet ether/ethyl acetate = 4:1); **eluent composition** petroleum ether/ethyl acetate = 9:1; **mp** 159-161 °C; **^{1}H NMR** (300 MHz, $CDCl_3$) δ 2.13 (s, 3H), 2.56 (s, 3 H), 7.23 (d, *J* = 1.6 Hz, 1H), 7.37 (d, *J* = 1.6 Hz, 1H), 7.42-7.49 (comp, 3H), 7.52-7.57 (comp, 2H), 7.59-7.64 (comp, 2H), 8.19 (dd, *J* = 8.1 Hz, 1.5 Hz, 1H), 8.79 (dd, *J* = 4.2 Hz, 1.8 Hz, 1H), 8.95 (dd, *J* = 6.6 Hz, 2.4 Hz, 1H), 10.08 (br s, 1H); **^{13}C NMR** (150 MHz, $CDCl_3$) δ 19.9, 20.9, 116.9, 119.0, 121.8, 122.2, 126.9, 127.4, 128.0, 128.5, 129.1, 129.6, 134.2, 134.3, 136.3, 138.0, 138.2, 138.5, 142.1, 148.0, 148.5, 164.6, 169.6; **HRMS** (ESI, m/z) calcd for $C_{25}H_{29}ClN_2O_3$ $[M + H]^+$ 431.1162, found 431.1164.

4'-(tert-butyl)-5-methyl-4-(quinolin-8-ylcarbamoyl)-[1,1'-biphenyl]-3-yl acetate (2v):

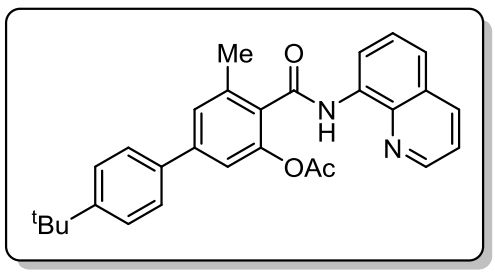

Yield 59% (53.0 mg); colorless solid; **R_f** 0.25 (pet ether/ethyl acetate = 4:1); **eluent composition** petroleum ether/ethyl acetate = 9:1; **mp** 194-196 °C; **^{1}H NMR** (300 MHz, $CDCl_3$) δ 1.37 (s, 9H), 2.13 (s, 3H), 2.56 (s, 3H), 7.25 (d, *J* = 1.5 Hz, 1H), 7.41 (d, *J*

= 1.5 Hz, 1H), 7.44-7.50 (comp, 3H), 7.54 (app s, 1H), 7.56-7.64 (comp, 3H), 8.19 (dd, *J* = 8.4 Hz, 1.8 Hz, 1H), 8.80 (dd, *J* = 4.2 Hz, 1.5 Hz, 1H), 8.96 (dd, *J* = 6.9 Hz, 2.1 Hz, 1H), 10.10 (br s, 1H); **^{13}C NMR** (150 MHz, $CDCl_3$) δ 20.0, 20.9, 31.4, 34.6, 116.8, 118.9, 121.8, 122.1, 125.9, 126.9, 127.0, 127.4, 128.0, 129.0, 134.4, 136.3, 136.7, 137.9, 138.5, 143.3, 147.9, 148.5, 151.2, 164.8, 169.6; **HRMS** (ESI, m/z) calcd for $C_{29}H_{28}N_2O_3$ $[M + H]^+$ 453.2178, found 453.2191.

3-fluoro-2-(quinolin-8-ylcarbamoyl)phenyl acetate (2w):

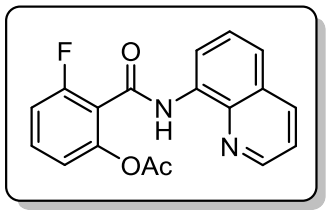

Yield 29% (18.6 mg); colorless solid; **R_f** 0.18 (pet ether/ethyl acetate = 4:1); **eluent composition** petroleum ether/ethyl acetate = 9:1; **mp** 96-98 °C; **^{1}H NMR** (300 MHz, $CDCl_3$) δ 2.25 (s, 3H), 7.05 (dd, *J* = 8.4 Hz, 1.2 Hz, 1H), 7.14 (app t, *J* = 9.0 Hz, 1H), 7.44-7.52 (comp, 2H), 7.56-7.62 (comp, 2H), 8.18 (dd, *J* = 8.4 Hz, 1.8 Hz, 1H), 8.81 (dd, *J* = 4.2 Hz, 1.8 Hz, 1H), 8.90 (dd, *J* = 6.0 Hz, 3.0 Hz, 1H), 10.33 (br s, 1H); **^{13}C NMR** (150 MHz, $CDCl_3$) δ 20.9, 114.0 (d, $^2J_{F\text{-}C}$ = 22.5 Hz), 117.0, 119.1 (d, $^2J_{F\text{-}C}$ = 19.5 Hz), 119.4 (d, $^4J_{F\text{-}C}$ = 3.0 Hz), 121.8, 122.3, 127.4, 128.0, 131.6 (d, $^3J_{F\text{-}C}$ = 10.5 Hz), 134.3, 136.3, 138.5, 148.4, 149.4 (d, $^3J_{F\text{-}C}$ = 6.0 Hz), 159.7, 160.0 (d, $^1J_{F\text{-}C}$ = 250.5 Hz), 169.2; **HRMS** (ESI, m/z) calcd for $C_{18}H_{13}FN_2O_3$ $[M + H]^+$ 325.0988, found 325.0996.

3-chloro-2-(quinolin-8-ylcarbamoyl)phenyl acetate (2x):[8f]

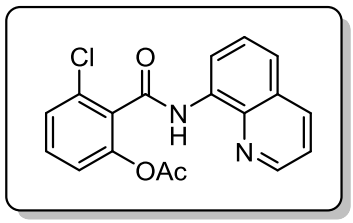

Yield 64% (43.9 mg); colorless solid; **R_f** 0.19 (pet ether/ethyl acetate = 4:1); **eluent composition** petroleum ether/ethyl acetate = 9:1; **mp** 122-124 °C; **^{1}H NMR** (300 MHz, $CDCl_3$) δ 2.15 (s, 3H), 7.17 (dd, *J* = 7.5 Hz, 1.8 Hz, 1H), 7.37-7.43 (comp, 2H), 7.44-7.46 (dd, *J* = 8.1 Hz, 4.2 Hz, 1H), 7.57-7.63 (comp, 2H), 8.18 (dd, *J* = 8.4 Hz, 1.8 Hz, 1H), 8.79 (dd, *J* = 4.2 Hz, 1.8 Hz, 1H), 8.92 (dd, *J* = 5.7 Hz, 3.0 Hz, 1H), 10.07 (br s, 1H); **^{13}C NMR** (75 MHz, $CDCl_3$) δ 20.9, 117.2, 121.9 (x 2), 122.5, 127.4, 127.6, 128.1, 130.6, 130.9, 132.3, 134.2, 136.4, 138.6, 148.6, 148.7, 162.0, 169.2; **HRMS** (ESI, m/z) calcd for $C_{18}H_{13}ClN_2O_3$ $[M + H]^+$ 341.0693, found 341.0692.

3-bromo-2-(quinolin-8-ylcarbamoyl)phenyl acetate (2y):

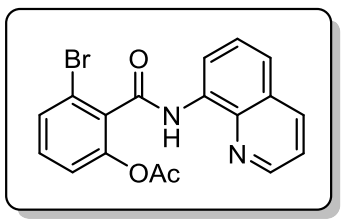

Yield 57% (43.9 mg); colorless solid; **R_f** 0.19 (pet ether/ethyl acetate = 4:1); **eluent composition** petroleum ether/ethyl acetate = 9:1; **mp** 122-124 °C; **^{1}H NMR** (300 MHz, $CDCl_3$) δ 2.13 (s, 3H), 7.19-7.26 (m, 1H), 7.32-7.38 (m, 1H), 7.46 (dd, *J* = 8.1 Hz, 4.2 Hz, 1H), 7.54-7.63 (comp, 3H), 8.18 (app dt, *J* = 8.4 Hz, 1.2 Hz, 1H), 8.79 (dd, *J* = 4.8 Hz, 1.8 Hz, 1H), 8.92 (dd, *J* = 6.0 Hz, 3.0 Hz, 1H), 10.04 (br s, 1H); **^{13}C NMR** (75 MHz, $CDCl_3$)

δ 20.8, 117.2 120.6, 121.9, 122.4, 122.5, 127.4, 128.1, 130.7, 131.2, 132.7, 134.1, 136.4, 138.6, 148.5, 148.6, 162.9, 169.2; **HRMS** (ESI, m/z) calcd for $C_{18}H_{13}BrN_2O_3$ $[M + H]^+$ 385.0188, found 385.0192.

3-iodo-2-(quinolin-8-ylcarbamoyl)phenyl acetate (2z):

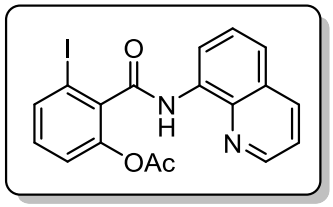

Yield 75% (65.1 mg); colorless solid; **R_f** 0.20 (pet ether/ethyl acetate = 4:1); **eluent composition** petroleum ether/ethyl acetate = 9:1; **mp** 118-120 °C (crystallization from DCM and hexane); **^{1}H NMR** (600 MHz, $CDCl_3$) δ 2.14 (s, 3H), 7.22 (app t, *J* = 8.4 Hz, 1H), 7.26 (dd, *J* = 8.4 Hz, 1.2 Hz, 1H), 7.49 (dd, *J* = 8.4 Hz, 4.2 Hz, 1H), 7.61-7.65 (comp, 2H), 7.83 (dd, *J* = 8.4 Hz, 1.2 Hz, 1H), 8.21 (dd, *J* = 8.4 Hz, 1.8 Hz, 1H), 8.82 (dd, *J* = 4.2 Hz, 1.8 Hz, 1H), 8.94 (app dt, *J* = 7.2 Hz, 1.2 Hz, 1H), 10.02 (br s, 1H); **^{13}C NMR** (150 MHz, $CDCl_3$) δ 20.8, 93.4, 117.1, 121.8, 122.4, 123.1, 127.4, 128.0, 131.5, 134.0, 136.3, 136.5, 137.0, 138.5, 147.6, 148.6, 164.5, 169.2; **HRMS** (ESI, m/z) calcd for $C_{18}H_{13}IN_2O_3$ $[M + H]^+$ 433.0049, found 433.0056.

Crystal data and structure refinement for 2z, CCDC No. 1819212

Empirical formula	$C_{18}H_{13}N_2O_3I$
Formula weight	432.20
Temperature/K	296.15
Crystal system	monoclinic
Space group	$P2_1/c$
a/Å	12.7681(14)
b/Å	13.9419(14)
c/Å	9.4448(10)
α/°	90
β/°	97.068(4)
γ/°	90
Volume/Å^3	1668.5(3)
Z	4
ρ_{calc}g/cm^3	1.721
μ/mm^{-1}	1.937
F(000)	848.0
Crystal size/mm^3	0.64 × 0.26 × 0.1
Radiation	Mo Kα (λ = 0.71073)
2Θ range for data collection/°	5.236 to 55.212
Index ranges	$-16 \le h \le 16$, $-18 \le k \le 18$, $-12 \le l \le 12$
Reflections collected	22466
Independent reflections	3860 [R_{int} = 0.0488, R_{sigma} = 0.0281]
Data/restraints/parameters	3860/0/218
Goodness-of-fit on F^2	1.059

Final R indexes [I>=2σ (I)]	R_1 = 0.0427, wR_2 = 0.1121
Final R indexes [all data]	R_1 = 0.0533, wR_2 = 0.1221
Largest diff. peak/hole / e Å^{-3}	1.11/-0.54

3-nitro-2-(quinolin-8-ylcarbamoyl)phenyl acetate (2aa):

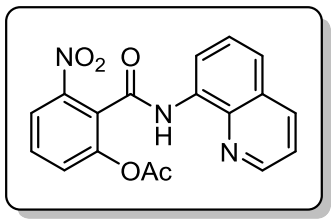

Yield 31% (21.7 mg); colorless solid; **R_f** 0.12 (pet ether/ethyl acetate = 4:1); **eluent composition** petroleum ether/ethyl acetate = 4:1; **mp** 158-160 ºC; **^{1}H NMR** (600 MHz, $CDCl_3$) δ 2.16 (s, 3H),7.49 (dd, *J* = 7.8 Hz, 4.2 Hz, 1H), 7.60-7.62 (m, 1H), 7.62-7.66 (comp, 2H), 7.69 (app t, *J* = 4.2 Hz, 1H), 8.16 (app dt, *J* = 4.2 Hz, 1.2 Hz, 1H) 8.22 (dd, *J* = 4.2 Hz, 1.8 Hz, 1H), 8.79 (dd, *J* = 4.2 Hz, 1.2 Hz, 1H), 8.90 (dd, *J* = 6.0 Hz, 2.4 Hz, 1H), 10.09 (br s, 1H); **^{13}C NMR** (150 MHz, $CDCl_3$) δ 20.7, 117.2, 121.8, 122.2, 122.6, 126.8, 127.4, 128.0, 129.3, 130.6, 134.0, 136.4, 138.4, 146.9, 148.4, 148.5, 160.7, 168.9; **HRMS** (ESI, m/z) calcd for $C_{18}H_{13}N_3O_5$ $[M + H]^+$ 352.0933, found 352.0939.

2-(quinolin-8-ylcarbamoyl)-3-(trifluoromethyl)phenyl acetate (2ab):

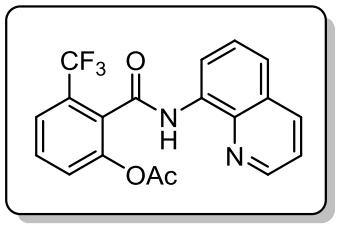

Yield 60% (45.1 mg); colorless solid; **R_f** 0.15 (pet ether/ethyl acetate = 4:1); **eluent composition** petroleum ether/ethyl acetate = 4:1; **mp** 138-140 ºC; **^{1}H NMR** (600 MHz, $CDCl_3$) δ 2.14 (s, 3H), 7.45-7.47 (comp, 2H), 7.60-7.63 (comp, 2H), 7.64 (d, *J* = 8.4 Hz, 1 H), 7.68 (d, *J* = 7.8 Hz, 1H), 8.19 (app d, *J* = 7.8 Hz, 1H), 8.78 (app d, *J* = 4.2 Hz, 1H), 8.90 (dd, *J* = 6.0 Hz, 2.4 Hz, 1H), 10.05 (br s, 1H); **^{13}C NMR** (150 MHz, $CDCl_3$) δ 20.7, 117.0, 121.8, 122.5, 123.1 (q, *J* = 273.0 Hz), 124.0 (q, *J* = 6.0 Hz), 127.1, 127.3, 127.9, 129.0 (q, *J* = 33.0 Hz), 129.2, 130.5, 134.0, 136.3, 138.3, 148.1, 148.5, 161.9, 169.1; **HRMS** (ESI, m/z) calcd for $C_{19}H_{13}F_3N_2O_3$ $[M + H]^+$ 375.0957, found 375.0968.

2-(quinolin-8-ylcarbamoyl)-[1,1'-biphenyl]-3-yl acetate (2ac):

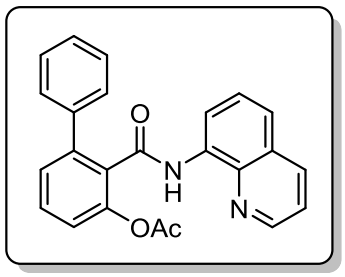

Yield 52% (39.7 mg); colorless oil; **R_f** 0.19 (pet ether/ethyl acetate = 4:1); **eluent composition** petroleum ether/ethyl acetate = 9:1; **^{1}H NMR** (300 MHz, $CDCl_3$) δ 2.19 (s, 3 H), 7.11-7.18 (m, 1H), 7.21-7.27 (comp, 3H), 7.36-7.40 (comp, 2H), 7.46-7.58 (comp, 5H), 8.09 (dd, *J* = 8.4 Hz, 1.8 Hz, 1H), 8.63 (dd, *J* = 4.5 Hz, 1.8 Hz, 1H), 8.71 (dd, *J* = 6.3 Hz, 2.7 Hz, 1H), 9.74 (br s, 1H); **^{13}C NMR** (75 MHz, $CDCl_3$) δ 20.8, 116.5, 121.5, 121.8, 122.0, 127.2, 127.7, 127.9, 128.3, 128.3, 128.6, 129.9, 130.3, 134.2, 136.0, 138.3, 139.2, 141.7, 148.0, 148.1, 164.4, 169.6; **HRMS** (ESI, m/z) calcd for $C_{24}H_{16}N_2O_3$ $[M + H]^+$ 383.1396, found 383.1396.

3,4-dichloro-2-(quinolin-8-ylcarbamoyl)phenyl acetate (2ad):

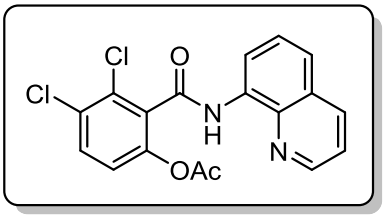

Yield 54% (40.6 mg); colorless solid; **R_f** 0.16 (pet ether/ethyl acetate = 4:1); **eluent composition** petroleum ether/ethyl acetate = 4:1; **mp** 126-128 ^oC; **^{1}H NMR** (300 MHz, $CDCl_3$) δ 2.14 (s, 3H), 7.15 (d, *J* = 9.0 Hz, 1H), 7.47 (dd, *J* = 8.4 Hz, 4.2 Hz, 1H), 7.58 (comp, 2H), 7.61 (app d, *J* = 0.9 Hz, 1H), 8.20 (dd, *J* = 8.1 Hz, 1.5 Hz, 1H), 8.80 (dd, *J* = 4.2 Hz, 1.8 Hz, 1H), 8.90 (app t, *J* = 4.5 Hz, 1H), 10.06 (br s, 1H); **^{13}C NMR** (150 MHz, $CDCl_3$) δ 20.7, 117.1, 121.9, 122.6, 122.8, 127.3, 128.0, 130.7, 131.1, 131.3, 132.1, 133.8, 136.4, 138.4, 146.7, 148.6, 161.1, 169.0; **HRMS** (ESI, m/z) calcd for $C_{18}H_{12}Cl_2N_2O_3$ $[M + H]^+$ 375.0303, found 375.0312.

3,5-dichloro-2-(naphthalen-1-ylcarbamoyl)phenyl acetate (2ae):

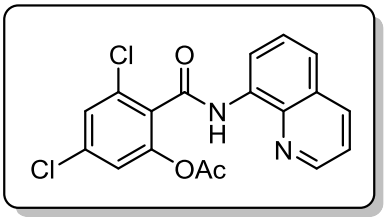

Yield 31% (23.6 mg); colorless oil; **R_f** 0.21 (pet ether/ethyl acetate = 4:1); **eluent composition** petroleum ether/ethyl acetate = 9:1; **^{1}H NMR** (300 MHz, $CDCl_3$) δ 2.15 (s, 3H), 7.21 (d, *J* = 1.8 Hz, 1H), 7.40 (d, *J* = 1.8 Hz, 1H), 7.46 (dd, *J* = 8.4 Hz, 4.2 Hz, 1H), 7.58 (s, 1H), 7.60 (app d, *J* = 0.9 Hz, 1H), 8.18 (dd, *J* = 8.4 Hz, 1.8 Hz, 1H), 8.79 (dd, *J* = 4.2 Hz, 1.5 Hz, 1H), 8.88 (app t, *J* = 4.5 Hz, 1H), 10.07 (br s, 1H); **^{13}C NMR** (150 MHz, $CDCl_3$) δ 20.7, 117.0, 121.8, 122.5, 122.5, 127.3, 127.5, 127.9, 129.1, 132.9, 133.8, 136.0, 136.3, 138.4, 148.5, 148.8, 161.0, 168.7; **HRMS** (ESI, m/z) calcd for $C_{18}H_{12}Cl_2N_2O_3$ $[M + H]^+$ 375.0303, found 375.0320.

3-bromo-4-methyl-2-(quinolin-8-ylcarbamoyl)phenyl acetate (2af):

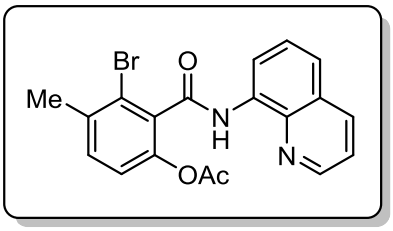

Yield 56% (44.3 mg); colorless solid; **R_f** 0.18 (pet ether/ethyl acetate = 4:1); **eluent composition** petroleum ether/ethyl acetate = 9:1; **mp** 134-136 ^oC; **^{1}H NMR** (300 MHz, $CDCl_3$) δ 2.12 (s, 3H), 2.47 (s, 3H), 7.11 (d, *J* = 8.4 Hz, 1H), 7.36 (d, *J* = 8.4 Hz, 1H), 7.46 (dd, *J* = 8.4 Hz, 4.2 Hz, 1H), 7.57-7.64 (comp, 2H), 8.18 (dd, *J* = 8.4 Hz, 1.8 Hz, 1H), 8.79 (dd, *J* = 4.2 Hz, 1.5 Hz, 1H), 8.93 (dd, *J* = 6.0 Hz, 3.0 Hz, 1H), 10.00 (br s, 1H); **^{13}C NMR** (75 MHz, $CDCl_3$) δ 20.7, 22.9, 116.9, 121.7, 121.9, 122.3, 122.4, 127.3, 127.9, 131.5, 132.9, 134.0, 136.2, 136.8, 138.4, 145.9, 148.4, 163.3, 169.3; **HRMS** (ESI, m/z) calcd for $C_{19}H_{15}BrN_2O_3$ $[M + H]^+$ 399.0344, found 399.0354.

3-bromo-5-methyl-2-(quinolin-8-ylcarbamoyl)phenyl acetate (2ag):

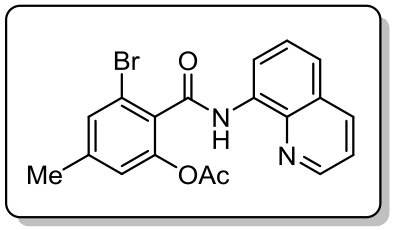

Yield 62% (49.4 mg); colorless solid; **R_f** 0.18 (pet ether/ethyl acetate = 4:1); **eluent composition** petroleum ether/ethyl acetate = 9:1; **mp** 138-140 °C; **^{1}H NMR** (300 MHz, $CDCl_3$) δ 2.12 (s, 3H), 2.40 (s, 3H), 7.00 (d, *J* = 1.2 Hz, 1H), 7.39 (d, *J* = 1.5 Hz, 1H), 7.46 (dd, *J* = 8.4 Hz, 4.2 Hz, 1H), 7.56-7.63 (comp, 2H), 8.18 (dd, *J* = 8.4 Hz, 1.8 Hz, 1H), 8.79 (dd, *J* = 4.2 Hz, 1.5 Hz, 1H), 8.91 (dd, *J* = 6.0 Hz, 2.7 Hz, 1H), 10.02 (br s, 1H); **^{13}C NMR** (150 MHz, $CDCl_3$) δ 20.8, 21.1, 116.9, 120.2, 121.8, 122.3, 122.9, 127.4, 128.0, 129.8, 131.2, 134.1, 136.3, 138.5, 142.1, 148.2, 148.5, 162.9, 169.3; **HRMS** (ESI, m/z) calcd for $C_{19}H_{15}BrN_2O_3$ $[M + H]^+$ 399.0344, found 399.0355.

3-bromo-5-chloro-2-(quinolin-8-ylcarbamoyl)phenyl acetate (2ah):

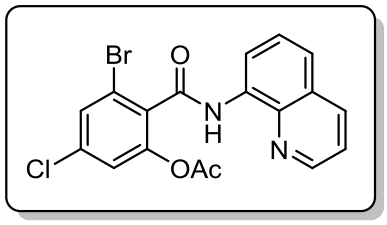

Yield 41% (34.7 mg); colorless solid; **R_f** 0.22 (pet ether/ethyl acetate = 4:1); **eluent composition** petroleum ether/ethyl acetate = 9:1; **mp** 124-126 °C; **^{1}H NMR** (300 MHz, $CDCl_3$) δ 2.14 (s, 3H), 7.26 (app d, *J* = 2.1 Hz, 1H), 7.47 (dd, *J* = 8.4 Hz, 4.2 Hz, 1H), 7.58-7.61 (comp, 3H), 8.19 (dd, *J* = 8.4 Hz, 1.2 Hz, 1H), 8.80 (dd, *J* = 4.2 Hz, 1.8 Hz, 1H), 8.88 (app t, *J* = 4.5 Hz, 1H), 10.03 (br s, 1H); **^{13}C NMR** (150 MHz, $CDCl_3$) δ 20.7, 117.0, 121.0, 121.9, 122.6, 123.0, 127.3, 128.0, 130.5, 131.2, 133.8, 136.2, 136.3, 138.4, 148.6, 148.6, 161.9, 168.7; **HRMS** (ESI, m/z) calcd for $C_{18}H_{12}BrClN_2O_3$ $[M + H]^+$ 418.9798, found 418.9803.

5-fluoro-3-iodo-2-(quinolin-8-ylcarbamoyl)phenyl acetate (2ai):

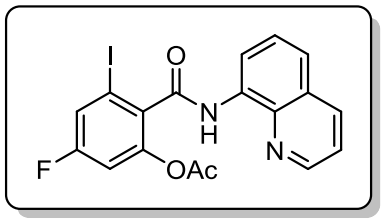

Yield 46% (41.6 mg); colorless solid; **R_f** 0.20 (pet ether/ethyl acetate = 4:1); **eluent composition** petroleum ether/ethyl acetate = 9:1; **mp** 152-154 °C; **^{1}H NMR** (300 MHz, $CDCl_3$) δ 2.12 (s, 3H), 7.04 (dd, *J* = 8.7 Hz, 2.4 Hz, 1H), 7.47 (dd, *J* = 8.4 Hz, 4.2 Hz, 1H), 7.56 (dd, *J* = 7.5 Hz, 2.4 Hz, 1H), 7.55-7.64 (comp, 2H), 8.20 (dd, *J* = 8.4 Hz, 1.8 Hz, 1H), 8.80 (dd, *J* = 4.2 Hz, 1.5 Hz, 1H), 8.89 (dd, *J* = 5.4 Hz, 3.6 Hz, 1H), 9.98 (br s, 1H); **^{13}C NMR** (150 MHz, $CDCl_3$) δ 20.8, 93.0 (d, $^3J_{F\text{-}C}$ = 10.5 Hz), 111.4 (d, $^2J_{F\text{-}C}$ = 24.0 Hz), 117.1, 121.9, 122.6, 124.4 (d, $^2J_{F\text{-}C}$ = 24.0 Hz), 127.4, 128.0, 133.0 (d, $^4J_{F\text{-}C}$ = 4.5 Hz), 133.9, 136.4, 138.4, 148.3 (d, $^3J_{F\text{-}C}$ = 10.5 Hz), 148.6, 162.3 (d, $^1J_{F\text{-}C}$ = 253.5 Hz), 163.8, 168.7; **HRMS** (ESI, m/z) calcd for $C_{18}H_{13}FIN_2O_3$ $[M + H]^+$ 450.9955, found 450.9969.

3-iodo-4-methyl-2-(quinolin-8-ylcarbamoyl)phenyl acetate (2aj):

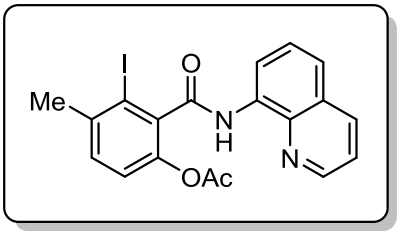

Yield 64% (57.1 mg); colorless solid; **R_f** 0.17 (pet ether/ethyl acetate = 4:1); **eluent composition** petroleum ether/ethyl acetate = 9:1; **mp** 160-162 ^oC; **^{1}H NMR** (300 MHz, $CDCl_3$) δ 2.10 (s, 3H), 2.52 (s, 3H), 7.14 (d, *J* = 8.4 Hz, 1H), 7.37 (d, *J* = 8.1 Hz, 1H), 7.46 (dd, *J* = 8.4 Hz, 4.2 Hz, 1H), 7.57-7.64 (comp, 2H), 8.18 (dd, *J* = 8.4 Hz, 1.8 Hz, 1H), 8.79 (dd, *J* = 4.2 Hz, 1.8 Hz, 1H), 8.92 (dd, *J* = 6.3 Hz, 2.7 Hz, 1H), 9.96 (br s, 1H); **^{13}C NMR** (75 MHz, $CDCl_3$) δ 20.7, 28.4, 99.8, 117.0, 121.8, 122.4, 122.7, 127.3, 128.0, 130.5, 134.1, 136.2, 137.2, 138.5, 140.5, 145.0, 148.5, 165.2, 169.4; **HRMS** (ESI, m/z) calcd for $C_{19}H_{15}IN_2O_3$ $[M + H]^+$ 447.0206, found 447.0218.

4-methoxy-2-(quinolin-8-ylcarbamoyl)phenyl acetate (2ak):

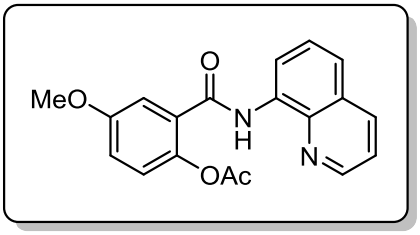

Yield 24% (16.4 mg); colorless solid; **R_f** 0.20 (pet ether/ethyl acetate = 4:1); **eluent composition** petroleum ether/ethyl acetate = 9:1; **mp** 110-112 ^oC; **^{1}H NMR** (600 MHz, $CDCl_3$) δ 2.46 (s, 3H), 3.92 (s, 3H), 7.12 (dd, *J* = 8.4 Hz, 3.6 Hz, 1H), 7.18 (d, *J* = 9.0 Hz, 1H), 7.52 (dd, *J* = 8.4 Hz, 4.2 Hz, 1H), 7.59 (app d, *J* = 7.8 Hz, 1H), 7.63 (app t, *J* = 7.8 Hz, 1H), 7.71 (app d, *J* = 3.0 Hz, 1H), 8.23 (app d, *J* = 8.4 Hz, 1H), 8.86 (app d, *J* = 4.2 Hz, 1H), 9.02 (app d, *J* = 7.8 Hz, 1H), 11.08 (br s, 1H); **^{13}C NMR** (150 MHz, $CDCl_3$) δ 21.4, 55.8, 114.6, 117.3, 119.0, 121.7, 122.0, 124.4, 127.6, 128.1, 128.2, 134.8, 136.5, 138.8, 141.6, 148.1, 157.4, 163.0, 169.5; **HRMS** (ESI, m/z) calcd for $C_{19}H_{16}N_2O_4$ $[M + H]^+$ 359.1008, found 359.1005.

4-bromo-2-(quinolin-8-ylcarbamoyl)phenyl acetate (2al):

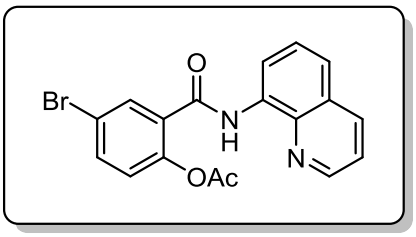

Yield 24% (16.4 mg); colorless solid; **R_f** 0.30 (pet ether/ethyl acetate = 4:1); **eluent composition** petroleum ether/ethyl acetate = 9:1; **mp** 174-176 ^oC; **^{1}H NMR** (600 MHz, $CDCl_3$) δ 2.46 (s, 3H), 7.17 (d, *J* = 9.0 Hz, 1H), 7.53 (dd, *J* = 8.4 Hz, 4.2 Hz, 1H), 7.60-7.65 (comp, 2H), 7.68 (dd, *J* = 8.4 Hz, 2.4 Hz, 1H), 8.24 (dd, *J* = 8.4 Hz, 1.2 Hz, 1H), 8.32 (d, *J* = 2.4 Hz, 1H), 8.86 (dd, *J* = 4.2 Hz, 1.8 Hz, 1H), 8.98 (dd, *J* = 7.2 Hz, 1.2 Hz, 1H), 11.02 (br s, 1H); **^{13}C NMR** (150 MHz, $CDCl_3$) δ 21.4, 117.4, 119.6, 121.8, 122.3, 125.2, 127.6, 128.1, 129.4, 134.0, 134.5, 135.2, 136.6, 138.7, 147.1, 148.2, 161.7, 168.7; **HRMS** (ESI, m/z) calcd for $C_{18}H_{13}BrN_2O_3$ $[M + H]^+$ 385.0188, found 385.0192.

1-(quinolin-8-ylcarbamoyl)naphthalen-2-yl acetate(2am):[8f]

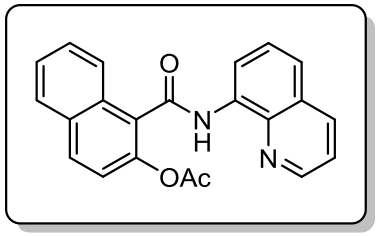

Yield 62% (44.3 mg); colorless oil; **R_f** 0.20 (pet ether/ethyl acetate = 4:1); **eluent composition** petroleum ether/ethyl acetate = 9:1; **^{1}H NMR** (300 MHz, $CDCl_3$) δ 2.18 (s, 3H), 7.35 (app d, *J* = 9.0 Hz, 1H), 7.44 (dd, *J* = 8.4 Hz, 4.2 Hz, 1H), 7.52-7.58 (comp, 2H), 7.61 (app d, *J* = 1.8 Hz, 1H), 7.64 (d, *J* = 7.2 Hz, 1H), 7.90-7.93 (m, 1H), 7.98 (app d, *J* = 9.0 Hz, 1H), 8.16 (app d, *J* = 5.4 Hz, 1H), 8.19 (dd, *J* = 8.4 Hz, 1.8 Hz, 1H), 8.74 (dd, *J*= 4.2 Hz, 1.8 Hz, 1H), 9.07 (dd, *J* = 7.2 Hz, 1.8 Hz, 1H), 10.24 (br s, 1H); **^{13}C NMR** (150 MHz, $CDCl_3$) δ 20.9, 117.0, 121.6, 121.8, 122.3, 125.3, 126.3, 126.4, 127.4, 127.8, 128.0, 128.2, 131.0, 131.2, 131.7, 134.4, 136.3, 138.5, 145.2, 148.5, 164.3, 169.7; **HRMS** (ESI, m/z) calcd for $C_{22}H_{16}N_2O_3$ $[M + H]^+$ 357.1239, found 357.1238.

2-(quinolin-8-ylcarbamoyl)thiophen-3-yl acetate (2an):

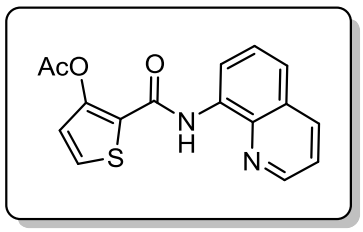

Yield 40% (12.4 mg); colorless solid; **R_f** 0.16 (pet ether/ethyl acetate = 4:1); **eluent composition** petroleum ether/ethyl acetate = 4:1; **mp** 188-190 ^{o}C; **^{1}H NMR** (300 MHz, $CDCl_3$) δ 2.71 (s, 3H), 7.27 (d, *J* = 5.7 Hz, 1H), 7.47-7.52 (comp, 2H), 7.54-7.62 (comp, 2H), 8.20 (dd, *J* = 8.4 Hz, 1.8 Hz, 1H), 8.79 (dd, *J* = 4.2 Hz, 1.8 Hz, 1H), 8.94 (dd, *J* = 6.9 Hz, 2.1 Hz, 1H), 11.14 (br s, 1H); **^{13}C NMR** (75 MHz, $CDCl_3$) δ 21.3, 117.2, 121.6, 121.8, 122.6, 125.4, 127.5, 128.0, 128.8, 134.6, 136.5, 138.5, 145.4, 147.8, 158.8, 167.3; **HRMS** (ESI, m/z) calcd for $C_{16}H_{12}N_2O_3S$ $[M + H]^+$ 313.0647, found 313.0647.

2-(quinolin-8-ylcarbamoyl)phenyl acetate (2ao):

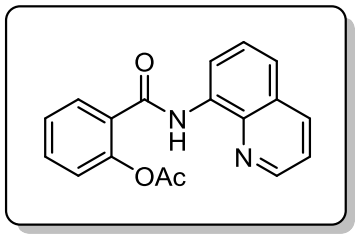

Yield 22% (13.5 mg); colorless solid; **R_f** 0.25 (pet ether/ethyl acetate = 4:1); **eluent composition** petroleum ether/ethyl acetate = 9:1; **mp** 142-144 ^{o}C; **^{1}H NMR** (300 MHz, $CDCl_3$) δ 2.44 (s, 3H), 7.25 (app d, *J* = 8.1 Hz, 1H), 7.41 (app t, *J* = 7.5 Hz, 1H), 7.48 (dd, *J* = 8.4 Hz, 4.2 Hz , 1H), 7.53-7.63 (comp, 3H), 8.14 (dd, *J* = 7.5 Hz, 1.5 Hz, 1H), 8.20 (dd, *J* = 8.4 Hz, 4.2 Hz, 1H), 8.83 (dd, *J* = 4.2 Hz, 1.8 Hz, 1H), 8.99 (dd, *J* = 7.2 Hz, 1.8 Hz, 1H), 10.98 (br s, 1H); **^{13}C NMR** (150 MHz, $CDCl_3$) δ 21.4, 117.2, 121.7, 122.0, 123.4, 126.4, 127.6, 127.8, 128.1, 131.1, 132.4, 134.8, 136.5, 138.7, 148.1, 148.2, 163.2, 169.1; **HRMS** (ESI, m/z) calcd for $C_{18}H_{14}N_2O_3$ $[M + Na]^+$ 329.0902, found 329.0892.

2-(quinolin-8-ylcarbamoyl)-1,3-phenylene diacetate (2ap):[8f]

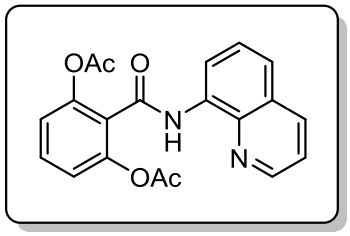

Yield 14% (10.1 mg); colorless solid; **R_f** 0.15 (pet ether/ethyl acetate = 4:1); **eluent composition** petroleum ether/ethyl acetate = 4:1; **mp** 94-96 ^oC; **^{1}H NMR** (300 MHz, $CDCl_3$) δ 2.19 (s, 6H), 7.15 (d, *J* = 8.1 Hz, 2H), 7.44-7.48 (m, 1H), 7.52 (d, *J* = 8.4 Hz, 1H), 7.53-7.61 (comp, 2H), 8.18 (dd, *J* = 8.1 Hz, 1.8 Hz, 1H), 8.81 (dd, *J* = 4.2 Hz, 1.8 Hz, 1H), 8.87 (dd, *J* = 6.0 Hz, 3.0 Hz, 1H), 10.21 (br s, 1H); **^{13}C NMR** (150 MHz, $CDCl_3$) δ 20.9, 116.9, 120.8 (x 2), 121.8, 122.2, 123.9, 127.4, 128.0, 130.9, 134.3, 136.3, 138.5, 148.4, 148.7, 161.0, 169.0; **HRMS** (ESI, m/z) calcd for $C_{20}H_{16}N_2O_5$ $[M + Na]^+$ 387.0957, found 387.0944.

2.5.5. Synthetic Transformation of the Acetoxylated Product 2a

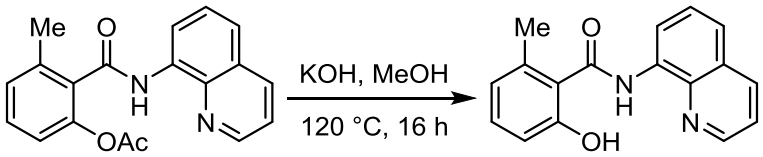

2a **3**, 95%

Following literature procedure,[21] in a 15 mL round bottomed flask, equipped with condenser, **2a** (64 mg, 0.2 mmol, 1.0 equiv) was taken and to it KOH (673 mg, 12 mmol, 60.0 equiv) and MeOH (5 mL) were added. The reaction mixture was kept for stirring in an oil bath by slowly raising temperature upto 120 ^oC for 16 h. After completion of reaction (checked by TLC), the reaction mixture was quenched with aq. HCl to make pH 6-7 and then it was extracted with ethyl acetate. The combined organic layers were given brine wash, and the organic phase was separated and concentrated under vacuo. The crude reaction mixture was subjected to column chromatography on silica gel using petroleum ether/ethyl acetate (9:1) as eluent to give **3** in 95% yield (53.0 mg).

Yield 95% (53.0 mg); colorless solid; **R_f** 0.18 (pet ether/ethyl acetate = 9:1); **eluent composition** petroleum ether/ethyl acetate = 9:1; **mp** 190-192 ^oC; **^{1}H NMR** (600 MHz, $CDCl_3$) δ 2.86 (s, 3H), 6.86 (d, *J* = 7.8 Hz, 1H), 6.93 (d, *J* = 7.8 Hz, 1H), 7.31 (app t, *J* = 7.8 Hz, 1H), 7.51 (dd, *J* = 7.8 Hz, 4.2 Hz , 1H), 7.61-7.65 (comp, 2H), 8.23 (app d, *J* = 7.8 Hz, 1H), 8.84 (app d, *J* = 4.2 Hz, 1H), 8.92 (dd, *J* = 6.6 Hz, 1.8 Hz, 1H), 10.64 (br s, 1H), 10.90 (br s, 1H); **^{13}C NMR** (150 MHz $CDCl_3$) δ 22.9, 115.8, 117.3, 118.5, 121.9, 122.5, 123.0, 127.4, 128.0, 132.6, 134.0, 136.1, 136.5, 138.8, 148.6, 160.5, 168.9; **HRMS** (ESI, m/z) calcd for $C_{17}H_{14}N_2O_2$ $[M + H]^+$ 279.1134, found 279.1140.

2.5.6. Mechanistic Experiments

(a) Procedure for H/D exchange experiments:

Procedure for H/D exchange experiment: (in presence of $Mn(OAc)_3.2H_2O$)

An oven-dried 10 mL Schlenk tube was charged with *N*-(quinolin-8-yl)benzamide **1ao** (49.7 mg, 0.2 mmol, 1.0 equiv) and catalyst $Co(acac)_2$ (5.1 mg, 0.02 mmol, 0.1 equiv), $Mn(OAc)_3.2H_2O$ (214.5 mg, 0.8 mmol, 4.0 equiv) and CD_3OD (0.16 mL, 4.0 mmol, 20.0 equiv). The tube was evacuated and backfilled with nitrogen and to it was added anhydrous DCE (2.0 mL, 0.1 M) under nitrogen atmosphere. The reaction mixture was degassed and backfilled with nitrogen 3 times. The tube was closed with a teflon-lined cap and kept on stirring in an oil bath. The bath temperature was slowly increased to 100 ^oC. After 12 h, the reaction was stopped and cooled to room temperature. The reaction mixture was filtered through a short pad of celite and concentrated under vacuo. The starting material **1ao**-d_n was recovered (6.9 mg, 14%), also the mono acetoxy product **2ao**-d_n was isolated (5.9 mg, 10%) by purifying through column chromatography on silica gel using ethyl acetate/petroleum ether as eluent. The deuterium incorporation was observed (24%) in case of **1ao**-d_n and (32%) in case of **2ao**-d_n by ^1H NMR spectroscopy.

Procedure for H/D exchange experiment: (in absence of $Mn(OAc)_3.2H_2O$)

An oven-dried 10 mL Schlenk tube was charged with *N*-(quinolin-8-yl)benzamide **1ao** (49.7 mg, 0.2 mmol, 1.0 equiv) and catalyst $Co(acac)_2$ (5.1 mg, 0.02 mmol, 0.1 equiv), $Mn(OAc)_3.2H_2O$ (214.5 mg, 0.8 mmol, 4.0 equiv) and CD_3OD (0.16 mL, 4.0 mmol, 20.0 equiv). The tube was evacuated and backfilled with nitrogen and to it was added anhydrous DCE (2.0 mL, 0.1 M) under nitrogen atmosphere. The reaction mixture was degassed and backfilled with nitrogen 3 times. The tube was closed with a teflon-lined cap and kept on stirring in an oil bath. The bath temperature was slowly increased to 100 ^oC. After 12 h, the reaction was stopped and cooled to room temperature. The reaction mixture was filtered through a short pad of celite and concentrated under vacuo. The starting material **1ao**-d_n was recovered (6.9 mg, 14%), also the mono acetoxy product **2ao**-d_n was isolated (5.9 mg, 10%) by purifying through column chromatography on silica gel using ethyl acetate/petroleum ether as eluent. The deuterium incorporation was observed (24%) in case of **1ao**-d_n and (32%) in case of **2ao**-d_n by ^1H NMR spectroscopy.

(b) Procedure for competitive experiment between 1ao and 1ao-d_5:

To an oven dried 10 mL Schlenk tube, a mixture of **1ao** and **1ao**-d_5 (0.1 mmol each) were subjected under standard condition. After 30 min, the reaction was stopped and cooled to room temperature. The reaction mixture was filtered through a short pad of celite and concentrated under vacuo. The crude reaction mixture was directly purified by column chromatography on silica gel using ethyl acetate/petroleum ether as eluent. The ratio of **2ao** and **2ao**-d_4 was determined by ^{1}H NMR spectroscopy.

Primary Kinetic Isotopic Effect ($\boldsymbol{k_H/k_D}$) = 0.72/0.28 = 2.6.

(c) Procedure for parallel experiment between 1ao and 1ao-d_5:

In two separate oven-dried 10 mL Schlenk tubes, **1ao** and **1ao**-d_5 (0.1 mmol each) were subjected under standard condition. After 30 min, the reaction was stopped and cooled to room temperature. Both the reaction mixtures were filtered through a short pad of celite, mixed and concentrated under vacuo. The crude reaction mixture was directly purified by column chromatography on silica gel using ethyl acetate/petroleum ether as eluent. The ratio of **2ao** and **2ao**-d_4 was determined by ^{1}H NMR spectroscopy.

Primary Kinetic Isotopic Effect ($\boldsymbol{k_H/k_D}$) = 0.73/0.27 = 2.7.

(d) Procedure for competitive experiment between 1q and 1n:

To an oven-dried 10 mL Schlenk tube, a mixture of **1q** and **1n** (0.1 mmol each) were subjected under standard condition. After 2 h, the reaction was stopped and cooled to room temperature. The reaction mixture was filtered through a short pad of celite and concentrated under vacuo. The crude reaction mixture was directly purified by column chromatography on silica gel using petroleum ether/ethyl acetate as eluent to obtain pure **2q** and **2n** in 36% and 35% yields respectively.

(e) Procedure for the preparation of complex C_1:

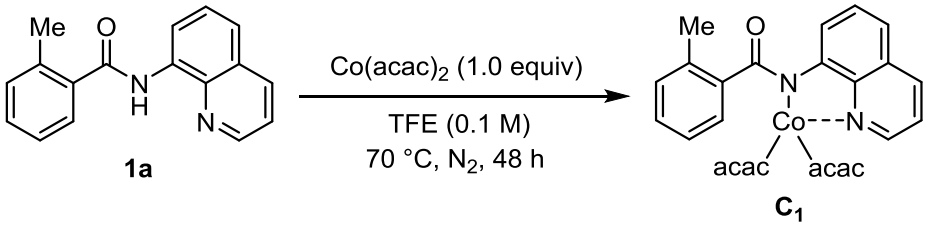

Following literature procedure,[13n] an oven-dried 10 mL Schlenk tube was charged with 2-methyl-*N*-(quinolin-8-yl)benzamide (**1a**) (52.5 mg, 0.2 mmol, 1.0 equiv) and catalyst $Co(acac)_2$ (51.4 mg, 0.2 mmol, 1.0 equiv). The tube was evacuated and backfilled with nitrogen and to it was added anhydrous TFE (2.0 mL, 0.1 M) under nitrogen atmosphere. The reaction mixture was degassed and backfilled with nitrogen 3 times. The tube was closed with a teflon-lined cap and kept on stirring in an oil bath. The bath temperature was slowly increased to 70 ^oC. After 48 h, the reaction was stopped and cooled to room temperature. The reaction mixture was filtered through a short pad of celite and concentrated under vacuo. The crude reaction mixture was directly purified by column chromatography on silica gel using petroleum ether/ethyl acetate as eluent to obtain the intermediate complex**.** The formation of the desired complex **C_1** was indicated by mass analysis (ESI, m/z at 541.1171 $[M + Na]^+$).

(f) Procedure for the reaction with the intermediate complex C_1:

In an oven-dried 10 mL Schlenk tube, 2-methyl-*N*-(quinolin-8-yl)benzamide **1a** (26.2 mg, 0.1 mmol, 1.0 equiv), complex **C_1** (5.2 mg, 0.01 mmol, 0.1 equiv) and $Mn(OAc)_3.2H_2O$ (107.2 mg, 0.4 mmol, 4.0 equiv) were added and reaction mixture was degassed and backfilled with nitrogen. Under nitrogen 1.0 mL (0.1 M) of anhydrous DCE was added. Then it was degassed and backfilled with nitrogen (3 times). The tube was closed with a teflon-lined cap and kept on stirring in an oil bath. The bath temperature was slowly increased to 100 ^oC. After 24 h, the reaction was stopped and cooled to room temperature. The reaction mixture was filtered through a short pad of celite and concentrated under vacuo. The crude reaction mixture was directly purified by column chromatography on silica gel using petroleum ether/ethyl acetate as eluent to give 3-methyl-2-(quinolin-8-ylcarbamoyl)phenyl acetate **2a** (80% yield).

2.6. ^{1}H and ^{13}C NMR Spectra of Representative Compounds

^{1}H NMR of **1a** (400 MHz, $CDCl_3$):[13g]

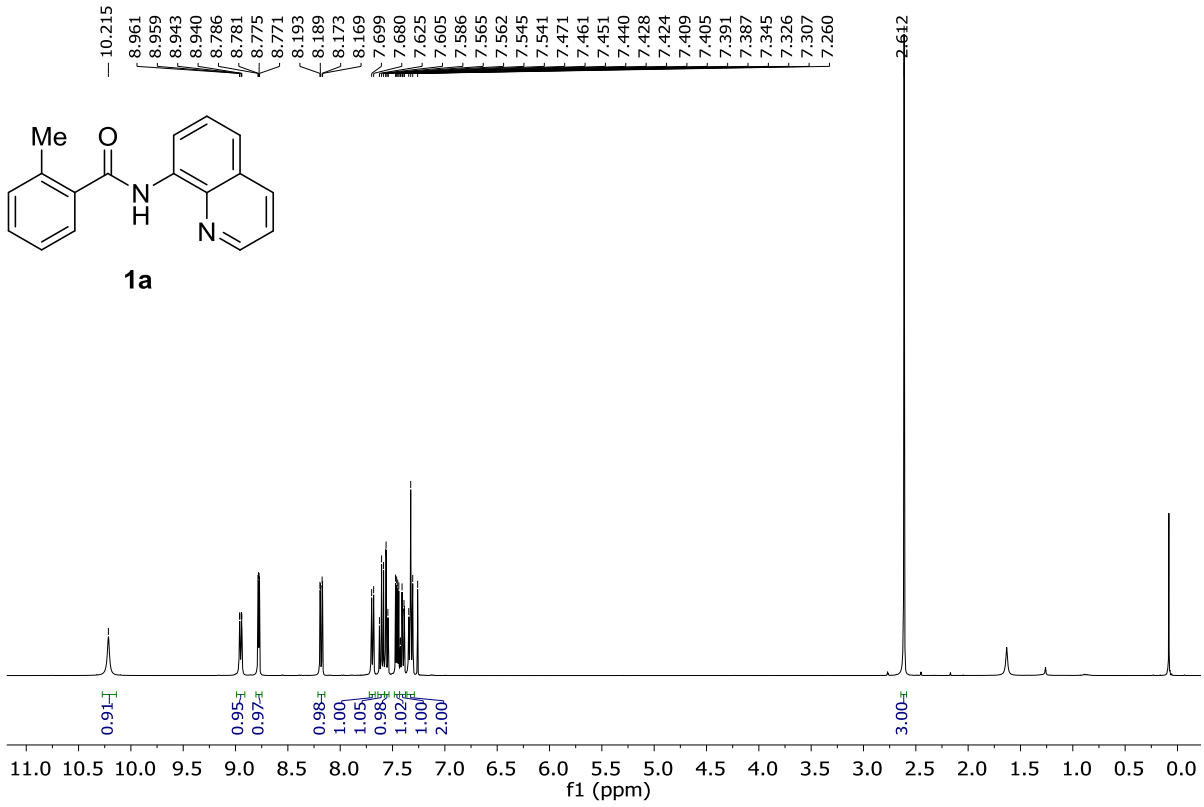

^{13}C NMR of **1a** (100 MHz, $CDCl_3$):

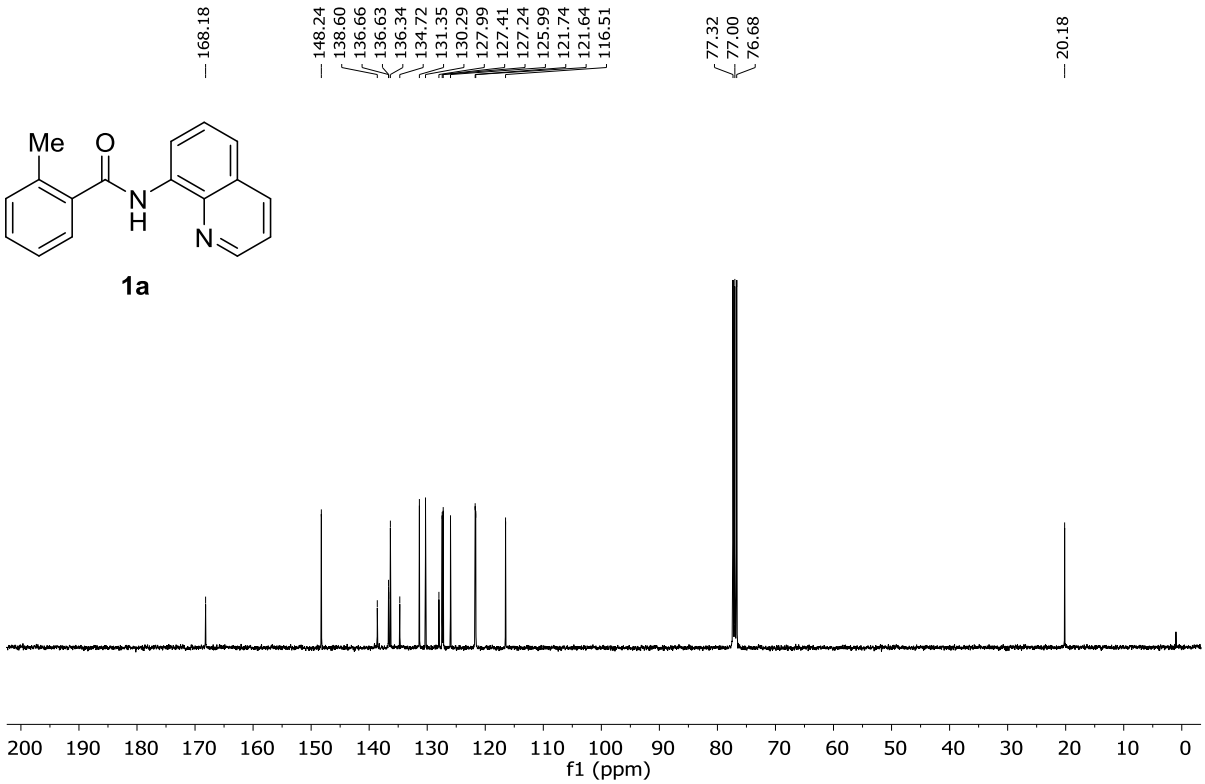

^{1}H NMR of **2a** (300 MHz, $CDCl_3$):

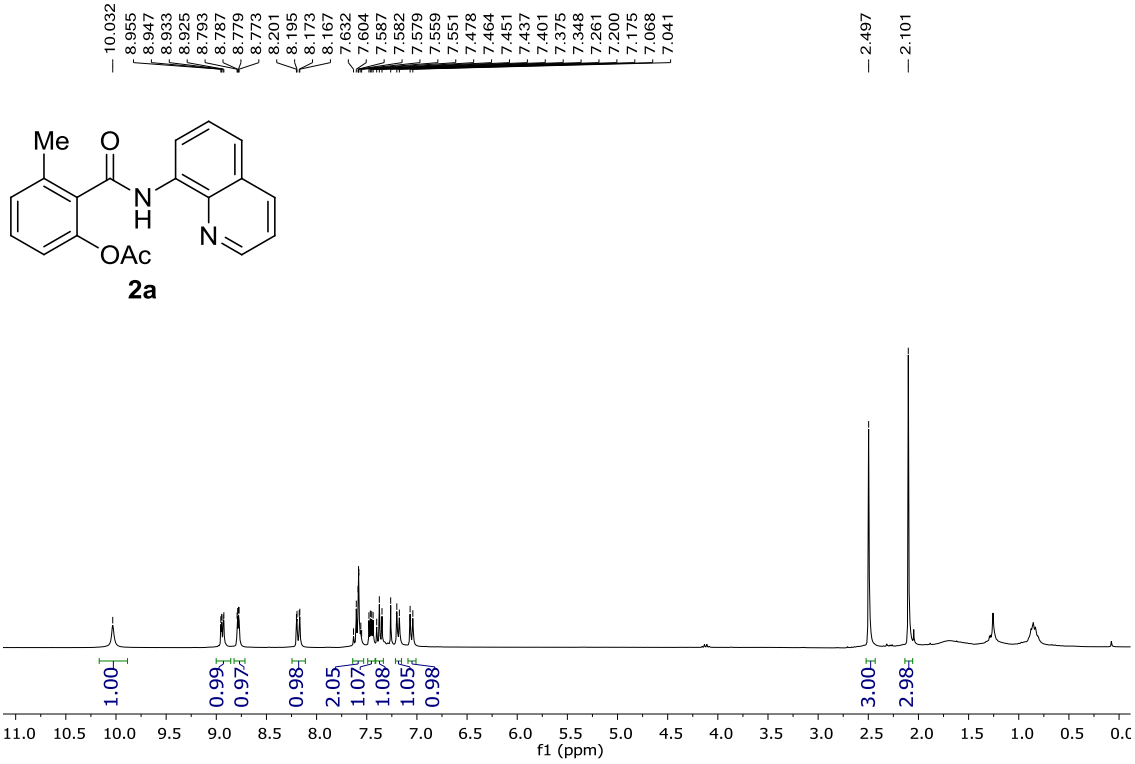

^{13}C NMR of **2a** (75 MHz, $CDCl_3$):

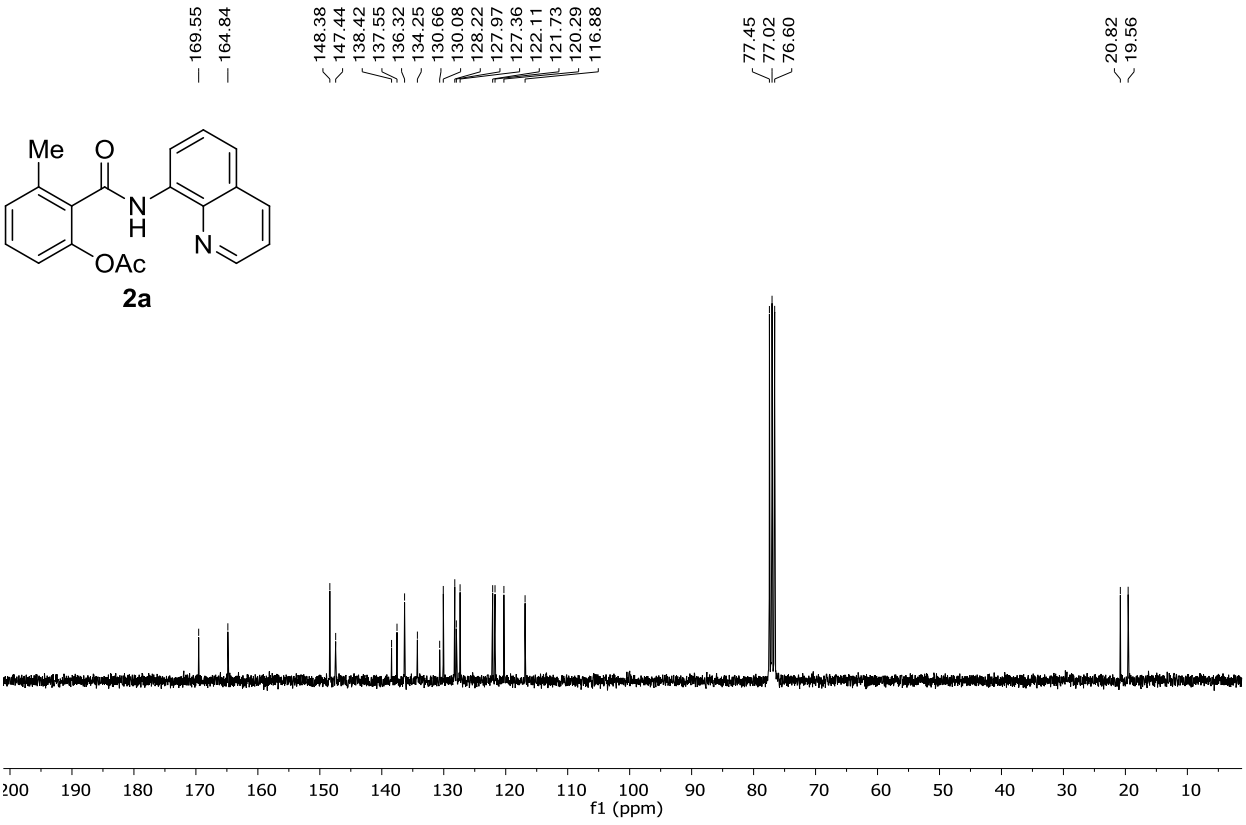

^{1}H NMR of **2d** (300 MHz, $CDCl_3$):

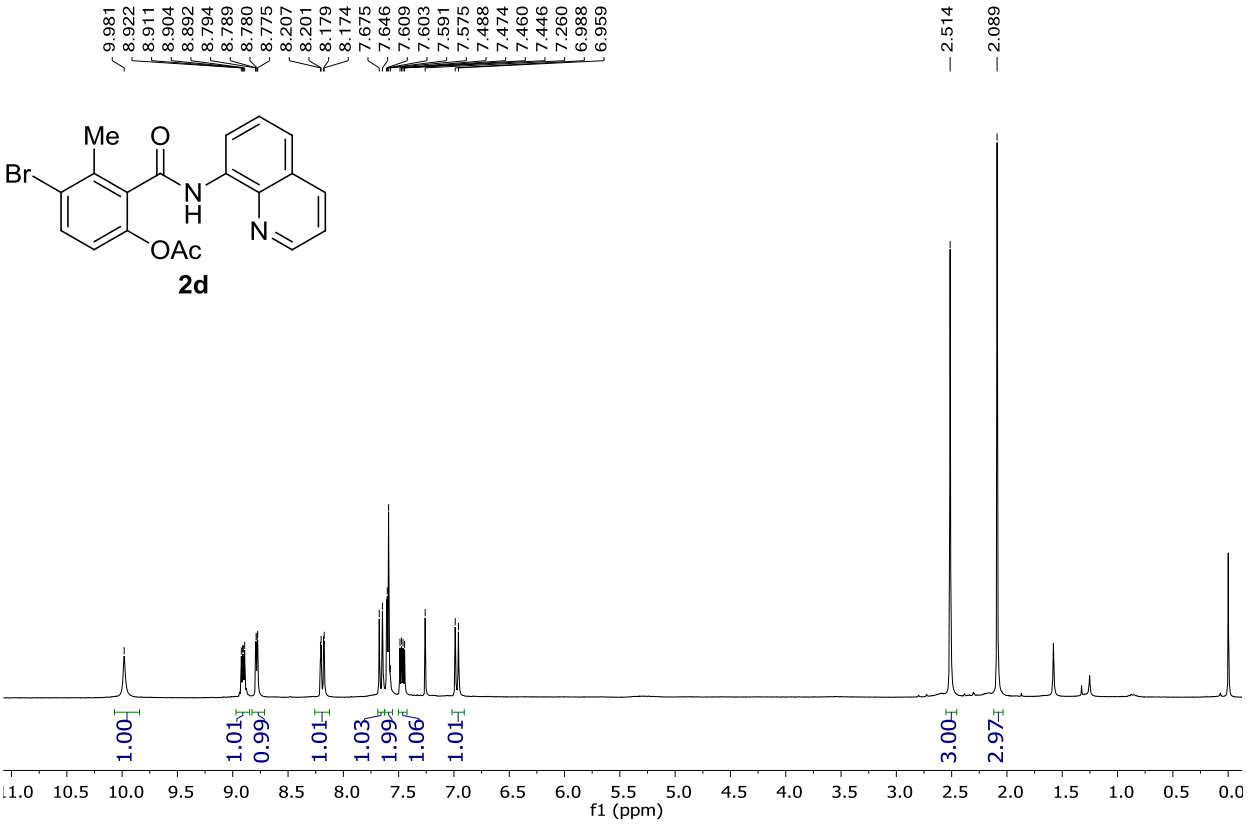

^{13}C NMR of **2d** (75 MHz, $CDCl_3$):

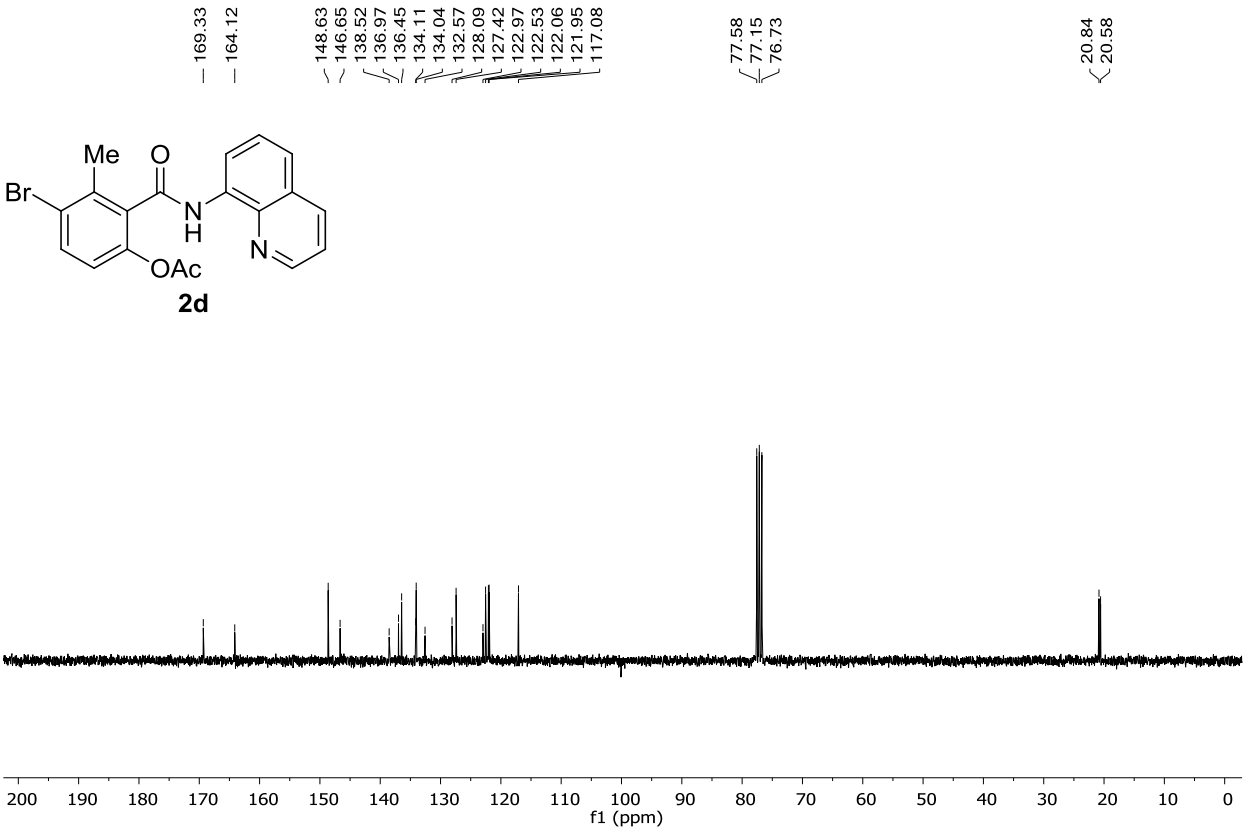

^{1}H NMR of **2g** (300 MHz, $CDCl_3$):

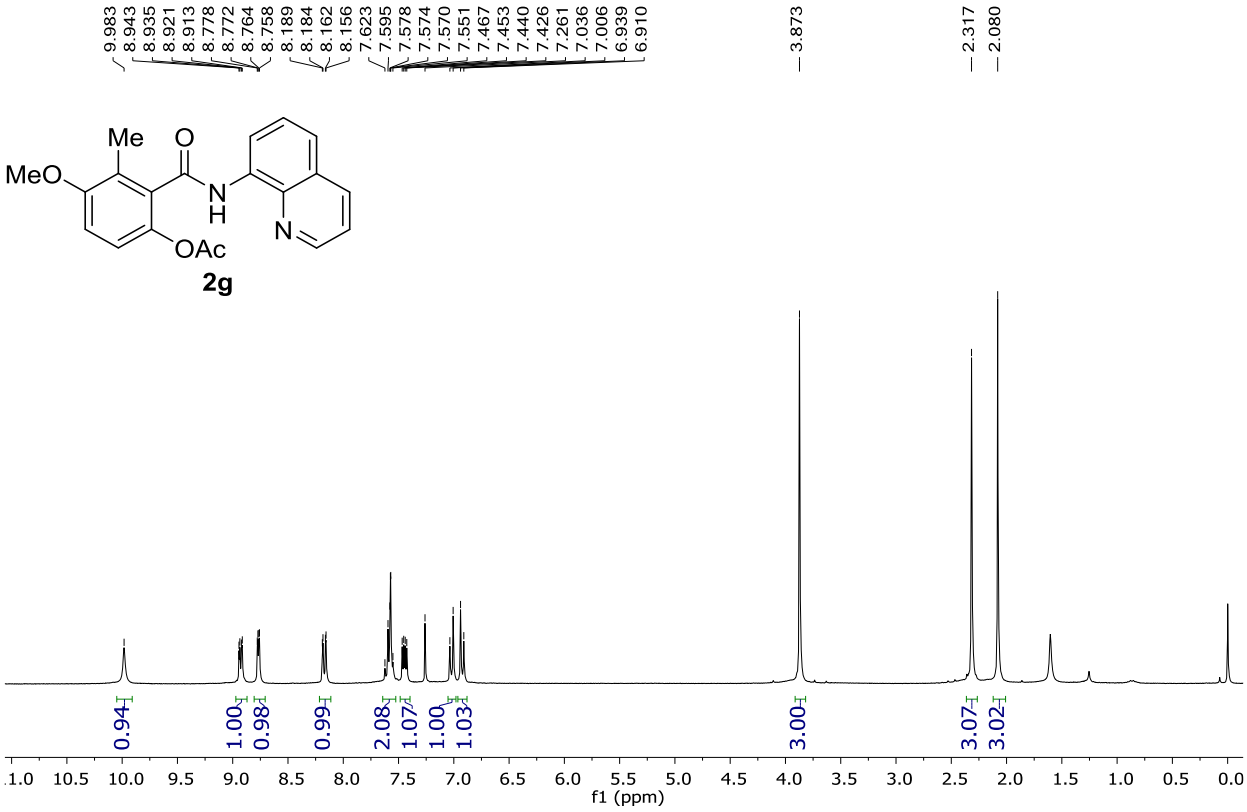

^{13}C NMR of **2g** (150 MHz, $CDCl_3$):

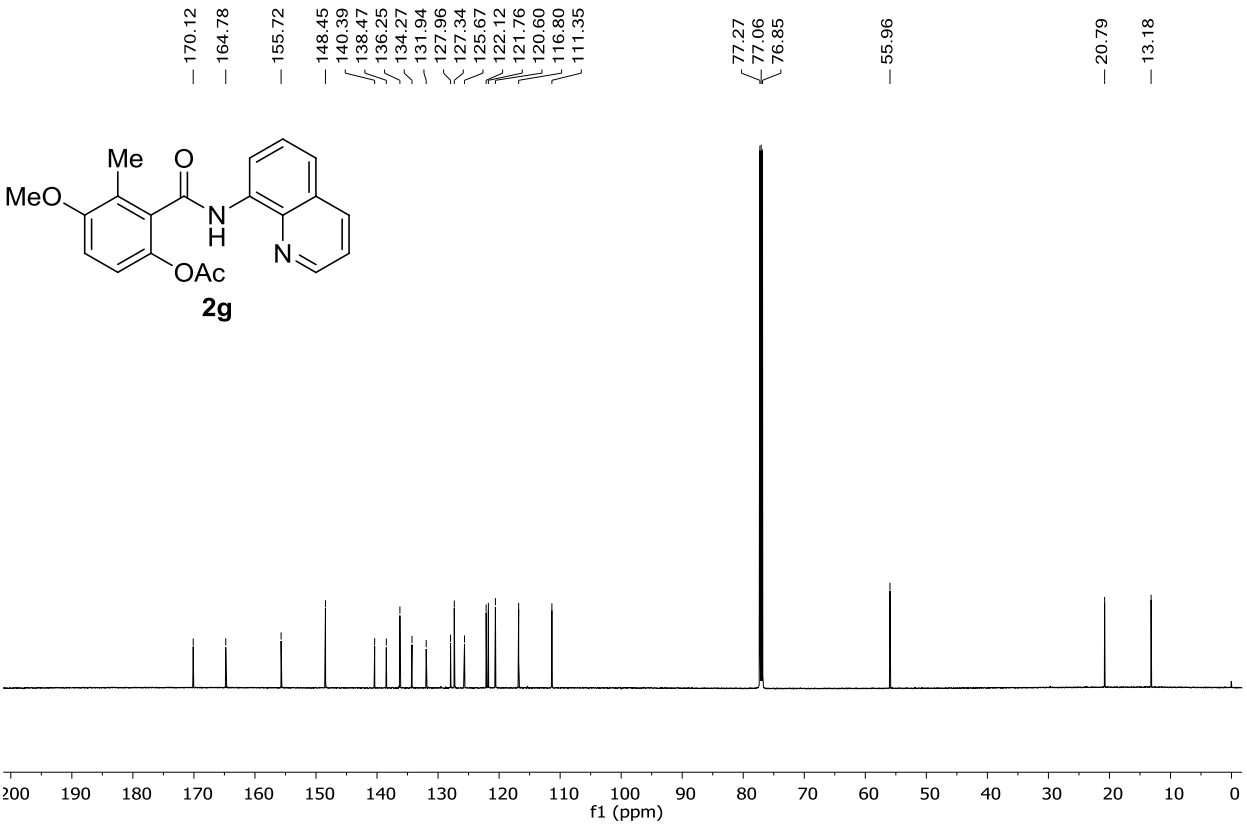

^{1}H NMR of **2j** (300 MHz, $CDCl_3$):

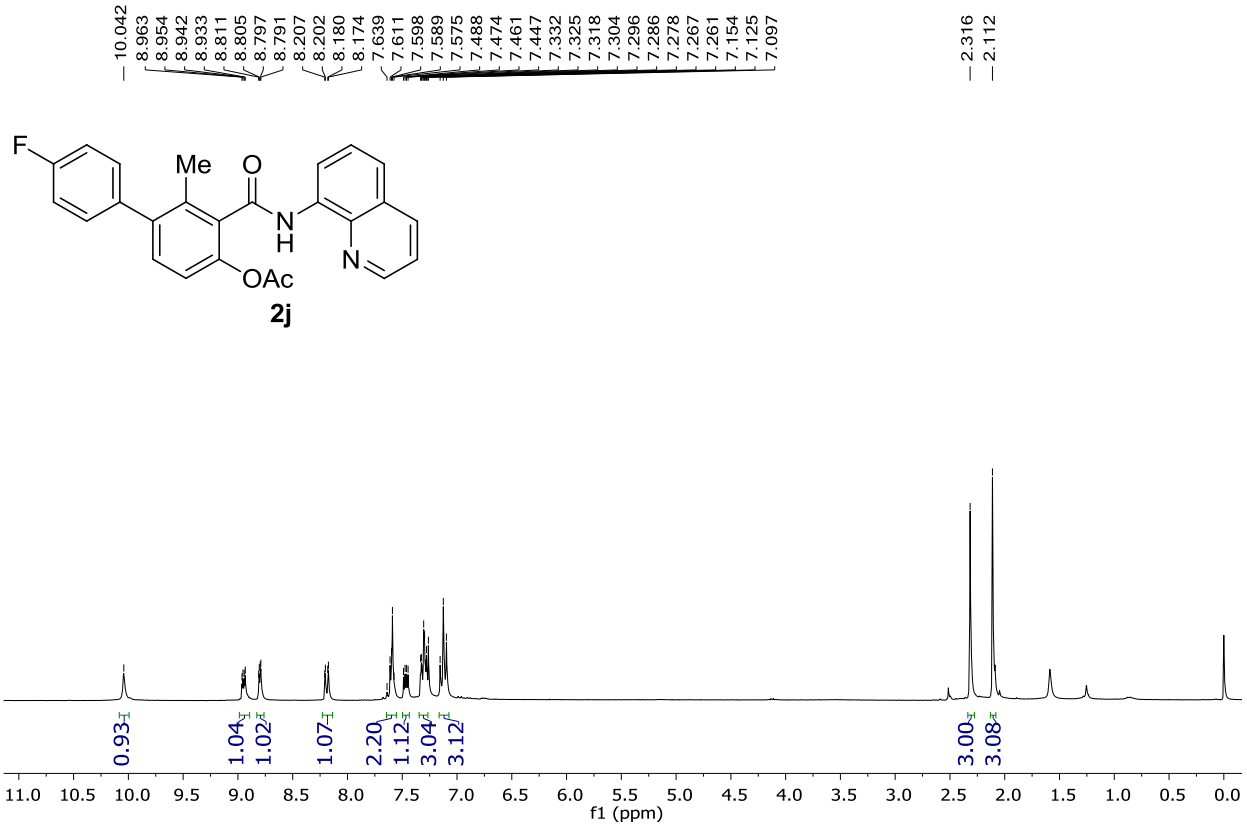

^{13}C NMR of **2j** (75 MHz, $CDCl_3$):

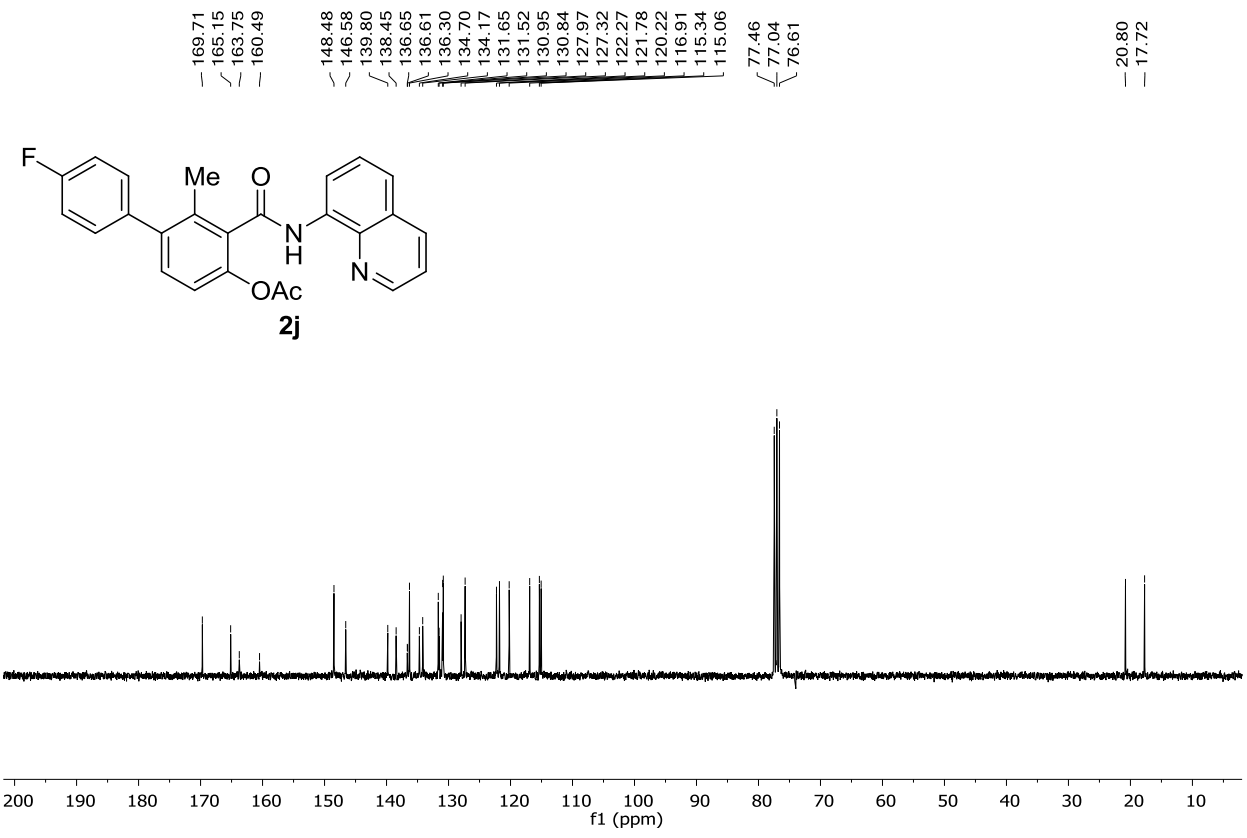

^{1}H NMR of **2l** (300 MHz, $CDCl_3$):

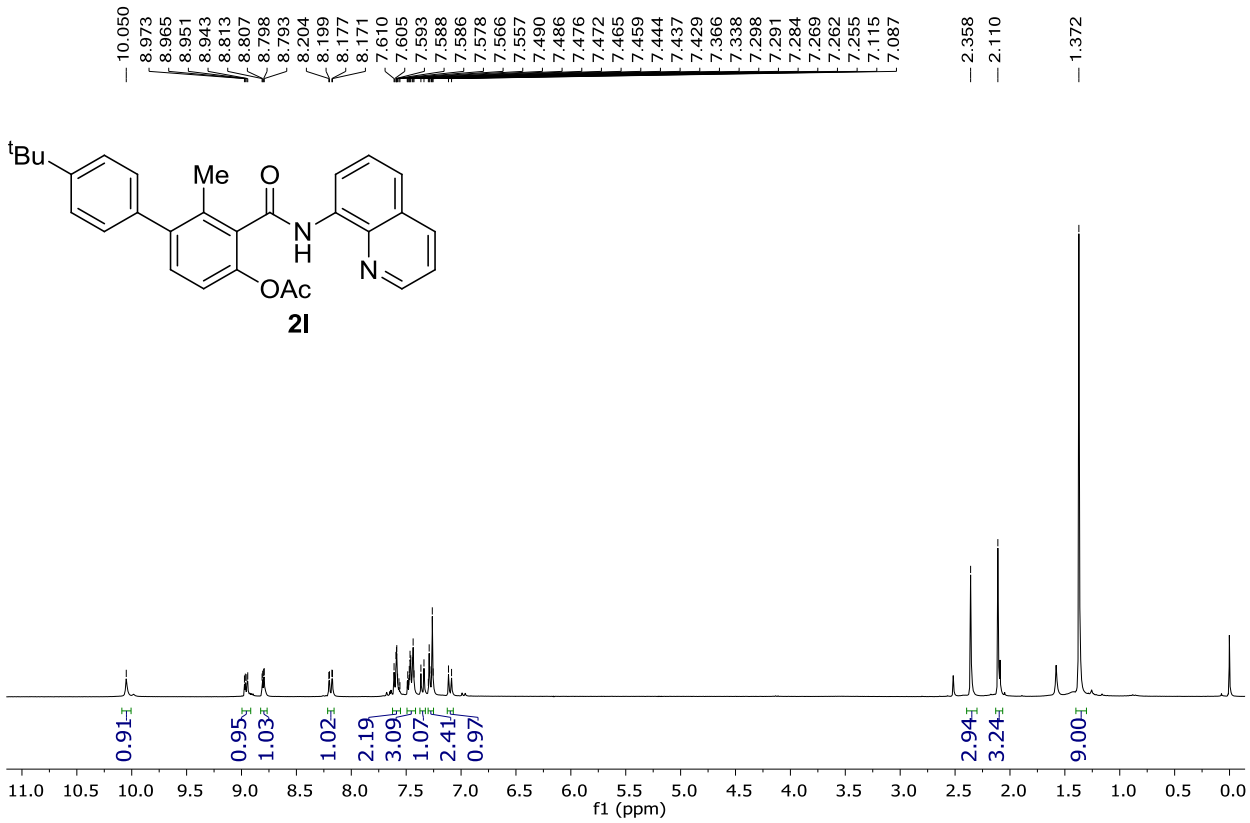

^{13}C NMR of **2l** (75 MHz, $CDCl_3$):

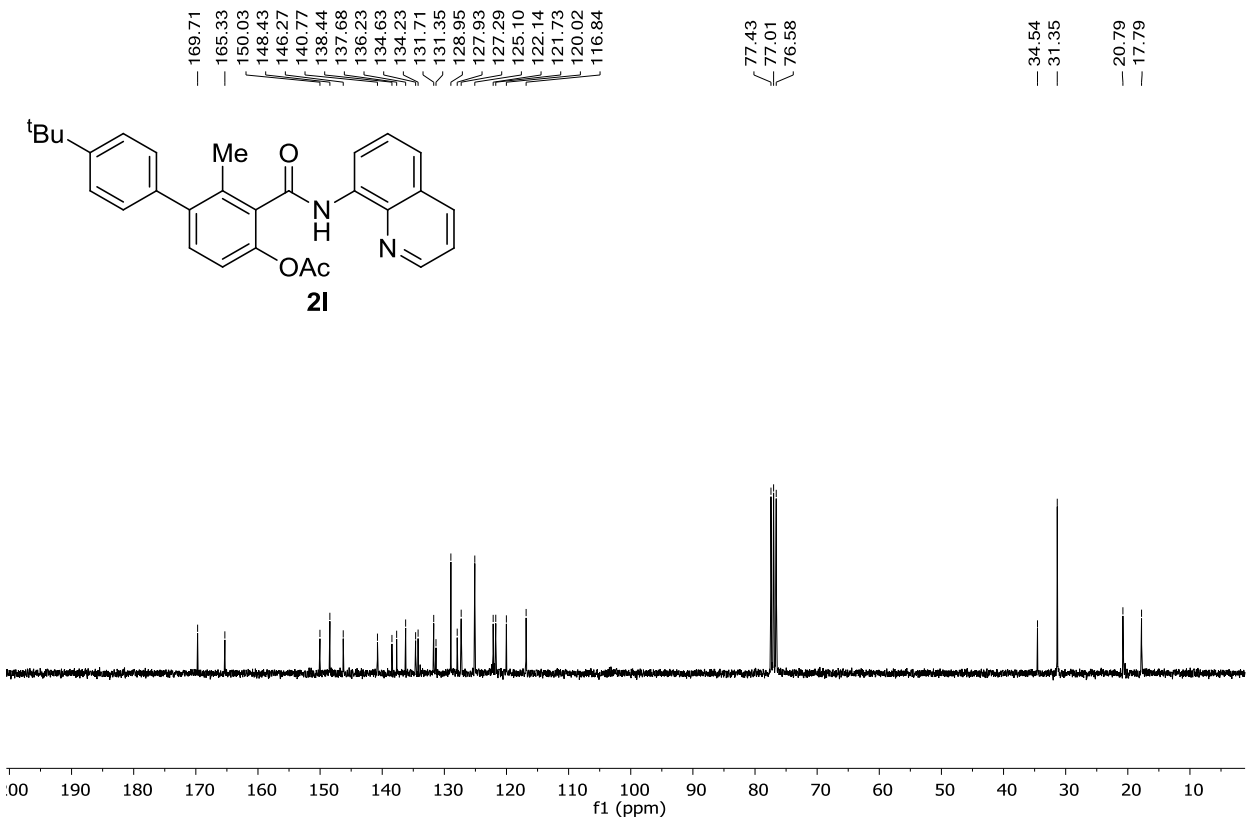

^{1}H NMR of **2n** (300 MHz, $CDCl_3$):

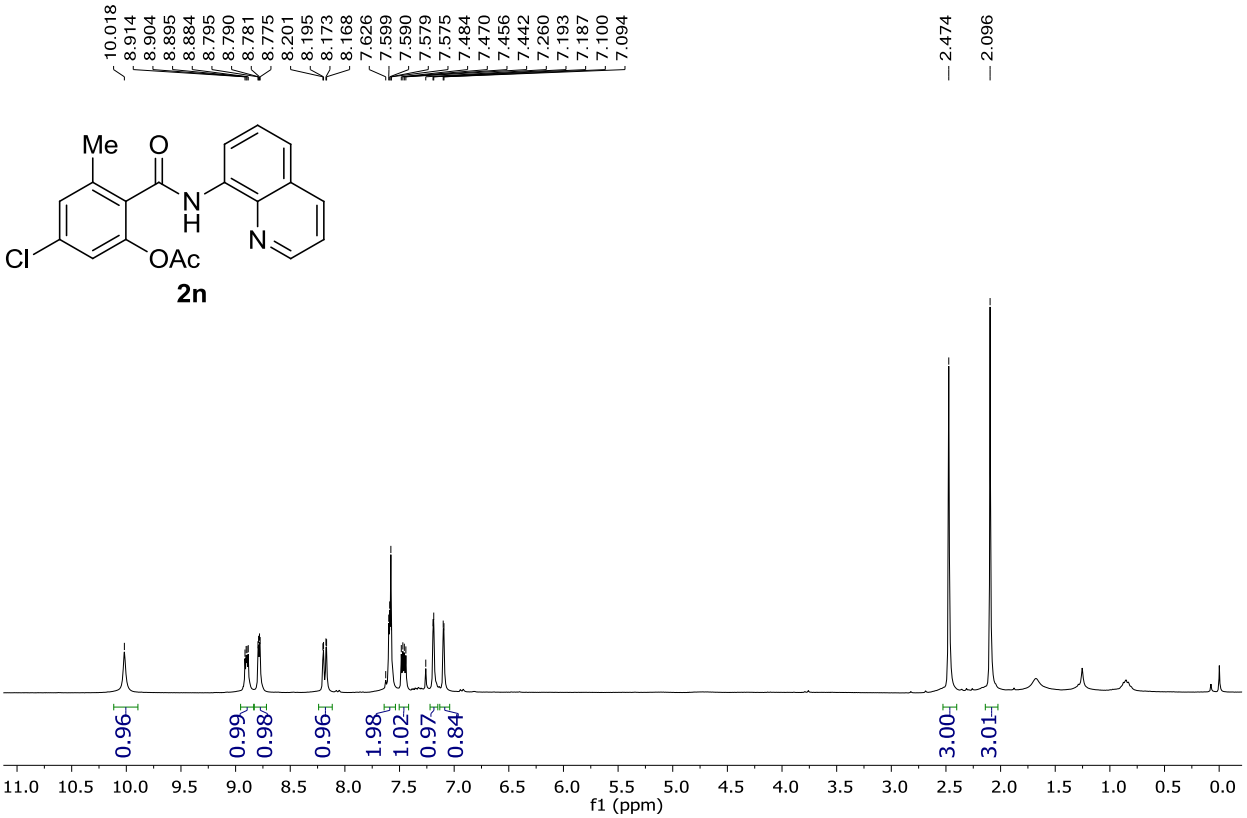

^{13}C NMR of **2n** (75 MHz, $CDCl_3$):

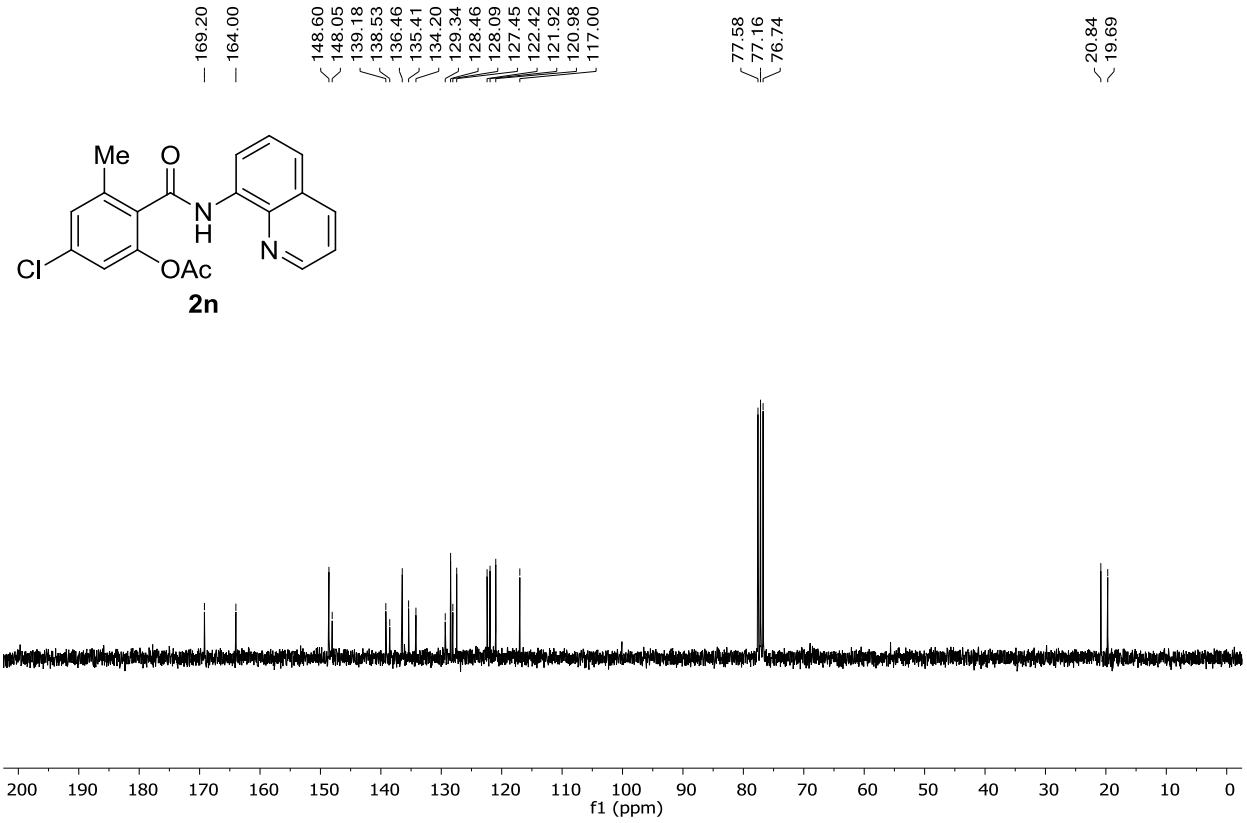

^{1}H NMR of **2p** (300 MHz, $CDCl_3$):

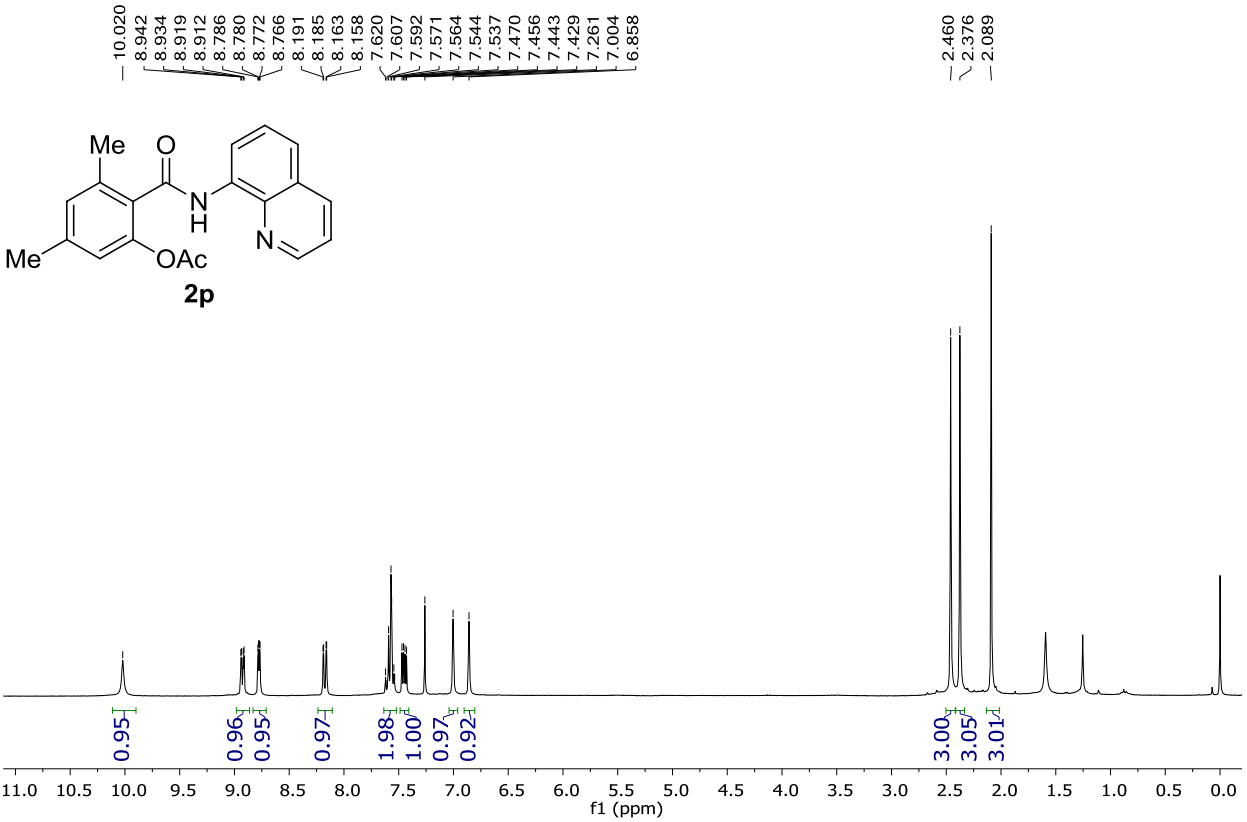

^{13}C NMR of **2p** (75 MHz, $CDCl_3$):

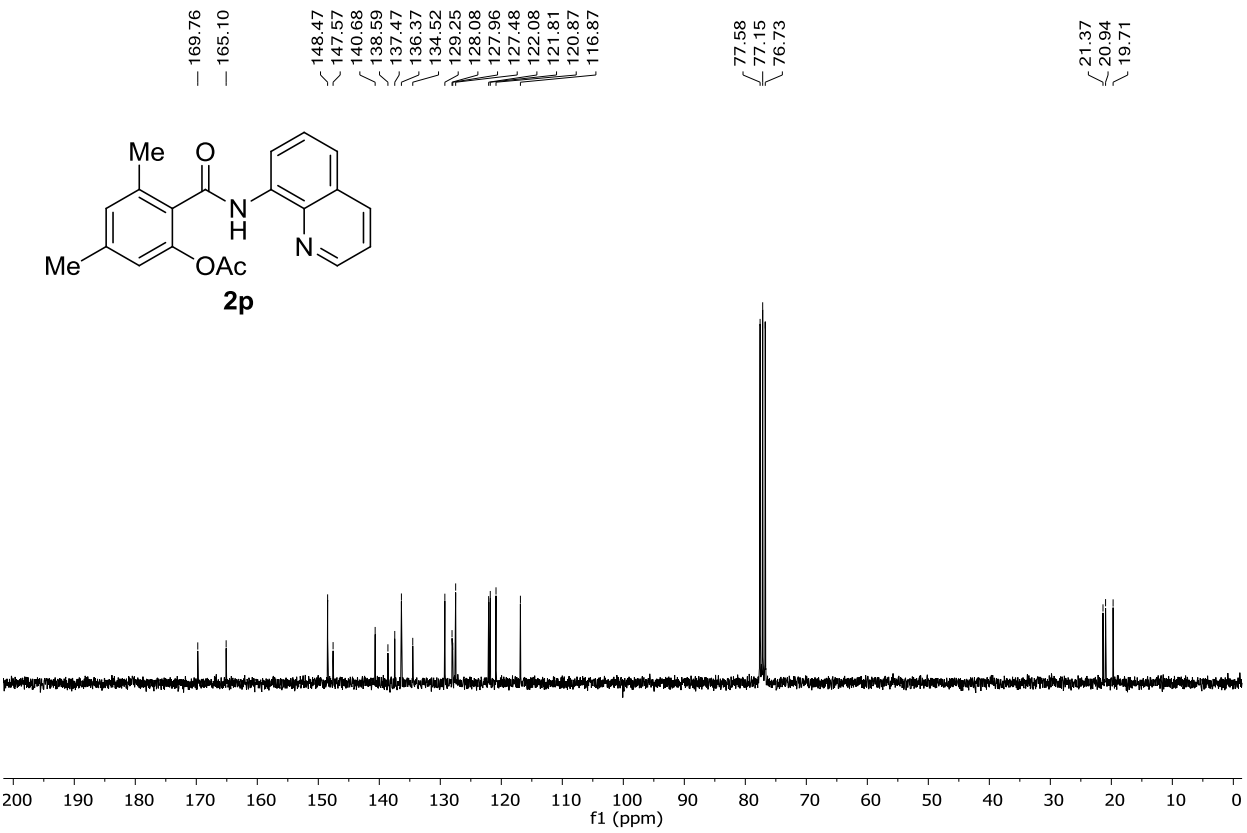

^{1}H NMR of **2s** (300 MHz, $CDCl_3$):

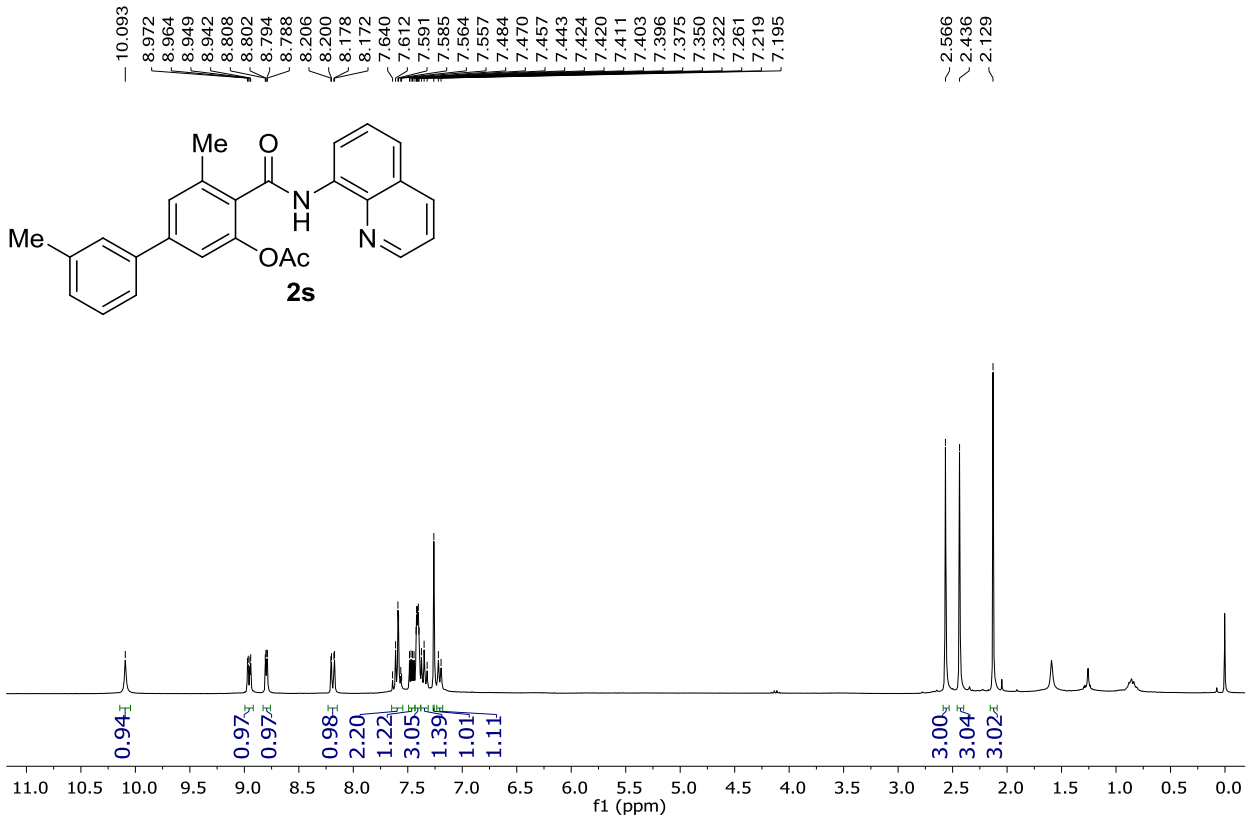

^{13}C NMR of **2s** (150 MHz, $CDCl_3$):

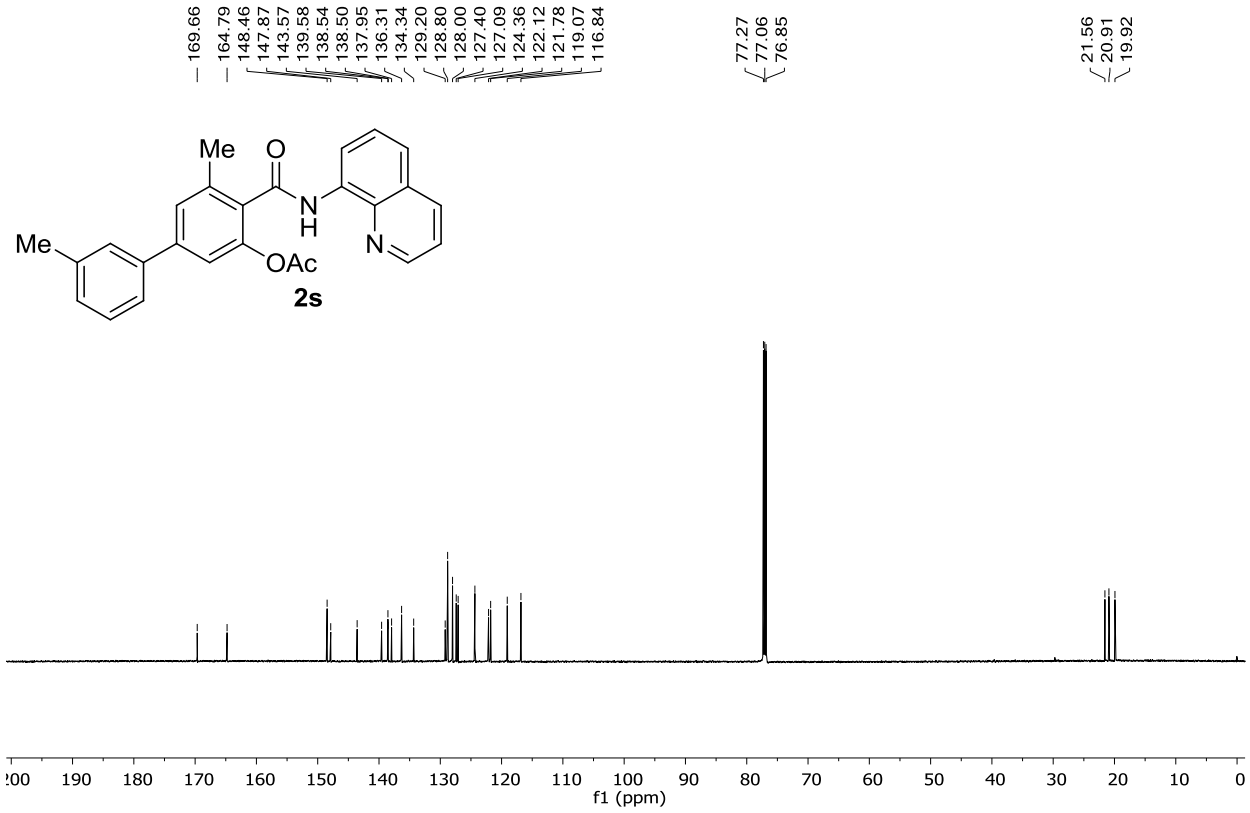

^{1}H NMR of **2u** (300 MHz, $CDCl_3$):

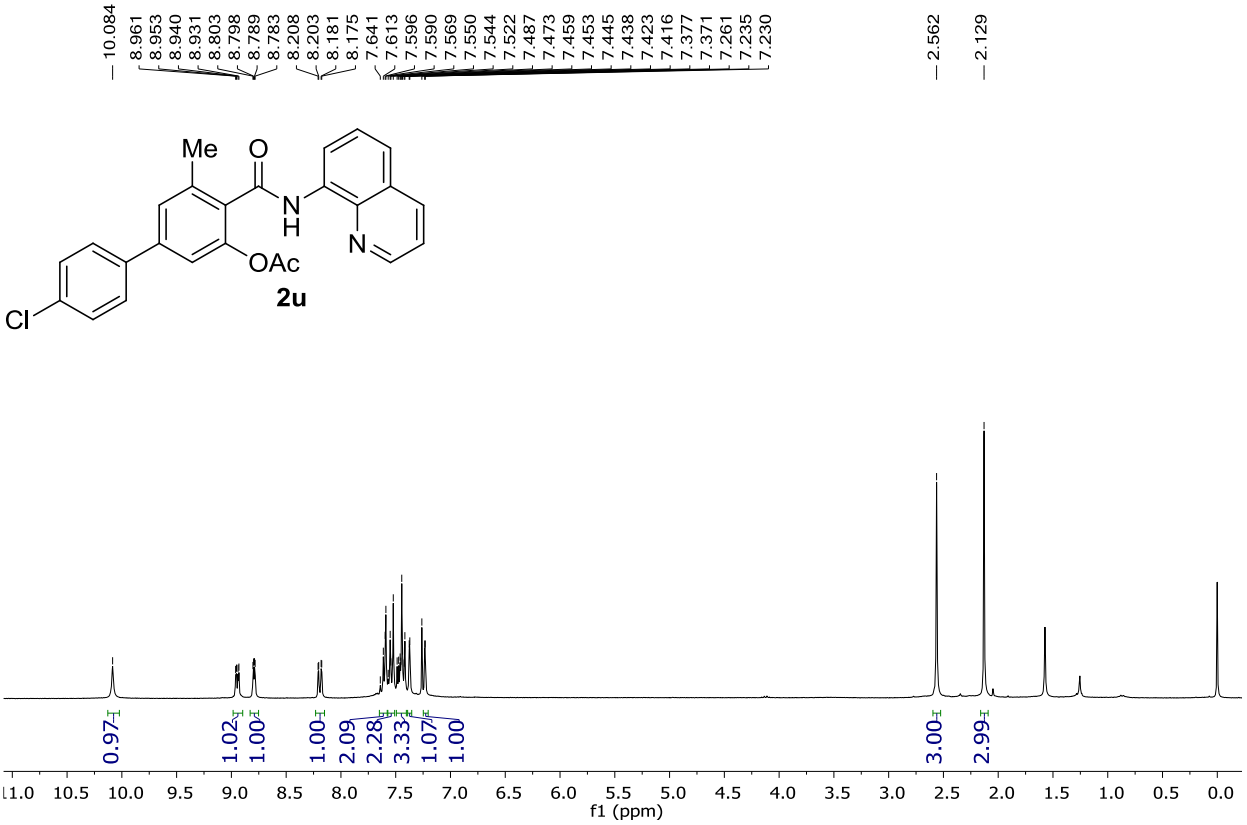

^{13}C NMR of **2u** (150 MHz, $CDCl_3$):

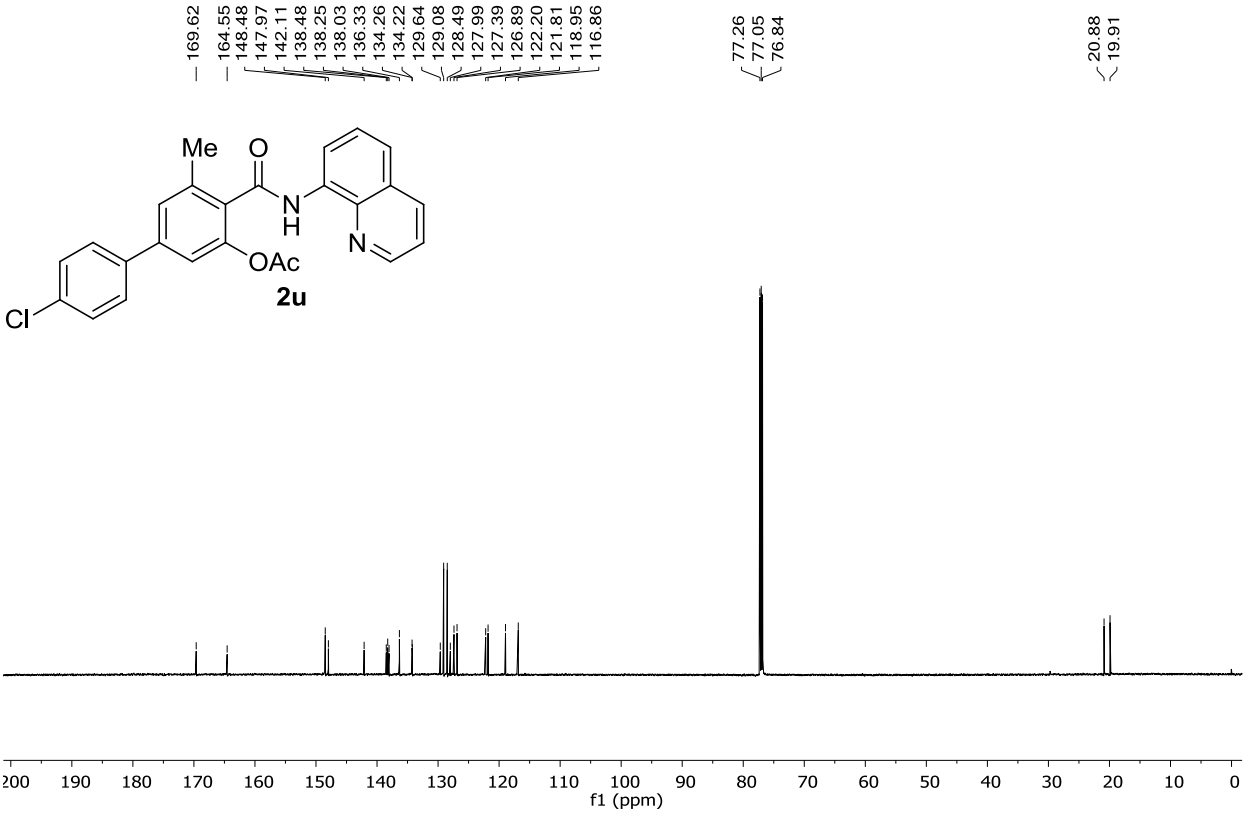

^{1}H NMR of **2ab** (600 MHz, $CDCl_3$):

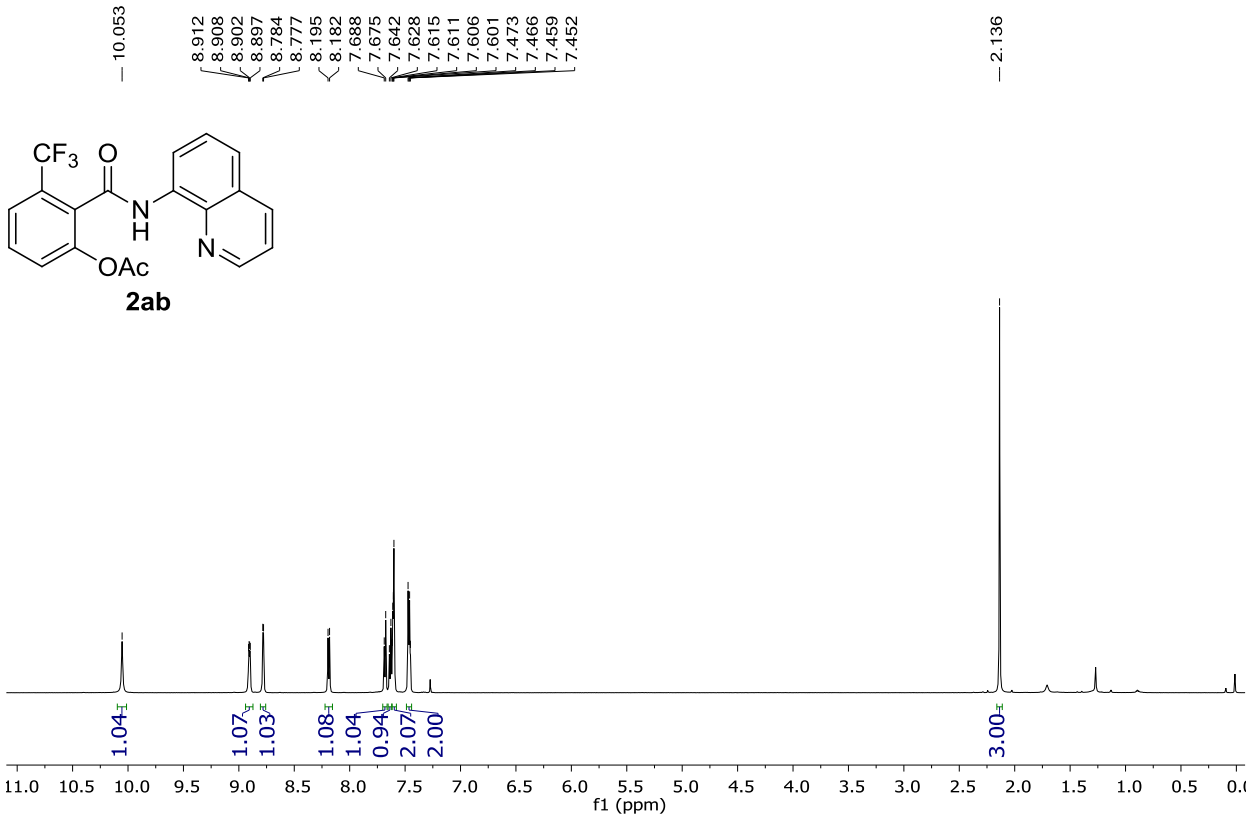

^{13}C NMR of **2ab** (150 MHz, $CDCl_3$):

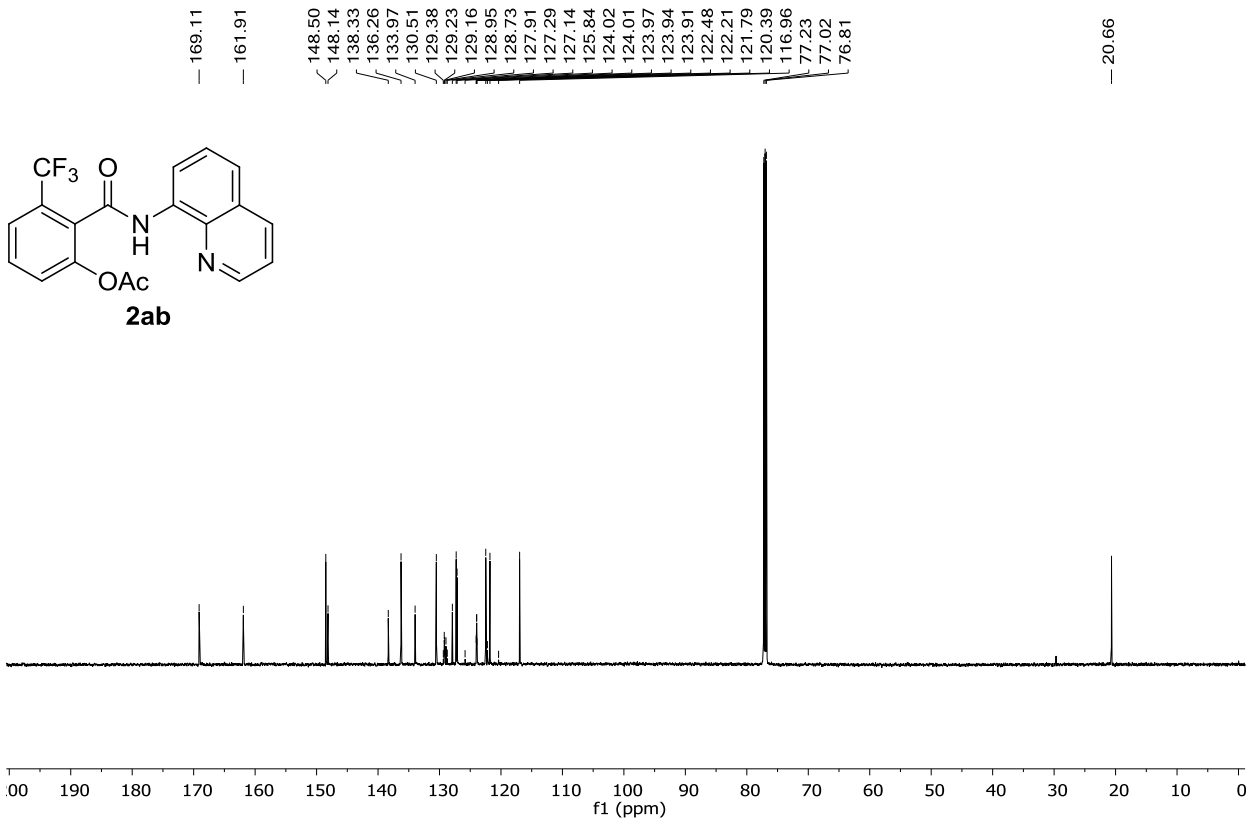

^{1}H NMR of **2ac** (300 MHz, $CDCl_3$):

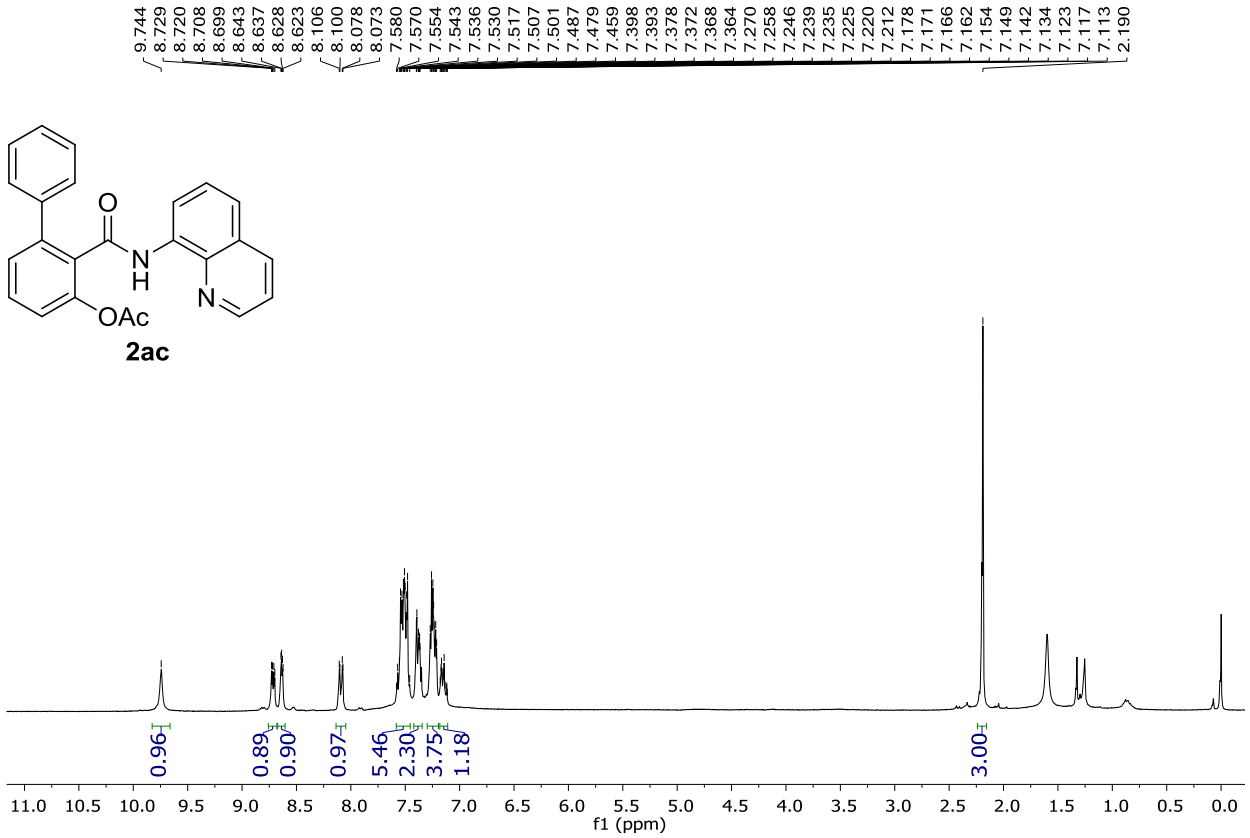

^{13}C NMR of **2ac** (75 MHz, $CDCl_3$):

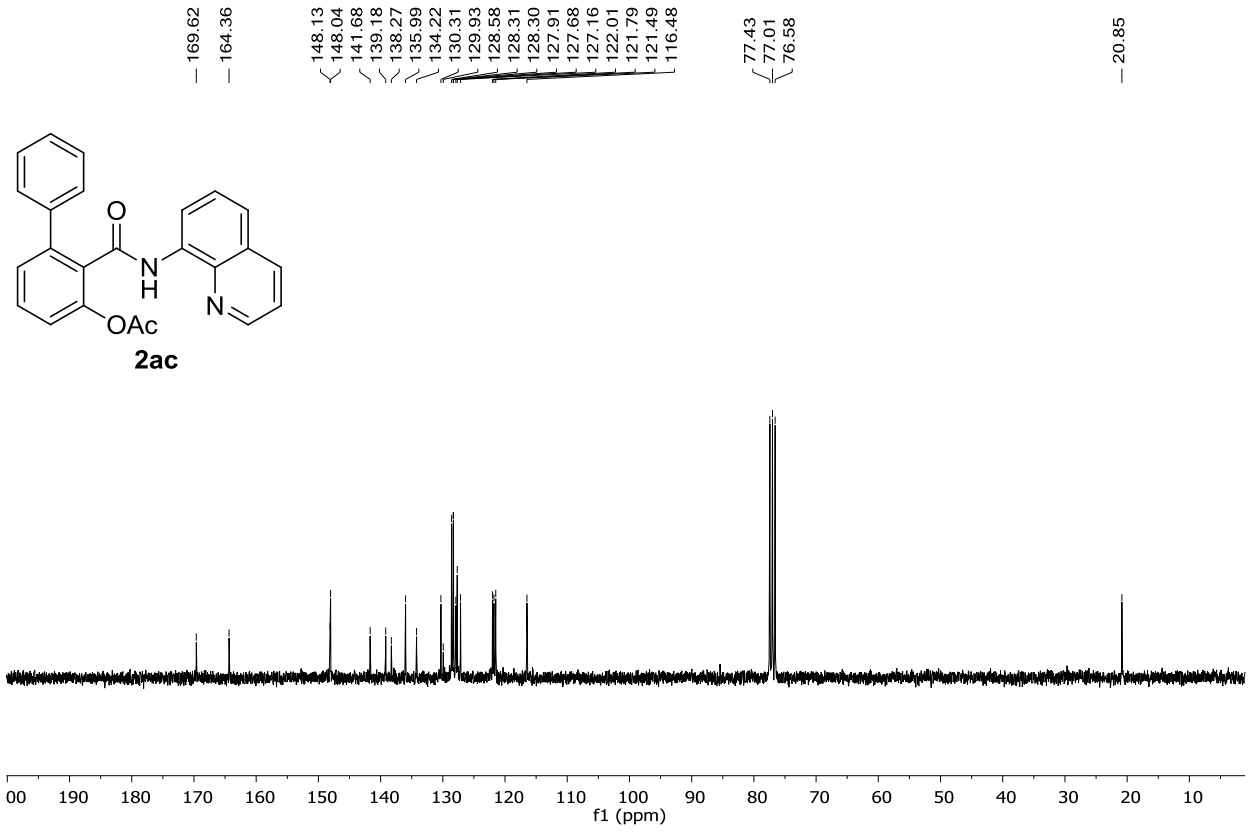

^{1}H NMR of **2ag** (300 MHz, $CDCl_3$):

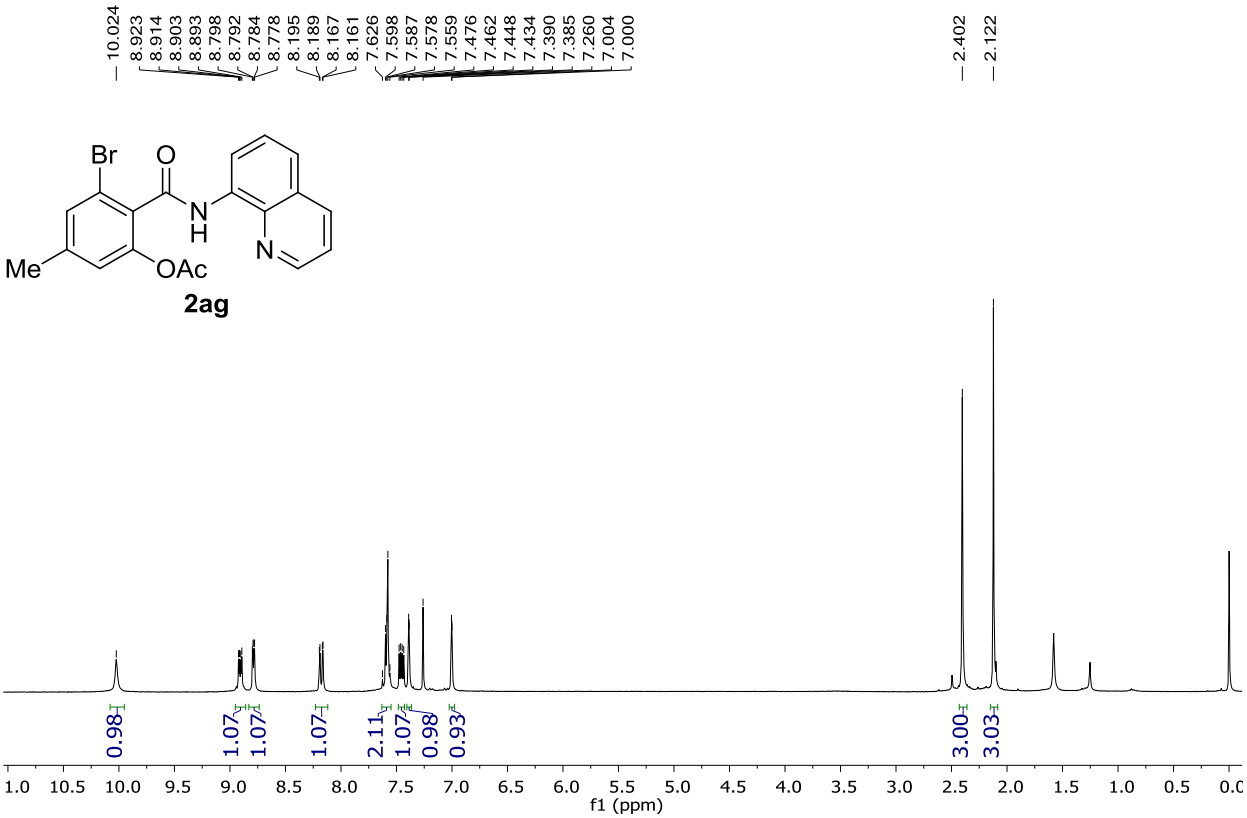

^{13}C NMR of **2ag** (150 MHz, $CDCl_3$):

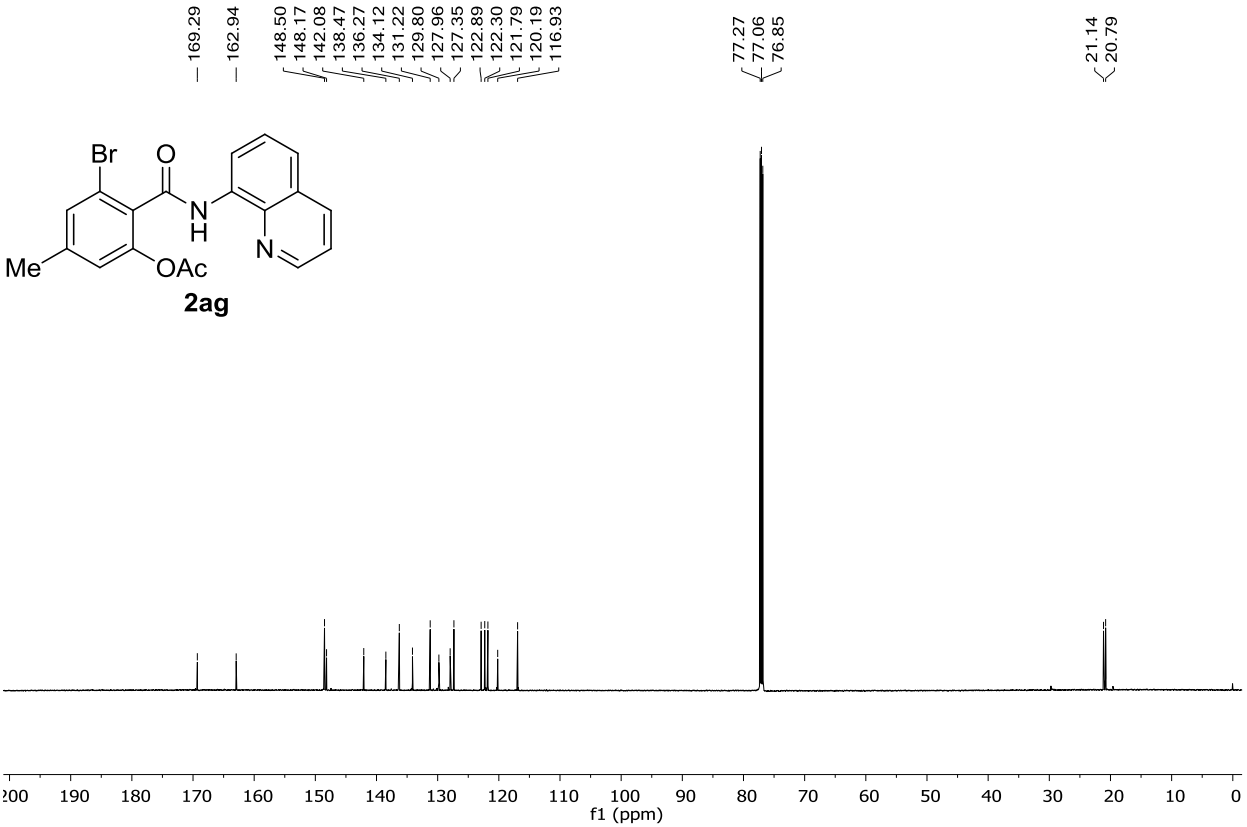

^{1}H NMR of **2ai** (300 MHz, $CDCl_3$):

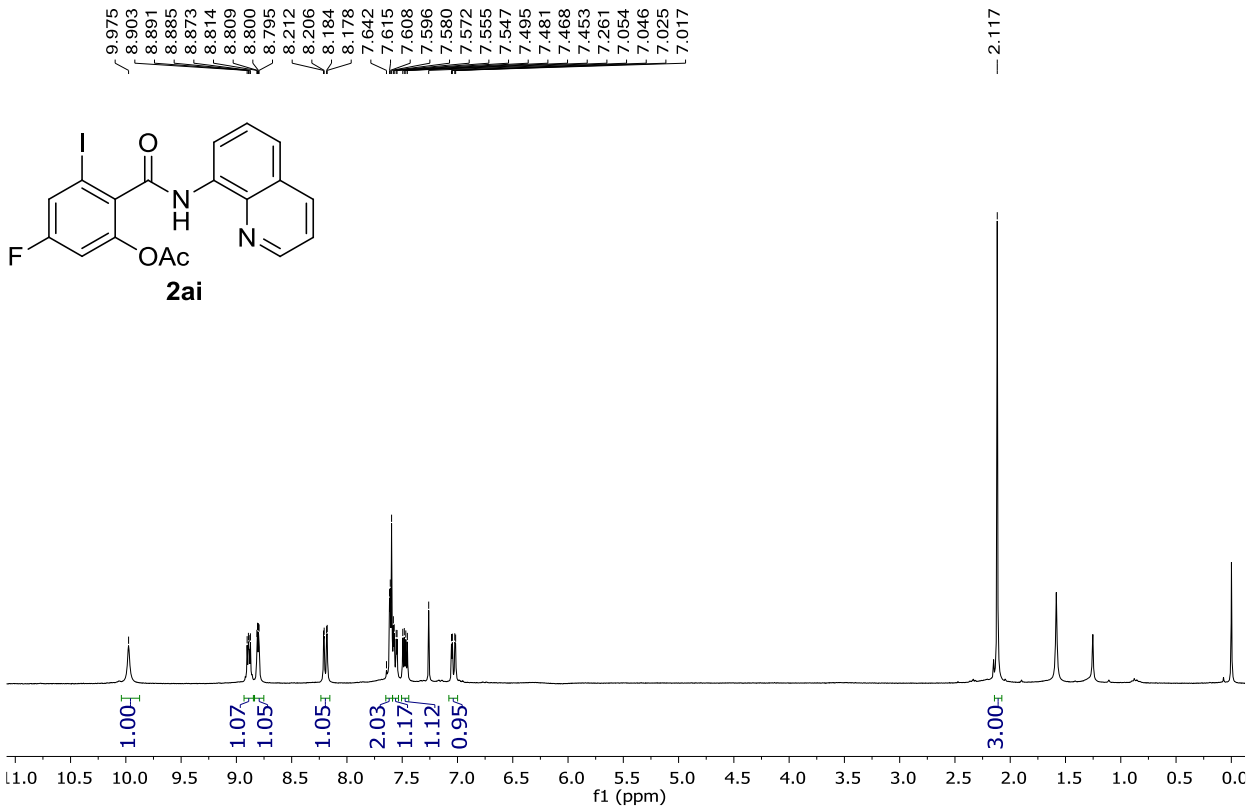

^{13}C NMR of **2ai** (150 MHz, $CDCl_3$):

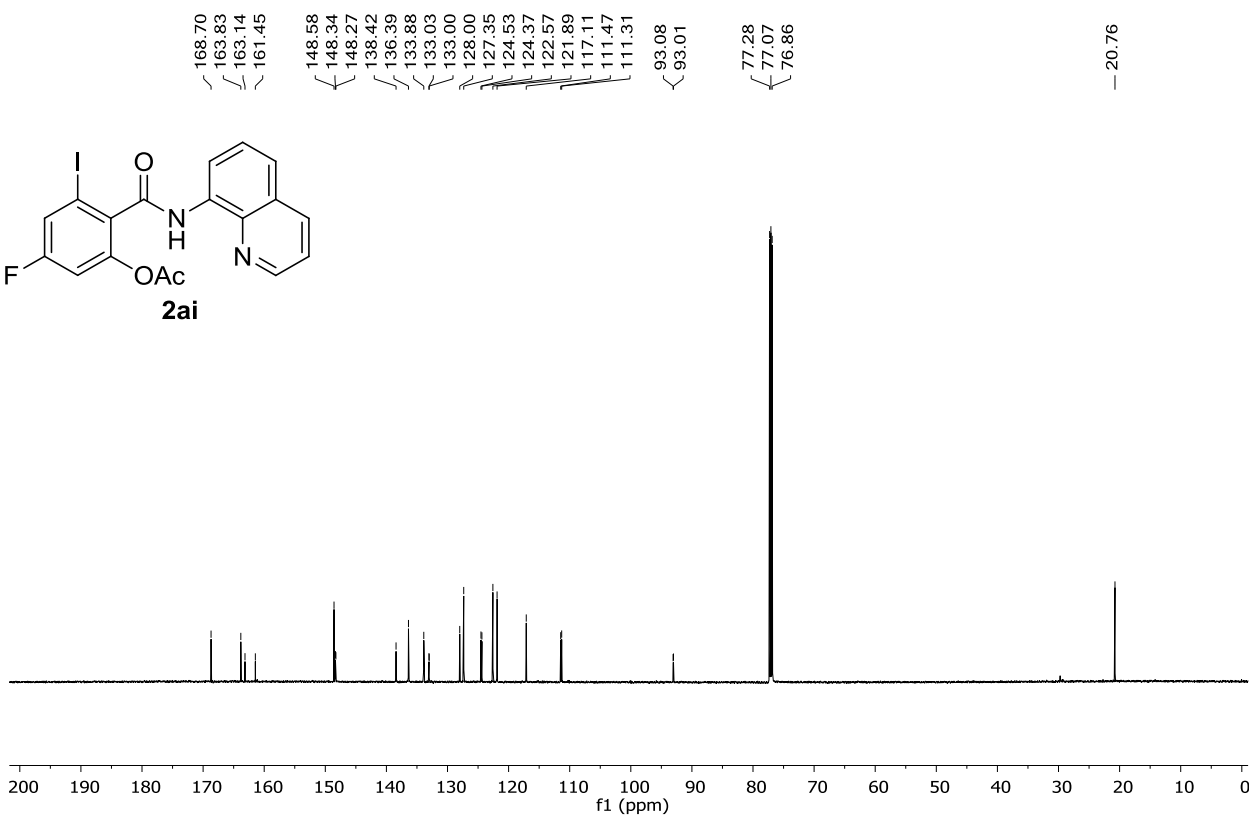

^{1}H NMR of **2ak** (600 MHz, $CDCl_3$):

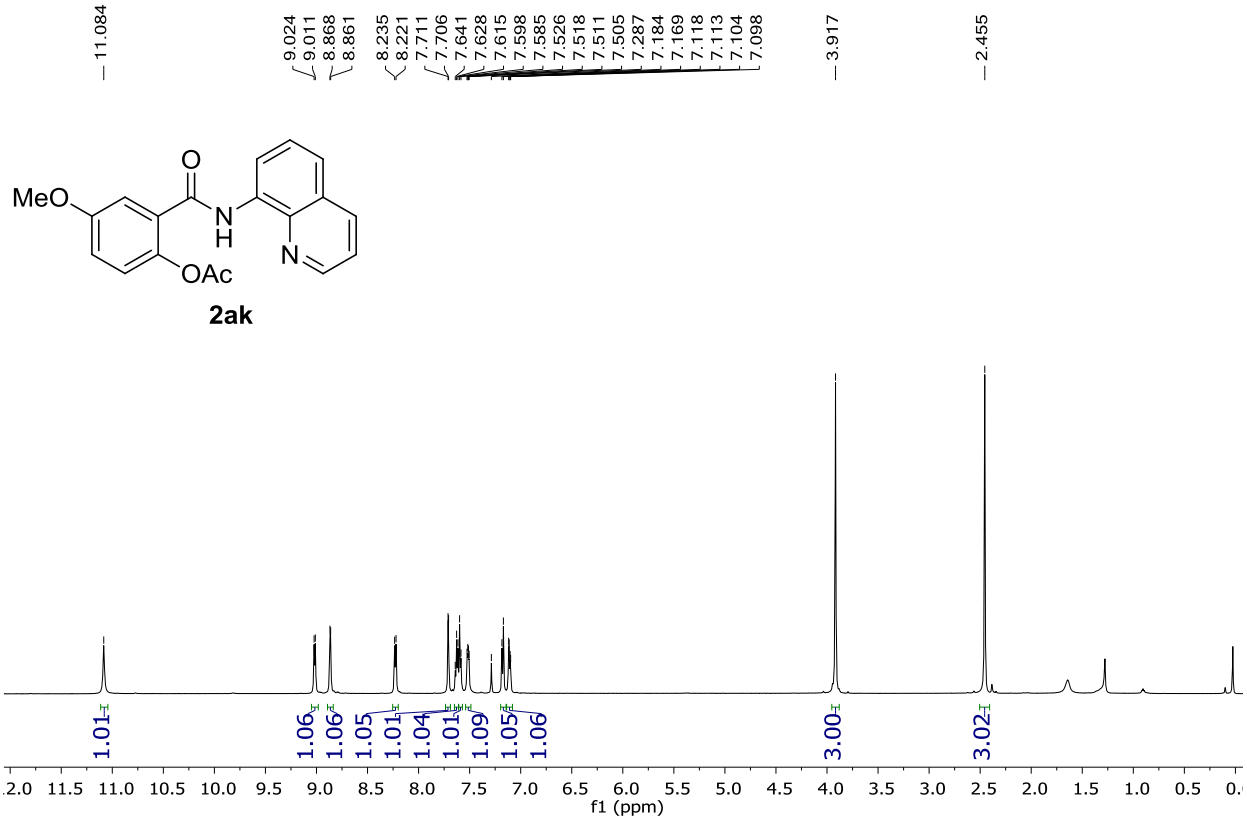

^{13}C NMR of **2ak** (150 MHz, $CDCl_3$):

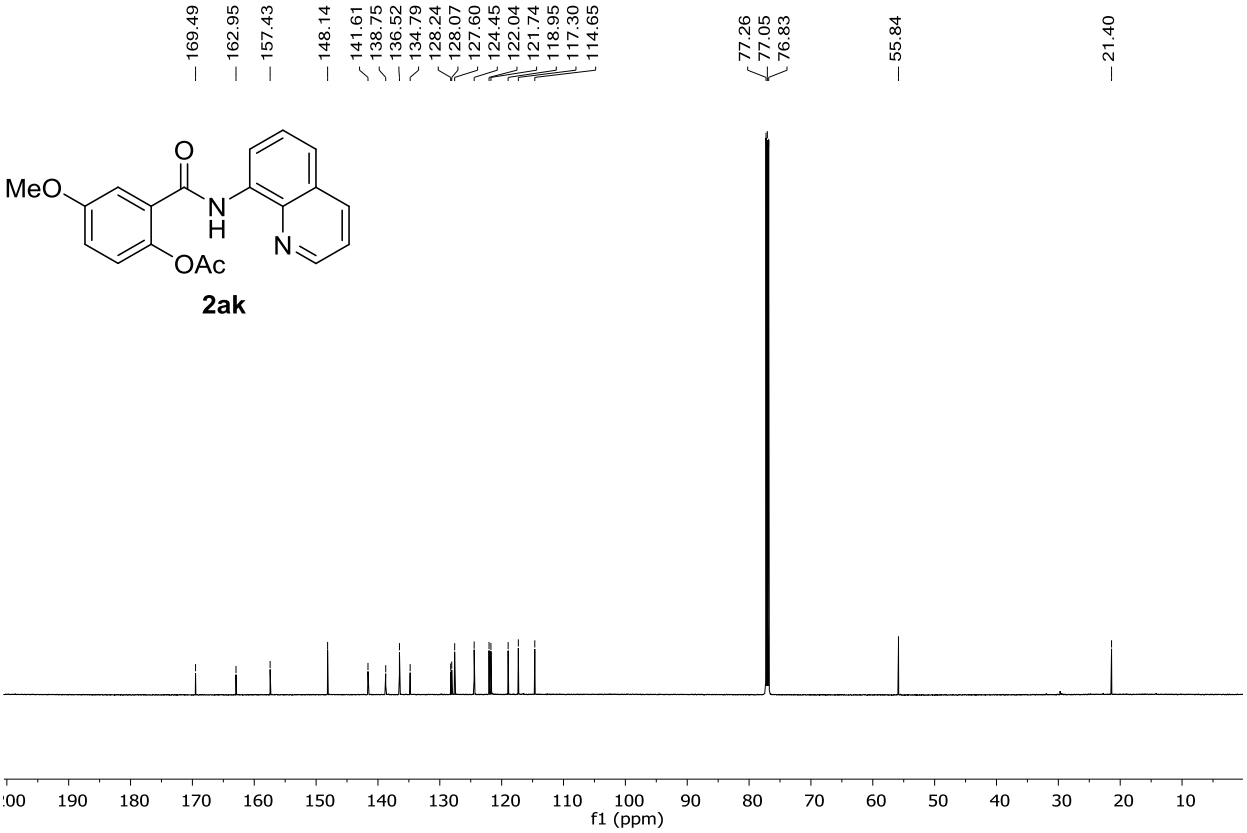

^{1}H NMR of **2al** (600 MHz, $CDCl_3$):

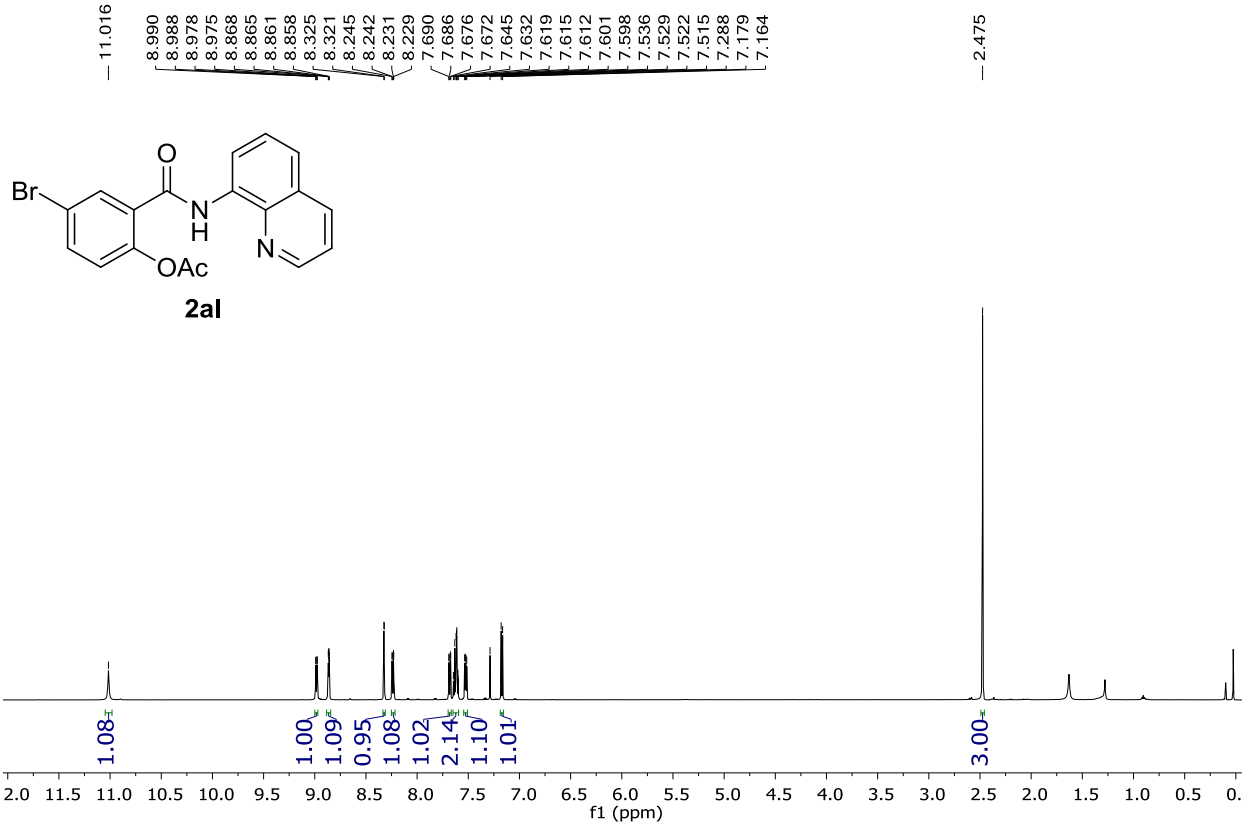

^{13}C NMR of **2al** (150 MHz, $CDCl_3$):

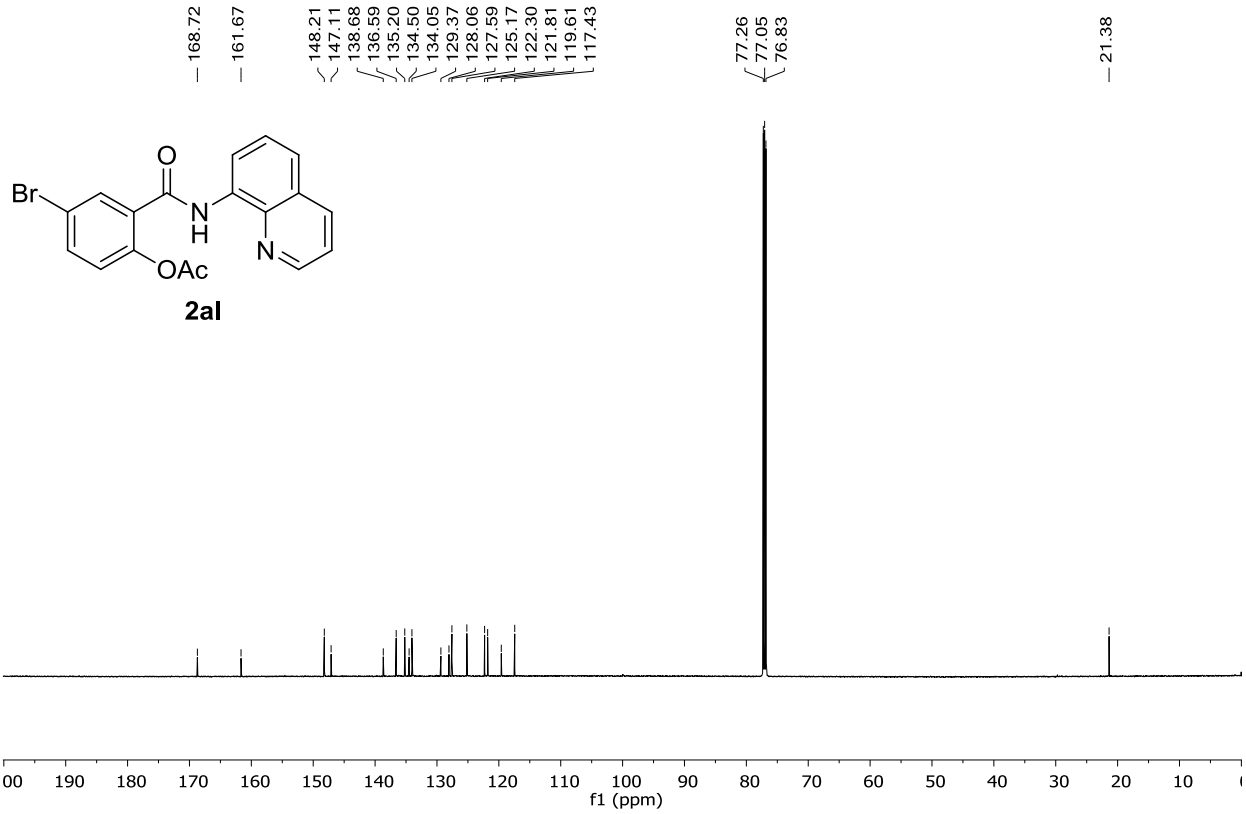

^{1}H NMR of **2am** (300 MHz, $CDCl_3$):

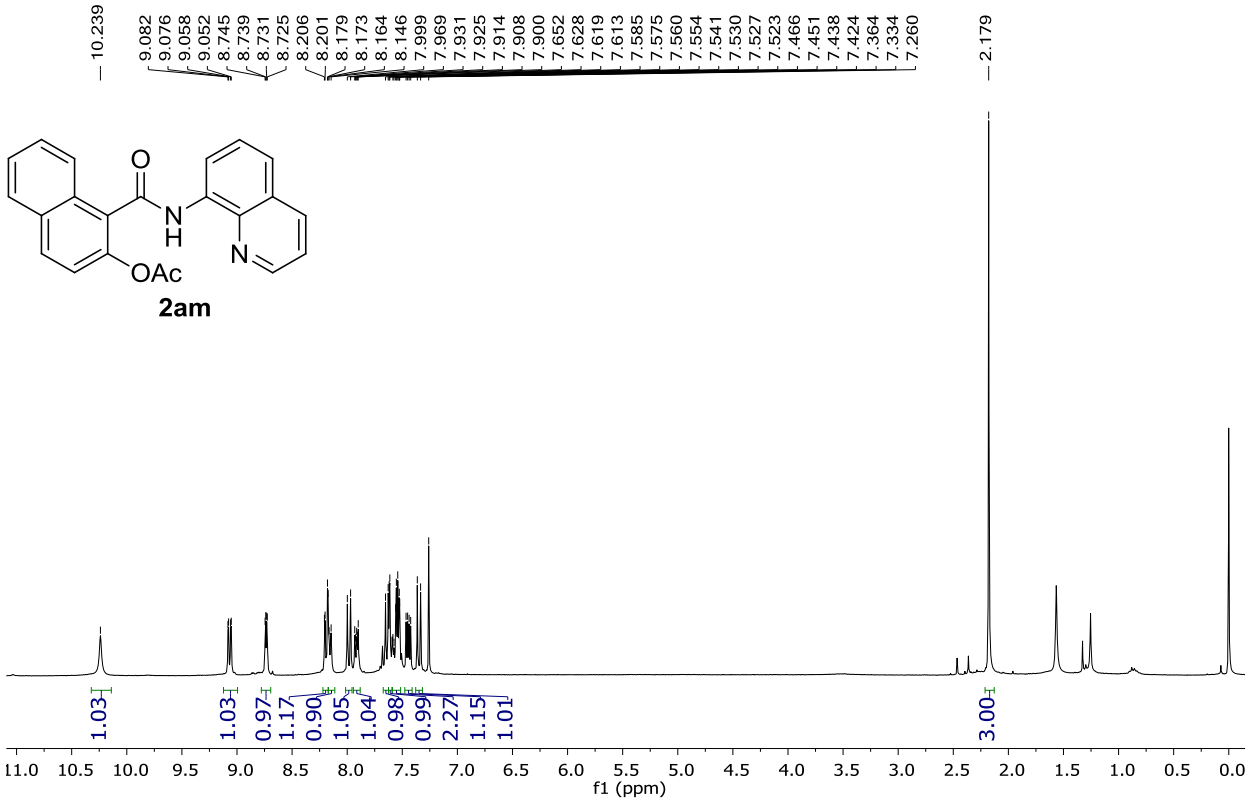

^{13}C NMR of **2am** (150 MHz, $CDCl_3$):

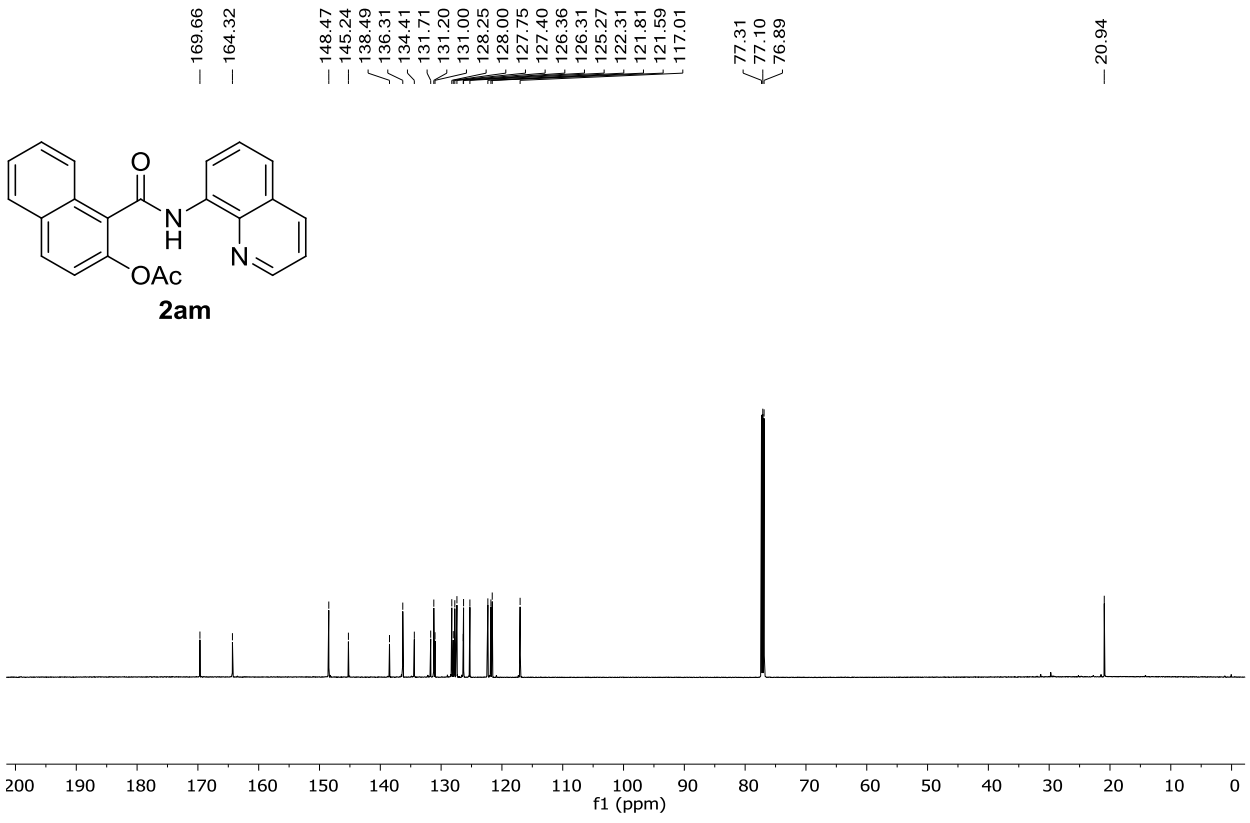

^{1}H NMR of **2an** (300 MHz, $CDCl_3$):

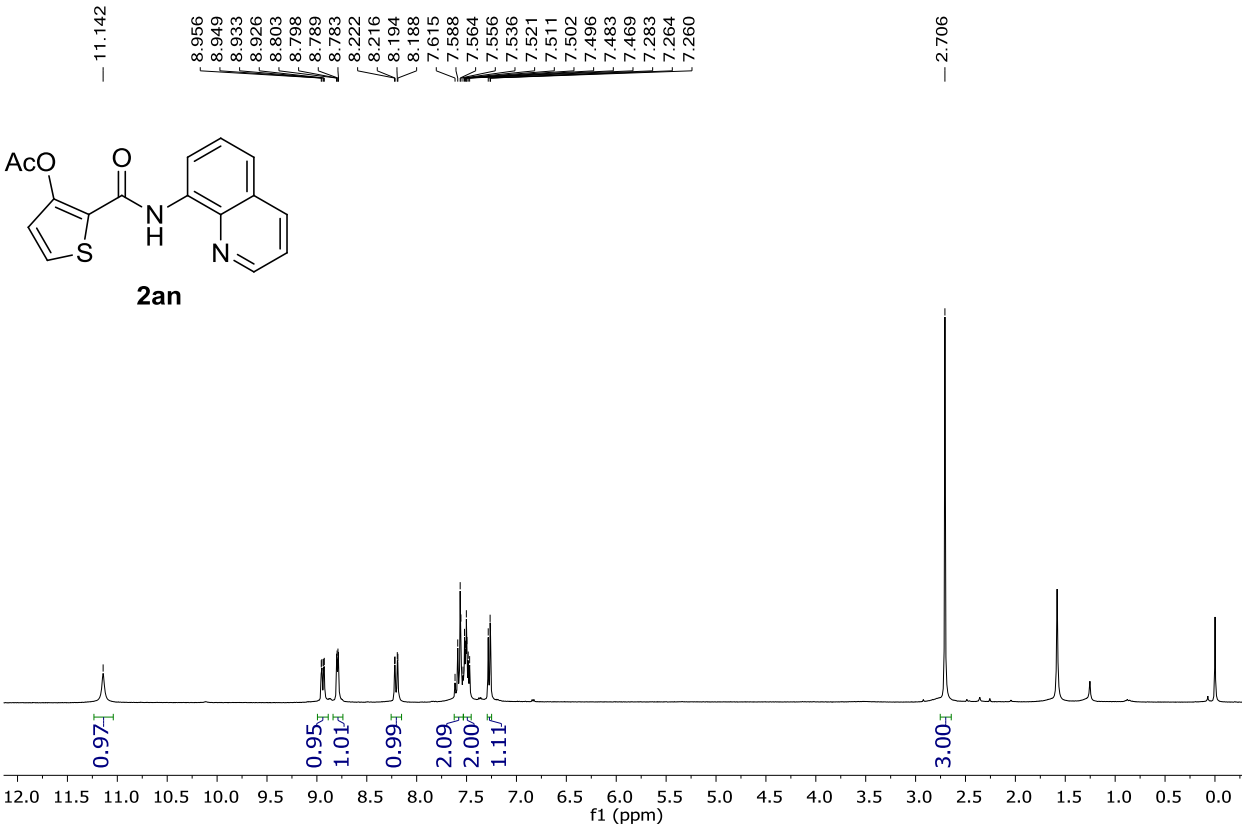

^{13}C NMR of **2an** (75 MHz, $CDCl_3$):

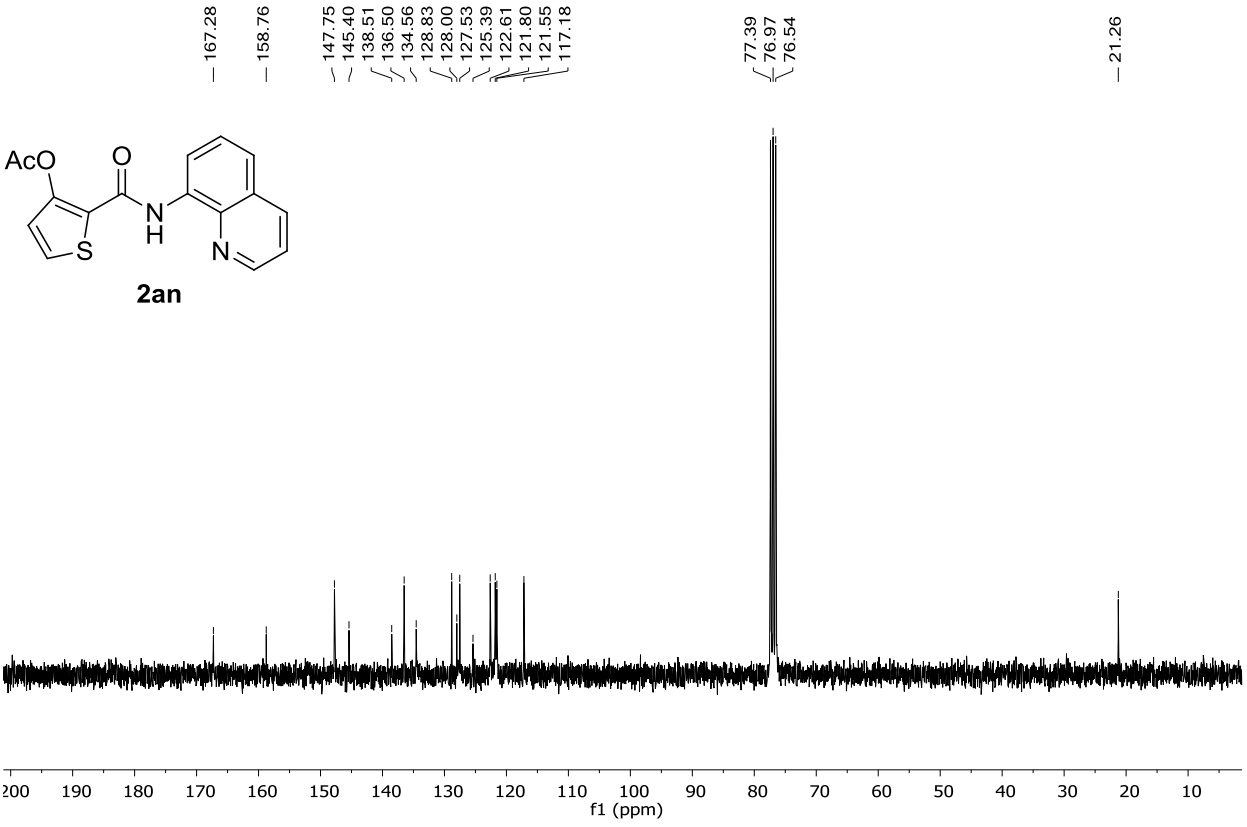

^{1}H NMR of **2ao** (300 MHz, $CDCl_3$):

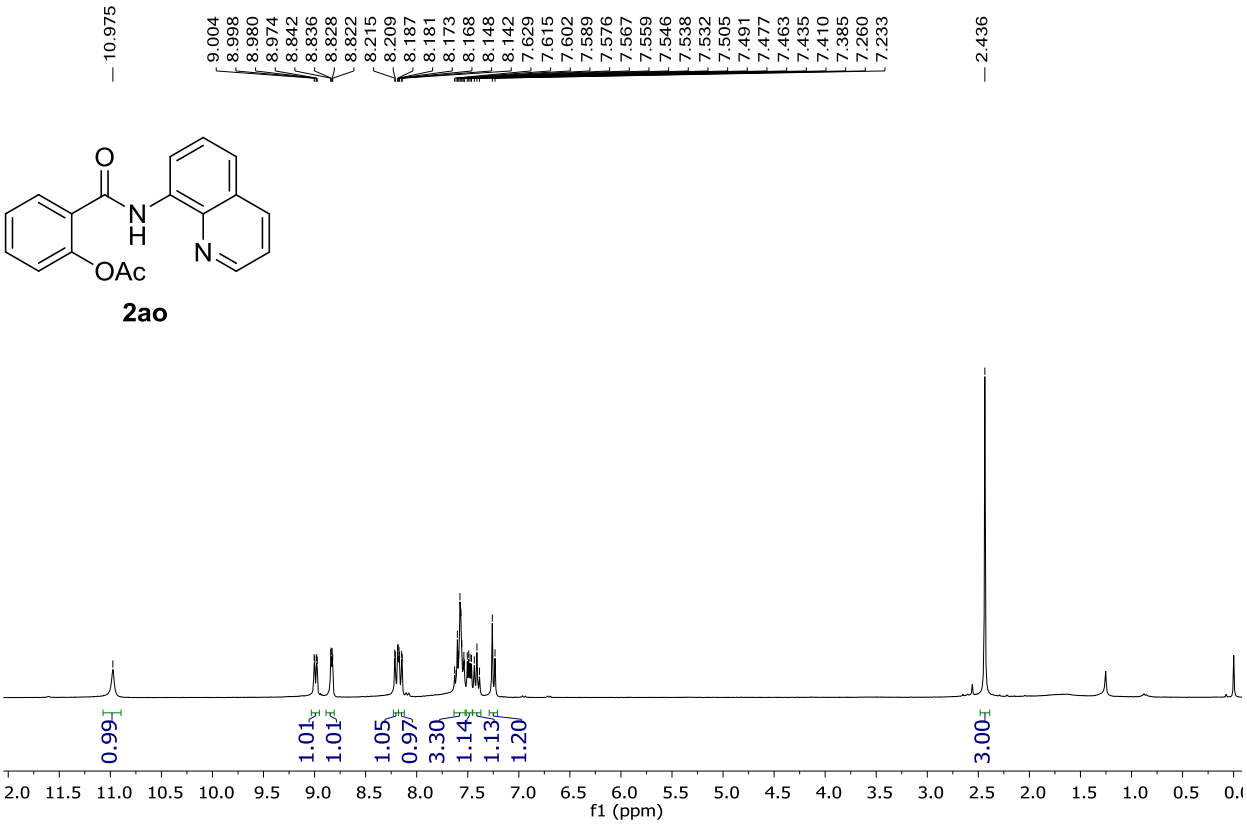

^{13}C NMR of **2ao** (150 MHz, $CDCl_3$):

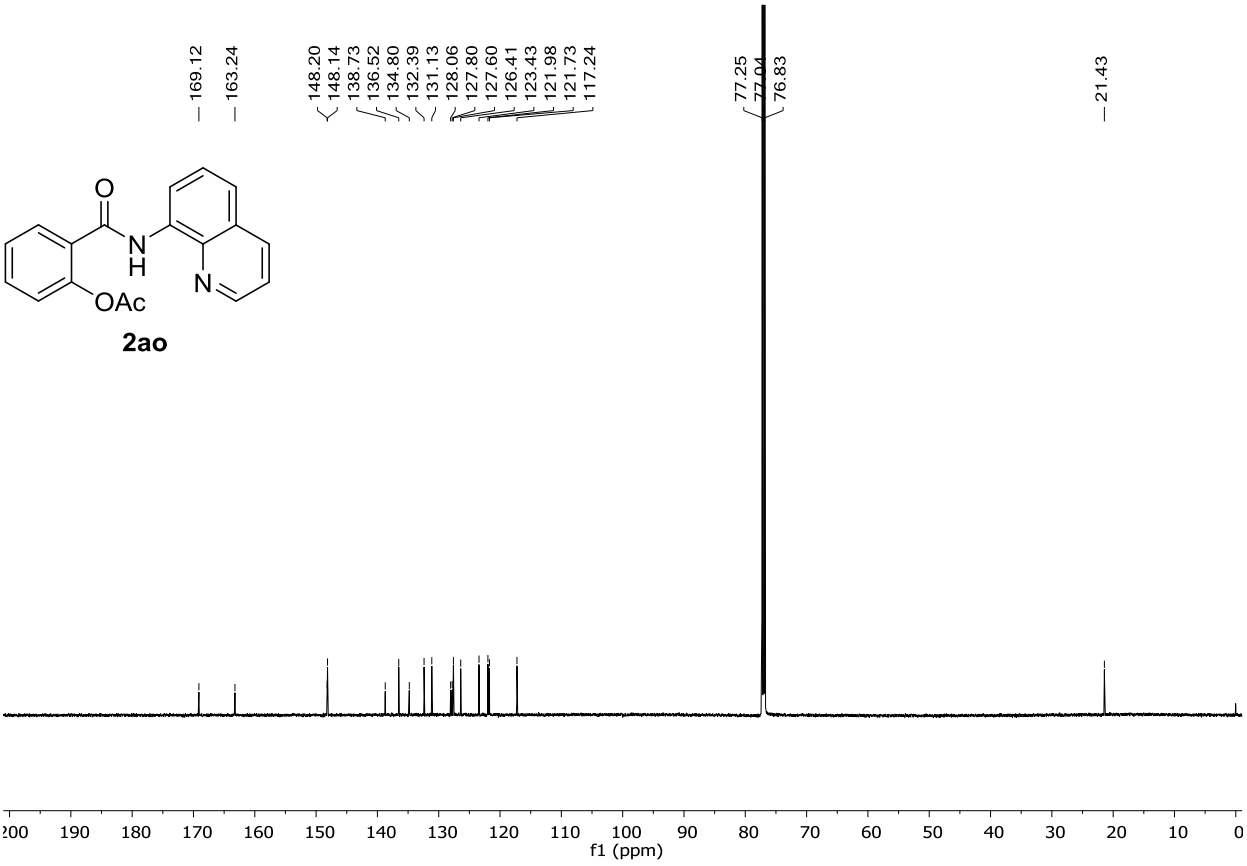

^{1}H NMR of **2ap** (300 MHz, $CDCl_3$):

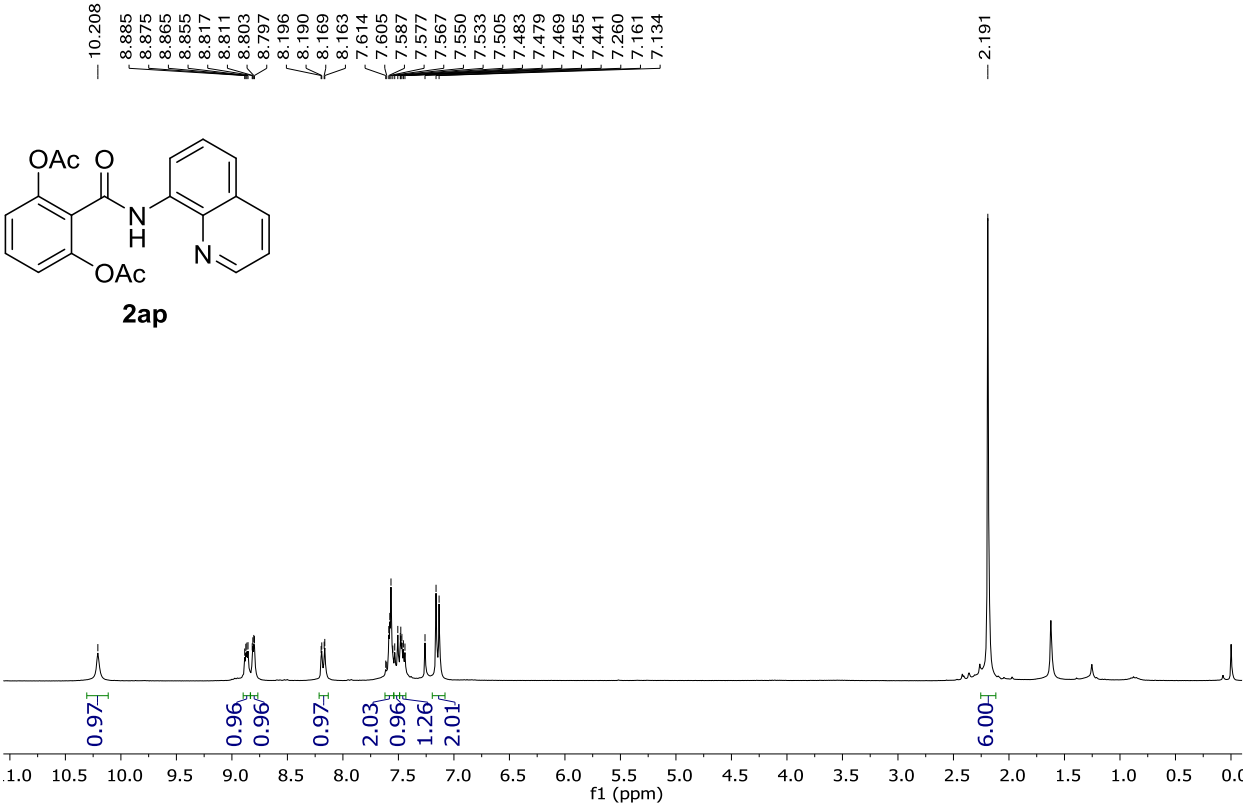

^{13}C NMR of **2ap** (150 MHz, $CDCl_3$):

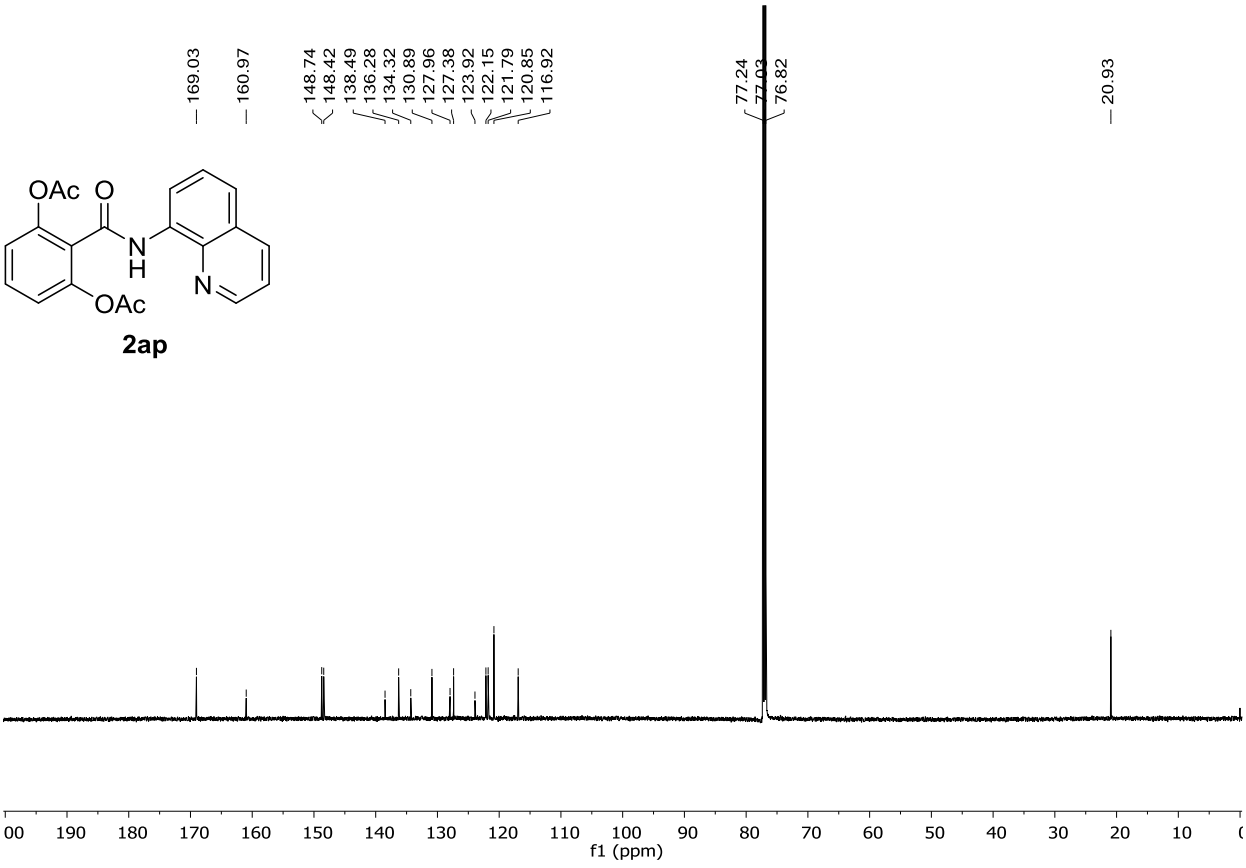

^{1}H NMR of **3** (600 MHz, $CDCl_3$):[6m]

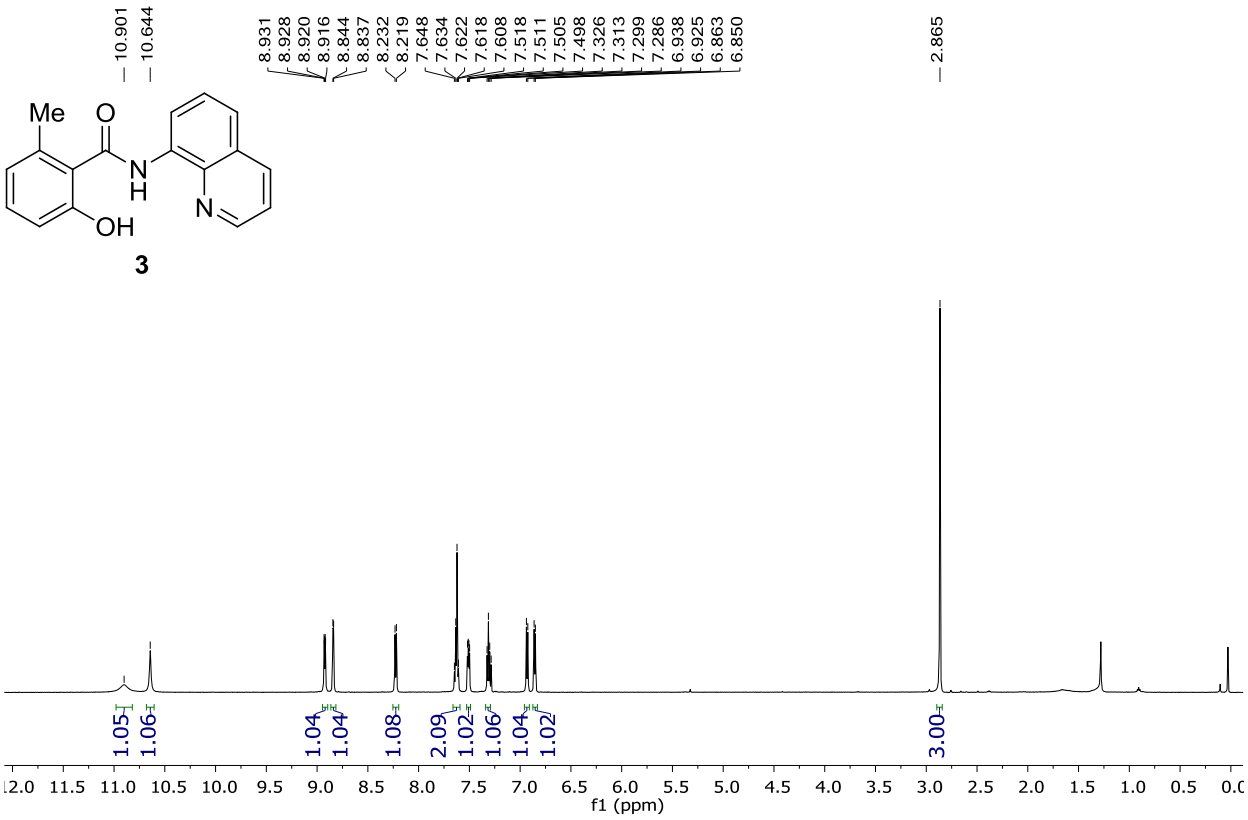

^{13}C NMR of **3** (150 MHz, $CDCl_3$):[6m]

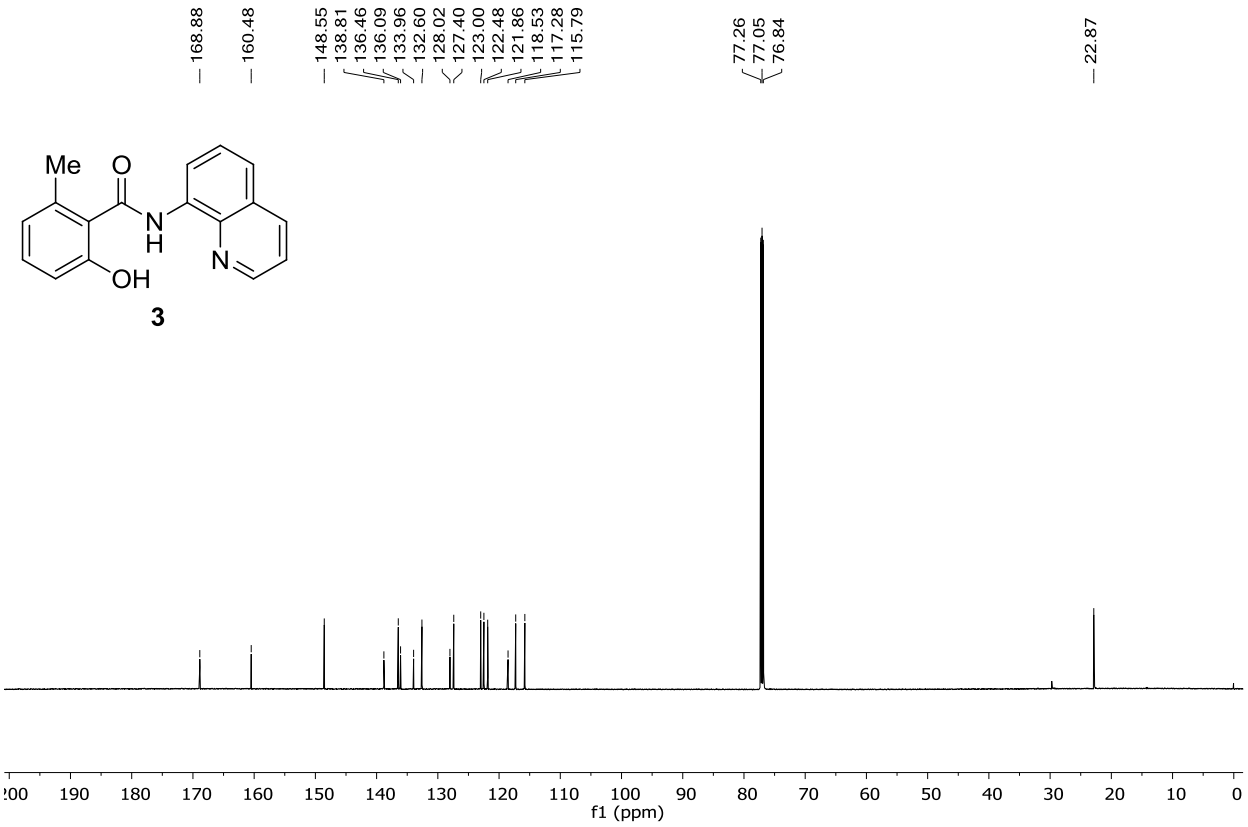

2.7. References

1. Vane, J. R.; Botting, R. M. *Thromb. Res.* **2003**, *110*, 255.
2. O'Connor, S. E.; Grosset, A.; Janiak, P. *Fundam. Clin. Pharmacol.* **1999**, *13*, 145.
3. (a) Ortega, A.; Blount, J. F.; Manchand, P. S. *J. Chem. Soc., Perkin Trans. 1* **1982**, 2505. (b) Fuerst, E. P.; Arntzen, C. J.; Pfister, K.; Donald, P. *Weed Sci.* **1986**, *34*, 344. (c) Murakami, A.; Kitazono, Y.; Jiwajinda, S.; Koshimizu, K.; Ohigashi, H. *Planta Med.* **1998**, *64*, 319. (d) May, J. A.; Ratan, H.; Glenn, J. R.; Losche, W.; Spangenberg, P.; Heptinstall, S. *Platelets* **1998**, *9*, 227. (e) Nichols, D. E.; Frescas, S. *Synthesis* **1999**, *1999*, 935. (f) Patterson, L. D.; Miller, M. J. *J. Org. Chem.* **2010**, *75*, 1289. (g) Deb, J.; Dibra, H.; Shan, S.; Rajan, S.; Manneh, J.; Kankipati, C. S.; Perry, C. J.; Nicholl, I. D. *Oncol. Rep.* **2011**, *26*, 557. (h) Rossignol, J.-F. J. A. r. *Antiviral Res.* **2014**, *110*, 94. (i) Klessig, D. F.; Tian, M.; Choi, H. W. *Front. Immunol.* **2016**, *7*, 206. (j) Zhang, B.; Guo, R.; Hu, Y.; Dong, X.; Lin, N.; Dai, X.; Wu, H.; Ma, S.; Yang, B. *RSC Adv.* **2017**, *7*, 31899. (k) Rais, R.; Vávra, J.; Tichý, T.; Dash, R. P.; Gadiano, A. J.; Tenora, L.; Monincová, L.; Bařinka, C.; Alt, J.; Zimmermann, S. C.; Slusher, C. E.; Wu, Y.; Wozniak, K.; Majer, P.; Tsukamoto, T.; Slusher, B. S. *J. Med. Chem.* **2017**, *60*, 7799-7809.
4. For reviews, see: (a) Lyons, T. W.; Sanford, M. S. *Chem. Rev.* **2010**, *110*, 1147. (b) Moghimi, S.; Mahdavi, M.; Shafiee, A.; Foroumadi, A. *Eur. J. Org. Chem.* **2016**, *2016*, 3282.
5. For selected examples, see: (a) Dick, A. R.; Kampf, J. W.; Sanford, M. S. *J. Am. Chem. Soc.* **2005**, *127*, 12790. (b) Ye, Z.; Wang, W.; Luo, F.; Zhang, S.; Cheng, J. *Org. Lett.* **2009**, *11*, 3974. (c) Wang, W.; Luo, F.; Zhang, S.; Cheng, J. *J. Org. Chem.* **2010**, *75*, 2415. (d) Sun, C.-L.; Liu, J.; Wang, Y.; Zhou, X.; Li, B.-J.; Shi, Z.-J. *Synlett* **2011**, *2011*, 883. (e) Wang, W.; Pan, C.; Chen, F.; Cheng, J. *Chem. Commun.* **2011**, *47*, 3978. (f) Rit, R. K.; Yadav, M. R.; Sahoo, A. K. *Org. Lett.* **2012**, *14*, 3724. (g) Hu, C.-J.; Zhang, X.-H.; Ding, Q.-P.; Lv, T.; Ge, S.-P.; Zhong, P. *Tetrahedron Lett.* **2012**, *53*, 2465. (h) Chen, X.; Zhu, C.; Cui, X.; Wu, Y. *Chem. Commun.* **2013**, *49*, 6900. (i) Padala, K.; Jeganmohan, M. *Chem. Commun.* **2013**, *49*, 9651. (j) Padala, K.; Jeganmohan, M. *Chem. Eur. J.* **2014**, *20*, 4092. (k) Rout, S. K.; Guin, S.; Gogoi, A.; Majji, G.; Patel, B. K. *Org. Lett.* **2014**, *16*, 1614. (l) Raghuvanshi, K.; Zell, D.; Ackermann, L. *Org. Lett.* **2017**, *19*, 1278. (m) Wang, F.; Hu, Q.; Shu, C.; Lin, Z.; Min, D.; Shi, T.; Zhang, W. *Org. Lett.* **2017**, *19*, 3636.

6. For selected examples, see: (a) Zhang, Y.-H.; Yu, J.-Q. *J. Am. Chem. Soc.* **2009**, *131*, 14654. (b) Shan, G.; Yang, X.; Ma, L.; Rao, Y. *Angew. Chem. Int. Ed.* **2012**, *51*, 13070. (c) Yan, Y.; Feng, P.; Zheng, Q.-Z.; Liang, Y.-F.; Lu, J.-F.; Cui, Y.; Jiao, N. *Angew. Chem. Int. Ed.* **2013**, *52*, 5827. (d) Zhang, H.-Y.; Yi, H.-M.; Wang, G.-W.; Yang, B.; Yang, S.-D. *Org. Lett.* **2013**, *15*, 6186. (e) Seth, K.; Nautiyal, M.; Purohit, P.; Parikh, N.; Chakraborti, A. K. *Chem. Commun.* **2015**, *51*, 191. (f) Dong, J.; Liu, P.; Sun, P. *J. Org. Chem.* **2015**, *80*, 2925. (g) Das, P.; Saha, D.; Saha, D.; Guin, J. *ACS Catal.* **2016**, *6*, 6050. (h) Chen, X.-Y.; Ozturk, S.; Sorensen, E. J. *Org. Lett.* **2017**, *19*, 6280. (i) Thirunavukkarasu, V. S.; Hubrich, J.; Ackermann, L. *Org. Lett.* **2012**, *14*, 4210. (j) Yang, F.; Rauch, K.; Kettelhoit, K.; Ackermann, L. *Angew. Chem. Int. Ed.* **2014**, *53*, 11285. (k) Li, X.; Liu, Y.-H.; Gu, W.-J.; Li, B.; Chen, F.-J.; Shi, B.-F. *Org. Lett.* **2014**, *16*, 3904. (l) Sun, S.-Z.; Shang, M.; Wang, H.-L.; Lin, H.-X.; Dai, H.-X.; Yu, J.-Q. *J. Org. Chem.* **2015**, *80*, 8843. (m) Singh, B. K.; Jana, R. *J. Org. Chem.* **2016**, *81*, 831.

7. For selected examples, see: (a) Wang, G.-W.; Yuan, T.-T. *J. Org. Chem.* **2010**, *75*, 476. (b) Zhang, S.-Y.; He, G.; Zhao, Y.; Wright, K.; Nack, W. A.; Chen, G. *J. Am. Chem. Soc.* **2012**, *134*, 7313. (c) Shi, S.; Kuang, C. *J. Org. Chem.* **2014**, *79*, 6105. (d) Yang, L.; Li, S.; Cai, L.; Ding, Y.; Fu, L.; Cai, Z.; Ji, H.; Li, G. *Org. Lett.* **2017**, *19*, 2746. (e) Li, S.; Zhu, W.; Gao, F.; Li, C.; Wang, J.; Liu, H. *J. Org. Chem.* **2017**, *82*, 126. (f) Roane, J.; Daugulis, O. *Org. Lett.* **2013**, *15*, 5842. (g) Hao, X.-Q.; Chen, L.-J.; Ren, B.; Li, L.-Y.; Yang, X.-Y.; Gong, J.-F.; Niu, J.-L.; Song, M.-P. *Org. Lett.* **2014**, *16*, 1104. (h) Bhadra, S.; Dzik, W. I.; Gooßen, L. J. *Angew. Chem. Int. Ed.* **2013**, *52*, 2959. (i) Zhang, L.-B.; Hao, X.-Q.; Zhang, S.-K.; Liu, Z.-J.; Zheng, X.-X.; Gong, J.-F.; Niu, J.-L.; Song, M.-P. *Angew. Chem. Int. Ed.* **2015**, *54*, 272.

8. For selected examples, see: (a) Dick, A. R.; Hull, K. L.; Sanford, M. S. *J. Am. Chem. Soc.* **2004**, *126*, 2300. (b) Desai, L. V.; Hull, K. L.; Sanford, M. S. *J. Am. Chem. Soc.* **2004**, *126*, 9542. (c) Giri, R.; Liang, J.; Lei, J.-G.; Li, J.-J.; Wang, D.-H.; Chen, X.; Naggar, I. C.; Guo, C.; Foxman, B. M.; Yu, J.-Q. *Angew. Chem. Int. Ed.* **2005**, *44*, 7420. (d) Desai, L. V.; Malik, H. A.; Sanford, M. S. *Org. Lett.* **2006**, *8*, 1141. (e) Wang, G.-W.; Yuan, T.-T.; Wu, X.-L. *J. Org. Chem.* **2008**, *73*, 4717. (f) Gou, F.-R.; Wang, X.-C.; Huo, P.-F.; Bi, H.-P.; Guan, Z.-H.; Liang, Y.-M. *Org. Lett.* **2009**, *11*, 5726. (g) Neufeldt, S. R.; Sanford, M. S. *Org. Lett.* **2010**, *12*, 532. (h) Vickers, C. J.; Mei, T.-S.; Yu, J.-Q. *Org. Lett.* **2010**, *12*, 2511. (i) Richter, H.; Beckendorf, S.; Mancheño, O. G. *Adv. Syn. Catal.* **2011**, *353*, 295. (j) Ren, Z.; Mo, F.; Dong, G. *J. Am. Chem. Soc.* **2012**, *134*, 16991. (k) Yadav, M. R.; Rit, R. K.; Sahoo, A. K. *Chem. Eur. J.* **2012**, *18*, 5541. (l) Reddy, B. V.

S.; Narasimhulu, G.; Umadevi, N.; Yadav, J. S. *Synlett* **2012**, *23*, 1364. (m) Chan, L. Y.; Meng, X.; Kim, S. *J. Org. Chem.* **2013**, *78*, 8826. (n) Rit, R. K.; Yadav, M. R.; Sahoo, A. K. *Org. Lett.* **2014**, *16*, 968. (o) Wang, M.; Yang, Y.; Fan, Z.; Cheng, Z.; Zhu, W.; Zhang, A. *Chem. Commun.* **2015**, *51*, 3219. (p) Chen, K.; Wang, D.; Li, Z.-W.; Liu, Z.; Pan, F.; Zhang, Y.-F.; Shi, Z.-J. *Org. Chem. Front.* **2017**, *4*, 2097.

9. Okada, T.; Nobushige, K.; Satoh, T.; Miura, M. *Org. Lett.* **2016**, *18*, 1150.
10. (a) Yu, W.; Chen, J.; Gao, K.; Liu, Z.; Zhang, Y. *Org. Lett.* **2014**, *16*, 4870. (b) Wu, Y.; Zhou, B. *Org. Lett.* **2017**, *19*, 3532. (c) Mishra, A.; Vats, T. K.; Nair, M. P.; Das, A.; Deb, I. *J. Org. Chem.* **2017**, *82*, 12406.
11. (a) Chen, X.; Hao, X.-S.; Goodhue, C. E.; Yu, J.-Q. *J. Am. Chem. Soc.* **2006**, *128*, 6790. (b) Wang, Z.; Kuninobu, Y.; Kanai, M. *Org. Lett.* **2014**, *16*, 4790. (c) Wu, X.; Zhao, Y.; Ge, H. *Chem. Asian J.* **2014**, *9*, 2736.
12. Zaitsev, V. G.; Shabashov, D.; Daugulis, O. *J. Am. Chem. Soc.* **2005**, *127*, 13154.
13. For selected examples of 8-aminoquinoline directed C–H functionalization, see: (a) Rouquet, G.; Chatani, N. *Angew. Chem. Int. Ed.* **2013**, *52*, 11726. (b) Corbet, M.; De Campo, F. *Angew. Chem. Int. Ed.* **2013**, *52*, 9896. (c) Daugulis, O.; Roane, J.; Tran, L. D. *Acc. Chem. Res.* **2015**, *48*, 1053. (d) Shabashov, D.; Daugulis, O. *J. Am. Chem. Soc.* **2010**, *132*, 3965. (e) Shibata, K.; Chatani, N. *Org. Lett.* **2014**, *16*, 5148. (f) Aihara, Y.; Chatani, N. *Chem. Sci.* **2013**, *4*, 664. (g) Tran, L. D.; Popov, I.; Daugulis, O. *J. Am. Chem. Soc.* **2012**, *134*, 18237. (h) Asako, S.; Ilies, L.; Nakamura, E. *J. Am. Chem. Soc.* **2013**, *135*, 17755. (i) Truong, T.; Klimovica, K.; Daugulis, O. *J. Am. Chem. Soc.* **2013**, *135*, 9342. (j) Aihara, Y.; Chatani, N. *J. Am. Chem. Soc.* **2013**, *135*, 5308. (k) Aihara, Y.; Chatani, N. *J. Am. Chem. Soc.* **2014**, *136*, 898. (l) Grigorjeva, L.; Daugulis, O. *Angew. Chem. Int. Ed.* **2014**, *53*, 10209. (m) Miura, W.; Hirano, K.; Miura, M. *Org. Lett.* **2015**, *17*, 4034. (n) Maity, S.; Kancherla, R.; Dhawa, U.; Hoque, E.; Pimparkar, S.; Maiti, D. *ACS Catal.* **2016**, *6*, 5493-5499.
14. For reviews on cobalt-catalyzed C–H functionalization, see: (a) Gao, K.; Yoshikai, N. *Acc. Chem. Res.* **2014**, *47*, 1208. (b) Yoshikai, N. *Bull. Chem. Soc. Jpn.* **2014**, *87*, 843. (c) Moselage, M.; Li, J.; Ackermann, L. *ACS Catal.* **2016**, *6*, 498. (d) Wei, D.; Zhu, X.; Niu, J.-L.; Song, M.-P. *ChemCatChem* **2016**, *8*, 1242. (e) Yoshino, T.; Matsunaga, S. *Adv. Syn. Catal.* **2017**, *359*, 1245. (f) Wang, S.; Chen, S.-Y.; Yu, X.-Q. *Chem. Commun.* **2017**, *53*, 3165.

15. For selected examples on low-valent cobalt-catalyzed C–H functionalization, see: (a) Gao, K.; Lee, P.-S.; Fujita, T.; Yoshikai, N. *J. Am. Chem. Soc.* **2010**, *132*, 12249. (b) Gao, K.; Yoshikai, N. *Angew. Chem. Int. Ed.* **2011**, *50*, 6888. (c) Gao, K.; Yoshikai, N. *J. Am. Chem. Soc.* **2011**, *133*, 400. (d) Chen, Q.; Ilies, L.; Nakamura, E. *J. Am. Chem. Soc.* **2011**, *133*, 428. (e) Song, W.; Ackermann, L. *Angew. Chem. Int. Ed.* **2012**, *51*, 8251. (f) Gao, K.; Yoshikai, N. *Chem. Commun.* **2012**, *48*, 4305. (g) Gao, K.; Paira, R.; Yoshikai, N. *Angew. Chem. Int. Ed.* **2014**, *356*, 1486. (h) Moselage, M.; Sauermann, N.; Richter, S. C.; Ackermann, L. *Angew. Chem. Int. Ed.* **2015**, *54*, 6352. (i) Xu, W.; Yoshikai, N. *Angew. Chem. Int. Ed.* **2016**, *55*, 12731.

16. For selected examples on high-valent Cp*Co(III) catalyzed C–H functionalization, see: (a) Yoshino, T.; Ikemoto, H.; Matsunaga, S.; Kanai, M. *Angew. Chem. Int. Ed.* **2013**, *52*, 2207. (b) Yoshino, T.; Ikemoto, H.; Matsunaga, S.; Kanai, M. *Chem. Eur. J.* **2013**, *19*, 9142. (c) Yu, D.-G.; Gensch, T.; de Azambuja, F.; Vásquez-Céspedes, S.; Glorius, F. *J. Am. Chem. Soc.* **2014**, *136*, 17722. (d) Sun, B.; Yoshino, T.; Matsunaga, S.; Kanai, M. *Adv. Syn. Catal.* **2014**, *356*, 1491. (e) Li, J.; Ackermann, L. *Angew. Chem. Int. Ed.* **2015**, *54*, 3635. (f) Pawar, A. B.; Chang, S. *Org. Lett.* **2015**, *17*, 660. (g) Sen, M.; Emayavaramban, B.; Barsu, N.; Premkumar, J. R.; Sundararaju, B. *ACS Catal.* **2016**, *6*, 2792. (h) Gensch, T.; Klauck, F. J. R.; Glorius, F. *Angew. Chem. Int. Ed.* **2016**, *55*, 11287. (i) Yoshida, M.; Kawai, K.; Tanaka, R.; Yoshino, T.; Matsunaga, S. *Chem. Commun.* **2017**, *53*, 5974. (j) Sk, M. R.; Bera, S. S.; Maji, M. S. *Org. Lett.* **2018**, *20*, 134.

17. For selected examples on affordable cobalt-catalyzed C–H functionalization, see: (a) Grigorjeva, L.; Daugulis, O. *Org. Lett.* **2014**, *16*, 4684. (b) Kalsi, D.; Sundararaju, B. *Org. Lett.* **2015**, *17*, 6118. (c) Du, C.; Li, P.-X.; Zhu, X.; Suo, J.-F.; Niu, J.-L.; Song, M.-P. *Angew. Chem. Int. Ed.* **2016**, *55*, 13571. (d) Yan, Q.; Xiao, T.; Liu, Z.; Zhang, Y. *Adv. Syn. Catal.* **2016**, *358*, 2707. (e) Yamaguchi, T.; Kommagalla, Y.; Aihara, Y.; Chatani, N. *Chem. Commun.* **2016**, *52*, 10129. (f) Manoharan, R.; Sivakumar, G.; Jeganmohan, M. *Chem. Commun.* **2016**, *52*, 10533. (g) Landge, V. G.; Midya, S. P.; Rana, J.; Shinde, D. R.; Balaraman, E. *Org. Lett.* **2016**, *18*, 5252. (h) Li, Q.; Hu, W.; Hu, R.; Lu, H.; Li, G. *Org. Lett.* **2017**, *19*, 4676. (i) Zhu, X.; Su, J.-H.; Du, C.; Wang, Z.-L.; Ren, C.-J.; Niu, J.-L.; Song, M.-P. *Org. Lett.* **2017**, *19*, 596.

18. (a) Lan, J.; Xie, H.; Lu, X.; Deng, Y.; Jiang, H.; Zeng, W. *Org. Lett.* **2017**, *19*, 4279. (b) Lin, C.; Chen, Z.; Liu, Z.; Zhang, Y. *Adv. Syn. Catal.* **2018**, *360*, 519. (c) Ueno, R.; Natsui, S.; Chatani, N. *Org. Lett.* **2018**, *20*, 1062.

19. Planas, O.; Whiteoak, C. J.; Martin-Diaconescu, V.; Gamba, I.; Luis, J. M.; Parella, T.; Company, A.; Ribas, X. *J. Am. Chem. Soc.* **2016**, *138*, 14388.
20. Qian, G.; Hong, X.; Liu, B.; Mao, H.; Xu, B. *Org. Lett.* **2014**, *16*, 5294.
21. Grigorjeva, L.; Daugulis, O. *Org. Lett.* **2015**, *17*, 1204.

Chapter 3: Copper || Thiolation

Copper-Mediated Direct and Selective C–H Thiolation of Quinazolinones

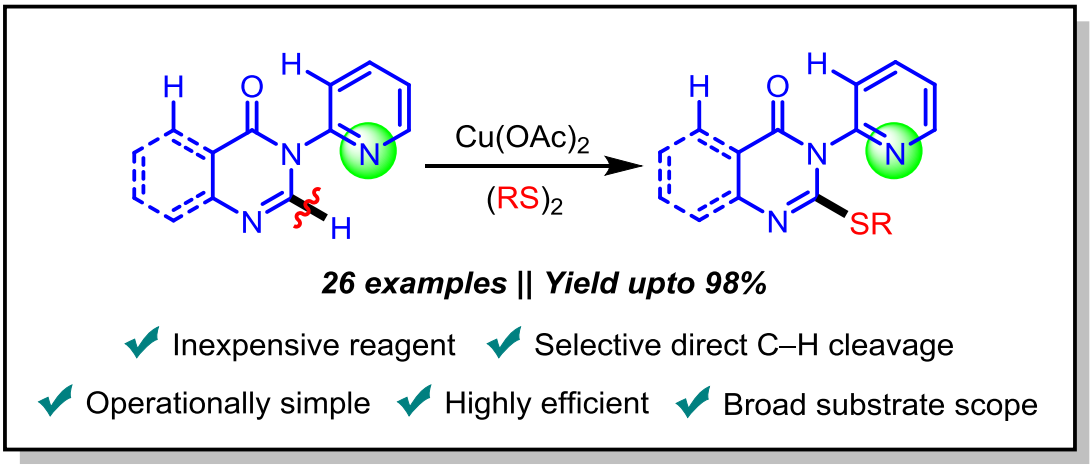

26 examples || Yield upto 98%

✔ Inexpensive reagent ✔ Selective direct C–H cleavage

✔ Operationally simple ✔ Highly efficient ✔ Broad substrate scope

3.1. Introduction

3.1.1. Relevance of Quinazolinones and Sulfur Based Compounds

Quinazolinones represent one of the most privileged scaffolds in organic chemistry with a wide array of bioactivities widespread in a number of pharmaceutically relevant molecules and drug candidates. 4-Quinazolinone derivatives such as sedatives afloqualone, methaqualone, piriqualone, diproqualone and cloroqualone, antimalarial febrifugine, and diuretic metolazone are among the commercially available marketed drugs (Figure 3.1.1.1).

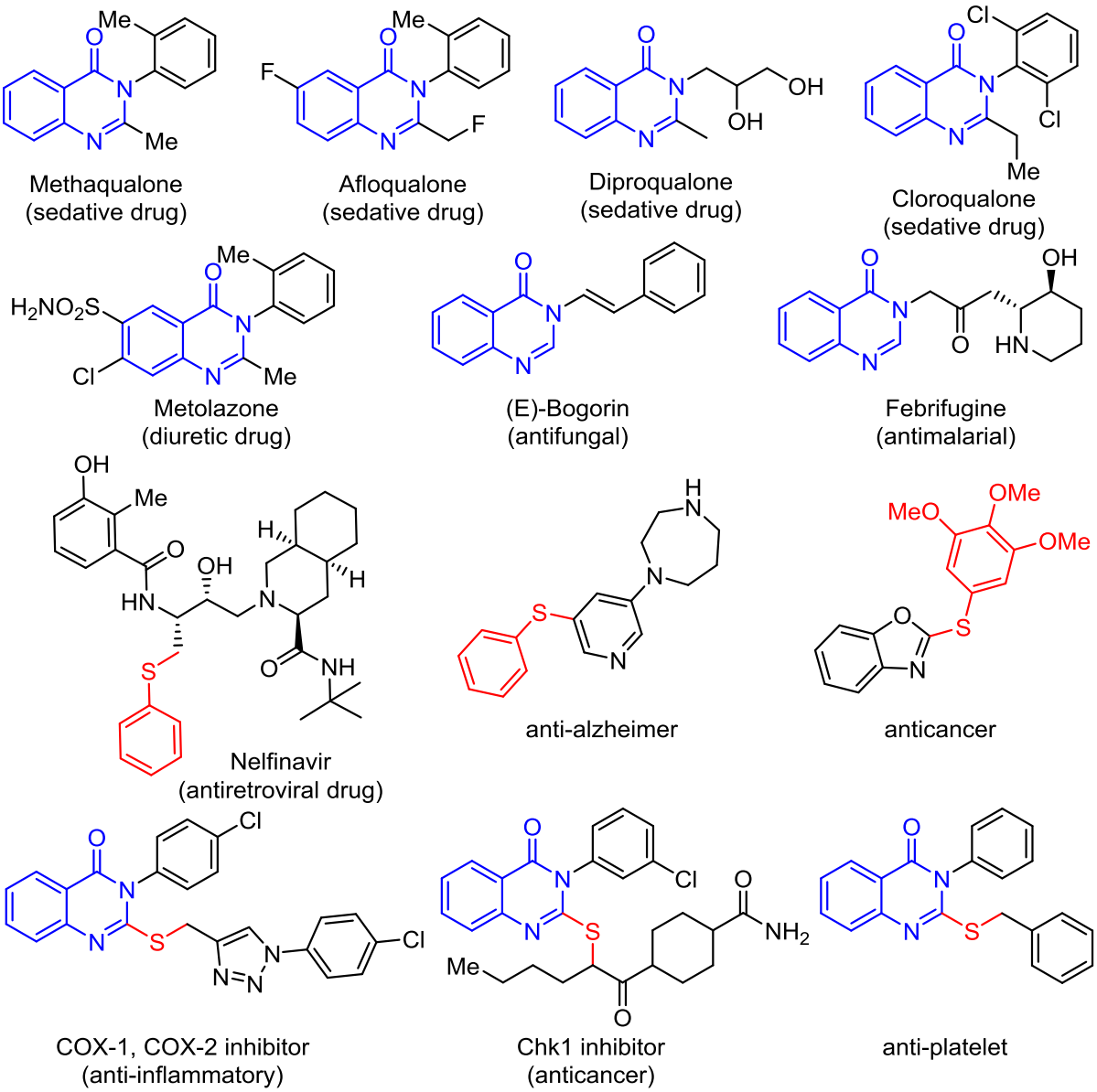

Figure 3.1.1.1. Representative examples of related biologically relevant molecules.

Also, some quinazolinone derivatives show antimitotic anticancer activities, act as lipophilic inhibitor of thymidylate synthase and show high cytotoxic activity against tumour cells. Among

other properties, quinazolinone derivatives also show analgesic activities and can act as antifungal, anti-allergic and anti-inflammatory agents.[1] On the other hand, organosulfur molecules are an important class of compounds having the antimicrobial property known since ages and form a part of many marketed sulfa drugs as well as useful building blocks in synthetic organic chemistry. Among various organosulfur molecules, aryl sulfides are ubiquitously prevalent in many bioactive and pharmaceutically relevant molecules. Thioethers comprise a unique class of structural elements present in a number of drugs such as nelfinavir (antiretroviral drug, inhibitor of HIV-1 protease), albendazole (antimicrosporidial activity), cimetidine (inhibits stomach acid production), and tiodazosin (antihypertensive), among others (Figure 3.1.1.1). Additionally, organothioethers are common building blocks in organic synthesis and organochalcogens like organo-sulfur, selenium, tellurium compounds have also become highly useful as fluorescent probes.[2] In recent times, quinazolinone tethered thioethers possessing anti-inflammatory, anticancer, and anti-platelet activities have also been reported (Figure 3.1.1.1),[3] underlining the immense importance in developing strategic routes for the synthesis of thioquinazolinones.

3.1.2. Strategies for Thioquinazolinone Synthesis

The synthesis of thioquinazolinones has seen many different ways over the years, but most of the practised methods involve the isothiocyanate intermediates and suffer from major limitations such as the use of electronically biased substrates, toxic starting materials, organolithium and other highly reactive reagents (Scheme 3.1.2.1).[4]

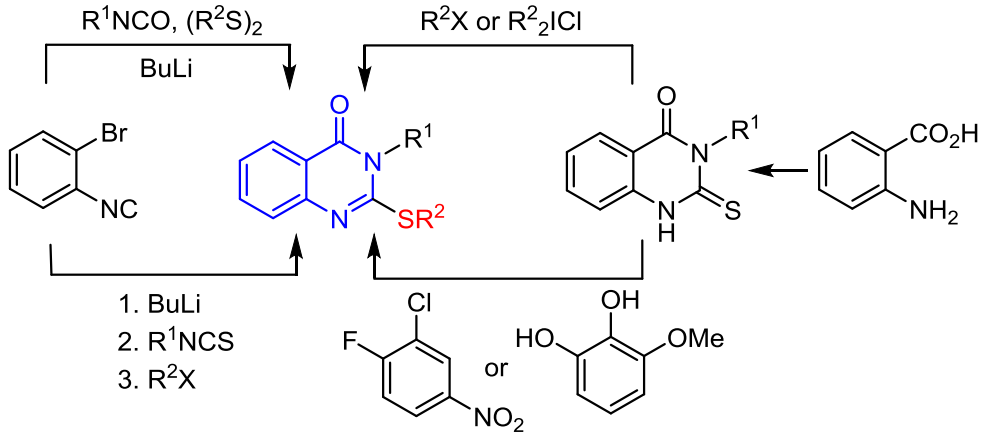

Scheme 3.1.2.1. Synthetic routes toward thioquinazolinones.

Additionally, these procedures demand stringent reaction conditions, some of which include microreactor or electrochemical oxidation conditions, offer low yields, and thus lead to low

atom and step economy. The drawbacks of these existing procedures, therefore, call for newer and more efficient approaches toward the synthesis of thioquinazolinones.

3.1.3. Transition Metal-Catalyzed/-Mediated C–S Bond Formation

Various transition metal-catalyzed cross-coupling reactions, especially with Pd, Ni and Cu catalysts provide convenient routes towards diarylsulfides which is largely dependent on sulfenylation of aryl halides and aryl boronic acids (typically known as Chan-Lam coupling). Aryl amines have also been employed for this purpose via diazotisation followed by heating (Sandmeyer reaction). Despite the advancements, all these methods suffer from the drawback of requirement of prefunctionalized starting materials (Scheme 3.1.3.1).[5] Recent literature has also seen a number of reports on thiolation of reactive C–H bonds.

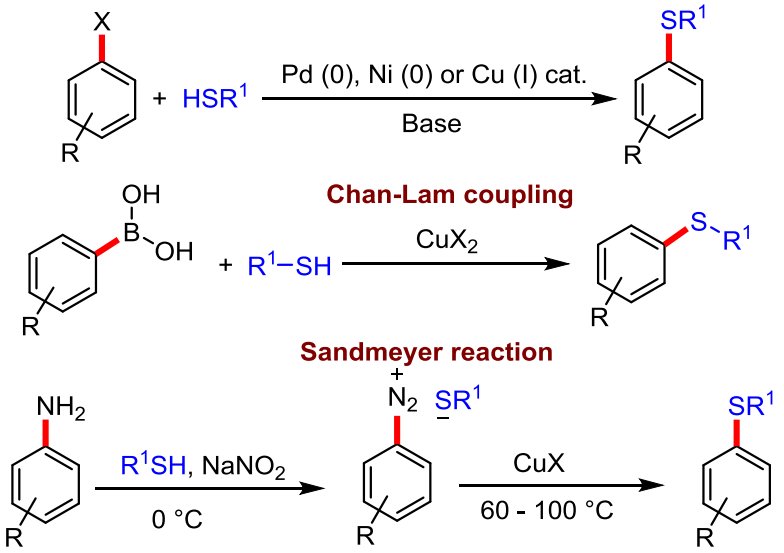

Scheme 3.1.3.1. Selected generalized classical routes towards diarylsulfides.

In the past two decades, various transition metal-catalyzed or mediated direct C–H activation methods have been developed for selective functionalization of unactivated and inert C–H bonds accomplishing numerous challenging synthetic tasks through shorter routes and exploiting readily available starting materials. However, direct C–H sulfenylation has been much of an underdeveloped area due to the fact that sulfur can coordinate with the reactive metal center and kill its catalytic activity (also called "catalyst poisoning"). Despite this fact, both expensive noble metals Pd, Rh, Ru as well as earth abundant base metals Cu, Co, Ni, etc. have turned up as highly utilized transition metals for direct sulfenylation as well selenylation reactions.[6] Some of the representative examples of transition metal-catalyzed C–H sulfenylation reactions are depicted in Scheme 3.1.3.2.

In 2006, Yu and co-workers first developed a copper-promoted direct C–H sulfenylation reaction of 2-phenylpyridines with thiols using O_2 as a stoichiometric oxidant (Scheme 3.1.3.2a).[6b] In 2012, Daugulis extended the C–H sulfenylation strategy to bidentate DG system employing sub-stoichiometric copper salt (Scheme 3.1.3.2b).[6c] In 2014, Nishihara *et al.* achieved the first palladium-catalyzed sulfenylation methodologies in both monodentate and bidentate systems employing disulfides (Scheme 3.1.3.2c, 3.1.3.2d).[6d,e]

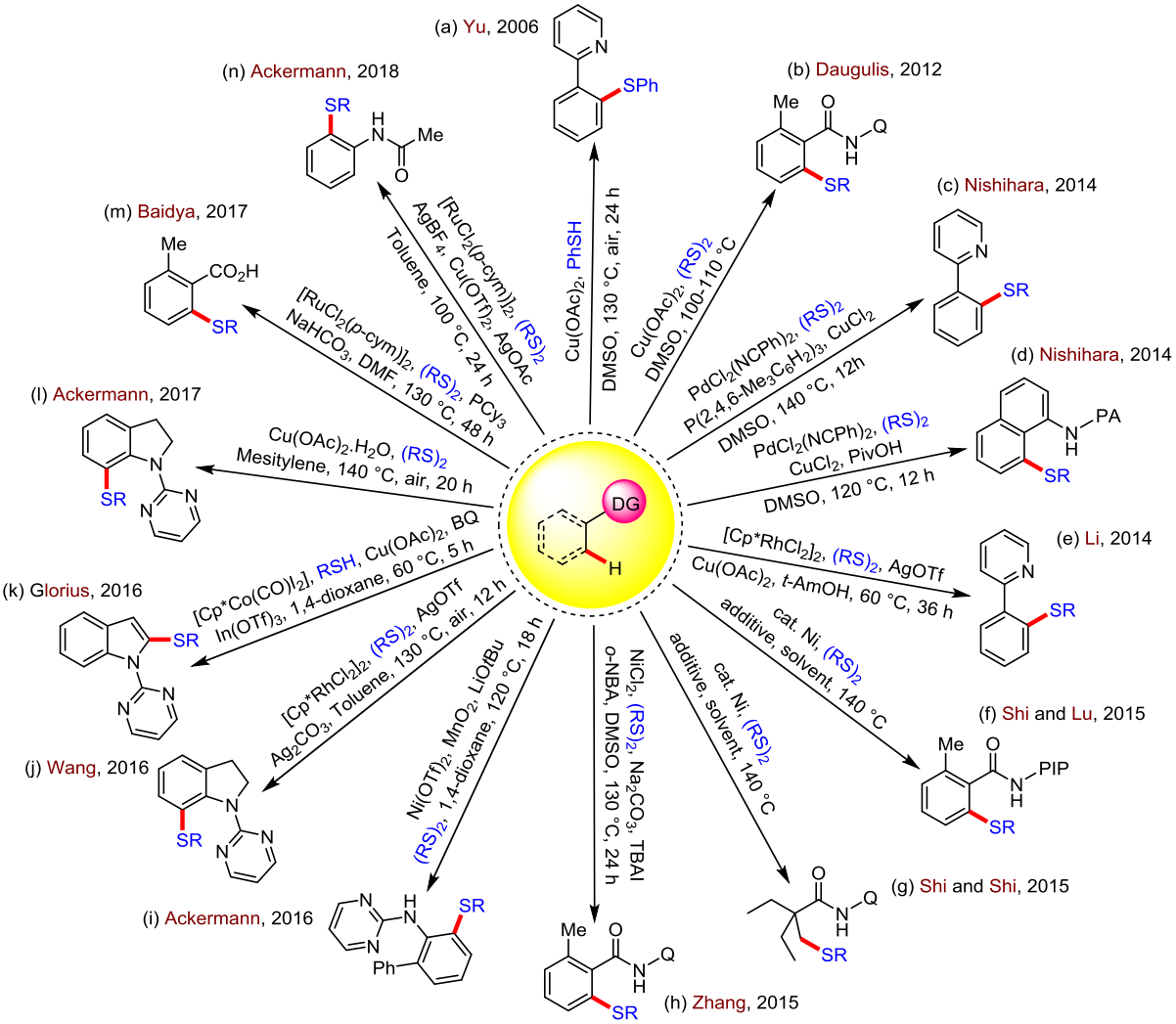

Scheme 3.1.3.2. Various transition metal-catalyzed directed C–H sulfenylation reactions.

Rhodium catalysis for C–H sulfenylation was put forward by Li group, when they reported the first direct C–H thiolation of various directing arenes with wide functional group tolerance and excellent selectivity over mono and dithiolation on simple tuning of reaction conditions (Scheme 3.1.3.2e).[6f] In between 2015 and 2016, the groups of Shi, Lu, Shi, and Ackermann independently demonstrated nickel-catalyzed sulfenylation of both sp^2 and sp^3 C–H bonds assisted by a bidentate or monodentate directing group (Scheme 3.1.3.2f-3.1.3.2i).[6g-j,6p] Till

now, the chalcogenation protocols described are largely limited to the 2-arylpyridine and arenecarboxamide scaffolds. In 2016, Wang and co-workers delineated a C7-selective thiolation and selenylation of indolines under Rh(III)-catalyzed conditions (Scheme 3.1.3.2j).[6q] Concurrently, Glorious *et al.* devised the first Cp*Co(III)-catalyzed regioselective C–H thiolation of indoles with thiols or disulfides (Scheme 3.1.3.2k).[6r] Indoles and Indolines could also be chalcogenated selectively at C2 and C7 positions respectively with disulfides or diselenides by Ackermann group employing copper catalysis (Scheme 3.1.3.2l).[6t] Baidya and co-workers utilized carboxylic acids as viable substrates for *ortho* chalcogenation reaction under ruthenium-catalyzed conditions without the need for any externally attached DG (Scheme 3.1.3.2m).[6w] Ru(II)-catalyzed C–H chalcogenation was also successfully applied to anilides by Ackermann *et al.* with readily available disulfides and diselenides (Scheme 3.1.3.2n).[6x] Apart from these notable works, in between a few other groups have also contributed in this area utilising other DGs.

3.1.4. Quinazolinones in C–H Activation

In recent times, the implementation of quinazolinones in transition metal-catalyzed C–H activation has been largely restricted to as a directing group for effective functionalization of sp^2 C–H bonds (Scheme 3.1.4.1).[7] In 2017, Cui *et al*. reported a Pd-catalyzed oxidative sequential [4+2] and [3+2] annulation reaction between 2-phenylquinazolin-4(*3H*)-one and alkyne to form novel fused polycyclic systems containing tetrahydropyridine and dihydrofuran rings (Scheme 3.1.4.1a).[7a] In the same year, Hong and Mhaske group independently developed methodologies for coupling quinazolinones with diaryliodonium triflates to afford different kind of products under palladium-catalyzed conditions (Scheme 3.1.4.1b).[7b,c] Cui and co-workers again devised a protocol for bis-sulfamidation of quinazolinones with sulfonyl azides employing iridium catalysis (Scheme 3.1.4.1c).[7d] In 2018, Peng and Jana group independently demonstrated annulation strategies for synthesizing diversely fused quinazolinones using vinyl trifluoroacetates and allyl acetates respectively under rhodium and ruthenium catalysis in the same order (Scheme 3.1.4.1d, 3.1.4.1e).[7e,f]

Apart from their use as an inherent directing group, minimal reports on direct C–H functionalization of quinazolinones have come up (only one sole example in each) by Samanta *et al.* using a suitable directing pyridine auxiliary employing rhodium catalysis.[8]

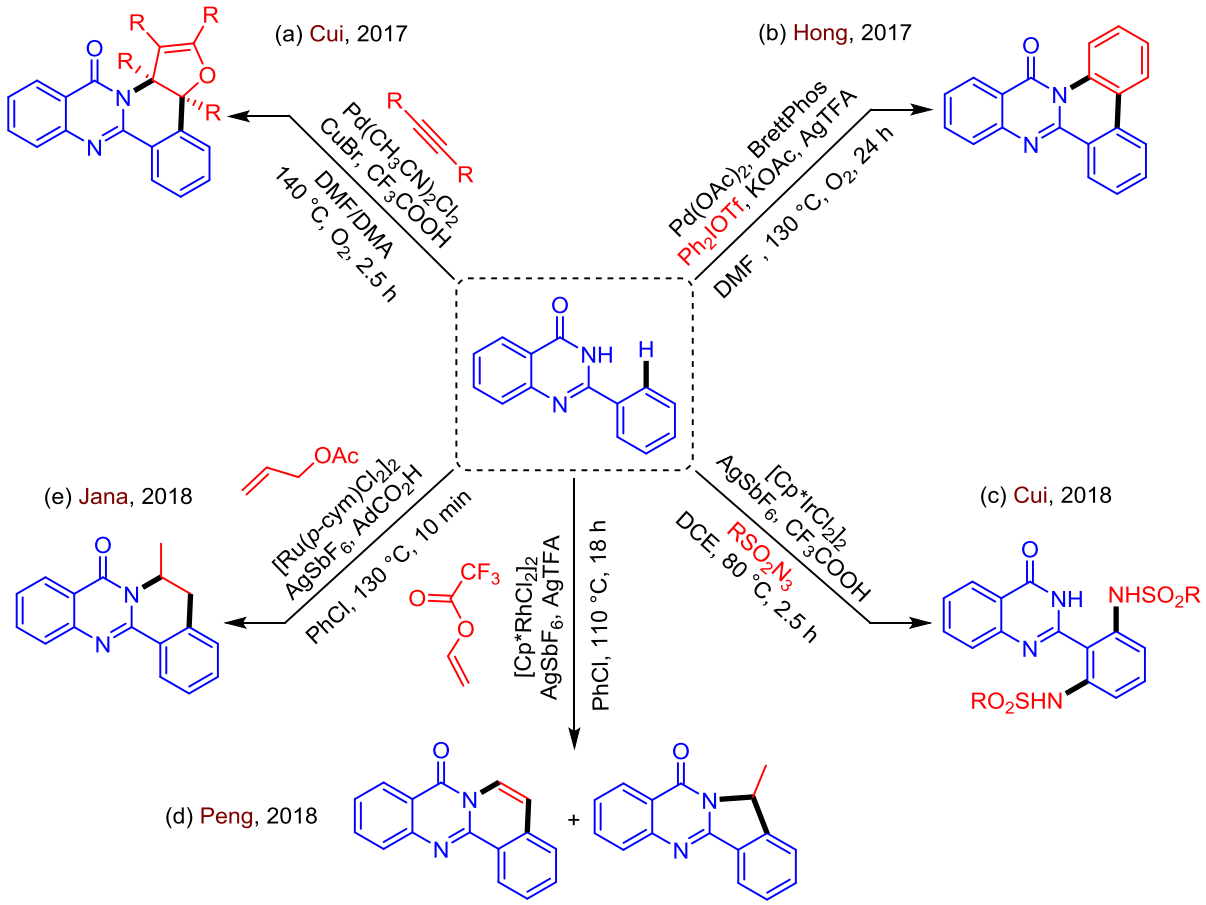

Scheme 3.1.4.1. Selected examples of quinazolinones acting as DG in C–H functionalization.

3.2. Objective

It is a given fact that organosulfur compounds have broad applications in pharmaceutics and transition metal-catalyzed direct and selective sulfenylation of inert C–H bonds is a growing field of research. Thus, newer approaches towards the construction of heterocycle tethered aryl thioethers are highly sought-after. In continuation with our research interest in quinazolinone substrates and the underlying importance in synthesizing thioquinazolinones, transition metal-catalyzed C–H sulfenylation would be another attractive topic for this purpose. Till date, direct C–H functionalization of quinazolinones has been confined to C–C bond formation reactions only. Hence, the development of a C–S bond forming reaction in quinazolinones could be highly valuable in terms of both academic and industrial purpose. Inspired by the recent trend of aryl thioether construction by means of atom and step economic transition metal catalysis and also to harness the power of cheap and benign first-row transition metal for this objective, we postulated that a thiophenyl group could be introduced selectively in quinazolinones with the aid of a suitable DG employing copper-mediated conditions (Scheme 3.2.1).

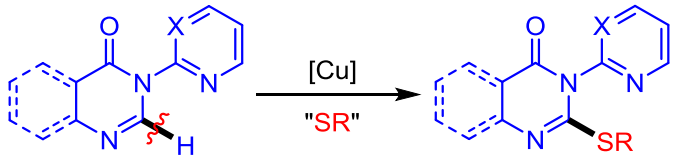

Scheme 3.2.1. Objective of this work: copper-mediated sp^2 C–H thiolation of quinazolinones.

3.3. Results and Discussion

3.3.1. Optimization Studies

We initiated our study by taking 3-(pyridin-2-yl)quinazolin-4(3*H*)-one (**1a**) as the model substrate for our methodology (Table 3.3.1.1). To our delight, the desired thiolated product 2-(phenylthio)-3-(pyridin-2-yl)quinazolin-4(3*H*)-one (**3aa**) was formed, although in a mere 12% yield in the presence of 1.0 equiv of diphenyl disulfide (**2a**) as the thiolating reagent, 2.0 equiv of $CuCl_2$ as catalyst in DMSO solvent at 140 ℃ for 24 h under N_2 atmosphere (Table 3.3.1.1, entry 1). Then, we surveyed various copper sources (Table 3.3.1.1, entries 2-5) with all of them providing comparatively similar yields, but $Cu(OAc)_2$ gave a slightly better yield of 14% (Table 3.3.1.1, entry 4). So, $Cu(OAc)_2$ was found to be the catalyst of choice for this reaction. To our curiousness, we then decreased the reaction temperature to 110 ℃ resulting in a slight uprise in the yield upto 17% (Table 3.3.1.1, entry 6). Next, we moved onto standardise the best solvent for the reaction by screening a series of polar and non-polar solvents such as DCE, 1,4-dioxane, DMF, MeCN, Toluene (Table 3.3.1.1, entries 7-11) ending up with DCE as the best solvent affording the desired product in an increased 32% yield (Table 3.3.1.1, entry 7).

Then, we went forward to check the influence of various additives in the present reaction, *viz.* Ag_2CO_3, AgO, AgOAc, $K_2S_2O_8$, $PhI(OAc)_2$, *p*-BQ, NMO (Table 3.3.1.1, entries 12-18). A significant improvement in the yield of **3aa** was observed up to 61% in case of 2.0 equiv of *p*-BQ (Table 3.3.1.1, entry 17). The yield of the thiolated product reached up to 67% when the reaction temperature was slightly elevated to 120 ℃ (Table 3.3.1.1, entry 19). Again, we increased the loading of the partner diphenyl disulfide (**2a**) to 1.5 equiv and observed a further increment in the yield up to 74% (Table 3.3.1.1, entry 20), which ultimately became the optimized condition for the current protocol. More elevated temperatures up to 130 ℃ led to slightly diminished yields (Table 3.3.1.1, entry 21). A decrease in the loading of $Cu(OAc)_2$ produced a reduced yield of the thiolated product (Table 3.3.1.1, entry 22). Finally, control experiment showed that $Cu(OAc)_2$ was necessary for this reaction since it did not take place in its absence (Table 3.3.1.1, entry 23). However, the attempts towards the development of catalytic version of this reaction using catalytic amount of $Cu(OAc)_2$ remained unsuccessful.

Table 3.3.1.1. Optimization of reaction conditions[a]

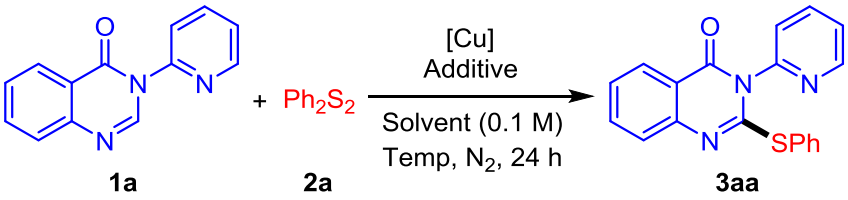

Entry	[Cu] (2.0 equiv)	Additive (x equiv)	Solvent (0.1 M)	Temp (°C)	Yield of **2a**[b] (%)
1	$CuCl_2$	-	DMSO	140	12
2	$CuBr_2$	-	DMSO	140	trace
3	CuF_2	-	DMSO	140	10
4	$Cu(OAc)_2$	-	DMSO	140	14
5	CuO	-	DMSO	140	nr
6	$Cu(OAc)_2$	-	DMSO	110	17
7	$Cu(OAc)_2$	-	DCE	110	32
8	$Cu(OAc)_2$	-	1,4-dioxane	110	nr
9	$Cu(OAc)_2$	-	DMF	110	26
10	$Cu(OAc)_2$	-	MeCN	110	30
11	$Cu(OAc)_2$	-	Toluene	110	trace
12	$Cu(OAc)_2$	Ag_2CO_3	DCE	110	trace
13	$Cu(OAc)_2$	AgO	DCE	110	trace
14	$Cu(OAc)_2$	AgOAc	DCE	110	15
15	$Cu(OAc)_2$	$K_2S_2O_8$	DCE	110	trace
16	$Cu(OAc)_2$	$PhI(OAc)_2$	DCE	110	34
17	$Cu(OAc)_2$	*p*-BQ	DCE	110	61
18	$Cu(OAc)_2$	NMO	DCE	110	59
19	$Cu(OAc)_2$	*p*-BQ	DCE	120	67
20[c]	**$Cu(OAc)_2$**	***p*-BQ**	**DCE**	**120**	**74 (74)**[d]
21[c]	$Cu(OAc)_2$	*p*-BQ	DCE	130	68
22[c,e]	$Cu(OAc)_2$	*p*-BQ	DCE	120	53
23[c]	-	*p*-BQ	DCE	120	nr

[a]Reaction conditions: Unless otherwise mentioned, substrate **1a** (0.1 mmol, 1.0 equiv), Ph_2S_2 (1.0 equiv), [Cu] (2.0 equiv), Solvent (1.0 mL), 140 °C, N_2, 24 h. [b]Isolated yield. [c]Ph_2S_2 (0.15 mmol). [d]in 0.2 mmol scale. [e]$Cu(OAc)_2$ (1.0 equiv). nr: no reaction.

3.3.2. Scope of the Reaction

A series of quinazolinones (**1**) were prepared depicted in Table 3.3.2.1 following literature procedures, discussed in the experimental section. *N*-pyridylquinazolinones (**1a-1j**) and *N*-pyridylpyrimidinone (**1l**) were prepared following literature procedure by arylation of substituted 4-hydroxyquinazolinones with 2-bromopyridine in the presence of CuI and K_2CO_3 in DMSO at 150 °C. *N*-pyrimidylquinazolinone (**1k**) was prepared following literature

procedure by arylation of 4-hydroxyquinazolinone with 2-bromopyrimidine in the presence of CuI and K_2CO_3 in DMF at 150 °C.

Table 3.3.2.1. List of quinazolinone and pyrimidinone substrates prepared[a]

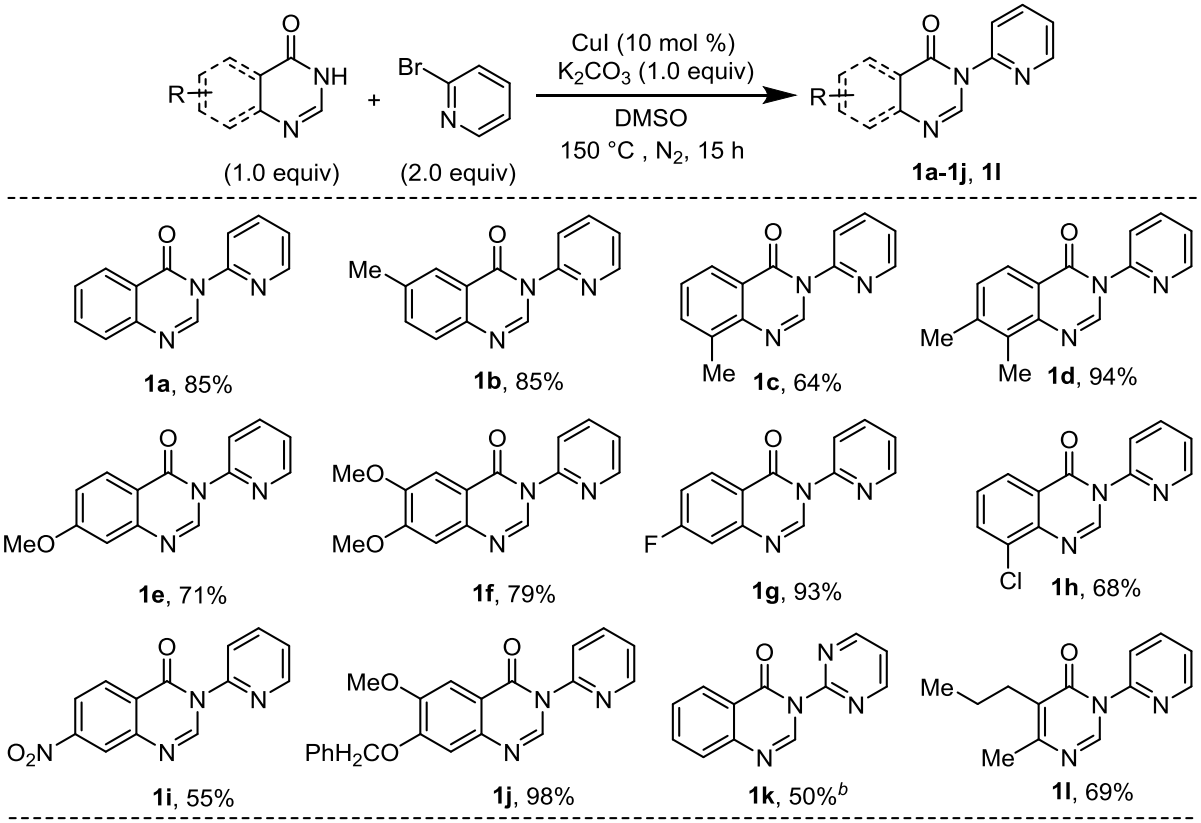

[a]Unless otherwise mentioned, all reactions were performed with substituted 4-hydroxyquinazoline as limiting reagent, 2.0 equiv of 2-bromopyridine, 10 mol % CuI, 1.0 equiv K_2CO_3 in DMSO at 150 °C for 15 h under N_2. [b]2.0 equiv of 2-bromopyridine, 20 mol % CuI in DMF.

After the preparation of the substituted quinazolinones and pyrimidinones (**1**), they were subjected to the thiolation reaction under the optimized condition to evaluate the scope of the reaction. First, the parent quinazolinone **1a** was tested with differently substituted disulfides (Table 3.3.2.2). In general, both aromatic as well as aliphatic disulfides gave very good results. Unsubstituted or electron-withdrawing group bearing aromatic disulfides such as F, Cl, or NO_2 gave their respective sulfenylated products **3aa**-**3ad** in good yields (57-75%). Dibenzyl disulfide proved to be a formidable partner furnishing the product **3ae** in 79% yield. Gratefully, aliphatic disulfides carrying cyclohexyl, *n*-butyl, or *n*-propyl groups, when subjected to the standard reaction condition also furnished the corresponding sulfenylated products **3af**-**3ah** in good to excellent yields (up to 82% yield).

Table 3.3.2.2. Scope of thiolation of *N*-pyridylquinazolinone with various disulfides[a]

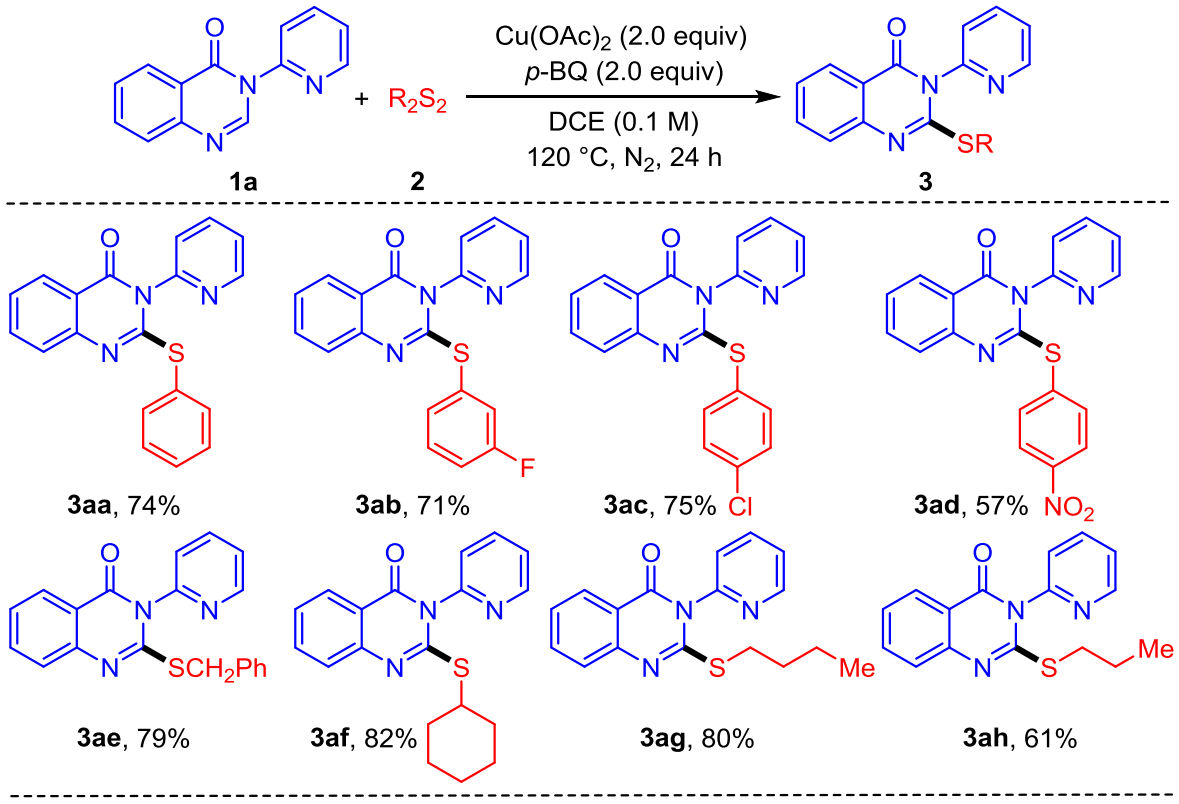

[a]Unless otherwise mentioned, all reactions were performed with 0.2 mmol **1a** at 0.1 M conc., 1.5 equiv of **2**, 2.0 equiv of $Cu(OAc)_2$ and 2.0 equiv of *p*-BQ in DCE at 120 °C for 24 h under N_2.

After investigating the various disulfides, we progressed to the diversely substituted quinazolinones (Table 3.3.2.3). In general, both electron-donating and electron-withdrawing substituents at various positions of the aryl ring of quinazolinone substrates were well tolerated and afforded the thiolated products with diphenyl disulfide (**2a**) in good to excellent yields. Electron-donating groups like Me or OMe bearing substrates at different positions of the phenyl ring provided the desired products (**3ba-3fa**) in yields up to 96%. Even those possessing electron-withdrawing groups like F, Cl, or NO_2 (**1g-1i**) reacted smoothly, generating their respective sulfenylated products (**3ga-3ia)** in very good yields (up to 87%). Another substrate **1j**, containing both OMe and *O*-benzyl groups, was reacted with some electron-rich as well as electron-poor disulfides yielding the desired thiolated products (**3ja**, **3jb**, **3jc**, **3jd**, and **3ji**) in good to excellent yields (up to 97%). Finally, when a pyrimidine group was positioned in place of the pyridine moiety in the quinazolinone substrate (**1k**), it gave the corresponding sulfenylated product **3ka** in 74% yield under the optimized condition, thus emphasizing the potency of the pyrimidine system acting as a suitable directing group.

Table 3.3.2.3. Scope of thiolation of quinazolinones with various diaryl disulfides[a]

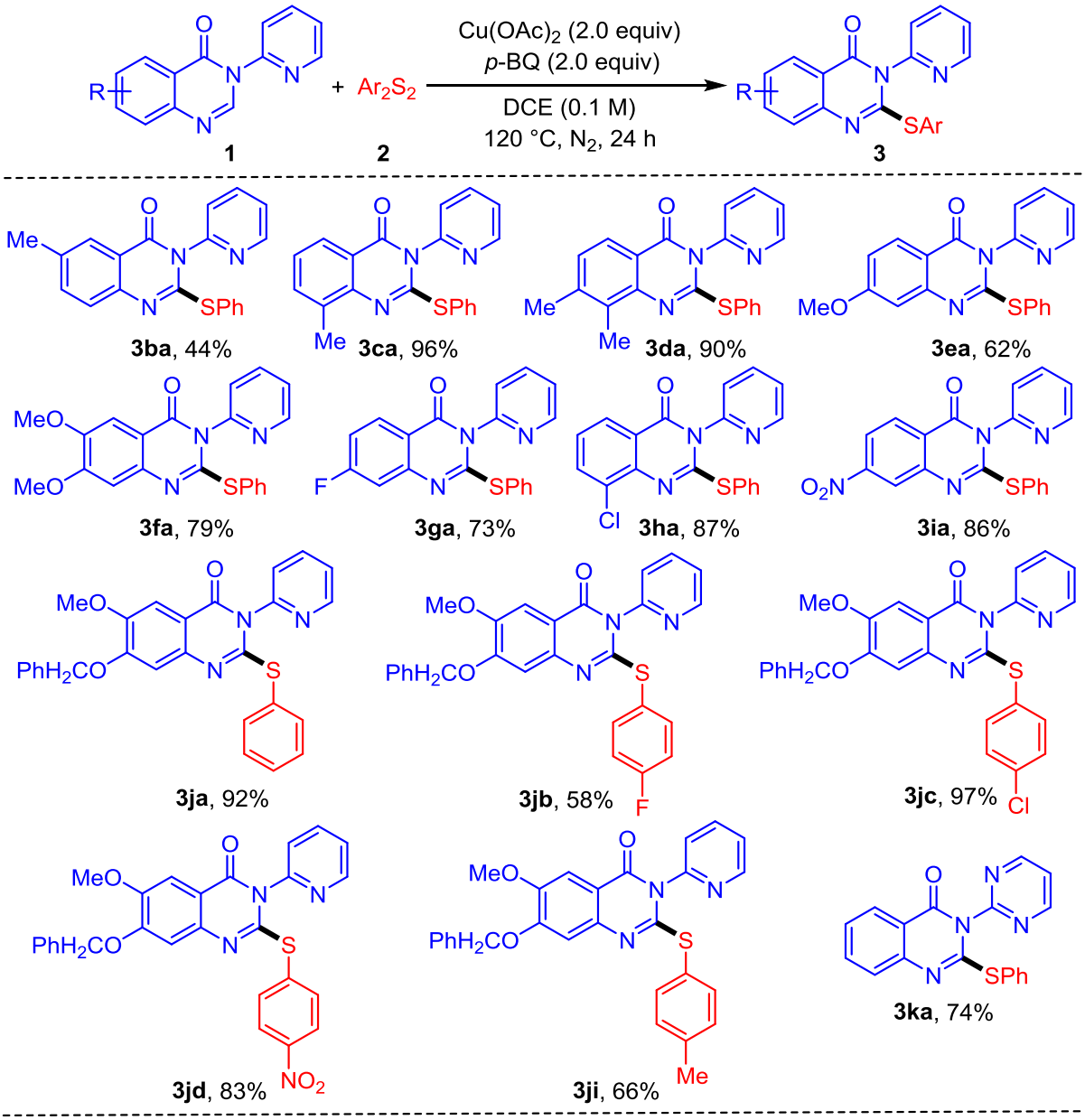

[a]Unless otherwise mentioned, all reactions were performed with 0.2 mmol **1** at 0.1 M conc., 1.5 equiv of Ar_2S_2, 2.0 equiv of $Cu(OAc)_2$ and 2.0 equiv of *p*-BQ in DCE at 120 °C for 24 h under N_2.

In order to expand the scope of the present protocol, we prepared the related pyrimidinone **1l** and treated it under standard reaction conditions with substituted disulfides including both the aromatic and aliphatic diversities (Table 3.3.2.4). To our pleasure, all of them delivered the desired products (**3la**, **3lc**, **3ld**, and **3lf**) in good to excellent yields (69-98%).

Table 3.3.2.4. Scope of thiolation of *N*-pyridylpyrimidinone with various disulfides[a]

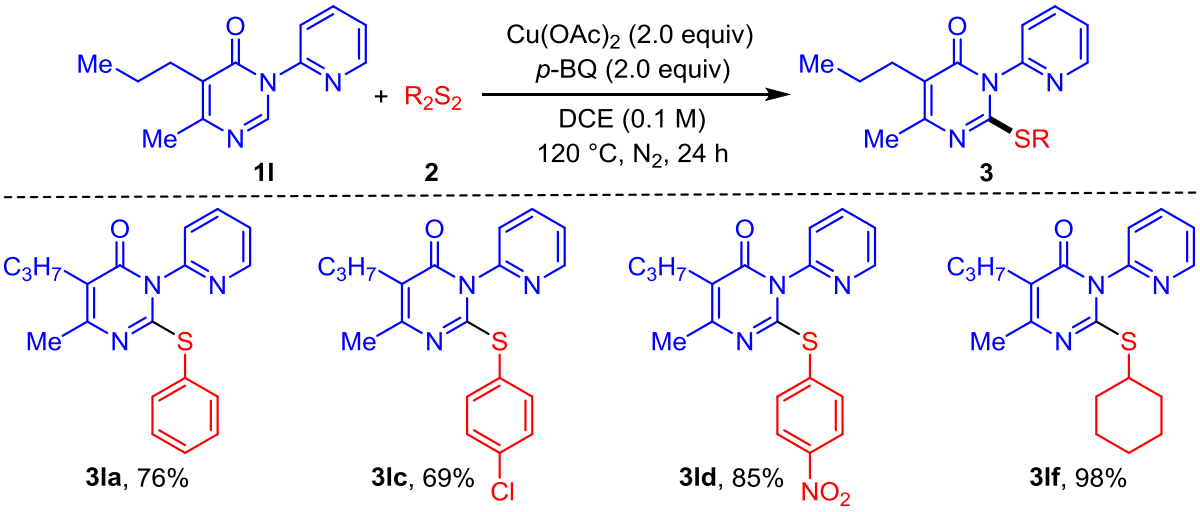

[a]Unless otherwise mentioned, all reactions were performed with 0.2 mmol **1l** at 0.1 M conc., 1.5 equiv of **2**, 2.0 equiv of $Cu(OAc)_2$ and 2.0 equiv of *p*-BQ in DCE at 120 °C for 24 h under N_2.

All the sulfenylated products (**3**) are duly characterised by ^{1}H, ^{13}C NMR and HRMS. Single-crystal X-ray analysis of **3ca** and **3ia** further confirmed their structures (Figure 3.3.2.1).

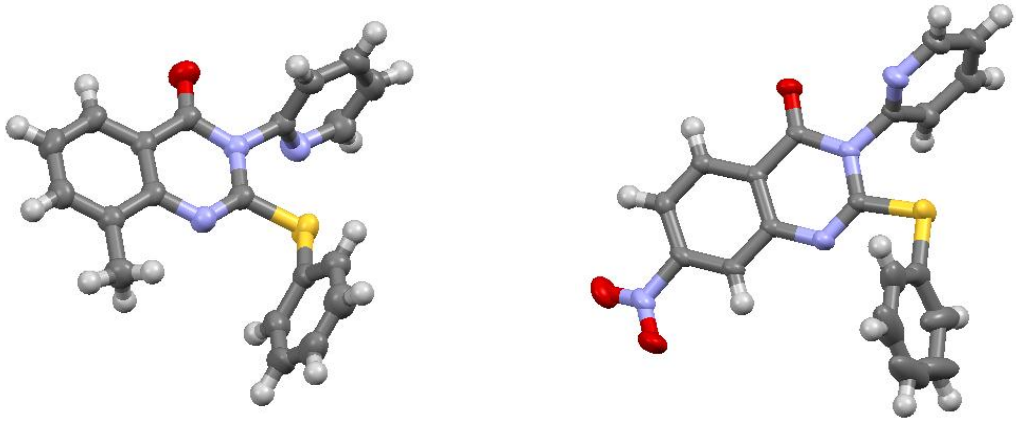

3ca
CCDC No. 1888207

3ia
CCDC No. 1888348

Figure 3.3.2.1. X-ray crystal structures of **3ca** and **3ia** (ellipsoid contour at 50% probability level).

3.3.3. Gram-Scale Reaction

To illustrate the scalability of our present methodology, we conducted a gram-scale experiment using the substrate **1a** (1.0 g) under the standard condition, but a comparatively moderate yield of 36% (0.539 g) of the sulfenylated product **3aa** was obtained (Scheme 3.3.3.1).

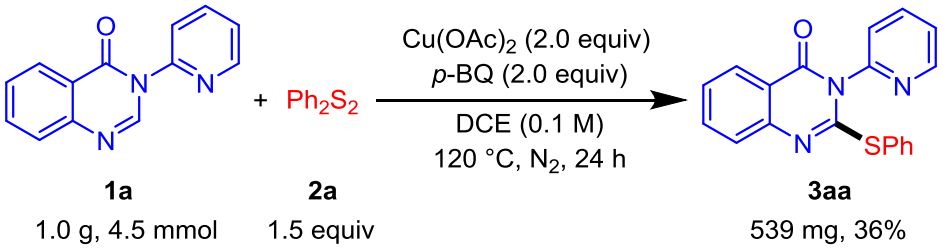

Scheme 3.3.3.1. Gram-scale reaction.

3.3.4. Control Experiment and Radical Scavenging Experiments

To understand the mechanism of the thiolation reaction, a series of control experiment and radical scavenging experiments were performed.

Our hypothesis for this protocol involved that the pyridine or the pyrimidine group might be acting as a directing group for chelation with the metal catalyst required for the C–H activation reaction. To confirm this, we examined the importance of the pyridine or the pyrimidine moiety by preparing the substrate **1m** devoid of pyridine or pyrimidine-*N* and then subjected it to the standard reaction conditions (Scheme 3.3.4.1). Results showed that without this group, the reaction does not take place at all, thereby confirming the fact that the pyridine or pyrimidine-*N* atom indeed acts as a coordinating entity to chelate with the copper metal salt in order for the reaction to take place.

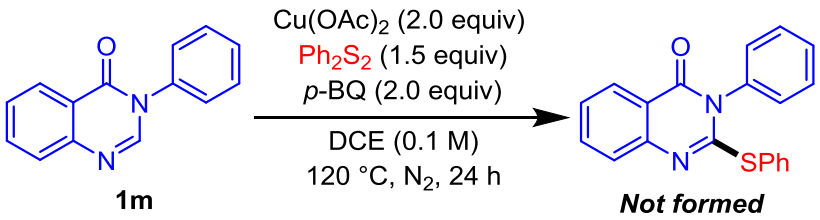

Scheme 3.3.4.1. Utility of pyridine or pyrimidine functionality.

Next, we performed radical quenching experiments on the parent substrate **1a** to verify our hypothesis that the reaction might involve a radical mechanistic pathway (Scheme 3.3.4.2). Radical trapping agents like TEMPO and BHT were used for this purpose. On adding 3.0 equiv of TEMPO as the radical quencher, a sizeable decrease in the yield of **3aa** (up to 22%) was observed. When BHT was used instead, a further decrease in the yield occurred up to 9%. These results suggested that the reaction might be going through a radical mechanism. However, attempts for the isolation or detection of any radical adduct failed.

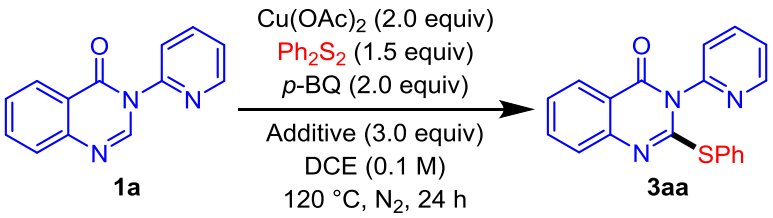

Exp. No.	Additive	Equiv	Yield
1	-	-	74%
2	TEMPO	3.0	22%
3	BHT	3.0	9%

Scheme 3.3.4.2. Radical scavenging experiments.

3.3.5. Plausible Mechanism

On the basis of above experimental results and literature precedents,[6b,o] a plausible reaction pathway is proposed as depicted in Scheme 3.3.5.1. It can be speculated that the reaction may proceed via initial coordination of pyridine-*N* with Cu(II) species giving intermediate **A**, followed by an intramolecular one-electron transfer (SET) process to generate intermediates **B** and then **C**. Next, oxidative addition of PhSSPh occurs in presence of excess $Cu(OAc)_2$ which aids the cleavage of the S–S bond, followed by reductive elimination and simultaneous deprotonation steps to furnish the desired thiolated product **3aa**. However, the role of excess amounts of *p*-BQ is still not clear.

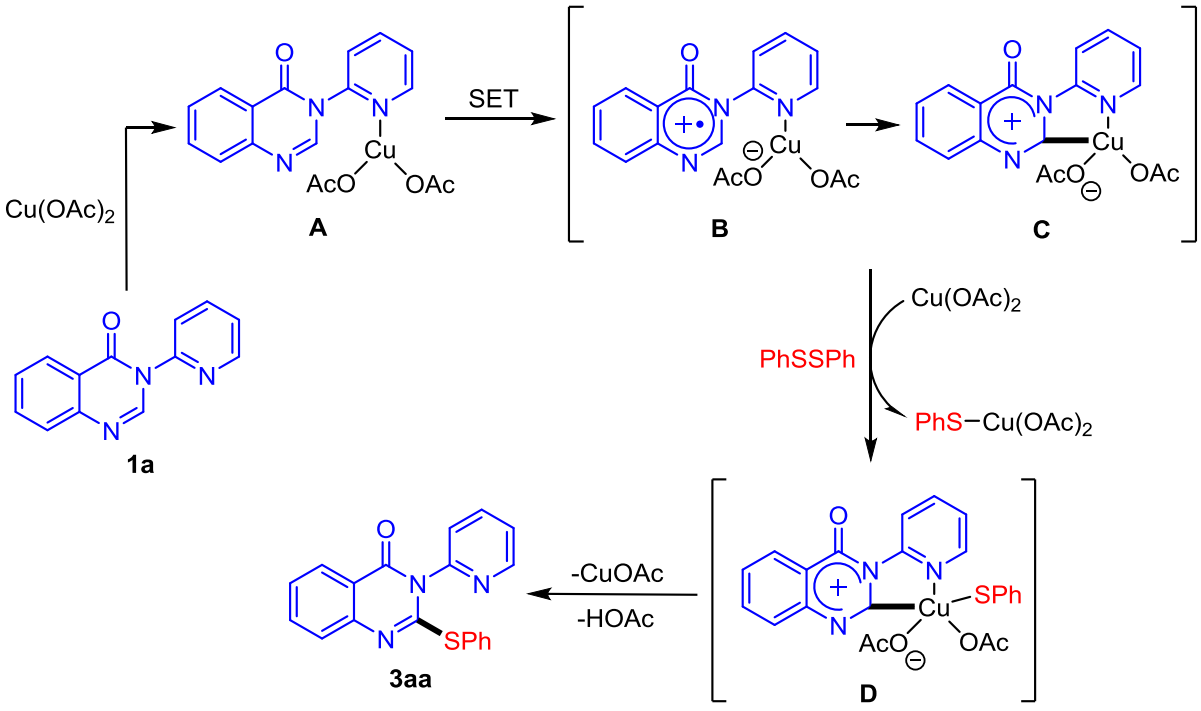

Scheme 3.3.5.1. Plausible reaction mechanism.

In order to get the deprotected thioquinazolinone product, we also performed several reactions for the removal of the pyrimidine directing group[9] from the sulfenylated product **3ka**. But, none of the attempts led to the successful elimination of the pyrimidine directing group.

3.4. Summary

In conclusion, we have developed a copper-mediated *ortho* sp^2 C–H sulfenylation of quinazolinones and pyrimidinones using diaryl disulfides and dialkyl disulfides, assisted by a pyridine or pyrimidine directing group. This reaction protocol is attractive due to the simple reaction conditions, use of the cheap and benign copper source to synthesize a wide array of biologically important thioquinazolinones. The methodology is applicable to a broad range of substrates and tolerates a wide array of functional groups and the utility of the method has been demonstrated by a gram scale reaction. A series of control experiments and radical quenching experiments were performed in order to understand the mechanism of the reaction. It was inferred that the present reaction may proceed through a radical pathway.

3.5. Experimental Section

3.5.1. General Information

All the information is same as that provided in Section 2.5.1 of Chapter 2 unless otherwise mentioned. The CIF files were submitted to CCDC (1888207 and 1888348) and can be obtained at https://summary.ccdc.cam.ac.uk/structure-summary-form.

3.5.2. General Procedure for the Preparation of Starting Materials

All the *N*-pyridylquinazolinones (**1a-1j**, **1l**) were prepared following the literature method.[10] Different quinazolin-4(3*H*)-ones were coupled with 2-bromopyridine to get the desired *N*-pyridylquinazolinones (Scheme 3.5.2.1).

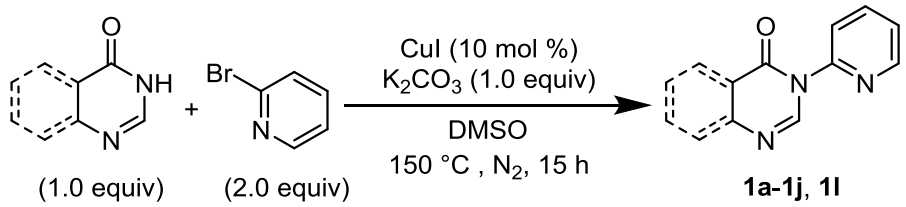

Scheme 3.5.2.1. Preparation of *N*-pyridylquinazolinones via Ullmann coupling.

To an oven-dried round bottom flask equipped with a reflux condenser, substituted 4-hydroxyquinazoline (1.0 equiv), CuI (10 mol %, 0.1 equiv), and K_2CO_3 (1.0 equiv) were added to anhydrous DMSO (0.15 M), and then 2-bromopyridine (2.0 equiv) was added. Then it was degassed and backfilled with nitrogen. The mixture was stirred at 150 °C for 15 h under nitrogen atmosphere. The resulting mixture was allowed to cool to room temperature and then extracted with ethyl acetate, washed with water and brine, passed over anhydrous Na_2SO_4 and

concentrated under vacuo. The reaction mixture was directly purified by column chromatography on silica gel using petroleum ether/ethyl acetate as eluent affording **1a-1j** and **1l** in 28-94% yield.

N-pyrimidylquinazolinone (**1k**) was prepared following the literature method (Scheme 3.5.2.2).[10] To an oven-dried round bottom flask equipped with a reflux condenser 4-hydroxyquinazoline (1.0 equiv), CuI (20 mol %, 0.2 equiv), and K_2CO_3 (1.0 equiv) were added to anhydrous DMF (0.15 M), and then 2-bromopyrimidine (2.0 equiv) was added. Then it was degassed and backfilled with nitrogen. The mixture was stirred at 150 °C for 15 h under nitrogen atmosphere. The resulting mixture was allowed to cool to room temperature and then extracted with ethyl acetate, washed with water and brine, passed over anhydrous Na_2SO_4 and concentrated under vacuo. The reaction mixture was directly purified by column chromatography on silica gel using ethyl acetate/petroleum ether as eluent affording 3-(pyrimidin-2-yl)quinazolin-4(3*H*)-one (**1k**) in 50% yield.

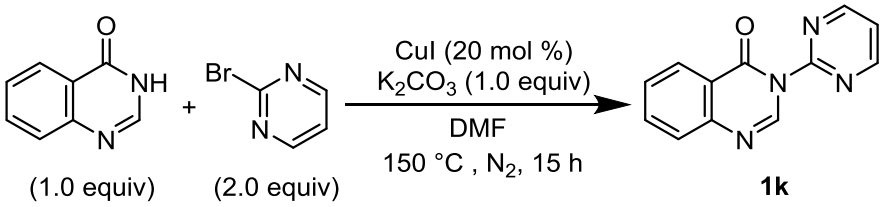

Scheme 3.5.2.2. Preparation of *N*-pyrimidylquinazolinones via Ullmann coupling.

3.5.3. General Procedure for Thiolation

(0.2 mmol scale):

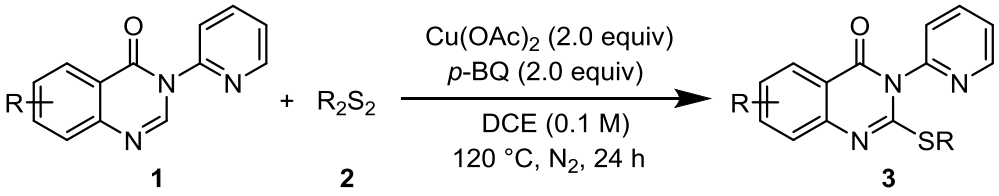

In an oven dried 10 mL Schlenk tube, the substrate (0.2 mmol, 1.0 equiv), R_2S_2 (0.3 mmol, 1.5 equiv), $Cu(OAc)_2$ (72.7 mg, 0.4 mmol, 2.0 equiv) and *p*-BQ (43.2 mg, 0.4 mmol, 2.0 equiv) were added and reaction mixture was degassed and backfilled with nitrogen. Under nitrogen 2.0 mL (0.1 M) of anhydrous DCE was added. Then it was degassed and backfilled with nitrogen (3 times). The tube was closed with a teflon-lined cap and kept on stirring in an oil bath. The bath temperature was slowly increased to 120 ^oC. After 24 h, the reaction was stopped and cooled to room temperature. The reaction mixture was filtered through a short pad of celite

and concentrated under vacuo. The crude reaction mixture was directly purified by column chromatography on silica gel using petroleum ether/ethyl acetate as eluent.

(gram-scale):

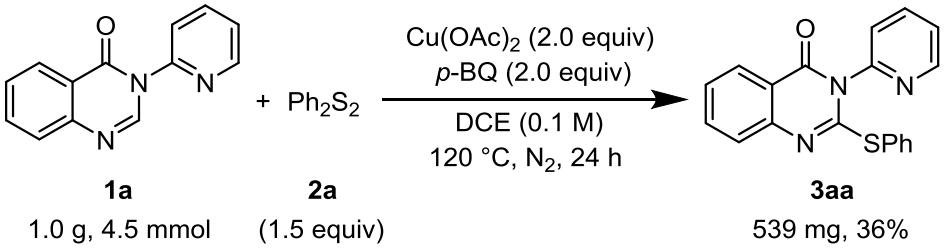

1a 1.0 g, 4.5 mmol | **2a** (1.5 equiv) | **3aa** 539 mg, 36%

To an oven-dried 100 mL round bottom flask equipped with a reflux condenser 3-(pyridin-2-yl)quinazolin-4(3*H*)-one (**1a**) (1.0 g, 4.5 mmol, 1.0 equiv), Ph_2S_2 (1.47 g, 6.75 mmol, 1.5 equiv), $Cu(OAc)_2$ (1.63 g, 9.0 mmol, 2.0 equiv) and *p*-BQ (968 mg, 9.0 mmol, 2.0 equiv) were added. Next it was degassed and backfilled with nitrogen. Under nitrogen 45 mL (0.1 M) of anhydrous DCE was added. Then it was degassed and backfilled with nitrogen (3 times). The reaction mixture was kept on stirring in an oil bath. The bath temperature was slowly increased to 120 ^{o}C. After 24 h, the reaction was stopped and cooled to room temperature. The reaction mixture was filtered through a short pad of celite and concentrated under vacuo. The crude reaction mixture was directly purified by column chromatography on silica gel using petroleum ether/ethyl acetate as eluent to give 2-(phenylthio)-3-(pyridin-2-yl)quinazolin-4(3*H*)-one (**3aa**) (0.539 g, 36% yield).

3.5.4. Characterization Data for the Unknown Substrates and Sulfenylated Products

Characterization Data for the Unknown Substrates

6-methyl-3-(pyridin-2-yl)quinazolin-4(3*H*)-one (1b):

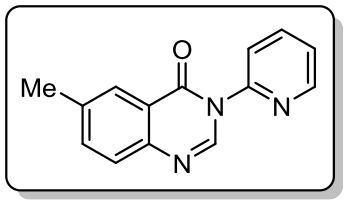

Yield 28%; pale yellow solid; $\mathbf{R_f}$ 0.25 (pet ether/ethyl acetate = 1:1); **eluent composition** petroleum ether/ethyl acetate = 7:3; **mp** 156-158 ^{o}C; **^{1}H NMR** (300 MHz, d_6-DMSO) δ 2.46 (s, 3H), 7.52-7.57 (m, 1H), 7.64 (d, *J* = 8.4 Hz, 1H), 7.71 (dd, *J* = 8.1 Hz, 2.1 Hz, 1H), 7.81 (d, *J* = 8.1 Hz, 1H), 8.01-8.03 (m, 1H), 8.06 (dd, *J* = 7.8 Hz, 1.8 Hz, 1H), 8.49 (s, 1H), 8.64 (dd, *J* = 5.1 Hz, 1.8 Hz, 1H); **^{13}C NMR** (150 MHz, d_6-DMSO) δ 21.3, 121.8, 122.7, 124.6, 126.4, 127.7, 136.7, 138.0, 139.0, 145.4, 145.9, 149.7, 150.1, 160.1; **HRMS** (ESI, m/z) calcd for $C_{14}H_{11}N_3O$ $[M + H]^+$ 238.0980, found 238.0977.

8-methyl-3-(pyridin-2-yl)quinazolin-4(3*H*)-one (1c):

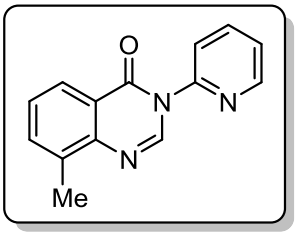

Yield 64%; colourless solid; **R_f** 0.40 (pet ether/ethyl acetate = 1:1); **eluent composition** petroleum ether/ethyl acetate = 9:1; **mp** 128-130 ^oC; **^{1}H NMR** (300 MHz, $CDCl_3$) δ 2.66 (s, 3H), 7.36-7.40 (m, 1H), 7.43 (app t, *J* = 6.9 Hz, 1H), 7.65 (app d, *J* = 7.5 Hz, 1H), 7.89-7.91 (comp, 2H), 8.23 (dd, *J* = 8.1 Hz, 1.5 Hz, 1H), 8.61-8.64 (comp, 2H); **^{13}C NMR** (150 MHz, $CDCl_3$) δ 17.5, 121.6, 122.1, 123.5, 124.9, 127.2, 135.5, 136.2, 138.0, 143.7, 146.2, 149.2, 149.8, 160.8; **HRMS** (EI, m/z) calcd for $C_{14}H_{11}N_3O$ [M^+] 237.0902, found 237.0901.

8-methyl-3-(pyridin-2-yl)quinazolin-4(3*H*)-one (1d):

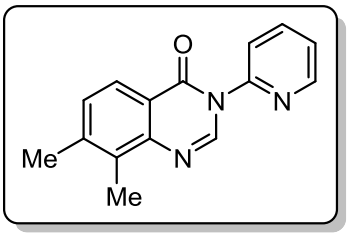

Yield 64%; colourless solid; **R_f** 0.40 (pet ether/ethyl acetate = 1:1); **eluent composition** petroleum ether/ethyl acetate = 9:1; **mp** 128-130 ^oC; **^{1}H NMR** (300 MHz, $CDCl_3$) δ 2.66 (s, 3H), 7.36-7.40 (m, 1H), 7.43 (app t, *J* = 6.9 Hz, 1H), 7.65 (app d, *J* = 7.5 Hz, 1H), 7.89-7.91 (comp, 2H), 8.23 (dd, *J* = 8.1 Hz, 1.5 Hz, 1H), 8.61-8.64 (comp, 2H); **^{13}C NMR** (150 MHz, $CDCl_3$) δ 17.5, 121.6, 122.1, 123.5, 124.9, 127.2, 135.5, 136.2, 138.0, 143.7, 146.2, 149.2, 149.8, 160.8; **HRMS** (EI, m/z) calcd for $C_{14}H_{11}N_3O$ [M^+] 237.0902, found 237.0901.

7-methoxy-3-(pyridin-2-yl)quinazolin-4(3*H*)-one (1e):

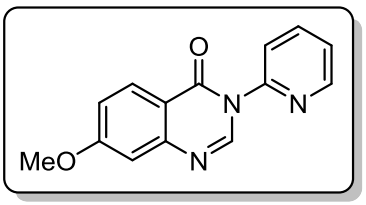

Yield 71%; colourless solid; **R_f** 0.12 (pet ether/ethyl acetate = 1:1); **eluent composition** petroleum ether/ethyl acetate = 7:3; **mp** 62-64 ^oC; **^{1}H NMR** (300 MHz, $CDCl_3$) δ 3.95 (s, 3 H), 7.10 (dd, *J* = 9.0 Hz, 2.4 Hz, 1H), 7.16 (d, *J* = 2.7 Hz, 1H), 7.36-7.40 (m, 1H), 7.88-7.90 (comp, 2H), 8.27 (d, *J* = 8.7 Hz, 1H), 8.61-8.63 (comp, 2H); **^{13}C NMR** (75 MHz, $CDCl_3$) δ 55.7, 108.5, 115.4, 117.2, 121.5, 123.4, 128.7, 137.9, 145.5, 149.0, 149.6, 149.8, 159.9, 164.8; **HRMS** (ESI, m/z) calcd for $C_{14}H_{11}N_3O_2$ [M + Na]$^+$ 276.0749, found 276.0750.

6,7-dimethoxy-3-(pyridin-2-yl)quinazolin-4(3*H*)-one (1f):

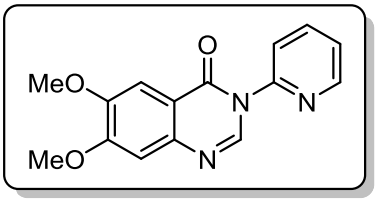

Yield 86%; colourless solid; **R_f** 0.08 (pet ether/ethyl acetate = 1:1); **eluent composition** petroleum ether/ethyl acetate = 1:1; **mp** 140-142 ^oC; **^{1}H NMR** (300 MHz, $CDCl_3$) δ 4.04 (s, 3H), 4.05 (s, 3H), 7.20 (s, 1H), 7.37-7.45 (m, 1H), 7.72 (s, 1H),

7.91-7.93 (comp, 2H), 8.56 (s, 1H), 8.64 (dt, *J* = 4.8 Hz, 1.5 Hz, 1H); **^{13}C NMR** (75 MHz, $CDCl_3$) δ 56.3, 56.3, 106.0, 108.1, 115.3, 121.6, 123.4, 138.0, 143.8, 143.8, 149.1, 149.4, 149.8, 155.1, 159.8; **HRMS** (ESI, m/z) calcd for $C_{15}H_{13}N_3O_3$ $[M + H]^+$ 284.1035, found 284.1034.

7-fluoro-3-(pyridin-2-yl)quinazolin-4(3*H*)-one (1g):

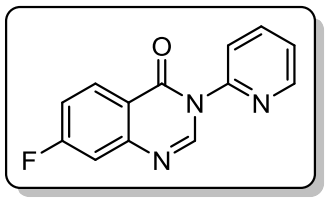

Yield 59%; colourless solid; **R_f** 0.32 (pet ether/ethyl acetate = 1:1); **eluent composition** petroleum ether/ethyl acetate = 4:1; **mp** 148-150 ^oC; **^{1}H NMR** (300 MHz, $CDCl_3$) δ 7.25-7.32 (m, 1H), 7.41-7.47 (comp, 2H), 7.89-7.97 (comp, 2H), 8.42 (dd, *J* = 9.0 Hz, 6.0 Hz, 1H), 8.64-8.67 (comp, 2H); **^{13}C NMR** (75 MHz, $CDCl_3$) δ 113.2 (d, $^2J_{F\text{-}C}$ = 21.75 Hz), 116.3 (d, $^2J_{F\text{-}C}$ = 23.25 Hz), 118.8, 121.4, 123.7, 130.0 (d, $^3J_{F\text{-}C}$ = 10.5 Hz), 138.1, 146.2, 149.2, 149.3 (d, $^4J_{F\text{-}C}$ = 7.5 Hz), 149.8 (d, $^3J_{F\text{-}C}$ = 12.75 Hz), 159.7, 166.6 (d, $^1J_{F\text{-}C}$ = 253.5 Hz); **HRMS** (ESI, m/z) calcd for $C_{13}H_8FN_3O$ $[M + H]^+$ 242.0730, found 242.0733.

8-chloro-3-(pyridin-2-yl)quinazolin-4(3*H*)-one (1h):

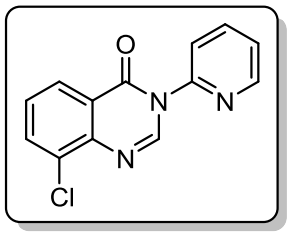

Yield 69%; colourless solid; **R_f** 0.45 (pet ether/ethyl acetate = 1:1); **eluent composition** petroleum ether/ethyl acetate = 9:1; **mp** 144-146 ^oC; **^{1}H NMR** (300 MHz, $CDCl_3$) δ 7.38-7.43 (m, 1H), 7.46 (app t, *J* = 7.8 Hz, 1H), 7.86-7.94 (comp, 3H), 8.30 (dd, *J* = 7.8 Hz, 1.5 Hz, 1H), 8.63 (dt, *J* = 4.8 Hz, 1.2 Hz, 1H), 8.73 (s, 1H); **^{13}C NMR** (150 MHz, $CDCl_3$) δ 121.4, 123.8, 123.8, 126.1, 127.7, 132.0, 135.1, 138.2, 144.3, 145.7, 149.3, 149.4, 159.8; **HRMS** (ESI, m/z) calcd for $C_{13}H_8ClN_3O$ $[M + H]^+$ 258.0434, found 258.0443.

7-nitro-3-(pyridin-2-yl)quinazolin-4(3*H*)-one (1i):

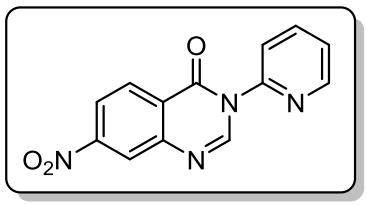

Yield 55%; yellow solid; **R_f** 0.30 (pet ether/ethyl acetate = 1:1); **eluent composition** petroleum ether/ethyl acetate = 4:1; **mp** 184-186 ^oC; **^{1}H NMR** (300 MHz, $CDCl_3$) δ 7.43-7.47 (m, 1H), 7.90-7.98 (comp, 2H), 8.32 (dd, *J* = 8.7 Hz, 2.1 Hz, 1H), 8.56 (d, *J* = 8.7 Hz, 1H), 8.62 (d, *J* = 2.4 Hz, 1H), 8.66 (dt, *J* = 4.8 Hz, 1.2 Hz, 1H), 8.76 (s, 1H); **^{13}C NMR** (150 MHz, $CDCl_3$) δ 121.3, 121.4, 123.3, 124.1, 126.5, 129.2, 138.4, 147.0, 148.3, 149.0, 149.4, 151.8, 159.3; **HRMS** (EI, m/z) calcd for $C_{13}H_8N_4O_3$ $[M^+]$ 268.0596, found 268.0590.

7-(benzyloxy)-6-methoxy-3-(pyridin-2-yl)quinazolin-4(3*H*)-one (1j):

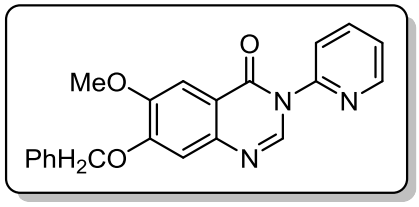

Yield 84%; colourless solid; **R$_f$** 0.15 (pet ether/ethyl acetate = 1:1); **eluent composition** petroleum ether/ethyl acetate = 7:3; **mp** 128-130 ^oC; **^{1}H NMR** (300 MHz, $CDCl_3$) δ 4.04 (s, 3H), 5.32 (s, 2H), 7.23 (s, 1H), 7.34-7.44 (comp, 4H), 7.49-7.52 (comp, 2H), 7.73 (s, 1H), 7.90-7.92 (comp, 2H), 8.54 (s, 1H), 8.63 (dt, *J* = 4.8 Hz, 1.5 Hz, 1 H); **^{13}C NMR** (75 MHz, $CDCl_3$) δ 56.4, 70.9, 106.3, 109.7, 115.5, 121.6, 123.4, 127.4, 128.2, 128.7, 135.7, 138.0, 143.7, 143.7, 149.1, 149.8, 149.9, 154.2, 159.8; **HRMS** (ESI, m/z) calcd for $C_{21}H_{17}N_3O_3$ $[M + H]^+$ 360.1348, found 360.1350.

3-(pyrimidin-2-yl)quinazolin-4(3*H*)-one (1k):

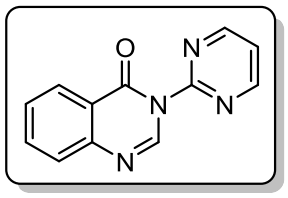

Yield 50%; yellow solid; **R$_f$** 0.07 (pet ether/ethyl acetate = 1:1); **eluent composition** petroleum ether/ethyl acetate = 1:1; **mp** 136-138 ^oC; **^{1}H NMR** (300 MHz, $CDCl_3$) δ 7.46 (app t, *J* = 4.8 Hz, 1H), 7.53-7.58 (m, 1H),7.75-7.84 (comp, 2H), 8.40 (dd, *J* = 8.1 Hz, 1.8 Hz, 1H), 8.49 (s, 1H), 8.95 (app d, *J* = 4.8 Hz, 2H); **^{13}C NMR** (150 MHz, $CDCl_3$) δ 120.7, 122.5, 127.4, 127.7, 127.9, 135.0, 144.4, 147.3, 157.3, 159.2 (x 2), 160.0; **HRMS** (ESI, m/z) calcd for $C_{12}H_8N_4O$ $[M + H]^+$ 225.0776, found 225.0774.

6-methyl-5-propyl-3-(pyridin-2-yl)pyrimidin-4(3*H*)-one (1l):

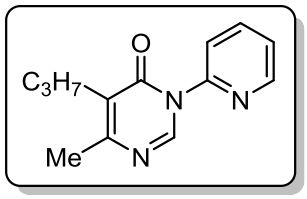

Yield 84%; colourless solid; **R$_f$** 0.20 (pet ether/ethyl acetate = 1:1); **eluent composition** petroleum ether/ethyl acetate = 7:3; **mp** 58-60 ^oC; **^{1}H NMR** (300 MHz, $CDCl_3$) δ 1.02 (t, *J* = 7.2 Hz, 3H), 1.53-1.63 (comp, 2H), 2.39 (s, 3H), 2.56-2.61 (comp, 2H), 7.35-7.43 (m, 1H), 7.85-7.92 (comp, 2H), 8.48 (s, 1H), 8.61 (dt, *J* = 5.1 Hz, 1.5 Hz, 1H); **^{13}C NMR** (75 MHz, $CDCl_3$) δ 14.2, 21.4, 21.4, 28.2, 121.5, 123.7, 125.6, 137.9, 145.5, 149.1, 149.6, 158.7, 160.7; **HRMS** (ESI, m/z) calcd for $C_{13}H_{15}N_3O$ $[M + H]^+$ 230.1293, found 230.1296.

Characterization Data for the Sulfenylated Products

2-(phenylthio)-3-(pyridin-2-yl)quinazolin-4(3*H*)-one (3aa):

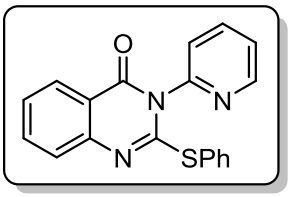

Yield 74% (48.8 mg); colourless solid; **R_f** 0.40 (pet ether/ethyl acetate = 1:1); **eluent composition** petroleum ether/ethyl acetate = 9:1; **mp** 122-126 ^oC; **^{1}H NMR** (300 MHz, $CDCl_3$) δ 7.35-7.39 (comp, 2H), 7.41-7.47 (comp, 3H), 7.52-7.59 (comp, 4H), 7.65 (td, *J* = 7.8 Hz, 1.8 Hz, 1H), 8.00 (td, *J* = 7.8 Hz, 1.8 Hz, 1H), 8.23 (dd, *J* = 7.8 Hz, 1.5 Hz, 1H), 8.79 (dd, *J* = 5.7 Hz, 1.8 Hz, 1H); **^{13}C NMR** (150 MHz, $CDCl_3$) δ 120.0, 124.7, 125.0, 126.1, 126.8, 127.0, 128.1, 129.0, 129.6, 134.6, 135.6, 138.8, 147.7, 149.8, 150.2, 155.5, 161.9; **HRMS** (ESI, m/z) calcd for $C_{19}H_{13}N_3OS$ $[M + H]^+$ 332.0858, found 332.0862.

2-((3-fluorophenyl)thio)-3-(pyridin-2-yl)quinazolin-4(3*H*)-one (3ab):

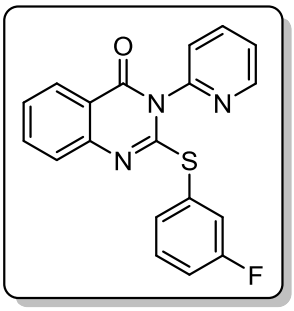

Yield 71% (49.5 mg); colourless solid; **R_f** 0.45 (pet ether/ethyl acetate = 1:1); **eluent composition** petroleum ether/ethyl acetate = 9:1; **mp** 130-134 ^oC; **^{1}H NMR** (300 MHz, $CDCl_3$) δ 7.12-7.18 (m, 1H), 7.31-7.35 (comp, 2H), 7.37-7.42 (comp, 3H), 7.51-7.55 (comp, 2H), 7.64-7.69 (m, 1H), 7.99 (td, *J* = 7.8 Hz, 1.8 Hz, 1H), 8.23 (dd, *J* = 8.4 Hz, 1.8 Hz, 1H), 8.77 (dd, *J* = 5.4 Hz, 1.8 Hz, 1H); **^{13}C NMR** (75 MHz, $CDCl_3$) δ 116.8 (d, $^2J_{F\text{-}C}$ = 21.0 Hz), 120.0, 122.5 (d, $^2J_{F\text{-}C}$ = 22.5 Hz), 124.7, 125.1, 126.4, 126.8, 127.0, 129.9 (d, $^3J_{F\text{-}C}$ = 8.25 Hz), 130.2 (d, $^3J_{F\text{-}C}$ = 7.5 Hz), 131.2 (d, $^4J_{F\text{-}C}$ = 3.0 Hz), 134.8, 138.9, 147.5, 149.6, 150.2, 154.7, 161.8, 162.4 (d, $^1J_{F\text{-}C}$ = 246.75 Hz); **HRMS** (EI, m/z) calcd for $C_{19}H_{18}ClN_3OS$ $[M^+]$ 349.0685, found 349.0684.

2-((4-chlorophenyl)thio)-3-(pyridin-2-yl)quinazolin-4(3*H*)-one (3ac):

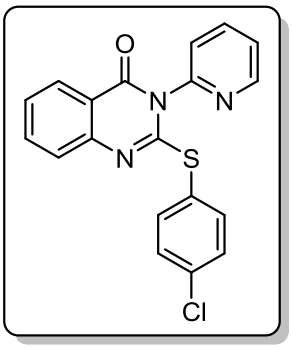

Yield 75% (55.2 mg); colourless solid; **R_f** 0.45 (pet ether/ethyl acetate = 1:1); **eluent composition** petroleum ether/ethyl acetate = 9:1; **mp** 90-94 ^oC; **^{1}H NMR** (300 MHz, $CDCl_3$) δ 7.37-7.43 (comp, 4H), 7.49-7.57 (comp, 4H), 7.68 (td, *J* = 7.8 Hz, 1.8 Hz, 1H), 8.01 (td, *J* = 7.8 Hz, 1.8 Hz, 1H), 8.24 (dd, *J* = 7.8 Hz, 1.5 Hz, 1H), 8.78 (dd, *J* = 4.8 Hz, 1.8 Hz, 1H); **^{13}C NMR** (150 MHz, $CDCl_3$) δ 120.0, 124.7, 125.2, 126.4, 126.6, 126.8, 127.1, 129.3, 134.8, 136.1, 137.0, 139.0, 147.6, 149.6, 150.2, 155.0, 161.8; **HRMS** (ESI, m/z) calcd for $[M + Na]^+$ 388.0287, found 388.0294.

2-((4-nitrophenyl)thio)-3-(pyridin-2-yl)quinazolin-4(3*H*)-one (3ad):

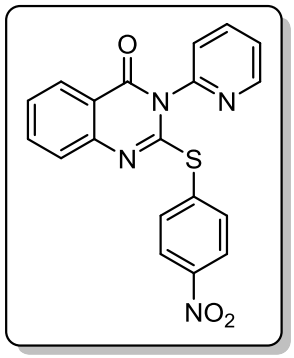

Yield 57% (43.2 mg); pale yellow solid; **R_f** 0.35 (pet ether/ethyl acetate = 1:1); **eluent composition** petroleum ether/ethyl acetate = 4:1; **mp** 122-124 ^oC; **^{1}H NMR** (300 MHz, $CDCl_3$) δ 7.38 (app d, *J* = 8.4 Hz, 1H), 7.44 (app t, *J* = 7.8 Hz, 1H), 7.54-7.58 (comp, 2H), 7.66-7.72 (m, 1H), 7.76 (app d, *J* = 8.7 Hz, 2H), 8.02 (td, *J* = 7.8 Hz, 1.8 Hz, 1H), 8.23-8.28 (comp, 3H), 8.78 (dd, *J* = 5.4 Hz, 1.8 Hz, 1H); **^{13}C NMR** (150 MHz, $CDCl_3$) δ 120.1, 123.8, 124.7, 125.3, 126.7, 126.8, 127.2, 135.0, 135.8, 136.9, 139.0, 147.3, 148.2, 149.4, 150.2, 153.5, 161.6; **HRMS** (EI, m/z) calcd for $C_{19}H_{12}N_4O_3S$ [M^+] 376.0630, found 376.0632.

2-(benzylthio)-3-(pyridin-2-yl)quinazolin-4(3*H*)-one (3ae):

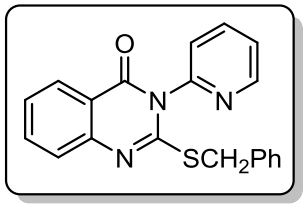

Yield 79% (54.9 mg); colourless solid; **R_f** 0.45 (pet ether/ethyl acetate = 1:1); **eluent composition** petroleum ether/ethyl acetate = 9:1; **mp** 128-130 ^oC; **^{1}H NMR** (300 MHz, $CDCl_3$) δ 4.47 (s, 2 H),7.23-7.31 (comp, 3H), 7.36-7.43 (comp, 4H), 7.44-7.47 (m, 1H), 7.68 (dd, *J* = 8.4 Hz, 1.2 Hz, 1H), 7.73-7.79 (m, 1H), 7.91 (td, *J* = 7.8 Hz, 1.8 Hz, 1H), 8.24 (dd, *J* = 8.1 Hz, 1.5 Hz, 1H), 8.69 (dd, *J* = 5.1 Hz, 1.8 Hz, 1H); **^{13}C NMR** (75 MHz, $CDCl_3$) δ 36.9, 120.0, 124.6, 125.0, 126.0, 126.3, 127.2, 127.5, 128.5, 129.4, 134.8, 136.0, 138.8, 147.7, 149.5, 150.2, 155.6, 161.8; **HRMS** (EI, m/z) calcd for $C_{20}H_{15}N_3OS$ [M^+] 345.0936, found 345.0940.

2-(cyclohexylthio)-3-(pyridin-2-yl)quinazolin-4(3*H*)-one (3af):

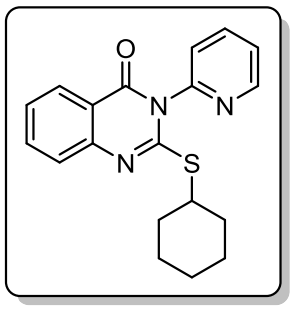

Yield 82% (55.4 mg); colourless solid; **R_f** 0.50 (pet ether/ethyl acetate = 1:1); **eluent composition** petroleum ether/ethyl acetate = 9:1; **mp** 122-124 ^oC; **^{1}H NMR** (300 MHz, $CDCl_3$) δ 1.37-1.55 (comp, 5H), 1.60-1.68 (m, 1H), 1.71-1.79 (comp, 2H), 2.09-2.16 (comp, 2H), 3.95-4.04 (m, 1H), 7.38-7.44 (comp, 2H), 7.49 (dd, *J* = 7.8 Hz, 4.8 Hz, 1H), 7.62 (d, *J* = 8.1 Hz, 1H), 7.74 (td, *J* = 8.1 Hz, 1.5 Hz, 1H), 7.95 (td, *J* = 7.8 Hz, 1.8 Hz, 1H), 8.24 (dd, *J* = 8.1 Hz, 1.5 Hz, 1H), 8.74 (dd, *J* = 5.1 Hz, 1.8 Hz, 1H); **^{13}C NMR** (150 MHz, $CDCl_3$) δ 25.7, 26.1, 32.7, 45.7, 119.9, 124.7, 124.8, 125.8, 126.4, 127.1, 134.7, 138.8, 148.0, 149.9, 150.2, 155.8, 162.0; **HRMS** (ESI, m/z) calcd for $C_{19}H_{19}N_3OS$ [M + Na]$^+$ 360.1147, found 360.1154.

2-(butylthio)-3-(pyridin-2-yl)quinazolin-4(3*H*)-one (3ag):

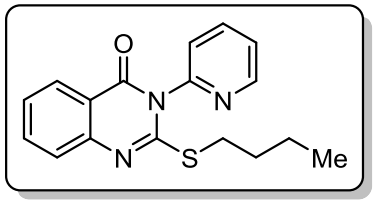

Yield 80% (49.8 mg); colourless solid; **R_f** 0.50 (pet ether/ethyl acetate = 1:1); **eluent composition** petroleum ether/ethyl acetate = 9:1; **mp** 152-154 °C; **^{1}H NMR** (300 MHz, $CDCl_3$) δ 0.93 (t, *J* = 7.2 Hz, 3H), 1.36-1.48 (comp, 2H), 1.63-1.73 (comp, 2H), 3.21 (t, *J* = 7.2 Hz, 2H), 7.36-7.44 (comp, 2H), 7.46-7.50 (m, 1H), 7.61 (dd, *J* = 8.1 Hz, 1.2 Hz, 1H), 7.70-7.76 (m, 1H), 7.94 (td, *J* = 7.8 Hz, 1.8 Hz, 1H), 8.23 (dd, *J* = 8.4 Hz, 1.8 Hz, 1H), 8.72 (dd, *J* = 4.8 Hz, 1.8 Hz, 1H); **^{13}C NMR** (150 MHz, $CDCl_3$) δ 13.7, 22.0, 30.7, 32.1, 119.9, 124.7, 124.9, 125.8, 126.3, 127.2, 134.8, 138.8, 147.9, 149.8, 150.2, 156.1, 161.9; **HRMS** (ESI, m/z) calcd for $C_{17}H_{17}N_3OS$ $[M + Na]^+$ 334.0990, found 334.0977.

2-(propylthio)-3-(pyridin-2-yl)quinazolin-4(3*H*)-one (3ah):

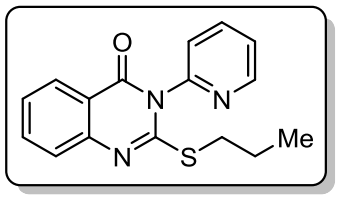

Yield 61% (36.2 mg); brown oil; **R_f** 0.35 (pet ether/ethyl acetate = 1:1); **eluent composition** petroleum ether/ethyl acetate = 4:1; **^{1}H NMR** (600 MHz, $CDCl_3$) δ 1.03 (t, *J* = 7.2 Hz, 3H), 1.72-1.78 (comp, 2H), 3.21 (t, *J* = 7.2 Hz, 2H), 7.42 (td, *J* = 7.2 Hz, 1.2 Hz, 1H), 7.46 (d, *J* = 7.8 Hz, 1H), 7.50-7.52 (m, 1H), 7.64 (dd, *J* = 8.4 Hz, 1.2 Hz, 1H), 7.74-7.77 (m, 1H), 7.97 (td, *J* = 7.8 Hz, 1.8 Hz, 1H), 8.26 (dd, *J* = 7.8 Hz, 1.8 Hz, 1H), 8.74-8.75 (m, 1H); **^{13}C NMR** (150 MHz, $CDCl_3$) δ 13.6, 22.1, 34.3, 119.9, 124.7, 125.0, 125.9, 126.4, 127.2, 134.8, 138.8, 147.9, 149.8, 150.2, 156.1, 162.0; **HRMS** (ESI, m/z) calcd for $C_{16}H_{15}N_3OS$ $[M + Na]^+$ 320.0834, found 320.0831.

6-methyl-2-(phenylthio)-3-(pyridin-2-yl)quinazolin-4(3*H*)-one (3ba):

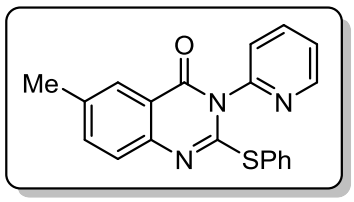

Yield 44% (30.4 mg); colourless solid; **R_f** 0.40 (pet ether/ethyl acetate = 1:1); **eluent composition** petroleum ether/ethyl acetate = 9:1; **mp** 148-150 °C; **^{1}H NMR** (300 MHz, $CDCl_3$) δ 2.43 (s, 3H), 7.26 (d, *J* = 8.4 Hz, 1H), 7.37-7.47 (comp, 4H), 7.49-7.57 (comp, 4H), 7.96 (dd, *J* = 7.8 Hz, 1.8 Hz, 1H), 8.00 (app t, *J* = 1.8 Hz, 1H), 8.77 (dd, *J* = 5.4 Hz, 1.8 Hz, 1H); **^{13}C NMR** (75 MHz, $CDCl_3$) δ 21.2, 119.6, 124.7, 124.9, 126.3, 126.6, 128.2, 129.0, 129.5, 135.5, 136.0, 136.2, 138.8, 145.7, 149.8, 150.1, 154.3, 161.9; **HRMS** (EI, m/z) calcd for $C_{20}H_{15}N_3OS$ $[M^+]$ 345.0936, found 345.0935.

8-methyl-2-(phenylthio)-3-(pyridin-2-yl)quinazolin-4(3*H*)-one (3ca):

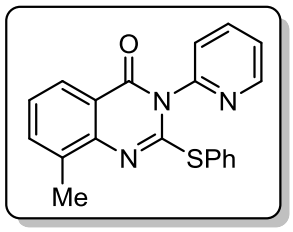

Yield 96% (66.2 mg); colourless solid; **R_f** 0.40 (pet ether/ethyl acetate = 1:1); **eluent composition** petroleum ether/ethyl acetate = 9:1; **mp** 136-138 ^oC (crystallization from DCM and hexane); **^{1}H NMR** (600 MHz, $CDCl_3$) δ 2.14 (s, 3H), 7.28 (d, *J* = 8.4 Hz, 1H), 7.43-7.48 (comp, 3H), 7.50 (d, *J* = 7.8 Hz, 1H), 7.54-7.56 (comp, 2H), 7.62 (app d, *J* = 7.2 Hz, 2H), 8.02 (app t, *J* = 7.8 Hz, 1H), 8.08 (d, *J* = 8.4 Hz, 1H), 8.80 (d, *J* = 4.8 Hz, 1H); **^{13}C NMR** (150 MHz, $CDCl_3$) δ 16.6, 119.8, 124.6, 124.7, 125.0, 125.7, 128.4, 128.9, 129.7, 135.2, 135.3, 136.1, 138.9, 146.1, 149.8, 150.2, 154.5, 162.3; **HRMS** (EI, m/z) calcd for $C_{20}H_{15}N_3OS$ [M^+] 345.0936, found 345.0935.

Crystal data and structure refinement for 3ca, CCDC No. 1888207

Empirical formula	$C_{20}H_{15}N_3OS$
Formula weight	345.41
Temperature/K	296.15
Crystal system	Monoclinic
Space group	$P2_1/c$
a/Å	10.4213(12)
b/Å	14.9525(18)
c/Å	11.3162(14)
α/°	90
β/°	104.032(2)
γ/°	90
Volume/Å^3	1710.7(4)
Z	4
ρ_{calc}g/cm^3	1.341
μ/mm^{-1}	0.202
F(000)	720.0
Crystal size/mm^3	0.45 × 0.28 × 0.13
Radiation	Mo Kα (λ = 0.71073)
2Θ range for data collection/°	4.602 to 49.992
Index ranges	$-12 \le h \le 12$, $-17 \le k \le 17$, $-10 \le l \le 13$
Reflections collected	8174
Independent reflections	2995 [R_{int} = 0.0480, R_{sigma} = 0.0522]
Data/restraints/parameters	2995/0/227
Goodness-of-fit on F^2	1.037
Final R indexes [I>=2σ (I)]	R_1 = 0.0424, wR_2 = 0.1011
Final R indexes [all data]	R_1 = 0.0571, wR_2 = 0.1126
Largest diff. peak/hole / e Å^{-3}	0.24/-0.27

7,8-dimethyl-2-(phenylthio)-3-(pyridin-2-yl)quinazolin-4(3*H*)-one (3da):

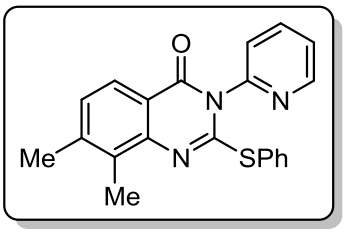

Yield 90% (65.2 mg); pale yellow solid; **R_f** 0.35 (pet ether/ethyl acetate = 1:1); **eluent composition** petroleum ether/ethyl acetate = 4:1; **mp** 122-124 °C; **^{1}H NMR** (300 MHz, $CDCl_3$) δ 2.04 (s, 3H), 2.32 (s, 3H), 7.16 (d, *J* = 8.1 Hz, 1H), 7.40-7.46 (comp, 3H), 7.49-7.54 (comp, 2H), 7.58-7.61 (comp, 2H), 7.95-8.01 (comp, 2H), 8.77 (dd, *J* = 5.1 Hz, 1.8 Hz, 1H); **^{13}C NMR** (150 MHz, $CDCl_3$) δ 12.4, 20.9, 117.7, 123.9, 124.8, 125.0, 128.1, 128.5, 129.0, 129.6, 133.1, 136.2, 138.9, 143.9, 145.8, 149.9, 150.1, 154.2, 162.4; **HRMS** (ESI, m/z) calcd for $C_{21}H_{17}N_3OS$ $[M + Na]^+$ 382.0990, found 382.0998.

7-methoxy-2-(phenylthio)-3-(pyridin-2-yl)quinazolin-4(3*H*)-one (3ea):

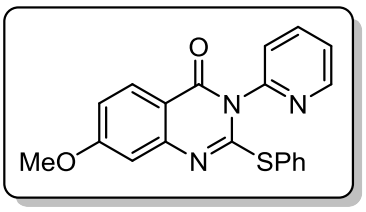

Yield 62% (44.7 mg); pale yellow solid; **R_f** 0.32 (pet ether/ethyl acetate = 1:1); **eluent composition** petroleum ether/ethyl acetate = 4:1; **mp** 170-172 °C; **^{1}H NMR** (300 MHz, $CDCl_3$) δ 3.84 (s, 3H), 6.72 (d, *J* = 2.4 Hz, 1H), 6.94 (dd, *J* = 9.0 Hz, 2.4 Hz, 1H), 7.42-7.45 (comp, 3H), 7.49-7.58 (comp, 4H), 7.98 (td, *J* = 7.8 Hz, 2.1 Hz, 1H), 8.11 (d, *J* = 8.7 Hz, 1H), 8.75-8.78 (m, 1H); **^{13}C NMR** (75 MHz, $CDCl_3$) δ 55.6, 107.7, 113.4, 116.1, 124.8, 125.0, 128.2, 128.6, 129.1, 129.6, 135.6, 138.8, 149.8, 149.9, 150.1, 156.2, 161.4, 164.9; **HRMS** (EI, m/z) calcd for $C_{20}H_{15}N_3O_2S$ $[M^+]$ 361.0885, found 361.0873.

6,7-dimethoxy-2-(phenylthio)-3-(pyridin-2-yl)quinazolin-4(3*H*)-one (3fa):

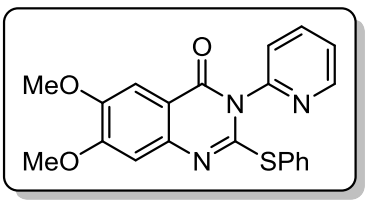

Yield 79% (51.5 mg); colourless solid; **R_f** 0.15 (pet ether/ethyl acetate = 1:1); **eluent composition** petroleum ether/ethyl acetate = 7:3; **mp** 130-132 °C; **^{1}H NMR** (300 MHz, $CDCl_3$) δ 3.94 (s, 3H), 3.97 (s, 3H), 6.78 (s, 1H), 7.42-7.47 (comp, 3H), 7.52-7.59 (comp, 5H), 8.00 (td, *J* = 7.8 Hz, 1.8 Hz, 1H), 8.78 (dd, *J* = 5.4 Hz, 1.8 Hz, 1H); **^{13}C NMR** (150 MHz, $CDCl_3$) δ 56.3, 56.3, 105.9, 107.6, 113.1, 124.8, 125.0, 128.4, 129.2, 129.5, 135.5, 138.8, 144.2, 148.5, 150.0, 150.1, 153.9, 155.1, 161.4; **HRMS** (EI, m/z) calcd for $C_{21}H_{17}ClN_3O_3S$ $[M^+]$ 391.0991, found 391.0997.

7-fluoro-2-(phenylthio)-3-(pyridin-2-yl)quinazolin-4(3*H*)-one (3ga):

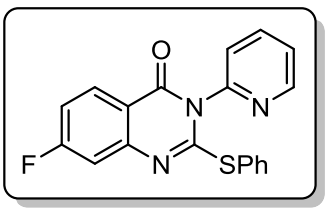

Yield 73% (51.1 mg); colourless solid; **R_f** 0.40 (pet ether/ethyl acetate = 1:1); **eluent composition** petroleum ether/ethyl acetate = 9:1; **mp** 134-136 °C; **^{1}H NMR** (600 MHz, $CDCl_3$) δ 7.01 (dd, *J* = 9.6 Hz, 2.4 Hz, 1H), 7.10 (td, *J* = 8.4 Hz, 2.4 Hz, 1H), 7.44-7.46

(comp, 2H), 7.47-7.50 (m, 1H), 7.55-7.58 (comp, 4H), 8.02 (td, *J* = 7.8 Hz, 1.8 Hz, 1H), 8.24 (dd, *J* = 8.4 Hz, 6.0 Hz, 1H), 8.80 (dd, *J* = 5.4 Hz, 1.8 Hz, 1H); **^{13}C NMR** (150 MHz, $CDCl_3$) δ 112.2 (d, $^2J_{F-C}$ = 22.5 Hz), 114.8 (d, $^2J_{F-C}$ = 24.0 Hz), 116.6 (d, $^4J_{F-C}$ = 3.0 Hz), 124.7, 125.2, 127.7, 129.2, 129.8 (d, $^3J_{F-C}$ = 10.5 Hz), 129.9, 135.8, 139.0, 149.5, 149.8 (d, $^3J_{F-C}$ = 13.5 Hz), 150.3, 157.5, 161.2, 166.8 (d, $^1J_{F-C}$ = 253.5 Hz); **HRMS** (ESI, m/z) calcd for $C_{19}H_{12}FN_3OS$ $[M + H]^+$ 370.0763, found 370.0767.

8-chloro-2-(phenylthio)-3-(pyridin-2-yl)quinazolin-4(3*H*)-one (3ha):

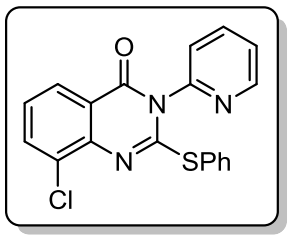

Yield 87% (64.0 mg); brown solid; **R_f** 0.40 (pet ether/ethyl acetate = 1:1); **eluent composition** petroleum ether/ethyl acetate = 9:1; **mp** 162-164 °C; **^{1}H NMR** (600 MHz, $CDCl_3$) δ 7.29 (app t, *J* = 7.8 Hz, 1H), 7.45-7.50 (comp, 3H), 7.54 (app d, *J* = 7.8 Hz, 1 H), 7.56-7.58 (m, 1H), 7.65-7.66 (comp, 2H), 7.73 (dd, *J* = 7.8 Hz, 1.8 Hz, 1H), 8.03 (td, *J* = 7.8 Hz, 1.8 Hz, 1H), 8.14 (dd, *J* = 7.8 Hz, 1.2 Hz, 1H), 8.14 (dd, *J* = 4.8 Hz, 2.4 Hz, 1H); **^{13}C NMR** (150 MHz, $CDCl_3$) δ 121.4, 124.6, 125.3, 125.8, 126.1, 127.6, 129.0, 129.8, 131.2, 135.0, 135.8,139.0, 144.3, 149.4, 150.4, 157.2, 161.4; **HRMS** (ESI, m/z) calcd for $C_{19}H_{12}ClN_3OS$ $[M + H]^+$ 366.0468, found 366.0469.

7-nitro-2-(phenylthio)-3-(pyridin-2-yl)quinazolin-4(3*H*)-one (3ia):

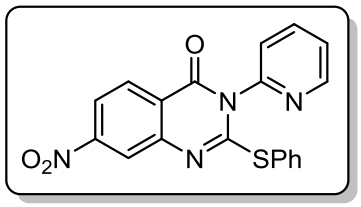

Yield 86% (65.0 mg); pale yellow solid; **R_f** 0.30 (pet ether/ethyl acetate = 1:1); **eluent composition** petroleum ether/ethyl acetate = 4:1; **mp** 182-184 °C (crystallization from DCM and hexane); **^{1}H NMR** (300 MHz, $CDCl_3$) δ 7.44-7.52 (comp, 3H), 7.54-7.60 (comp, 4H), 8.04 (td, *J* = 7.8 Hz, 1.8 Hz, 1H), 8.12 (dd, *J* = 8.4 Hz, 2.4 Hz, 1H), 8.15 (d, *J* = 2.1 Hz, 1H),8.37 (d, *J* = 8.4 Hz, 1H), 8.80 (dd, *J* = 5.1 Hz, 1.8 Hz, 1H); **^{13}C NMR** (150 MHz, $CDCl_3$) δ 119.6, 122.3, 124.1, 124.5, 125.5, 127.0, 128.9, 129.4, 130.3, 135.9, 139.2, 148.2, 149.0, 150.5, 151.8, 159.3, 160.6; **HRMS** (ESI, m/z) calcd for $C_{19}H_{12}N_4O_3S$ $[M + H]^+$ 377.0708, found 377.0695.

Crystal data and structure refinement for 3ia, CCDC No. 1888348

Empirical formula	$C_{19}H_{12}N_4O_3S$
Formula weight	376.39
Temperature/K	296.15
Crystal system	Monoclinic
Space group	C2/c
a/Å	23.0252(11)
b/Å	12.5983(6)

c/Å	13.4670(7)
α/°	90
β/°	118.554(2)
γ/°	90
Volume/Å^3	3431.3(3)
Z	8
ρ_{calc}g/cm^3	1.457
μ/mm^{-1}	0.218
F(000)	1552.0
Crystal size/mm^3	0.31 × 0.14 × 0.13
Radiation	Mo Kα (λ = 0.71073)
2Θ range for data collection/°	4.028 to 55.06
Index ranges	-29 ≤ h ≤ 29, -16 ≤ k ≤ 16, -17 ≤ l ≤ 17
Reflections collected	32629
Independent reflections	3945 [R_{int} = 0.0412, R_{sigma} = 0.0231]
Data/restraints/parameters	3945/228/245
Goodness-of-fit on F^2	1.059
Final R indexes [I>=2σ (I)]	R_1 = 0.0421, wR_2 = 0.1157
Final R indexes [all data]	R_1 = 0.0573, wR_2 = 0.1366
Largest diff. peak/hole / e Å^{-3}	0.38/-0.33

7-(benzyloxy)-6-methoxy-2-(phenylthio)-3-(pyridin-2-yl)quinazolin-4(3*H*)-one (3ja):

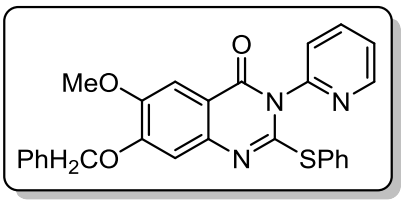

Yield 92% (86.0 mg); brown solid; **R$_f$** 0.40 (pet ether/ethyl acetate = 1:1); **eluent composition** petroleum ether/ethyl acetate = 9:1; **mp** 178-180 ^{o}C; **^{1}H NMR** (300 MHz, $CDCl_3$) δ 3.96 (s, 3H), 5.15 (s, 2H), 6.87 (s, 1H), 7.34-7.41 (comp, 3H), 7.42-7.47 (comp, 5H), 7.51 (s, 1H), 7.53-7.57 (comp, 4H), 7.99 (td, *J* = 7.8 Hz, 1.8 Hz, 1H), 8.78 (dt, *J* = 4.2 Hz, 1.2 Hz, 1H); **^{13}C NMR** (75 MHz, $CDCl_3$) δ 56.2, 70.8, 106.2, 108.9, 113.2, 124.7, 124.9, 127.6, 128.2, 128.5, 128.6, 129.1, 129.4, 135.4, 135.8, 138.7, 144.0, 148.8, 150.0, 150.0, 153.6, 154.3, 161.4; **HRMS** (ESI, m/z) calcd for $C_{27}H_{21}N_3O_3S$ $[M + H]^+$ 468.1382, found 468.1375.

7-(benzyloxy)-2-((3-fluorophenyl)thio)-6-methoxy-3-(pyridin-2-yl)quinazolin-4(3*H*)-one (3jb):

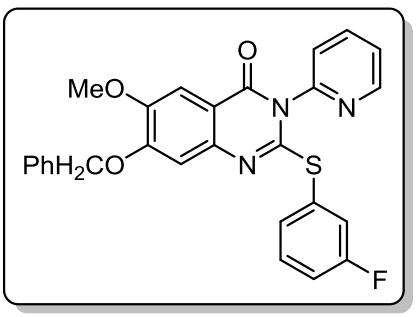

Yield 58% (56.6 mg); colourless solid; **R$_f$** 0.20 (pet ether/ethyl acetate = 1:1); **eluent composition** petroleum ether/ethyl acetate = 7:3; **mp** 158-160 ^{o}C; **^{1}H NMR** (300 MHz, $CDCl_3$) δ 3.94 (s, 3H), 5.15 (s, 2H), 6.88 (s, 1H), 7.10-7.16 (m, 1H), 7.29-7.35 (comp, 4H), 7.38-7.46 (comp, 4H), 7.48-7.52 (comp, 2H), 7.56 (s, 1H), 7.96 (td, *J* = 7.8

Hz, 1.8 Hz, 1H), 8.74 (dd, *J* = 5.4 Hz, 1.8 Hz, 1H); **^{13}C NMR** (75 MHz, $CDCl_3$) δ 56.3, 70.9, 106.2, 109.0, 113.3, 116.7 (d, $^2J_{F-C}$ = 21.0 Hz), 122.2 (d, $^2J_{F-C}$ = 22.5 Hz), 124.7, 125.0, 127.7, 128.2, 128.6, 130.2 (d, $^3J_{F-C}$ = 8.25 Hz), 130.4 (d, $^3J_{F-C}$ = 8.25 Hz), 130.8 (d, $^4J_{F-C}$ = 3.0 Hz), 135.7, 138.8, 143.9, 149.0, 149.9, 150.1, 152.8, 154.4, 161.3, 162.4 (d, $^1J_{F-C}$ = 246.75 Hz); **HRMS** (ESI, m/z) calcd for $C_{27}H_{20}FN_3O_3S$ $[M + H]^+$ 486.1288, found 486.1297.

7-(benzyloxy)-2-((4-chlorophenyl)thio)-6-methoxy-3-(pyridin-2-yl)quinazolin-4(3*H*)-one (3jc):

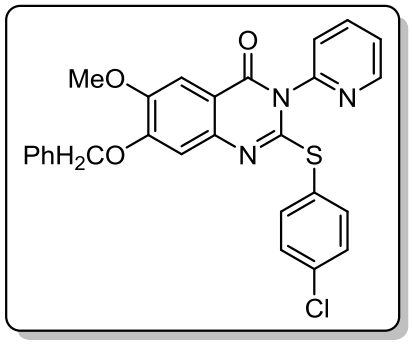

Yield 97% (97.2 mg); colourless solid; **R_f** 0.20 (pet ether/ethyl acetate = 1:1); **eluent composition** petroleum ether/ethyl acetate = 7:3; **mp** 164-166 °C; **^{1}H NMR** (300 MHz, $CDCl_3$) δ 3.94 (s, 3H), 5.16 (s, 2H), 6.85 (s, 1H), 7.33-7.38 (comp, 2H), 7.39-7.47 (comp, 6H), 7.48-7.51 (comp, 2H), 7.52-7.55 (comp, 2H), 7.97 (td, *J* = 7.8 Hz, 1.8 Hz, 1H), 8.75 (dt, *J* = 4.2 Hz, 1.5 Hz, 1H); **^{13}C NMR** (75 MHz, $CDCl_3$) δ 56.3, 70.9, 106.2, 108.9, 113.2, 124.7, 125.0, 126.9, 127.6, 128.2, 128.6, 129.3, 135.8, 135.8, 136.8, 138.8, 143.9, 149.0, 149.9, 150.1, 153.2, 154.4, 161.3; **HRMS** (ESI, m/z) calcd for $C_{27}H_{20}ClN_3O_3S$ $[M + H]^+$ 502.0992, found 502.0990.

7-(benzyloxy)-6-methoxy-2-((4-nitrophenyl)thio)-3-(pyridin-2-yl)quinazolin-4(3*H*)-one (3jd):

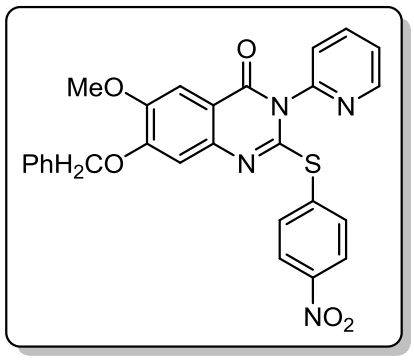

Yield 83% (85.1 mg); pale yellow solid; **R_f** 0.18 (pet ether/ethyl acetate = 1:1); **eluent composition** petroleum ether/ethyl acetate = 7:3; **mp** 178-180 °C; **^{1}H NMR** (300 MHz, $CDCl_3$) δ 3.96 (s, 3H), 5.17 (s, 2H), 6.84 (s, 1H), 7.31-7.45 (comp, 5H), 7.51-7.57 (comp, 3H), 7.69-7.73 (comp, 2H), 7.99 (td, *J* = 7.8 Hz, 2.1 Hz, 1H), 8.22-8.25 (comp, 2H), 8.75 (app d, *J* = 4.8 Hz, 1H); **^{13}C NMR** (75 MHz, $CDCl_3$) δ 56.3, 70.9, 106.2, 108.8, 113.4, 123.8, 124.5, 125.1, 127.5, 128.2, 128.6, 135.2, 135.6, 137.4, 138.8, 143.5, 148.0, 149.3, 149.6, 150.0, 151.5, 154.5, 161.0; **HRMS** (ESI, m/z) calcd for $C_{27}H_{20}N_4O_5S$ $[M + H]^+$ 513.1233, found 513.1230.

7-(benzyloxy)-6-methoxy-3-(pyridin-2-yl)-2-(p-tolylthio)quinazolin-4(3*H*)-one (3ji):

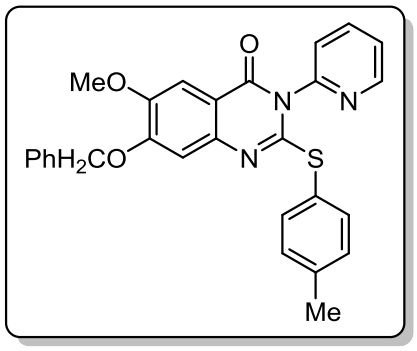

Yield 66% (63.3 mg); colourless solid; **R_f** 0.08 (pet ether/ethyl acetate = 1:1); **eluent composition** petroleum ether/ethyl acetate = 1:1; **mp** 138-140 ^oC; **^{1}H NMR** (300 MHz, $CDCl_3$) δ 2.41 (s, 3H), 3.93 (s, 3H), 5.13 (s, 2H), 6.87 (s, 1H), 7.22 (d, *J* = 7.8 Hz, 2H), 7.30-7.46 (comp, 7H), 7.48-7.53 (comp, 2H), 7.55 (s, 1H), 7.96 (td, *J* = 7.8 Hz, 1.8 Hz, 1H), 8.76 (dd, *J* = 5.4 Hz, 1.8 Hz, 1H); **^{13}C NMR** (75 MHz, $CDCl_3$) δ 21.4, 56.2, 70.8, 106.2, 109.0, 113.2, 124.8, 124.8, 124.9, 127.7, 128.2, 128.6, 129.9, 135.4, 135.8, 138.7, 139.7, 144.1, 148.8, 150.1 (x 2), 154.1, 154.3, 161.4; **HRMS** (ESI, m/z) calcd for $C_{28}H_{23}N_3O_3S$ $[M+H]^+$ 482.1538, found 482.1549.

2-(phenylthio)-3-(pyrimidin-2-yl)quinazolin-4(3*H*)-one (3ka):

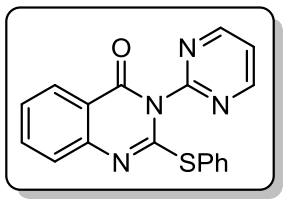

Yield 74% (48.6 mg); brown solid; **R_f** 0.30 (pet ether/ethyl acetate = 1:1); **eluent composition** petroleum ether/ethyl acetate = 4:1; **mp** 144-146 ^oC; **^{1}H NMR** (600 MHz, $CDCl_3$) δ 7.39-7.46 (comp, 5H), 7.55 (app t, *J* = 4.8 Hz, 1H), 7.59 (app d, *J* = 7.2 Hz, 2H), 7.67 (app t, *J* = 7.8 Hz, 1H), 8.25 (d, *J* = 7.8 Hz, 1H), 9.04 (app d, *J* = 5.4 Hz, 2H); **^{13}C NMR** (150 MHz, $CDCl_3$) δ 120.0, 121.7, 126.4, 126.9, 127.0, 127.8, 129.2, 129.7, 134.8, 135.6, 147.6, 154.0, 157.3, 159.8, 161.8; **HRMS** (EI, m/z) calcd for $C_{18}H_{12}N_4OS$ $[M^+]$ 332.0732, found 332.0731.

6-methyl-2-(phenylthio)-5-propyl-3-(pyridin-2-yl)pyrimidin-4(3*H*)-one (3la):

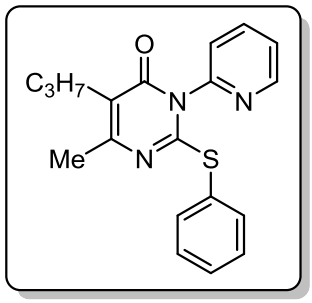

Yield 72% (48.6 mg); brown solid; **R_f** 0.45 (pet ether/ethyl acetate = 1:1); **eluent composition** petroleum ether/ethyl acetate = 9:1; **mp** 108-110 ^oC; **^{1}H NMR** (300 MHz, $CDCl_3$) δ 0.94 (t, *J* = 7.2 Hz, 3H), 1.45-1.58 (comp, 2H), 2.11 (s, 3H), 2.44 (t, *J* = 7.8 Hz, 2H), 7.34-7.41 (comp, 3H), 7.45-7.51 (comp, 4H), 7.94 (td, *J* = 7.8 Hz, 2.1 Hz, 1H), 8.73 (dd, *J* = 5.1 Hz, 1.8 Hz, 1H); **^{13}C NMR** (75 MHz, $CDCl_3$) δ 14.2, 21.5, 21.5, 28.0, 121.2, 124.2, 124.8, 128.0, 128.9, 129.5, 135.5, 138.8, 150.0, 150.1, 156.2, 158.8, 162.6; **HRMS** (ESI, m/z) calcd for $C_{19}H_{19}N_3OS$ $[M + Na]^+$ 360.1147, found 360.1153.

2-((4-chlorophenyl)thio)-6-methyl-5-propyl-3-(pyridin-2-yl)pyrimidin-4(3*H*)-one (3lc):

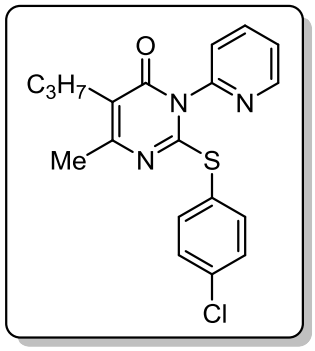

Yield 69% (51.2 mg); colourless solid; **R_f** 0.35 (pet ether/ethyl acetate = 1:1); **eluent composition** petroleum ether/ethyl acetate = 4:1; **mp** 128-130 ºC; **^{1}H NMR** (300 MHz, $CDCl_3$) δ 0.94 (t, *J* = 7.2 Hz, 3H), 1.45-1.57 (comp, 2H), 2.12 (s, 3H), 2.44 (t, *J* = 7.8 Hz, 2H), 7.33-7.37 (comp, 2H), 7.40-7.46 (comp, 3H), 7.47-7.50 (m, 1H), 7.95 (td, *J* = 7.8 Hz, 1.8 Hz, 1H), 8.72 (dd, *J* = 5.1 Hz, 1.8 Hz, 1H); **^{13}C NMR** (75 MHz, $CDCl_3$) δ 14.2, 21.4, 21.5, 28.0, 121.3, 124.2, 124.9, 126.4, 129.2, 135.9, 136.8, 138.8, 149.8, 150.1, 155.6, 158.8, 162.5; **HRMS** (EI, m/z) calcd for $C_{19}H_{18}ClN_3OS$ [M^+] 371.0859, found 371.0858.

6-methyl-2-((4-nitrophenyl)thio)-5-propyl-3-(pyridin-2-yl)pyrimidin-4(3*H*)-one (3ld):

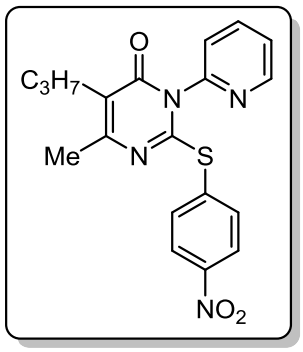

Yield 85% (64.6 mg); pale yellow solid; **R_f** 0.30 (pet ether/ethyl acetate = 1:1); **eluent composition** petroleum ether/ethyl acetate = 4:1; **mp** 136-138 ºC; **^{1}H NMR** (300 MHz, $CDCl_3$) δ 0.96 (t, *J* = 7.2 Hz, 3H), 1.49-1.56 (comp, 2H), 2.14 (s, 3H), 2.46 (t, *J* = 7.8 Hz, 2H), 7.46-7.53 (comp, 2H), 7.66-7.72 (comp, 2H), 7.97 (td, *J* = 7.8 Hz, 1.8 Hz, 1H), 8.19-8.24 (comp, 2H), 8.73 (dd, *J* = 5.4 Hz, 1.8 Hz, 1H); **^{13}C NMR** (150 MHz, $CDCl_3$) δ 14.2, 21.4, 21.5, 28.1, 122.2, 123.7, 124.2, 125.2, 135.6, 136.9, 138.9, 148.1, 149.6, 150.1, 154.2, 158.6, 162.3; **HRMS** (EI, m/z) calcd for $C_{19}H_{18}N_4O_3S$ [M^+] 382.1100, found 382.1093.

2-(cyclohexylthio)-6-methyl-5-propyl-3-(pyridin-2-yl)pyrimidin-4(3*H*)-one (3lf):

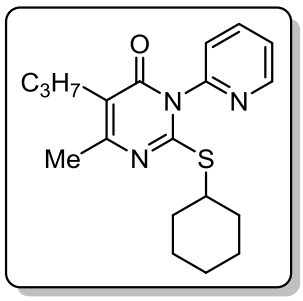

Yield 91% (64.2 mg); colourless solid; **R_f** 0.45 (pet ether/ethyl acetate = 1:1); **eluent composition** petroleum ether/ethyl acetate = 9:1; **mp** 110-112 ºC; **^{1}H NMR** (300 MHz, $CDCl_3$) δ 0.95 (t, *J* = 7.2 Hz, 3H), 1.33-1.42 (comp, 4H), 1.48-1.59 (comp, 3H), 1.66-1.72 (comp, 3H), 1.99-2.05 (comp, 2H), 2.30 (s, 3H), 2.46 (t, *J* = 7.8 Hz, 2H), 3.77-3.84 (m, 1H), 7.32 (d, *J* = 7.8 Hz, 1H), 7.39-7.43 (m, 1H), 7.87 (td, *J* = 7.8 Hz, 1.8 Hz, 1H), 8.67 (dd, *J* = 5.1 Hz, 1.8 Hz, 1H); **^{13}C NMR** (75 MHz, $CDCl_3$) δ 14.2, 21.5, 21.6, 25.6, 25.9, 27.9, 32.6, 45.4, 120.3, 124.2, 124.6, 138.6, 150.0 (x 2), 156.6, 158.5, 162.7; **HRMS** (ESI, m/z) calcd for $C_{19}H_{25}N_3OS$ [M + H]$^+$ 344.1797, found 344.1801.

3.5.5. Radical Scavenging Experiments

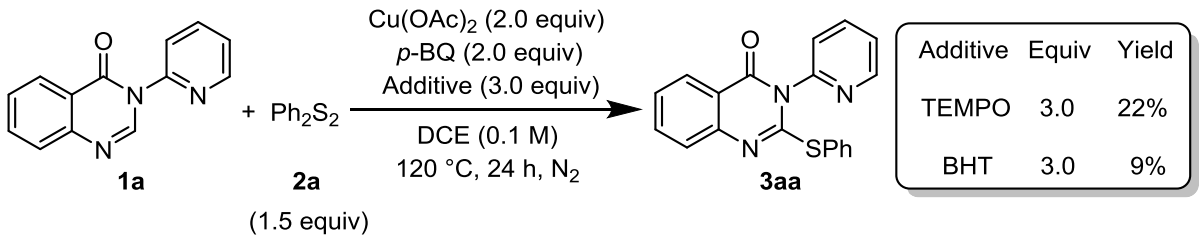

Scheme 3.5.5.1. Radical scavenging experiments.

In an oven-dried 10 mL Schlenk tube, substrate **1a** (0.1 mmol, 1.0 equiv), Ph_2S_2 (65.5 mg, 0.3 mmol, 1.5 equiv), $Cu(OAc)_2$ (36.3 mg, 0.2 mmol, 2.0 equiv), *p*-BQ (21.6 mg, 0.2 mmol, 2.0 equiv) and additive (0.3 mmol, 3.0 equiv) were added and the reaction mixture was degassed and backfilled with nitrogen. Under nitrogen, 2.0 mL (0.1 M) of anhydrous DCE was added. Then it was again degassed and backfilled with nitrogen (3 times). The tube was closed with a teflon-lined cap and kept on stirring in an oil bath. The bath temperature was slowly increased to 120 ^{o}C. After 24 h, the reaction was stopped and cooled to room temperature. The reaction mixture was filtered through a short pad of celite and concentrated under vacuo. The crude reaction mixture was directly purified by column chromatography on silica gel using petroleum ether/ethyl acetate ether as eluent.

3.6. ^{1}H and ^{13}C NMR Spectra of Representative Compounds

^{1}H NMR of **1b** (300MHz, d_6-DMSO):

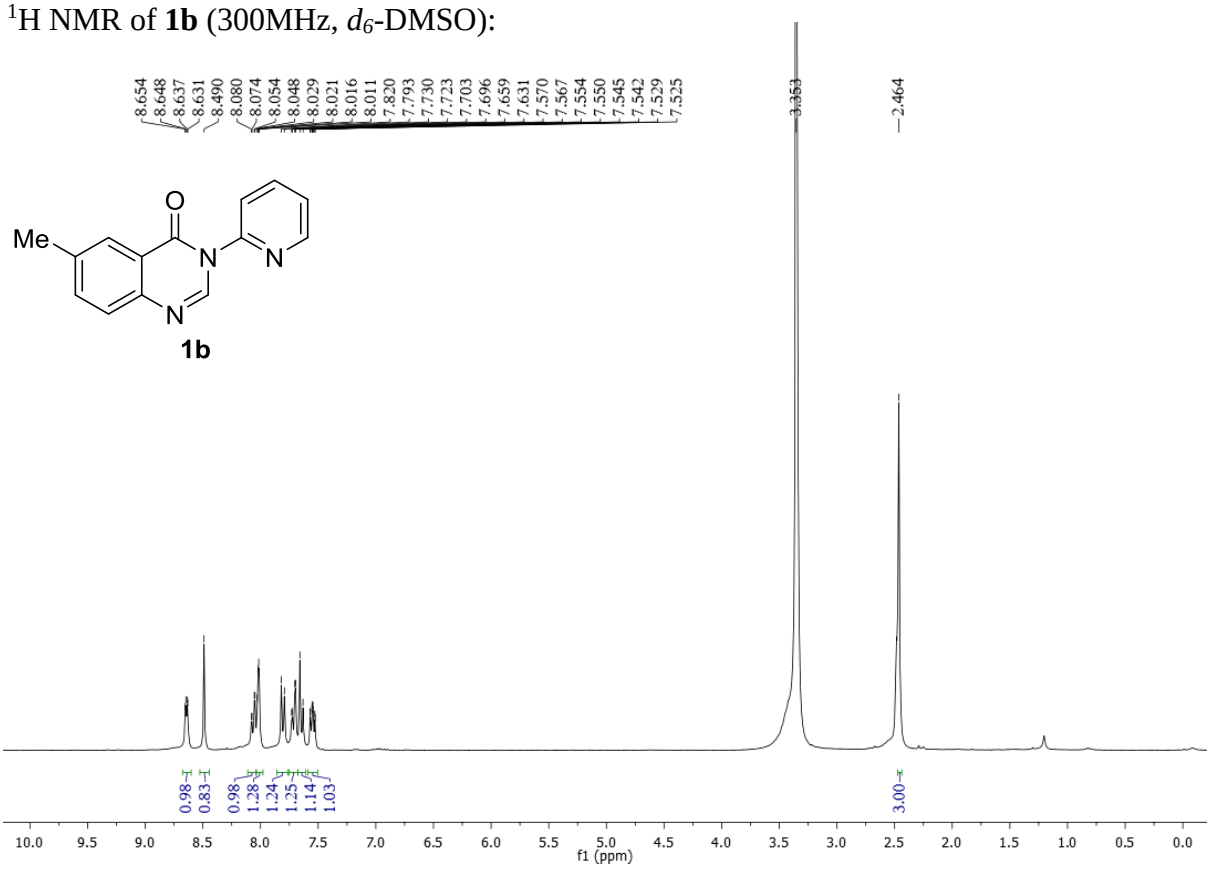

^{13}C NMR of **1b** (150MHz, d_6-DMSO):

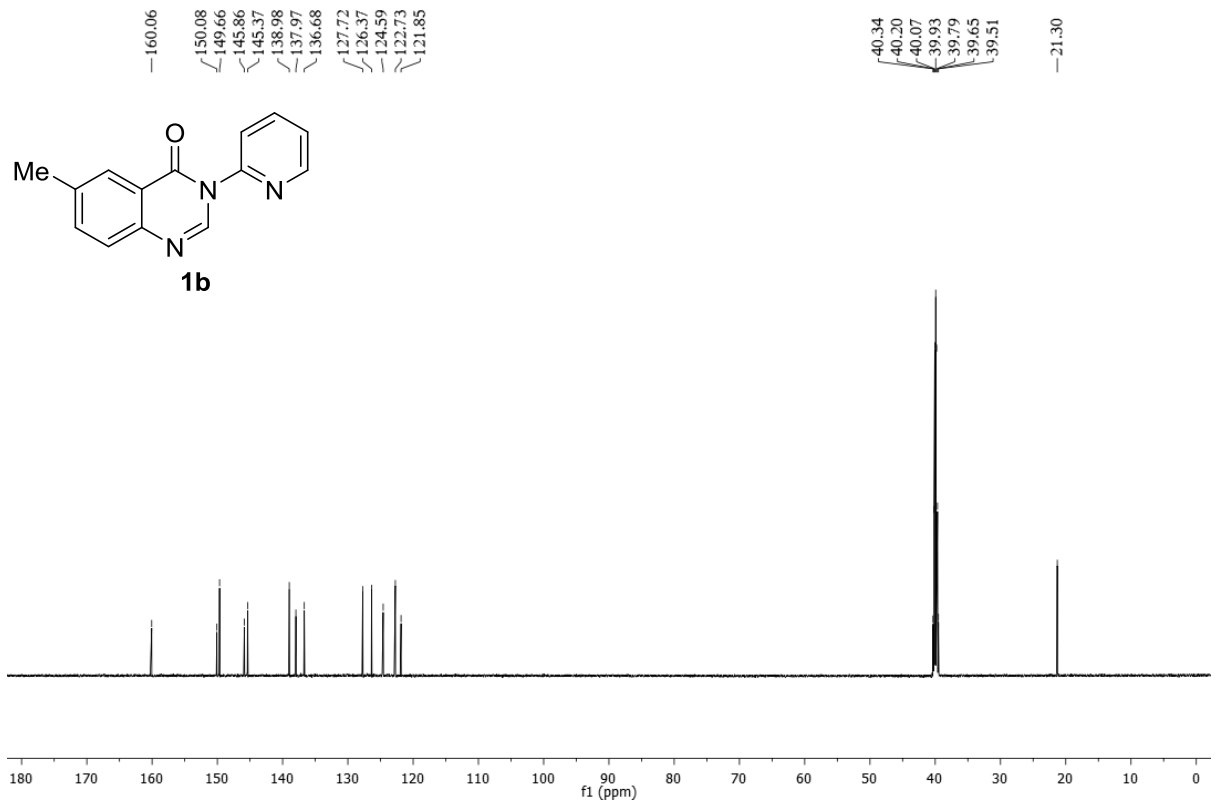

^{1}H NMR of **1e** (300MHz, $CDCl_3$):

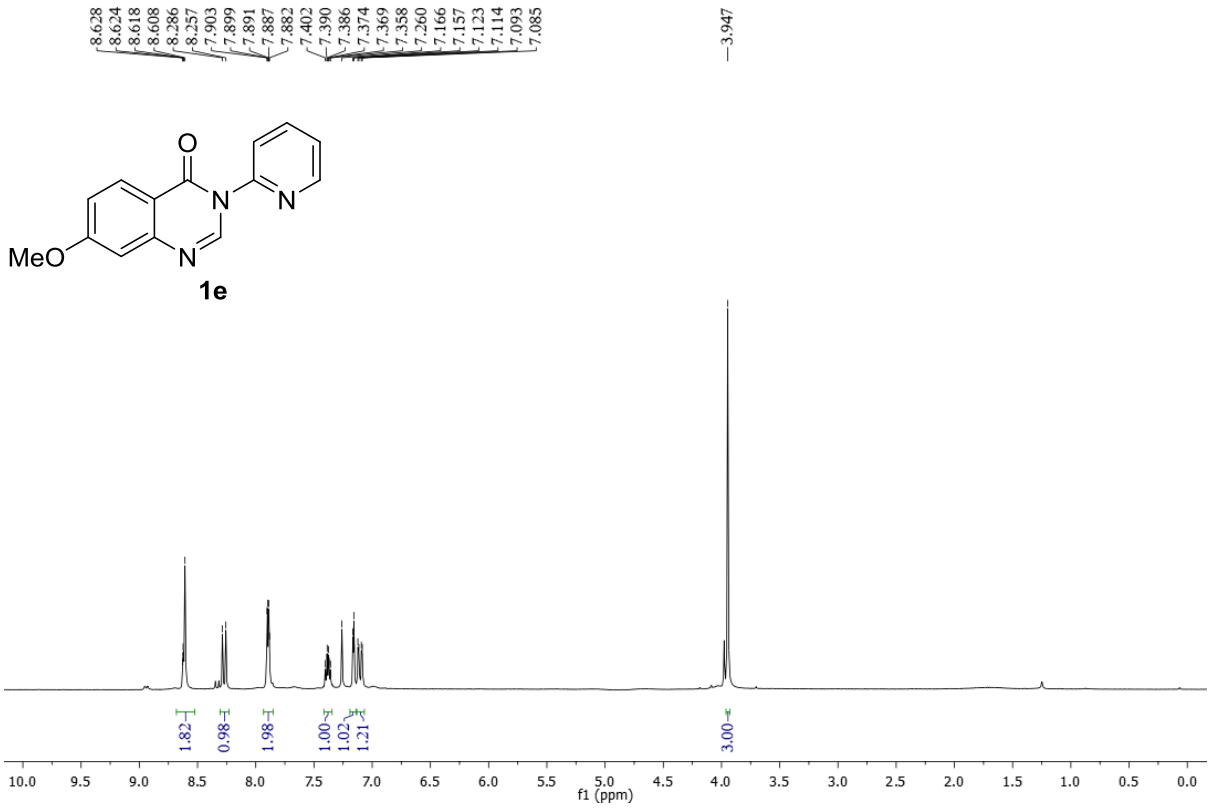

^{13}C NMR of **1e** (75MHz, $CDCl_3$):

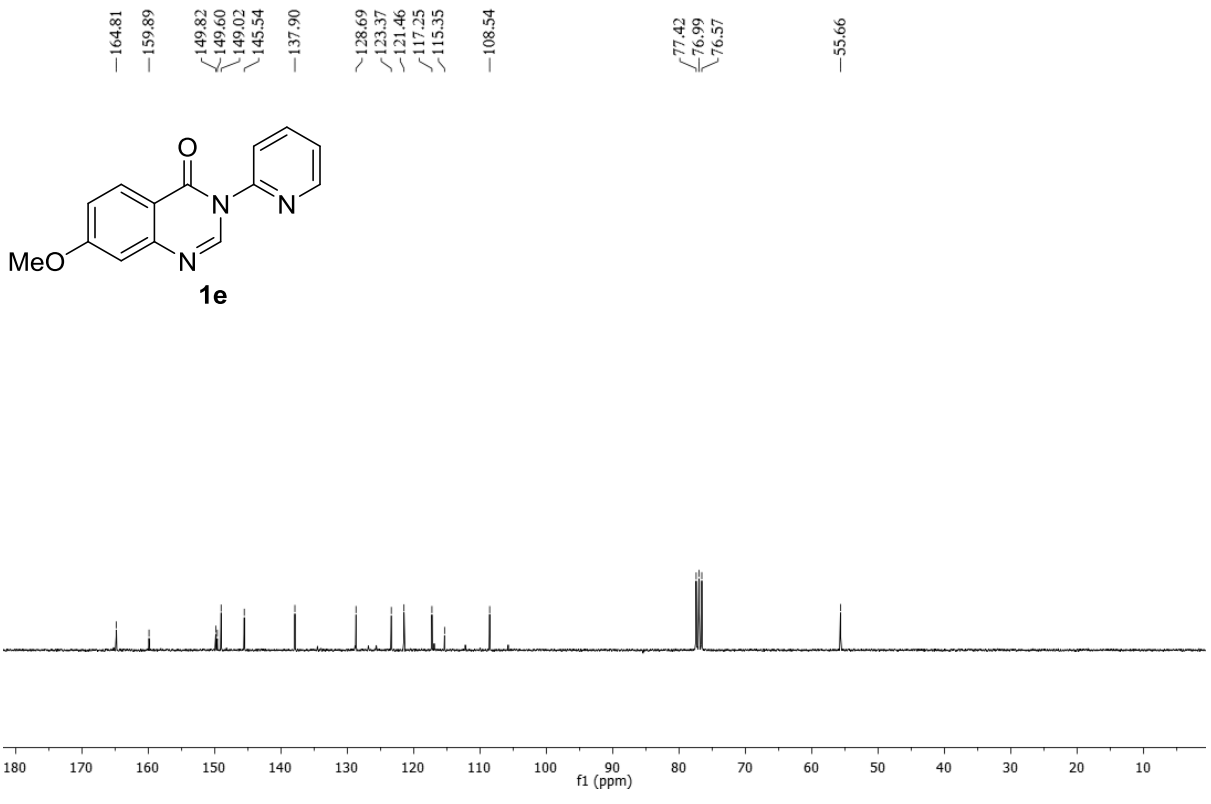

^{1}H NMR of **1g** (300MHz, $CDCl_3$):

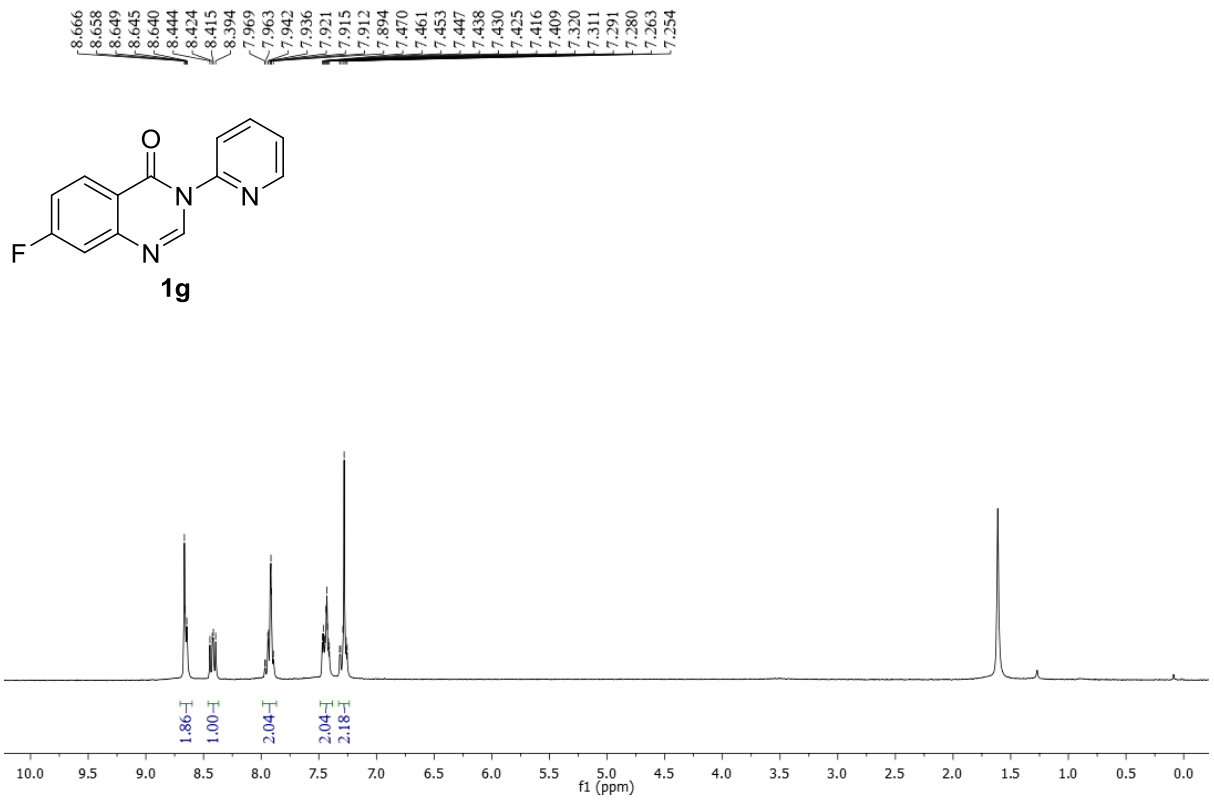

^{13}C NMR of **1g** (75MHz, $CDCl_3$):

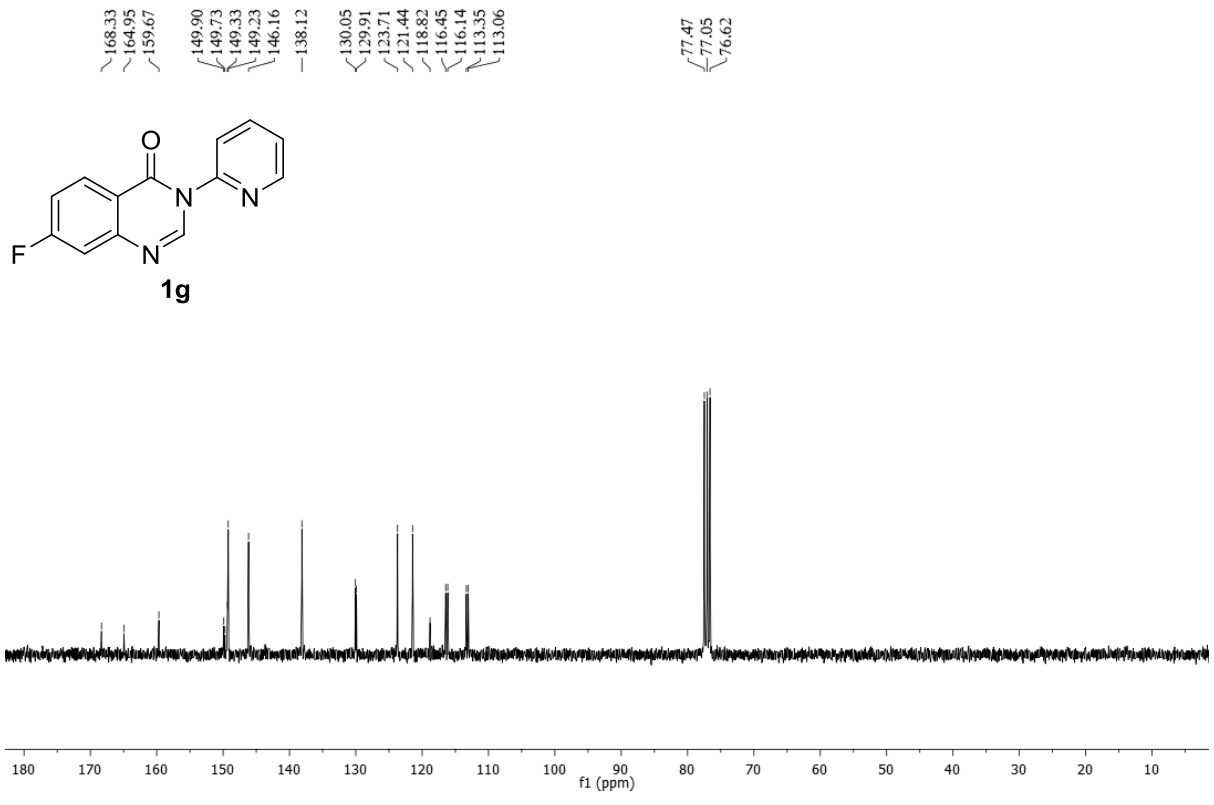

^{1}H NMR of **1h** (300MHz, $CDCl_3$):

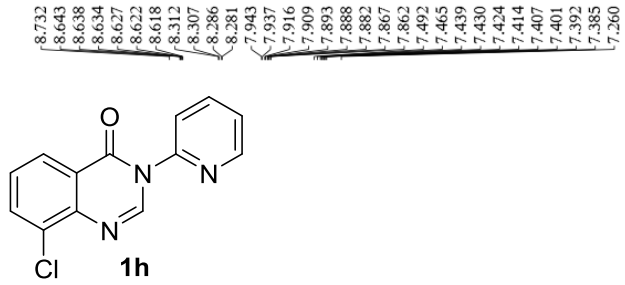

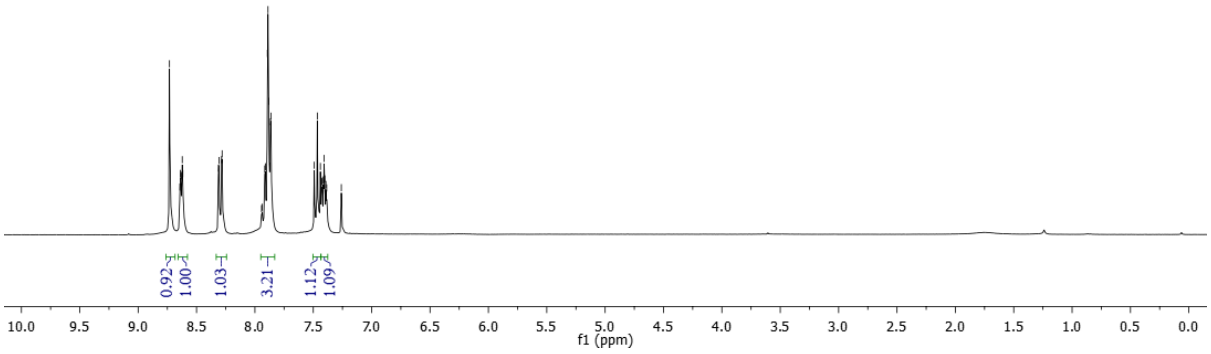

^{13}C NMR of **1h** (150MHz, $CDCl_3$):

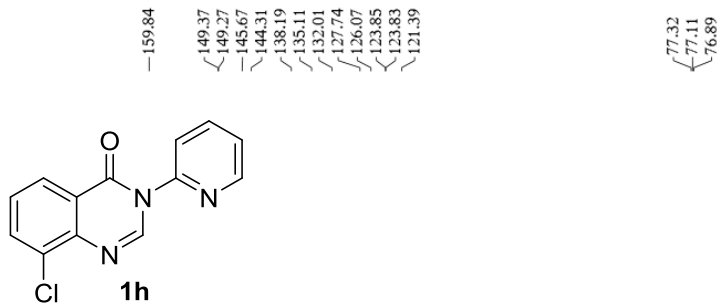

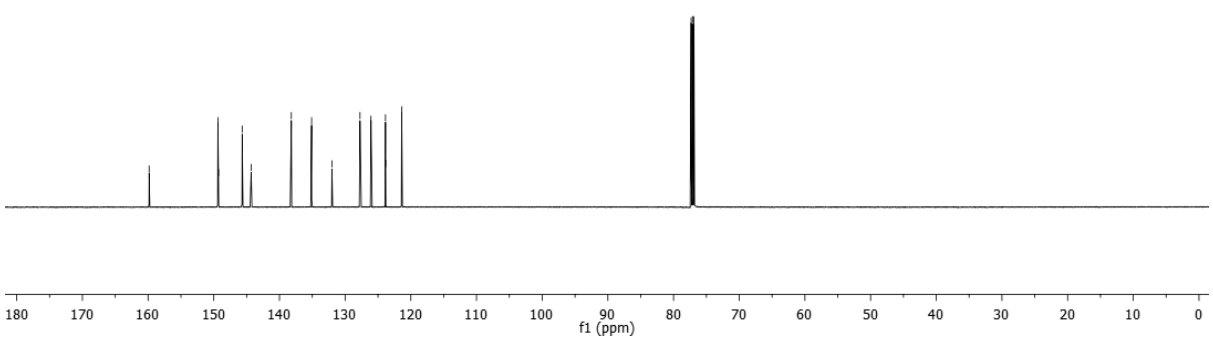

^{1}H NMR of **1j** (300MHz, $CDCl_3$):

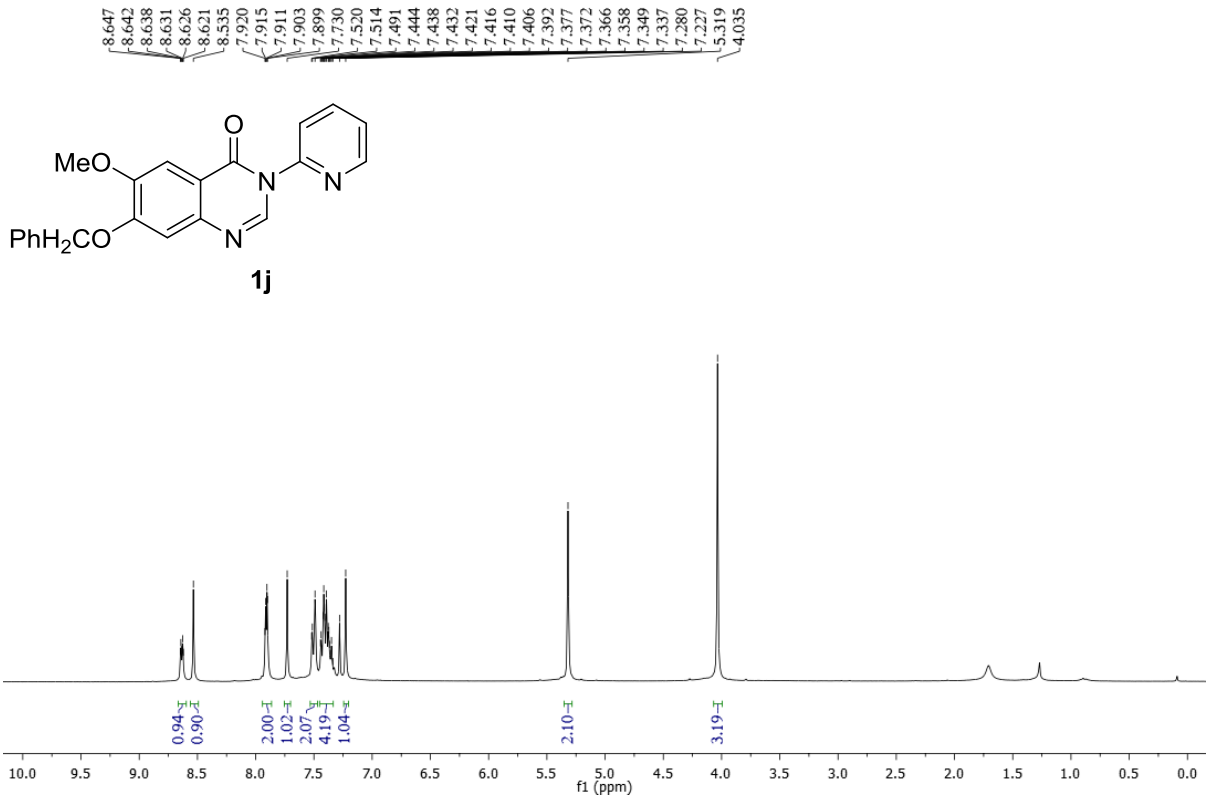

^{13}C NMR of **1j** (75MHz, $CDCl_3$):

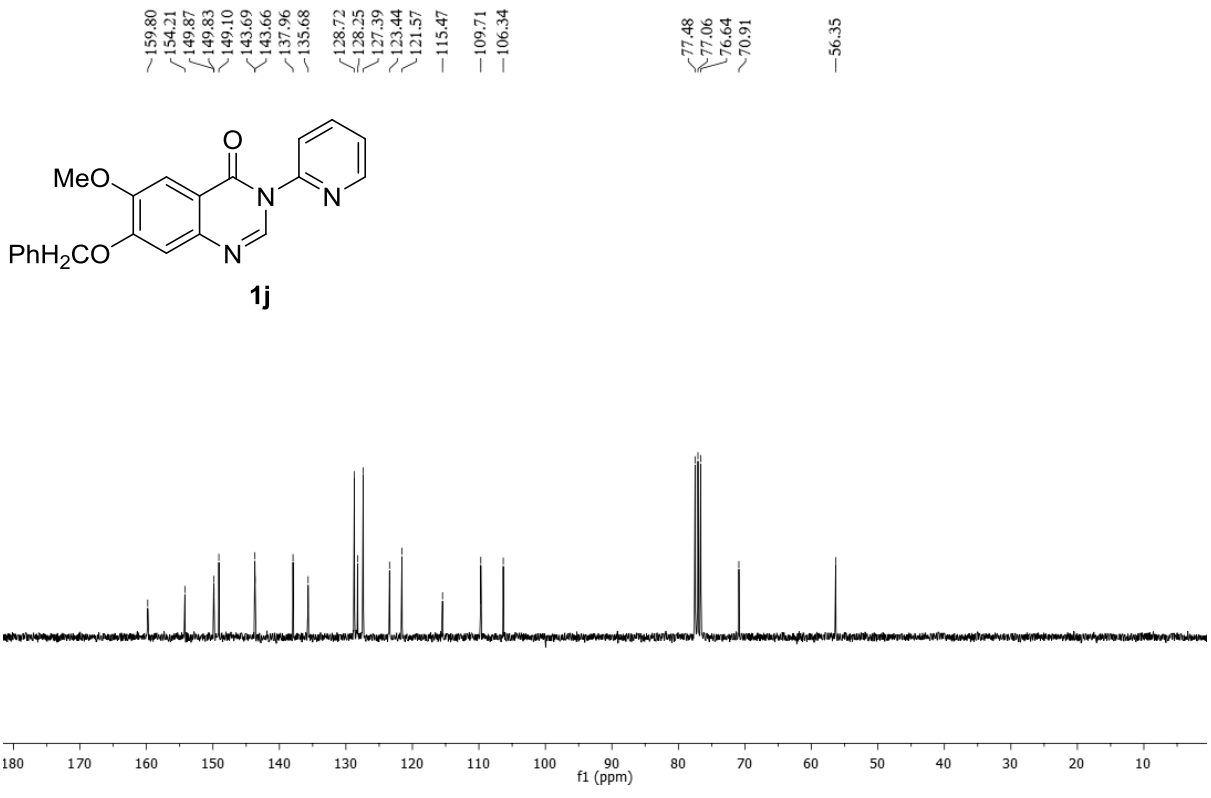

^{1}H NMR of **1k** (300MHz, $CDCl_3$):

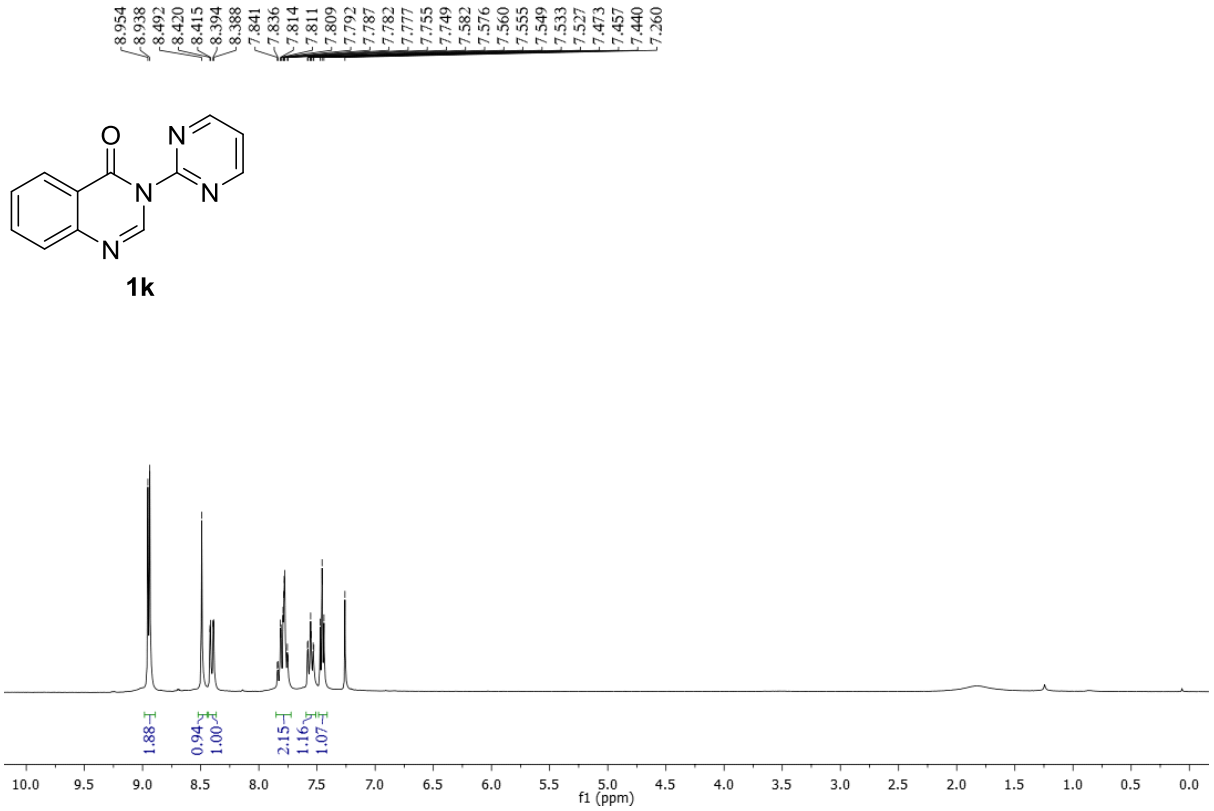

^{13}C NMR of **1k** (150MHz, $CDCl_3$):

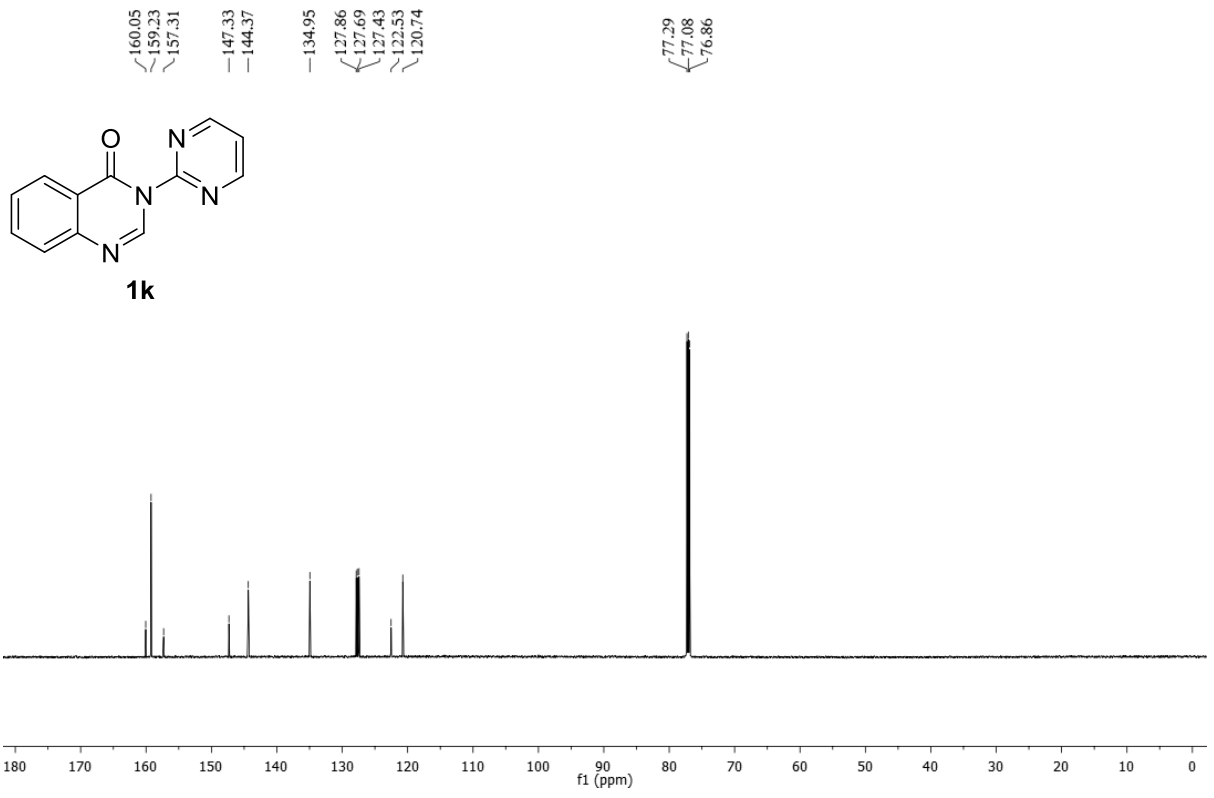

^{1}H NMR of **1l** (300MHz, $CDCl_3$):

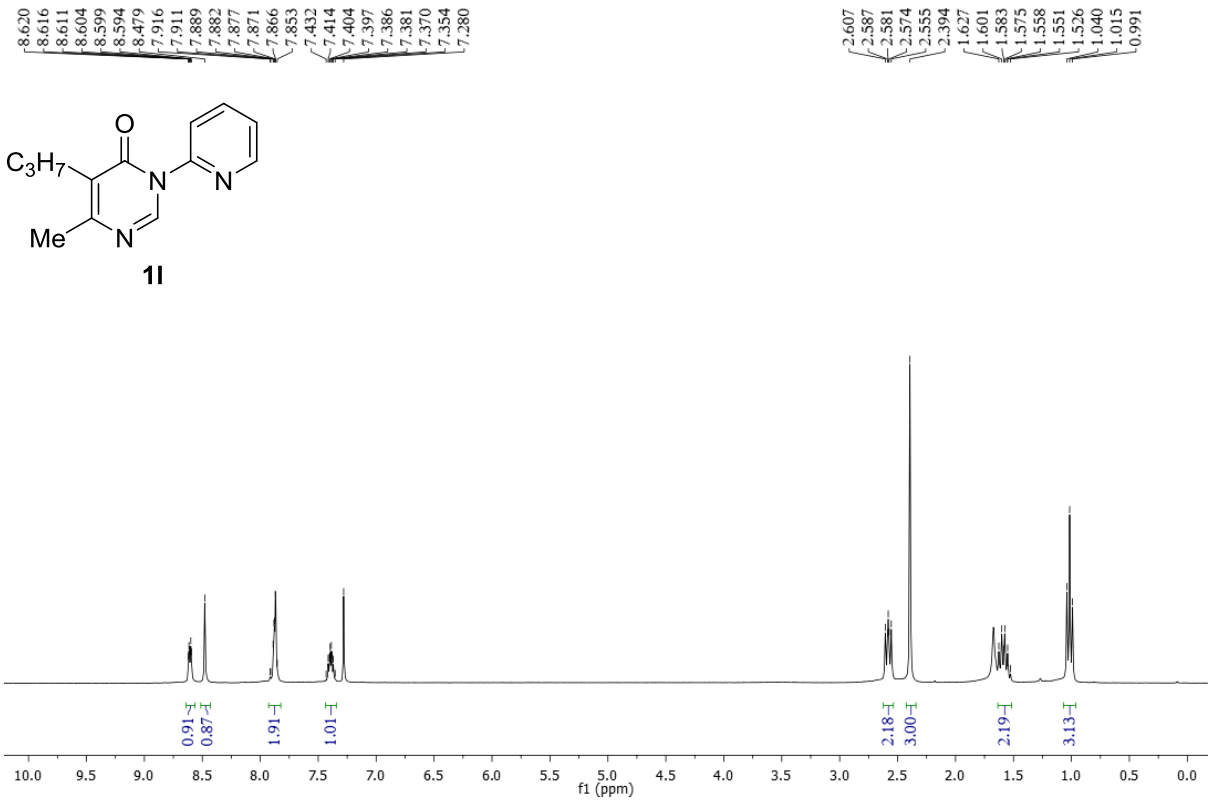

1l

^{13}C NMR of **1l** (75MHz, $CDCl_3$):

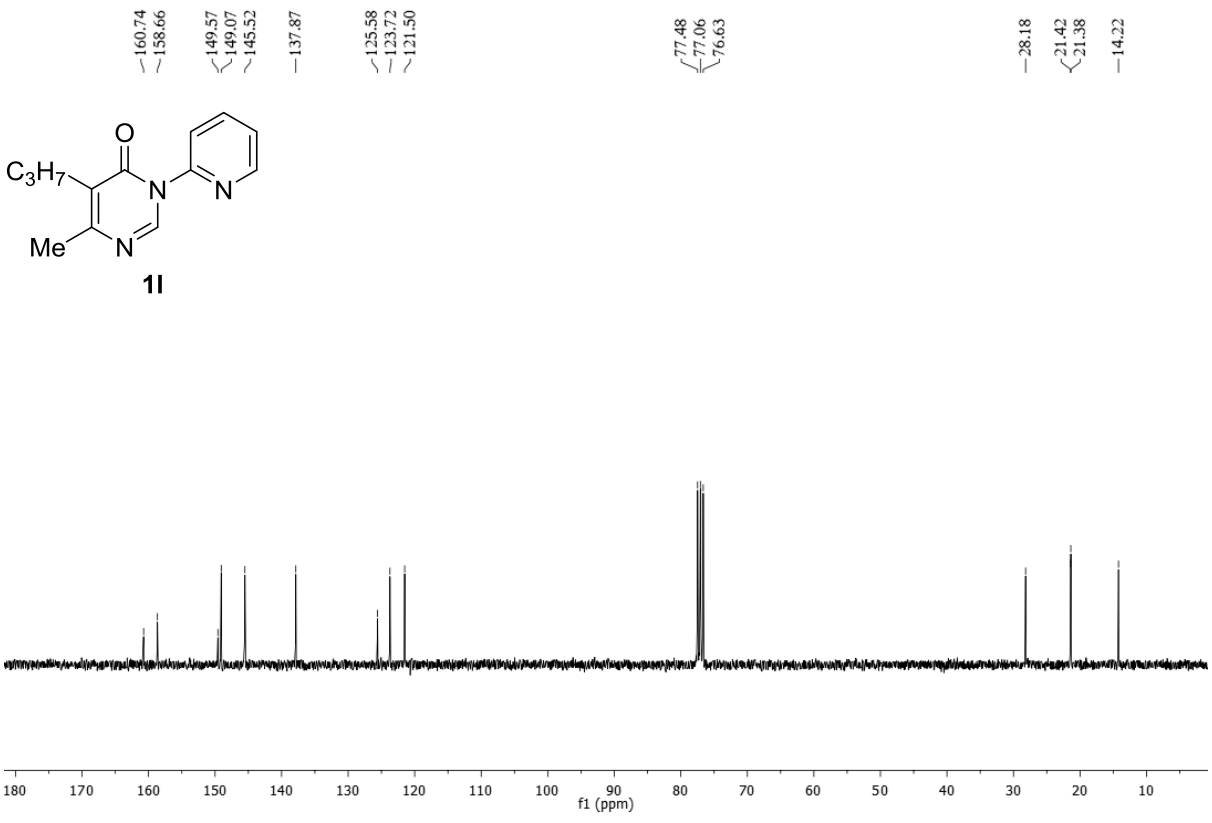

1l

^{1}H NMR of **3aa** (300MHz, $CDCl_3$):

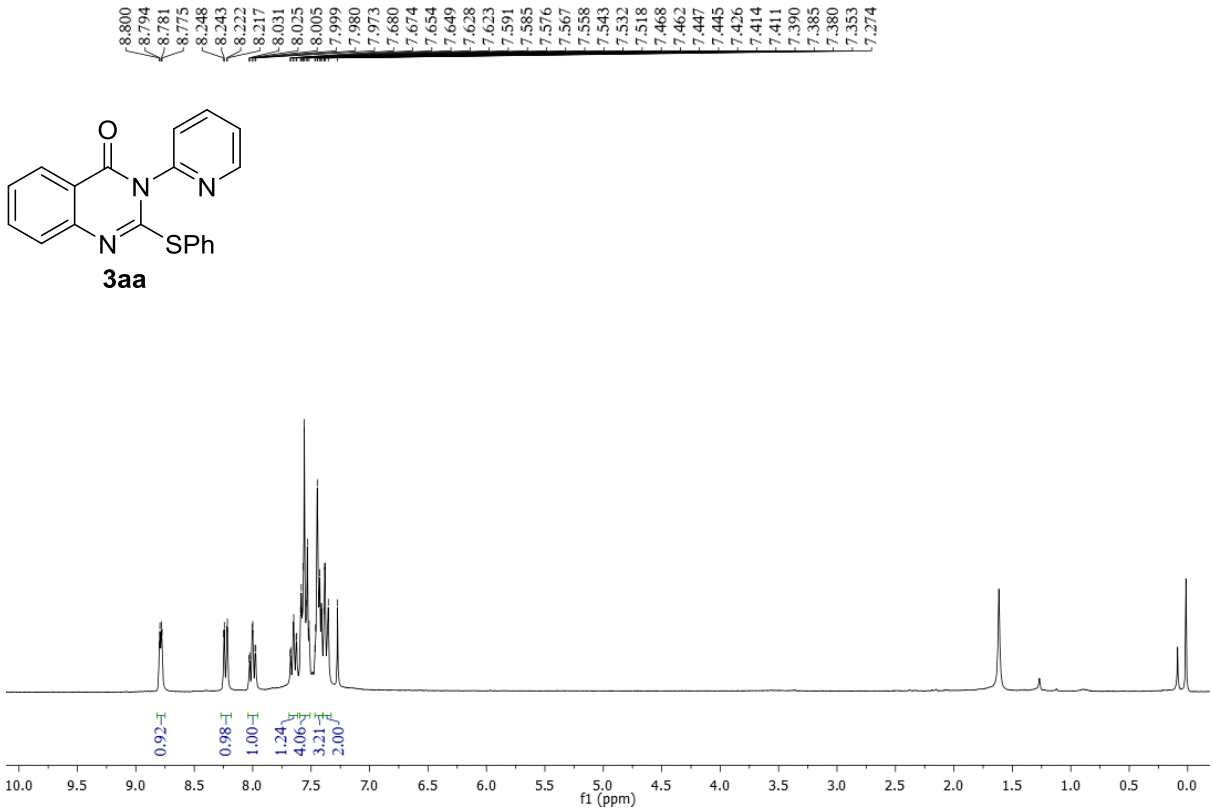

^{13}C NMR of **3aa** (150MHz, $CDCl_3$):

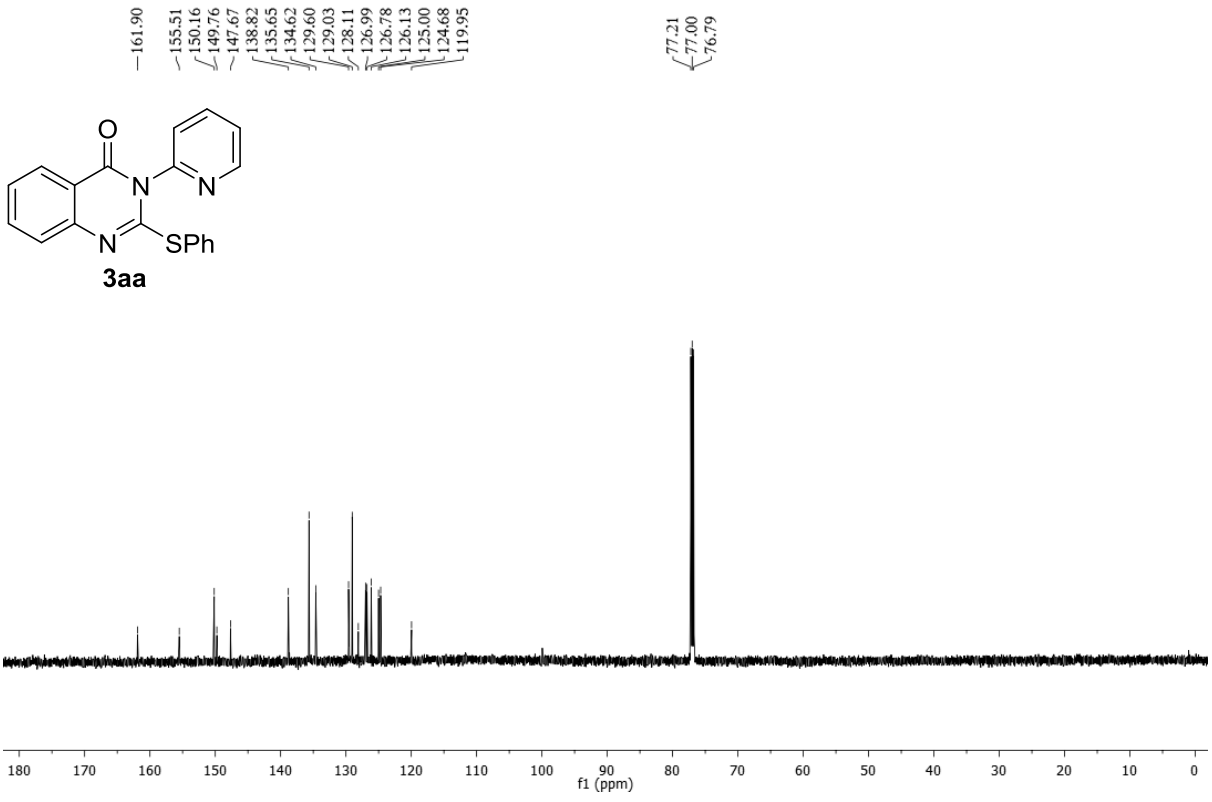

^{1}H NMR of **3ac** (300MHz, $CDCl_3$):

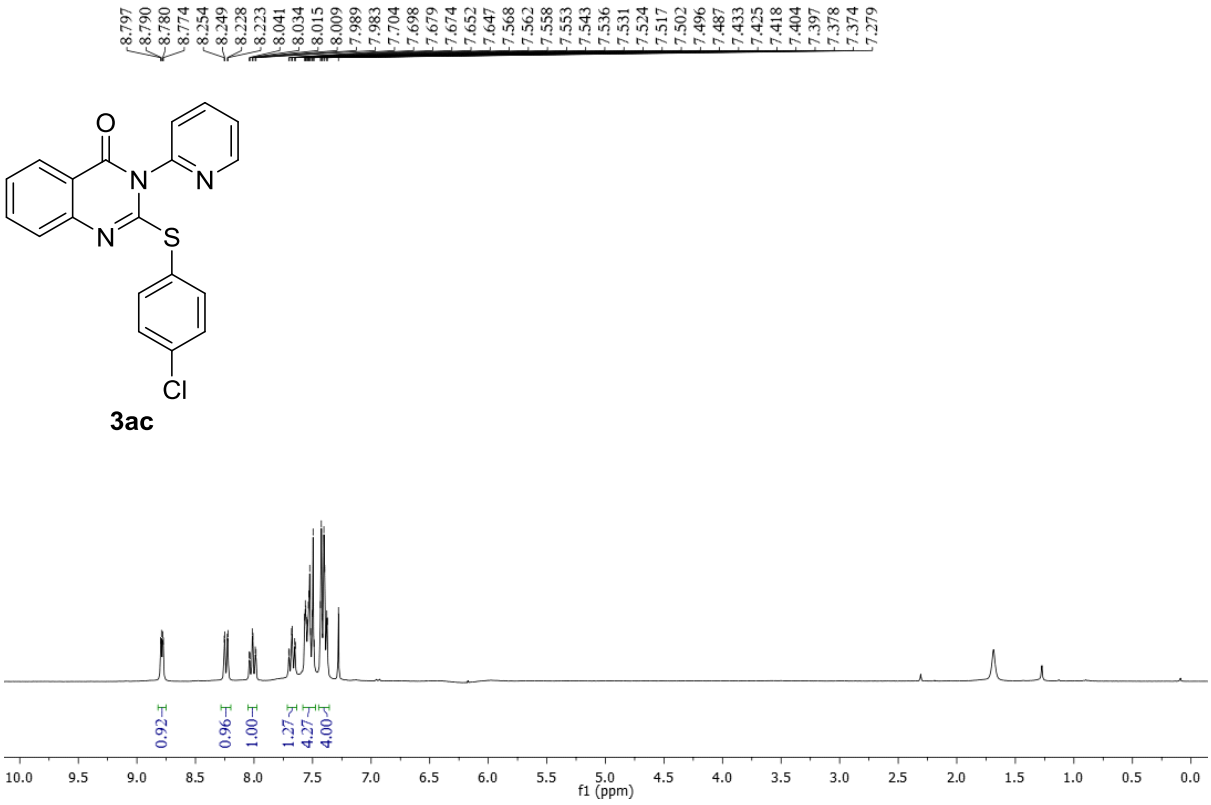

^{13}C NMR of **3ac** (150MHz, $CDCl_3$):

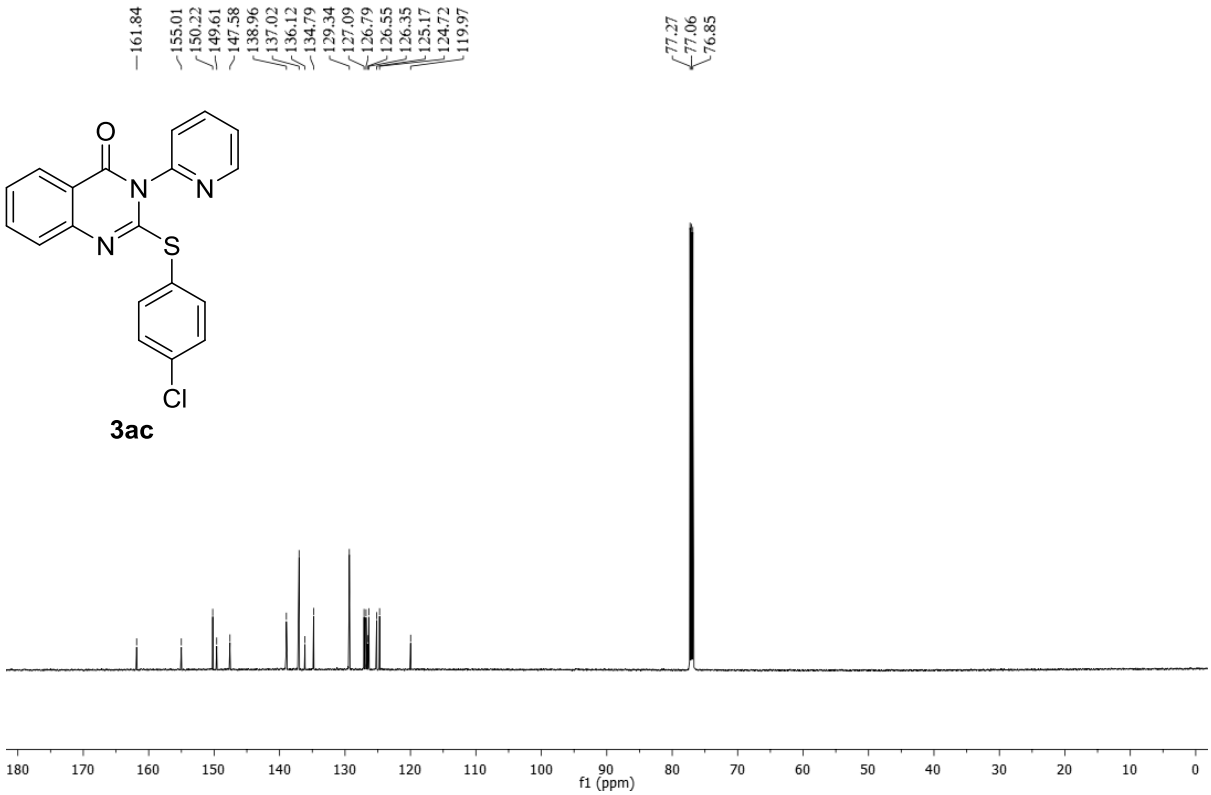

^{1}H NMR of **3ae** (300MHz, $CDCl_3$):

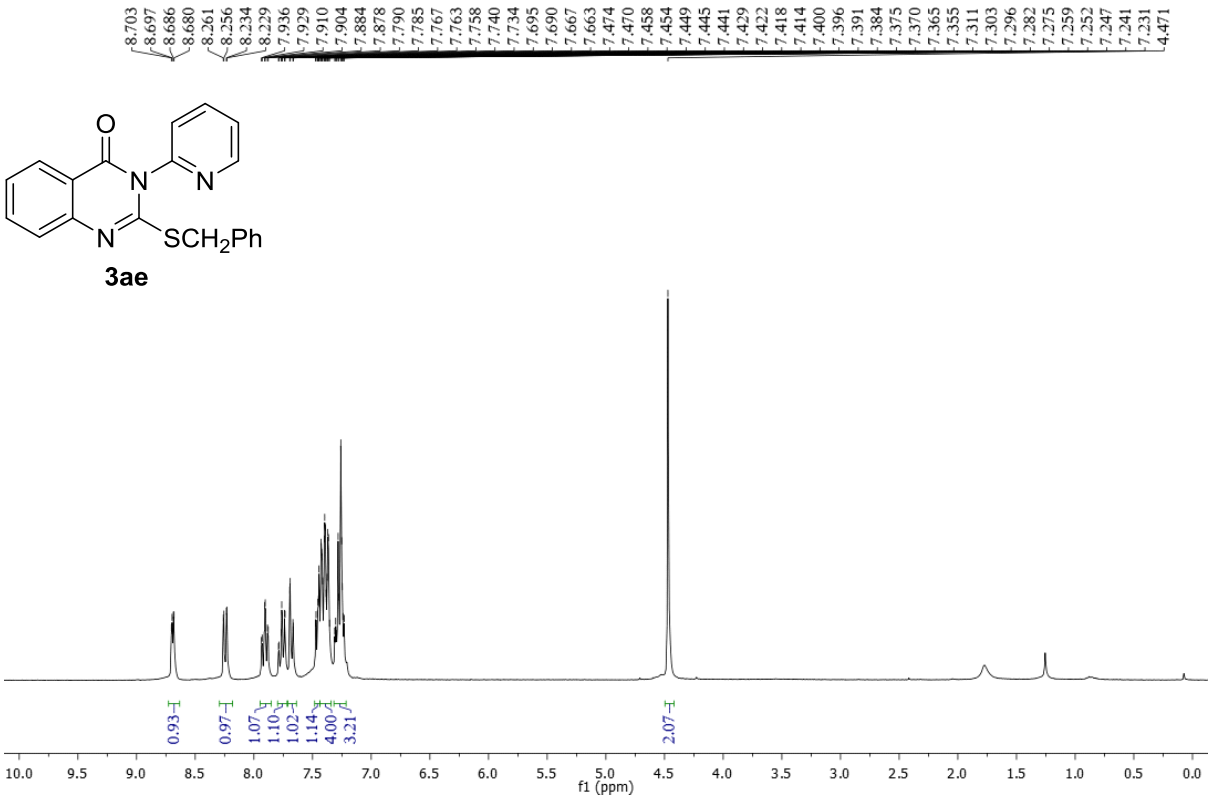

^{13}C NMR of **3ae** (75MHz, $CDCl_3$):

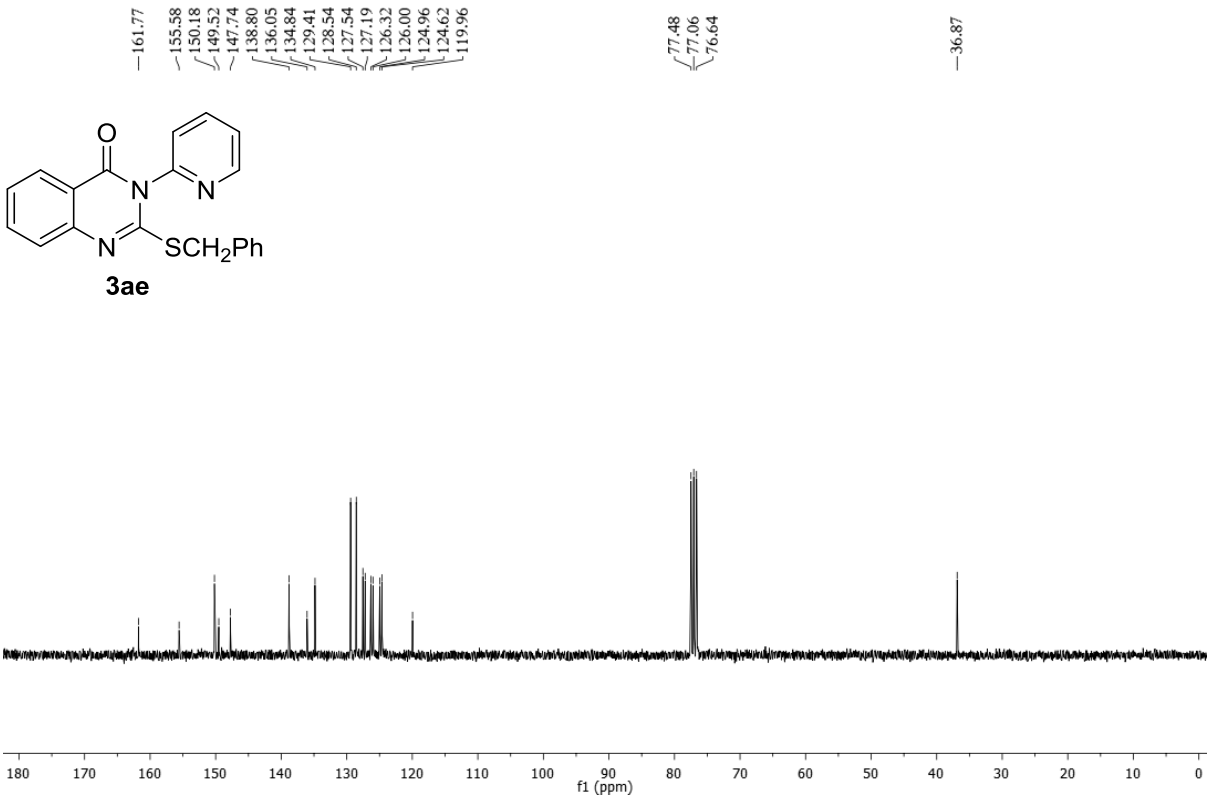

^{1}H NMR of **3ag** (300MHz, $CDCl_3$):

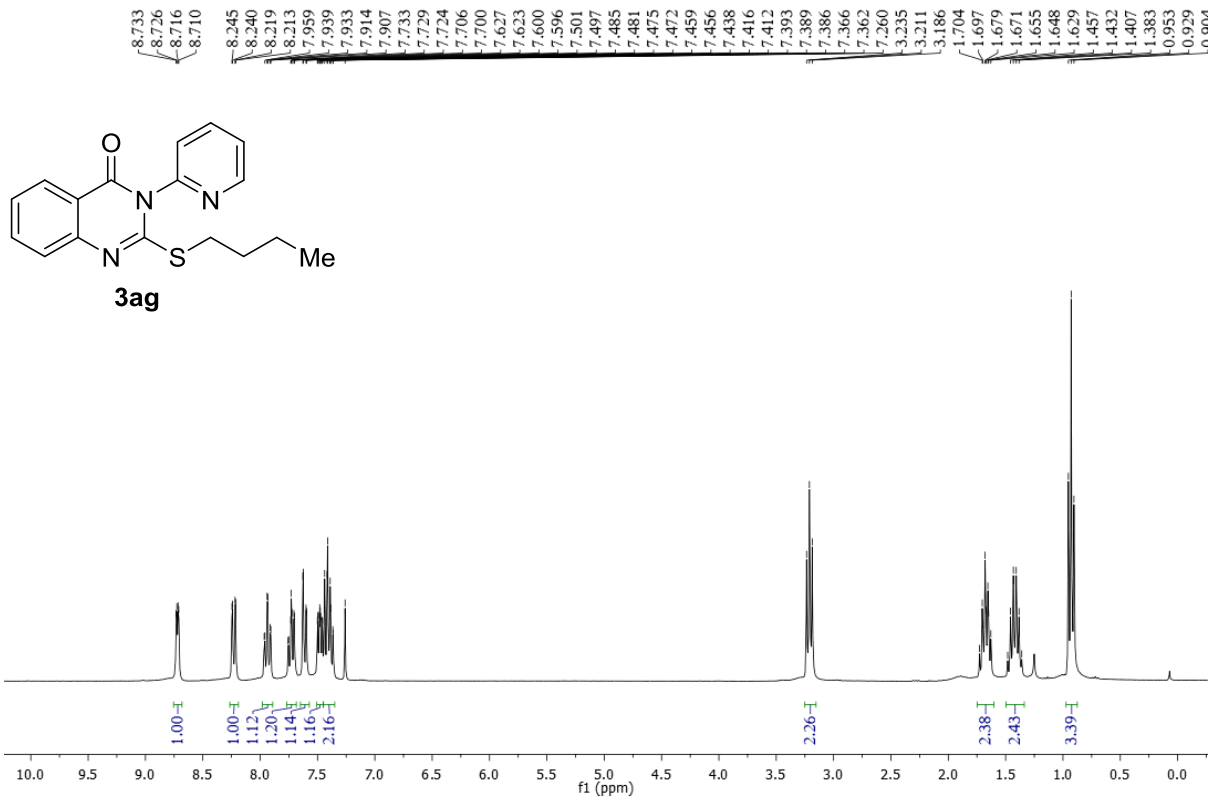

^{13}C NMR of **3ag** (150MHz, $CDCl_3$):

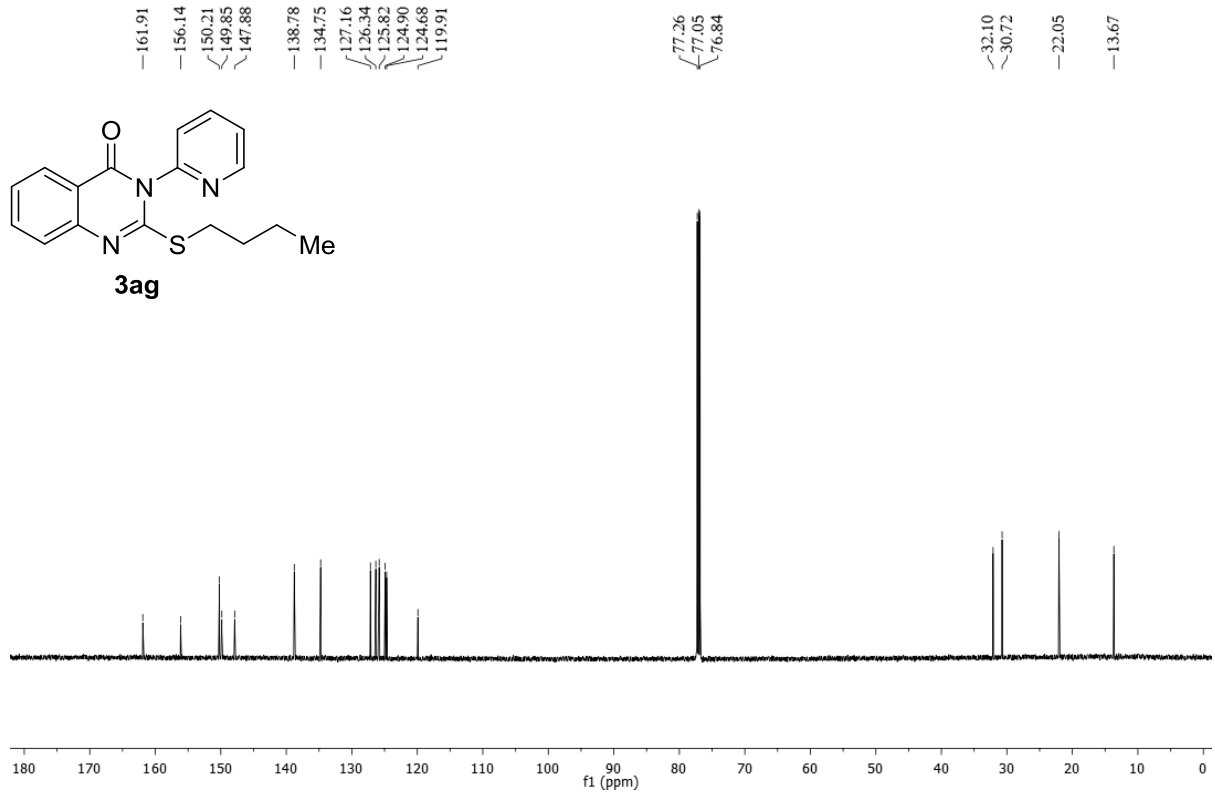

^{1}H NMR of **3ca** (600MHz, $CDCl_3$):

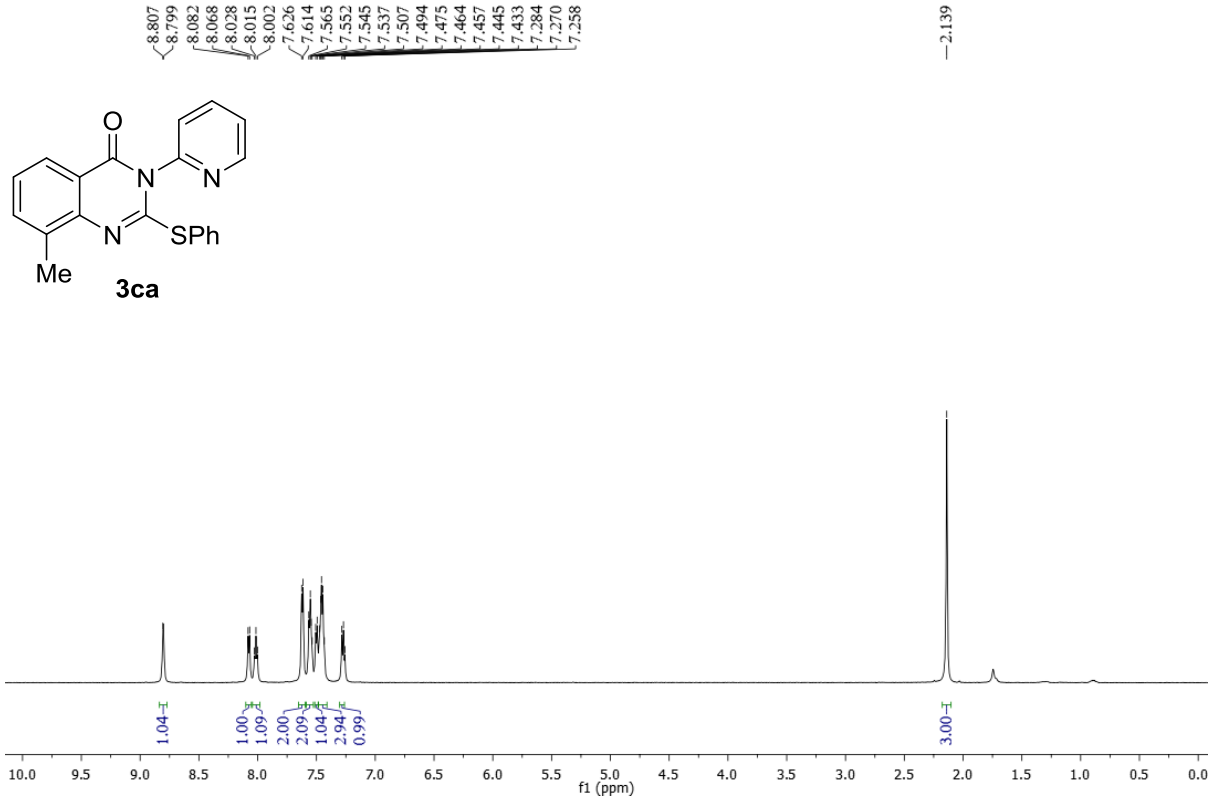

^{13}C NMR of **3ca** (150MHz, $CDCl_3$):

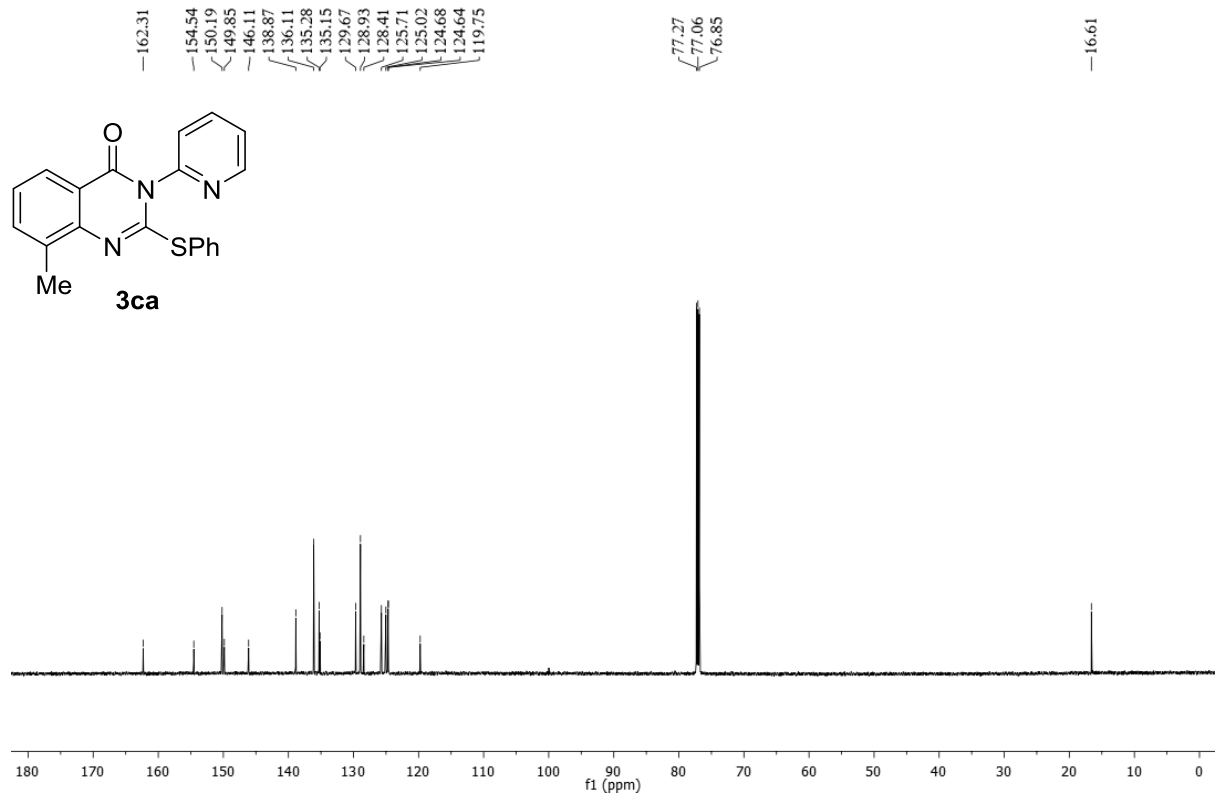

^{1}H NMR of **3da** (300MHz, $CDCl_3$):

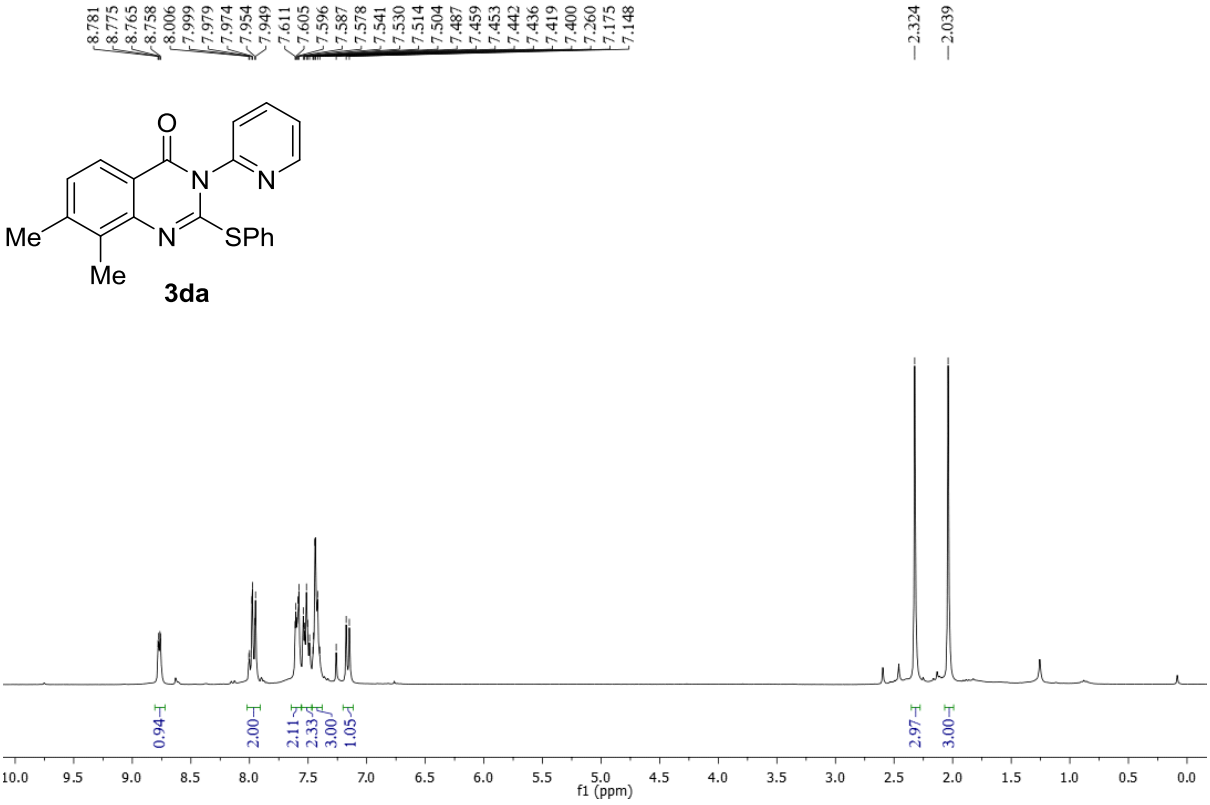

^{13}C NMR of **3ca** (150MHz, $CDCl_3$):

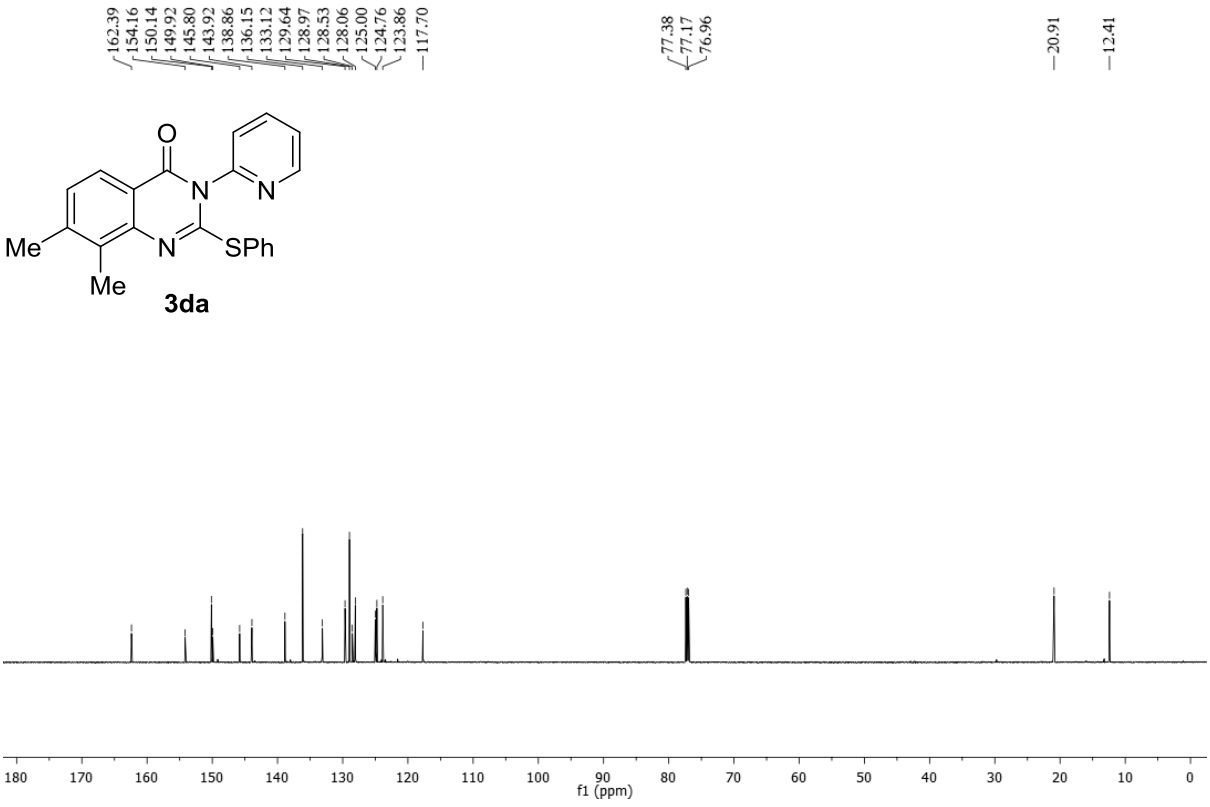

^{1}H NMR of **3ga** (600MHz, $CDCl_3$):

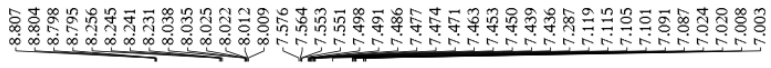

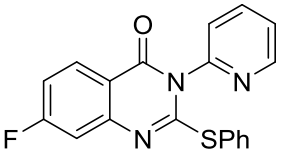

3ga

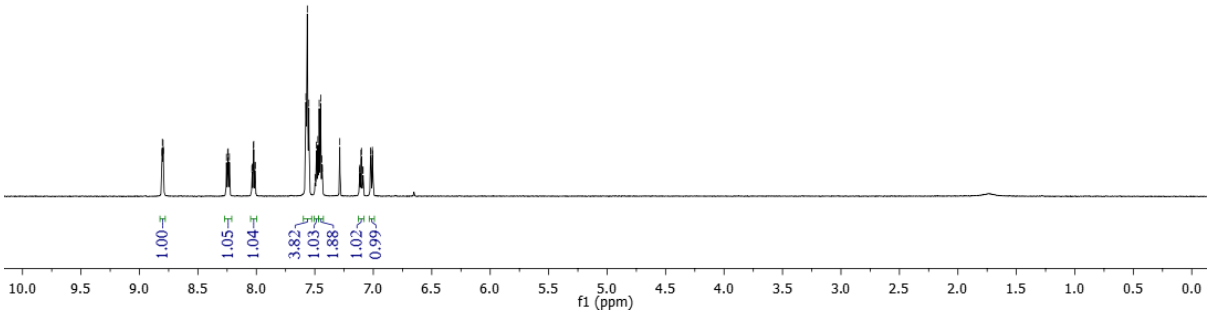

^{13}C NMR of **3ga** (150MHz, $CDCl_3$):

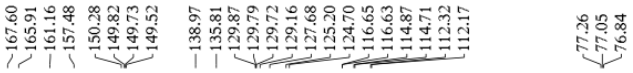

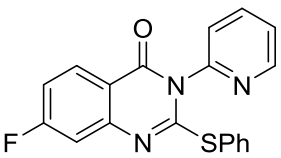

3ga

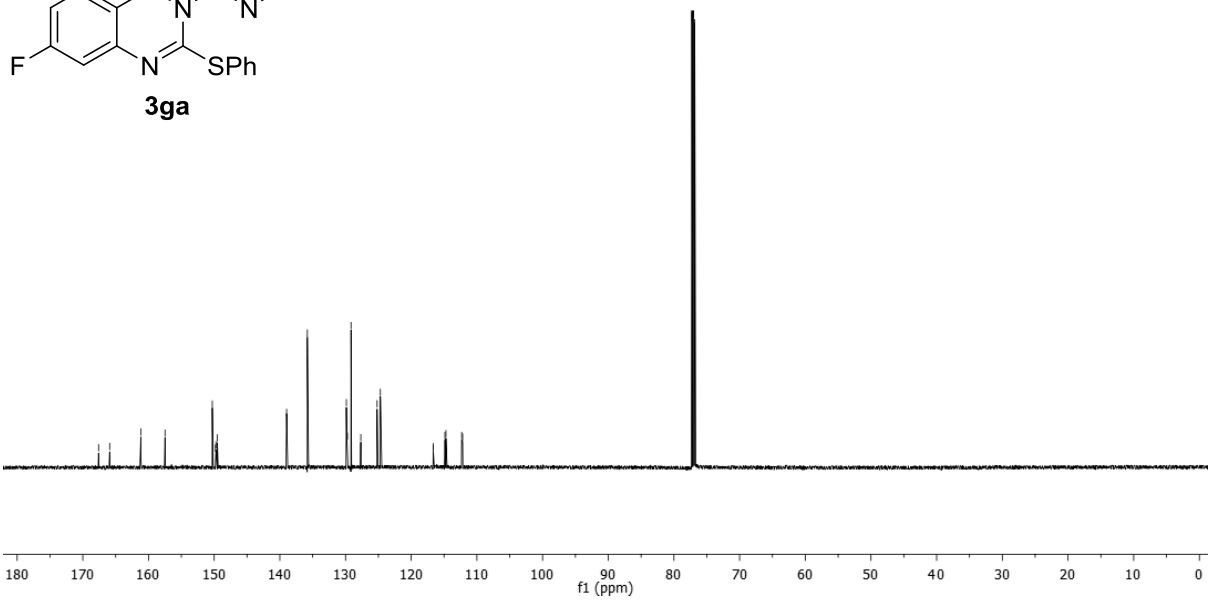

^{1}H NMR of **3ji** (300MHz, $CDCl_3$):

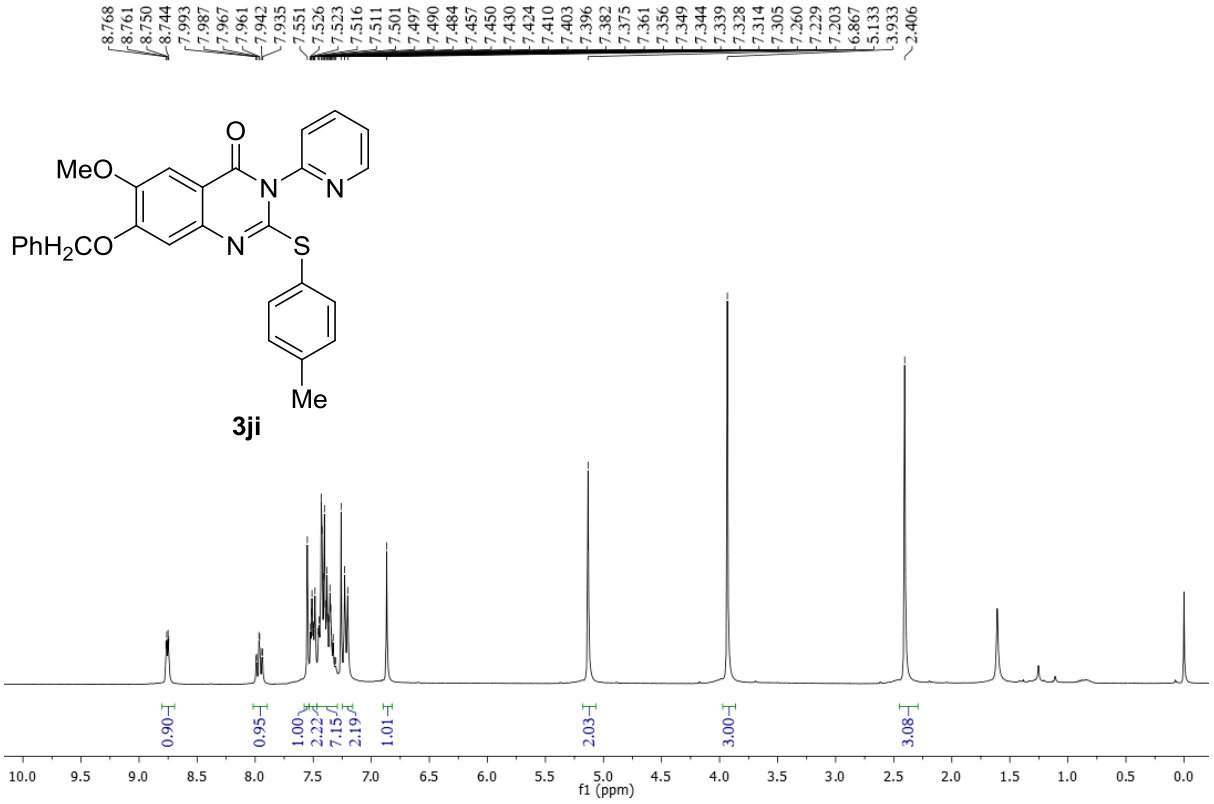

^{13}C NMR of **3ji** (75MHz, $CDCl_3$):

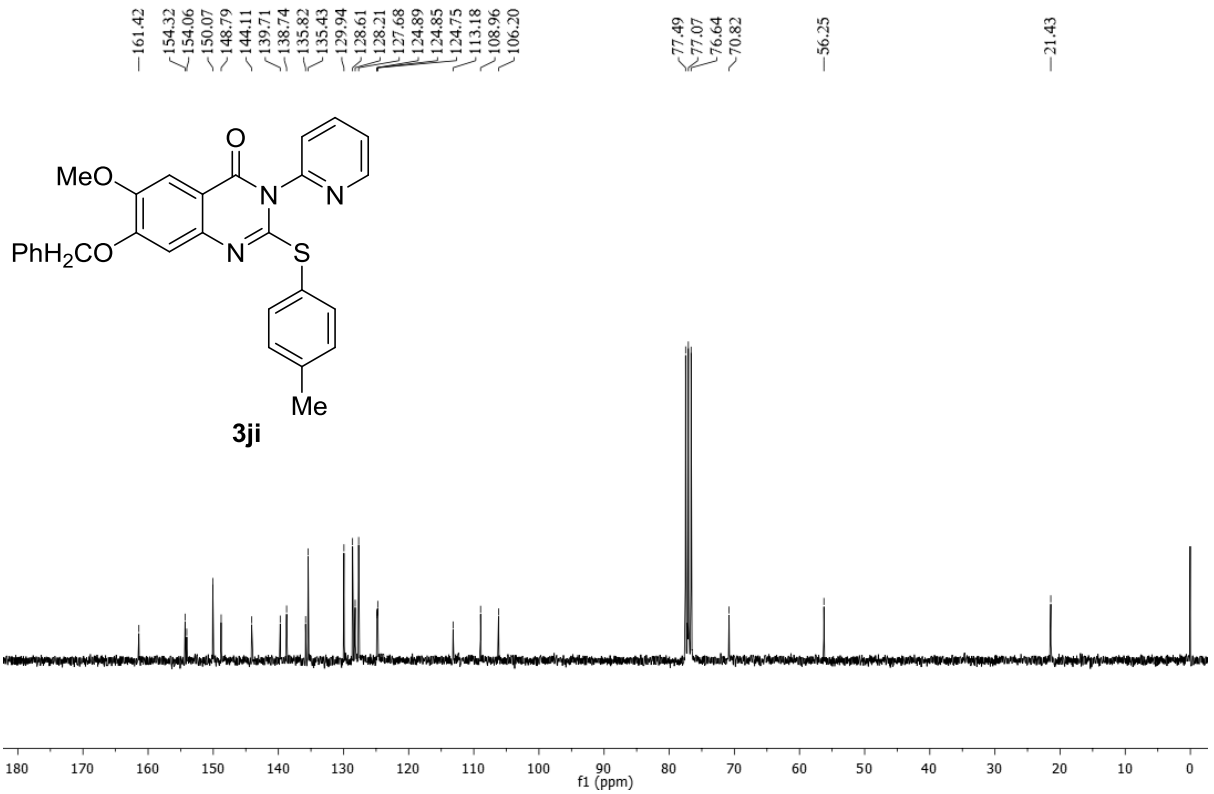

^{1}H NMR of **3jc** (300MHz, $CDCl_3$):

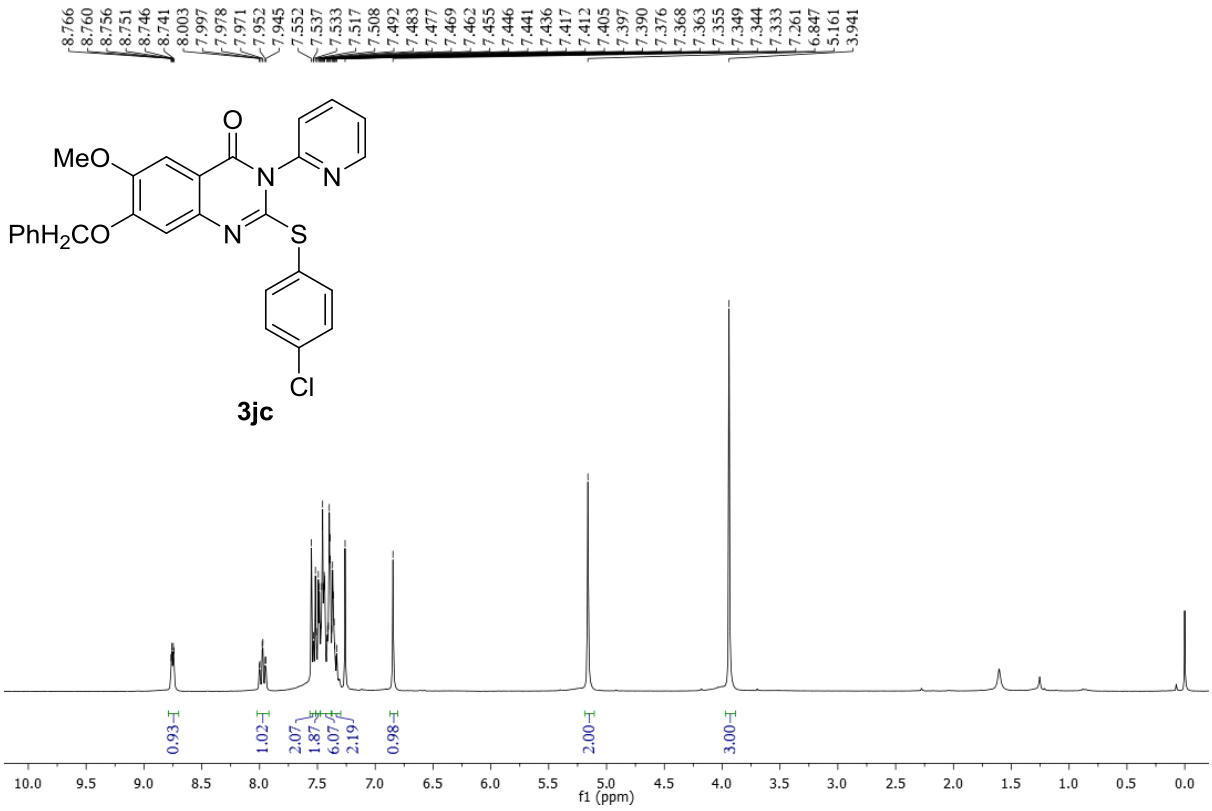

^{13}C NMR of **3jc** (75MHz, $CDCl_3$):

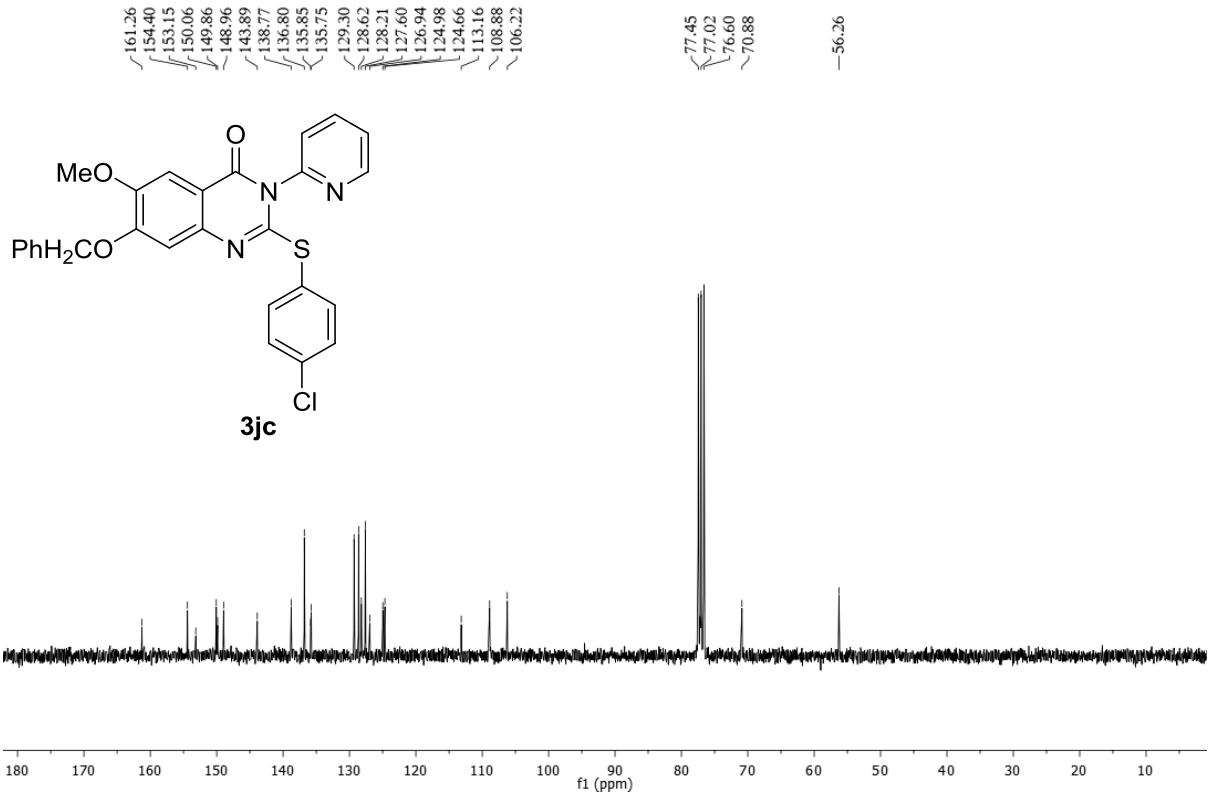

^{1}H NMR of **3ka** (600MHz, $CDCl_3$):

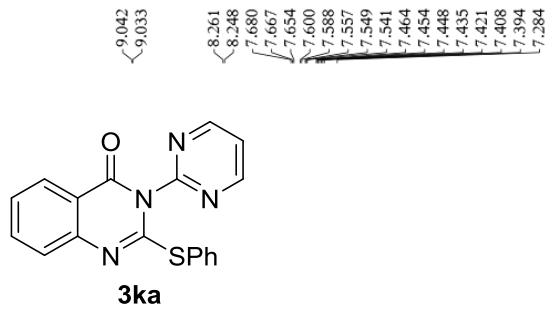

3ka

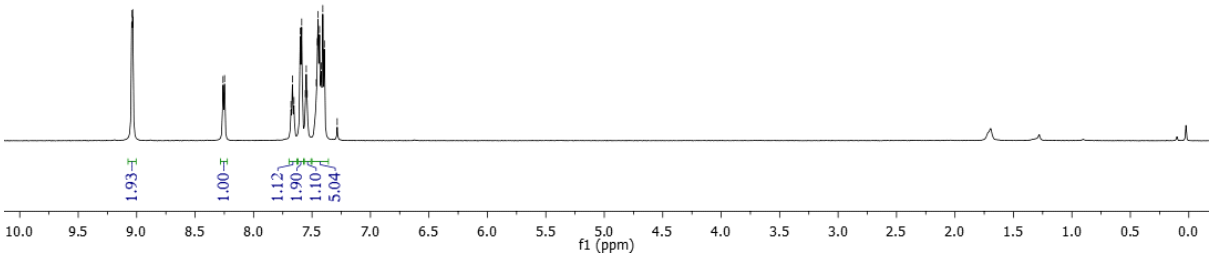

^{13}C NMR of **3ka** (150MHz, $CDCl_3$):

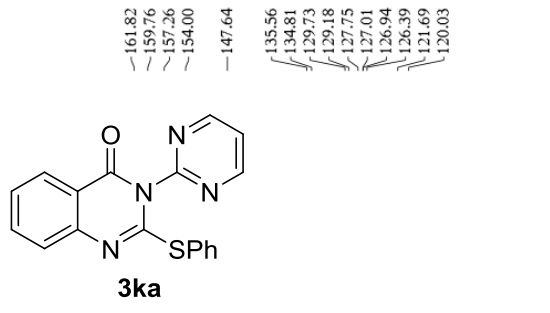

3ka

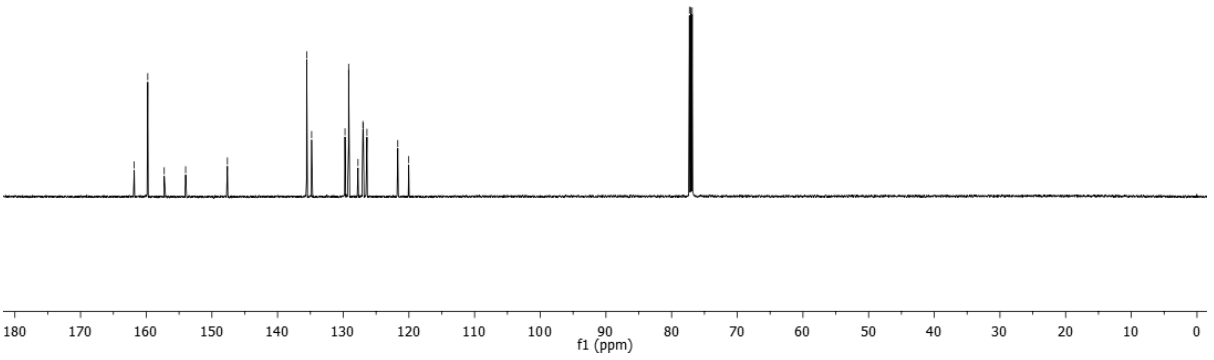

^{1}H NMR of **3la** (300MHz, $CDCl_3$):

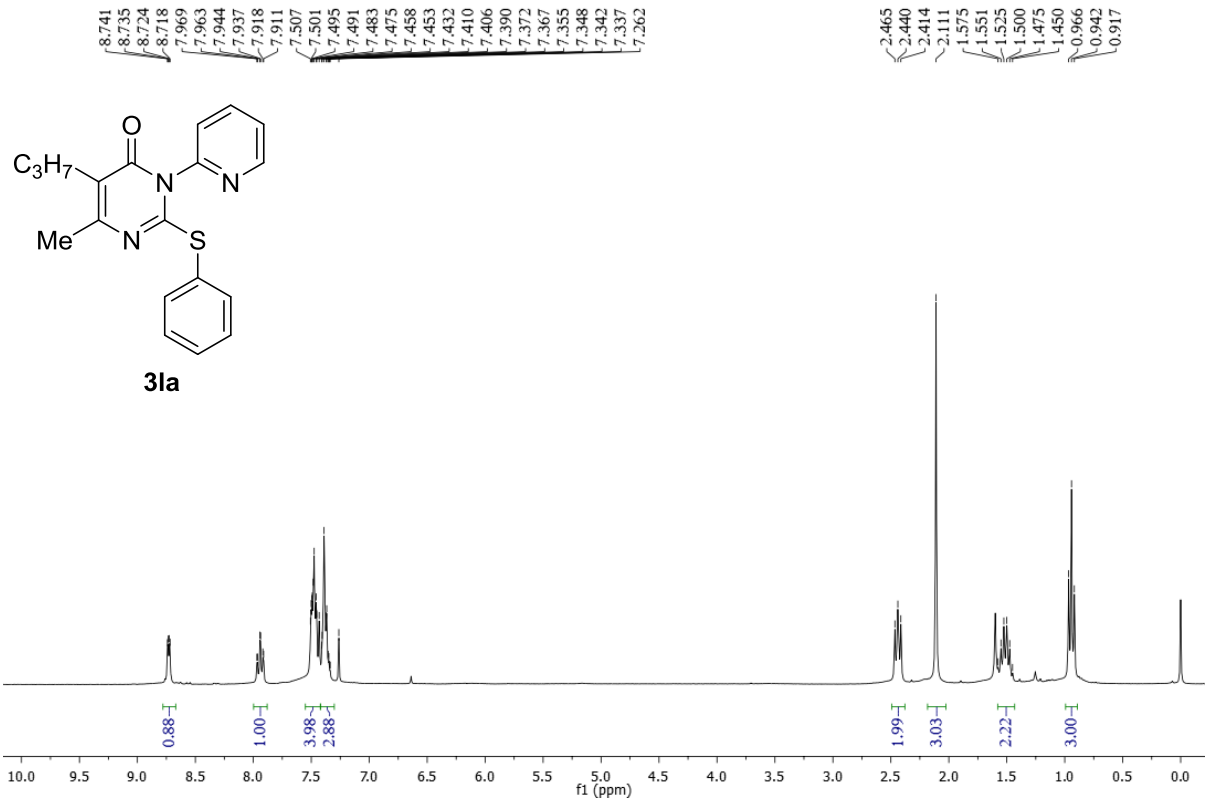

3la

^{13}C NMR of **3la** (75MHz, $CDCl_3$):

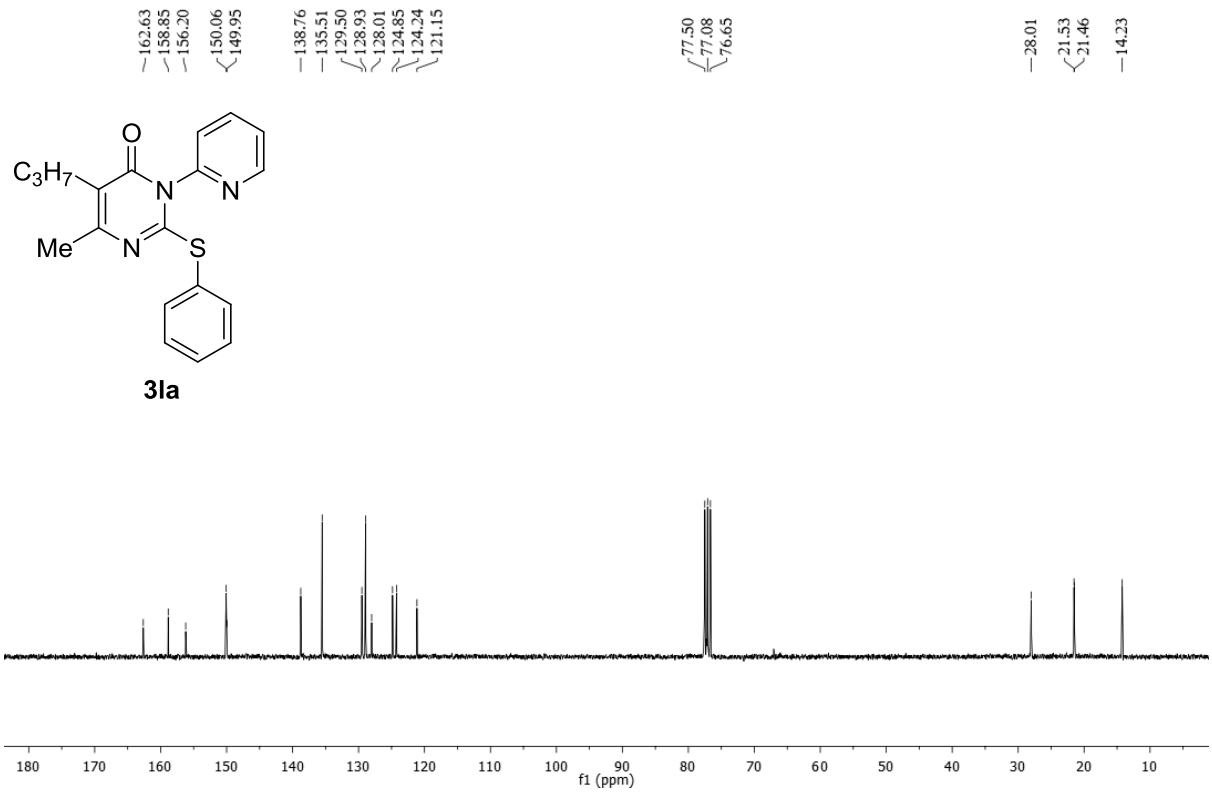

3la

^{1}H NMR of **3ld** (300MHz, $CDCl_3$):

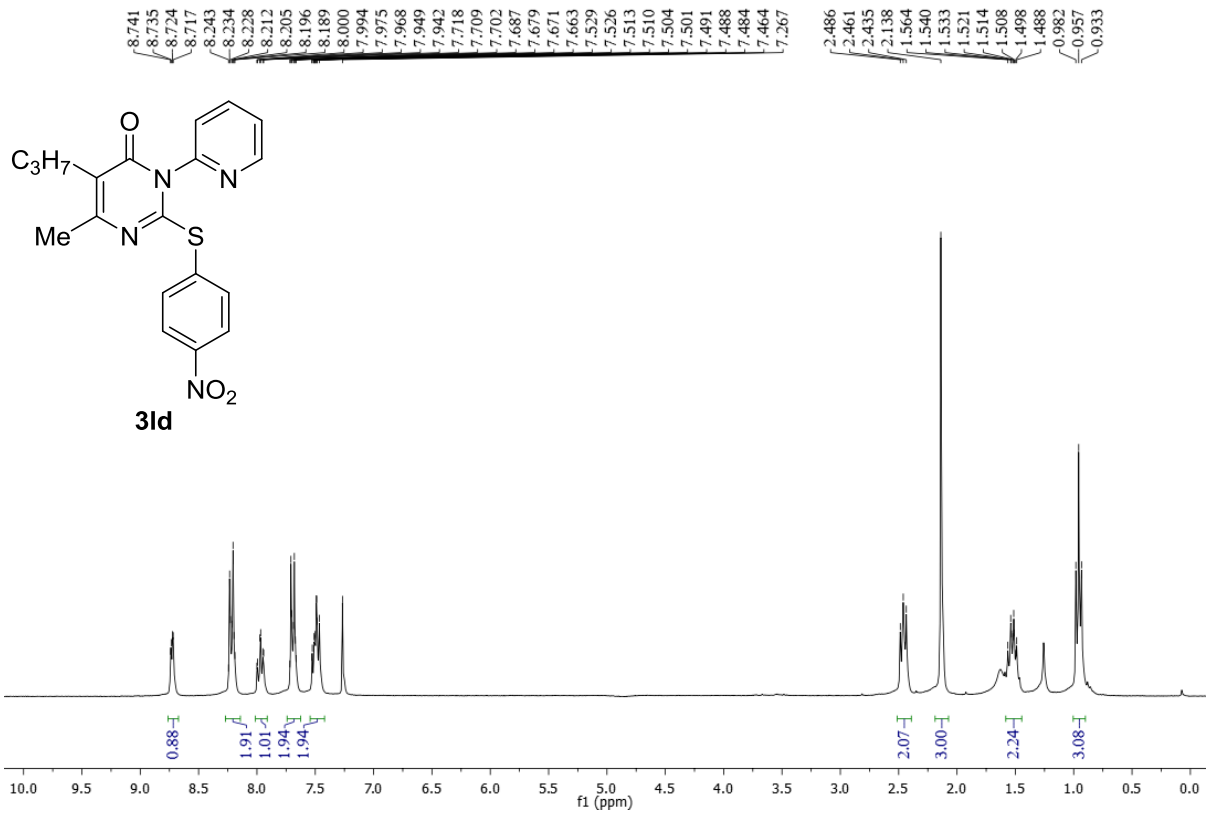

^{13}C NMR of **3ld** (150MHz, $CDCl_3$):

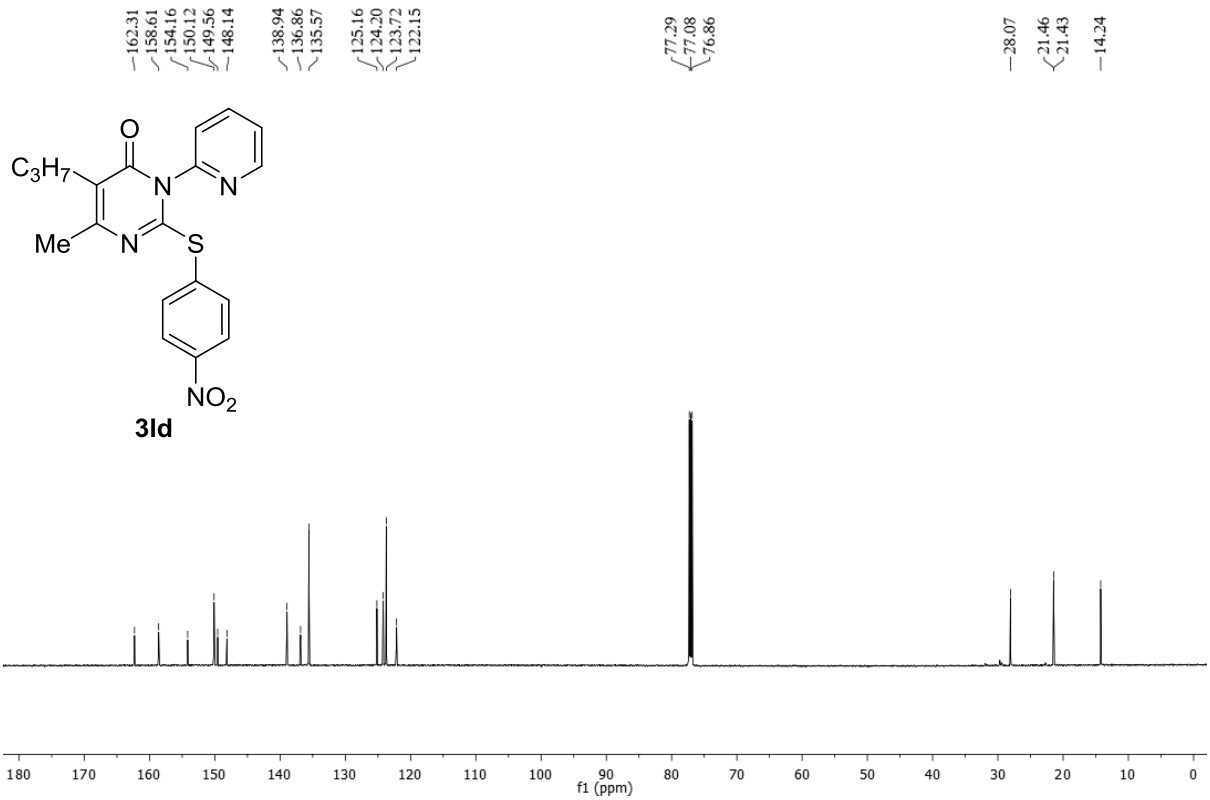

^{1}H NMR of **3lf** (300MHz, $CDCl_3$):

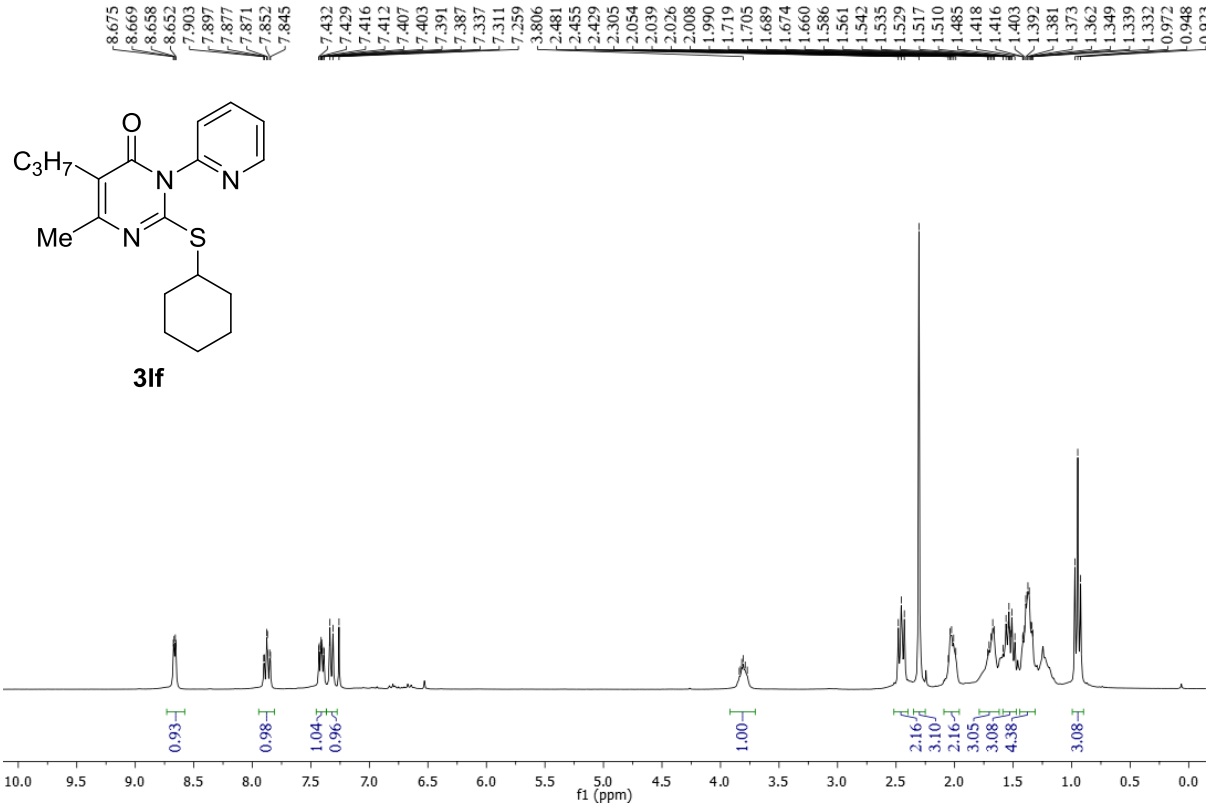

^{13}C NMR of **3lf** (75MHz, $CDCl_3$):

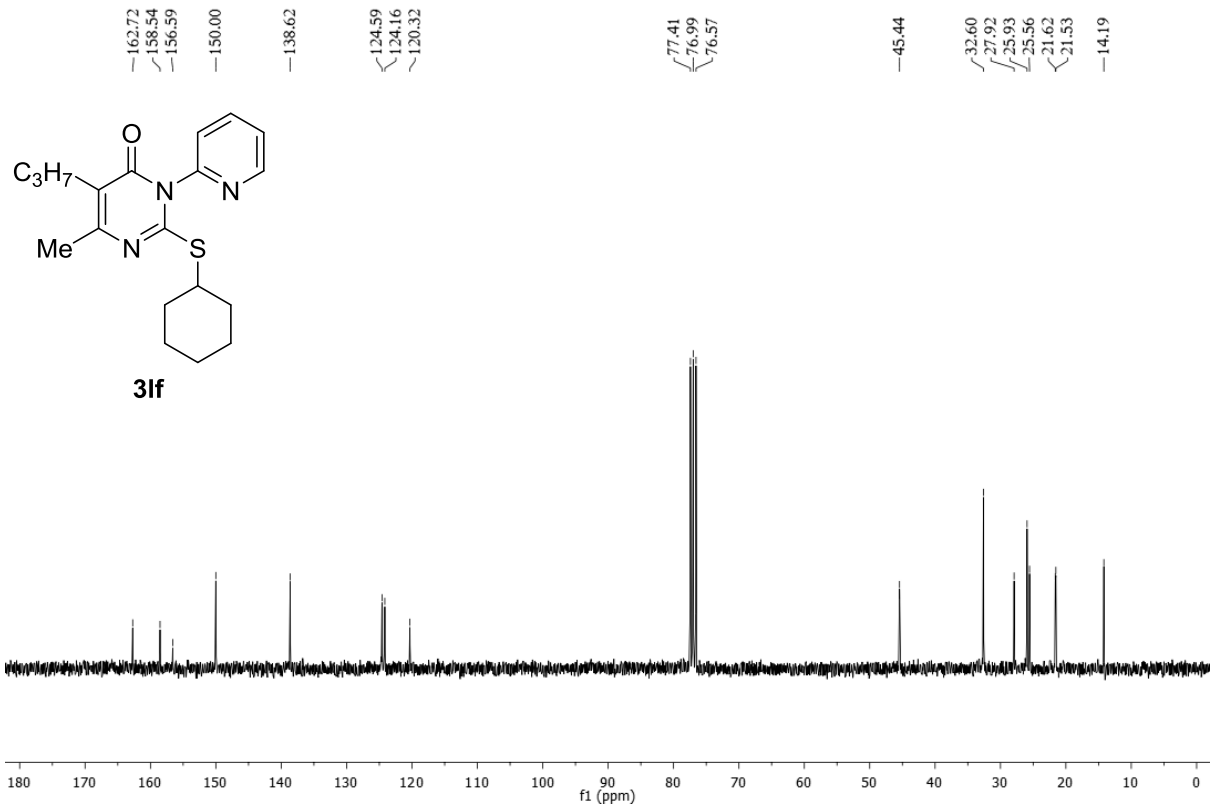

3.7. References

1. For representative examples of bioactive quinazolinones, see: (a) Ochiai, T.; Ishida, R. *Jpn. J. Pharmacol.* **1982**, *32*, 427. (b) Wolfe, J. F.; Rathman, T. L.; Sleevi, M. C.; Campbell, J. A.; Greenwood, T. D. *J. Med. Chem.* **1990**, *33*, 161. (c) Turcant, A.; Premel-Cabic, A.; Cailleux, A.; Allain, P. *Clin. Chem.* **1991**, *37*, 1210. (d) Jiang, S.; Zeng, Q.; Gettayacamin, M.; Tungtaeng, A.; Wannaying, S.; Lim, A.; Hansukjariya, P.; Okunji, C. O.; Zhu, S.; Fang, D. *Antimicrob. Agents Chemother.* **2005**, *49*, 1169. (e) Gunstone, R. F.; Shani, H. G. P.; Njemo, D.; Wing, A. J.; Sabuka, E. M. W. *Postgrad. Med. J.* **1971**, *47*, 789. (f) Jiang, J. B.; Hesson, D. P.; Dusak, B. A.; Dexter, D. L.; Kang, G. J.; Hamel, E. *J. Med. Chem.* **1990**, *33*, 1721. (g) Baek, D.-J.; Park, Y.-K.; Heo, H. I.; Lee, M.; Yang, Z.; Choi, M. *Bioorg. Med. Chem. Lett.* **1998**, *8*, 3287. (h) Rádl, S.; Hezky, P.; Proška, J.; Krejcí, I. *Arch. Pharm. Pharm. Med. Chem.* **2000**, *333*, 381. (i) Peet, N. P.; Baugh, L. E.; Sunder, S.; Lewis, J. E.; Matthews, E. H.; Olberding, E. L.; Shah, D. N. *J. Med. Chem.* **1986**, *29*, 2403. (j) Chao, Q.; Deng, L.; Shih, H.; Leoni, L. M.; Genini, D.; Carson, D. A.; Cottam, H. B. *J. Med. Chem.* **1999**, *42*, 3860.
2. For representative examples and reviews on application of organochalcogens, see: (a) Kaldor, S. W.; Kalish, V. J.; Davies, J. F.; Shetty, B. V.; Fritz, J. E.; Appelt, K.; Burgess, J. A.; Campanale, K. M.; Chirgadze, N. Y.; Clawson, D. K.; Dressman, B. A.; Hatch, S. D.; Khalil, D. A.; Kosa, M. B.; Lubbehusen, P. P.; Muesing, M. A.; Patick, A. K.; Reich, S. H.; Su, K. S.; Tatlock, J. H. *J. Med. Chem.* **1997**, *40*, 3979. (b) Gangjee, A.; Zeng, Y.; Talreja, T.; McGuire, J. J.; Kisliuk, R. L.; Queener, S. F. *J. Med. Chem.* **2007**, *50*, 3046. (c) Haque, M. A.; Hollister, W. S.; Willcox, A.; Canning, E. U. *J. Invertebr. Pathol.* **1993**, *62*, 171. (d) Collen, M. J.; Howard, J. M.; McArthur, K. E.; Raufman, J.-P.; Cornelius, M. J.; Ciarleglio, C. A.; Gardner, J. D.; Jensen, R. T. *Ann. Intern. Med.* **1984**, *100*, 52. (e) Mugesh, G.; du Mont, W.-W.; Sies, H. *Chem. Rev.* **2001**, *101*, 2125. (f) Chaudhary, S.; Umar, A.; Mehta, S. K. *Prog. Mater. Sci.* **2016**, *83*, 270. (g) Uetake, Y.; Niwa, T.; Hosoya, T. *Org. Lett.* **2016**, *18*, 2758. (h) Pan, F.; Wang, H.; Shen, P.-X.; Zhao, J.; Shi, Z.-J. *Chem. Sci.* **2013**, *4*, 1573. (i) Manjare, S. T.; Kim, Y.; Churchill, D. G. *Acc. Chem. Res.* **2014**, *47*, 2985.
3. (a) Converso, A.; Hartingh, T.; Garbaccio, R. M.; Tasber, E.; Rickert, K.; Fraley, M. E.; Yan, Y.; Kreatsoulas, C.; Stirdivant, S.; Drakas, B.; Walsh, E. S.; Hamilton, K.; Buser, C. A.; Mao, X.; Abrams, M. T.; Beck, S. C.; Tao, W.; Lobell, R.; Sepp-Lorenzino, L.; Zugay-Murphy, J.; Sardana, V.; Munshi, S. K.; Jezequel-Sur, S. M.; Zuck, P. D.;

Hartman, G. D. *Bioorg. Med. Chem. Lett.* **2009**, *19*, 1240. (b) Eskandariyan, Z.; Esfahani Zadeh, M.; Haj Mohammad Ebrahim Tehrani, K.; Mashayekhi, V.; Kobarfard, F. *Arch. Pharm. Res.* **2014**, *37*, 332. (c) Moussa, G.; Alaaeddine, R.; Alaeddine, L. M.; Nassra, R.; Belal, A. S. F.; Ismail, A.; El-Yazbi, A. F.; Abdel-Ghany, Y. S.; Hazzaa, A. *Eur. J. Med. Chem.* **2018**, *144*, 635.

4. For selected reviews and examples, see: (a) Szabó, Z.; Ősz, E.; Lóránd, T. *J. Biochem. Biophys. Methods* **2004**, *61*, 77. (b) Al-Rashood, S. T.; Aboldahab, I. A.; Nagi, M. N.; Abouzeid, L. A.; Abdel-Aziz, A. A. M.; Abdel-hamide, S. G.; Youssef, K. M.; Al-Obaid, A. M.; El-Subbagh, H. I. *Bioorg. Med. Chem.* **2006**, *14*, 8608. (c) Fakhari, A. R.; Hasheminasab, K.; Ahmar, H.; Alizadeh, A. *Synthesis* **2008**, *2008*, 3963. (d) Lygin, A. V.; de Meijere, A. *Org. Lett.* **2009**, *11*, 389. (e) Kim, H.; Lee, H.-J.; Kim, D.-P. *Angew. Chem. Int. Ed.* **2015**, *54*, 1877.

5. For selected reviews and examples, see: (a) Kondo, T.; Mitsudo, T.-a. *Chem. Rev.* **2000**, *100*, 3205. (b) Prim, D.; Campagne, J.-M.; Joseph, D.; Andrioletti, B. *Tetrahedron* **2002**, *58*, 2041. (c) Ley, S. V.; Thomas, A. W. *Angew. Chem. Int. Ed.* **2003**, *42*, 5400. (d) Hartwig, J. F. *Acc. Chem. Res.* **2008**, *41*, 1534. (e) Beletskaya, I. P.; Ananikov, V. P. *Chem. Rev.* **2011**, *111*, 1596. (f) Bates, C. G.; Gujadhur, R. K.; Venkataraman, D. *Org. Lett.* **2002**, *4*, 2803. (g) Xu, H.-J.; Zhao, Y.-Q.; Feng, T.; Feng, Y.-S. *J. Org. Chem.* **2012**, *77*, 2878. (h) Li, Y.; Pu, J.; Jiang, X. *Org. Lett.* **2014**, *16*, 2692.

6. For selected reviews and examples, see: (a) Iwasaki, M.; Nishihara, Y. *Dalton Trans.* **2016**, *45*, 15278. (b) Chen, X.; Hao, X.-S.; Goodhue, C. E.; Yu, J.-Q. *J. Am. Chem. Soc.* **2006**, *128*, 6790. (c) Tran, L. D.; Popov, I.; Daugulis, O. *J. Am. Chem. Soc.* **2012**, *134*, 18237. (d) Iwasaki, M.; Iyanaga, M.; Tsuchiya, Y.; Nishimura, Y.; Li, W.; Li, Z.; Nishihara, Y. *Chem. Eur. J.* **2014**, *20*, 2459. (e) Iwasaki, M.; Kaneshika, W.; Tsuchiya, Y.; Nakajima, K.; Nishihara, Y. *J. Org. Chem.* **2014**, *79*, 11330. (f) Yang, Y.; Hou, W.; Qin, L.; Du, J.; Feng, H.; Zhou, B.; Li, Y. *Chem. Eur. J.* **2014**, *20*, 416. (g) Yan, S.-Y.; Liu, Y.-J.; Liu, B.; Liu, Y.-H.; Shi, B.-F. *Chem. Commun.* **2015**, *51*, 4069. (h) Yang, K.; Wang, Y.; Chen, X.; Kadi, A. A.; Fun, H.-K.; Sun, H.; Zhang, Y.; Lu, H. *Chem. Commun.* **2015**, *51*, 3582. (i) Yan, S.-Y.; Liu, Y.-J.; Liu, B.; Liu, Y.-H.; Zhang, Z.-Z.; Shi, B.-F. *Chem. Commun.* **2015**, *51*, 7341. (j) Ye, X.; Petersen, J. L.; Shi, X. *Chem. Commun.* **2015**, *51*, 7863. (k) Lin, C.; Li, D.; Wang, B.; Yao, J.; Zhang, Y. *Org. Lett.* **2015**, *17*, 1328. (l) Lin, C.; Yu, W.; Yao, J.; Wang, B.; Liu, Z.; Zhang, Y. *Org. Lett.* **2015**, *17*, 1340. (m) Wang, X.; Qiu, R.; Yan, C.; Reddy, V. P.; Zhu, L.; Xu, X.; Yin, S.-F. *Org. Lett.* **2015**, *17*, 1970. (n) Qiu, R.; Reddy, V. P.; Iwasaki, T.; Kambe, N. *J. Org. Chem.* **2015**, *80*, 367.

(o) Zhu, L.; Cao, X.; Qiu, R.; Iwasaki, T.; Reddy, V. P.; Xu, X.; Yin, S.-F.; Kambe, N. *RSC Adv.* **2015**, *5*, 39358. (p) Müller, T.; Ackermann, L. *Chem. Eur. J.* **2016**, *22*, 14151. (q) Xie, W.; Li, B.; Wang, B. *J. Org. Chem.* **2016**, *81*, 396. (r) Gensch, T.; Klauck, F. J. R.; Glorius, F. *Angew. Chem. Int. Ed.* **2016**, *55*, 11287. (s) Gao, F.; Zhu, W.; Zhang, D.; Li, S.; Wang, J.; Liu, H. *J. Org. Chem.* **2016**, *81*, 9122. (t) Gandeepan, P.; Koeller, J.; Ackermann, L. *ACS Catal.* **2017**, *7*, 1030. (u) Yang, S.; Feng, B.; Yang, Y. *J. Org. Chem.* **2017**, *82*, 12430. (v) Maity, S.; Karmakar, U.; Samanta, R. *Chem. Commun.* **2017**, *53*, 12197. (w) Mandal, A.; Dana, S.; Sahoo, H.; Grandhi, G. S.; Baidya, M. *Org. Lett.* **2017**, *19*, 2430. (x) Ma, W.; Weng, Z.; Rogge, T.; Gu, L.; Lin, J.; Peng, A.; Luo, X.; Gou, X.; Ackermann, L. *Adv. Syn. Catal.* **2018**, *360*, 704. (y) Vats, T. K.; Mishra, A.; Deb, I. *Adv. Syn. Catal.* **2018**, *360*, 2291.

7. For representative examples, see: (a) Feng, Y.; Tian, N.; Li, Y.; Jia, C.; Li, X.; Wang, L.; Cui, X. *Org. Lett.* **2017**, *19*, 1658. (b) Lee, J. B.; Kang, M. E.; Kim, J.; Lee, C. Y.; Kee, J.-M.; Myung, K.; Park, J.-U.; Hong, S. Y. *Chem. Commun.* **2017**, *53*, 10394. (c) Garad, D. N.; Viveki, A. B.; Mhaske, S. B. *J. Org. Chem.* **2017**, *82*, 6366. (d) Feng, Y.; Li, Y.; Yu, Y.; Wang, L.; Cui, X. *RSC Adv.* **2018**, *8*, 8450. (e) Lou, M.; Deng, Z.; Mao, X.; Fu, Y.; Yang, Q.; Peng, Y. *Org. Biomol. Chem.* **2018**, *16*, 1851. (f) Bairy, G.; Das, S.; Begam, H. M.; Jana, R. *Org. Lett.* **2018**, *20*, 7107.
8. (a) Das, D.; Biswas, A.; Karmakar, U.; Chand, S.; Samanta, R. *J. Org. Chem.* **2016**, *81*, 842. (b) Das, D.; Poddar, P.; Maity, S.; Samanta, R. *J. Org. Chem.* **2017**, *82*, 3612.
9. (a) Li, J.; Ackermann, L. *Angew. Chem. Int. Ed.* **2015**, *54*, 3635. (b) Mishra, N. K.; Jeong, T.; Sharma, S.; Shin, Y.; Han, S.; Park, J.; Oh, J. S.; Kwak, J. H.; Jung, Y. H.; Kim, I. S. *Adv. Syn. Catal.* **2015**, *357*, 1293. (c) Yu, K.; Liang, Y.; Li, B.; Wang, B. *Adv. Syn. Catal.* **2016**, *358*, 661. (d) Mishra, A.; Vats, T. K.; Nair, M. P.; Das, A.; Deb, I. *J. Org. Chem.* **2017**, *82*, 12406.
10. Sughara, M.; Ukita, T. *Chem. Pharm. Bull.* **1997**, *45*, 719.

Chapter 4: Copper || Silylation

Copper-Catalyzed Direct sp^2 C–H Silylation of Arylamides Using Disilanes

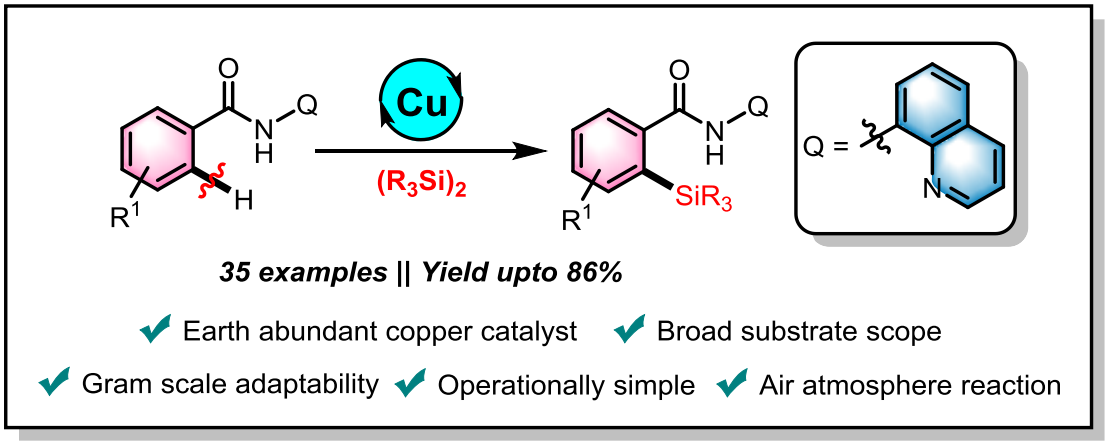

4.1. Introduction

4.1.1. Relevance of Silyl Functional Group Containing Compounds

C–Si bond formation is indispensable in synthetic organic chemistry by virtue of its unique physical, chemical, and bioactive properties. These inherent properties make them valuable building blocks and thus have numerous applications in organic chemistry.[1] Due to the easy transformability of organosilicon compounds into versatile organic functionalities through the different types of reactions, like cross-coupling[1c,d,i,n,p] or *ipso* substitution[1g,j] chemistry, they are considered to be valuable precursors for late-stage modifications in organic synthesis. Recently, their application in natural product synthesis has become a powerful tool in synthetic organic chemistry.[1c] Apart from their immense synthetic utility, organosilicon compounds have also found potential uses in the fields of material science and polymer chemistry.[2] Because of their low cost, high abundance and environmentally benign nature, they are often opted as suitable and readily acceptable components for preparing advanced materials and alternating copolymers.

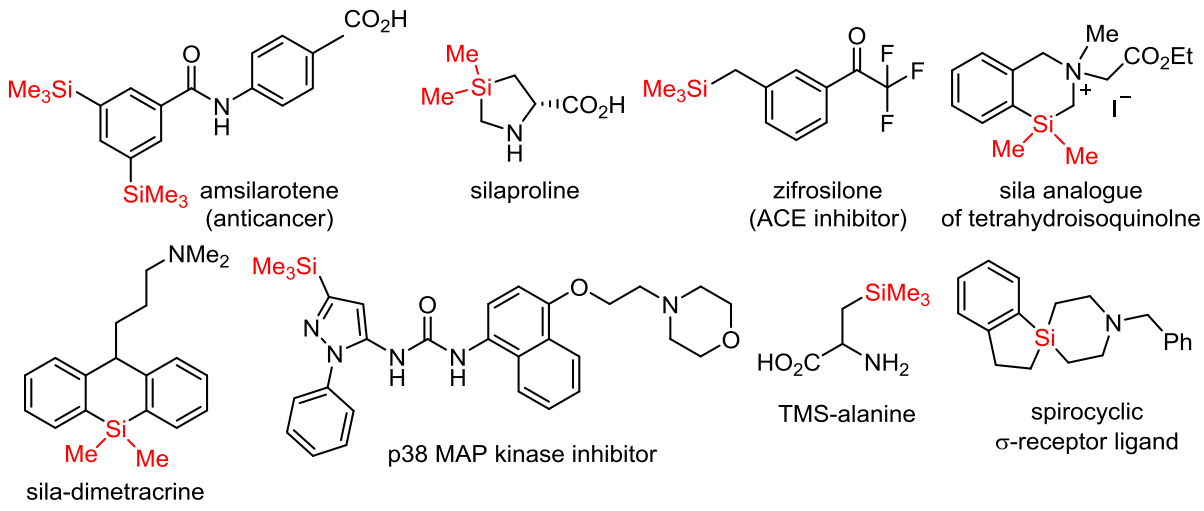

Figure 4.1.1.1. Representative examples of biologically relevant organosilicon compounds.

In the vivid research area of drug discovery, the incorporation of silicon groups in drug candidates have led to modified biological properties, hence a growing number of reports from medicinal chemistry studies have suggested the incorporation of silicon groups in diverse drug candidates.[3] From literature, many organosilicon compounds in therapeutically relevant molecules and medicinal chemistry have been found as depicted in Figure 4.1.1.1. Therefore, organosilicon compounds have found potential uses in the pharmaceutical industry.[4] Also, they have discovered their involvement in the agrochemical industry.[5]

4.1.2. Strategies For Transition Metal-Catalyzed C–Si bond Formation

These the enormous importance of the silyl functional group have led to the development of several methodologies to introduce silyl moiety in different organic frameworks. To this end, in recent years many research groups have made significant efforts towards the strategic installation of silyl groups into organic molecules. Conventional approaches of C–Si bond formation include transition metal-catalyzed (mostly Pd and Rh) coupling reactions between aryl or acyl halides with diverse organosilicon reagents.[6] On the other hand, transition metal-free techniques have also been exercised for the incorporation of silicon group in different organic molecules.[7] But these existing methods suffer from the viewpoints of pre-functionalized starting material requirement, poor selectivities, drastic reaction conditions, and costly organosilicon partners in some cases. To overcome these limitations, synthesis of organosilanes through transition metal-catalyzed direct C–H functionalization as compared to the traditional approaches, be it using metal catalyst or metal-free conditions, have emerged as the most demanded protocol from the perspective of atom-economy and high efficiency.[8] In addition, high abundance, low cost, and environmentally benign nature of silicon have also allowed the development of catalytic silylation methods via C–H bond activation.

In the past decades, major advances have been made in this field with second-row as well as third-row noble transition metals Ru,[9] Rh,[10] Ir,[11] Sc,[12] and Pt[13] as catalysts for the silylation of C(sp^2)–H as well as C(sp^3)–H bonds. Some of these methodologies utilized the directing group strategy whereas some of them were undirected silylation reactions employing various organosilicon partners like disilanes, silanes, etc. More recently, palladium catalysis entered the picture utilizing the directed C–H activation strategy for the direct silylation of both sp^2 and sp^3 C–H bonds (Scheme 4.1.2.1).[14] In 2014, Kuninobu and Kanai group disclosed the first palladium-catalyzed direct silylation of diverse benzamides and carboxamides with commercially available disilanes as silicon source with the aid of removable bidentate 8-aminoquinoline DG (Scheme 4.1.2.1a).[14a] Under the same reaction conditions, germanylation was also successful with digermanes. Following this pioneering work, Zhao and co-workers utilized oxalyl amide functional group as a potent DG for direct *ortho*-silylation and germanylation of phenylmethanamines and phenethylamines with disilanes (Scheme 4.1.2.1b).[14b] In 2016, the first Pd-catalyzed silylation methodologies of both primary and secondary aliphatic β-C(sp^3)–H bonds with readily available hexamethyl disilane were devised independently by the groups of Zhang and Shi giving access to a wide array of organosilanes

(Scheme 4.1.2.1c, 4.1.2.1.d).[14c,d] Direct silylation of aliphatic C–H bonds was next impressively extended to distal γ-C(sp^3)–H silylation by Maiti *et al*. employing Pd(II) catalysis in a highly regioselective fashion (Scheme 4.1.2.1e).[14e] DFT studies along with isolation of a Pd(II) intermediate and other detailed mechanistic experiments were performed to have a thorough understanding of the reaction mechanism.

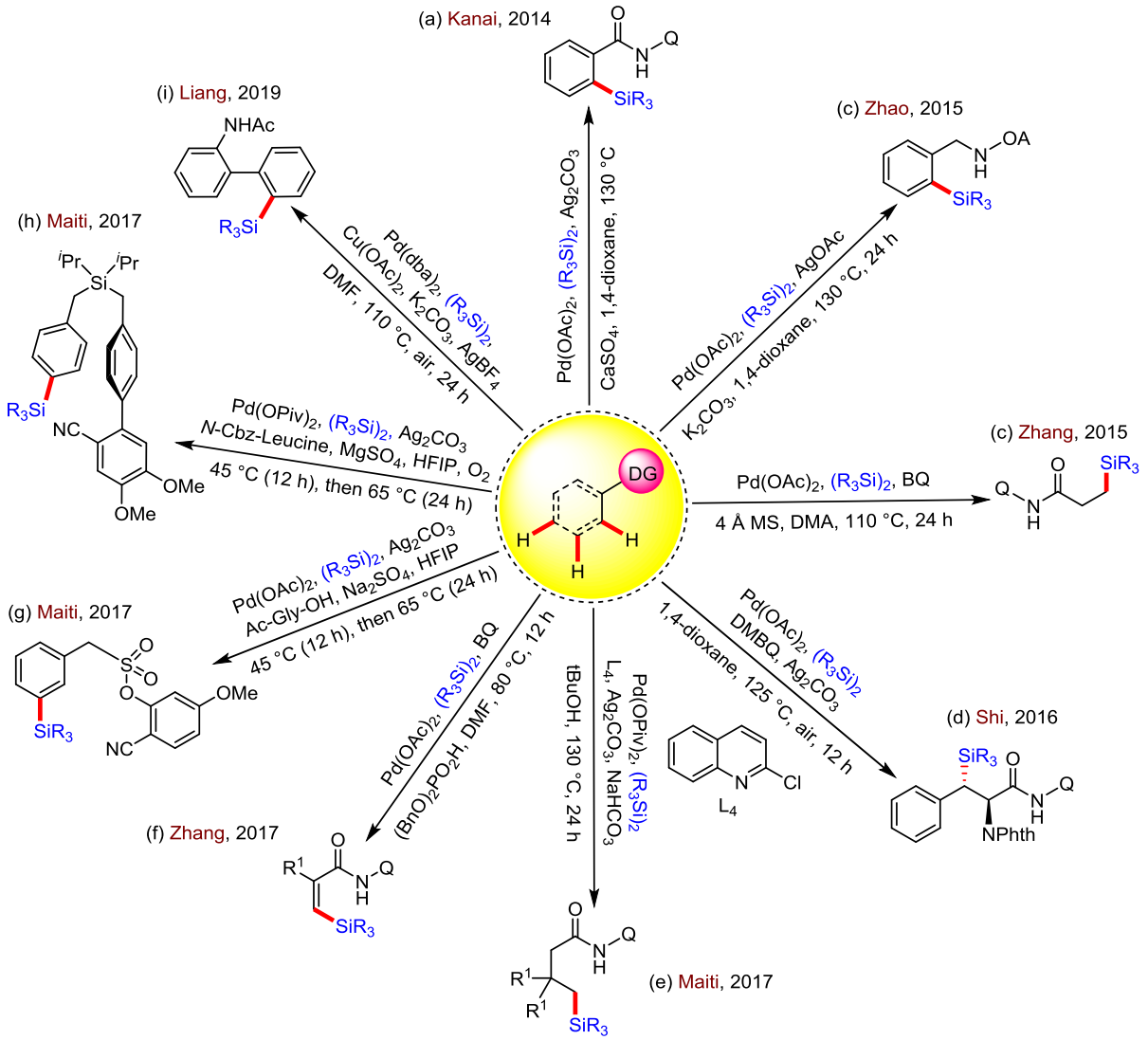

Scheme 4.1.2.1. DG-assisted Pd-catalyzed direct C–H silylation reactions.

In 2017, Zhang group demonstrated an efficient Pd-catalyzed intermolecular silylation protocol of vinylic sp^2 C–H bonds with disilanes affording *Z*-vinyl silanes excluisively in a regio- and stereoselective fashion (Scheme 4.1.2.1f).[14f] Apart from *ortho* C–H silylation, Maiti and Liu made spectacular breakthroughs in unprecedented regioselective *meta* and *para* C–H silylation techniques employing palladium catalysis (Scheme 4.1.2.1g, 4.1.2.1h).[14g,h] These distal positions which are otherwise difficult to functionalize, were made possible to react with the

help of judiciously designed directing templates suitable for remote C–H bond activation. In 2019, Yang *et al.* devised another Pd-catalyzed approach for the synthesis divergent silicon-containing 1,1′-biaryl-2-acetamides which relies on the use of norbornene (NBE) derivatives as a reactivity switch for *ortho* or *meta* C–H silylation to take place (Scheme 4.1.2.1i).[14i]

All these previous reports, despite their efficacy use transition metal catalysts that suffer from significant drawbacks such as low earth abundance, high cost and bio-incompatibility. Naturally this demands for developing catalytic silylation routes using a complimentary more effective, earth-abundant, and cost-efficient 3d transition metal. Therefore, a first-row transition metal-catalyzed direct C–H silylation method is highly solicited in organic synthesis. In this realm, copper is a universally accepted earth-abundant transition metal possessing tremendous potency in the selective functionalization of directed C–H bonds well explored by diverse research groups.[15] The high bench stability and low cost of copper salts allow them to be used in both stoichiometric and more preferably in a catalytic fashion. Complimentarily, the catalytic reactivity and efficacy of copper catalysts is commendable as compared to the noble transition metal catalysts, especially palladium. Henceforth, we envisioned that copper catalysis might be convenient for this transformation and a methodology for the generation of C–Si bond in a catalytic fashion rather than stoichiometric is highly coveted.

4.1.3. 8-Aminoquinoline Directing Group in C–H Activation

As discussed in chapter 2 (Section 2.1.3), 8-aminoquinoline (8-AQ) is a versatile bidentate directing group for regioselective sp^2 and sp^3 C–H functionalization employing different transition metal catalysts, like Pd, Ru, Rh, Cu, Co, Fe, Ni, which is well explored by various research groups all over the world.[8c,14a,14c-f,15a,15f-h,k,15n-r,16] The easy installation and removable nature of this moiety also provides an added advantage for the diverse synthetic manipulations performed. For example, some of the notable works using this DG are depicted in Scheme 4.1.3.1. In 2005, representing one of the pioneering research works in the field of C–H activation, Daugulis first introduced the use 8-aminoquinoline as an efficient auxiliary which serves as a directing group for regioselective C–H functionalization. They reported a palladium-catalyzed regioselective C–H arylation of aliphatic as well as aromatic amides using aryl iodides assisted by 8-AQ directing group (Scheme 4.1.3.1a).[16d] After a long gap, Ru catalysis was employed by Chatani and co-workers for *ortho* selective arylation of 8-AQ tethered aromatic amides with aryl bromides (Scheme 4.1.3.1b).[16e] It was observed from Hammett calculations that presence of electron-withdrawing groups on the arylamides

facilitated the reaction, whereas aryl bromides bearing both electron-donating as well as electron-withdrawing groups accelerated the reaction. The same group described a strategy for regioselective alkylation of benzamides containing 8-AQ chelating moiety with a series of α,β-unsaturated carbonyl compounds under rhodium-catalyzed conditions (Scheme 4.1.3.1c).[16f]

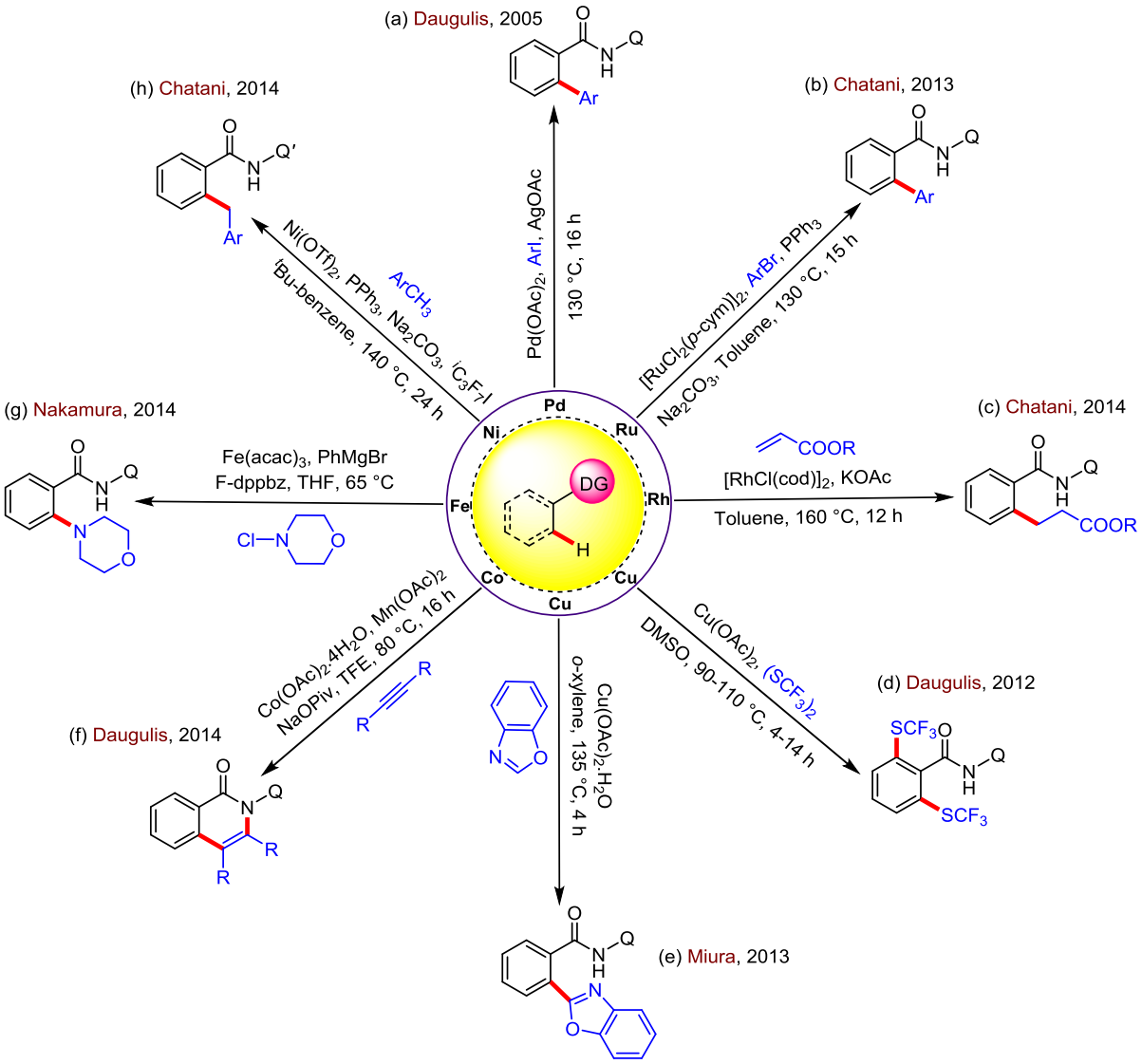

Scheme 4.1.3.1. Representative examples of 8-aminoquinoline DG-assisted transition metal-catalyzed C–H functionalization reactions.

8-aminoquinoline auxiliary has also been fruitfully employed in C–H functionalization reactions under base metal catalysis. In 2012, Daugulis *et al*. demonstrated a copper-promoted 8-AQ directed β-sp^2 C–H trifluoromethylsulfenylation and sulfenylation of benzoic acid derivatives using disulfide reagents (Scheme 4.1.3.1d).[16h] Following year, Miura group established a direct heterobiaryl coupling strategy between 8-aminoquinoline based benzamides and 1,3-azoles under copper-mediated conditions (Scheme 4.1.3.1e).[15g] In 2014,

Daugulis and co-workers again reported a cobalt-catalyzed alkenylation/annulation of 8-AQ tethered arylamides with both internal as well as terminal alkynes with good yields and high functional group tolerance (Scheme 4.1.3.1f).[16i] Concurrently, Nakamura *et al*. delineated an iron/diphosphine-catalyzed *ortho* amination of arenes possessing 8-AQ chelating group with *N*-chloroamines and *N*-benzoyloxyamines furnishing anthranilic acid derivatives (Scheme 4.1.3.1g).[16j] In the same year, Chatani group discovered a C(sp^2)–H/C(sp^3)–H oxidative coupling protocol for Ni(II)-catalyzed *ortho* benzylation of modified 8-aminoquinoline directed aromatic amides with toluene derivatives using heptafluoroisopropyl iodide as oxidant (Scheme 4.1.3.1h).[16l] Despite all these unique methodologies, catalytic silylation of arenes directed by a bidentate DG like 8-AQ employing first-row transition metal catalysis was yet to be unearthed to the best of our knowledge.

4.2. Objective

The omnipresence of silyl functional group in various fields of science such as pharmaceutical and drug industry, polymer industry, material science industry, as well as the transformative nature of this group to other functionalities makes it a universal target for its incorporation in different molecules. In this realm, chemists over the past decades have been successful in many ways but recently, transition metal-catalyzed direct C–H silylation technique has been the go-to target. Literature reports show methodologies predominantly involving Pd catalysis on bidentate directing groups. Apart from that, there are very few reports on silylation reactions with other noble transition metal catalysts. More importantly, a direct and efficient C–H silylation reaction employing first-row transition metal catalysis was not known till that time. So, we envisioned that a cheap, environmentally benign and earth-abundant first-row transition metal catalyst can be utilized for developing a complementary silylation method. Inspired by the pioneering works depicted above and to harness the potential of copper catalysis for this task, we, therefore, explored a simple copper-catalyzed *ortho* selective direct silylation of carboxamides assisted by 8-aminoquinoline DG using disilanes as organosilicon source under air atmosphere (Scheme 4.2.1).

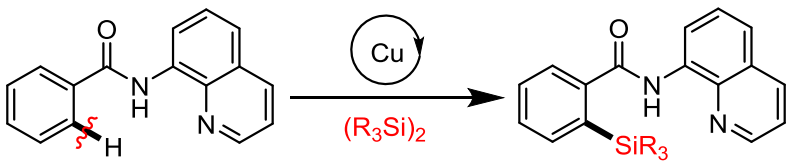

Scheme 4.2.1. Objective of this work: copper-catalyzed sp^2 C–H silylation of benzamides.

4.3. Results and Discussion

4.3.1. Optimization Studies

We started off our optimization studies with 2-methyl-*N*-(quinolin-8-yl)benzamide (**1a**) as the model substrate and hexamethyldisilane (HMDS, **2a**) as the silyl partner (Table 4.3.1.1). To our delight, with 2.0 equiv of HMDS, the desired product 2-methyl-*N*-(quinolin-8-yl)-6-(trimethylsilyl)benzamide (**3a**) was obtained in 27% yield in presence of 20 mol % of $Cu(OAc)_2$ catalyst and 1.5 equiv of Ag_2CO_3 oxidant in DMF solvent at 120 °C for 21 h under N_2 atmosphere (Table 4.3.1.1, entry 1). A thorough screening of different polar, as well as nonpolar protic and aprotic solvents displayed a diminishing effect with either poor yields in DMA and 1,4-dioxane, or no reaction in DMSO, MeCN, and DCE (Table 4.3.1.1, entries 2-6), keeping DMF as our solvent of choice. An increased amount of Ag_2CO_3 led to a slight decrease in the yield of the reaction (Table 4.3.1.1, entry 7). So, we continued with 1.5 equiv of the silver oxidant. In order to better the yield, we surveyed a string of additives in the reaction, *viz.* CsF, KF, $MgSO_4$, Na_2SO_4, $CaSO_4$, K_2CO_3 (Table 4.3.1.1, entries 8-13). Gratifyingly, on using 2.0 equiv of $MgSO_4$ there was a significant uplift in the yield of the silylation product furnishing **3a** in 51% yield (Table 4.3.1.1, entry 10).

Next, we turned our attention to investigate the effect of several oxidants, but none of the metal or non-metal-based oxidants resulted in an enhancement of the yield (Table 4.3.1.1, entries 14-16). So, Ag_2CO_3 remained the best oxidant for this protocol. Following this, an array of other Cu catalysts was screened (Table 4.3.1.1, entries 17-19) but all of these had detrimental effect on the yield of the reaction. So, we stayed on with $Cu(OAc)_2$ as our prime catalyst for the present reaction. An elevated amount of the $MgSO_4$ (3.0 equiv) did not result in an increased yield of the reaction (Table 4.3.1.1, entry 20), thus the additive amount was fixed to 2.0 equiv. To enhance the efficiency of the reaction, when the loading of HMDS was increased to 5.0 equiv, the yield of **3a** went up to 56% (Table 4.3.1.1, entry 21). Further increase to 10.0 equiv of HMDS notched up the yield of the silylation product to 70% (Table 4.3.1.1, entry 22). Thereafter, we continued the optimization with 10.0 equiv of **2a**. We also wanted to check if commonly used monodentate and bidentate ligands (PPh_3 and 1,10 phen) had an advantageous effect on this reaction, but no improvements in the yield was observed. Rather, the yields declined which led us to conclude that ligands had no effect on the current protocol (Table 4.3.1.1, entries 23-24). To our curiosity, when the catalyst loading was decreased from 20 mol % to 10 mol %, the yield of the silylated product was marginally bettered (Table 1, entry 25). Therefore, we moved forward with 10 mol % $Cu(OAc)_2$.

Table 4.3.1.1. Optimization of reaction conditions[a]

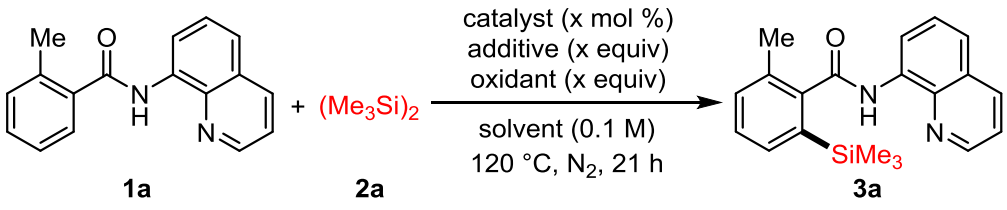

1a **2a** **3a**

entry	catalyst (x mol %)	additive (x equiv)	oxidant (x equiv)	solvent (0.1 M)	yield of **3a**[b] (%)
1	$Cu(OAc)_2$ (20)	-	Ag_2CO_3 (1.5)	DMF	27
2	$Cu(OAc)_2$ (20)	-	Ag_2CO_3 (1.5)	DMSO	nr
3	$Cu(OAc)_2$ (20)	-	Ag_2CO_3 (1.5)	MeCN	nr
4	$Cu(OAc)_2$ (20)	-	Ag_2CO_3 (1.5)	DMA	16
5	$Cu(OAc)_2$ (20)	-	Ag_2CO_3 (1.5)	1,4-Dioxane	7
6	$Cu(OAc)_2$ (20)	-	Ag_2CO_3 (1.5)	DCE	nr
7	$Cu(OAc)_2$ (20)	-	Ag_2CO_3 (2.0)	DMF	20
8	$Cu(OAc)_2$ (20)	CsF (2.0)	Ag_2CO_3 (1.5)	DMF	nr
9	$Cu(OAc)_2$ (20)	KF (2.0)	Ag_2CO_3 (1.5)	DMF	nr
10	$Cu(OAc)_2$ (20)	$MgSO_4$ (2.0)	Ag_2CO_3 (1.5)	DMF	51
11	$Cu(OAc)_2$ (20)	Na_2SO_4 (2.0)	Ag_2CO_3 (1.5)	DMF	29
12	$Cu(OAc)_2$ (20)	$CaSO_4$ (2.0)	Ag_2CO_3 (1.5)	DMF	19
13	$Cu(OAc)_2$ (20)	K_2CO_3 (2.0)	Ag_2CO_3 (1.5)	DMF	nr
14	$Cu(OAc)_2$ (20)	$MgSO_4$ (2.0)	Ag_2SO_4 (1.5)	DMF	34
15	$Cu(OAc)_2$ (20)	$MgSO_4$ (2.0)	NMO (1.5)	DMF	nr
16	$Cu(OAc)_2$ (20)	$MgSO_4$ (2.0)	$Mn(OAc)_2.4H_2O$ (1.5)	DMF	nr
17	$CuBr_2$ (20)	$MgSO_4$ (2.0)	Ag_2CO_3 (1.5)	DMF	8
18	CuF_2 (20)	$MgSO_4$ (2.0)	Ag_2CO_3 (1.5)	DMF	7
19	CuO (20)	$MgSO_4$ (2.0)	Ag_2CO_3 (1.5)	DMF	nr
20	$Cu(OAc)_2$ (20)	$MgSO_4$ (3.0)	Ag_2CO_3 (1.5)	DMF	49
21[c]	$Cu(OAc)_2$ (20)	$MgSO_4$ (2.0)	Ag_2CO_3 (1.5)	DMF	56
22[d]	$Cu(OAc)_2$ (20)	$MgSO_4$ (2.0)	Ag_2CO_3 (1.5)	DMF	70
23[d,e]	$Cu(OAc)_2$ (20)	$MgSO_4$ (2.0)	Ag_2CO_3 (1.5)	DMF	51
24[d,f]	$Cu(OAc)_2$ (20)	$MgSO_4$ (2.0)	Ag_2CO_3 (1.5)	DMF	20
25[d]	$Cu(OAc)_2$ (10)	$MgSO_4$ (2.0)	Ag_2CO_3 (1.5)	DMF	72
26[d,g]	$Cu(OAc)_2$ (10)	$MgSO_4$ (2.0)	Ag_2CO_3 (1.5)	DMF	69
27[d,h]	$Cu(OAc)_2$ (10)	$MgSO_4$ (2.0)	Ag_2CO_3 (1.5)	DMF	68
28[d,i]	$Cu(OAc)_2$ (10)	$MgSO_4$ (2.0)	Ag_2CO_3 (1.5)	DMF	74
29[d,i]	-	$MgSO_4$ (2.0)	Ag_2CO_3 (1.5)	DMF	nr
30[d,i]	$Cu(OAc)_2$ (10)	$MgSO_4$ (2.0)	-	DMF	nr
31[d,i,j]	**$Cu(OAc)_2$ (10)**	**$MgSO_4$ (2.0)**	**Ag_2CO_3 (1.5)**	**DMF**	**88 (86)[k]**
32[d,i,l]	$Cu(OAc)_2$ (10)	$MgSO_4$ (2.0)	Ag_2CO_3 (1.5)	DMF	74

[a]Reaction condition: Unless otherwise mentioned, substrate **1a** (0.1 mmol, 1.0 equiv), **2a** (2.0 equiv), catalyst (x mol %), oxidant (x equiv), additive (x equiv), and solvent (1.0 mL, 0.1 M) at 120 °C under N_2 for 21 h. [b]Isolated yield. [c]**2a** (5.0 equiv), [d]**2a** (10.0 equiv), [e]PPh_3 (0.4 equiv), [f]1,10-phen (0.2 equiv), [g]140 °C, [h]100 °C, [i]Under air atmosphere, [j]Reaction run for 36 h. [k]Yield for 0.2 mmol scale. [l]Reaction run for 48 h. nr: no reaction.

Elevated and subdued reaction temperatures gave similar yields for the silylated product **3a** (Table 4.3.1.1, entries 26-27), so we continued with 120 ℃ as the optimum reaction temperature. When we removed the inert condition and subjected our reaction to air atmosphere, to our pleasure there was no drop in the yield of the reaction, in fact a slight increase up to 74% was observed (Table 4.3.1.1, entry 28). Control experiments proved the pivotal roles played by the copper catalyst and silver oxidant (Table 4.3.3.1, entries 29-30) for the silylation reaction, since without them there was no formation of the desired product **3a**. Again, on continuing the reaction up to 36 h, there was a noteworthy rise in the yield of the reaction up to 88% (Table 4.3.1.1, entry 31), which also proved to be our optimized reaction condition for the present methodology. It was confirmed by performing the reaction in 0.2 mmol scale delivering **3a** in 86% yield. A further longer reaction time up to 48 h led to slightly diminished yields (Table 4.3.1.1, entry 32). As evident from literature precedents which requires super-stoichiometric amounts of disilanes as reaction partner for effective silylation of unactivated C–H bonds,[12] the present methodology also asked for excess amount of disilanes. This might be due to the lesser reactivity of strong non-polar Si–Si bond, since in case of substrate scope with disilanes like $(PhMe_2Si)_2$ and $(Ph_2MeSi)_2$, they remained unreacted in considerable amounts, discussed in the next section.

4.3.2. Scope of the Reaction

All the benzamides (**1**) (Table 2.3.2.1, Chapter 2) were prepared following the literature procedure, discussed in the experimental section. Some substrates (**1g-1n**, **1t-1aa**) were prepared by Suzuki cross-coupling method (Table 2.3.2.2, Chapter 2) following the literature procedure, discussed in the experimental section. Deuterated starting material **1a**-d_1 was also prepared according to the literature procedure, discussed in the experimental section.

After the preparation of the substituted benzamides (**1**), they were subjected to silylation under the optimized condition to check the generality and limitations of the reaction (Table 4.3.2.1). Overall, it was prevalent that *ortho* position of the benzamides had to be substituted in all cases, otherwise the outcome of the reaction was not very fruitful. To generalise, it was observed that the reactivity of both *para*-substituted electron-donating and electron-withdrawing groups was slightly more efficient than that of the *meta*-substituted amides. Various functional groups like Me, OMe, F, Cl, Br, CF_3, ^{t}Bu were all well tolerated. We started off by examining the *meta*-substituted amides of corresponding *o*-toluic acid (**1b**-**1f**). It was found that electron-donating groups such as Me and OMe gave the desired products **3b** and **3c** in high yields (73% and 78%

respectively); in case of electron-withdrawing substituent like fluoro, the silylated product **3d** was obtained in a very good yield of 75%, while chloro and bromo substituents furnished the corresponding products **3e** and **3f** in moderate yields (54% and 37% respectively). Various aryl groups decorated with both electron-rich and electron-deficient substituents such as Me, OMe, ^{t}Bu, F, Cl, CF_3 (**1g**-**1n**) at this position showed moderate to satisfactory conversion with yields ranging between 36%-50%. When we investigated the reactivity of different substituents at the *para* position featuring electron-donating methyl, methoxy groups (**1o**-**1p**) and electron-withdrawing fluoro, chloro, bromo (**1q**-**1s**), all of them were well tolerated delivering their respective silylated products (**3o**-**3s**) in moderate to high yields (up to 82% yield). In a similar manner, on moving to different aryl groups at this position bearing diverse substituents such as Me, OMe, ^{t}Bu, F, Cl, CF_3, they showed good conversion delivering the products (**3t**-**3aa**) in the range of 45%-71% yields.

Till now, we tested the substrate scope with methyl substituent at *ortho* position of the benzamides, but on changing it to phenyl, ethyl and isopropyl groups (**1ab**-**1ad**), it was revealed that the desired products (**3ab**-**3ad**) were obtained in satisfactory yields (31-57% yields). Notably the current protocol also tolerated the challenging heterocyclic thiophene substrate **1af**, but the yield turned out to be poor (**3af**, 15%). But when unsubstituted benzamide **1ag** was subjected under the standard reaction condition, only mono silylated product **3ag** was formed in a mere 11% yield showing the limitation of this method to *ortho*-substituted benzamides. The reason behind this could be the better chelating property of the substrate with the catalyst for facile C–H activation when an *ortho* substituent is present.

Next, we pursued to inspect the scope of other organosilicon sources. Using relatively sterically hindered disilanes $(Me_2PhSi)_2$ and $(MePh_2Si)_2$ in place of $(Me_3Si)_2$, moderate to good conversion was seen, affording the corresponding silylated products **3ah** and **3ai** in 67% and 47% yields respectively. Very interestingly, the current silylation reaction worked successfully with a sp^3 variant aliphatic benzamide at the β-position under the optimized condition, although with a paltry yield (**3ai**, 13%). The 1-naphthyl variant was regioselectively silylated at 2-position (**S3a**) with a below par yield of 20%. Only *meta*-substituted benzamide with electron-donating methyl substituent produced its silylated product (**S3b**) in a poor 14% yield, whereas that containing electron-withdrawing fluoro substituent furnished trace amounts of the silylated analogue (**S3d**). These evidences again surmised the requirement for an *ortho* substituent in the benzamide substrate for a better reaction. Moreover, the present reaction conditions could also promote the silylation of olefinic carboxamide, but not in an efficient manner giving a

mere 12% yield of the product (**S3c**). These promising results showcased the capability of copper catalysis in sp^3 and sp^2 olefinic silylation of 8-AQ assisted carboxamides for getting enhanced yields which is being investigated in our laboratory.

Table 4.3.2.1. Scope of silylation of arylamides[a]

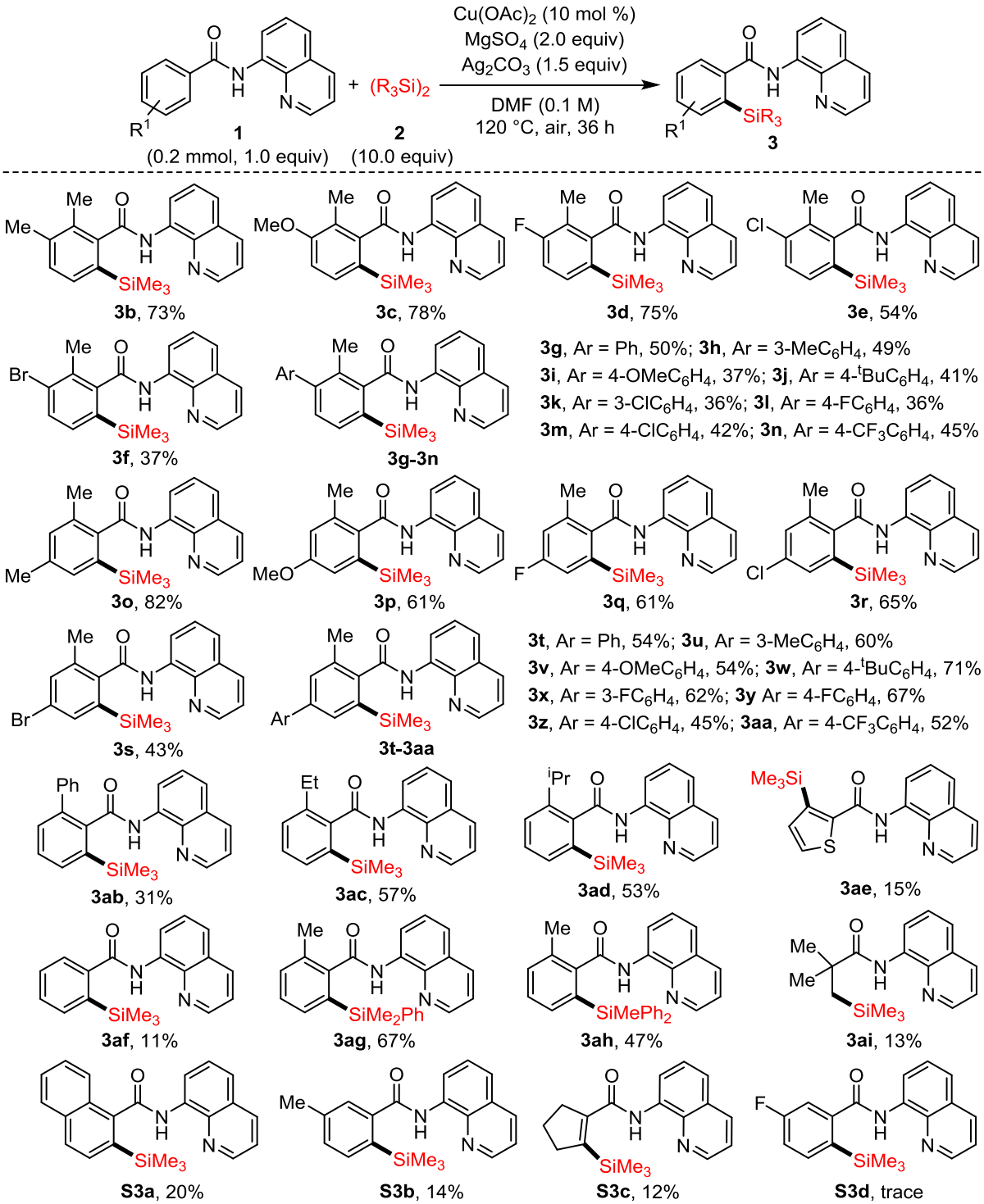

[a]Reaction condition: Unless otherwise mentioned, **1** (0.2 mmol, 1.0 equiv), **2** (10.0 equiv), $Cu(OAc)_2$ (10 mol %), $MgSO_4$ (2.0 equiv), Ag_2CO_3 (1.5 equiv) in DMF (2.0 mL) at 120 °C for 36 h under air.

All the silylated products (**3**) were duly characterised by ^{1}H, ^{13}C NMR and HRMS. Single-crystal X-ray analysis of **3a**, **3b**, **3c**, **3d**, **3e**, **3q**, **3s**, **3t**, **3ac** and **3ag** further confirmed their structures (Figure 4.3.2.1).

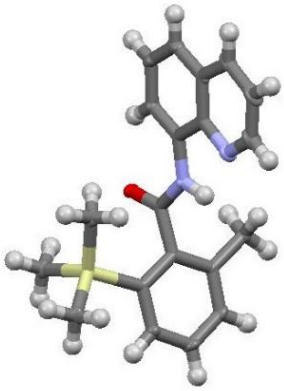

3a
CCDC No. 2054613

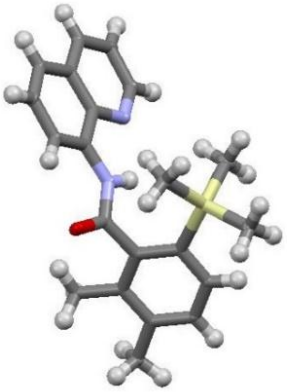

3b
CCDC No. 2054616

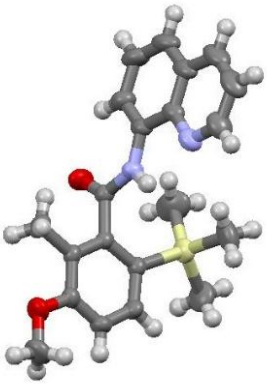

3c
CCDC No. 2054617

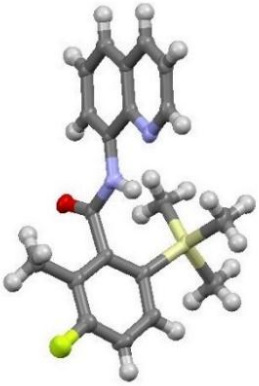

3d
CCDC No. 2054618

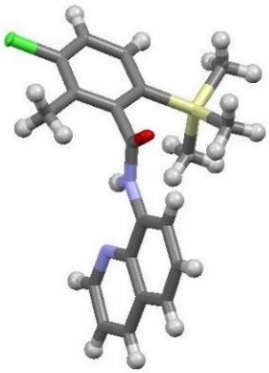

3e
CCDC No. 2054619

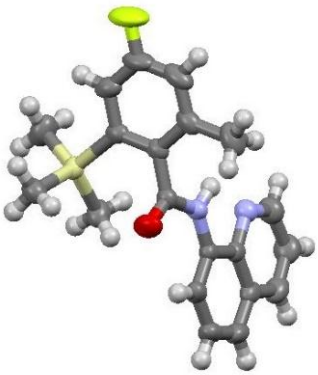

3q
CCDC No. 2054620

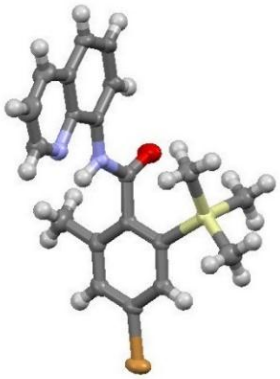

3s
CCDC No. 2054621

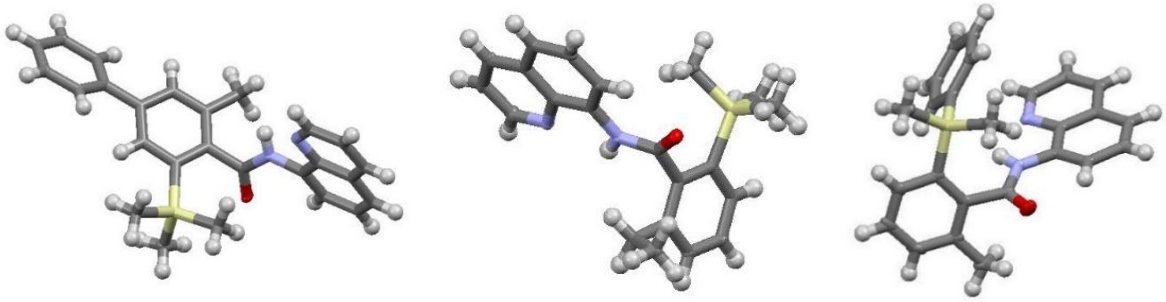

3t
CCDC No. 2054622

3ac
CCDC No. 2054614

3ag
CCDC No. 2054615

Figure 4.3.2.1. X-ray crystal structures of **3a**, **3b**, **3c**, **3d**, **3e**, **3q**, **3s**, **3t**, **3ac** and **3ag** (ellipsoid contour at 50% probability level).

A few substrates which did not fare well under the standard reaction conditions and failed to deliver the desired products are represented in Figure 4.3.2.2. Olefinic carboxamides did not provide the corresponding silylated products **S3e** and **S3f** probably due to weak coordinating properties of the olefinic sp^2 C–H bond with the copper catalyst. Other heterocyclic variants, *viz*. furan and benzofuran based carboxamides could not be silylated (**S3g** and **S3h**) under the present catalytic condition possibly because of electronic reasons. On the disilane side, bulky hexaphenyl disilane did not furnish the desired silylated benzamide (**S3i**) probably on account of steric reasons.

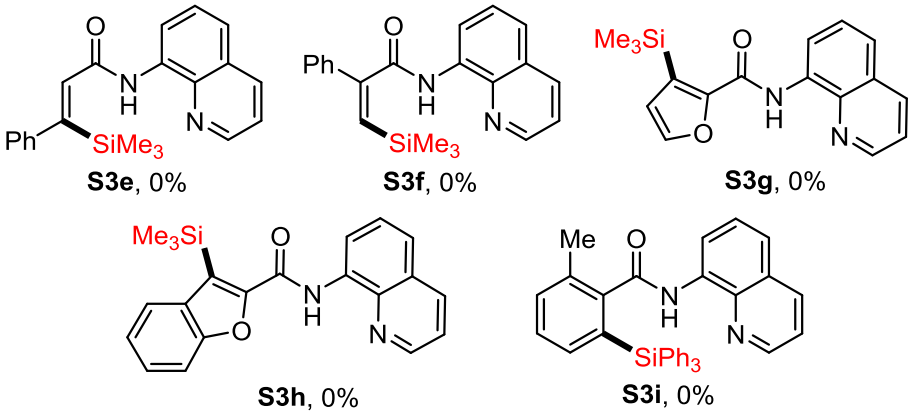

Figure 4.3.2.2. List of failed substrates.

Also, we attempted the present silylation reaction on various commonly used bidentate DG attached substrates (**I-VI**) in the field of C–H activation. But either they showed poor conversion or did not participate under the optimized condition (Figure 4.3.2.3). Substrate **VI** did not undergo the reaction, thus emphasizing the fact that bidentate coordination takes place between the substrate and copper catalyst before the occurrence of the C–H activation step.

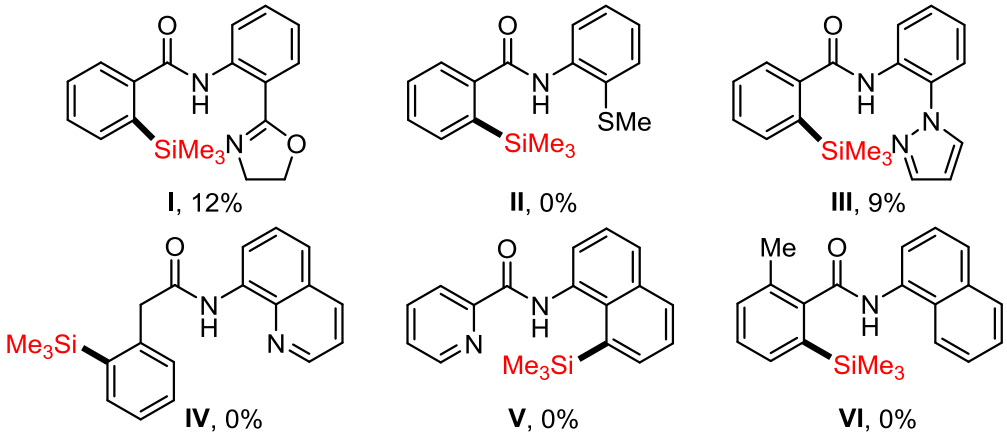

Figure 4.3.2.3. List of unsuccessful bidentate DG attached substrates.

4.3.3. Gram-Scale Reaction

To illustrate the effectiveness of this catalytic process and broaden the synthetic utility of the methodology, a gram-scale reaction was conducted under standard condition using 1.0 g of **1a** (3.8 mmol) with HMDS (**2a**), and the desired product **3a** was obtained in an impressive 79% yield (1.0 g) (Scheme 4.3.3.1).

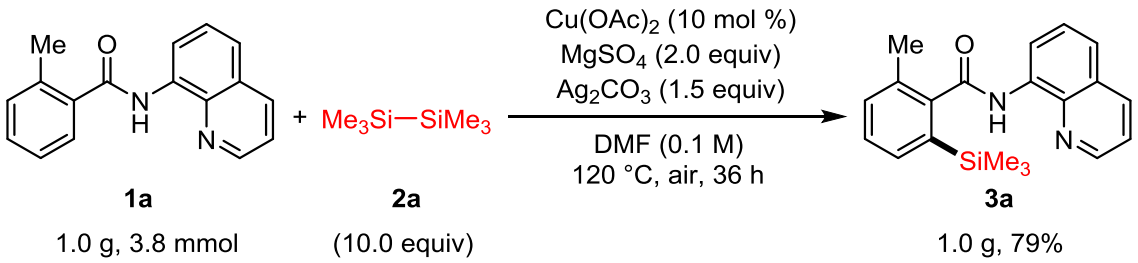

Scheme 4.3.3.1. Gram-scale reaction.

4.3.4. Mechanistic Experiments and Plausible Mechanism

In order to gain an insight to the reaction mechanism and catalytic cycle of the silylation reaction, few kinetic experiments were performed.

First, H/D exchange experiment was conducted with the parent benzamide **1a** (Scheme 4.3.4.1a). When **1a** was subjected to the standard conditions in absence of HMDS and quenched with excess CD_3OD, no deuterium-proton exchange was observed in the recovered starting material. ^1H NMR study showed <5% D-incorporation in case of **1a**-d_n (Figure 4.3.4.1). The result suggested that the C–H bond cleavage step is irreversible in nature.

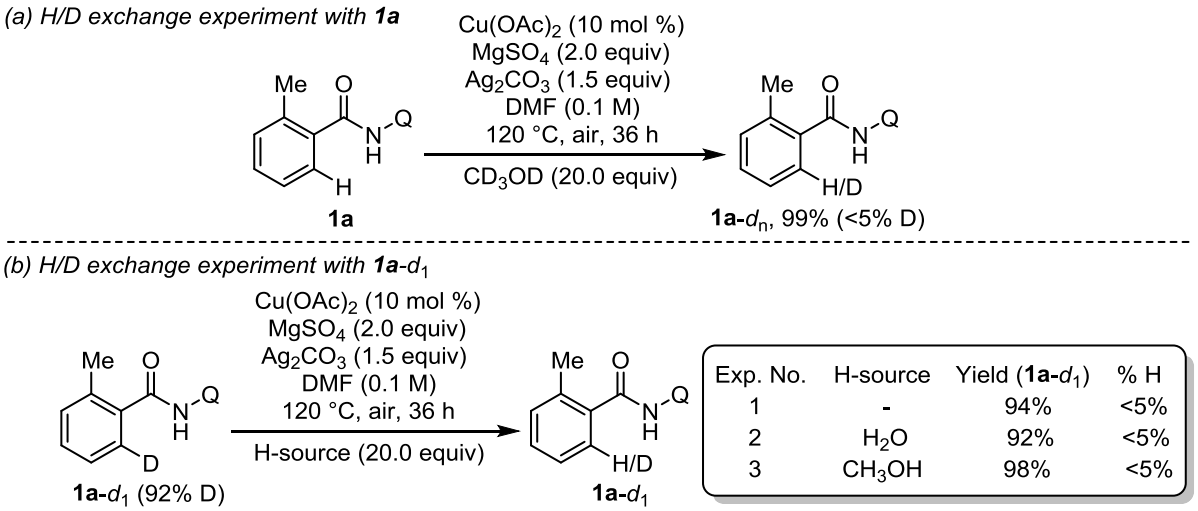

Scheme 4.3.4.1. H/D exchange experiments with **1a** and **1a**-d_1.

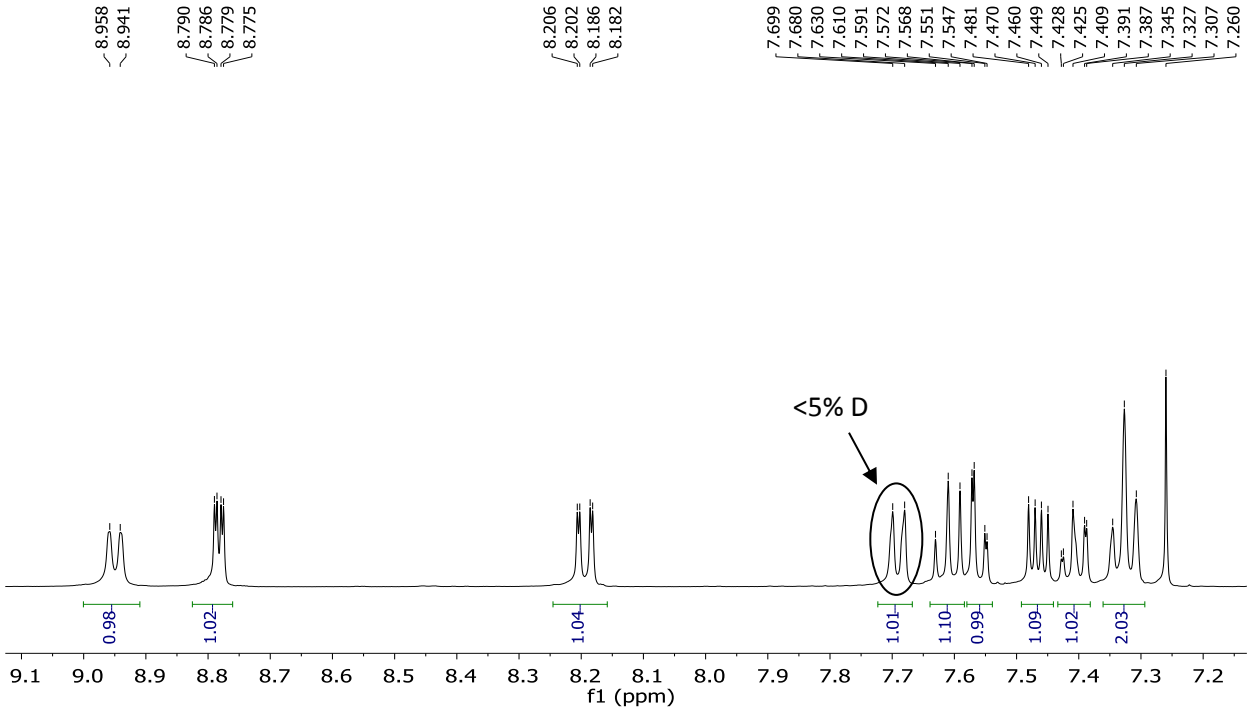

Figure 4.3.4.1. ^{1}H NMR spectrum of recovered **1a**-d_n after H/D exchange experiment in presence of excess CD_3OD.

When the deuterated benzamide **1a**-d_1 (^{1}H NMR, Figure 4.3.4.2) was subjected to the standard conditions in absence of HMDS and quenched with either no external H-source or with excess H-sources like H_2O and CH_3OH, no deuterium-proton exchange was observed in the recovered starting material in all the experiments (Scheme 4.3.4.1b). ^{1}H NMR studies showed <5% H-incorporation in case of recovered **1a**-d_1 in all the cases (Figure 4.3.4.3, 4.3.4.4, 4.3.4.5). The

result reassured the previous conclusion that C–H bond cleavage step is irreversible in nature since no substantial H-incorporation was observed at the *ortho* C–H bond of the recovered starting material.

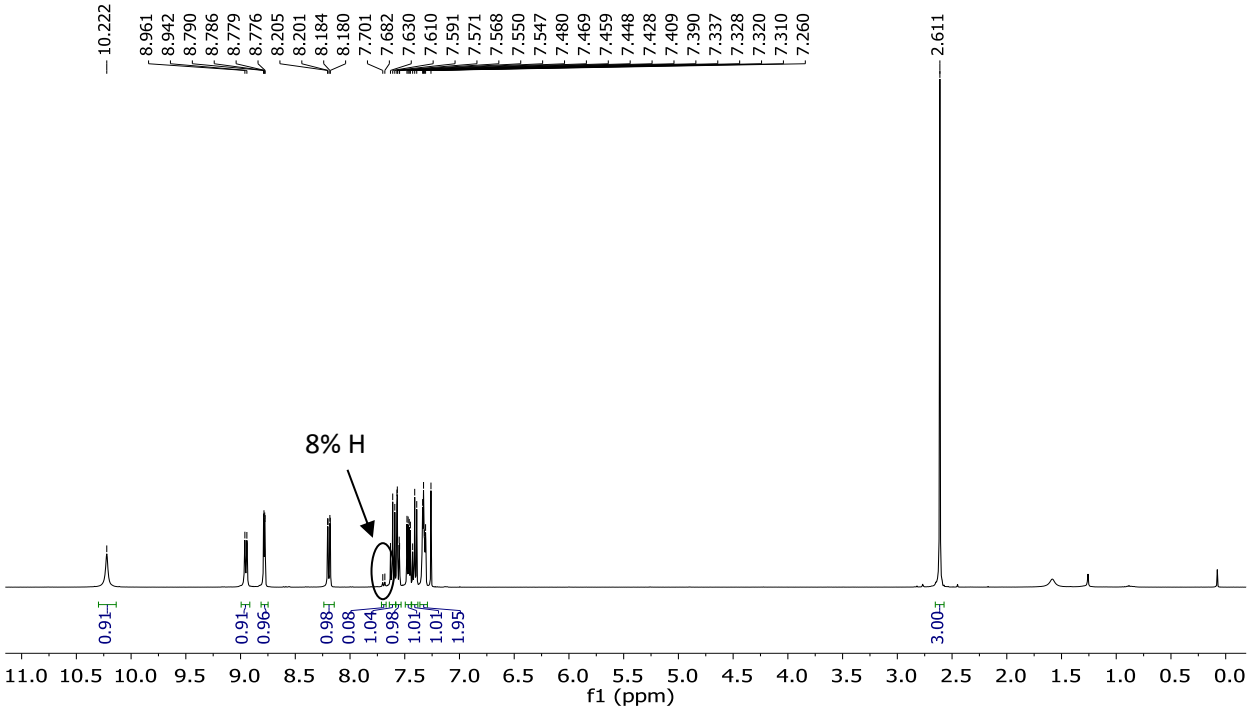

Figure 4.3.4.2. ^{1}H NMR spectrum of deuterated benzamide **1a**-d_1 (92% D).

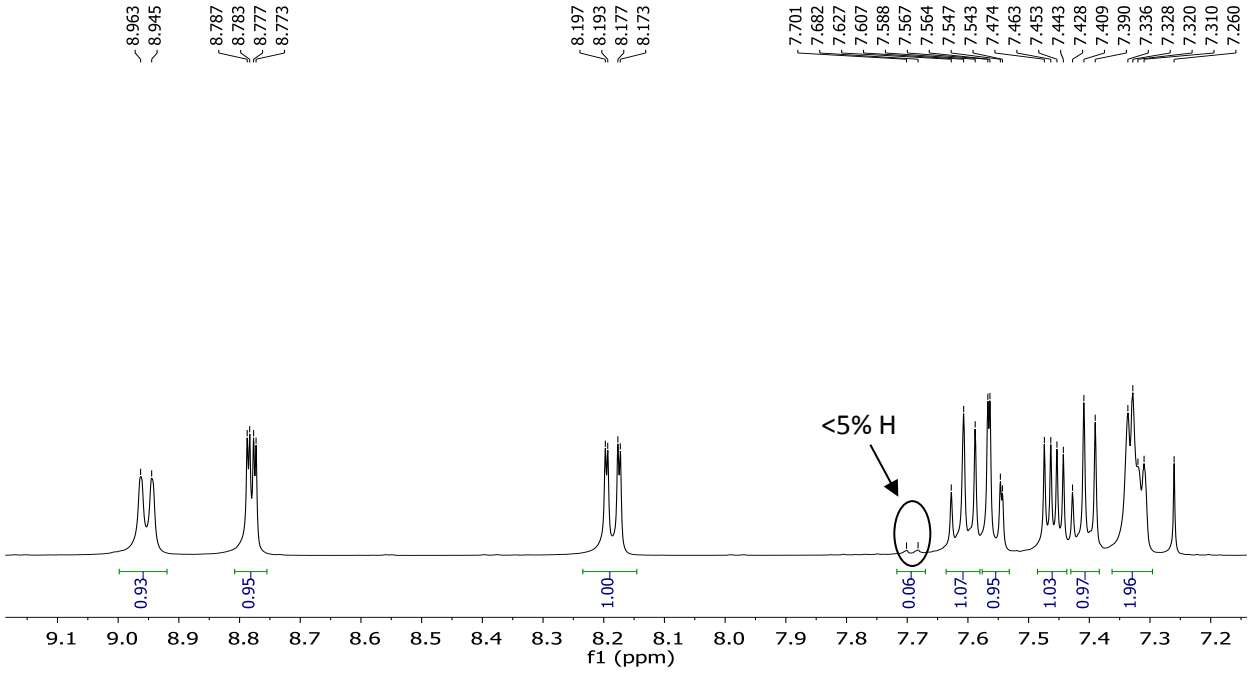

Figure 4.3.4.3. ^{1}H NMR spectrum of recovered **1a**-d_1 after H/D exchange experiment in absence of any external H-source.

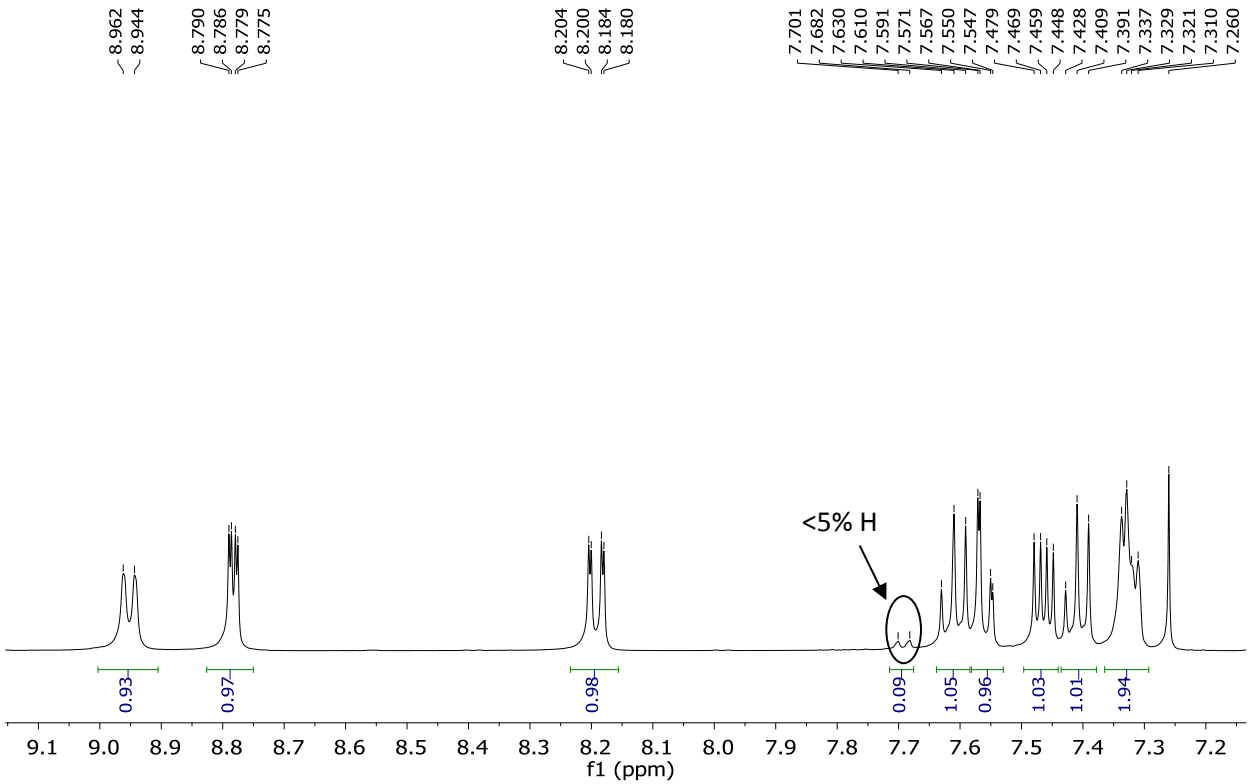

Figure 4.3.4.4. ^{1}H NMR spectra of recovered **1a**-d_1 after H/D exchange experiment in presence of H_2O as external H-source.

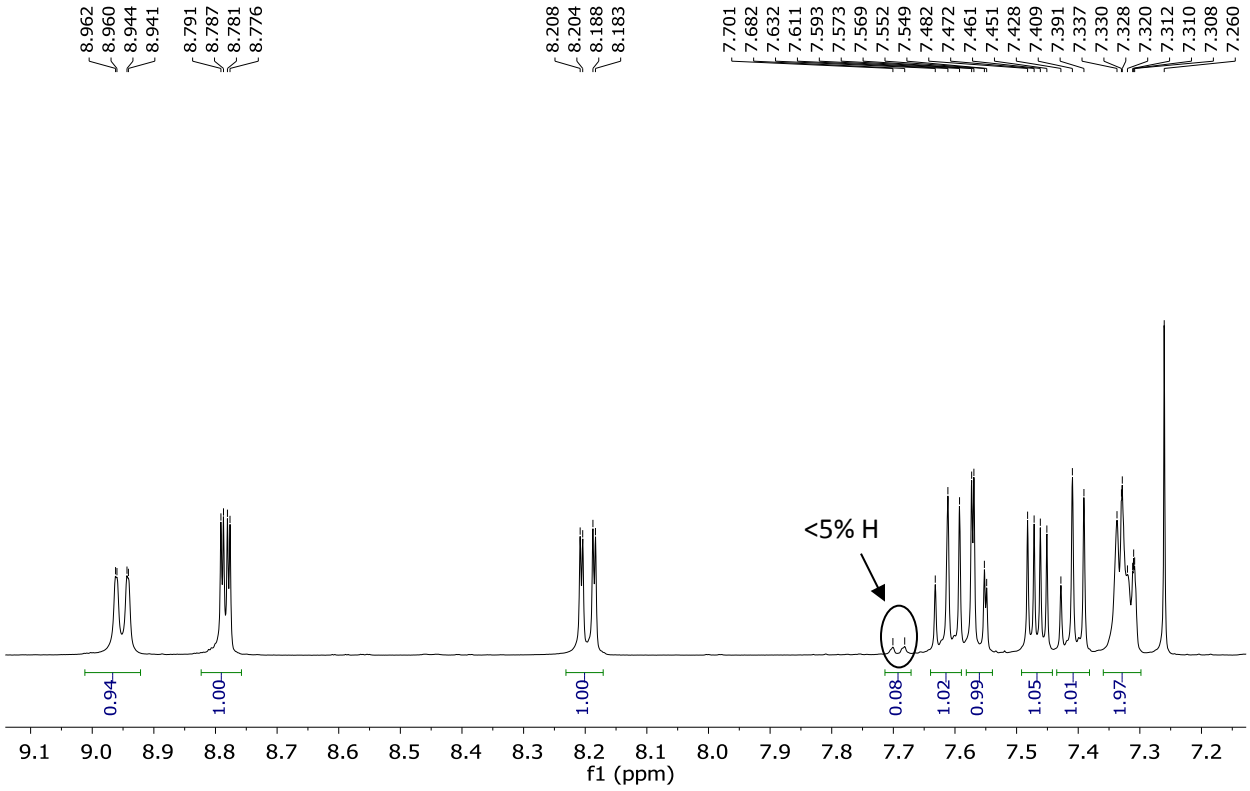

Figure 4.3.4.5. ^{1}H NMR spectra of recovered **1a**-d_1 after H/D exchange experiment in presence of CH_3OH as external H-source.

To have an understanding of the electronic effects of substituents on the benzamides in the present protocol, we performed competitive experiments between substrates bearing electron-donating and electron-withdrawing functional groups at both the *meta* and *para* positions of the amide bond under optimized reaction conditions (Scheme 4.3.4.2). When a mixture of *meta*-substituted electron-donating group (Me) containing substrate **1b** and electron-withdrawing group (F) containing substrate **1d** (1:1 ratio) was reacted, the corresponding silylated products **3b** and **3d** were isolated in 17% and 47% yields respectively (Scheme 4.3.4.2a). Similarly, when a mixture of *para*-substituted electron-donating group (OMe) containing substrate **1p** and electron-withdrawing group (Cl) containing substrate **1r** (1:1 ratio) was reacted, their respective silylated products **3p** and **3r** were isolated in 14% and 33% yields respectively (Scheme 4.3.4.2b). These results indicated the presence of a prominent substituent effect with electron-withdrawing group bearing substrates undergoing the silylation reaction at a faster rate than the electron-donating counterparts at both the *meta* and *para* positions.

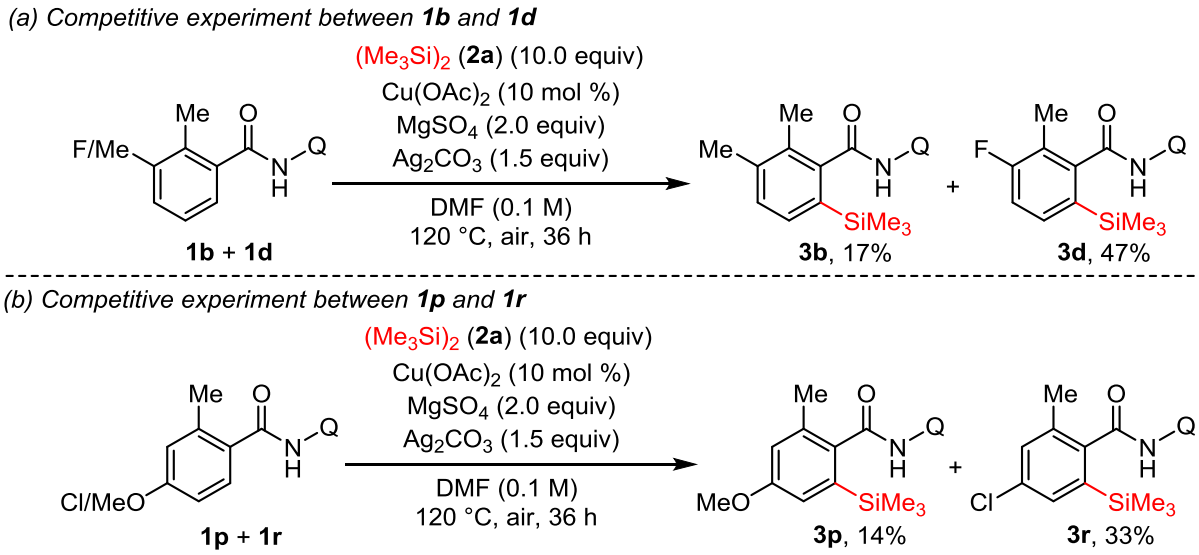

Scheme 4.3.4.2. Competitive experiments between electron-rich and electron-deficient benzamide substrates.

Based on the above experimental results and previous literature reports,[14-16] we put forward a plausible reaction pathway depicted in Scheme 4.3.4.3. In accordance with the known coordination properties of Cu(II) species with bidentate DG attached arenes, firstly benzamide **1a** in presence of $Cu(X)_2$ (X = acetate/carbonate) generates the intermediate **A** with the aid of chelation by *N*,*N*-bidentate 8-aminoquinoline directing group. This is succeeded by a chelate-directed *ortho* C(sp^2)–H activation via a concerted metalation-deprotonation (CMD) process to form the key metalacyclic intermediate complex **B**. Subsequently, on treatment with HMDS

2a, it undergoes disproportionation/oxidation affording intermediate **C** with the insertion of Si–Si bond and concomitant transfer of a trimethylsilyl group.[14a-c,14f] Finally, reductive elimination occurs to yield the desired silylated product **3a** upon hydrolysis and generates the Cu(I) species. Reoxidation of Cu(I) to Cu(II) by Ag_2CO_3 which here acts as the terminal oxidant, then continues the catalytic cycle.

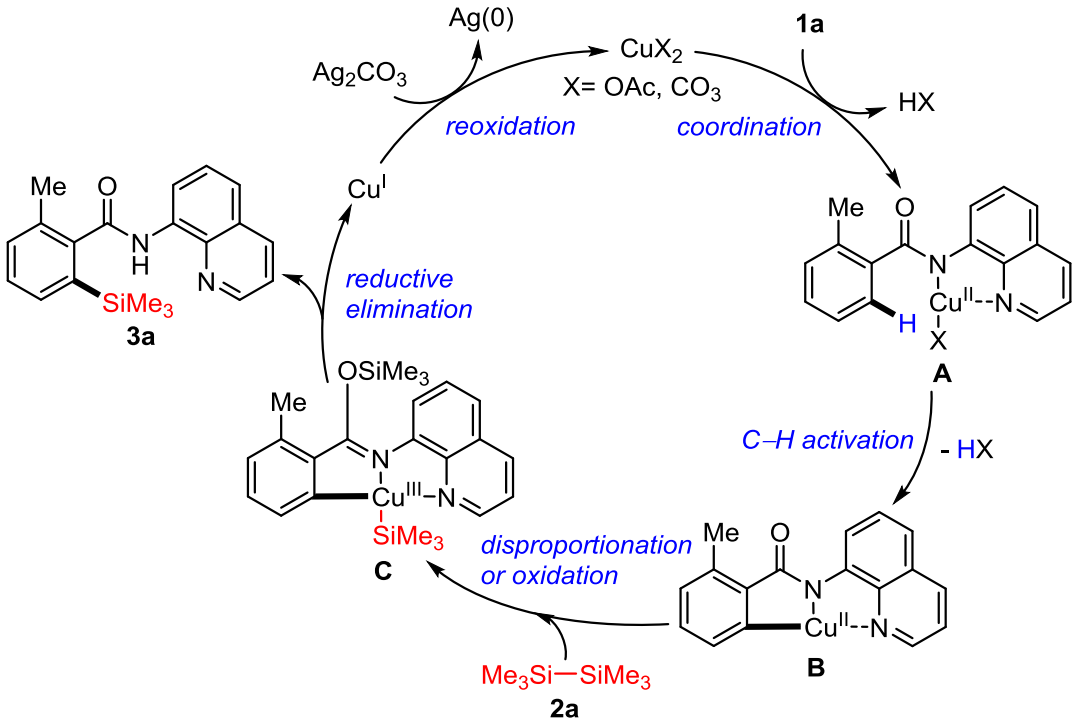

Scheme 4.3.4.3. Plausible reaction mechanism.

4.4. Summary

In summary, we have developed the first practical and convenient copper-catalyzed direct *ortho* silylation of unactivated arenes using disilanes as readily available organosilicon source, assisted by 8-aminoquinoline directing group. The prime features of the methodology include the applicability to a broad substrate scope, tolerance of a wide array of functional groups, and scalability to gram scale without yield reduction. This reaction protocol is attractive since the strategy gives an efficient access to structural C–Si bonds fundamental in organic synthesis, with the help of cheap copper catalyst and inexpensive hexamethyldisilane overcoming the cost ineffective and harsh palladium-catalyzed conditions. A series of kinetic experiments were conducted in order to understand the mechanism of the reaction. It was concluded that an irreversible cleavage of the C−H bond may be involved in the reaction pathway and significant substituent effect was present for the substrates under the present reaction conditions.

4.5. Experimental Section

4.5.1. General Information

All the information is same as that provided in Section 2.5.1 of Chapter 2 unless otherwise mentioned. All reactions were carried out in oven-dried reaction vessels under air atmosphere unless otherwise mentioned. The CIF files were submitted to CCDC (2054613-2054622) and can be obtained at https://summary.ccdc.cam.ac.uk/structure-summary-form. Single crystals of the silylated compounds were obtained taking 5-10 mg of the sample in 5 mL vials using either a mono-solvent system by solvent evaporation method or using a bi-solvent system applying solvent diffusion technique. The choice of solvent systems and methods for crystal growth for each compound (**3a**-**3e**, **3q**, **3s**, **3t**, **3ac**, **3ag**) are provided in the characterization data section.

4.5.2. General Procedure for the Preparation of Starting Materials

All the benzamides (**1**) were prepared following the literature method (Scheme 2.5.2.1, Chapter 2).[16h,i,n] Some substrates (**1g-1n**, **1t-1aa**) were prepared by the Suzuki cross-coupling method by taking suitable bromo-benzamides (**1f** and **1s**) and arylboronic acids (Scheme 2.5.2.2, Chapter 2) following the literature method.[17]

Benzamide **1a**-d_1 was prepared according to the literature method (Scheme 4.5.2.1).[18] In a sealed tube, benzamide **1a** (0.52 g, 2.0 mmol, 1.0 equiv), $Pd(OAc)_2$ (89.8 mg, 0.4 mmol, 0.2 equiv) and D_2O (99.8% D content, 10 mL) were added. The reaction was stirred at 140 °C for 48 h. Then, the reaction mixture was cooled to room temperature and extracted with water (15 mL)-ethyl acetate (3 × 20 mL). The combined organic phase was washed with saturated brine solution and dried over anhydrous Na_2SO_4 and concentrated under vacuo. The crude mixture was purified by column chromatography on silica gel using pet ether/ethyl acetate (9:1) as eluent to give the deuterated benzamide **1a**-d_1 (0.38 g, 72% yield, 92% D incorporation).

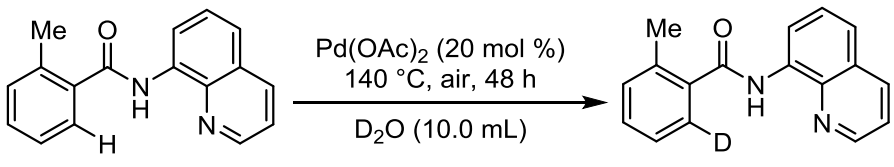

1a
0.52 g, 3.8 mmol

1a-d_1 (92% D)
0.38 g, 72%

Scheme 4.5.2.1. Preparation of deuterated benzamide **1a**-d_1.

4.5.3. General Procedure for Silylation

(0.2 mmol scale):

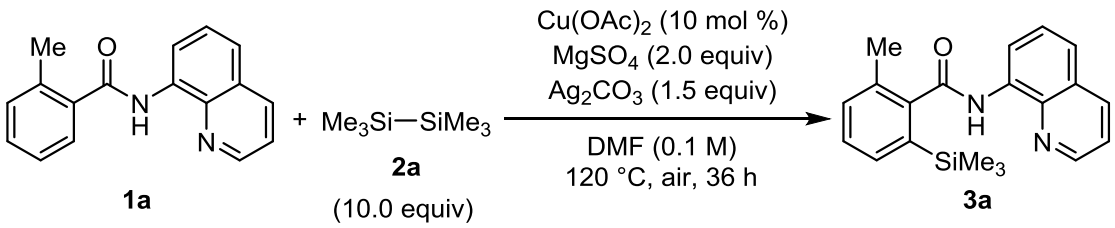

In an oven-dried 10 mL Schlenk tube, 2-methyl-*N*-(quinolin-8-yl)benzamide (**1a**) (52.5 mg, 0.2 mmol, 1.0 equiv), $Cu(OAc)_2$ (3.6 mg, 0.02 mmol, 0.1 equiv), $MgSO_4$ (48.2 mg, 0.4 mmol, 2.0 equiv), and Ag_2CO_3 (82.8 mg, 0.3 mmol, 1.5 equiv) were taken. Then hexamethyldisilane (0.41 mL, 2.0 mmol, 10.0 equiv) and 2.0 mL (0.1 M) of anhydrous DMF was added. The tube was closed with a teflon-lined cap and kept on stirring in an oil bath. The bath temperature was slowly increased to 120 ^oC. After 36 h, the reaction was stopped and cooled to room temperature. The reaction mixture was filtered through a short pad of celite, poured to water (20 mL) and extracted with ethyl acetate (3 x 5 mL). The combined organic layers were washed with brine solution (2 x 5 mL). The organic phase was separated, dried over anhydrous Na_2SO_4, filtered and concentrated under vacuo. The crude reaction mixture was directly purified by column chromatography on silica gel using pet ether/ethyl acetate as eluent to obtain 2-methyl-*N*-(quinolin-8-yl)-6-(trimethylsilyl)benzamide (**3a**) (57.4 mg, 86% yield).

(gram-scale):

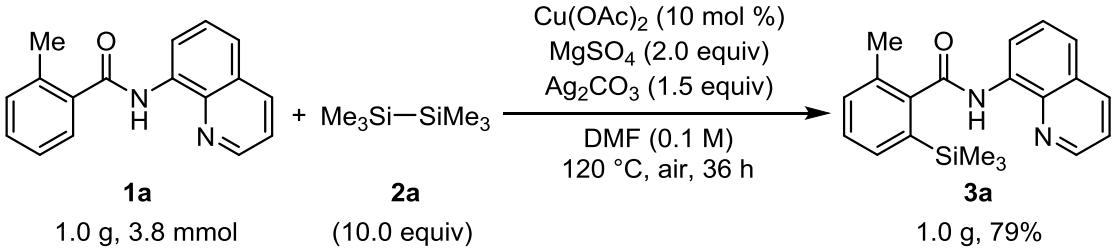

To an oven-dried 100 mL round bottom flask equipped with a reflux condenser, 2-methyl-*N*-(quinolin-8-yl)benzamide (**1a**) (1.0 g, 3.8 mmol, 1.0 equiv), $Cu(OAc)_2$ (69.2 mg, 0.38 mmol, 0.1 equiv), $MgSO_4$ (0.92 g, 7.6 mmol, 2.0 equiv), and Ag_2CO_3 (1.58 g, 5.7 mmol, 1.5 equiv) were taken. Then hexamethyldisilane (7.8 mL, 38.1 mmol, 10.0 equiv) and 38.0 mL (0.1 M) of anhydrous DMF was added. The tube was closed with a teflon-lined cap and kept on stirring in an oil bath. The bath temperature was slowly increased to 120 ^oC. After 36 h, the reaction was stopped and cooled to room temperature. The reaction mixture was filtered through a short

pad of celite, poured to water (400 mL) and extracted with ethyl acetate (3 x 80 mL). The combined organic layers were washed with brine solution (2 x 25 mL). The organic phase was separated, dried over anhydrous Na_2SO_4, filtered and concentrated under vacuo. The crude reaction mixture was directly purified by column chromatography on silica gel using pet ether/ethyl acetate as eluent to obtain 2-methyl-*N*-(quinolin-8-yl)-6-(trimethylsilyl)benzamide (**3a**) (1.0 g, 79% yield).

4.5.4. Characterization Data for the Silylated Products

2-methyl-*N*-(quinolin-8-yl)-6-(trimethylsilyl)benzamide (3a):[14a]

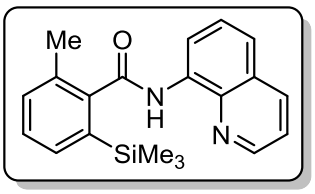

Yield 86% (57.4 mg); colorless solid; $\mathbf{R_f}$ 0.30 (pet ether/ethyl acetate = 9:1); **eluent composition** petroleum ether/ethyl acetate = 19:1; **mp** 106-108 ºC (crystallization from DCM and hexane using solvent diffusion method); **^{1}H NMR** (400 MHz, $CDCl_3$) δ 9.96 (br s, 1H), 9.00 (app d, *J* = 7.2 Hz, 1H), 8.73 (app d, *J* = 4.0 Hz, 1H), 8.18 (app d, *J* = 8.4 Hz, 1H), 7.62 (app t, *J* = 8.0 Hz, 1H), 7.57 (app d, *J* = 8.4 Hz, 1H), 7.50 (app d, *J* = 7.2 Hz, 1H), 7.44 (dd, *J* = 8.0 Hz, 4.0 Hz, 1H), 7.35 (app t, *J* = 7.2 Hz, 1H), 7.29 (app d, *J* = 7.2 Hz, 1H), 2.46 (s, 3H), 0.28 (s, 9H); **^{13}C NMR** (100 MHz, $CDCl_3$) δ 170.0, 148.4, 143.4, 138.6, 137.4, 136.5, 134.6, 134.2, 132.4, 131.3, 128.7, 128.2, 127.6, 122.0, 121.8, 116.9, 19.8, 0.1; **HRMS** (ESI, m/z) calcd for $C_{20}H_{22}N_2OSi$ $[M + Na]^+$ 357.1399, found 357.1400.

Crystal data and structure refinement for 3a, CCDC No. 2054613

Empirical formula	$C_{20}H_{22}N_2OSi$
Formula weight	334.48
Temperature/K	100.0
Crystal system	monoclinic
Space group	$P2_1/n$
a/Å	10.1808(4)
b/Å	13.5406(5)
c/Å	13.5834(5)
α/°	90
β/°	95.202(2)
γ/°	90
Volume/Å^3	1864.82(12)
Z	4
ρ_{calc}g/cm^3	1.191
μ/mm^{-1}	1.165
F(000)	712.0
Crystal size/mm^3	0.35 × 0.275 × 0.2
Radiation	Cu Kα (λ = 1.54178)
2Θ range for data collection/°	9.24 to 144.214

Index ranges	$-12 \leq h \leq 12, -16 \leq k \leq 16, -16 \leq l \leq 16$
Reflections collected	26183
Independent reflections	3614 [R_{int} = 0.0627, R_{sigma} = 0.0384]
Data/restraints/parameters	3614/0/221
Goodness-of-fit on F^2	1.142
Final R indexes [I>=2σ (I)]	R_1 = 0.0528, wR_2 = 0.1204
Final R indexes [all data]	R_1 = 0.0548, wR_2 = 0.1214
Largest diff. peak/hole / e $Å^{-3}$	0.28/-0.37

2,3-dimethyl-*N*-(quinolin-8-yl)-6-(trimethylsilyl)benzamide (3b):

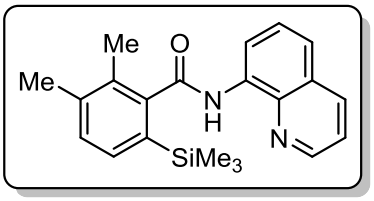

Yield 73% (51.0 mg); colorless solid; **R_f** 0.40 (pet ether/ethyl acetate = 9:1); **eluent composition** petroleum ether/ethyl acetate = 19:1; **mp** 150-152 ^oC (crystallization from $CDCl_3$ using solvent evaporation method); **^{1}H NMR** (400 MHz, $CDCl_3$) δ 9.97 (br s, 1H), 9.01 (dd, *J* = 7.2 Hz, 1.6 Hz, 1H), 8.73 (dd, *J* = 4.0 Hz, 1.6 Hz, 1H), 8.19 (dd, *J* = 8.4 Hz, 1.6 Hz, 1H), 7.63 (app t, *J* = 8.0 Hz, 1H), 7.57 (dd, *J* = 8.4 Hz, 1.2 Hz, 1H), 7.44 (dd, *J* = 8.4 Hz, 4.0 Hz, 1H), 7.40 (d, *J* = 7.6 Hz, 1H), 7.25 (d, *J* = 7.6 Hz, 1H), 2.35 (s, 3H), 2.34 (s, 3H), 0.25 (s, 9H); **^{13}C NMR** (150 MHz, $CDCl_3$) δ 170.5, 148.3, 143.7, 138.5 (x 2), 136.6, 134.6, 134.4, 132.8, 132.3, 130.1, 128.2, 127.7, 122.0, 121.8, 117.0, 20.5, 16.5, 0.1; **HRMS** (ESI, m/z) calcd for $C_{21}H_{24}N_2OSi$ $[M + H]^+$ 349.1736, found 349.1739.

Crystal data and structure refinement for 3b, CCDC No. 2054616

Empirical formula	$C_{21}H_{24}N_2OSi$
Formula weight	348.51
Temperature/K	100.0
Crystal system	monoclinic
Space group	$P2_1/n$
a/Å	12.3232(8)
b/Å	10.8891(8)
c/Å	14.1794(9)
α/°	90
β/°	97.493(3)
γ/°	90
Volume/$Å^3$	1886.5(2)
Z	4
ρ_{calc}g/cm^3	1.227
μ/mm^{-1}	1.171
F(000)	744.0
Crystal size/mm^3	0.5 × 0.315 × 0.275
Radiation	Cu Kα (λ = 1.54178)
2Θ range for data collection/°	10.192 to 127.54
Index ranges	$-14 \leq h \leq 14, -12 \leq k \leq 12, -16 \leq l \leq 16$
Reflections collected	43942

Independent reflections	2998 [R_{int} = 0.0566, R_{sigma} = 0.0236]
Data/restraints/parameters	2998/0/231
Goodness-of-fit on F^2	1.079
Final R indexes [I>=2σ (I)]	R_1 = 0.0432, wR_2 = 0.1126
Final R indexes [all data]	R_1 = 0.0434, wR_2 = 0.1128
Largest diff. peak/hole / e $Å^{-3}$	0.21/-0.30

3-methoxy-2-methyl-*N*-(quinolin-8-yl)-6-(trimethylsilyl)benzamide (3c):

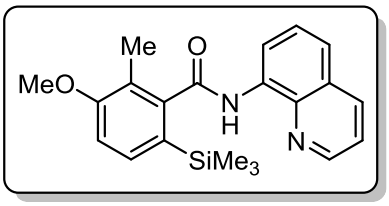

Yield 78% (56.9 mg); colorless solid; **R_f** 0.30 (pet ether/ethyl acetate = 9:1); **eluent composition** petroleum ether/ethyl acetate = 19:1; **mp** 122-124 °C (crystallization from $CHCl_3$ and hexane using solvent diffusion method); **^{1}H NMR** (600 MHz, $CDCl_3$) δ 9.97 (br s, 1H), 8.99 (dd, *J* = 7.8 Hz, 1.2 Hz, 1H), 8.72 (dd, *J* = 4.2 Hz, 1.8 Hz, 1H), 8.18 (dd, *J* = 7.8 Hz, 1.8 Hz, 1H), 7.62 (app t, *J* = 7.8 Hz, 1H), 7.57 (dd, *J* = 8.4 Hz, 1.2 Hz, 1H), 7.47 (d, *J* = 7.8 Hz, 1H), 7.44 (dd, *J* = 8.4 Hz, 4.2 Hz, 1H), 6.93 (d, *J* = 8.4 Hz, 1H), 3.88 (s, 3H), 2.31 (s, 3H), 0.25 (s, 9H); **^{13}C NMR** (150 MHz, $CDCl_3$) δ 169.7, 158.6, 148.3, 144.7, 138.5, 136.5, 134.6, 133.8, 128.2, 127.8, 127.7, 123.4, 122.0, 121.8, 117.0, 110.3, 55.6, 12.9, 0.2; **HRMS** (ESI, m/z) calcd for $C_{21}H_{24}N_2O_2Si$ $[M + H]^+$ 365.1685, found 365.1691.

Crystal data and structure refinement for 3c, CCDC No. 2054617

Empirical formula	$C_{21}H_{24}N_2O_2Si$
Formula weight	364.51
Temperature/K	296.15
Crystal system	monoclinic
Space group	$P2_1/n$
a/Å	12.6160(10)
b/Å	11.1461(10)
c/Å	14.1882(12)
α/°	90
β/°	96.307(2)
γ/°	90
Volume/$Å^3$	1983.1(3)
Z	4
ρ_{calc}g/cm^3	1.221
μ/mm^{-1}	0.135
F(000)	776.0
Crystal size/mm^3	0.2 × 0.2 × 0.2
Radiation	MoKα (λ = 0.71073)
2Θ range for data collection/°	4.578 to 60.012
Index ranges	-17 ≤ h ≤ 17, -15 ≤ k ≤ 15, -19 ≤ l ≤ 19
Reflections collected	33353
Independent reflections	5588 [R_{int} = 0.0493, R_{sigma} = 0.0332]
Data/restraints/parameters	5588/0/240

Goodness-of-fit on F^2	1.023
Final R indexes [I>=2σ (I)]	R_1 = 0.0475, wR_2 = 0.1234
Final R indexes [all data]	R_1 = 0.0767, wR_2 = 0.1423
Largest diff. peak/hole / e $Å^{-3}$	0.24/-0.22

3-fluoro-2-methyl-*N*-(quinolin-8-yl)-6-(trimethylsilyl)benzamide (3d):

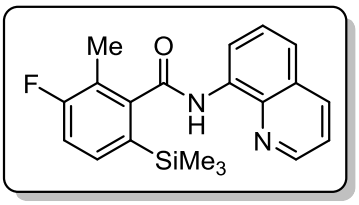

Yield 75% (53.1 mg); colorless solid; **R_f** 0.40 (pet ether/ethyl acetate = 9:1); **eluent composition** petroleum ether/ethyl acetate = 19:1; **mp** 108-110 ºC (crystallization from $CHCl_3$ using solvent evaporation method); **^{1}H NMR** (600 MHz, $CDCl_3$) δ 9.98 (br s, 1H), 8.98 (dd, *J* = 7.2 Hz, 1.2 Hz, 1H), 8.75 (dd, *J* = 4.2 Hz, 1.8 Hz, 1H), 8.20 (dd, *J* = 8.4 Hz, 1.2 Hz, 1H), 7.63 (app t, *J* = 7.8 Hz, 1H), 7.59 (dd, *J* = 8.4 Hz, 1.2 Hz, 1H), 7.47-7.45 (comp, 2H), 7.13-7.10 (m, 1H), 2.36 (app d, *J* = 2.4 Hz, 3H), 0.26 (s, 9H); **^{13}C NMR** (150 MHz, $CDCl_3$) δ 168.6 (d, *J* = 3.0 Hz), 162.0 (d, $^1J_{F-C}$ = 246.0 Hz), 148.4, 145.6 (d, $^4J_{F-C}$ = 3.0 Hz), 138.5, 136.6, 134.3, 134.1 (d, $^3J_{F-C}$ = 7.5 Hz), 132.8 (d, $^3J_{F-C}$ = 4.5 Hz), 128.2, 127.6, 122.3, 122.0 (d, $^2J_{F-C}$ = 16.5 Hz), 121.9, 117.1, 115.4 (d, $^2J_{F-C}$ = 21.0 Hz), 11.7 (d, *J* = 4.5 Hz), 0.0; **HRMS** (ESI, m/z) calcd for $C_{20}H_{21}FN_2OSi$ $[M + H]^+$ 353.1485, found 353.1488.

Crystal data and structure refinement for 3d, CCDC No. 2054618

Empirical formula	$C_{20}H_{21}FN_2OSi$
Formula weight	352.48
Temperature/K	100.0
Crystal system	monoclinic
Space group	$P2_1/c$
a/Å	8.5937(9)
b/Å	12.5787(12)
c/Å	16.9182(16)
α/°	90
β/°	93.235(4)
γ/°	90
Volume/$Å^3$	1825.9(3)
Z	4
ρ_{calc}g/cm^3	1.282
μ/mm^{-1}	1.299
F(000)	744.0
Crystal size/mm^3	0.402 × 0.25 × 0.12
Radiation	Cu Kα (λ = 1.54178)
2Θ range for data collection/°	8.764 to 125.102
Index ranges	$-9 \le h \le 9$, $-14 \le k \le 14$, $-17 \le l \le 19$
Reflections collected	19963
Independent reflections	2905 [R_{int} = 0.2155, R_{sigma} = 0.1175]
Data/restraints/parameters	2905/0/230

Goodness-of-fit on F^2	1.327
Final R indexes [I>=2σ (I)]	R_1 = 0.1575, wR_2 = 0.3389
Final R indexes [all data]	R_1 = 0.1659, wR_2 = 0.3511
Largest diff. peak/hole / e $Å^{-3}$	0.94/-1.30

3-chloro-2-methyl-*N*-(quinolin-8-yl)-6-(trimethylsilyl)benzamide (3e):

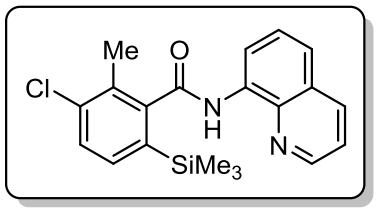

Yield 54% (39.8 mg); colorless solid; **R_f** 0.40 (pet ether/ethyl acetate = 9:1); **eluent composition** petroleum ether/ethyl acetate = 19:1; **mp** 146-148 °C (crystallization from DCM and hexane using solvent diffusion method); **^{1}H NMR** (600 MHz, $CDCl_3$) δ 9.96 (br s, 1H), 8.97 (dd, *J* = 7.2 Hz, 1.2 Hz, 1H), 8.75 (dd, *J* = 4.2 Hz, 1.8 Hz, 1H), 8.20 (dd, *J* = 8.4 Hz, 1.8 Hz, 1H), 7.63 (app t, *J* = 7.8 Hz, 1H), 7.59 (dd, *J* = 8.4 Hz, 1.2 Hz, 1H), 7.46 (dd, *J* = 8.4 Hz, 4.2 Hz, 1H), 7.44 (dd, *J* = 7.8 Hz, 4.2 Hz, 1H), 7.41 (d, *J* = 7.8 Hz, 1H), 2.48 (s, 3H), 0.26 (s, 9H); **^{13}C NMR** (150 MHz, $CDCl_3$) δ 168.9, 148.5, 145.1, 138.5, 136.6, 136.5, 136.0, 134.3, 133.5, 132.4, 129.4, 128.2, 127.6, 122.3, 121.9, 117.0, 17.2, -0.1; **HRMS** (ESI, m/z) calcd for $C_{20}H_{21}ClN_2OSi$ $[M + H]^+$ 369.1190, found 369.1195.

Crystal data and structure refinement for 3e, CCDC No. 2054619

Empirical formula	$C_{20}H_{21}ClN_2OSi$
Formula weight	368.93
Temperature/K	100.0
Crystal system	monoclinic
Space group	$P2_1/c$
a/Å	8.4502(2)
b/Å	12.8498(2)
c/Å	17.2023(3)
α/°	90
β/°	93.0220(10)
γ/°	90
Volume/$Å^3$	1865.29(6)
Z	4
ρ_{calc}g/cm^3	1.314
μ/mm^{-1}	2.503
F(000)	776.0
Crystal size/mm^3	0.54 × 0.45 × 0.4
Radiation	Cu Kα (λ = 1.54178)
2Θ range for data collection/°	8.594 to 133.266
Index ranges	$-10 \le h \le 9$, $-15 \le k \le 15$, $-20 \le l \le 20$
Reflections collected	30755
Independent reflections	3277 [R_{int} = 0.0642, R_{sigma} = 0.0312]
Data/restraints/parameters	3277/0/230
Goodness-of-fit on F^2	1.093
Final R indexes [I>=2σ (I)]	R_1 = 0.0426, wR_2 = 0.1006

Final R indexes [all data]	R_1 = 0.0431, wR_2 = 0.1010
Largest diff. peak/hole / e Å^{-3}	0.27/-0.37

3-bromo-2-methyl-*N*-(quinolin-8-yl)-6-(trimethylsilyl)benzamide (3f):

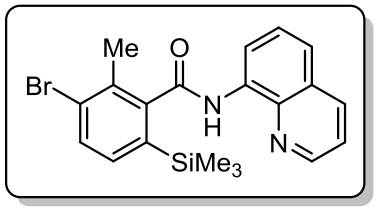

Yield 37% (30.3 mg); colorless solid; **R_f** 0.40 (pet ether/ethyl acetate = 9:1); **eluent composition** petroleum ether/ethyl acetate = 19:1; **mp** 134-136 °C; **^{1}H NMR** (600 MHz, $CDCl_3$) δ 9.97 (br s, 1H), 8.97 (dd, *J* = 7.2 Hz, 1.2 Hz, 1H), 8.75 (dd, *J* = 4.8 Hz, 1.2 Hz, 1H), 8.20 (dd, *J* = 8.4 Hz, 1.2 Hz, 1H), 7.63 (app t, *J* = 7.2 Hz, 2H), 7.59 (dd, *J* = 8.4 Hz, 1.2 Hz, 1H), 7.46 (dd, *J* = 8.4 Hz, 4.2 Hz, 1H), 7.32 (d, *J* = 7.8 Hz, 1H), 2.51 (s, 3H), 0.26 (s, 9H); **^{13}C NMR** (150 MHz, $CDCl_3$) δ 168.9, 148.4, 144.9, 138.5, 136.7, 136.6, 134.3, 134.0, 133.7, 132.8, 128.2, 127.6, 127.5, 122.4, 121.9, 117.1, 20.3, -0.1; **HRMS** (ESI, m/z) calcd for $C_{20}H_{21}BrN_2OSi$ $[M + H]^+$ 413.0685, found 413.0694.

2-methyl-*N*-(quinolin-8-yl)-4-(trimethylsilyl)-[1,1'-biphenyl]-3-carboxamide (3g):

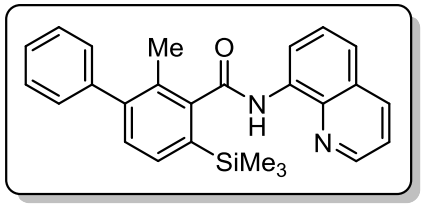

Yield 50% (41.1 mg); colorless oil; **R_f** 0.40 (pet ether/ethyl acetate = 9:1); **eluent composition** petroleum ether/ethyl acetate = 19:1; **^{1}H NMR** (400 MHz, $CDCl_3$) δ 10.00 (br s, 1H), 9.02 (dd, *J* = 7.2 Hz, 1.6 Hz, 1H), 8.76 (dd, *J* = 4.4 Hz, 1.6 Hz, 1H), 8.20 (dd, *J* = 8.4 Hz, 1.6 Hz, 1H), 7.63 (app t, *J* = 8.0 Hz, 1H), 7.58 (dd, *J* = 8.0 Hz, 1.6 Hz, 1H), 7.54 (d, *J* = 7.6 Hz, 1H), 7.48-7.42 (comp, 3H), 7.38-7.34 (comp, 3H), 7.32 (d, *J* = 7.6 Hz, 1H), 2.34 (s, 3H), 0.30 (s, 9H); **^{13}C NMR** (100 MHz, $CDCl_3$) δ 170.1, 148.3, 144.3, 143.7, 141.7, 138.5, 136.6, 136.3, 134.6, 132.3, 131.6, 130.1, 129.4 (x 2), 128.3 (x 2), 128.2, 127.7, 127.2, 122.1, 121.8, 117.2, 17.6, 0.1; **HRMS** (ESI, m/z) calcd for $C_{26}H_{26}N_2OSi$ $[M + H]^+$ 411.1893, found 411.1897.

2,3'-dimethyl-*N*-(quinolin-8-yl)-4-(trimethylsilyl)-[1,1'-biphenyl]-3-carboxamide (3h):

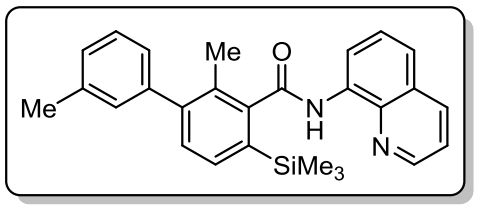

Yield 49% (41.2 mg); colorless solid; **R_f** 0.40 (pet ether/ethyl acetate = 9:1); **eluent composition** petroleum ether/ethyl acetate = 19:1; **mp** 58-60 °C; **^{1}H NMR** (400 MHz, $CDCl_3$) δ 10.05 (br s, 1H), 9.03 (dd, *J* = 7.2 Hz, 1.6 Hz, 1H), 8.77 (dd, *J* = 4.0 Hz, 1.6 Hz, 1H), 8.19 (dd, *J* = 8.4 Hz, 1.6 Hz, 1H), 7.64 (app t, *J* = 8.0 Hz, 1H), 7.58 (dd, *J* = 8.0 Hz, 1.2 Hz, 1H), 7.54 (d, *J* = 7.6 Hz, 1H), 7.46 (dd, *J* = 8.0 Hz, 4.0 Hz, 1H), 7.35-7.31 (comp, 2H), 7.19-7.16 (comp, 3H), 2.42 (s, 3H), 2.35 (s, 3H), 0.31 (s, 9H); **^{13}C NMR** (100 MHz, $CDCl_3$) δ 170.3, 148.4, 144.3, 143.8, 141.6, 138.6, 137.9, 136.5, 136.1, 134.6, 132.2, 131.6, 130.1 (x 2), 128.2, 128.2, 127.9, 127.7, 126.4, 122.1,

121.8, 117.0, 21.6, 17.6, 0.1; **HRMS** (ESI, m/z) calcd for $C_{27}H_{28}N_2OSi$ [M + H]$^+$ 425.2049, found 425.2050.

4'-methoxy-2-methyl-*N*-(quinolin-8-yl)-4-(trimethylsilyl)-[1,1'-biphenyl]-3-carboxamide (3i):

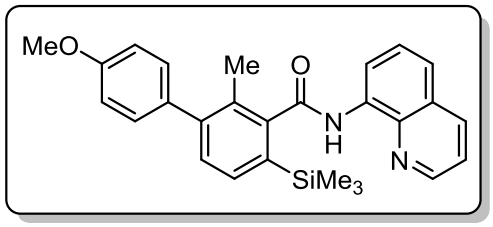

Yield 37% (32.5 mg); colorless solid; **R_f** 0.30 (pet ether/ethyl acetate = 9:1); **eluent composition** petroleum ether/ethyl acetate = 19:1; **mp** 126-128 ^oC; **^{1}H NMR** (400 MHz, $CDCl_3$) δ 10.04 (br s, 1H), 9.02 (dd, *J* = 7.6 Hz, 1.2 Hz, 1H), 8.76 (dd, *J* = 4.4 Hz, 1.6 Hz, 1H), 8.19 (dd, *J* = 8.0 Hz, 1.6 Hz, 1H), 7.63 (app t, *J* = 8.0 Hz, 1H), 7.58 (dd, *J* = 8.0 Hz, 0.8 Hz, 1H), 7.53 (d, *J* = 7.6 Hz, 1H), 7.46 (dd, *J* = 8.4 Hz, 4.4 Hz, 1H), 7.31 (d, *J* = 7.6 Hz, 1H), 7.30-7.27 (comp, 2H), 6.99-6.96 (comp, 2H), 3.86 (s, 3H), 2.35 (s, 3H), 0.30 (s, 9H); **^{13}C NMR** (100 MHz, $CDCl_3$) δ 170.3, 158.9, 148.4, 144.3, 143.3, 138.6, 136.6, 135.9, 134.6, 134.0, 132.3, 131.8, 130.5 (x 2), 130.3, 128.2, 127.7, 122.1, 121.8, 117.1, 113.8 (x 2), 55.4, 17.6, 0.1; **HRMS** (ESI, m/z) calcd for $C_{27}H_{28}N_2O_2Si$ [M + H]$^+$ 441.1998, found 441.2001.

4'-(tert-butyl)-2-methyl-*N*-(quinolin-8-yl)-4-(trimethylsilyl)-[1,1'-biphenyl]-3-carboxamide (3j):

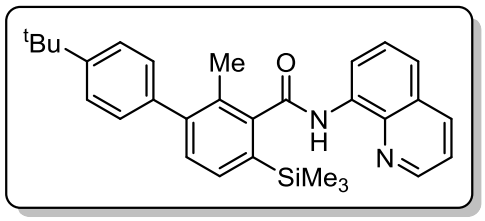

Yield 41% (38.6 mg); colorless oil; **R_f** 0.40 (pet ether/ethyl acetate = 9:1); **eluent composition** petroleum ether/ethyl acetate = 19:1; **^{1}H NMR** (400 MHz, $CDCl_3$) δ 10.04 (br s, 1H), 9.02 (dd, *J* = 7.2 Hz, 1.6 Hz, 1H), 8.76 (dd, *J* = 4.4 Hz, 1.6 Hz, 1H), 8.19 (dd, *J* = 8.0 Hz, 1.6 Hz, 1H), 7.63 (app t, *J* = 8.0 Hz, 1H), 7.58 (dd, *J* = 8.4 Hz, 1.2 Hz, 1H), 7.53 (d, *J* = 8.0 Hz, 1H), 7.48-7.44 (comp, 3H), 7.33 (d, *J* = 7.6 Hz, 1H), 7.31-7.28 (comp, 2H), 2.36 (s, 3H), 1.37 (s, 9H), 0.30 (s, 9H); **^{13}C NMR** (100 MHz, $CDCl_3$) δ 170.4, 150.1, 148.3, 144.3, 143.6, 138.6, 138.5, 136.6, 136.0, 134.6, 132.3, 131.7, 130.2, 129.0 (x 2), 128.2, 127.7, 125.2 (x 2), 122.1, 121.8, 117.1, 34.7, 31.5, 17.6, 0.1; **HRMS** (ESI, m/z) calcd for $C_{30}H_{34}N_2OSi$ [M + H]$^+$ 467.2519, found 467.2516.

3'-chloro-2-methyl-*N*-(quinolin-8-yl)-4-(trimethylsilyl)-[1,1'-biphenyl]-3-carboxamide (3k):

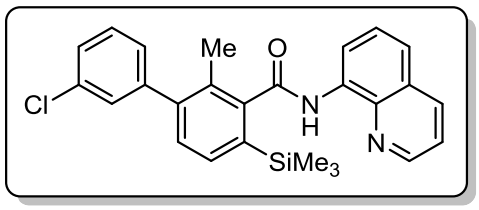

Yield 36% (32.0 mg); colorless solid; **R_f** 0.30 (pet ether/ethyl acetate = 9:1); **eluent composition** petroleum ether/ethyl acetate = 19:1; **mp** 112-114 °C; **^{1}H NMR** (400 MHz, $CDCl_3$) δ 10.04 (br s, 1H), 9.02 (dd, *J* = 7.2 Hz, 1.6 Hz, 1H), 8.77 (dd, *J* = 4.4 Hz, 1.6 Hz, 1H), 8.20 (dd, *J* = 8.4 Hz, 1.6 Hz, 1H), 7.63 (app t, *J* = 8.0 Hz, 1H), 7.58 (dd, *J* = 4.0 Hz, 1.6 Hz, 1H), 7.54 (d, *J* = 7.6 Hz, 1H), 7.47 (dd, *J* = 8.0 Hz, 4.0 Hz, 1H), 7.38-7.33 (comp, 3H), 7.28 (d, *J* = 7.6 Hz, 1H), 7.24-7.22 (m, 1H), 2.32 (s, 3H), 0.30 (s, 9H); **^{13}C NMR** (100 MHz, $CDCl_3$) δ 170.0, 148.4, 144.4, 143.5, 142.2, 138.5, 136.7, 134.5, 134.2, 132.4, 131.6, 129.9, 129.6, 129.4, 128.2, 127.7, 127.6, 127.4, 125.2, 122.2, 121.9, 117.2, 17.5, 0.0; **HRMS** (ESI, m/z) calcd for $C_{26}H_{25}ClN_2OSi$ $[M + H]^+$ 445.1503, found 445.1505.

4'-fluoro-2-methyl-*N*-(quinolin-8-yl)-4-(trimethylsilyl)-[1,1'-biphenyl]-3-carboxamide (3l):

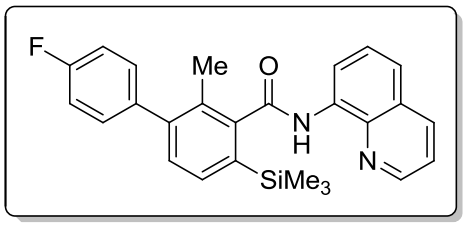

Yield 36% (31.0 mg); colorless solid; **R_f** 0.40 (pet ether/ethyl acetate = 9:1); **eluent composition** petroleum ether/ethyl acetate = 19:1; **mp** 160-162 °C; **^{1}H NMR** (400 MHz, $CDCl_3$) δ 10.03 (br s, 1H), 9.01 (dd, *J* = 7.2 Hz, 1.6 Hz, 1H), 8.76 (dd, *J* = 4.4 Hz, 1.6 Hz, 1H), 8.20 (dd, *J* = 8.0 Hz, 1.6 Hz, 1H), 7.63 (app t, *J* = 8.0 Hz, 1H), 7.58 (dd, *J* = 4.4 Hz, 1.6 Hz, 1H), 7.54 (d, *J* = 8.0 Hz, 1H), 7.46 (dd, *J* = 8.0 Hz, 4.0 Hz, 1H), 7.34-7.28 (comp, 3H), 7.15-7.09 (comp, 2H), 2.32 (s, 3H), 0.30 (s, 9H); **^{13}C NMR** (100 MHz, $CDCl_3$) δ 170.2, 162.2 (d, $^1J_{F\text{-}C}$ = 245.0 Hz), 148.4, 144.4, 142.6, 138.6, 137.6 (d, $^4J_{F\text{-}C}$ = 3.0 Hz), 136.6, 136.6 (d, $^3J_{F\text{-}C}$ = 5.0 Hz), 134.5, 132.4, 131.7, 130.9 (d, $^3J_{F\text{-}C}$ = 7.0 Hz), 130.1, 128.2, 127.7, 122.2, 121.9, 117.1, 115.3 (d, $^2J_{F\text{-}C}$ = 21.0 Hz), 17.6, 0.0; **HRMS** (ESI, m/z) calcd for $C_{26}H_{25}FN_2OSi$ $[M + H]^+$ 429.1798, found 429.1806.

4'-chloro-2-methyl-*N*-(quinolin-8-yl)-4-(trimethylsilyl)-[1,1'-biphenyl]-3-carboxamide (3m):

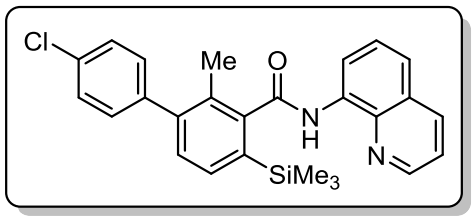

Yield 42% (37.7 mg); colorless solid; **R_f** 0.40 (pet ether/ethyl acetate = 9:1); **eluent composition** petroleum ether/ethyl acetate = 19:1; **mp** 152-154 °C; **^{1}H NMR** (400 MHz, $CDCl_3$) δ 10.03 (br s, 1H), 9.01 (dd, *J* = 7.6 Hz, 1.6 Hz, 1H), 8.76 (dd, *J* = 4.4 Hz, 1.6 Hz, 1H), 8.20 (dd, *J* = 8.4 Hz, 1.6 Hz,

1H), 7.63 (app t, *J* = 8.0 Hz, 1H), 7.58 (dd, *J* = 8.0 Hz, 1.2 Hz, 1H), 7.54 (d, *J* = 7.6 Hz, 1H), 7.47 (dd, *J* = 8.0 Hz, 4.0 Hz, 1H), 7.42-7.39 (comp, 2H), 7.30-7.28 (comp, 3H), 2.32 (s, 3H), 0.30 (s, 9H); **^{13}C NMR** (100 MHz, $CDCl_3$) δ 170.1, 148.4, 144.4, 142.4, 140.1, 138.5, 136.8, 136.6, 134.5, 133.3, 132.4, 131.6, 130.7 (x 2), 130.0, 128.6 (x 2), 128.2, 127.7, 122.2, 121.9, 117.1, 17.5, 0.0; **HRMS** (ESI, m/z) calcd for $C_{26}H_{25}ClN_2OSi$ $[M + H]^+$ 445.1503, found 445.1504.

2-methyl-*N*-(quinolin-8-yl)-4'-(trifluoromethyl)-4-(trimethylsilyl)-[1,1'-biphenyl]-3-carboxamide (3n):

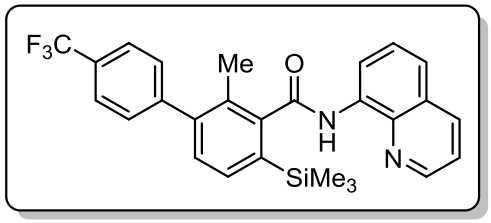

Yield 45% (42.6 mg); colorless solid; **R_f** 0.30 (pet ether/ethyl acetate = 9:1); **eluent composition** petroleum ether/ethyl acetate = 19:1; **mp** 136-138 °C; **^{1}H NMR** (400 MHz, $CDCl_3$) δ 10.05 (br s, 1H), 9.02 (dd, *J* = 7.2 Hz, 1.6 Hz, 1H), 8.77 (dd, *J* = 4.0 Hz, 1.6 Hz, 1H), 8.20 (dd, *J* = 8.4 Hz, 1.6 Hz, 1H), 7.72-7.70 (comp, 2H), 7.64 (app t, *J* = 8.0 Hz, 1H), 7.60-7.57 (comp, 2H), 7.49-7.45 (comp, 3H), 7.30 (d, *J* = 7.6 Hz, 1H), 2.33 (s, 3H), 0.32 (s, 9H); **^{13}C NMR** (100 MHz, $CDCl_3$) δ 170.0, 148.4, 145.4, 144.5, 142.2, 138.6, 137.3, 136.6, 134.5, 132.5, 131.5, 129.8, 129.7 (x 2), 129.1 (q, *J* = 41.0 Hz), 128.2, 127.7, 127.1 (q, *J* = 282.0 Hz), 125.3 (q, *J* = 4.0 Hz), 122.3, 121.9, 117.1, 17.5, 0.0; **HRMS** (ESI, m/z) calcd for $C_{27}H_{25}F_3N_2OSi$ $[M + H]^+$ 479.1766, found 479.1768.

2,4-dimethyl-*N*-(quinolin-8-yl)-6-(trimethylsilyl)benzamide (3o):

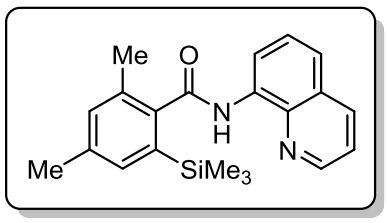

Yield 82% (57.0 mg); colorless solid; **R_f** 0.40 (pet ether/ethyl acetate = 9:1); **eluent composition** petroleum ether/ethyl acetate = 19:1; **mp** 82-84 °C; **^{1}H NMR** (400 MHz, $CDCl_3$) δ 9.96 (br s, 1H), 8.99 (dd, *J* = 7.6 Hz, 1.2 Hz, 1H), 8.72 (dd, *J* = 4.4 Hz, 1.6 Hz, 1H), 8.17 (dd, *J* = 8.0 Hz, 1.6 Hz, 1H), 7.62 (app t, *J* = 8.0 Hz, 1H), 7.56 (dd, *J* = 8.0 Hz, 1.6 Hz, 1H), 7.44 (dd, *J* = 8.0 Hz, 4.0 Hz, 1H), 7.29 (app s, 1H), 7.11 (app s, 1H), 2.44 (s, 3H), 2.39 (s, 3H), 0.28 (s, 9H); **^{13}C NMR** (100 MHz, $CDCl_3$) δ 170.2, 148.3, 140.8, 138.6, 138.2, 137.4, 136.4, 134.7, 134.2, 133.0, 132.0, 128.2, 127.6, 121.9, 121.8, 116.8, 21.5, 19.7, 0.1; **HRMS** (ESI, m/z) calcd for $C_{21}H_{24}N_2OSi$ $[M + H]^+$ 349.1736, found 349.1746.

4-methoxy-2-methyl-*N*-(quinolin-8-yl)-6-(trimethylsilyl)benzamide (3p):

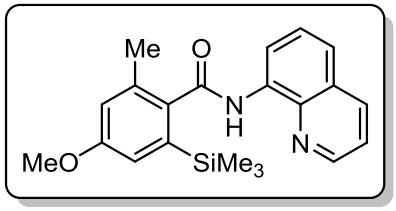

Yield 61% (44.2 mg); colorless solid; **R_f** 0.20 (pet ether/ethyl acetate = 9:1); **eluent composition** petroleum ether/ethyl acetate = 19:1; **mp** 116-118 °C; **^{1}H NMR** (400 MHz, $CDCl_3$) δ 9.95 (br s, 1H), 8.98 (dd, *J* = 7.6 Hz, 1.2 Hz, 1H), 8.73 (dd, *J* = 4.0 Hz, 1.6 Hz, 1H), 8.17 (dd, *J* = 8.4 Hz, 1.6 Hz, 1H), 7.61 (app t, *J* = 8.0 Hz, 1H), 7.55 (dd, *J* = 8.0 Hz, 1.6 Hz, 1H), 7.44 (dd, *J* = 8.4 Hz, 4.0 Hz, 1H), 7.02 (d, *J* = 2.8 Hz, 1H), 6.80 (d, *J* = 2.4 Hz, 1H), 3.86 (s, 3H), 2.46 (s, 3H), 0.28 (s, 9H); **^{13}C NMR** (100 MHz, $CDCl_3$) δ 170.1, 159.3, 148.3, 139.7, 138.6, 136.4 (x 2), 136.3, 134.7, 128.2, 127.6, 121.9, 121.8, 118.3, 116.8, 115.7, 55.3, 20.2, 0.0; **HRMS** (ESI, m/z) calcd for $C_{21}H_{24}N_2O_2Si$ $[M + Na]^+$ 387.1505, found 387.1514.

4-fluoro-2-methyl-*N*-(quinolin-8-yl)-6-(trimethylsilyl)benzamide (3q):[14a]

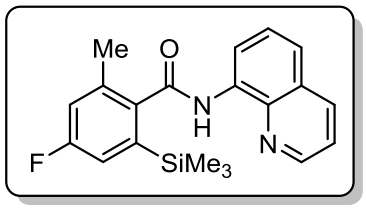

Yield 61% (43.2 mg); colorless solid; **R_f** 0.40 (pet ether/ethyl acetate = 9:1); **eluent composition** petroleum ether/ethyl acetate = 19:1; **mp** 110-112 °C (crystallization from $CHCl_3$ and hexane using solvent diffusion method); **^{1}H NMR** (600 MHz, $CDCl_3$) δ 9.96 (br s, 1H), 8.97 (dd, *J* = 7.2 Hz, 1.2 Hz, 1H), 8.75 (dd, *J* = 4.2 Hz, 1.8 Hz, 1H), 8.20 (dd, *J* = 8.4 Hz, 1.8 Hz, 1H), 7.62 (app t, *J* = 8.4 Hz, 1H), 7.58 (dd, *J* = 8.4 Hz, 1.2 Hz, 1H), 7.46 (dd, *J* = 8.4 Hz, 4.2 Hz, 1H), 7.15 (dd, *J* = 9.6 Hz, 2.4 Hz, 1H), 6.97 (dd, *J* = 8.4 Hz, 2.4 Hz, 1H), 2.46 (s, 3H), 0.27 (s, 9H); **^{13}C NMR** (150 MHz, $CDCl_3$) δ 169.4, 162.5 (d, $^1J_{F\text{-}C}$ = 249.0 Hz), 148.4, 141.1 (d, $^3J_{F\text{-}C}$ = 4.5 Hz), 139.5 (d, $^4J_{F\text{-}C}$ = 3.0 Hz), 138.4, 137.5 (d, $^3J_{F\text{-}C}$ = 7.5 Hz), 136.6, 134.4, 128.2, 127.7, 122.2, 121.9, 118.7 (d, $^2J_{F\text{-}C}$ = 18.0 Hz), 117.8 (d, $^2J_{F\text{-}C}$ = 21.0 Hz), 117.0, 19.9, 0.1; **HRMS** (ESI, m/z) calcd for $C_{20}H_{21}FN_2OSi$ $[M + H]^+$ 353.1485, found 353.1487.

Crystal data and structure refinement for 3q, CCDC No. 2054620

Empirical formula	$C_{20}H_{21}FN_2OSi$
Formula weight	352.48
Temperature/K	296.15
Crystal system	orthorhombic
Space group	Pbca
a/Å	8.859(4)
b/Å	16.866(8)
c/Å	24.048(12)
α/°	90
β/°	90
γ/°	90

Volume/Å^3	3593(3)
Z	8
ρ_{calc}g/cm^3	1.303
μ/mm^{-1}	0.151
F(000)	1488.0
Crystal size/mm^3	0.48 × 0.32 × 0.18
Radiation	Mo Kα (λ = 0.71073)
2Θ range for data collection/°	3.388 to 51.314
Index ranges	-10 ≤ h ≤ 10, -20 ≤ k ≤ 20, -29 ≤ l ≤ 29
Reflections collected	35360
Independent reflections	3352 [R_{int} = 0.0397, R_{sigma} = 0.0197]
Data/restraints/parameters	3352/0/230
Goodness-of-fit on F^2	1.042
Final R indexes [I>=2σ (I)]	R_1 = 0.0370, wR_2 = 0.1005
Final R indexes [all data]	R_1 = 0.0492, wR_2 = 0.1108
Largest diff. peak/hole / e Å^{-3}	0.18/-0.21

4-chloro-2-methyl-*N*-(quinolin-8-yl)-6-(trimethylsilyl)benzamide (3r):

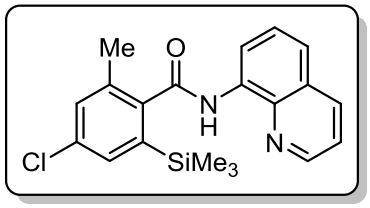

Yield 65% (47.6 mg); colorless solid; **R_f** 0.40 (pet ether/ethyl acetate = 9:1); **eluent composition** petroleum ether/ethyl acetate = 19:1; **mp** 134-136 ^oC; **^{1}H NMR** (600 MHz, $CDCl_3$) δ 9.95 (br s, 1H), 8.96 (dd, *J* = 7.2 Hz, 1.6 Hz, 1H), 8.74 (dd, *J* = 4.4 Hz, 1.6 Hz, 1H), 8.18 (dd, *J* = 8.4 Hz, 1.6 Hz, 1H), 7.62 (app t, *J* = 8.0 Hz, 1H), 7.56 (dd, *J* = 8.0 Hz, 1.6 Hz, 1H), 7.45 (dd, *J* = 8.0 Hz, 4.0 Hz, 1H), 7.43 (d, *J* = 1.6 Hz, 1H), 7.28 (d, *J* = 1.6 Hz, 1H), 2.44 (s, 3H), 0.28 (s, 9H); **^{13}C NMR** (150 MHz, $CDCl_3$) δ 161.9, 148.5, 141.7, 140.3, 138.5, 136.5 (x 2), 134.8, 134.3, 132.1, 131.0, 128.2, 127.6, 122.3, 121.9, 116.9, 19.6, -0.1; **HRMS** (ESI, m/z) calcd for $C_{20}H_{21}ClN_2OSi$ $[M + H]^+$ 369.1190, found 369.1198.

4-bromo-2-methyl-*N*-(quinolin-8-yl)-6-(trimethylsilyl)benzamide (3s):

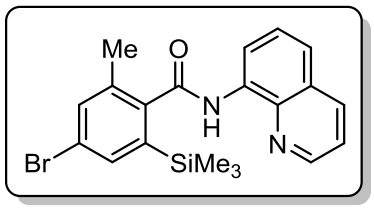

Yield 43% (35.4 mg); colorless solid; **R_f** 0.40 (pet ether/ethyl acetate = 9:1); **eluent composition** petroleum ether/ethyl acetate = 19:1; **mp** 132-134 ^oC (crystallization from DCM and hexane using solvent diffusion method); **^{1}H NMR** (400 MHz, $CDCl_3$) δ 9.94 (br s, 1H), 8.95 (dd, *J* = 7.2 Hz, 1.6 Hz, 1H), 8.74 (dd, *J* = 4.4 Hz, 1.6 Hz, 1H), 8.19 (dd, *J* = 8.4 Hz, 1.6 Hz, 1H), 7.62 (app t, *J* = 8.0 Hz, 1H), 7.59-7.57 (comp, 2H), 7.48-7.44 (comp, 2H), 2.43 (s, 3H), 0.28 (s, 9H); **^{13}C NMR** (100 MHz, $CDCl_3$) δ 169.1, 148.5, 142.1, 140.6, 138.5, 136.7, 136.5, 134.9, 134.3, 133.9, 128.2, 127.6, 123.6, 122.3, 121.9, 116.9, 19.6, -0.1; **HRMS** (ESI, m/z) calcd for $C_{20}H_{21}BrN_2OSi$ $[M + H]^+$ 413.0685, found 413.0691.

Crystal data and structure refinement for 3s, CCDC No. 2054621

Empirical formula	$C_{20}H_{21}BrN_2OSi$
Formula weight	413.39
Temperature/K	296.15
Crystal system	triclinic
Space group	P-1
a/Å	8.7091(13)
b/Å	9.3209(14)
c/Å	12.996(2)
α/°	87.899(3)
β/°	78.083(3)
γ/°	70.996(3)
Volume/Å^3	975.4(3)
Z	2
ρ_{calc}g/cm^3	1.407
μ/mm^{-1}	2.178
F(000)	424.0
Crystal size/mm^3	0.75 × 0.375 × 0.235
Radiation	Mo Kα (λ = 0.71073)
2Θ range for data collection/°	4.624 to 60.12
Index ranges	-11 ≤ h ≤ 12, -13 ≤ k ≤ 12, -18 ≤ l ≤ 18
Reflections collected	54434
Independent reflections	5434 [R_{int} = 0.0667, R_{sigma} = 0.0396]
Data/restraints/parameters	5434/0/230
Goodness-of-fit on F^2	1.138
Final R indexes [I>=2σ (I)]	R_1 = 0.0567, wR_2 = 0.1026
Final R indexes [all data]	R_1 = 0.0930, wR_2 = 0.1211
Largest diff. peak/hole / e Å^{-3}	0.83/-0.66

3-methyl-*N*-(quinolin-8-yl)-5-(trimethylsilyl)-[1,1'-biphenyl]-4-carboxamide (3t):

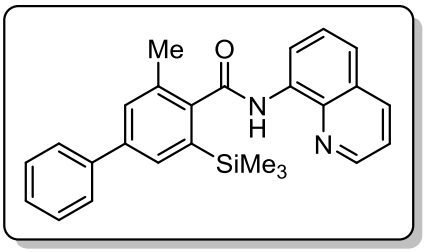

Yield 54% (44.0 mg); colorless solid; **R_f** 0.40 (pet ether/ethyl acetate = 9:1); **eluent composition** petroleum ether/ethyl acetate = 19:1; **mp** 150-152 ^oC (crystallization from DCM and hexane using solvent diffusion method); **^{1}H NMR** (400 MHz, $CDCl_3$) δ 10.05 (br s, 1H), 9.03 (dd, *J* = 7.6 Hz, 1.2 Hz, 1H), 8.76 (dd, *J* = 4.4 Hz, 1.6 Hz, 1H), 8.19 (dd, *J* = 8.4 Hz, 1.6 Hz, 1H), 7.71 (d, *J* = 1.6 Hz, 1H), 7.66-7.63 (comp, 3H), 7.59 (dd, *J* = 8.0 Hz, 1.6 Hz, 1H), 7.51-7.48 (comp, 3H), 7.46 (dd, *J* = 8.8 Hz, 4.8 Hz, 1H), 7.42-7.38 (m, 1H), 2.56 (s, 3H), 0.34 (s, 9H); **^{13}C NMR** (100 MHz, $CDCl_3$) δ 170.0, 148.4, 142.3, 141.5, 141.2, 138.6, 138.2, 136.5, 134.7, 134.6, 131.3, 130.2, 129.0 (x 2), 128.2, 127.7 (x 2), 127.4 (x 2), 122.1, 121.8, 117.0, 20.0, 0.1; **HRMS** (ESI, m/z) calcd for $C_{26}H_{26}N_2OSi$ $[M + H]^+$ 411.1893, found 411.1911.

Crystal data and structure refinement for 3t, CCDC No. 2054622

Empirical formula	$C_{26}H_{26}N_2OSi$
Formula weight	410.58
Temperature/K	100.0
Crystal system	triclinic
Space group	P-1
a/Å	8.1234(10)
b/Å	11.3451(14)
c/Å	12.8468(16)
α/°	82.183(4)
β/°	74.803(5)
γ/°	74.099(4)
Volume/Å^3	1096.2(2)
Z	2
ρ_{calc}g/cm^3	1.244
μ/mm^{-1}	1.090
F(000)	436.0
Crystal size/mm^3	0.5 × 0.365 × 0.25
Radiation	Cu Kα (λ = 1.54178)
2Θ range for data collection/°	7.148 to 128.018
Index ranges	$-9 \leq h \leq 9$, $-13 \leq k \leq 12$, $-14 \leq l \leq 14$
Reflections collected	23938
Independent reflections	3578 [R_{int} = 0.0734, R_{sigma} = 0.0452]
Data/restraints/parameters	3578/0/275
Goodness-of-fit on F^2	1.071
Final R indexes [I>=2σ (I)]	R_1 = 0.0469, wR_2 = 0.1191
Final R indexes [all data]	R_1 = 0.0496, wR_2 = 0.1212
Largest diff. peak/hole / e Å^{-3}	0.29/-0.40

3,3'-dimethyl-*N*-(quinolin-8-yl)-5-(trimethylsilyl)-[1,1'-biphenyl]-4-carboxamide (3u):

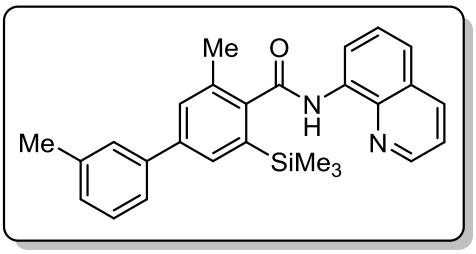

Yield 60% (51.3 mg); colorless oil; **R_f** 0.40 (pet ether/ethyl acetate = 9:1); **eluent composition** petroleum ether/ethyl acetate = 19:1; **^{1}H NMR** (400 MHz, $CDCl_3$) δ 10.05 (br s, 1H), 9.03 (dd, *J* = 7.6 Hz, 0.8 Hz, 1H), 8.76 (dd, *J* = 4.0 Hz, 1.6 Hz, 1H), 8.20 (dd, *J* = 8.4 Hz, 1.2 Hz, 1H), 7.70 (d, *J* = 1.2 Hz, 1H), 7.65 (app t, *J* = 8.0 Hz, 1H), 7.59 (dd, *J* = 8.0 Hz, 0.8 Hz, 1H), 7.50 (d, *J* = 0.8 Hz, 1H), 7.47-7.44 (comp, 3H), 7.39 (app t, *J* = 8.0 Hz, 1H), 7.22 (d, *J* = 7.6 Hz, 1H), 2.55 (s, 3H), 2.48 (s, 3H), 0.34 (s, 9H); **^{13}C NMR** (100 MHz, $CDCl_3$) δ 170.0, 148.4, 142.3, 141.6, 141.2, 138.6, 138.1, 136.5, 134.7, 134.6, 131.3, 130.2, 128.9 (x 2), 128.4, 128.2 (x 2), 127.7, 124.6, 122.1, 121.8, 117.0, 21.7, 19.9, 0.1; **HRMS** (ESI, m/z) calcd for $C_{27}H_{28}N_2OSi$ $[M + H]^+$ 425.2049, found 425.2038.

4'-methoxy-3-methyl-*N*-(quinolin-8-yl)-5-(trimethylsilyl)-[1,1'-biphenyl]-4-carboxamide (3v):

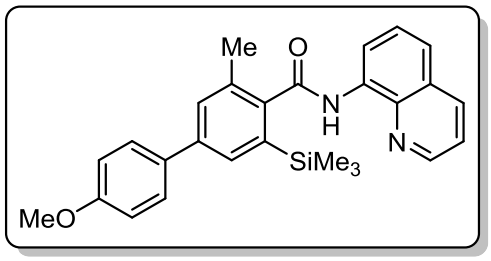

Yield 54% (47.2 mg); colorless solid; **R_f** 0.30 (pet ether/ethyl acetate = 9:1); **eluent composition** petroleum ether/ethyl acetate = 19:1; **mp** 142-144 °C; **^{1}H NMR** (400 MHz, $CDCl_3$) δ 10.03 (br s, 1H), 9.02 (dd, *J* = 7.6 Hz, 1.2 Hz, 1H), 8.74 (dd, *J* = 4.4 Hz, 1.6 Hz, 1H), 8.19 (dd, *J* = 8.4 Hz, 1.6 Hz, 1H), 7.66 (d, *J* = 2.0 Hz, 1H), 7.63 (d, *J* = 8.0 Hz, 1H), 7.59-7.56 (comp, 3H), 7.47-7.43 (comp, 2H), 7.04-7.01 (comp, 2H), 3.88 (s, 3H), 2.53 (s, 3H), 0.33 (s, 9H); **^{13}C NMR** (100 MHz, $CDCl_3$) δ 170.0, 159.5, 148.4, 141.8, 141.0, 138.6, 138.1, 136.5, 134.7, 134.6, 133.6, 130.9, 129.8, 128.5 (x 2), 128.2, 127.6, 122.0, 121.8, 116.9, 114.4 (x 2), 55.5, 20.0, 0.1; **HRMS** (ESI, m/z) calcd for $C_{27}H_{28}N_2O_2Si$ $[M + H]^+$ 441.1998, found 441.2014.

4'-(tert-butyl)-3-methyl-*N*-(quinolin-8-yl)-5-(trimethylsilyl)-[1,1'-biphenyl]-4-carboxamide (3w):

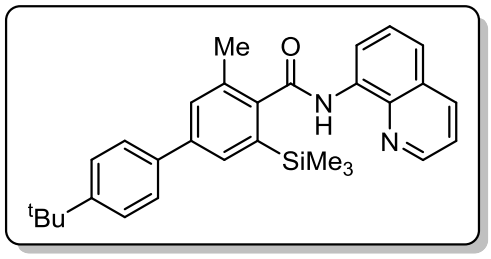

Yield 71% (66.1 mg); colorless solid; **R_f** 0.40 (pet ether/ethyl acetate = 9:1); **eluent composition** petroleum ether/ethyl acetate = 19:1; **mp** 166-168 °C; **^{1}H NMR** (400 MHz, $CDCl_3$) δ 10.05 (br s, 1H), 9.04 (dd, *J* = 7.2 Hz, 1.2 Hz, 1H), 8.76 (dd, *J* = 4.0 Hz, 1.6 Hz, 1H), 8.19 (dd, *J* = 8.0 Hz, 1.6 Hz, 1H), 7.71 (d, *J* = 0.8 Hz, 1H), 7.64 (app t, *J* = 8.0 Hz, 1H), 7.60-7.58 (comp, 3H), 7.54-7.51 (comp, 3H), 7.46 (dd, *J* = 8.4 Hz, 4.0 Hz, 1H), 2.55 (s, 3H), 1.41 (s, 9H), 0.34 (s, 9H); **^{13}C NMR** (100 MHz, $CDCl_3$) δ 170.1, 150.7, 148.4, 142.1, 141.4, 138.6, 138.3, 138.0, 136.5, 134.6, 134.6, 131.3, 130.1, 128.2, 127.7, 127.1 (x 2), 125.9 (x 2), 122.0, 121.8, 117.0, 34.7, 31.5, 20.0, 0.1; **HRMS** (ESI, m/z) calcd for $C_{30}H_{34}N_2OSi$ $[M + H]^+$ 467.2519, found 467.2510.

3'-fluoro-3-methyl-*N*-(quinolin-8-yl)-5-(trimethylsilyl)-[1,1'-biphenyl]-4-carboxamide (3x):

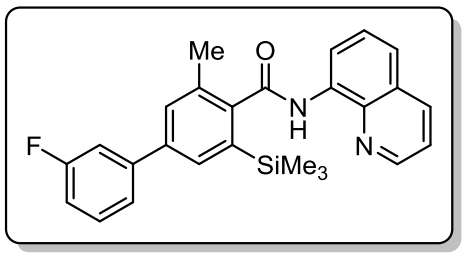

Yield 62% (53.5 mg); colorless solid; **R_f** 0.20 (pet ether/ethyl acetate = 9:1); **eluent composition** petroleum ether/ethyl acetate = 19:1; **mp** 116-118 °C; **^{1}H NMR** (400 MHz, $CDCl_3$) δ 10.04 (br s, 1H), 9.02 (dd, *J* = 7.6 Hz, 1.2 Hz, 1H), 8.75 (dd, *J* = 4.0 Hz, 1.6

Hz, 1H), 8.19 (dd, *J* = 8.0 Hz, 1.6 Hz, 1H), 7.67 (d, *J* = 1.2 Hz, 1H), 7.64 (app t, *J* = 8.0 Hz, 1H), 7.59 (dd, *J* = 8.0 Hz, 0.8 Hz, 1H), 7.49 (app s, 1H), 7.47-7.40 (comp, 3H), 7.33 (dd, *J* = 6.4 Hz, 1.6 Hz, 1H), 7.11-7.06 (m, 1H), 2.54 (s, 3H), 0.34 (s, 9H); **^{13}C NMR** (100 MHz, $CDCl_3$) δ 169.8, 163.3 (d, $^1J_{F\text{-}C}$ = 244.0 Hz), 148.4, 143.4 (d, $^3J_{F\text{-}C}$ = 8.0 Hz), 142.9, 140.2, 138.6, 138.5, 136.5, 134.9, 134.5, 131.2, 130.4 (d, $^3J_{F\text{-}C}$ = 9.0 Hz), 130.1, 128.2, 127.6, 123.1 (d, $^3J_{F\text{-}C}$ = 4.5 Hz), 122.2, 121.9, 117.0, 114.4 (d, $^2J_{F\text{-}C}$ = 21.0 Hz), 114.3 (d, $^2J_{F\text{-}C}$ = 22.0 Hz), 19.9, 0.1; **HRMS** (ESI, m/z) calcd for $C_{26}H_{25}FN_2OSi$ $[M + H]^+$ 429.1798, found 429.1802.

4'-fluoro-3-methyl-*N*-(quinolin-8-yl)-5-(trimethylsilyl)-[1,1'-biphenyl]-4-carboxamide (3y):

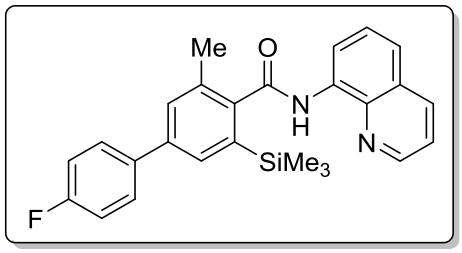

Yield 67% (57.3 mg); colorless solid; **R_f** 0.40 (pet ether/ethyl acetate = 9:1); **eluent composition** petroleum ether/ethyl acetate = 19:1; **mp** 166-168 ºC; **^{1}H NMR** (400 MHz, $CDCl_3$) δ 10.04 (br s, 1H), 9.02 (dd, *J* = 7.2 Hz, 0.8 Hz, 1H), 8.75 (dd, *J* = 4.0 Hz, 1.6 Hz, 1H), 8.19 (dd, *J* = 8.0 Hz, 1.6 Hz, 1H), 7.66-7.62 (comp, 2H), 7.60-7.56 (comp, 3H), 7.47-7.44 (comp, 2H), 7.20-7.14 (comp, 2H), 2.54 (s, 3H), 0.34 (s, 9H),; **^{13}C NMR** (100 MHz, $CDCl_3$) δ 169.9, 162.8 (d, $^1J_{F\text{-}C}$ = 245.0 Hz), 148.4, 142.4, 140.5, 138.6, 138.3, 137.2 (d, $^4J_{F\text{-}C}$ = 4.5 Hz), 136.5, 134.8, 134.5, 131.1, 130.0, 129.0 (d, $^3J_{F\text{-}C}$ = 8.0 Hz), 128.2, 127.7 (x 2), 122.0 (d, $^2J_{F\text{-}C}$ = 28.0 Hz), 117.0, 115.8 (d, $^2J_{F\text{-}C}$ = 21.0 Hz), 19.9, 0.1; **HRMS** (ESI, m/z) calcd for $C_{26}H_{25}FN_2OSi$ $[M + H]^+$ 429.1798, found 429.1801.

4'-chloro-3-methyl-*N*-(quinolin-8-yl)-5-(trimethylsilyl)-[1,1'-biphenyl]-4-carboxamide (3z):

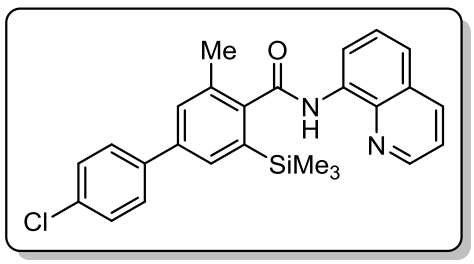

Yield 45% (40.2 mg); colorless solid; **R_f** 0.30 (pet ether/ethyl acetate = 9:1); **eluent composition** petroleum ether/ethyl acetate = 19:1; **mp** 148-150 ºC; **^{1}H NMR** (400 MHz, $CDCl_3$) δ 10.03 (br s, 1H), 9.02 (dd, *J* = 7.2 Hz, 1.6 Hz, 1H), 8.75 (dd, *J* = 4.0 Hz, 1.6 Hz, 1H), 8.19 (dd, *J* = 8.0 Hz, 1.6 Hz, 1H), 7.66-7.64 (m, 1H), 7.63 (d, *J* = 7.6 Hz, 1H), 7.59 (dd, *J* = 8.0 Hz, 1.6 Hz, 1H), 7.56-7.54 (comp, 2H), 7.46-7.44 (comp, 4H), 2.54 (s, 3H), 0.33 (s, 9H); **^{13}C NMR** (100 MHz, $CDCl_3$) δ 169.8, 148.4, 142.6, 140.2, 139.6, 138.6, 138.4, 136.5, 134.9, 134.5, 133.8, 131.1, 130.0, 129.1 (x 2), 128.7 (x 2), 128.2, 127.7, 122.1, 121.8, 117.0, 19.9, 0.1; **HRMS** (ESI, m/z) calcd for $C_{26}H_{25}ClN_2OSi$ $[M + H]^+$ 445.1503, found 445.1507.

3-methyl-*N*-(quinolin-8-yl)-4'-(trifluoromethyl)-5-(trimethylsilyl)-[1,1'-biphenyl]-4-carboxamide (3aa):

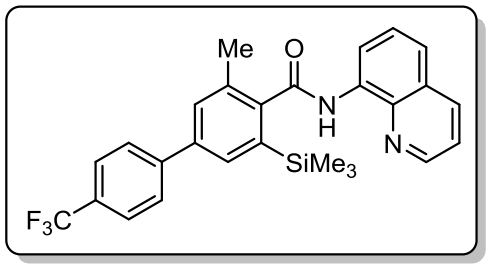

Yield 52% (50.0 mg); colorless solid; **R_f** 0.30 (pet ether/ethyl acetate = 9:1); **eluent composition** petroleum ether/ethyl acetate = 19:1; **mp** 142-144 ^oC; **^1H NMR** (400 MHz, $CDCl_3$) δ 10.05 (br s, 1H), 9.03 (dd, *J* = 7.6 Hz, 1.2 Hz, 1H), 8.76 (dd, *J* = 4.0 Hz, 1.6 Hz, 1H), 8.20 (dd, *J* = 8.4 Hz, 1.6 Hz, 1H), 7.76-7.72 (comp, 4H), 7.70 (d, *J* = 1.6 Hz, 1H), 7.65 (app t, *J* = 8.0 Hz, 1H), 7.60 (dd, *J* = 8.4 Hz, 1.2 Hz, 1H), 7.51 (d, *J* = 0.8 Hz, 1H), 7.46 (dd, *J* = 8.4 Hz, 4.0 Hz, 1H), 2.56 (s, 3H), 0.34 (s, 9H); **^{13}C NMR** (100 MHz, $CDCl_3$) δ 169.7, 148.4, 144.7, 143.2, 140.0, 138.6, 138.6, 136.6, 135.1, 134.5, 131.4, 130.3, 129.7 (q, *J* = 32.0 Hz), 128.2, 127.7 (x 2), 127.7, 125.9 (q, *J* = 3.0 Hz), 124.4 (q, *J* = 271.0 Hz), 122.2, 121.9, 117.0, 19.9, 0.1; **HRMS** (ESI, m/z) calcd for $C_{27}H_{25}F_3N_2OSi$ $[M + H]^+$ 479.1766, found 479.1765.

***N*-(quinolin-8-yl)-3-(trimethylsilyl)-[1,1'-biphenyl]-2-carboxamide (3ab):**

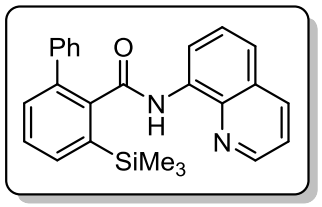

Yield 31% (24.3 mg); colorless solid; **R_f** 0.40 (pet ether/ethyl acetate = 9:1); **eluent composition** petroleum ether/ethyl acetate = 19:1; **mp** 146-148 ^oC; **^1H NMR** (400 MHz, $CDCl_3$) δ 9.62 (br s, 1H), 8.75 (dd, *J* = 7.2 Hz, 1.6 Hz, 1H), 8.57 (dd, *J* = 8.0 Hz, 1.6 Hz, 1H), 8.07 (dd, *J* = 8.0 Hz, 1.6 Hz, 1H), 7.69 (dd, *J* = 8.0 Hz, 1.6 Hz, 1H), 7.54-7.48 (comp, 4H), 7.47 (dd, *J* = 8.0 Hz, 1.6 Hz, 1H), 7.44 (dd, *J* = 8.0 Hz, 1.2 Hz, 1H), 7.34 (dd, *J* = 8.0 Hz, 4.0 Hz, 1H), 7.20-7.17 (comp, 2H), 7.07-7.03 (m, 1H), 0.35 (s, 9H); **^{13}C NMR** (100 MHz, $CDCl_3$) δ 169.5, 147.9, 142.5, 140.7, 139.4, 139.3, 138.4, 136.1, 134.6, 134.1, 131.0, 128.9 (x 2), 128.8, 128.2 (x 2), 127.9, 127.4, 127.3, 121.6, 121.5, 116.4, 0.2; **HRMS** (ESI, m/z) calcd for $C_{25}H_{24}N_2OSi$ $[M + H]^+$ 397.1736, found 397.1753.

2-ethyl-*N*-(quinolin-8-yl)-6-(trimethylsilyl)benzamide (3ac):

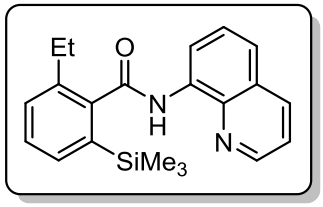

Yield 57% (39.8 mg); colorless solid; **R_f** 0.30 (pet ether/ethyl acetate = 9:1); **eluent composition** petroleum ether/ethyl acetate = 19:1; **mp** 110-112 ^oC (crystallization from $CHCl_3$ using solvent evaporation method); **^1H NMR** (400 MHz, $CDCl_3$) δ 9.99 (br s, 1H), 9.01 (dd, *J* = 7.2 Hz, 0.8 Hz, 1H), 8.73 (dd, *J* = 8.0 Hz, 1.6 Hz, 1H), 8.18 (dd, *J* = 7.6 Hz, 1.6 Hz, 1H), 7.63 (app t, *J* = 8.0 Hz, 1H), 7.57 (dd, *J* = 8.0 Hz, 0.8 Hz, 1H), 7.51 (dd, *J* = 7.2 Hz, 0.8 Hz, 1H), 7.44 (dd, *J* = 8.0 Hz, 4.0 Hz, 1H), 7.40 (app t, *J* = 7.2 Hz, 1H), 7.35 (d, *J* =

7.2 Hz, 1H), 2.79 (q, *J* = 7.6 Hz, 2H), 1.29 (t, *J* = 7.6 Hz, 3H), 0.28 (s, 9H); **^{13}C NMR** (100 MHz, $CDCl_3$) δ 170.0, 148.4, 142.9, 140.3, 138.6, 137.4, 136.4, 134.6, 132.4, 129.7, 128.8, 128.2, 127.6, 122.0, 121.8, 116.9, 26.6, 16.1, 0.1; **HRMS** (ESI, m/z) calcd for $C_{21}H_{24}N_2OSi$ $[M + H]^+$ 349.1736, found 349.1735.

Crystal data and structure refinement for 3ac, CCDC No. 2054614

Empirical formula	$C_{21}H_{24}N_2OSi$
Formula weight	348.51
Temperature/K	100.0
Crystal system	monoclinic
Space group	$P2_1/n$
a/Å	10.3889(6)
b/Å	13.8214(14)
c/Å	13.617(2)
α/°	90
β/°	94.158(7)
γ/°	90
Volume/Å^3	1950.1(4)
Z	4
ρ_{calc}g/cm^3	1.187
μ/mm^{-1}	1.133
F(000)	744.0
Crystal size/mm^3	0.35 × 0.25 × 0.2
Radiation	Cu Kα (λ = 1.54178)
2Θ range for data collection/°	9.128 to 133.466
Index ranges	$-11 \le h \le 12$, $-16 \le k \le 16$, $-16 \le l \le 16$
Reflections collected	28695
Independent reflections	3437 [R_{int} = 0.0586, R_{sigma} = 0.0314]
Data/restraints/parameters	3437/0/230
Goodness-of-fit on F^2	1.077
Final R indexes [I>=2σ (I)]	R_1 = 0.0399, wR_2 = 0.0946
Final R indexes [all data]	R_1 = 0.0416, wR_2 = 0.0958
Largest diff. peak/hole / e Å^{-3}	0.20/-0.29

2-isopropyl-*N*-(quinolin-8-yl)-6-(trimethylsilyl)benzamide (3ad):

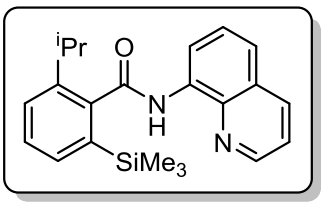

Yield 53% (38.4 mg); colorless solid; **R_f** 0.40 (pet ether/ethyl acetate = 9:1); **eluent composition** petroleum ether/ethyl acetate = 19:1; **mp** 154-156 °C; **^{1}H NMR** (400 MHz, $CDCl_3$) δ 10.00 (br s, 1H), 9.00 (app d, *J* = 7.2 Hz, 1H), 8.72 (dd, *J* = 8.0 Hz, 1.6 Hz, 1H), 8.18 (dd, *J* = 8.4 Hz, 1.2 Hz, 1H), 7.63 (app t, *J* = 8.0 Hz, 1H), 7.57 (d, *J* = 7.6 Hz, 1H), 7.51-7.49 (m, 1H), 7.46-7.42 (comp, 3H), 3.27-3.17 (m, 1H), 1.29 (d, *J* = 6.8 Hz, 6H), 0.27 (s, 9H); **^{13}C NMR** (100 MHz, $CDCl_3$) δ 170.0, 148.3, 145.0, 142.3, 138.5, 137.2, 136.5, 134.6,

132.5, 128.9, 128.2, 127.7, 126.7, 122.0, 121.8, 116.9, 30.8, 24.7, 0.1; **HRMS** (ESI, m/z) calcd for $C_{22}H_{26}N_2OSi$ $[M + H]^+$ 363.1893, found 363.1894.

***N*-(quinolin-8-yl)-3-(trimethylsilyl)thiophene-2-carboxamide (3ae):**[14a]

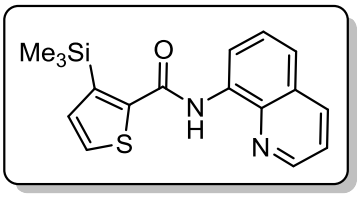

Yield 15% (9.6 mg); colorless solid; **R_f** 0.40 (pet ether/ethyl acetate = 9:1); **eluent composition** petroleum ether/ethyl acetate = 19:1; **mp** 118-120 °C; **^{1}H NMR** (400 MHz, $CDCl_3$) δ 10.44 (br s, 1H), 8.84-8.86 (comp, 2H), 8.18 (dd, *J* = 8.0 Hz, 1.6 Hz, 1H), 7.58 (app t, *J* = 8.0 Hz, 1H), 7.54 (dd, *J* = 8.0 Hz, 1.6 Hz, 1H), 7.49-7.46 (comp, 2H), 7.25 (d, *J* = 4.8 Hz, 1H), 0.41 (s, 9H); **^{13}C NMR** (100 MHz, $CDCl_3$) δ 161.4, 148.4, 147.3, 143.2, 138.7, 136.5, 135.1, 134.9, 128.2, 127.6, 127.3, 121.8, 121.7, 116.8, -0.0; **HRMS** (ESI, m/z) calcd for $C_{17}H_{18}N_2OSSi$ $[M + H]^+$ 327.0987, found 327.0986.

***N*-(quinolin-8-yl)-2-(trimethylsilyl)benzamide (3af):**[14a]

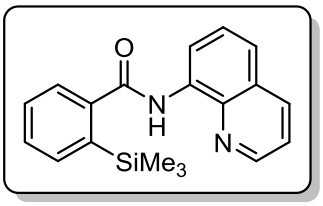

Yield 11% (7.2 mg); colorless solid; **R_f** 0.40 (pet ether/ethyl acetate = 9:1); **eluent composition** petroleum ether/ethyl acetate = 19:1; **mp** 106-108 °C; **^{1}H NMR** (400 MHz, $CDCl_3$) δ 10.32 (br s, 1H), 8.94 (dd, *J* = 7.2 Hz, 1.6 Hz, 1H), 8.79 (dd, *J* = 4.0 Hz, 1.6 Hz, 1H), 8.19 (dd, *J* = 8.4 Hz, 1.6 Hz, 1H), 7.80-7.75 (m, 1H), 7.74-7.71 (m, 1H), 7.61 (app t, *J* = 8.0 Hz, 1H), 7.56 (dd, *J* = 8.4 Hz, 1.6 Hz, 1H), 7.53-7.49 (comp, 2H), 7.47 (dd, *J* = 8.4 Hz, 4.4 Hz, 1H), 0.36 (s, 9H); **^{13}C NMR** (100 MHz, $CDCl_3$) δ 169.4, 148.3, 142.9, 140.2, 138.7, 136.6, 135.7, 134.9, 129.9, 129.1, 128.2, 127.7, 126.5, 121.9, 121.8, 116.8, 0.3; **HRMS** (ESI, m/z) calcd for $C_{19}H_{20}N_2OSi$ $[M + H]^+$ 321.1423, found 321.1422.

2-(dimethyl(phenyl)silyl)-6-methyl-*N*-(quinolin-8-yl)benzamide (3ag):

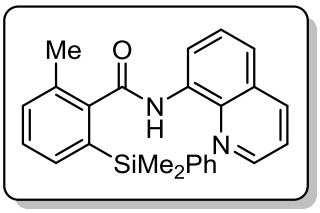

Yield 67% (53.4 mg); colorless solid; **R_f** 0.30 (pet ether/ethyl acetate = 9:1); **eluent composition** petroleum ether/ethyl acetate = 19:1; **mp** 132-134 °C (crystallization from $CHCl_3$ using solvent evaporation method); **^{1}H NMR** (400 MHz, $CDCl_3$) δ 9.71 (br s, 1H), 8.84 (dd, *J* = 7.2 Hz, 1.6 Hz, 1H), 8.61 (dd, *J* = 4.4 Hz, 1.6 Hz, 1H), 8.15 (dd, *J* = 8.0 Hz, 1.6 Hz, 1H), 7.58 (app t, *J* = 8.0 Hz, 1H), 7.54 (dd, *J* = 8.0 Hz, 1.6 Hz , 1H), 7.45 (dd, *J* = 6.8 Hz, 1.6 Hz, 1H), 7.44-7.39 (comp, 3H), 7.36-7.30 (comp, 2H), 7.06-7.02 (comp, 3H), 2.43 (s, 3H), 0.58 (s, 6H); **^{13}C NMR** (100 MHz, $CDCl_3$) δ 169.6, 148.1, 143.8, 138.5, 138.2, 136.3, 135.6, 134.4, 134.4, 134.2 (x 2), 133.5, 131.6, 128.6, 128.6, 128.0, 127.6 (x 2), 127.5, 121.9,

121.6, 116.9, 19.8, -1.3; **HRMS** (ESI, m/z) calcd for $C_{25}H_{24}N_2OSi$ $[M + H]^+$ 397.1736, found 397.1739.

Crystal data and structure refinement for 3ag, CCDC No. 2054615

Empirical formula	$C_{25}H_{24}N_2OSi$
Formula weight	396.55
Temperature/K	100.0
Crystal system	monoclinic
Space group	$P2_1/c$
a/Å	12.9104(3)
b/Å	11.5100(3)
c/Å	15.1097(4)
α/°	90
β/°	114.9740(10)
γ/°	90
Volume/Å^3	2035.35(9)
Z	4
ρ_{calc}g/cm^3	1.294
μ/mm^{-1}	1.156
F(000)	840.0
Crystal size/mm^3	0.25 × 0.18 × 0.12
Radiation	Cu Kα (λ = 1.54178)
2Θ range for data collection/°	7.554 to 127.608
Index ranges	$-15 \leq h \leq 14$, $-13 \leq k \leq 13$, $-13 \leq l \leq 17$
Reflections collected	15965
Independent reflections	3297 [R_{int} = 0.0730, R_{sigma} = 0.0568]
Data/restraints/parameters	3297/0/265
Goodness-of-fit on F^2	1.061
Final R indexes [I>=2σ (I)]	R_1 = 0.0603, wR_2 = 0.1655
Final R indexes [all data]	R_1 = 0.0652, wR_2 = 0.1707
Largest diff. peak/hole / e Å^{-3}	0.37/-0.62

2-methyl-6-(methyldiphenylsilyl)-*N*-(quinolin-8-yl)benzamide (3ah):

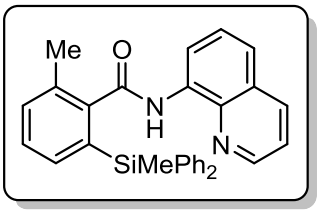

Yield 47% (42.9 mg); colorless solid; **R_f** 0.30 (pet ether/ethyl acetate = 9:1); **eluent composition** petroleum ether/ethyl acetate = 19:1; **mp** 160-162 °C; **^{1}H NMR** (400 MHz, $CDCl_3$) δ 9.58 (br s, 1H), 8.66-8.61 (m, 1H), 8.49 (dd, *J* = 4.0 Hz, 1.6 Hz, 1H), 8.11 (dd, *J* = 8.0 Hz, 1.6 Hz, 1H), 7.50-7.48 (comp, 2H), 7.43-7.41 (comp, 4H), 7.38-7.27 (comp, 4H), 7.15-7.08 (comp, 6H), 2.47 (s, 3H), 0.85 (s, 3H); **^{13}C NMR** (100 MHz, $CDCl_3$) δ 169.2, 147.8, 144.3, 138.2, 136.4, 136.3, 135.2 (x 4), 135.0, 134.7, 134.2, 133.6, 132.0, 129.0 (x 2), 128.5, 127.8, 127.7 (x 4), 127.4, 121.8, 121.3, 117.0, 19.9, -2.6; **HRMS** (ESI, m/z) calcd for $C_{30}H_{26}N_2OSi$ $[M + H]^+$ 459.1893, found 459.1896.

2,2-dimethyl-*N*-(quinolin-8-yl)-3-(trimethylsilyl)propanamide (3ai):

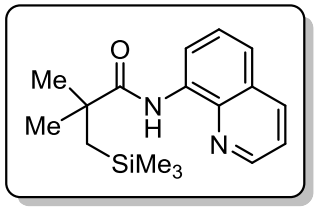

Yield 13% (8.0 mg); colorless oil; **R_f** 0.30 (pet ether/ethyl acetate = 9:1); **eluent composition** petroleum ether/ethyl acetate = 19:1; **^{1}H NMR** (400 MHz, $CDCl_3$) δ 10.27 (br s, 1H), 8.82 (dd, *J* = 4.0 Hz, *J* = 1.6 Hz, 1H), 8.79 (dd, *J* = 7.2 Hz, *J* = 1.6 Hz, 1H), 8.16 (dd, *J* = 8.0 Hz, *J* = 1.6 Hz, 1H), 7.54 (app t, *J* = 8.0 Hz, 1H), 7.48 (dd, *J* = 8.8 Hz, 1.2 Hz, 1H), 7.45 (dd, *J* = 8.0 Hz, 4.0 Hz, 1H), 1.47 (s, 6H), 1.20 (s, 2H), 0.03 (s, 9H); **^{13}C NMR** (100 MHz, $CDCl_3$) δ 177.5, 148.3, 138.9, 136.5, 134.9, 128.1, 127.7, 121.6, 121.3, 116.4, 43.0, 31.0, 29.1, 0.3; **HRMS** (ESI, m/z) calcd for $C_{17}H_{24}N_2OSi$ $[M + H]^+$ 301.1736, found 301.1738.

***N*-(quinolin-8-yl)-2-(trimethylsilyl)-1-naphthamide (S3a):**[14a]

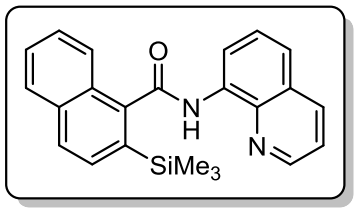

Yield 20% (14.9 mg); colorless solid; **R_f** 0.40 (pet ether/ethyl acetate = 9:1); **eluent composition** petroleum ether/ethyl acetate = 19:1; **mp** 156-158 °C; **^{1}H NMR** (400 MHz, $CDCl_3$) δ 10.20 (br s, 1H), 9.13 (app d, *J* = 7.6 Hz, 1H), 8.66 (app d, *J* = 2.8 Hz, 1H), 8.19 (app d, *J* = 7.6 Hz, 1H), 8.10 (app d, *J* = 8.0 Hz, 1H), 7.93 (app d, *J* = 8.4 Hz, 1H), 7.78 (app d, *J* = 7.6 Hz, 1H), 7.72 (d, *J* = 8.0 Hz, 1H), 7.68 (app t, *J* = 8.0 Hz, 1H), 7.61 (d, *J* = 7.6 Hz, 1H), 7.54-7.46 (comp, 2H), 7.43 (dd, *J* = 8.4 Hz, 4.0 Hz, 1H), 0.36 (s, 9H); **^{13}C NMR** (100 MHz, $CDCl_3$) δ 169.6, 148.4, 142.0, 138.5, 136.5, 135.1, 134.7, 133.7, 130.5, 130.0, 128.4, 128.2, 128.1, 127.7, 127.1, 126.8, 125.4, 122.2, 121.8, 117.5, 0.0; **HRMS** (ESI, m/z) calcd for $C_{23}H_{22}N_2OSi$ $[M + H]^+$ 371.1580, found 371.1574.

***N*-(quinolin-8-yl)-2-(trimethylsilyl)benzamide (S3b):**[14a]

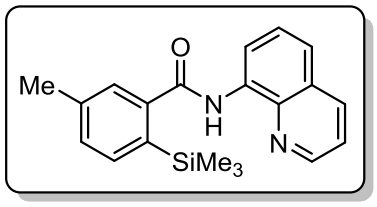

Yield 14% (9.3 mg); colorless solid; **R_f** 0.30 (pet ether/ethyl acetate = 9:1); **eluent composition** petroleum ether/ethyl acetate = 19:1; **mp** 110-112 °C; **^{1}H NMR** (400 MHz, $CDCl_3$) δ 10.26 (br s, 1H), 8.94 (dd, *J* = 7.2 Hz, 1.6 Hz, 1H), 8.80 (dd, *J* = 4.4 Hz, 1.6 Hz, 1H), 8.20 (dd, *J* = 8.4 Hz, 1.6 Hz, 1H), 7.63-7.59 (comp, 2H), 7.57-7.54 (comp, 2H), 7.47 (dd, *J* = 8.0 Hz, 4.0 Hz , 1H), 7.32 (dd, *J* = 7.6 Hz, 0.8 Hz, 1H), 2.45 (s, 3H), 0.33 (s, 9H); **^{13}C NMR** (100 MHz, $CDCl_3$) δ 169.7, 148.3, 143.1, 139.1, 138.7, 136.6, 136.4, 135.7, 135.0, 130.6, 128.2, 127.7, 127.3, 121.8, 121.8, 116.8, 21.5, 0.3; **HRMS** (ESI, m/z) calcd for $C_{20}H_{22}N_2OSi$ $[M + H]^+$ 335.1580, found 335.1590.

***N*-(quinolin-8-yl)-2-(trimethylsilyl)cyclopent-1-ene-1-carboxamide (S3c):**[14f]

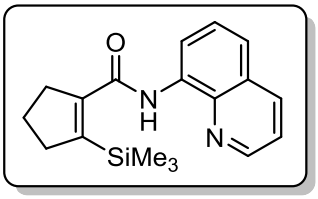

Yield 12% (7.4 mg); colorless solid; **R_f** 0.40 (pet ether/ethyl acetate = 9:1); **eluent composition** petroleum ether/ethyl acetate = 19:1; **mp** 122-124 °C; **^{1}H NMR** (400 MHz, $CDCl_3$) δ 10.02 (br s, 1H), 8.85 (dd, *J* = 7.6 Hz, *J* = 1.6 Hz, 1H), 8.81 (dd, *J* = 4.4 Hz, *J* = 1.6 Hz, 1H), 8.17 (dd, *J* = 8.4 Hz, *J* = 1.6 Hz, 1H), 7.56 (app t, *J* = 8.0 Hz, 1H), 7.51 (dd, *J* = 8.0 Hz, 1.6 Hz, 1H), 7.46 (dd, *J* = 8.4 Hz, 4.4 Hz, 1H), 2.98-2.92 (m, 2H), 2.69-2.64 (m, 2H), 2.05-1.98 (m, 2H), 0.22 (s, 9H); **^{13}C NMR** (100 MHz, $CDCl_3$) δ 165.7, 155.0, 148.2, 147.2, 138.5, 136.7, 134.8, 128.2, 127.7, 121.7, 121.5, 117.0, 39.8, 36.0, 24.1, -0.7; **HRMS** (ESI, m/z) calcd for $C_{18}H_{22}N_2OSi$ $[M + H]^+$ 311.1580, found 311.1589.

4.5.5. Mechanistic Experiments

(a) Procedure for H/D exchange experiments:

Procedure for H/D exchange experiment (with 1a):

An oven-dried 10 mL Schlenk tube was charged with 2-methyl-*N*-(quinolin-8-yl)benzamide (**1a**) (52.5 mg, 0.2 mmol, 1.0 equiv) $Cu(OAc)_2$ (3.6 mg, 0.02 mmol, 0.1 equiv), $MgSO_4$ (48.2 mg, 0.4 mmol, 2.0 equiv), Ag_2CO_3 (82.8 mg, 0.3 mmol, 1.5 equiv). Then CD_3OD (0.16 mL, 4.0 mmol, 20.0 equiv) and 2.0 mL (0.1 M) of anhydrous DMF was added. The tube was closed with a teflon-lined cap and kept on stirring in an oil bath. The bath temperature was slowly increased to 120 °C. After 36 h, the reaction was stopped and cooled to room temperature. The reaction mixture was filtered through a short pad of celite, poured to water (20 mL) and extracted with ethyl acetate (3 x 5 mL). The combined organic layers were washed with brine solution (2 x 5 mL). The organic phase was separated, dried over anhydrous Na_2SO_4, filtered and concentrated under vacuo. The starting material (**1a**-d_n) was recovered (51.7 mg, 99%) by purifying through column chromatography on silica gel using ethyl acetate/pet ether as eluent. The deuterium incorporation (<5%) was determined by ^{1}H NMR spectroscopy.

Procedure for H/D exchange experiment (with 1a-d_1):

An oven-dried 10 mL Schlenk tube was charged with 2-methyl-*N*-(quinolin-8-yl)benzamide-6-*d* (**1a**-d_1, 92% D) (52.5 mg, 0.2 mmol, 1.0 equiv) $Cu(OAc)_2$ (3.6 mg, 0.02 mmol, 0.1 equiv), $MgSO_4$ (48.2 mg, 0.4 mmol, 2.0 equiv), Ag_2CO_3 (82.8 mg, 0.3 mmol, 1.5 equiv). Then a H-source (4.0 mmol, 20.0 equiv) and 2.0 mL (0.1 M) of anhydrous DMF was added. The tube was closed with a teflon-lined cap and kept on stirring in an oil bath. The bath temperature was slowly increased to 120 °C. After 36 h, the reaction was stopped and cooled to room

temperature. The reaction mixture was filtered through a short pad of celite, poured to water (20 mL) and extracted with ethyl acetate (3 x 5 mL). The combined organic layers were washed with brine solution (2 x 5 mL). The organic phase was separated, dried over anhydrous Na_2SO_4, filtered and concentrated under vacuo. The starting material (**1a**-d_1) was recovered by purifying through column chromatography on silica gel using ethyl acetate/pet ether as eluent. The hydrogen incorporation was determined by ^{1}H NMR spectroscopy.

(b) Procedure for competitive experiment between 1b and 1d:

To an oven-dried 10 mL Schlenk tube a mixture of **1b** and **1d** (0.1 mmol each) were subjected under standard condition. After 36 h, the reaction was stopped and cooled to room temperature. The reaction mixture was filtered through a short pad of celite and concentrated under vacuo. The crude reaction mixture was directly purified by column chromatography on silica gel using pet ether/ethyl acetate as eluent to obtain pure **3b** and **3d** in 17% and 47% yields respectively.

(c) Procedure for competitive experiment between 1p and 1r:

To an oven-dried 10 mL Schlenk tube a mixture of **1p** and **1r** (0.1 mmol each) were subjected under standard condition. After 36 h, the reaction was stopped and cooled to room temperature. The reaction mixture was filtered through a short pad of celite and concentrated under vacuo. The crude reaction mixture was directly purified by column chromatography on silica gel using pet ether/ethyl acetate as eluent to obtain pure **3p** and **3r** in 14% and 33% yields respectively.

4.6. ^{1}H and ^{13}C NMR Spectra of Representative Compounds

^{1}H NMR of **1a** (400 MHz, $CDCl_3$):[16h]

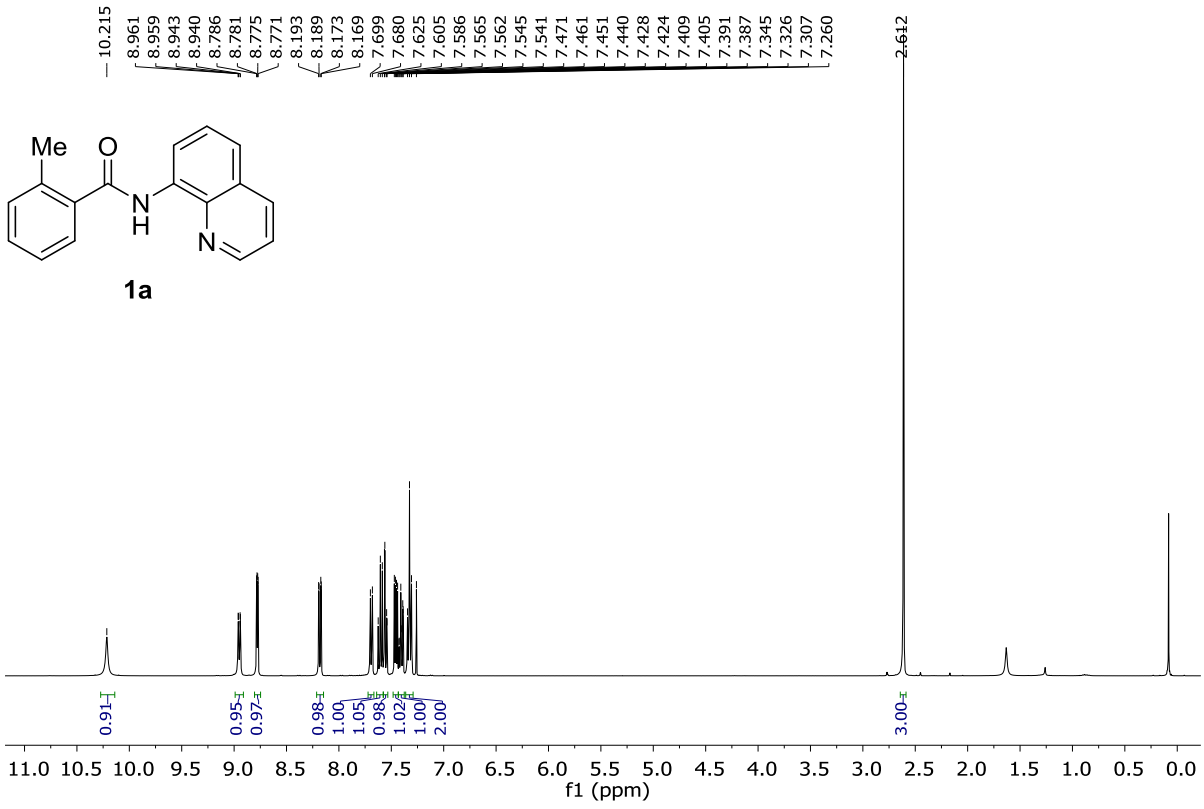

^{13}C NMR of **1a** (100 MHz, $CDCl_3$):

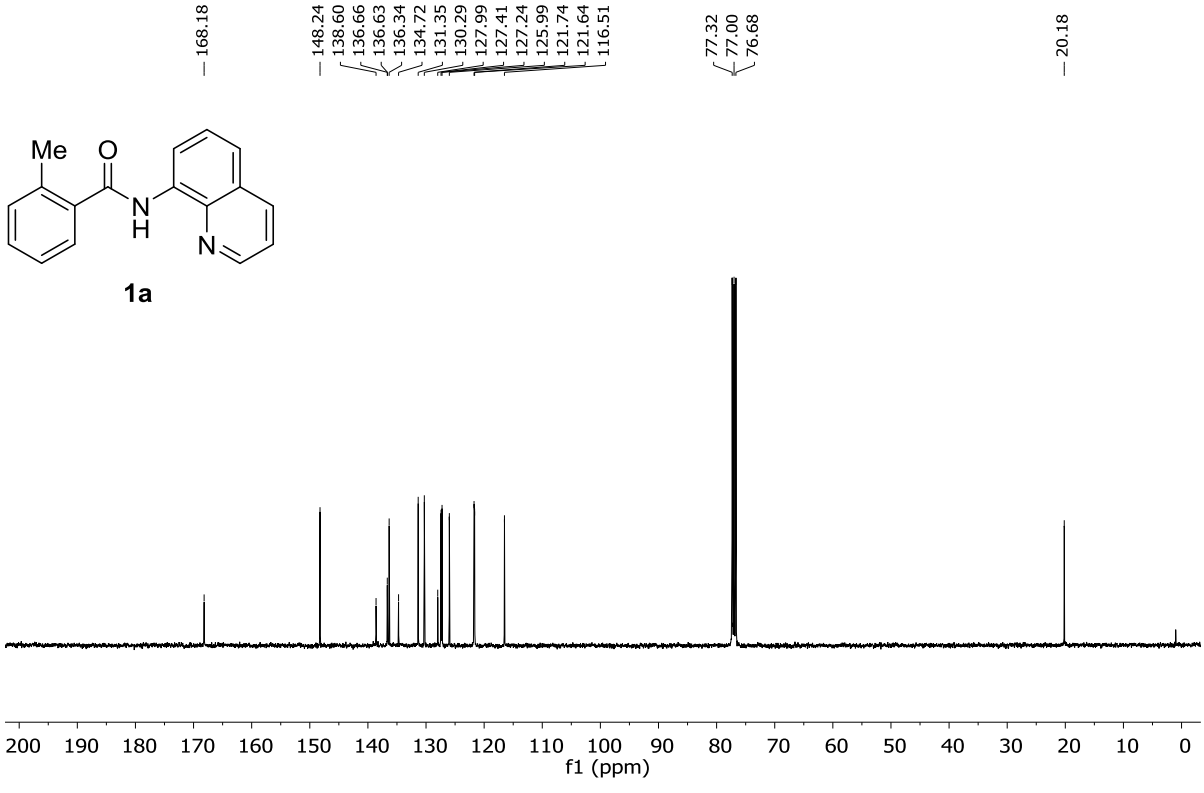

^{1}H NMR of **3a** (400 MHz, $CDCl_3$):

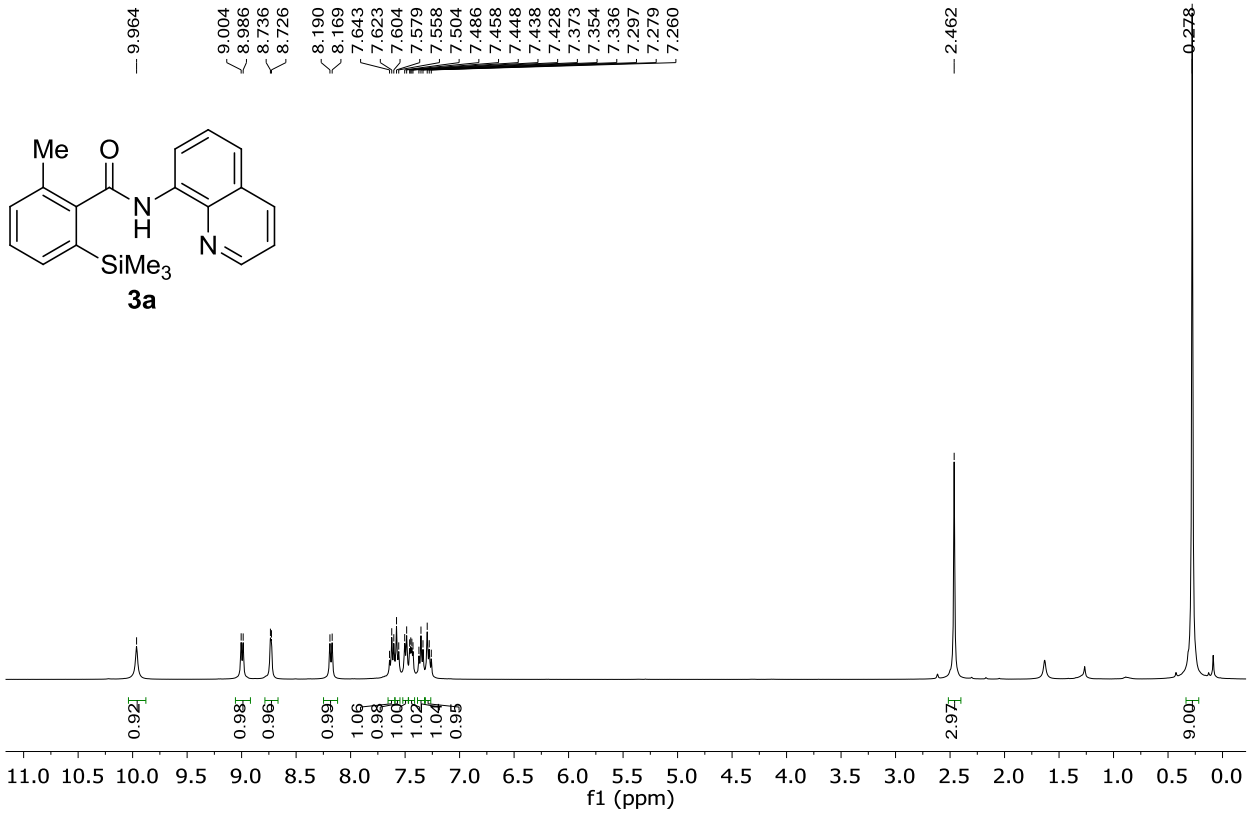

^{13}C NMR of **3a** (100 MHz, $CDCl_3$):

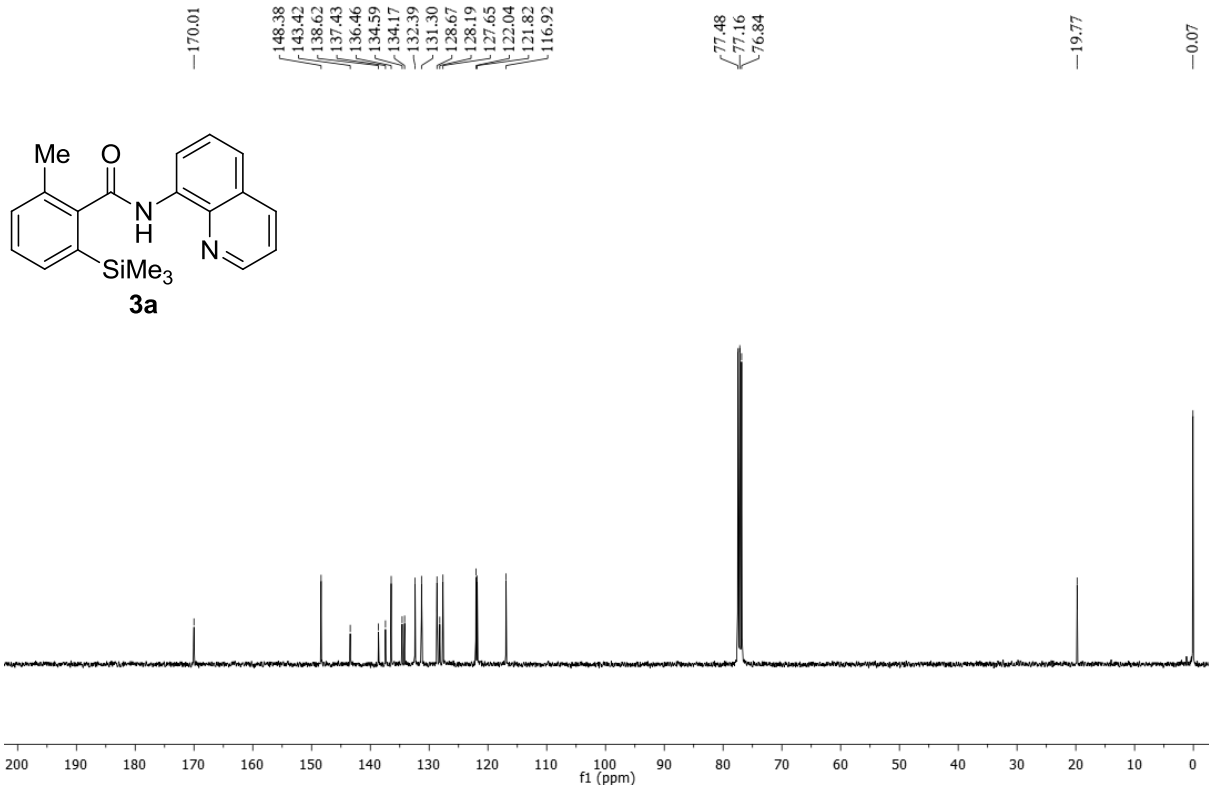

^{1}H NMR of **3c** (400 MHz, $CDCl_3$):

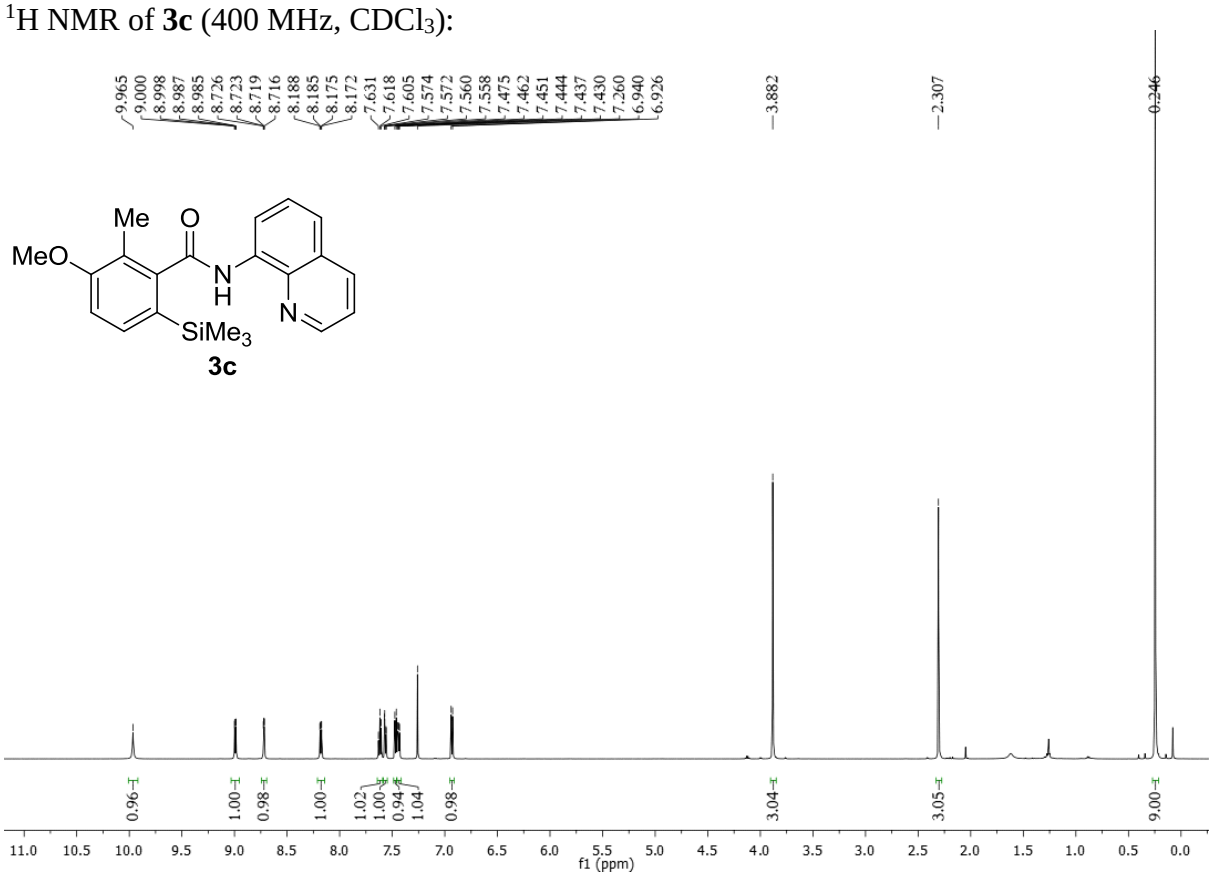

^{13}C NMR of **3c** (100 MHz, $CDCl_3$):

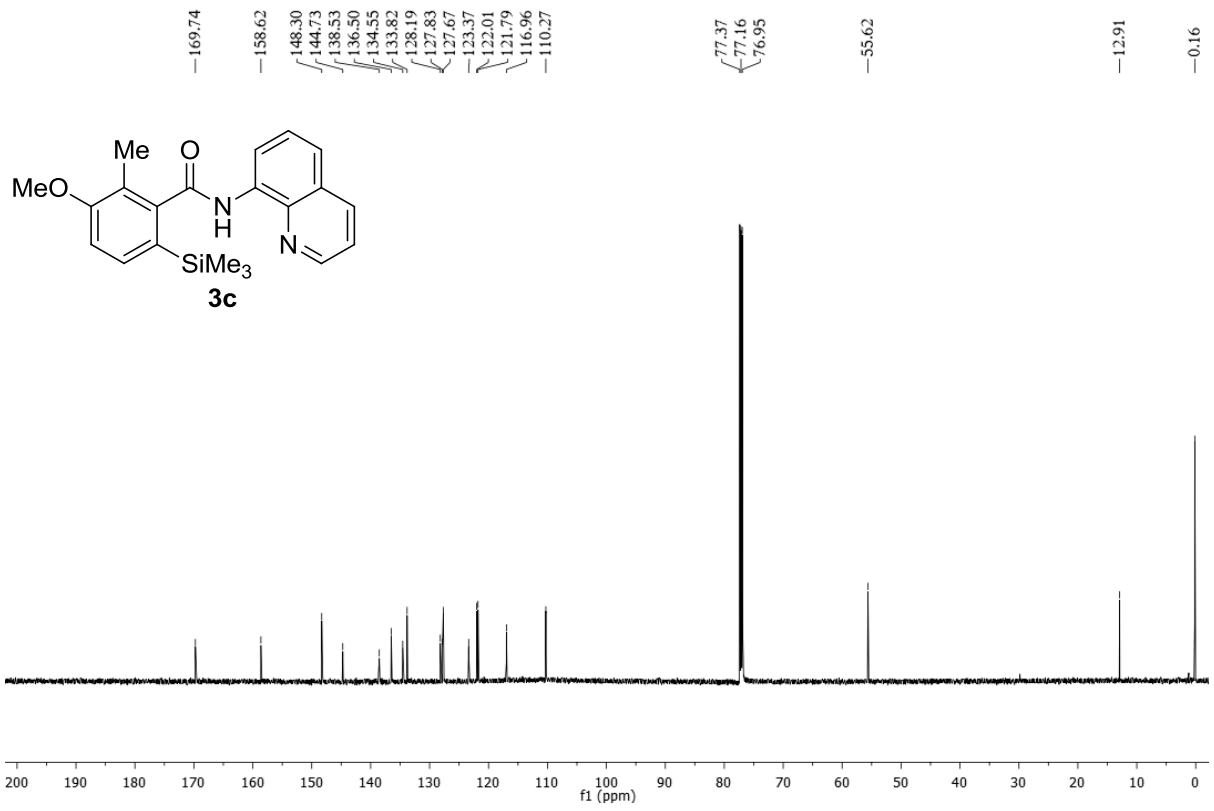

^{1}H NMR of **3f** (600 MHz, $CDCl_3$):

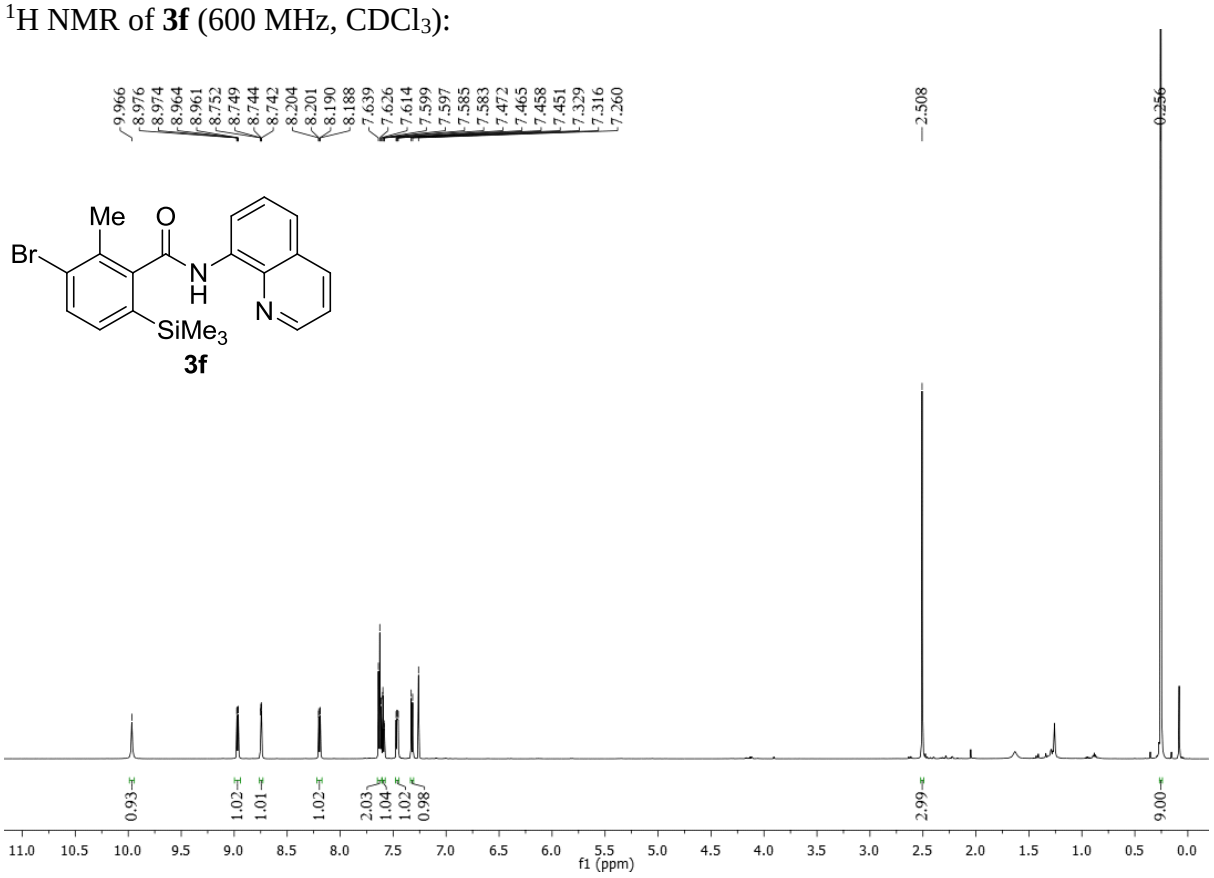

^{13}C NMR of **3f** (150 MHz, $CDCl_3$):

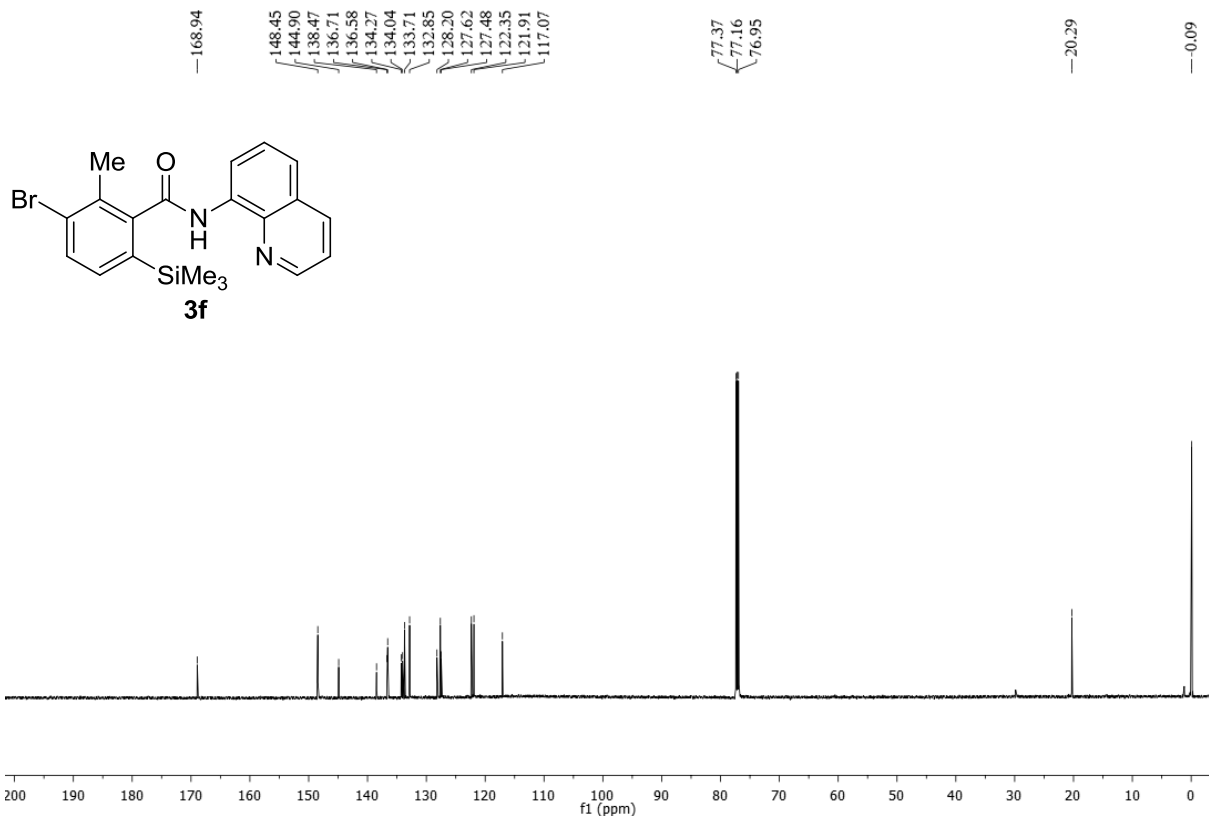

^{1}H NMR of **3g** (400 MHz, $CDCl_3$):

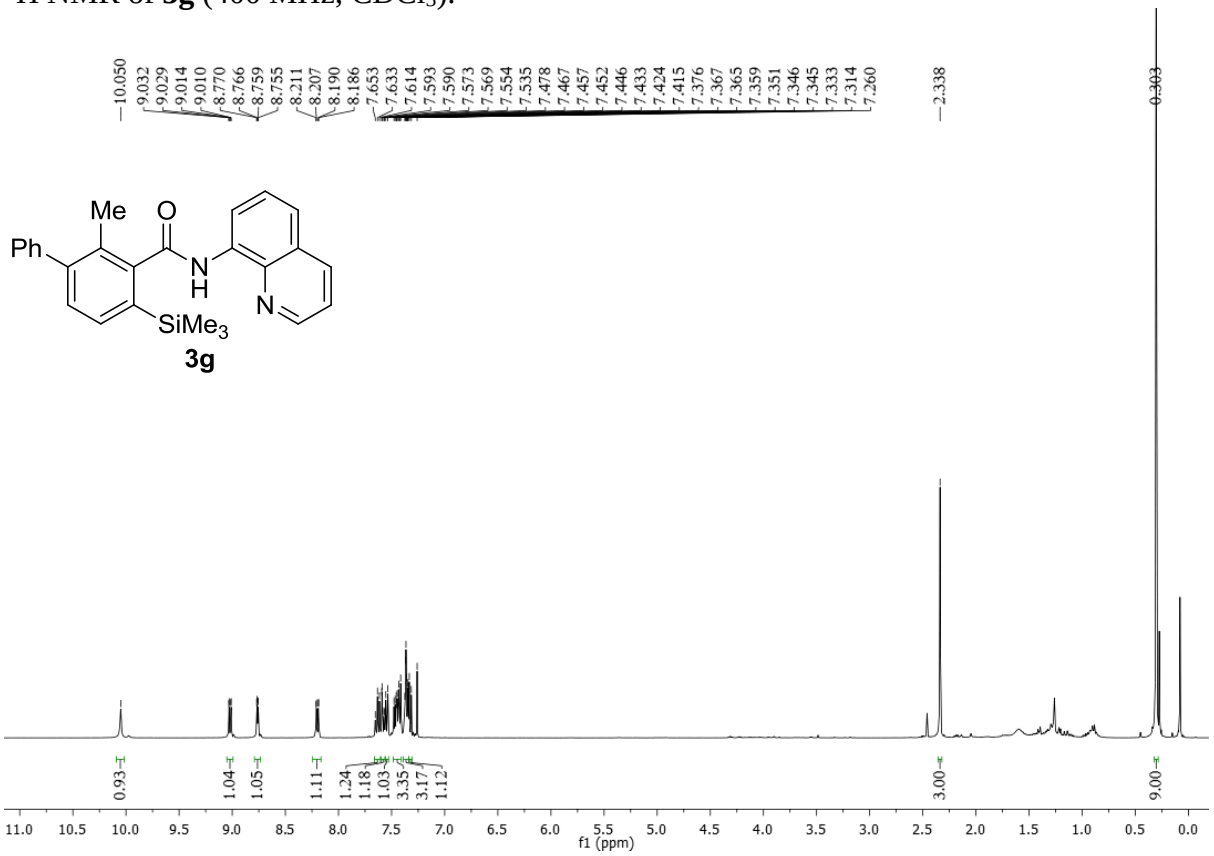

^{13}C NMR of **3g** (100 MHz, $CDCl_3$):

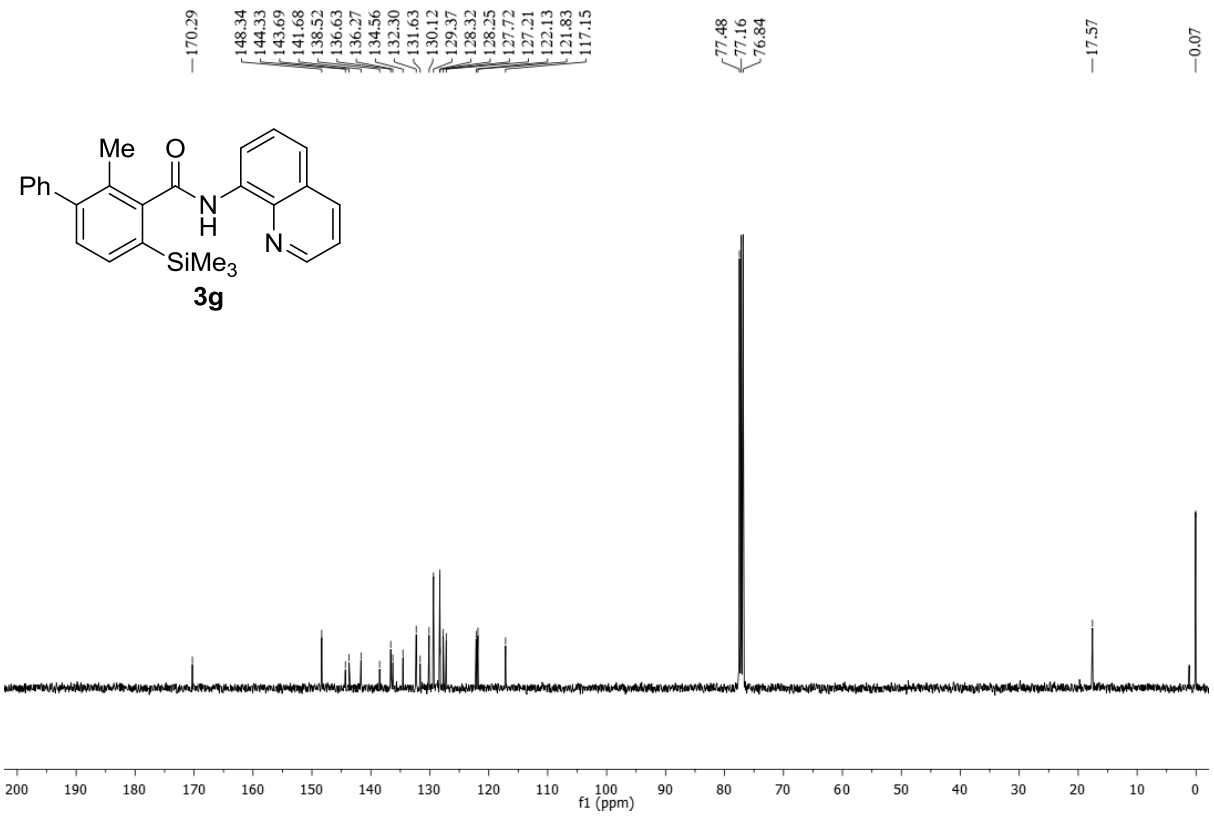

^{1}H NMR of **3j** (400 MHz, $CDCl_3$):

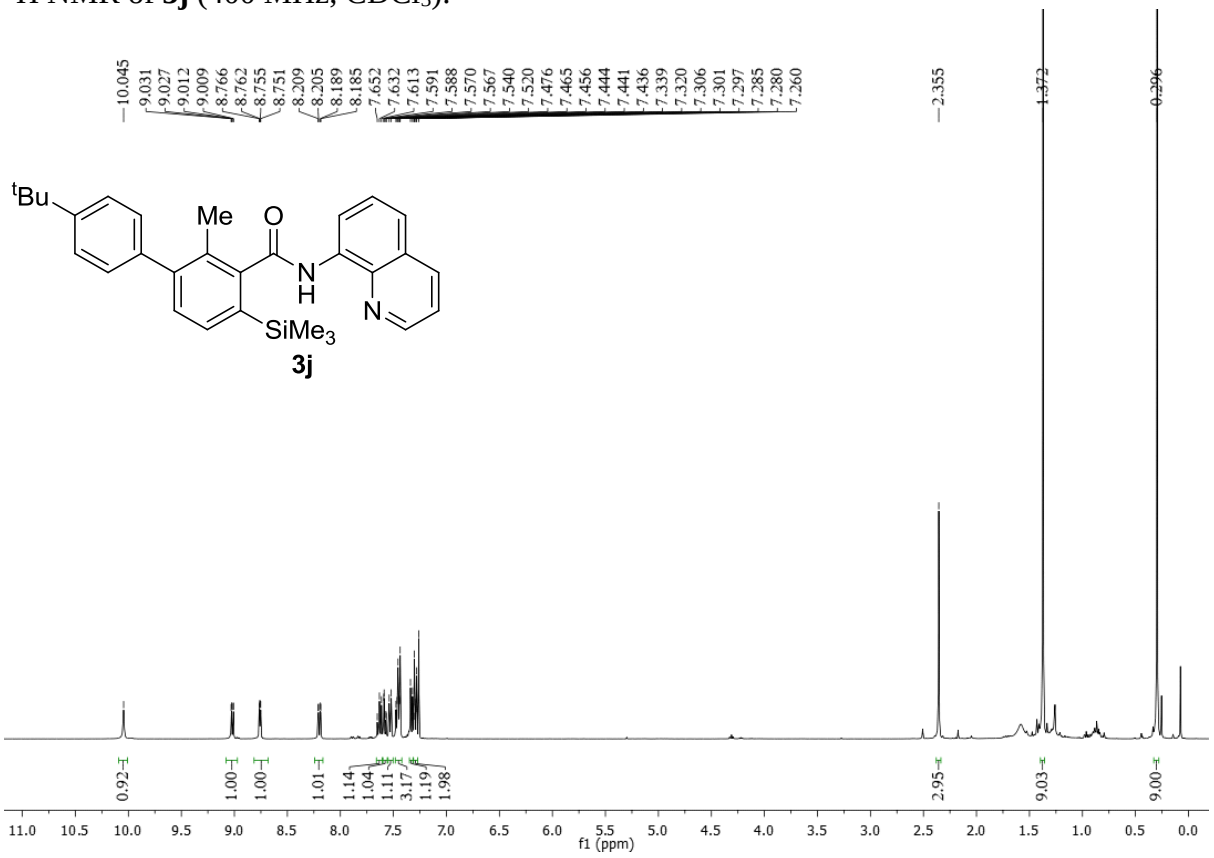

^{13}C NMR of **3j** (100 MHz, $CDCl_3$):

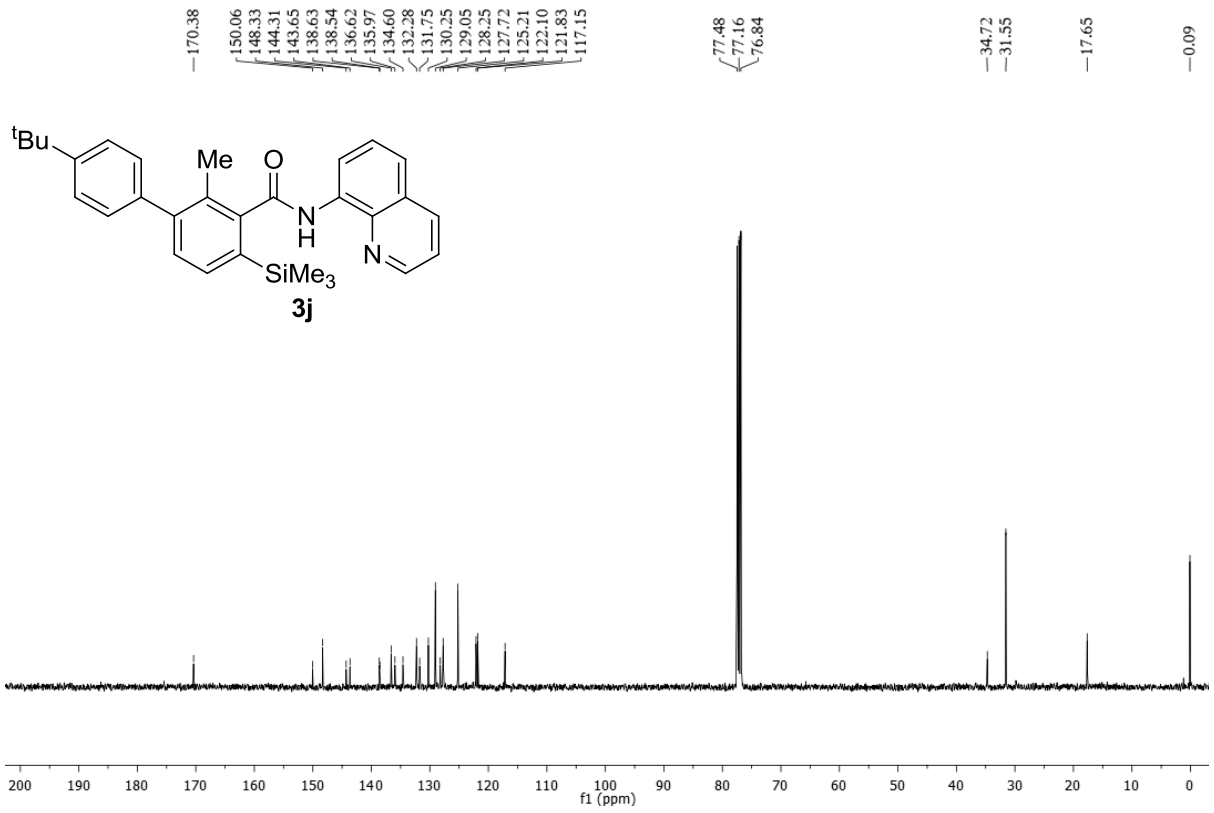

^{1}H NMR of **3l** (400 MHz, $CDCl_3$):

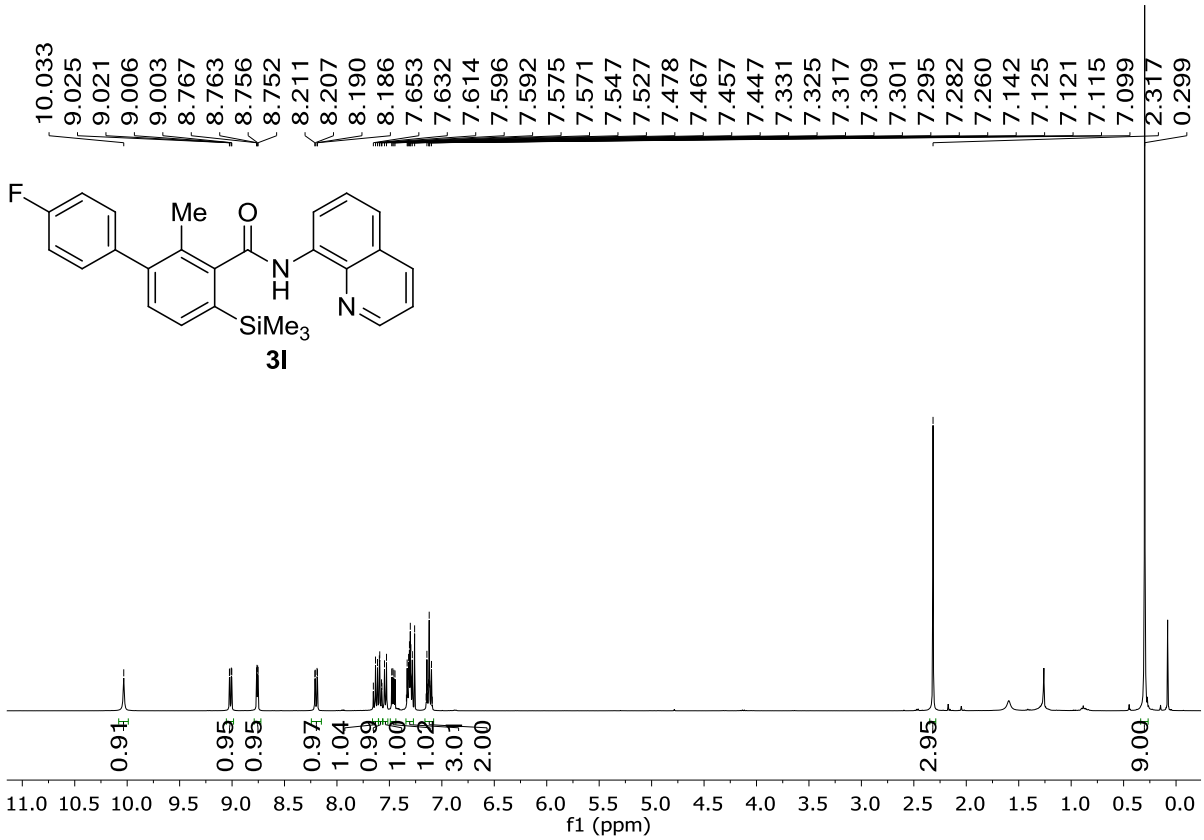

^{13}C NMR of **3l** (100 MHz, $CDCl_3$):

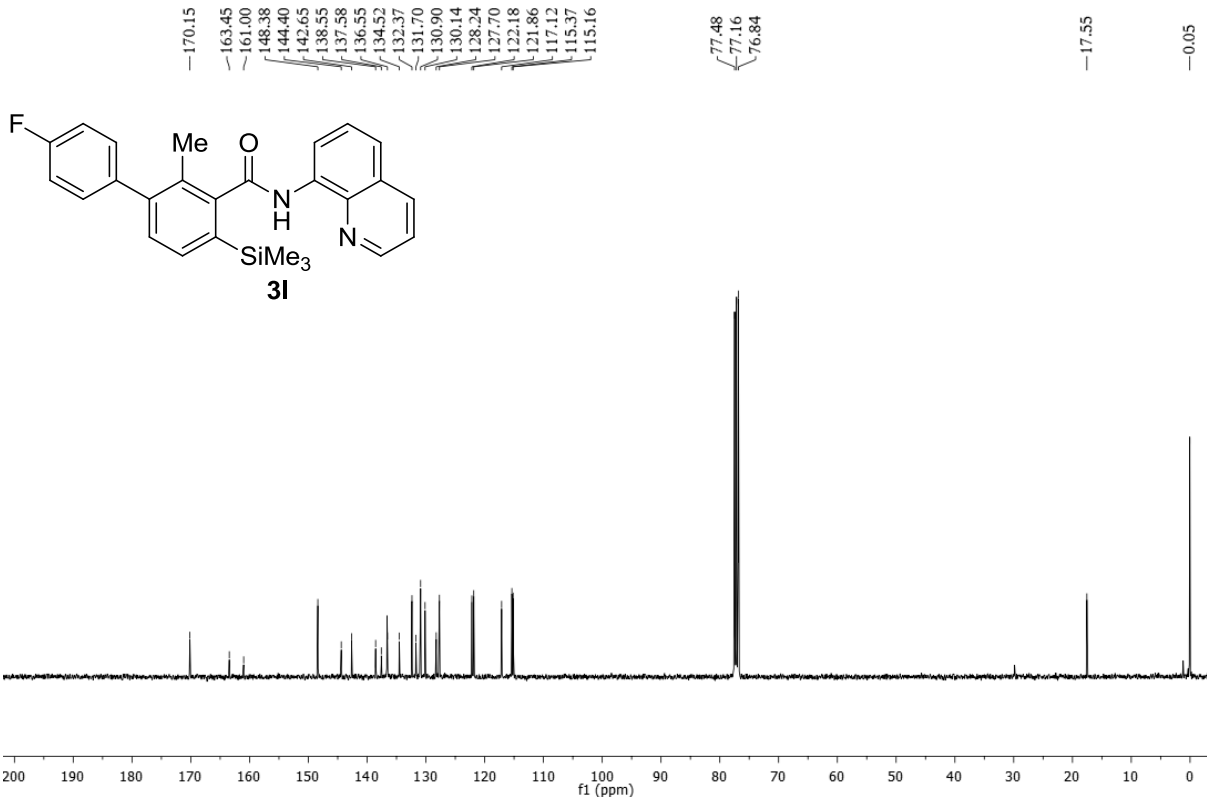

^{1}H NMR of **3o** (400 MHz, $CDCl_3$):

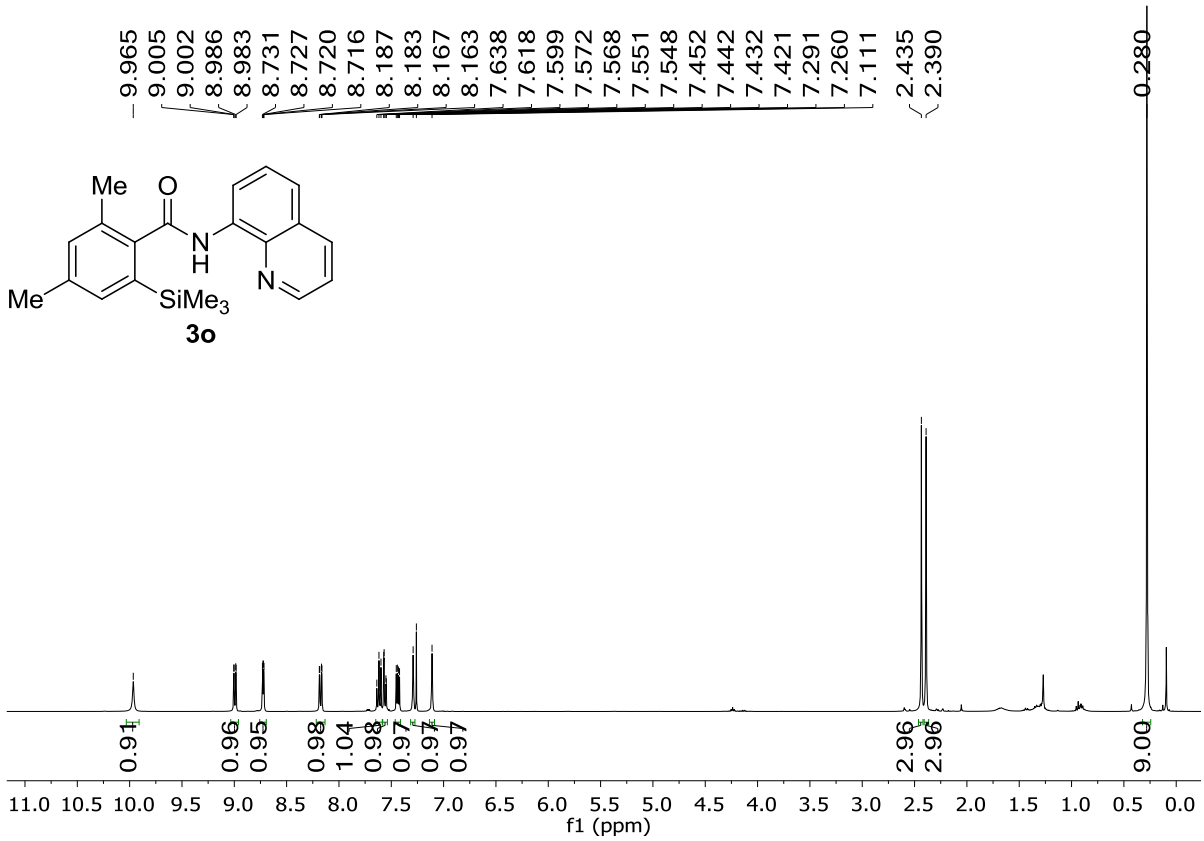

^{13}C NMR of **3o** (100 MHz, $CDCl_3$):

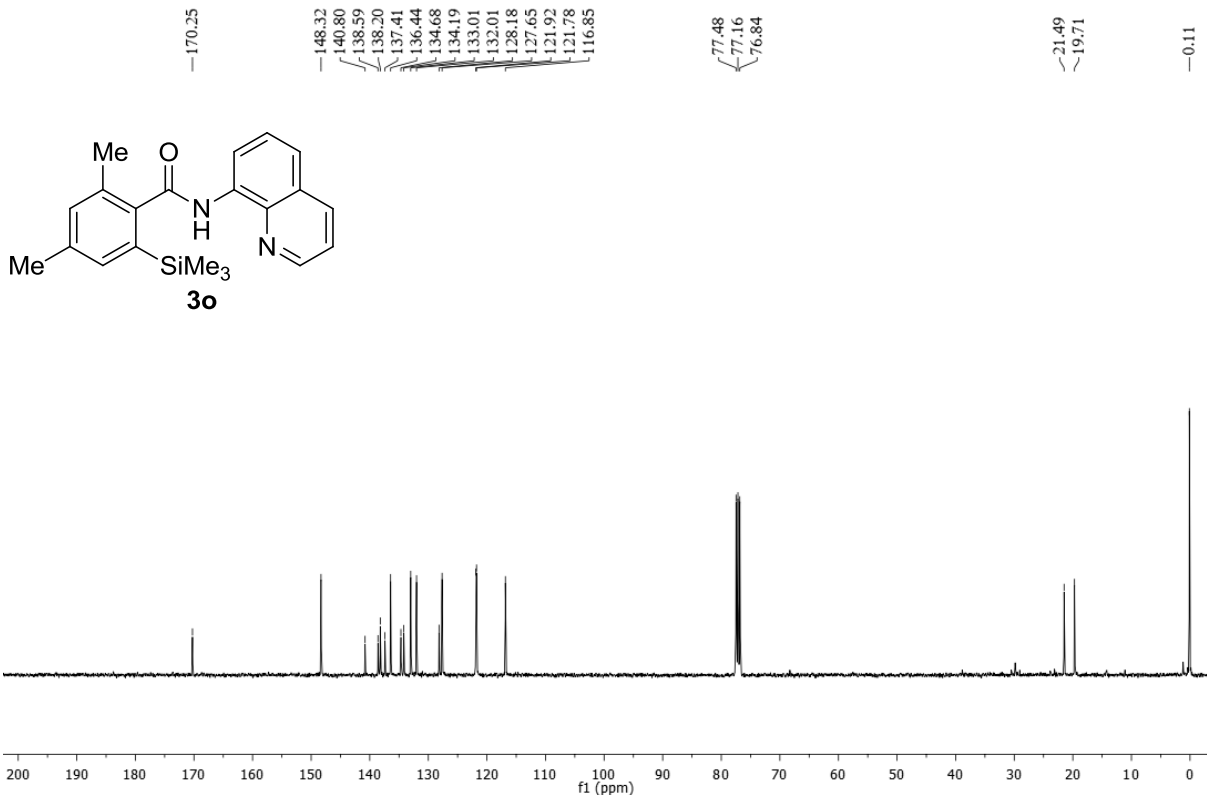

^{1}H NMR of **3r** (400 MHz, $CDCl_3$):

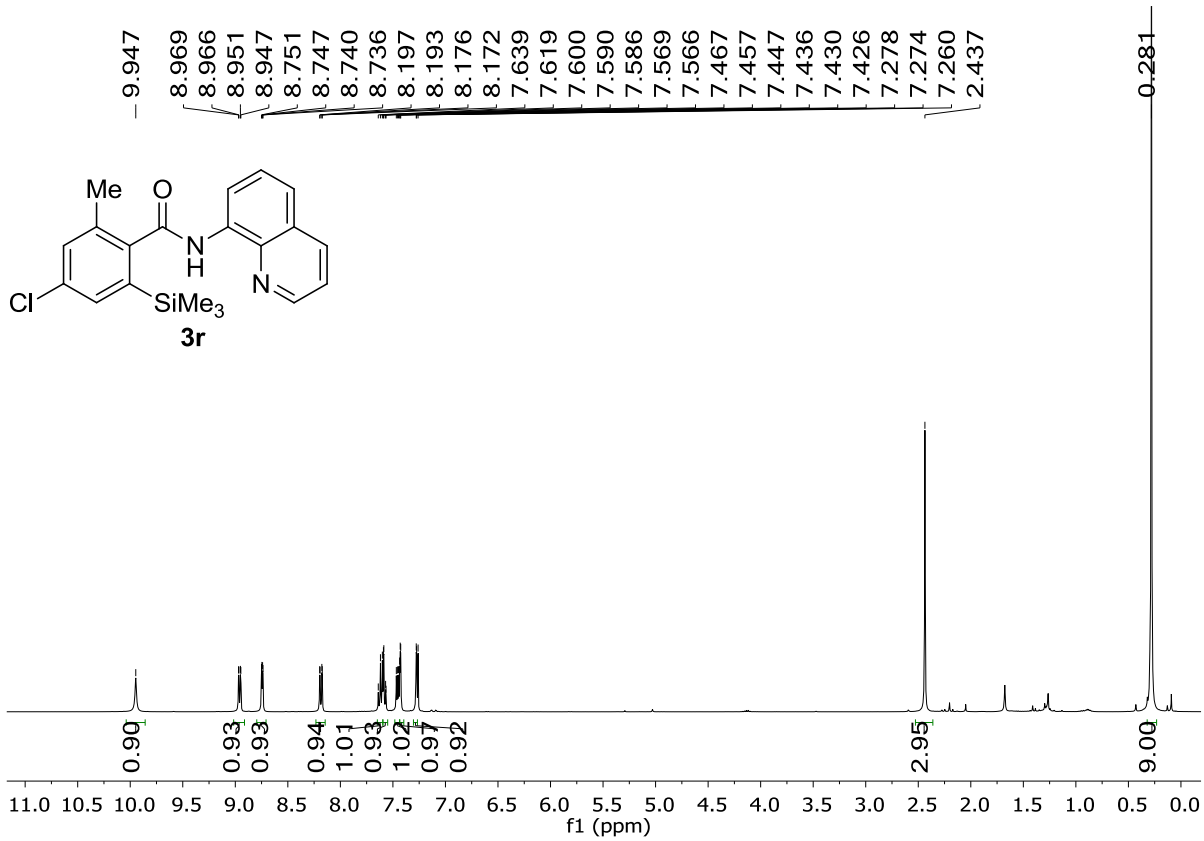

^{13}C NMR of **3r** (100 MHz, $CDCl_3$):

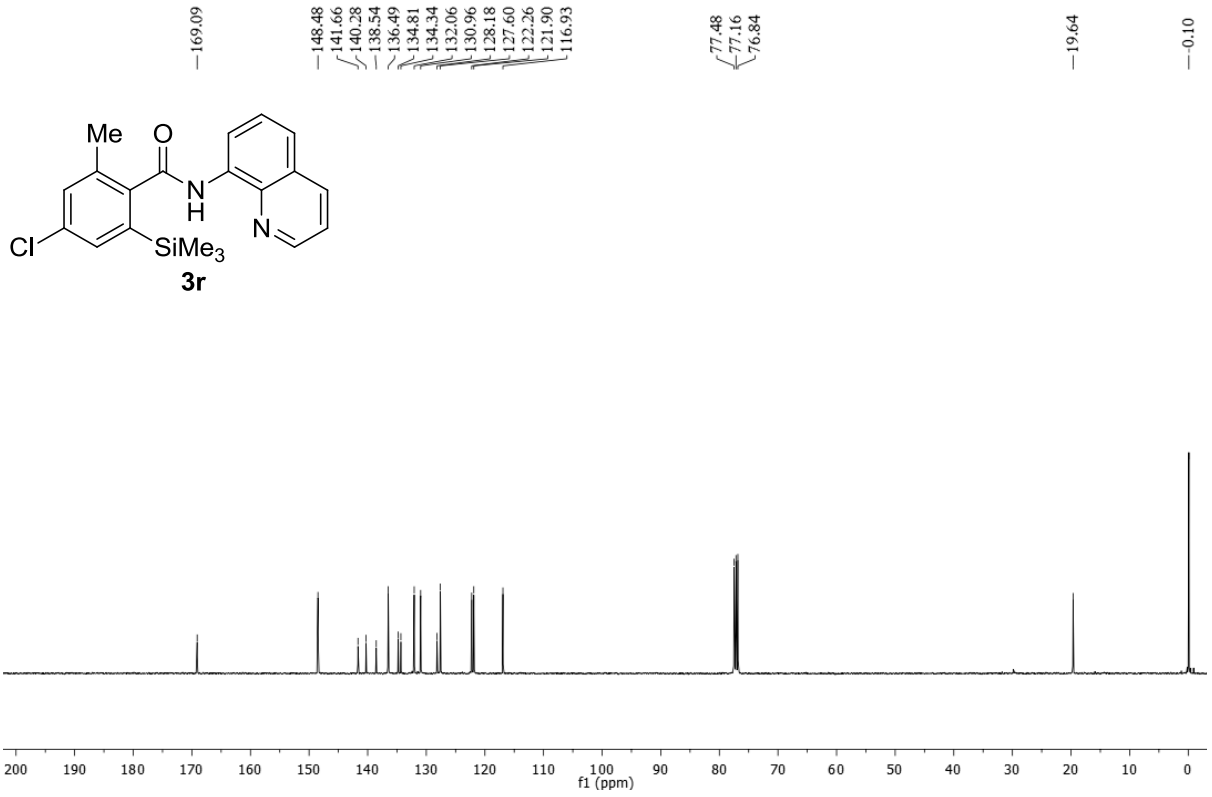

^{1}H NMR of **3v** (400 MHz, $CDCl_3$):

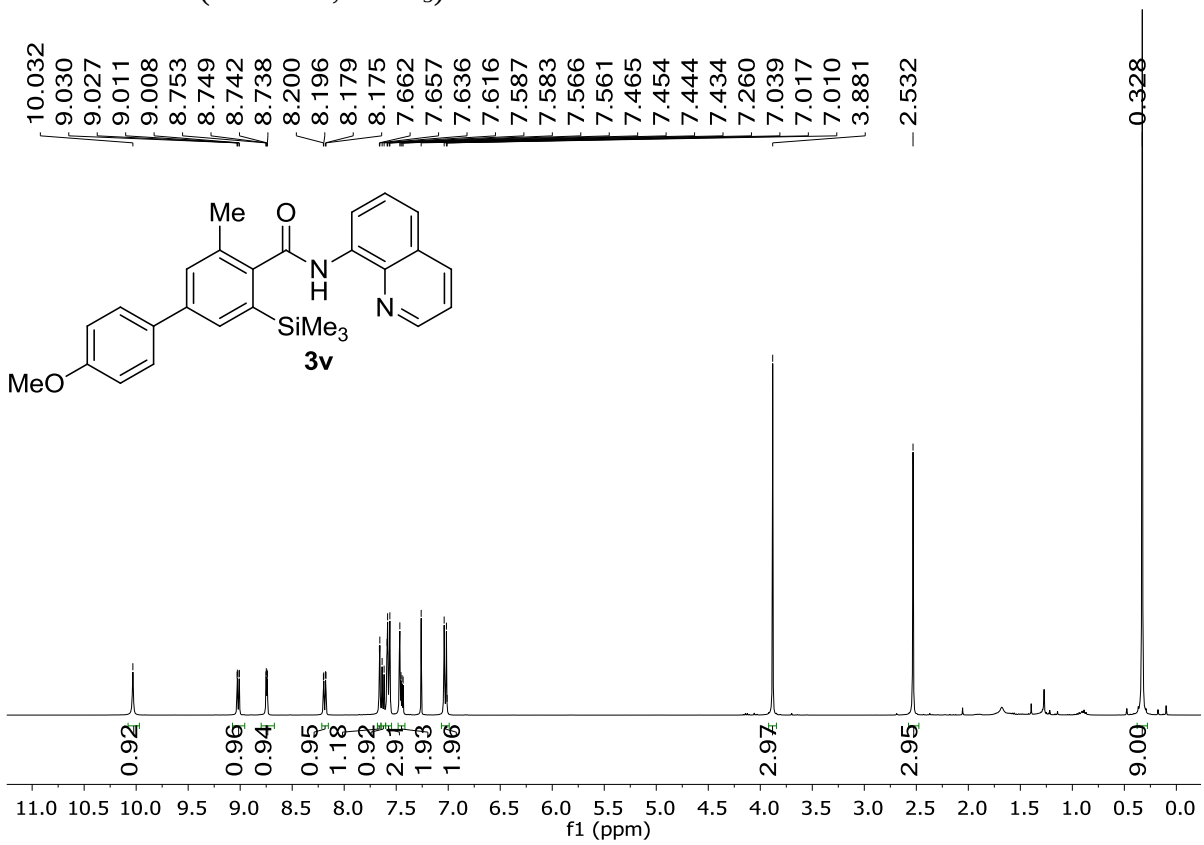

^{13}C NMR of **3v** (100 MHz, $CDCl_3$):

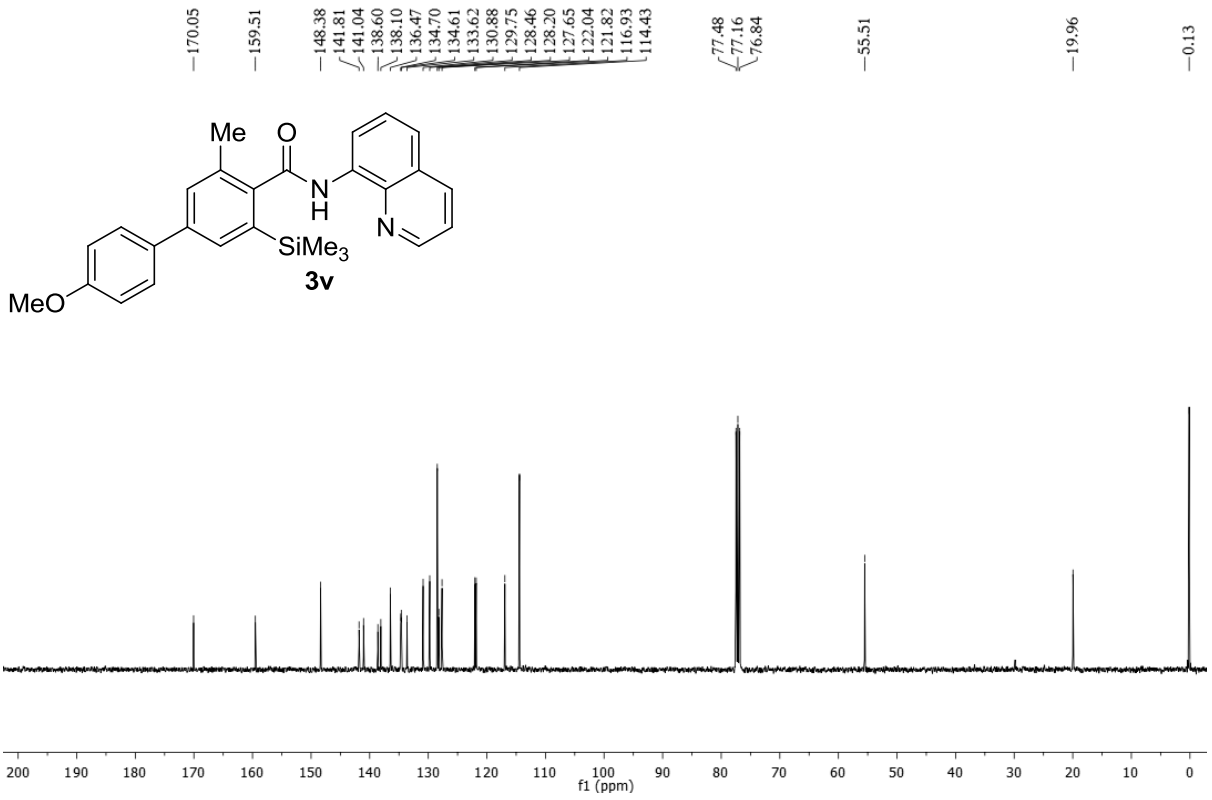

^{1}H NMR of **3aa** (400 MHz, $CDCl_3$):

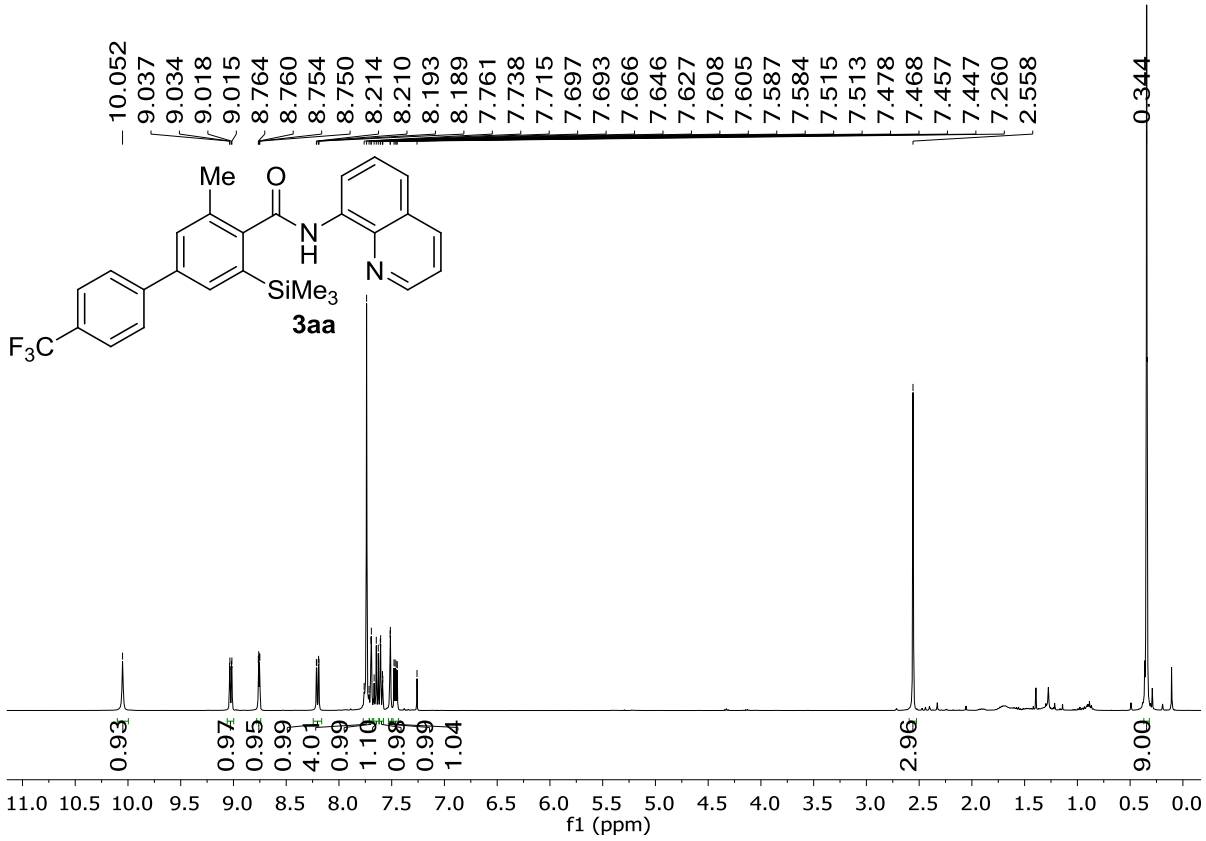

^{13}C NMR of **3aa** (100 MHz, $CDCl_3$):

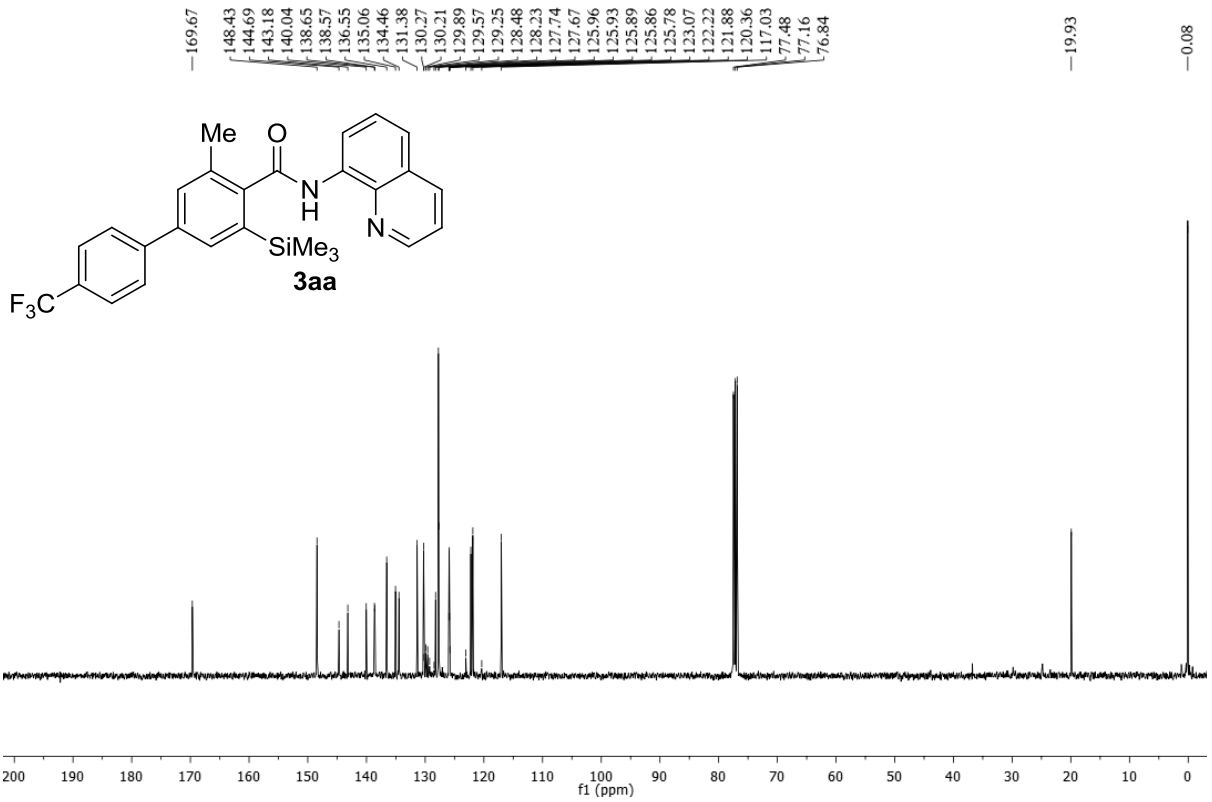

^{1}H NMR of **3ad** (400 MHz, $CDCl_3$):

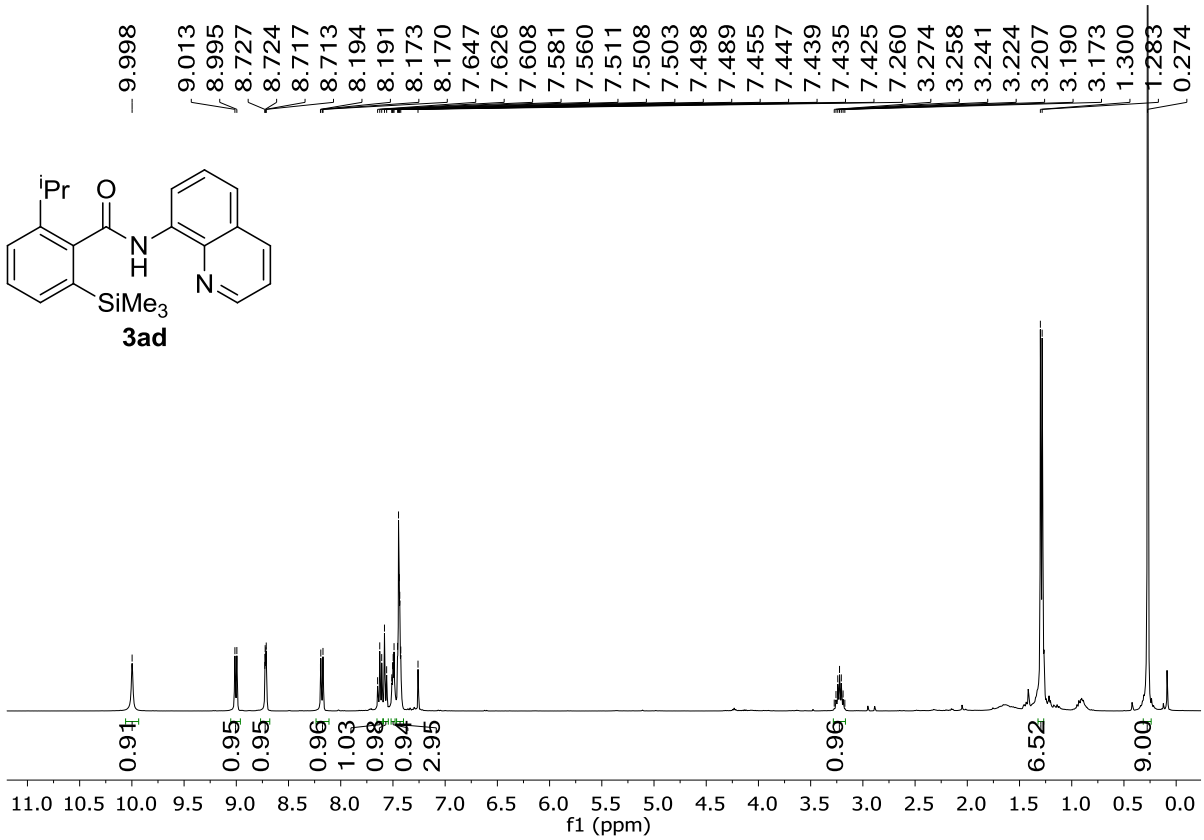

^{13}C NMR of **3ad** (100 MHz, $CDCl_3$):

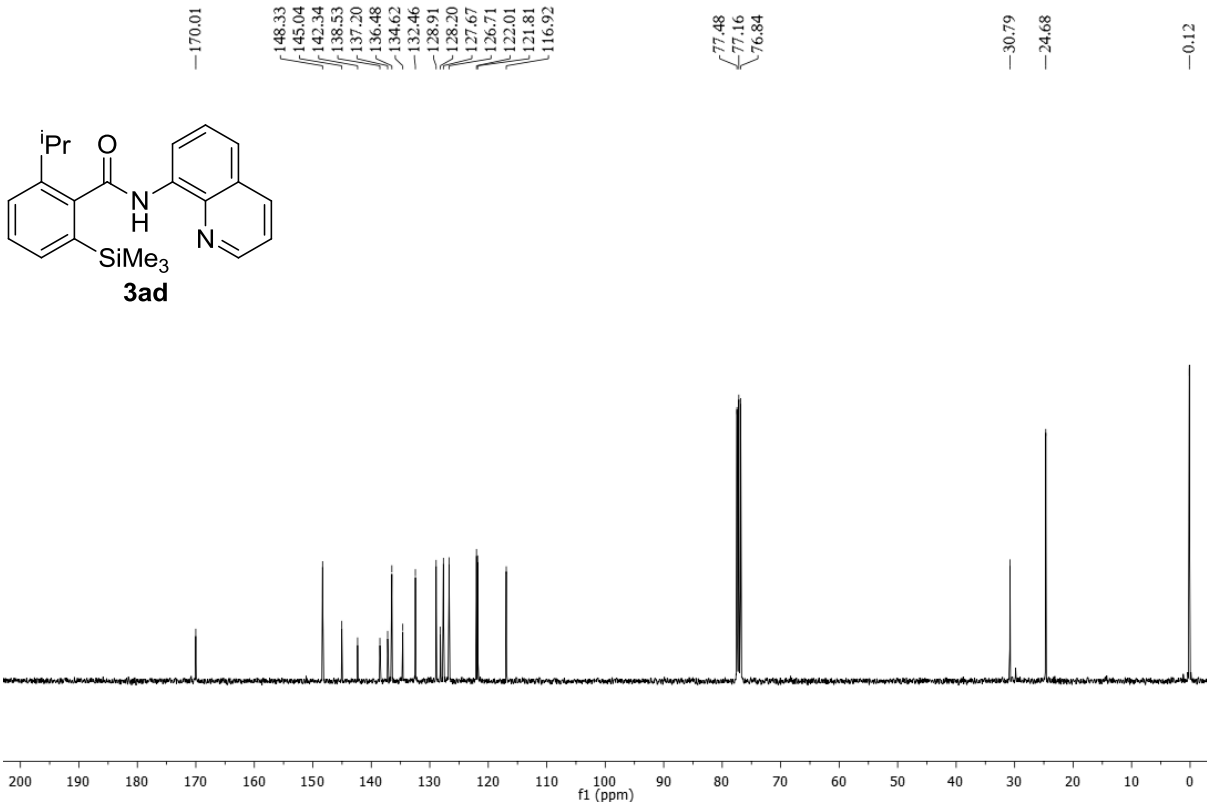

^{1}H NMR of **3ae** (400 MHz, $CDCl_3$):

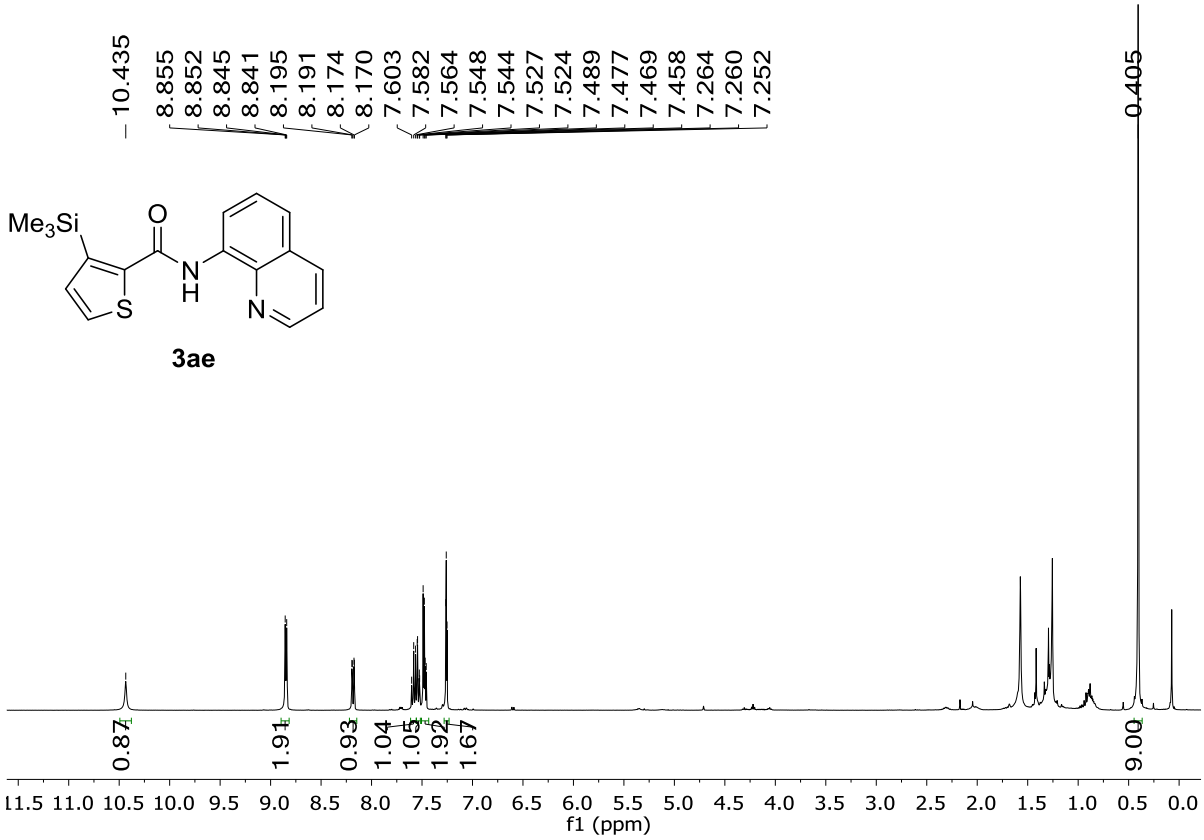

^{13}C NMR of **3ae** (100 MHz, $CDCl_3$):

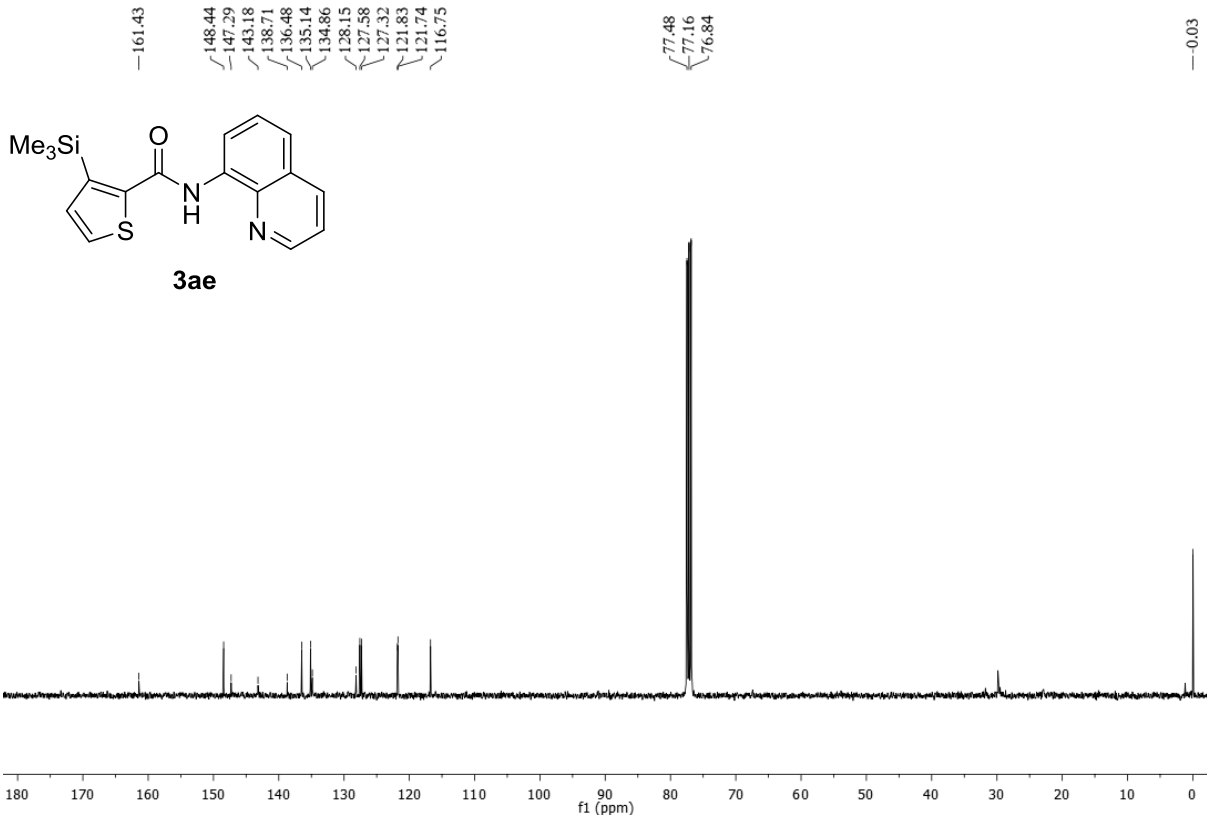

^{1}H NMR of **3af** (400 MHz, $CDCl_3$):

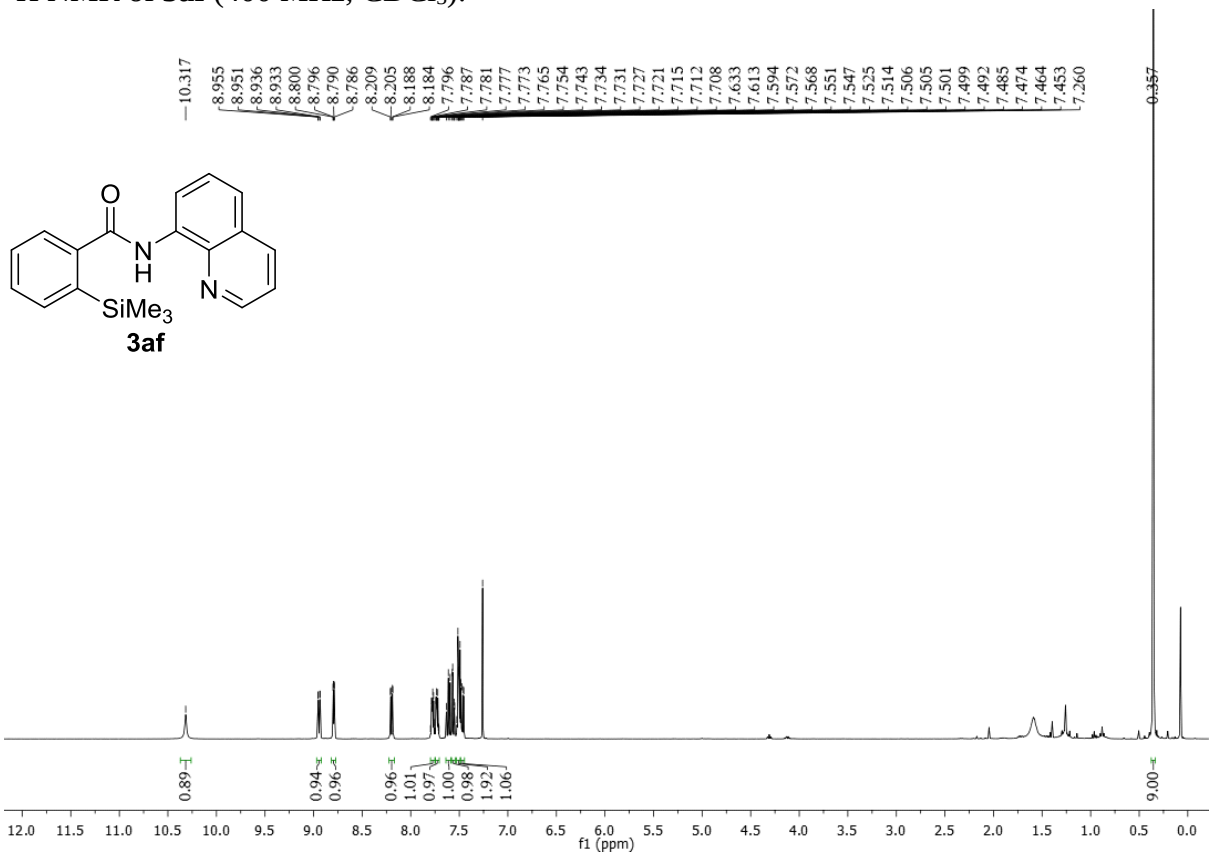

^{13}C NMR of **3af** (100 MHz, $CDCl_3$):

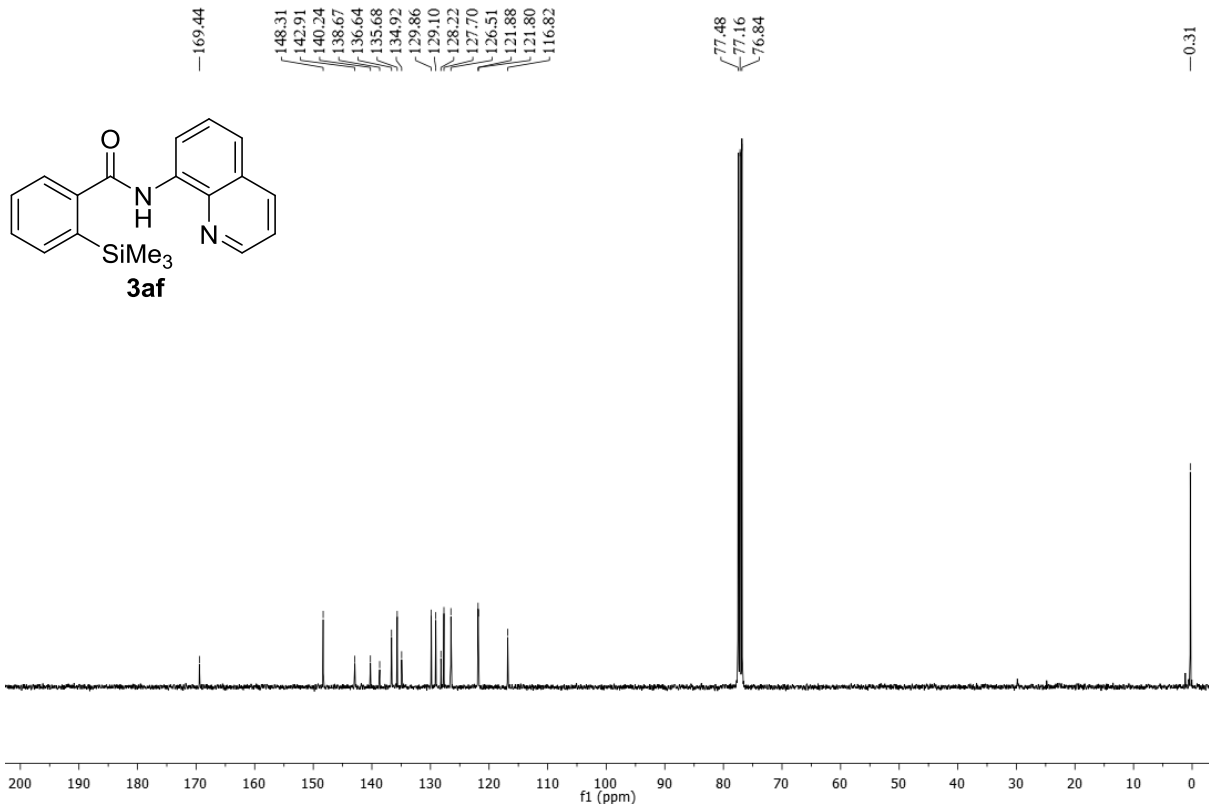

^{1}H NMR of **3ah** (400 MHz, $CDCl_3$):

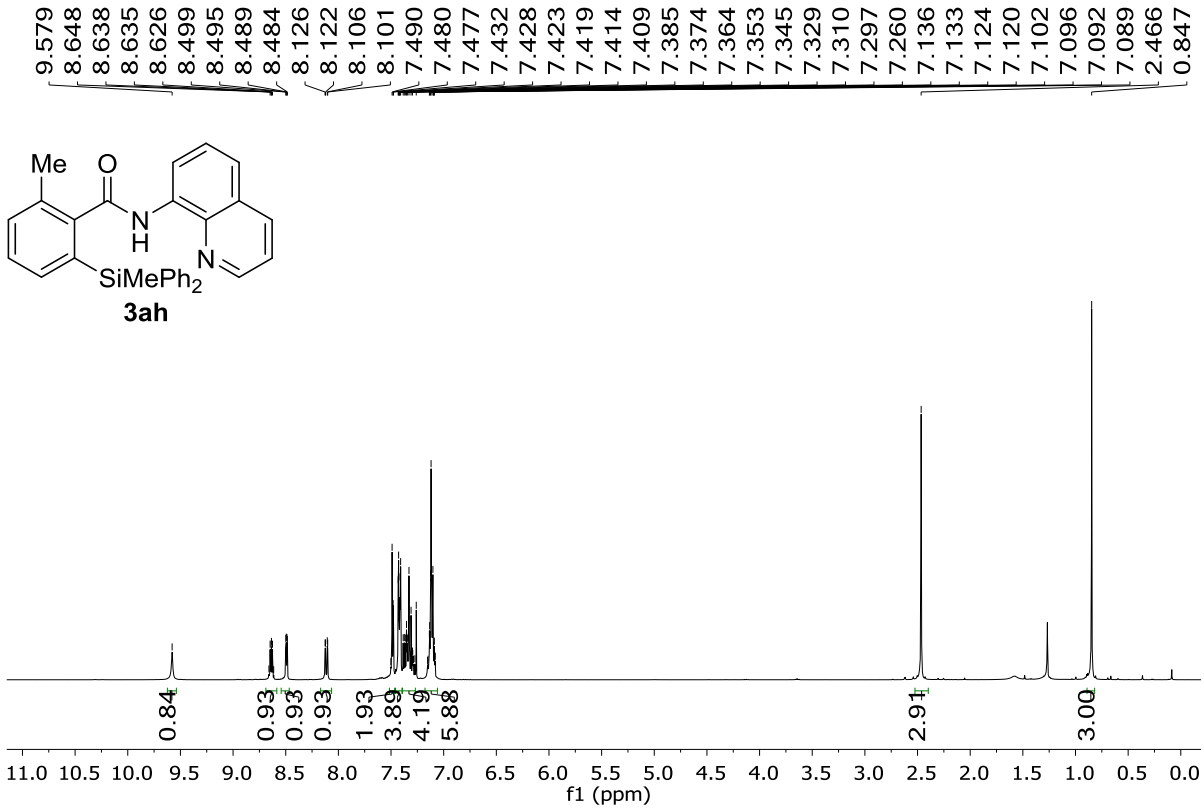

^{13}C NMR of **3ah** (100 MHz, $CDCl_3$):

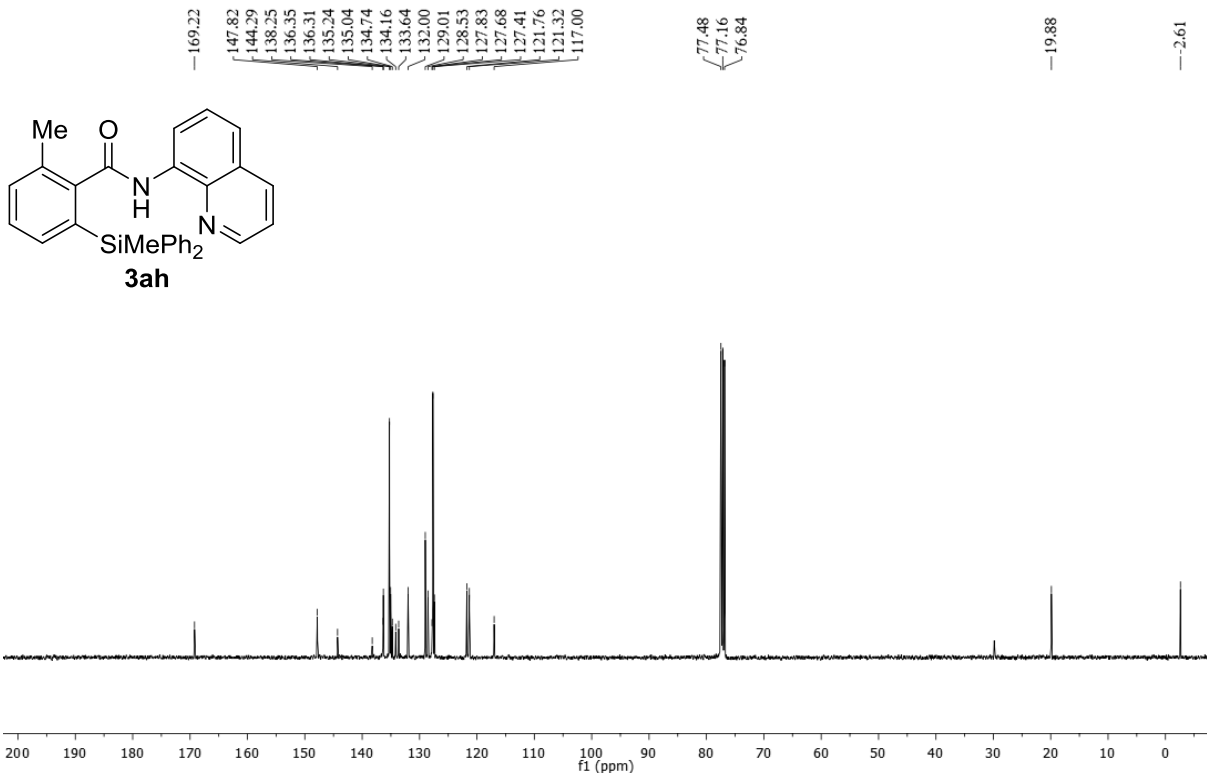

^{1}H NMR of **3ai** (400 MHz, $CDCl_3$):

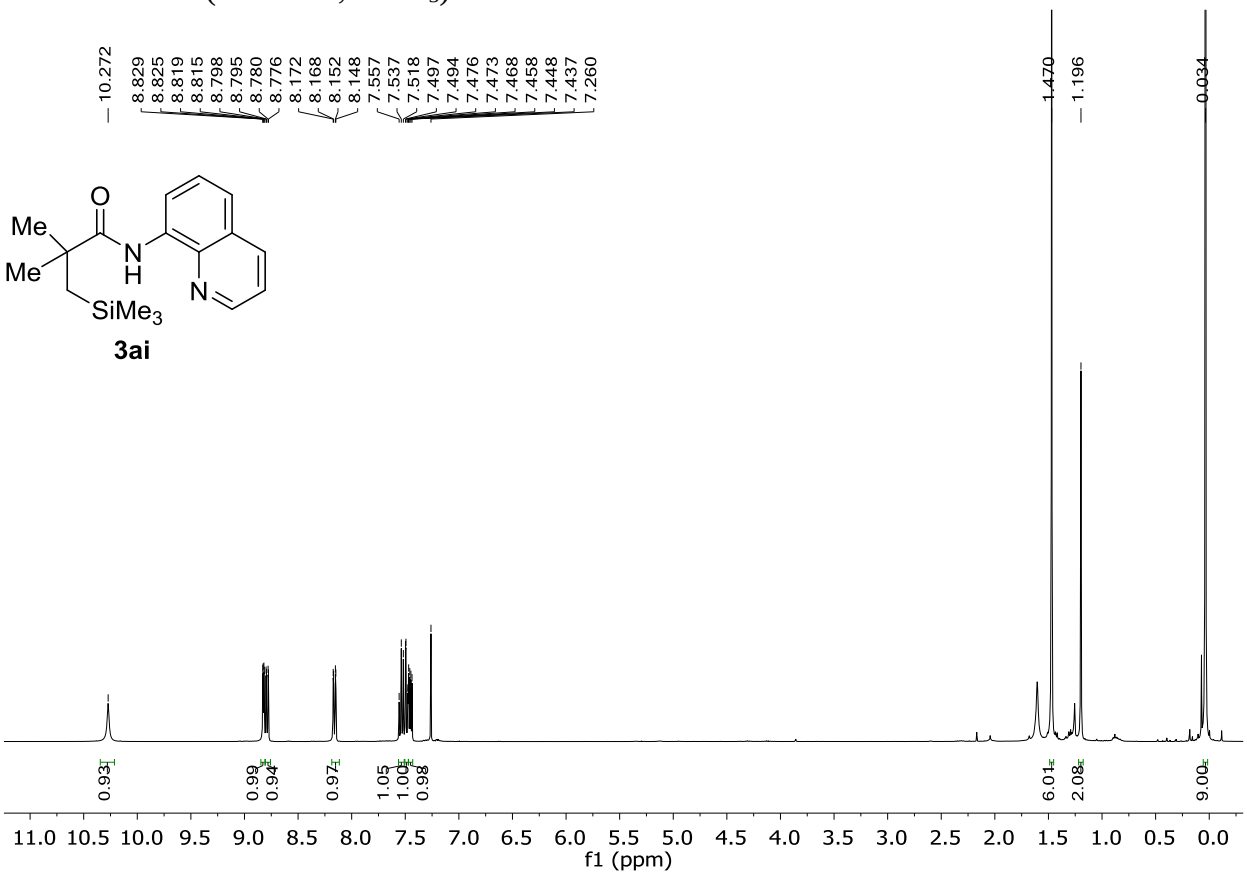

^{13}C NMR of **3ai** (100 MHz, $CDCl_3$):

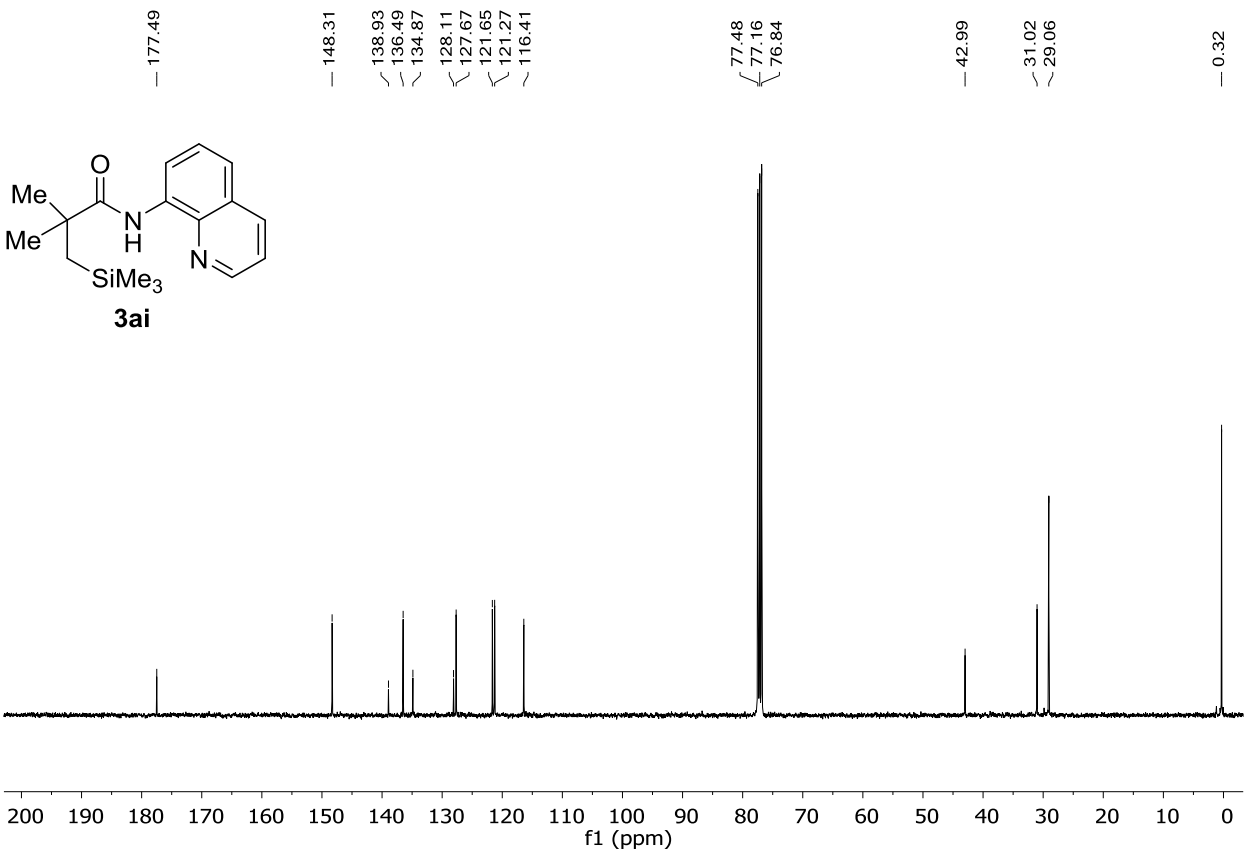

^{1}H NMR of **S3a** (400 MHz, $CDCl_3$):

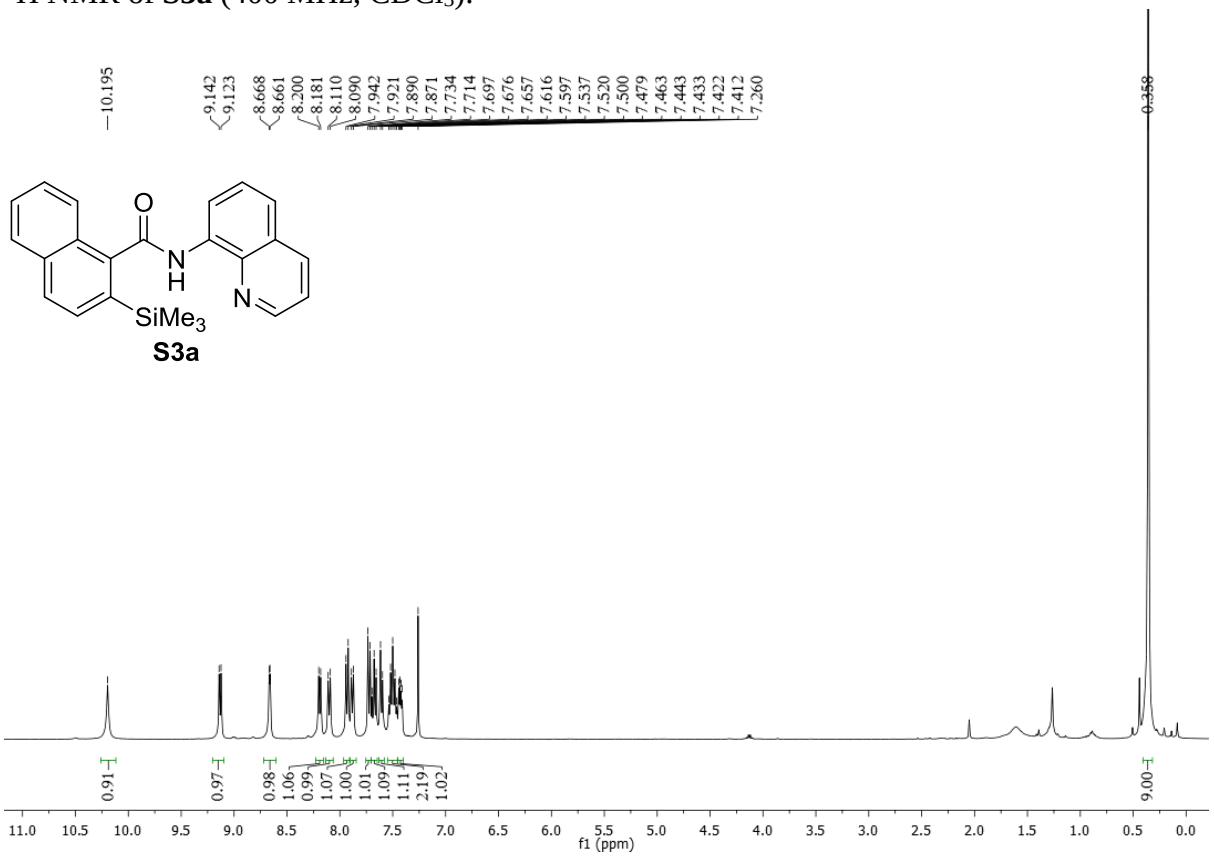

^{13}C NMR of **S3a** (100 MHz, $CDCl_3$):

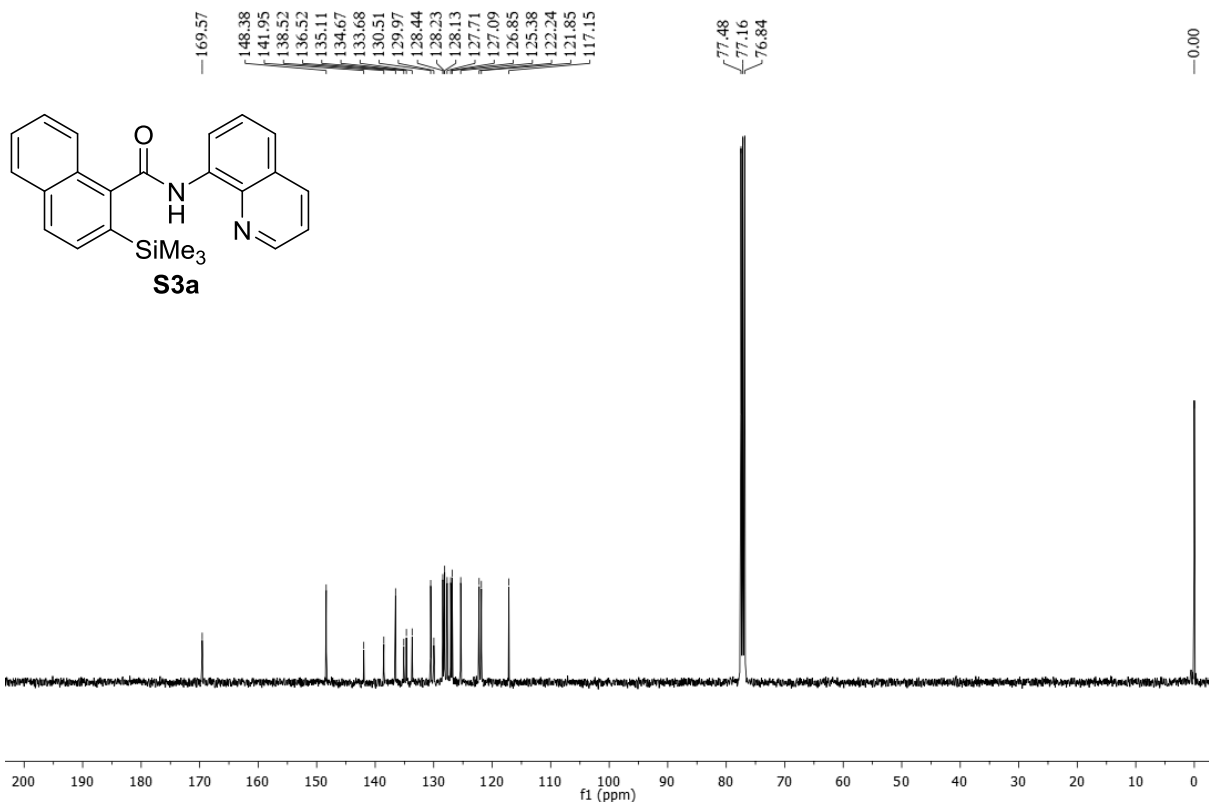

^{1}H NMR of **S3b** (400 MHz, $CDCl_3$):

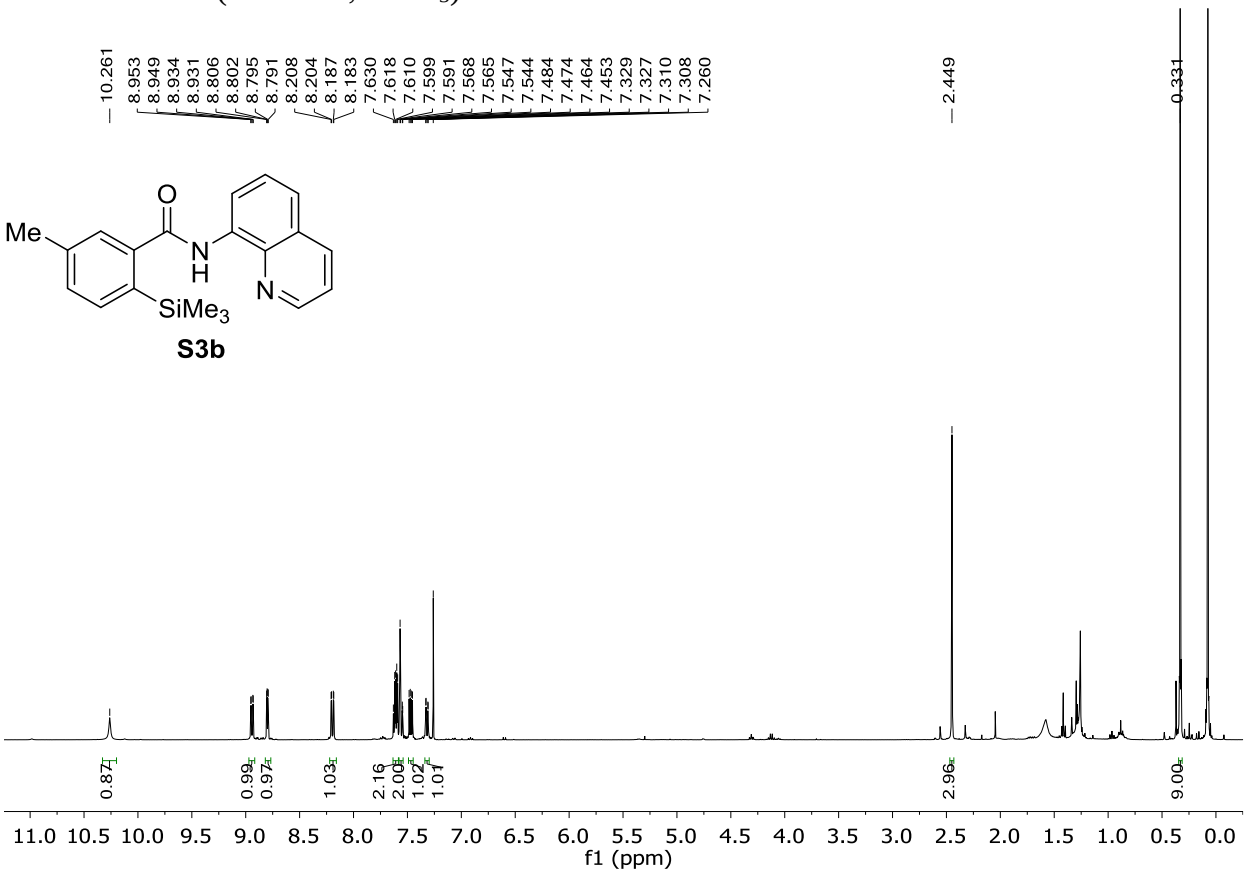

^{13}C NMR of **S3b** (100 MHz, $CDCl_3$):

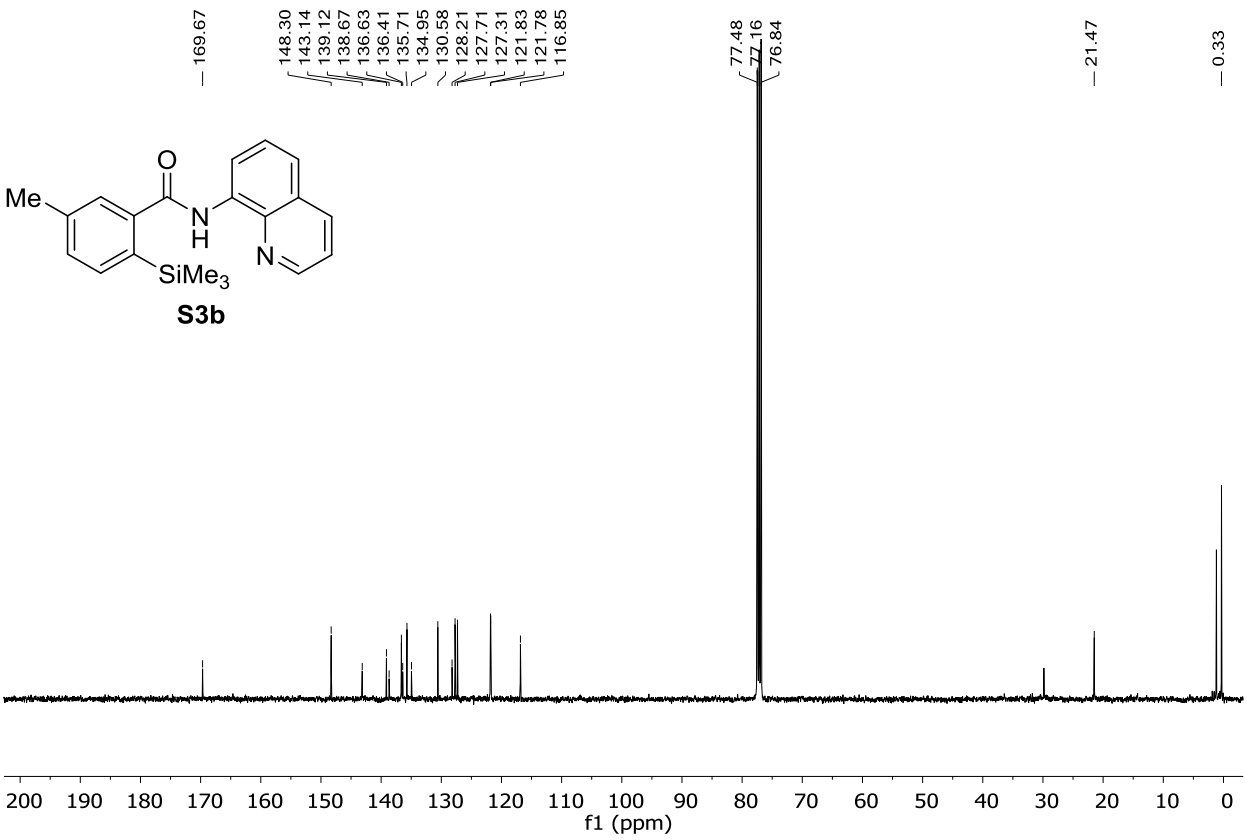

^{1}H NMR of **S3c** (400 MHz, $CDCl_3$):

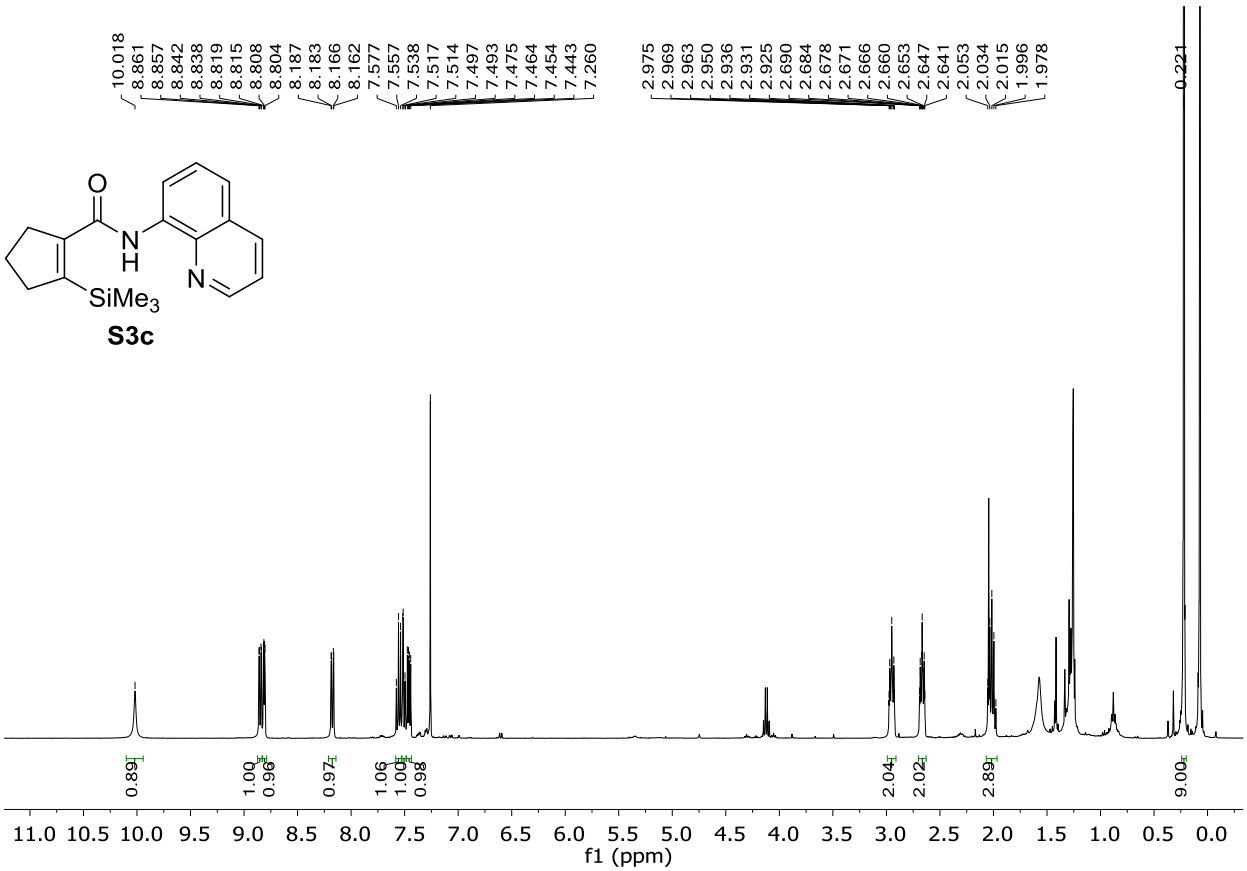

^{13}C NMR of **S3c** (100 MHz, $CDCl_3$):

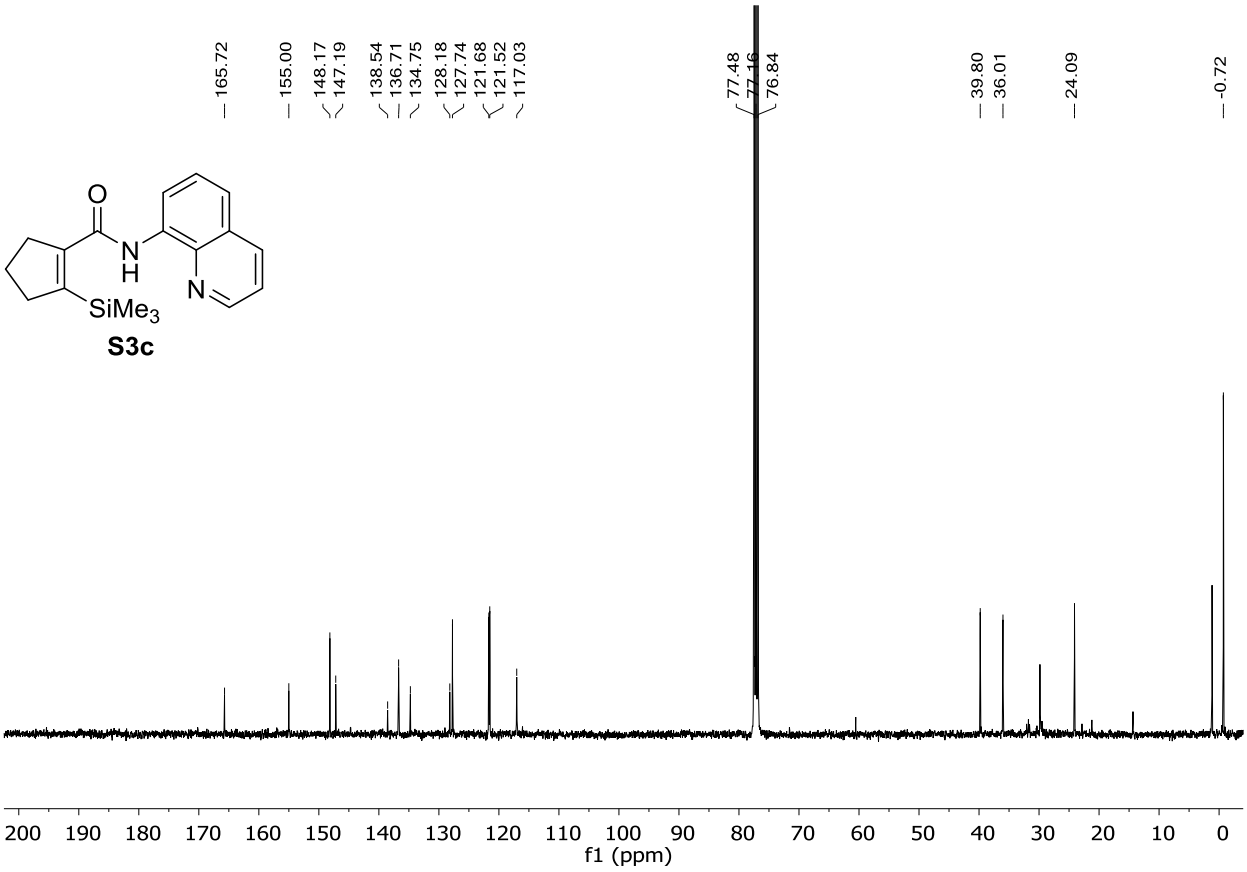

4.7. References

1. (a) Colvin, E. W. *Silicon Reagents in Organic Synthesis*. Academic Press: London, 1988. (b) Hatanaka, Y.; Hiyama, T. *J. Org. Chem.* **1988**, *53*, 918. (c) Langkopf, E.; Schinzer, D. *Chem. Rev.* **1995**, *95*, 1375. (d) Jones, G. R.; Landais, Y. *Tetrahedron* **1996**, *52*, 7599. (e) Corey, J. Y.; Braddock-Wilking, J. *Chem. Rev.* **1999**, *99*, 175. (f) Rappoport, Z.; Apeloig, Y.; Eds. *Chemistry of Organosilicon Compounds*. Wiley-VCH: New York, 2001; Vol. 3. (g) Manoso, A. S.; DeShong, P. *J. Org. Chem.* **2001**, *66*, 7449. (h) Zhao, Z.; Snieckus, V. *Org. Lett.* **2005**, *7*, 2523. (i) Denmark, S. E.; Baird, J. D. *Chem. Eur. J.* **2006**, *12*, 4954. (j) Denmark, S. E.; Regens, C. S. *Acc. Chem. Res.* **2008**, *41*, 1486. (k) Mochida, K.; Shimizu, M.; Hiyama, T. *J. Am. Soc. Chem.* **2009**, *131*, 8350. (l) Liang, Y.; Zhang, S.; Xi, Z. *J. Am. Soc. Chem.* **2011**, *133*, 9204. (m) Nakao, Y.; Hiyama, T. *Chem. Soc. Rev.* **2011**, *40*, 4893. (n) Ball, L. T.; Lloyd-Jones, G. C.; Russell, C. A. J. S. *Science* **2012**, *337*, 1644. (o) Gulevich, A. V.; Melkonyan, F. S.; Sarkar, D.; Gevorgyan, V. *J. Am. Soc. Chem.* **2012**, *134*, 5528. (p) Zarate, C.; Nakajima, M.; Martin, R. *J. Am. Soc. Chem.* **2017**, *139*, 1191.
2. (a) Jung, S.-H.; Kim, H. K.; Kim, S.-H.; Kim, Y. H.; Jeoung, S. C.; Kim, D. *Macromolecules* **2000**, *33*, 9277. (b) Kumagai, T.; Itsuno, S. *Macromolecules* **2002**, *35*, 5323. (c) Liu, X.-M.; He, C.; Huang, J.; Xu, J. *Chem. Mater.* **2005**, *17*, 434. (d) You, Y.; An, C.-G.; Kim, J.-J.; Park, S. Y. *J. Org. Chem.* **2007**, *72*, 6241.
3. For selected examples and reviews, see: (a) Sieburth, S. M.; Nittoli, T.; Mutahi, A. M.; Guo, L. *Angew. Chem. Int. Ed.* **1998**, *37*, 812. (b) Showell, G. A.; Mills, J. S. *Drug Discovery Today* **2003**, *8*, 551. (c) Tacke, R.; Heinrich, T.; Bertermann, R.; Burschka, C.; Hamacher, A.; Kassack, M. U. *Organometallics* **2004**, *23*, 4468. (d) Barnes, M. J.; Conroy, R.; Miller, D. J.; Mills, J. S.; Montana, J. G.; Pooni, P. K.; Showell, G. A.; Walsh, L. M.; Warneck, J. B. H. *Bioorg. Med. Chem. Lett.* **2007**, *17*, 354. (e) Franz, A. K.; Wilson, S. O. *J. Med. Chem.* **2013**, *56*, 388. (f) Tacke, R.; Handmann, V. I.; Bertermann, R.; Burschka, C.; Penka, M.; Seyfried, C. *Organometallics* **2003**, *22*, 916.
4. For selected reviews and examples, see: (a) Mortensen, M.; Husmann, R.; Veri, E.; Bolm, C. *Chem. Soc. Rev.* **2009**, *38*, 1002. (b) Mita, T.; Chen, J.; Sugawara, M.; Sato, Y. *Org. Lett.* **2012**, *14*, 6202. (c) Yonemoto-Kobayashi, M.; Inamoto, K.; Tanaka, Y.; Kondo, Y. *Org. Biomol. Chem.* **2013**, *11*, 3773.

5. (a) Moberg, W. K.; Basarab, G. S.; Cuomo, J.; Liang, P. H.; In *Synthesis and Chemistry of Agrochemicals*. American Chemical Society: Washington DC, 1987, *355*, 288. (b) Eckert, M. R.; Rossall, S.; Selley, A.; Fitt, B. D. *Pest Manage. Sci.* **2010**, *66*, 396.
6. (a) Lickiss, P. D. *Adv. Inorg. Chem.* **1995**, *42*, 147. (b) Geng, F.; Maleczka, R. E. *Tetrahedron Lett.* **1999**, *40*, 3113. (c) Murata, M.; Ishikura, M.; Nagata, M.; Watanabe, S.; Masuda, Y. *Org. Lett.* **2002**, *4*, 1843. (d) Hayashi, S.; Hirano, K.; Yorimitsu, H.; Oshima, K. *J. Am. Soc. Chem.* **2007**, *129*, 12650. (e) Guo, H.; Chen, X.; Zhao, C.; He, W. *Chem. Commun.* **2015**, *51*, 17410.
7. For selected reviews and examples, see: (a) Tyagi, A.; Yadav, N.; Khan, J.; Singh, S.; Kumar Hazra, C. *Asian J. Org. Chem.* **2021**, *10*, 334. (b) Toutov, A. A.; Liu, W.-B.; Betz, K. N.; Fedorov, A.; Stoltz, B. M.; Grubbs, R. H. *Nature* **2015**, *518*, 80. (c) Ma, Y.; Wang, B.; Zhang, L.; Hou, Z. *J. Am. Soc. Chem.* **2016**, *138*, 3663.
8. For reviews, see: (a) Lyons, T. W.; Sanford, M. S. *Chem. Rev.* **2010**, *110*, 1147. (b) Hartwig, J. F. *Acc. Chem. Res.* **2012**, *45*, 864. (c) Rouquet, G.; Chatani, N. *Angew. Chem. Int. Ed.* **2013**, *52*, 11726. (d) Cheng, C.; Hartwig, J. F. *Chem. Rev.* **2015**, *115*, 8946. (e) Yang, Y.; Wang, C. *Sci. China: Chem.* **2015**, *58*, 1266. (f) Sharma, R.; Kumar, R.; Kumar, I.; Singh, B.; Sharma, U. *Synthesis* **2015**, *47*, 2347. (g) Gensch, T.; Hopkinson, M. N.; Glorius, F.; Wencel-Delord, J. *Chem. Soc. Rev.* **2016**, *45*, 2900.
9. For selected examples, see: (a) Fumitoshi, K.; Kimitaka, I.; Mitsutaka, M.; Naoto, C.; Shinji, M. *Chem. Lett.* **2001**, *30*, 422. (b) Kakiuchi, F.; Tsuchiya, K.; Matsumoto, M.; Mizushima, E.; Chatani, N. *J. Am. Soc. Chem.* **2004**, *126*, 12792. (c) Ihara, H.; Suginome, M. *J. Am. Soc. Chem.* **2009**, *131*, 7502. (d) Sakurai, T.; Matsuoka, Y.; Hanataka, T.; Fukuyama, N.; Namikoshi, T.; Watanabe, S.; Murata, M. *Chem. Lett.* **2012**, *41*, 374.
10. For selected examples, see: (a) Toshiyasu, S.; Yuko, T.; Touru, S.; Masato, T. *Chem. Lett.* **1987**, *16*, 2375. (b) Tobisu, M.; Ano, Y.; Chatani, N. *Chem. Asian J.* **2008**, *3*, 1585. (c) Kuninobu, Y.; Nakahara, T.; Takeshima, H.; Takai, K. *Org. Lett.* **2013**, *15*, 426. (d) Cheng, C.; Hartwig, J. F. *Science* **2014**, *343*, 853.
11. For selected examples, see: (a) Ishiyama, T.; Sato, K.; Nishio, Y.; Miyaura, N. *Angew. Chem. Int. Ed.* **2003**, *42*, 5346. (b) Saiki, T.; Nishio, Y.; Ishiyama, T.; Miyaura, N. *Organometallics* **2006**, *25*, 6068. (c) Simmons, E. M.; Hartwig, J. F. *Nature* **2012**, *483*, 70. (d) Choi, G.; Tsurugi, H.; Mashima, K. *J. Am. Soc. Chem.* **2013**, *135*, 13149. (e) Cheng, C.; Hartwig, J. F. *J. Am. Soc. Chem.* **2015**, *137*, 592.
12. Oyamada, J.; Nishiura, M.; Hou, Z. *Angew. Chem. Int. Ed.* **2011**, *50*, 10720.

13. For selected examples, see: (a) Uchimaru, Y.; El Sayed, A. M. M.; Tanaka, M. *Organometallics* **1993**, *12*, 2065. (b) Williams, N. A.; Uchimaru, Y.; Tanaka, M. *J. Chem. Soc., Chem. Commun.* **1995**, 1129. (c) Tsukada, N.; Hartwig, J. F. *J. Am. Soc. Chem.* **2005**, *127*, 5022.

14. (a) Kanyiva, K. S.; Kuninobu, Y.; Kanai, M. *Org. Lett.* **2014**, *16*, 1968. (b) Chen, C.; Guan, M.; Zhang, J.; Wen, Z.; Zhao, Y. *Org. Lett.* **2015**, *17*, 3646. (c) Pan, J.-L.; Li, Q.-Z.; Zhang, T.-Y.; Hou, S.-H.; Kang, J.-C.; Zhang, S.-Y. *Chem. Commun.* **2016**, *52*, 13151. (d) Liu, Y.-J.; Liu, Y.-H.; Zhang, Z.-Z.; Yan, S.-Y.; Chen, K.; Shi, B.-F. *Angew. Chem. Int. Ed.* **2016**, *55*, 13859. (e) Deb, A.; Singh, S.; Seth, K.; Pimparkar, S.; Bhaskararao, B.; Guin, S.; Sunoj, R. B.; Maiti, D. *ACS Catal.* **2017**, *7*, 8171-8175. (f) Pan, J.-L.; Chen, C.; Ma, Z.-G.; Zhou, J.; Wang, L.-R.; Zhang, S.-Y. *Org. Lett.* **2017**, *19*, 5216. (g) Modak, A.; Patra, T.; Chowdhury, R.; Raul, S.; Maiti, D. *Organometallics* **2017**, *36*, 2418. (h) Maji, A.; Guin, S.; Feng, S.; Dahiya, A.; Singh, V. K.; Liu, P.; Maiti, D. *Angew. Chem. Int. Ed.* **2017**, *56*, 14903. (i) Li, W.; Chen, W.; Zhou, B.; Xu, Y.; Deng, G.; Liang, Y.; Yang, Y. *Org. Lett.* **2019**, *21*, 2718.

15. For selected reviews and examples of copper-catalyzed/-mediated C–H functionalization, see: (a) Liu, J.; Chen, G.; Tan, Z. *Adv. Syn. Catal.* **2016**, *358*, 1174. (b) Rao, W.-H.; Shi, B.-F. *Org. Chem. Front.* **2016**, *3*, 1028. (c) Chen, X.; Hao, X.-S.; Goodhue, C. E.; Yu, J.-Q. *J. Am. Soc. Chem.* **2006**, *128*, 6790. (d) Chu, L.; Yue, X.; Qing, F.-L. *Org. Lett.* **2010**, *12*, 1644. (e) Kitahara, M.; Umeda, N.; Hirano, K.; Satoh, T.; Miura, M. *J. Am. Soc. Chem.* **2011**, *133*, 2160. (f) Truong, T.; Klimovica, K.; Daugulis, O. *J. Am. Soc. Chem.* **2013**, *135*, 9342. (g) Nishino, M.; Hirano, K.; Satoh, T.; Miura, M. *Angew. Chem. Int. Ed.* **2013**, *52*, 4457. (h) Tran, L. D.; Roane, J.; Daugulis, O. *Angew. Chem. Int. Ed.* **2013**, *52*, 6043. (i) Shang, M.; Sun, S.-Z.; Wang, H.-L.; Laforteza, B. N.; Dai, H.-X.; Yu, J.-Q. *Angew. Chem. Int. Ed.* **2014**, *53*, 10439. (j) Li, X.; Liu, Y.-H.; Gu, W.-J.; Li, B.; Chen, F.-J.; Shi, B.-F. *Org. Lett.* **2014**, *16*, 3904. (k) Wang, S.; Guo, R.; Wang, G.; Chen, S.-Y.; Yu, X.-Q. *Chem. Commun.* **2014**, *50*, 12718. (l) Shang, M.; Wang, H.-L.; Sun, S.-Z.; Dai, H.-X.; Yu, J.-Q. *J. Am. Soc. Chem.* **2014**, *136*, 11590. (m) Li, Q.; Zhang, S.-Y.; He, G.; Ai, Z.; Nack, W. A.; Chen, G. *Org. Lett.* **2014**, *16*, 1764. (n) Wang, Z.; Ni, J.; Kuninobu, Y.; Kanai, M. *Angew. Chem. Int. Ed.* **2014**, *53*, 3496. (o) Wang, Z.; Kuninobu, Y.; Kanai, M. *Org. Lett.* **2014**, *16*, 4790. (p) Liu, J.; Yu, L.; Zhuang, S.; Gui, Q.; Chen, X.; Wang, W.; Tan, Z. *Chem. Commun.* **2015**, *51*, 6418. (q) Mandal, A.; Sahoo, H.; Baidya, M. *Org. Lett.* **2016**, *18*, 3202. (r) Hu, L.; Chen, X.; Gui, Q.; Tan,

Z.; Zhu, G. *Chem. Commun.* **2016**, *52*, 6845. (s) Gandeepan, P.; Koeller, J.; Ackermann, L. *ACS Catal.* **2017**, *7*, 1030. (t) Roy, S.; Pradhan, S.; Punniyamurthy, T. *Chem. Commun.* **2018**, *54*, 3899. (u) Takamatsu, K.; Hayashi, Y.; Kawauchi, S.; Hirano, K.; Miura, M. *ACS Catal.* **2019**, *9*, 5336. (v) Li, G.-J.; Pan, Y.-L.; Liu, Y.-L.; Xu, H.-F.; Chen, J.-Z. *Org. Lett.* **2019**, *21*, 1740.

16. For representative reviews and examples of 8-aminoquinoline directed C–H functionalization, see: (a) Corbet, M.; De Campo, F. *Angew. Chem. Int. Ed.* **2013**, *52*, 9896. (b) Daugulis, O.; Roane, J.; Tran, L. D. *Acc. Chem. Res.* **2015**, *48*, 1053. (c) Rej, S.; Ano, Y.; Chatani, N. *Chem. Rev.* **2020**, *120*, 1788. (d) Zaitsev, V. G.; Shabashov, D.; Daugulis, O. *J. Am. Soc. Chem.* **2005**, *127*, 13154. (e) Aihara, Y.; Chatani, N. *Chem. Sci.* **2013**, *4*, 664. (f) Shibata, K.; Chatani, N. *Org. Lett.* **2014**, *16*, 5148. (g) Shabashov, D.; Daugulis, O. *J. Am. Soc. Chem.* **2010**, *132*, 3965. (h) Tran, L. D.; Popov, I.; Daugulis, O. *J. Am. Soc. Chem.* **2012**, *134*, 18237. (i) Grigorjeva, L.; Daugulis, O. *Angew. Chem. Int. Ed.* **2014**, *53*, 10209. (j) Matsubara, T.; Asako, S.; Ilies, L.; Nakamura, E. *J. Am. Soc. Chem.* **2014**, *136*, 646. (k) Wu, X.; Zhao, Y.; Ge, H. *J. Am. Soc. Chem.* **2014**, *136*, 1789. (l) Aihara, Y.; Tobisu, M.; Fukumoto, Y.; Chatani, N. *J. Am. Soc. Chem.* **2014**, *136*, 15509. (m) Thrimurtulu, N.; Dey, A.; Maiti, D.; Volla, C. M. R. *Angew. Chem. Int. Ed.* **2016**, *55*, 12361. (n) Maity, S.; Kancherla, R.; Dhawa, U.; Hoque, E.; Pimparkar, S.; Maiti, D. *ACS Catal.* **2016**, *6*, 5493. (o) Barsu, N.; Bolli, S. K.; Sundararaju, B. *Chem. Sci.* **2017**, *8*, 2431.

17. Qian, G.; Hong, X.; Liu, B.; Mao, H.; Xu, B. *Org. Lett.* **2014**, *16*, 5294.

18. Zhao, D.; Luo, H.; Chen, B.; Chen, W.; Zhang, G.; Yu, Y. *J. Org. Chem.* **2018**, *83*, 7860.

Chapter 5: Introduction || Part-II

A Brief Overview of Rhodium and Iridium-Catalyzed C–H Activation

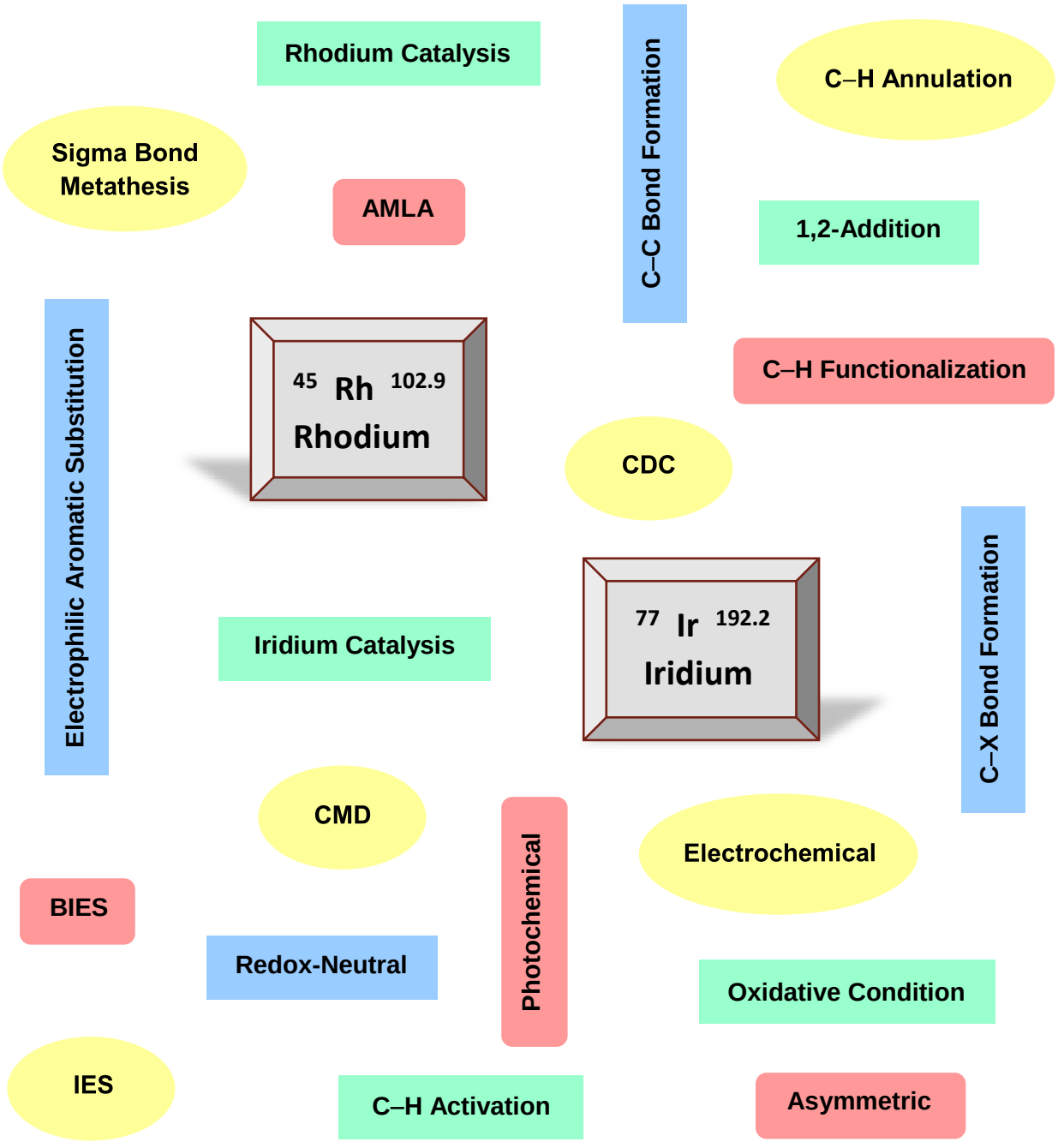

5.1. Transition Metal-Catalyzed C–H Activation/Functionalization

The pioneering work of Murahashi in 1955,[1] disclosed the first example of C–C bond formation via cobalt-catalyzed C–H activation (Chapter 1, Scheme 1.6.1), followed by the groundbreaking work of Murai and Chatani in 1993,[2] who first reported directing group assisted C–C bond formation under ruthenium catalysis (Chapter 1, Scheme 1.6.3). Since these works, several research groups have explored the field of directing group aided C–H activation/functionalization using various 3d base metal catalysts (Co, Cu, Ni, Mn, Fe)[3] as well as noble 4d and 5d noble metal catalysts (Pd, Rh, Ru, Ir).[4] In chapter 1, a glimpse of the modern era of C–H functionalization moving onto first-row transition metal catalysis, and a thorough description of cobalt and copper-catalyzed C–H activation has been provided. In continuation with the evolvement of C–H activation chemistry, rhodium and iridium catalysis has also participated heavily in the development of C–C and C–X (X = heteroatom) bonds. In this chapter, a detailed report of rhodium and iridium-catalyzed C–H activation/functionalization is provided. Mostly, C–C bond formation reactions and annulation reactions have been discussed with a brief insight into the C–X bond formation reactions.

5.2. Rhodium-Catalyzed C–H Activation

Driven by the desire in synthesizing complex structures and valuable building blocks, rhodium-catalyzed C–H bond activation has been cultivated extensively over the past few decades. In the area of C–C and C–X bond formation reactions, rhodium catalysis has played a pivotal role and stands out for its functional group tolerance and synthetic utility. As discussed in chapter 1, the issue of selectivity is of paramount importance in conjugation with developing C–H functionalization methodologies. To this end, the approach of using directing groups have found widespread success in selectively functionalizing specific C–H bonds. On surveying the examples of directing group-aided Rh-catalyzed C–H bond functionalization, mechanistically two distinct pathways are possible (Figure 5.2.1). In first case, a pendant heteroatom acts as a directing group or chelator to bind with the rhodium metal catalyst, thereby assisting in the activation of the proximal C–H bond (Figure 5.2.1a). The driving force for this reaction is the formation of a metalacyclic intermediate which induces the reaction at the proximal site by undergoing insertion or addition with π-systems like alkyne, alkene, etc. for C–C bond formations or reacting with electrophilic partners for C–X bond formations. In the second case, initial coordination between the heteroatom of the DG and Rh catalyst takes place, which

stabilizes the formation of metal-carbon bond at the proximal position (Figure 5.2.1b). In this chapter, the focus of discussion will be more on the first type.

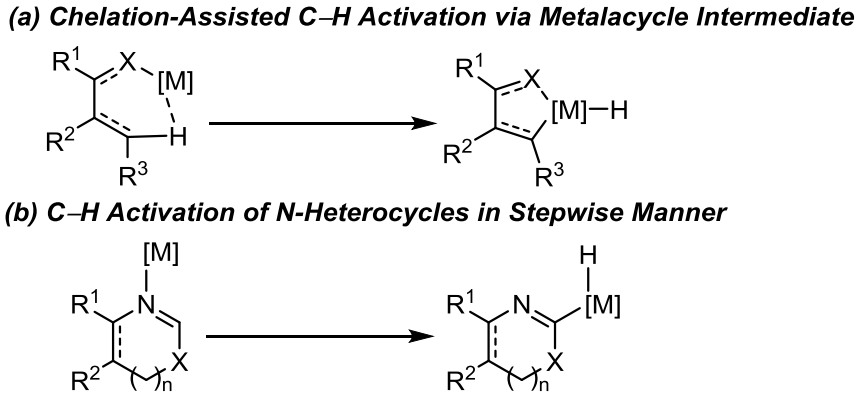

Figure 5.2.1. Modes of DG-assisted C–H bond activation.

A generally accepted catalytic cycle for rhodium-catalyzed C–H functionalization reactions is depicted in Scheme 5.2.1.[5] The detailed mechanistic steps may vary in different type of reactions. Generally, four main steps are involved- coordination between the heteroatom containing DG and Rh, C–H bond cleavage, C–Rh bond transformation, and regeneration of the active catalyst. Diverse modes of C–Rh bond transformation can take place like insertion of different partners (alkyne, olefin, CO, carbene, nitrene, etc.) and also heteroatom partners. The final step involves the C–C/C–heteroatom reductive elimination or protonation of the C–Rh bond, thereby regenerating the active catalyst.

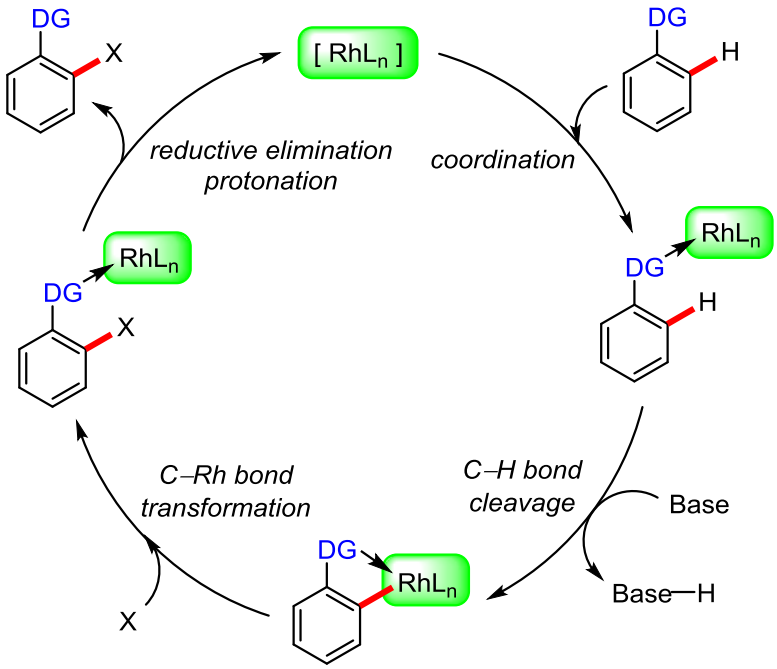

Scheme 5.2.1. General catalytic cycle for Rh-catalyzed C–H functionalizations.

For the initial C–H bond cleavage step in Rh-catalyzed processes, there are four possible modes of reaction represented in Figure 5.2.2. They are concerted metalation-deprotonation (CMD), oxidative addition (OA), Friedel-Crafts-type electrophilic aromatic substitution (S_EAr), and σ-complex assisted metathesis (σ-CAM). These C–H activation modes have been broadly discussed in Chapter 1, Section 1.3.

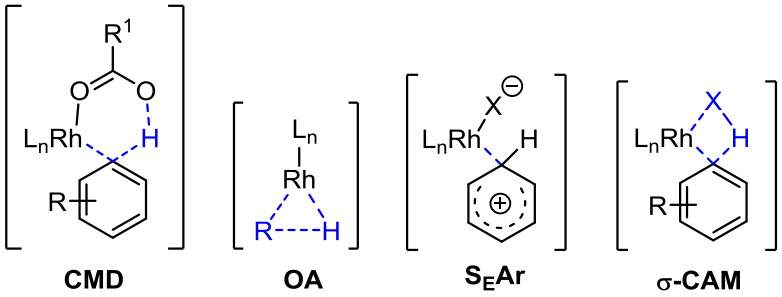

Figure 5.2.2. Possible Rh-catalyzed C–H activation modes.

5.2.1. C–C Bond Formation

The seminal work of Murai demonstrated a ruthenium-catalyzed *ortho* alkylation of aryl ketones to proceed exclusively with terminal, non-isomerizable olefins (Scheme 5.2.1.1a).[2] But, overalkylation remained a problem when *ortho* blocking substitution was absent. The pioneering works of Kim and co-workers showed that pyridine DG could be used efficiently for the regioselective cleavage of *ortho* C–H bonds of arenes under Rh(I) catalysis.[6] They reported the first Rh-catalyzed chelation-assisted direct C–H alkylation of 2-phenylpyridines with olefins.

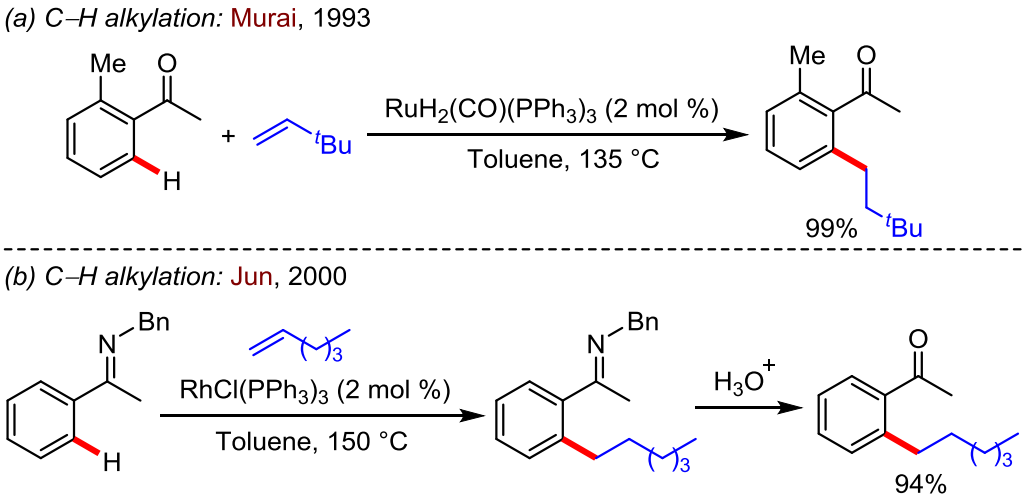

Scheme 5.2.1.1. Early examples of Rh-catalyzed C–H alkylation.

Following this, Jun *et al*. improved upon the results of the work of Murai by devising a protocol for Rh(I)-catalyzed *ortho* alkylation of *N*-benzyl aryl ketimines utilizing the directing ability of the imine functionality (Scheme 5.2.1.1b).[7] They employed air and moisture stable $RhCl(PPh_3)_3$ (Wilkinson's catalyst) as the optimized catalyst for the reaction which comprised a broad substrate scope tolerating a wide array of alkenes and also overcame the problem of overalkylation associated with the Ru-catalyzed alkylation process. Final hydrolysis of the alkylated imine products under acidic conditions furnished the corresponding alkylated aryl ketones, thus exhibiting the overall transformation analogous to Murai's reaction. Mechanistically, the rhodium-catalyzed alkylation pathway is outlined in Scheme 5.2.1.2. Initial coordination of the iminyl *N*-atom of aryl imine with the rhodium metal catalyst triggers the C–H activation step to generate a rhodacycle intermediate. This is followed by the dissociation of a phosphine ligand, olefin binding and hydride insertion via migratory insertion of the olefin to produce another metalacyclic intermediate. Finally, reductive elimination from this intermediate furnishes the desired alkylated product and closes the catalytic cycle.

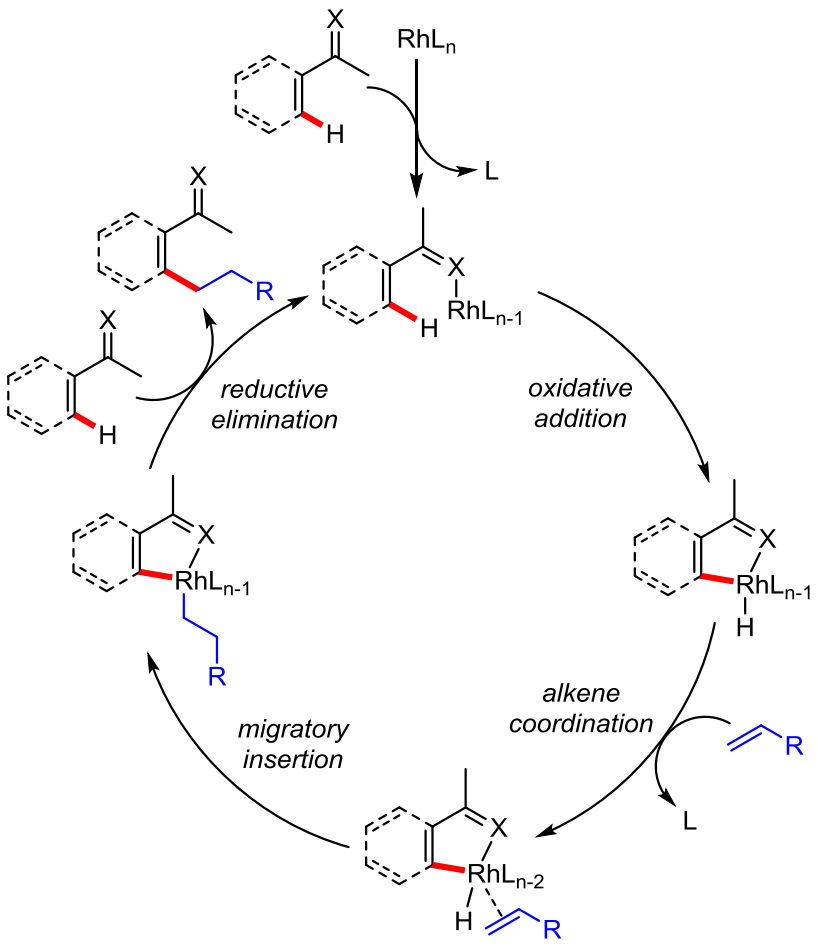

Scheme 5.2.1.2. Plausible mechanism of Rh-catalyzed C–H alkylation of aryl ketimines.

Following this, further alkylation reactions have been reported by the same group under different conditions employing Wilkinson catalyst.[8] They demonstrated an *ortho* alkylation reaction between aryl ketimines and electron-deficient olefins like α,β-unsaturated esters, amides, sulfones, and nitriles.[8a] Again, to improve on the existing methods involving high temperatures and longer reaction times and make an industrially viable methodology, they developed a procedure for imine formation of ketones (*in situ* generation of imines from ketones) and then *ortho* alkylation with both terminal and internal alkenes under solvent-free microwave conditions.[8b] Jun *et al*. also revealed the successful alkenylation of aryl ketimines with both internal as well as terminal alkynes, which could be extended to the synthesis of isoquinolines on increasing time and temperature of the reaction under Rh(I) catalysis.[9]

With time, rhodium-catalyzed C–H activation reactions have evolved and prospered with the upcoming of (pentamethylcyclopentadienyl)rhodium (Cp*Rh) based catalysts, *viz*. $[Cp^*RhCl_2]_2$, $[Cp^*Rh(MeCN)_3][SbF_6]_2$, and $[Cp^*Rh(MeCN)_3][BF_4]_2$. These high-valent Rh(III)-based catalysts have revolutionized the way rhodium chemistry is involved in C–H transformation reactions and new strategies for C–C and C–X bond formation have been discovered harnessing their novel reactivity. In this context, the initial findings of Davies,[10] Miura[11] and others[12] showed the scientific community the use of Cp*Rh-based catalysts for the direct activation of aromatic sp^2 C–H bonds and subsequent reaction with unsaturated coupling partners like alkenes and alkynes for the synthesis of structurally important moieties.[13] In addition, other π-systems, *viz*. activated alkenes, allenes, isocyanates, carbonyl compounds, carbon monoxide, imines, etc. have been successfully incorporated in C–H functionalization reactions with suitable DG attached substrates taking advantage of the reactivity of rhodacycle intermediate to undergo insertion or addition reaction with these unsaturated systems.[14] Apart from these works, various other methodologies have also been designed for the efficient synthesis of important structural motifs and heterocyclic scaffolds employing this versatile catalyst.[4b,f,15] Some of the examples on Rh-catalyzed C–C bond formation are depicted in Schemes 5.2.1.3-5.2.1.5.

In 2010, Fagnou group reported a rhodium(III)-catalyzed intermolecular hydroarylation of alkynes (Scheme 5.2.1.3a).[13a] The reaction occurred regioselectively at the C2 position of indole moiety. Concurrently, Glorius *et al*. demonstrated a Rh-catalyzed oxidative olefination of acetanilides with electronically neutral alkenes like styrenes and even ethylene under very low catalytic loading conditions (Scheme 5.2.1.3b).[13b] They devised another protocol for

Rh(III)-catalyzed oxidative olefination of *N*-methoxy benzamides with simple unactivated alkenes under redox-neutral conditions, where no external oxidant is required since the N–O bond acts as an internal oxidant (Scheme 5.2.1.3c).[13c] Following year, Ellman and Shi groups independently developed methodologies for addition of 2-arylpyridines to protected aldimines employing rhodium-catalyzed conditions (Scheme 5.2.1.3d, 5.2.1.3e).[14a,g]

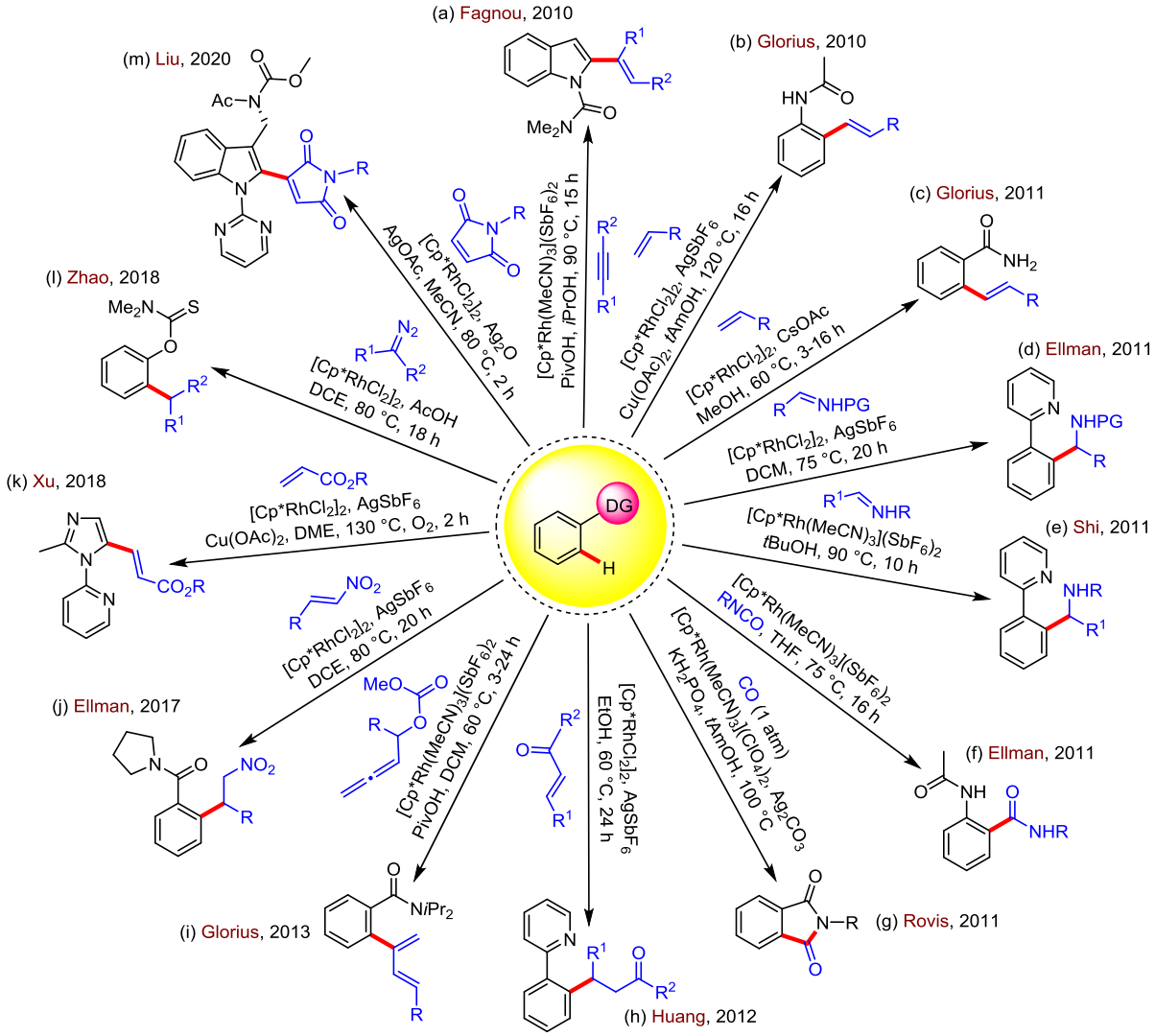

Scheme 5.2.1.3. Representative examples of Rh-catalyzed C–C bond formation with unsaturated coupling partners.

In the same year, isocyanates were efficiently utilized by Ellman and co-workers for a regioselective amidation of anilides and enamides employing rhodium catalysis affording valuable *N*-acyl anthranilamides and enamine amides (Scheme 5.2.1.3f).[14b] Rovis group achieved a Rh(III)-catalyzed oxidative carbonylation of arylamides with carbon monoxide to form phthalimides (Scheme 5.2.1.3g).[14d] In 2012, Huang *et al*. disclosed a 1,4-addition of 2-

phenylpyridines to α,β-unsaturated ketones under rhodium catalysis (Scheme 5.2.1.3h).[14h] Next year, Glorius *et al*. delineated a Rh(III)-catalyzed coupling reaction between benzamides and enamides with allenyl carbinol carbonates (Scheme 5.2.1.3i).[14m] In 2017, Ellman group elegantly employed electron-deficient nitroalkenes in an addition reaction with directing arenes employing rhodium catalysis (Scheme 5.2.1.3j).[14p] Xu and co-workers reported a rhodium-catalyzed regio and stereoselective olefination of pyrimidyl-directed imidazoles with activated alkenes (Scheme 5.2.1.3k).[14r] Zhao *et al*. revealed a strategy for thiocarbamate-directed *ortho* alkylation of phenol derivatives with diazo compounds under Rh-catalyzed conditions (Scheme 5.2.1.3l).[14u] Recently, in 2020, Liu group reported a Rh(III)-catalyzed C–H alkenylation of tryptophan derivatives with maleimides utilizing the chelation assistance of pyrimidine directing group (Scheme 5.2.1.3m).[14v]

In 2014, Cui group revealed a Rh(III)-catalyzed C2-selective direct arylation of *N*-methoxy-1*H*-indole-1-carboxamides with arylboronic acids as aryl source and cheap $Cu(OAc)_2$ as external oxidant (Scheme 5.2.1.4a).[16] Thereafter, several research groups have reported efficient procedures for direct C–H arylation employing rhodium catalysis.[17] The incorporation of alkyne fragment into C–H bond of unactivated arenes was first disclosed by Li and co-workers in 2014, when they reported a Rh(III)-catalyzed *ortho* alkynylation protocol of *N*-(pivaloyloxy)benzamides with electrophilic hypervalent iodine reagent, 1-silylethynyl-1,2-benziodoxol-3(1*H*)-ones (TIPS-EBX) (Scheme 5.2.1.4b).[18] The reaction is highly mono-selective and proceeds at room temperature featuring a wide functional group tolerance. Concurrently, Li group developed a chelation-assisted Rh(III) and Ir(III)-catalyzed alkynylation of (hetero)arenes with similar hypervalent iodine-alkyne reagents with controlled mono- and bis-alkynylation selectivity.[19] During the same time, Glorius *et al*. demonstrated a direct alkynylation reaction of alkenyl and aromatic amides using commercially available TIPS-EBX as alkynylating agent giving access to a series of conjugated enynes under rhodium-catalyzed conditions.[20] In the following years, further reports on Rh-catalyzed direct C–H alkynylation were observed using a variety of alkynyl sources.[15g,21]

In 2013, the first Rh-catalyzed direct C–H cyanation was demonstrated by the group of Fu utilizing the nature of Cp*Rh catalyst to undergo insertion type mechanism with π-systems. As an environmentally benign and bench-stable reagent, they used *N*-cyano-*N*-phenyl-*p*-toluenesulfonamide (NCTS) as cyanating agent for selective cyanation of diverse directing group attached arenes thereby providing a practicable method for the synthesis of aromatic

nitriles (Scheme 5.2.1.4c).[22] Almost at the same time, Anbarasan *et al*. devised a similar methodology for the cyanation of different chelating arenes allowing the synthesis of various benzonitrile derivatives in good to excellent yields employing a low Rh catalyst loading.[23] Owing to the importance of the cyano functionality in synthetic organic chemistry as it can be transformed to other functional groups, over the next years, several rhodium-catalyzed direct cyanation protocols have emerged.[24]

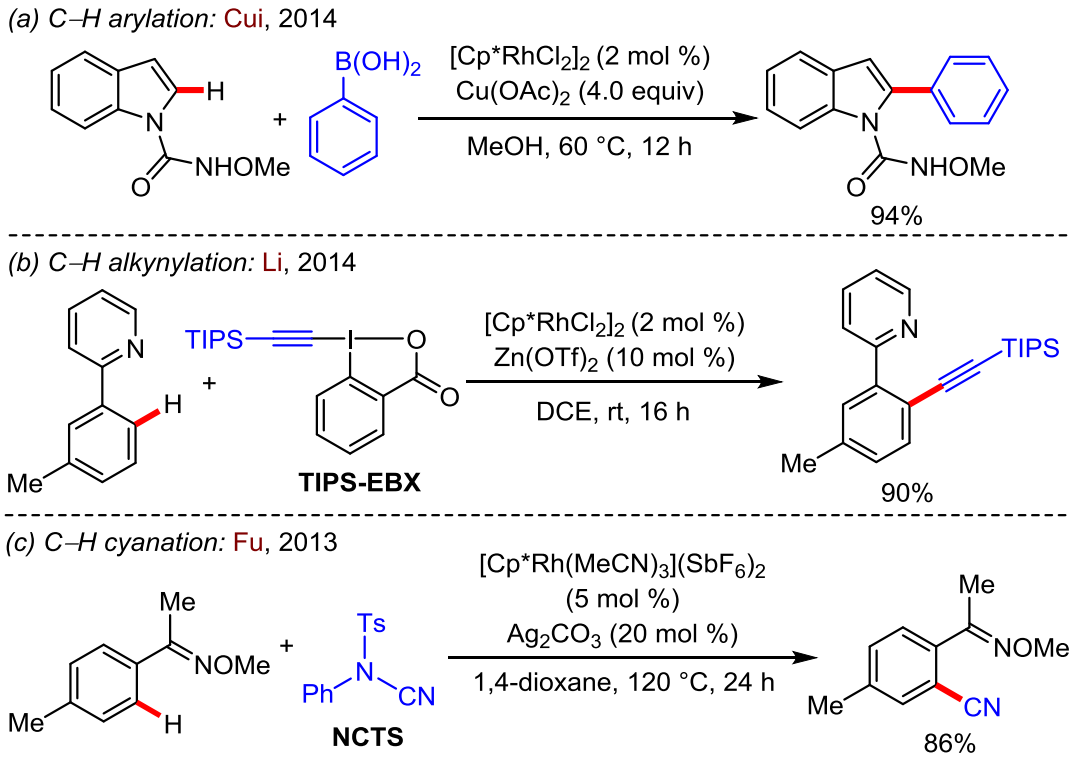

Scheme 5.2.1.4. Rh-catalyzed C–H arylation, alkynylation, and cyanation reactions.

As a part of the continuous development of Rh-catalyzed C–C bond formation, several other reactions have also been reported under external oxidant free conditions, also called redox-neutral reactions.[15g,25] A common characteristic of these type of reactions is the involvement of coupling reaction between an electrophilic partner containing a leaving group and the nucleophilic rhodacycle intermediate. Selected examples of these reactions are depicted in Scheme 5.2.1.5. In 2012, Yu group devised a protocol for Rh-catalyzed intermolecular coupling between directing arenes and diazomalonates with high regioselectivity and good functional group tolerance paving a new route to α-aryl carbonyl compounds (Scheme 5.2.1.5a).[25a] Following year, Li and co-workers achieved an aziridine ring-opening reaction for C–C bond formation of chelating group assisted arenes under rhodium-catalyzed redox-neutral conditions (Scheme 5.2.1.5b).[25b] Around the same time, they again revealed a Rh(III)-catalyzed

coupling reaction between (hetero)arenes and 7-oxabenzonorbornadienes leading to dehydrative naphthylation (Scheme 5.2.1.5c).[25c] In 2014, Wang *et al*. realized an intermolecular coupling reaction between *N*-phenoxyacetamides and *N*-tosylhydrazones under Rh catalysis (Scheme 5.2.1.5d).[25d] The reaction furnished a series of *ortho* alkenylated phenols in high regio- and stereoselective manner, and was proposed to proceed via a Rh-carbene migratory insertion step. Cui and co-workers demonstrated a methodology for the synthesis of functionalized cyclopentenes employing Rh(III)-catalyzed C–H activation/desymmetrization of dizabicycles with directing group tethered arenes (Scheme 5.2.1.5e).[25e] In the same year, Li group reported three elegant works on C–C bond formations between arenes containing diverse directing groups and 2-vinyloxiranes, cyclopropenones, and 4-hydroxycyclohexa-2,5-dienones employing redox-neutral Rh(III) catalysis (Scheme 5.2.1.5f-5.2.1.5h).[25f-h]

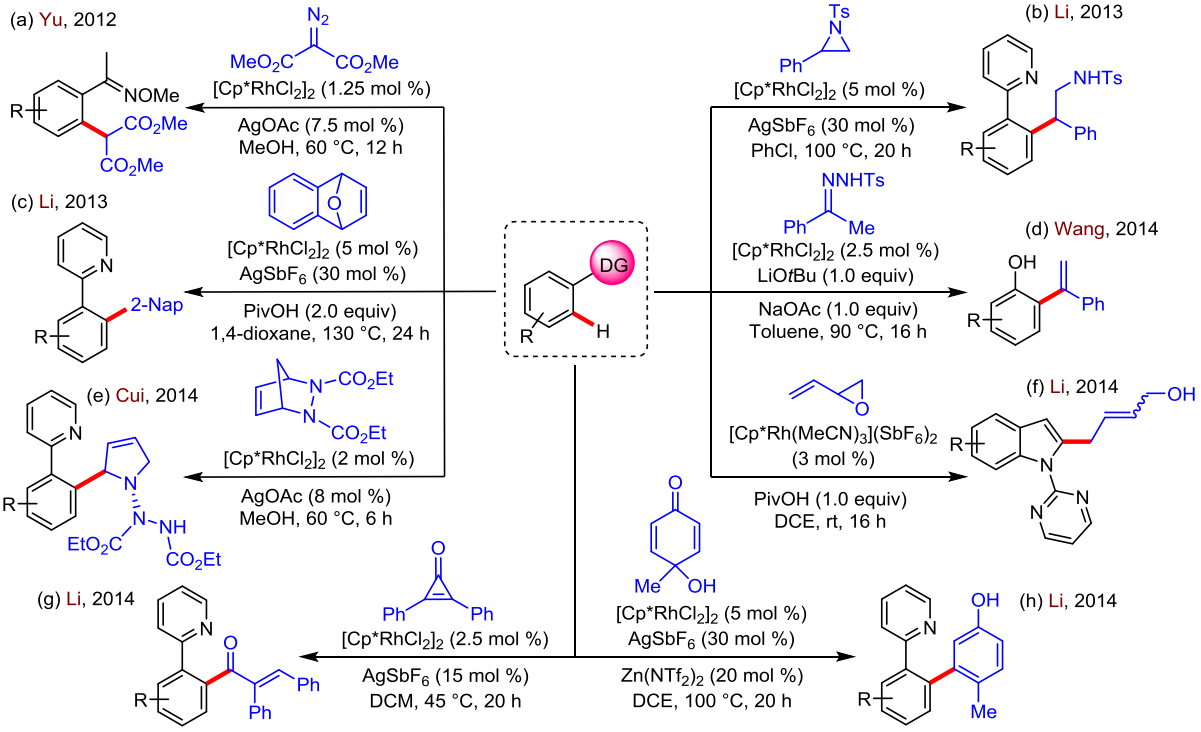

Scheme 5.2.1.5. Representative examples of Rh-catalyzed C–C bond formation under oxidant free conditions.

Apart from the aforementioned rhodium-catalyzed intermolecular coupling reactions in the presence or absence of external oxidant, another class of C–C bond forming reactions that has largely evolved in the past years is the two-fold oxidative cross-dehydrogenative coupling (CDC) reactions between DG attached arenes and (hetero)arenes or alkenes.[15g,26] In 2012, Glorius group disclosed a novel strategy for Cp*Rh(III)-catalyzed cross-dehydrogenative coupling between directed arenes and halogen-substituted benzene derivatives with a broad

scope generating biaryl fragments in moderate to good yields (Scheme 5.2.1.6).[26a] Thereafter, several groups have designed efficient CDC reactions employing Rh catalysis.

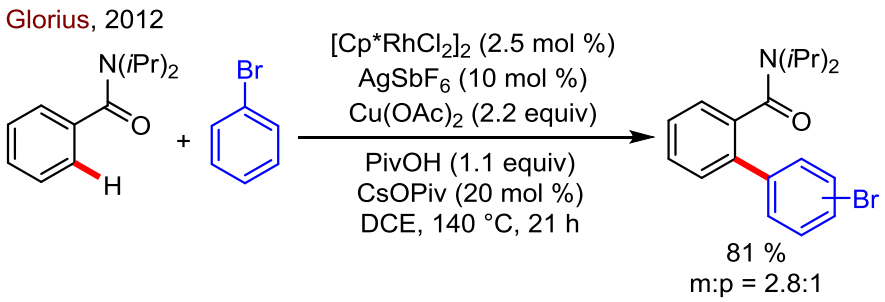

Scheme 5.2.1.6. Rh-catalyzed cross-dehydrogenative coupling reaction.

5.2.2. C–X Bond Formation

Carbon–Heteroatom (C–X) bond formations in the form of C–N, C–O, C–S, C–Z (Z = halogen, *viz*. Cl, Br, I), etc. have also been explored extensively over the years employing rhodium catalysis. In this section, some of the notable reports on C–N, C–O, C–S, C–Z, and other C–X bond formation reactions are discussed briefly.

➢ C–N bond formation

The generalized concept of Cp*Rh-catalyzed C–H activation reaction with electrophilic partners containing a leaving group has been efficiently utilized for the creation of C–N bonds by various research groups. Some of these examples are outlined in Scheme 5.2.2.1. In particular, Rh-catalyzed direct C–H amination and amidation has been thoroughly studied over the years with a plethora of reports on reactions using diverse coupling partners. In 2012, Chang *et al*. opened a new avenue for intermolecular C–N bond formation by coupling different chelating arenes with sulfonyl azides acting as the amino source (Scheme 5.2.2.1a).[27] The reaction went under external oxidant free conditions and N_2 was released as the sole byproduct making it a very practical method. The implementation of azides as capable aminating reagents was next extended to aryl as well as alkyl azides in selectively functionalizing aromatic C–H bonds of useful DG attached moieties like benzamides, ketones, and also 6-arylpurines to deliver the corresponding aminated products in good to excellent yields.[28] Almost at the same time, Chang and Glorius group independently developed mild methodologies for Rh(III)-catalyzed direct *ortho* amination of oximes and hydroxamic acid derivatives using chloride anion leaving group containing *N*-chloramines as the source of amine functionality (Scheme 5.2.2.1b, 5.2.2.1c).[29] In 2013, Glorius and co-workers devised a rhodium-catalyzed sp^2 C–H

amidation of pyridine and hydroxamic acid derivative directed arenes using electrophilic aroyloxycarbamates as efficient amidating agents giving access to *N*-Boc protected arylamines (Scheme 5.2.2.1d).[30]

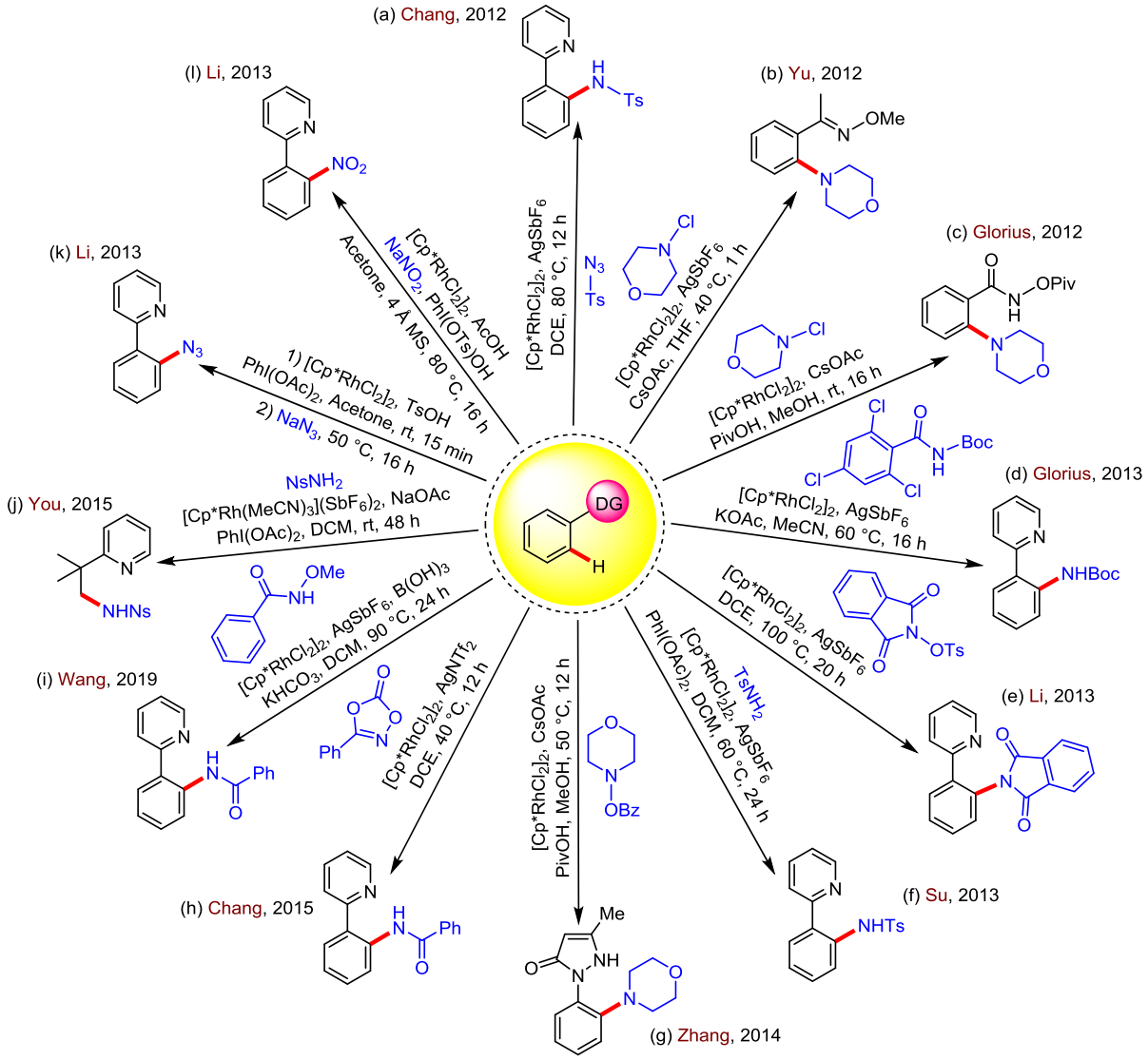

Scheme 5.2.2.1. Representative examples of Rh-catalyzed C–N bond formation.

Simultaneously, Li group revealed a C–H amidation reaction of diverse DG assisted arenes employing *N*-arenesulfonated imides as amidating reagent under base free Rh-catalyzed conditions (Scheme 5.2.2.1e).[31] Shortly after, Su *et al*. followed up with a report on Rh(III)-catalyzed intermolecular dehydrogenative aromatic C–H amidation of different chelating arenes with both aromatic and aliphatic sulfonamides (Scheme 5.2.2.1f).[32] Zhang and co-workers achieved another intermolecular C–H amination of 1-aryl-1*H*-pyrazol-5(4*H*)-ones with *N*-benzoate alkylamines under rhodium-catalyzed conditions (Scheme 5.2.2.1g).[33] In 2015, Chang group disclosed the use of 1,4,2-dioxazol-5-ones as an extremely efficient and

convenient to prepare and use amidating agent in comparison to the corresponding azides. They possessed increased amidation reactivity as compared to the azides on account of their strong affinity to cationic Rh(III) species. This newly developed reagent underwent direct a amidation reaction with a wide array of substrates with the concomitant release of CO_2 as a single byproduct (Scheme 5.2.2.1h).[34] In 2019, Wang *et al*. delineated the unusual reactivity of *N*-methoxyamides as an amidating reagent in a rhodium-catalyzed direct amidation reaction of various directing aromatic C–H bonds (Scheme 5.2.2.1i).[35]

Shifting the focus to aliphatic C–H activation, in 2015, You and co-workers demonstrated a Rh(III)-catalyzed sp^3 C–H amidation of pyridine-directed unactivated aliphatic C–H bonds with sulfonamides (Scheme 5.2.2.1j). The reaction took place at room temperature and proceeded with broad functional group tolerance and high selectivity.[36] Moving onto other C–N bond forming reactions, Li group in 2013, reported the first C–H azidation and nitration reactions employing rhodium catalysis. The methodology utilized hypervalent iodine reagent as an efficient oxidant and sodium azide and sodium nitrite as the sources of azide group and nitro group respectively for the direct functionalization of pyridine, pyrimidine, and pyrazole heterocycle directed arenes (Scheme 5.2.2.1k, 5.2.2.1l).[37] Apart from these examples, several other contributions on Rh-catalyzed C–N bond formations have also been observed.[38]

- **C–O bond formation**

C–O bonds are ubiquitous in nature owing to their presence in biologically active compounds, natural products, pharmaceuticals, and polymers. Thus, their construction is of utmost importance in synthetic organic chemistry. In this regard, Rh-catalyzed chelation assisted direct C–H oxygenations, *viz*. acetoxylation, acyloxylation and hydroxylation reactions have also been reported,[39] some of which are depicted in Scheme 5.2.2.2. The first DG assisted Rh(III)-catalyzed direct C–H acetoxylation reaction was revealed by Zhang group in 2014 for the efficient synthesis of *Z*-configured acetoxylated enamides using $Cu(OAc)_2$ as the acetate source as well as the oxidant (Scheme 5.2.2.2a).[39a] Following this report on vinylic sp^2 C–H oxygenation, in 2017, Zhou *et al*. disclosed an acetoxylation protocol for directing arenes under rhodium catalysis using PIDA as acetoxy source and $AcOH/Ac_2O$ as a solvent combination which promoted the reaction. In the same report, they showed that when H_2O was used as an additive, direct C–H hydroxylation could be achieved in very good yields (Scheme 5.2.2.2b).[39b] Around the same time, Li and co-workers devised a Rh-catalyzed direct *ortho* sp^2 C–H acyloxylation of diverse chelating group attached arenes and alkenes with a vast array of

readily available alkyl, alkenyl, and aryl carboxylic acids (Scheme 5.2.2.2c).[39f] Lu group demonstrated a Rh(III)-catalyzed sp^3 C–H acetoxylation of 8-methylquinolines employing a $PhI(OAc)_2/Ac_2O$ combination as the source of acetoxy group (Scheme 5.2.2.2d).[39h]

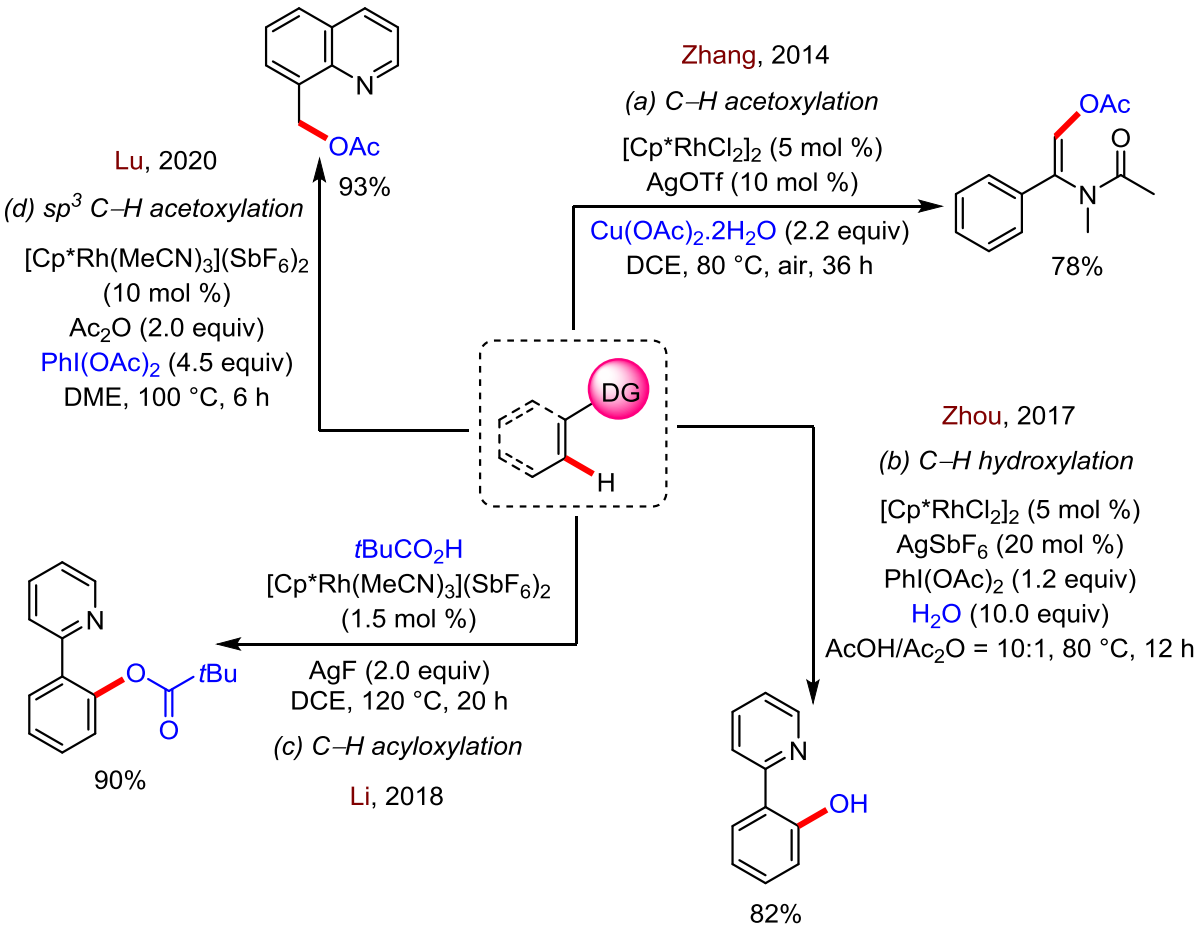

Scheme 5.2.2.2. Representative examples of Rh-catalyzed C–O bond formation.

➢ C–S and C–Se bond formation

The importance of organosulfur and organoselenium compounds in various fields of science has rendered the development of C–S and C–Se bond an attractive synthetic organic chemistry research area. Among various catalytic methods developed for their construction, DG assisted rhodium-catalyzed direct C–H chalcogenation reactions have become a highly utilized mode of approach by different research groups all over the world. A few examples are outlined in Scheme 5.2.2.3. In 2014, Zhou and Li group accomplished the first intermolecular C–S coupling via Rh-catalysis between different nitrogen heterocycle bearing arenes and aryl or alkyl disulfides (Scheme 5.2.2.3a).[40] The reaction produced a broad range of aryl thioethers or dithioethers depending upon the choice of oxidant employed. Following year, Li and co-

workers demonstrated a Rh(III)-catalyzed chelation-assisted C–H selenylation of directing arenes with electrophilic selenyl chlorides and diselenides as the source of selenyl functionality (Scheme 5.2.2.3b).[41] Concurrently, they devised a C2-selective direct trifluoromethylthiolation of indoles under rhodium catalysis using *N*-trifluoromethylthiosaccharin as an efficient electrophilic SCF_3 reagent (Scheme 5.2.2.3c).[42] In 2016, Li *et al*. again realized a Rh(III)-catalyzed C–S bond formation for the sulfonylation of 2-phenylpyridines using sodium *p*-toluenesulfinate as the source of sulfonyl group (Scheme 5.2.2.3d).[43] The reaction was proposed to proceed via an initial hyperiodination of the arene substrate followed by an uncatalyzed nucleophilic functionalization. Apart from these noteworthy works, several other reports on C–H chalcogenation have come up over the years.[44]

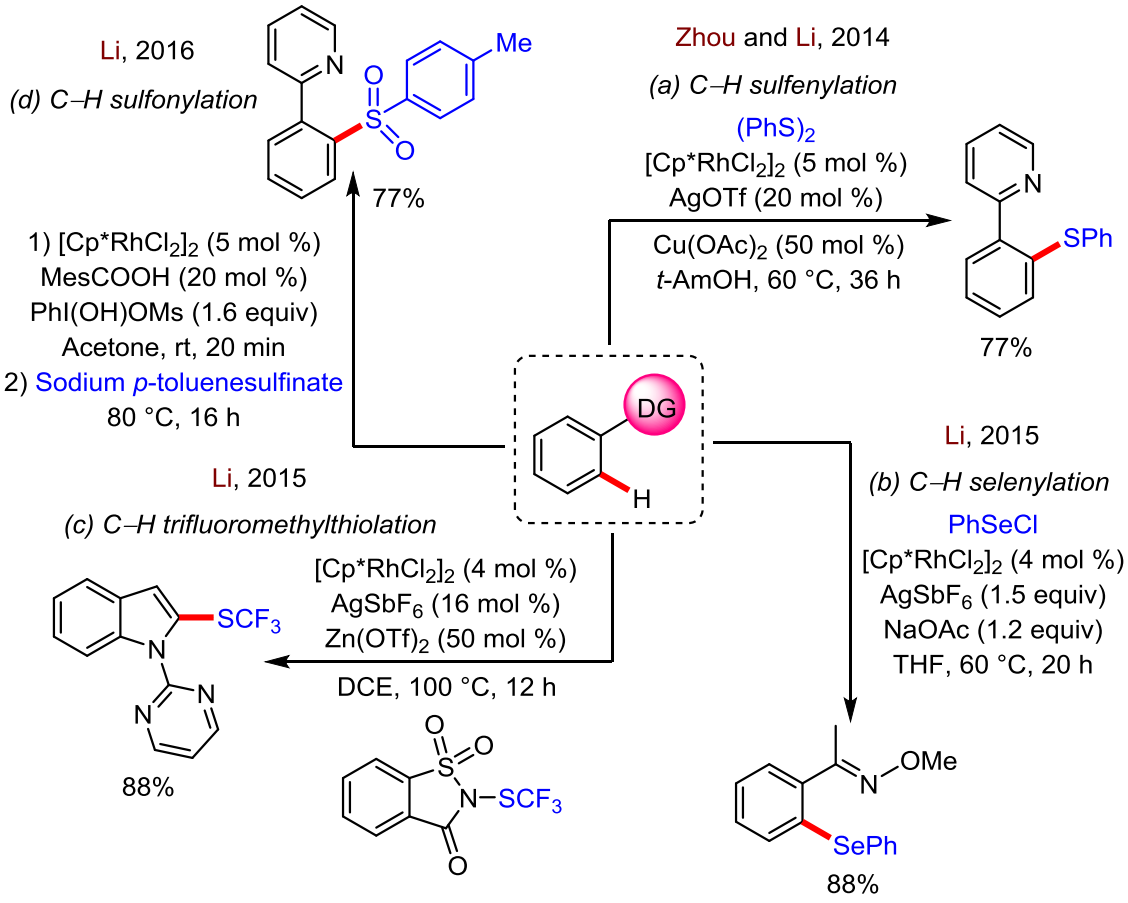

Scheme 5.2.2.3. Representative examples of Rh-catalyzed C–S and C–Se bond formation.

➢ C–Z (Z = Cl, Br, I) bond formation

Aromatic halides are an important class of compounds which play pivotal roles in synthetic organic chemistry, since they behave as valuable precursors to organometallic reagents and nucleophilic substitution reactions, and are also a core building block for cross-coupling

chemistry. Consequently, their synthesis remains highly valuable in which Rh-catalyzed C–H bond activation has also played its part very generously. In 2012, Glorius group disclosed the first chelation-aided Rh(III)-catalyzed *ortho* bromination and iodination of diverse arenes using readily available *N*-halosuccinimides (Scheme 5.2.2.4).[45] The reaction provided good to excellent yields with high functional group tolerance, where the use of chlorinated solvent and PivOH or $Cu(OAc)_2$ additive were essential for the reaction. Taking inspiration from this work, thereafter, many reports on directing group assisted C–H halogenation reactions employing rhodium catalysis have surfaced using different halogen sources like *N*-halosuccinimides, sodium halides, and 1,2-dichloroethane (DCE).[46]

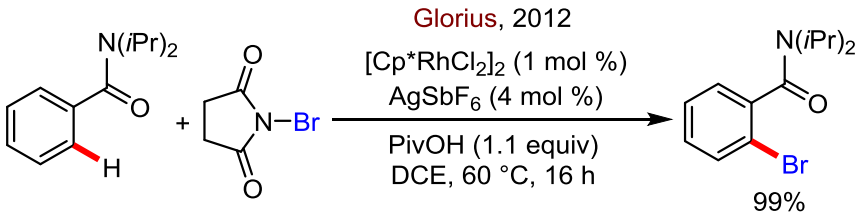

Scheme 5.2.2.4. Rh-catalyzed direct C–H halogenation.

➢ Other C–X bond formation

Apart from the above carbon–heteroatom bond formations designed frequently using rhodium catalysis, sporadic examples of other type of C–X bonds like C–P and C–B bond formation reactions have also been cleverly developed employing Rh(III) catalysis (Scheme 5.2.2.5).[47] In 2016, Hong group achieved a direct Rh(III)-catalyzed sp^2 C–H phosphorylation of diverse (hetero)arenes using dialkyl phosphonates, thus providing a straightforward route to a series of structurally and medicinally important aryl phosphonates (Scheme 5.2.2.5a).[47a]

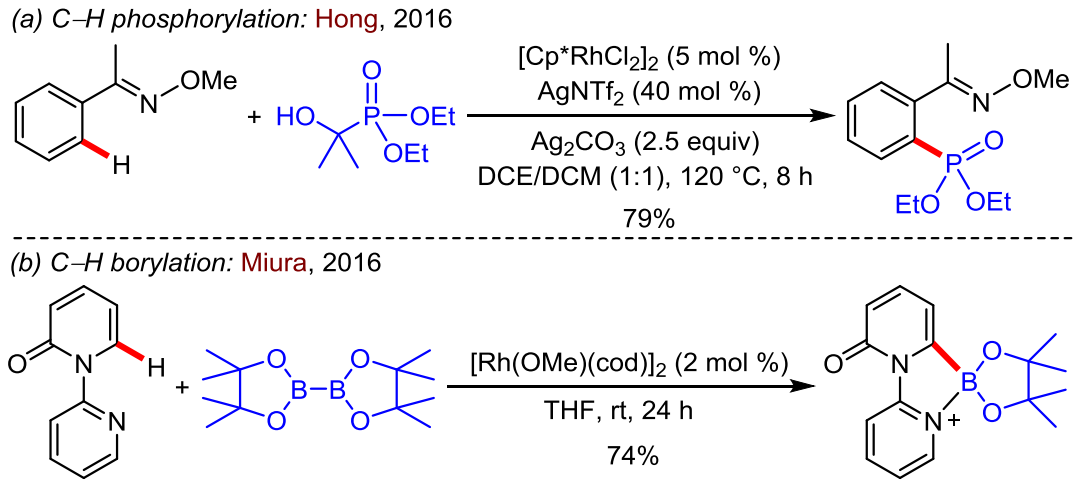

Scheme 5.2.2.5. Rh-catalyzed C–P and C–B bond formation.

Given the rich chemistry of organoboron compounds (for eg. Suzuki-Miyaura cross-coupling) in organic synthesis, the C–B bond serves as a useful synthetic platform for further manipulations in the synthesis of versatile compounds. In this context, Miura *et al*. disclosed a pyridine directed rhodium-catalyzed C6-selective direct C–H borylation of 2-pyridones with excellent site selectivity (Scheme 5.2.2.5b).[47b] Bis(pinacolato)diboron (B_2Pin_2) was used as the borylating reagent for the reaction.

5.2.3. C–H Annulation Reaction

Rhodium complexes are exceptionally significant in homogeneous catalysis. The synthetic community observed the rapid burgeoning of such rhodium catalysis since the discovery of Wilkinson's catalyst. After the discovery of pentamethylcyclopentadienylrhodium(III) chloride dimer, $[Cp^*RhCl_2]_2$, or simply Cp*Rh, several reports have appeared in literature in the last two decades exploring this as a potent catalyst in C–H functionalization reactions. The Cp*Rh(III) complex is often considered as a preferential catalyst for C–H activation, presumably because of the better π-acceptor ability of Rh(III) species with unsaturated bonds which activates the carbon–carbon multiple bonds. The presence of an electron-rich Cp* ligand stabilizes the organorhodium complex and facilitates oxidative addition on the metal, and also favours the reductive elimination step due to its bulkiness.

In this context, annulation reactions through tandem C–H activation/cyclization have become a dominant class of reactions to make (hetero)cyclic products by harnessing the power of organorhodium catalysis owing to its high efficiency, functional group tolerance, bench-stability, easy handling, thus making it a superior catalyst. Annulation strategy refers to the formation of a ring involving the fusion of two molecular fragments that are united to generate two new bonds and it finds numerous applications in the synthesis of many natural products, medicinally relevant compounds, and is particularly useful when more than one C–C or C–X bond needs to be formed. Directing group (DG) tethered substrates undergo smooth annulation reactions with alkynes/alkenes and other unsaturated partners, thus making it a powerful tool for the synthesis of fused (hetero)aromatic compounds.[15a,48] A series of diverse directing groups bearing heteroatoms like *N*, *O*, *P*, *S* have been studied for this purpose. This section provides a brief account on different rhodium-catalyzed annulation strategies, namely, oxidative, redox-neutral, photoredox, and electrochemical transformations. In addition, the enantioselective synthesis of annulated molecules using chiral rhodium catalysts is also highlighted.

A typical rhodium-catalyzed C–H activation/annulation strategy consists of the following sequence of processes: (i) Lewis base dissociation/formation of active catalytic species (ii) Ligand combination (iii) Oxidative addition/C–H activation (iv) Unsaturated coupling partner coordination/insertion/cyclization and (v) Reductive elimination followed by regeneration of Rh(III) species from insitu generated Rh(I) in the presence of external or internal oxidant (Scheme 5.2.3.1). Depending upon the reaction conditions, reaction mechanism, kind of products formed, annulation reactions have been classified in the following categories, such as- (a) redox-active/oxidative annulation where the active Rh(III) species regenerates from Rh(I) in presence of an external oxidant (b) redox-neutral annulation where external oxidant is not needed to regenerate the active Rh(III) catalyst since the heteroatom bond (mostly N–O bond) present in the substrate acts as a built-in oxidant (c) photochemical annulation where the active catalytic Rh species is regenerated using a photocatalyst (d) electrocatalytic annulation where the active catalytic Rh species regenerates via an electrochemical reaction at the surface of a suitable electrode (e) enantioselective annulation where active chiral Rh(III) complex is involved in the reaction.

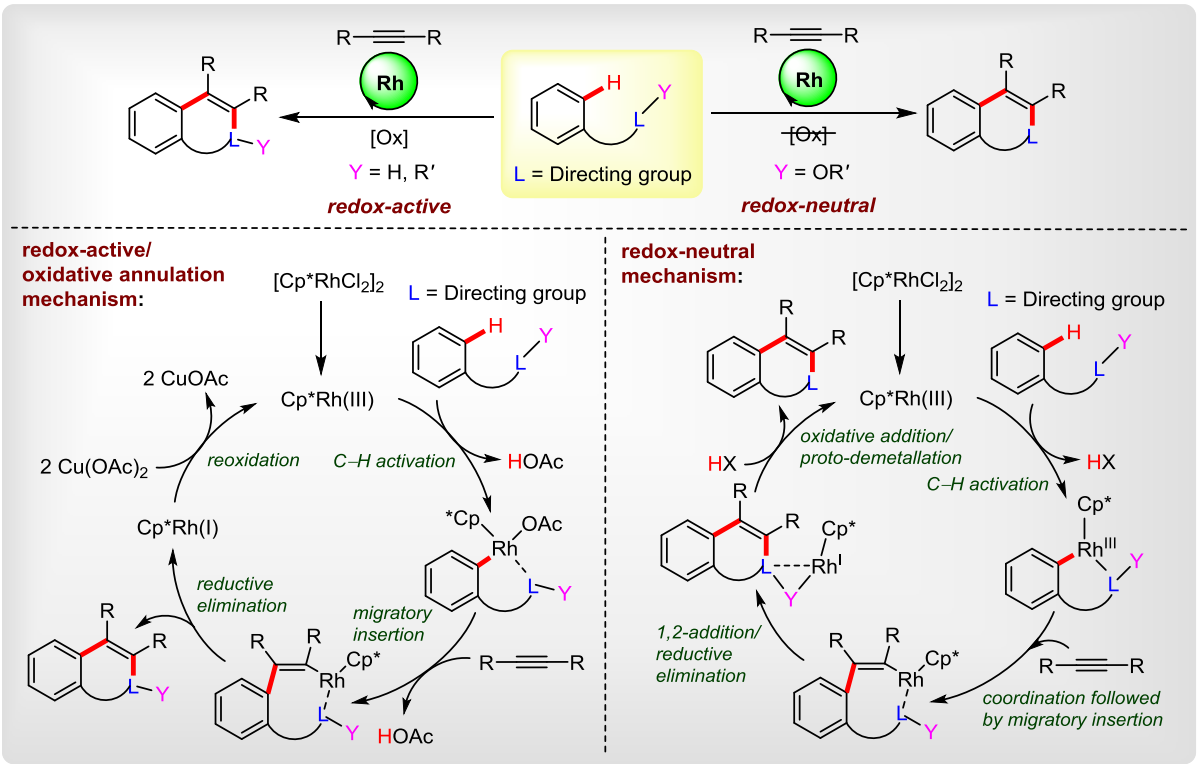

Scheme 5.2.3.1. General reaction mechanism of Rh(III)-catalyzed C–H bond activation/annulation.

The annulation/cyclization reactions can be further divided into different sub-types depending upon the number of atoms or π-bonds involved in the reaction between the two coupling partners, *viz*. [4+2], [3+2], [4+1], [5+1], etc. annulation reactions.

- **Redox-active/Oxidative annulation**

The majority of [4+2] annulation reactions developed by several research groups involve alkyne as one of the most convenient coupling partners in combination with various substrates. The type of coupled products formed in these cases depend on whether an anionic directing group (L–Y) or a neutral directing group (L) is present. Substrates with nitrogen or oxygen-containing weakly chelating DGs such as imines, amides, carboxylic acids, ketones, aldehydes, alcohols can undergo oxidative annulation with alkynes, which enhances the versatility of the methodology for practical uses. The presence of heteroatoms, either *O*- or *N*-coordinated with Rh(III) species allow to form a rhodacycle intermediate via C–H activation, which then encounters alkyne insertion and subsequent reductive elimination occurs to furnish the corresponding annulated product and Rh(I) species, and on using a suitable external oxidant the active Rh(III) species is again regenerated by oxidation (Scheme 5.2.3.1, redox-active). Commonly, AgOAc and $Cu(OAc)_2$, $Cu(OAc)_2$-air/O_2 combination are the natural choice of external oxidants used for the reoxidation of Rh(I) to Rh(III). Furthermore, the OAc^- anion associated with these oxidants helps to accelerate the C–H breaking process as well. Different solvents, including 1,2-DCE, acetone, DMF, *o*-xylene, *t*-BuOH and *t*-AmOH are generally used in this type of transformation. A variety of isocoumarins, chromones, benzamides, indoles, indenols and their analogues have been synthesized efficiently utilizing this rhodium(III)-catalyzed oxidative annulation strategy.

In this realm, the pioneering work of Miura and Satoh led many research groups to devote themselves to this field employing rhodium-catalyzed C–H activation/annulation cascade using aromatic compounds with alkynes, depicted in Schemes 5.2.3.2 and 5.2.3.3. In 2007, Miura and Satoh group elegantly employed benzoic acids to combine with alkynes in 1:1 ratio to synthesize [4+2] annulated isocoumarin derivatives using $[Cp^*RhCl_2]_2$ as catalyst and $Cu(OAc)_2.H_2O$ as oxidant (Scheme 5.2.3.2a).[11] Following year, the coupling of salicylaldehydes with internal alkynes was also achieved by them to obtain the corresponding [4+2] annulated chromone derivatives with the cleavage of aldehyde C–H bond in an efficient manner employing a combination of a rhodium catalyst, cyclopentadiene ligand and copper oxidant (Scheme 5.2.3.2b).[49]

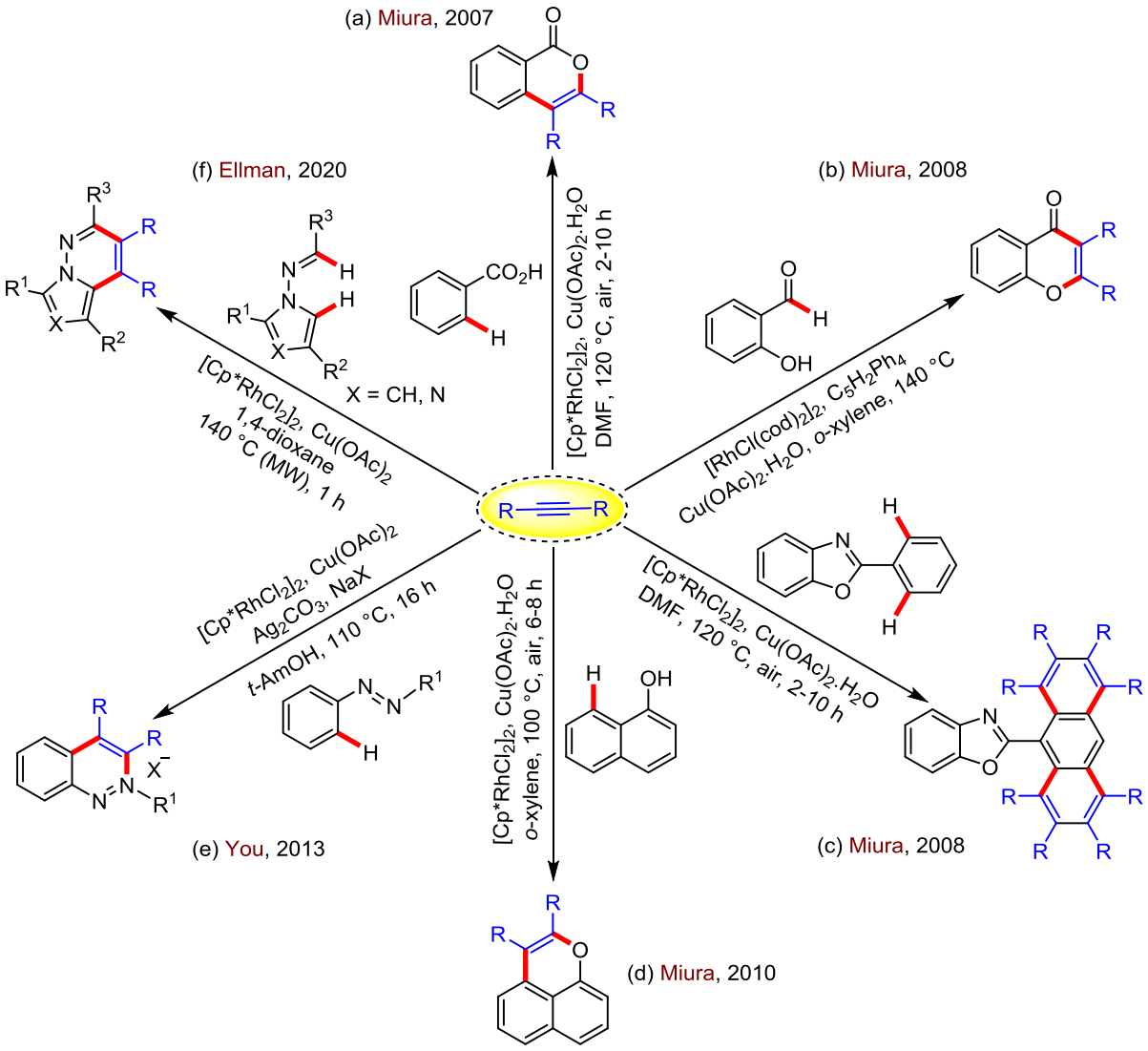

Scheme 5.2.3.2. Selected examples of oxidative annulation with alkynes.

Concurrently, they made possible a direct coupling reaction between phenylazoles and internal alkynes to yield 1-naphthyl- or 1-anthrylazole derivatives depending on the ratio of alkyne in presence of a rhodium catalyst and copper oxidant through the cleavage of multiple C–H bonds (Scheme 5.2.3.2c).[50] In 2010, they continued their pursuit with alkyne partners by reacting them with 1-naphthols or other phenolic and alcoholic substrates to give regioselective [4+2] annulated products such as naphtho[1,8-*bc*]pyran derivatives and related polycyclic compounds exercising rhodium catalysis, where the hydroxy group plays as a key functional group for the regioselective oxidative annulation reaction (Scheme 5.2.3.2d).[51] In 2013, You (Scheme 5.2.3.2e) and Cheng group independently showcased the synthesis of pharmaceutically relevant cinnolinium salts by chelate-assisted C–H activation/annulation of azobenzenes with alkynes, which was again very recently extended to 2-phenylindalzoles for

the generation of cinnolinium and fluoranthenium salts under rhodium catalysis by Maheswari group.[52] Recently, Ellman and co-workers explored the [4+2] annulation of alkynes with hydrazones via a dual C–H activation technique employing Rh(III) catalysis to generate pyrrolopyridazines or azolopyridazines under microwave heating conditions (Scheme 5.2.3.2f).[53] Also, fastening the alkyne to the hydrazone moiety resulted in the formation of complicated tricyclic products using an intramolecular version of this methodology.

Apart from *O*- and *N*-based directing groups, other *S*- and *P*-based directing groups, *viz.* sulfonamides, sulfoximines, phosphinic acids, sulfonic acids, and simple thiols have been explored for rhodium-catalyzed oxidative C–H/X–H annulation with alkynes for the synthesis of diverse heterocycles (Scheme 5.2.3.3).[54]

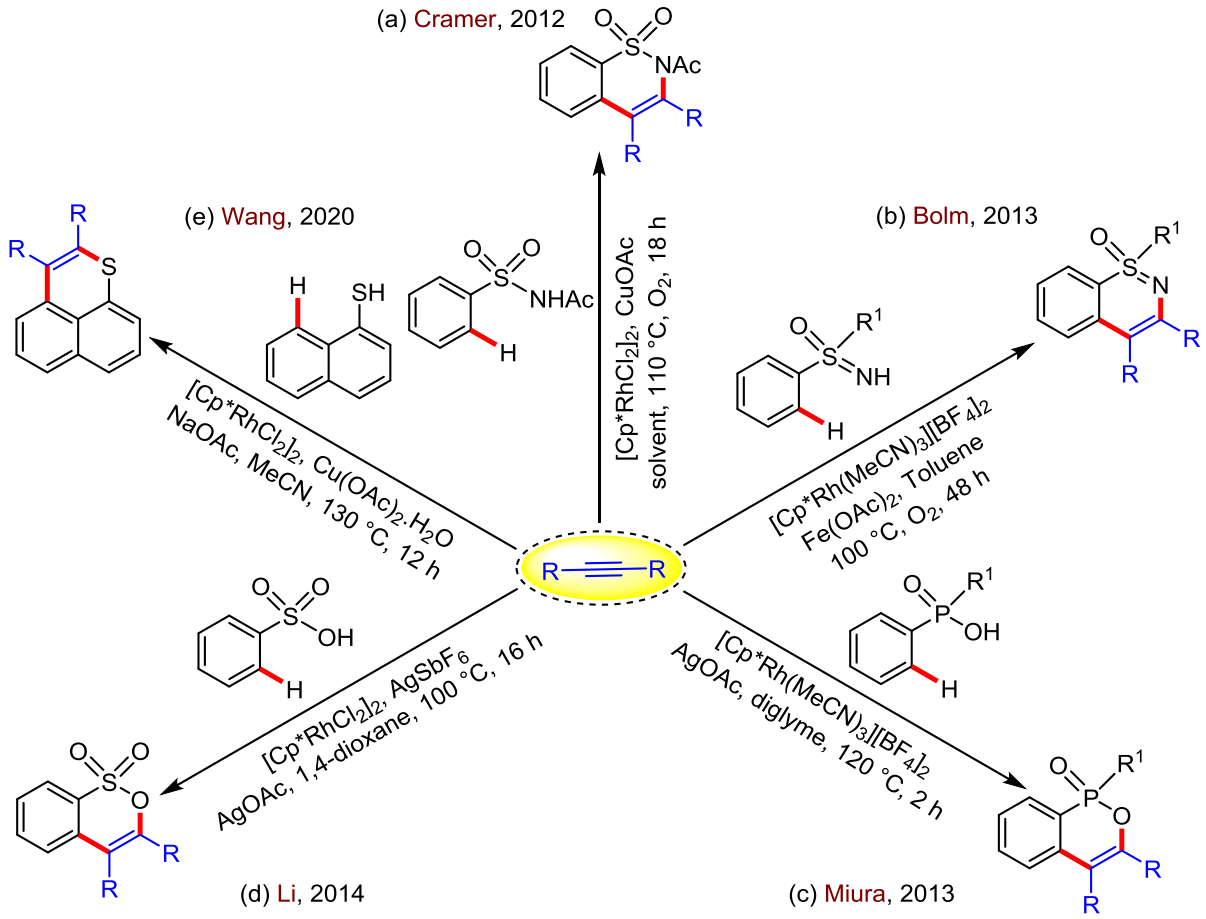

Scheme 5.2.3.3. Other heteroatom based DGs in oxidative annulation with alkynes.

In 2016, Perumal group devised a Rh(III)-catalyzed dehydrogenative C–H/N–H annulation strategy to construct photophysically important phthalazino[2,3-a]- or indazolo[1,2-a]cinnolines from the reaction of *N*-phenyl phthalazine or indazole derivative with alkynes under oxidative conditions (Scheme 5.2.3.4a).[55] On the contrary, in 2018, Sakhuja and co-

workers disclosed a redox-neutral methodology for the synthesis of similar phthalazino-fused cinnoline scaffolds via a [4+2] annulation reaction between 2-arylphthalazine-1,4-diones and α-diazo carbonyl compounds employing rhodium catalysis.[56] Very recently, propargyl alcohols have been used for [4+2] annulation with *N*-arylbenzimidines for the generation of functionalized isoquinolines (Scheme 5.2.3.4b).[57]

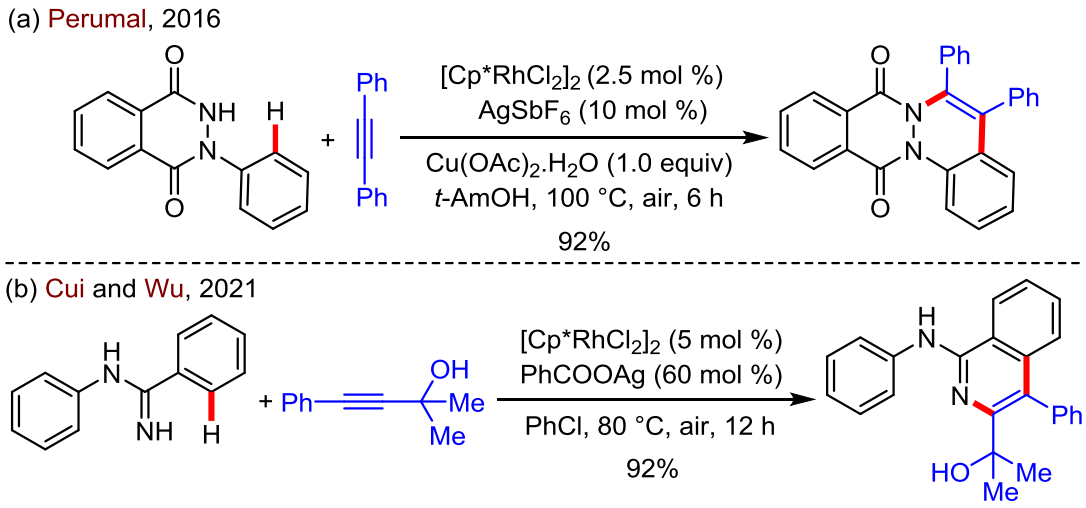

Scheme 5.2.3.4. Other examples of [4+2] annulation with different *N*-based DG.

Activated olefins are also commonly used as appropriate coupling partners for Rh-catalyzed [4+2] annulation reactions using various directing group attached substrates. Among them, maleimides and α,β-unsaturated esters have always been the go-to coupling partners to furnish diverse annulated products (5.2.3.5).[58] In 2020, Li and Fan *et al.* offered a sustainable synthetic approach for the synthesis of pharmaceutically useful maleimide-fused complex heterocycles, like benzocarbazoles/imidazo[1,2-*a*]pyridines through a rhodium(III)-catalyzed oxidative [4+2] annulation reaction of 2-arylindoles/2-arylimidazo[1,2-*a*]pyridines with *N*-substituted maleimides (Scheme 5.2.3.5a).[58a] Later, Zhou and Lee have also used maleimides to construct a series of benzimidazoisoquinolines on coupling with 2-arylbenzimidazoles.[58b,c] In the following year, Li group devised a protocol for the formation of fused quinoline scaffolds via annulation of 4-aminoquinolines at the rarely studied 5-position with acrylates through two successive C–H activations (Scheme 5.2.3.5b).[58d] Acrylates as a coupling partner have also been employed in other types of annulation reactions discussed later under appropriate sections. Other activated alkenes like cyclic enones (Scheme 5.2.3.5d) and silyl enol ethers (Scheme 5.2.3.5e) have also been utilized for oxidative [4+2] annulation reactions with 2-arylindazoles and *N*-carbamoylindoles by the groups of Reddy and Ji respectively.[59]

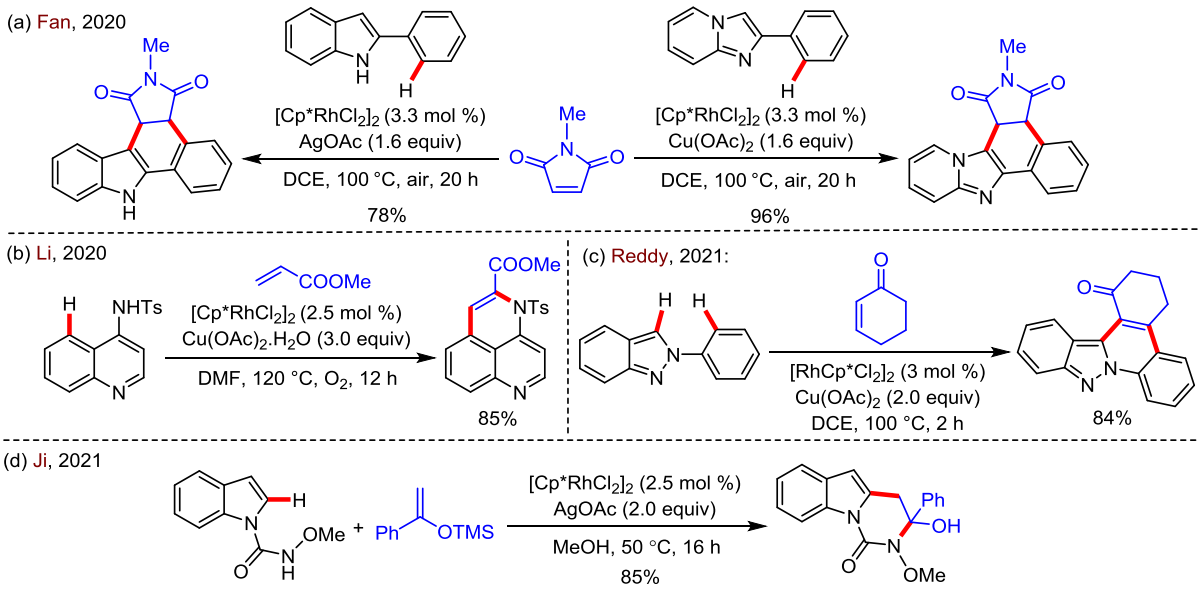

Scheme 5.2.3.5. Selected examples of [4+2] annulation with activated olefins.

[3+2] annulation as well as spirocyclization reactions have also been exploited using oxidative Rh(III) catalysis. In 2008 and 2010 successively, Fagnou group developed Rh-catalyzed oxidative [3+2] annulation reactions for the synthesis of indoles from easily accessible aniline derivatives and alkynes (Scheme 5.2.3.6a).[12b,60] In 2014, Liu *et al*. accomplished a rhodium-catalyzed [3+2] annulation of hydrazine derivatives with alkynes under oxidative conditions furnishing 1-aminoindole derivatives using 1,3-dinitrobenzene as an external oxidant to regenerate the active catalytic species Rh(III) from Rh(I) (Scheme 5.2.3.6b).[61] In between, Miura and Satoh group devised a protocol for rhodium-catalyzed oxidative coupling between aromatic imines and internal alkynes which coherently produced indenone imine and isoquinoline derivatives via C–H bond cleavage (Scheme 5.2.3.6c).[62]

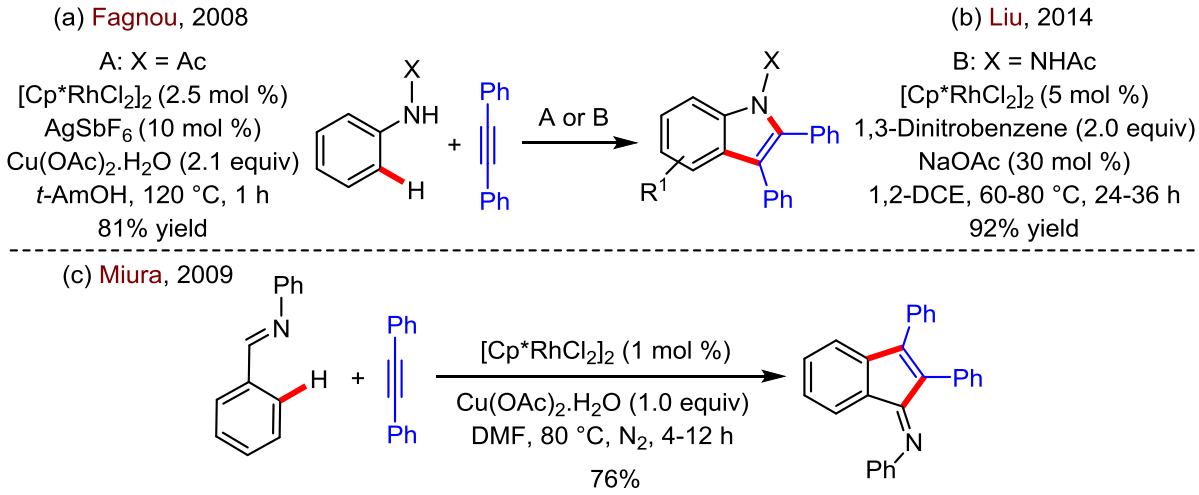

Scheme 5.2.3.6. [3+2] annulation with alkynes.

Synthesis of spirocyclic scaffolds is another compelling facet in the area of annulation chemistry and indeed several groups have achieved this feat by [3+2] spirocyclization via Rh catalysis, some of which are depicted in Scheme 5.2.3.7.[63] In 2014, Mascareñas and Gulías *et al*. unveiled an excellent chemo and regioselective method for making spirocycles using substituted 2-alkenylphenols which undergo a formal [3+2] annulation with alkynes employing oxidative Rh(III) catalysis (Scheme 5.2.3.7a).[63a] Cleavage of the terminal C–H bond of the alkenyl moiety and the dearomatization of phenol are the key steps of this reaction to produce highly appealing spirocyclic scaffolds. At the same time, Xia and Li group described a rhodium(III)-catalyzed regioselective [3+2] annulation of 5-aryl-2,3-dihydro-1*H*-pyrroles with internal alkynes to construct a spiro[indene-1,2'-pyrrolidine] architecture in high yields (Scheme 5.2.3.7b).[63b] In 2016, Wei and co-workers devised a cross-dehydrogenative coupling/annulation strategy between weakly directing cyclic *N*-sulfonyl ketimines and thiophenes for the synthesis of structurally fascinating and synthetically relevant spirocyclic sultams (Scheme 5.2.3.7c).[63c]

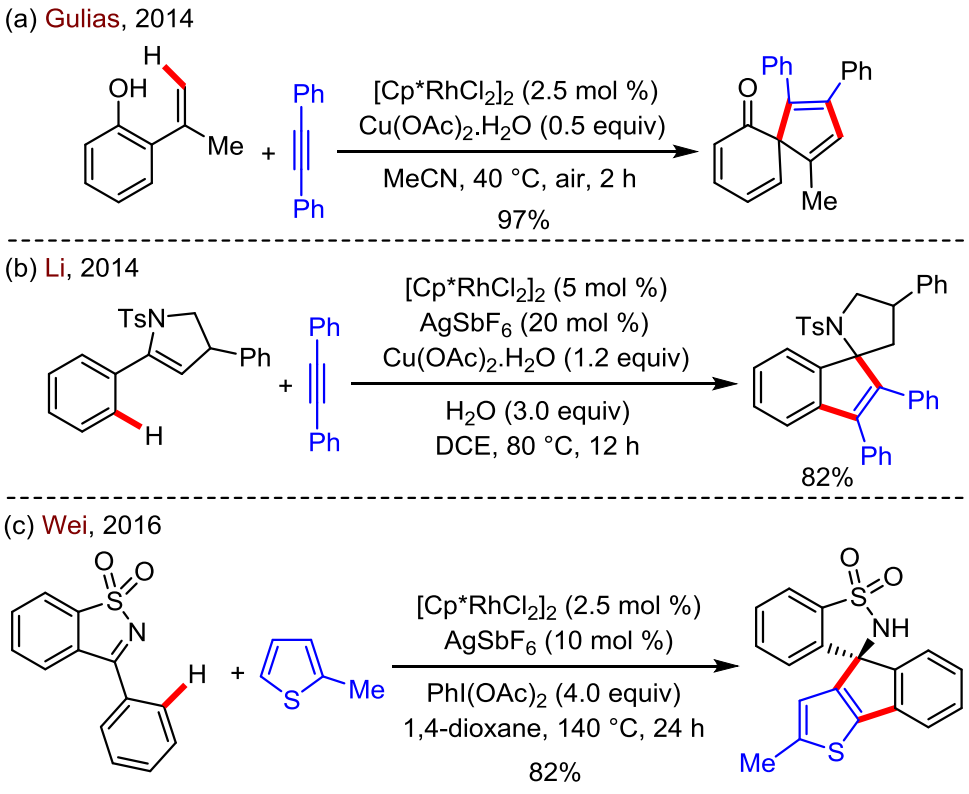

Scheme 5.2.3.7. [3+2] spirocyclization with different coupling partners.

Different types of couplings partners have been applied in Rh(III)-catalyzed [4+1] annulation reactions by several research groups (Scheme 5.2.3.8).[64] In 2014, Carretero group delineated a highly stereoselective cascade olefination/annulation reaction between picolinamides and

unsaturated esters (Scheme 5.2.3.8a).[64a] Ji and co-workers employed propargyl alcohols to undergo [4+1] annulation with various heterocycles giving access to a wide range of quaternary carbon centers containing fused heterocyclic scaffolds (Scheme 5.2.3.8b).[64b] Here, no external metal oxidants were used and air atmosphere was employed where O_2 reoxidized the Rh(I) species to the active Rh(III) species to continue the catalytic cycle. Next, in 2019, Li *et al.* developed an efficient strategy to synthetically manipulate various classes of aromatic substrates with 1,3-enynes in order to produce diversified heterocycles under relatively mild reaction conditions (Scheme 5.2.3.8c).[64c]

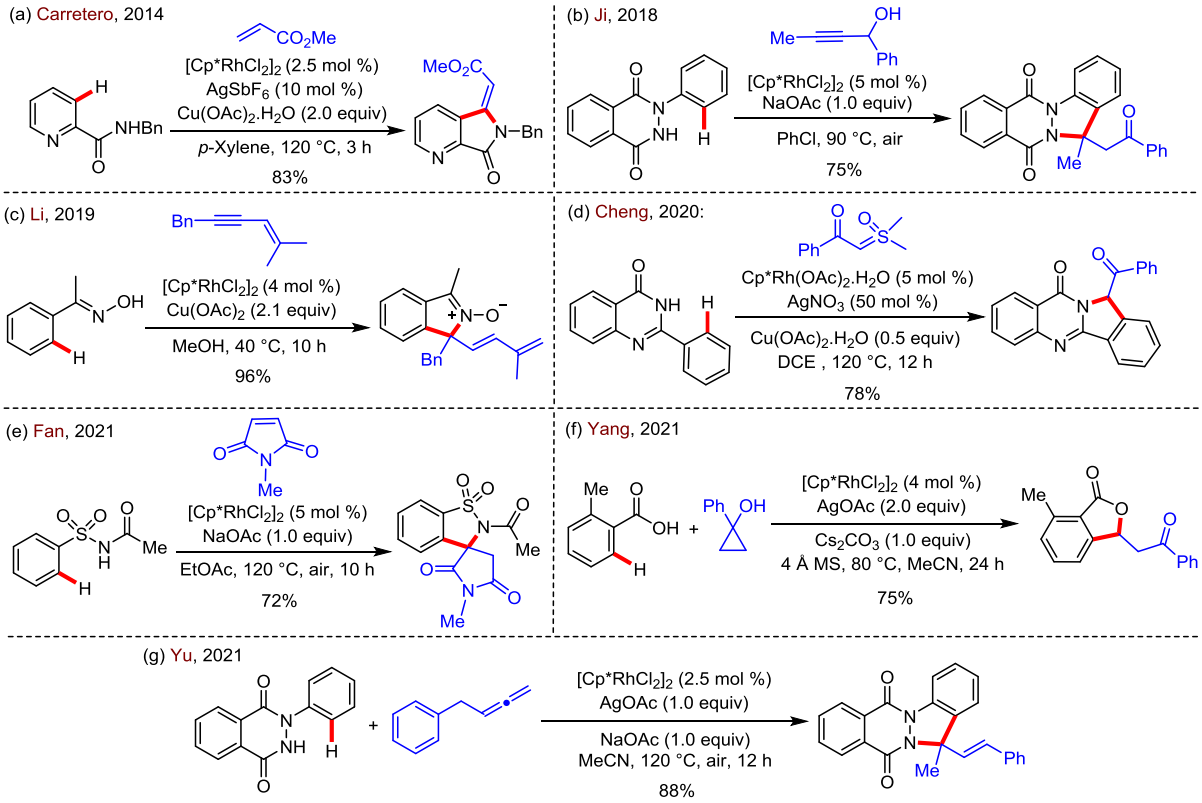

Scheme 5.2.3.8. [4+1] annulation with different partners under Rh(III) catalysis.

In the following year, Cheng and co-workers impressively extended the [4+1] annulation technique to 2-aryl quinazolin-4(3*H*)-ones and sulfoxonium ylides, leading to the formation of 12-aroyl isoindolo[1,2-*b*]quinazolin-10(12*H*)-ones in good yields (Scheme 5.2.3.8d).[64d] Very recently, Fan group disclosed a protocol for the synthesis of spiro-fused sultams from sulfonyl acetamides and maleimides through a series of cascade processes (Scheme 5.2.3.8e).[64e] Again, a Rh(III)-catalyzed tandem C–H activation/ring-opening/cyclization of carboxylic acids was achieved employing cyclopropanols as a suitable coupling partner (Scheme 5.2.3.8f).[64f] Allenes have also recently been utilized as coupling partners to synthesize indazole derivatives

with high *Z*-selectivity on annulation with phthalazinones and pyridazinones (Scheme 5.2.3.8g).[64g]

Other classes of not so common Rh-catalyzed oxidative annulation reactions are the [5+1], [5+2] and [3+1+1] annulation reactions. [5+1] annulation has been exercised for the preparation of fused heterocyclic as well as carbocyclic rings.[65] Among these reports, in 2021, Zhou and co-workers devised a protocol for the synthesis of six-membered 1,7-fused indolines bearing an all-carbon quarternary stereogenic center by C7-selective C–H activation/annulation of indolines with 1,3-enynes under rhodium-catalyzed conditions (Scheme 5.2.3.9a).[65d] On the other hand, [5+2] annulation reactions allow for the direct synthesis of attractive and rarely observed larger ring frameworks. In 2018, Gao and Zhou group described a unique oxidative Rh(III)-catalyzed [5+2]-annulation reaction of 2-alkenylphenols with propargyl carbonates in 2018 (Scheme 5.2.3.9b).[66] The two *O*-atoms of both the counterparts acted as traceless assisting groups. In the context of [3+1+1] annulation reaction, very recently, Xie *et al.* described a Rh-catalyzed three-component dehydrogenative cascade cyclization reaction involving diarylimines, vinyl ketones, and simple amines, where, four C–H bonds and two N–H bonds are broken and one new C–C bond and two new C–N bonds are formed in one-pot (Scheme 5.2.3.9c).[67]

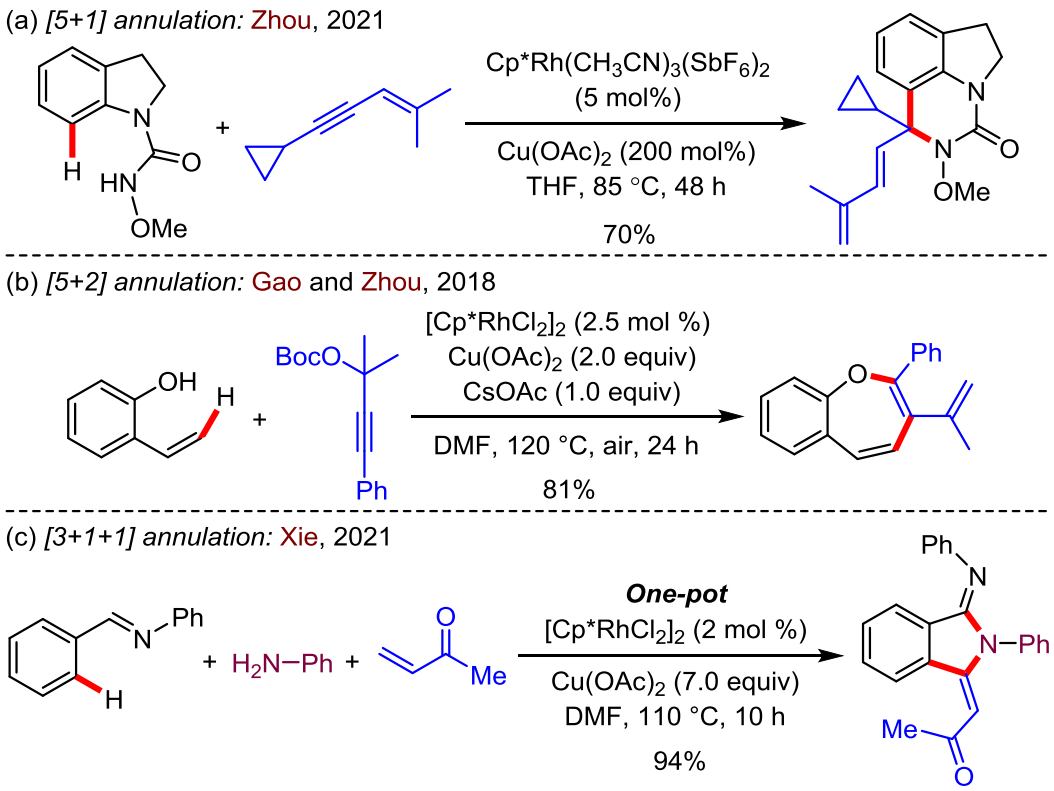

Scheme 5.2.3.9. Selected examples of Rh-catalyzed [5+1], [5+2] and [3+1+1] annulation.

➢ Redox-neutral annulation

In 2010, a conceptually new approach was developed by Fagnou and co-workers to access isoquinolones via a Rh(III)-catalyzed redox-neutral annulation strategy using both internal and terminal alkynes as well as alkenes with substrates containing different directing groups in absence of any external oxidant (Scheme 5.2.3.10).[68]

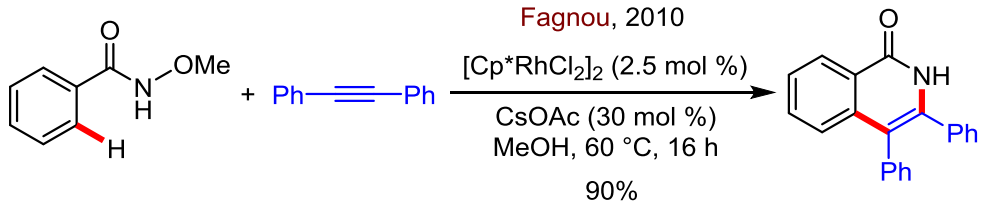

Scheme 5.2.3.10. First example of Rh-catalyzed redox-neutral annulation.

The prime difference of this strategy from the oxidative annulation reactions is the masterful choice of nitrogen-based directing groups where the N–O bond plays the instrumental role of an internal oxidant (Scheme 5.2.3.1, redox-neutral), thus eliminating the use of stoichiometric external oxidants needed in the previous concept. Inspired by this pioneering work, thereafter several types of redox-neutral annulations catalyzed by Rh(III) catalysts have been reported by various research groups for the synthesis of diverse ring systems discussed briefly.

One class of annulation reactions extensively studied under redox-neutral rhodium catalysis is the [3+2] annulation chemistry.

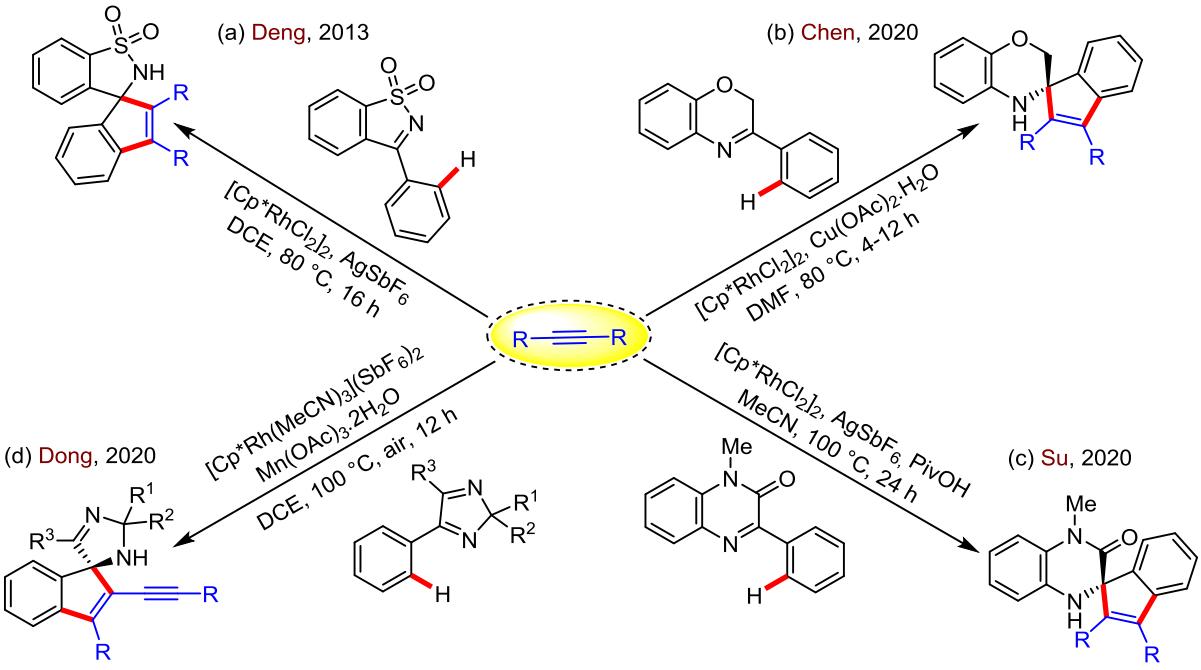

Scheme 5.2.3.11. [3+2] spirocyclization with alkynes via rhodium catalysis.

In 2013, spirocyclic benzosultams via [3+2] annulation were furnished by Deng *et al*. using a combination of *N*-sulfonyl ketimines and internal alkynes (Scheme 5.2.3.11a).[69] Among latest reports, recently, employing this protocol, methods for spiro-indenylbenzoxazine starting from 3-Aryl-2*H*-Benzo[*b*][1,4]oxazines and spiroquinoxalinone derivatives from 3-arylquinoxalin-2(1*H*)-ones and [imidazole-4,1′-indene] from 2*H*-imidazoles using alkynes or dialkynes as coupling partners were disclosed by Chen, Su, and Dong groups, independently (Scheme 5.2.3.11b-5.2.3.11d).[70] Like simple alkynes, dialkynes have also been employed in [3+2] cyclization with indole derivatives.[71]

Shifting focus to unsaturated coupling partners from triple bonds to double bonds, activated alkenes like CF_3-substituted enones were also employed in a similar fashion by Li and co-workers in 2017. These activated olefins underwent a Rh(III)-catalyzed diastereodivergent redox-neutral spiroannulation reaction with cyclic *N*-sulfonyl as well as *N*-acyl ketimines smoothly (Scheme 5.2.3.12a).[72] The diastereoselectivity is guided by the type of silver additives used.

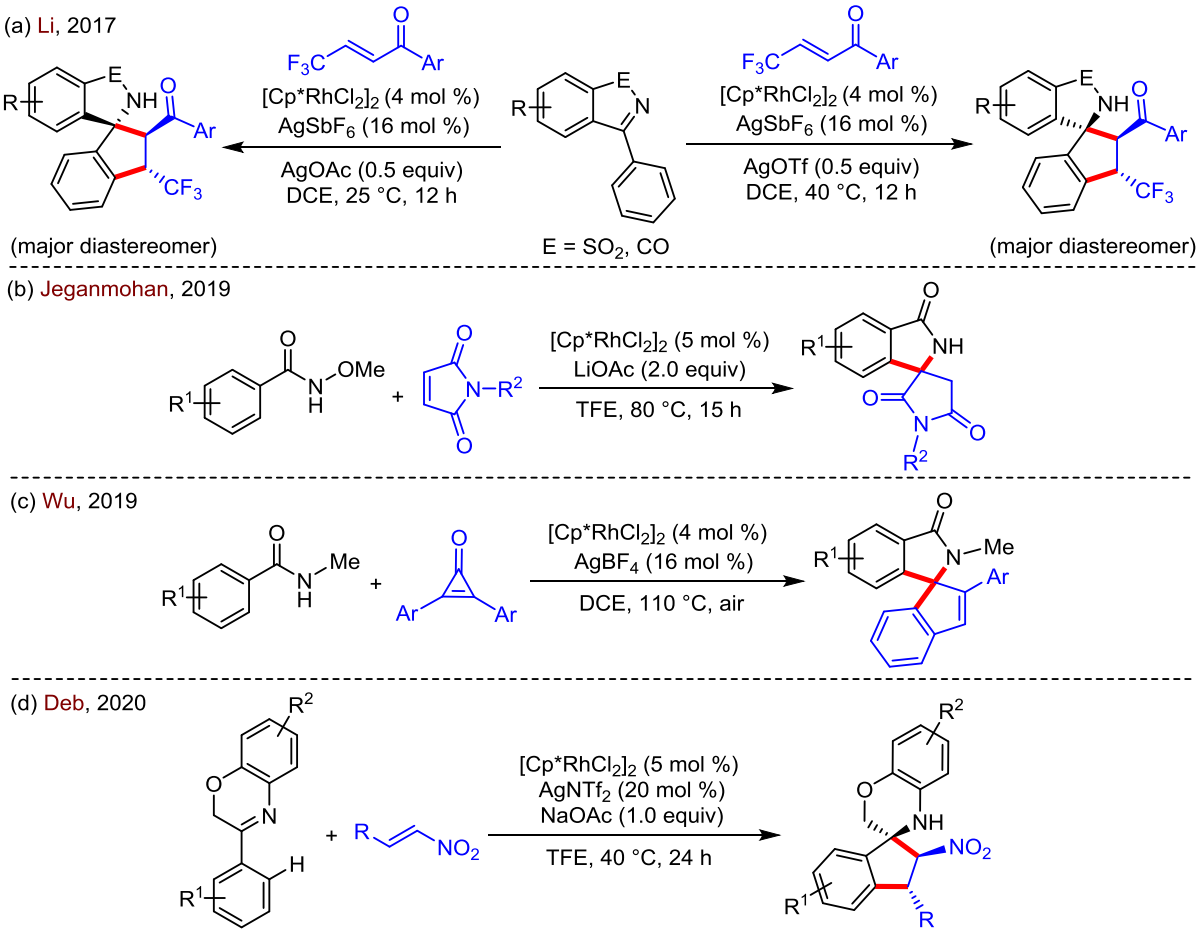

Scheme 5.2.3.12. Rh-catalyzed spirocyclization with activated alkenes.

In 2019, maleimides were applied thoughtfully by Jeganmohan *et al*. in a redox-neutral spiroannulation reaction with *N*-methoxy benzamides providing a set of isoindolinone spirosuccinimides with a wide substrate scope. Computational studies revealed that the *in situ* generated AcOH plays the pivotal role of N−OMe bond cleavage and reoxidation of Rh(I) to Rh(III) species (Scheme 5.2.3.12b).[73] Wu and co-workers described a rhodium-catalyzed redox-neutral cascade annulation exploring the reactivity of cyclopropenones to achieve spiroisoindolinones using benzamides (Scheme 5.2.3.12c).[74] α,β-unsaturated nitroolefins are value-added electrophilic synthon for 1,4-conjugate addition reactions and Diels−Alder reactions. In 2020, Deb group showcased a unique method for redox-neutral spirocyclization of benzoxazines with nitroolefins in excellent yields with high diastereoselectivity under Rh(III) catalysis (Scheme 5.2.3.12d).[75] This example was probably the first account of nitroalkenes being used as a capable unsaturated coupling partner in transition metal-catalyzed annulation chemistry for the synthesis of novel spirocycles containing a nitro group. In this context, another rhodium-catalyzed [3+2] spiroannulation reaction between cyclic ketimines and chalcones has been developed very recently which is a part of this thesis work and discussed in Chapter 6 in detail.

Another common class of annulation reaction is depicted in Scheme 5.2.3.13, i.e. [4+2] annulation has also been explored employing rhodium catalysis using various coupling partners.[76] In 2014, Marsden and co-workers illustrated that vinyl acetate can be used as a convenient acetylene equivalent, and upon reaction with *N*-(pivaloyloxy)benzamide it facilitated the synthesis of 3,4-unsubstituted isoquinolones and heteroaryl-fused pyridines under Rh(III) catalysis (Scheme 5.2.3.13a).[76a] Loh group in 2015, showed a Rh-catalyzed redox-neutral C–H functionalization/annulation cascade of *N*-carbamoyl indolines with internal alkynes to make a pyrroloquinoline framework. The plausible catalytic cycle showed that the reaction involves a sequential C–H/C–N cleavage from the indoline and urea motifs respectively for the rapid access to fused-ring pyrroloquinolinone derivatives via alkenylation/annulation pathway (Scheme 5.2.3.13b).[76b] On the other hand, ketenes were used as capable coupling partners for Rh-catalyzed redox-neutral [4+2] annulation with *O*-pivaloyl oximes (Scheme 5.2.3.13c).[76c] This methodology gives direct access to quarternary-carbon-stereocenter-containing (QCSC) isoquinolinones. *O*-pivaloyl oximes were again used in annulation reaction with acryloyl silanes for the synthesis of 3-acylsubstituted isoquinolines (Scheme 5.2.3.13d).[76d] Sulfoxonium ylides are another class of activated alkenes used in [4+2] annulation with pyrazolidinones under Rh(III) catalysis (Scheme 5.2.3.13e).[76e] Very recently,

Sakhuja group developed a method for the synthesis of hydroxyamino-decorated indazolo[1,2-a]cinnolines and phthalazino[2,3-a]cinnolines via reductive [4+2] annulation of 1-arylindazolones and 2-aryl-2,3-dihydrophthalazine-1,4-diones with α,β-unsaturated nitroolefins under Rh(III)-catalyzed conditions (Scheme 5.2.3.13f).[76f]

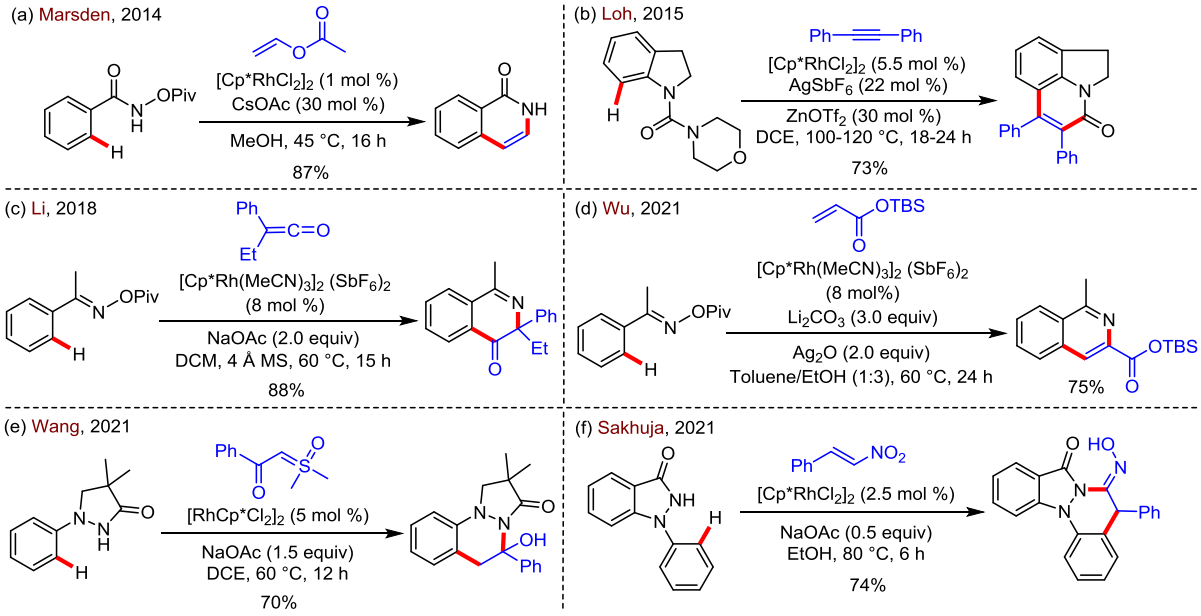

Scheme 5.2.3.13. Rh-catalyzed [4+2] annulation with activated alkenes.

Relatively less common [5+1] annulation has been very recently described by the group of Volla employing rhodium catalysis.[77] They reported a non-oxidative Rh(III)-catalyzed [5+1] vinylic C–H annulation reaction between 2-alkenylanilides and allenyl acetates furnishing 1,2-dihydroquinoline derivatives (Scheme 5.2.3.14a). Chromene derivatives could also be manufactured starting from 2-alkenylphenols. In this protocol, the allene serves as a one carbon source, and the acetate group associated with it facilitates the β-oxy elimination step of the reaction and also plays an important role in controlling the chemo- and regioselectivity of the reaction. Reddy *et al.* have studied Rh-catalyzed redox-neutral domino annulation reactions for the synthesis of fused heterocycles using different DG tethered substrates and coupling partners containing two unsaturated fragments.[78] In 2018, they delineated a cascade annulation methodology by coupling *N*-(pivaloyloxy)benzamides with 2-alkynyl aldehydes for the synthesis of 7-hydroxyisoindolo[2,1-*b*]isoquinolin-5(7*H*)-ones (Scheme 5.2.3.14a).[78a] The reaction pathway follows the steps of sequential alkyne insertion and then addition of the amide nitrogen to the aldehyde, thereby generating products with an aminal functional group which could act as a useful handle for further derivatizations.

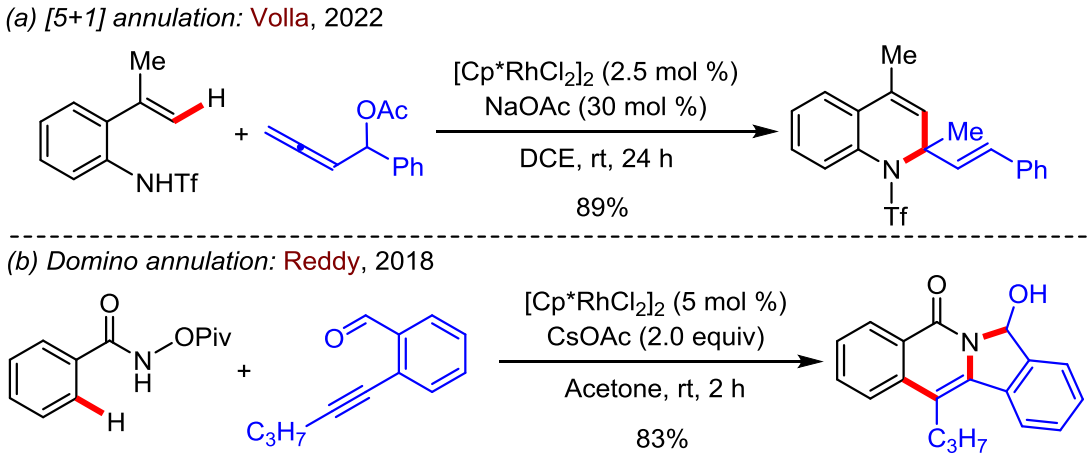

Scheme 5.2.3.14. Rh-catalyzed [5+1] and cascade annulation reactions.

Outside of these notable works, there are several other important contributions by different research groups on Rh-catalyzed redox-neutral annulation strategy using a wide variety of directing group attached substrates and capable coupling partners, like dioxazolones, diazo compounds, propargyl alcohols/acetates, gem-difluoro alkenes, allyl alcohols, etc. giving access to biologically relevant (spiro)cyclic components of different ring sizes.[79]

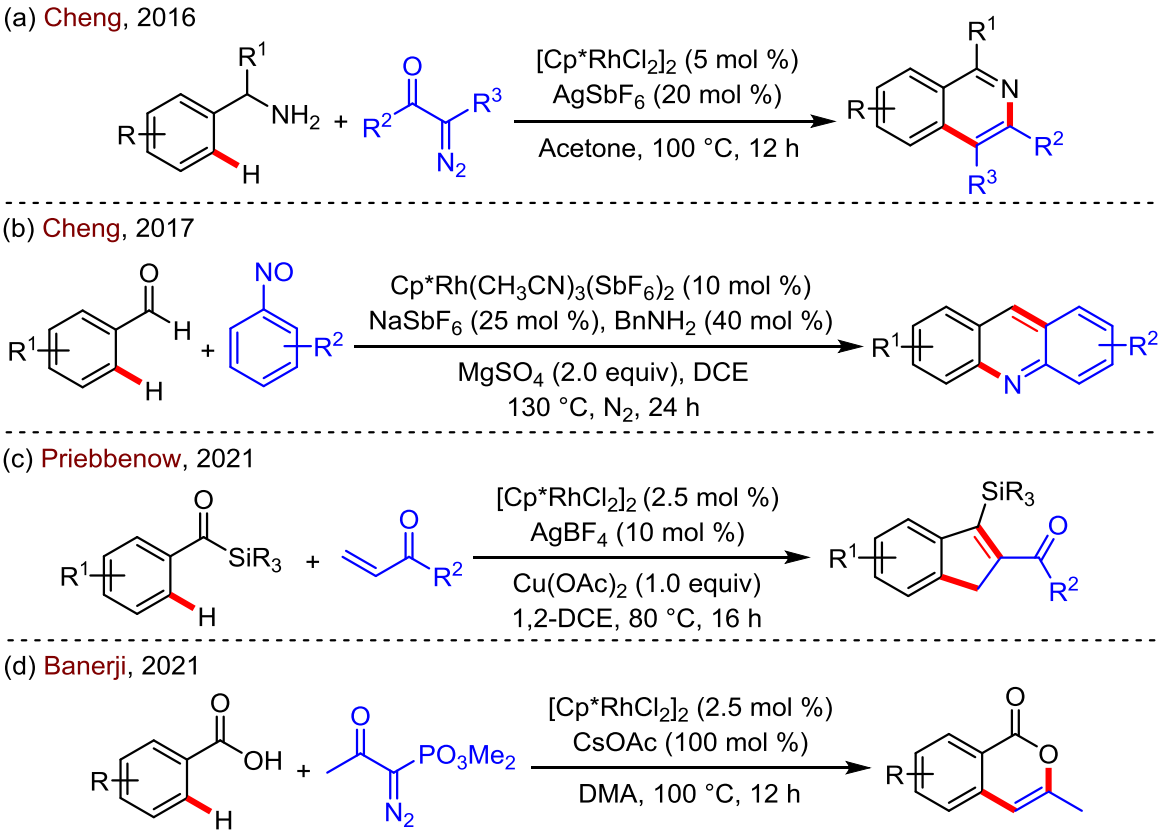

Scheme 5.2.3.15. Selected examples of other diverse DGs in redox-neutral annulations.

Also, other common functional groups (aldehydes, benzylamines, acylsilanes, and carboxylic acids) acting as directing groups, have been applied in Rh(III)-catalyzed redox-neutral annulation reactions with appropriate coupling partners by the groups of Cheng, Priebbenow, and Banerji (Scheme 5.2.3.15).[80] Another type of Rh(III)-catalyzed annulation reaction recently explored by Zhang *et al*. is the three-component intermolecular cyclization reaction involving acrylic acids, formaldehyde, and malonates to afford cyclopentenones in one-pot via vinylic C–H activation.[81]

➢ **Photochemical and Electrochemical annulation**

In the last few years, photoredox catalysis has come to the forefront replacing traditional approaches owing to its environmentally benign nature.[82] Traditional approaches like oxidative annulations make use of external oxidants and harsh conditions, whereas the redox-neutral technique remains specific to some functional directed molecules bearing an internal oxidant handle. These limitations somewhat diminish the general applicability of these reactions for the synthesis of varieties of functionalized molecules. As a result, to overcome these drawbacks and invent a more sustainable approach, various research groups have meticulously employed photoredox catalysis, either to activate the substrate or to regenerate the active catalytic species. In this realm, in 2019, Rueping group disclosed a photoredox/Rh(III)-catalyzed annulation strategy for synthesizing nitrogen-containing heterocycles starting from *N*-acetanilides and alkynes using a Ru-based photocatalyst under visible light conditions (Scheme 5.2.3.16).[83]

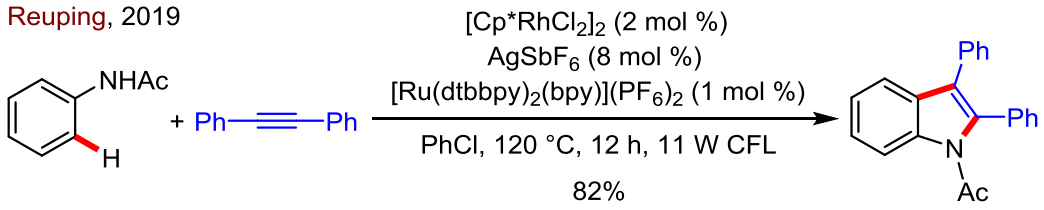

Scheme 5.2.3.16. Annulation through Rh(III)/photoredox catalysis.

More recently, electrochemistry has come to the limelight in the field of transition metal-catalyzed C–H activation and opened the door for another greener and environmentally friendly approach for direct C–H functionalization chemistry, where sustainable electrical energy/electricity is replacing the use of stoichiometric toxic external oxidants in traditional approaches.[84] In this context, in 2018, Ackermann and co-workers developed the first rhodium-catalyzed cross-dehydrogenative two-fold C–H/C–H functionalization followed by annulation by electrocatalysis for the synthesis of cyclic esters and amides without using any hazardous

external chemical oxidants (Scheme 5.2.3.17a).[85] Next year, they reported a metalaelectro-catalyzed C–H activation followed by annulation to synthesize isoquinoline derivatives from imidates and alkynes under Rh(III) catalysis using an electro-flow cell composed of porous graphite felt anode (Scheme 5.2.3.17b).[86] Following this, other rhoda-electrocatalyzed methodologies for the synthesis of heterocyclic scaffolds have also been developed by them and Mei group.[87]

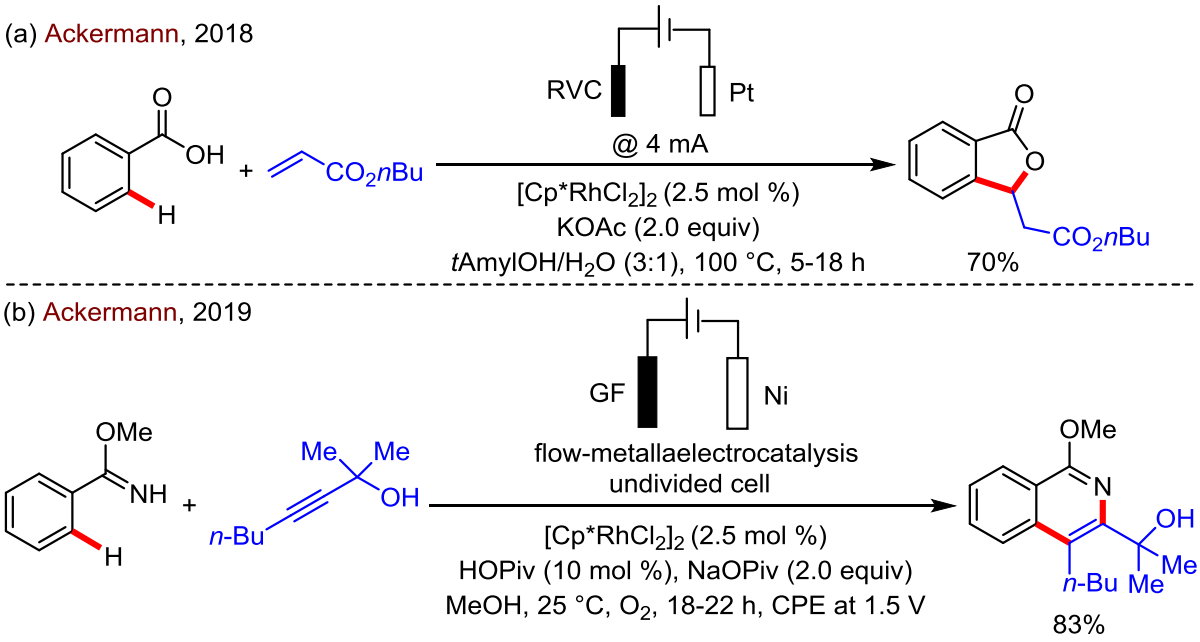

Scheme 5.2.3.17. Rhoda-electrocatalyzed annulation reactions.

➢ Enantioselective annulation

Several research groups have been engaged in developing methods for the enantioselective version of Rh(III)-catalyzed C–H bond functionalization followed by cyclization for the synthesis of enantioenriched cyclic molecules.[48b] The mainstay of developing chiral versions is to manipulate the cyclopentadienyl unit which stores the chiral information of the catalyst. With this, an efficient set of flexible and adjustable chiral Cp^x ligands need to be devised which could function as powerful navigating ligands for the application of Rh(III)-catalyzed enantioselective annulation reactions. To achieve the enantioselectivity, various chiral derivatives of cyclopentadienyl (Cp) and pentamethylcyclopentadienyl (Cp*) ligands have been designed and widely used by several research groups to incorporate asymmetric induction in annulation reactions (Figure 5.2.3.1).[88] In this regard, a wide array of different DG containing substrates have been coupled in an enantioselective fashion with various type of unsaturated coupling partners generating chiral heterocyclic or carbocyclic frameworks.

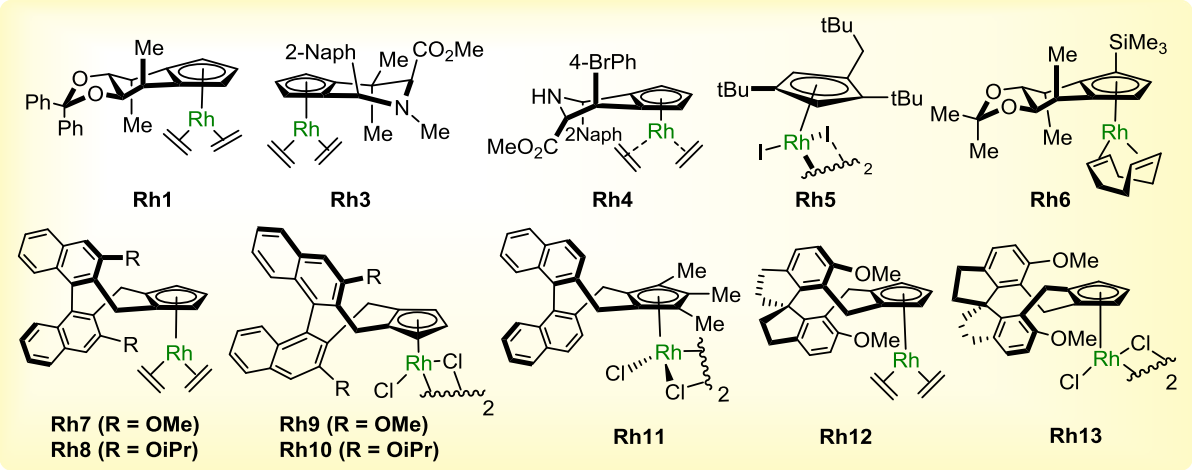

Figure 5.2.3.1. Representative examples of chiral cyclopentadienyl based Rh catalysts.

In 2012, concurrently Ward and Rovis, and Cramer groups independently reported the pioneering works on hydroxamic acid derivative directed C–H activation/annulation with different olefins for the enantioselective synthesis of dihydroisoquinolones using a new class of bifunctional artificial metalloenzyme streptavidin and biotinylated rhodium(III) complex **Rh2** catalyst[89] and chiral Cp containing Rh-complex **Rh1** catalyst[90] respectively (Scheme 5.2.3.18). This transformation then became a standard reaction to screen the activity of different chiral cyclopentadienyl based Rh-complexes **Rh3**, **Rh5**, and **Rh6** to achieve the enantioselectivity (Scheme 5.2.3.18).[91] These findings opened a new area of enantioselective C–H activation/annulation reaction employing chiral Cp containing Rh complexes (mainly **Rh1-Rh13** and others) for the synthesis of structurally divergent chiral (spiro)cycles.[92]

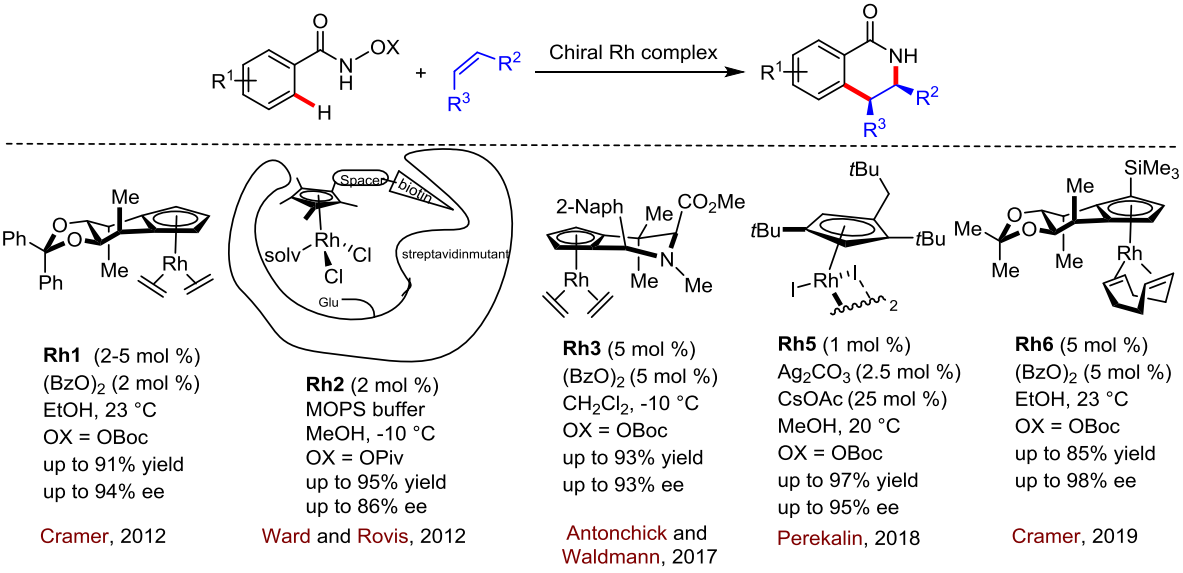

Scheme 5.2.3.18. Early examples of chiral Cp-based Rh-catalyzed enantioselective annulation.

Over the past few years, employing these Rh catalysts **Rh1-Rh13**, various enantioselective methods for the synthesis of chiral spirocycles such as spiroenones (Scheme 5.2.3.19a),[92a] spirosultams (Scheme 5.2.3.19b),[92b] and spiropyrazolones (Scheme 5.2.3.19c, 5.2.3.19d)[92c,f] via [3+2] annulation with alkynes as coupling partner; spironitrones (Scheme 5.2.3.19e)[92h] and spiroimines (Scheme 5.2.3.19f)[92m] via [4+1] annulation with diazo coupling partner, have been developed by the groups of You, Antonchick and Waldmann, Cramer, and Li. Very recently, Li *et al.* again used alkynes in an asymmetric [3+2] annulation fashion with arylnitrones where the nitrone group acts as an electrophilic directing group.[92n] Diverse axially and centrally chiral indenes/indenones were synthesized with high yields and excellent enantioselectivity.

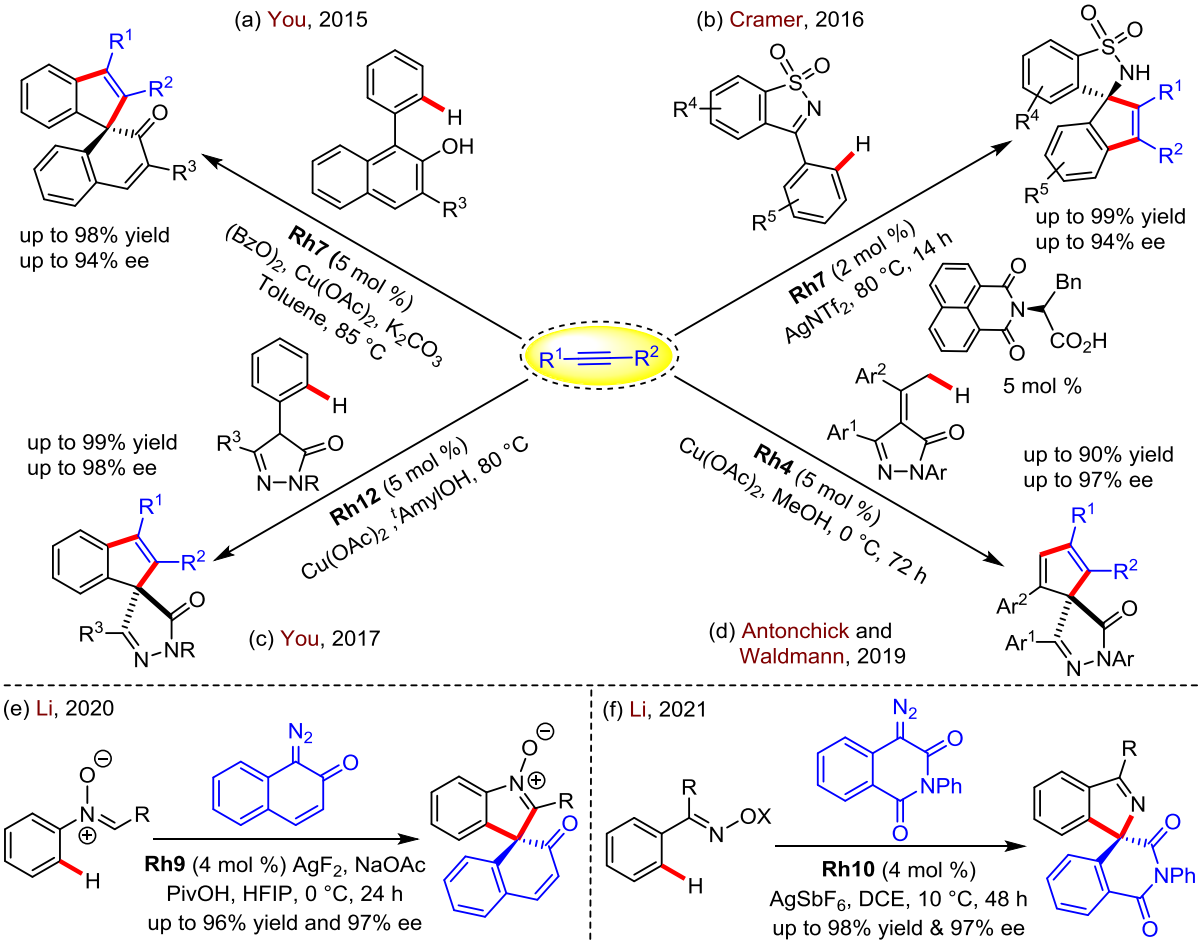

Scheme 5.2.3.19. Representative enantioselective Rh-catalyzed spiroannulation reactions.

Among other types of [4+2], [3+2] and [4+1] annulation reactions, chiral tricyclic hydrophenanthridinones (Scheme 5.2.3.20a),[92i] chiral 3-substituted phthalides (Scheme 5.2.3.20b),[92l] and chiral isoindolinones (Scheme 5.2.3.20c, 5.2.3.20d)[92j,k] have been synthesized employing chiral CpRh(III)-catalyzed enantioselective C−H activation/annulation strategies by Wang, You and Li groups, independently.

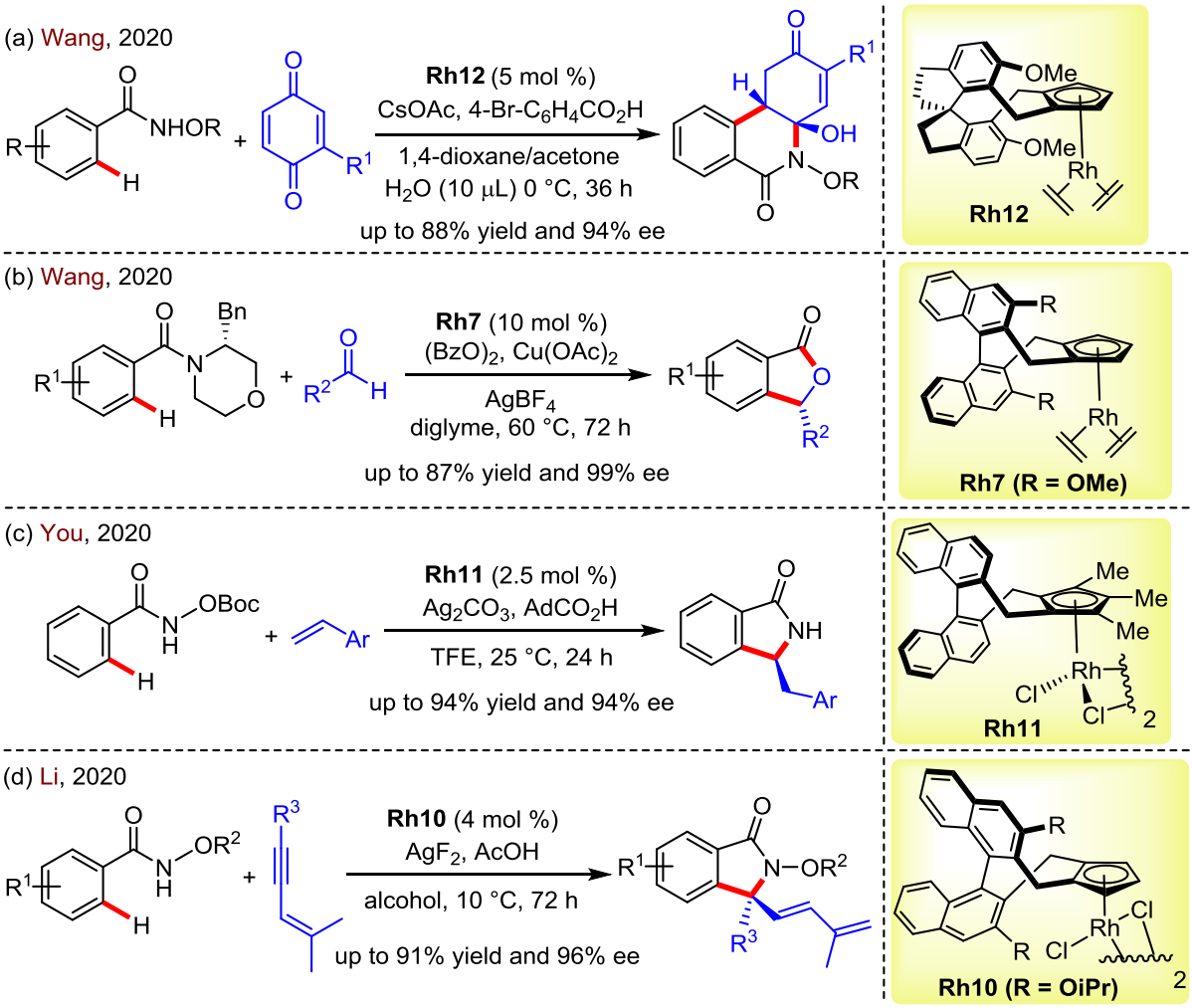

Scheme 5.2.3.20. Selected examples of enantioselective [4+2], [3+2] and [4+1] annulation.

5.3. Iridium-Catalyzed C–H Activation

Iridium is a rare precious metal and its outer electronic structure allow it to exhibit a wide range of oxidation states. In the past decades, there has been a rapid surge in the use of iridium complexes as versatile catalysts in a variety of reactions, *viz*. asymmetric hydrogen transfer reactions, oxidation, reductive amination, allylic substitutions, borylation, photoredox and electrocatalytic reactions. As a result, they have been applied enormously in the synthesis of natural products and biologically active molecules.[93] In the field of C–H bond functionalization, the advancement of iridium catalysis has been progressing at a rather slower rate. Although Ir(III) complexes have shown great reactivity for stoichiometric reactions towards C–H oxidative addition, but the high stability of iridacycle intermediates generated from C–H activation and the difficulty in the reductive elimination steps for getting the desired

product from the internal oxidant of iridacycle might be the major issues associated with the less number of reports on Ir-catalyzed C–H functionalization reactions.

In 1968, Maitlis successfully synthesized and characterized high-valent $[Cp^*IrCl_2]_2$ and $[Cp^*RhCl_2]_2$ complexes.[94] Since these pioneering works, there has been great research interest in exercising the reactivity of these complexes in a plethora of reactions.[12a,95] Utilizing the robust nature of Cp*-based iridium catalysts, C–H functionalization reactions have proven an efficient tool for delivering various heteroatom containing functionalized molecules (Scheme 5.3.1). After a decade, in the early 1980s, Bergman's landmark work[96] on alkane C–H activation using Ir(III) complex inspired a generation of chemists all over the world that C–H functionalization can indeed be performed using stoichiometric high-valent Ir(III) complexes.[97] Although stoichiometric C–H bond transformations came to the ascendency using half-sandwich cyclometalated Cp*Ir(III) complexes, but owing to their high stability and sensitivity towards oxidants, their applications in catalytic C–H functionalization reactions advanced relatively at a slower rate.

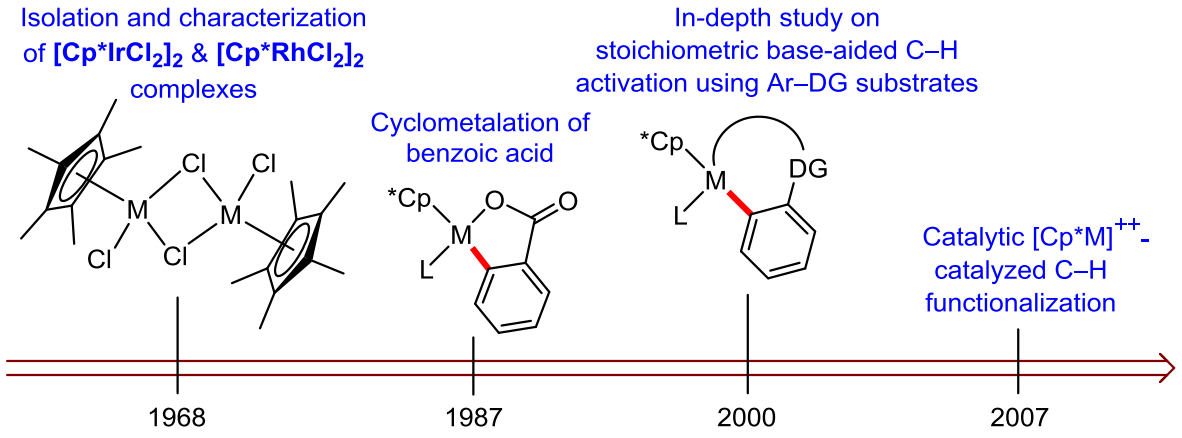

Scheme 5.3.1. Developments of [Cp*M] (M = Rh, Ir) complexes in organic synthesis.

It was found that in the presence of heteroatom containing directing group attached arenes or aliphatic scaffolds with polar unsaturated C=N or C=O bonds, Cp*Ir(III) complexes could form five-membered iridacycles through heteroatom chelation with the proximal sp^2 or sp^3 C–H bonds thereby initiating their activation assisted by a suitable base (Scheme 5.3.2a).[98] These five-membered iridacycles fabricated from a stoichiometric C–H activation could then undergo ready insertion with diverse reaction partners like alkynes, olefins, carbonyl groups, diazo compounds, heteroatom coupling partners, etc. demonstrating rich chemical transformations (Scheme 5.3.2b). Encouraged by the successes of Bergman's seminal works, thereafter several

reports on directing group assisted C–H functionalization reactions employing cationic Cp*Ir(III) complexes and other high-valent Ir(III) salts have been disclosed.[4g,98d,e,99] The C–H functionalization reactions are classified into few sub-categories- C–C bond formation, C–X (X = heteroatom) bond formation, annulation, and electrochemical reactions discussed below.

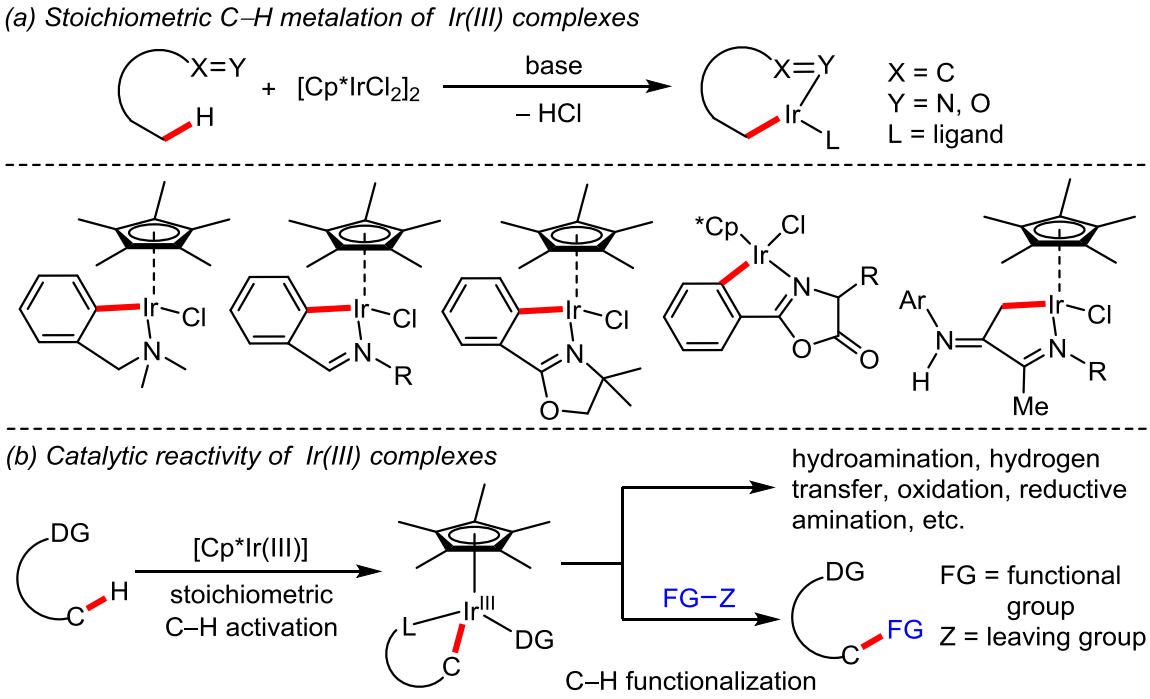

Scheme 5.3.2. Modes of C–H metalation and functionalization by Ir(III) complexes.

5.3.1. C–C Bond Formation

C–C bond formation remains one of the most fundamental reactions in synthetic organic chemistry. Advancing from the widely applied Heck, Suzuki, Negishi, Tsuji-Trost, Stille coupling reactions, sustainable methodologies using transition metal catalyzed C–H activation strategy have gained tremendous attraction in recent times. Iridium-catalyzed C–H functionalization reactions have also formed an integral part of this journey for C–C bond forming reactions. Among them, direct C–H arylation and heteroarylation reactions utilizing directing group assistance harnessing iridium catalysis has played a crucial part in recent years.[100] Different arylating agents have been used for this purpose. Some of these examples are depicted in Scheme 5.3.1.1.

In 2013, Miura group disclosed an intramolecular arylation/cyclization reaction of triarylmethanols in presence of Cp*Ir(III) salts and copper oxidant with the aid of hydroxy DG to afford a series of fluorene molecules (Scheme 5.3.1.1a).[100a] Two years later, Chang and co-

workers demonstrated a procedure for Ir(III)-catalyzed direct arylation of aromatic as well as olefinic amides using aryldiazonium tetrafluoroborates, which performed the dual roles of aryl source and oxidant via C–N_2 bond cleavage, thus rendering the reaction to proceed under mild and external oxidant free conditions (Scheme 5.3.1.1b).[100b] In the same year, Gooβen *et al.* devised a similar protocol for *ortho* arylation of benzoic acids with arenediazonium salts to furnish diaryl-2-carboxylates (Scheme 5.3.1.1c).[100c] Quinone diazides were also used as capable coupling partners for direct arylation of diverse directing arenes.[100d] In 2018, Chang group devised an Ir-catalyzed *ortho* arylation of diverse arenes with arylsiloxanes as a suitable aryl group source (Scheme 5.3.1.1d).[100e] Aliphatic C–H arylation was also achieved under iridium catalysis by Shi group employing diaryliodonium triflate salts (Scheme 5.3.1.1e).[100g] Mechanistic investigation through DFT studies showed that the sp^3 C–H activation occurs via a triflate-involved CMD process and a favourable oxidation of Ir(III) to Ir(V) takes place when a bistriflimide is contained in the diaryliodonium salt. Along this line, another methodology for DG aided direct *ortho* C–H arylation employing iridium catalysis was developed which is a part of this thesis work, discussed in detail in Chapter 7.

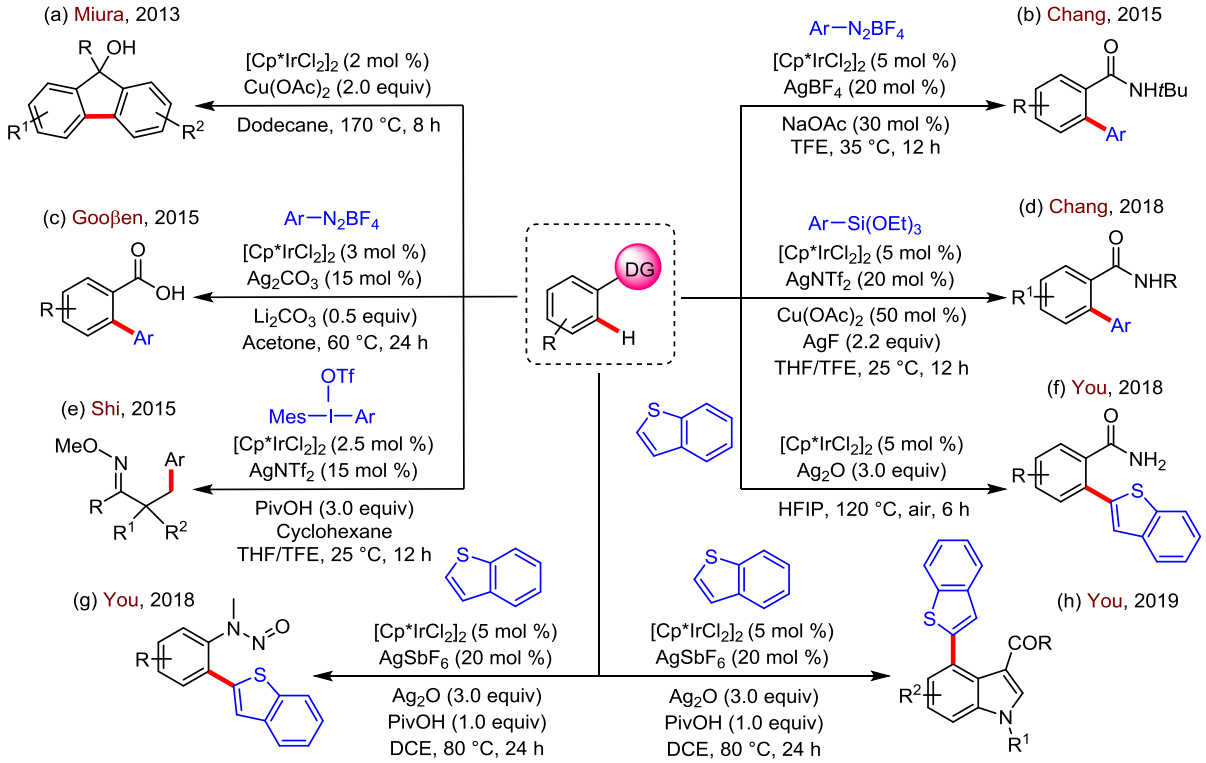

Scheme 5.3.1.1. Representative examples of Ir-catalyzed C–H (hetero)arylation reaction.

Heteroarylation reactions have also been discovered in this context, when You and co-workers showcased an Ir-catalyzed Ar–H/Ar–H cross-coupling reaction between primary benzamides

and thiophenes giving access to (2-thienyl)benzamides. (Scheme 5.3.1.1f).[100h] Simultaneously, they also developed a protocol for oxidative *ortho* C–H heteroarylation of up to 16 directing group attached arenes with thiophene derivatives via cross-dehydrogenative coupling (Scheme 5.3.1.1g).[100i] In case of olefinic amides, it was observed that heteroarylation occurred leading to *Z*-selective coupled products. Following year, the same group reported a Cp*Ir(III)-catalyzed regiodivergent C2 and C4 heteroarylation of 3-pivaloyl indoles with diverse heteroarenes (Scheme 5.3.1.1h).[100j] The choice of oxidants played the key role in altering the reactivity, where, on using $Cu(OAc)_2.H_2O$ as oxidant, C2 selectivity was observed via a concerted metalation-deprotonation (CMD) mechanism, whereas Ag_2O as oxidant gave C4 selectivity via a trimolecular electrophilic substitution (S_E3) pathway.

As a representative example, the mechanism of the iridium-catalyzed arylation of benzoic acids by Gooβen is outlined in Scheme 5.3.1.2. The mechanistic experiments performed in this reaction in presence of radical scavengers suggested the involvement of a single-electron transfer mechanism.

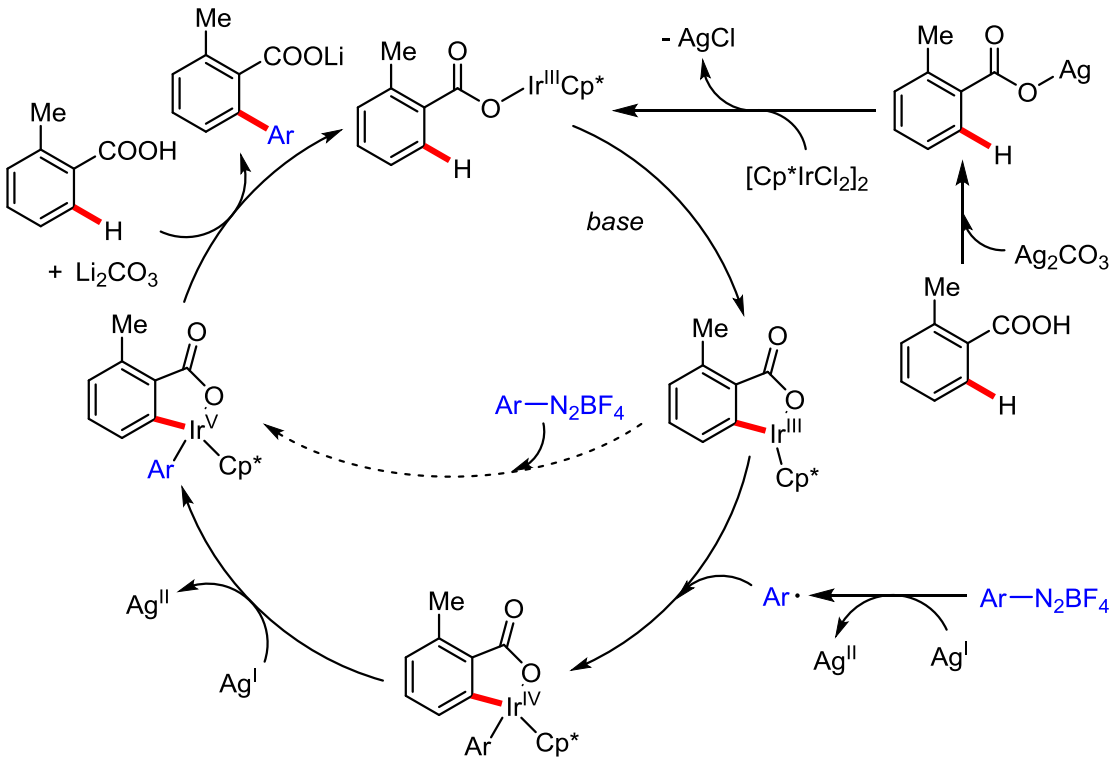

Scheme 5.3.1.2. Plausible mechanism of Ir-catalyzed C–H arylation of carboxylic acids.

The $[Cp^*IrCl_2]_2$ dimer is cleaved in the presence of silver salt and carboxylic acid ligand to generate an active species. Next, in presence of base, a cyclometalated Ir(III) complex is generated or a direct conversion to Ir(V) species may take place by oxidative addition of the

diazonium salt. The mechanistic experiments showed that the oxidation of the iridium species might be a stepwise phenomenon rather than a direct process which is rather difficult. Finally, reductive elimination and salt metathesis with another benzoic acid substrate delivers the biaryl product and regenerates the Ir(III) species to continue the catalytic cycle.

Moving to direct C–H alkenylation and alkylation with appropriate coupling partners, iridium catalysis has shown its potency outlined in Scheme 5.3.1.3. In 2015, Chang *et al*. showcased a strategy for Cp*Ir(III)-catalyzed regioselective alkenylation and alkylation reactions with activated alkenes like acrylates by switching the directing groups, where amide DG furnished alkenylation and 2-pyridine DG provided oxidative C–H alkylation (Scheme 5.3.1.3a).[101] Unactivated olefins like simple styrenes were applied in the synthesis of 7-alkenylindolines from *N*-carbonyl or carbamoyl indolines employing Ir(III) catalysis in combination with catalytic silver and copper additives (Scheme 5.3.1.3b).[102] Following this, other iridium-catalyzed alkenylation reactions have been performed judiciously using alkynes, vinyl phosphonates, and vinyl sulfones as capable coupling partners.[103]

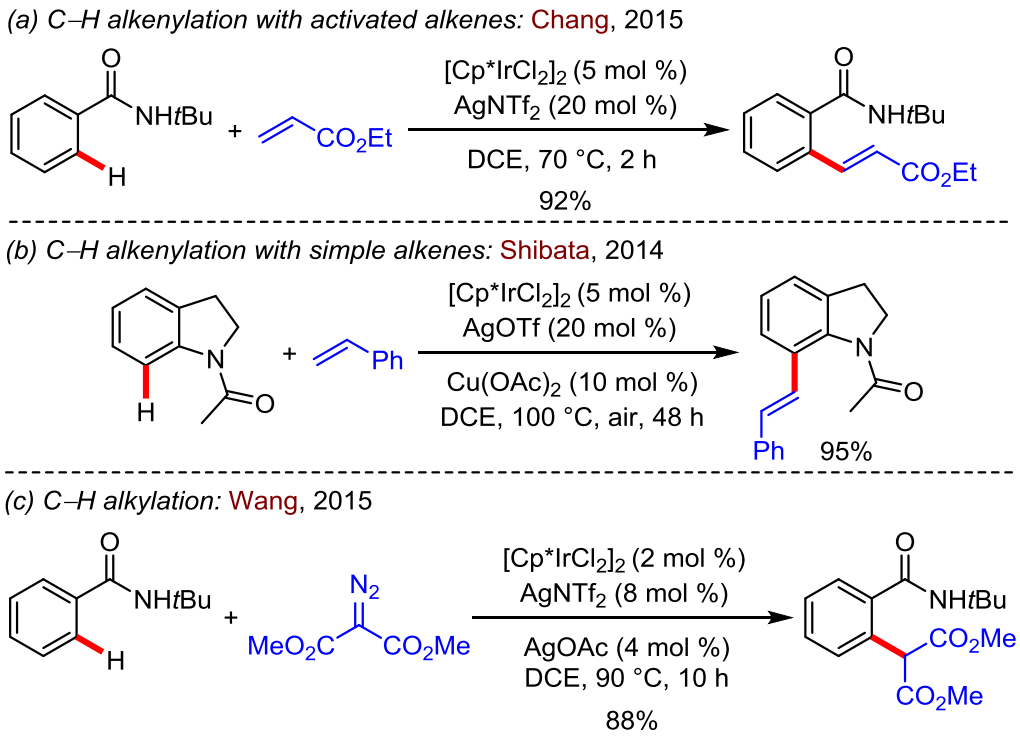

Scheme 5.3.1.3. Iridium-catalyzed C–H alkenylation and alkylation.

In 2015, Wang and co-workers incorporated diazomalonates through a metal carbenoid migratory insertion for *ortho* C–H alkylation of carbamoyl group directing (hetero)arenes under iridium catalysis (Scheme 5.3.1.3c).[104] Sorensen and Wang groups then devised new

Cp*Ir(III)-catalyzed alkylation protocols using alkyl boron reagents and maleimides respectively.[105] Very recently, diverse α-diazo compounds were again utilized by Kapur group in direct C(3)–H alkylation of *N*-acetyl-1,2-dihydroisoquinolines to create a series of substituted isoquinoline derivatives.[106] In 2019, Zhong *et al.* reported Ir-catalyzed direct C–H allylation of acrylamides with conjugated dienes.[107]

C–H alkynylation employing iridium catalysis was first explored by Li group in 2014, when they disclosed a Ir(III)-catalyzed direct C–H alkynylation reaction of different chelating arenes and heteroarenes under relatively mild conditions (Scheme 5.3.1.4).[19] They used electrophilic hypervalent iodine-alkyne reagent (TIPS-EBX) as a suitable alkynylating reagent for this purpose. After this notable work, several other groups have contributed immensely in C–H alkynylation reactions under iridium catalysis with different class of alkynylating agents like alkynyl bromides as well as terminal alkynes.[108]

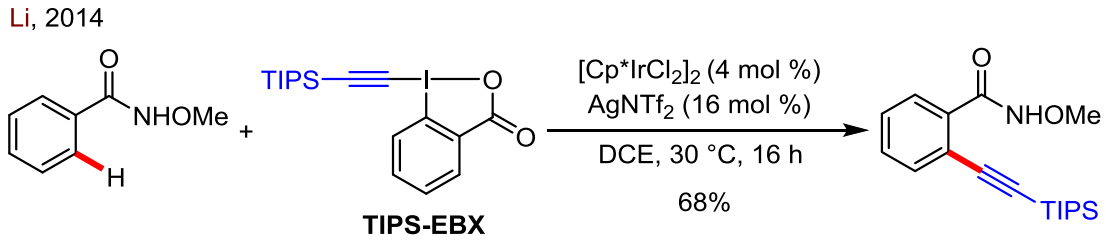

Scheme 5.3.1.4. Iridium-catalyzed C–H alkynylation.

5.3.2. C–X Bond Formation

The wide utility of Carbon–Heteroatom (C–X) bond containing molecules, like C–N, C–Z (Z = halogen, *viz*. Cl, Br, I), C–S, etc. in various fields of science has led to its creation via directing group aided iridium-catalyzed C–H activation also. In this section, some of the noteworthy reports on C–N, C–Z, C–S, and other C–X bond formation reactions are discussed in a brief manner.

Among these, direct C–N bond forming reactions have been mostly studied employing Cp*Ir(III)-catalyzed C–H activation/functionalization.[109] There are many improvements on Ir-catalyzed C–H amidation/amination methodologies over the existing traditional protocols, predominantly on account of its increased selectivity. The important factors associated with these are the relatively stable half-sandwich iridacycle complexes and the incompatibility of external oxidants, and thus the choice of aminating reagent plays a crucial role. Many different

kinds of amidating/aminating sources have been exploited for developing C–N bond forming reactions using iridium catalysis (Scheme 5.3.2.1).[110]

In 2013, Chang group demonstrated the first Ir(III)-catalyzed direct regio- and stereoselective C–H amidation of aromatic as well as alkenyl amides with a variety of acyl azides as nitrogen source under mild reaction conditions (Scheme 5.3.2.1a).[110a] The reaction conditions were also environmentally benign since it did not require any external oxidants and molecular nitrogen was simply released as a single byproduct. Since then, Chang and co-workers have worked tremendously on Ir-catalyzed C–H functionalization, especially, C–N bond formation. Following year, they devised a strategy for the synthesis of phosphoramidates by C–H amidation of different DG-containing substrates with phosphoryl azides under Ir(III)-catalyzed conditions (Scheme 5.3.2.1b).[110b] In the same year, they reported an iridium-catalyzed remote C8-amidation of quinoline-*N*-oxides with sulfonyl azides, whose regioselectivity was ascertained from the formation of *N*-oxide-chelated iridacycle (Scheme 5.3.2.1c).[110c] Concurrently, they developed a protocol for C–H amidation of weakly coordinating ketones and esters with sulfonyl azides using a combination of $[Cp^*IrCl_2]_2$/AcOH/Li_2CO_3 catalytic system (Scheme 5.3.2.1d).[110d] The same group again delineated a methodology for coupling different directing arenes with *N*-substituted hydroxylamines like aryloxy- or alkyloxycarbamates employing iridium catalysis to furnish *N*-substituted arylamine products under mild reaction conditions (Scheme 5.3.2.1e).[110e] Chang *et al.* delivered a room temperature direct C–H amination reaction between benzamides and anilines where an iridium catalyst was used in combination with external oxidant (Scheme 5.3.2.1f).[110f]

In 2015, Bolm and co-workers reported an Ir-catalyzed *ortho* amidation of aroylsilanes with sulfonyl azides in very quick reaction times (Scheme 5.3.2.1g).[110g] The products could be further transformed to *N*-heterocycles after proper functionalization and treatment under photochemical or thermal conditions. Chang group utilized the weak coordinating nature of keto functionality for Ir(III)-catalyzed room temperature regioselective C7-amidation of *N*-substituted indoles with sulfonyl azides to generate biologically important 7-aminoindoles on deprotection (Scheme 5.3.2.1h).[110h] Shi *et al.* accomplished an Ir-catalyzed direct and selective amidation of aldehydes with sulfonyl azides using various anilines as a catalytic or stoichiometric directing group (Scheme 5.3.2.1i).[110i] In 2017, You group devised a strategy for highly efficient C4-amidation of C3-functionalized indoles with sulfonyl azides under iridium-catalyzed mild reaction conditions (Scheme 5.3.2.1j).[110j]

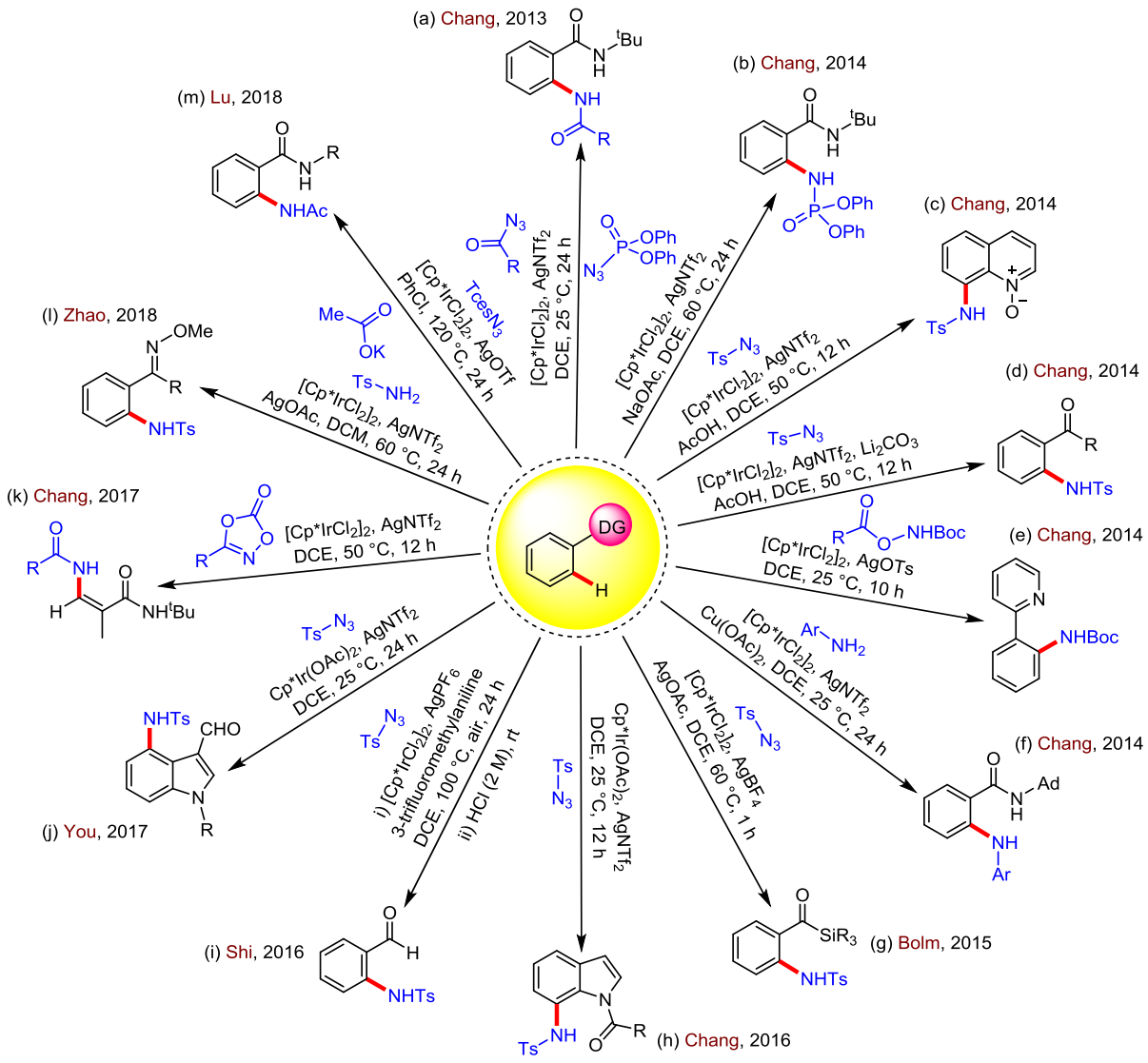

Scheme 5.3.2.1. Representative examples of Ir-catalyzed C–N bond formation.

In the same year, Chang and co-workers discovered a new amidating reagent in the form of 1,4,2-dioxazol-5-one as an efficient source for amide functionality which is much more reactive with iridacyclic intermediates than previously used acyl azides on account of its easy decarboxylation. They reported an Ir-catalyzed direct C–H amidation reaction of a broad range of diversely directed aromatic as well as olefinic substrates with dioxazolones under relatively mild reaction conditions (Scheme 5.3.2.1k).[110k] Zhao group applied both aromatic and aliphatic sulfonamides as efficient nitrogen sources for *ortho* sp^2 C–H amidation of *O*-methyl ketoximes via Ir(III)-catalyzed C–H activation (Scheme 5.3.2.1l).[110l] Lu *et al.* reported an iridium-catalyzed sequential aryl and amidyl C–N bond formation reaction using trichloroethoxysulfonyl azide ($TcesN_3$) as a bifunctional nitrogen source (Scheme 5.3.2.1m).[110m] This reaction was applicable to a variety of readily available benzamides and

carboxylates and did not require any external oxidants or coupling reagents. Apart from these representative examples, a plethora of other Ir-catalyzed C(sp^2)–H amidation/amination reactions have also been disclosed till date.[111]

More stringent sp^3 C–H amidation was achieved by Chang group in 2014, where they described an iridium-catalyzed direct amidation of unactivated aliphatic C–H bonds with sulfonyl and acyl azides (Scheme 5.3.2.2).[112] Late-stage functionalization was also exemplified using this protocol. In 2016, Zeng *et al.* reported a novel Ir(III)-catalyzed sulfonylamidation of secondary sp^3 C–H bonds with sulfonyl azides using the assistance of a *N*,*N*-bis-chelating ligand in iridium-nitrene insertion to the remote aliphatic C–H bond to eventually give access to structurally diverse γ-sulfonamido-substituted aliphatic amines.[113]

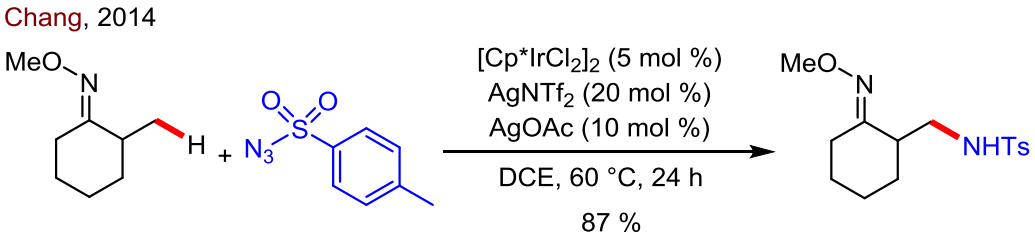

Scheme 5.3.2.2. Iridium-catalyzed sp^3 C–H amidation.

Apart from C–N bond forming reactions, a relatively fewer number of examples on iridium-catalyzed C–Z,[114] C–S,[115] C–B,[116] and C–Si[117] bond formation have also been disclosed by different research groups, out of which one representative example of each is depicted in Scheme 5.3.2.3. In 2017, Nicholls and co-workers reported the first mono-protected L-amino acid (L-MPAA) accelerated Ir-catalyzed *ortho* selective C–H halogenation protocol of (hetero)anilides using *N*-halosuccinimides/phthalimides as halogen source at room temperature employing very low catalyst loadings (Scheme 5.3.2.3a).[114a] Very recently, the same group demonstrated an Ir(III)-catalyzed decarbonylative bis-arylsulfenylation strategy at C2 and C4 positions of indoles bearing a traceless adamantoyl directing group at C3-position using disulfides (Scheme 5.3.2.3b).[115] In terms of direct borylation reactions, iridium catalysis has been well studied, when Hartwig *et al.* in 2008, reported a study on the direct *ortho* C–H borylation of diverse arenes with good regioselectivity using hydrosilanes as directing group employing $[Ir(cod)Cl]_2$ as catalyst and bis(pinacolato)diboron (B_2Pin_2)/pinacolborane (HBPin) combination as boron source (Scheme 5.3.2.3c).[116b] In early 2016, Chattopadhyay group demonstrated a methodology for *ortho* and *meta* selective C–H borylation of aromatic

aldehydes under ligand enabled iridium catalysis.[116k] They envisaged that on employing *tert*-butylamine as a traceless DG, *ortho* borylation occurs, whereas, meta borylation takes place via an electrostatic interaction and secondary interaction between the ligand of the catalyst and the substrate. Ir-catalyzed C–Si bond formation has also been explored. In 2013, Mashima and co-workers devised a hemilabile Ir(carbene)-catalyzed direct dehydrogenative C–H silylation of pyridyl and iminyl arenes with triethylsilanes yielding mono *ortho* silylated products selectively (Scheme 5.3.2.3d).[117b]

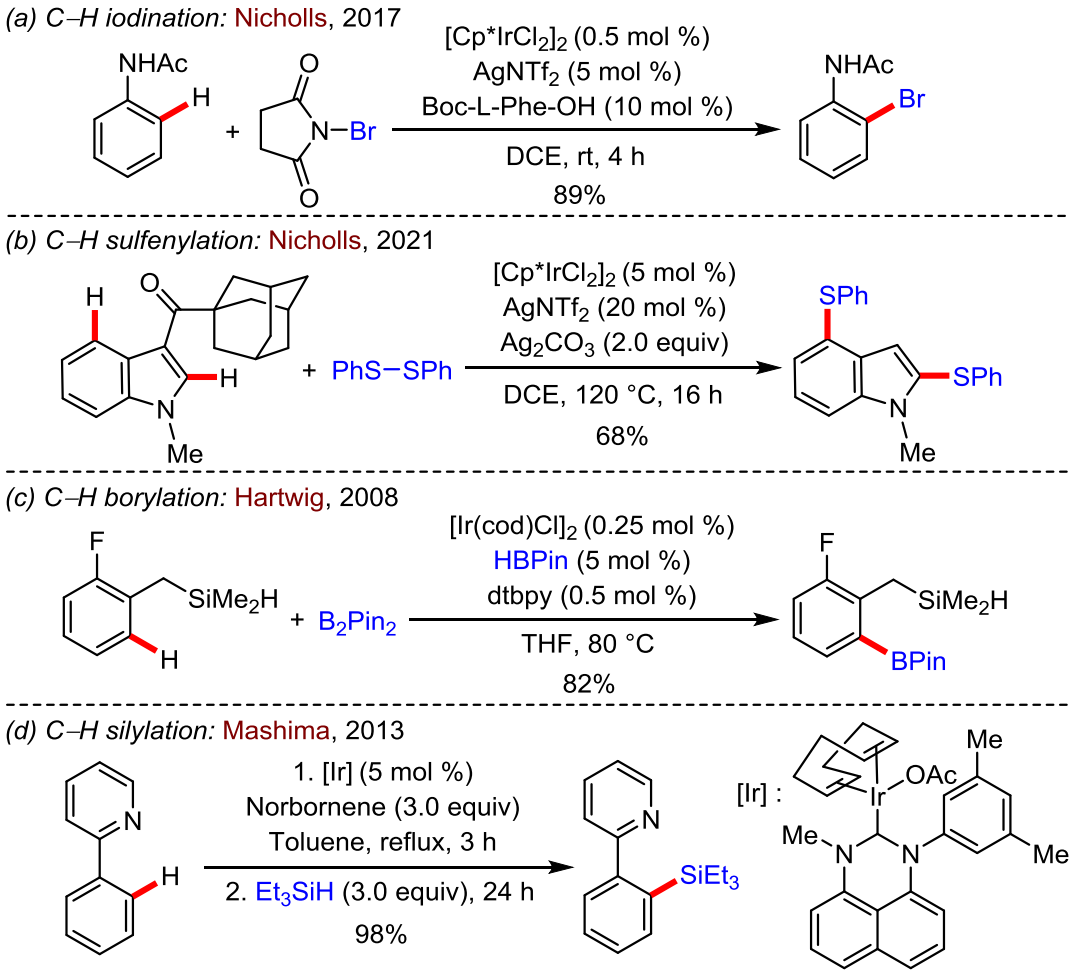

Scheme 5.3.2.3. Ir-catalyzed C–Z, C–S, C–B, and C–Si bond formation.

5.3.3. C–H Annulation Reaction

Iridium-catalyzed C–H activation/annulation reactions are also a well-explored route for constructing (spiro)annulated structures in highly efficient manner,[11,48e,g,100a,118] also in an enantioselective manner.[119] Both redox-neutral and oxidative conditions have been applied in this context for the creation of unique cyclic motifs using a combination of the different directing group attached substrates and varied coupling partners. Cp*Ir(III) catalysts show

different reactivity from its counterparts Cp*Rh(III) and Cp*Co(III) catalysts, owing to the possible stability of the iridacycle intermediates and the incompatibility of an internal oxidant with an iridacycle, thus providing complementary choices in new C–H activation reactions. Some of the representative C–H annulation reactions employing iridium catalysis is depicted in Scheme 5.3.3.1 and discussed below.

In 2007, Miura group reported an Ir(III)-catalyzed 1:2 coupling reaction between aromatic acids and internal alkynes to deliver naphthalene derivatives exclusively under oxidative conditions (Scheme 5.3.3.1a).[11] After a long gap, in 2013, Nishimura *et al.* described 1,5-cyclooctadiene coordinated cationic iridium complex-catalyzed [3+2] spiroannulation of *N*-sulfonyl ketimines with 1,3-dienes to give spirocyclic aminoindane scaffolds in high yields and high regio- and diastereoselectivity (Scheme 5.3.3.1b).[118c] In 2015, Miura and co-workers designed a methodology for the synthesis of N–H carbazoles via Ir-catalyzed intramolecular C–H amination/dehydrogenative cyclization sequence from 2-aminobiphenyls using copper co-catalyst and air as terminal oxidant (Scheme 5.3.3.1c).[118f] In the same year, Wang group delineated an Ir(III)-catalyzed spiroannulation reaction between NH-isoquinolones and 1,4-benzoquinones in near quantitative yields (Scheme 5.3.3.1d).[118g]

Following year, Ramana and co-workers realized an efficient annulation reaction between aryloximes and α-diazocarbonyl compounds generating a series of isoquinoline *N*-oxides employing iridium-catalyzed mild reaction conditions releasing N_2 and H_2O as byproducts (Scheme 5.3.3.1e).[118h] Concurrently, Dong *et al.* reported a highly stereoselective Ir-catalyzed cascade C–H activation/[3+2] spiroannulation reaction between *N*-phosphoryl imines and internal alkynes (Scheme 5.3.3.1f).[118j] In 2018, Shi and co-workers demonstrated an Ir(III)-catalyzed C–H annulation between readily available benzimidates and hydroxylisopropylalkynes to deliver biologically important isoquinolines under mild reaction conditions (Scheme 5.3.3.1g).[118m] Next year, Gooβen group disclosed a straightforward annulation reaction between benzoic acids and α,β-unsaturated carbonyl compounds to give substituted indanones under iridium catalysis (Scheme 5.3.31h).[118n] Simultaneously, Deb and co-workers achieved an iridium(III)-catalyzed redox-neutral [3+2] spiroannulation reaction between weakly directing *N*-sulfonyl ketimines and demanding nitroalkenes furnishing spirocycles with three consecutive stereogenic centers in high yields and excellent diastereoselectivity (Scheme 5.3.3.1i).[118o]

Zhou *et al.* reported an unprecedented Ir-catalyzed cyclization of benzoic acid derivatives with trifluoromethylated alkynes under oxidative conditions in a highly regioselective manner (Scheme 5.3.3.1j).[118p] Wu group realized a strategy for the synthesis of 2-alkyl indoles via a Cp*Ir(III)-catalyzed C–H alkylation/intramolecular annulation pathway between *N*-aryl-2-aminopyridines and sulfoxonium ylides (Scheme 5.3.3.1k).[118q] The reaction showcased the utility of carbene precursors like sulfoxonium ylides as a useful surrogate of diazo compounds. In 2020, You *et al.* demonstrated an iridium-catalyzed tandem C–H/C–H cross-coupling/cyclization methodology between oxime ethers and heteroarenes to deliver polycyclic heteroaromatic compounds (Scheme 5.3.3.1l).[118w] Very recently, Sun and co-workers devised a highly regioselective Ir-catalyzed dual C2 and C3 dual functionalization of indoles with nitrones via sequential multiple C–H bond cleavage and C–C bond formation where nitrones serve both as a building block and as an oxidant (Scheme 5.3.3.1m).[118x]

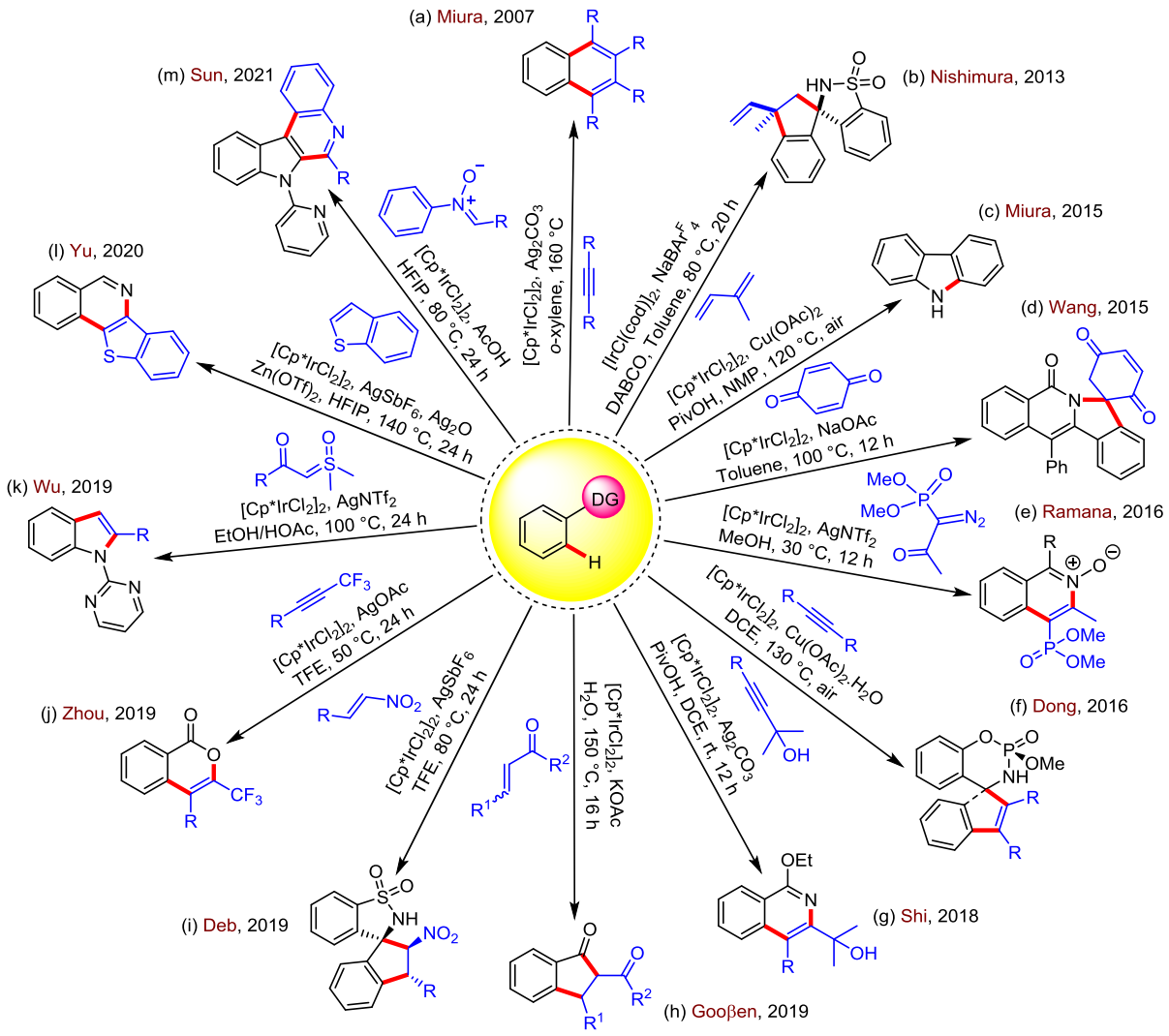

Scheme 5.3.3.1. Representative examples of iridium-catalyzed C–H annulation.

5.3.4. Electrochemical C–H Activation

Merging electrocatalysis with transition metal catalysis has been a significant boon over the recent years attracting considerable attention by different research groups on account of its several environmentally benign advantages.[84] To this end, iridium catalysis has also made a considerable contribution starting in 2018, when Ackermann group accomplished an iridium-electrocatalyzed C–H alkenylation/annulation cascade between aromatic acids and acrylates through weak *O*-coordination (Scheme 5.3.4.1a).[120] The reaction features the use of a metal-free redox mediator and electricity as a sustainable terminal oxidant. Following year, Mei and co-workers reported a C–H/O–H annulation of acrylic acids with alkynes for the efficient synthesis of α-pyrones via Ir-catalyzed electrochemical vinylic C–H functionalization in an undivided cell (Scheme 5.3.4.1b).[121] Since then, a few other C–H functionalization protocols have been reported collaborating iridium catalysis and electrocatalysis.[122] Among them, very recently, Chang *et al.* disclosed an intramolecular version of dehydrogenative C–H/N–H coupling of 2-alkenyl anilines furnishing an array of 3-substituted NH-indoles under Ir-catalyzed electrochemical conditions (Scheme 5.3.4.1c).[122c] The reaction proceeds via an electro-oxidation induced reductive elimination pathway.

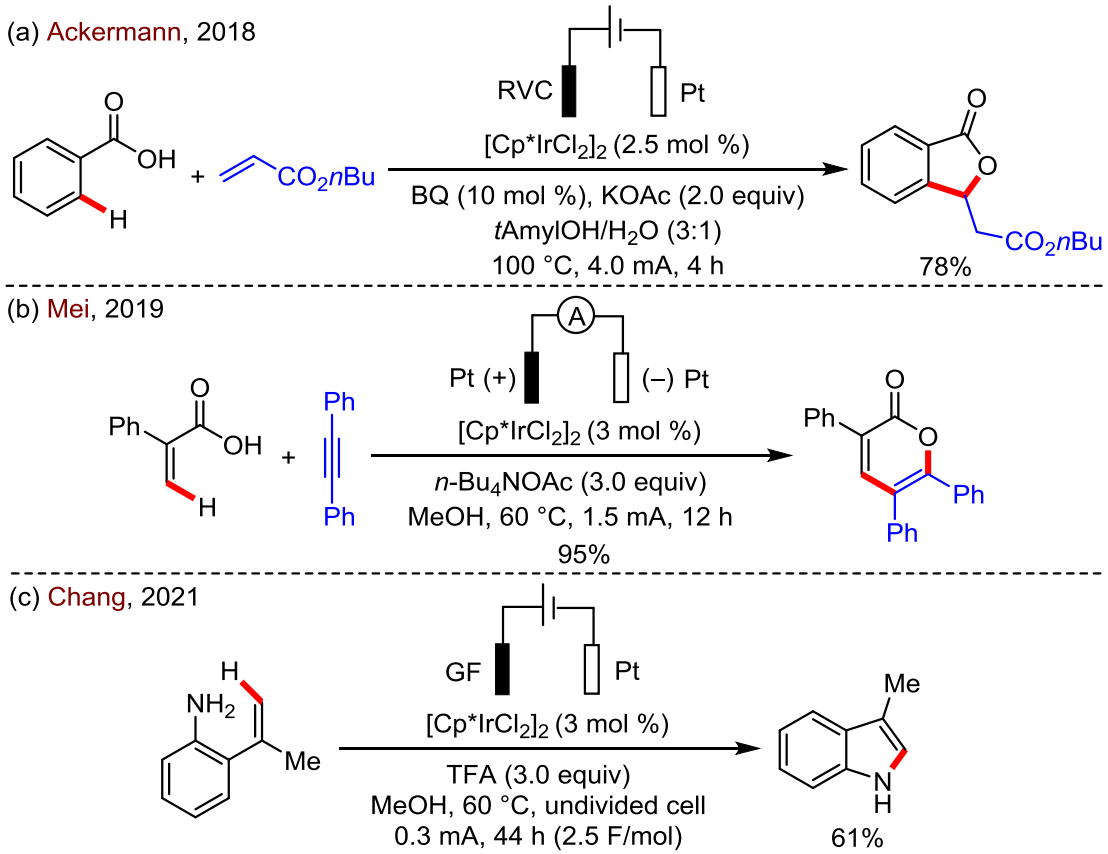

Scheme 5.3.4.1. Selected examples of Ir-catalyzed electrochemical annulation.

5.4. References

1. Murahashi, S. *J. Am. Chem. Soc.* **1955**, *77*, 6403.
2. Murai, S.; Kakiuchi, F.; Sekine, S.; Tanaka, Y.; Kamatani, A.; Sonoda, M.; Chatani, N. *Nature* **1993**, *366*, 529.
3. For selected reviews, see: (a) Gao, K.; Yoshikai, N. *Acc. Chem. Res.* **2014**, *47*, 1208. (b) Moselage, M.; Li, J.; Ackermann, L. *ACS Catal.* **2016**, *6*, 498. (c) Wei, D.; Zhu, X.; Niu, J.-L.; Song, M.-P. *ChemCatChem* **2016**, *8*, 1242. (d) Liu, J.; Chen, G.; Tan, Z. *Adv. Syn. Catal.* **2016**, *358*, 1174. (e) Rao, W.-H.; Shi, B.-F. *Org. Chem. Front.* **2016**, *3*, 1028. (f) Yamaguchi, J.; Muto, K.; Itami, K. *Top. Curr. Chem.* **2016**, *374*, 55. (g) Liu, W.; Ackermann, L. *ACS Catal.* **2016**, *6*, 3743. (h) Shang, R.; Ilies, L.; Nakamura, E. *Chem. Rev.* **2017**, *117*, 9086.
4. For selected reviews, see: (a) Lyons, T. W.; Sanford, M. S. *Chem. Rev.* **2010**, *110*, 1147. (b) Colby, D. A.; Bergman, R. G.; Ellman, J. A. *Chem. Rev.* **2010**, *110*, 624. (c) Yeung, C. S.; Dong, V. M. *Chem. Rev.* **2011**, *111*, 1215. (d) Arockiam, P. B.; Bruneau, C.; Dixneuf, P. H. *Chem. Rev.* **2012**, *112*, 5879. (e) Ackermann, L. *Acc. Chem. Res.* **2014**, *47*, 281. (f) Kuhl, N.; Schröder, N.; Glorius, F. *Adv. Syn. Catal.* **2014**, *356*, 1443. (g) Li, X.; Ouyang, W.; Nie, J.; Ji, S.; Chen, Q.; Huo, Y. *ChemCatChem* **2020**, *12*, 2358.
5. Qi, X.; Li, Y.; Bai, R.; Lan, Y. *Acc. Chem. Res.* **2017**, *50*, 2799.
6. (a) Lim, Y.-G.; Kim, Y. H.; Kang, J.-B. *J. Chem. Soc., Chem. Commun.* **1994**, 2267. (b) Lim, Y.-G.; Kang, J.-B.; Kim, Y. H. *J. Chem. Soc., Perkin Trans 1* **1996**, 2201. (c) Lim, Y.-G.; Kang, J.-B. *Bull. Korean Chem. Soc.* **1997**, *18*, 1213. (d) Lim, Y.-G.; Han, J.-S.; Kang, J.-B. *Bull. Korean Chem. Soc.* **1998**, *19*, 1143. (e) Lim, Y.-G.; Han, J.-S.; Koo, B. T.; Kang, J.-B. *Bull. Korean Chem. Soc.* **1999**, *20*, 1097.
7. Jun, C.-H.; Hong, J.-B.; Kim, Y.-H.; Chung, K.-Y. *Angew. Chem. Int. Ed.* **2000**, *39*, 3440.
8. (a) Lim, S.-G.; Ahn, J.-A.; Jun, C.-H. *Org. Lett.* **2004**, *6*, 4687. (b) Vo-Thanh, G.; Lahrache, H.; Loupy, A.; Kim, I.-J.; Chang, D.-H.; Jun, C.-H. *Tetrahedron* **2004**, *60*, 5539.
9. Lim, S.-G.; Lee, J. H.; Moon, C. W.; Hong, J.-B.; Jun, C.-H. *Org. Lett.* **2003**, *5*, 2759.
10. Davies, D. L.; Al-Duaij, O.; Fawcett, J.; Giardiello, M.; Hilton, S. T.; Russell, D. R. *Dalton Trans.* **2003**, 4132.
11. Ueura, K.; Satoh, T.; Miura, M. *J. Org. Chem.* **2007**, *72*, 5362.

12. (a) Li, L.; Brennessel, W. W.; Jones, W. D. *J. Am. Chem. Soc.* **2008**, *130*, 12414. (b) Stuart, D. R.; Bertrand-Laperle, M.; Burgess, K. M. N.; Fagnou, K. *J. Am. Chem. Soc.* **2008**, *130*, 1647.

13. For representative examples, see: (a) Schipper, D. J.; Hutchinson, M.; Fagnou, K. *J. Am. Chem. Soc.* **2010**, *132*, 6910. (b) Patureau, F. W.; Glorius, F. *J. Am. Chem. Soc.* **2010**, *132*, 9982. (c) Rakshit, S.; Grohmann, C.; Besset, T.; Glorius, F. *J. Am. Chem. Soc.* **2011**, *133*, 2350. (d) Xue, X.; Xu, J.; Zhang, L.; Xu, C.; Pan, Y.; Xu, L.; Li, H.; Zhang, W. *Adv. Syn. Catal.* **2016**, *358*, 573. (e) Jambu, S.; Jeganmohan, M. *Org. Lett.* **2020**, *22*, 5057.

14. For representative examples, see: (a) Tsai, A. S.; Tauchert, M. E.; Bergman, R. G.; Ellman, J. A. *J. Am. Chem. Soc.* **2011**, *133*, 1248. (b) Hesp, K. D.; Bergman, R. G.; Ellman, J. A. *J. Am. Chem. Soc.* **2011**, *133*, 11430. (c) Yang, L.; Correia, C. A.; Li, C.-J. *Org. Biomol. Chem.* **2011**, *9*, 7176. (d) Du, Y.; Hyster, T. K.; Rovis, T. *Chem. Commun.* **2011**, *47*, 12074. (e) Feng, C.; Loh, T.-P. *Chem. Commun.* **2011**, *47*, 10458. (f) Gong, T.-J.; Xiao, B.; Liu, Z.-J.; Wan, J.; Xu, J.; Luo, D.-F.; Fu, Y.; Liu, L. *Org. Lett.* **2011**, *13*, 3235. (g) Li, Y.; Li, B.-J.; Wang, W.-H.; Huang, W.-P.; Zhang, X.-S.; Chen, K.; Shi, Z.-J. *Angew. Chem. Int. Ed.* **2011**, *50*, 2115. (h) Yang, L.; Qian, B.; Huang, H. *Chem. Eur. J.* **2012**, *18*, 9511. (i) Zhou, B.; Yang, Y.; Li, Y. *Chem. Commun.* **2012**, *48*, 5163. (j) Tauchert, M. E.; Incarvito, C. D.; Rheingold, A. L.; Bergman, R. G.; Ellman, J. A. *J. Am. Chem. Soc.* **2012**, *134*, 1482. (k) Li, Y.; Zhang, X.-S.; Zhu, Q.-L.; Shi, Z.-J. *Org. Lett.* **2012**, *14*, 4498. (l) Li, Y.; Zhang, X.-S.; Li, H.; Wang, W.-H.; Chen, K.; Li, B.-J.; Shi, Z.-J. *Chem. Sci.* **2012**, *3*, 1634. (m) Wang, H.; Beiring, B.; Yu, D.-G.; Collins, K. D.; Glorius, F. *Angew. Chem. Int. Ed.* **2013**, *52*, 12430. (n) Han, S. H.; Choi, M.; Jeong, T.; Sharma, S.; Mishra, N. K.; Park, J.; Oh, J. S.; Kim, W. J.; Lee, J. S.; Kim, I. S. *J. Org. Chem.* **2015**, *80*, 11092. (o) Tian, P.; Feng, C.; Loh, T.-P. *Nat. Commun.* **2015**, *6*, 7472. (p) Potter, T. J.; Kamber, D. N.; Mercado, B. Q.; Ellman, J. A. *ACS Catal.* **2017**, *7*, 150. (q) Zhou, L.; Zhu, C.; Loh, T.-P.; Feng, C. *Chem. Commun.* **2018**, *54*, 5618. (r) Zhao, H.; Xu, J.; Chen, C.; Xu, X.; Pan, Y.; Zhang, Z.; Li, H.; Xu, L. *Adv. Syn. Catal.* **2018**, *360*, 985. (s) Han, Q.; Guo, X.; Tang, Z.; Su, L.; Yao, Z.; Zhang, X.; Lin, S.; Xiang, S.; Huang, Q. *Adv. Syn. Catal.* **2018**, *360*, 972. (t) Pradhan, S.; De, P. B.; Punniyamurthy, T. *Org. Lett.* **2019**, *21*, 9898. (u) Jin, S.; Chen, Z.; Zhao, Y. *Adv. Syn. Catal.* **2019**, *361*, 4674. (v) Peng, J.; Li, C.; Khamrakulov, M.; Wang, J.; Liu, H. *Org. Lett.* **2020**, *22*, 1535.

15. (a) Song, G.; Wang, F.; Li, X. *Chem. Soc. Rev.* **2012**, *41*, 3651. (b) Colby, D. A.; Tsai, A. S.; Bergman, R. G.; Ellman, J. A. *Acc. Chem. Res.* **2012**, *45*, 814. (c) Patureau, F. W.; Wencel- Delord, J.; Glorius, F. *Aldrichimica Acta* **2012**, *45*, 31-41. (d) Song, G.; Li, X.

Acc. Chem. Res. **2015**, *48*, 1007. (e) Wencel-Delord, J.; Patureau, F. W.; Glorius, F. *Top Organomet. Chem.* **2015**, *55*, 1-27. (f) Li, S.-S.; Qin, L.; Dong, L. *Org. Biomol. Chem.* **2016**, *14*, 4554. (g) Rej, S.; Chatani, N. *Angew. Chem. Int. Ed.* **2019**, *58*, 8304. (h) Wang, R.; Xie, X.; Liu, H.; Zhou, Y. J. C. *Catalysts* **2019**, *9*, 823. (i) Dhiman, A. K.; Thakur, A.; Kumar, R.; Sharma, U. *Asian J. Org. Chem.* **2020**, *9*, 1502.

16. Zheng, J.; Zhang, Y.; Cui, S. *Org. Lett.* **2014**, *16*, 3560.
17. Yang, Z.; Yu, J.-T.; Pan, C. *Org. Biomol. Chem.* **2021**, *19*, 8442.
18. Feng, C.; Loh, T.-P. *Angew. Chem. Int. Ed.* **2014**, *53*, 2722.
19. Xie, F.; Qi, Z.; Yu, S.; Li, X. *J. Am. Chem. Soc.* **2014**, *136*, 4780.
20. Collins, K. D.; Lied, F.; Glorius, F. *Chem. Commun.* **2014**, *50*, 4459.
21. (a) Hou, H.; Zhao, Y.; Pu, S.; Chen, J. *Org. Biomol. Chem.* **2019**, *17*, 2948. (b) Du, X.; Hou, H.; Zhao, Y.; Sheng, S.; Chen, J. *Eur. J. Org. Chem.* **2020**, *2020*, 1100.
22. Gong, T.-J.; Xiao, B.; Cheng, W.-M.; Su, W.; Xu, J.; Liu, Z.-J.; Liu, L.; Fu, Y. *J. Am. Chem. Soc.* **2013**, *135*, 10630.
23. Chaitanya, M.; Yadagiri, D.; Anbarasan, P. *Org. Lett.* **2013**, *15*, 4960.
24. Soumya, P. K.; Vaishak, T. B.; Saranya, S.; Anilkumar, G. *Appl. Organomet. Chem.* **2021**, *35*, e6340.
25. For representative examples, see: (a) Chan, W.-W.; Lo, S.-F.; Zhou, Z.; Yu, W.-Y. *J. Am. Chem. Soc.* **2012**, *134*, 13565. (b) Li, X.; Yu, S.; Wang, F.; Wan, B.; Yu, X. *Angew. Chem. Int. Ed.* **2013**, *52*, 2577. (c) Qi, Z.; Li, X. *Angew. Chem. Int. Ed.* **2013**, *52*, 8995. (d) Hu, F.; Xia, Y.; Ye, F.; Liu, Z.; Ma, C.; Zhang, Y.; Wang, J. *Angew. Chem. Int. Ed.* **2014**, *53*, 1364. (e) Zhang, Y.; Wu, Q.; Cui, S. *Chem. Sci.* **2014**, *5*, 297. (f) Yu, S.; Li, X. *Org. Lett.* **2014**, *16*, 1200. (g) Yu, S.; Li, X. *Org. Lett.* **2014**, *16*, 1220. (h) Zhang, X.; Wang, F.; Qi, Z.; Yu, S.; Li, X. *Org. Lett.* **2014**, *16*, 1586.
26. For selected examples, see: (a) Wencel-Delord, J.; Nimphius, C.; Patureau, F. W.; Glorius, F. *Angew. Chem. Int. Ed.* **2012**, *51*, 2247. (b) Wencel-Delord, J.; Nimphius, C.; Wang, H.; Glorius, F. *Angew. Chem. Int. Ed.* **2012**, *51*, 13001. (c) Qin, X.; Liu, H.; Qin, D.; Wu, Q.; You, J.; Zhao, D.; Guo, Q.; Huang, X.; Lan, J. *Chem. Sci.* **2013**, *4*, 1964. (d) Dong, J.; Long, Z.; Song, F.; Wu, N.; Guo, Q.; Lan, J.; You, J. *Angew. Chem. Int. Ed.* **2013**, *52*, 580. (e) Reddy, V. P.; Qiu, R.; Iwasaki, T.; Kambe, N. *Org. Lett.* **2013**, *15*, 1290.
27. Kim, J. Y.; Park, S. H.; Ryu, J.; Cho, S. H.; Kim, S. H.; Chang, S. *J. Am. Chem. Soc.* **2012**, *134*, 9110.

28. (a) Ryu, J.; Shin, K.; Park, S. H.; Kim, J. Y.; Chang, S. *Angew. Chem. Int. Ed.* **2012**, *51*, 9904. (b) Shin, K.; Baek, Y.; Chang, S. *Angew. Chem. Int. Ed.* **2013**, *52*, 8031. (c) Kim, H. J.; Ajitha, M. J.; Lee, Y.; Ryu, J.; Kim, J.; Lee, Y.; Jung, Y.; Chang, S. *J. Am. Chem. Soc.* **2014**, *136*, 1132. (d) Park, S. H.; Kwak, J.; Shin, K.; Ryu, J.; Park, Y.; Chang, S. *J. Am. Chem. Soc.* **2014**, *136*, 2492.
29. (a) Ng, K.-H.; Zhou, Z.; Yu, W.-Y. *Org. Lett.* **2012**, *14*, 272. (b) Grohmann, C.; Wang, H.; Glorius, F. *Org. Lett.* **2012**, *14*, 656.
30. Grohmann, C.; Wang, H.; Glorius, F. *Org. Lett.* **2013**, *15*, 3014.
31. Yu, S.; Wan, B.; Li, X. *Org. Lett.* **2013**, *15*, 3706.
32. Zhao, H.; Shang, Y.; Su, W. *Org. Lett.* **2013**, *15*, 5106.
33. Wu, K.; Fan, Z.; Xue, Y.; Yao, Q.; Zhang, A. *Org. Lett.* **2014**, *16*, 42.
34. Park, Y.; Park, K. T.; Kim, J. G.; Chang, S. *J. Am. Chem. Soc.* **2015**, *137*, 4534.
35. Zhou, C.; Zhao, J.; Guo, W.; Jiang, J.; Wang, J. *Org. Lett.* **2019**, *21*, 9315.
36. Huang, X.; Wang, Y.; Lan, J.; You, J. *Angew. Chem. Int. Ed.* **2015**, *54*, 9404.
37. Xie, F.; Qi, Z.; Li, X. *Angew. Chem. Int. Ed.* **2013**, *52*, 11862.
38. For selected examples, see: (a) Ng, K.-H.; Zhou, Z.; Yu, W.-Y. *Chem. Commun.* **2013**, *49*, 7031. (b) Ng, F.-N.; Zhou, Z.; Yu, W.-Y. *Chem. Eur. J.* **2014**, *20*, 4474. (c) Tang, R.-J.; Luo, C.-P.; Yang, L.; Li, C.-J. *Adv. Syn. Catal.* **2013**, *355*, 869. (d) Maiden, T. M. M.; Swanson, S.; Procopiou, P. A.; Harrity, J. P. A. *J. Org. Chem.* **2016**, *81*, 10641. (e) Jeon, M.; Park, J.; Dey, P.; Oh, Y.; Oh, H.; Han, S.; Um, S. H.; Kim, H. S.; Mishra, N. K.; Kim, I. S. *Adv. Syn. Catal.* **2017**, *359*, 3471. (f) Wang, H.-W.; Lu, Y.; Zhang, B.; He, J.; Xu, H.-J.; Kang, Y.-S.; Sun, W.-Y.; Yu, J.-Q. *Angew. Chem. Int. Ed.* **2017**, *56*, 7449. (g) Ding, J.; Jiang, W.; Bai, H.-Y.; Ding, T.-M.; Gao, D.; Bao, X.; Zhang, S.-Y. *Chem. Commun.* **2018**, *54*, 8889. (h) Gogula, T.; Zhang, J.-Q.; Zou, H.-B. *Org. Lett.* **2019**, *21*, 5933. (i) Shi, H.; Dixon, D. J. *Chem. Sci.* **2019**, *10*, 3733. (j) Samanta, S.; Mondal, S.; Ghosh, D.; Hajra, A. *Org. Lett.* **2019**, *21*, 4905. (k) Khake, S. M.; Chatani, N. *Org. Lett.* **2020**, *22*, 3655.
39. For representative examples, see: (a) Yu, W.; Chen, J.; Gao, K.; Liu, Z.; Zhang, Y. *Org. Lett.* **2014**, *16*, 4870. (b) Wu, Y.; Zhou, B. *Org. Lett.* **2017**, *19*, 3532. (c) Mishra, A.; Vats, T. K.; Nair, M. P.; Das, A.; Deb, I. *J. Org. Chem.* **2017**, *82*, 12406. (d) Li, C.-X.; Zhang, H.-Y.; Wong, T.-Y.; Cao, H.-J.; Yan, H.; Lu, C.-S. *Org. Lett.* **2017**, *19*, 5178. (e) Kim, K.; Hyun, J.; Kim, J.; Kim, H. *Asian J. Org. Chem.* **2017**, *6*, 907. (f) Chen, C.; Pan, Y.; Zhao, H.; Xu, X.; Xu, J.; Zhang, Z.; Xi, S.; Xu, L.; Li, H. *Org. Chem. Front.* **2018**, *5*, 415. (g) Zhai, W.; Li, B.; Wang, B. *ChemistrySelect* **2018**, *3*, 8035. (h) Chen, Y.-K.;

Kang, Y.-S.; Xu, H.-J.; Zhang, P.; Zhao, J.; Li, T.; Sun, W.-Y.; Lu, Y. *Org. Lett.* **2020**, *22*, 5390. (i) Hazra, S.; Hirano, K.; Miura, M. *Heterocycles* **2020**, *101*, 223. (j) Pan, G.; Lu, L.; Zhuang, W.; Huang, Q. *J. Org. Chem.* **2021**, *86*, 16753.

40. Yang, Y.; Hou, W.; Qin, L.; Du, J.; Feng, H.; Zhou, B.; Li, Y. *Chem. Eur. J.* **2014**, *20*, 416.
41. Yu, S.; Wan, B.; Li, X. *Org. Lett.* **2015**, *17*, 58.
42. Wang, Q.; Xie, F.; Li, X. *J. Org. Chem.* **2015**, *80*, 8361.
43. Wang, F.; Yu, X.; Qi, Z.; Li, X. *Chem. Eur. J.* **2016**, *22*, 511.
44. For selected reviews and examples, see: (a) Di Giuseppe, A.; Castarlenas, R.; Oro, L. A. *Top. Organomet. Chem.* **2016**, *61*, 31. (b) Ma, W.; Kaplaneris, N.; Fang, X.; Gu, L.; Mei, R.; Ackermann, L. *Org. Chem. Front.* **2020**, *7*, 1022. (c) Wen, J.; Wu, A.; Wang, M.; Zhu, J. *J. Org. Chem.* **2015**, *80*, 10457. (d) Xie, W.; Li, B.; Wang, B. *J. Org. Chem.* **2016**, *81*, 396. (e) Yang, S.; Feng, B.; Yang, Y. *J. Org. Chem.* **2017**, *82*, 12430. (f) Maity, S.; Karmakar, U.; Samanta, R. *Chem. Commun.* **2017**, *53*, 12197. (g) Vats, T. K.; Mishra, A.; Deb, I. *Adv. Syn. Catal.* **2018**, *360*, 2291. (h) Liu, C.; Fang, Y.; Wang, S.-Y.; Ji, S.-J. *Org. Lett.* **2018**, *20*, 6112. (i) Yang, J.; Deng, B.; Guo, X.; Li, Z.; Xiang, H.; Zhou, X. *Asian J. Org. Chem.* **2018**, *7*, 439. (j) Kang, Y.-S.; Zhang, P.; Li, M.-Y.; Chen, Y.-K.; Xu, H.-J.; Zhao, J.; Sun, W.-Y.; Yu, J.-Q.; Lu, Y. *Angew. Chem. Int. Ed.* **2019**, *58*, 9099. (k) Wang, D.; Zhou, K.; Zhang, J.; Zhao, Y. *Org. Chem. Front.* **2020**, *7*, 3229. (l) Shi, G.; Khan, R.; Zhang, X.; Yang, Y.; Zhan, Y.; Li, J.; Luo, Y.; Fan, B. *Asian J. Org. Chem.* **2020**, *9*, 788. (m) Lin, J.; Hu, L.; Chen, C.; Feng, H.; Yu, Y.; Yang, Y.; Zhou, B. *Org. Lett.* **2021**, *23*, 1194.
45. Schröder, N.; Wencel-Delord, J.; Glorius, F. *J. Am. Chem. Soc.* **2012**, *134*, 8298.
46. For selected examples, see: (a) Kuhl, N.; Schröder, N.; Glorius, F. *Org. Lett.* **2013**, *15*, 3860. (b) Qian, G.; Hong, X.; Liu, B.; Mao, H.; Xu, B. *Org. Lett.* **2014**, *16*, 5294. (c) Zhang, P.; Hong, L.; Li, G.; Wang, R. *Adv. Syn. Catal.* **2015**, *357*, 345. (d) Ding, Q.; Zhou, X.; Pu, S.; Cao, B. *Tetrahedron* **2015**, *71*, 2376. (e) Hernández, J. G.; Bolm, C. *Chem. Commun.* **2015**, *51*, 12582. (f) Kim, K.; Hyun, J.; Kim, J.; Kim, H. *Asian J. Org. Chem.* **2016**, *5*, 1107. (g) Huestis, M. P. *J. Org. Chem.* **2016**, *81*, 12545. (h) Zhang, T.; Qi, X.; Liu, S.; Bai, R.; Liu, C.; Lan, Y. *Chem. Eur. J.* **2017**, *23*, 2690. (i) Peng, Q.; Hu, J.; Huo, J.; Yuan, H.; Xu, L.; Pan, X. *Org. Biomol. Chem.* **2018**, *16*, 4471. (j) Dhiman, A. K.; Gupta, S. S.; Sharma, R.; Kumar, R.; Sharma, U. *J. Org. Chem.* **2019**, *84*, 12871. (k) Tanaka, J.; Shibata, Y.; Joseph, A.; Nogami, J.; Terasawa, J.; Yoshimura, R.; Tanaka, K. *Chem. Eur. J.* **2020**, *26*, 5774.

47. (a) Min, M.; Kang, D.; Jung, S.; Hong, S. *Adv. Syn. Catal.* **2016**, *358*, 1296. (b) Miura, W.; Hirano, K.; Miura, M. *Org. Lett.* **2016**, *18*, 3742. (c) Wen, J.; Wang, D.; Qian, J.; Wang, D.; Zhu, C.; Zhao, Y.; Shi, Z. *Angew. Chem. Int. Ed.* **2019**, *58*, 2078.

48. (a) Satoh, T.; Miura, M. *Chem. Eur. J.* **2010**, *16*, 11212. (b) Ye, B.; Cramer, N. *Acc. Chem. Res.* **2015**, *48*, 1308. (c) Yang, Y.; Li, K.; Cheng, Y.; Wan, D.; Li, M.; You, J. *Chem. Commun.* **2016**, *52*, 2872. (d) Gulías, M.; Mascareñas, J. L. *Angew. Chem. Int. Ed.* **2016**, *55*, 11000. (e) Nishii, Y.; Miura, M. *ACS Catal.* **2020**, *10*, 9747. (f) Wang, C.; Chen, F.; Qian, P.; Cheng, J. *Org. Biomol. Chem.* **2021**, *19*, 1705. (g) Song, L.; Van der Eycken, E. V. *Chem. Eur. J.* **2021**, *27*, 121.

49. Shimizu, M.; Tsurugi, H.; Satoh, T.; Miura, M. *Chem. Asian J.* **2008**, *3*, 881.

50. Umeda, N.; Hirano, K.; Satoh, T.; Shibata, N.; Sato, H.; Miura, M. *J. Org. Chem.* **2011**, *76*, 13.

51. Mochida, S.; Shimizu, M.; Hirano, K.; Satoh, T.; Miura, M. *Chem. Asian J.* **2010**, *5*, 847.

52. (a) Zhao, D.; Wu, Q.; Huang, X.; Song, F.; Lv, T.; You, J. *Chem. Eur. J.* **2013**, *19*, 6239. (b) Muralirajan, K.; Cheng, C.-H. *Chem. Eur. J.* **2013**, *19*, 6198. (c) Mayakrishnan, S.; Tamizmani, M.; Balachandran, C.; Aoki, S.; Maheswari, N. U. *Org. Biomol. Chem.* **2021**, *19*, 5413.

53. Streit, A. D.; Zoll, A. J.; Hoang, G. L.; Ellman, J. A. *Org. Lett.* **2020**, *22*, 1217.

54. For representative examples, see: (a) Pham, M. V.; Ye, B.; Cramer, N. *Angew. Chem. Int. Ed.* **2012**, *51*, 10610. (b) Dong, W.; Wang, L.; Parthasarathy, K.; Pan, F.; Bolm, C. *Angew. Chem. Int. Ed.* **2013**, *52*, 11573. (c) Unoh, Y.; Hashimoto, Y.; Takeda, D.; Hirano, K.; Satoh, T.; Miura, M. *Org. Lett.* **2013**, *15*, 3258. (d) Qi, Z.; Wang, M.; Li, X. *Chem. Commun.* **2014**, *50*, 9776. (e) Yan, K.; Liu, M.; Wen, J.; Wang, S.; Li, J.; Wang, H. *Org. Lett.* **2020**, *22*, 7825.

55. Mayakrishnan, S.; Arun, Y.; Balachandran, C.; Emi, N.; Muralidharan, D.; Perumal, P. T. *Org. Biomol. Chem.* **2016**, *14*, 1958.

56. Karishma, P.; Mahesha, C. K.; Agarwal, D. S.; Mandal, S. K.; Sakhuja, R. *J. Org. Chem.* **2018**, *83*, 11661.

57. Ren, J.; Pi, C.; Cui, X.; Wu, Y. *Org. Lett.* **2021**, *23*, 6628.

58. For representative examples, see: (a) Li, B.; Guo, C.; Shen, N.; Zhang, X.; Fan, X. *Org. Chem. Front.* **2020**, *7*, 3698. (b) Deng, C.; Li, C.; Yao, J.; Jin, Q.; Miao, M.; Zhou, H. *Eur. J. Org. Chem.* **2021**, *2021*, 3552. (c) Aslam, M.; Mohandoss, S.; Lee, Y. R. *Org. Lett.* **2021**, *23*, 6206. (d) Liu, J.; Gao, Y.; Zhu, Y.; Zhu, J.; Wang, C.; Rui, X.; Yang, K.; Si, D.; Lin, J.; Yuan, D.; Wen, H.; Li, W. *Org. Lett.* **2020**, *22*, 2657.

59. (a) Chary, D. Y.; Chaitanya, I.; Balasubramanian, S.; Reddy, B. V. S. *Eur. J. Org. Chem.* **2021**, *2021*, 3083. (b) Chen, L.; Wang, Z.; Pang, B.; Wang, Y.; Xu, X.; Wu, G.; Ji, Y. *Asian J. Org. Chem.* **2021**, *10*, 2603.
60. Stuart, D. R.; Alsabeh, P.; Kuhn, M.; Fagnou, K. *J. Am. Chem. Soc.* **2010**, *132*, 18326.
61. Li, D. Y.; Chen, H. J.; Liu, P. N. *Org. Lett.* **2014**, *16*, 6176.
62. Fukutani, T.; Umeda, N.; Hirano, K.; Satoh, T.; Miura, M. *Chem. Commun.* **2009**, 5141.
63. (a) Seoane, A.; Casanova, N.; Quiñones, N.; Mascareñas, J. L.; Gulías, M. *J. Am. Chem. Soc.* **2014**, *136*, 7607. (b) Zhou, M.-B.; Pi, R.; Hu, M.; Yang, Y.; Song, R.-J.; Xia, Y.; Li, J.-H. *Angew. Chem. Int. Ed.* **2014**, *53*, 11338. (c) Mei, S.-T.; Liang, H.-W.; Teng, B.; Wang, N.-J.; Shuai, L.; Yuan, Y.; Chen, Y.-C.; Wei, Y. *Org. Lett.* **2016**, *18*, 1088.
64. (a) Martínez, Á. M.; Rodríguez, N.; Gómez Arrayás, R.; Carretero, J. C. *Chem. Commun.* **2014**, *50*, 6105. (b) Wu, X.; Ji, H. *J. Org. Chem.* **2018**, *83*, 4650. (c) Bai, D.; Xia, J.; Song, F.; Li, X.; Liu, B.; Liu, L.; Zheng, G.; Yang, X.; Sun, J.; Li, X. *Chem. Sci.* **2019**, *10*, 3987. (d) Wang, C.; Qian, P.-C.; Chen, F.; Cheng, J. *Tetrahedron Lett.* **2020**, *61*, 152441. (e) Hu, B.; Chen, G.; Zhao, J.; Xue, L.; Jiang, Y.; Zhang, X.; Fan, X. *J. Org. Chem.* **2021**, *86*, 10330. (f) Wang, S.; Miao, E.; Wang, H.; Song, B.; Huang, W.; Yang, W. *Chem. Commun.* **2021**, *57*, 5929. (g) Yin, C.; Zhong, T.; Zheng, X.; Li, L.; Zhou, J.; Yu, C. *Org. Biomol. Chem.* **2021**, *19*, 7701.
65. For selected examples, see: (a) Li, G.; Ding, Z.; Xu, B. *Org. Lett.* **2012**, *14*, 5338. (b) Zhou, T.; Wang, Y.; Li, B.; Wang, B. *Org. Lett.* **2016**, *18*, 5066. (c) Liang, G.; Rong, J.; Sun, W.; Chen, G.; Jiang, Y.; Loh, T.-P. *Org. Lett.* **2018**, *20*, 7326. (d) Shi, Y.; Chen, C.; Yang, Y.; Zhou, B. *Tetrahedron Lett.* **2021**, *72*, 153065.
66. Yi, W.; Li, L.; Chen, H.; Ma, K.; Zhong, Y.; Chen, W.; Gao, H.; Zhou, Z. *Org. Lett.* **2018**, *20*, 6812.
67. Lyu, H.; Quan, Y.; Cheng, B.; Xie, Z. *Chem. Commun.* **2021**, *57*, 7930.
68. (a) Guimond, N.; Gouliaras, C.; Fagnou, K. *J. Am. Chem. Soc.* **2010**, *132*, 6908. (b) Guimond, N.; Gorelsky, S. I.; Fagnou, K. *J. Am. Chem. Soc.* **2011**, *133*, 6449.
69. Dong, L.; Qu, C.-H.; Huang, J.-R.; Zhang, W.; Zhang, Q.-R.; Deng, J.-G. *Chem. Eur. J.* **2013**, *19*, 16537.
70. (a) Tan, H.; Laishram, R. D.; Zhang, X.; Shi, G.; Li, K.; Chen, J. *Eur. J. Org. Chem.* **2020**, *2020*, 4542. (b) Zhang, Y.; Huang, T.; Li, X.; Zhang, M.; Song, Y.; Huang, K.; Su, W. *RSC Adv.* **2020**, *10*, 22216-. (c) Luo, Y.; Liu, H.; Zhang, J.; Liu, M.; Dong, L. *Org. Lett.* **2020**, *22*, 7604.

71. Kumar, S.; Nunewar, S.; Usama, K. M.; Kanchupalli, V. *Eur. J. Org. Chem.* **2021**, *2021*, 2223.
72. Liu, B.; Hu, P.; Zhang, Y.; Li, Y.; Bai, D.; Li, X. *Org. Lett.* **2017**, *19*, 5402.
73. Ramesh, B.; Tamizmani, M.; Jeganmohan, M. *J. Org. Chem.* **2019**, *84*, 4058.
74. Yuan, T.; Pi, C.; You, C.; Cui, X.; Du, S.; Wan, T.; Wu, Y. *Chem. Commun.* **2019**, *55*, 163.
75. Mishra, A.; Bhowmik, A.; Samanta, S.; Sarkar, W.; Das, S.; Deb, I. *Org. Lett.* **2020**, *22*, 1340.
76. For representative examples, see: (a) Webb, N. J.; Marsden, S. P.; Raw, S. A. *Org. Lett.* **2014**, *16*, 4718. (b) Yang, X.-F.; Hu, X.-H.; Loh, T.-P. *Org. Lett.* **2015**, *17*, 1481. (c) Yang, X.; Liu, S.; Yu, S.; Kong, L.; Lan, Y.; Li, X. *Org. Lett.* **2018**, *20*, 2698. (d) Yang, Z.; Zhou, H.; He, M.; Li, J.; Yang, Z.; Wu, Y. *Asian J. Org. Chem.* **2021**, *10*, 1683. (e) Hu, S.; Han, X.; Xie, X.; Fang, F.; Wang, Y.; Saidahmatov, A.; Liu, H.; Wang, J. *Adv. Syn. Catal.* **2021**, *363*, 3311. (f) Karishma, P.; Mahesha, C. K.; Mandal, S. K.; Sakhuja, R. *J. Org. Chem.* **2021**, *86*, 2734.
77. Singh, A.; Shukla, R. K.; Volla, C. M. R. *Chem. Sci.* **2022**, *13*, 2043.
78. (a) Reddy, C. R.; Mallesh, K. *Org. Lett.* **2018**, *20*, 150. (b) Reddy, C. R.; Mallesh, K.; Bodasu, S.; Donthiri, R. R. *J. Org. Chem.* **2020**, *85*, 7905. (c) Reddy, C. R.; Bodasu, S.; Mallesh, K.; Prapurna, Y. L. *Synthesis* **2021**, *53*, 1127.
79. For selected examples, see: (a) Liang, Y.; Yu, K.; Li, B.; Xu, S.; Song, H.; Wang, B. *Chem. Commun.* **2014**, *50*, 6130. (b) Zhou, B.; Chen, Z.; Yang, Y.; Ai, W.; Tang, H.; Wu, Y.; Zhu, W.; Li, Y. *Angew. Chem. Int. Ed.* **2015**, *54*, 12121. (c) Sun, P.; Wu, Y.; Huang, Y.; Wu, X.; Xu, J.; Yao, H.; Lin, A. *Org. Chem. Front.* **2016**, *3*, 91. (d) Liu, H.; Song, S.; Wang, C.-Q.; Feng, C.; Loh, T.-P. *ChemSusChem* **2017**, *10*, 58. (e) Wang, C.-Q.; Ye, L.; Feng, C.; Loh, T.-P. *J. Am. Chem. Soc.* **2017**, *139*, 1762. (f) Wu, X.; Sun, S.; Xu, S.; Cheng, J. *Adv. Syn. Catal.* **2018**, *360*, 1111. (g) Pan, J.-L.; Xie, P.; Chen, C.; Hao, Y.; Liu, C.; Bai, H.-Y.; Ding, J.; Wang, L.-R.; Xia, Y.; Zhang, S.-Y. *Org. Lett.* **2018**, *20*, 7131. (h) Zhou, J.; Li, J.; Li, Y.; Wu, C.; He, G.; Yang, Q.; Zhou, Y.; Liu, H. *Org. Lett.* **2018**, *20*, 7645. (i) Lv, N.; Chen, Z.; Liu, Z.; Zhang, Y. *J. Org. Chem.* **2019**, *84*, 13013. (j) Ghosh, K.; Nishii, Y.; Miura, M. *Org. Lett.* **2020**, *22*, 3547. (k) Li, Y.; Fang, F.; Zhou, J.; Li, J.; Wang, R.; Liu, H.; Zhou, Y. *Adv. Syn. Catal.* **2021**, *363*, 3305. (l) Li, J.; Fang, F.; Wang, R.; Li, Y.; Xu, B.; Liu, H.; Zhou, Y. *Org. Chem. Front.* **2021**, *8*, 3876. (m) Jiang, Z.; Zhou, J.; Zhu, H.; Liu, H.; Zhou, Y. *Org. Lett.* **2021**, *23*, 4406. (n) Ko, G. H.; Maeng, C.; Jeong, H.; Han, S. H.; Han, G. U.; Lee, K.; Noh, H. C.; Lee, P. H. *Chem.*

Asian J. **2021**, *16*, 3179. (o) Luo, Y.; Pu, W.-Y.; Xu, Y.-J.; Dong, L. *Org. Chem. Front.* **2021**, *8*, 4549. (p) Wang, T.-T.; Jin, H.-S.; Cao, M.-M.; Wang, R.-B.; Zhao, L.-M. *Org. Lett.* **2021**, *23*, 5952. (q) Singh, A.; Dey, A.; Volla, C. M. R. *J. Org. Chem.* **2021**, *86*, 10474. (r) Wang, L.; Jiang, K.-c.; Zhang, N.; Zhang, Z.-h. *Asian J. Org. Chem.* **2021**, *10*, 1671. (s) Wang, Y.-J.; Wang, T.-T.; Liang, C.-C.; Li, Z.-H.; Zhao, L.-M. *Org. Lett.* **2021**, *23*, 6272. (t) Zhang, Y.; Chen, Z.-N.; Su, W. *Tetrahedron Lett.* **2021**, *72*, 153049.

80. For representative examples, see: (a) Chu, H.; Xue, P.; Yu, J.-T.; Cheng, J. *J. Org. Chem.* **2016**, *81*, 8009. (b) Hu, W.; Zheng, Q.; Sun, S.; Cheng, J. *Chem. Commun.* **2017**, *53*, 6263. (c) Priebbenow, D. L.; Hua, C. *Chem. Commun.* **2021**, *57*, 7938. (d) Bera, S.; Mondal, P.; Sarkar, D.; Pathi, V. B.; Pakrashy, S.; Datta, A.; Banerji, B. *J. Org. Chem.* **2021**, *86*, 7069.
81. Yu, S.; Hong, C.; Liu, Z.; Zhang, Y. *Org. Lett.* **2021**, *23*, 5054.
82. For selected reviews, see: (a) Fabry, D. C.; Rueping, M. *Acc. Chem. Res.* **2016**, *49*, 1969. (b) Levin, M. D.; Kim, S.; Toste, F. D. *ACS Cent. Sci.* **2016**, *2*, 293. (c) Wang, C.-S.; Dixneuf, P. H.; Soulé, J.-F. *Chem. Rev.* **2018**, *118*, 7532.
83. Kim, H. J.; Fabry, D. C.; Mader, S.; Rueping, M. *Org. Chem. Front.* **2019**, *6*, 2319.
84. For selected reviews, see: (a) Jiang, Y.; Xu, K.; Zeng, C. *Chem. Rev.* **2018**, *118*, 4485. (b) Tang, S.; Liu, Y.; Lei, A. *Chem* **2018**, *4*, 27. (c) Yuan, Y.; Lei, A. *Acc. Chem. Res.* **2019**, *52*, 3309. (d) Gandeepan, P.; Finger, L. H.; Meyer, T. H.; Ackermann, L. *Chem. Soc. Rev.* **2020**, *49*, 4254. (e) Jiao, K.-J.; Xing, Y.-K.; Yang, Q.-L.; Qiu, H.; Mei, T.-S. *Acc. Chem. Res.* **2020**, *53*, 300. (f) Siu, J. C.; Fu, N.; Lin, S. *Acc. Chem. Res.* **2020**, *53*, 547.
85. Qiu, Y.; Kong, W.-J.; Struwe, J.; Sauermann, N.; Rogge, T.; Scheremetjew, A.; Ackermann, L. *Angew. Chem. Int. Ed.* **2018**, *57*, 5828.
86. Kong, W.-J.; Finger, L. H.; Messinis, A. M.; Kuniyil, R.; Oliveira, J. C. A.; Ackermann, L. *J. Am. Chem. Soc.* **2019**, *141*, 17198.
87. (a) Kong, W.-J.; Finger, L. H.; Oliveira, J. C. A.; Ackermann, L. *Angew. Chem. Int. Ed.* **2019**, *58*, 6342. (b) Wang, Y.; Oliveira, J. C. A.; Lin, Z.; Ackermann, L. *Angew. Chem. Int. Ed.* **2021**, *60*, 6419. (c) Xing, Y.-K.; Chen, X.-R.; Yang, Q.-L.; Zhang, S.-Q.; Guo, H.-M.; Hong, X.; Mei, T.-S. *Nat. Commun.* **2021**, *12*, 930.
88. For selected reviews and examples, see: (a) Newton, C. G.; Wang, S.-G.; Oliveira, C. C.; Cramer, N. *Chem. Rev.* **2017**, *117*, 8908. (b) Mas-Roselló, J.; Herraiz, A. G.; Audic, B.; Laverny, A.; Cramer, N. *Angew. Chem. Int. Ed.* **2021**, *60*, 13198. (c) Newton, C. G.; Kossler, D.; Cramer, N. *J. Am. Chem. Soc.* **2016**, *138*, 3935.

89. Hyster, T. K.; Knörr, L.; Ward, T. R.; Rovis, T. *Science* **2012**, *338*, 500.

90. Ye, B.; Cramer, N. *Science* **2012**, *338*, 504.

91. (a) Jia, Z.-J.; Merten, C.; Gontla, R.; Daniliuc, C. G.; Antonchick, A. P.; Waldmann, H. *Angew. Chem. Int. Ed.* **2017**, *56*, 2429. (b) Trifonova, E. A.; Ankudinov, N. M.; Mikhaylov, A. A.; Chusov, D. A.; Nelyubina, Y. V.; Perekalin, D. S. *Angew. Chem. Int. Ed.* **2018**, *57*, 7714. (c) Audic, B.; Wodrich, M. D.; Cramer, N. *Chem. Sci.* **2019**, *10*, 781.

92. For representative examples, see: (a) Zheng, J.; Wang, S.-B.; Zheng, C.; You, S.-L. *J. Am. Chem. Soc.* **2015**, *137*, 4880. (b) Pham, M. V.; Cramer, N. *Chem. Eur. J.* **2016**, *22*, 2270. (c) Zheng, J.; Wang, S.-B.; Zheng, C.; You, S.-L. *Angew. Chem. Int. Ed.* **2017**, *56*, 4540. (d) Sun, Y.; Cramer, N. *Angew. Chem. Int. Ed.* **2017**, *56*, 364. (e) Shen, B.; Wan, B.; Li, X. *Angew. Chem. Int. Ed.* **2018**, *57*, 15534. (f) Li, H.; Gontla, R.; Flegel, J.; Merten, C.; Ziegler, S.; Antonchick, A. P.; Waldmann, H. *Angew. Chem. Int. Ed.* **2019**, *58*, 307. (g) Mi, R.; Zheng, G.; Qi, Z.; Li, X. *Angew. Chem. Int. Ed.* **2019**, *58*, 17666. (h) Kong, L.; Han, X.; Liu, S.; Zou, Y.; Lan, Y.; Li, X. *Angew. Chem. Int. Ed.* **2020**, *59*, 7188. (i) Yan, X.; Zhao, P.; Liang, H.; Xie, H.; Jiang, J.; Gou, S.; Wang, J. *Org. Lett.* **2020**, *22*, 3219. (j) Cui, W.-J.; Wu, Z.-J.; Gu, Q.; You, S.-L. *J. Am. Chem. Soc.* **2020**, *142*, 7379. (k) Sun, J.; Yuan, W.; Tian, R.; Wang, P.; Zhang, X.-P.; Li, X. *Angew. Chem. Int. Ed.* **2020**, *59*, 22706. (l) Chen, W.; Li, J.; Xie, H.; Wang, J. *Org. Lett.* **2020**, *22*, 3586. (m) Sun, L.; Liu, B.; Zhao, Y.; Chang, J.; Kong, L.; Wang, F.; Deng, W.-Q.; Li, X. *Chem. Commun.* **2021**, *57*, 8268. (n) Wang, F.; Jing, J.; Zhao, Y.; Zhu, X.; Zhang, X.-P.; Zhao, L.; Hu, P.; Deng, W.-Q.; Li, X. *Angew. Chem. Int. Ed.* **2021**, *60*, 16628. (o) Wang, Q.; Zhang, W.-W.; Zheng, C.; Gu, Q.; You, S.-L. *J. Am. Chem. Soc.* **2021**, *143*, 114.

93. (a) Yuan, C.; Liu, B. *Org. Chem. Front.* **2018**, *5*, 106. (b) Chen, P.; Wu, Y.; Zhu, S.; Jiang, H.; Ma, Z. *Org. Chem. Front.* **2018**, *5*, 132.

94. (a) Kang, J. W.; Maitlis, P. M. *J. Am. Chem. Soc.* **1968**, *90*, 3259. (b) Kang, J. W.; Moseley, K.; Maitlis, P. M. *J. Am. Chem. Soc.* **1969**, *91*, 5970.

95. (a) Albrecht, M. *Chem. Rev.* **2010**, *110*, 576. (b) Kisenyi, J. M.; Sunley, G. J.; Cabeza, J. A.; Smith, A. J.; Adams, H.; Salt, N. J.; Maitlis, P. M. *J. Chem. Soc., Dalton Trans.* **1987**, 2459. (c) Davies, D. L.; Donald, S. M. A.; Al-Duaij, O.; Macgregor, S. A.; Pölleth, M. *J. Am. Chem. Soc.* **2006**, *128*, 4210. (d) Hull, J. F.; Balcells, D.; Blakemore, J. D.; Incarvito, C. D.; Eisenstein, O.; Brudvig, G. W.; Crabtree, R. H. *J. Am. Chem. Soc.* **2009**, *131*, 8730. (e) Kashiwame, Y.; Kuwata, S.; Ikariya, T. *Chem. Eur. J.* **2010**, *16*, 766. (f) Wang, C.; Pettman, A.; Bacsa, J.; Xiao, J. *Angew. Chem. Int. Ed.* **2010**, *49*, 7548. (g) Wang, C.; Villa-Marcos, B.; Xiao, J. *Chem. Commun.* **2011**, *47*, 9773.

96. Janowicz, A. H.; Bergman, R. G. *J. Am. Chem. Soc.* **1982**, *104*, 352.

97. (a) Arndtsen, B. A.; Bergman, R. G.; Mobley, T. A.; Peterson, T. H. *Acc. Chem. Res.* **1995**, *28*, 154. (b) Hoyano, J. K.; McMaster, A. D.; Graham, W. A. G. *J. Am. Chem. Soc.* **1983**, *105*, 7190. (c) Arndtsen, B. A.; Bergman, R. G. *Science* **1995**, *270*, 1970. (d) Lohrenz, J. C. W.; Jacobsen, H. *Angew. Chem. Int. Ed.* **1996**, *35*, 1305. (e) Young, K. J. H.; Mironov, O. A.; Periana, R. A. *Organometallics* **2007**, *26*, 2137.

98. (a) Mkhalid, I. A. I.; Barnard, J. H.; Marder, T. B.; Murphy, J. M.; Hartwig, J. F. *Chem. Rev.* **2010**, *110*, 890. (b) Bower, J. F.; Krische, M. J. J. I. C. *Top Organomet. Chem.* **2011**, *34*, 107. (c) Hashiguchi, B. G.; Bischof, S. M.; Konnick, M. M.; Periana, R. A. *Acc. Chem. Res.* **2012**, *45*, 885. (d) Hartwig, J. F. *Acc. Chem. Res.* **2012**, *45*, 864. (e) Ros, A.; Fernández, R.; Lassaletta, J. M. *Chem. Soc. Rev.* **2014**, *43*, 3229.

99. Haldar, C.; Hoque, M. E.; Chaturvedi, J.; Hassan, M. M. M.; Chattopadhyay, B. *Chem. Commun.* **2021**, *57*, 13059.

100. For representative examples, see: (a) Itoh, M.; Hirano, K.; Satoh, T.; Shibata, Y.; Tanaka, K.; Miura, M. *J. Org. Chem.* **2013**, *78*, 1365. (b) Shin, K.; Park, S.-W.; Chang, S. *J. Am. Chem. Soc.* **2015**, *137*, 8584. (c) Huang, L.; Hackenberger, D.; Gooßen, L. J. *Angew. Chem. Int. Ed.* **2015**, *54*, 12607. (d) Zhang, S.-S.; Jiang, C.-Y.; Wu, J.-Q.; Liu, X.-G.; Li, Q.; Huang, Z.-S.; Li, D.; Wang, H. *Chem. Commun.* **2015**, *51*, 10240. (e) Shin, K.; Park, Y.; Baik, M.-H.; Chang, S. *Nat. Chem.* **2018**, *10*, 218. (f) Kim, J.; Shin, K.; Jin, S.; Kim, D.; Chang, S. *J. Am. Chem. Soc.* **2019**, *141*, 4137. (g) Gao, P.; Guo, W.; Xue, J.; Zhao, Y.; Yuan, Y.; Xia, Y.; Shi, Z. *J. Am. Chem. Soc.* **2015**, *137*, 12231. (h) Tan, G.; Ran, C.; You, J. *Org. Chem. Front.* **2018**, *5*, 2930. (i) Tan, G.; You, Q.; You, J. *ACS Catal.* **2018**, *8*, 8709. (j) Chen, S.; Zhang, M.; Su, R.; Chen, X.; Feng, B.; Yang, Y.; You, J. *ACS Catal.* **2019**, *9*, 6372. (k) Chen, Y.; Quan, Y.; Xie, Z. *Chem. Commun.* **2020**, *56*, 7001.

101. Kim, J.; Park, S.-W.; Baik, M.-H.; Chang, S. *J. Am. Chem. Soc.* **2015**, *137*, 13448.

102. Pan, S.; Wakaki, T.; Ryu, N.; Shibata, T. *Chem. Asian J.* **2014**, *9*, 1257.

103. (a) Quan, Y.; Xie, Z. *J. Am. Chem. Soc.* **2014**, *136*, 15513. (b) Sun, Y.; Meng, K.; Zhang, J.; Jin, M.; Huang, N.; Zhong, G. *Org. Lett.* **2019**, *21*, 4868. (c) Meng, K.; Sun, Y.; Zhang, J.; Zhang, K.; Ji, X.; Ding, L.; Zhong, G. *Org. Lett.* **2019**, *21*, 8219.

104. Xia, Y.; Liu, Z.; Feng, S.; Zhang, Y.; Wang, J. *J. Org. Chem.* **2015**, *80*, 223.

105. (a) Chen, X.-Y.; Sorensen, E. J. *Chem. Sci.* **2018**, *9*, 8951. (b) Tian, T.; Dong, A.-S.; Chen, D.; Cao, X.-T.; Wang, G. *Org. Biomol. Chem.* **2019**, *17*, 7664.

106. Jha, N.; Singh, R. P.; Saxena, P.; Kapur, M. *Org. Lett.* **2021**, *23*, 8694.

107. Xu, L.; Meng, K.; Zhang, J.; Sun, Y.; Lu, X.; Li, T.; Jiang, Y.; Zhong, G. *Chem. Commun.* **2019**, *55*, 9757.

108. For selected examples, see: (a) Zhou, J.; Shi, J.; Qi, Z.; Li, X.; Xu, H. E.; Yi, W. *ACS Catal.* **2015**, *5*, 6999. (b) Li, X.; Wu, G.; Liu, X.; Zhu, Z.; Huo, Y.; Jiang, H. *J. Org. Chem.* **2017**, *82*, 13003. (c) Chen, C.; Liu, P.; Tang, J.; Deng, G.; Zeng, X. *Org. Lett.* **2017**, *19*, 2474. (d) Li, G.; Hu, J.; Zeng, R.; Shi, D.-Q.; Zhao, Y. *Org. Lett.* **2018**, *20*, 2454. (e) Kona, C. N.; Nishii, Y.; Miura, M. *Angew. Chem. Int. Ed.* **2019**, *58*, 9856. (f) Wu, G.; Ouyang, W.; Chen, Q.; Huo, Y.; Li, X. *Org. Chem. Front.* **2019**, *6*, 284. (g) Sun, X.; Zhao, W.; Li, B.-J. *Chem. Commun.* **2020**, *56*, 1298.

109. (a) Shin, K.; Kim, H.; Chang, S. *Acc. Chem. Res.* **2015**, *48*, 1040. (b) Sk, M. R.; Bera, S. S.; Basuli, S.; Metya, A.; Maji, M. S. *Asian J. Org. Chem.* **2020**, *9*, 1701.

110. For representative examples, see: (a) Ryu, J.; Kwak, J.; Shin, K.; Lee, D.; Chang, S. *J. Am. Chem. Soc.* **2013**, *135*, 12861. (b) Kim, H.; Park, J.; Kim, J. G.; Chang, S. *Org. Lett.* **2014**, *16*, 5466. (c) Hwang, H.; Kim, J.; Jeong, J.; Chang, S. *J. Am. Chem. Soc.* **2014**, *136*, 10770. (d) Kim, J.; Chang, S. *Angew. Chem. Int. Ed.* **2014**, *53*, 2203. (e) Patel, P.; Chang, S. *Org. Lett.* **2014**, *16*, 3328. (f) Kim, H.; Shin, K.; Chang, S. *J. Am. Chem. Soc.* **2014**, *136*, 5904. (g) Becker, P.; Pirwerdjan, R.; Bolm, C. *Angew. Chem. Int. Ed.* **2015**, *54*, 15493. (h) Kim, Y.; Park, J.; Chang, S. *Org. Lett.* **2016**, *18*, 1892. (i) Zhang, Y.-F.; Wu, B.; Shi, Z.-J. *Chem. Eur. J.* **2016**, *22*, 17808. (j) Chen, S.; Feng, B.; Zheng, X.; Yin, J.; Yang, S.; You, J. *Org. Lett.* **2017**, *19*, 2502. (k) Hwang, Y.; Park, Y.; Chang, S. *Chem. Eur. J.* **2017**, *23*, 11147. (l) Zhang, W.; Yang, D.; Wang, W.; Wang, S.; Zhao, H. *Eur. J. Org. Chem.* **2018**, *2018*, 2071. (m) Yu, M.; Zhang, T.; Jalani, H. B.; Dong, X.; Lu, H.; Li, G. *Org. Lett.* **2018**, *20*, 4828.

111. For selected examples, see: (a) Figg, T. M.; Park, S.; Park, J.; Chang, S.; Musaev, D. G. *Organometallics* **2014**, *33*, 4076. (b) Shin, K.; Chang, S. *J. Org. Chem.* **2014**, *79*, 12197. (c) Pan, C.; Jin, N.; Zhang, H.; Han, J.; Zhu, C. *J. Org. Chem.* **2014**, *79*, 9427. (d) Gwon, D.; Lee, D.; Kim, J.; Park, S.; Chang, S. *Chem. Eur. J.* **2014**, *20*, 12421. (e) Pi, C.; Cui, X.; Wu, Y. *J. Org. Chem.* **2015**, *80*, 7333. (f) Park, Y.; Heo, J.; Baik, M.-H.; Chang, S. *J. Am. Chem. Soc.* **2016**, *138*, 14020. (g) Li, Y.; Feng, Y.; Xu, L.; Wang, L.; Cui, X. *Org. Lett.* **2016**, *18*, 4924. (h) Xu, L.; Tan, L.; Ma, D. *J. Org. Chem.* **2016**, *81*, 10476. (i) Kim, S.; Chakrasali, P.; Suh, H. S.; Mishra, N. K.; Kim, T.; Han, S. H.; Kim, H. S.; Lee, B. M.; Han, S. B.; Kim, I. S. *J. Org. Chem.* **2017**, *82*, 7555. (j) Mu, D.; Wang, X.; Chen, G.; He, G. *J. Org. Chem.* **2017**, *82*, 4497. (k) Xu, L.; Wang, L.; Feng, Y.; Li, Y.; Yang, L.; Cui, X. *Org. Lett.* **2017**, *19*, 4343. (l) Xia, J.; Yang, X.; Li, Y.; Li, X. *Org. Lett.* **2017**, *19*,

3243. (m) Zhang, W.; Deng, H.; Li, H. *Org. Chem. Front.* **2017**, *4*, 2202. (n) Wang, L.; Yang, Z.; Yang, M.; Zhang, R.; Kuai, C.; Cui, X. *Org. Biomol. Chem.* **2017**, *15*, 8302. (o) Pan, C.; Wang, Y.; Wu, C.; Yu, J.-T. *Org. Biomol. Chem.* **2018**, *16*, 3711. (p) Li, W.-H.; Dong, L. *Adv. Syn. Catal.* **2018**, *360*, 1104. (q) Mishra, A.; Mukherjee, U.; Vats, T. K.; Deb, I. *J. Org. Chem.* **2018**, *83*, 3756. (r) Das, D.; Samanta, R. *Adv. Syn. Catal.* **2018**, *360*, 379. (s) Hou, H.; Zhao, Y.; Sheng, S.; Chen, J. *Adv. Syn. Catal.* **2019**, *361*, 4393. (t) Xiong, H.; Gu, Y.; Zhang, S.; Lu, F.; Ji, Q.; Liu, L.; Ma, P.; Yang, G.; Hou, W.; Xu, H. *Chem. Commun.* **2020**, *56*, 4692. (u) Hwang, S.-H.; Choi, T.-L. *Org. Lett.* **2020**, *22*, 2935. (v) Feng, Y.; Zhang, Z.; Fu, Q.; Yao, Q.; Huang, H.; Shen, J.; Cui, X. *Chin. Chem. Lett.* **2020**, *31*, 58. (w) Yoo, K.; Hong, E. J.; Huynh, T. Q.; Kim, B.-S.; Kim, J. G. *ACS Sustainable Chem. Eng.* **2021**, *9*, 8679.

112. Kang, T.; Kim, Y.; Lee, D.; Wang, Z.; Chang, S. *J. Am. Chem. Soc.* **2014**, *136*, 4141.
113. Xiao, X.; Hou, C.; Zhang, Z.; Ke, Z.; Lan, J.; Jiang, H.; Zeng, W. *Angew. Chem. Int. Ed.* **2016**, *55*, 11897.
114. (a) Kathiravan, S.; Nicholls, I. A. *Chem. Eur. J.* **2017**, *23*, 7031. (b) Erbing, E.; Sanz-Marco, A.; Vázquez-Romero, A.; Malmberg, J.; Johansson, M. J.; Gómez-Bengoa, E.; Martín-Matute, B. *ACS Catal.* **2018**, *8*, 920. (c) Guzmán Santiago, A. J.; Brown, C. A.; Sommer, R. D.; Ison, E. A. *Dalton Trans.* **2020**, *49*, 16166.
115. Kathiravan, S.; Anaspure, P.; Zhang, T.; Nicholls, I. A. *Org. Lett.* **2021**, *23*, 3331.
116. For selected reviews and examples, see: (a) Hartwig, J. F. *Chem. Soc. Rev.* **2011**, *40*, 1992. (b) Boebel, T. A.; Hartwig, J. F. *J. Am. Chem. Soc.* **2008**, *130*, 7534. (c) Kawamorita, S.; Ohmiya, H.; Hara, K.; Fukuoka, A.; Sawamura, M. *J. Am. Chem. Soc.* **2009**, *131*, 5058. (d) Kawamorita, S.; Ohmiya, H.; Sawamura, M. *J. Org. Chem.* **2010**, *75*, 3855. (e) Ishiyama, T.; Isou, H.; Kikuchi, T.; Miyaura, N. *Chem. Commun.* **2010**, *46*, 159. (f) Yamazaki, K.; Kawamorita, S.; Ohmiya, H.; Sawamura, M. *Org. Lett.* **2010**, *12*, 3978. (g) Ros, A.; Estepa, B.; López-Rodríguez, R.; Álvarez, E.; Fernández, R.; Lassaletta, J. M. *Angew. Chem. Int. Ed.* **2011**, *50*, 11724. (h) Ros, A.; López-Rodríguez, R.; Estepa, B.; Álvarez, E.; Fernández, R.; Lassaletta, J. M. *J. Am. Chem. Soc.* **2012**, *134*, 4573. (i) Larsen, M. A.; Hartwig, J. F. *J. Am. Chem. Soc.* **2014**, *136*, 4287. (j) Kuninobu, Y.; Ida, H.; Nishi, M.; Kanai, M. *Nat. Chem.* **2015**, *7*, 712. (k) Bisht, R.; Chattopadhyay, B. *J. Am. Chem. Soc.* **2016**, *138*, 84. (l) Davis, H. J.; Mihai, M. T.; Phipps, R. J. *J. Am. Chem. Soc.* **2016**, *138*, 12759. (m) Davis, H. J.; Genov, G. R.; Phipps, R. J. *Angew. Chem. Int. Ed.* **2017**, *56*, 13351. (n) Hoque, M. E.; Bisht, R.; Haldar, C.; Chattopadhyay, B. *J. Am. Chem. Soc.* **2017**, *139*, 7745.

117. For selected reviews and examples, see: (a) Cheng, C.; Hartwig, J. F. *Chem. Rev.* **2015**, *115*, 8946. (b) Choi, G.; Tsurugi, H.; Mashima, K. *J. Am. Chem. Soc.* **2013**, *135*, 13149. (c) Cheng, C.; Hartwig, J. F. *J. Am. Chem. Soc.* **2015**, *137*, 592. (d) Fukumoto, Y.; Hirano, M.; Chatani, N. *ACS Catal.* **2017**, *7*, 3152. (e) Karmel, C.; Rubel, C. Z.; Kharitonova, E. V.; Hartwig, J. F. *Angew. Chem. Int. Ed.* **2020**, *59*, 6074. (f) Yan, Z.-B.; Peng, M.; Chen, Q.-L.; Lu, K.; Tu, Y.-Q.; Dai, K.-L.; Zhang, F.-M.; Zhang, X.-M. *Chem. Sci.* **2021**, *12*, 9748.

118. For representative examples, see: (a) Nishimura, T.; Yasuhara, Y.; Hayashi, T. *J. Am. Chem. Soc.* **2007**, *129*, 7506. (b) Shibata, T.; Hashimoto, Y.-k.; Otsuka, M.; Tsuchikama, K.; Endo, K. *Synlett* **2011**, *22*, 2075. (c) Nishimura, T.; Ebe, Y.; Hayashi, T. *J. Am. Chem. Soc.* **2013**, *135*, 2092. (d) Nagamoto, M.; Nishimura, T. *Chem. Commun.* **2014**, *50*, 6274. (e) Nagata, T.; Hirano, K.; Satoh, T.; Miura, M. *J. Org. Chem.* **2014**, *79*, 8960. (f) Suzuki, C.; Hirano, K.; Satoh, T.; Miura, M. *Org. Lett.* **2015**, *17*, 1597. (g) Zhou, T.; Li, L.; Li, B.; Song, H.; Wang, B. *Org. Lett.* **2015**, *17*, 4204. (h) Phatake, R. S.; Patel, P.; Ramana, C. V. *Org. Lett.* **2016**, *18*, 292. (i) Phatake, R. S.; Patel, P.; Ramana, C. V. *Org. Lett.* **2016**, *18*, 2828. (j) Li, S.-S.; Wu, L.; Qin, L.; Zhu, Y.-Q.; Su, F.; Xu, Y.-J.; Dong, L. *Org. Lett.* **2016**, *18*, 4214. (k) Yan, K.; Li, B.; Wang, B. *Adv. Syn. Catal.* **2018**, *360*, 2272. (l) Mahesha, C. K.; Agarwal, D. S.; Karishma, P.; Markad, D.; Mandal, S. K.; Sakhuja, R. *Org. Biomol. Chem.* **2018**, *16*, 8585. (m) Liu, M.; Gong, W.; You, E.; Zhang, H.; Shi, L.; Cao, W.; Shi, J. *Eur. J. Org. Chem.* **2018**, *2018*, 4991. (n) Zhang, G.; Hu, Z.; Bertoli, G.; Gooßen, L. J. *ACS Catal.* **2019**, *9*, 8153. (o) Mishra, A.; Mukherjee, U.; Sarkar, W.; Meduri, S. L.; Bhowmik, A.; Deb, I. *Org. Lett.* **2019**, *21*, 2056. (p) Liu, G.; Kuang, G.; Zhang, X.; Lu, N.; Fu, Y.; Peng, Y.; Zhou, Y. *Org. Lett.* **2019**, *21*, 3043. (q) Luo, Y.; Guo, L.; Yu, X.; Ding, H.; Wang, H.; Wu, Y. *Eur. J. Org. Chem.* **2019**, *2019*, 3203. (r) Zhang, L.; Chen, J.; Chen, J.; Jin, L.; Zheng, X.; Jiang, X.; Yu, C. *Tetrahedron Lett.* **2019**, *60*, 1053. (s) Sihag, P.; Jeganmohan, M. *J. Org. Chem.* **2019**, *84*, 2699. (t) Zhou, K.; Geng, J.; Wang, D.; Zhang, J.; Zhao, Y. *Org. Lett.* **2020**, *22*, 5109. (u) Tomita, E.; Yamada, K.; Shibata, Y.; Tanaka, K.; Kojima, M.; Yoshino, T.; Matsunaga, S. *Angew. Chem. Int. Ed.* **2020**, *59*, 10474. (v) Maeng, C.; Son, J.-Y.; Lee, S. C.; Baek, Y.; Um, K.; Han, S. H.; Ko, G. H.; Han, G. U.; Lee, K.; Lee, K.; Lee, P. H. *J. Org. Chem.* **2020**, *85*, 3824. (w) Yu, Z.; Zhang, Y.; Tang, J.; Zhang, L.; Liu, Q.; Li, Q.; Gao, G.; You, J. *ACS Catal.* **2020**, *10*, 203. (x) Li, M.; Dong, Y.; Zhou, C.; Bai, J.; Cheng, J.; Sun, J.; Sun, S. *Org. Lett.* **2021**, *23*, 8229.

119. For selected reviews and examples, see: (a) Woźniak, Ł.; Tan, J.-F.; Nguyen, Q.-H.; Madron du Vigné, A.; Smal, V.; Cao, Y.-X.; Cramer, N. *Chem. Rev.* **2020**, *120*, 10516. (b) Yoshino, T.; Matsunaga, S. *ACS Catal.* **2021**, *11*, 6455. (c) Nishimura, T.; Yasuhara, Y.; Nagaosa, M.; Hayashi, T. *Tetrahedron: Asymmetry* **2008**, *19*, 1778. (d) Nishimura, T.; Nagamoto, M.; Ebe, Y.; Hayashi, T. *Chem. Sci.* **2013**, *4*, 4499. (e) Nagamoto, M.; Yamauchi, D.; Nishimura, T. *Chem. Commun.* **2016**, *52*, 5876.

120. Qiu, Y.; Stangier, M.; Meyer, T. H.; Oliveira, J. C. A.; Ackermann, L. *Angew. Chem. Int. Ed.* **2018**, *57*, 14179.

121. Yang, Q.-L.; Xing, Y.-K.; Wang, X.-Y.; Ma, H.-X.; Weng, X.-J.; Yang, X.; Guo, H.-M.; Mei, T.-S. *J. Am. Chem. Soc.* **2019**, *141*, 18970.

122. For selected examples, see: (a) Ye, X.; Wang, C.; Zhang, S.; Wei, J.; Shan, C.; Wojtas, L.; Xie, Y.; Shi, X. *ACS Catal.* **2020**, *10*, 11693. (b) Yang, Q.-L.; Jia, H.-W.; Liu, Y.; Xing, Y.-K.; Ma, R.-C.; Wang, M.-M.; Qu, G.-R.; Mei, T.-S.; Guo, H.-M. *Org. Lett.* **2021**, *23*, 1209. (c) Kim, Y.; Kim, D.; Chang, S. *Chem. Commun.* **2021**, *57*, 12309.

Chapter 6: Rhodium || Spirocyclization

Regio- and Diastereoselective [3+2]-Spiroannulation of Benzoxazines with Chalcones: A Rh(III)-Catalyzed Redox-Neutral Approach to α-Aroyl Spiro-Indanamines

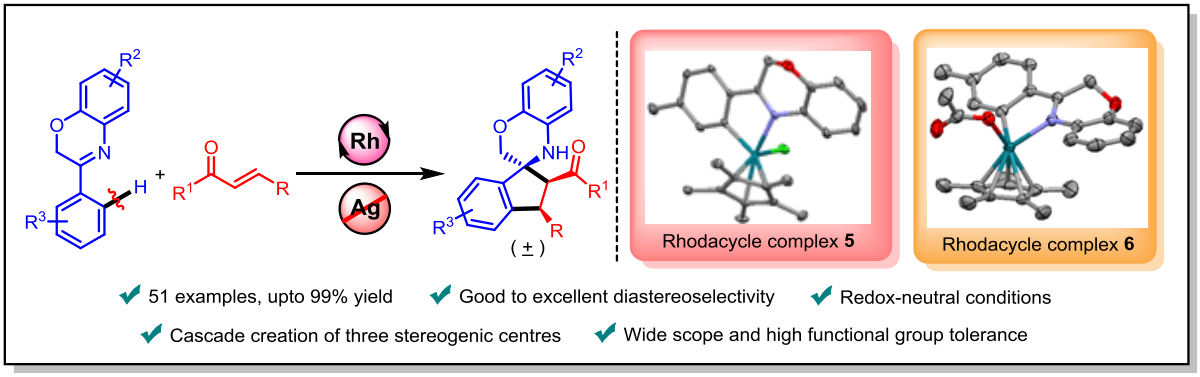

6.1. Introduction

6.1.1. Relevance of Benzoxazine and Indane/Indene Frameworks

2,3-dihydro-1,4-benzoxazine core as well as other benzoxazine derivatives remain one of the most important scaffolds in synthetic organic chemistry with diverse biological and ecological activities and therefore constitute a part of a wide spectrum of biologically active small molecules. The biological activities include anticancer, antibiotic, antibacterial, antifungal, phytotoxic, anti-arrythmic, antithrombotic, antihyperlipidemic, calcium antagonism, 5-HT3 receptor antagonism, inhibiting nature of CETP enzyme, among others.[1] 1,4-Benzoxazine scaffold is present in many natural products, for e.g. Obscurinervidine, a natural alkaloid, and also form a part of many commercially available drugs like Levofloxacin and Ofloxacin which are commercially available antibiotics. Some of the representative biologically relevant benzoxazine derivatives are depicted in Figure 6.1.1.1. Owing to their thermal characteristics, benzoxazine derivatives also find their use in material science and polymer chemistry. Consequently, there is an immense need for their synthesis and application in synthetic organic chemistry research field and has hence attracted the attention of chemists all over the world.

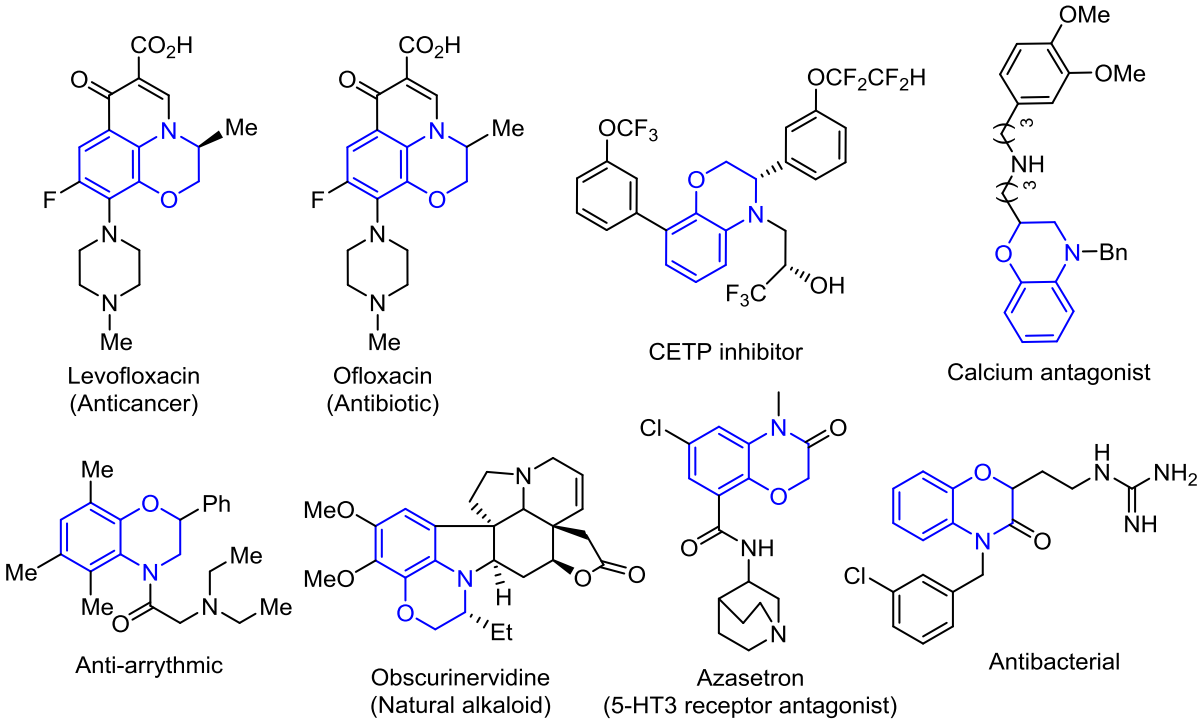

Figure 6.1.1.1. Representative examples of biologically relevant benzoxazine derivatives.

On the other end, indane and its multiple analogues like indene, 1-indanamine, 1-indenone, 1,3-indanedione, etc. represent an appealing biological profile providing a useful assay for the

rational development of therapeutically and medicinally important molecules designed and deliberated at diversified biological targets showing varied properties like anti-proliferative, anticancer, anti-inflammatory, anti-arrythmic, among others.[2] They along with pharmacophores based out of them serve as functional scaffolds for the development of commercially available drugs and pharmaceuticals, *viz.* Indinavir, Sulindac, donepezil, etc. and in addition to the development of neuroleptics and neuroprotective molecules. They also show properties such as CGRP receptor antagonists, calcium antagonists, carbonic anhydrase inhibitory properties and many more.

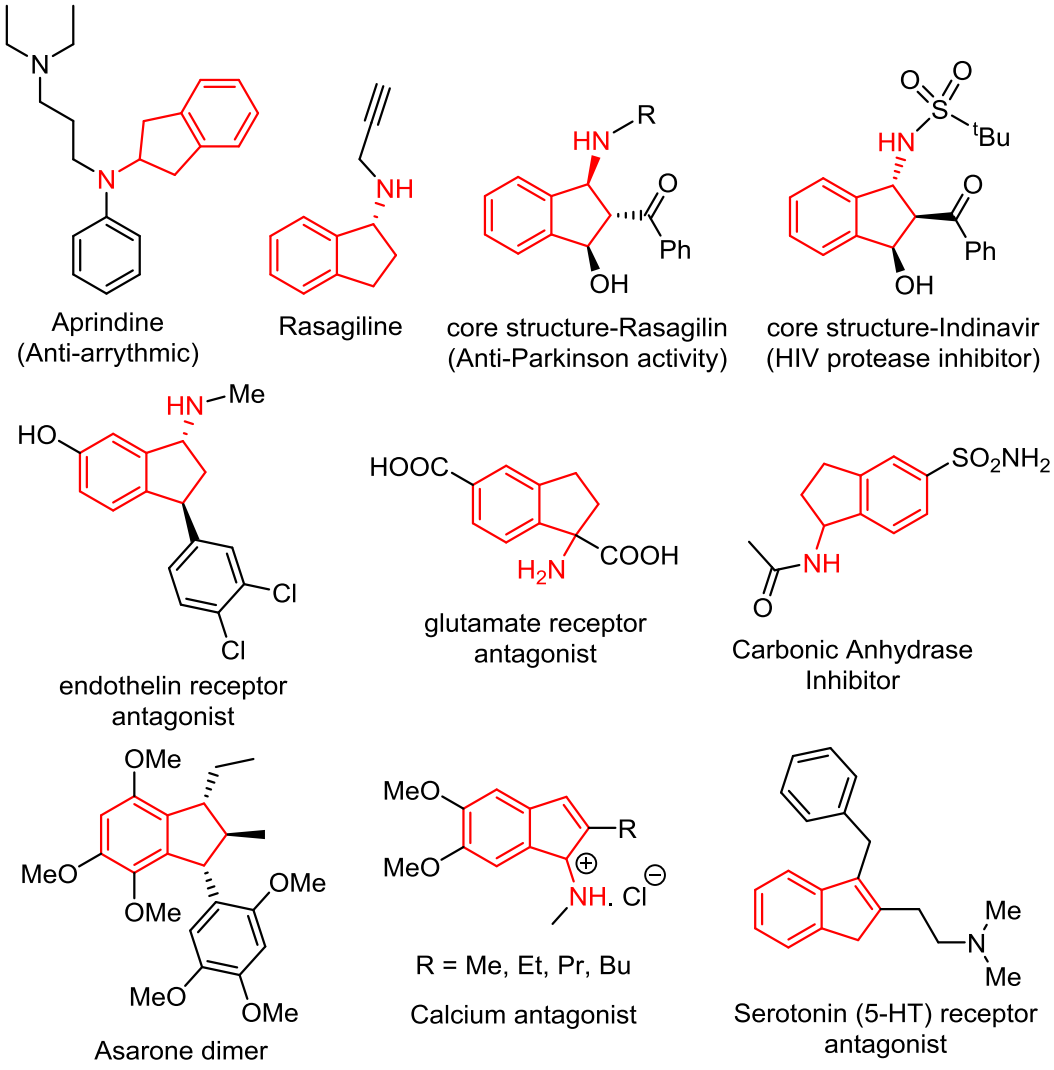

Figure 6.1.1.2. Representative examples of biologically relevant indane/indene derivatives.

The oxidized form, indene moieties in conjuncture showcase their usefulness in developing anticancer drugs. Besides, these indane frameworks constitute an array of natural products which also show therapeutic properties making them prospective drug candidates. They reflect core structure of a broad spectrum of natural products, as a result, various synthetic methods

have been applied for their synthesis and they are also used as valuable precursors for many different biologically and synthetically important heterocycles. Some of the biologically important indanyl/indenyl derivatives are shown in Figure 6.1.1.2. Owing to the huge importance of indane and its analogous nuclei in a plethora of scientific fields, their synthesis and incorporation is highly desirable in organic synthesis.

6.1.2. Strategies For Transition Metal-Catalyzed [3+2]-Annulation

C–C and C–X (X = heteroatom) bond formation has been the fundamental pillar of strengths for the synthetic organic chemistry community. Along this line, from its inception transition metal-catalyzed C–H activation over the past two to three decades has become a master strategy for the direct manufacturing of functionalized molecules owing to the ubiquitous nature of C–H bonds in numerous organic frameworks.[3] Apart from simple C–H functionalization reactions to get cross-coupled products using the help of directing groups, annulation chemistry is one of the chief components of this technique whose successful implementation has paved way to diverse multifaceted cyclic structures.[4] On account of the importance of carbocyclic skeletons like (spiro)indanes/indenes, more so, (spiro)indanamines/indenamines as discussed in the previous section, their creation via C–H activation triggered intermolecular tandem [3+2]-annulation reactions using Re,[5] Rh,[6] Ru,[7] Ir,[8] Co,[9] and Mn[10] as transition metal catalysts under oxidative as well as redox-neutral conditions has seen a consistent rise in application by several research groups. This has been achieved utilizing the directing strategy of various class of imines and other electrophilic C=N bond containing diverse directing substrates to combine with a wide array of suitable unsaturated hydrocarbon coupling partners *viz.* alkynes, allenes, maleimides, acrylates, among others. Some of the representative examples on [3+2]-annulation of imines are depicted in Scheme 6.1.2.1.

In 2005, Takai group reported the first [3+2]-annulation between aromatic aldimines and phenyl acetylenes via rhenium-catalyzed C–H activation giving rise to indene frameworks (Scheme 6.1.2.1a).[5a] Since then, several research groups have developed unique methodologies on C–H activation assisted [3+2]-annulation chemistry exploiting the imine functionality. In 2010, they again devised a Re-catalyzed diastereoselective synthesis of aminoindanes treating aromatic imines with allenes through an intermolecular insertion/intramolecular nucleophilic cyclization sequence (Scheme 6.1.2.1b).[5c] Rhodium catalysis in [3+2]-annulation of imines was first exemplified by Miura *et al.* in 2009, when they demonstrated an oxidative coupling between aromatic imines and alkynes in a regioselective fashion providing indenone imines

(Scheme 6.1.2.1c).[6a] Following year, Zhao group described a rhodium-catalyzed [3+2]-annulation of *N*-unsubstituted arylimines and internal alkynes leading to the synthesis of indene-based tertiary carbinamines (Scheme 6.1.2.1d).[6b] In 2013, Dong and co-workers employed cyclic *N*-sulfonyl ketimines in [3+2]-spiroannulation with internal alkynes to furnish spirocyclic sultam scaffolds under Rh-catalyzed conditions (Scheme 6.1.2.1e).[6d] In 2017, Li *et al.* delineated a Rh(III)-catalyzed diastereodivergent synthesis of spirocyclic indanamines coupling cyclic *N*-acyl or *N*-sulfonyl ketimines with activated alkenes under redox-neutral mild reaction conditions (Scheme 6.1.2.1f).[6i] Simultaneously, Kim group disclosed a highly diastereoselective [3+2]-annulation of *N*-sulfonyl aldimines with maleimides and other activated olefins for the synthesis of 1-aminoindanes via rhodium-catalyzed C–H alkylation/intramolecular cyclization chain of events (Scheme 6.1.2.1g).

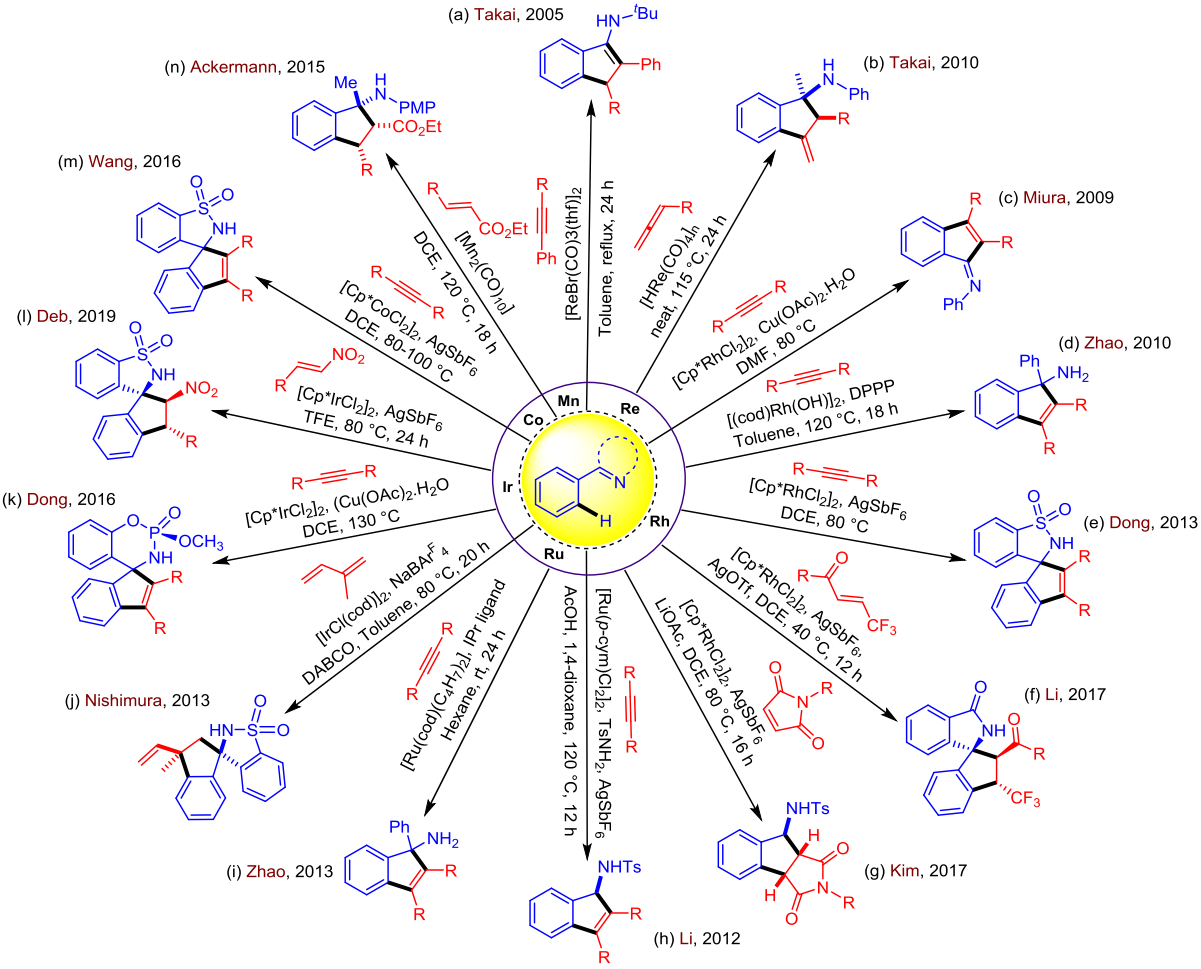

Scheme 6.1.2.1. Imines as DG in [3+2]-(spiro)annulation reactions.

Ruthenium catalysis has also been applied in imine-directed [3+2]-annulation reactions. In 2012, Li and co-workers achieved a Ru(II)-catalyzed [3+2]-annulation of *N*-sulfonyl aldimines

with alkynes producing indenamines needing a sulfonamide cocatalyst (Scheme 6.1.2.1h).[7a] Next year, Zhao group developed a cross-coupled carbocyclization strategy between unsubstituted aromatic ketimines with alkynes under ambient reaction conditions using a combination of Ru(II)/π-allyl catalyst precursor and NHC ligands (Scheme 6.1.2.1i).[7b] In 2013, Nishimura and co-workers reported the first iridium-catalyzed highly regio- and diastereoselective synthesis of aminoindane derivatives via a [3+2]-spiroannulation of cyclic *N*-sulfonyl ketimines with 1,3-dienes (Scheme 6.1.2.1j).[8a] In 2016, Dong *et al.* revealed an Ir(III)-catalyzed cascade C–H activation/Grignard-type [3+2]-annulation of *N*-phosphoryl ketimines with alkynes forming spirocyclic phosphoramide derivatives with high efficiency and selectivity (Scheme 6.1.2.1k).[8b] In 2019, Deb group described an iridium-catalyzed redox-neutral [3+2]-spirocyclization reaction between cyclic *N*-sulfonyl ketimines and nitroalkenes with high yields and diastereoselectivity which led to the synthesis of nitro-substituted novel spirocyclic benzosultams (Scheme 6.1.2.1l).[8c] Shifting attention to first-row transition metal catalysis in [3+2]-annulation reaction using imines as directing substrates, in 2016, Wang *et al.* demonstrated a Cp*Co(III)-catalyzed cascade C–H alkenylation/[3+2]-annulation of weakly coordinating cyclic *N*-sulfonyl ketimines with alkynes generating a series of spirocyclic indenyl benzosultams (Scheme 6.1.2.1m).[9a] In 2015, Ackermann group reported the first Mn-catalyzed highly regio- and chemoselective C–H activation/alkene annulation of aromatic ketimines with activated olefinic esters for the expedient synthesis of functionalized β-amino acid ester derivatives with unusual cis-stereoselectivity (Scheme 6.1.2.1n).[10]

Over the years, few reports have also surfaced even successfully accomplishing the enantioselective annulation versions.[11] In 2011, Cramer group described a Rh(I)-catalyzed enantioselective [3+2]-annulation of unsubstituted ketimines with internal alkynes using a chiral bisphosphine based biphenyl ligand giving access to a broad range of chiral 1-aminoindenes with good yields and high enantiomeric ratio (Scheme 6.1.2.2).[11a] The reaction is highly regioselective with respect to unsymmetrical alkynes and tolerates a wide array of functional groups and heterocycles.

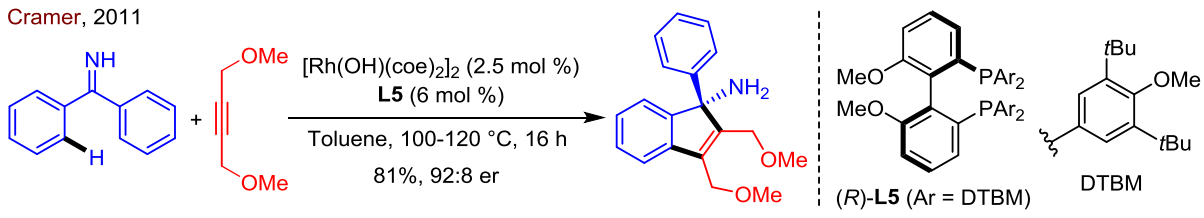

Scheme 6.1.2.2. Imine as DG in enantioselective [3+2]-annulation.

6.1.3. Benzoxazines and Chalcones in C–H Activation

From the previous section, it is evident that most of the imines used in transition metal-catalyzed C–H activation/annulation are either activated ketimines carrying electron-withdrawing groups like acyl, sulfonyl, and phosphonyl groups, or aromatic aldimines bearing a tosyl group. On the flip side, the use of unactivated ketimines is somewhat limited in this area.[5c,10,12] Recently, relatively less reactive general aromatic imines devoid of an activating group like cyclic ketimines such as 2*H*-benzo[*b*][1,4]oxazines, or simply benzoxazines, have been rarely used in [3+2]-spirocyclization reactions.[12] Their imine functionality has been nurtured as a robust chelating entity in transition metal-catalyzed C–H activation/[3+2]-annulation cascade to deliver densely functionalized spiro-indanamines/indenamines on coupling with appropriate partners (Scheme 6.1.3.1).

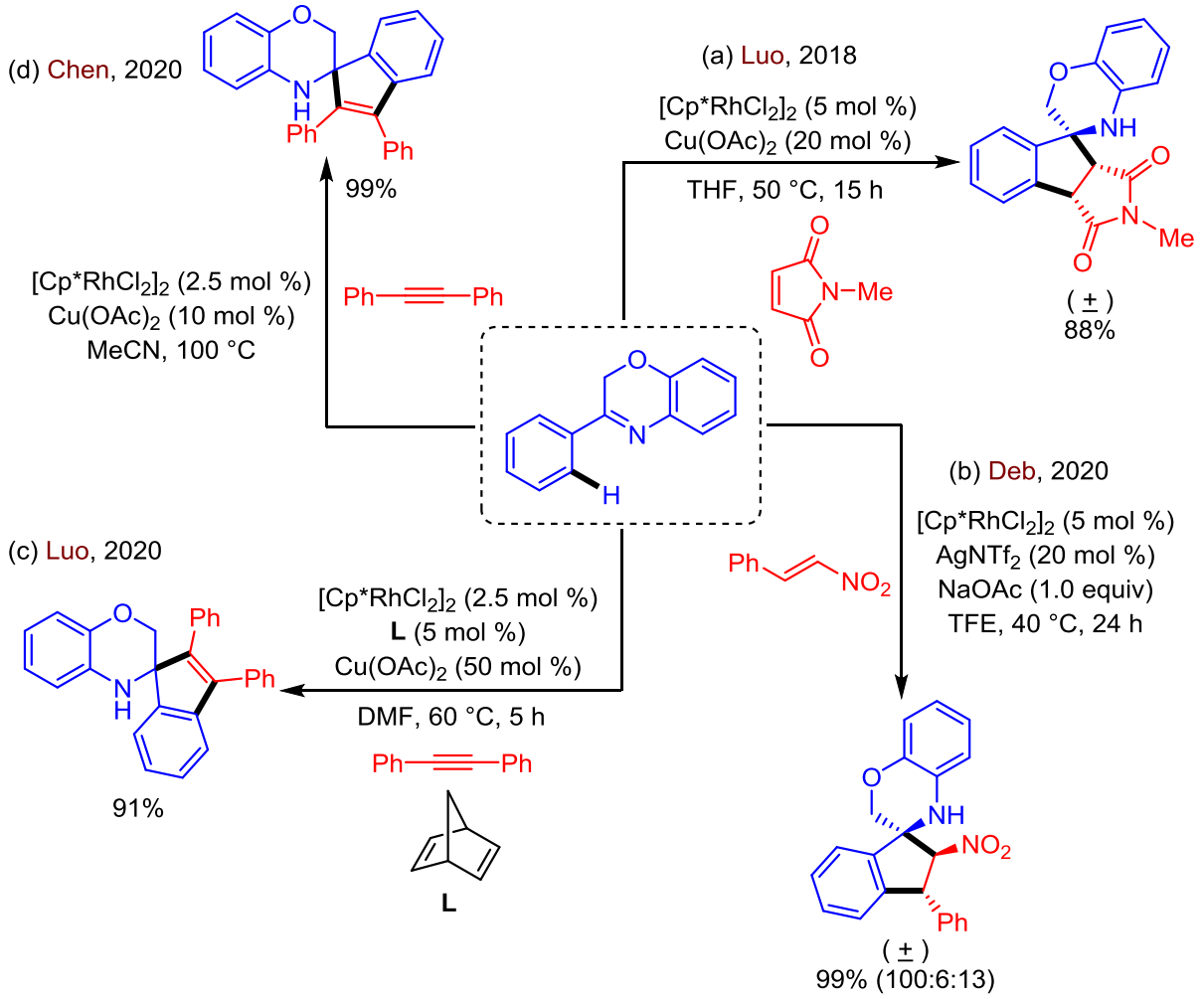

Scheme 6.1.3.1. Benzoxazine as DG in C–H functionalizations.

In 2018, Luo group disclosed the first example of the use of unactivated cyclic ketimines, benzoxazines in a Rh(III)-catalyzed [3+2]-annulation reaction with *N*-substituted maleimides to afford spirocyclic multichiral-centered indanyl amines in high yields and excellent diastereoselectivity (Scheme 6.1.3.1a).[12a] In 2020, Deb *et al.* described a mild redox-neutral Cp*Rh-catalyzed C–H activation triggered [3+2]-spirocyclization of benzoxazines with α,β-unsaturated nitroolefins giving access to a novel class of biologically relevant nitro-substituted spirocyclic 2,3-dihydro-1,4-benzoxazine derivatives in good yields accompanying high diastereoselectivity (Scheme 6.1.3.1b).[12b] In the same year, Luo and co-workers again developed a strategy for rhodium-catalyzed [3+2]-annulation of benzoxazines with alkynes (Scheme 6.1.3.1c).[12c] This reaction showed the importance of externally added olefin-based ligands which accelerated the reaction by increasing the turnover rate and promoting the conversion of $[Cp^*RhCl_2]_2$ in forming the rhodacycle intermediate in the C–H activation step. Concurrently, Chen group delineated a Rh-catalyzed [3+2]-spiroannulation between 3-Aryl-2*H*-benzo[*b*][1,4]oxazines and alkynes giving rise to benzoxazine-indene derivatives in high yields via an imine-directed C–H alkenylation/annulation cascade (Scheme 6.1.3.1d).[12d]

Chalcones or α,β-unsaturated ketones are medicinally privileged compounds and form a central core of many biologically relevant compounds possessing a broad spectrum of biological activities like anticancer, anti-inflammatory, antidiabetic, antioxidant, antiviral, antimicrobial properties and can also act as fluorescent materials.[13] Hence, they have found renowned interests for their synthetic manipulations in both academia and industry. Chalcones are easily accessible scaffolds whose application has been primarily restricted to 1,4-addition partners in the realm of transition metal-catalyzed C–H activation (Scheme 6.1.3.2).[3i,l,14]

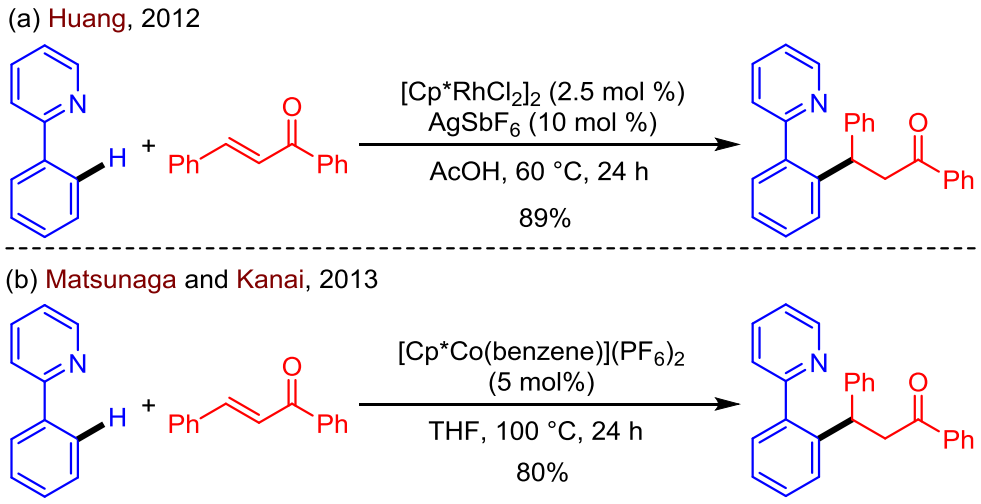

Scheme 6.1.3.2. Chalcones as 1,4-addition coupling partner in C–H functionalizations.

In 2012, Huang and co-workers revealed a Rh-catalyzed C–H activation/conjugate addition of 2-phenylpyridines to chalcones and other α,β-unsaturated ketones to furnish *ortho*-alkylated products (Scheme 6.1.3.1a).[14a] In this reaction, AcOH plays a crucial role in the proton-transfer effect associated with the conjugate addition. Following year, Matsunaga and Kanai group demonstrated a Cp*Co(III)-catalyzed 1,4-addition of 2-arylpyridines to chalcones and other polar electrophiles without using any external additives (Scheme 6.1.3.2b).[14b]

6.2. Objective

It is apparent from literature that benzoxazines, chalcones and (spiro)indanamines are all biologically and synthetically important scaffolds. The use of benzoxazines has been limited in [3+2]-spirocyclization reactions, on the other hand, with the presence of the activated double bond, there is ample scope for the application of chalcones in annulation reactions via C–H activation which is also not very well explored. We hypothesized that both these entities can be coupled together to form attractive spirocyclic scaffolds possessing polysubstituted indanyl amine cores containing an acyl group at C2-position, which could be biologically and structurally important in synthesizing further important molecules. This can be achieved via a cascade annulation reaction (β-arylation followed by α-aminomethylation) employing sterically challenging β-substituted α,β-unsaturated ketones in combination with 1,4-benzoxazines which is not known to the best of our knowledge.

As evident from previous sections, rhodium-catalyzed C–H activation has played a key role in [3+2]-annulation chemistry generating unique cyclic structures in a regio- and stereoselective manner. Encouraged by these observations, we aimed to develop a methodology for the spirocyclization between the rarely used benzoxazines and easily accessible chalcones employing rhodium catalysis. Persistent with our research interests in transition metal-catalyzed C–H functionalization for the efficient and sustainable synthesis of functionalized heterocycles, we therefore described a tandem C–H activation/[3+2]-annulation cascade reaction between benzoxazines and chalcones under redox-neutral rhodium-catalyzed conditions for the synthesis of a series of novel spirocycles containing three consecutive stereogenic centers in a highly diastereoselective manner (Scheme 6.2.1). In the process, imine-ligated half-sandwich rhodacycle complex intermediates have also been synthesized and their catalytic activity has been harnessed in this spiroannulation strategy.

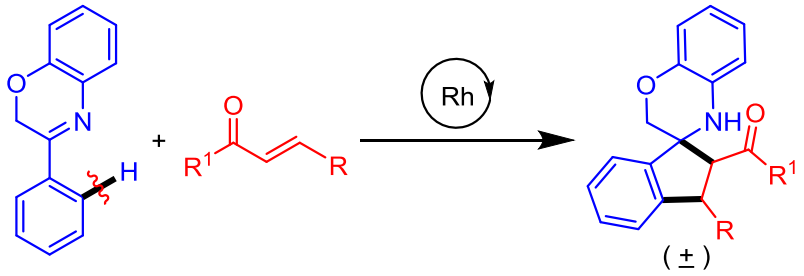

Scheme 6.2.1. Objective of this work: rhodium-catalyzed [3+2]-spiroannulation of benzoxazines with chalcones.

6.3. Results and Discussion

6.3.1. Optimization Studies

We initiated the reaction taking 3-phenyl-2*H*-benzo[*b*][1,4]oxazine (**1a**) as the parent cyclic imine substrate and (*E*)-chalcone (**2a**) as the suitable α,β-unsaturated carbonyl compound reaction partner using a catalytic system of $[Cp^*RhCl_2]_2/AgNTf_2$ (5 mol %/20 mol %), NaOAc (1.0 equiv) as additive in TFE solvent (0.1 M) at 100 °C for 24 h under N_2 atmosphere. Under these conditions, spiroannulated product phenyl(3'-phenyl-2,2',3',4-tetrahydrospiro[benzo[*b*][1,4]oxazine-3,1'-inden]-2'-yl)methanone was obtained as a mixture of three inseparable diastereomers (**3a**/**3a′**/**3a″**) in an overall combined yield of 71% with excellent diastereoselectivity (100:10:1) (Table 6.3.1.1, entry 1). The major diastereomer was obtained exclusively by crystallization from hot EtOH/$CHCl_3$ mixture and its relative geometry was established unambiguously by single crystal X-ray analysis of related products during substrate scope of the reaction shown in a later section. Inquisitive of whether the halide scavenger $AgNTf_2$ salt is needed for the reaction, delightfully in its absence the product was obtained in an excellent yield of 93% maintaining the superior diastereoselectivity (100:5:6), ascertaining the fact that the reaction does not require toxic silver salts for its progress (Table 6.3.1.1, entry 2). Changing solvents ranging from polar to non-polar as well as protic to aprotic ones like DCE, HFIP, Toluene, MeCN, 1,4-dioxane, DMF, THF, and $PhCF_3$ (Table 6.3.1.1, entries 3-10) proved to be fruitless since none of them gave the desired product, except for another fluorinated solvent HFIP which delivered the product in a reduced combined yield of 76% with a moderately good diastereomeric ratio of 100:28:23. So, TFE continued to be our solvent of choice. Next, a series of different acetate sources and sodium salts were screened as additives like LiOAc, KOAc, CsOAc, $Cu(OAc)_2$, AgOAc, NaOBz, NaOPiv, and NaOTf but except for $Cu(OAc)_2$ and AgOAc which yielded no product, rest of them had a detrimental effect on the reaction without hampering much of the selectivity (Table 6.3.1.1, entries 11-18).

Table 6.3.1.1. Optimization of reaction conditions[a]

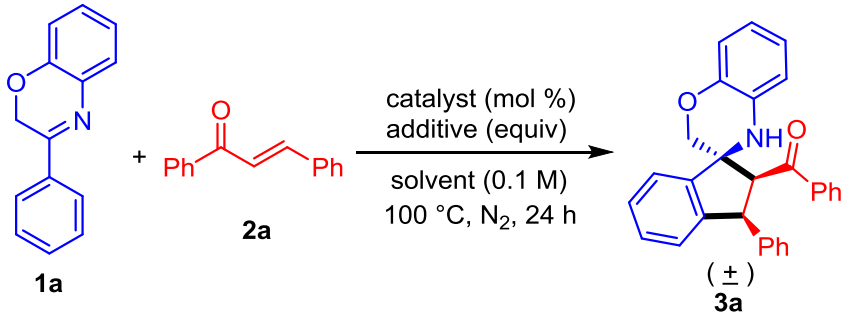

entry	catalyst (mol %)	additive (equiv)	solvent (0.1 M)	yield (%) of **3a**[b] (dr)
1	$[Cp^*RhCl_2]_2$ (5)/$AgNTf_2$ (20)	NaOAc (1.0)	TFE	71 (100:10:1)
2	$[Cp^*RhCl_2]_2$ (5)	NaOAc (1.0)	TFE	93 (100:5:6)
3	$[Cp^*RhCl_2]_2$ (5)	NaOAc (1.0)	DCE	nd
4	$[Cp^*RhCl_2]_2$ (5)	NaOAc (1.0)	HFIP	76 (100:28:23)
5	$[Cp^*RhCl_2]_2$ (5)	NaOAc (1.0)	Toluene	nd
6	$[Cp^*RhCl_2]_2$ (5)	NaOAc (1.0)	MeCN	nd
7	$[Cp^*RhCl_2]_2$ (5)	NaOAc (1.0)	1,4-dioxane	nd
8	$[Cp^*RhCl_2]_2$ (5)	NaOAc (1.0)	DMF	nd
9	$[Cp^*RhCl_2]_2$ (5)	NaOAc (1.0)	THF	nd
10	$[Cp^*RhCl_2]_2$ (5)	NaOAc (1.0)	$PhCF_3$	nd
11	$[Cp^*RhCl_2]_2$ (5)	LiOAc (1.0)	TFE	36 (100:15:3)
12	$[Cp^*RhCl_2]_2$ (5)	KOAc (1.0)	TFE	62 (100:11:7)
13	$[Cp^*RhCl_2]_2$ (5)	CsOAc (1.0)	TFE	58 (100:14:9)
14	$[Cp^*RhCl_2]_2$ (5)	$Cu(OAc)_2$ (1.0)	TFE	nd
15	$[Cp^*RhCl_2]_2$ (5)	AgOAc (1.0)	TFE	nd
16	$[Cp^*RhCl_2]_2$ (5)	NaOBz (1.0)	TFE	63 (100:7:4)
17	$[Cp^*RhCl_2]_2$ (5)	NaOPiv (1.0)	TFE	78 (100:5:4)
18	$[Cp^*RhCl_2]_2$ (5)	NaOTf (1.0)	TFE	nd
19	$[Cp^*RhCl_2]_2$ (5)	NaOAc (0.5)	TFE	82 (100:6:6)
20	$[Cp^*RhCl_2]_2$ (5)	NaOAc (1.5)	TFE	92 (100:4:4)
21	$[Cp^*RhCl_2]_2$ (3)	NaOAc (1.0)	TFE	53 (100:2:1)
22[c]	$[Cp^*RhCl_2]_2$ (5)	NaOAc (1.0)	TFE	70 (100:3:1)
23[d]	$[Cp^*RhCl_2]_2$ (5)	NaOAc (1.0)	TFE	96 (100:18:8)
24[e]	$[Cp^*RhCl_2]_2$ (5)	NaOAc (1.0)	TFE	89 (100:3:2)
25[f]	$[Cp^*RhCl_2]_2$ (5)	NaOAc (1.0)	TFE	96 (100:2:2)
26[g]	**$[Cp^*RhCl_2]_2$ (5)**	**NaOAc (1.0)**	**TFE**	**98 (100:4:5)**
27[h]	$[Cp^*RhCl_2]_2$ (5)	NaOAc (1.0)	TFE	47 (100:5:2)
28	$[Cp^*Rh(MeCN)_3](SbF_6)_2$ (5)	NaOAc (1.0)	TFE	83 (100:14:9)
29	$[Cp^*IrCl_2]_2$ (5)	NaOAc (1.0)	TFE	nd
30	$[Ru(p\text{-}cym)Cl_2]_2$ (5)	NaOAc (1.0)	TFE	nd
31	$[Cp^*Co(CO)I_2]$ (5)	NaOAc (1.0)	TFE	nd
32[i]	$[Cp^{*}RhCl_2]_2$ (5)	NaOAc (1.0)	TFE	91 (100:6:4)
33	-	NaOAc (1.0)	TFE	nd
34	$[Cp^*RhCl_2]_2$ (5)	-	TFE	nd

[a]Reaction conditions: Unless otherwise mentioned, all reactions were performed with **1a** (0.2 mmol, 1.0 equiv), **2a** (1.1 equiv), catalyst (mol %) and additive (equiv) in solvent (2.0 mL, 0.1 M) at 100 °C for 24 h under N_2. [b]Combined isolated yield of all the diastereomers, only major diastereomer is shown and dr given within parenthesis is calculated by ^1H NMR. [c]Reaction was run at 80 °C. [d]Reaction was run at 120 °C. [e]Reaction was run for 18 h. [f]**2a** (1.3 equiv). [g]**2a** (1.5 equiv). [h]Reaction was performed under air. [i]**1a** (1.5 equiv) and **2a** (0.2 mmol, 1.0 equiv). "nd" stands for "not detected".

When the loading of NaOAc was decreased to 0.5 equiv, a fall in the yield of the reaction was observed; whereas on increasing the loading to 1.5 equiv, the product was obtained in similar yield of 92% (Table 6.3.1.1, entries 19-20). Lowering the loading of the rhodium catalyst to 3 mol % led to a sharp dip in the yield of the product to 53% (Table 6.3.1.1, entry 21). On decreasing the reaction temperature to 80 °C, the yield dropped to 70%, while increasing it to 120 °C, the yield remained similar (96%); on the other hand, running the reaction for a lesser time of 18 h furnished the product in a slightly diminished yield of 89% (Table 6.3.1.1, entries 22-24). Interestingly, on increasing the loading of **2a** to 1.3 equiv, the yield increased slightly to 96% keeping up the good diastereoslectivity (Table 6.3.1.1, entry 25); further increament to 1.5 equiv led to the formation of the spirocyclized product **3a** in almost quantitative yield of 98% with an excellent diastereomeric ratio of 100:4:5 (Table 6.3.1.1, entry 26), which ultimately proved to be our optimized reaction condition. On performing the reaction under an air atmosphere, it saw a significant drop in the yield of the reaction to 47% (Table 6.3.1.1, entry 27), which established the need for an inert atmosphere for the present methodology. Screening a different rhodium catalyst $[Cp^*Rh(MeCN)_3](SbF_6)_2$ resulted in a decreased yield of 83% (Table 6.3.1.1, entry 28). When other similar Cp*-based catalysts like $[Cp^*IrCl_2]_2$, $[Ru(p\text{-}cym)Cl_2]_2$, $[Cp^*Co(CO)I_2]$ were tested under the present conditions, none of them succeeded in producing the spiroannulated product **3a** (Table 6.3.1.1, entries 29-31).

Since the product was difficult to separate from the (*E*)-chalcone (**2a**), we checked the fate of the reaction reversing the ratio of the substrate (**1a**) and chalcone partner (**2a**), making **2a** the limiting reagent this time. The reaction yielded the product in 91% yield with a diastereoselectivity of 100:6:4 (Table 6.3.1.1, entry 32). This reverse ratio experiment could be successfully exploited in cases where the product separation would be difficult using a normal ratio. In general, all the cases gave good to excellent diastereoselective results. Finally, control experiments suggested that the use of both the Rh(III) catalyst and NaOAc additive are of utmost importance for the current protocol since the desired product was not formed in their absence (Table 6.3.1.1, entries 33-34).

6.3.2. Scope of the Reaction

A series of benzoxazines (**1**) and chalcones (**2**) were prepared following literature procedures, discussed in the experimental section.

Benzoxazines (**1a-1t**) were prepared following the literature procedure by a condensation reaction between 2-aminophenols and phenacyl bromides in DCM solvent at room temperature (Table 6.3.2.1).

Table 6.3.2.1. List of benzoxazine substrates prepared

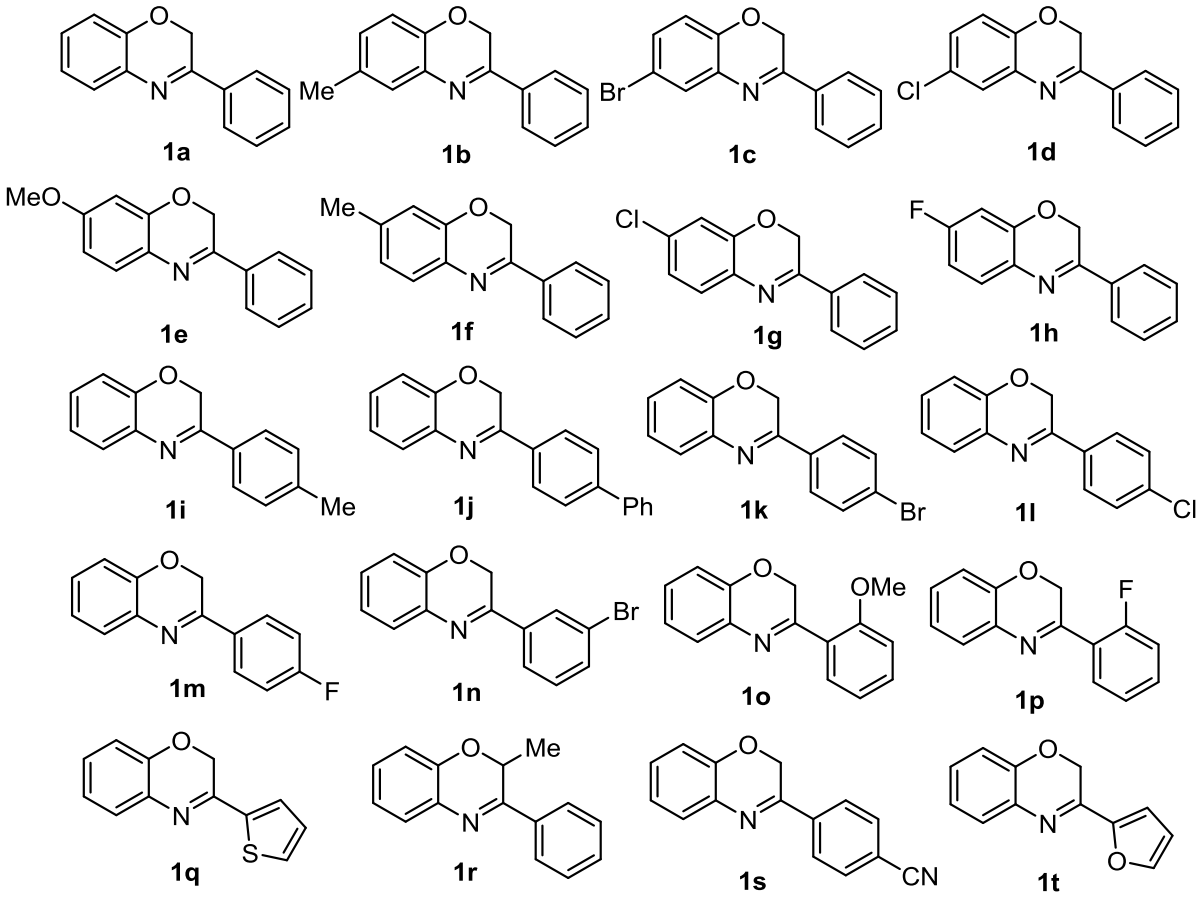

Chalcones and α,β-unsaturated carbonyl compounds (**2a-2at**) were prepared following the literature procedure by a condensation reaction between different aldehydes and acetophenones in EtOH solvent at room temperature (Table 6.3.2.2).

Table 6.3.2.2. List of chalcones and other α,β-unsaturated carbonyl compounds prepared

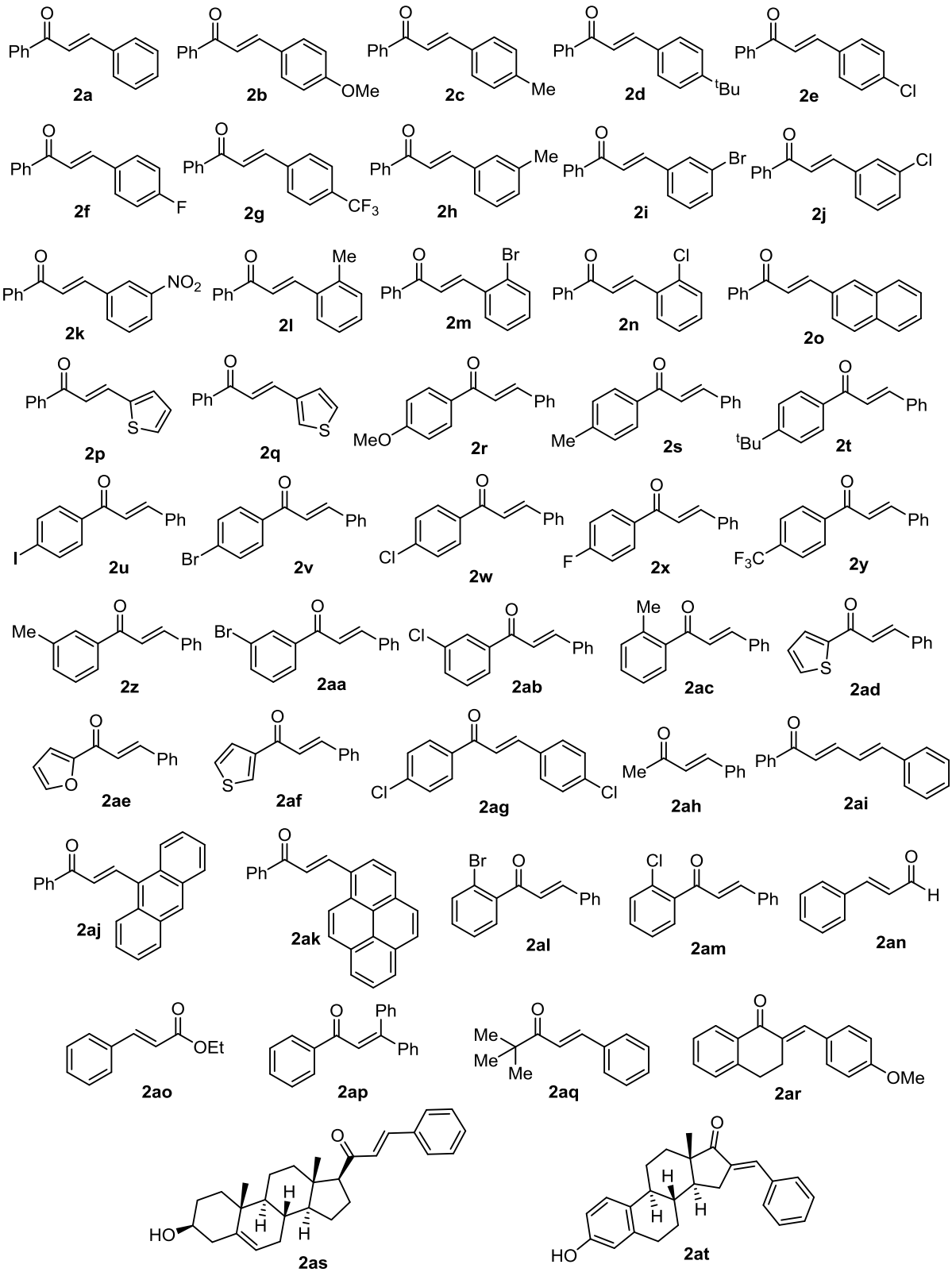

After the preparation of the benzoxazine (**1**) and chalcone (**2**) derivatives, they were subjected to the [3+2]-spiroannulation reaction under the optimized condition to evaluate the scope and

generality of the reaction (Table 6.3.2.3-6.3.2.5). At first, we went on to explore a series of diverse chalcones **2** with substitutions on the aldehyde side by reacting with 3-phenyl-2*H*-benzo[*b*][1,4]oxazine (**1a**) (Table 6.3.2.3).

Table 6.3.2.3. Scope of Cyclization of Benzoxazine **1a** and Substituted Chalcones **2**[a]

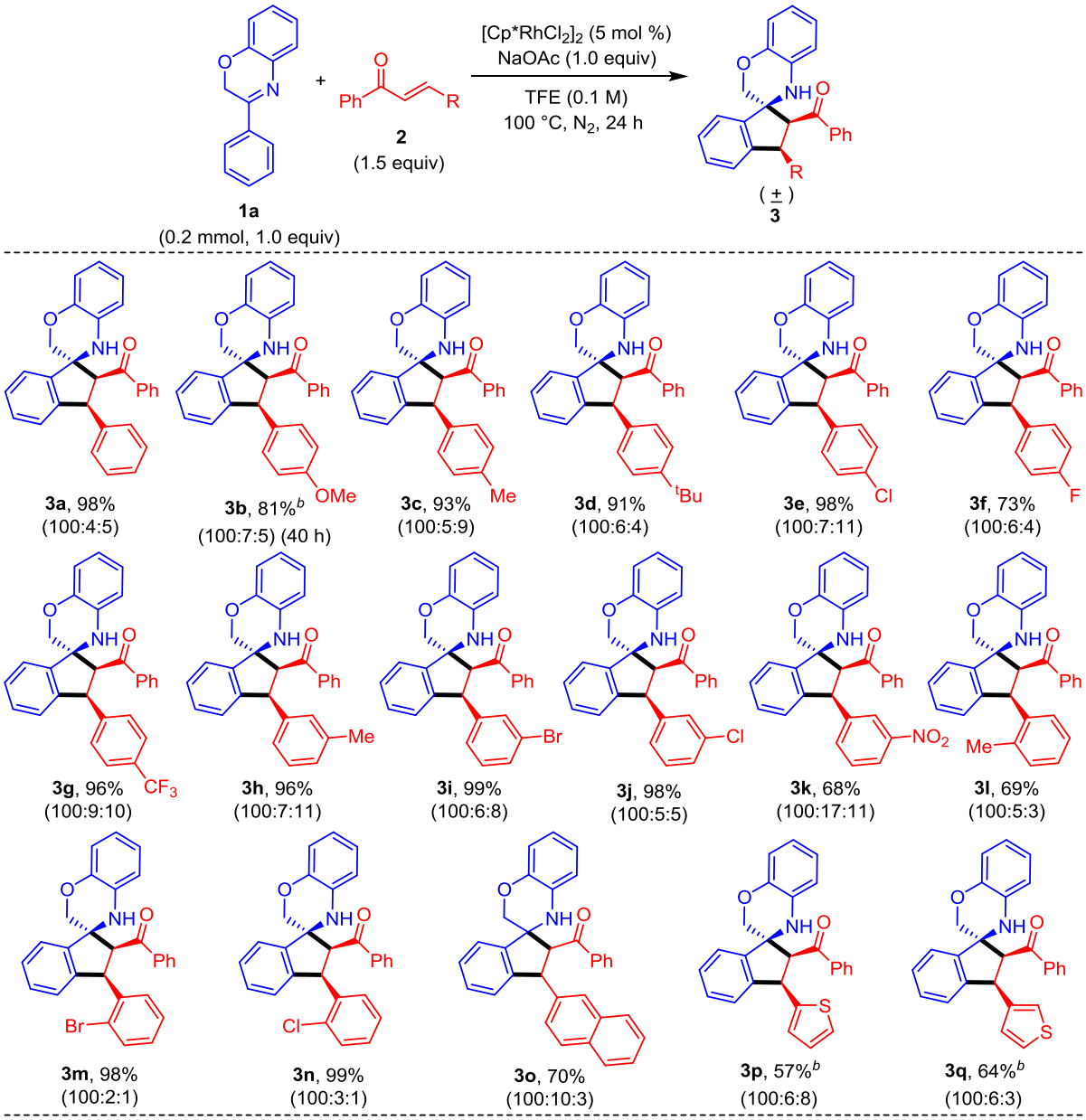

[a]Combined isolated yield of all the diastereomers; only the major diastereomer is shown (except for **3o** as it could not be crystallized); dr given within parenthesis is calculated by ^{1}H NMR. [b]**1a** (1.5 equiv) and **2** (0.2 mmol, 1.0 equiv) were taken.

Generally, the electronic effects of the substituents on the aromatic ring at β-position of the chalcones did not have any substantial impact, with both electron-donating and -withdrawing groups at all positions being tolerated well. Electron-donating group containing substrates

carrying methoxy, methyl, and tert-butyl substitutions at the *para* position delivered the products in yields up to 93% with excellent selectivity (**3b**-**3d**). Substrates carrying electron-withdrawing substituents like chloro, fluoro, and trifluoromethyl produced similar results in terms of both yield (up to 98%) and diastereoselectivity (**3e**-**3g**). Moving forward to *meta*-substituted chalcones, there was a perceptible rise in the yield of the products (up to 99%) for all kinds of substitutions (**3h**-**3j**) except for the highly electron-withdrawing nitro substituent which furnished the spirocyclized product **3k** in a moderately good yield (68%) though maintaining a good selectivity (100:17:11). Next, the *ortho*-substituted chalcones containing electron-withdrawing group successfully generated the desired products in excellent yields and diastereoselectivity with electron-withdrawing chalcones faring splendidly (**3m**, 98%; **3n**, 99%) over electron-donating chalcone (**3l**, 69%). Pleasingly, bulky naphthyl chalcone and heterocyclic variant like thiophene-tethered chalcone produced the corresponding spirocyclized products (**3o**-**3q**) in moderate to good yields (up to 70%) keeping up with the impressive diastereoselectivity.

The scope of chalcones was subsequently extended to chalcones **2** with variations in the aryl group on the ketone side (Table 6.3.2.4). First, *para*-substituted chalcones bearing a wide array of functional groups like methoxy, methyl, tert-butyl, iodo, bromo, chloro, fluoro, trifluoromethyl were tested under the optimized reaction condition, and all of them were well tolerated yielding the targeted compounds (**3r**-**3y**) in good to excellent yields (73-99%) along with promising selectivity. A yield range of 94-96% was achieved when *meta*-substituted reactants were screened carrying electron-donating methyl group and electron-withdrawing bromo and chloro groups (**3z**-**3ab**). However, there was a sharp decline in the yield of the reaction for o*rtho*-methyl substituted chalcone producing 45% of the product **3ac** while continuing with a good diastereomeric ratio (100:7:6). Once again to our delight, the presence of heterocycles like thiophene and furan in place of the phenyl group of the chalcones handed the desired products (**3ad**-**3af**) in excellent yields (93-99%) with very good selectivity. Changing both sides of the chalcone by taking a doubly *para* chloro substituted derivative continued to carry the baton affording the spirocyclized product **3ag** in 88% yield with an excellent diastereomeric ratio of 100:4:4. Gratifyingly, when we replaced the phenyl group on the ketone side of the chalcone with a methyl group, *viz.* (*E*)-4-phenylbut-3-en-2-one and subjected it to the standard condition, it awarded the desired product **3ah** as a single diastereomer, albeit in a lower yield of 25%.

Table 6.3.2.4. Scope of Cyclization of Benzoxazine **1a** and Substituted Chalcones **2**[a]

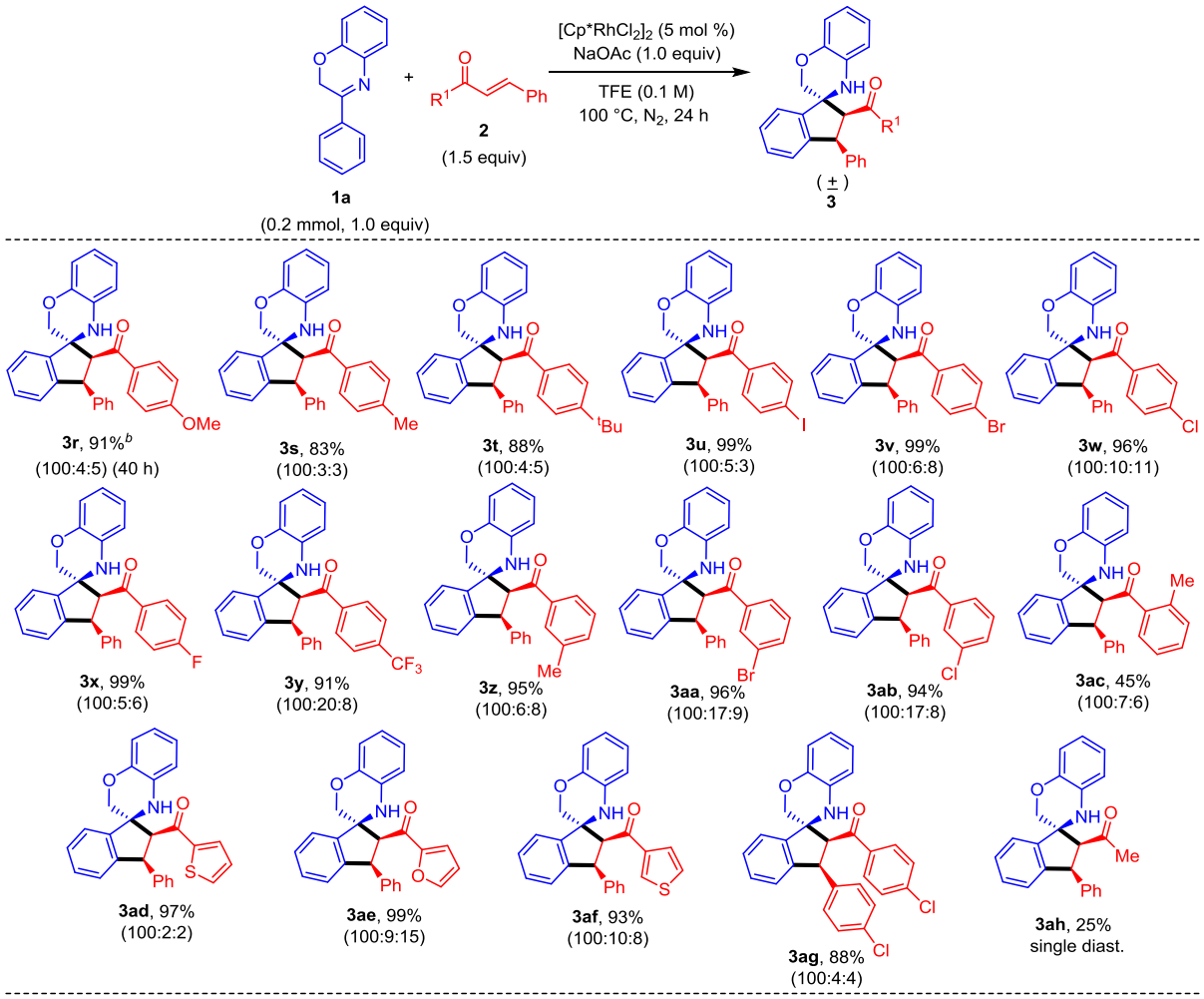

[a]Combined isolated yield of all the diastereomers; only the major diastereomer is shown; dr given within parenthesis is calculated by ^{1}H NMR. [b]**1a** (1.5 equiv) and **2** (0.2 mmol, 1.0 equiv) were taken.

Thereafter, we turned our attention towards the substituted benzoxazines (**1b-1r**) with varied functional groups at different positions of both the aryl rings, which were made to react with (*E*)-chalcone (**2a**) as the coupling partner (Scheme 6.3.2.5). First, substituents on the benzoxazine ring comprising of both electron-donating and electron-withdrawing groups (**1b-1h**) were tested. All of them reacted smoothly and the desired products (**4a-4g**) were obtained in good to excellent yields (up to 93%) complemented by good to excellent diastereoselectivity, except for the bromo equivalent which reacted poorly to give its corresponding product in slightly lower yield (**4b**, 44%). Next, substituents on the phenyl ring of the benzoxazine substrate were screened. Methyl and phenyl groups at the *para* position of the ring performed excellently, whereas bromo, chloro, and fluoro groups gave slightly below par yields (38-96%) of their spirocyclized products (**4h-4l**) though with very good selectivity.

Table 6.3.2.5. Scope of Cyclization of Benzoxazine **1** and (*E*)-chalcone **2a**[a]

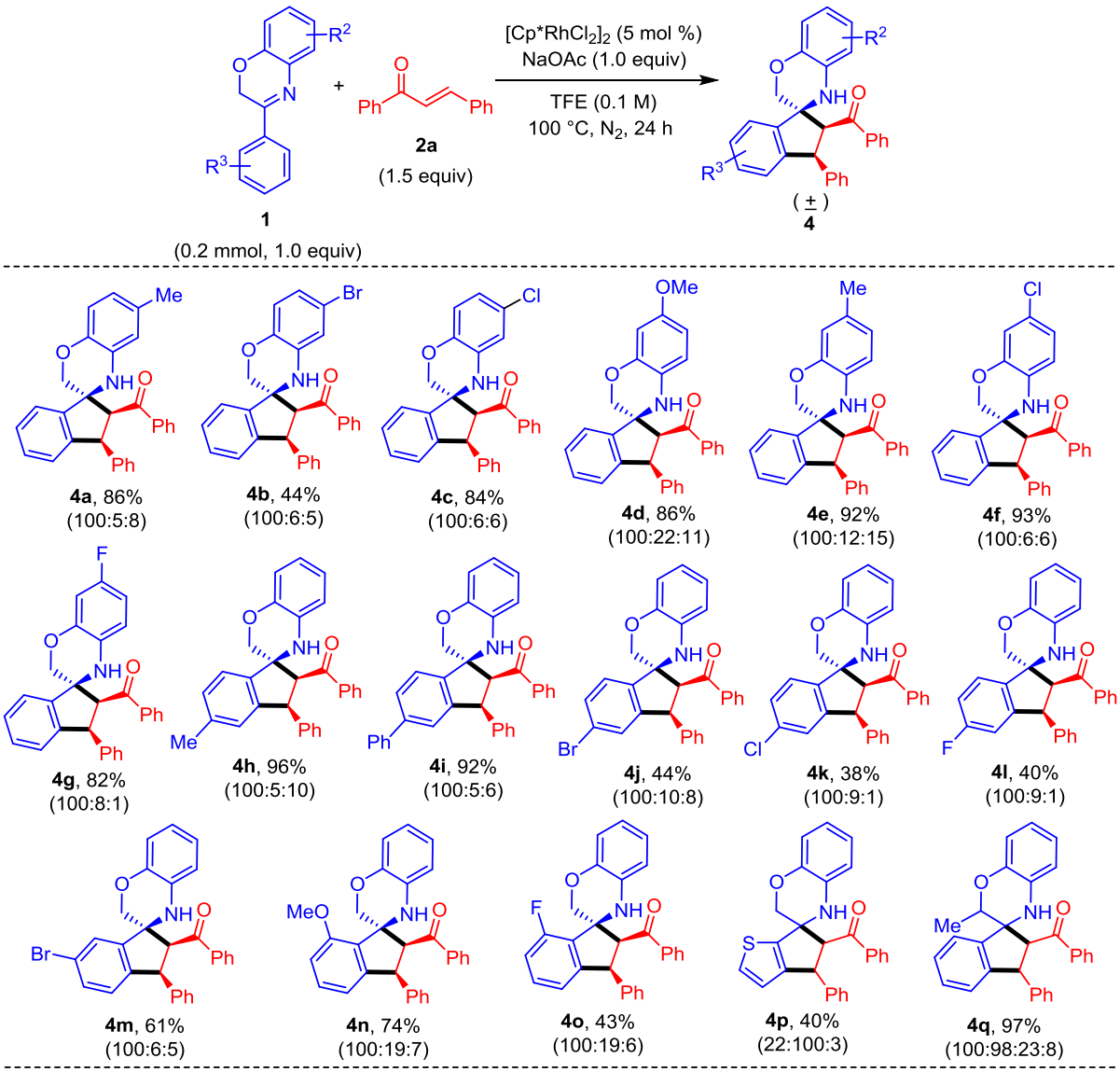

[a]Combined isolated yield of all the diastereomers; only the major diastereomer is shown (except for **4p** and **4q** as they could not be crystallized); dr given within parenthesis is calculated by ^{1}H NMR.

A bromo substitution at the *meta* position of the phenyl ring reacted regioselectively to yield 61% of the spiroannulated product **4m** with high diastereoselectivity (100:6:5). Contrasting reactivities were observed with *ortho* methoxy and fluoro-substituted benzoxazines, with the electron-donating methoxy group giving 74% of the product (**4n**) but electron-withdrawing fluoro substituent producing a lower yield (43%, **4o**). Delightfully, when the phenyl ring of the benzoxazine substrate was replaced by a heterocyclic (thiophene) ring, the corresponding spiroannulated product (**4p**) was obtained in a satisfactory yield of 40%. However, in this case, the diastereomeric ratio was altered (to 22:100:3) to get the other isomer in major amounts. Interestingly, when a methyl group was placed on the cyclic imine ring (**1q**), the product (**4q**)

was encountered in an excellent yield of 97% with a diastereomeric ratio of 100:98:23:8 due to concomitant generation of a fourth chiral center.

Some of the benzoxazines, chalcones and other α,β-unsaturated carbonyl compound derivatives did not undergo the [3+2]-spiroannulation when subjected to the standard reaction conditions and failed to deliver the desired spirocyclized products. Those are represented in Figure 6.3.2.1. Highly electron-withdrawing cyano group at the *para* position of the phenyl ring of benzoxazine substrate (**1s**) and furyl ring containing benzoxazine (**1t**) did not participate in the spirocyclization reaction with **2a** possibly because of electronic reasons. Among chalcones, on reacting with **1a**, extensively conjugated cinnamyl derived chalcone (**2ai**) and sterically imposed chalcones like anthrachene and pyrene derivatives (**2aj** and **2ak**) were not successful under the present reaction conditions. *Ortho* halo substituted chalcones like **2al** and **2am** produced trace amounts of their respective annulated products. All these could be pointed to the electronic effects and steric effects of the substituents. Again, on account of electronic reasons and bulkiness, various kinds of α,β-unsaturated carbonyl compounds (**2an**-**2at**) did not fare well and the formation of the corresponding spiroannulated products was not observed.

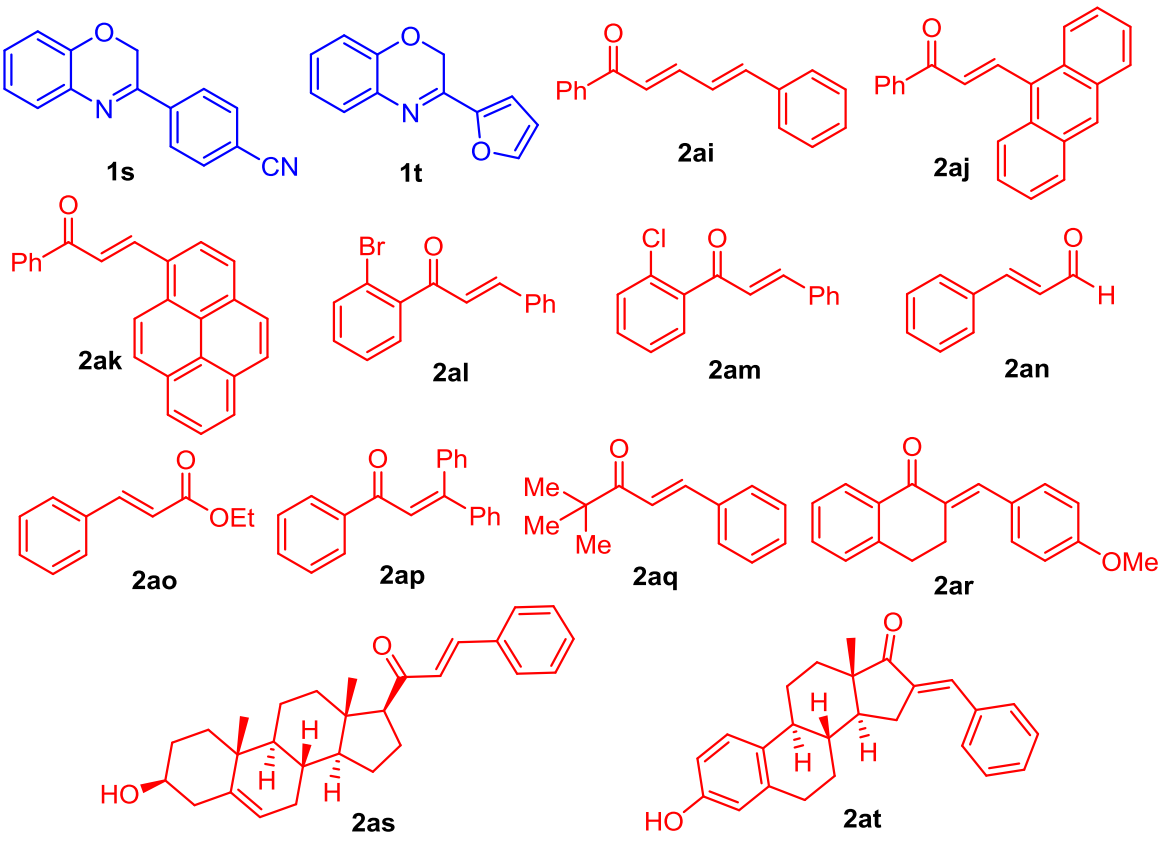

Figure 6.3.2.1. List of unsuccessful benzoxazines, chalcones and other α,β-unsaturated carbonyl compounds.

6.3.3. Gram-Scale Reaction

To illustrate the feasibility and generality of this synthetic methodology, a scale-up experiment was performed under standard conditions using 4.8 mmol (1.0 g) of **1a** with (*E*)-chalcone **2a** furnishing the desired spirocyclized product **3a** in a satisfactory yield of 63% maintaining the excellent diastereoselectivity (Scheme 6.3.3.1).

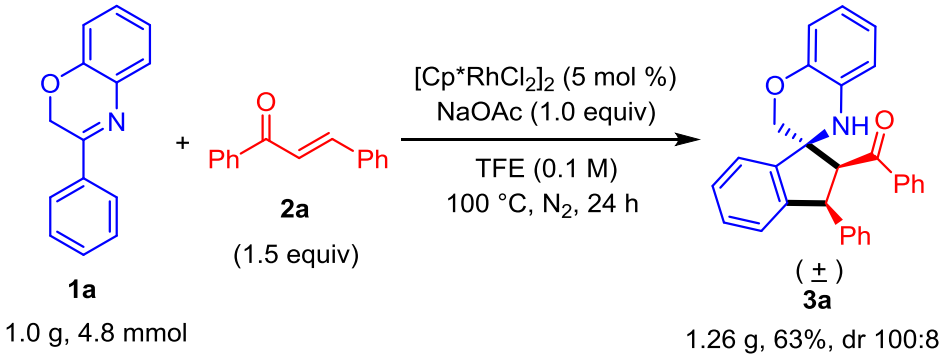

Scheme 6.3.3.1. Gram-scale reaction.

6.3.4. Interchange of the Diastereomers

Intrigued to know the nature and relative stereochemistry of the minor diastereomers, we studied the reactivity of the diastereoisomers under basic (in presence of DBU) or acidic conditions (in presence of conc. H_2SO_4/H_2O mixture) and hypothesized a probable mechanistic pathway for the transformations (Scheme 6.3.4.1).

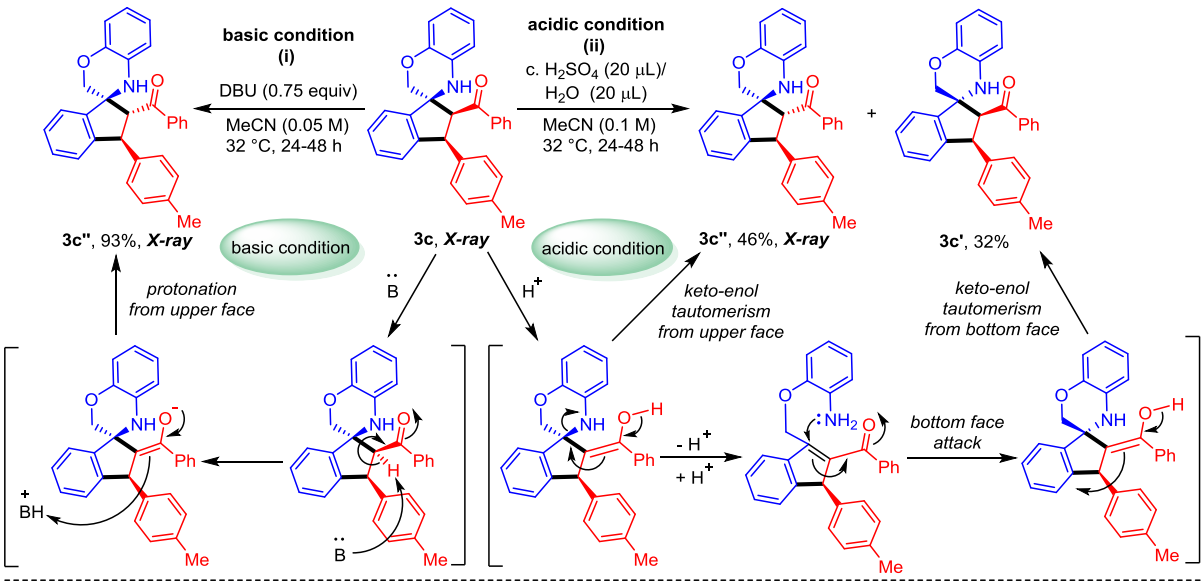

[a]Isolated yield.

Scheme 6.3.4.1. Route to the minor diastereomers and its plausible mechanism.[a]

When the major diastereomer **3c** was exposed to DBU in MeCN solvent, it was exclusively converted into **3c″**, one of the minor isomers. This transformation could possibly take place solely due to epimerization of the C2-center via an enolization process. On the contrary, treating **3c** with catalytic amount of conc. H_2SO_4/H_2O mixture transformed **3c** to both the minor isomers **3c′** and **3c″** in 32% and 46% yields respectively. In this case, **3c″** is again formed maybe simply via a facile keto-enol tautomerism leading to inversion of stereochemistry at the C2-position. The other isomer **3c′** is formed possibly via enolization and subsequent ring-opening/ring-closing pathway from opposite face again via enolization. These results led us to an important conclusion that the minor diastereomers could be easily obtained and isolated from the major diastereomer when put under appropriate conditions.

6.3.5. Determination of the Relative Stereochemistry of the Spirocyclized Products

The relative stereochemistry of the three diastereomers **3c**, **3c′**, **3c″** (Figure 6.3.5.1) was determined by analyzing a series of 1D and 2D NMR techniques and finally confirmed by single crystal X-ray analysis. The structural analysis is discussed below.

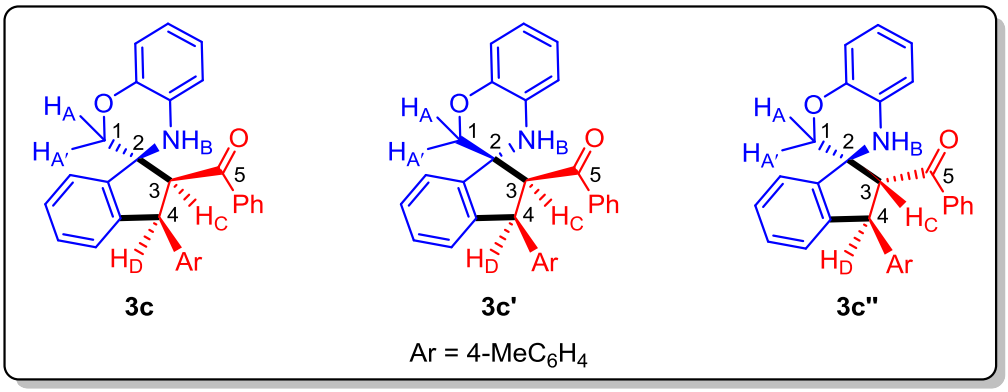

Figure 6.3.5.1. Three diastereomers of compound (±) **3c**.

First, the ^1H, ^{13}C, and DEPT-135 NMR data were recorded for the three pure diastereomers which gave us a preliminary idea of the structure of the spirocyclized products (Figure 6.3.5.2-6.3.5.4). The corresponding data of ^1H and ^{13}C NMR for each of the diastereomers is provided in the experimental section later. The DEPT-135 NMR showed the relative peak positions of the corresponding CH and CH_2 and CH_3 carbon atoms. We were particularly interested to understand the positioning and relative geometry of the protons (H_A, $H_{A'}$, H_B, H_C and H_D) and carbons (C1, C2, C3, C4 and C5) of the 6,5-spiro-fused system of the spirocyclic 1,4-benzoxazine derivatives. For this, we took the help of 2D NMR spectroscopic techniques like ^1H-^1H COSY, ^1H-^1H NOESY, ^1H-^{13}C HMQC, ^1H-^{13}C HSQC, ^1H-^{13}C HMBC.

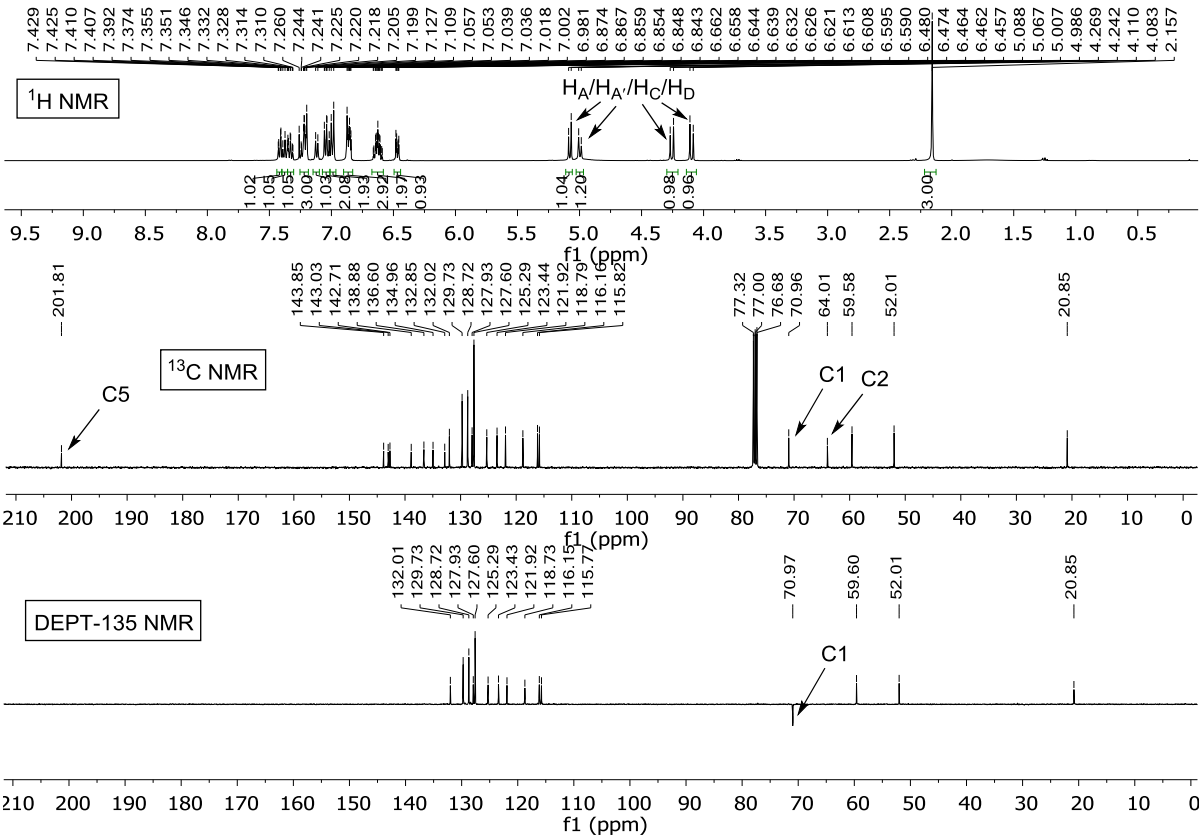

Figure 6.3.5.2. ^{1}H, ^{13}C, and DEPT-135 NMR spectra of **3c**.

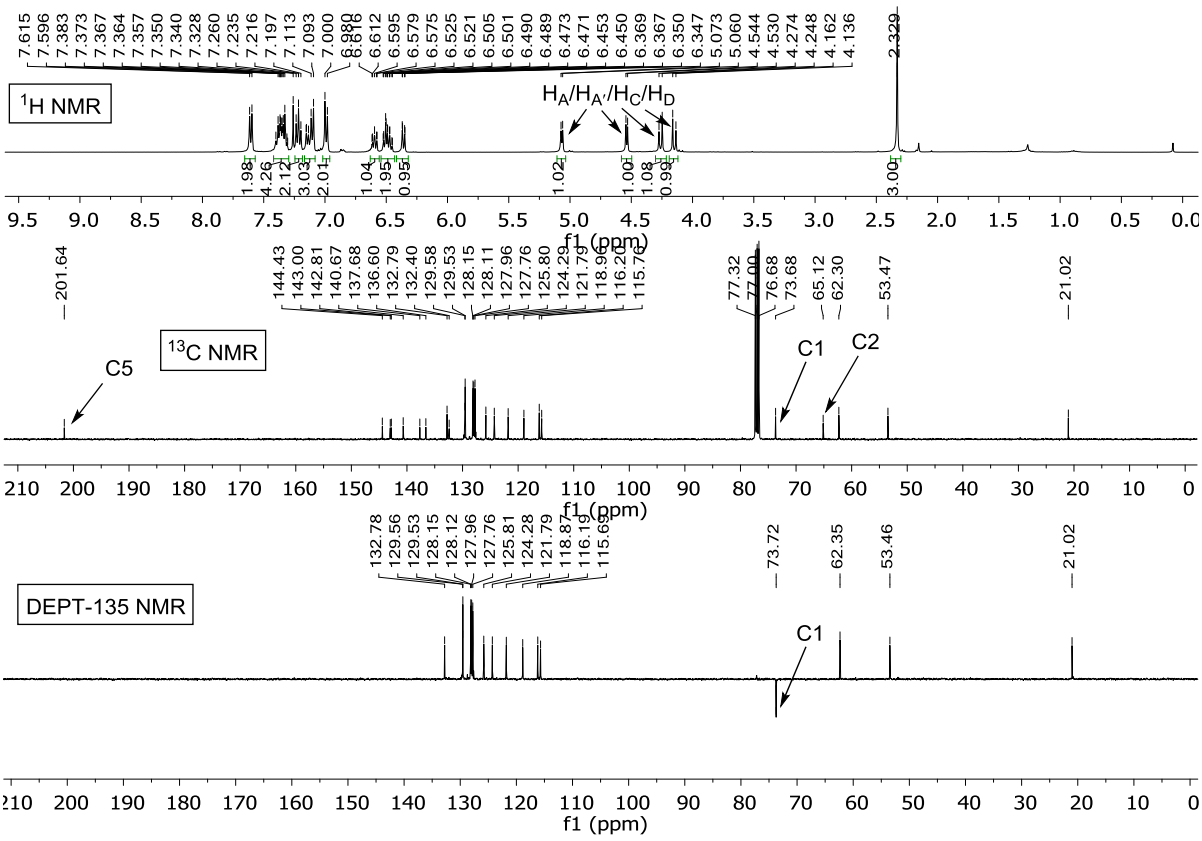

Figure 6.3.5.3. ^{1}H, ^{13}C, and DEPT-135 NMR spectra of **3c′**.

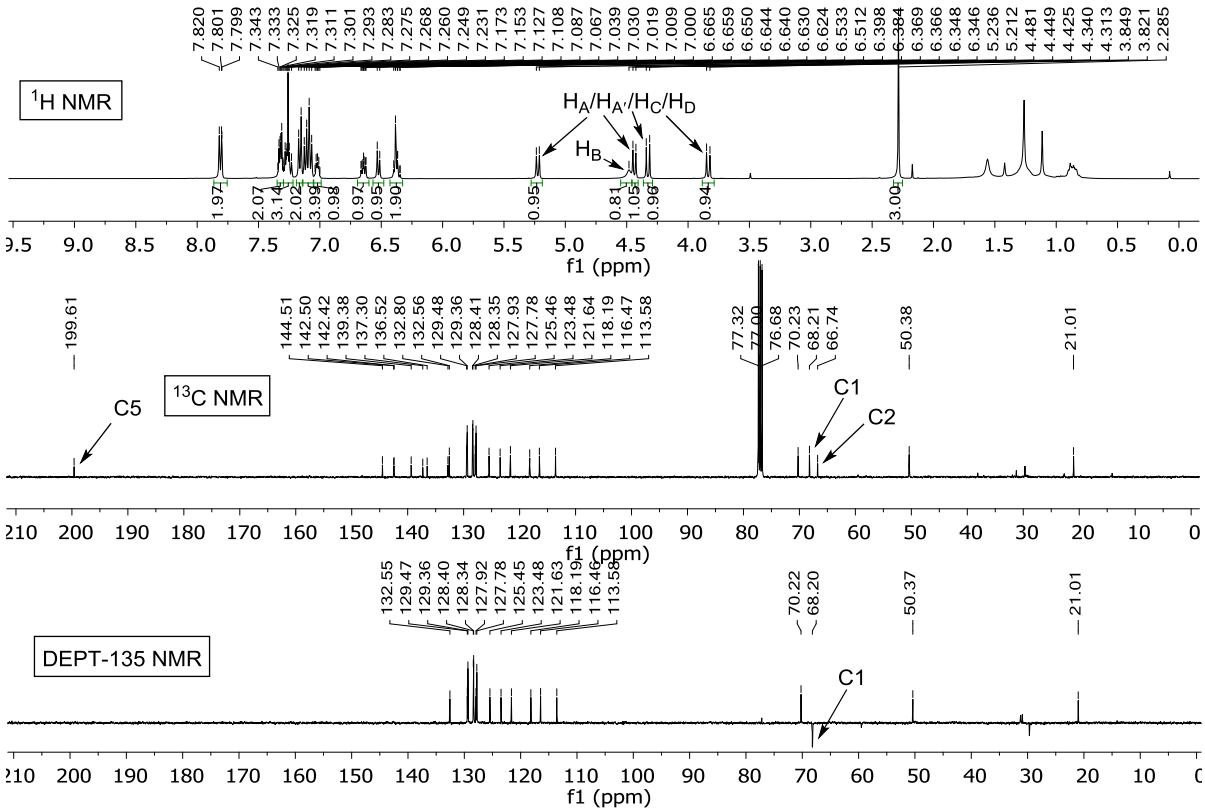

Figure 6.3.5.4. ^{1}H, ^{13}C, and DEPT-135 NMR spectra of **3c″**.

The protons were preliminarily assigned by ^{1}H and ^{1}H-^{1}H 2D-COSY NMR data (Figure 6.3.5.5-6.3.5.7). From ^{1}H NMR data, we found out the peak positions of H_A, $H_{A'}$, H_B (N–H proton which was observed in some cases, got overlapped in some cases, and not in other cases), H_C and H_D and their coupling constant (*J*) values for each of the doublets observed. On taking the ^{1}H-^{1}H 2D-COSY NMR data of the three diastereomers, and matching the peak positions with the *J* values, we observed two cross peaks and hence correlation for the combination $H_A/H_{A'}$ and H_C/H_D. The correlation was observed for the pair of protons with same *J* values. But it was not conclusive from this technique that which of the correlations is for which combination. Henceforth, we moved forward to ^{1}H-^{13}C 2D-HMQC, ^{1}H-^{13}C 2D-HSQC, and ^{1}H-^{13}C 2D-HMBC NMR spectroscopy to get an idea of which proton is attached to which carbon atom of the fragment of interest.

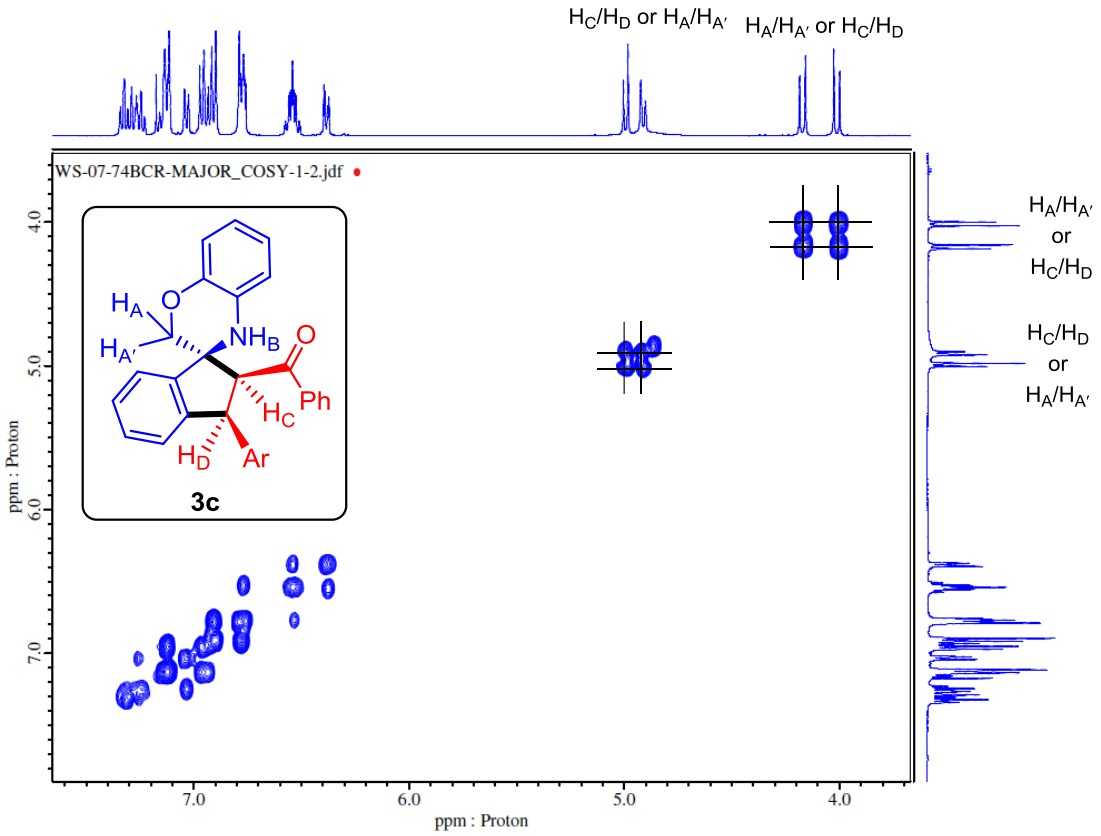

Figure 6.3.5.5. ^{1}H-^{1}H COSY NMR spectrum of **3c**.

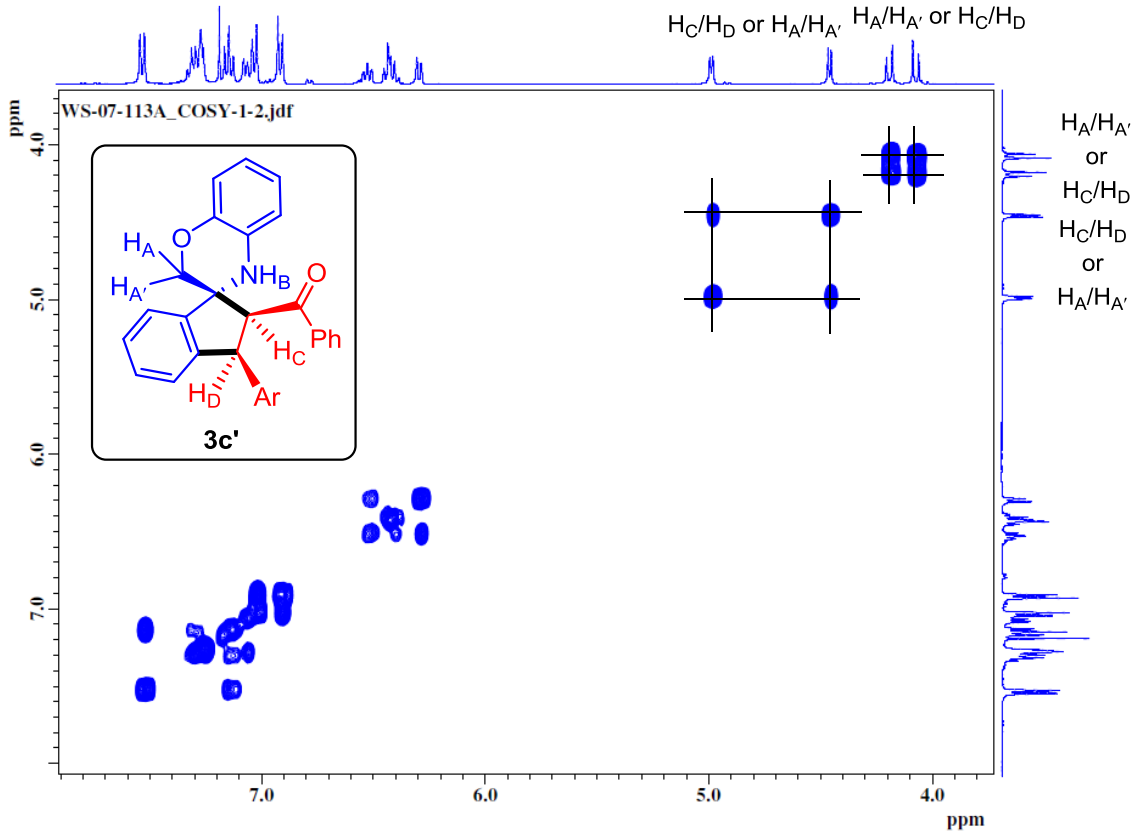

Figure 6.3.5.6. ^{1}H-^{1}H COSY NMR spectrum of **3c′**.

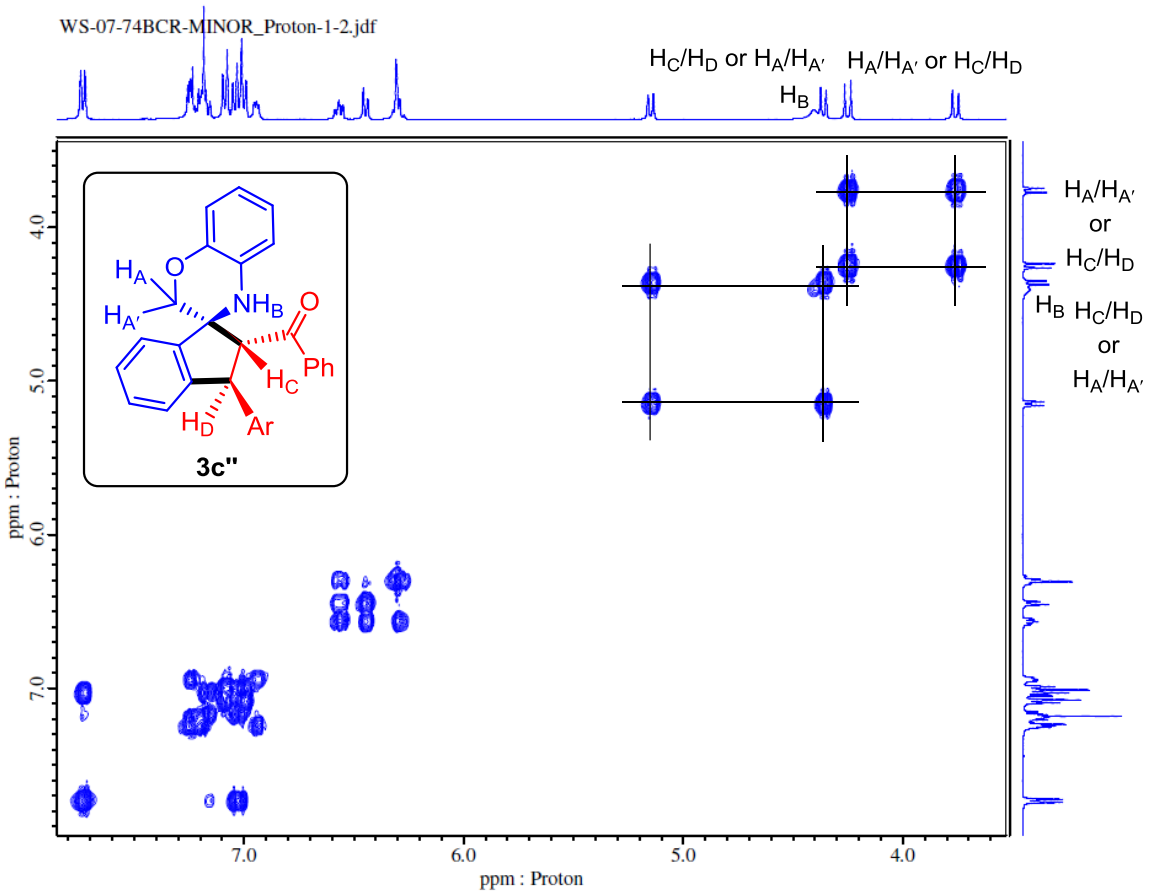

Figure 6.3.5.7. ^{1}H-^{1}H COSY NMR spectrum of **3c″**.

The analysis of ^{1}H-^{13}C HMQC NMR data (Figure 6.3.5.8-6.3.5.10) and ^{1}H-^{13}C HSQC NMR data (Figure 6.3.5.11-6.3.5.13) for the three diastereomers **3c**, **3c′**, **3c″** showed the 1-bond correlations present in the molecule, meaning which proton is directly attached to which carbon atom. They showed a correlation between protons H_A and $H_{A'}$ with C1 carbon atom from where we concluded that H_A and $H_{A'}$ are diastereotopic protons which are both directly attached to the same carbon atom C1. There were no correlations with C2 indicating that it is quaternary carbon atom (which was also confirmed from DEPT-135 NMR data). Two other correlations were observed for each proton out of H_C and H_D with C3 and C4 carbon atoms but the exact correlation could not be concluded from here. For this, next we recorded the ^{1}H-^{13}C HMBC NMR data for the three diastereomers (Figure 6.3.5.14-6.3.5.16).

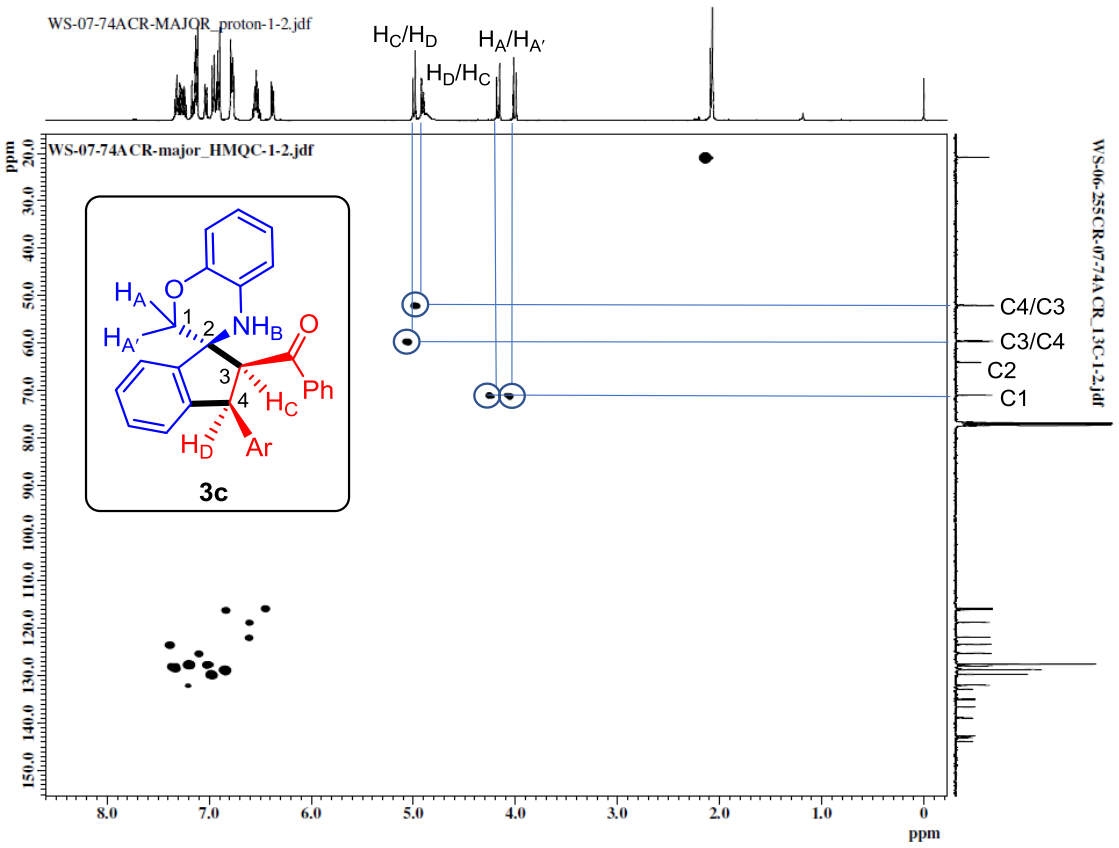

Figure 6.3.5.8. ^{1}H-^{13}C HMQC NMR spectrum of **3c**.

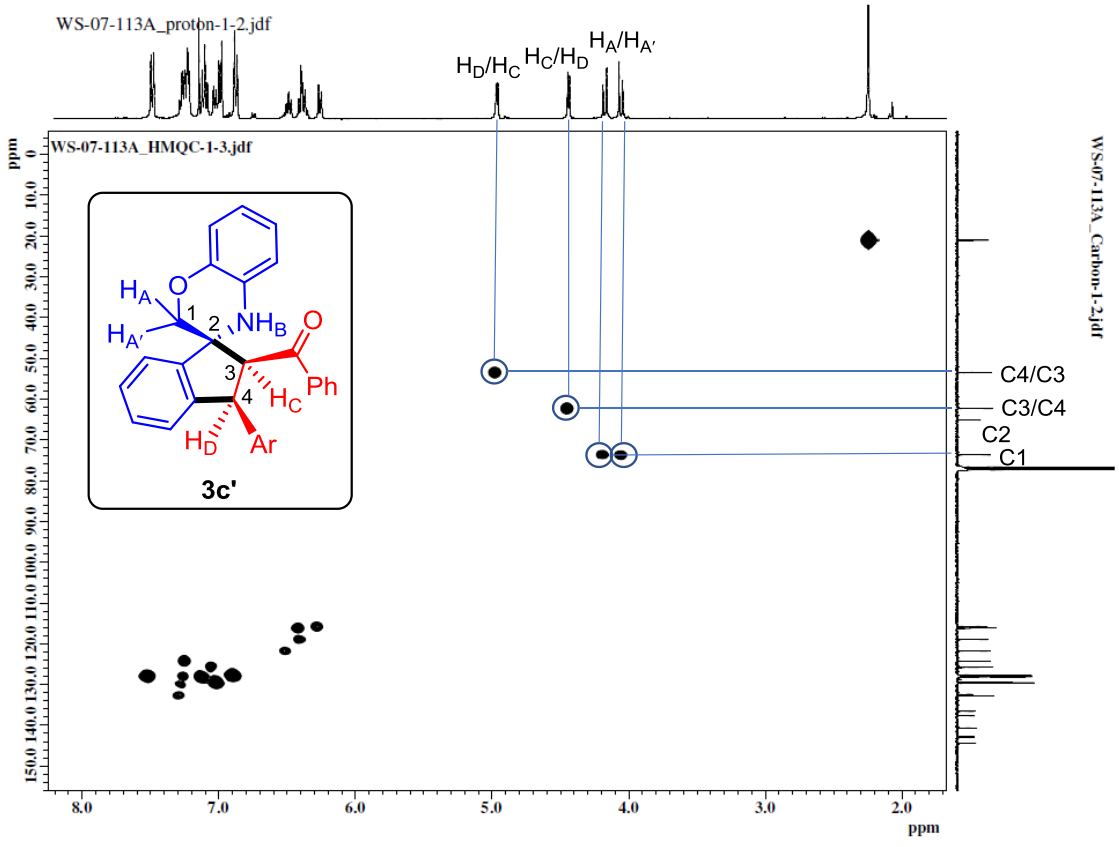

Figure 6.3.5.9. ^{1}H-^{13}C HMQC NMR spectrum of **3c′**.

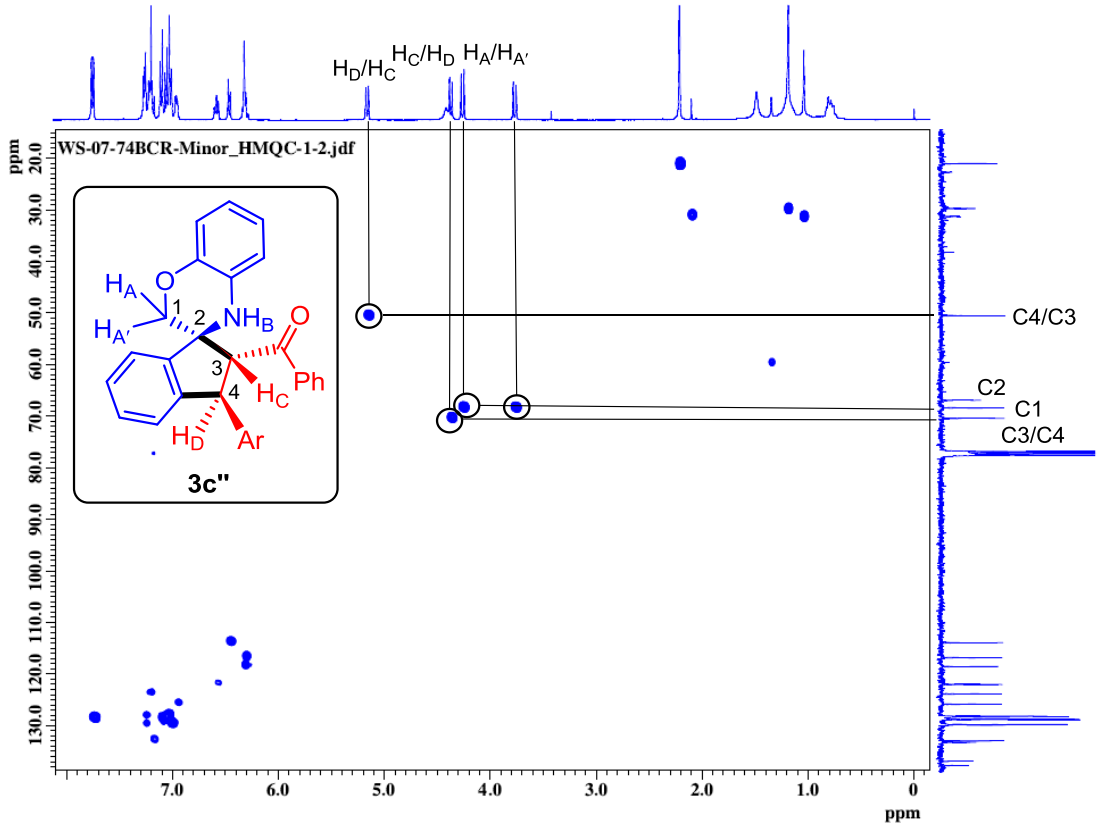

Figure 6.3.5.10. ^{1}H-^{13}C HMQC NMR spectrum of **3c″**.

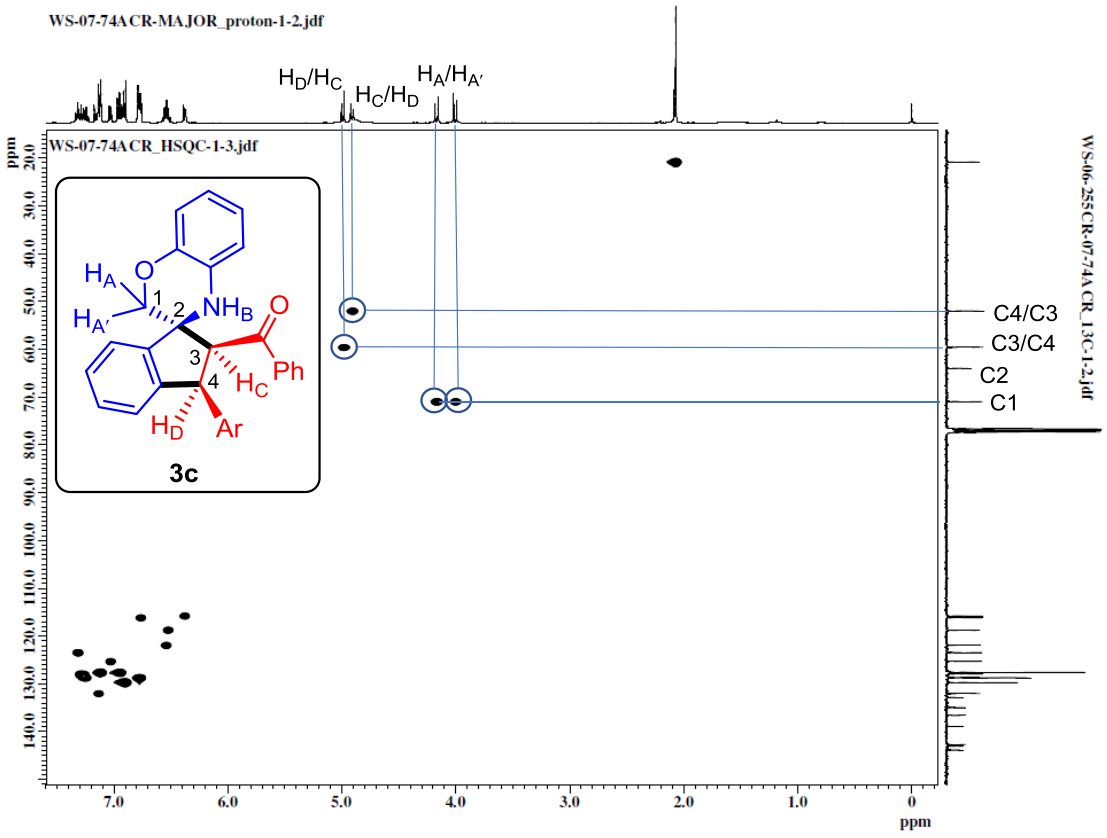

Figure 6.3.5.11. ^{1}H-^{13}C HSQC NMR spectrum of **3c**.

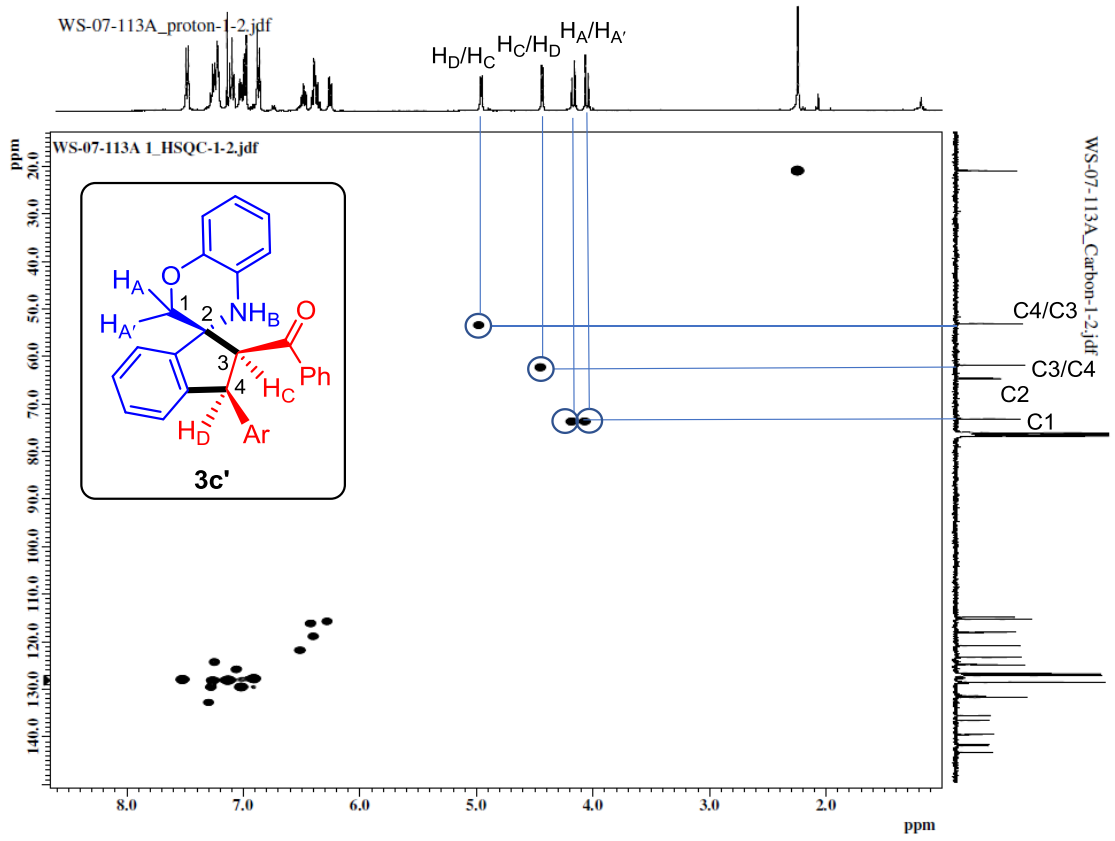

Figure 6.3.5.12. ^{1}H-^{13}C HSQC NMR spectrum of **3c′**.

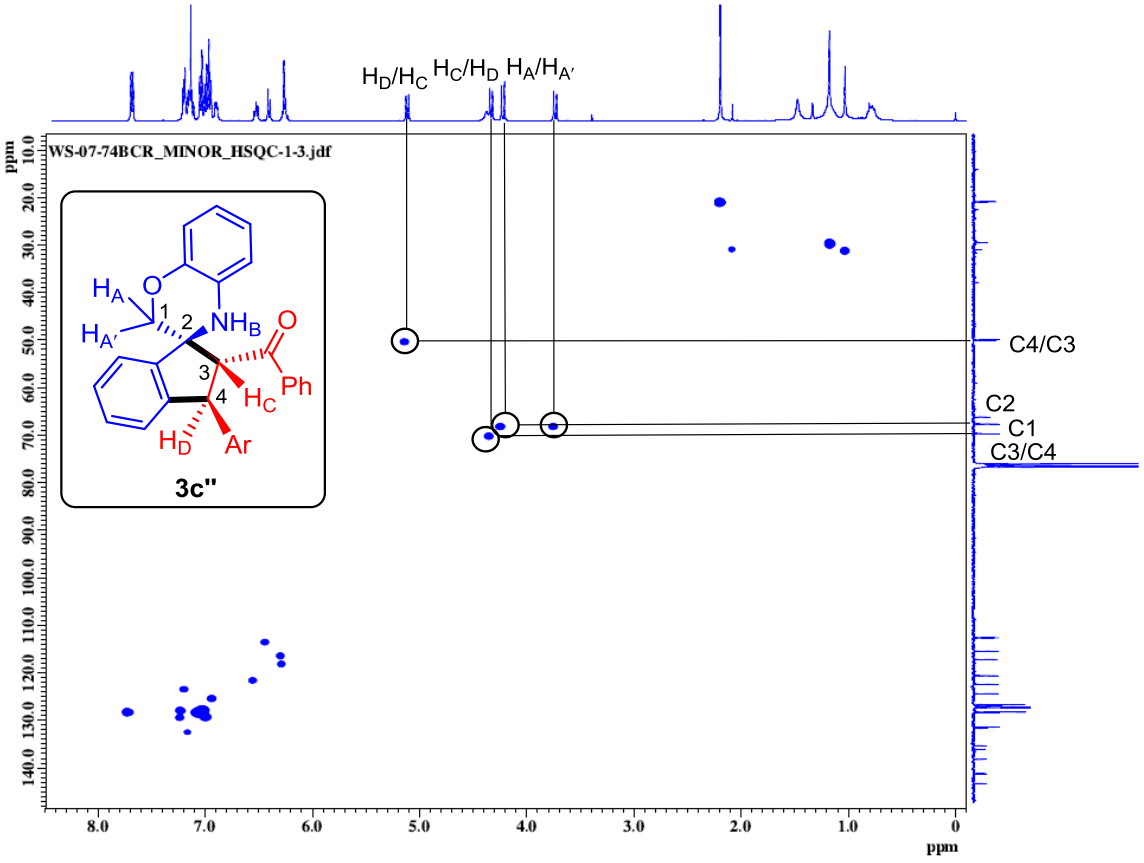

Figure 6.3.5.13. ^{1}H-^{13}C HSQC NMR spectrum of **3c″**.

This ^{1}H-^{13}C HMBC 2D-NMR spectroscopic technique shows the 2-bond and 3-bond correlations (sometimes 4-bond correlations) between protons and carbons and direct 1-bond correlations are suppressed, thus unfolding the structural pattern and bond connectivity present in a molecule. Generally (but not always), the 3-bond couplings are slightly stronger than the 2-bond couplings which is reflected in the intensities of their cross peaks. In our case, in all the ^{1}H-^{13}C HMBC data for the three diastereomers, correlations were observed for- (i) H_A/$H_{A'}$ with C3, (ii) H_C with C1, C2, C4 and C5, (iii) H_D with C_3 and C_5. These observations led us to the conclusive peak positions of protons H_C, H_D, and carbons C_3 and C_4. Therefore, from these spectra analysis, we found out the relative positions of the protons (H_A, $H_{A'}$, H_B, H_C and H_D) and carbons (C1, C2, C3, C4 and C5) and how they are connected to each other, thereby giving us an idea of the structure of the spirocyclic molecule.

In major diastereomer **3c**, the assignments are as follows- H_A/$H_{A'}$ at δ 4.10 (d, *J* = 10.8 Hz, 1H) and 4.26 (d, *J* = 10.8 Hz, 1H) attached to C1 at δ 71.0, H_C at δ 5.00 (d, *J* = 8.4 Hz, 1H) attached to C3 at δ 59.6, H_D at δ 5.08 (d, *J* = 8.4 Hz, 1H) attached to C4 at δ 52.0.

In minor diastereomer **3c′**, the assignments are as follows- H_A/$H_{A'}$ at δ 4.15 (d, *J* = 10.4 Hz, 1H) and 4.26 (d, *J* = 10.4 Hz, 1H) attached to C1 at δ 73.7, H_C at δ 4.54 (d, *J* = 5.6 Hz, 1H) attached to C3 at δ 62.3, H_D at δ 5.07 (d, *J* = 5.2 Hz, 1H) attached to C4 at δ 53.5.

In minor diastereomer **3c″**, the assignments are as follows- H_A/$H_{A'}$ at δ 3.84 (d, *J* = 11.2 Hz, 1H) and 4.33 (d, *J* = 10.8 Hz, 1H) attached to C1 at δ 68.2, H_C at δ 4.44 (d, *J* = 9.6 Hz, 1H) attached to C3 at δ 70.3, H_D at δ 5.22 (d, *J* = 9.6 Hz, 1H) attached to C4 at δ 50.4.

Now, we have a clear idea of the structure of the spirocyclic molecules based on the findings of the through-bond spectroscopic techniques described above. But we still have to assign and elucidate the relative geometry of the diastereomers to fulfil our objective of understanding its stereochemical orientation. For this purpose, we took the help of ^{1}H-^{1}H 2D-NOESY NMR spectroscopy. We recorded the ^{1}H-^{1}H NOESY NMR data for the three diastereomers **3c**, **3c′** and **3c″** (Figure 6.3.5.17-6.3.5.19). ^{1}H-^{1}H NOESY 2D-NMR spectroscopy is a through-space technique which provides an idea about the spatial arrangements of protons close to each other even if they are not bonded to each other. This helps in understanding the stereochemical relationships present within a molecule, and hence is important for stereoisomers where all atoms are connected exactly in the same fashion.

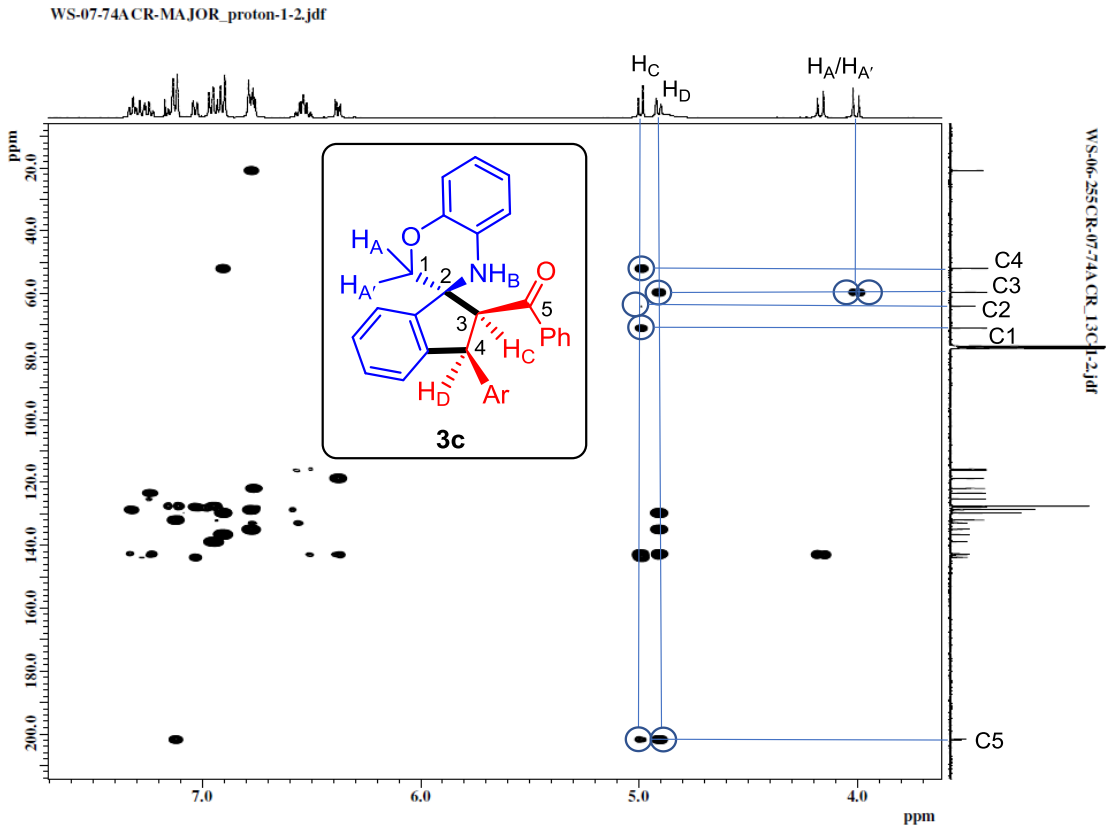

Figure 6.3.5.14. ^{1}H-^{13}C HMBC NMR spectrum of **3c**.

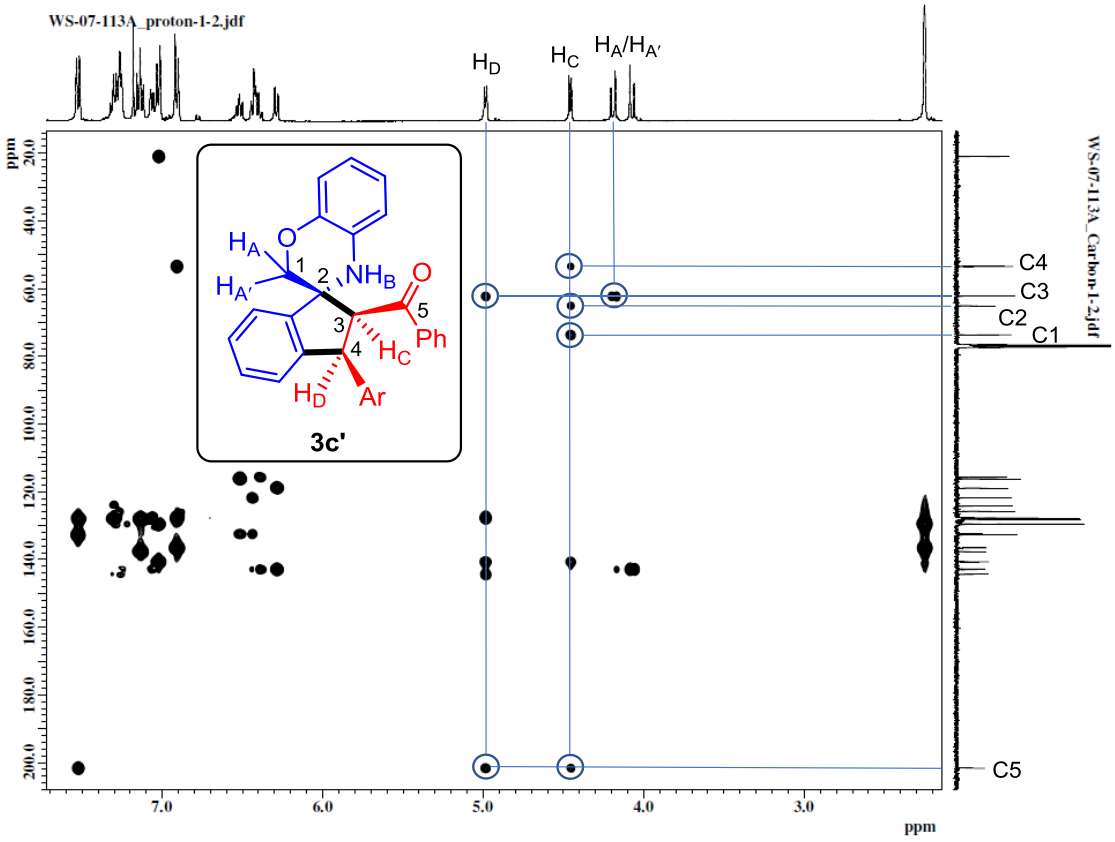

Figure 6.3.5.15. ^{1}H-^{13}C HMBC NMR spectrum of **3c′**.

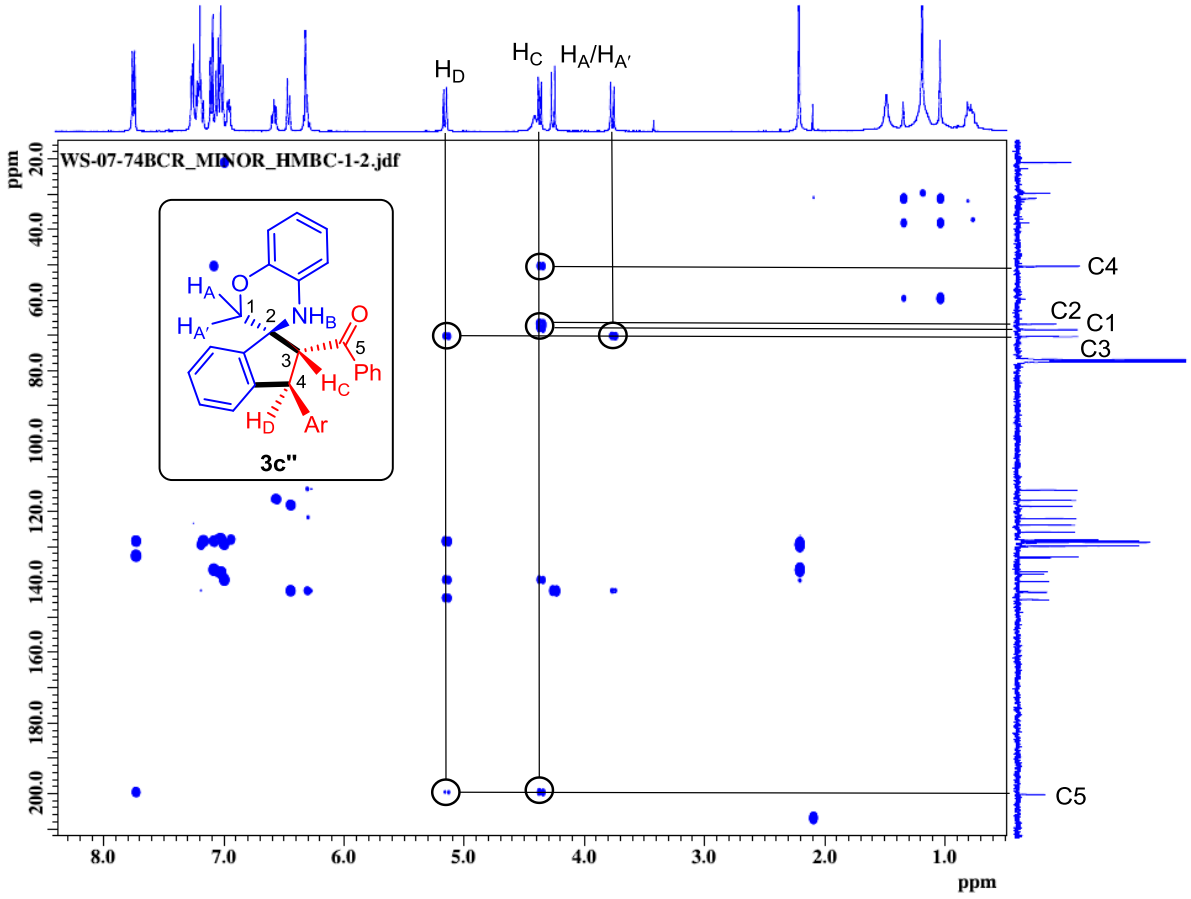

Figure 6.3.5.16. ^{1}H-^{13}C HMBC NMR spectrum of **3c″**.

^{1}H-^{1}H NOESY NMR data for the major diastereomer **3c** showed a strong NOE interaction between H_C and H_D suggesting that these two protons might be *syn* to each other (Figure 6.3.5.17). For the minor diastereomer **3c′**, we again observed a strong NOE interaction between H_C and H_D suggesting that they might be *syn* to each other in this isomer also (Figure 6.3.5.18). But for the other minor diastereomer **3c″**, a weak NOE interaction between H_C and H_D was observed suggesting here these two protons might be *anti* to each other (Figure 6.3.5.19). But we did not observe any NOE interaction of H_C or H_D with H_B (maybe due to the absence of N–H_B proton peak in ^{1}H NMR spectra of many compounds) in any of the diastereomers. Thus, from here we got an idea of the geometrical relationship between H_C and H_D, but could not establish the stereochemical relationship of them with the NH_B group. Finally, to understand this aspect and confirm the relative stereochemistry of the diastereomers, we crystallized them and recorded their single-crystal X-ray analysis data. We successfully crystallized the major diastereomer **3c** and one of the minor diastereomers **3c″** and hence assigned their structures based on the X-ray data, but we were unable to crystallize the other minor diastereomer **3c′** and hence its structure is given based on the 1D and 2D-NMR spectroscopic data analysis.

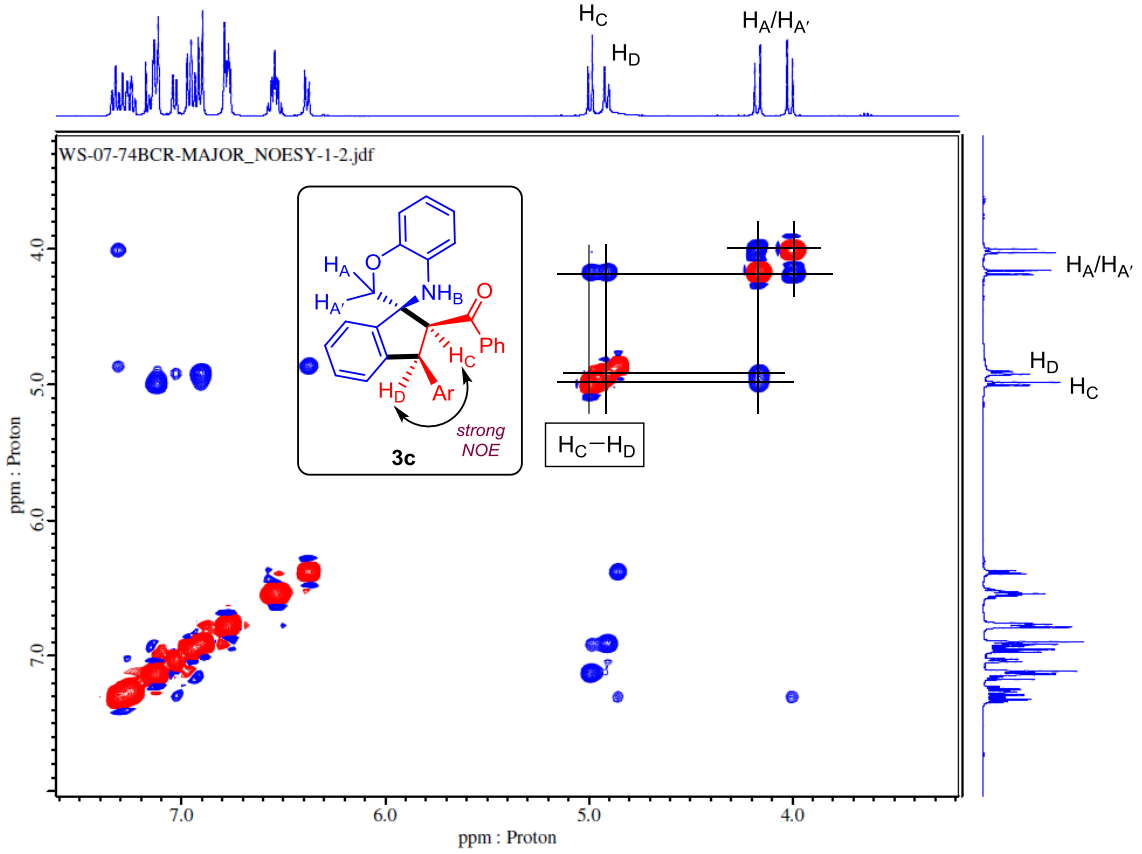

Figure 6.3.5.17. ^{1}H-^{1}H NOESY NMR spectrum of **3c**.

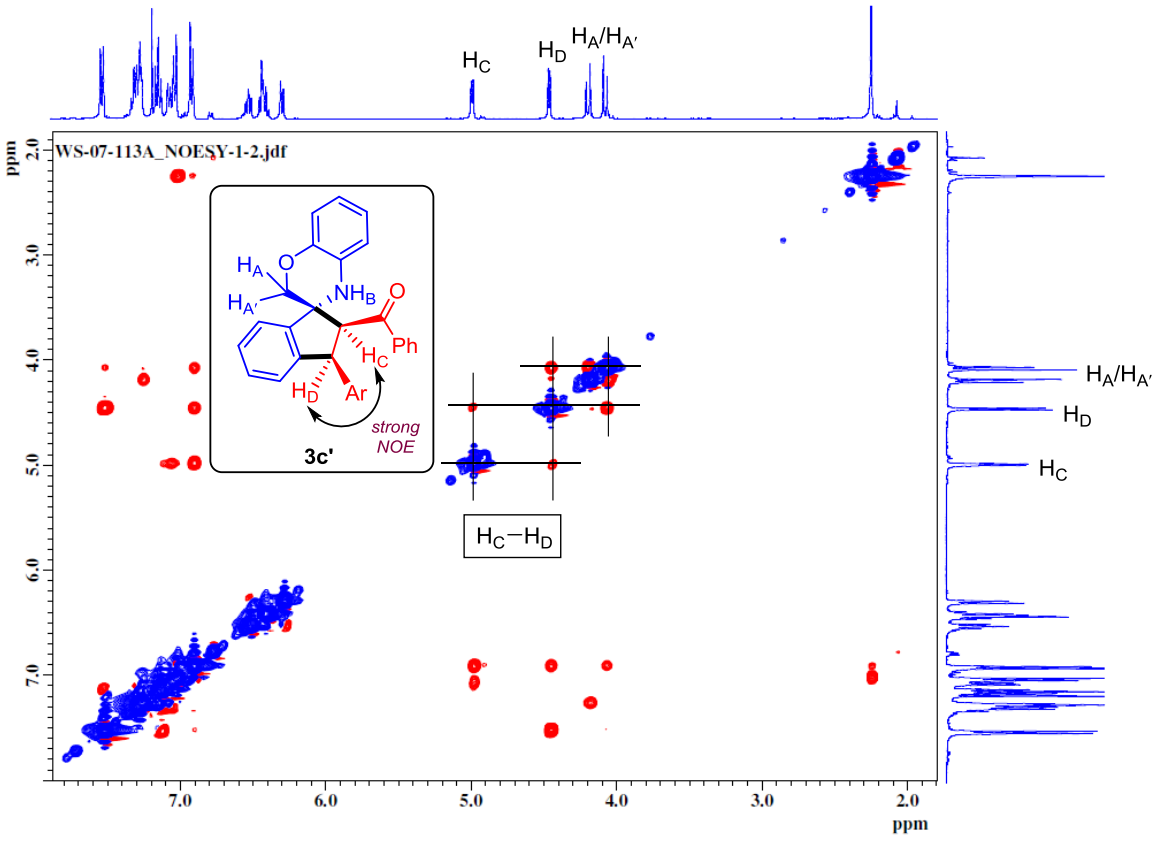

Figure 6.3.5.18. ^{1}H-^{1}H NOESY NMR spectrum of **3c′**.

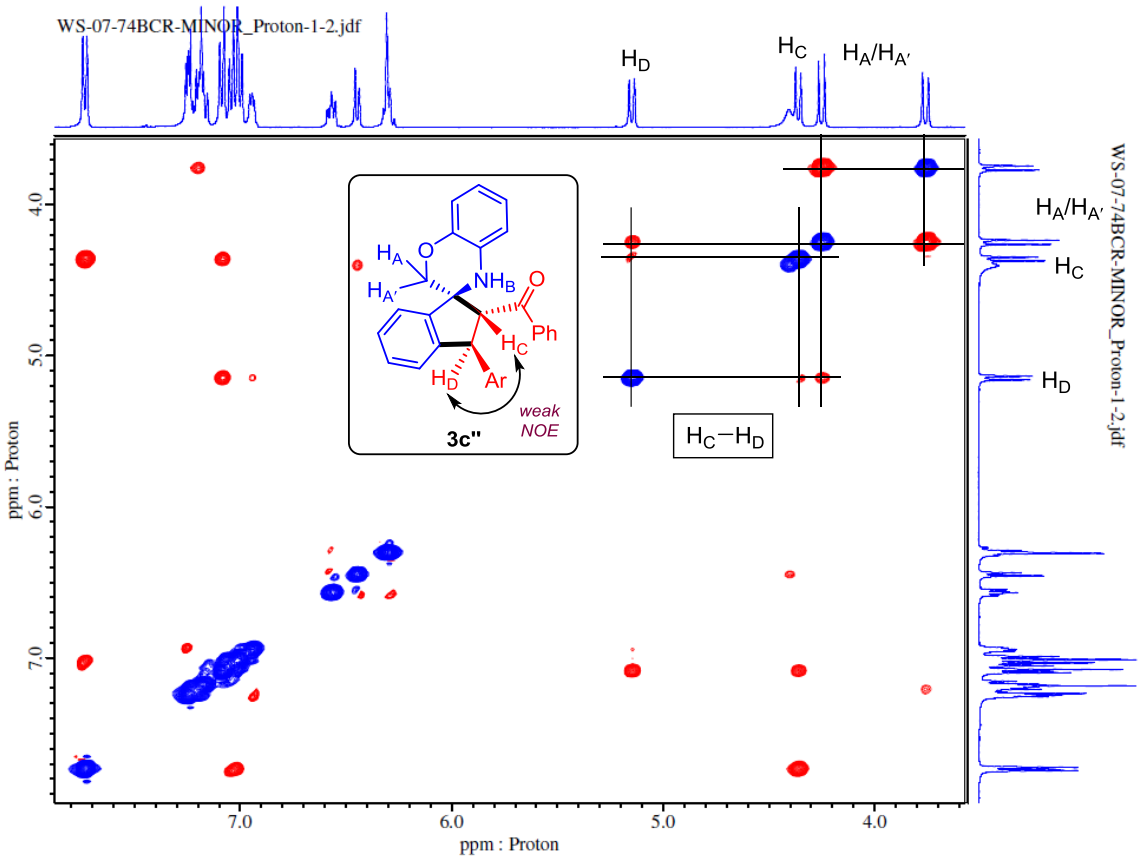

Figure 6.3.5.19. ^{1}H-^{1}H NOESY NMR spectrum of **3c″**.

All the spirocyclized products (**3** and **4**) were duly characterised by ^{1}H, ^{13}C NMR and HRMS. Single-crystal X-ray analysis of **3c**, **3c″**, **3l**, **3aa** and **4d** further confirmed their structures (Figure 6.5.3.20).

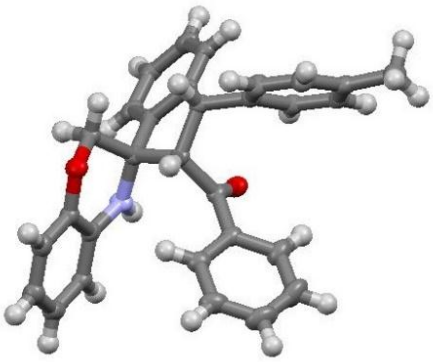

3c
(major diastereomer)
CCDC No. 2090973

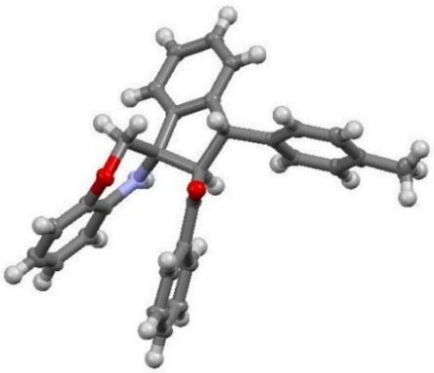

3c″
(minor diastereomer)
CCDC No. 2090974

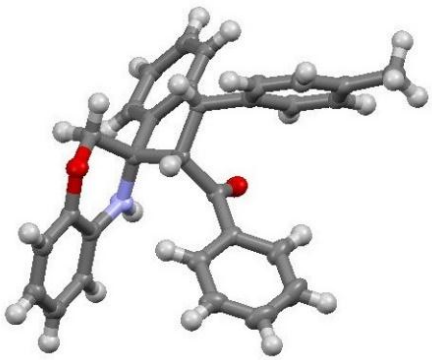

3l
CCDC No. 2090975

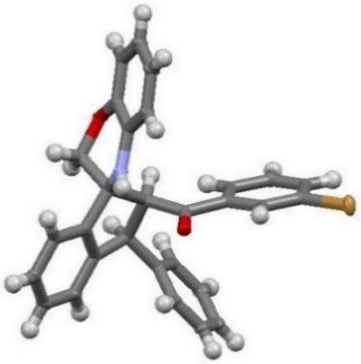

3aa
CCDC No. 2090976

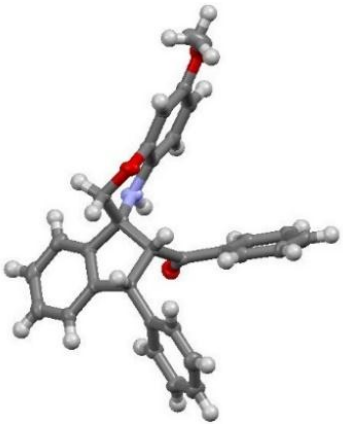

4d
CCDC No. 2090977

Figure 6.3.5.20. X-ray crystal structures of **3c**, **3c″**, **3l**, **3aa** and **4d** (ellipsoid contour at 50% probability level).

6.3.6. Mechanistic Experiments and Plausible Mechanism

In order to gain knowledge about the mechanism of the present [3+2]-spirocyclization reaction and study how its catalytic cycle works, several kinetic experiments were performed.

First, to understand the nature of the C–H cleavage step, H/D exchange experiments were conducted on **1a** taking D_2O and CD_3OD as external deuterated sources under the standard conditions (Scheme 6.3.6.1a). From ^1H NMR studies, significant D-incorporation was noticed at the *ortho* positions of the phenyl ring, but it was more prominent at the $-CH_2$ position adjacent to the *O*-atom of the cyclic imine ring of **1a** (Figure 6.3.6.1, 6.3.6.2). This could be presumably due to the possibility of imine-enamine tautomerism in the presence of polar protic TFE solvent. When the same reaction was performed at a lower temperature of 40 °C taking D_2O as external deuterated source (Scheme 6.3.6.1b), ^1H NMR study showed substantial D-incorporation at the *ortho* positions, but none was observed at the $-CH_2$ position (Figure

6.3.6.3). This again could be addressed to the phenomenon that the imine-enamine transformation might be more feasible at higher temperatures. All these results indicated that the *ortho* C–H bond cleavage step of this reaction might be reversible in nature.

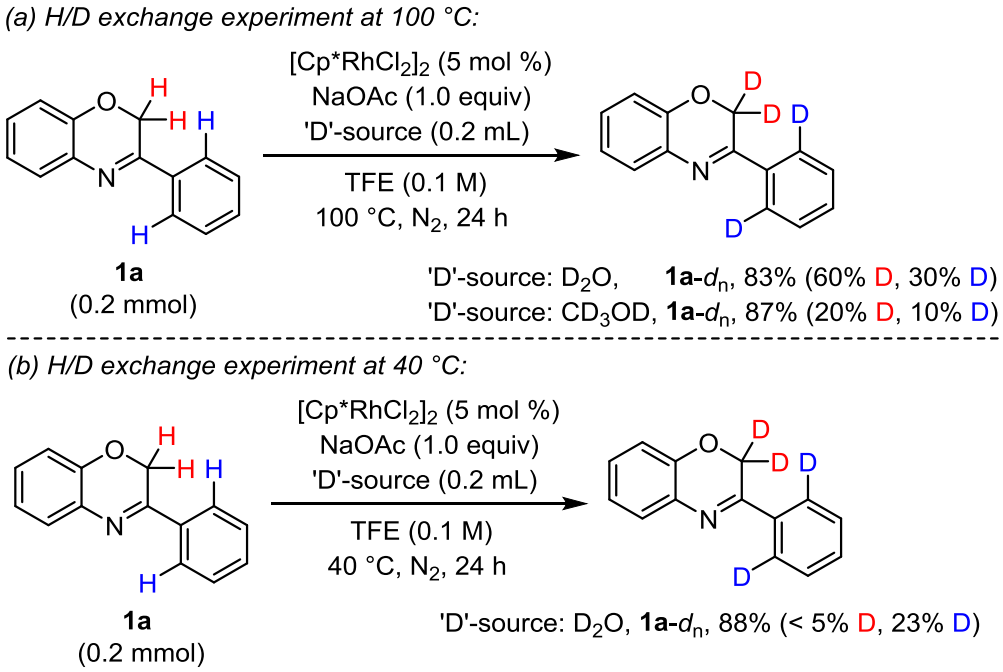

Scheme 6.3.6.1. H/D exchange experiments.

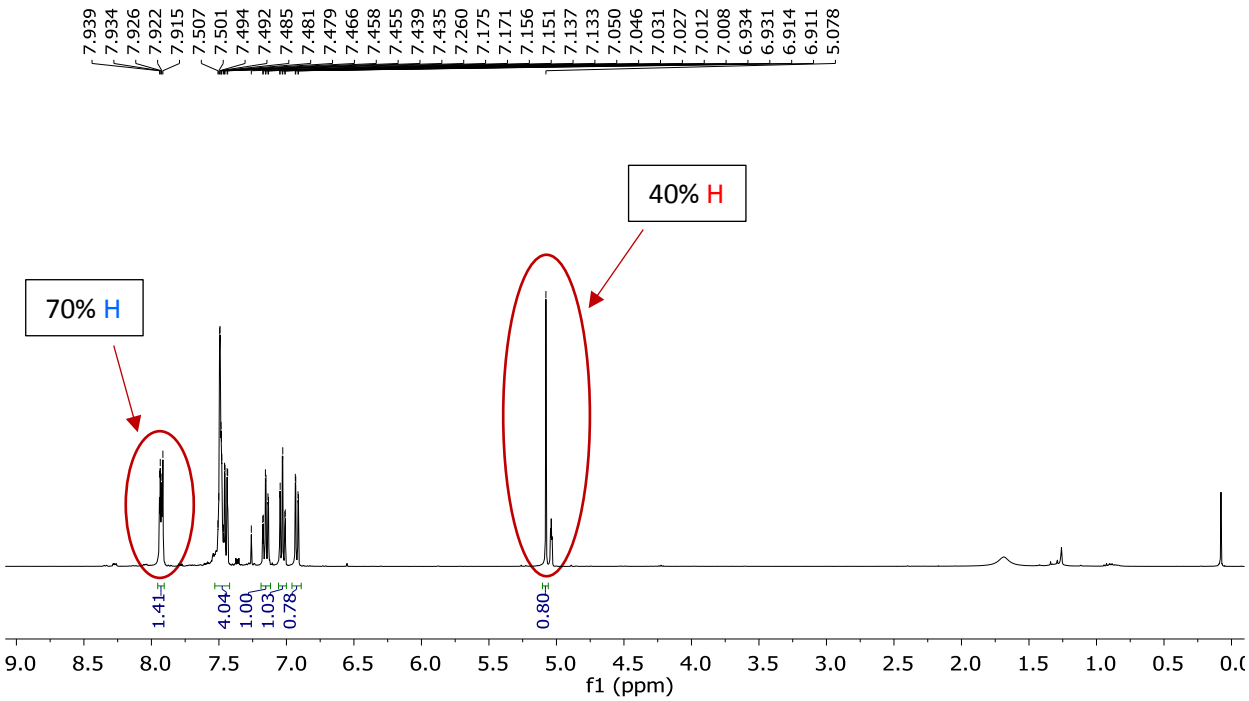

Figure 6.3.6.1. ^{1}H NMR spectrum of **1a**-d_n after H/D exchange experiment (D_2O as D-source at 100 ^{o}C oil bath temperature).

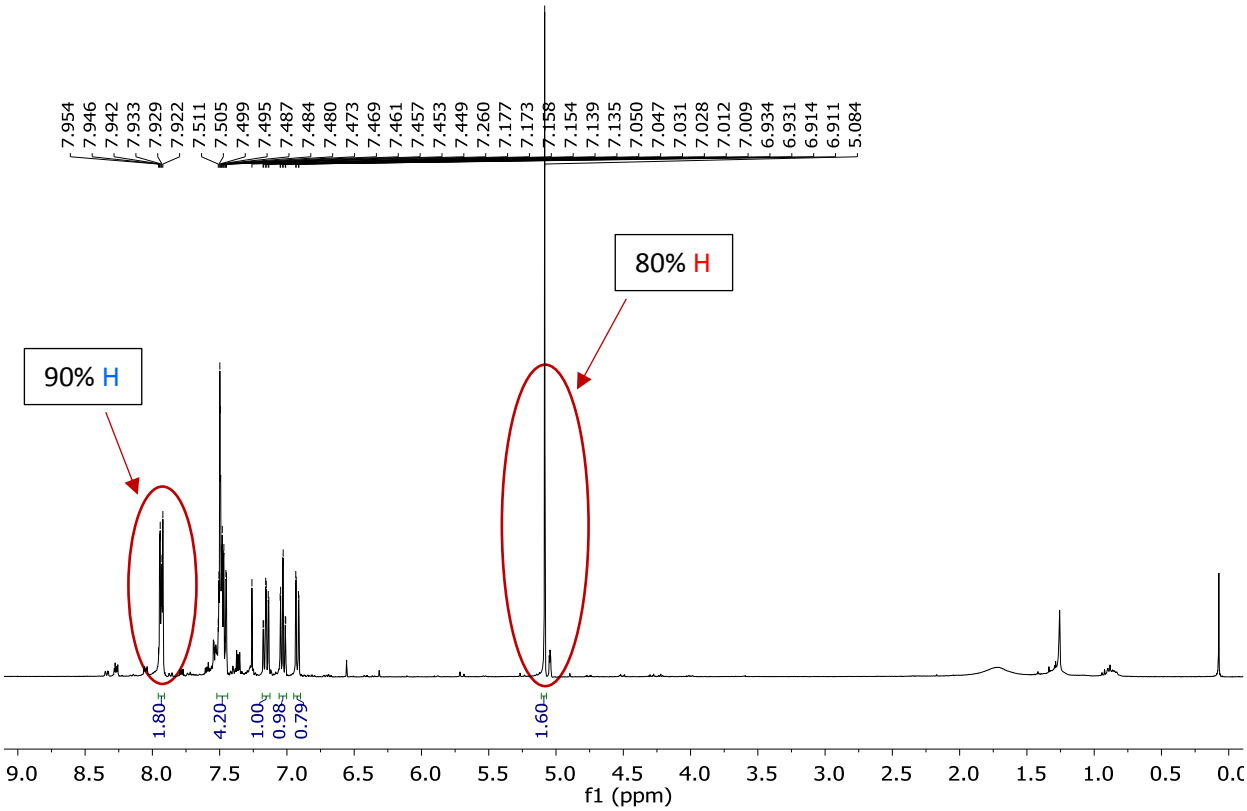

Figure 6.3.6.2. ^{1}H NMR spectrum of **1a**-d_n after H/D exchange experiment (CD_3OD as D-source at 100 ^{o}C oil bath temperature).

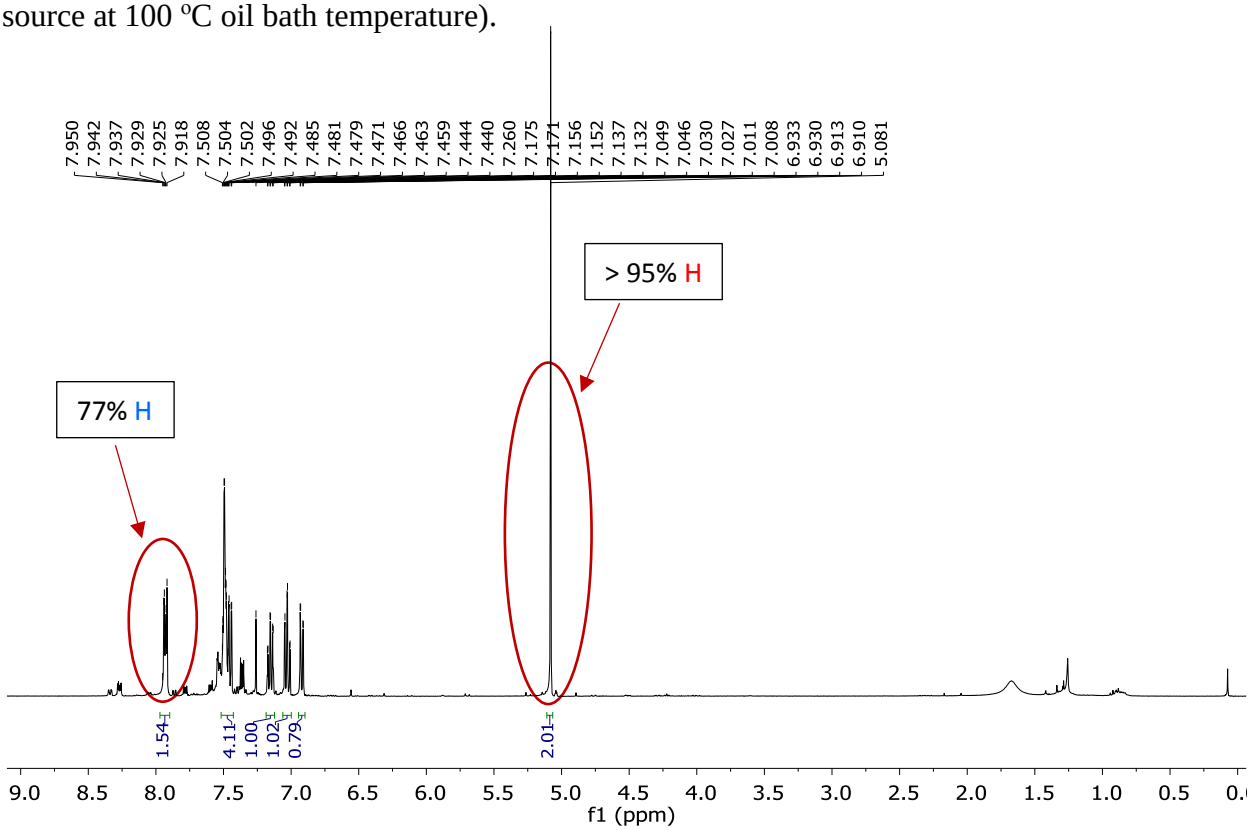

Figure 6.3.6.3. ^{1}H NMR spectrum of **1a**-d_n after H/D exchange experiment (D_2O as D-source at 40 ^{o}C oil bath temperature).

Next, competition experiments were performed taking differently substituted chalcones (**2**) and benzoxazines (**1**) to understand the effects of substituents on the reaction pathway and mechanistically how the C–H activation step proceeds (Scheme 6.3.6.2-6.3.6.5). First, a detailed investigation of the electronic effects of electron-donating (methyl) and electron-withdrawing (trifluoromethyl) substituents at *para* positions of both the aryl rings of chalcones were performed with **1a** under the standard conditions (Scheme 6.3.6.2, 6.3.6.3). ^{1}H NMR studies (with respect to major isomers) showed that in both cases electron-deficient partners reacted slightly favourably at a faster rate over the electron-rich ones (Figure 6.3.6.4, 6.3.6.5).

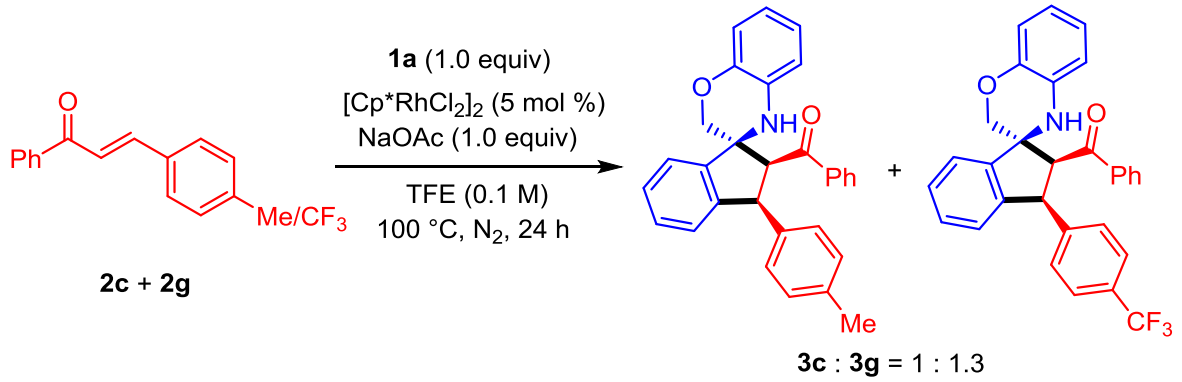

Scheme 6.3.6.2. Competitive experiment between chalcones **2c** and **2g** with **1a**.

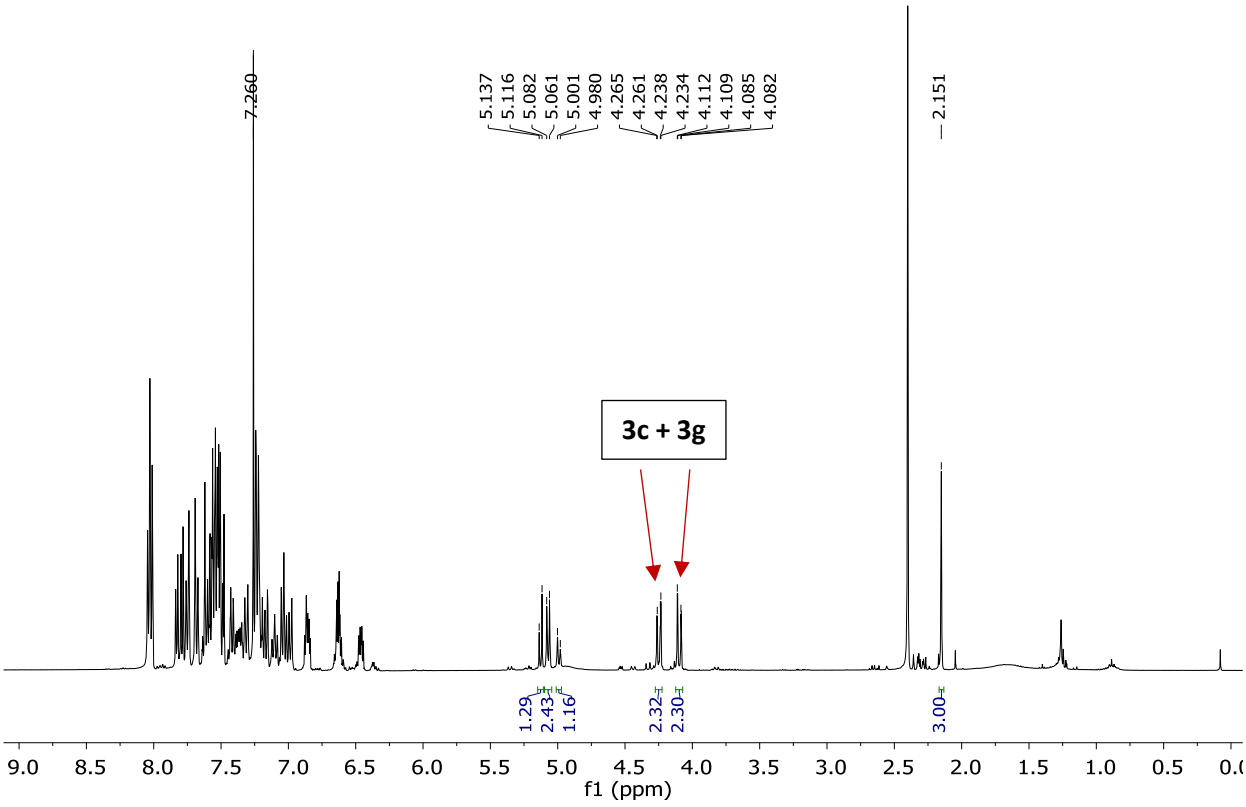

Figure 6.3.6.4. ^{1}H NMR spectrum for competitive experiment between chalcones **2c** and **2g**.

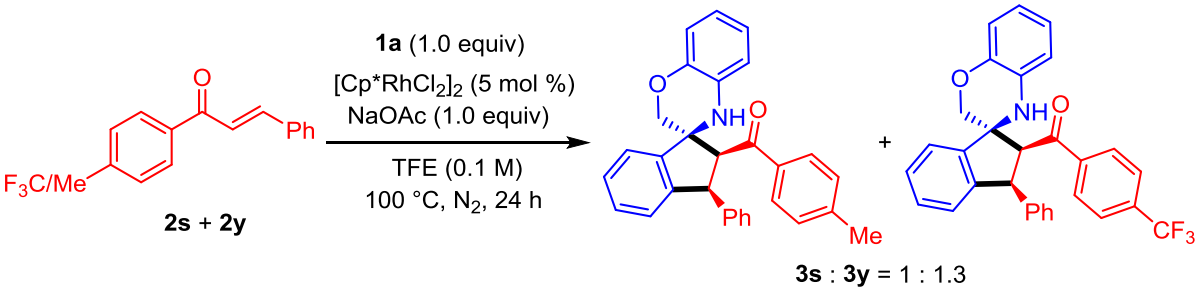

Scheme 6.3.6.3. Competitive experiment between chalcones **2s** and **2y** with **1a**.

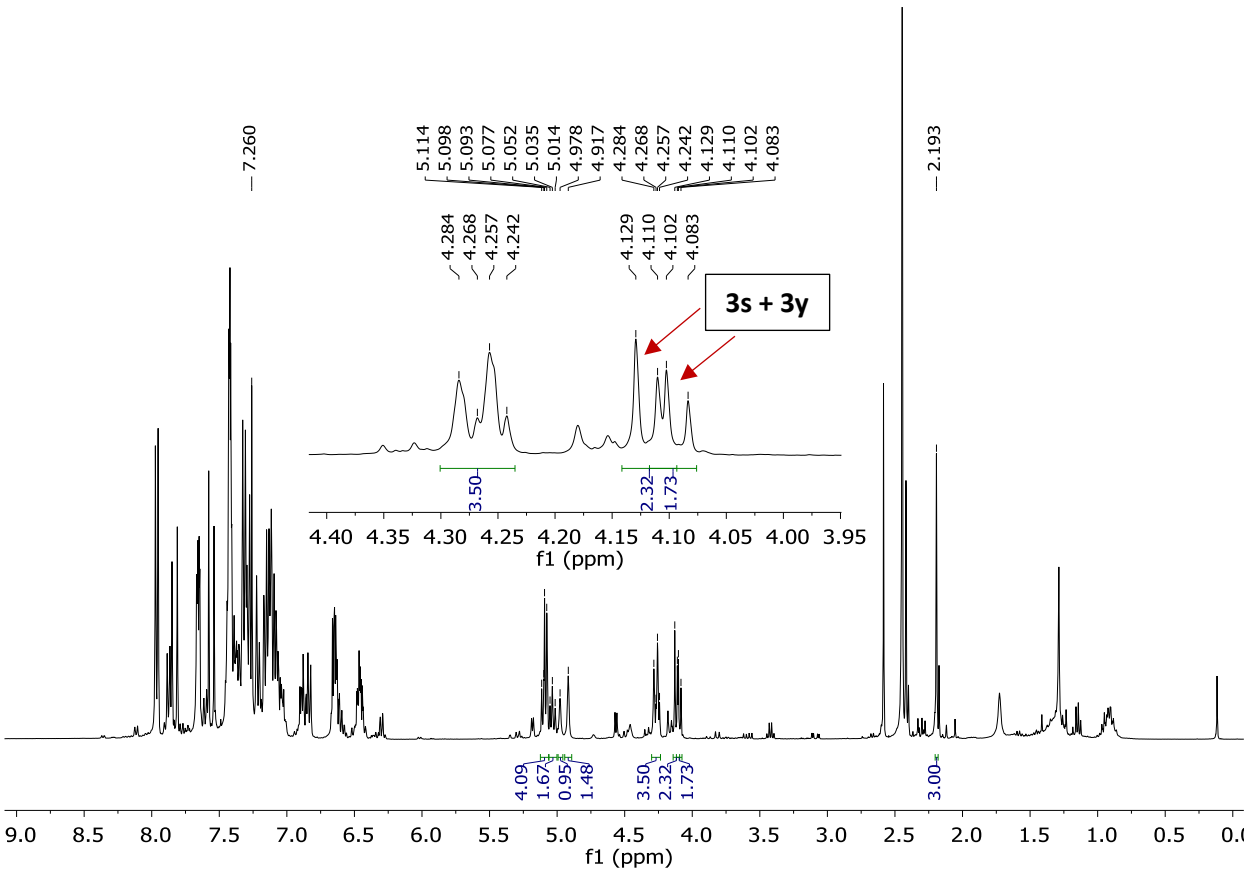

Figure 6.3.6.5. ^{1}H NMR spectrum for competitive experiment between chalcones **2s** and **2y**.

Again, a similar inspection was conducted between electron-rich benzoxazines (methyl-substituted on either of the aryl rings) and electron-poor ones (fluoro-substituted) with **2a** under the standard conditions (Scheme 6.3.6.4, 6.3.6.5). In contrast from the previous scenario, in both these cases, ^{1}H NMR studies (with respect to major isomers) showed that electron-donating group substituted benzoxazines reacted somewhat better than the electron-withdrawing group substituted ones (Figure 6.3.6.6, 6.3.6.7).

Combining these observations, they made us realize that the C–H activation step might undergo via a base-aided internal electrophilic substitution (BIES) type of mechanism.

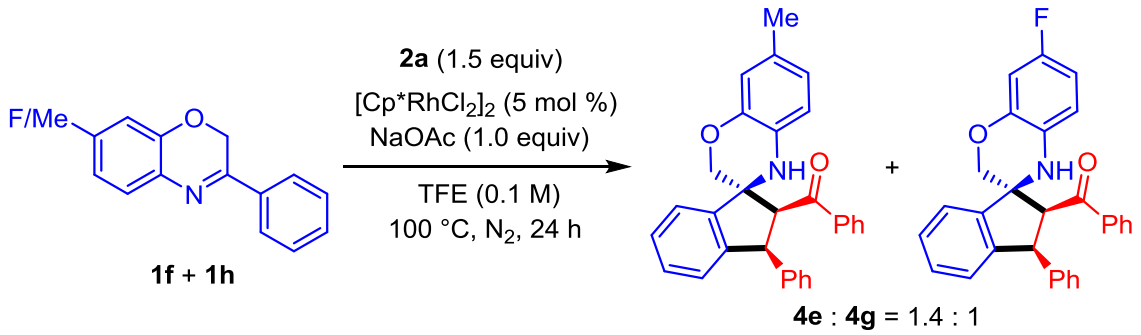

Scheme 6.3.6.4. Competitive experiment between between benzoxazines **1f** and **1h**.

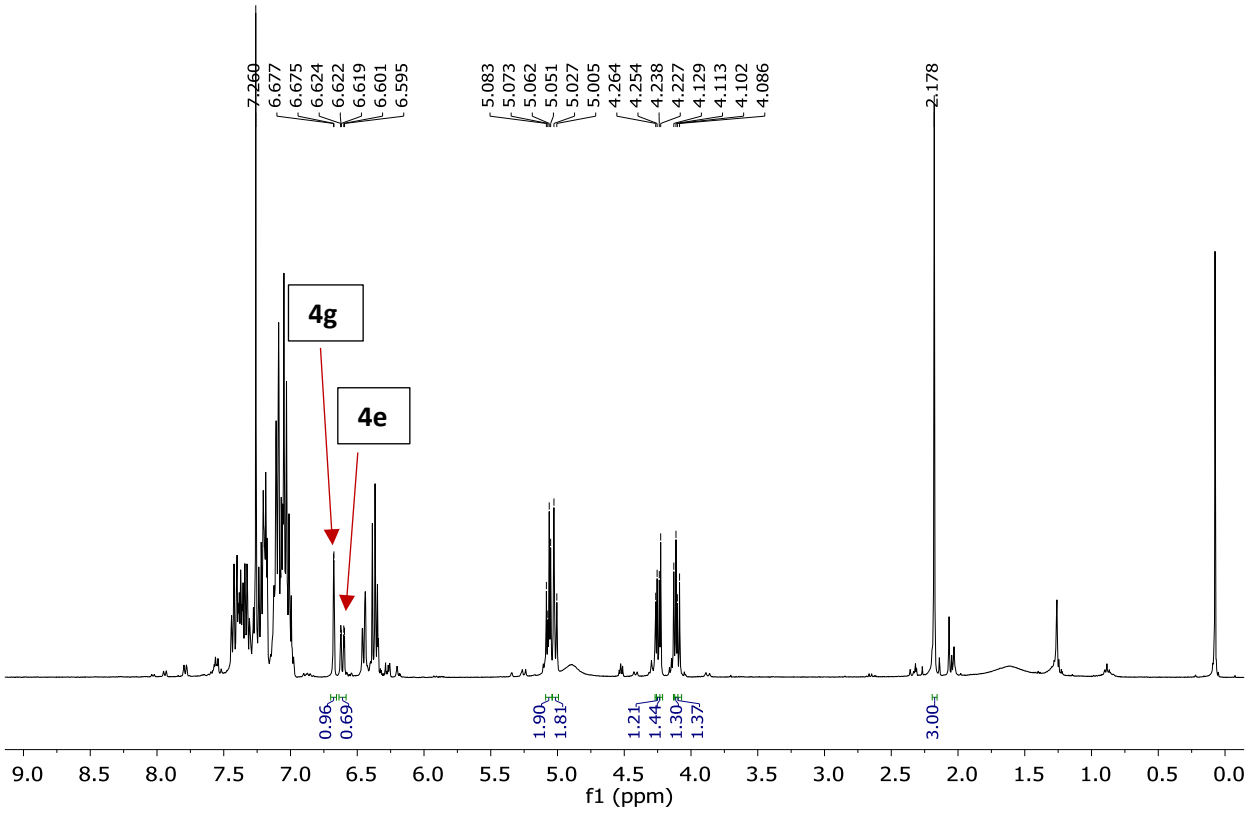

Figure 6.3.6.6. ^{1}H NMR spectrum for competitive experiment between benzoxazines **1f** and **1h**.

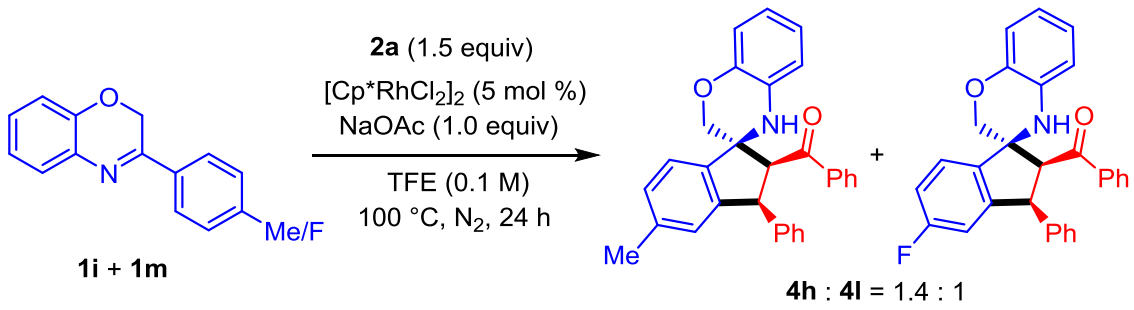

Scheme 6.3.6.5. Competitive experiment between between benzoxazines **1i** and **1m**.

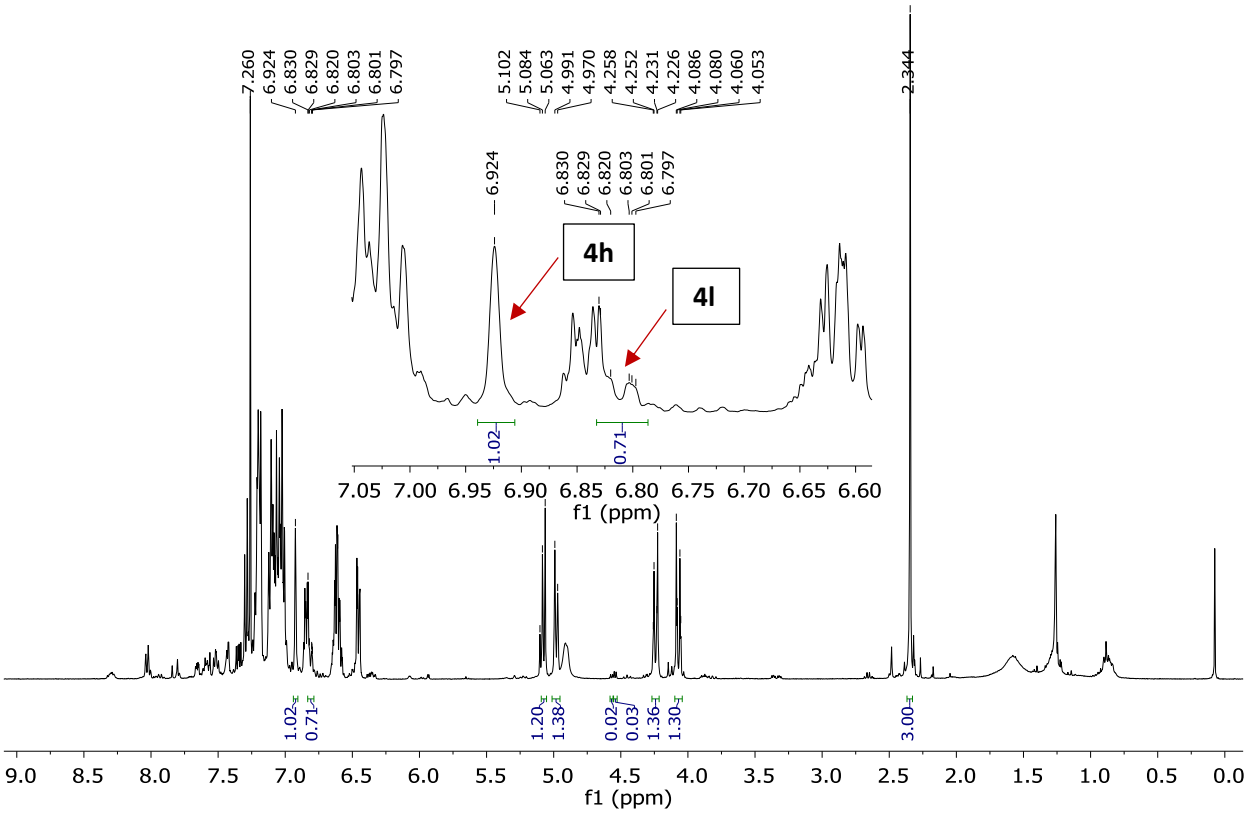

Figure 6.3.6.7. ^{1}H NMR spectrum for competitive experiment between benzoxazines **1i** and **1m**.

To further seek a perception of what kind of possible intermediates might be involved in the reaction pathway, we took up the synthesis of probable metalacyclic intermediates of the reaction and study its participation in the process (Scheme 6.3.6.6). For this objective, on performing a stoichiometric reaction between substrate **1i** and $[Cp^*RhCl_2]_2$ dimer, rhodacycle complex **5** was synthesized in an almost quantitative 99% yield, which was further easily converted to another rhodacycle half-sandwich complex **6** (96% yield) (Scheme 6.3.6.6a). The structures of these rhodacyclic complexes were confirmed by single-crystal X-ray analysis (Figure 6.3.6.8).

When complexes **5** or **6** were employed as catalysts for the current spiroannulation reaction between **1a**/**1i** and **2a**, the corresponding products **3a** and **4h** were formed respectively in very good yields and excellent diastereomeric ratios (Scheme 6.3.6.6b). This manifested the catalytic prowess of the rhodacyclic intermediates suggesting that the reaction could be initiated from the rhodacycle complexes. Finally, when complex **5** and chalcone **2a** were made to react in a stoichiometric reaction under standard conditions, a mere 25% yield of the product **4h** was obtained with poor selectivity (Scheme 6.3.6.6c). All these outcomes were in total support of the assumption that an elementary reaction between the rhodacycle intermediate and

chalcone followed by annulation maybe likely involved as a part of a simple carborhodation step, which is accelerated when an extra free imine substrate is present in the reaction medium along with NaOAc additive.

(a) Preparation of the rhodacycle complex intermediates:

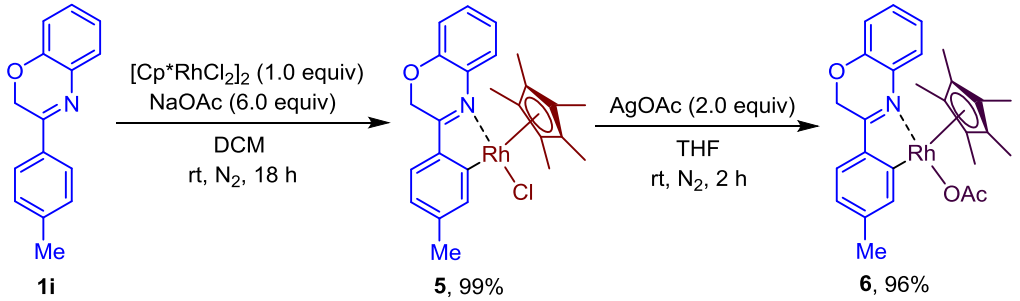

*(b) Treatment of the cyclometalated intermediates **5** and **6** as catalysts:*

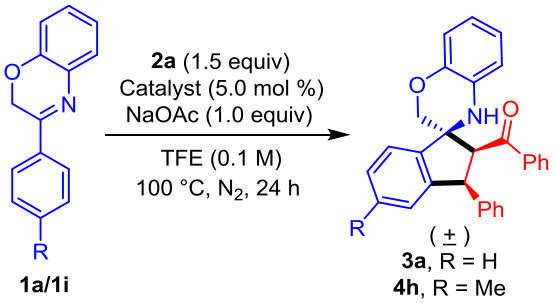

Substrate	Catalyst	Combined Yield (**3a/4h**)	dr
1a	$[Cp^*RhCl_2]_2$	98%	100:4:5
R = H	**5**	65%	100:2:1
(0.2 mmol)	**6**	84%	100:2:1
1i	$[Cp^*RhCl_2]_2$	96%	100:5:10
R = Me	**5**	76%	100:2:1
(0.1 mmol)	**6**	98%	100:1:1

*(c) Stoichiometric reaction between intermediate **5** and chalcone **2a**:*

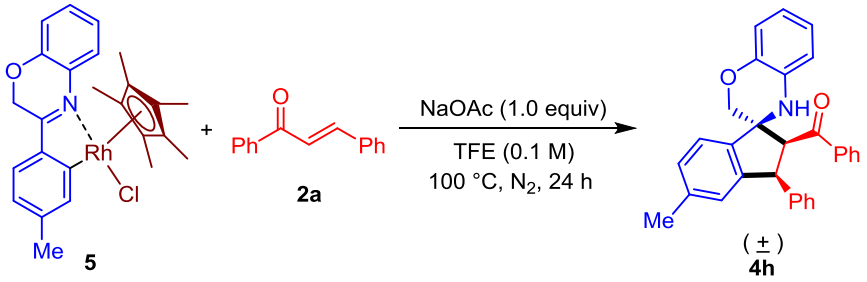

Scheme 6.3.6.6. Preparation and participation of cyclometalated intermediates.

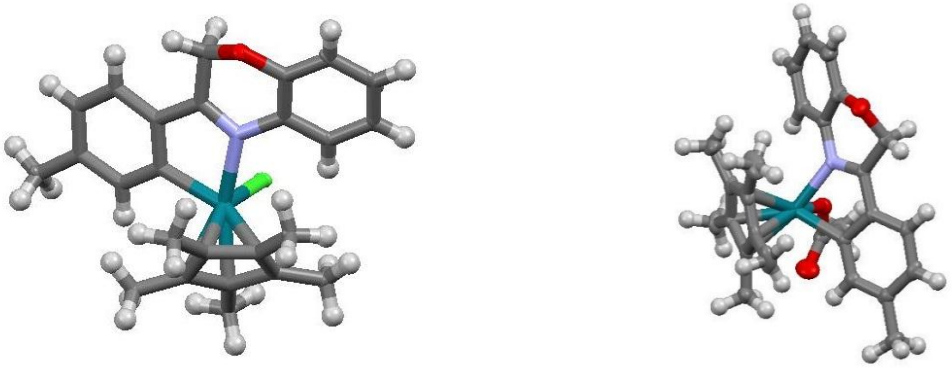

5
CCDC No. 2090978

6
CCDC No. 2090979

Figure 6.3.6.8. X-ray crystal structures of **5** and **6** (ellipsoid contour at 50% probability level).

On the basis of the above experimental results and previous literature reports,[6,10] a plausible reaction mechanism is outlined in Scheme 6.3.6.7. First, in the presence of NaOAc additive an active cationic monomeric Rh(III) species **A** can be formed from its predecessor $[Cp^*RhCl_2]_2$ dimer. This potent catalytic species **A** can coordinate with the iminyl *N*-atom of substrate **1a** generating rhodacycle intermediate **5** or **6** through a reversible C–H activation step. Subsequently, carborhodation may occur via tandem coordination/migratory insertion of the chalcone **2a** into the Rh–C bond of this intermediate in a regioselective manner. This can lead to a rhodium enolate intermediate **B** which may gain stabilization by the weakly chelating keto-enol oxygen atom[15] which supports the observation of the regioselective product. Next, the electrophilic imine carbon atom can undergo an intramolecular nucleophilic attack that leads to 1,2-addition of the C–Rh bond into the imine bond thereby affording intermediate **C**. Both the iminyl nitrogen and keto-carbonyl oxygen atoms may help in simultaneous chelation with the rhodium metal which is thought to be the key factor in accelerating the cyclization step and hence may be the reason for the formation of the cis-diastereomer as the major product. Finally, proto-demetalation of **C** can lead to the formation of the desired spiroannulated product **3a** with simultaneous regeneration of the active Rh(III) species **A**. This species again chelates with another free imine molecule **1a** and continues the catalytic cycle.

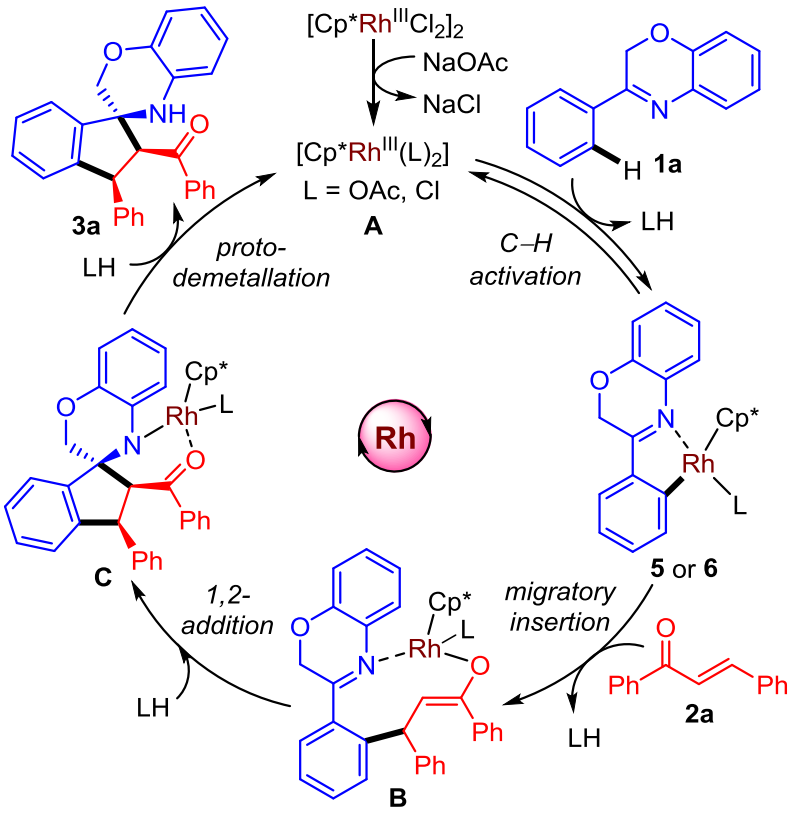

Scheme 6.3.6.7. Plausible reaction mechanism.

6.4. Summary

In summary, we have demonstrated a novel approach for a highly efficient and atom-economical synthesis of multi-substituted spiro-indanamines via a one-pot spirocyclization reaction between benzoxazines and chalcones employing redox-neutral Rh(III) catalysis in a highly stereoselective manner. This tandem C–H activation/[3+2]-annulation strategy features an environmentally benign technique which takes place under toxic silver additive-free and external oxidant-free conditions making it a synthetically viable and operationally simple process. The protocol presents a broad substrate scope applicable to a wide range of cyclic ketimines and chalcones with high functional group tolerance, furnishing densely functionalized spirocyclized products in excellent yields and high diastereoselectivity. This methodology guarantees access to a vast spectrum of α-keto-substituted indanamines containing spiro-1,4-benzoxazine derivatives with potential biological applications.

6.5. Experimental Section

6.5.1. General Information

All the information is same as that provided in Section 2.5.1 of Chapter 2 unless otherwise mentioned. The CIF files were submitted to CCDC (**2090973-2090979**) and can be obtained at https://summary.ccdc.cam.ac.uk/structure-summary-form. Major diastereomers and single crystals of the spirocyclized compounds were obtained taking 50-60 mg of the sample in 10 mL round bottom flasks using hot EtOH/$CHCl_3$ mixture applying solvent evaporation method. Single crystals of the cyclometallated compounds were obtained taking 5-10 mg of the sample in 5 mL vials using a bi-solvent system applying solvent diffusion technique. The choice of solvent systems and the method for crystal growth for each compound (**3c**, **3c″**, **3l**, **3aa**, **4d**, **5**, **6**) are provided in the characterization data section.

6.5.2. General Procedure for the Preparation of Starting Materials

All the benzoxazines[16] and chalcones and other α,β-unsaturated carbonyl compounds[17] were prepared following literature method (Scheme 6.5.2.1, 6.5.2.2).

To a solution of substituted 2-aminophenols (1.0 equiv) in DCM (0.167 M) was added K_2CO_3 solution (20% aqueous) and $^nBu_4HSO_4$ (1.0 equiv). The resulting two layers (aq. K_2CO_3/DCM) were magnetically stirred. To the emulsion formed, a solution of different phenacylbromides (1.0 equiv in DCM) was added dropwise over a period of 15 minutes. The resulting reaction mixture was stirred for 48 h at room temperature. After completion of reaction, the organic

layer was separated using DCM as eluent and washed with water, dried over anhydrous Na_2SO_4 and concentrated under vacuo. The resulting residue was purified by silica gel column chromatography to give the desired benzoxazines (**1**) (Scheme 6.5.2.1).

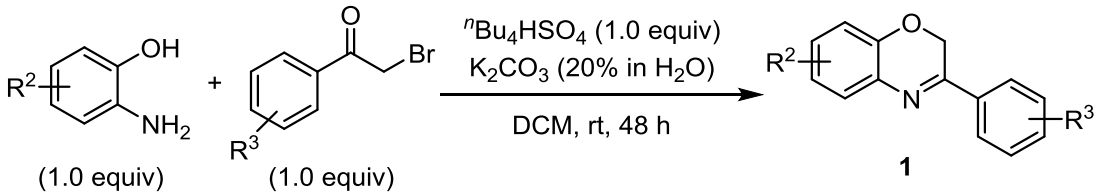

Scheme 6.5.2.1. Preparation of benzoxazines **1**.

Chalcones (**2**) were prepared by dissolving substituted acetophenones (1.0 equiv) in EtOH solvent (0.83 M) in a single-necked round bottom flask fitted on a magnetic stirrer. To it was added NaOH (0.2 equiv) and the resulting mixture was stirred for 10 minutes. Then, different aldehydes (1.0 equiv) were added separately while stirring and the reaction mixture was stirred for 6 to 8 h at room temperature and reaction progress was monitored by TLC. If precipitate was observed, then it was filtered by washing with cold water and the vaccum dried. Thereafter the crude products were recrystallized from EtOH to give the desired chalcones (**2**). In some cases where no precipitate was formed, the reaction mixture was eluted with ethyl acetate and washed with water and brine solution, dried over anhydrous Na_2SO_4 and concentrated under vacuo. Purification the resulting residue was done by silica gel column chromatography to give the corresponding chalcones (**2**) (Scheme 6.5.2.2).

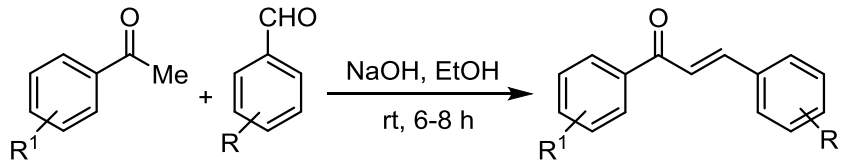

Scheme 6.5.2.2. Preparation of chalcones **2**.

6.5.3. General Procedure for Spirocyclization

(0.2 mmol scale):

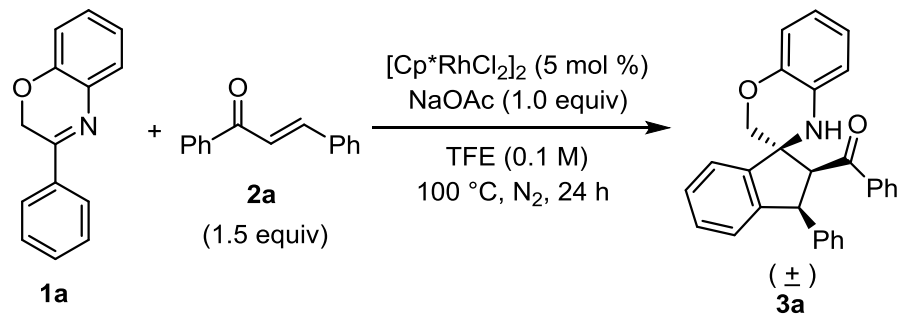

In an oven-dried 10 mL Schlenk tube, 3-phenyl-2*H*-benzo[*b*][1,4]oxazine (**1a**) (41.8 mg, 0.2 mmol, 1.0 equiv), (*E*)-chalcone (**2a**) (62.5 mg, 0.3 mmol, 1.5 equiv), $[Cp^*RhCl_2]_2$ (6.2 mg, 0.01 mmol, 0.05 equiv), and NaOAc (16.4 mg, 0.2 mmol, 1.0 equiv) were taken and the reaction mixture was degassed and backfilled with nitrogen. Under nitrogen 2.0 mL (0.1 M) of TFE was added. Then it was degassed and backfilled with nitrogen 3 times. The tube was closed with a teflon-lined cap and kept on stirring in a preheated oil bath at 100 °C. After 24 h, the reaction was stopped and cooled to room temperature. The reaction mixture was filtered through a short pad of celite and concentrated under vacuo. The crude reaction mixture was directly purified by column chromatography on silica gel using pet ether/ethyl acetate (19:1) as eluent to obtain phenyl(3'-phenyl-2',3'-dihydro-2*H*,4*H*-spiro[benzo[*b*][1,4]oxazine-3,1'-inden]-2'-yl)methanone (**3a**) (82.0 mg, 98% combined yield) as an inseparable mixture of three diastereomers (**3a**+**3a′**+**3a″**). The dr was calculated by ^{1}H NMR spectroscopy (100:4:5) (Figure 6.5.3.1).

82.0 mg of isolated mixture was dissolved in approx. 3-5 mL hot EtOH/$CHCl_3$ mixture and kept at room temperature. The crystal of the major diastereomer (**3a**) formed exclusively upon slow evaporation of the solvent which was collected by filtration and dried under vacuo (43.2 mg, 53% crystallization yield).

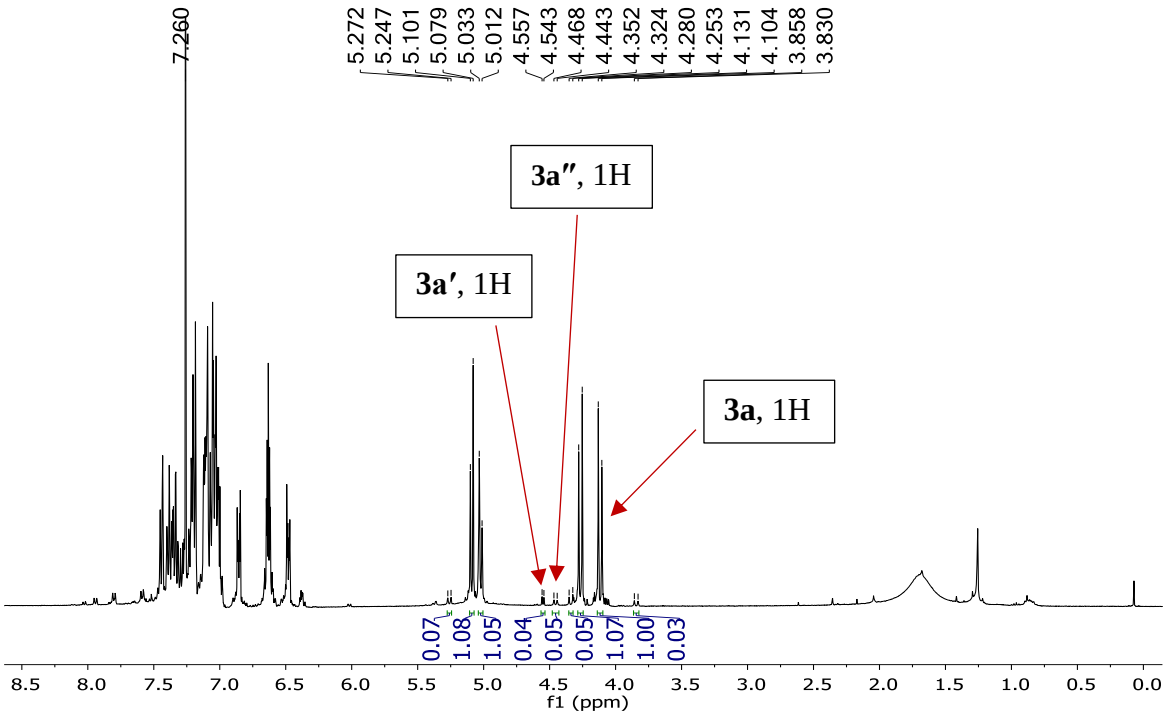

Figure 6.5.3.1. ^{1}H NMR spectrum of inseparable mixture of **3a**, **3a′** and **3a″**.

(gram-scale):

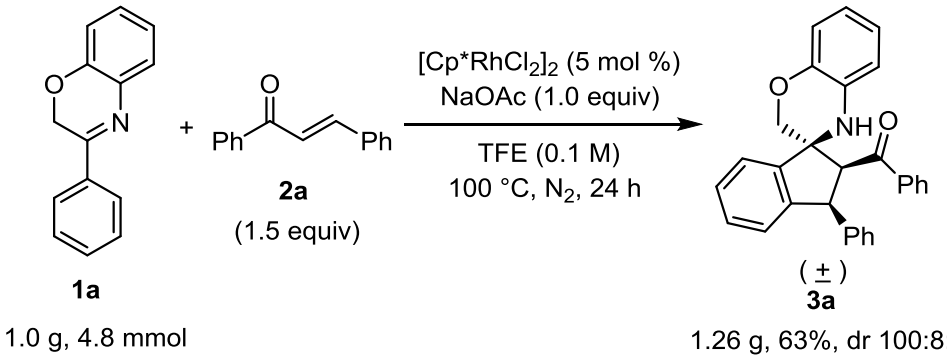

To an oven-dried 100 mL round bottom flask equipped with a reflux condenser, 3-phenyl-2*H*-benzo[*b*][1,4]oxazine (**1a**) (1.0 g, 4.8 mmol, 1.0 equiv), (*E*)-chalcone (**2a**) (1.5 g, 0.3 mmol, 1.5 equiv), $[Cp^*RhCl_2]_2$ (147.7 mg, 0.24 mmol, 0.05 equiv), and NaOAc (392.0 mg, 4.8 mmol, 1.0 equiv) were taken and the reaction mixture was degassed and backfilled with nitrogen. Under nitrogen 48.0 mL (0.1 M) of TFE was added. Then it was degassed and backfilled with nitrogen 3 times. The mouth of the round bottom flask was closed with a glass stopper and kept on stirring in a preheated oil bath at 100 ^{o}C. After 24 h, the reaction was stopped and cooled to room temperature. The reaction mixture was filtered through a short pad of celite and concentrated under vacuo. The crude reaction mixture was directly purified by column chromatography on silica gel using pet ether/ethyl acetate (19:1) as eluent to obtain phenyl(3'-phenyl-2',3'-dihydro-2*H*,4*H*-spiro[benzo[*b*][1,4]oxazine-3,1'-inden]-2'-yl)methanone (**3a**) (1.26 g, 63% combined yield) as an inseparable mixture of three diastereomers (**3a**+**3a′**+**3a″**). The dr was calculated by ^{1}H NMR spectroscopy (100:7:8).

Compounds **3b**, **3p**-**3r** were prepared using chalcone **2** (0.2 mmol, 1.0 equiv) and substrate **1a** (0.3 mmol, 1.5 equiv) employing the same procedure. The reaction for the synthesis of compounds **3b** and **3r** were run for 40 h.

The characterization data for all the major diastereomers is given below.

6.5.4. Characterization Data for the Spirocyclized Products

phenyl(3'-phenyl-2',3'-dihydro-2*H*,4*H*-spiro[benzo[*b*][1,4]oxazine-3,1'-inden]-2'-yl)methanone:

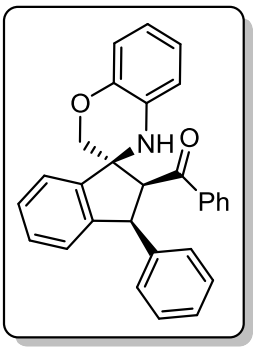

Combined Yield 98% (82.0 mg, dr 100:4:5)

Major diastereomer **3a**:

Light yellow solid; **R_f** 0.25 (pet ether/ethyl acetate = 19:1); **eluent composition** petroleum ether/ethyl acetate = 19:1; **mp** 202-204 ^oC (crystallization from hot EtOH/$CHCl_3$ mixture using solvent evaporation method); **^{1}H NMR** (400 MHz, $CDCl_3$) δ 7.43-7.41 (m, 1H), 7.38 (app t, *J* = 7.2 Hz, 1H), 7.36-7.32 (m, 1H), 7.24-7.19 (comp, 3H), 7.12-7.10 (comp, 3H), 7.08-7.00 (comp, 5H), 6.87-6.84 (m, 1H), 6.66-6.59 (comp, 2H), 6.48-6.46 (m, 1H), 5.09 (d, *J* = 8.8 Hz, 1H), 5.02 (d, *J* = 8.4 Hz, 1H), 4.95 (br s, 1H), 4.26 (d, *J* = 10.8 Hz, 1H), 4.10 (d, *J* = 10.4 Hz, 1H); **^{13}C NMR** (100 MHz, $CDCl_3$) δ 201.7, 143.9, 143.0, 142.5, 138.8, 138.1, 132.8, 132.1, 129.9 (x 2), 128.8, 128.1 (x 2), 128.0, 127.7 (x 2), 127.6 (x 2), 127.0, 125.3, 123.5, 122.0, 118.8, 116.2, 115.8, 71.0, 64.0, 59.5, 52.4; **HRMS** (ESI, m/z) calcd for $C_{29}H_{23}NO_2$ $[M + H]^+$ 418.1807, found 418.1806.

(3'-(4-methoxyphenyl)-2',3'-dihydro-2*H*,4*H*-spiro[benzo[*b*][1,4]oxazine-3,1'-inden]-2'-yl)(phenyl)methanone:

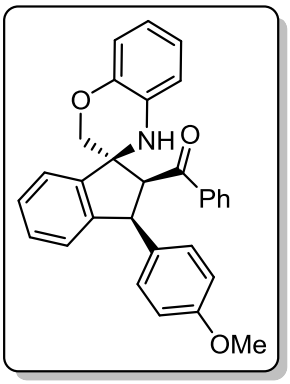

Combined Yield 81% (72.7 mg, dr 100:7:5)

Major diastereomer **3b**:

Light yellow solid; **R_f** 0.10 (pet ether/ethyl acetate = 19:1); **eluent composition** petroleum ether/ethyl acetate = 19:1; **mp** 166-168 ^oC (crystallization from hot EtOH/$CHCl_3$ mixture using solvent evaporation method); **^{1}H NMR** (400 MHz, $CDCl_3$) δ 7.42-7.31 (comp, 3H), 7.25-7.22 (comp, 3H), 7.10 (app d, *J* = 7.2 Hz, 1H), 7.07-7.01 (comp, 4H), 6.86-6.84 (m, 1H), 6.66-6.59 (comp, 4H), 6.47 (dd, *J* = 7.2 Hz, 1.6 Hz, 1H), 5.07 (d, *J* = 8.4 Hz, 1H), 4.99 (d, *J* = 8.4 Hz, 1H), 4.25 (d, *J* = 10.8 Hz, 1H), 4.09 (d, *J* = 10.8 Hz, 1H), 3.66 (s, 3H); **^{13}C NMR** (100 MHz, $CDCl_3$) δ 201.9, 158.6, 143.8, 143.0, 142.9, 138.9, 132.9, 132.1, 130.9 (x 2), 130.2, 128.8, 128.0, 127.7 (x 2), 127.6 (x 2), 125.2, 123.4, 121.9, 118.8, 116.2, 115.8, 113.5 (x 2), 71.0, 64.0, 59.5, 55.2, 51.6; **HRMS** (ESI, m/z) calcd for $C_{30}H_{25}NO_3$ $[M + H]^+$ 448.1913, found 448.1926.

phenyl(3'-(*p*-tolyl)-2',3'-dihydro-2*H*,4*H*-spiro[benzo[*b*][1,4]oxazine-3,1'-inden]-2'-yl)methanone:

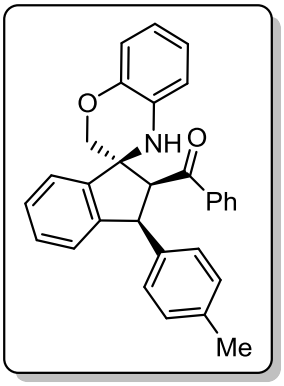

Combined Yield 93% (79.8 mg, dr 100:5:9)

Major diastereomer **3c**:

Light yellow solid; **R_f** 0.30 (pet ether/ethyl acetate = 19:1); **eluent composition** petroleum ether/ethyl acetate = 19:1; **mp** 198-200 ^oC (crystallization from hot EtOH/$CHCl_3$ mixture using solvent evaporation method); **^{1}H NMR** (400 MHz, $CDCl_3$) δ 7.42 (dd, *J* = 7.2 Hz, 1.6 Hz, 1H), 7.37 (app t, *J* = 7.2 Hz, 1H), 7.33 (td, *J* = 7.2 Hz, 1.6 Hz, 1H), 7.24-7.20 (comp, 3H), 7.12 (app d, *J* = 7.2 Hz, 1H), 7.06-7.02 (comp, 2H), 7.00-6.98 (comp, 2H), 6.87-6.84 (comp, 3H), 6.66-6.59 (comp, 2H), 6.48-6.46 (m, 1H), 5.08 (d, *J* = 8.4 Hz, 1H), 5.00 (d, *J* = 8.4 Hz, 1H), 4.26 (d, *J* = 10.8 Hz, 1H), 4.10 (d, *J* = 10.8 Hz, 1H), 2.16 (s, 3H); **^{13}C NMR** (100 MHz, $CDCl_3$) δ 201.8, 143.8, 143.0, 142.7, 138.9, 136.6, 135.0, 132.8, 132.0, 129.7 (x 2), 128.7 (x 3), 127.9, 127.6 (x 4), 125.3, 123.4, 121.9, 118.8, 116.2, 115.8, 71.0, 64.0, 59.6, 52.0, 20.8; **HRMS** (ESI, m/z) calcd for $C_{30}H_{25}NO_2$ $[M + H]^+$ 432.1964, found 432.1975.

Crystal data and structure refinement for 3c, CCDC No. 2090973

Empirical formula	$C_{30}H_{25}NO_2$
Formula weight	431.51
Temperature/K	100.0
Crystal system	triclinic
Space group	P-1
a/Å	9.6057(5)
b/Å	11.3540(6)
c/Å	11.9640(6)
α/°	72.192(2)
β/°	66.978(2)
γ/°	83.414(2)
Volume/Å^3	1143.35(10)
Z	2
ρ_{calc}g/cm^3	1.253
μ/mm^{-1}	0.611
F(000)	456.0
Crystal size/mm^3	0.2 × 0.19 × 0.13
Radiation	Cu Kα (λ = 1.54178)
2Θ range for data collection/°	8.178 to 130.096
Index ranges	$-11 \le h \le 11$, $-13 \le k \le 12$, $-14 \le l \le 14$
Reflections collected	46421
Independent reflections	3885 [R_{int} = 0.0838, R_{sigma} = 0.0429]

Data/restraints/parameters	3885/0/300
Goodness-of-fit on F^2	1.111
Final R indexes [I>=2σ (I)]	R_1 = 0.0557, wR_2 = 0.1317
Final R indexes [all data]	R_1 = 0.0595, wR_2 = 0.1345
Largest diff. peak/hole / e $Å^{-3}$	0.25/-0.30

(3'-(4-(tert-butyl)phenyl)-2',3'-dihydro-2*H*,4*H*-spiro[benzo[*b*][1,4]oxazine-3,1'-inden]-2'-yl)(phenyl)methanone:

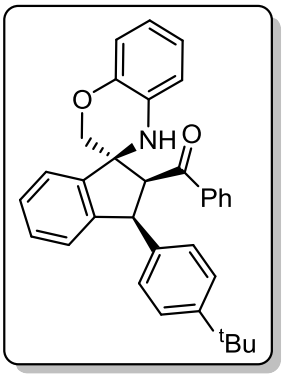

Combined Yield 91% (86.0 mg, dr 100:6:4)

Major diastereomer **3d**:

Colorless solid; **R_f** 0.30 (pet ether/ethyl acetate = 19:1); **eluent composition** petroleum ether/ethyl acetate = 19:1; **mp** 158-160 °C (crystallization from hot EtOH/$CHCl_3$ mixture using solvent evaporation method); **^{1}H NMR** (400 MHz, $CDCl_3$) δ 7.43 (dd, *J* = 7.2 Hz, 0.8 Hz, 1H), 7.38 (app t, *J* = 7.2 Hz, 1H), 7.34 (td, *J* = 7.2 Hz, 1.6 Hz, 1H), 7.20-7.16 (comp, 2H), 7.14-7.12 (comp, 2H), 7.05-6.98 (comp, 6H), 6.88-6.86 (m, 1H), 6.68-6.61 (comp, 2H), 6.51-6.49 (m, 1H), 5.06 (d, *J* = 8.4 Hz, 1H), 5.02 (d, *J* = 8.4 Hz, 1H), 4.26 (d, *J* = 10.8 Hz, 1H), 4.10 (d, *J* = 10.8 Hz, 1H), 1.16 (s, 9H); **^{13}C NMR** (100 MHz, $CDCl_3$) δ 202.0, 149.9, 144.0, 143.1, 142.3, 139.0, 134.8, 132.9, 131.8, 129.4 (x 2), 128.7, 128.0, 127.6 (x 2), 127.6 (x 2), 125.4, 124.9 (x 2), 123.4, 121.9, 118.8, 116.2, 115.9, 70.9, 63.8, 59.6, 52.0, 34.2, 31.2; **HRMS** (ESI, m/z) calcd for $C_{33}H_{31}NO_2$ $[M + H]^+$ 474.2433, found 474.2429.

(3'-(4-chlorophenyl)-2',3'-dihydro-2*H*,4*H*-spiro[benzo[*b*][1,4]oxazine-3,1'-inden]-2'-yl)(phenyl)methanone:

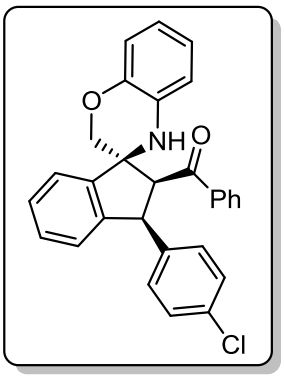

Combined Yield 98% (88.2 mg, dr 100:7:11)

Major diastereomer **3e**:

Light yellow solid; **R_f** 0.20 (pet ether/ethyl acetate = 19:1); **eluent composition** petroleum ether/ethyl acetate = 19:1; **mp** 202-204 °C (crystallization from hot EtOH/$CHCl_3$ mixture using solvent evaporation method); **^{1}H NMR** (400 MHz, $CDCl_3$) δ 7.43-7.37 (comp, 2H), 7.34 (td, *J* = 7.2 Hz, 2.0 Hz, 1H), 7.29-7.21 (comp, 3H), 7.10-7.02 (comp, 7H), 6.88-6.83 (m, 1H), 6.66-6.59 (comp, 2H), 6.48-6.43 (m, 1H), 5.10 (d, *J* = 8.4 Hz, 1H), 4.99 (d, *J* = 8.4 Hz, 1H), 4.91 (br s, 1H), 4.23 (d, *J* = 10.8 Hz, 1H), 4.09 (d, *J* = 10.8 Hz, 1H); **^{13}C NMR** (100 MHz, $CDCl_3$) δ 201.4, 143.8, 143.0, 142.0, 138.6, 136.8, 132.9, 132.7, 132.4, 131.2 (x 2), 128.9, 128.2 (x 3), 127.9 (x 2), 127.5 (x 2), 125.1, 123.6, 122.0, 118.9,

116.2, 115.8, 71.0, 64.1, 59.4, 51.6; **HRMS** (ESI, m/z) calcd for $C_{29}H_{22}ClNO_2$ $[M + H]^+$ 452.1417, found 452.1411.

(3'-(4-fluorophenyl)-2',3'-dihydro-2*H*,4*H*-spiro[benzo[*b*][1,4]oxazine-3,1'-inden]-2'-yl)(phenyl)methanone:

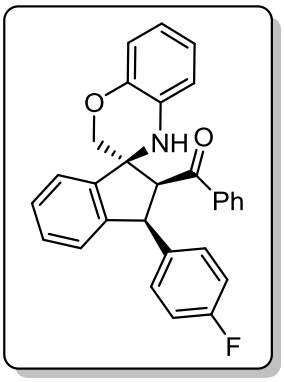

Combined Yield 73% (63.7 mg, dr 100:6:4)

Major diastereomer **3f**:

Light yellow solid; **R_f** 0.20 (pet ether/ethyl acetate = 19:1); **eluent composition** petroleum ether/ethyl acetate = 19:1; **mp** 154-156 ºC (crystallization from hot EtOH/$CHCl_3$ mixture using solvent evaporation method); **^{1}H NMR** (400 MHz, $CDCl_3$) δ 7.42 (dd, *J* = 7.2 Hz, 1.2 Hz, 1H), 7.39 (app t, *J* = 7.2 Hz, 1H), 7.34 (td, *J* = 7.2 Hz, 1.6 Hz, 1H), 7.28-7.22 (comp, 3H), 7.10-7.05 (comp, 5H), 6.88-6.83 (m, 1H), 6.78-6.73 (comp, 2H), 6.66-6.59 (comp, 2H), 6.49-6.44 (m, 1H), 5.09 (d, *J* = 8.4 Hz, 1H), 5.01 (d, *J* = 8.4 Hz, 1H), 4.93 (br s, 1H), 4.24 (d, *J* = 10.8 Hz, 1H), 4.09 (d, *J* = 10.8 Hz, 1H); **^{13}C NMR** (100 MHz, $CDCl_3$) δ 201.6, 161.8 (d, $^1J_{C–F}$ = 245.0 Hz), 143.8, 143.0, 142.4, 138.7, 133.9 (d, $^4J_{C–F}$ = 3.0 Hz), 132.8, 132.4, 131.4 (d, $^3J_{C–F}$ = 8.0 Hz), 128.9, 128.2, 127.8 (x 3), 127.6 (x 3), 125.1, 123.6, 122.0, 118.9, 116.2, 115.8, 114.9 (d, $^2J_{C–F}$ = 21.0 Hz), 71.0, 64.1, 59.4, 51.5; **HRMS** (ESI, m/z) calcd for $C_{29}H_{22}FNO_2$ $[M + H]^+$ 436.1713, found 436.1703.

phenyl(3'-(4-(trifluoromethyl)phenyl)-2',3'-dihydro-2*H*,4*H*-spiro[benzo[*b*][1,4]oxazine-3,1'-inden]-2'-yl)methanone:

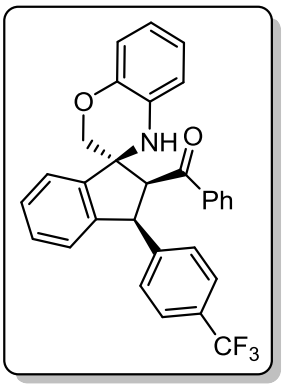

Combined Yield 96% (93.0 mg, dr 100:9:10)

Major diastereomer **3g**:

Light yellow solid; **R_f** 0.20 (pet ether/ethyl acetate = 19:1); **eluent composition** petroleum ether/ethyl acetate = 19:1; **mp** 154-156 ºC (crystallization from hot EtOH/$CHCl_3$ mixture using solvent evaporation method); **^{1}H NMR** (400 MHz, $CDCl_3$) δ 7.45-7.39 (comp, 2H), 7.36 (td, *J* = 7.2 Hz, 2.0 Hz, 1H), 7.32-7.30 (comp, 2H), 7.24-7.22 (comp, 3H), 7.18-7.15 (comp, 2H), 7.09 (app d, *J* = 7.6 Hz, 1H), 7.06-7.02 (comp, 2H), 6.88-6.83 (m, 1H), 6.66-6.60 (comp, 2H), 6.47-6.43 (m, 1H), 5.13 (d, *J* = 8.4 Hz, 1H), 5.07 (d, *J* = 8.8 Hz, 1H), 4.92 (br s, 1H), 4.25 (d, *J* = 10.8 Hz, 1H), 4.09 (d, *J* = 10.8 Hz, 1H); **^{13}C NMR** (100 MHz, $CDCl_3$) δ 201.3, 143.9, 142.9, 142.4, 141.5, 138.6, 132.8, 132.5, 130.2 (x 2), 129.3 (app d, *J* = 32.0 Hz), 129.0, 128.4, 127.9 (x 2), 127.5 (x 2), 126.6 (q, *J* = 255.0 Hz), 125.1,

125.0 (q, *J* = 3.0 Hz), 123.7, 122.0, 118.9, 116.2, 115.8, 71.0, 64.2, 59.3, 52.0; **HRMS** (ESI, m/z) calcd for $C_{30}H_{22}F_3NO_2$ $[M + H]^+$ 486.1681, found 486.1675.

phenyl(3'-(*m*-tolyl)-2',3'-dihydro-2*H*,4*H*-spiro[benzo[*b*][1,4]oxazine-3,1'-inden]-2'-yl)methanone:

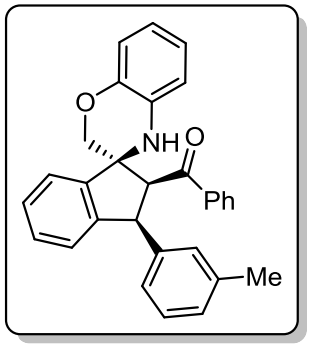

Combined Yield 96% (82.7 mg, dr 100:7:11)

Major diastereomer **3h**:

Light yellow solid; **R_f** 0.25 (pet ether/ethyl acetate = 19:1); **eluent composition** petroleum ether/ethyl acetate = 19:1; **mp** 142-144 ^oC (crystallization from hot EtOH/$CHCl_3$ mixture using solvent evaporation method); **^{1}H NMR** (400 MHz, $CDCl_3$) δ 7.42 (dd, *J* = 7.2 Hz, 1.6 Hz, 1H), 7.38 (app t, *J* = 7.2 Hz, 1H), 7.34 (td, *J* = 7.2 Hz, 1.6 Hz, 1H), 7.24-7.20 (comp, 3H), 7.13 (app d, *J* = 7.6 Hz, 1H), 7.06-7.02 (comp, 2H), 6.96-6.89 (comp, 3H), 6.85 (dd, *J* = 7.2 Hz, 1.6 Hz, 1H), 6.79 (app d, *J* = 6.8 Hz, 1H), 6.67-6.59 (comp, 2H), 6.48 (dd, *J* = 7.2 Hz, 1.6 Hz, 1H), 5.07 (d, *J* = 8.4 Hz, 1H), 4.99 (d, *J* = 7.2 Hz, 2H), 4.25 (dd, *J* = 10.8 Hz, 2.0 Hz, 1H), 4.08 (d, *J* = 10.8 Hz, 1H), 2.12 (s, 3H); **^{13}C NMR** (100 MHz, $CDCl_3$) δ 201.6, 144.0, 143.0, 142.4, 138.8, 137.9, 137.6, 133.0, 132.0, 130.6, 128.7, 128.0 (x 2), 127.7, 127.6 (x 2), 127.6 (x 2), 126.8, 125.4, 123.4, 121.9, 118.7, 116.2, 115.8, 70.9, 63.9, 59.4, 52.3, 21.1; **HRMS** (ESI, m/z) calcd for $C_{30}H_{25}NO_2$ $[M + H]^+$ 432.1964, found 432.1955.

(3'-(3-bromophenyl)-2',3'-dihydro-2*H*,4*H*-spiro[benzo[*b*][1,4]oxazine-3,1'-inden]-2'-yl)(phenyl)methanone:

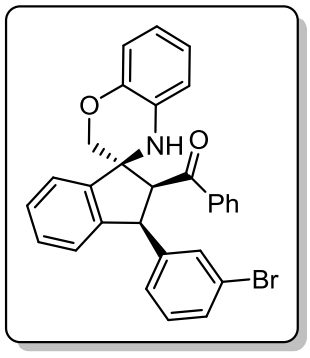

Combined Yield 99% (98.6 mg, dr 100:6:8)

Major diastereomer **3i**:

Yellow solid; **R_f** 0.20 (pet ether/ethyl acetate = 19:1); **eluent composition** petroleum ether/ethyl acetate = 19:1; **mp** 184-186 ^oC (crystallization from hot EtOH/$CHCl_3$ mixture using solvent evaporation method); **^{1}H NMR** (400 MHz, $CDCl_3$) δ 7.44-7.38 (comp, 2H), 7.35 (td, *J* = 7.2 Hz, 1.6 Hz, 1H), 7.28-7.24 (comp, 4H), 7.14-7.07 (comp, 4H), 7.03 (app d, *J* = 8.0 Hz, 1H), 6.91 (app t, *J* = 8.0 Hz, 1H), 6.87-6.85 (m, 1H), 6.67-6.60 (comp, 2H), 6.49-6.46 (m, 1H), 5.08 (d, *J* = 8.4 Hz, 1H), 4.97 (d, *J* = 8.4 Hz, 1H), 4.23 (d, *J* = 10.8 Hz, 1H), 4.09 (d, *J* = 10.8 Hz, 1H); **^{13}C NMR** (100 MHz, $CDCl_3$) δ 201.2, 143.9, 143.0, 141.6, 140.6, 138.5, 133.0, 132.7, 132.5, 130.1, 129.6, 129.0, 128.4, 128.3,

127.8 (x 2), 127.6 (x 2), 125.1, 123.6, 122.2, 122.0, 119.0, 116.2, 115.9, 70.9, 64.0, 59.1, 51.8; **HRMS** (ESI, m/z) calcd for $C_{29}H_{22}BrNO_2$ $[M + H]^+$ 496.0912, found 496.0908.

(3'-(3-chlorophenyl)-2',3'-dihydro-2*H*,4*H*-spiro[benzo[*b*][1,4]oxazine-3,1'-inden]-2'-yl)(phenyl)methanone:

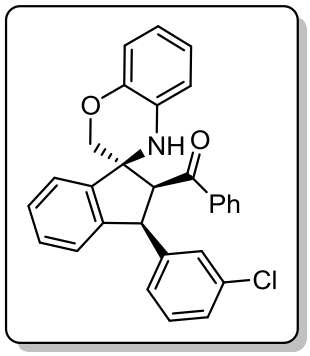

Combined Yield 98% (88.8 mg, dr 100:5:5)

Major diastereomer **3j**:

Yellow solid; **R_f** 0.25 (pet ether/ethyl acetate = 19:1); **eluent composition** petroleum ether/ethyl acetate = 19:1; **mp** 174-176 ^oC (crystallization from hot EtOH/$CHCl_3$ mixture using solvent evaporation method); **^{1}H NMR** (400 MHz, $CDCl_3$) δ 7.44-7.38 (comp, 2H), 7.35 (td, *J* = 7.2 Hz, 2.0 Hz, 1H), 7.28-7.24 (comp, 3H), 7.11-7.06 (comp, 4H), 7.01-6.97 (comp, 3H), 6.87-6.85 (m, 1H), 6.67-6.60 (comp, 2H), 6.50-6.45 (m, 1H), 5.09 (d, *J* = 8.4 Hz, 1H), 4.99 (d, *J* = 8.4 Hz, 1H), 4.24 (d, *J* = 10.8 Hz, 1H), 4.09 (d, *J* = 10.8 Hz, 1H); **^{13}C NMR** (100 MHz, $CDCl_3$) δ 201.2, 143.9, 143.0, 141.6, 140.3, 138.6, 134.0, 132.8, 132.4, 130.0, 129.3, 129.0, 128.3, 128.0, 127.8 (x 2), 127.6 (x 2), 127.2, 125.1, 123.6, 122.0, 118.9, 116.2, 115.8, 70.9, 64.0, 59.2, 51.9; **HRMS** (ESI, m/z) calcd for $C_{29}H_{22}BrNO_2$ $[M + H]^+$ 452.1417, found 452.1409.

(3'-(3-nitrophenyl)-2',3'-dihydro-2*H*,4*H*-spiro[benzo[*b*][1,4]oxazine-3,1'-inden]-2'-yl)(phenyl)methanone:

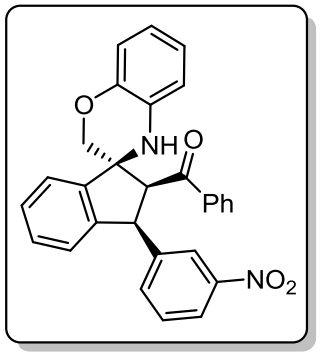

Combined Yield 68% (62.3 mg, dr 100:17:11)

Major diastereomer **3k**:

Yellow solid; **R_f** 0.15 (pet ether/ethyl acetate = 19:1); **eluent composition** petroleum ether/ethyl acetate = 19:1; **mp** 168-170 ^oC (crystallization from hot EtOH/$CHCl_3$ mixture using solvent evaporation method); **^{1}H NMR** (400 MHz, $CDCl_3$) δ 8.02 (app t, *J* = 1.6 Hz, 1H), 7.89-7.86 (m, 1H), 7.47-7.43 (comp, 3H), 7.41-7.36 (m, 1H), 7.28-7.22 (comp, 4H), 7.08-7.03 (comp, 3H), 6.89-6.83 (m, 1H), 6.65-6.59 (comp, 2H), 6.45-6.40 (m, 1H), 5.18 (d, *J* = 8.4 Hz, 1H), 5.13 (d, *J* = 8.4 Hz, 1H), 4.88 (br s, 1H), 4.24 (d, *J* = 10.8 Hz, 1H), 4.09 (d, *J* = 10.8 Hz, 1H); **^{13}C NMR** (100 MHz, $CDCl_3$) δ 200.7, 147.9, 143.9, 142.9, 141.1, 140.7, 138.2, 135.8, 132.8, 132.6, 129.2, 129.0, 128.6, 128.0 (x 2), 127.6 (x 2), 125.0, 124.8, 123.9, 122.1, 122.0, 118.9, 116.2, 115.7, 71.0, 64.3, 59.0, 51.7; **HRMS** (ESI, m/z) calcd for $C_{29}H_{22}N_2O_4$ $[M + H]^+$ 463.1658, found 463.1653.

phenyl(3'-(*o*-tolyl)-2',3'-dihydro-2*H*,4*H*-spiro[benzo[*b*][1,4]oxazine-3,1'-inden]-2'-yl)methanone:

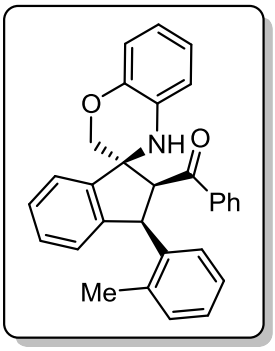

Combined Yield 69% (59.3 mg, dr 100:5:3)

Major diastereomer **3l**:

Light yellow solid; **R_f** 0.25 (pet ether/ethyl acetate = 19:1); **eluent composition** petroleum ether/ethyl acetate = 19:1; **mp** 184-186 °C (crystallization from hot EtOH/$CHCl_3$ mixture using solvent evaporation method); **^{1}H NMR** (400 MHz, $CDCl_3$) δ 7.44 (dd, *J* = 7.2 Hz, 1.2 Hz, 1H), 7.41-7.33 (comp, 2H), 7.24-7.20 (m, 1H), 7.14 (app d, *J* = 7.2 Hz, 1H), 7.07-7.00 (comp, 6H), 6.95-6.87 (comp, 2H), 6.77 (app d, *J* = 7.6 Hz, 1H), 6.67-6.62 (comp, 2H), 6.50-6.46 (m, 1H), 5.20 (d, *J* = 8.4 Hz, 1H), 5.14 (d, *J* = 8.4 Hz, 1H), 5.01 (br s, 1H), 4.25 (d, *J* = 10.8 Hz, 1H), 4.13 (d, *J* = 10.8 Hz, 1H), 2.26 (s, 3H); **^{13}C NMR** (100 MHz, $CDCl_3$) δ 202.2, 143.7, 143.1, 142.6, 139.1, 136.7, 136.2, 132.8, 132.0, 129.6, 129.6, 128.8, 127.9, 127.7 (x 2), 127.0 (x 2), 126.8, 125.8, 125.6, 123.6, 122.0, 119.0, 116.2, 116.0, 71.3, 64.0, 57.4, 48.2, 19.8; **HRMS** (ESI, m/z) calcd for $C_{30}H_{25}NO_2$ $[M + H]^+$ 432.1964, found 432.1954.

Crystal data and structure refinement for 3l, CCDC No. 2090975

Empirical formula	$C_{30}H_{25}NO_2$
Formula weight	431.51
Temperature/K	100.0
Crystal system	triclinic
Space group	P-1
a/Å	9.521(2)
b/Å	11.402(4)
c/Å	11.575(3)
α/°	98.51(2)
β/°	99.544(14)
γ/°	111.134(15)
Volume/Å^3	1125.9(5)
Z	2
ρ_{calc}g/cm^3	1.273
μ/mm^{-1}	0.621
F(000)	456.0
Crystal size/mm^3	0.3 × 0.2 × 0.15
Radiation	Cu Kα (λ = 1.54184)
2Θ range for data collection/°	7.95 to 134.132
Index ranges	$-11 \le h \le 11$, $-13 \le k \le 13$, $-13 \le l \le 12$
Reflections collected	39144
Independent reflections	3925 [R_{int} = 0.0453, R_{sigma} = 0.0253]
Data/restraints/parameters	3925/0/299

Goodness-of-fit on F^2	1.074
Final R indexes [I>=2σ (I)]	R_1 = 0.0445, wR_2 = 0.1108
Final R indexes [all data]	R_1 = 0.0458, wR_2 = 0.1120
Largest diff. peak/hole / e $Å^{-3}$	0.24/-0.39

(3'-(2-bromophenyl)-2',3'-dihydro-2*H*,4*H*-spiro[benzo[*b*][1,4]oxazine-3,1'-inden]-2'-yl)(phenyl)methanone:

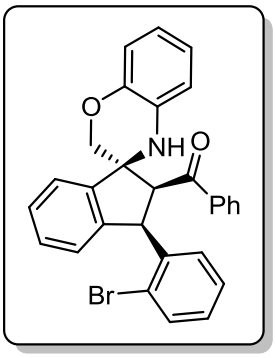

Combined Yield 98% (97.2 mg, dr 100:2:1)

Major diastereomer **3m**:

Light yellow solid; **R_f** 0.25 (pet ether/ethyl acetate = 19:1); **eluent composition** petroleum ether/ethyl acetate = 19:1; **mp** 156-158 °C (crystallization from hot EtOH/$CHCl_3$ mixture using solvent evaporation method); **^{1}H NMR** (400 MHz, $CDCl_3$) δ 7.43-7.39 (comp, 2H), 7.36 (app d, *J* = 8.4 Hz, 1H), 7.33-7.24 (comp, 3H), 7.21 (app d, *J* = 8.0 Hz, 1H), 7.12-7.05 (comp, 5H), 6.88-6.87 (comp, 2H), 6.65-6.60 (comp, 2H), 6.46-6.44 (m, 1H), 5.45 (d, *J* = 8.0 Hz, 1H), 5.29 (d, *J* = 8.4 Hz, 1H), 4.92 (br s, 1H), 4.29 (d, *J* = 10.8 Hz, 1H), 4.10 (d, *J* = 10.8 Hz, 1H); **^{13}C NMR** (100 MHz, $CDCl_3$) δ 201.4, 144.0, 143.0, 141.6, 138.2, 137.5, 132.8, 132.4, 132.2, 131.3, 128.8, 128.5, 128.1, 127.7 (x 2), 127.6 (x 2), 127.2, 126.2, 125.2, 123.7, 121.9, 118.8, 116.2, 115.7, 71.2, 63.9, 57.0, 51.4; **HRMS** (ESI, m/z) calcd for $C_{29}H_{22}BrNO_2$ $[M + H]^+$ 496.0912, found 496.0910.

(3'-(2-chlorophenyl)-2',3'-dihydro-2*H*,4*H*-spiro[benzo[*b*][1,4]oxazine-3,1'-inden]-2'-yl)(phenyl)methanone:

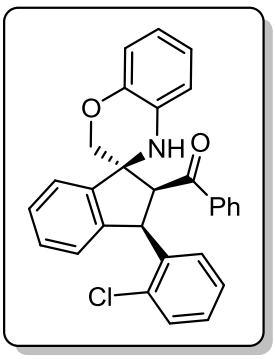

Combined Yield 99% (89.8 mg, dr 100:3:1)

Major diastereomer **3n**:

Colorless solid; **R_f** 0.25 (pet ether/ethyl acetate = 19:1); **eluent composition** petroleum ether/ethyl acetate = 19:1; **mp** 144-146 °C (crystallization from hot EtOH/$CHCl_3$ mixture using solvent evaporation method); **^{1}H NMR** (400 MHz, $CDCl_3$) δ 7.45-7.34 (comp, 3H), 7.31-7.24 (comp, 3H), 7.15-7.04 (comp, 5H), 7.03-7.01 (m, 1H), 6.97-6.93 (m, 1H), 6.90-6.86 (m, 1H), 6.66-6.60 (comp, 2H), 6.48-6.44 (m, 1H), 5.48 (d, *J* = 8.4 Hz, 1H), 5.28 (d, *J* = 8.4 Hz, 1H), 4.96 (br s, 1H), 4.29 (d, *J* = 10.8 Hz, 1H), 4.11 (d, *J* = 10.8 Hz, 1H); **^{13}C NMR** (100 MHz, $CDCl_3$) δ 201.4, 144.0, 143.0, 141.4, 138.2, 136.0, 135.0, 132.8, 132.4, 131.0, 128.8 (x 2), 128.2, 128.1, 127.7 (x 2), 127.5 (x 2), 126.5, 125.2, 123.7, 121.9, 118.8, 116.2, 115.7, 71.2, 64.0, 57.0, 48.6; **HRMS** (ESI, m/z) calcd for $C_{29}H_{22}ClNO_2$ $[M + H]^+$ 452.1417, found 452.1417.

(3'-(naphthalen-2-yl)-2',3'-dihydro-2*H*,4*H*-spiro[benzo[*b*][1,4]oxazine-3,1'-inden]-2'-yl)(phenyl)methanone (3o): (data for the major diastereomer is given)

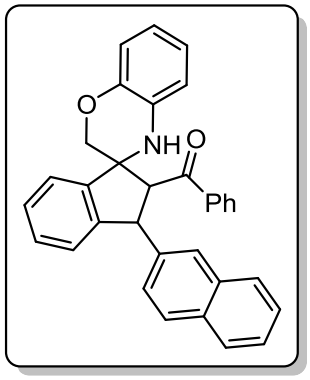

Combined Yield 70% (65.7 mg, dr 100:10:3)

Light yellow solid; **R_f** 0.20 (pet ether/ethyl acetate = 19:1); **eluent composition** petroleum ether/ethyl acetate = 19:1; **^{1}H NMR** (400 MHz, $CDCl_3$) δ 7.65-7.63 (comp, 2H), 7.51 (d, *J* = 8.4 Hz, 1H), 7.47-7.44 (comp, 2H), 7.42-7.36 (comp, 4H), 7.19 (dd, *J* = 8.4 Hz, 1.6 Hz, 1H), 7.16-7.12 (comp, 3H), 7.07-7.03 (m, 1H), 6.88-6.83 (comp, 3H), 6.66-6.59 (comp, 2H), 6.48-6.46 (m, 1H), 5.20 (d, *J* = 8.4 Hz, 1H), 5.18 (d, *J* = 8.4 Hz, 1H), 4.99 (br s, 1H), 4.31 (d, *J* = 10.8 Hz, 1H), 4.13 (d, *J* = 10.8 Hz, 1H); **^{13}C NMR** (100 MHz, $CDCl_3$) δ 201.7, 144.0, 143.0, 142.5, 138.7, 135.6, 133.1, 132.9, 132.4, 132.0, 128.9 (x 2), 128.1, 127.8, 127.7, 127.6, 127.5 (x 2), 127.4 (x 2), 127.3, 125.8, 125.6, 125.4, 123.6, 122.0, 118.8, 116.2, 115.8, 71.0, 64.1, 59.5, 52.5; **HRMS** (ESI, m/z) calcd for $C_{33}H_{25}NO_2$ $[M + H]^+$ 468.1964, found 468.1980.

phenyl(3'-(thiophen-2-yl)-2',3'-dihydro-2*H*,4*H*-spiro[benzo[*b*][1,4]oxazine-3,1'-inden]-2'-yl)methanone:

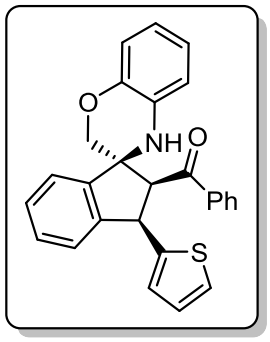

Combined Yield 58% (49.1 mg, dr 100:6:8)

Major diastereomer **3p**:

Light yellow solid; **R_f** 0.25 (pet ether/ethyl acetate = 19:1); **eluent composition** petroleum ether/ethyl acetate = 19:1; **mp** 174-176 ^oC (crystallization from hot EtOH/$CHCl_3$ mixture using solvent evaporation method); **^{1}H NMR** (400 MHz, $CDCl_3$) δ 7.40-7.34 (comp, 5H), 7.31-7.26 (comp, 2H), 7.13-7.09 (comp, 2H), 6.96 (dd, *J* = 4.8 Hz, 0.8 Hz, 1H), 6.88-6.84 (m, 1H), 6.80 (app d, *J* = 3.2 Hz, 1H), 6.74 (dd, *J* = 5.2 Hz, 3.6 Hz, 1H), 6.65-6.59 (comp, 2H), 6.45-6.41 (m, 1H), 5.28 (d, *J* = 8.0 Hz, 1H), 5.12 (d, *J* = 8.4 Hz, 1H), 4.85 (br s, 1H), 4.23 (d, *J* = 10.8 Hz, 1H), 4.08 (d, *J* = 10.8 Hz, 1H); **^{13}C NMR** (100 MHz, $CDCl_3$) δ 201.4, 143.1, 142.9, 142.5, 140.9, 138.7, 132.8, 132.4, 129.0, 128.3, 127.8 (x 2), 127.7 (x 3), 127.4, 126.6, 125.0, 124.5, 122.0, 118.8, 116.2, 115.7, 70.8, 64.0, 59.7, 47.0; **HRMS** (ESI, m/z) calcd for $C_{27}H_{21}NO_2S$ $[M + H]^+$ 424.1371, found 424.1365.

phenyl(3'-(thiophen-3-yl)-2',3'-dihydro-2*H*,4*H*-spiro[benzo[*b*][1,4]oxazine-3,1'-inden]-2'-yl)methanone:

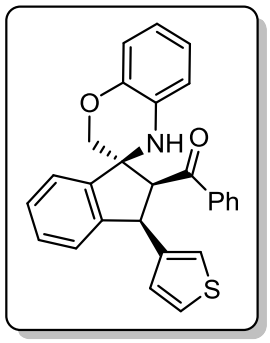

Combined Yield 64% (53.8 mg, dr 100:6:3)

Major diastereomer **3q**:

Light yellow solid; **R_f** 0.25 (pet ether/ethyl acetate = 19:1); **eluent composition** petroleum ether/ethyl acetate = 19:1; **mp** 190-192 ^oC (crystallization from hot EtOH/$CHCl_3$ mixture using solvent evaporation method); **^{1}H NMR** (400 MHz, $CDCl_3$) δ 7.42-7.33 (comp, 3H), 7.32-7.26 (comp, 3H), 7.17-7.15 (m, 1H), 7.12-7.08 (comp, 2H), 7.00 (dd, *J* = 2.8 Hz, 1.2 Hz, 1H), 6.97 (dd, *J* = 4.8 Hz, 3.2 Hz, 1H), 6.87-6.85 (m, 1H), 6.73 (dd, *J* = 4.8 Hz, 1.2 Hz, 1H), 6.67-6.60 (comp, 2H), 6.48-6.46 (m, 1H), 5.14 (d, *J* = 8.4 Hz, 1H), 5.06 (d, *J* = 8.4 Hz, 1H), 4.94 (br s, 1H), 4.23 (d, *J* = 10.8 Hz, 1H), 4.09 (d, *J* = 10.4 Hz, 1H); **^{13}C NMR** (100 MHz, $CDCl_3$) δ 201.8, 143.4, 143.0, 142.7, 139.0, 138.6, 132.9, 132.2, 128.9, 128.8, 128.1, 127.8 (x 2), 127.6 (x 3), 125.0, 123.9, 123.4, 122.0, 118.8, 116.2, 115.8, 70.8, 64.0, 59.0, 47.3; **HRMS** (ESI, m/z) calcd for $C_{27}H_{21}NO_2S$ $[M + H]^+$ 424.1371, found 424.1368.

(4-methoxyphenyl)(3'-phenyl-2',3'-dihydro-2*H*,4*H*-spiro[benzo[*b*][1,4]oxazine-3,1'-inden]-2'-yl)methanone:

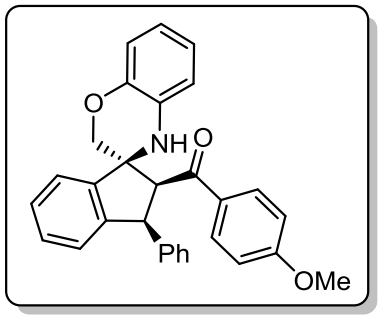

Combined Yield 91% (81.4 mg, dr 100:4:5)

Major diastereomer **3r**:

Colorless solid; **R_f** 0.10 (pet ether/ethyl acetate = 19:1); **eluent composition** petroleum ether/ethyl acetate = 19:1; **mp** 162-164 ^oC (crystallization from hot EtOH/$CHCl_3$ mixture using solvent evaporation method); **^{1}H NMR** (400 MHz, $CDCl_3$) δ 7.41 (dd, *J* = 7.2 Hz, 0.8 Hz, 1H), 7.37 (app t, *J* = 7.2 Hz, 1H), 7.32 (td, *J* = 7.2 Hz, 1.6 Hz, 1H), 7.29-7.26 (comp, 2H), 7.14-7.05 (comp, 5H), 7.03-6.99 (m, 1H), 6.84 (dd, *J* = 7.6 Hz, 2.0 Hz, 1H), 6.66-6.58 (comp, 2H), 6.54-6.50 (comp, 2H), 6.47 (dd, *J* = 7.6 Hz, 1.6 Hz, 1H), 5.04 (d, *J* = 8.4 Hz, 1H), 5.00 (d, *J* = 8.4 Hz, 1H), 4.96 (br s, 1H), 4.26 (d, *J* = 10.8 Hz, 1H), 4.09 (d, *J* = 10.8 Hz, 1H), 3.70 (s, 3H); **^{13}C NMR** (100 MHz, $CDCl_3$) δ 199.4, 162.8, 144.1, 143.0, 142.6, 138.2, 133.1, 131.8, 130.0 (x 2), 129.9 (x 2), 128.7, 128.0 (x 2), 127.9, 127.0, 125.2, 123.4, 121.9 (x 2), 118.6, 116.1, 115.7, 112.9, 70.9, 64.0, 59.0, 55.2, 52.4; **HRMS** (ESI, m/z) calcd for $C_{30}H_{25}NO_3$ $[M + H]^+$ 448.1913, found 448.1916.

(3'-phenyl-2',3'-dihydro-2*H*,4*H*-spiro[benzo[*b*][1,4]oxazine-3,1'-inden]-2'-yl)(*p*-tolyl)methanone:

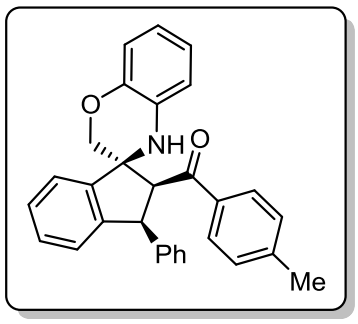

Combined Yield 83% (71.7 mg, dr 100:3:3)

Major diastereomer **3s**:

Colorless solid; **R_f** 0.20 (pet ether/ethyl acetate = 19:1); **eluent composition** petroleum ether/ethyl acetate = 19:1; **mp** 184-186 ^oC (crystallization from hot EtOH/$CHCl_3$ mixture using solvent evaporation method); **^{1}H NMR** (400 MHz, $CDCl_3$) δ 7.42-7.28 (comp, 3H), 7.15-7.00 (comp, 8H), 6.86-6.82 (comp, 3H), 6.66-6.58 (comp, 2H), 6.46 (dd, *J* = 7.2 Hz, 1.6 Hz, 1H), 5.06 (d, *J* = 8.4 Hz, 1H), 5.01 (d, *J* = 8.4 Hz, 1H), 4.95 (br s, 1H), 4.26 (d, *J* = 10.8 Hz, 1H), 4.09 (d, *J* = 10.8 Hz, 1H), 2.20 (s, 3H); **^{13}C NMR** (100 MHz, $CDCl_3$) δ 201.0, 144.0, 143.0, 142.9, 142.6, 138.2, 136.4, 133.0, 129.9 (x 2), 128.7, 128.4 (x 2), 128.0 (x 2), 127.9, 127.7(x 2), 127.0, 125.2, 123.4, 121.9, 118.6, 116.1, 115.7, 70.9, 64.0, 59.3, 52.4, 21.4; **HRMS** (ESI, m/z) calcd for $C_{30}H_{25}NO_2$ $[M + H]^+$ 432.1964, found 432.1954.

(4-(tert-butyl)phenyl)(3'-phenyl-2',3'-dihydro-2*H*,4*H*-spiro[benzo[*b*][1,4]oxazine-3,1'-inden]-2'-yl)methanone:

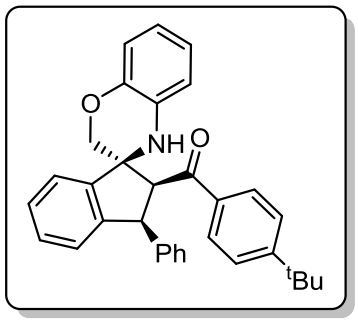

Combined Yield 88% (83.4 mg, dr 100:4:5)

Major diastereomer **3t**:

Light yellow solid; **R_f** 0.30 (pet ether/ethyl acetate = 19:1); **eluent composition** petroleum ether/ethyl acetate = 19:1; **mp** 194-196 ^oC (crystallization from hot EtOH/$CHCl_3$ mixture using solvent evaporation method); **^{1}H NMR** (400 MHz, $CDCl_3$) δ 7.42-7.31 (comp, 3H), 7.20-7.18 (comp, 2H), 7.13-7.11 (comp, 3H), 7.06-7.02 (comp, 4H), 7.00-6.97 (m, 1H), 6.85 (dd, *J* = 7.2 Hz, 2.0 Hz, 1H), 6.66-6.58 (comp, 2H), 6.45 (dd, *J* = 7.2 Hz, 1.6 Hz, 1H), 5.08 (d, *J* = 8.4 Hz, 1H), 5.01 (d, *J* = 8.4 Hz, 1H), 4.98 (br s, 1H), 4.27 (d, *J* = 10.8 Hz, 1H), 4.08 (d, *J* = 10.8 Hz, 1H), 1.19 (s, 9H); **^{13}C NMR** (100 MHz, $CDCl_3$) δ 200.9, 155.7, 144.0, 143.0, 142.5, 138.2, 136.1, 133.0, 129.9 (x 2), 128.7, 128.0 (x 2), 127.9, 127.7 (x 2), 126.9, 125.2, 124.6 (x 2), 123.4, 121.9, 118.6, 116.2, 115.7, 70.8, 64.0, 59.3, 52.3, 34.8, 30.9; **HRMS** (ESI, m/z) calcd for $C_{33}H_{31}NO_2$ $[M + H]^+$ 474.2433, found 474.2441.

(4-iodophenyl)(3'-phenyl-2',3'-dihydro-2*H*,4*H*-spiro[benzo[*b*][1,4]oxazine-3,1'-inden]-2'-yl)methanone:

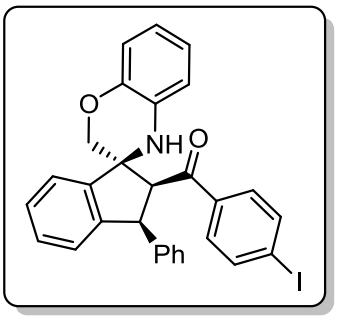

Combined Yield 99% (108.0 mg, dr 100:5:3)

Major diastereomer **3u**:

Yellow solid; **R_f** 0.30 (pet ether/ethyl acetate = 19:1); **eluent composition** petroleum ether/ethyl acetate = 19:1; **mp** 188-190 ^oC (crystallization from hot EtOH/$CHCl_3$ mixture using solvent evaporation method); **^{1}H NMR** (400 MHz, $CDCl_3$) δ 7.42-7.37 (comp, 4H), 7.34 (td, *J* = 6.8 Hz, 2.0 Hz, 1H), 7.13-7.05 (comp, 6H), 6.88-6.83 (comp, 3H), 6.67-6.60 (comp, 2H), 6.47-6.42 (m, 1H), 5.01 (app s, 2H), 4.89 (br s, 1H), 4.24 (d, *J* = 10.8 Hz, 1H), 4.09 (d, *J* = 10.8 Hz, 1H); **^{13}C NMR** (100 MHz, $CDCl_3$) δ 200.1, 143.6, 142.9, 142.4, 138.1, 137.9, 137.0 (x 2), 132.7, 129.8 (x 2), 128.9, 128.8 (x 2), 128.2 (x 2), 128.1, 127.2, 125.3, 123.5, 122.0, 119.0, 116.2, 115.8, 100.2, 71.0, 64.1, 59.5, 52.3; **HRMS** (ESI, m/z) calcd for $C_{29}H_{22}INO_2$ $[M + H]^+$ 544.0773, found 544.0777.

(4-bromophenyl)(3'-phenyl-2',3'-dihydro-2*H*,4*H*-spiro[benzo[*b*][1,4]oxazine-3,1'-inden]-2'-yl)methanone:

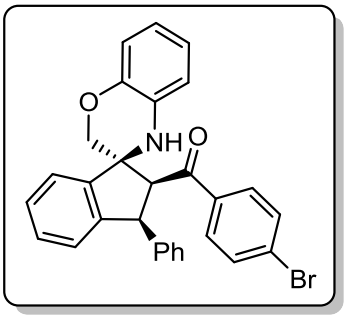

Combined Yield 99% (98.8 mg, dr 100:6:8)

Major diastereomer **3v**:

Yellow solid; **R_f** 0.25 (pet ether/ethyl acetate = 19:1); **eluent composition** petroleum ether/ethyl acetate = 19:1; **mp** 184-186 ^oC (crystallization from hot EtOH/$CHCl_3$ mixture using solvent evaporation method); **^{1}H NMR** (400 MHz, $CDCl_3$) δ 7.42-7.38 (comp, 2H), 7.34 (td, *J* = 7.2 Hz, 2.4 Hz, 1H), 7.18-7.16 (comp, 2H), 7.13-7.02 (comp, 8H), 6.87-6.84 (m, 1H), 6.67-6.60 (comp, 2H), 6.47-6.43 (m, 1H), 5.02 (app s, 2H), 4.89 (br s, 1H), 4.25 (d, *J* = 10.8 Hz, 1H), 4.09 (d, *J* = 10.8 Hz, 1H); **^{13}C NMR** (100 MHz, $CDCl_3$) δ 200.7, 143.7, 142.9, 142.4, 137.9, 137.6, 132.8, 131.0 (x 2), 129.8 (x 2), 129.0 (x 2), 128.9, 128.2 (x 2), 128.1, 127.3, 127.2, 125.3, 123.5, 122.0, 119.0, 116.2, 115.8, 71.0, 64.1, 59.5, 52.3; **HRMS** (ESI, m/z) calcd for $C_{29}H_{22}BrNO_2$ $[M + H]^+$ 496.0912, found 496.0907.

(4-chlorophenyl)(3'-phenyl-2',3'-dihydro-2*H*,4*H*-spiro[benzo[*b*][1,4]oxazine-3,1'-inden]-2'-yl)methanone:

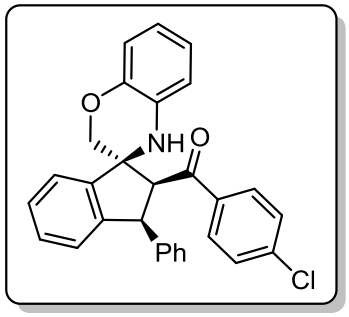

Combined Yield 96% (87.1 mg, dr 100:10:11)

Major diastereomer **3w**:

Yellow solid; **R_f** 0.25 (pet ether/ethyl acetate = 19:1); **eluent composition** petroleum ether/ethyl acetate = 19:1; **mp** 162-164 ^oC (crystallization from hot EtOH/$CHCl_3$ mixture using solvent evaporation method); **^{1}H NMR** (400 MHz, $CDCl_3$) δ 7.42-7.34 (comp, 3H), 7.14-7.06 (comp, 8H), 7.01-6.99 (comp, 2H), 6.87-6.84 (m, 1H), 6.66-6.58 (comp, 2H), 6.48-6.44 (m, 1H), 5.03 (app s, 2H), 4.90 (br s, 1H), 4.25 (d, *J* = 10.8 Hz, 1H), 4.09 (d, *J* = 10.8 Hz, 1H); **^{13}C NMR** (100 MHz, $CDCl_3$) δ 200.5, 143.7, 142.9, 142.4, 138.6, 138.0, 137.1, 132.8, 129.8 (x 2), 128.9 (x 3), 128.2 (x 2), 128.1, 128.0 (x 2), 127.2, 125.3, 123.5, 122.0, 118.9, 116.2, 115.8, 71.0, 64.1, 59.5, 52.3; **HRMS** (ESI, m/z) calcd for $C_{29}H_{22}ClNO_2$ $[M + H]^+$ 452.1417, found 452.1420.

(4-fluorophenyl)(3'-phenyl-2',3'-dihydro-2*H*,4*H*-spiro[benzo[*b*][1,4]oxazine-3,1'-inden]-2'-yl)methanone:

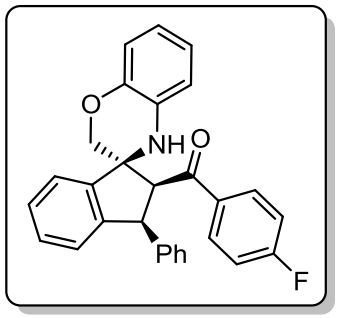

Combined Yield 99% (86.3 mg, dr 100:5:6)

Major diastereomer **3x**:

Light yellow solid; **R_f** 0.20 (pet ether/ethyl acetate = 19:1); **eluent composition** petroleum ether/ethyl acetate = 19:1; **mp** 150-152 ^oC (crystallization from hot EtOH/$CHCl_3$ mixture using solvent evaporation method); **^{1}H NMR** (400 MHz, $CDCl_3$) δ 7.43-7.32 (comp, 3H), 7.26-7.23 (comp, 2H), 7.13-7.01 (comp, 6H), 6.86 (dd, *J* = 6.8 Hz, 1.2 Hz, 1H), 6.72-6.68 (comp, 2H), 6.67-6.60 (comp, 2H), 6.46 (dd, *J* = 6.8 Hz, 1.2 Hz, 1H), 5.04 (app s, 2H), 4.94 (br s, 1H), 4.26 (d, *J* = 10.8 Hz, 1H), 4.10 (d, *J* = 10.4 Hz, 1H); **^{13}C NMR** (100 MHz, $CDCl_3$) δ 199.9, 165.0 (d, $^1J_{C–F}$ = 253.0 Hz), 143.8, 143.0, 142.4, 138.0, 135.2 (d, $^4J_{C–F}$ = 2.0 Hz), 132.8, 130.2 (d, $^3J_{C–F}$ = 10.0 Hz), 129.8 (x 3), 128.8, 128.1 (x 3), 128.1 (d, $^3J_{C–F}$ = 7.0 Hz), 127.1, 125.3, 123.5, 122.0, 118.8, 116.2, 115.8, 114.8 (d, $^2J_{C–F}$ = 21.0 Hz), 70.9, 64.0, 59.4, 52.3; **HRMS** (ESI, m/z) calcd for $C_{29}H_{22}FNO_2$ $[M + H]^+$ 436.1713, found 436.1706.

(3'-phenyl-2',3'-dihydro-2*H*,4*H*-spiro[benzo[*b*][1,4]oxazine-3,1'-inden]-2'-yl)(4-(trifluoromethyl)phenyl)methanone:

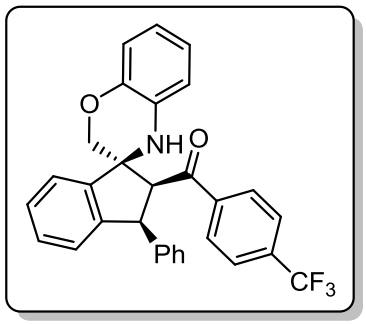

Combined Yield 91% (88.0 mg, dr 100:20:8)

Major diastereomer **3y**:

Yellow solid; **R_f** 0.30 (pet ether/ethyl acetate = 19:1); **eluent composition** petroleum ether/ethyl acetate = 19:1; **mp** 136-138 ^oC (crystallization from hot EtOH/$CHCl_3$ mixture using solvent evaporation method); **^{1}H NMR** (400 MHz, $CDCl_3$) δ 7.44-7.35 (comp, 3H), 7.29-7.27 (comp, 2H), 7.21-7.19 (comp, 2H), 7.16-7.03 (comp, 6H), 6.89-6.86 (m, 1H), 6.67-6.62 (comp, 2H), 6.47-6.44 (m, 1H), 5.09 (d, *J* = 8.4 Hz, 1H), 5.06 (d, *J* = 8.8 Hz, 1H), 4.90 (br s, 1H), 4.26 (d, *J* = 10.4 Hz, 1H), 4.11 (d, *J* = 10.4 Hz, 1H); **^{13}C NMR** (100 MHz, $CDCl_3$) δ 201.2, 143.5, 142.9, 142.2, 141.6, 137.8, 133.1 (app d, *J* = 32.0 Hz), 132.6, 129.8 (x 2), 129.0, 128.2 (x 3), 128.2, 127.6 (x 3), 127.3, 125.4, 124.7 (q, *J* = 4.0 Hz), 123.6, 122.0, 119.1, 116.2, 115.8, 71.0, 64.1, 60.0, 52.3; **HRMS** (ESI, m/z) calcd for $C_{30}H_{22}F_3NO_2$ $[M + H]^+$ 486.1681, found 486.1697.

(3'-phenyl-2',3'-dihydro-2*H*,4*H*-spiro[benzo[*b*][1,4]oxazine-3,1'-inden]-2'-yl)(*m*-tolyl)methanone:

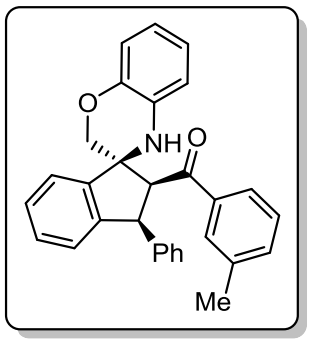

Combined Yield 95% (82.4 mg, dr 100:6:8)

Major diastereomer **3z**:

Light yellow solid; **R_f** 0.20 (pet ether/ethyl acetate = 19:1); **eluent composition** petroleum ether/ethyl acetate = 19:1; **mp** 196-198 ^oC (crystallization from hot EtOH/$CHCl_3$ mixture using solvent evaporation method); **^{1}H NMR** (400 MHz, $CDCl_3$) δ 7.43-7.32 (comp, 3H), 7.14-7.06 (comp, 5H), 7.04-6.99 (comp, 3H), 6.94-6.90 (comp, 2H), 6.87 (dd, *J* = 6.8 Hz, 2.0 Hz, 1H), 6.66-6.60 (comp, 2H), 6.48-6.46 (m, 1H), 5.08 (d, *J* = 8.4 Hz, 1H), 5.02 (d, *J* = 8.4 Hz, 1H), 4.95 (br s, 1H), 4.27 (d, *J* = 10.4 Hz, 1H), 4.10 (d, *J* = 10.8 Hz, 1H), 2.12 (s, 3H); **^{13}C NMR** (100 MHz, $CDCl_3$) δ 202.0, 143.9, 143.0, 142.5, 139.0, 138.2, 137.3, 133.0, 132.8, 129.9 (x 2), 128.8, 128.2, 128.0 (x 2), 128.0, 127.5, 127.0, 125.3, 124.6, 123.5, 121.9, 118.8, 116.1, 115.8, 71.0, 64.0, 59.8, 52.3, 21.0; **HRMS** (ESI, m/z) calcd for $C_{30}H_{25}NO_2$ $[M + H]^+$ 432.1964, found 432.1953.

(3-bromophenyl)(3'-phenyl-2',3'-dihydro-2*H*,4*H*-spiro[benzo[*b*][1,4]oxazine-3,1'-inden]-2'-yl)methanone:

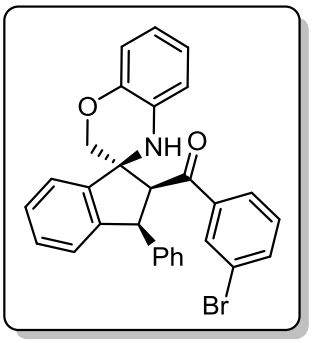

Combined Yield 96% (94.8 mg, dr 100:17:9)

Major diastereomer **3aa**:

Yellow solid; **R_f** 0.25 (pet ether/ethyl acetate = 19:1); **eluent composition** petroleum ether/ethyl acetate = 19:1; **mp** 182-184 ^oC (crystallization from hot EtOH/$CHCl_3$ mixture using solvent evaporation method); **^{1}H NMR** (400 MHz, $CDCl_3$) δ 7.41-7.32 (comp, 4H), 7.22-7.10 (comp, 8H), 6.92-6.87 (comp, 2H), 6.66-6.64 (comp, 2H), 6.48-6.46 (m, 1H), 5.04 (d, *J* = 8.4 Hz, 1H), 5.00 (d, *J* = 8.4 Hz, 1H), 4.91 (br s, 1H), 4.26 (d, *J* = 10.4 Hz, 1H), 4.10 (d, *J* = 10.4 Hz, 1H); **^{13}C NMR** (100 MHz, $CDCl_3$) δ 200.5, 143.6, 143.0, 142.2, 140.5, 137.8, 134.9, 132.7, 130.6, 129.8 (x 2), 129.2, 128.9, 128.9, 128.2 (x 2), 128.1, 127.3, 125.9, 125.4, 123.5, 122.0, 119.1, 116.2, 115.8, 71.0, 64.1, 59.8, 52.3; **HRMS** (ESI, m/z) calcd for $C_{29}H_{22}BrNO_2$ $[M + H]^+$ 496.0912, found 496.0905.

Crystal data and structure refinement for 3aa, CCDC No. 2090976

Empirical formula	$C_{29}H_{22}BrNO_2$
Formula weight	496.38
Temperature/K	100.0
Crystal system	triclinic
Space group	P-1
a/Å	10.5811(9)
b/Å	11.3432(10)
c/Å	11.6882(10)
α/°	76.041(2)
β/°	63.968(2)
γ/°	64.554(2)
Volume/$Å^3$	1135.85(17)
Z	2
$\rho_{calc}g/cm^3$	1.451
μ/mm^{-1}	2.677
F(000)	508.0
Crystal size/mm^3	0.4 × 0.18 × 0.15
Radiation	Cu Kα (λ = 1.54178)
2Θ range for data collection/°	8.436 to 136.652
Index ranges	$-12 \le h \le 12$, $-13 \le k \le 13$, $-13 \le l \le 14$
Reflections collected	28720
Independent reflections	4018 [R_{int} = 0.1767, R_{sigma} = 0.0726]
Data/restraints/parameters	4018/0/299
Goodness-of-fit on F^2	1.098
Final R indexes [I>=2σ (I)]	R_1 = 0.0597, wR_2 = 0.1606

Final R indexes [all data]	R_1 = 0.0605, wR_2 = 0.1612
Largest diff. peak/hole / e Å^{-3}	0.88/-1.72

(3-chlorophenyl)(3'-phenyl-2',3'-dihydro-2*H*,4*H*-spiro[benzo[*b*][1,4]oxazine-3,1'-inden]-2'-yl)methanone:

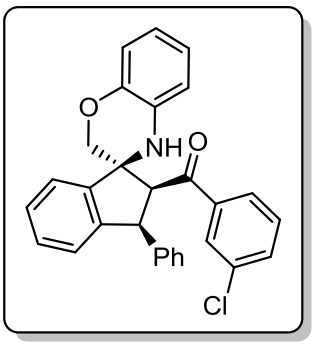

Combined Yield 94% (84.6 mg, dr 100:17:8)

Major diastereomer **3ab**:

Yellow solid; **R_f** 0.25 (pet ether/ethyl acetate = 19:1); **eluent composition** petroleum ether/ethyl acetate = 19:1; **mp** 172-174 ºC (crystallization from hot EtOH/$CHCl_3$ mixture using solvent evaporation method); **^{1}H NMR** (400 MHz, $CDCl_3$) δ 7.43-7.34 (comp, 3H), 7.18 (app d, *J* = 8.0 Hz, 1H), 7.14-7.06 (comp, 8H), 6.97 (app t, *J* = 8.0 Hz, 1H), 6.89-6.87 (m, 1H), 6.68-6.64 (comp, 2H), 6.48-6.46 (m, 1H), 5.04 (d, *J* = 8.4 Hz, 1H), 5.01 (d, *J* = 8.4 Hz, 1H), 4.92 (br s, 1H), 4.26 (d, *J* = 10.8 Hz, 1H), 4.10 (d, *J* = 10.4 Hz, 1H); **^{13}C NMR** (100 MHz, $CDCl_3$) δ 200.5, 143.6, 143.0, 142.2, 140.3, 137.9, 134.0, 132.7, 132.0, 129.8 (x 2), 129.0, 128.9, 128.2 (x 2), 128.1, 127.6, 127.2, 125.5, 125.4, 123.5, 122.0, 119.0, 116.2, 115.8, 71.0, 64.1, 59.8, 52.3; **HRMS** (ESI, m/z) calcd for $C_{29}H_{22}ClNO_2$ $[M + H]^+$ 452.1417, found 452.1404.

(3'-phenyl-2',3'-dihydro-2*H*,4*H*-spiro[benzo[*b*][1,4]oxazine-3,1'-inden]-2'-yl)(*o*-tolyl)methanone:

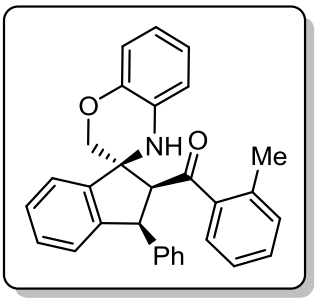

Combined Yield 45% (40.1 mg, dr 100:7:6)

Major diastereomer **3ac**:

Colorless solid; **R_f** 0.30 (pet ether/ethyl acetate = 19:1); **eluent composition** petroleum ether/ethyl acetate = 19:1; **mp** 184-186 ºC (crystallization from hot EtOH/$CHCl_3$ mixture using solvent evaporation method); **^{1}H NMR** (400 MHz, $CDCl_3$) δ 7.42-7.34 (comp, 3H), 7.22-7.12 (comp, 6H), 7.09-7.03 (comp, 2H), 6.89 (dd, *J* = 7.6 Hz, 1.6 Hz, 1H), 6.86-6.82 (comp, 2H), 6.71-6.62 (comp, 2H), 6.50 (dd, *J* = 7.2 Hz, 1.6 Hz, 1H), 5.06 (d, *J* = 8.8 Hz, 1H), 5.03 (d, *J* = 8.4 Hz, 1H), 4.86 (br s, 1H), 4.25 (d, *J* = 10.8 Hz, 1H), 4.07 (d, *J* = 10.8 Hz, 1H), 1.88 (s, 3H); **^{13}C NMR** (100 MHz, $CDCl_3$) δ 204.4, 144.0, 143.0, 142.4, 138.6, 138.5, 138.2, 133.0, 131.4, 131.0, 129.9 (x 2), 129.2, 128.8, 128.3 (x 2), 128.0, 127.1, 125.4, 125.0, 123.6, 122.1, 118.8, 116.3, 115.5, 71.2, 64.7, 61.7, 52.3, 20.5; **HRMS** (ESI, m/z) calcd for $C_{30}H_{25}NO_2$ $[M + H]^+$ 432.1964, found 432.1964.

(3'-phenyl-2',3'-dihydro-2*H*,4*H*-spiro[benzo[*b*][1,4]oxazine-3,1'-inden]-2'-yl)(thiophen-2-yl)methanone:

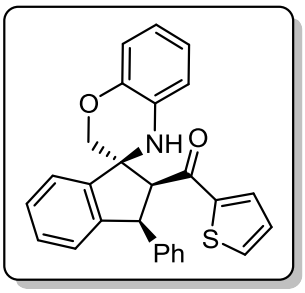

Combined Yield 97% (82.2 mg, dr 100:2:2)

Major diastereomer **3ad**:

Colorless solid; **R_f** 0.20 (pet ether/ethyl acetate = 19:1); **eluent composition** petroleum ether/ethyl acetate = 19:1; **mp** 180-182 °C (crystallization from hot EtOH/$CHCl_3$ mixture using solvent evaporation method); **^{1}H NMR** (400 MHz, $CDCl_3$) δ 7.41-7.37 (comp, 2H), 7.33 (td, *J* = 7.2 Hz, 2.0 Hz, 1H), 7.29 (dd, *J* = 4.8 Hz, 0.8 Hz, 1H), 7.19-7.15 (comp, 3H), 7.14-7.10 (comp, 3H), 7.07-7.04 (m, 1H), 6.84 (dd, *J* = 8.0 Hz, 1.6 Hz, 1H), 6.71-6.69 (m, 1H), 6.66 (td, *J* = 7.6 Hz, 1.2 Hz, 1H), 6.60 (td, *J* = 7.6 Hz, 1.6 Hz, 1H), 6.50 (dd, *J* = 7.6 Hz, 1.6 Hz, 1H), 5.02 (d, *J* = 8.0 Hz, 1H), 4.97 (br s, 1H), 4.85 (d, *J* = 8.0 Hz, 1H), 4.27 (d, *J* = 10.8 Hz, 1H), 4.06 (d, *J* = 10.8 Hz, 1H); **^{13}C NMR** (100 MHz, $CDCl_3$) δ 192.6, 145.7, 143.8, 142.9, 142.4, 138.0, 133.9, 133.0, 132.4, 129.9 (x 2), 128.8, 128.1 (x 2), 128.0, 127.5, 127.1, 125.2, 123.4, 121.9, 118.5, 116.2, 115.5, 70.6, 64.0, 61.4, 52.4; **HRMS** (ESI, m/z) calcd for $C_{27}H_{21}NO_2S$ $[M + H]^+$ 424.1371, found 424.1376.

furan-2-yl(3'-phenyl-2',3'-dihydro-2*H*,4*H*-spiro[benzo[*b*][1,4]oxazine-3,1'-inden]-2'-yl)methanone:

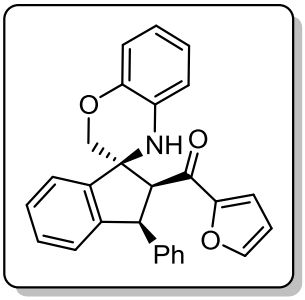

Combined Yield 99% (80.8 mg, dr 100:9:15)

Major diastereomer **3ae**:

Colorless solid; **R_f** 0.10 (pet ether/ethyl acetate = 19:1); **eluent composition** petroleum ether/ethyl acetate = 19:1; **mp** 178-180 °C (crystallization from hot EtOH/$CHCl_3$ mixture using solvent evaporation method); **^{1}H NMR** (400 MHz, $CDCl_3$) δ 7.40-7.36 (comp, 2H), 7.32 (td, *J* = 7.2 Hz, 2.0 Hz, 1H), 7.19-7.16 (comp, 3H), 7.14-7.04 (comp, 4H), 6.84 (dd, *J* = 8.0 Hz, 1.6 Hz, 1H), 6.69 (td, *J* = 7.6 Hz, 1.2 Hz, 1H), 6.63-6.59 (comp, 2H), 6.53 (dd, *J* = 8.0 Hz, 1.6 Hz, 1H), 6.11 (dd, *J* = 3.6 Hz, 1.6 Hz, 1H), 5.00 (d, *J* = 8.4 Hz, 2H), 4.82 (d, *J* = 8.0 Hz, 1H), 4.24 (d, *J* = 10.8 Hz, 1H), 4.04 (d, *J* = 10.8 Hz, 1H); **^{13}C NMR** (100 MHz, $CDCl_3$) δ 188.2, 153.1, 146.2, 144.0, 142.9, 142.3, 137.9, 133.0, 132.4, 129.7 (x 2), 128.8, 128.0 (x 2), 127.1, 125.2, 123.4, 121.9, 118.4, 117.7, 116.2, 115.5, 111.9, 70.6, 63.7, 59.9, 52.3; **HRMS** (ESI, m/z) calcd for $C_{27}H_{21}NO_3$ $[M + H]^+$ 408.1600, found 408.1604.

(3'-phenyl-2',3'-dihydro-2*H*,4*H*-spiro[benzo[*b*][1,4]oxazine-3,1'-inden]-2'-yl)(thiophen-3-yl)methanone:

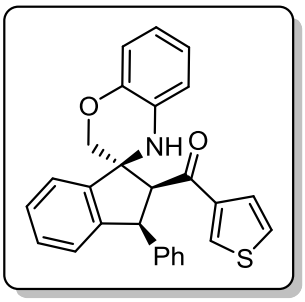

Combined Yield 93% (78.6 mg, dr 100:10:8)

Major diastereomer **3af**:

Light yellow solid; **R$_f$** 0.20 (pet ether/ethyl acetate = 19:1); **eluent composition** petroleum ether/ethyl acetate = 19:1; **mp** 184-186 ^oC (crystallization from hot EtOH/$CHCl_3$ mixture using solvent evaporation method); **^{1}H NMR** (400 MHz, $CDCl_3$) δ 7.44-7.317 (comp, 4H), 7.16-7.03 (comp, 6H), 6.94 (app d, *J* = 4.8 Hz, 1H), 6.89-6.84 (comp, 2H), 6.69-6.59 (comp, 2H), 6.48 (app d, *J* = 7.6 Hz, 1H), 5.01 (d, *J* = 8.0 Hz, 1H), 4.96 (br s, 1H), 4.83 (d, *J* = 8.0 Hz, 1H), 4.25 (d, *J* = 10.8 Hz, 1H), 4.06 (d, *J* = 10.8 Hz, 1H); **^{13}C NMR** (100 MHz, $CDCl_3$) δ 194.6, 143.8, 143.7, 142.9, 142.4, 138.1, 133.1, 132.3, 129.8 (x 2), 128.8, 128.1 (x 2), 128.0, 127.1, 126.4, 125.2, 125.2, 123.4, 122.0, 118.6, 116.2, 115.6, 70.7, 63.9, 61.5, 52.3; **HRMS** (ESI, m/z) calcd for $C_{27}H_{21}NO_2S$ $[M + H]^+$ 424.1371, found 424.1352.

(4-chlorophenyl)(3'-(4-chlorophenyl)-2',3'-dihydro-2*H*,4*H*-spiro[benzo[*b*][1,4]oxazine-3,1'-inden]-2'-yl)methanone:

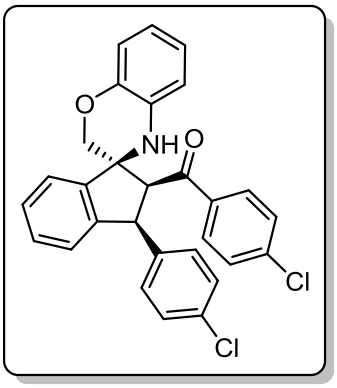

Combined Yield 88% (85.1 mg, dr 100:4:4)

Major diastereomer **3ag**:

Yellow solid; **R$_f$** 0.20 (pet ether/ethyl acetate = 19:1); **eluent composition** petroleum ether/ethyl acetate = 19:1; **mp** 214-216 ^oC (crystallization from hot EtOH/$CHCl_3$ mixture using solvent evaporation method); **^{1}H NMR** (400 MHz, $CDCl_3$) δ 7.41-7.33 (comp, 3H), 7.17-7.14 (comp, 2H), 7.10-7.03 (comp, 7H), 6.87-6.83 (m, 1H), 6.65-6.61 (comp, 2H), 6.44-6.40 (m, 1H), 5.03 (d, *J* = 8.4 Hz, 1H), 4.98 (d, *J* = 8.4 Hz, 1H), 4.83 (br s, 1H), 4.22 (d, *J* = 10.8 Hz, 1H), 4.08 (d, *J* = 10.8 Hz, 1H); **^{13}C NMR** (100 MHz, $CDCl_3$) δ 200.2, 143.5, 142.9, 142.0, 139.0, 137.0, 136.7, 133.1, 132.6, 131.2 (x 2), 129.0, 128.8 (x 2), 128.3 (x 2), 128.3, 128.2 (x 2), 125.1, 123.7, 122.0, 119.1, 116.2, 115.8, 71.0, 64.3, 59.4, 51.6; **HRMS** (ESI, m/z) calcd for $C_{29}H_{21}Cl_2NO_2$ $[M + H]^+$ 486.1028, found 486.1019.

1-(3'-phenyl-2',3'-dihydro-2*H*,4*H*-spiro[benzo[*b*][1,4]oxazine-3,1'-inden]-2'-yl)ethan-1-one:

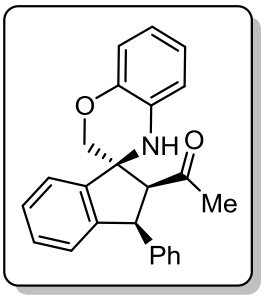

Yield 25% (18.0 mg)

Single diastereomer **3ah**:

Colorless solid; **R_f** 0.25 (pet ether/ethyl acetate = 19:1); **eluent composition** petroleum ether/ethyl acetate = 19:1; **mp** 162-164 ^oC; **^{1}H NMR** (400 MHz, $CDCl_3$) δ 7.35-7.31 (comp, 4H), 7.31-7.26 (comp, 2H), 7.24-7.22 (comp, 2H), 7.08 (dd, *J* = 7.2 Hz, 0.8 Hz, 1H), 6.85 (dd, *J* = 8.0 Hz, 1.2 Hz, 1H), 6.78 (td, *J* = 7.6 Hz, 1.2 Hz, 1H), 6.68 (td, *J* = 8.0 Hz, 1.6 Hz, 1H), 6.60 (dd, *J* = 8.0 Hz, 1.6 Hz, 1H), 4.90 (d, *J* = 8.4 Hz, 1H), 4.88 (br s, 1H), 4.18 (d, *J* = 8.4 Hz, 1H), 4.12 (d, *J* = 10.8 Hz, 1H), 4.00 (d, *J* = 10.8 Hz, 1H), 1.28 (s, 3H); **^{13}C NMR** (100 MHz, $CDCl_3$) δ 200.8, 143.8, 142.9, 141.9, 138.2, 132.9, 129.6 (x 2), 128.8, 128.7 (x 2), 128.0, 127.6, 125.2, 123.4, 122.0, 118.8, 116.3, 115.7, 70.6, 64.4, 63.3, 51.6, 33.4; **HRMS** (ESI, m/z) calcd for $C_{24}H_{21}NO_2$ $[M + H]^+$ 356.1651, found 356.1651.

(6-methyl-3'-phenyl-2',3'-dihydro-2*H*,4*H*-spiro[benzo[*b*][1,4]oxazine-3,1'-inden]-2'-yl)(phenyl)methanone:

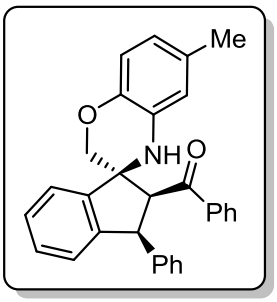

Combined Yield 86% (73.8 mg, dr 100:5:8)

Major diastereomer **4a**:

Light yellow solid; **R_f** 0.25 (pet ether/ethyl acetate = 19:1); **eluent composition** petroleum ether/ethyl acetate = 19:1; **mp** 152-154 ^oC (crystallization from hot EtOH/$CHCl_3$ mixture using solvent evaporation method); **^{1}H NMR** (400 MHz, $CDCl_3$) δ 7.39-7.32 (comp, 3H), 7.28-7.24 (comp, 3H), 7.13-7.04 (comp, 7H), 7.03-6.99 (m, 1H), 6.73 (d, *J* = 8.0 Hz, 1H), 6.41-6.39 (m, 1H), 6.29 (d, *J* = 1.2 Hz, 1H), 5.09 (d, *J* = 8.4 Hz, 1H), 5.01 (d, *J* = 8.4 Hz, 1H), 4.90 (br s, 1H), 4.23 (d, *J* = 10.8 Hz, 1H), 4.04 (d, *J* = 10.4 Hz, 1H), 2.07 (s, 3H); **^{13}C NMR** (100 MHz, $CDCl_3$) δ 201.6, 144.1, 142.4, 140.8, 138.8, 138.1, 132.6, 132.1, 131.4, 129.9 (x 2), 128.7, 128.0 (x 2), 128.0, 127.6 (x 4), 127.0, 125.3, 123.4, 119.2, 116.2, 115.9, 71.0, 64.1, 59.5, 52.3, 20.6; **HRMS** (ESI, m/z) calcd for $C_{30}H_{25}NO_2$ $[M + H]^+$ 432.1964, found 432.1963.

(6-bromo-3'-phenyl-2',3'-dihydro-2*H*,4*H*-spiro[benzo[*b*][1,4]oxazine-3,1'-inden]-2'-yl)(phenyl)methanone:

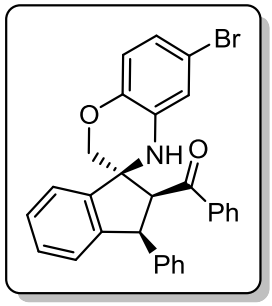

Combined Yield 44% (43.7 mg, dr 100:6:5)

Major diastereomer **4b**:

Colorless solid; **R_f** 0.25 (pet ether/ethyl acetate = 19:1); **eluent composition** petroleum ether/ethyl acetate = 19:1; **mp** 192-194 ^oC (crystallization from hot EtOH/$CHCl_3$ mixture using solvent evaporation method); **^{1}H NMR** (400 MHz, $CDCl_3$) δ 7.41-7.32 (comp, 3H), 7.28-7.24 (comp, 3H), 7.12-6.98 (comp, 8H), 6.72-6.67 (comp, 2H), 6.60 (d, *J* = 1.6 Hz, 1H), 5.06 (d, *J* = 8.4 Hz, 1H), 5.04 (br s, 1H), 5.01 (d, *J* = 8.4 Hz, 1H), 4.25 (dd, *J* = 10.8 Hz, 0.8 Hz, 1H), 4.02 (d, *J* = 10.8 Hz, 1H); **^{13}C NMR** (100 MHz, $CDCl_3$) δ 201.2, 143.4, 142.4, 142.0, 138.5, 137.9, 134.4, 132.4, 129.9 (x 2), 128.9, 128.1 (x 3), 127.8 (x 2), 127.7 (x 2), 127.1, 125.4, 123.3, 121.1, 117.9, 117.6, 114.0, 70.8, 63.8, 59.4, 52.4; **HRMS** (ESI, m/z) calcd for $C_{29}H_{22}BrNO_2$ $[M + H]^+$ 496.0912, found 496.0916.

(6-chloro-3'-phenyl-2',3'-dihydro-2*H*,4*H*-spiro[benzo[*b*][1,4]oxazine-3,1'-inden]-2'-yl)(phenyl)methanone:

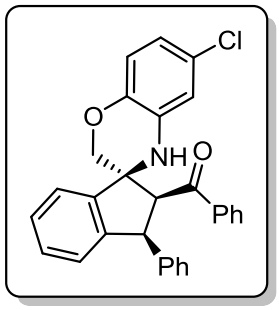

Combined Yield 84% (75.7 mg, dr 100:6:6)

Major diastereomer **4c**:

Colorless solid; **R_f** 0.25 (pet ether/ethyl acetate = 19:1); **eluent composition** petroleum ether/ethyl acetate = 19:1; **mp** 168-170 ^oC (crystallization from hot EtOH/$CHCl_3$ mixture using solvent evaporation method); **^{1}H NMR** (400 MHz, $CDCl_3$) δ 7.41-7.32 (comp, 3H), 7.28-7.24 (comp, 3H), 7.12-6.98 (comp, 8H), 6.76 (d, *J* = 8.8 Hz, 1H), 6.55 (dd, *J* = 8.8 Hz, 2.4 Hz, 1H), 6.47 (d, *J* = 2.4 Hz, 1H), 5.07 (d, *J* = 8.4 Hz, 2H), 5.02 (d, *J* = 8.4 Hz, 1H), 4.25 (dd, *J* = 10.8 Hz, 0.8 Hz, 1H), 4.03 (d, *J* = 11.2 Hz, 1H); **^{13}C NMR** (100 MHz, $CDCl_3$) δ 201.2, 143.4, 142.4, 141.5, 138.5, 137.9, 134.0, 132.4, 129.9 (x 2), 128.9, 128.1 (x 3), 127.8 (x 2), 127.7 (x 2), 127.1, 126.6, 125.4, 123.3, 118.2, 117.1, 115.1, 70.8, 63.8, 59.4, 52.4; **HRMS** (ESI, m/z) calcd for $C_{29}H_{22}ClNO_2$ $[M + H]^+$ 452.1417, found 452.1410.

(7-methoxy-3'-phenyl-2',3'-dihydro-2*H*,4*H*-spiro[benzo[*b*][1,4]oxazine-3,1'-inden]-2'-yl)(phenyl)methanone:

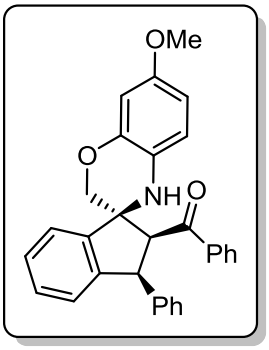

Combined Yield 86% (77.4 mg, dr 100:22:11)

Major diastereomer **4d**:

Light yellow solid; **R_f** 0.25 (pet ether/ethyl acetate = 19:1); **eluent composition** petroleum ether/ethyl acetate = 19:1; **mp** 138-140 ^oC (crystallization from hot EtOH/$CHCl_3$ mixture using solvent evaporation method); **^{1}H NMR** (400 MHz, $CDCl_3$) δ 7.45 (app d, *J* = 7.2 Hz, 1H), 7.38 (app t, *J* = 7.2 Hz, 1H), 7.33 (td, *J* = 7.2 Hz, 1.2 Hz, 1H), 7.22 (app t, *J* = 7.2 Hz, 1H), 7.18-7.16 (comp, 2H), 7.11-6.98 (comp, 8H), 6.49 (d, *J* = 2.8 Hz, 1H), 6.39 (d, *J* = 8.8 Hz, 1H), 6.23 (dd, *J* = 8.8 Hz, 2.4 Hz, 1H), 5.07 (d, *J* = 8.8 Hz, 1H), 5.02 (d, *J* = 8.8 Hz, 1H), 4.86 (br s, 1H), 4.24 (d, *J* = 10.8 Hz, 1H), 4.15 (d, *J* = 10.4 Hz, 1H), 3.67 (s, 3H); **^{13}C NMR** (100 MHz, $CDCl_3$) δ 201.8, 153.4, 143.9, 142.6, 138.9, 138.1, 132.1, 129.9 (x 2), 128.8, 128.1 (x 2), 128.0, 127.7 (x 2), 127.5 (x 3), 127.0, 126.2, 125.3, 123.7, 116.7, 107.5, 102.6, 71.3, 64.2, 58.9, 55.7, 52.4; **HRMS** (ESI, m/z) calcd for $C_{30}H_{25}NO_3$ $[M + H]^+$ 448.1913, found 448.1914.

Crystal data and structure refinement for 4d, CCDC No. 2090977

Empirical formula	$C_{30}H_{25}NO_3$
Formula weight	447.51
Temperature/K	100.0
Crystal system	monoclinic
Space group	$P2_1/c$
a/Å	14.5915(6)
b/Å	6.1948(2)
c/Å	25.4400(10)
α/°	90
β/°	96.413(2)
γ/°	90
Volume/$Å^3$	2285.17(15)
Z	4
$\rho_{calc}g/cm^3$	1.301
μ/mm^{-1}	0.665
F(000)	944.0
Crystal size/mm^3	0.7 × 0.18 × 0.16
Radiation	Cu Kα (λ = 1.54178)
2Θ range for data collection/°	6.096 to 136.228
Index ranges	$-17 \leq h \leq 17$, $-6 \leq k \leq 7$, $-30 \leq l \leq 30$
Reflections collected	100408
Independent reflections	4111 [R_{int} = 0.0520, R_{sigma} = 0.0194]

Data/restraints/parameters	4111/0/309
Goodness-of-fit on F^2	1.057
Final R indexes [I>=2σ (I)]	R_1 = 0.0429, wR_2 = 0.1044
Final R indexes [all data]	R_1 = 0.0437, wR_2 = 0.1051
Largest diff. peak/hole / e $Å^{-3}$	0.28/-0.23

(7-methyl-3'-phenyl-2',3'-dihydro-2*H*,4*H*-spiro[benzo[*b*][1,4]oxazine-3,1'-inden]-2'-yl)(phenyl)methanone:

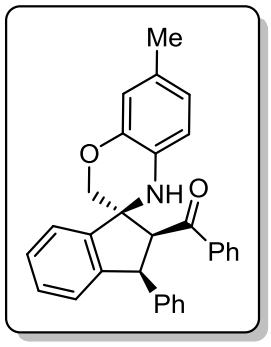

Combined Yield 92% (79.0 mg, dr 100:12:15)

Major diastereomer **4e**:

Light yellow solid; **R_f** 0.25 (pet ether/ethyl acetate = 19:1); **eluent composition** petroleum ether/ethyl acetate = 19:1; **mp** 182-184 °C (crystallization from hot EtOH/$CHCl_3$ mixture using solvent evaporation method); **^{1}H NMR** (400 MHz, $CDCl_3$) δ 7.42 (app d, *J* = 7.2 Hz, 1H), 7.37 (app t, *J* = 7.2 Hz, 1H), 7.33 (td, *J* = 7.2 Hz, 1.2 Hz, 1H), 7.24-7.19 (comp, 3H), 7.11-7.10 (comp, 3H), 7.07-6.98 (comp, 5H), 6.68 (d, *J* = 1.2 Hz, 1H), 6.45 (dd, *J* = 8.0 Hz, 1.2 Hz, 1H), 6.37 (d, *J* = 8.0 Hz, 1H), 5.08 (d, *J* = 8.4 Hz, 1H), 5.02 (d, *J* = 8.4 Hz, 1H), 4.86 (br s, 1H), 4.24 (d, *J* = 10.8 Hz, 1H), 4.09 (d, *J* = 10.8 Hz, 1H), 2.18 (s, 3H); **^{13}C NMR** (100 MHz, $CDCl_3$) δ 201.7, 144.2, 142.9, 142.4, 138.9, 138.2, 132.0, 130.3, 129.9 (x 2), 128.7, 128.4, 128.0 (x 2), 128.0, 127.6 (x 2), 127.6 (x 2), 127.0, 125.2, 123.5, 122.4, 116.7, 115.7, 71.1, 64.1, 59.4, 52.4, 20.5; **HRMS** (ESI, m/z) calcd for $C_{30}H_{25}NO_2$ $[M + H]^+$ 432.1964, found 432.1978.

(7-chloro-3'-phenyl-2',3'-dihydro-2*H*,4*H*-spiro[benzo[*b*][1,4]oxazine-3,1'-inden]-2'-yl)(phenyl)methanone:

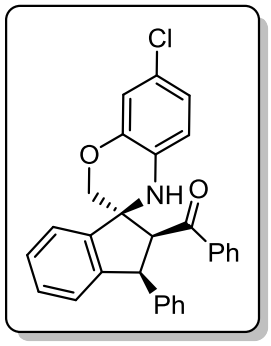

Combined Yield 93% (83.8 mg, dr 100:6:6)

Major diastereomer **4f**:

Light yellow solid; **R_f** 0.20 (pet ether/ethyl acetate = 19:1); **eluent composition** petroleum ether/ethyl acetate = 19:1; **mp** 192-194 °C (crystallization from hot EtOH/$CHCl_3$ mixture using solvent evaporation method); **^{1}H NMR** (400 MHz, $CDCl_3$) δ 7.42-7.32 (comp, 3H), 7.27-7.22 (comp, 3H), 7.13-7.04 (comp, 7H), 7.03-6.98 (m, 1H), 6.86 (d, *J* = 2.4 Hz, 1H), 6.61 (dd, *J* = 8.4 Hz, 2.4 Hz, 1H), 6.38 (d, *J* = 8.4 Hz, 1H), 5.06 (d, *J* = 8.4 Hz, 1H), 5.02 (d, *J* = 8.4 Hz, 1H), 4.86 (br s, 1H), 4.26 (d, *J* = 10.4 Hz, 1H), 4.07 (d, *J* = 10.8 Hz, 1H); **^{13}C NMR** (100 MHz, $CDCl_3$) δ 201.4, 143.5, 143.4, 142.5, 138.6, 137.9, 132.3, 131.7, 129.9 (x 2), 128.9, 128.1 (x 3), 127.8 (x 2), 127.6 (x 2), 127.1, 125.4, 123.4, 122.9,

121.8, 116.4, 116.3, 70.9, 63.8, 59.2, 52.4; **HRMS** (ESI, m/z) calcd for $C_{29}H_{22}ClNO_2$ $[M + H]^+$ 452.1417, found 452.1413.

(7-fluoro-3'-phenyl-2',3'-dihydro-2*H*,4*H*-spiro[benzo[*b*][1,4]oxazine-3,1'-inden]-2'-yl)(phenyl)methanone:

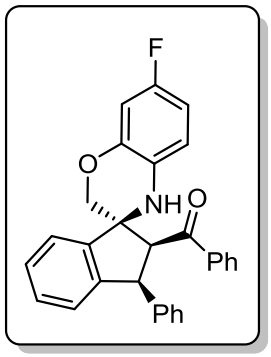

Combined Yield 82% (71.7 mg, dr 100:8:1)

Major diastereomer **4g**:

Colorless solid; **R_f** 0.20 (pet ether/ethyl acetate = 19:1); **eluent composition** petroleum ether/ethyl acetate = 19:1; **mp** 182-184 ^oC (crystallization from hot EtOH/$CHCl_3$ mixture using solvent evaporation method); **^{1}H NMR** (400 MHz, $CDCl_3$) δ 7.42-7.39 (comp, 2H), 7.34 (td, *J* = 7.2 Hz, 2.0 Hz, 1H), 7.24-7.18 (comp, 3H), 7.13-7.10 (comp, 3H), 7.08-6.99 (comp, 5H), 6.63-6.60 (m, 1H), 6.39-6.32 (comp, 2H), 5.07 (d, *J* = 8.8 Hz, 1H), 5.02 (d, *J* = 8.4 Hz, 1H), 4.89 (br s, 1H), 4.25 (d, *J* = 10.8 Hz, 1H), 4.12 (d, *J* = 10.4 Hz, 1H); **^{13}C NMR** (100 MHz, $CDCl_3$) δ 201.6, 156.2 (d, $^1J_{C–F}$ = 235.0 Hz), 143.7, 143.4 (d, $^3J_{C–F}$ = 11.0 Hz), 142.6, 138.8, 138.0, 132.2, 129.9 (x 2), 129.1 (d, $^4J_{C–F}$ = 1.0 Hz), 128.9, 128.1 (x 2), 128.0, 127.7 (x 2), 127.5 (x 2), 127.1, 125.3, 123.5, 115.9 (d, $^3J_{C–F}$ = 9.0 Hz), 108.2 (d, $^2J_{C–F}$ = 22.0 Hz), 103.7 (d, $^2J_{C–F}$ = 25.0 Hz), 71.2, 63.8, 59.0, 52.4; **HRMS** (ESI, m/z) calcd for $C_{29}H_{22}FNO_2$ $[M + H]^+$ 436.1713, found 436.1718.

(5'-methyl-3'-phenyl-2',3'-dihydro-2*H*,4*H*-spiro[benzo[*b*][1,4]oxazine-3,1'-inden]-2'-yl)(phenyl)methanone:

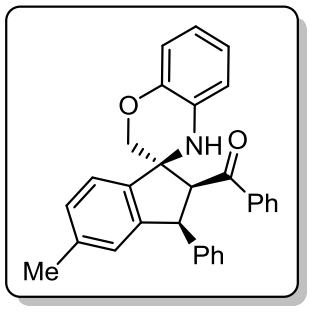

Combined Yield 96% (82.4 mg, dr 100:5:10)

Major diastereomer **4h**:

Light yellow solid; **R_f** 0.25 (pet ether/ethyl acetate = 19:1); **eluent composition** petroleum ether/ethyl acetate = 19:1; **mp** 196-198 ^oC (crystallization from hot EtOH/$CHCl_3$ mixture using solvent evaporation method); **^{1}H NMR** (400 MHz, $CDCl_3$) δ 7.30 (d, *J* = 7.6 Hz, 1H), 7.24-7.20 (comp, 4H), 7.14-7.12 (comp, 2H), 7.09-7.00 (comp, 5H), 6.94 (app s, 1H), 6.86 (dd, *J* = 7.2 Hz, 1.6 Hz, 1H), 6.66-6.59 (comp, 2H), 6.46 (dd, *J* = 7.2 Hz, 2.0 Hz, 1H), 5.09 (d, *J* = 8.4 Hz, 1H), 4.99 (d, *J* = 8.4 Hz, 1H), 4.93 (br s, 1H), 4.25 (d, *J* = 10.8 Hz, 1H), 4.08 (d, *J* = 10.8 Hz, 1H), 2.35 (s, 3H); **^{13}C NMR** (100 MHz, $CDCl_3$) δ 201.7, 143.0, 142.6, 141.1, 138.9, 138.7, 138.2, 133.0, 132.1, 129.9 (x 2), 128.9, 128.1 (x 2), 127.7 (x 2), 127.6 (x

2), 127.0, 125.8, 123.2, 121.9, 118.7, 116.1, 115.7, 71.0, 63.8, 59.6, 52.3, 21.4; **HRMS** (ESI, m/z) calcd for $C_{30}H_{25}NO_2$ $[M + H]^+$ 432.1964, found 432.1962.

(3',5'-diphenyl-2',3'-dihydro-2*H*,4*H*-spiro[benzo[*b*][1,4]oxazine-3,1'-inden]-2'-yl)(phenyl)methanone:

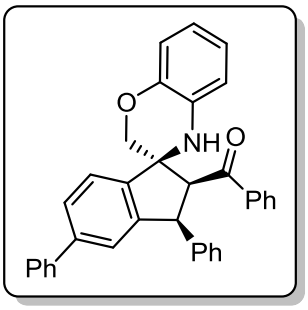

Combined Yield 92% (91.0 mg, dr 100:5:6)

Major diastereomer **4i**:

Light yellow solid; **R$_f$** 0.20 (pet ether/ethyl acetate = 19:1); **eluent composition** petroleum ether/ethyl acetate = 19:1; **mp** 198-200 ^oC (crystallization from hot EtOH/$CHCl_3$ mixture using solvent evaporation method); **^{1}H NMR** (400 MHz, $CDCl_3$) δ 7.62 (app d, *J* = 8.0 Hz, 1H), 7.56-7.54 (comp, 2H), 7.49 (d, *J* = 8.0 Hz, 1H), 7.43-7.39 (comp, 2H), 7.35-7.31 (comp, 2H), 7.25-7.22 (comp, 3H), 7.18-7.17 (comp, 2H), 7.10-7.01 (comp, 5H), 6.90-6.88 (m, 1H), 6.69-6.62 (comp, 2H), 6.52-6.49 (m, 1H), 5.15 (d, *J* = 8.4 Hz, 1H), 5.09 (d, *J* = 8.4 Hz, 1H), 5.01 (br s, 1H), 4.33 (d, *J* = 10.4 Hz, 1H), 4.16 (d, *J* = 10.8 Hz, 1H); **^{13}C NMR** (100 MHz, $CDCl_3$) δ 201.7, 143.1, 143.0 (x 2), 142.2, 141.0, 138.8, 138.0, 132.9, 132.2, 129.9 (x 2), 128.7 (x 2), 128.2 (x 2), 127.7 (x 2), 127.6 (x 2), 127.3, 127.3 (x 2), 127.2, 127.1, 124.1, 123.8, 122.0, 118.8, 116.2, 115.8, 70.9, 63.8, 59.7, 52.4; **HRMS** (ESI, m/z) calcd for $C_{35}H_{27}NO_2$ $[M + H]^+$ 494.2120, found 494.2132.

(5'-bromo-3'-phenyl-2',3'-dihydro-2*H*,4*H*-spiro[benzo[*b*][1,4]oxazine-3,1'-inden]-2'-yl)(phenyl)methanone:

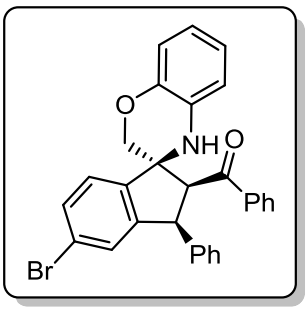

Combined Yield 44% (43.7 mg, dr 100:10:8)

Major diastereomer **4j**:

Light yellow solid; **R$_f$** 0.25 (pet ether/ethyl acetate = 19:1); **eluent composition** petroleum ether/ethyl acetate = 19:1; **mp** 200-202 ^oC (crystallization from hot EtOH/$CHCl_3$ mixture using solvent evaporation method); **^{1}H NMR** (400 MHz, $CDCl_3$) δ 7.50 (app d, *J* = 8.0 Hz, 1H), 7.28 (d, *J* = 8.0 Hz, 1H), 7.25-7.20 (comp, 4H), 7.10-7.02 (comp, 7H), 6.86-6.84 (m, 1H), 6.67-6.60 (comp, 2H), 6.47 (dd, *J* = 7.2 Hz, 2.4 Hz, 1H), 5.07 (d, *J* = 8.4 Hz, 1H), 4.99 (d, *J* = 8.4 Hz, 1H), 4.91 (br s, 1H), 4.24 (d, *J* = 10.8 Hz, 1H), 4.06 (d, *J* = 10.8 Hz, 1H); **^{13}C NMR** (100 MHz, $CDCl_3$) δ 201.4, 144.8, 143.1, 142.9, 138.5, 137.2, 132.6, 132.3, 131.2, 129.7 (x 2), 128.4, 128.3 (x 2), 127.8 (x 2), 127.6 (x 2), 127.3, 125.0, 122.7, 122.1, 119.0, 116.2, 115.8, 70.6, 63.6, 59.5, 52.1; **HRMS** (ESI, m/z) calcd for $C_{29}H_{22}BrNO_2$ $[M + H]^+$ 496.0912, found 496.0910.

(5'-chloro-3'-phenyl-2',3'-dihydro-2*H*,4*H*-spiro[benzo[*b*][1,4]oxazine-3,1'-inden]-2'-yl)(phenyl)methanone:

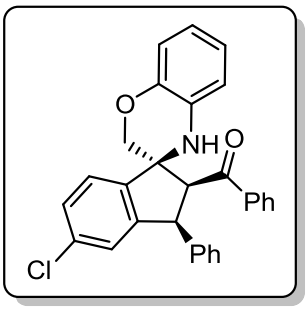

Combined Yield 38% (34.1 mg, dr 100:9:1)

Major diastereomer **4k**:

Light yellow solid; **R_f** 0.20 (pet ether/ethyl acetate = 19:1); **eluent composition** petroleum ether/ethyl acetate = 19:1; **mp** 210-212 ºC (crystallization from hot EtOH/$CHCl_3$ mixture using solvent evaporation method); **^{1}H NMR** (400 MHz, $CDCl_3$) δ 7.36-7.32 (comp, 2H), 7.25-7.20 (comp, 3H), 7.09-7.02 (comp, 8H), 6.86-6.84 (m, 1H), 6.67-6.60 (comp, 2H), 6.48-6.46 (m, 1H), 5.08 (d, *J* = 8.4 Hz, 1H), 4.98 (d, *J* = 8.4 Hz, 1H), 4.91 (br s, 1H), 4.24 (d, *J* = 10.8 Hz, 1H), 4.06 (d, *J* = 10.8 Hz, 1H); **^{13}C NMR** (100 MHz, $CDCl_3$) δ 201.4, 144.5, 142.9, 142.6, 138.6, 137.2, 134.7, 132.7, 132.3, 129.8 (x 2), 128.3, 128.3 (x 2), 127.8 (x 2), 127.6 (x 2), 127.3, 125.5, 124.6, 122.0, 119.0, 116.2, 115.8, 70.7, 63.6, 59.5, 52.1; **HRMS** (ESI, m/z) calcd for $C_{29}H_{22}ClNO_2$ $[M + H]^+$ 452.1417, found 452.1429.

(5'-fluoro-3'-phenyl-2',3'-dihydro-2*H*,4*H*-spiro[benzo[*b*][1,4]oxazine-3,1'-inden]-2'-yl)(phenyl)methanone:

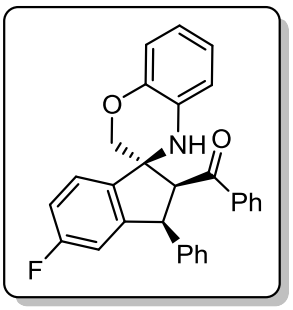

Combined Yield 40% (34.4 mg, dr 100:9:1)

Major diastereomer **4l**:

Colorless solid; **R_f** 0.25 (pet ether/ethyl acetate = 19:1); **eluent composition** petroleum ether/ethyl acetate = 19:1; **mp** 200-202 ºC (crystallization from hot EtOH/$CHCl_3$ mixture using solvent evaporation method); **^{1}H NMR** (400 MHz, $CDCl_3$) δ 7.35 (dd, *J* = 8.4 Hz, 5.2 Hz, 1H), 7.24-7.20 (comp, 3H), 7.12-7.00 (comp, 8H), 6.87-6.84 (m, 1H), 6.83-6.80 (m, 1H), 6.66-6.59 (comp, 2H), 6.48-6.44 (m, 1H), 5.10 (d, *J* = 8.4 Hz, 1H), 4.98 (d, *J* = 8.4 Hz, 1H), 4.90 (br s, 1H), 4.25 (d, *J* = 10.8 Hz, 1H), 4.07 (d, *J* = 10.8 Hz, 1H); **^{13}C NMR** (100 MHz, $CDCl_3$) δ 201.5, 163.5 (d, $^1J_{C-F}$ = 245.0 Hz), 144.9 (d, $^3J_{C-F}$ = 8.0 Hz), 143.0, 139.5 (d, $^4J_{C-F}$ = 2.0 Hz), 138.6, 137.4, 132.8, 132.3, 129.8 (x 2), 128.2 (x 2), 127.7 (x 2), 127.6 (x 2), 127.3, 124.7 (d, $^3J_{C-F}$ = 9.0 Hz), 122.0, 118.9, 116.2, 115.8, 115.1 (d, $^2J_{C-F}$ = 22.0 Hz), 112.6 (d, $^2J_{C-F}$ = 24.0 Hz), 70.9, 63.4, 59.6, 52.0; **HRMS** (ESI, m/z) calcd for $C_{29}H_{22}FNO_2$ $[M + H]^+$ 436.1713, found 436.1714.

(6'-bromo-3'-phenyl-2',3'-dihydro-2*H*,4*H*-spiro[benzo[*b*][1,4]oxazine-3,1'-inden]-2'-yl)(phenyl)methanone:

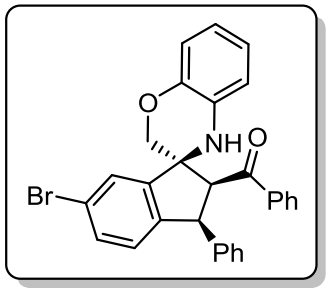

Combined Yield 61% (60.4 mg, dr 100:6:5)

Major diastereomer **4m**:

Light yellow solid; **R_f** 0.20 (pet ether/ethyl acetate = 19:1); **eluent composition** petroleum ether/ethyl acetate = 19:1; **mp** 176-178 ^oC (crystallization from hot EtOH/$CHCl_3$ mixture using solvent evaporation method); **^{1}H NMR** (400 MHz, $CDCl_3$) δ 7.55 (d, *J* = 2.0 Hz, 1H), 7.45 (d, *J* = 8.0 Hz, 1.6 Hz, 1H), 7.24-7.19 (comp, 3H), 7.09-7.01 (comp, 7H), 6.98 (dd, *J* = 8.0 Hz, 0.8 Hz, 1H), 6.87-6.84 (m, 1H), 6.68-6.60 (comp, 2H), 6.49-6.46 (m, 1H), 5.08 (d, *J* = 8.4 Hz, 1H), 4.95 (d, *J* = 8.4 Hz, 2H), 4.26 (d, *J* = 10.8 Hz, 1H), 4.07 (d, *J* = 10.8 Hz, 1H); **^{13}C NMR** (100 MHz, $CDCl_3$) δ 201.4, 146.3, 142.9, 141.5, 138.5, 137.4, 132.5, 132.3, 131.9, 129.8 (x 2), 128.2 (x 2), 127.7 (x 2), 127.6 (x 2), 127.3, 126.9, 126.8, 122.1, 121.8, 119.0, 116.2, 115.8, 70.7, 63.8, 59.6, 51.9; **HRMS** (ESI, m/z) calcd for $C_{29}H_{22}BrNO_2$ $[M + H]^+$ 496.0912, found 496.0914.

(7'-methoxy-3'-phenyl-2',3'-dihydro-2*H*,4*H*-spiro[benzo[*b*][1,4]oxazine-3,1'-inden]-2'-yl)(phenyl)methanone:

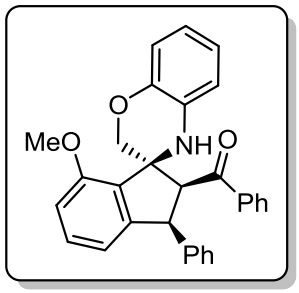

Combined Yield 74% (66.5 mg, dr 100:19:7)

Major diastereomer **4n**:

Light yellow solid; **R_f** 0.10 (pet ether/ethyl acetate = 19:1); **eluent composition** petroleum ether/ethyl acetate = 19:1; **mp** 170-172 ^oC (crystallization from hot EtOH/$CHCl_3$ mixture using solvent evaporation method); **^{1}H NMR** (400 MHz, $CDCl_3$) δ 7.31 (app t, *J* = 8.0 Hz, 1H), 7.26-7.19 (comp, 5H), 7.14-7.10 (comp, 2H), 7.07-7.01 (comp, 3H), 6.87-6.85 (comp, 2H), 6.78 (app d, *J* = 7.6 Hz, 1H), 6.64-6.55 (comp, 2H), 6.37 (dd, *J* = 7.6 Hz, 1.6 Hz, 1H), 5.05 (d, *J* = 8.0 Hz, 1H), 4.88 (d, *J* = 8.4 Hz, 1H), 4.27 (d, *J* = 10.8 Hz, 1H), 4.22 (d, *J* = 10.4 Hz, 1H), 3.81 (s, 3H); **^{13}C NMR** (100 MHz, $CDCl_3$) δ 201.0, 157.0, 145.5, 143.0, 139.2, 138.2, 132.9, 131.8, 130.2, 130.0 (x 2), 128.8, 128.0 (x 2), 127.6 (x 2), 127.4 (x 2), 126.8, 122.0, 117.8, 117.6, 116.2, 115.6, 110.1, 67.8, 66.6, 60.1, 55.3, 51.8; **HRMS** (ESI, m/z) calcd for $C_{30}H_{25}NO_3$ $[M + H]^+$ 448.1913, found 448.1912.

(7'-fluoro-3'-phenyl-2',3'-dihydro-2*H*,4*H*-spiro[benzo[*b*][1,4]oxazine-3,1'-inden]-2'-yl)(phenyl)methanone:

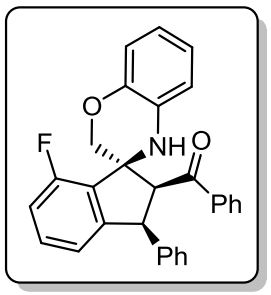

Combined Yield 43% (37.3 mg, dr 100:19:6)

Major diastereomer **4o**:

Light yellow solid; **R_f** 0.20 (pet ether/ethyl acetate = 19:1); **eluent composition** petroleum ether/ethyl acetate = 19:1; **mp** 172-174 ^oC (crystallization from hot EtOH/$CHCl_3$ mixture using solvent evaporation method); **^{1}H NMR** (400 MHz, $CDCl_3$) δ 7.32-7.27 (m, 1H), 7.24-7.20 (comp, 3H), 7.15-7.00 (comp, 8H), 6.92 (app d, *J* = 7.6 Hz, 1H), 6.85 (dd, *J* = 8.0 Hz, 1.6 Hz, 1H), 6.65-6.56 (comp, 2H), 6.42 (dd, *J* = 7.6 Hz, 1.6 Hz, 1H), 5.09 (d, *J* = 8.4 Hz, 1H), 5.01 (br s, 1H), 4.96 (d, *J* = 8.4 Hz, 1H), 4.38 (d, *J* = 10.4 Hz, 1H), 4.28 (d, *J* = 10.8 Hz, 1H); **^{13}C NMR** (100 MHz, $CDCl_3$) δ 201.3, 159.8 (d, $^1J_{C–F}$ = 251.0 Hz), 146.3 (d, $^3J_{C–F}$ = 5.0 Hz), 142.8, 138.8, 137.5, 132.4, 132.2, 130.5 (d, $^3J_{C–F}$ = 8.0 Hz), 129.9 (x 2), 128.9 (d, $^2J_{C–F}$ = 12.0 Hz), 128.2 (x 2), 127.8 (x 2), 127.5 (x 2), 127.2, 122.1, 121.1 (d, $^4J_{C–F}$ = 3.0 Hz), 118.4, 116.2, 115.5, 115.3 (d, $^2J_{C–F}$ = 20.0 Hz), 68.8, 65.0, 59.8, 52.4; **HRMS** (ESI, m/z) calcd for $C_{29}H_{22}FNO_2$ $[M + H]^+$ 436.1713, found 436.1705.

phenyl(4'-phenyl-4',5'-dihydro-2*H*,4*H*-spiro[benzo[*b*][1,4]oxazine-3,6'-cyclopenta[*b*]thiophen]-5'-yl)methanone (4p): (data for the major diastereomer is given)

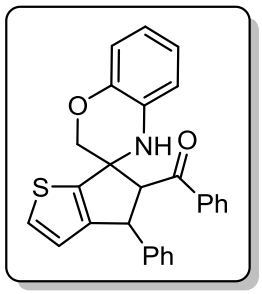

Combined Yield 40% (34.2 mg, dr 22:100:3)

Orange yellow solid; **R_f** 0.15 (pet ether/ethyl acetate = 19:1); **eluent composition** petroleum ether/ethyl acetate = 19:1; **^{1}H NMR** (400 MHz, $CDCl_3$) δ 7.64-7.62 (comp, 2H), 7.45-7.41 (m, 1H), 7.37 (d, *J* = 4.8 Hz, 1H), 7.31-7.25 (comp, 5H), 7.16-7.14 (comp, 2H), 6.75 (d, *J* = 4.8 Hz, 1H), 6.68-6.64 (m, 1H), 6.59-6.53 (comp, 2H), 6.42 (dd, *J* = 7.6 Hz, 1.2 Hz, 1H), 5.12 (d, *J* = 6.0 Hz, 1H), 4.73 (d, *J* = 6.0 Hz, 1H), 4.43 (br s, 1H), 4.36 (d, *J* = 10.8 Hz, 1H), 4.20 (d, *J* = 10.0 Hz, 1H); **^{13}C NMR** (100 MHz, $CDCl_3$) δ 200.0, 146.8, 143.1, 143.0, 142.9, 137.7, 133.0, 131.9, 131.4, 128.9 (x 2), 128.3 (x 2), 128.0 (x 2), 127.2 (x 2), 127.1, 122.1, 121.9, 119.4, 116.3, 116.0, 73.5, 67.1, 62.7, 50.2; **HRMS** (ESI, m/z) calcd for $C_{27}H_{21}NO_2S$ $[M + H]^+$ 424.1371, found 424.1379.

phenyl(4'-phenyl-4',5'-dihydro-2*H*,4*H*-spiro[benzo[*b*][1,4]oxazine-3,6'-cyclopenta[*b*]thiophen]-5'-yl)methanone (4p): (data for the major diastereomers is given)

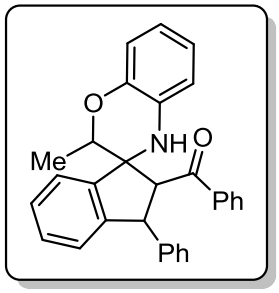

Combined Yield 97% (83.8 mg, dr 100:98:23:8)

Light yellow solid; **R_f** 0.20 (pet ether/ethyl acetate = 19:1); **eluent composition** petroleum ether/ethyl acetate = 19:1; **^{1}H NMR** (400 MHz, $CDCl_3$) δ 7.49-7.47 (m, 1H), 7.38-7.32 (comp, 5H), 7.21-7.16 (comp, 2H), 7.15-7.07 (comp, 12H), 7.06-7.04 (comp, 4H), 7.02-6.98 (comp, 4H), 6.87-6.83 (m, 1H), 6.82-6.78 (m, 1H), 6.64-6.58 (comp, 2H), 6.58-6.51 (comp, 2H), 6.46-6.41 (m, 1H), 6.41-6.37 (m, 1H), 5.10-5.07 (comp, 2H), 5.05-5.00 (comp, 3H), 4.87 (br s, 1H), 4.52 (q, *J* = 6.4 Hz, 1H), 4.46 (q, *J* = 6.4 Hz, 1H), 1.37 (d, *J* = 6.4 Hz, 3H), 1.29 (d, *J* = 6.8 Hz, 3H); **^{13}C NMR** (100 MHz, $CDCl_3$) δ 202.0, 201.9, 144.4, 144.2, 144.0, 143.7, 143.0, 141.4, 139.6, 139.1, 138.8, 138.2, 132.8, 132.0, 131.9, 131.8, 130.2 (x 2), 129.9 (x 2), 128.9, 128.5, 128.0 (x 2), 127.9 (x 2), 127.6 (x 2), 127.6 (x 3), 127.5, 127.4 (x 3), 127.1, 127.0, 126.8, 125.2, 125.1, 124.9, 123.9, 121.6, 121.5, 119.2, 119.1, 116.7, 116.0, 115.8, 115.8, 78.8, 73.7, 67.3, 66.9, 61.7, 56.9, 54.3, 52.1, 15.8, 14.8; **HRMS** (ESI, m/z) calcd for $C_{30}H_{25}NO_2$ $[M + H]^+$ 432.1964, found 432.1964.

6.5.5. General Procedure for the Interchange of the Diastereomers:

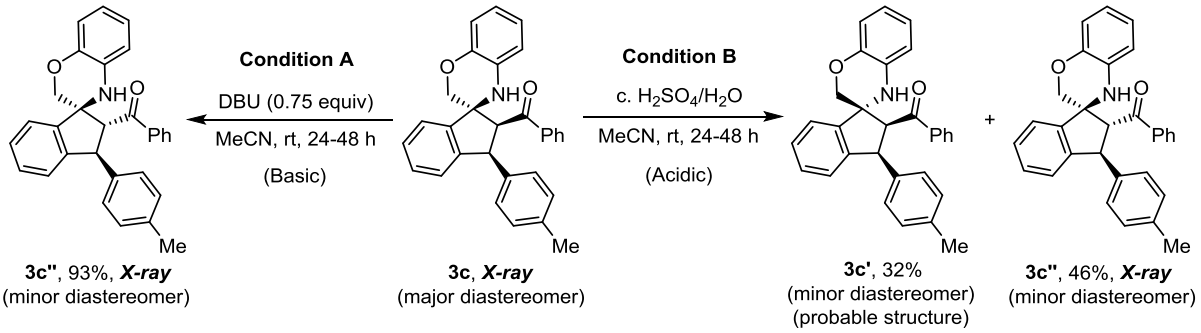

Condition A: A mixture of major diastereomer phenyl((2'*S*,3*S*,3'*S*)-3'-(*p*-tolyl)-2',3'-dihydro-2*H*,4*H*-spiro[benzo[*b*][1,4]oxazine-3,1'-inden]-2'-yl)methanone (**3c**) (43.2 mg, 0.1 mmol, 1.0 equiv) and DBU (10.3 µL, 0.075 mmol, 0.75 equiv) in 2.0 mL MeCN was allowed to stir at room temperature for 24-48 hours. After completion of reaction as checked by TLC, the reaction mixture was concentrated under under vacuo. The reaction mixture was quenched with 1M HCl (few drops), poured to water (20 mL) and extracted with ethyl acetate (3 x 5 mL). The combined organic layers were washed with brine solution (2 x 5 mL). The organic phase was separated, dried

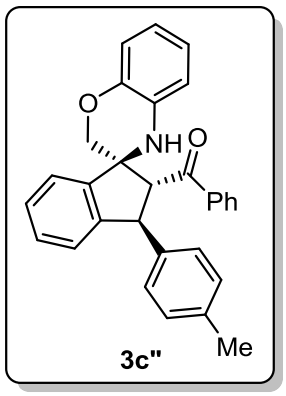

over anhydrous Na_2SO_4, filtered and concentrated under vacuo. The crude reaction mixture was directly purified by column chromatography on silica gel using pet ether/ethyl acetate as eluent (19:1) to obtain the minor diastereomer phenyl((2'*R*,3*S*,3'*S*)-3'-(*p*-tolyl)-2',3'-dihydro-2*H*,4*H*-spiro[benzo[*b*][1,4]oxazine-3,1'-inden]-2'-yl)methanone (**3c″**) exclusively (40.1 mg, 93% yield).

Light yellow solid; **R_f** 0.30 (pet ether/ethyl acetate = 19:1); **mp** 216-218 ^oC (crystallization from hot EtOH/$CHCl_3$ mixture using solvent evaporation method); **^{1}H NMR** (400 MHz, $CDCl_3$) δ 7.82-7.80 (comp, 2H), 7.34-7.30 (comp, 2H), 7.29-7.23 (comp, 2H), 7.17-7.15 (comp, 2H), 7.13-7.07 (comp, 4H), 7.04-7.00 (m, 1H), 6.66-6.62 (m, 1H), 6.52 (d, *J* = 8.4 Hz, 1H), 6.40-6.35 (comp, 2H), 5.22 (d, *J* = 9.6 Hz, 1H), 4.48 (br s, 1H), 4.44 (d, *J* = 9.6 Hz, 1H), 4.33 (d, *J* = 10.8 Hz, 1H), 3.84 (d, *J* = 11.2 Hz, 1H), 2.28 (s, 3H); **^{13}C NMR** (100 MHz, $CDCl_3$) δ 199.6, 144.5, 142.5, 142.4, 139.4, 137.3, 136.5, 132.8, 132.6, 129.5, 129.4 (x 2), 128.4 (x 2), 128.4 (x 2), 127.9, 127.8 (x 2), 125.5, 123.5, 121.6, 118.2, 116.5, 113.6, 70.2, 68.2, 66.7, 50.4, 21.0; **HRMS** (ESI, m/z) calcd for $C_{30}H_{25}NO_2$ $[M + H]^+$ 432.1964, found 432.1954.

Crystal data and structure refinement for 3c″, CCDC No. 2090974

Empirical formula	$C_{30}H_{25}NO_2$
Formula weight	431.51
Temperature/K	100.0
Crystal system	monoclinic
Space group	$P2_1/n$
a/Å	6.0754(3)
b/Å	15.6533(7)
c/Å	24.0657(11)
α/°	90
β/°	90.539(2)
γ/°	90
Volume/Å^3	2288.55(18)
Z	4
ρ_{calc}g/cm^3	1.252
μ/mm^{-1}	0.611
F(000)	912.0
Crystal size/mm^3	0.4 × 0.1 × 0.06
Radiation	Cu Kα (λ = 1.54178)
2Θ range for data collection/°	6.736 to 136.86
Index ranges	$-7 \le h \le 7$, $-18 \le k \le 18$, $-28 \le l \le 29$
Reflections collected	46345
Independent reflections	4159 [R_{int} = 0.1178, R_{sigma} = 0.0601]
Data/restraints/parameters	4159/0/300
Goodness-of-fit on F^2	1.079
Final R indexes [I>=2σ (I)]	R_1 = 0.0894, wR_2 = 0.2441

Final R indexes [all data]	R_1 = 0.0950, wR_2 = 0.2525
Largest diff. peak/hole / e Å^{-3}	0.53/-0.59

Condition B: A mixture of major diastereomer phenyl((2'*S*,3*S*,3'*S*)-3'-(*p*-tolyl)-2',3'-dihydro-2*H*,4*H*-spiro[benzo[*b*][1,4]oxazine-3,1'-inden]-2'-yl)methanone (**3c**) (43.2 mg, 0.1 mmol, 1.0 equiv), conc. H_2SO_4 (20 µL), and H_2O (20 µL) in 1.0 mL MeCN was allowed to stir at room temperature for 24-48 hours. After completion of reaction as checked by TLC, the reaction mixture was concentrated under under vacuo. The reaction mixture was quenched with saturated $NaHCO_3$ solution (5 mL), poured to water (20 mL) and extracted with ethyl acetate (3 x 5 mL). The combined organic layers were washed with brine solution (2 x 5 mL). The organic phase was separated, dried over anhydrous Na_2SO_4, filtered and concentrated under vacuo. The crude reaction mixture was directly purified by column chromatography on silica gel using pet ether/ethyl acetate as eluent (19:1) to obtain both the minor diastereomers phenyl((2'*S*,3*R*,3'*S*)-3'-(*p*-tolyl)-2',3'-dihydro-2*H*,4*H*-spiro[benzo[*b*][1,4]oxazine-3,1'-inden]-2'-yl)methanone (**3c′**) (14.0 mg, 32% yield) and phenyl((2'*R*,3*S*,3'*S*)-3'-(*p*-tolyl)-2',3'-dihydro-2*H*,4*H*-spiro[benzo[*b*][1,4]oxazine-3,1'-inden]-2'-yl)methanone (**3c″**) (20.0 mg, 46% yield).

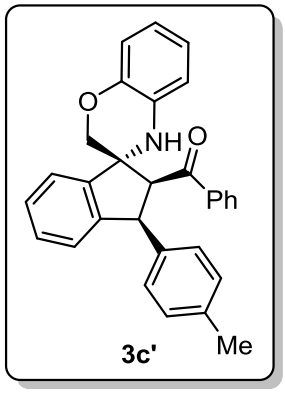

(probable structure is shown as it could not be crystallized) Light yellow solid; **R$_f$** 0.25 (pet ether/ethyl acetate = 19:1); **mp** 46-48 °C; **^{1}H NMR** (400 MHz, $CDCl_3$) δ 7.62-7.60 (comp, 2H), 7.40-7.30 (comp, 4H), 7.24-7.20 (comp, 2H), 7.15-7.09 (comp, 3H), 7.00-6.98 (comp, 2H), 6.62-6.58 (m, 1H), 6.52-6.45 (comp, 2H), 6.36 (dd, *J* = 8.0 Hz, 0.8 Hz, 1H), 5.07 (d, *J* = 5.2 Hz, 1H), 4.54 (d, *J* = 5.6 Hz, 1H), 4.26 (d, *J* = 10.4 Hz, 1H), 4.15 (d, *J* = 10.4 Hz, 1H), 2.33 (s, 3H); **^{13}C NMR** (100 MHz, $CDCl_3$) δ 201.6, 144.4, 143.0, 142.8, 140.7, 137.7, 136.6, 132.8, 132.4, 129.6, 129.5 (x 2), 128.2, 128.1 (x 2), 128.0 (x 2), 127.8 (x 2), 125.8, 124.3, 121.8, 119.0, 116.2, 115.8, 73.7, 65.1, 62.3, 53.5, 21.0; **HRMS** (ESI, m/z) calcd for $C_{30}H_{25}NO_2$ $[M + H]^+$ 432.1964, found 432.1961.

6.5.6. Mechanistic Experiments

(a) Procedure for H/D exchange experiment:

An oven-dried 10 mL Schlenk tube was charged with 3-phenyl-2*H*-benzo[*b*][1,4]oxazine (**1a**) (41.8 mg, 0.2 mmol, 1.0 equiv), $[Cp^*RhCl_2]_2$ (6.2 mg, 0.01 mmol, 0.05 equiv), and NaOAc (16.4 mg, 0.2 mmol, 1.0 equiv) were taken and the reaction mixture was degassed and backfilled with nitrogen. To it, 0.2 mL of a D-source (excess) and 2.0 mL (0.1 M) of TFE were added under nitrogen. Then it was degassed and backfilled with nitrogen 3 times. The tube was closed with a teflon-lined cap and kept on stirring in a preheated oil bath. After 24 h, the reaction was stopped and cooled to room temperature. The reaction mixture was filtered through a short pad of celite and concentrated under vacuo. The starting material (**1a**-d_n) was recovered by purifying through column chromatography on silica gel using ethyl acetate/pet ether as eluent. The deuterium incorporation was determined by ^{1}H NMR spectroscopy.

(b) Procedure for competitive experiments between benzoxazines and chalcones:

Procedure for competitive experiment between chalcones 2c and 2g:

In an oven-dried 10 mL Schlenk tube, 3-phenyl-2*H*-benzo[*b*][1,4]oxazine (**1a**) (41.8 mg, 0.2 mmol, 1.0 equiv), (*E*)-1-phenyl-3-(*p*-tolyl)prop-2-en-1-one (**2c**) (66.7 mg, 0.3 mmol, 1.5 equiv), (*E*)-1-phenyl-3-(4-(trifluoromethyl)phenyl)prop-2-en-1-one (**2g**) (82.9 mg, 0.3 mmol, 1.5 equiv), $[Cp^*RhCl_2]_2$ (6.2 mg, 0.01 mmol, 0.05 equiv), and NaOAc (16.4 mg, 0.2 mmol, 1.0 equiv) were taken and the reaction mixture was degassed and backfilled with nitrogen. Under nitrogen 2.0 mL (0.1 M) of TFE was added. Then it was degassed and backfilled with nitrogen 3 times. The tube was closed with a teflon-lined cap and kept on stirring in a preheated oil bath at 100 ^{o}C. After 24 h, the reaction was stopped and cooled to room temperature. The reaction mixture was filtered through a short pad of celite and concentrated under vacuo. The crude reaction mixture was directly purified through column chromatography on silica gel using pet ether/ethyl acetate (19:1) as eluent. The ratio of **3c** and **3g** (with respect to major diastereomer) was determined by ^{1}H NMR spectroscopy (1:1.3).

Procedure for competitive experiment between chalcones 2s and 2y:

In an oven-dried 10 mL Schlenk tube, 3-phenyl-2*H*-benzo[*b*][1,4]oxazine (**1a**) (41.8 mg, 0.2 mmol, 1.0 equiv), (*E*)-3-phenyl-1-(*p*-tolyl)prop-2-en-1-one (**2s**) (66.7 mg, 0.3 mmol, 1.5 equiv), (*E*)-3-phenyl-1-(4-(trifluoromethyl)phenyl)prop-2-en-1-one (**2y**) (82.9 mg, 0.3 mmol, 1.5 equiv), $[Cp^*RhCl_2]_2$ (6.2 mg, 0.01 mmol, 0.05 equiv), and NaOAc (16.4 mg, 0.2 mmol, 1.0

equiv) were taken and the reaction mixture was degassed and backfilled with nitrogen. Under nitrogen 2.0 mL (0.1 M) of TFE was added. Then it was degassed and backfilled with nitrogen 3 times. The tube was closed with a teflon-lined cap and kept on stirring in a preheated oil bath at 100 ^{o}C. After 24 h, the reaction was stopped and cooled to room temperature. The reaction mixture was filtered through a short pad of celite and concentrated under vacuo. The crude reaction mixture was directly purified through column chromatography on silica gel using pet ether/ethyl acetate (19:1) as eluent. The ratio of **3s** and **3y** (with respect to major diastereomer) was determined by ^{1}H NMR spectroscopy (1:1.3).

Procedure for competitive experiment between benzoxazines 1f and 1h:

In an oven-dried 10 mL Schlenk tube, 7-methyl-3-phenyl-2*H*-benzo[*b*][1,4]oxazine (**1f**) (44.7 mg, 0.2 mmol, 1.0 equiv), 7-fluoro-3-phenyl-2*H*-benzo[*b*][1,4]oxazine (**1h**) (45.4 mg, 0.2 mmol, 1.0 equiv), (*E*)-chalcone (**2a**) (62.5 mg, 0.3 mmol, 1.5 equiv), $[Cp^*RhCl_2]_2$ (6.2 mg, 0.01 mmol, 0.05 equiv), and NaOAc (16.4 mg, 0.2 mmol, 1.0 equiv) were taken and the reaction mixture was degassed and backfilled with nitrogen. Under nitrogen 2.0 mL (0.1 M) of TFE was added. Then it was degassed and backfilled with nitrogen 3 times. The tube was closed with a teflon-lined cap and kept on stirring in a preheated oil bath at 100 ^{o}C. After 24 h, the reaction was stopped and cooled to room temperature. The reaction mixture was filtered through a short pad of celite and concentrated under vacuo. The crude reaction mixture was directly purified through column chromatography on silica gel using pet ether/ethyl acetate (19:1) as eluent. The ratio of **4e** and **4g** (with respect to major diastereomer) was determined by ^{1}H NMR spectroscopy (1.4:1).

Procedure for competitive experiment between benzoxazines 1i and 1m:

In an oven-dried 10 mL Schlenk tube, 3-(*p*-tolyl)-2H-benzo[*b*][1,4]oxazine (**1i**) (44.7 mg, 0.2 mmol, 1.0 equiv), 3-(4-fluorophenyl)-2*H*-benzo[*b*][1,4]oxazine (**1m**) (45.4 mg, 0.2 mmol, 1.0 equiv), (*E*)-chalcone (**2a**) (62.5 mg, 0.3 mmol, 1.5 equiv), $[Cp^*RhCl_2]_2$ (6.2 mg, 0.01 mmol, 0.05 equiv), and NaOAc (16.4 mg, 0.2 mmol, 1.0 equiv) were taken and the reaction mixture was degassed and backfilled with nitrogen. Under nitrogen 2.0 mL (0.1 M) of TFE was added. Then it was degassed and backfilled with nitrogen 3 times. The tube was closed with a teflon-lined cap and kept on stirring in a preheated oil bath at 100 ^{o}C. After 24 h, the reaction was stopped and cooled to room temperature. The reaction mixture was filtered through a short pad of celite and concentrated under vacuo. The crude reaction mixture was directly purified through column chromatography on silica gel using pet ether/ethyl acetate (19:1) as eluent. The

ratio of **4h** and **4l** (with respect to major diastereomer) was determined by ^{1}H NMR spectroscopy (1.4:1).

(c) Procedure for the preparation of the rhodacyclic complexes 5 and 6:

Procedure for the preparation of complex 5: Following literature procedure,[18] a mixture of $[Cp^*RhCl_2]_2$ (25.0 mg, 0.04 mmol, 1 equiv), 3-(*p*-tolyl)-2*H*-benzo[*b*][1,4]oxazine (**1i**) (20.0 mg, 0.089 mmol, 2.2 equiv), and NaOAc (20.0 mg, 0.24 mmol, 6.0 equiv) in 10.0 mL of DCM, was allowed to stir at room temperature (approx. 32 ^{o}C) overnight. After completion of the reaction, the reaction mixture was passed through a short pad of celite and concentrated under vacuo, followed by washing with hexane and finally vaccum-dried to give the cyclometallated compound **5** (39.5 mg, 99% yield).

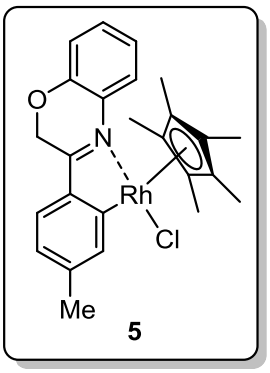

5

Orange yellow solid; **R$_f$** 0.40 (pet ether/ethyl acetate = 19:1); **mp** 238-240 ^{o}C (decomp.) (crystallization from DCM and hexane using solvent diffusion method); **^{1}H NMR** (400 MHz, $CDCl_3$) δ 7.96 (d, *J* = 7.6 Hz, 1H), 7.72 (app s, 1H), 7.22 (app d, *J* = 7.6 Hz, 1H), 7.16 (app t, *J* = 7.6 Hz, 1H), 7.08 (app t, *J* = 7.2 Hz, 1H), 6.96 (app d, *J* = 8.0 Hz, 1H), 6.82 (app d, *J* = 8.0 Hz, 1H), 5.37 (d, *J* = 15.6 Hz, 1H), 4.72 (d, *J* = 15.2 Hz, 1H), 2.41 (s, 3H), 1.52 (s, 15H); **^{13}C NMR** (100 MHz, $CDCl_3$) δ 172.4, 148.1, 142.2, 141.0, 138.0, 133.5, 128.1, 126.1, 126.0, 123.9, 122.9, 115.8, 96.4, 96.3, 64.2, 22.0, 9.3; **HRMS** (ESI, m/z) calcd for $C_{25}H_{27}ClNORh$ $[M + Na]^+$ 518.0734, found 518.0748.

Crystal data and structure refinement for 5, CCDC No. 2090978

Empirical formula	$C_{25}H_{27}ClNORh$
Formula weight	495.83
Temperature/K	100.0
Crystal system	orthorhombic
Space group	Pbca
a/Å	14.8911(5)
b/Å	16.3377(5)
c/Å	18.0100(6)
α/°	90
β/°	90
γ/°	90
Volume/Å^3	4381.6(2)
Z	8
ρ_{calc}g/cm^3	1.503
μ/mm^{-1}	7.537
F(000)	2032.0
Crystal size/mm^3	0.28 × 0.23 × 0.1

Radiation	Cu Kα (λ = 1.54178)
2Θ range for data collection/°	9.418 to 137.344
Index ranges	$-17 \leq h \leq 17$, $-19 \leq k \leq 18$, $-21 \leq l \leq 21$
Reflections collected	79802
Independent reflections	4029 [R_{int} = 0.0827, R_{sigma} = 0.0327]
Data/restraints/parameters	4029/0/268
Goodness-of-fit on F^2	1.168
Final R indexes [I>=2σ (I)]	R_1 = 0.0371, wR_2 = 0.0880
Final R indexes [all data]	R_1 = 0.0374, wR_2 = 0.0882
Largest diff. peak/hole / e $Å^{-3}$	0.89/-0.98

Procedure for the preparation of complex 6: Following literature procedure,[12a] a mixture of compound **5** (24.8 mg, 0.05 mmol, 1.0 equiv) and AgOAc (16.7 mg, 0.1 mmol, 2.0 equiv) in 10.0 mL THF was allowed to stir at room temperature (approx. 32 °C) for 2 hours. After completion of reaction, the reaction mixture was passed through a short pad of celite to remove AgCl and excess AgOAc and concentrated under vacuo, followed by washing with hexane and finally vaccum-dried to give the cyclometallated compound **6** (25.0 mg, 96% yield).

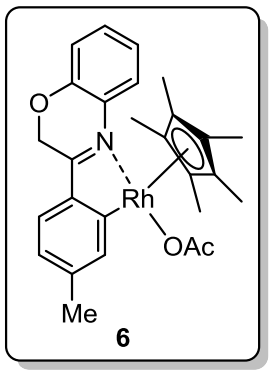

6

Reddish brown solid; **R_f** 0.40 (pet ether/ethyl acetate = 19:1); **mp** 130-132 °C (decomp.) (crystallization from DCM and hexane using solvent diffusion method); **^{1}H NMR** (400 MHz, $CDCl_3$) δ 8.30 (dd, *J* = 7.2 Hz, 2.4 Hz, 1H), 8.06 (app s, 1H), 7.22 (d, *J* = 8.0 Hz, 1H), 7.19-7.14 (comp, 2H), 6.96 (dd, *J* = 7.2 Hz, 1.6 Hz, 1H), 6.86 (app d, *J* = 7.6 Hz, 1H), 5.36 (d, *J* = 15.2 Hz, 1H), 4.72 (d, *J* = 15.2 Hz, 1H), 2.45 (s, 3H), 1.80 (s, 3H), 1.46 (s, 15H); **^{13}C NMR** (100 MHz, $CDCl_3$) δ 177.6, 172.3, 148.2, 141.8, 141.4, 138.2, 134.1, 128.1, 127.0, 125.9, 123.9, 123.0, 115.4, 95.2, 95.1, 63.8, 24.8, 22.2, 9.4; **HRMS** (EI, m/z) calcd for $C_{27}H_{30}NO_3Rh$ [M^+] 519.1281, found 519.1211.

Crystal data and structure refinement for 6, CCDC No. 2090979

Empirical formula	$C_{27}H_{30}NO_3Rh$
Formula weight	519.43
Temperature/K	100.0
Crystal system	monoclinic
Space group	$P2_1/n$
a/Å	13.3118(7)
b/Å	13.5542(7)
c/Å	13.3190(7)
α/°	90
β/°	103.355(2)
γ/°	90
Volume/$Å^3$	2338.2(2)
Z	4

ρ_{calc}g/cm^3	1.476
μ/mm^{-1}	6.130
F(000)	1072.0
Crystal size/mm^3	0.8 × 0.2 × 0.13
Radiation	Cu Kα (λ = 1.54178)
2Θ range for data collection/°	8.464 to 136.544
Index ranges	-16 ≤ h ≤ 14, -16 ≤ k ≤ 16, -16 ≤ l ≤ 15
Reflections collected	24042
Independent reflections	4232 [R_{int} = 0.0825, R_{sigma} = 0.0538]
Data/restraints/parameters	4232/0/296
Goodness-of-fit on F^2	1.051
Final R indexes [I>=2σ (I)]	R_1 = 0.0481, wR_2 = 0.1388
Final R indexes [all data]	R_1 = 0.0520, wR_2 = 0.1424
Largest diff. peak/hole / e Å^{-3}	1.14/-1.43

(d) Procedure for the treatment of the rhodacycle complexes 5 and 6 as catalyst for the spirocyclization reaction:

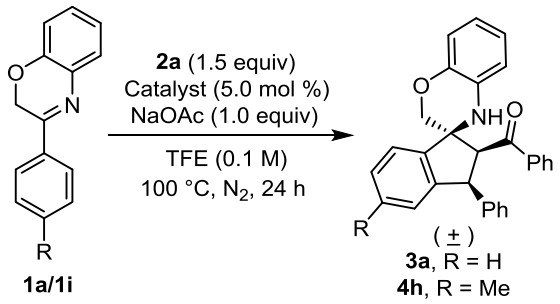

Substrate	Catalyst	Combined Yield (**3a/4h**)	dr
1a	$[Cp^*RhCl_2]_2$	98%	100:4:5
R = H	**5**	65%	100:2:1
(0.2 mmol)	**6**	84%	100:2:1
1i	$[Cp^*RhCl_2]_2$	96%	100:5:10
R = Me	**5**	76%	100:2:1
(0.1 mmol)	**6**	98%	100:1:1

In an oven-dried 10 mL Schlenk tube, substrate (**1a**/**1i**) (1.0 equiv), (*E*)-chalcone (**2a**) (1.5 equiv), catalyst (0.05 equiv), and NaOAc (1.0 equiv) were taken and the reaction mixture was degassed and backfilled with nitrogen. Under nitrogen (0.1 M) of TFE was added. Then it was degassed and backfilled with nitrogen 3 times. The tube was closed with a teflon-lined cap and kept on stirring in a preheated oil bath at 100 ^{o}C. After 24 h, the reaction was stopped and cooled to room temperature. The reaction mixture was filtered through a short pad of celite and concentrated under vacuo. The crude reaction mixture was directly purified by column chromatography on silica gel using pet ether/ethyl acetate (19:1) as eluent to obtain the corresponding product **3a**/**4h** as an inseparable mixture of three diastereomers. The dr was calculated by ^{1}H NMR spectroscopy.

(e) Procedure for the stoichiometric reaction between complex 5 and chalcone 2a:

In an oven-dried 10 mL Schlenk tube, cyclometallated intermediate (**5**) (24.8 mg, 0.05 mmol, 1.0 equiv), (*E*)-chalcone (**2a**) (14.0 mg, 0.05 mmol, 1.0 equiv), and NaOAc (4.1 mg, 0.05 mmol, 1.0 equiv) were taken and the reaction mixture was degassed and backfilled with

nitrogen. Under nitrogen 0.5 mL (0.1 M) of TFE was added. Then it was degassed and backfilled with nitrogen 3 times. The tube was closed with a teflon-lined cap and kept on stirring in a preheated oil bath at 100 ^{o}C. After 24 h, the reaction was stopped and cooled to room temperature. The reaction mixture was filtered through a short pad of celite and concentrated under vacuo. The crude reaction mixture was directly purified by column chromatography on silica gel using pet ether/ethyl acetate (19:1) as eluent to obtain (5'-methyl-3'-phenyl-2',3'-dihydro-2*H*,4*H*-spiro[benzo[*b*][1,4]oxazine-3,1'-inden]-2'-yl)(phenyl)methanone (**4h**) (5.3 mg, 25% combined yield) as an inseparable mixture of three diastereomers (**4h**+**4h′**+**4h″**). The dr was calculated by ^{1}H NMR spectroscopy (100:4:50).

6.6. ^{1}H and ^{13}C NMR Spectra of Representative Compounds

^{1}H NMR of **1a** (400 MHz, $CDCl_3$):

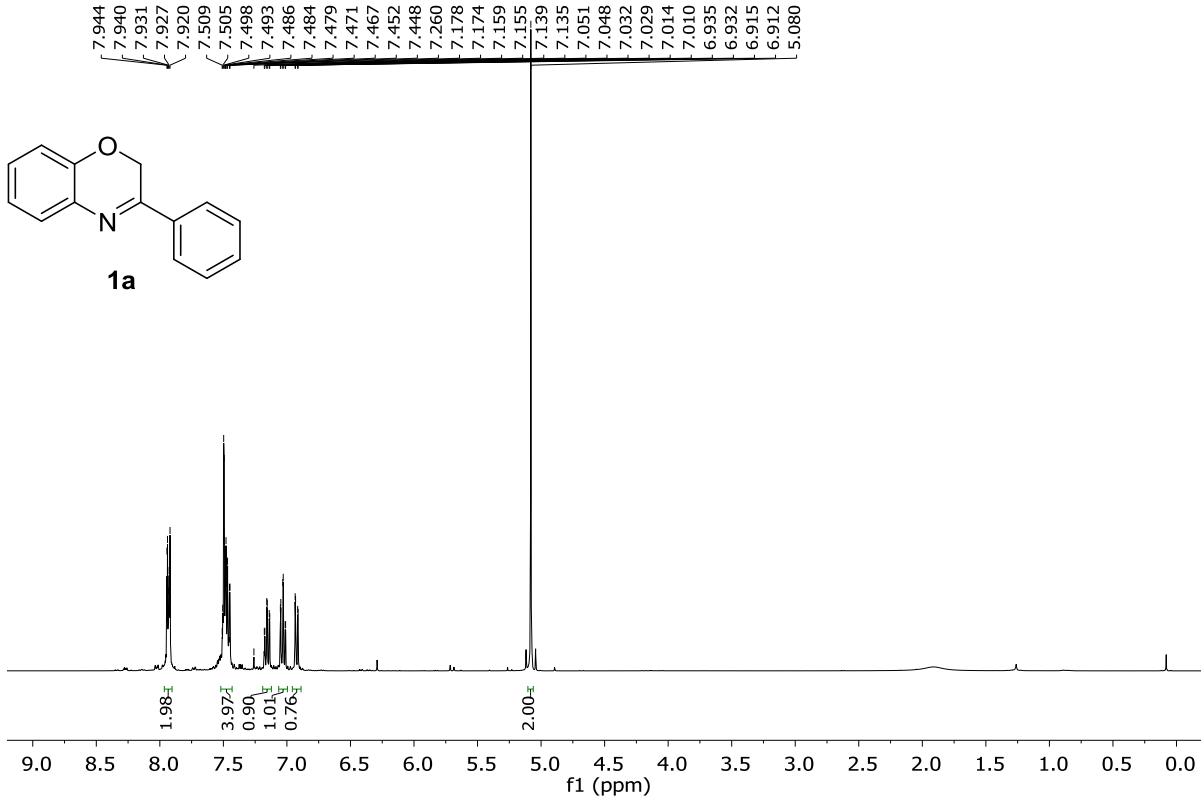

^{13}C NMR of **1a** (100 MHz, $CDCl_3$):

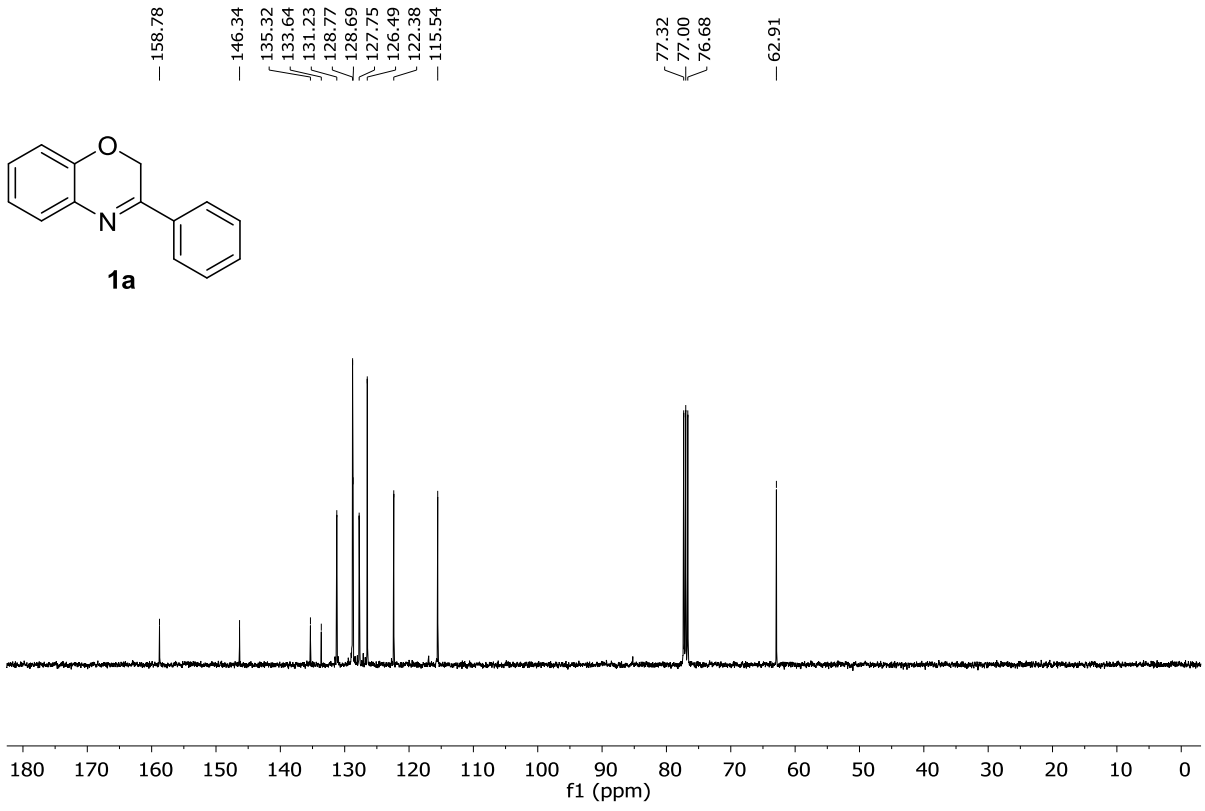

^{1}H NMR of **3a** (400 MHz, $CDCl_3$):

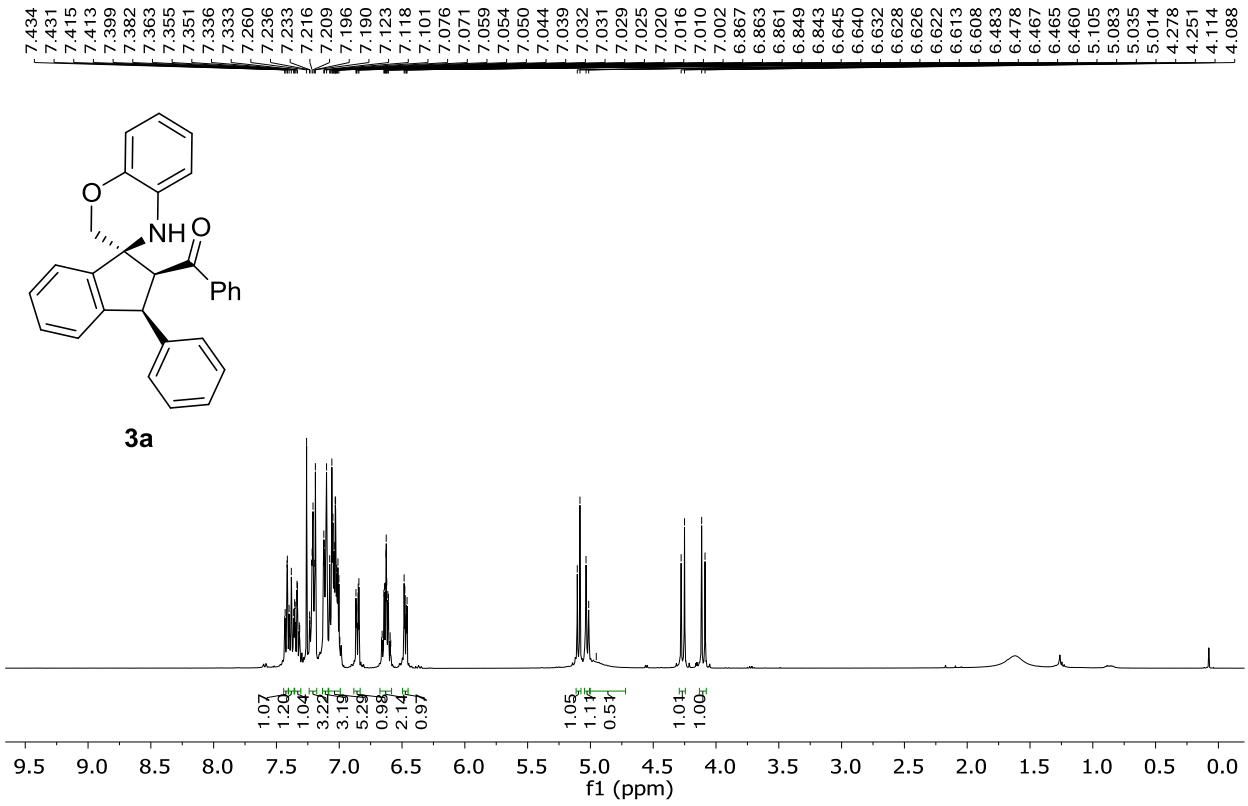

^{13}C NMR of **3a** (100 MHz, $CDCl_3$):

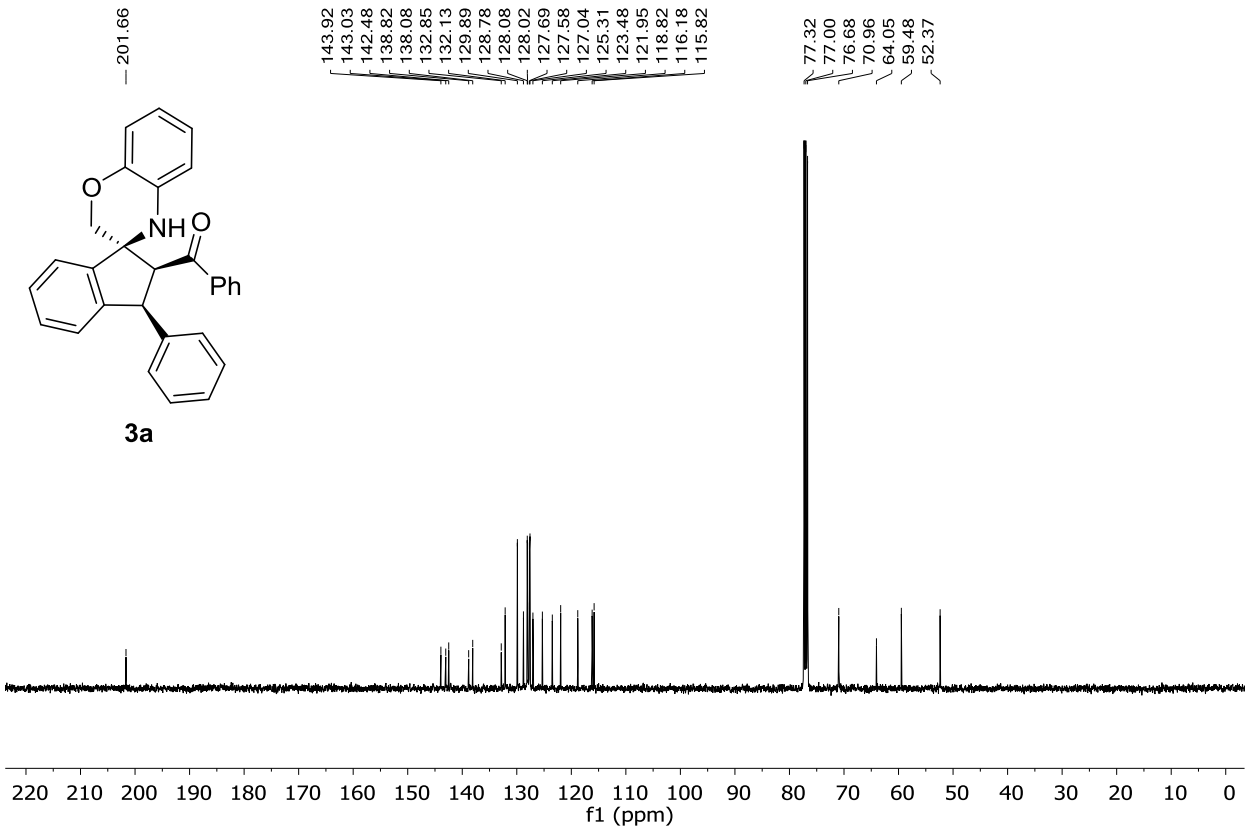

^{1}H NMR of **3c** (400 MHz, $CDCl_3$):

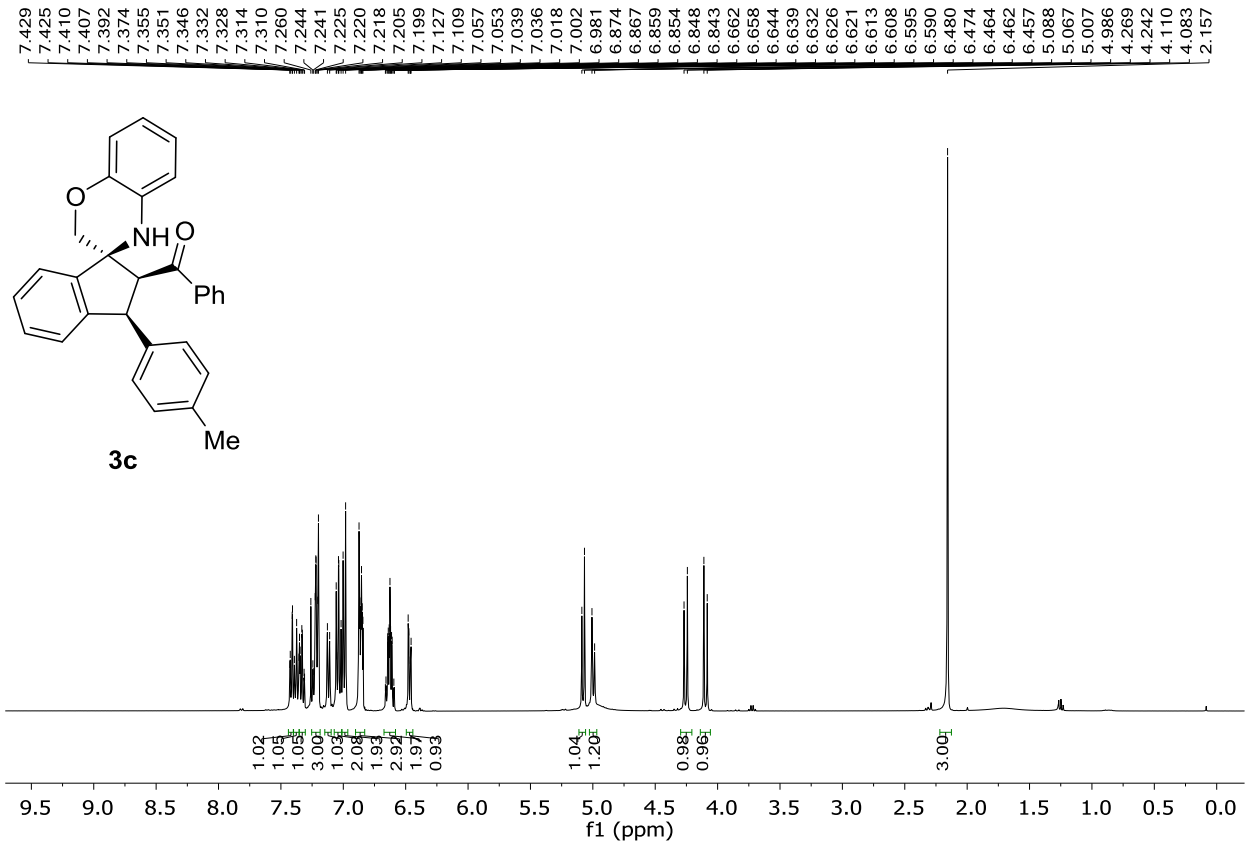

^{13}C NMR of **3c** (100 MHz, $CDCl_3$):

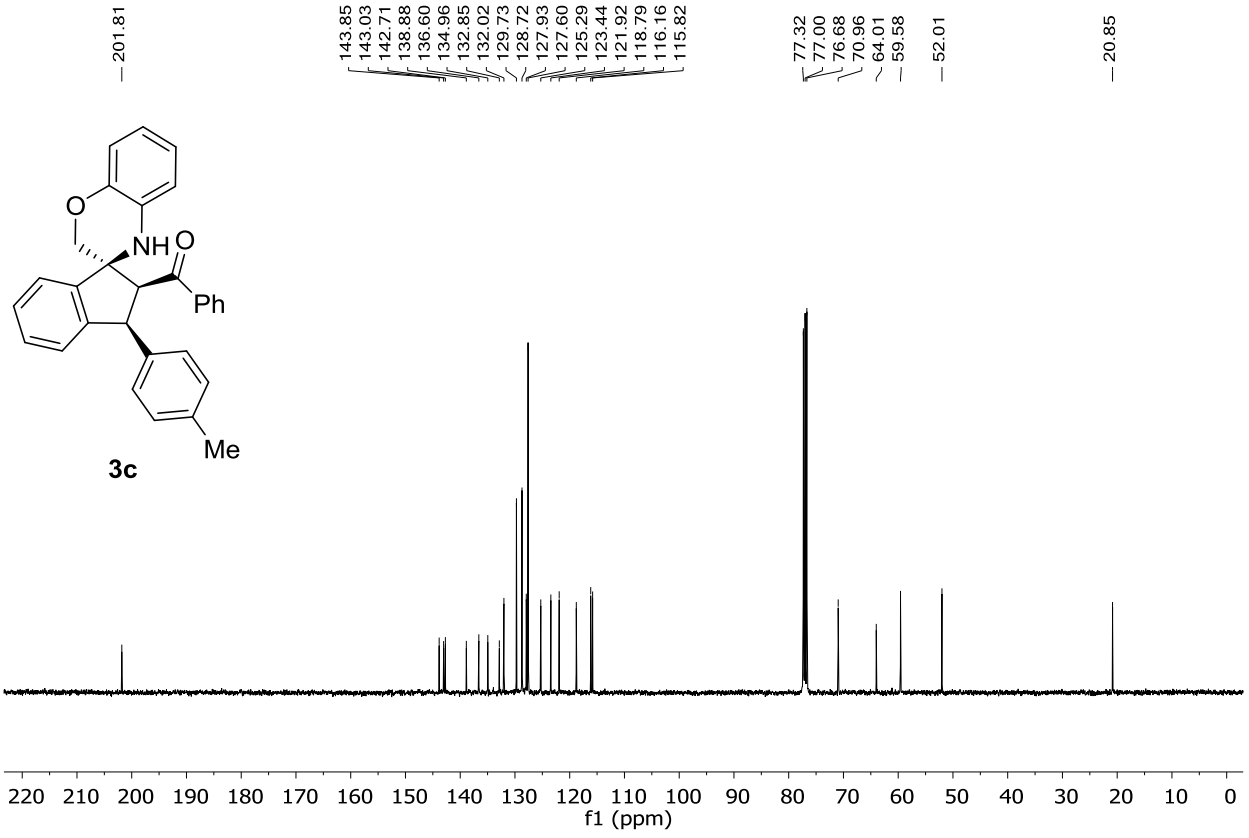

^{1}H NMR of **3c′** (400 MHz, $CDCl_3$):

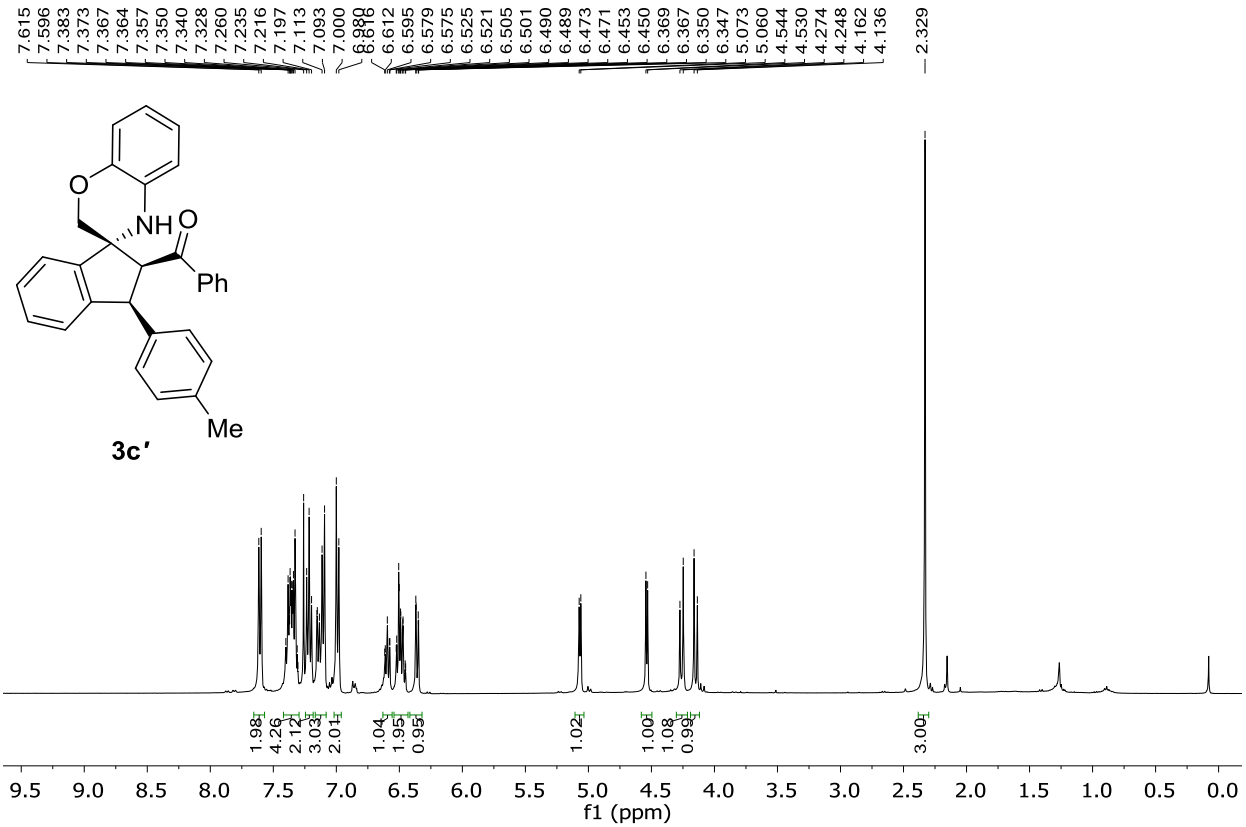

^{13}C NMR of **3c′** (100 MHz, $CDCl_3$):

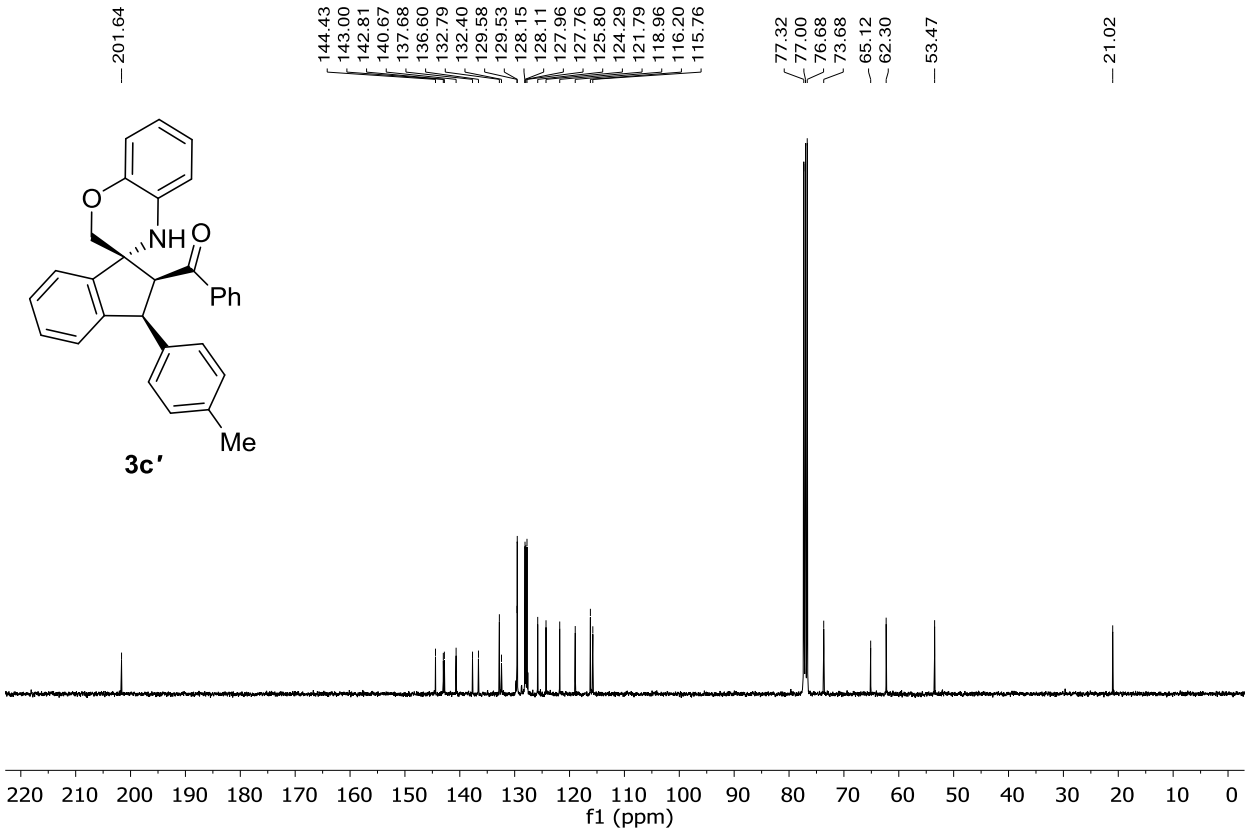

^{1}H NMR of **3c″** (400 MHz, $CDCl_3$):

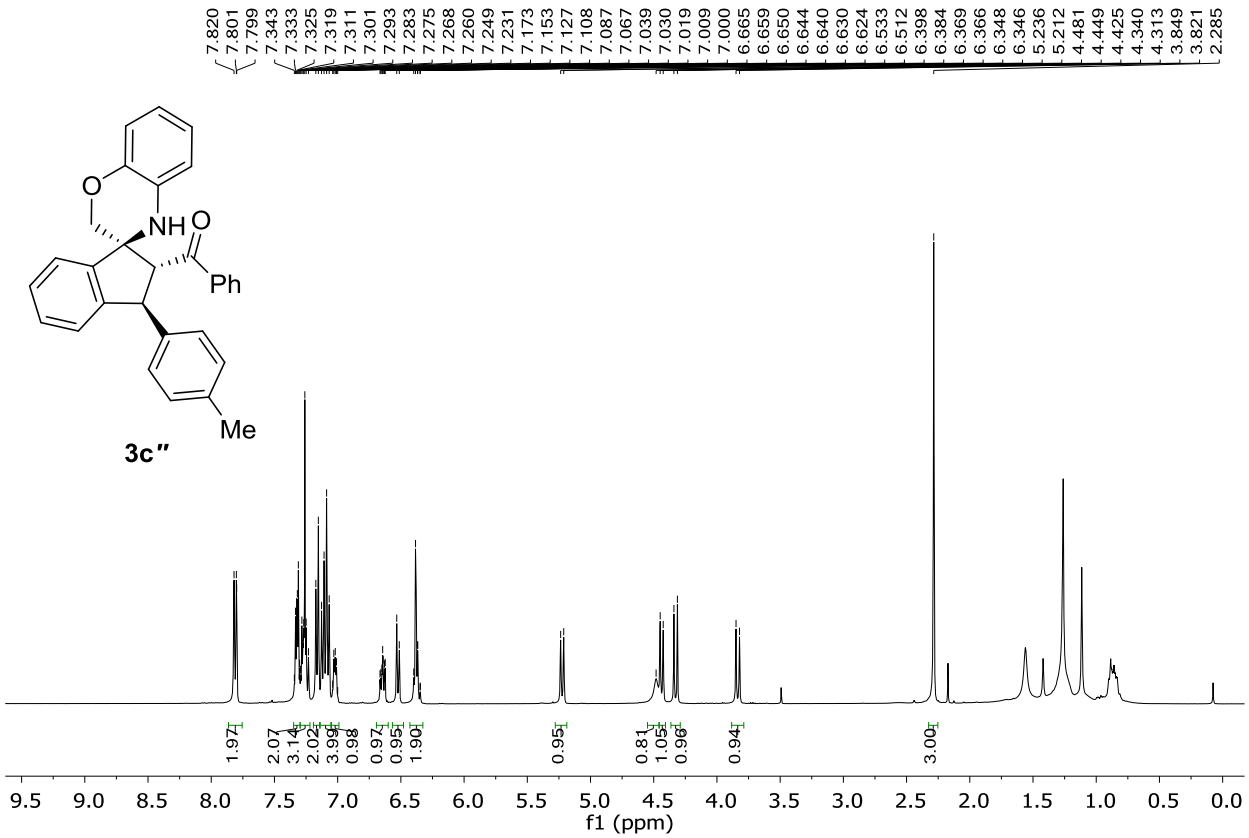

^{13}C NMR of **3c″** (100 MHz, $CDCl_3$):

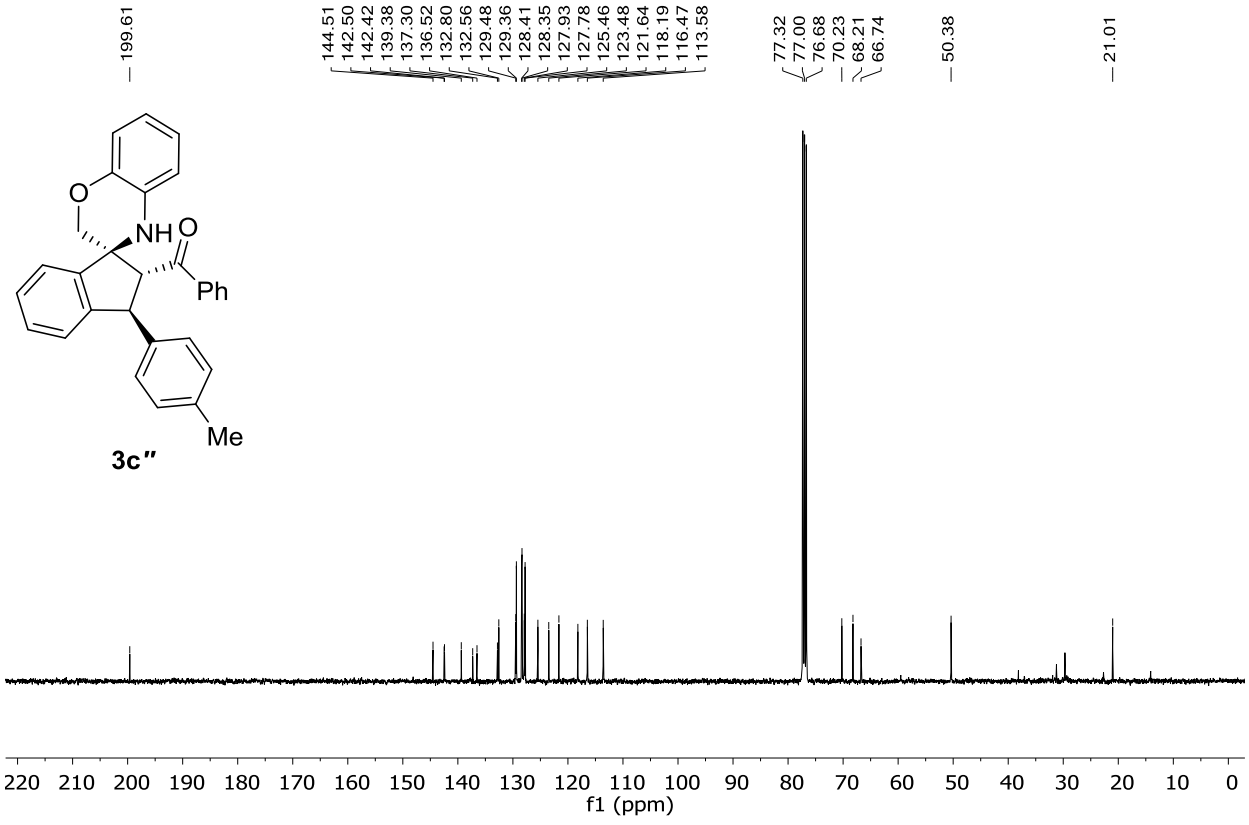

^{1}H NMR of **3d** (400 MHz, $CDCl_3$):

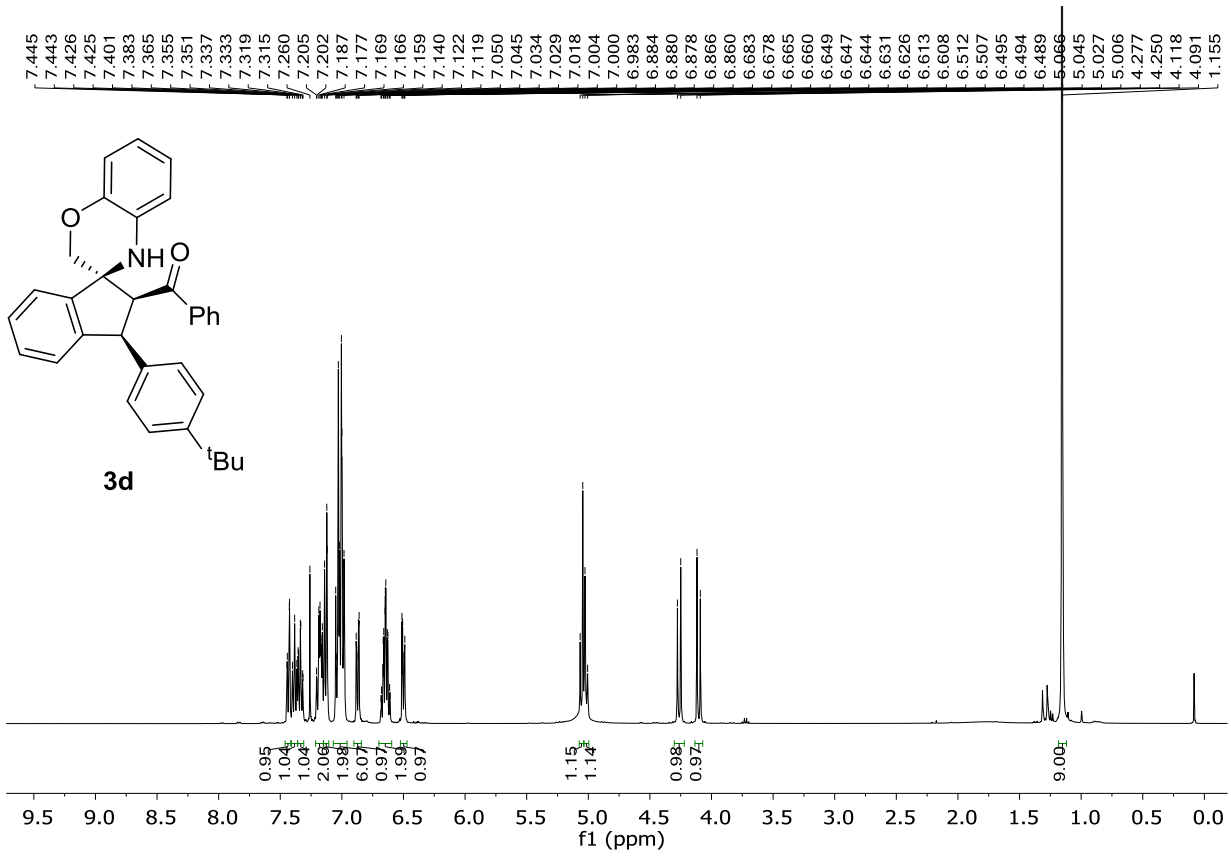

^{13}C NMR of **3d** (100 MHz, $CDCl_3$):

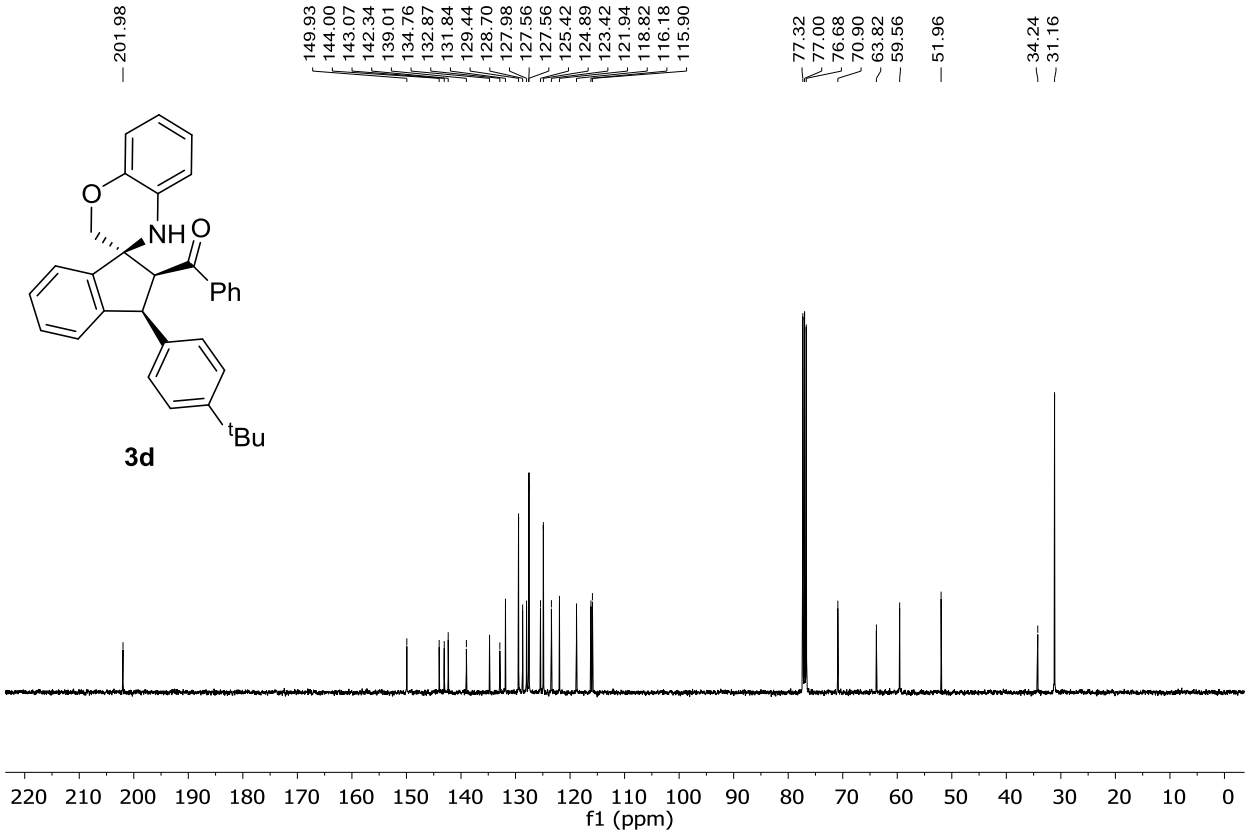

^{1}H NMR of **3f** (400 MHz, $CDCl_3$):

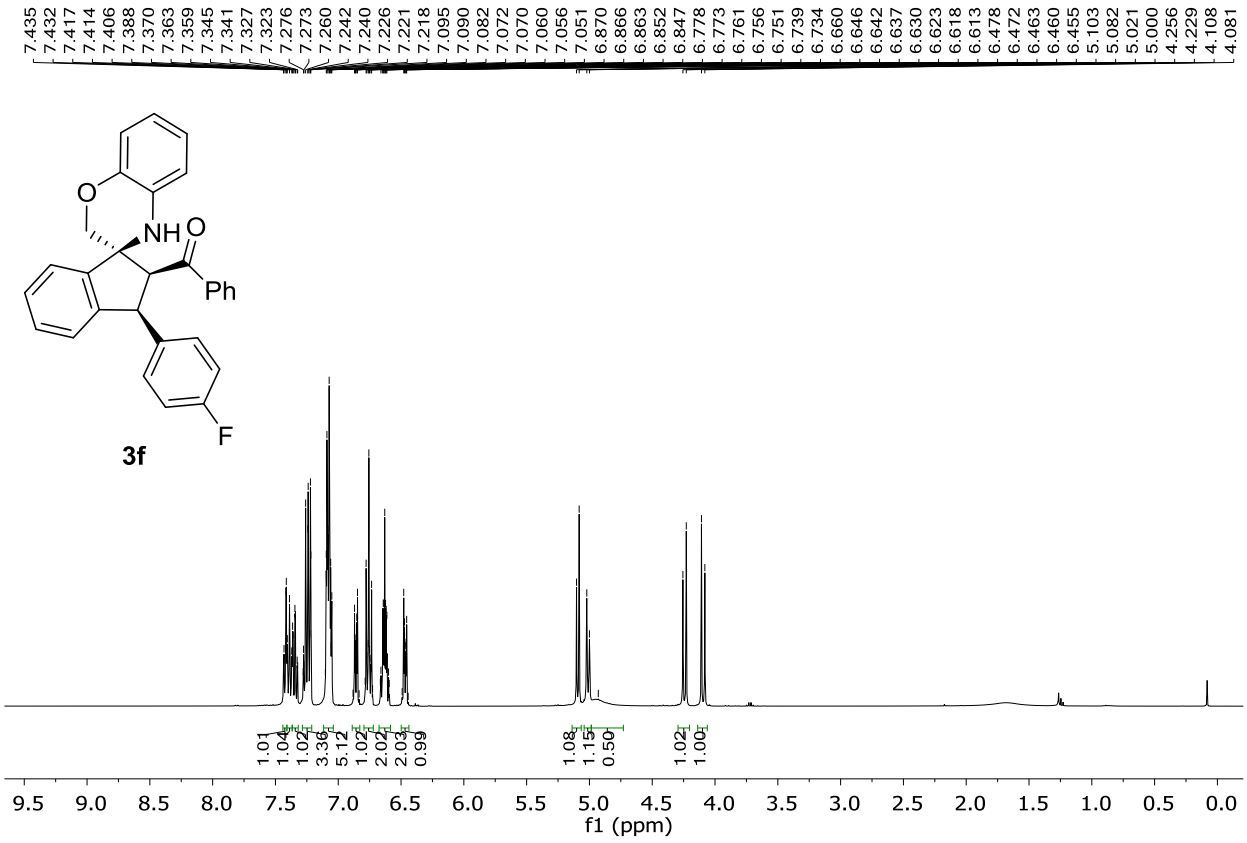

^{13}C NMR of **3f** (100 MHz, $CDCl_3$):

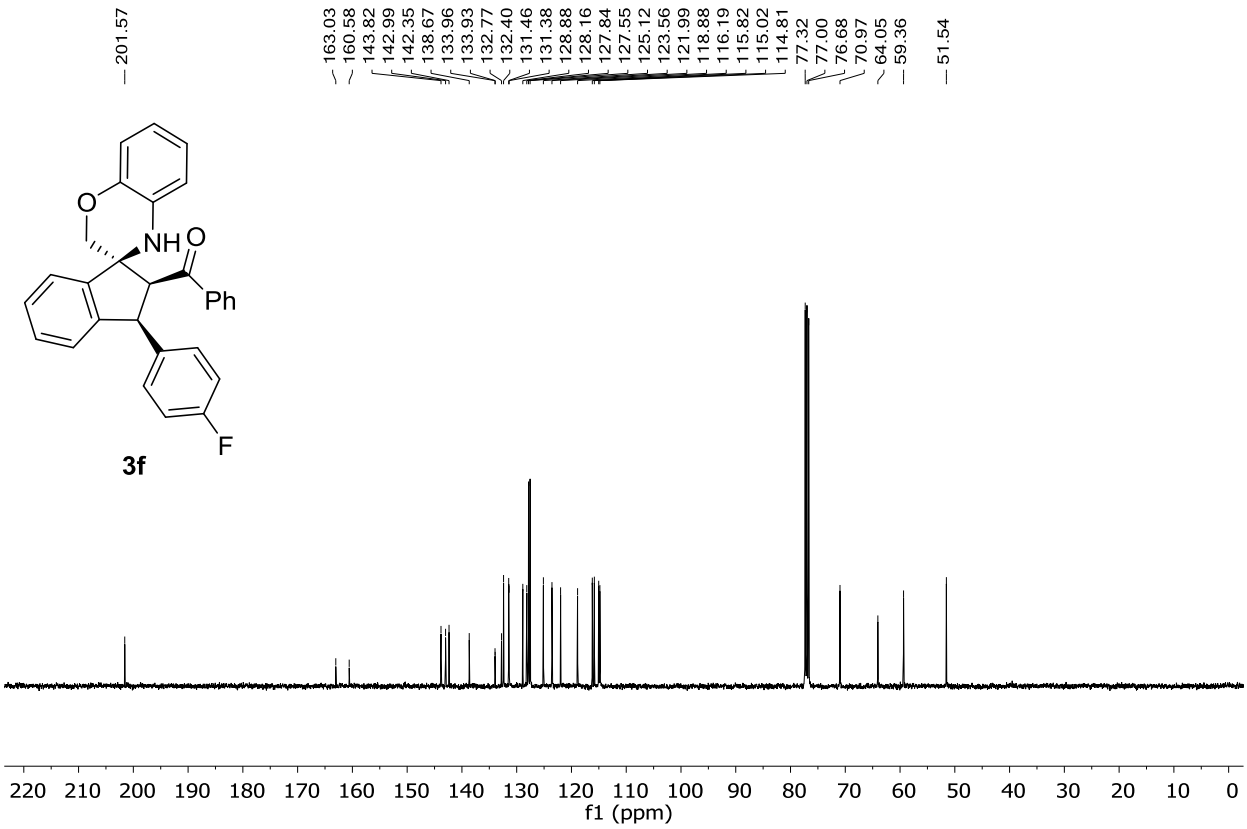

^{1}H NMR of **3i** (400 MHz, $CDCl_3$):

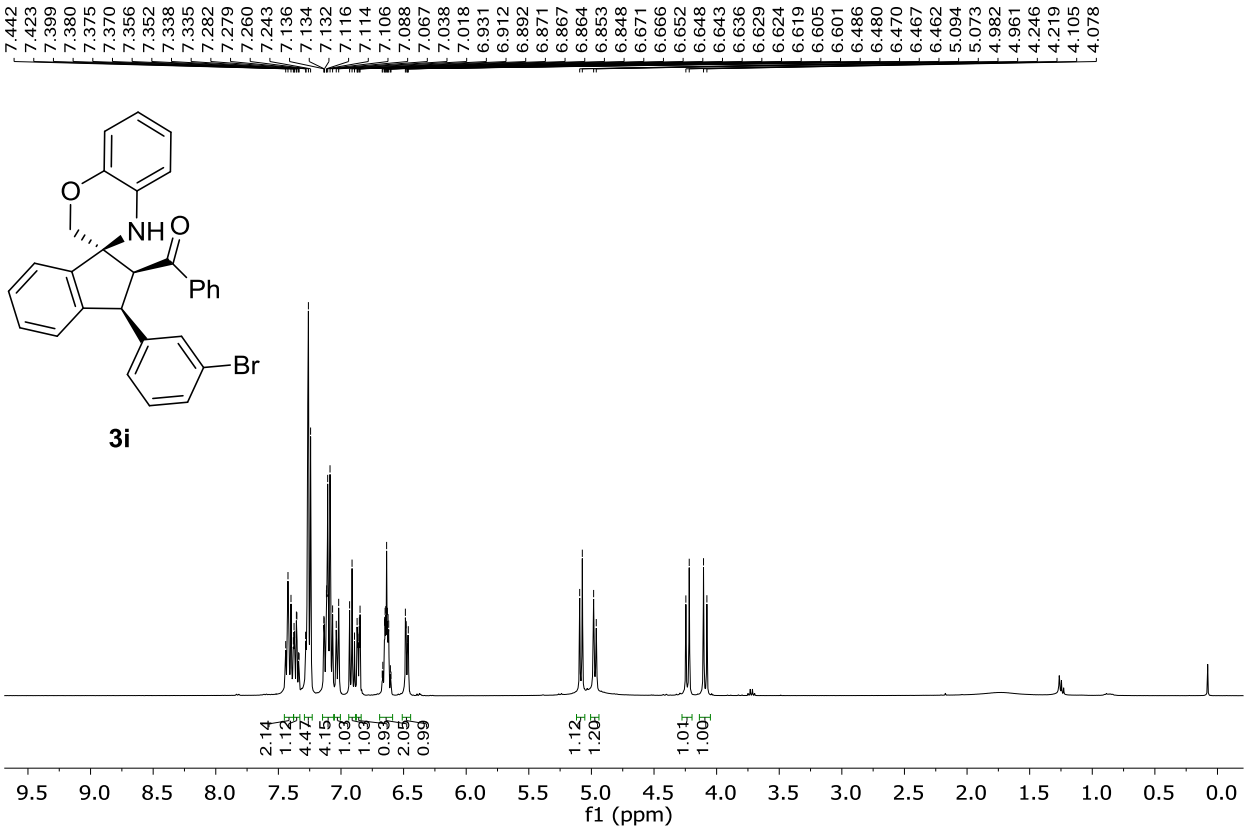

^{13}C NMR of **3i** (100 MHz, $CDCl_3$):

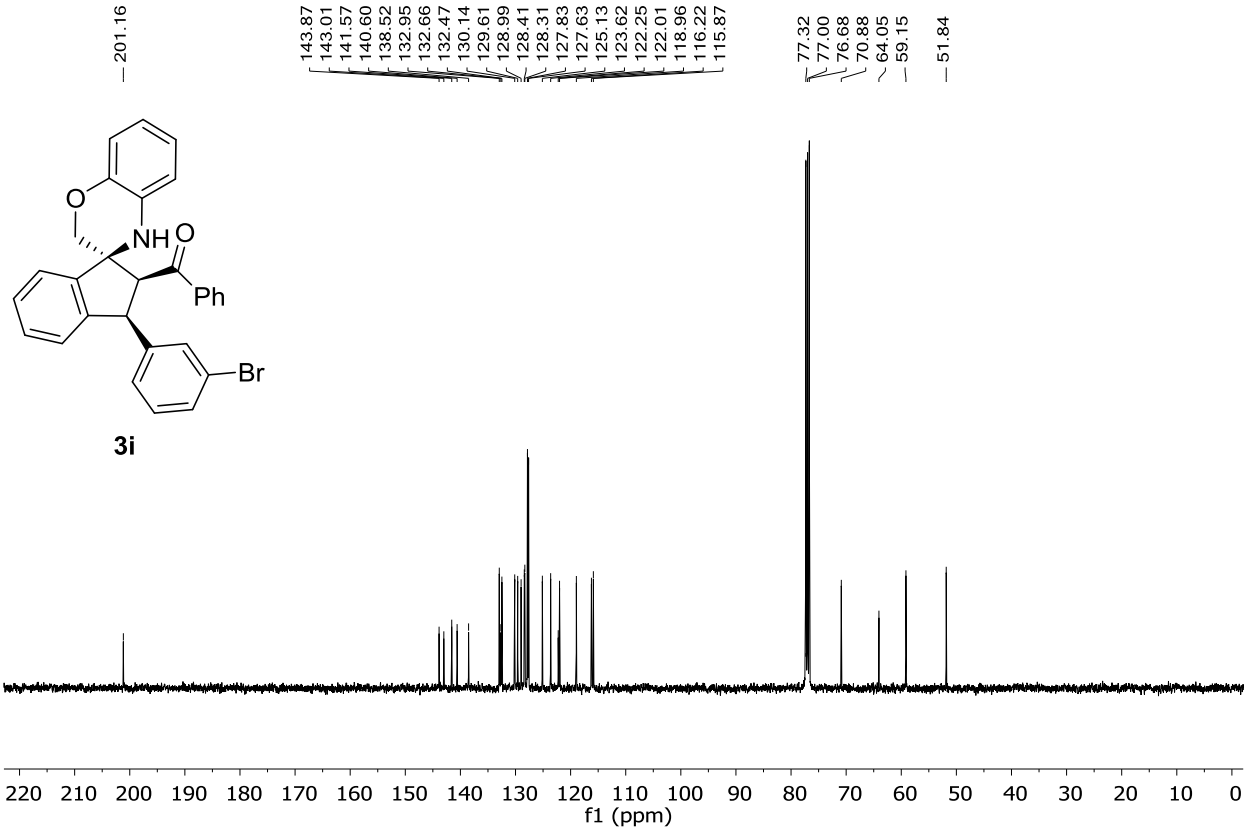

^{1}H NMR of **3l** (400 MHz, $CDCl_3$):

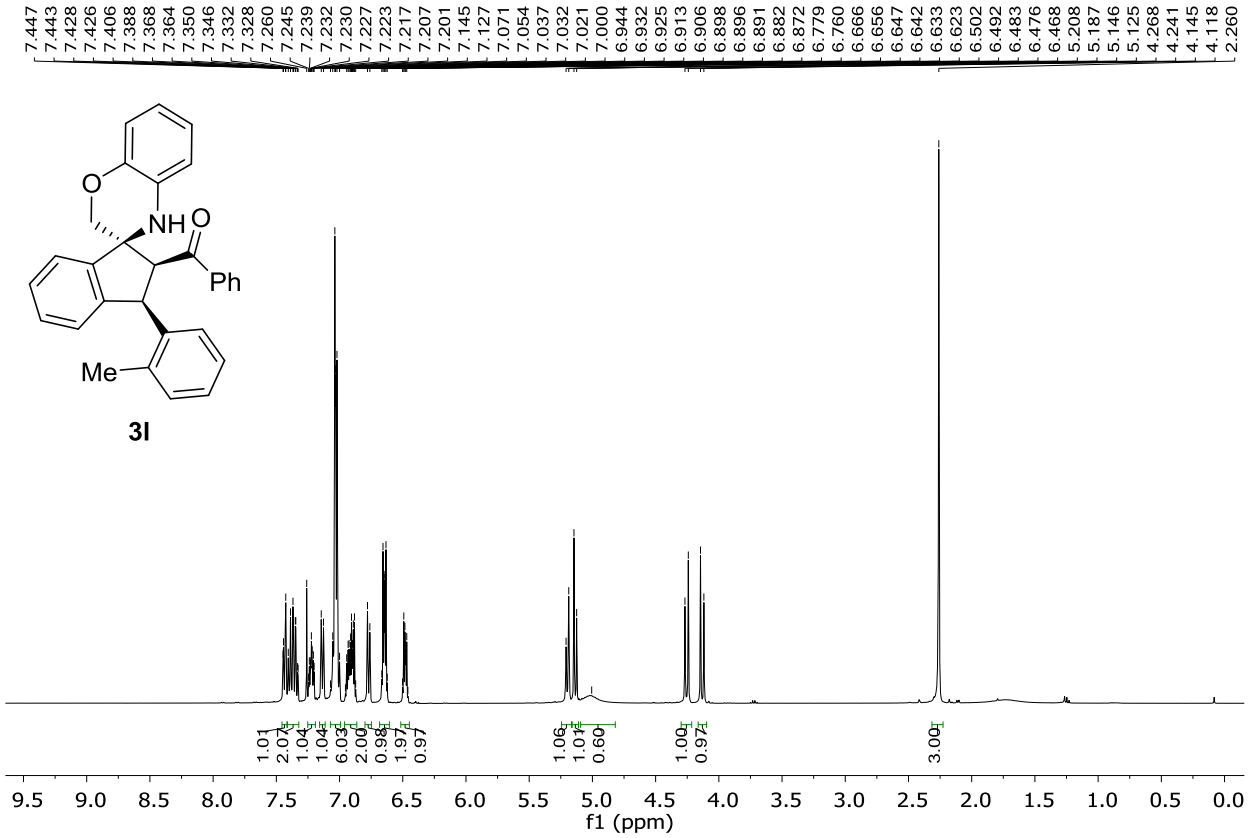

^{13}C NMR of **3l** (100 MHz, $CDCl_3$):

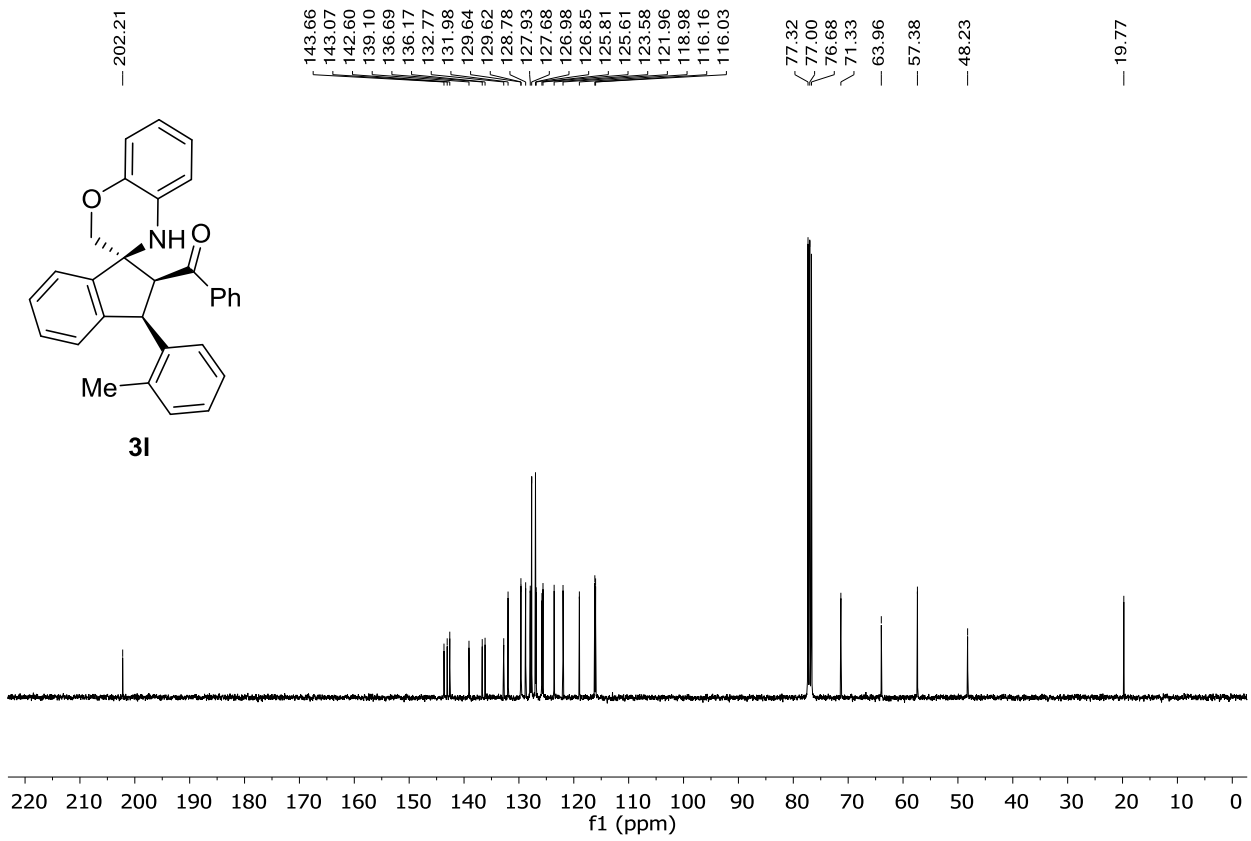

^{1}H NMR of **3n** (400 MHz, $CDCl_3$):

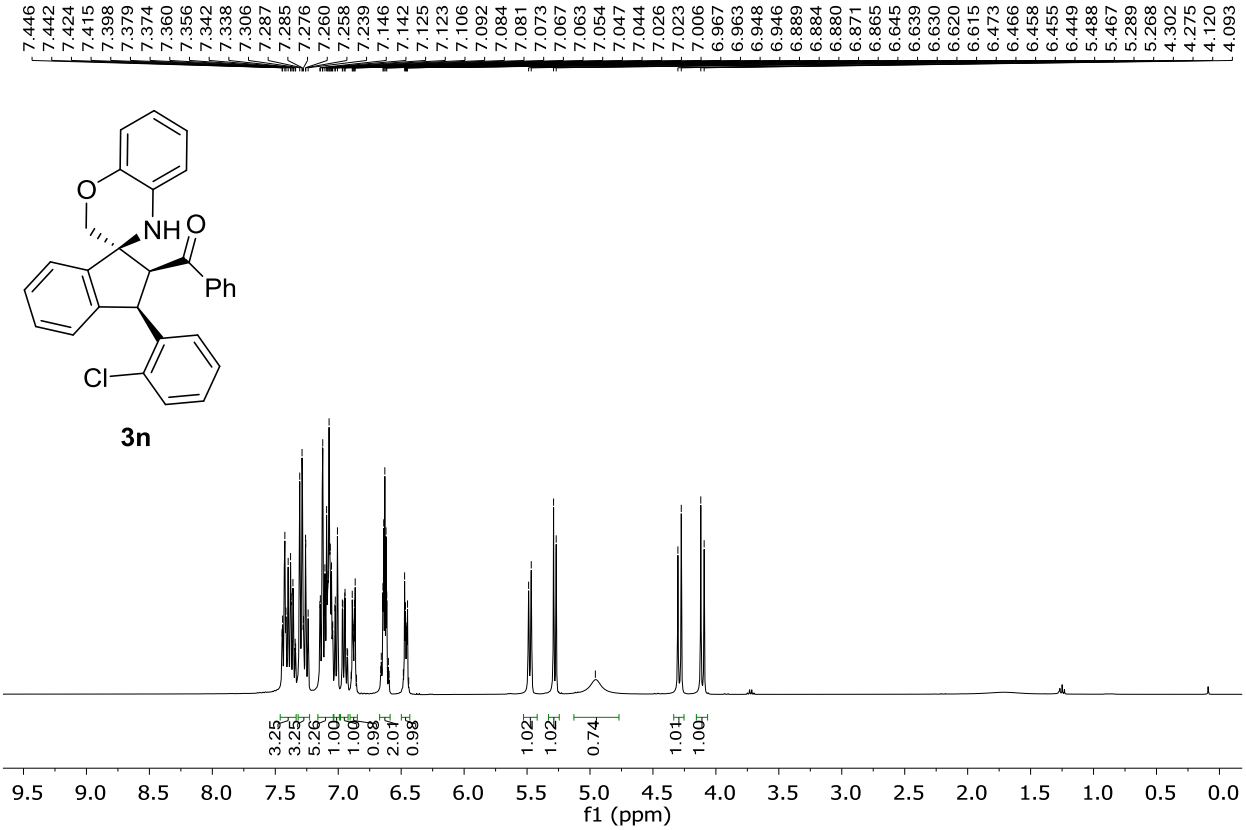

^{13}C NMR of **3n** (100 MHz, $CDCl_3$):

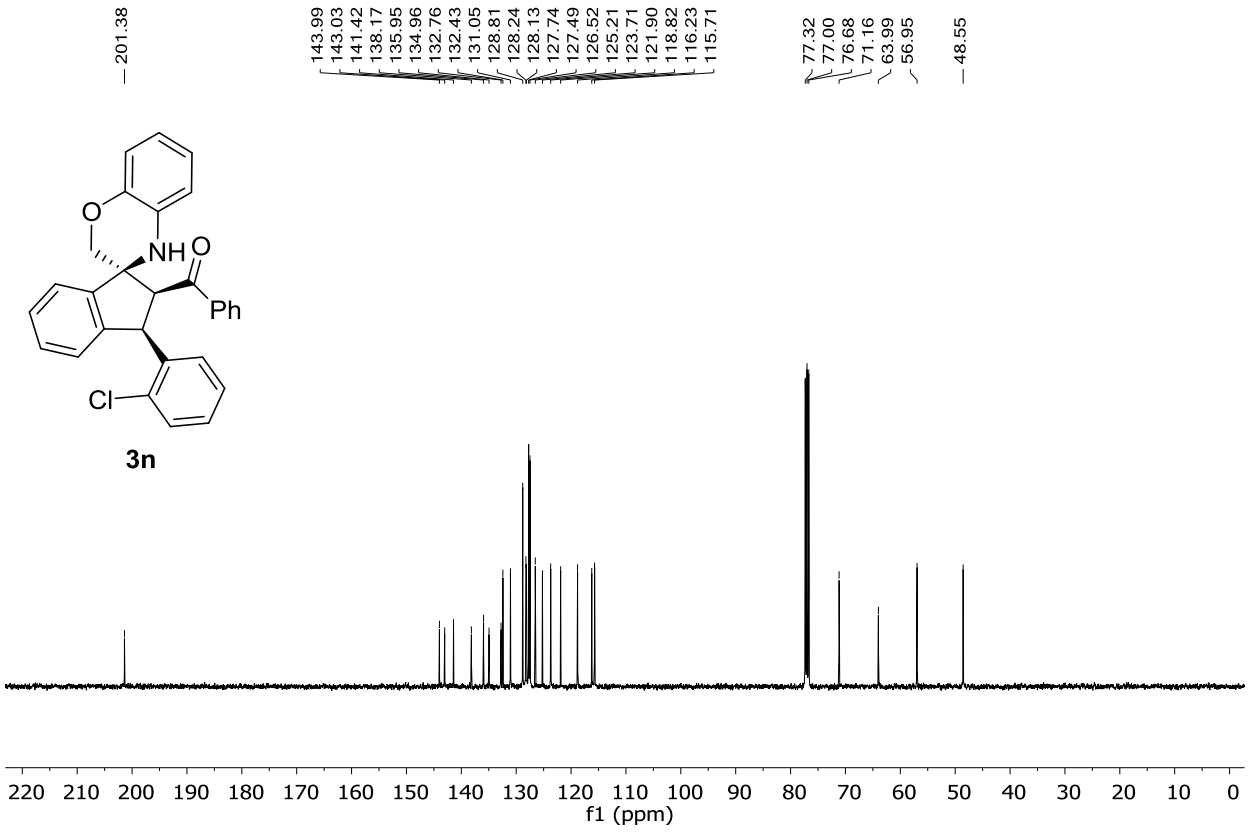

^{1}H NMR of **3o** (400 MHz, $CDCl_3$):

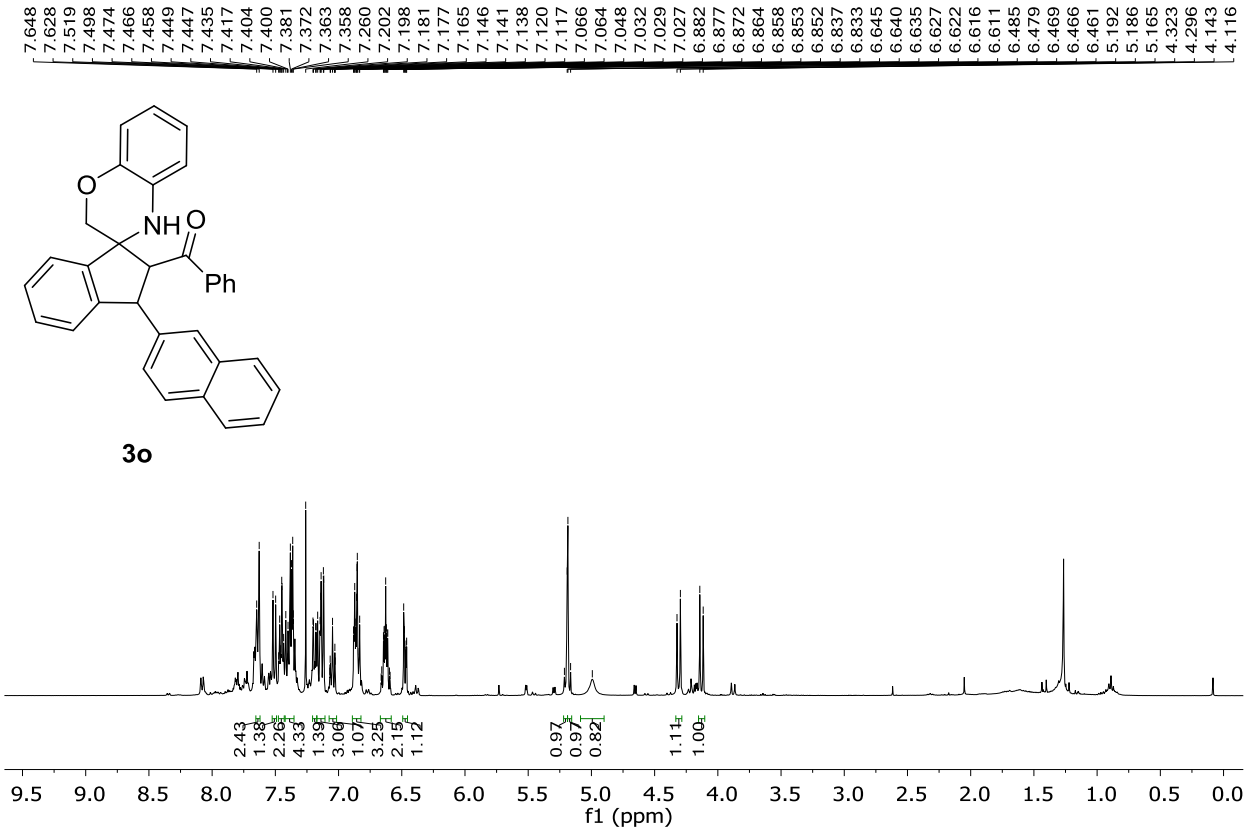

^{13}C NMR of **3o** (100 MHz, $CDCl_3$):

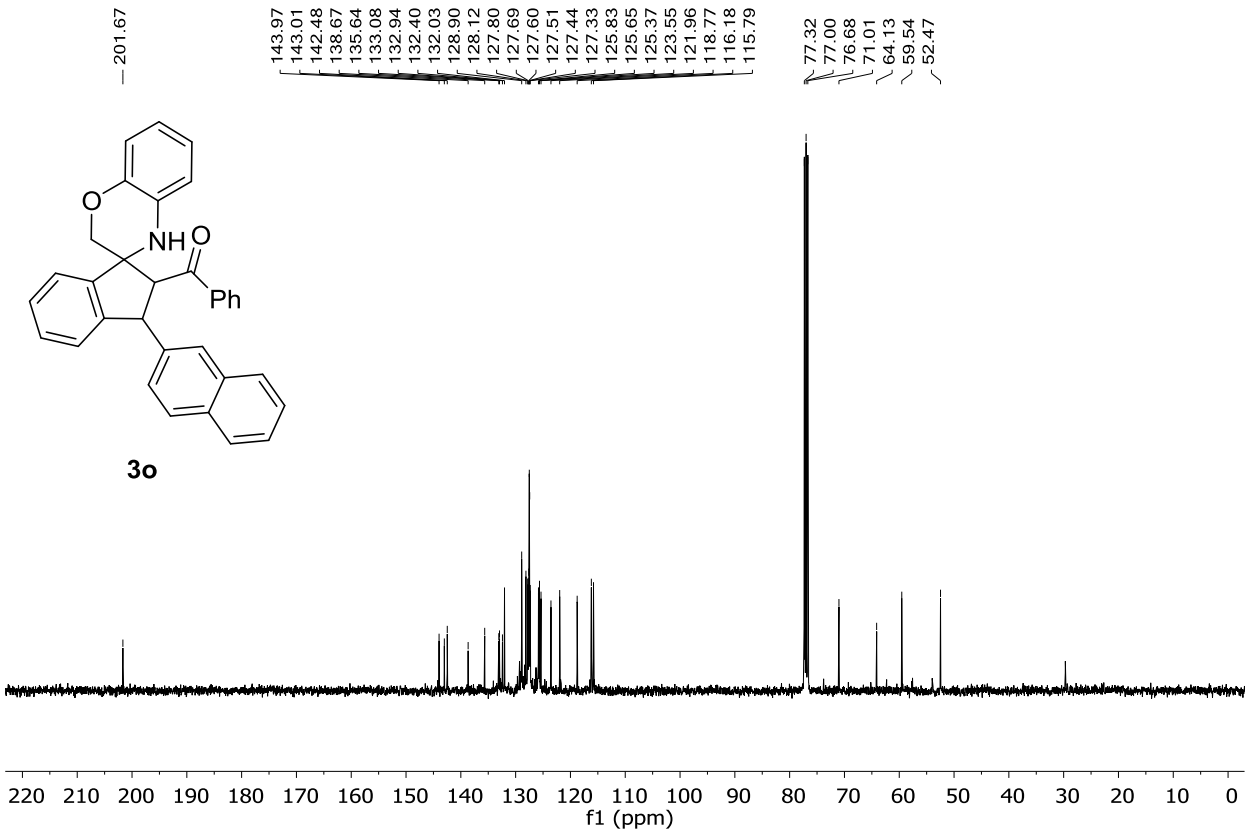

^{1}H NMR of **3q** (400 MHz, $CDCl_3$):

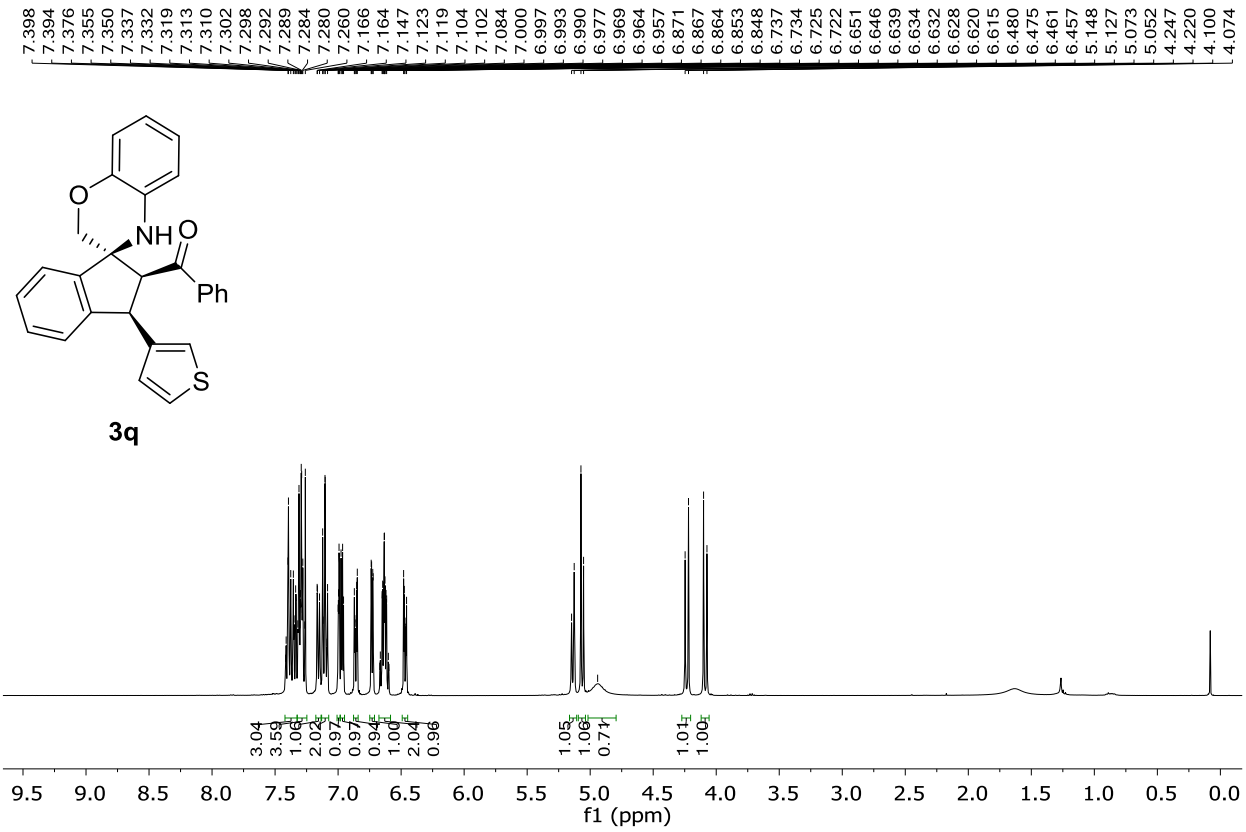

^{13}C NMR of **3q** (100 MHz, $CDCl_3$):

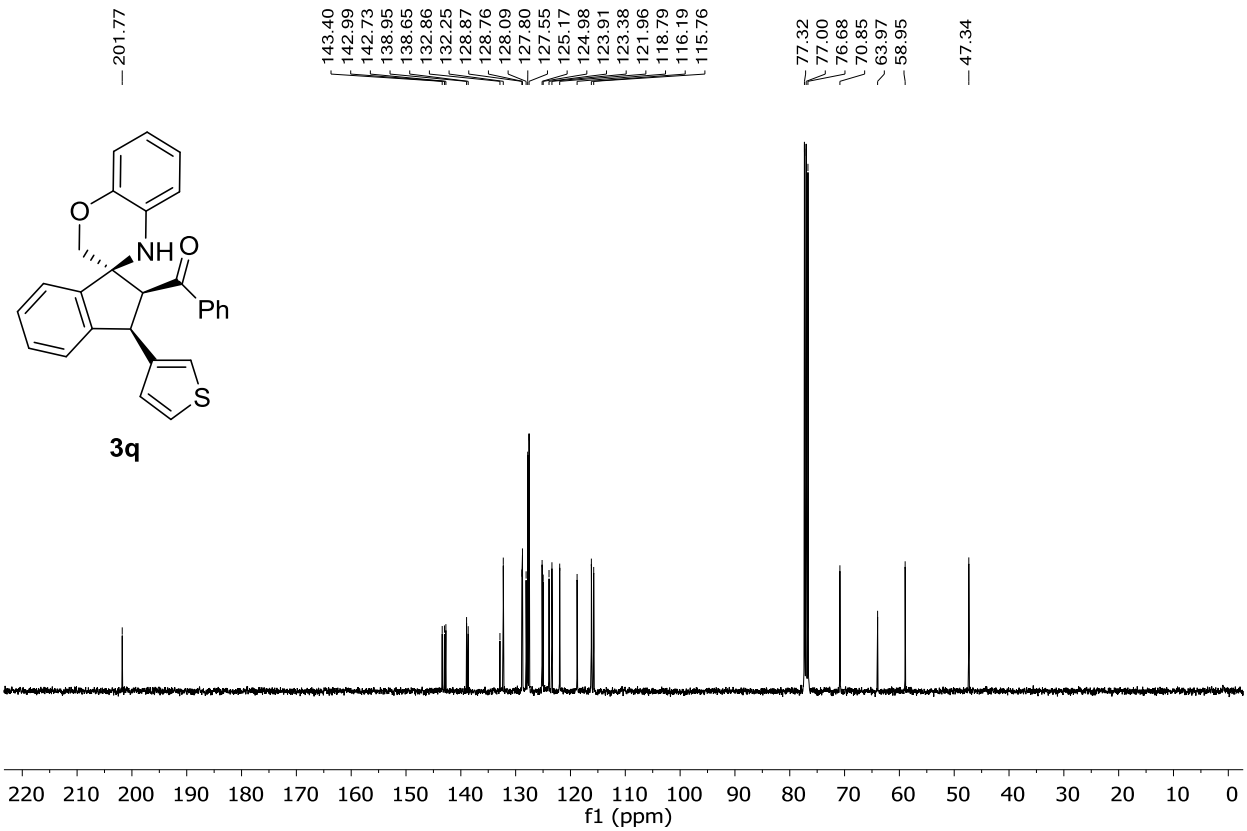

^{1}H NMR of **3r** (400 MHz, $CDCl_3$):

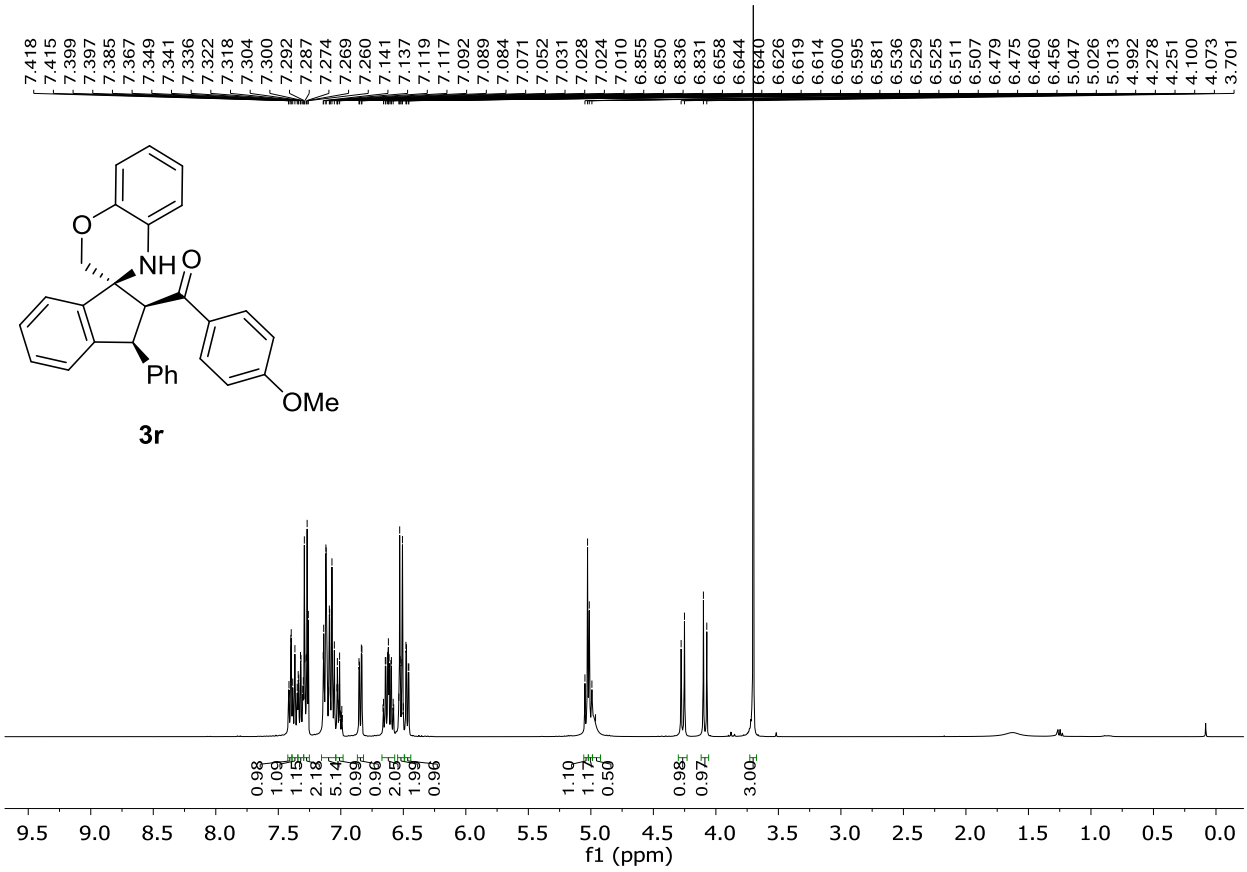

^{13}C NMR of **3r** (100 MHz, $CDCl_3$):

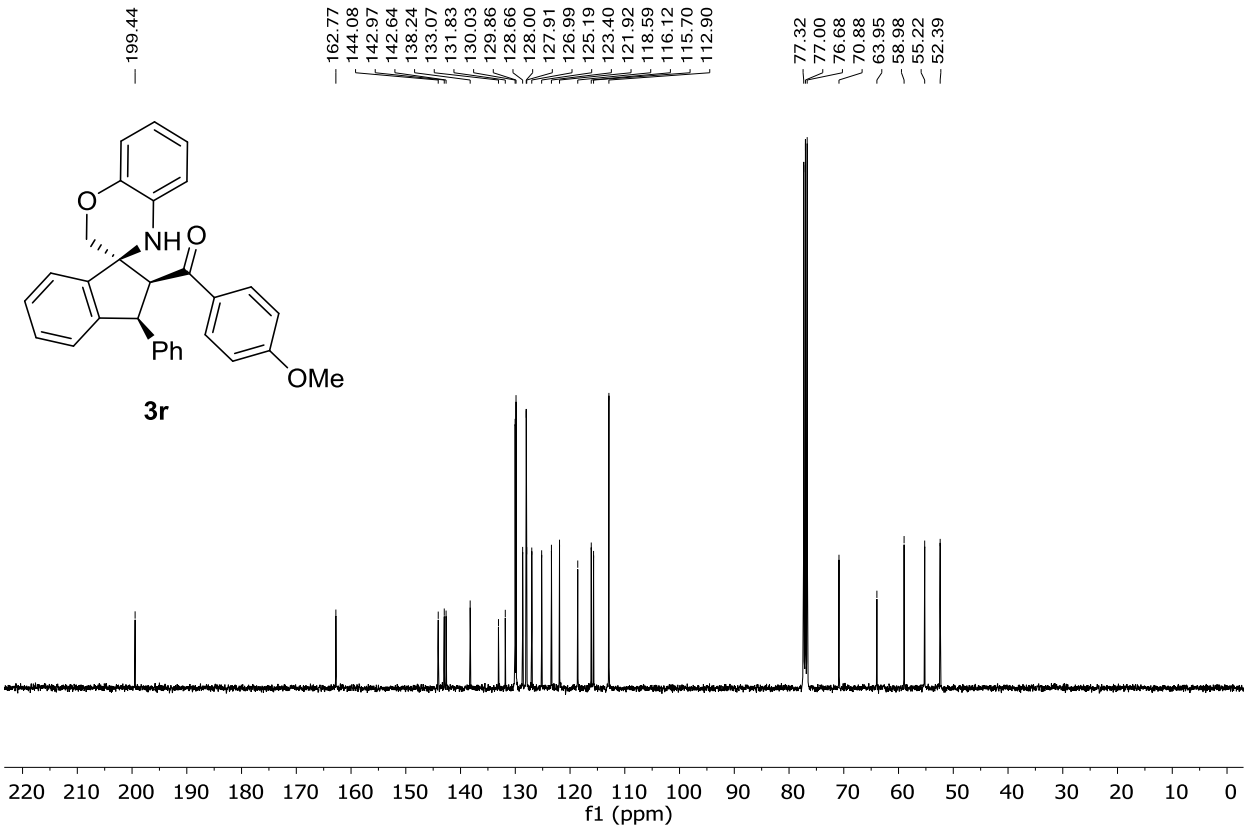

^{1}H NMR of **3u** (400 MHz, $CDCl_3$):

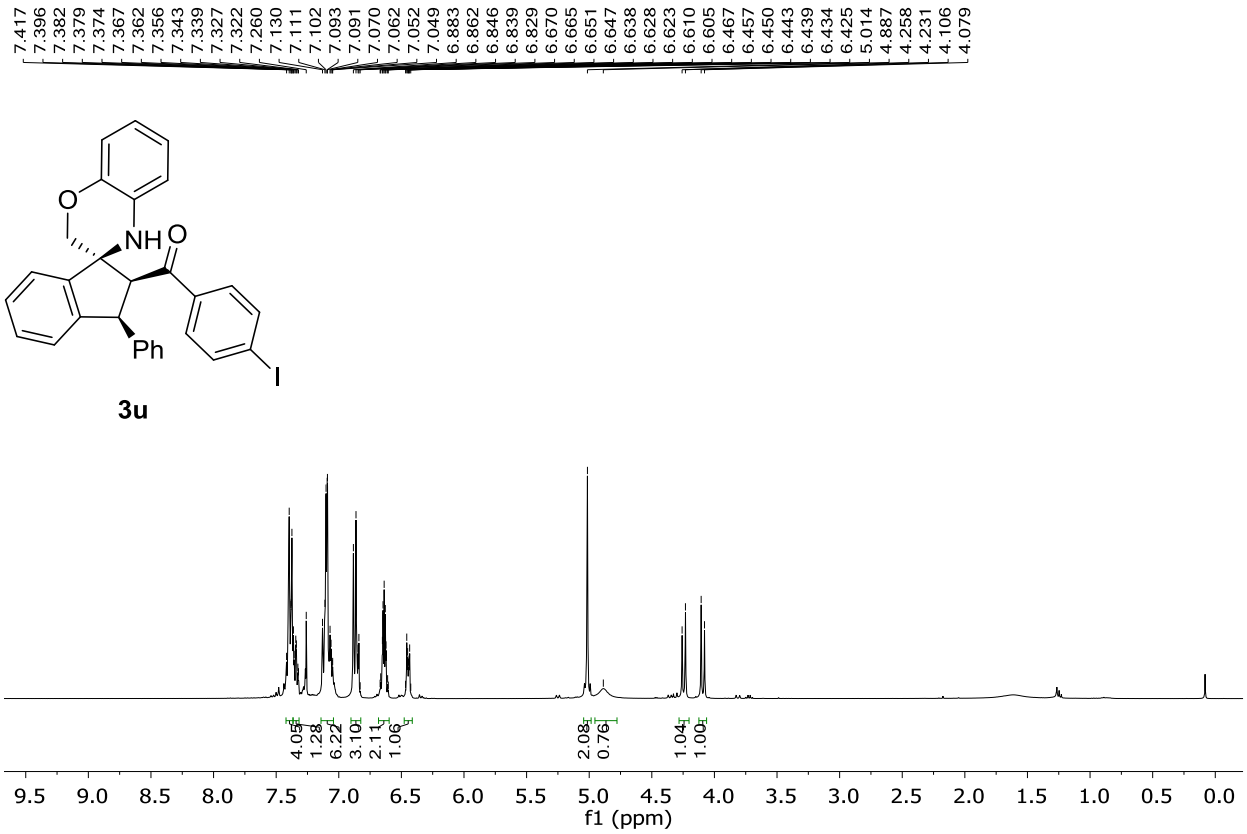

3u

^{13}C NMR of **3u** (100 MHz, $CDCl_3$):

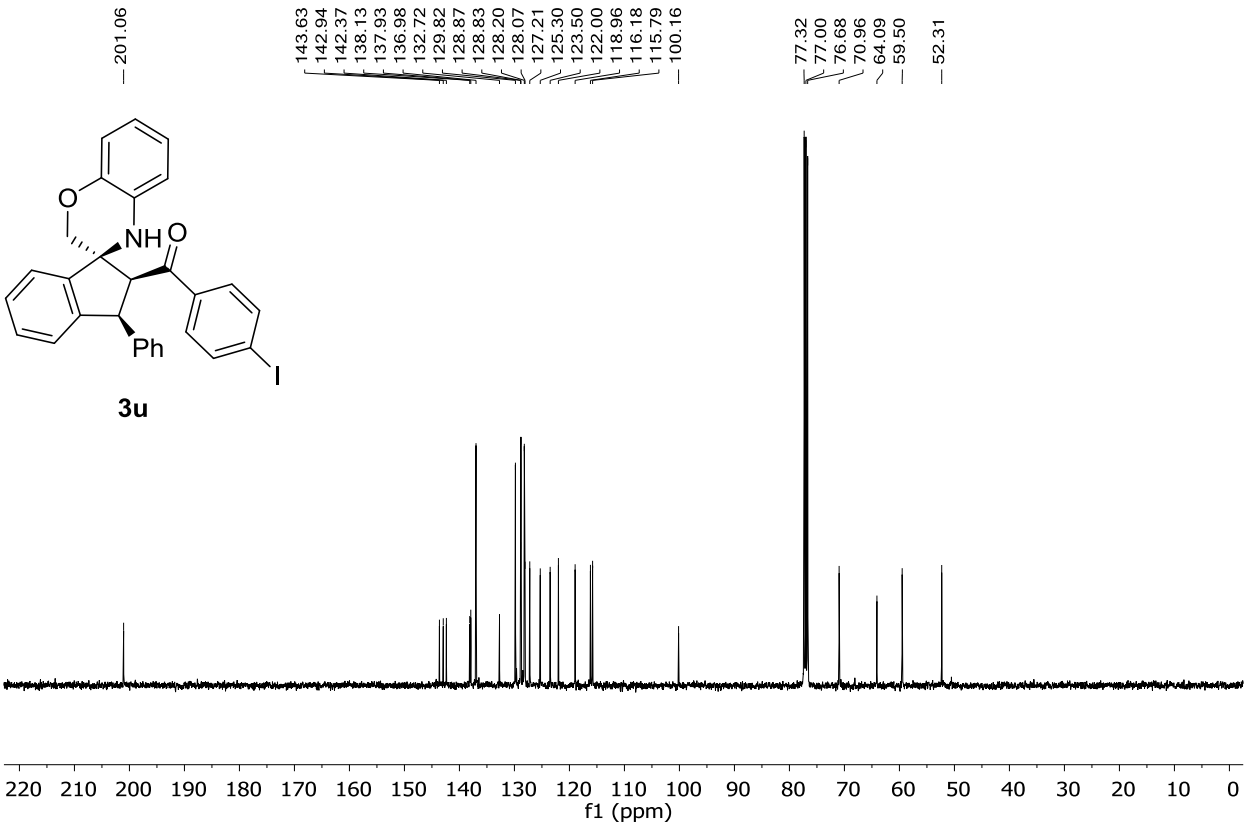

3u

^{1}H NMR of **3x** (400 MHz, $CDCl_3$):

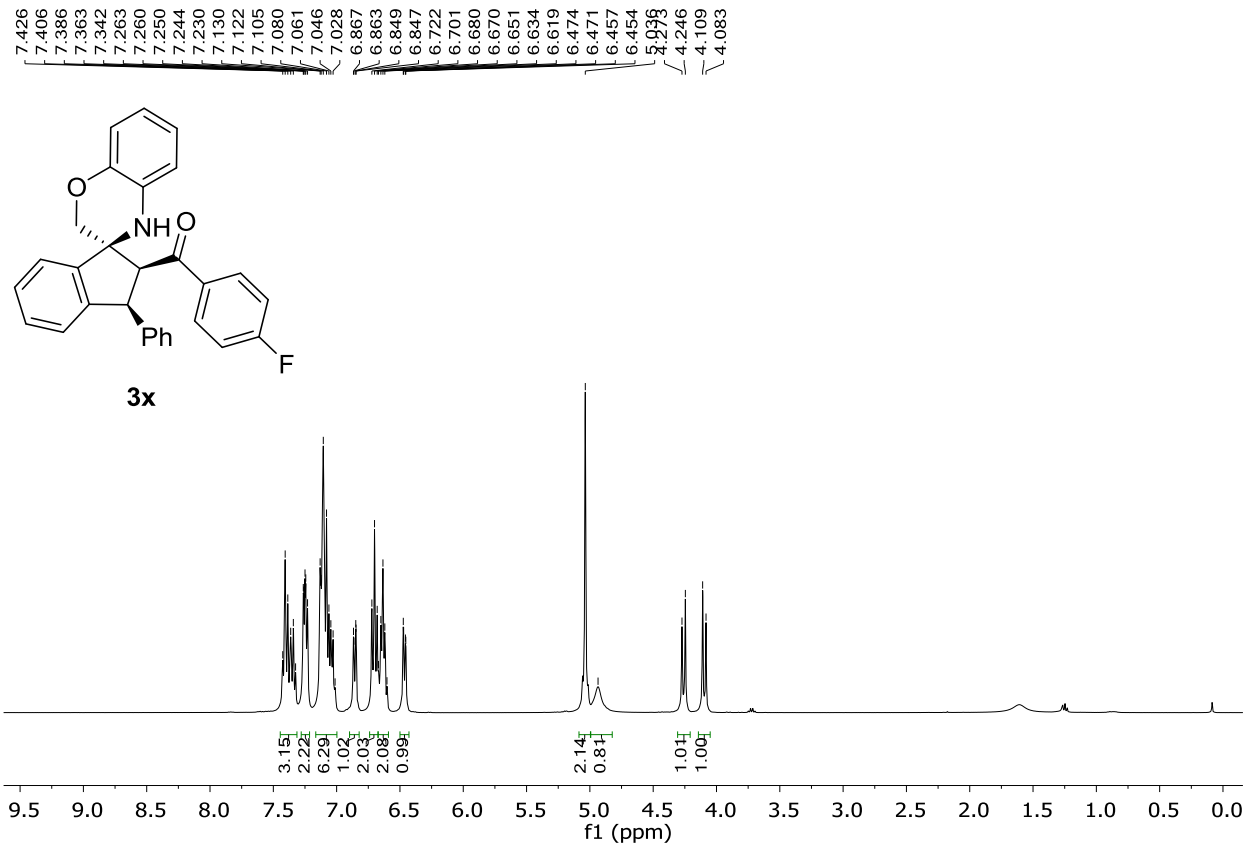

^{13}C NMR of **3x** (100 MHz, $CDCl_3$):

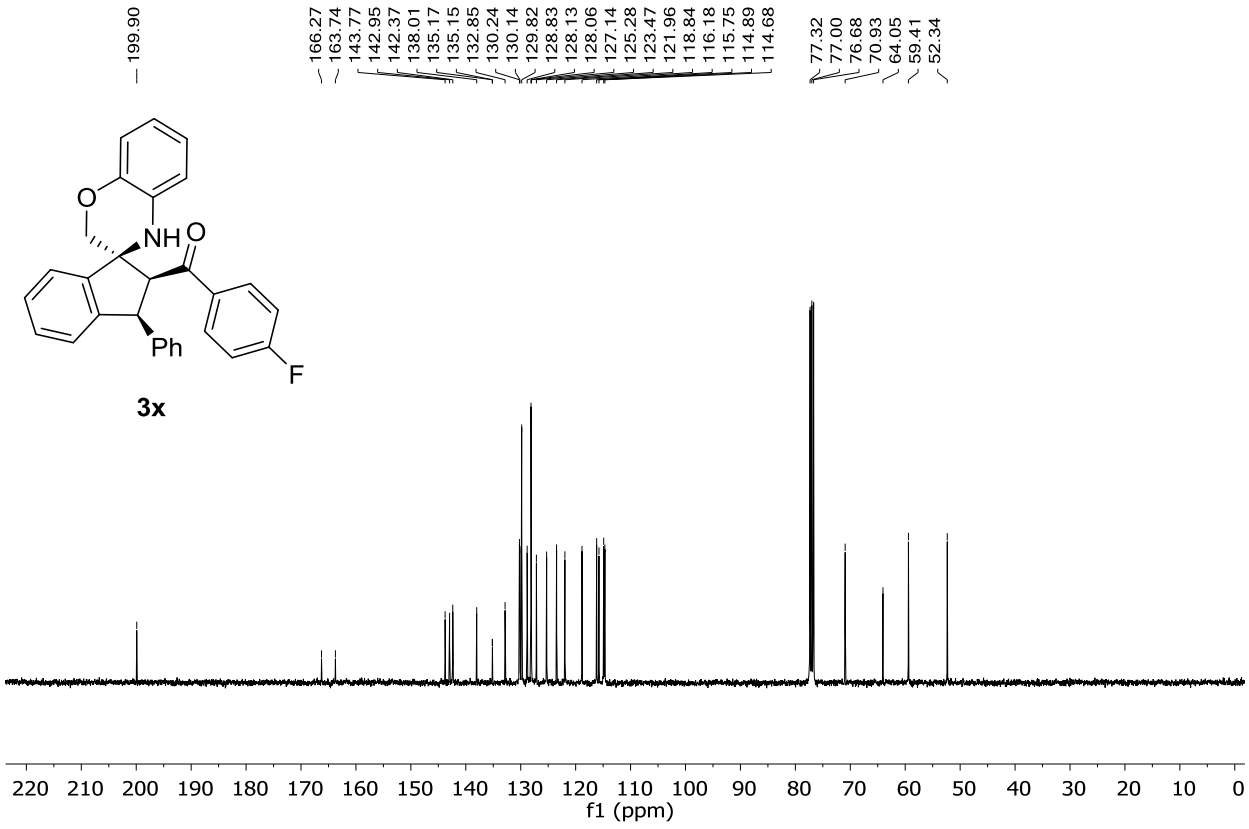

^{1}H NMR of **3y** (400 MHz, $CDCl_3$):

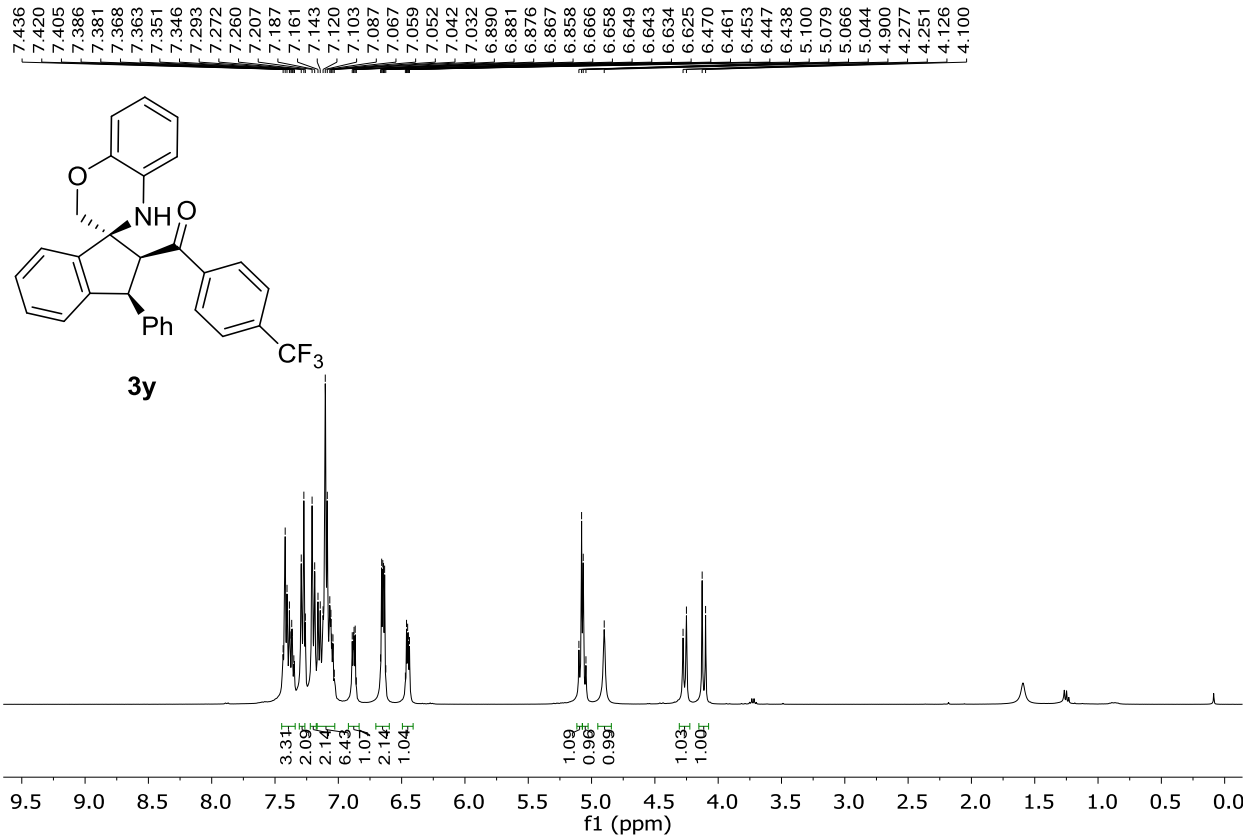

^{13}C NMR of **3y** (100 MHz, $CDCl_3$):

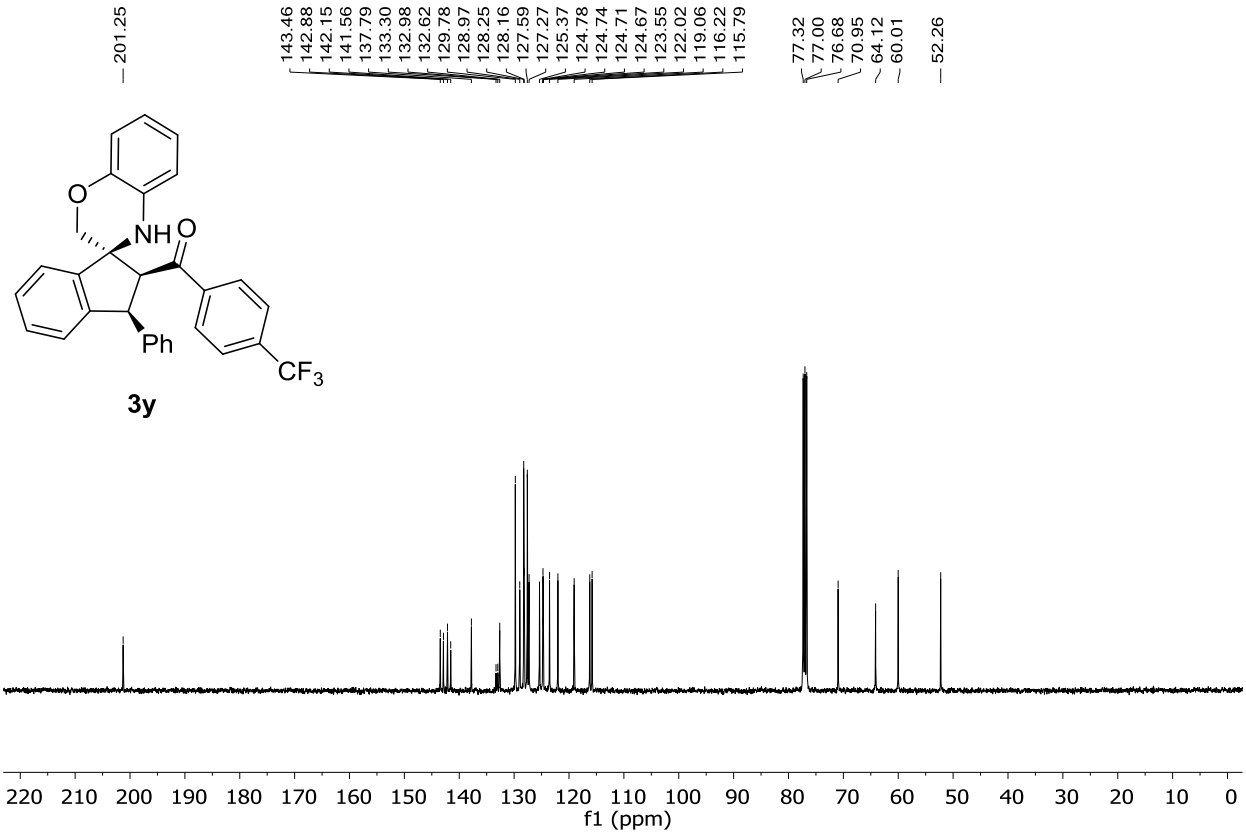

^{1}H NMR of **3ab** (400 MHz, $CDCl_3$):

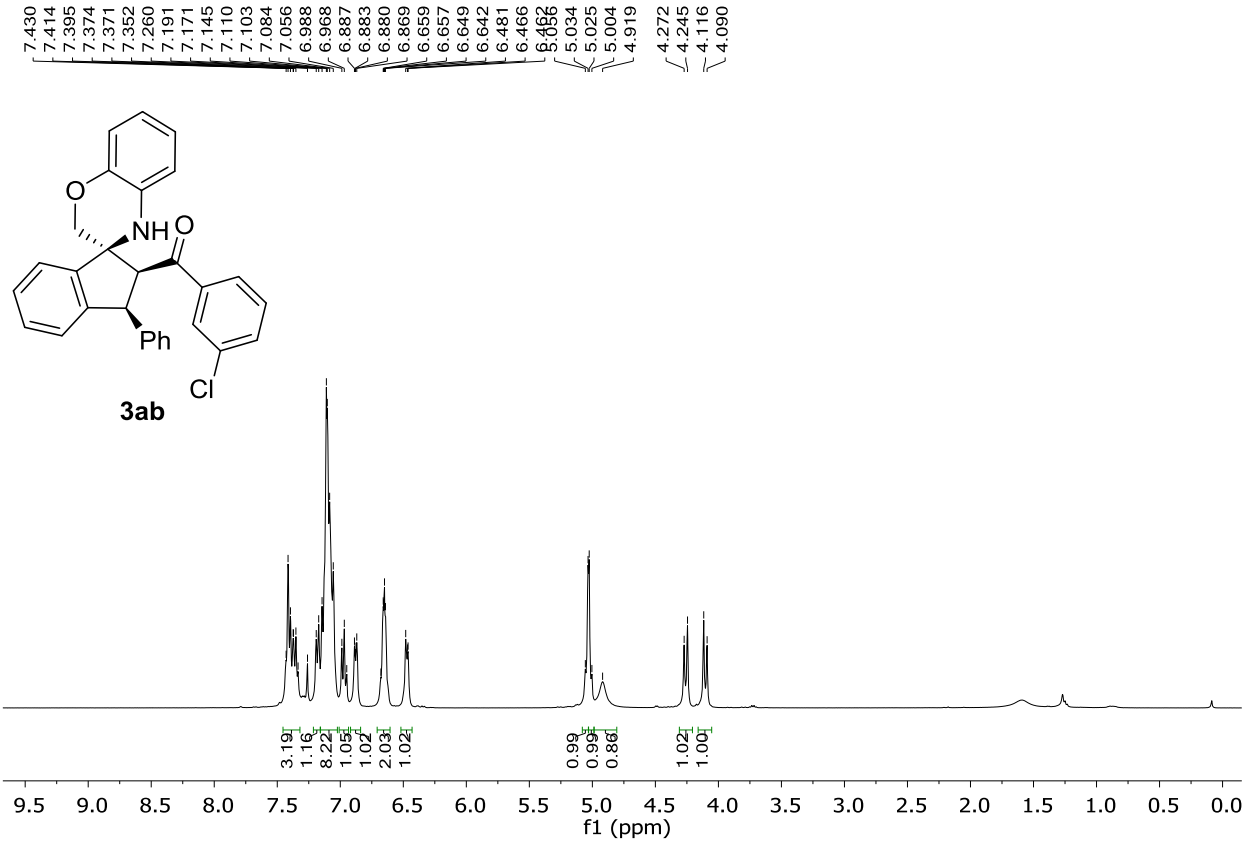

^{13}C NMR of **3ab** (100 MHz, $CDCl_3$):

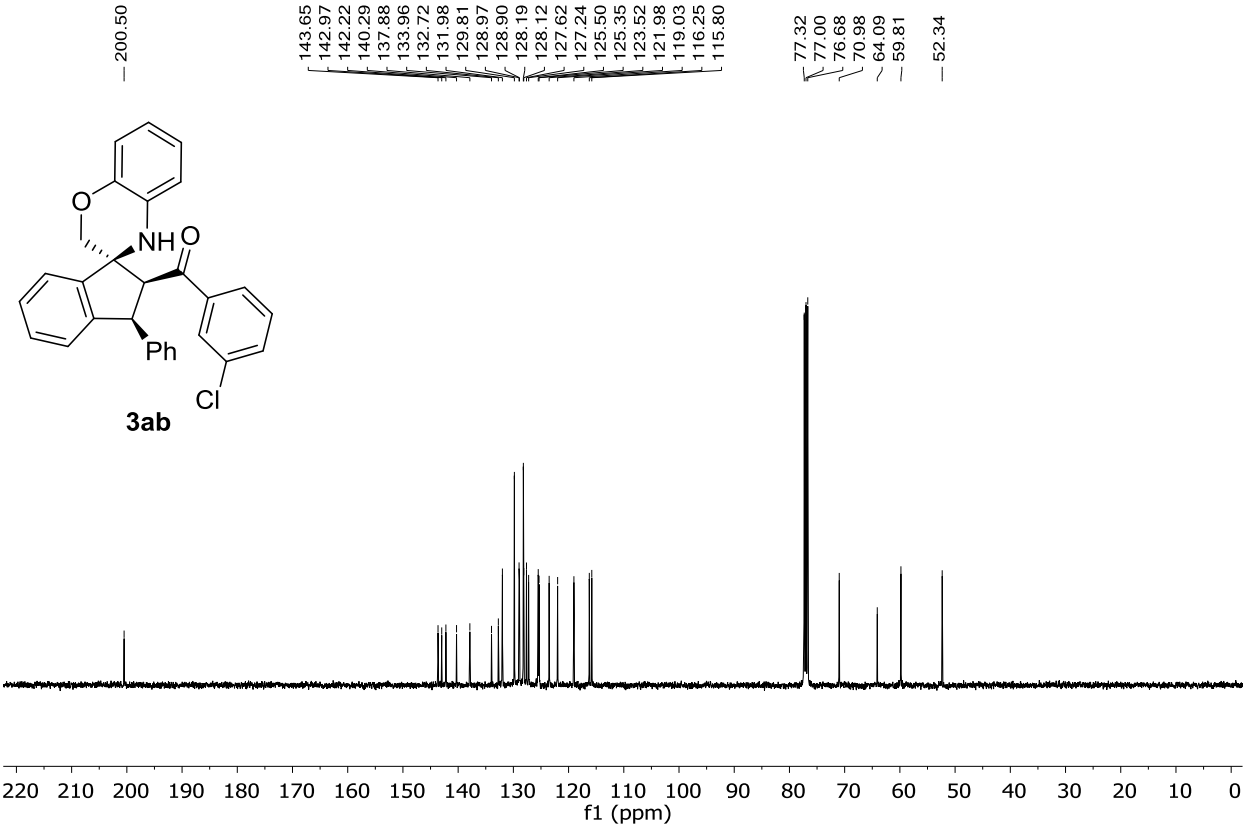

^{1}H NMR of **3ac** (400 MHz, $CDCl_3$):

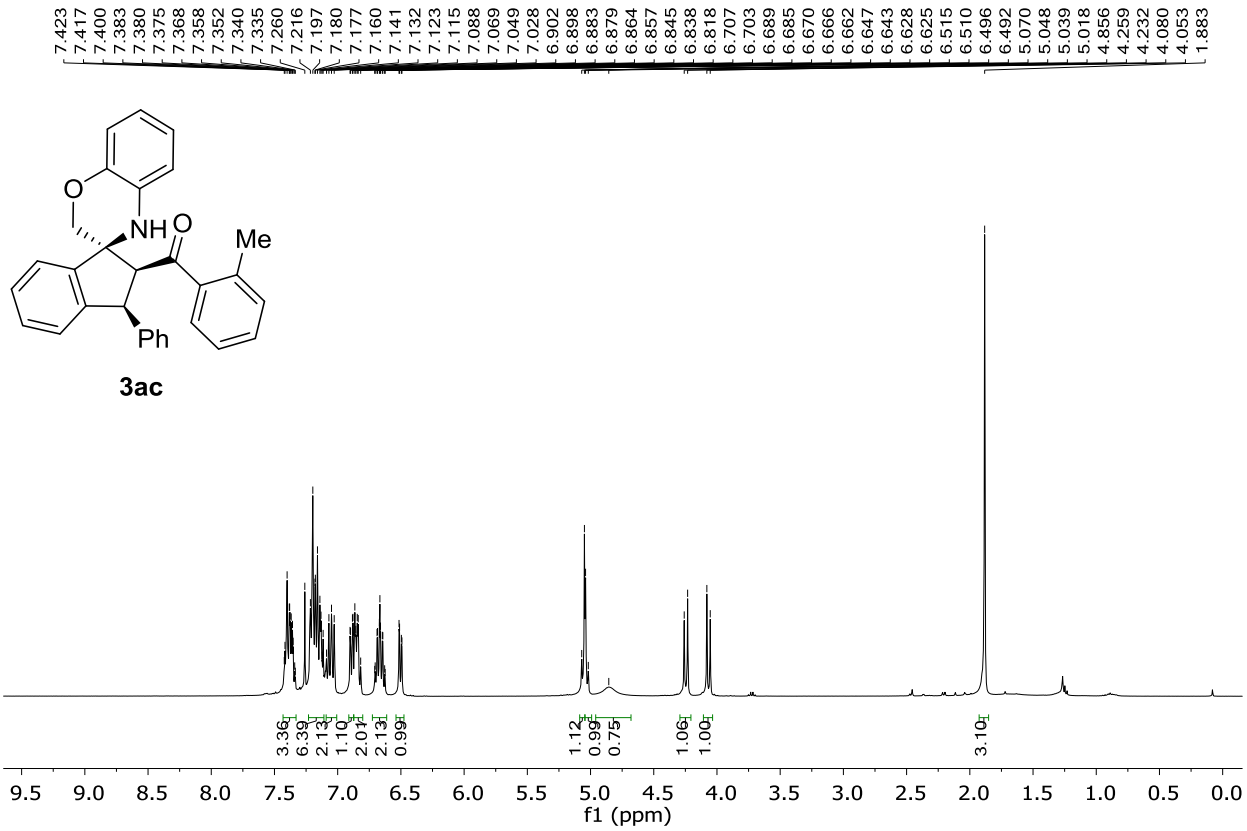

^{13}C NMR of **3ac** (100 MHz, $CDCl_3$):

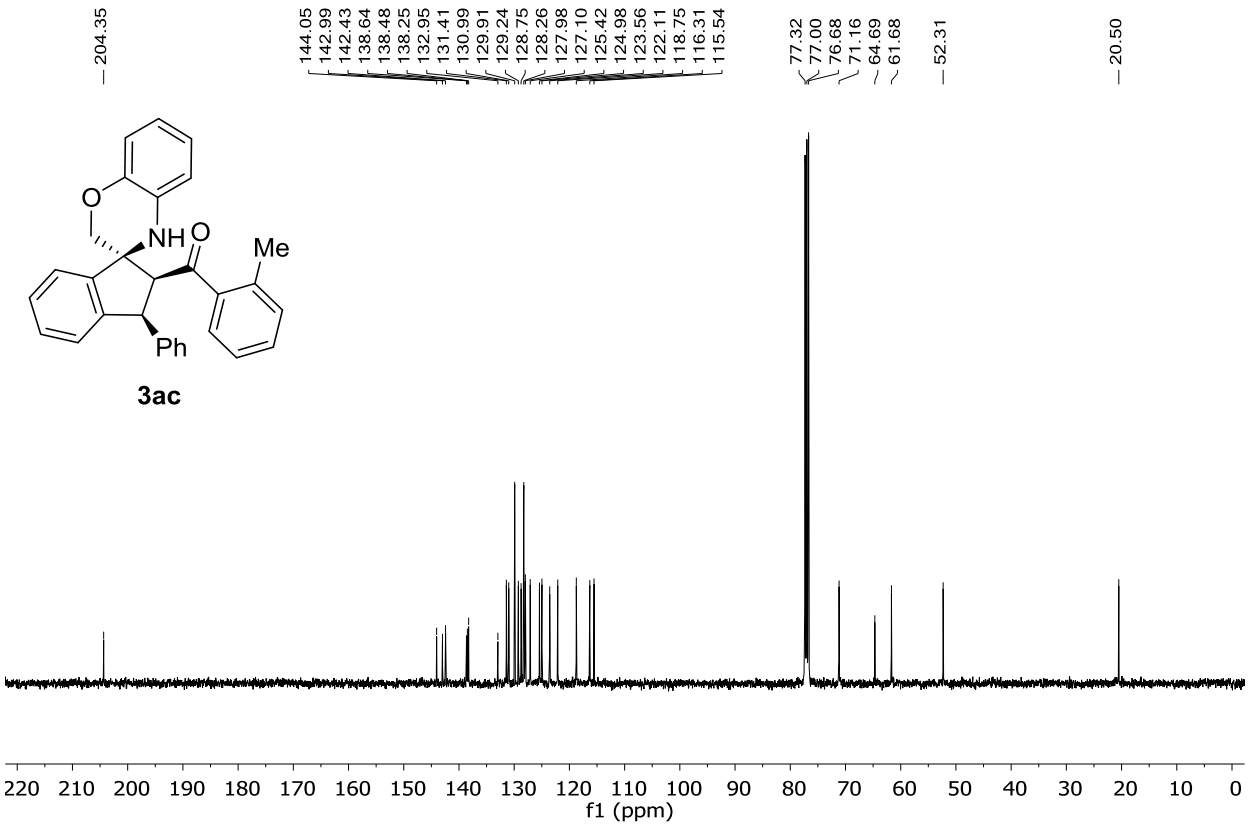

^{1}H NMR of **3ad** (400 MHz, $CDCl_3$):

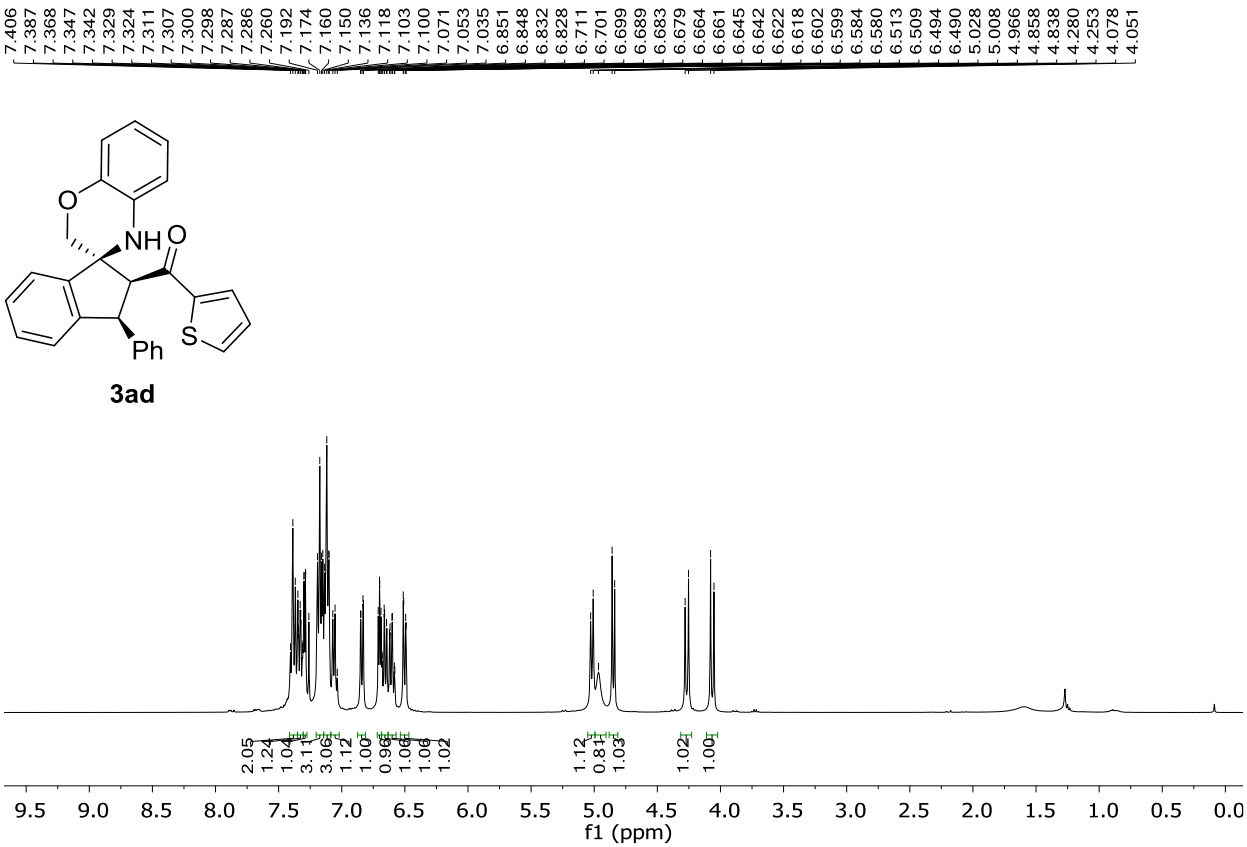

^{13}C NMR of **3ad** (100 MHz, $CDCl_3$):

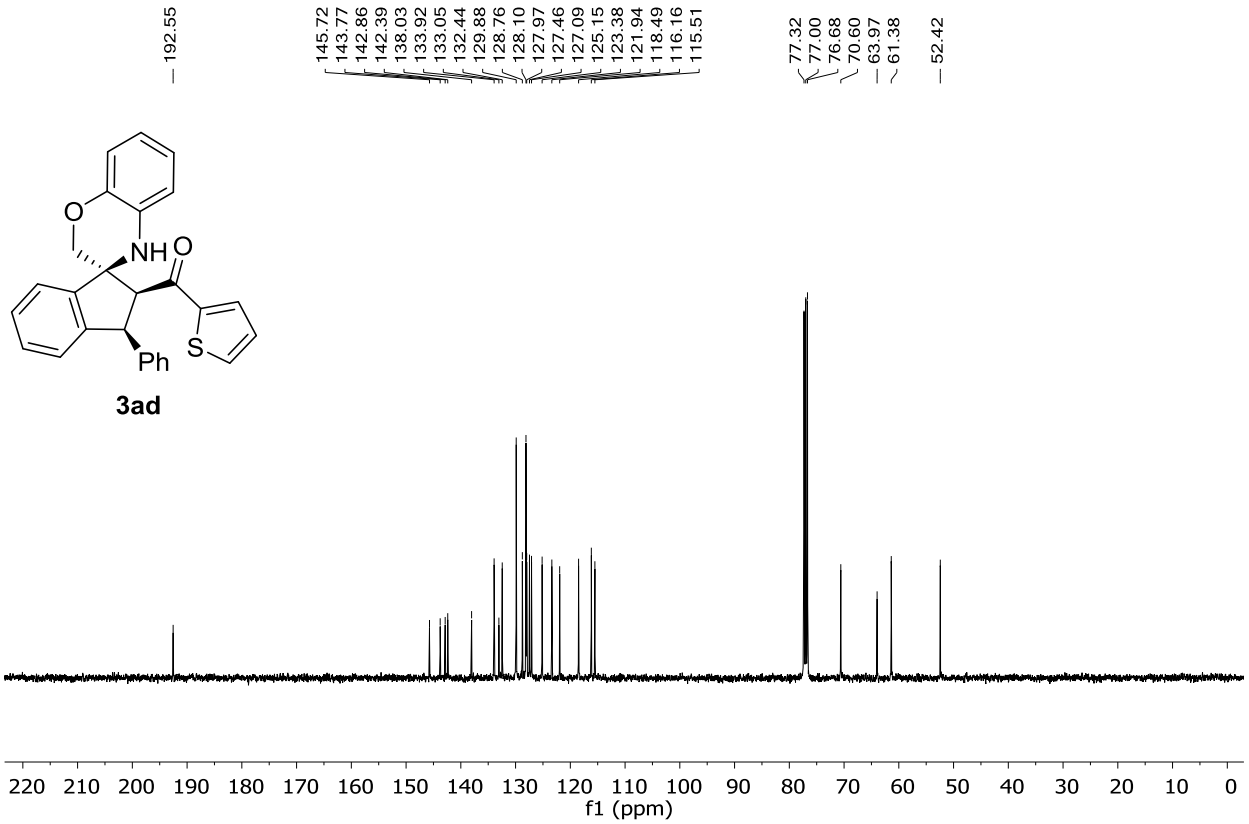

^{1}H NMR of **3ae** (400 MHz, $CDCl_3$):

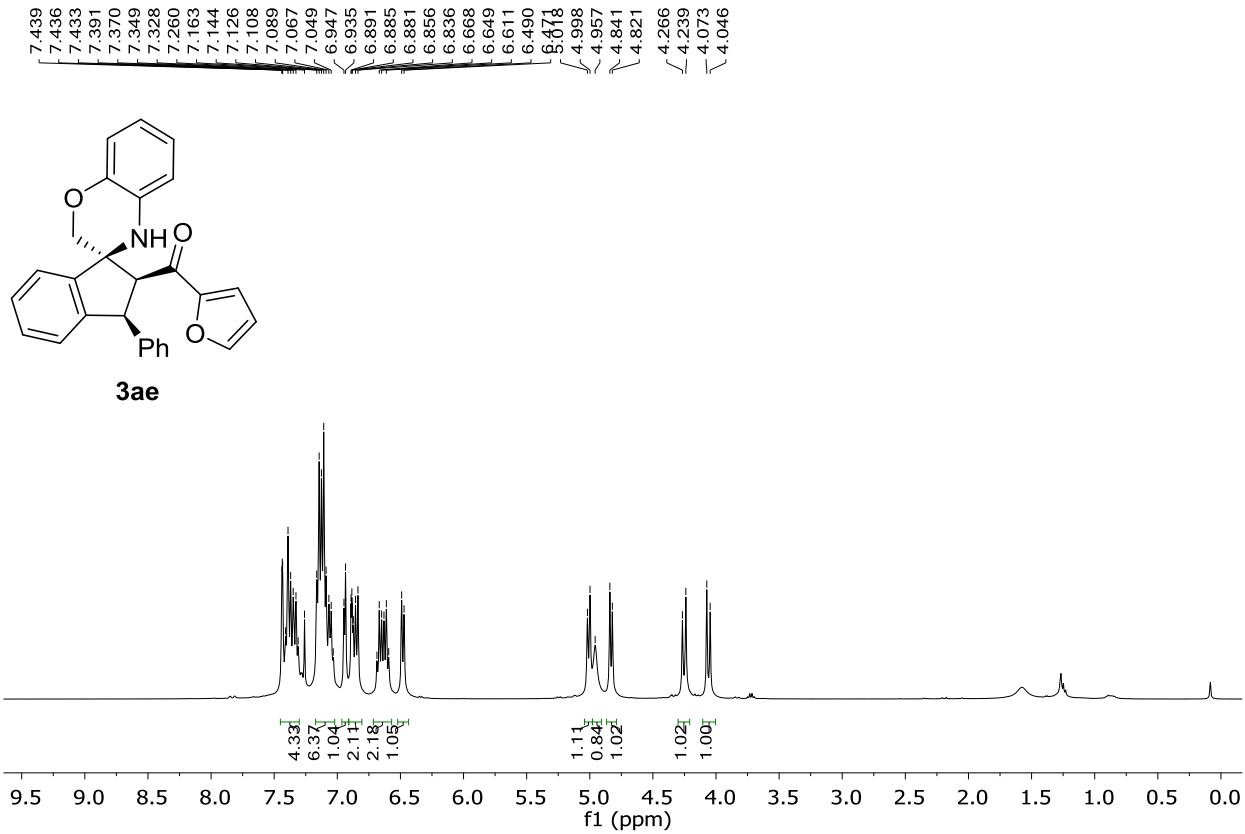

^{13}C NMR of **3ae** (100 MHz, $CDCl_3$):

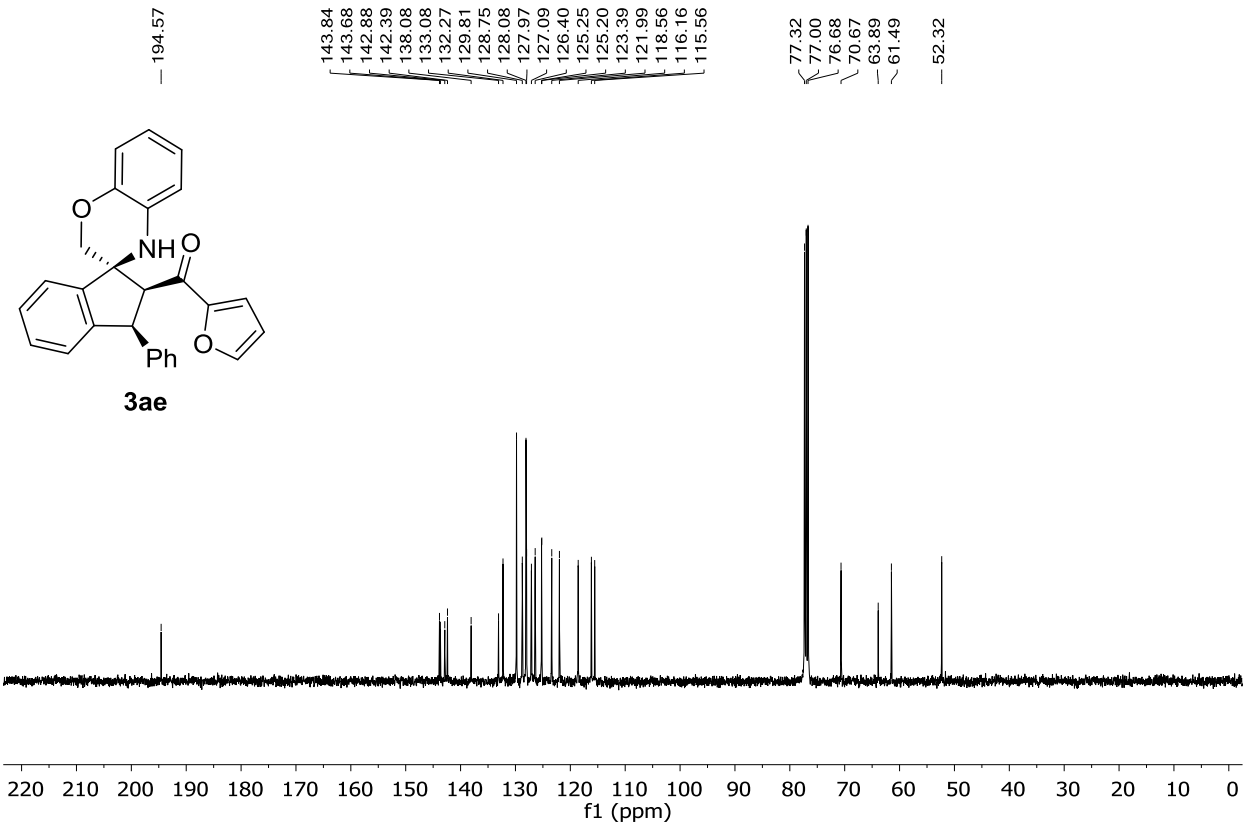

^{1}H NMR of **3ag** (400 MHz, $CDCl_3$):

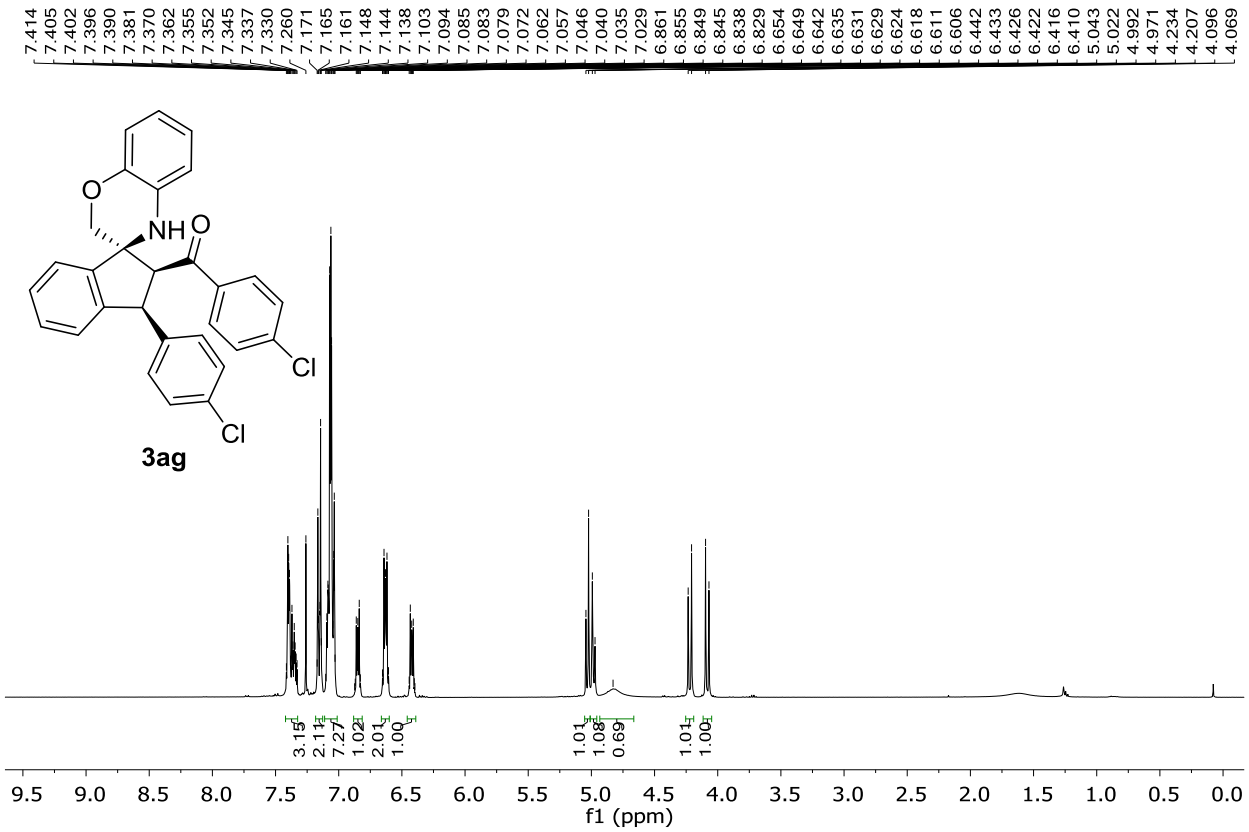

^{13}C NMR of **3ag** (100 MHz, $CDCl_3$):

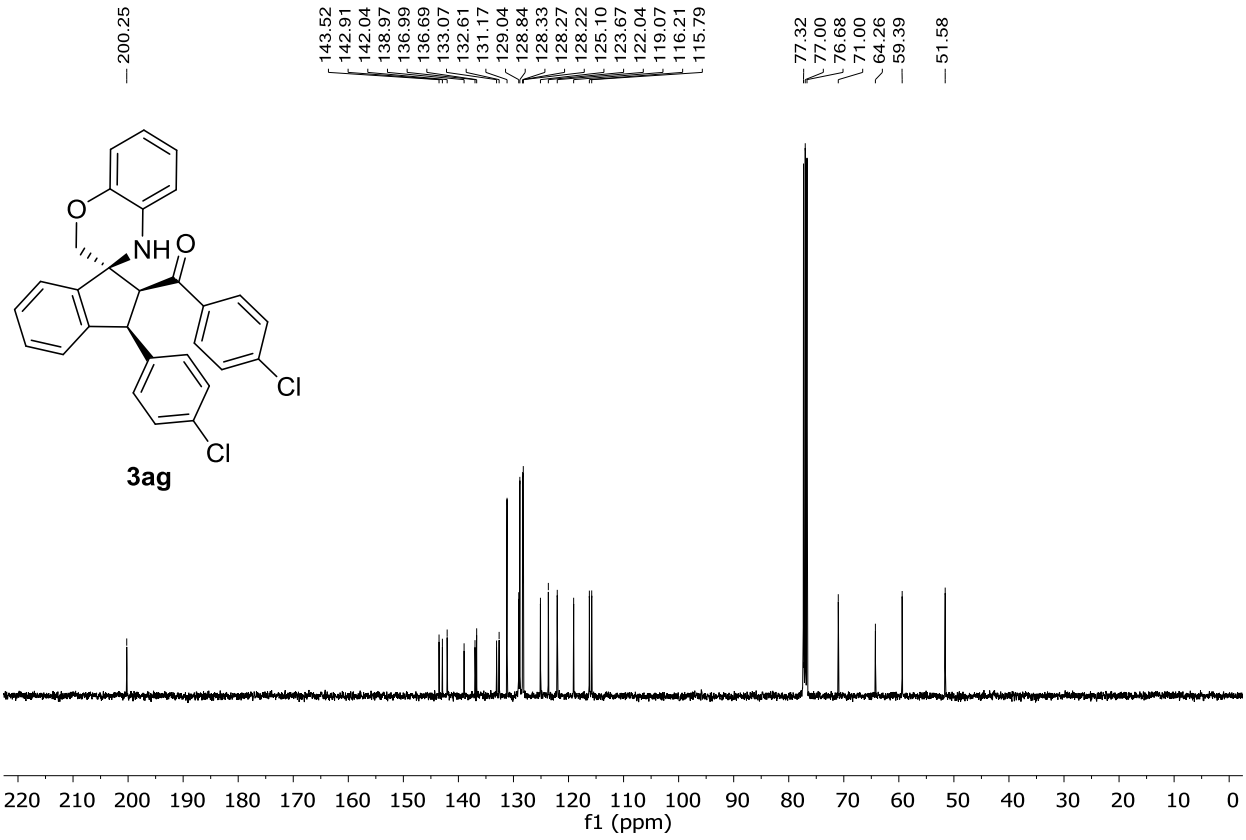

^{1}H NMR of **3ah** (400 MHz, $CDCl_3$):

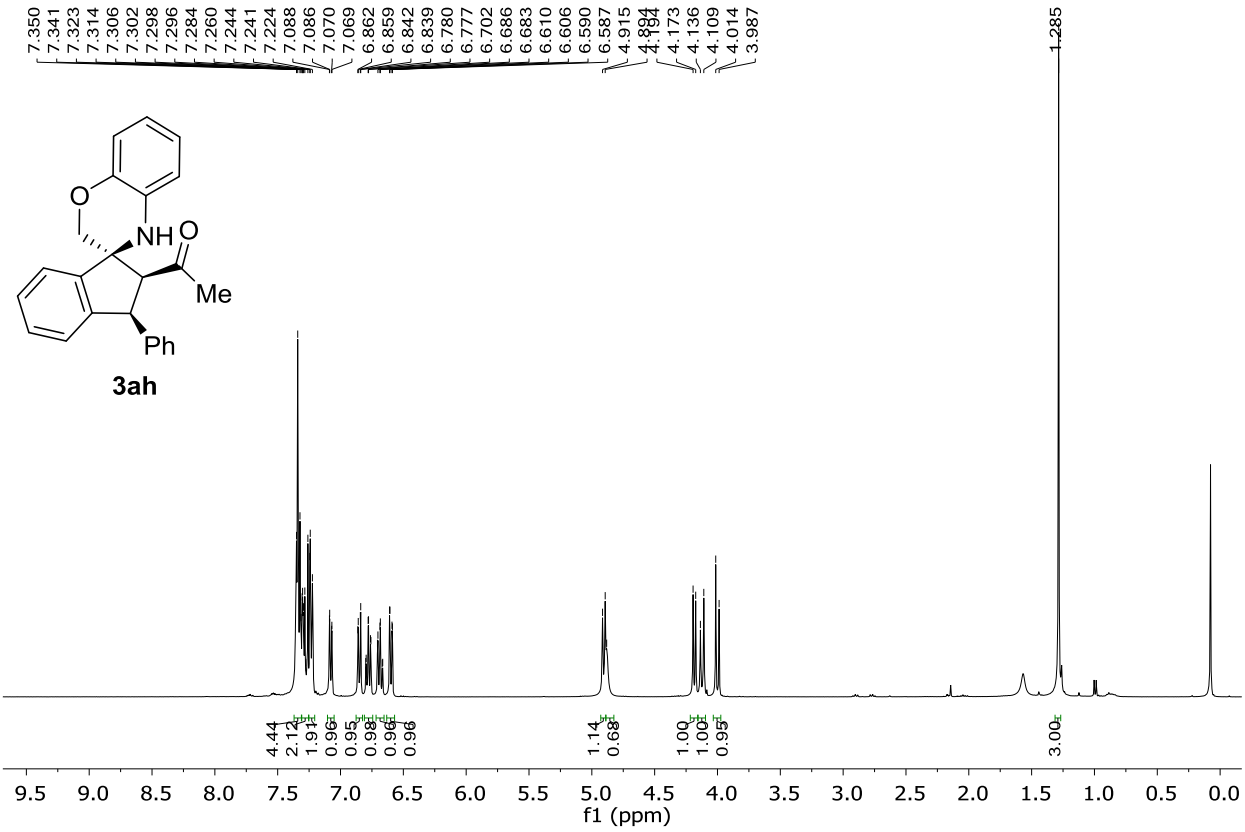

^{13}C NMR of **3ah** (100 MHz, $CDCl_3$):

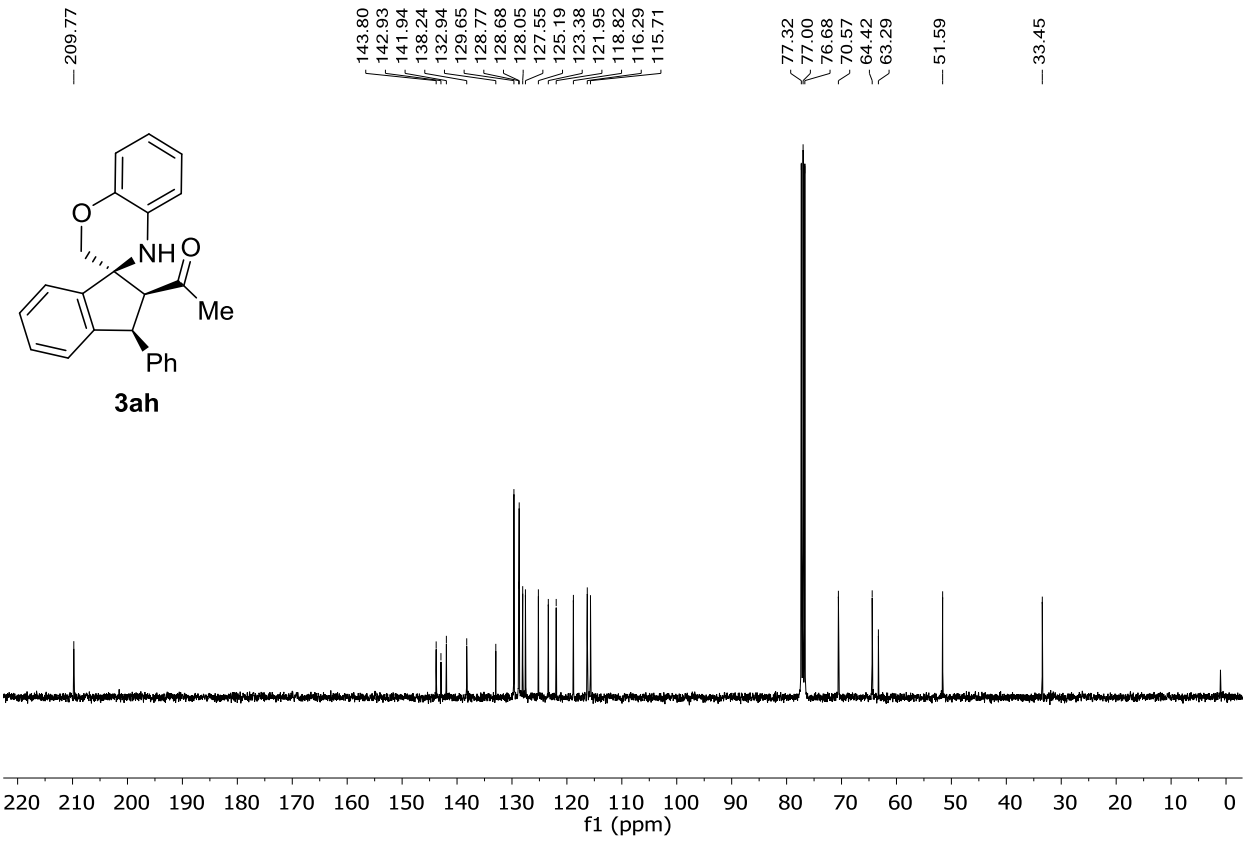

^{1}H NMR of **4a** (400 MHz, $CDCl_3$):

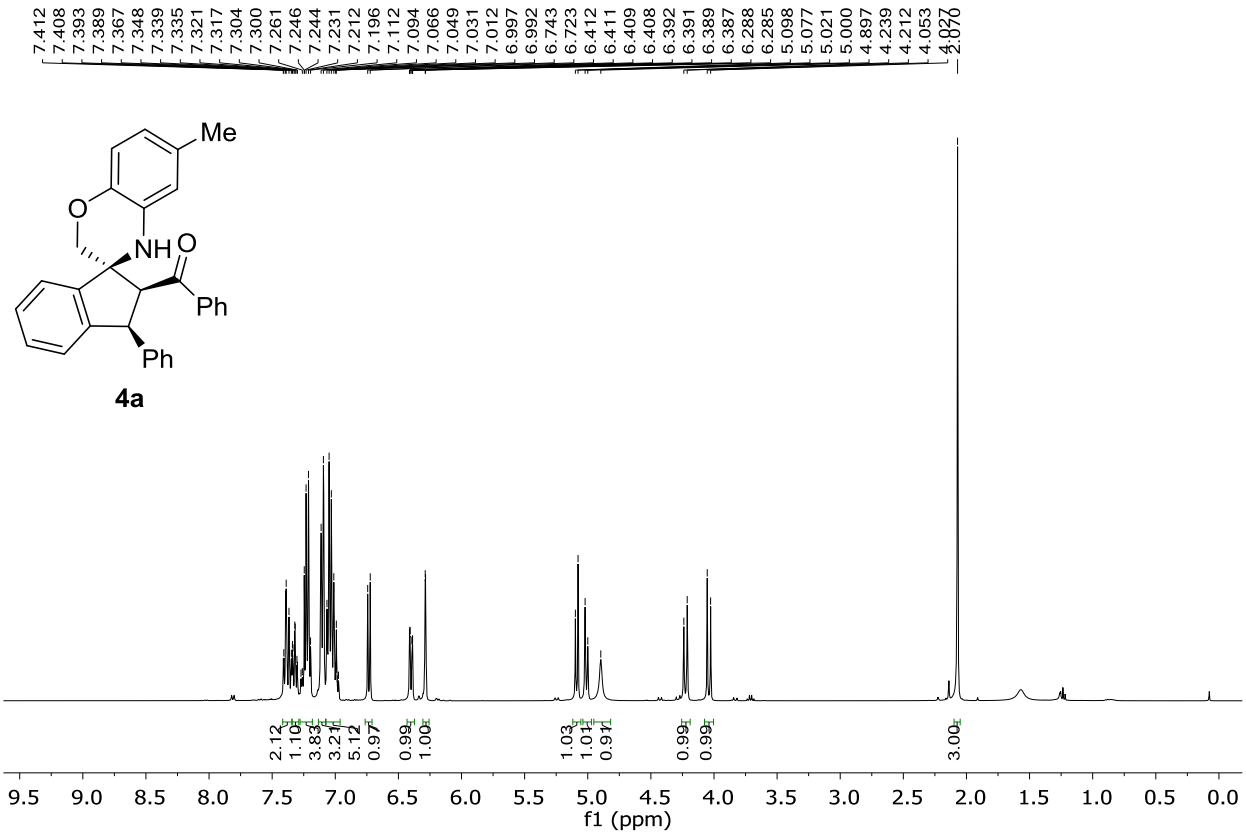

^{13}C NMR of **4a** (100 MHz, $CDCl_3$):

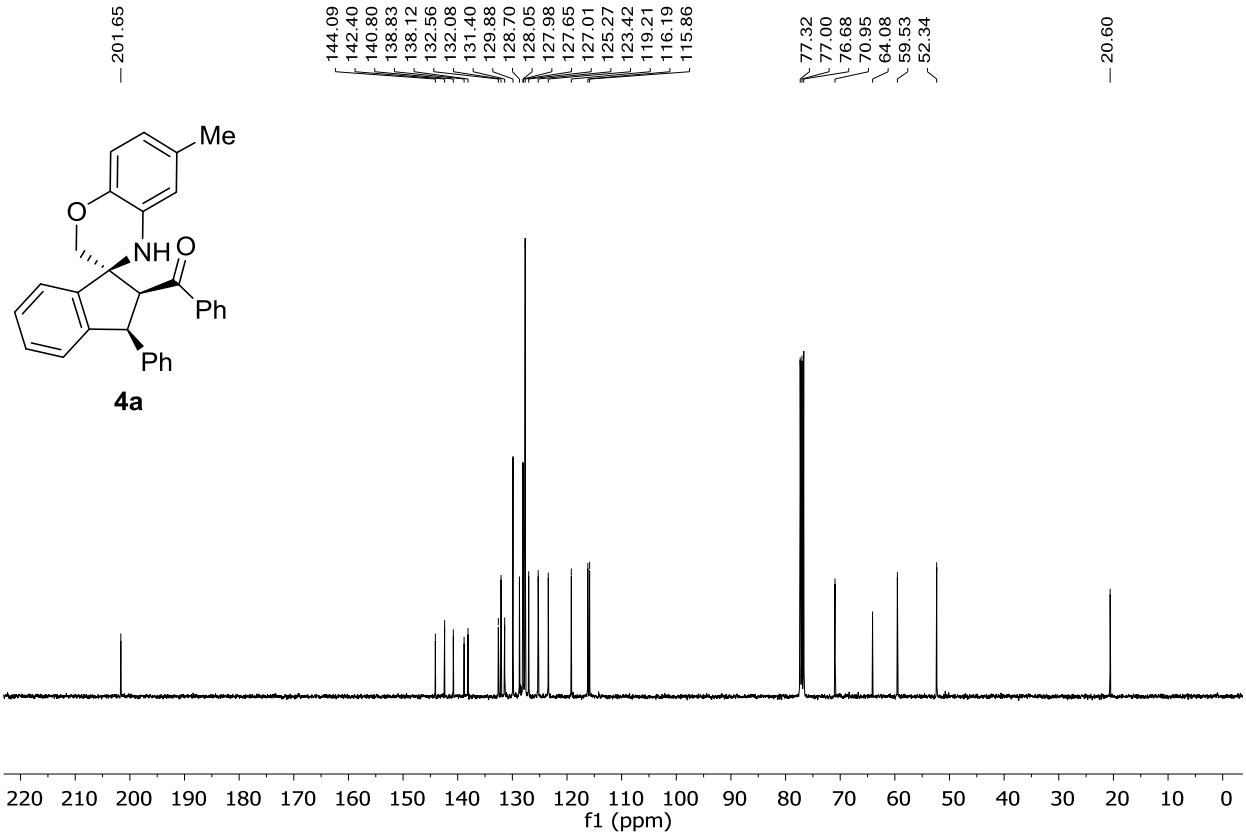

^{1}H NMR of **4b** (400 MHz, $CDCl_3$):

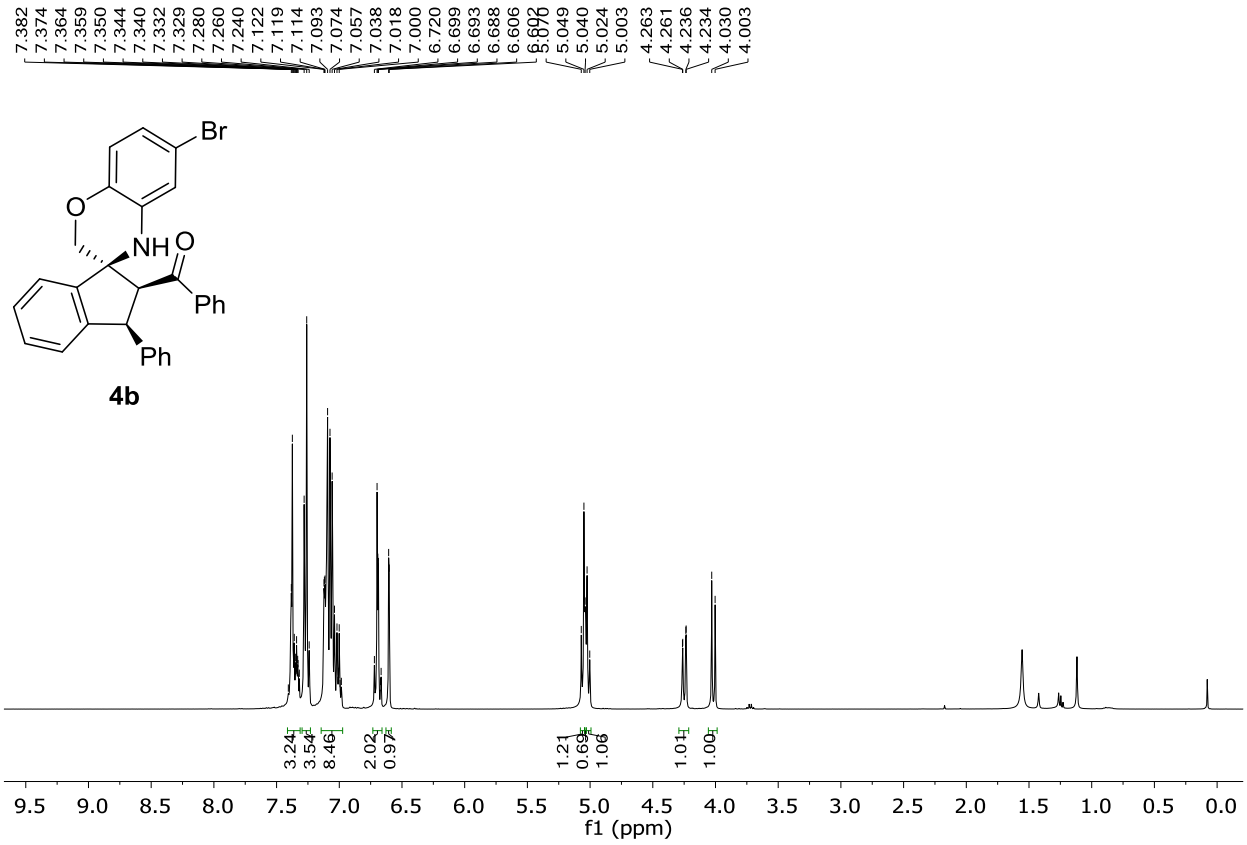

^{13}C NMR of **4b** (100 MHz, $CDCl_3$):

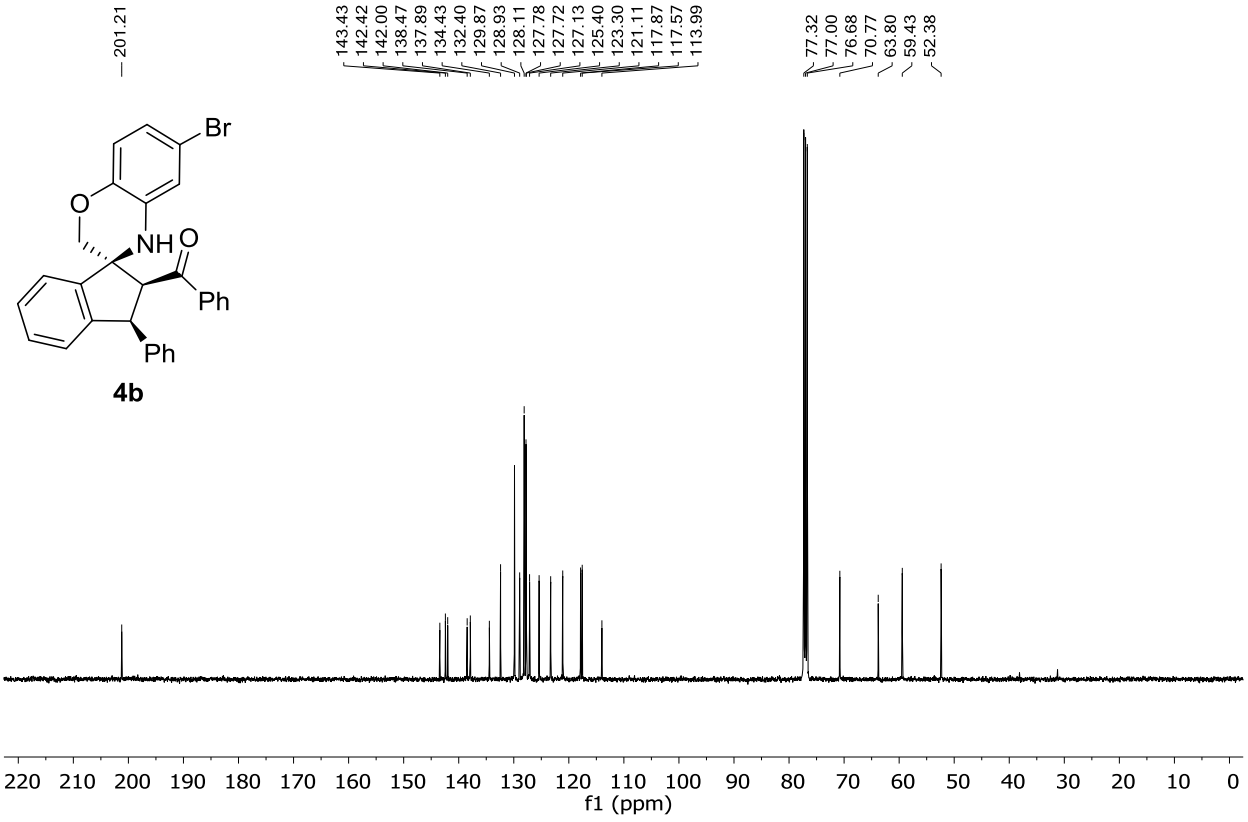

^{1}H NMR of **4d** (400 MHz, $CDCl_3$):

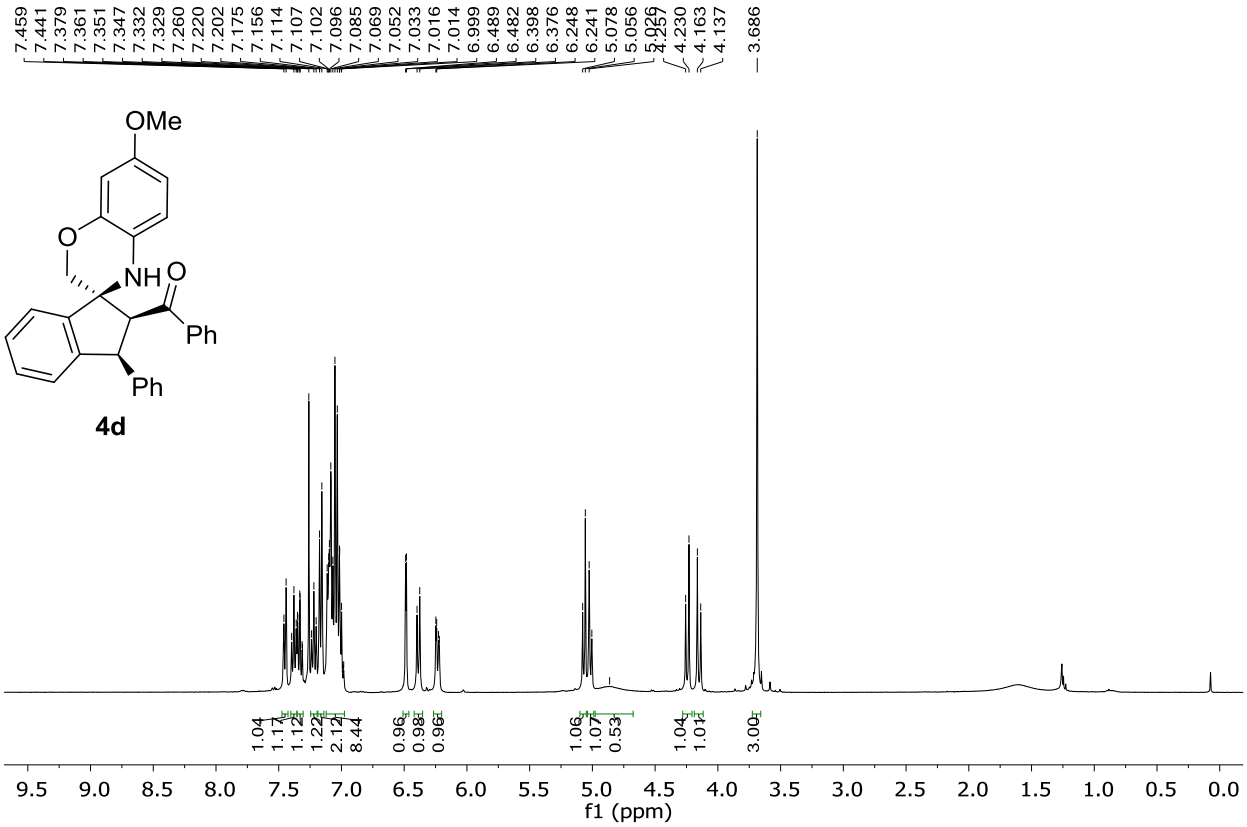

^{13}C NMR of **4d** (100 MHz, $CDCl_3$):

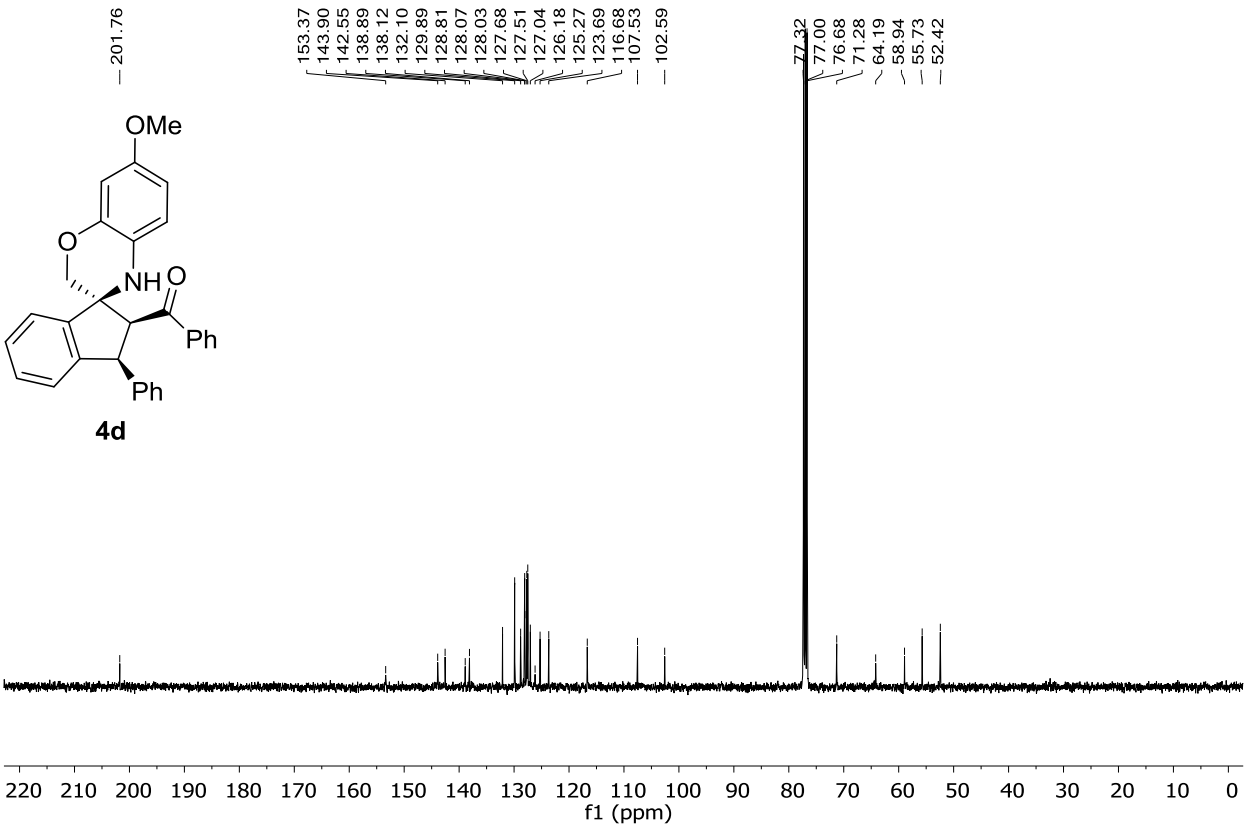

^{1}H NMR of **4g** (400 MHz, $CDCl_3$):

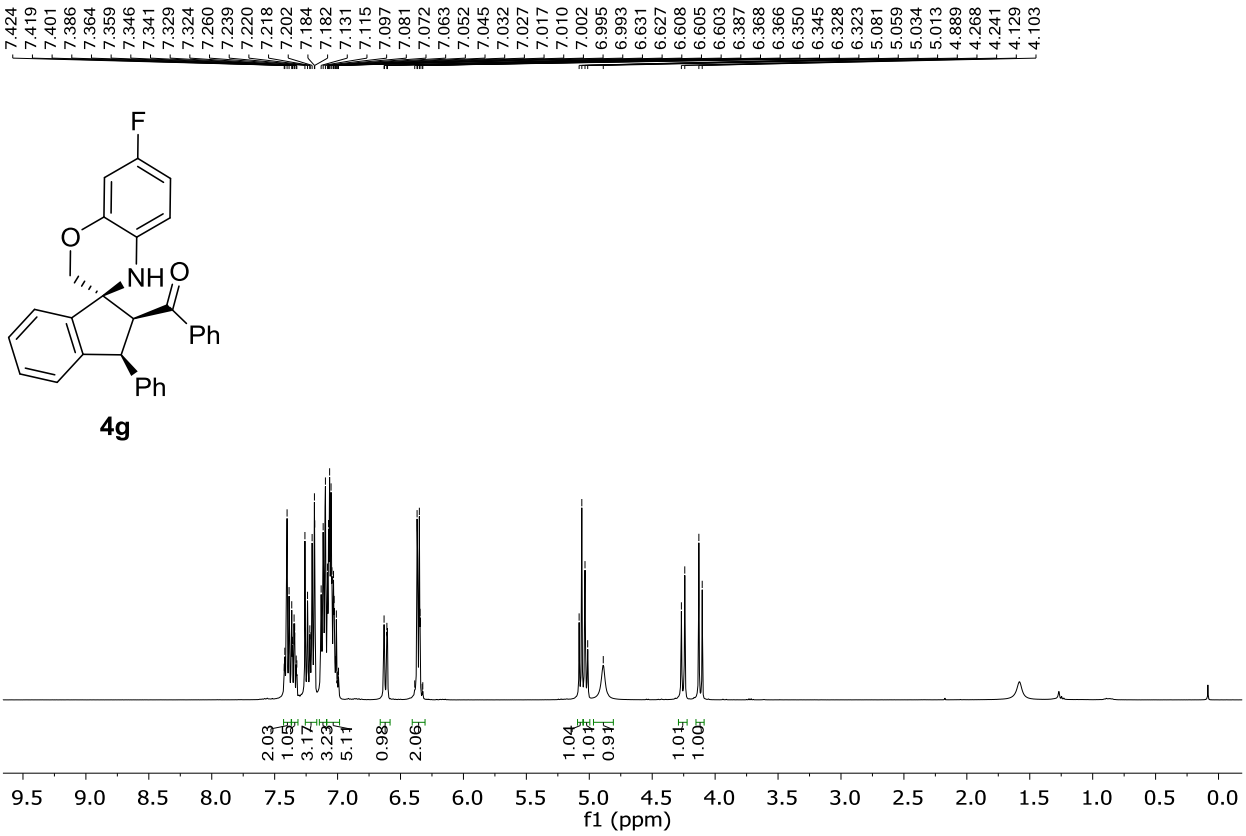

^{13}C NMR of **4g** (100 MHz, $CDCl_3$):

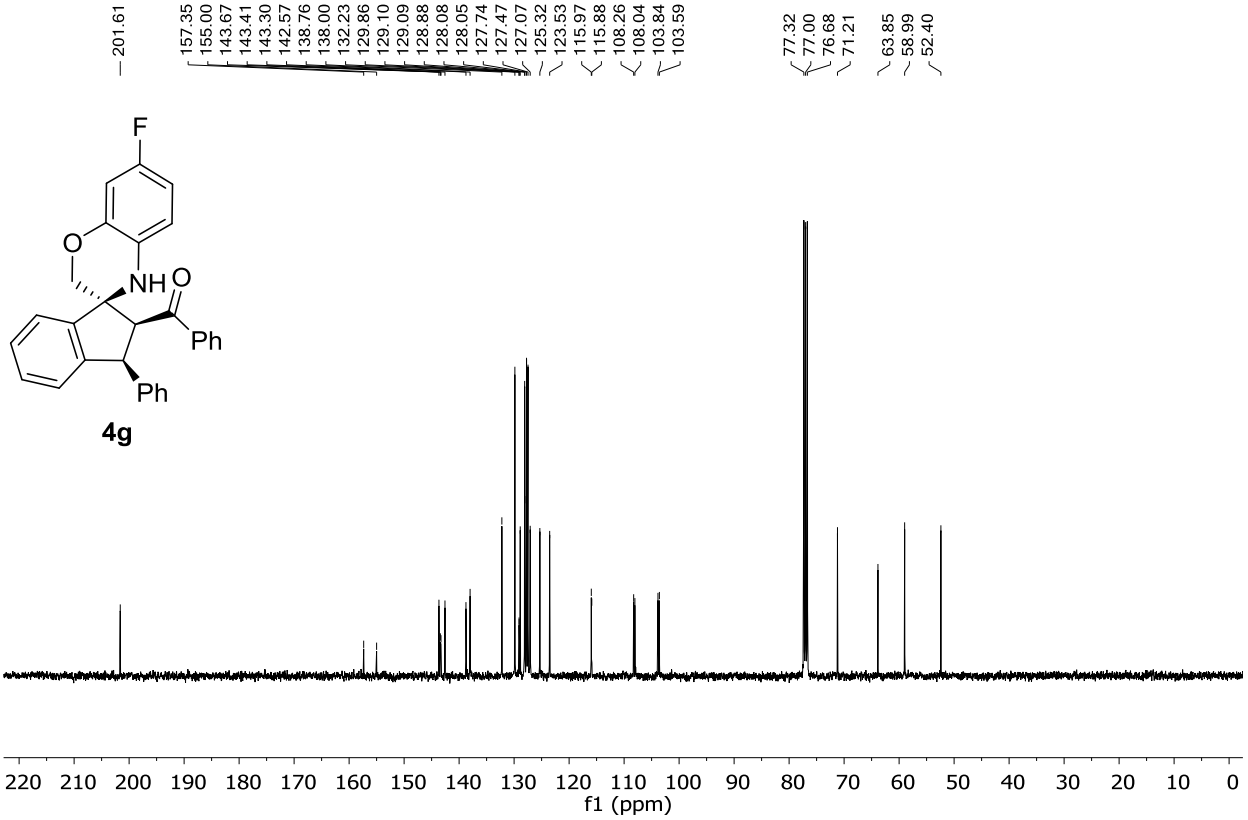

^{1}H NMR of **4i** (400 MHz, $CDCl_3$):

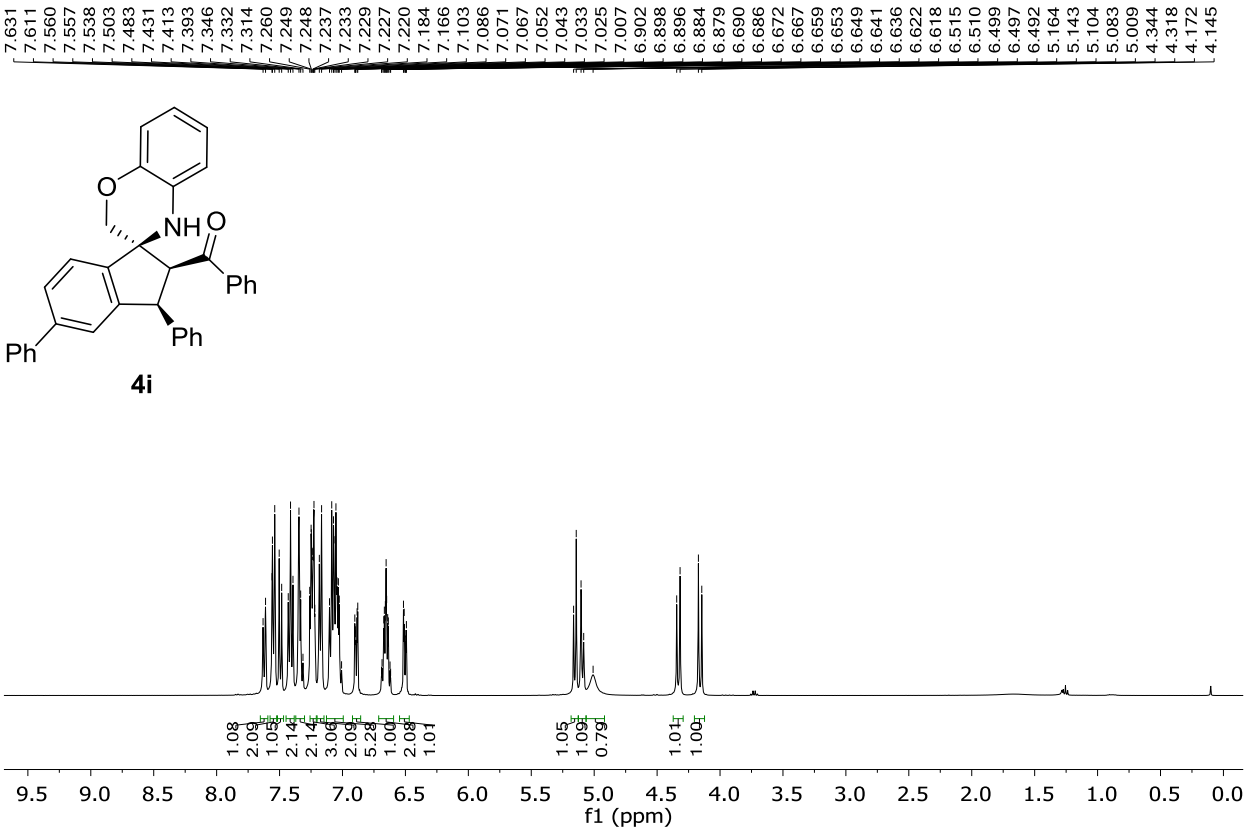

^{13}C NMR of **4i** (100 MHz, $CDCl_3$):

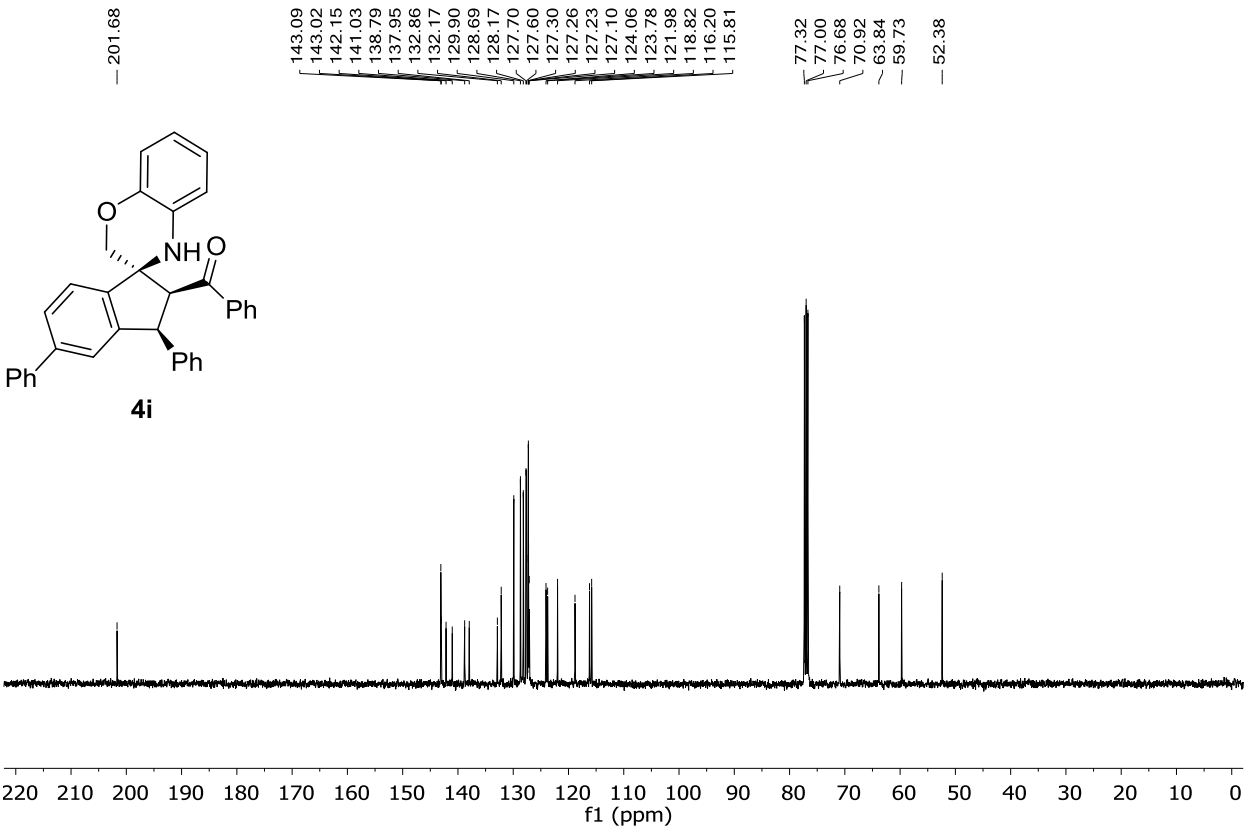

^{1}H NMR of **4k** (400 MHz, $CDCl_3$):

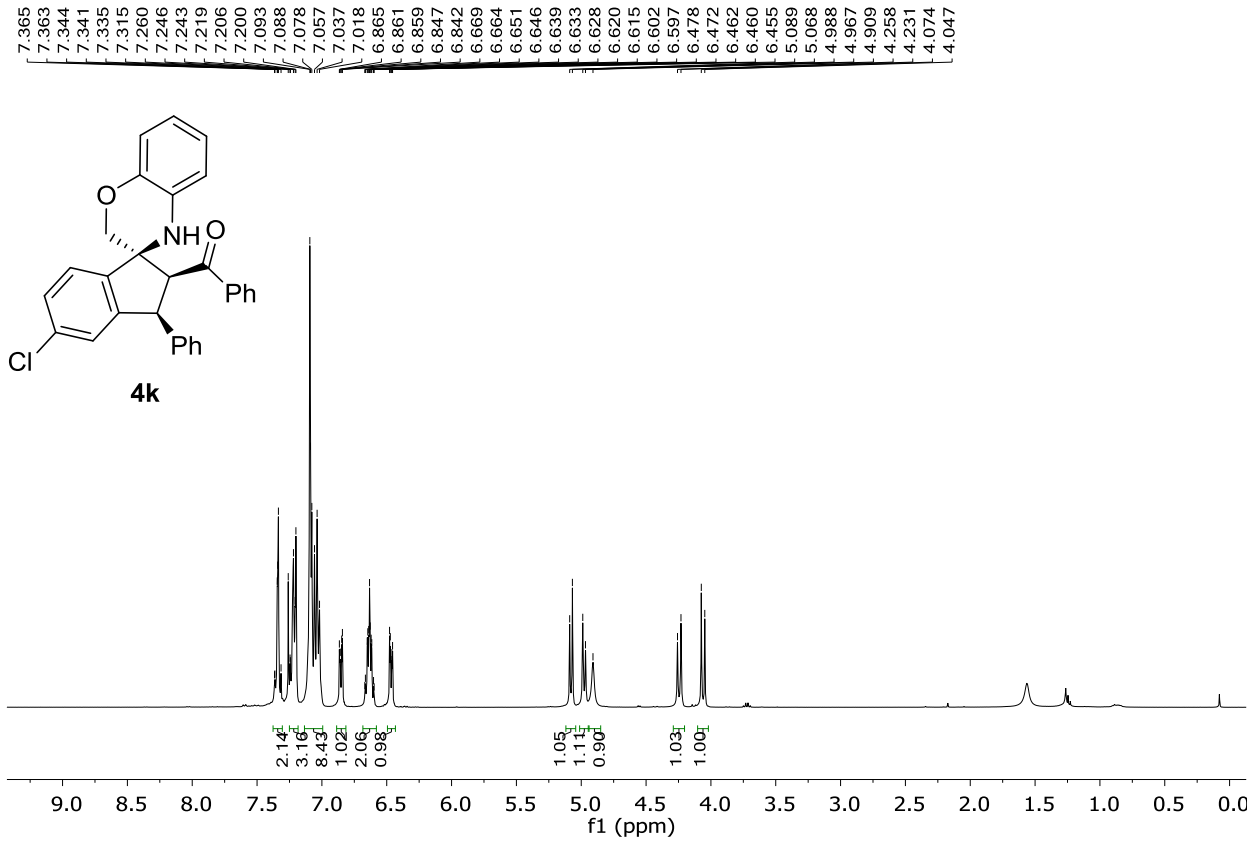

^{13}C NMR of **4k** (100 MHz, $CDCl_3$):

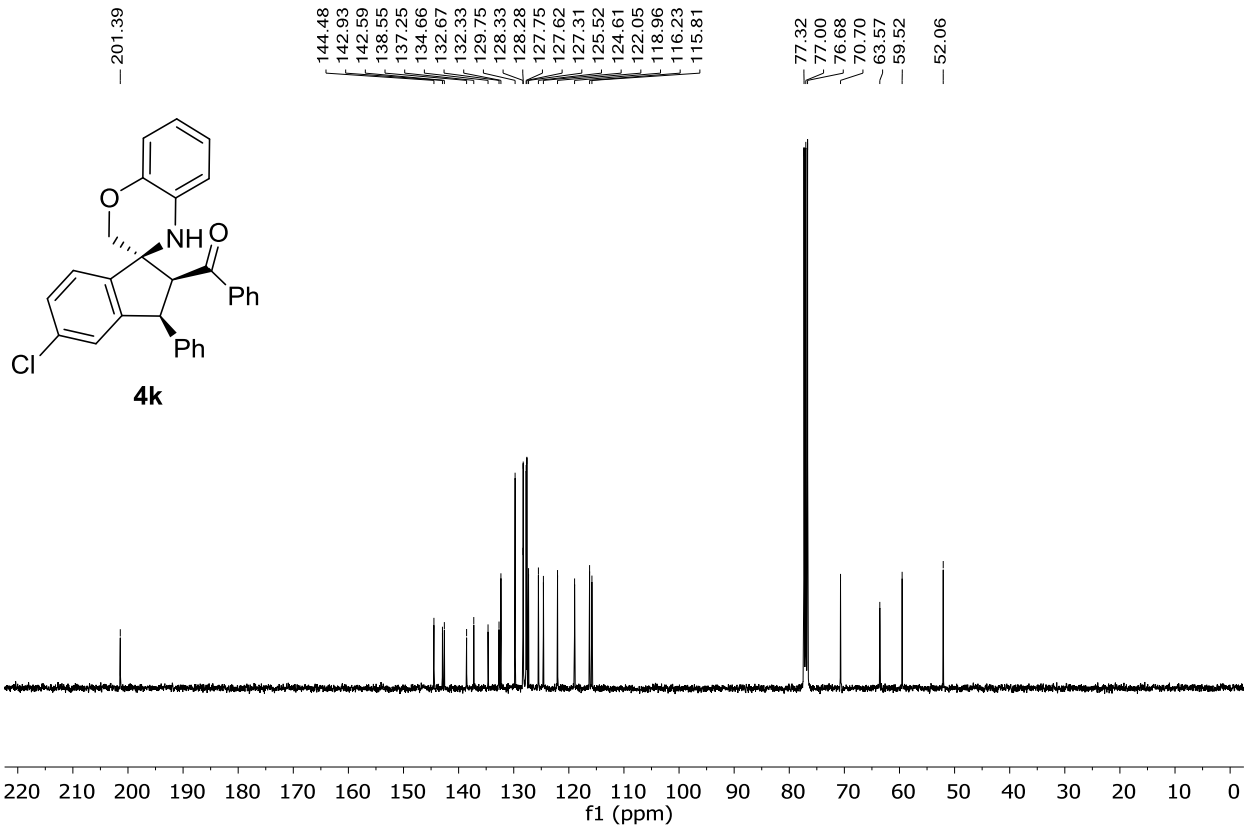

^{1}H NMR of **4m** (400 MHz, $CDCl_3$):

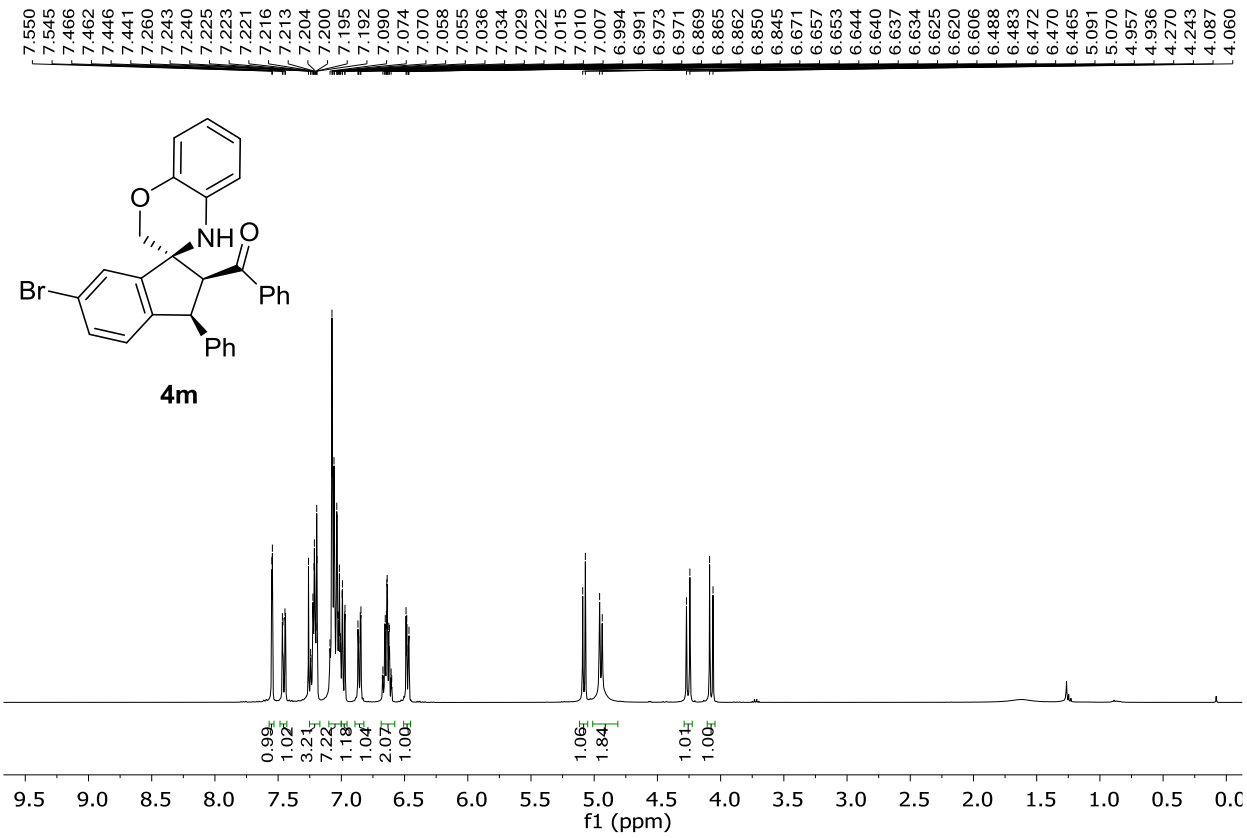

^{13}C NMR of **4m** (100 MHz, $CDCl_3$):

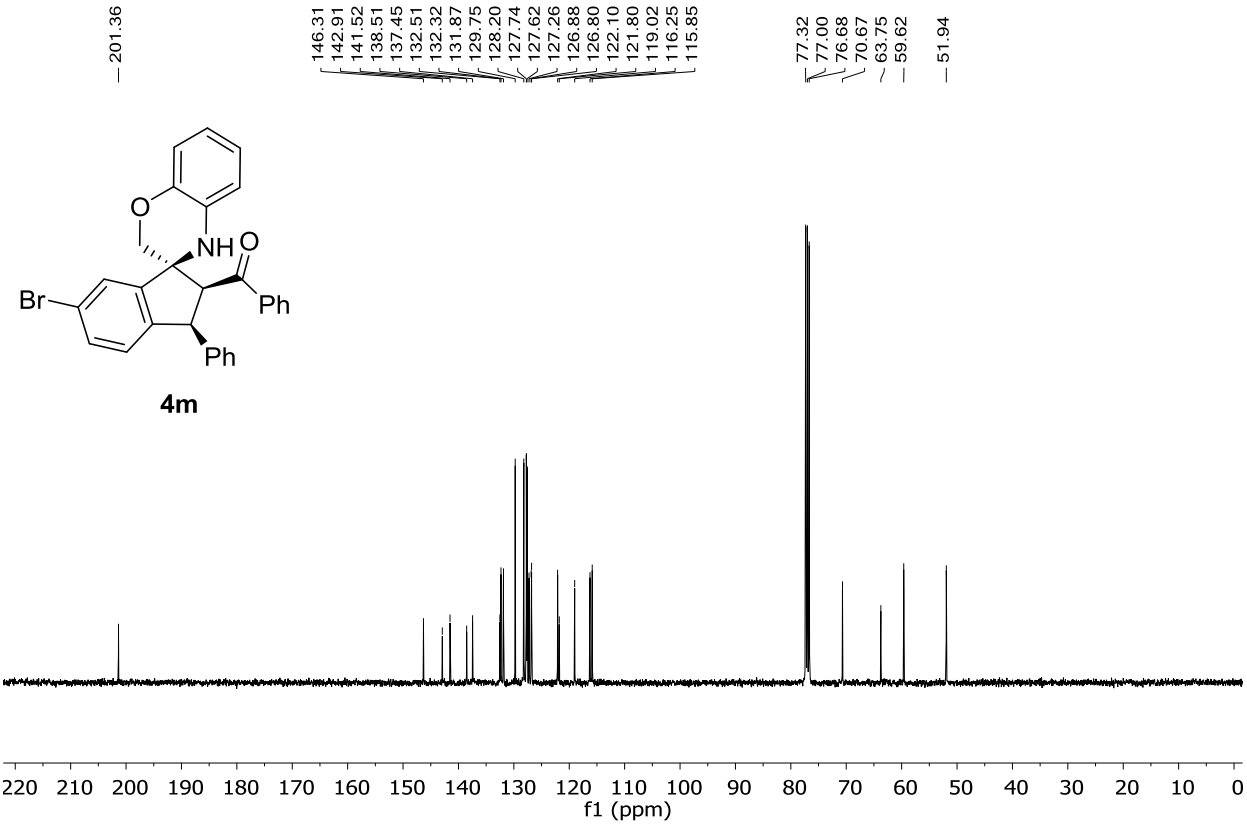

^{1}H NMR of **4n** (400 MHz, $CDCl_3$):

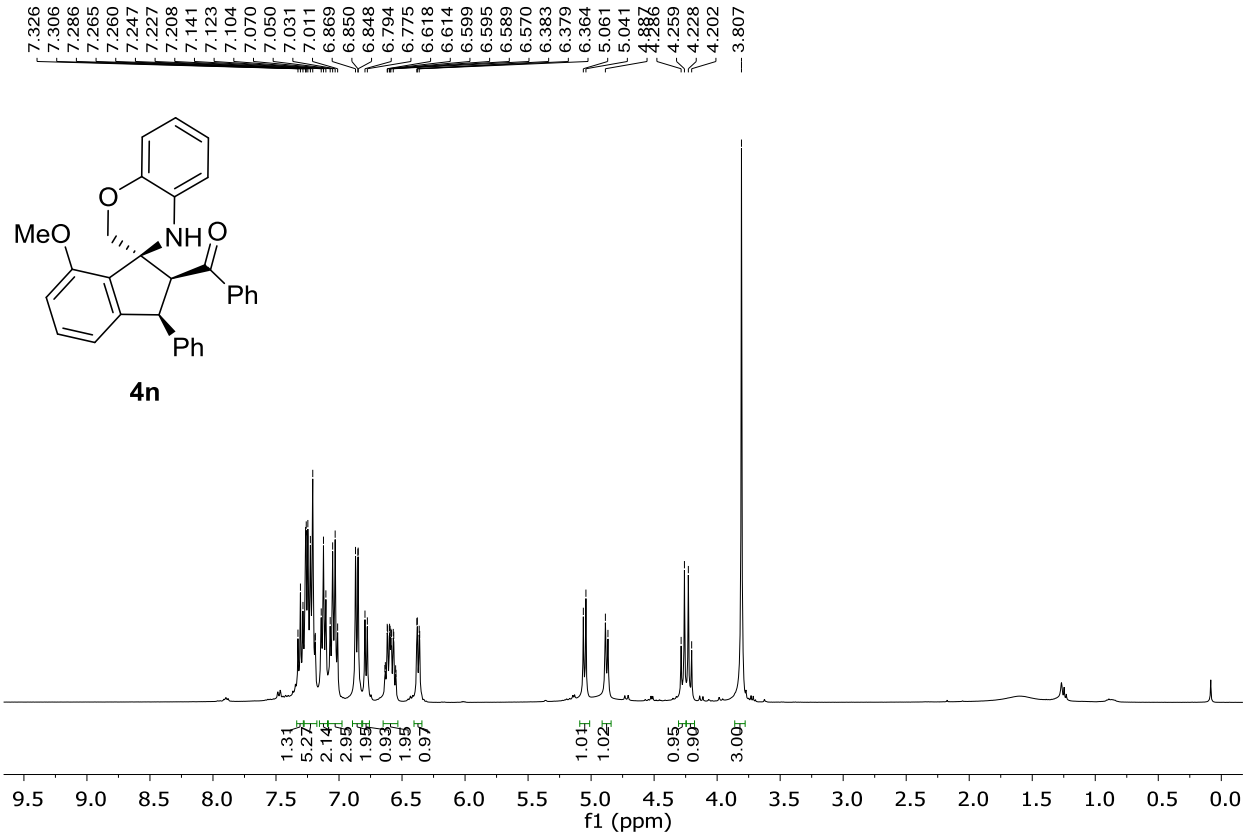

^{13}C NMR of **4n** (100 MHz, $CDCl_3$):

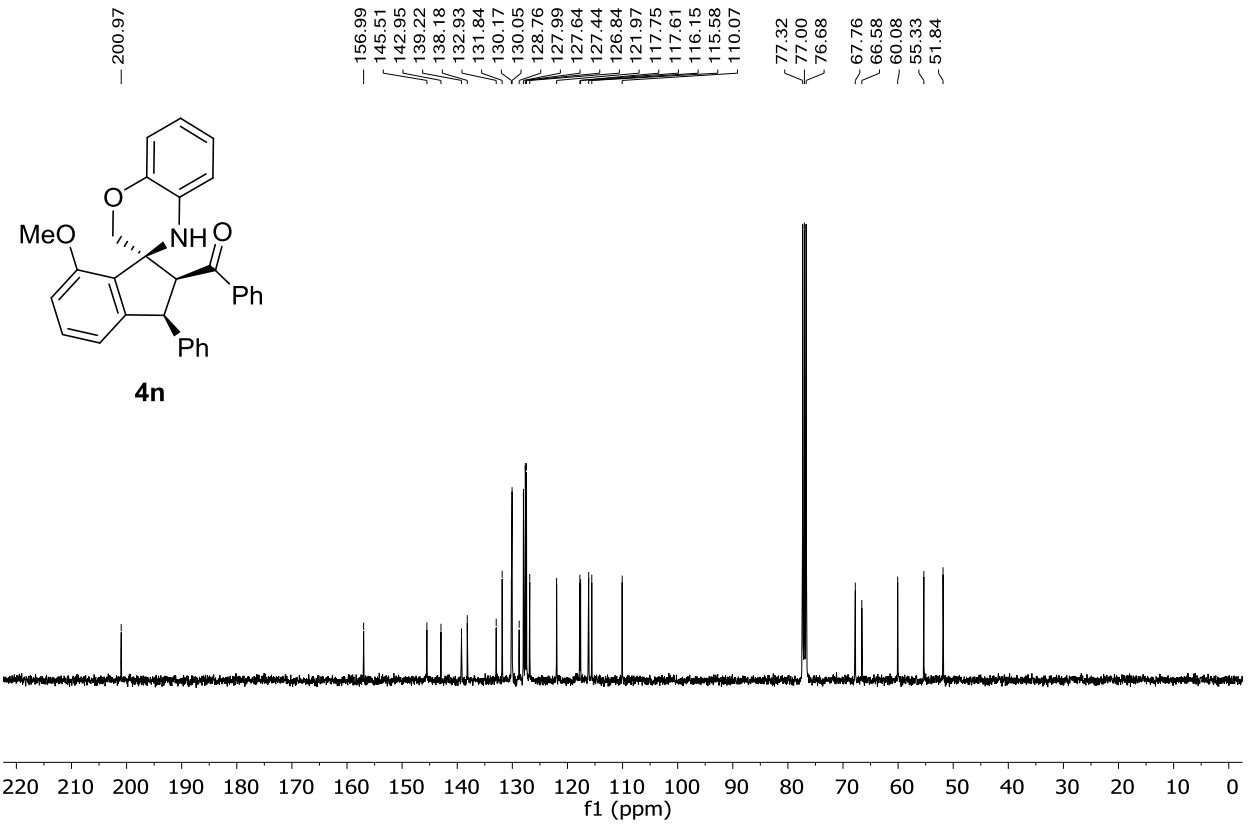

^{1}H NMR of **4p** (400 MHz, $CDCl_3$):

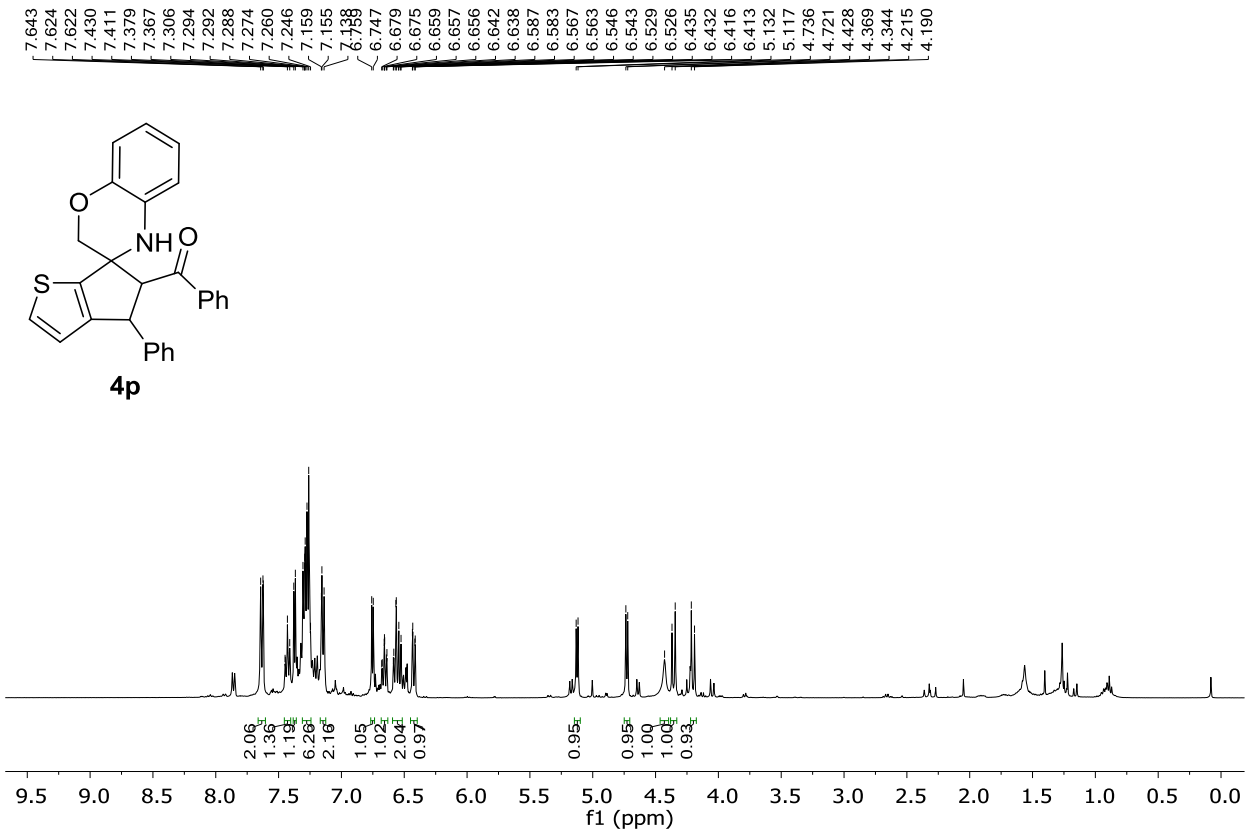

^{13}C NMR of **4p** (100 MHz, $CDCl_3$):

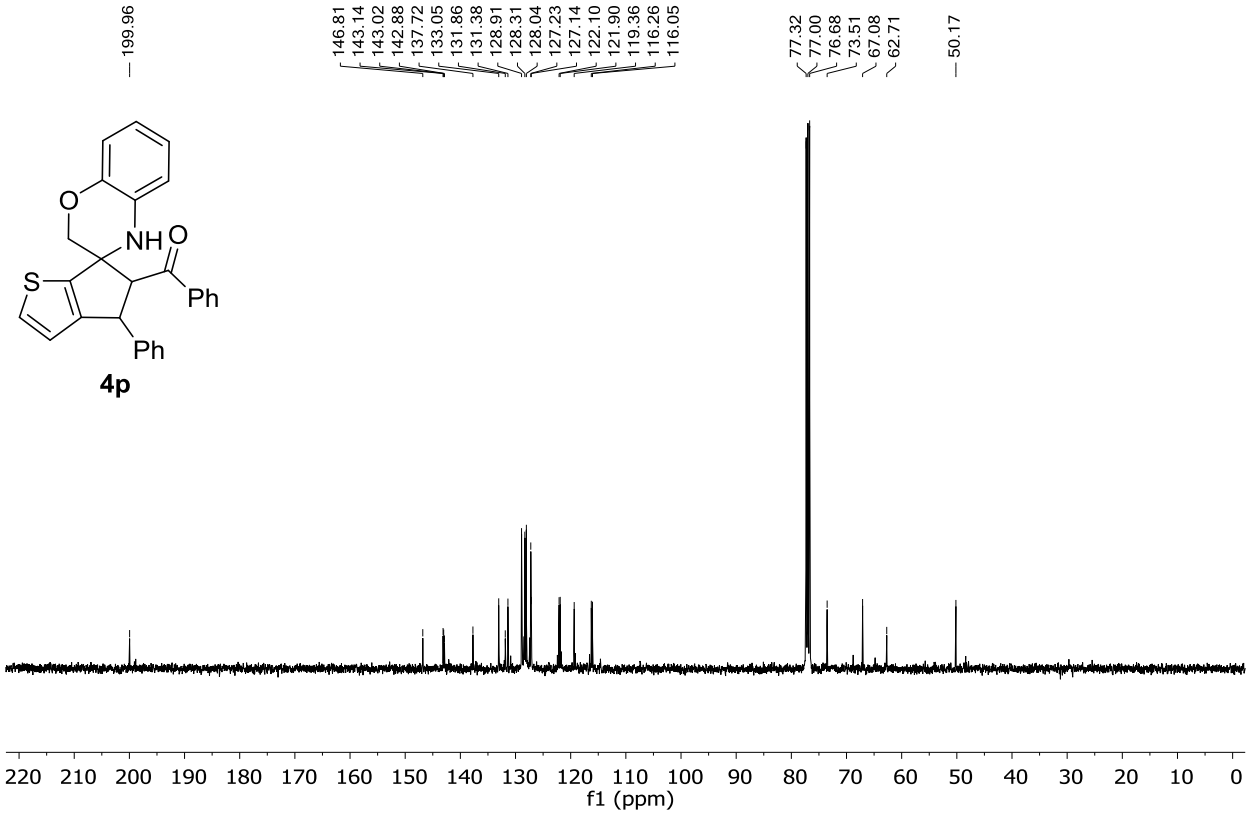

^{1}H NMR of **4q** (400 MHz, $CDCl_3$):

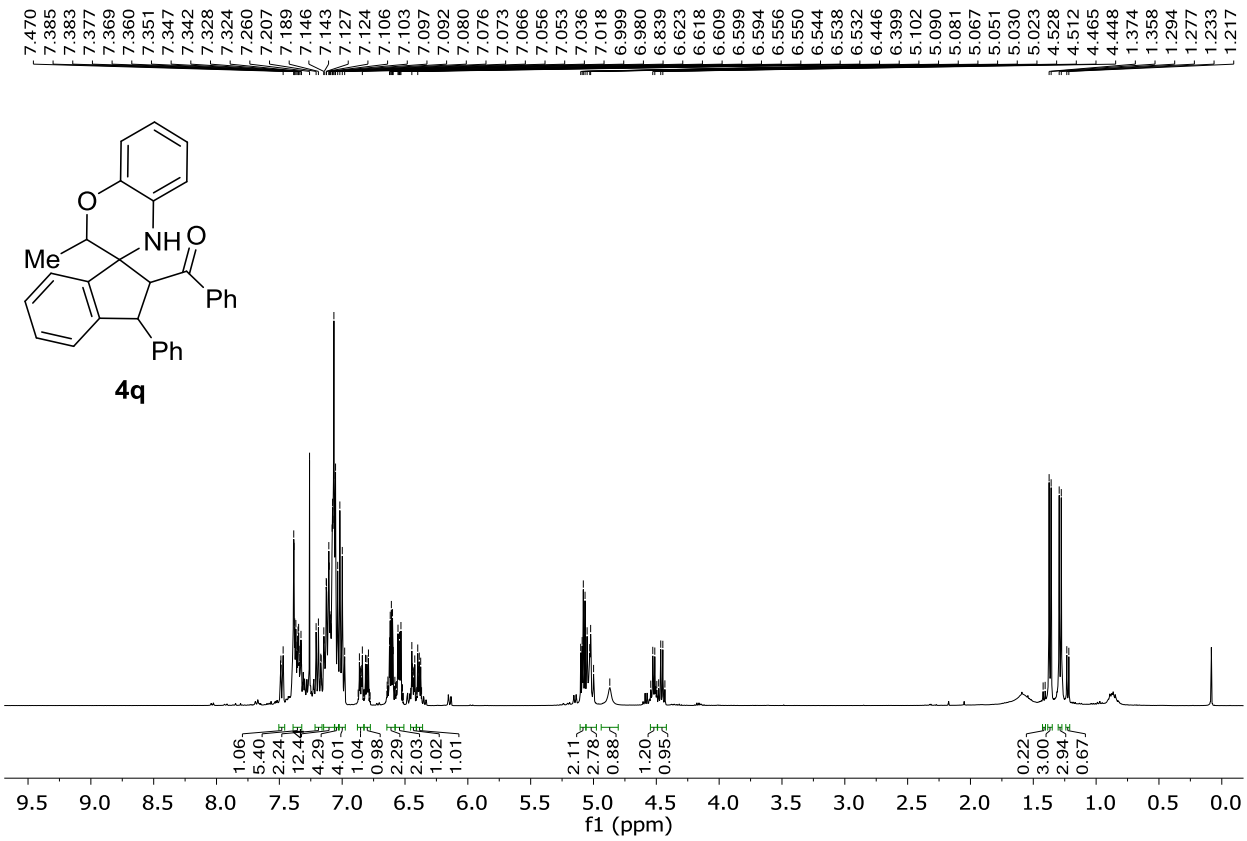

^{13}C NMR of **4q** (100 MHz, $CDCl_3$):

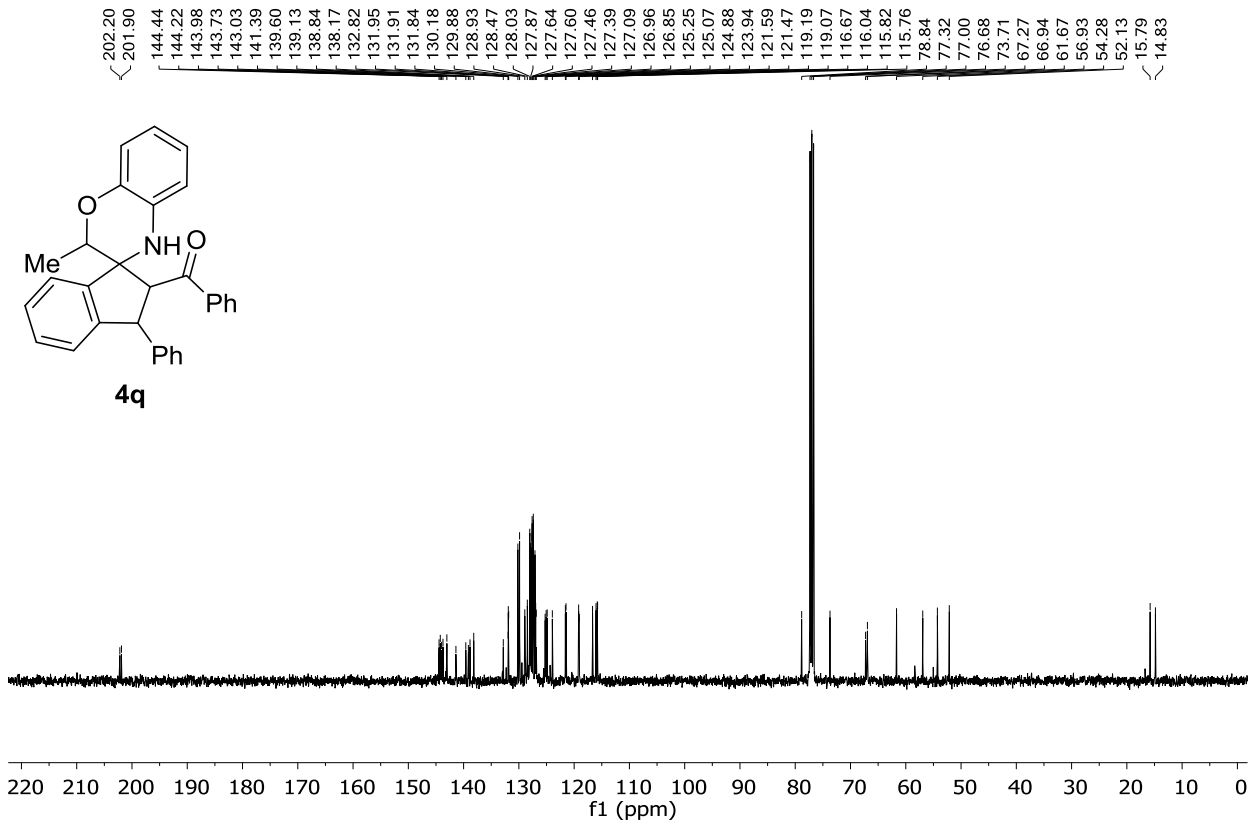

^{1}H NMR of **5** (400 MHz, $CDCl_3$):

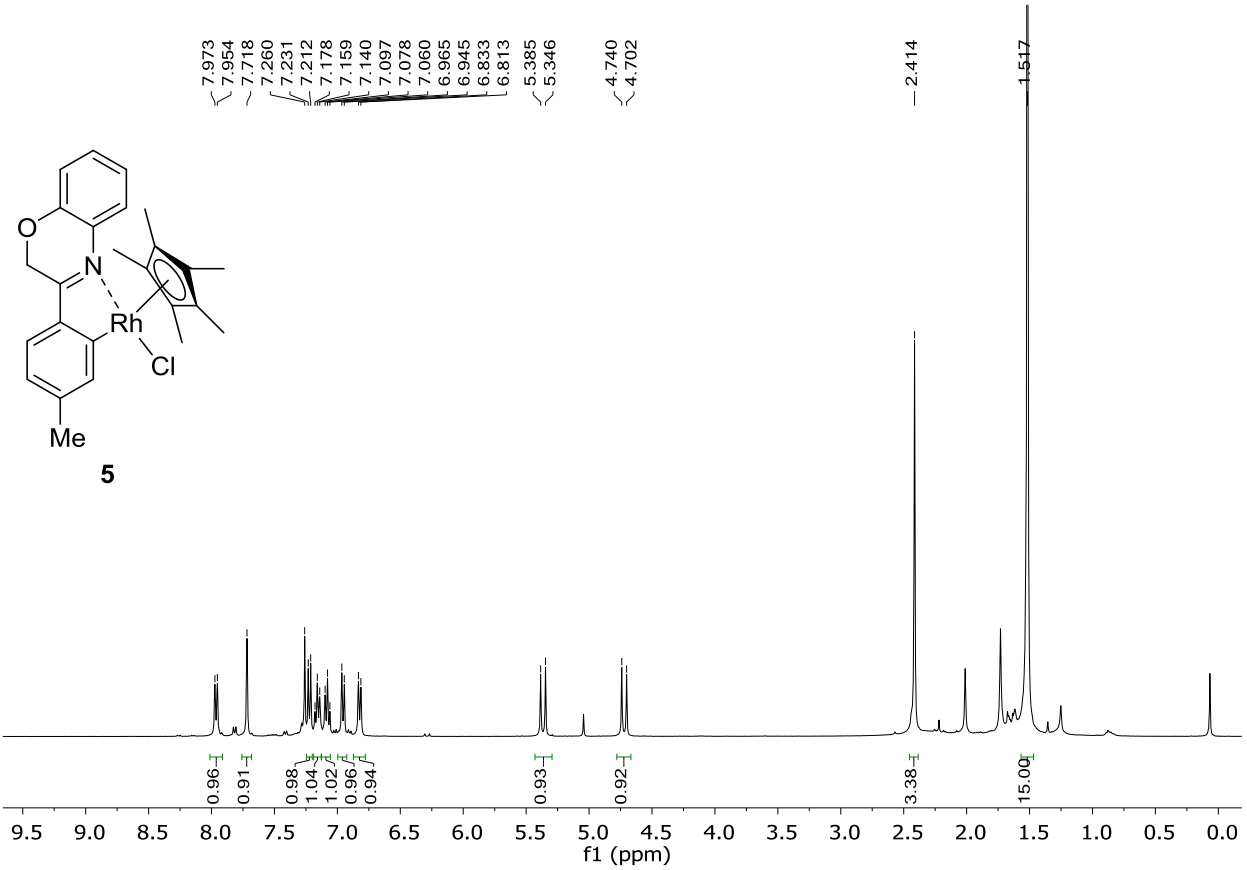

^{13}C NMR of **5** (100 MHz, $CDCl_3$):

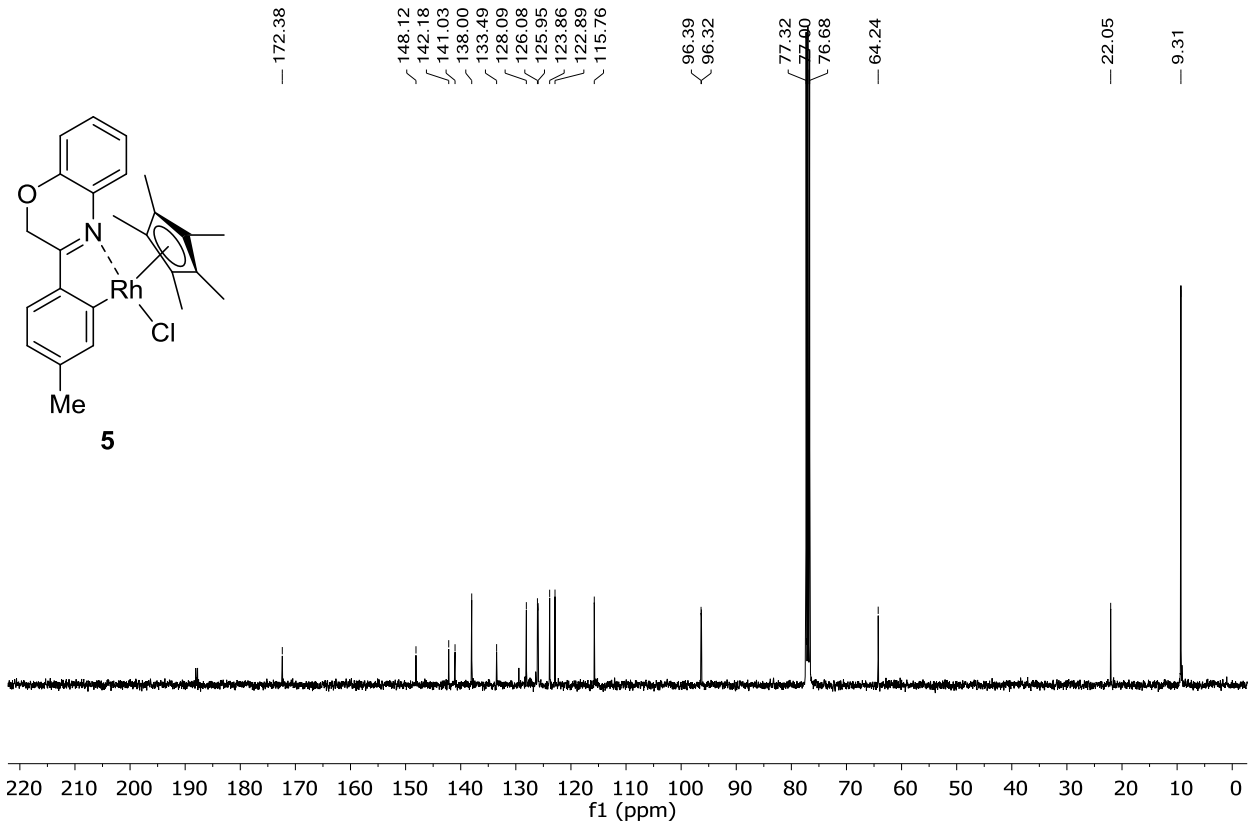

^{1}H NMR of **6** (400 MHz, $CDCl_3$):

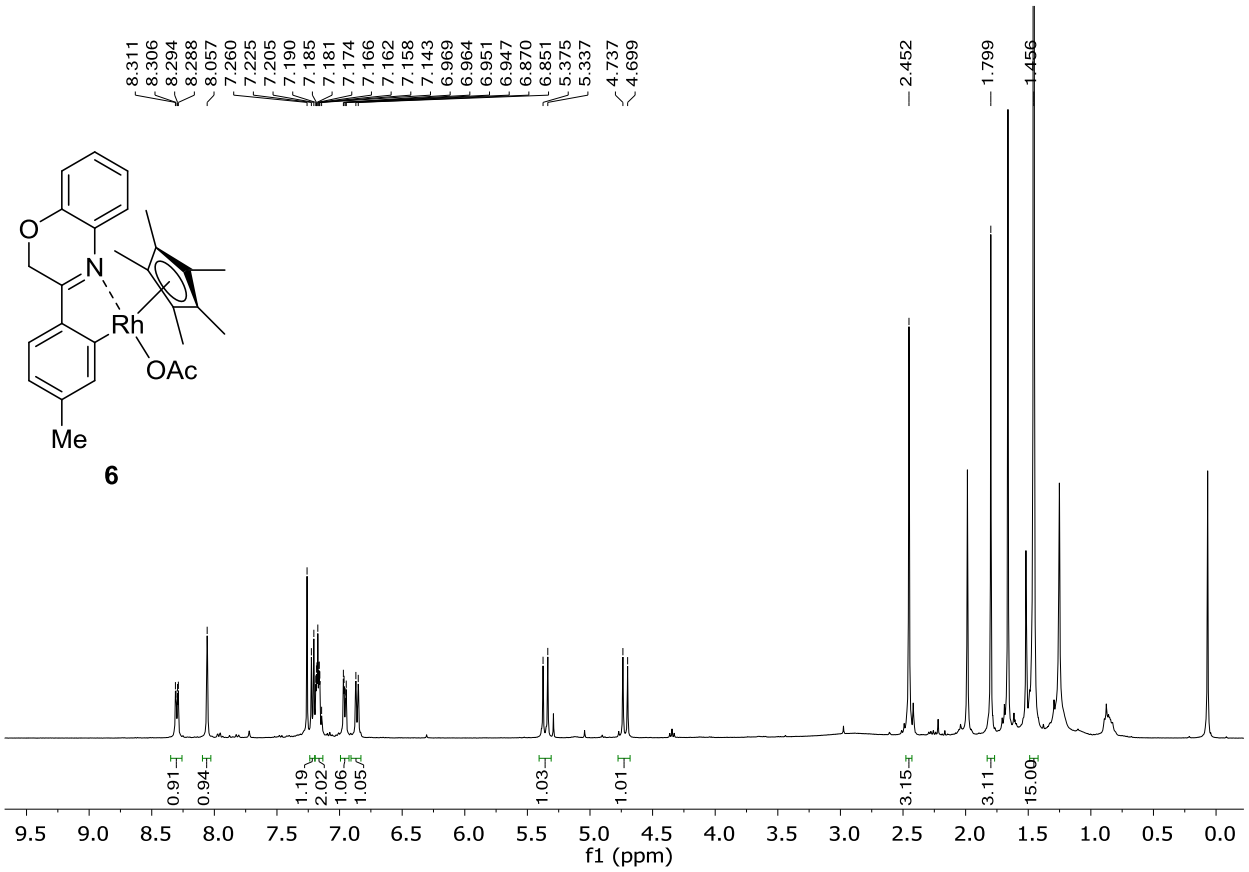

^{13}C NMR of **6** (100 MHz, $CDCl_3$):

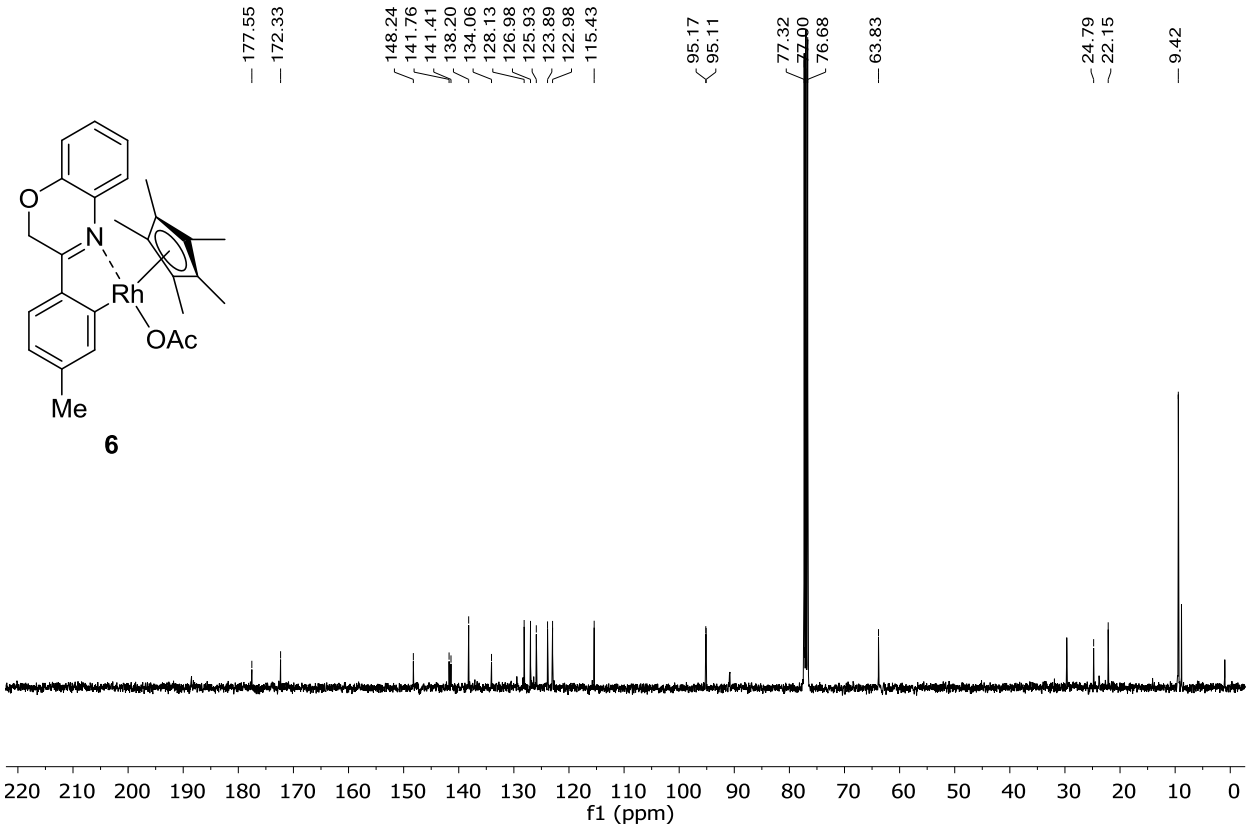

6.7. References

1. For selected reviews and examples, see: (a) Brown, K. S.; Djerassi, C. *J. Am. Chem. Soc.* **1964**, *86*, 2451. (b) Hayakawa, I.; Atarashi, S.; Yokohama, S.; Imamura, M.; Sakano, K.; Furukawa, M. *Antimicrob. Agents Chemother.* **1986**, *29*, 163. (c) Fu, K. P.; Lafredo, S. C.; Foleno, B.; Isaacson, D. M.; Barrett, J. F.; Tobia, A. J.; Rosenthale, M. E. *Antimicrob. Agents Chemother.* **1992**, *36*, 860. (d) Bourlot, A.-S.; Sánchez, I.; Dureng, G.; Guillaumet, G.; Massingham, R.; Monteil, A.; Winslow, E.; Pujol, M. D.; Mérour, J.-Y. *J. Med. Chem.* **1998**, *41*, 3142. (e) Ilaš, J.; Jakopin, Ž.; Borštnar, T.; Stegnar, M.; Kikelj, D. *J. Med. Chem.* **2008**, *51*, 5617. (f) Koini, E. N.; Papazafiri, P.; Vassilopoulos, A.; Koufaki, M.; Horváth, Z.; Koncz, I.; Virág, L.; Papp, G. J.; Varró, A.; Calogeropoulou, T. *J. Med. Chem.* **2009**, *52*, 2328. (g) Wang, A.; Prouty, C. P.; Pelton, P. D.; Yong, M.; Demarest, K. T.; Murray, W. V.; Kuo, G.-H. *Bioorg. Med. Chem. Lett.* **2010**, *20*, 1432. (h) Mathew, B. P.; Kumar, A.; Sharma, S.; Shukla, P. K.; Nath, M. *Eur. J. Med. Chem.* **2010**, *45*, 1502. (i) Waisser, K.; Petrlíková, E.; Peřina, M.; Klimešová, V.; Kuneš, J.; Palát, K.; Kaustová, J.; Dahse, H.-M.; Möllmann, U. *Eur. J. Med. Chem.* **2010**, *45*, 2719. (j) Ilić, M.; Kontogiorgis, C.; Hadjipavlou-Litina, D.; Ilaš, J.; Kikelj, D. *Bioorg. Med. Chem. Lett.* **2011**, *21*, 4705. (k) Matralis, A. N.; Katselou, M. G.; Nikitakis, A.; Kourounakis, A. P. *J. Med. Chem.* **2011**, *54*, 5583. (l) Sawaryn, C.; Landfester, K.; Taden, A. *Macromolecules* **2011**, *44*, 5650. (m) Blass, B. *ACS Med. Chem. Lett.* **2013**, *4*, 1020. (n) Liu, J.; Lu, X.; Xin, Z.; Zhou, C. *Langmuir* **2013**, *29*, 411. (o) Gacche, N.; Dawane, B. S. J. M. C. R. *Med. Chem. Res.* **2015**, *24*, 1077. (p) Konda, S.; Raparthi, S.; Bhaskar, K.; Munaganti, R. K.; Guguloth, V.; Nagarapu, L.; Akkewar, D. M. *Bioorg. Med. Chem. Lett.* **2015**, *25*, 1643. (q) Arslan, M.; Kiskan, B.; Yagci, Y. *Macromolecules* **2015**, *48*, 1329. (r) Roy, A.; Saha, D.; Mukherjee, A.; Talukdar, P. *Org. Lett.* **2016**, *18*, 5864. (s) Kirschbaum, S.; Landfester, K.; Taden, A. *Macromolecules* **2015**, *48*, 3811. (t) Sharma, P.; Lochab, B.; Kumar, D.; Roy, P. K. *ACS Sustainable Chem. Eng.* **2016**, *4*, 1085. (u) Sini, N. K.; Endo, T. *Macromolecules* **2016**, *49*, 8466. (v) Sharma, V.; Amarnath, N.; Shukla, S.; Ayana, R.; Kumar, N.; Yadav, N.; Kannan, D.; Sehrawat, S.; Pati, S.; Lochab, B.; Singh, S. *Bioorg. Med. Chem. Lett.* **2018**, *28*, 1629.
2. For selected reviews and examples, see: (a) Marson, C. M. *Chem. Soc. Rev.* **2011**, *40*, 5514. (b) Ahmed, N., Synthetic Advances in the Indane Natural Product Scaffolds as Drug Candidates: A Review. In *Studies in Natural Product Chemistry*; Atta-Ur-Rahaman, Ed.; Elsevier, 2016; Vol. 51, p. 383. (c) Prasher, P.; Sharma, M.

ChemistrySelect **2021**, *6*, 2658. (d) Bogeso, K. P.; Christensen, A. V.; Hyttel, J.; Liljefors, T. *J. Med. Chem.* **1985**, *28*, 1817. (e) Bertolini, G.; Vecchietti, V.; Mabilia, M.; Norcini, G.; Restelli, A.; Santangelo, F.; Villa, A. M.; Casagrande, C. *Eur. J. Med. Chem.* **1992**, *27*, 663. (f) Böhme, T. M.; Keim, C.; Kreutzmann, K.; Linder, M.; Dingermann, T.; Dannhardt, G.; Mutschler, E.; Lambrecht, G. *J. Med. Chem.* **2003**, *46*, 856. (g) McConathy, J.; Owens, M. J.; Kilts, C. D.; Malveaux, E. J.; Votaw, J. R.; Nemeroff, C. B.; Goodman, M. M. *Nuclear Med. Biol.* **2005**, *32*, 593. (h) Thiry, A.; Ledecq, M.; Cecchi, A.; Dogné, J.-M.; Wouters, J.; Supuran, C. T.; Masereel, B. *J. Med. Chem.* **2006**, *49*, 2743. (i) Macías, F. A.; Marín, D.; Oliveros-Bastidas, A.; Molinillo, J. M. G. *Nat. Prod. Rep.* **2009**, *26*, 478. (j) Ugliarolo, E. A.; Gagey, D.; Lantaño, B.; Moltrasio, G. Y.; Campos, R. H.; Cavallaro, L. V.; Moglioni, A. G. *Bioorg. Med. Chem. Lett.* **2012**, *20*, 5986. (k) Morales, A. R.; Frazer, A.; Woodward, A. W.; Ahn-White, H.-Y.; Fonari, A.; Tongwa, P.; Timofeeva, T.; Belfield, K. D. *J. Org. Chem.* **2013**, *78*, 1014. (l) Nagavelli, V. R.; Nukala, S. K.; Narsimha, S.; Battula, K. S.; Tangeda, S. J.; Reddy, Y. N. *Med. Chem. Res.* **2016**, *25*, 1781. (m) Gardelli, C.; Wada, H.; Ray, A.; Caffrey, M.; Llinas, A.; Shamovsky, I.; Tholander, J.; Larsson, J.; Sivars, U.; Hultin, L.; Andersson, U.; Sanganee, H. J.; Stenvall, K.; Leidvik, B.; Gedda, K.; Jinton, L.; Rydén Landergren, M.; Karabelas, K. *J. Med. Chem.* **2018**, *61*, 5974.

3. For selected reviews, see: Sames, D. *Science* **2006**, *312*, 67. (b) Chen, X.; Engle, K. M.; Wang, D.-H.; Yu, J.-Q. *Angew. Chem. Int. Ed.* **2009**, *48*, 5094. (c) Lyons, T. W.; Sanford, M. S. *Chem. Rev.* **2010**, *110*, 1147. (d) Ackermann, L. *Chem. Rev.* **2011**, *111*, 1315. (e) Wencel-Delord, J.; Dröge, T.; Liu, F.; Glorius, F. *Chem. Soc. Rev.* **2011**, *40*, 4740. (f) Gutekunst, W. R.; Baran, P. S. *Chem. Soc. Rev.* **2011**, *40*, 1976. (g) Yamaguchi, J.; Yamaguchi, A. D.; Itami, K. *Angew. Chem. Int. Ed.* **2012**, *51*, 8960. (h) Noisier, A. F. M.; Brimble, M. A. *Chem. Rev.* **2014**, *114*, 8775. (i) Yang, L.; Huang, H. *Chem. Rev.* **2015**, *115*, 3468. (j) Hartwig, J. F.; Larsen, M. A. *ACS Cent. Sci.* **2016**, *2*, 281. (k) Newton, C. G.; Wang, S.-G.; Oliveira, C. C.; Cramer, N. *Chem. Rev.* **2017**, *117*, 8908. (l) Hummel, J. R.; Boerth, J. A.; Ellman, J. A. *Chem. Rev.* **2017**, *117*, 9163. (m) Sambiagio, C.; Schönbauer, D.; Blieck, R.; Dao-Huy, T.; Pototschnig, G.; Schaaf, P.; Wiesinger, T.; Zia, M. F.; Wencel-Delord, J.; Besset, T.; Maes, B. U. W.; Schnürch, M. *Chem. Soc. Rev.* **2018**, *47*, 6603. (n) Gandeepan, P.; Müller, T.; Zell, D.; Cera, G.; Warratz, S.; Ackermann, L. *Chem. Rev.* **2019**, *119*, 2192. (o) Rej, S.; Ano, Y.; Chatani, N. *Chem. Rev.* **2020**, *120*, 1788. (p) Liu, B.; Romine, A. M.; Rubel, C. Z.; Engle, K. M.; Shi, B.-F. *Chem. Rev.* **2021**, *121*, 14957. (q) Dutta, U.; Maiti, S.; Bhattacharya, T.; Maiti,

D. *Science* **2021**, *372*, eabd5992. (r) Dalton, T.; Faber, T.; Glorius, F. *ACS Cent. Sci.* **2021**, *7*, 245. (s) Rogge, T.; Kaplaneris, N.; Chatani, N.; Kim, J.; Chang, S.; Punji, B.; Schafer, L. L.; Musaev, D. G.; Wencel-Delord, J.; Roberts, C. A.; Sarpong, R.; Wilson, Z. E.; Brimble, M. A.; Johansson, M. J.; Ackermann, L. *Nat. Rev. Methods Primers* **2021**, *1*, 43.

4. For selected reviews, see: (a) Colby, D. A.; Bergman, R. G.; Ellman, J. A. *Chem. Rev.* **2010**, *110*, 624. (b) Satoh, T.; Miura, M. *Chem. Eur. J.* **2010**, *16*, 11212. (c) Song, G.; Wang, F.; Li, X. *Chem. Soc. Rev.* **2012**, *41*, 3651. (d) Ackermann, L. *Acc. Chem. Res.* **2014**, *47*, 281. (e) Gulías, M.; Mascareñas, J. L. *Angew. Chem. Int. Ed.* **2016**, *55*, 11000. (f) Yang, Y.; Li, K.; Cheng, Y.; Wan, D.; Li, M.; You, J. *Chem. Commun.* **2016**, *52*, 2872. (g) Prakash, S.; Kuppusamy, R.; Cheng, C.-H. *ChemCatChem* **2018**, *10*, 683. (h) Satoh, T.; Miura, M. **2019**, *Rhodium Catalysis in Organic Synthesis: Methods and Reactions* (Ed.: K. Tanaka), Wiley-VCH, Weinheim, 2019, p. 487. (i) Nishii, Y.; Miura, M. *ACS Catal.* **2020**, *10*, 9747. (j) Song, L.; Van der Eycken, E. V. *Chem. Eur. J.* **2021**, *27*, 121. (k) Wang, C.; Chen, F.; Qian, P.; Cheng, J. *Org. Biomol. Chem.* **2021**, *19*, 1705.
5. For representative examples, see: (a) Kuninobu, Y.; Kawata, A.; Takai, K. *J. Am. Chem. Soc.* **2005**, *127*, 13498. (b) Kuninobu, Y.; Tokunaga, Y.; Kawata, A.; Takai, K. *J. Am. Chem. Soc.* **2006**, *128*, 202. (c) Kuninobu, Y.; Yu, P.; Takai, K. *Org. Lett.* **2010**, *12*, 4274.
6. For representative examples, see: (a) Fukutani, T.; Umeda, N.; Hirano, K.; Satoh, T.; Miura, M. *Chem. Commun.* **2009**, 5141. (b) Sun, Z.-M.; Chen, S.-P.; Zhao, P. *Chem. Eur. J.* **2010**, *16*, 2619. (c) Tran, D. N.; Cramer, N. *Angew. Chem. Int. Ed.* **2010**, *49*, 8181. (d) Dong, L.; Qu, C.-H.; Huang, J.-R.; Zhang, W.; Zhang, Q.-R.; Deng, J.-G. *Chem. Eur. J.* **2013**, *19*, 16537. (e) Chen, Y.; Wang, F.; Zhen, W.; Li, X. *Adv. Syn. Catal.* **2013**, *355*, 353. (f) Huang, J.-R.; Song, Q.; Zhu, Y.-Q.; Qin, L.; Qian, Z.-Y.; Dong, L. *Chem. Eur. J.* **2014**, *20*, 16882. (g) Huang, J.-R.; Qin, L.; Zhu, Y.-Q.; Song, Q.; Dong, L. *Chem. Commun.* **2015**, *51*, 2844. (h) Mei, S.-T.; Liang, H.-W.; Teng, B.; Wang, N.-J.; Shuai, L.; Yuan, Y.; Chen, Y.-C.; Wei, Y. *Org. Lett.* **2016**, *18*, 1088. (i) Liu, B.; Hu, P.; Zhang, Y.; Li, Y.; Bai, D.; Li, X. *Org. Lett.* **2017**, *19*, 5402. (j) Han, S. H.; Mishra, N. K.; Jeon, M.; Kim, S.; Kim, H. S.; Jung, S.-Y.; Jung, Y. H.; Ku, J.-M.; Kim, I. S. *Adv. Syn. Catal.* **2017**, *359*, 3900. (k) Sharma, S.; Oh, Y.; Mishra, N. K.; De, U.; Jo, H.; Sachan, R.; Kim, H. S.; Jung, Y. H.; Kim, I. S. *J. Org. Chem.* **2017**, *82*, 3359. (l) Chaudhary, B.; Auti, P.; Shinde, S. D.; Yakkala, P. A.; Giri, D.; Sharma, S. *Org. Lett.* **2019**, *21*, 2763. (m) Zhang, J.; Sun, J.-S.; Xia, Y.-Q.; Dong, L. *Adv. Syn. Catal.* **2019**, *361*, 2037. (n) Luo, Y.; Liu,

H.; Zhang, J.; Liu, M.; Dong, L. *Org. Lett.* **2020**, *22*, 7604. (o) Zhang, Y.; Huang, T.; Li, X.; Zhang, M.; Song, Y.; Huang, K.; Su, W. *RSC Adv.* **2020**, *10*, 22216.

7. For representative examples, see: (a) Zhao, P.; Wang, F.; Han, K.; Li, X. *Org. Lett.* **2012**, *14*, 5506. (b) Zhang, J.; Ugrinov, A.; Zhao, P. *Angew. Chem. Int. Ed.* **2013**, *52*, 6681. (c) Hung, C.-H.; Gandeepan, P.; Cheng, C.-H. *ChemCatChem* **2014**, *6*, 2692. (d) Song, Z.; Yang, Z.; Wang, P.; Shi, Z.; Li, T.; Cui, X. *Org. Lett.* **2020**, *22*, 6272.
8. For representative examples, see: (a) Nishimura, T.; Ebe, Y.; Hayashi, T. *J. Am. Chem. Soc.* **2013**, *135*, 2092. (b) Li, S.-S.; Wu, L.; Qin, L.; Zhu, Y.-Q.; Su, F.; Xu, Y.-J.; Dong, L. *Org. Lett.* **2016**, *18*, 4214. (c) Mishra, A.; Mukherjee, U.; Sarkar, W.; Meduri, S. L.; Bhowmik, A.; Deb, I. *Org. Lett.* **2019**, *21*, 2056.
9. (a) Liu, H.; Li, J.; Xiong, M.; Jiang, J.; Wang, J. *J. Org. Chem.* **2016**, *81*, 6093. (b) Dey, A.; Volla, C. M. R. *Org. Lett.* **2021**, *23*, 5018.
10. Liu, W.; Zell, D.; John, M.; Ackermann, L. *Angew. Chem. Int. Ed.* **2015**, *54*, 4092.
11. For selected examples, see: (a) Tran, D. N.; Cramer, N. *Angew. Chem. Int. Ed.* **2011**, *50*, 11098. (b) Tran, D. N.; Cramer, N. *Angew. Chem. Int. Ed.* **2013**, *52*, 10630. (c) Nishimura, T.; Nagamoto, M.; Ebe, Y.; Hayashi, T. *Chem. Sci.* **2013**, *4*, 4499. (d) Pham, M. V.; Cramer, N. *Chem. Eur. J.* **2016**, *22*, 2270. (e) Nagamoto, M.; Sakamoto, K.; Nishimura, T. *Adv. Syn. Catal.* **2018**, *360*, 791.
12. (a) Zhu, C.; Luan, J.; Fang, J.; Zhao, X.; Wu, X.; Li, Y.; Luo, Y. *Org. Lett.* **2018**, *20*, 5960. (b) Mishra, A.; Bhowmik, A.; Samanta, S.; Sarkar, W.; Das, S.; Deb, I. *Org. Lett.* **2020**, *22*, 1340. (c) Shi, Y.; Fang, Y.; Zhao, X.; Zhu, C.; Wu, X.; Yang, X.; Luo, Y. *Org. Lett.* **2020**, *22*, 4903. (d) Tan, H.; Laishram, R. D.; Zhang, X.; Shi, G.; Li, K.; Chen, J. *Eur. J. Org. Chem.* **2020**, *2020*, 4542.
13. For selected reviews and examples, see: (a) Singh, P.; Anand, A.; Kumar, V. *Eur. J. Med. Chem.* **2014**, *85*, 758. (b) Rozmer, Z.; Perjési, P. *Phytochem. Rev.* **2016**, *15*, 87. (c) Saxena, H. O.; Faridi, U.; Kumar, J. K.; Luqman, S.; Darokar, M. P.; Shanker, K.; Chanotiya, C. S.; Gupta, M. M.; Negi, A. S. *Steroids* **2007**, *72*, 892. (d) Zhuang, C.; Zhang, W.; Sheng, C.; Zhang, W.; Xing, C.; Miao, Z. *Chem. Rev.* **2017**, *117*, 7762. (e) Niu, C.; Tuerxuntayi, A.; Li, G.; Kabas, M.; Dong, C.-Z.; Aisa, H. A. *Chin. Chem. Lett.* **2017**, *28*, 1533. (f) Rammohan, A.; Reddy, J. S.; Sravya, G.; Rao, C. N.; Zyryanov, G. V. *Environ. Chem. Lett.* **2020**, *18*, 433.
14. For representative examples, see: (a) Yang, L.; Qian, B.; Huang, H. *Chem. Eur. J.* **2012**, *18*, 9511. (b) Yoshino, T.; Ikemoto, H.; Matsunaga, S.; Kanai, M. *Angew. Chem. Int. Ed.* **2013**, *52*, 2207.

15. (a) Engle, K. M.; Mei, T.-S.; Wasa, M.; Yu, J.-Q. *Acc. Chem. Res.* **2012**, *45*, 788. (b) De Sarkar, S.; Liu, W.; Kozhushkov, S. I.; Ackermann, L. *Adv. Syn. Catal.* **2014**, *356*, 1461.
16. Sabitha, M. G.; Rao, A. V. S. *Synth. Commun.* **1987**, *17*, 341.
17. (a) Zhang, X.; Kang, J.; Niu, P.; Wu, J.; Yu, W.; Chang, J. *J. Org. Chem.* **2014**, *79*, 10170. (b) Yu, W.; Goddard, C.; Clearfield, E.; Mills, C.; Xiao, T.; Guo, H.; Morrey, J. D.; Motter, N. E.; Zhao, K.; Block, T. M.; Cuconati, A.; Xu, X. *J. Med. Chem.* **2011**, *54*, 5660. (c) Bashary, R.; Khatik, G. L. *Bioorg. Chem.* **2019**, *82*, 156. (d) Katila, P.; Shrestha, A.; Shrestha, A.; Shrestha, R.; Park, P.-H.; Lee, E.-S. *Bioorg. Chem.* **2019**, *87*, 495. (e) Onishi, Y.; Yoneda, Y.; Nishimoto, Y.; Yasuda, M.; Baba, A. *Org. Lett.* **2012**, *14*, 5788. (f) Arenas-González, A.; Mendez-Delgado, L. A.; Merino-Montiel, P.; Padrón, J. M.; Montiel-Smith, S.; Vega-Báez, J. L.; Meza- Reyes, S. *Steroids* **2016**, *116*, 13. (g) da Costa, R. G. M.; Farias, F. R. L.; Back, D.; Limberger, J. *Tetrahedron Lett.* **2018**, *59*, 771.
18. Li, L.; Brennessel, W. W.; Jones, W. D. *Organometallics* **2009**, *28*, 3492.

Chapter 7: Iridium || Arylation

Iridium-Catalyzed Direct C–H Arylation of Cyclic *N*-Sulfonyl Ketimines with Arylsiloxanes at Ambient Temperature

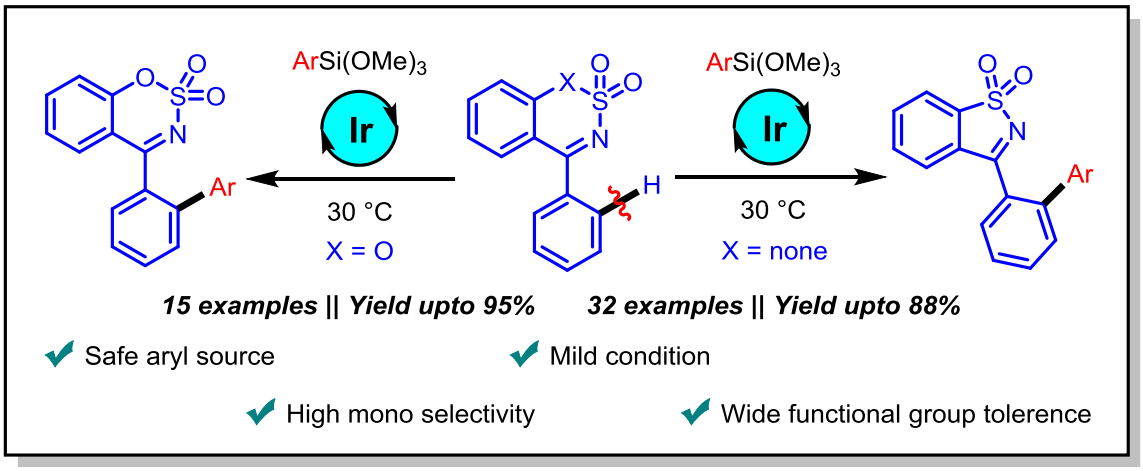

7.1. Introduction

7.1.1. Relevance of Biaryls and *N*-Sulfonyl Ketimines and Benzosultams

The biaryl framework is one of the most privileged scaffolds in synthetic organic chemistry. It is an important substructure of many bioactive scaffolds and functional molecules. This biaryl core is known to be present in many commercially available drugs and medicinally important compounds, *viz.* antitumor, anti-hypertensive, antibiotic, anticancer, anti-inflammatory, antifungal, anti-atherosclerotic agents, among others.[1] The biphenyl substructure constitutes 4.3% of all known drugs.[2] Owing to its aromatic nature, it shows versatility in binding interactions and diversity in receptor selectivity, thus making it an integral part of the pharmaceutical industry.

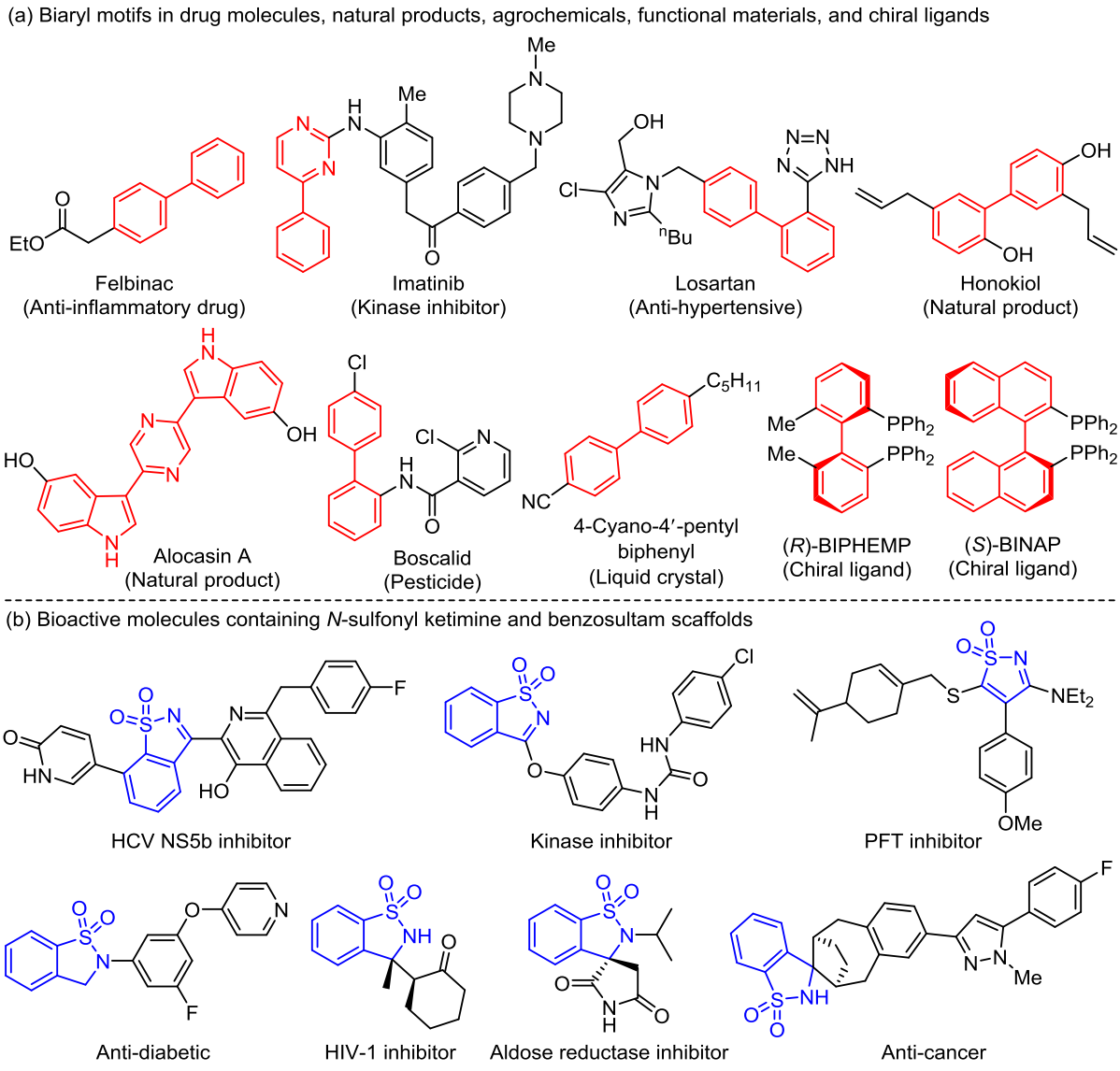

Figure 7.1.1.1. Representative examples of biologically relevant compounds.

Also, biaryl motifs are ubiquitous in natural products, agrochemicals, liquid crystal displays, and are also incorporated into molecular motors and switches. In addition, they also constitute many chiral ligands and catalysts commonly used in organic synthesis.[3] Some of the biologically and synthetically important biaryl fragment containing molecules is depicted in Figure 7.1.1.1a. Consequently, in the dimension of C–C bond formation reactions in synthetic organic chemistry, the construction of biaryl compounds has always been one of the top targets for organic chemists all over the world.

On the flip side, functionalized cyclic *N*-sulfonyl ketimine motifs[4] are another class of compounds with unique structural architecture widely prevalent in many biologically active compounds including potential inhibitors against Hepatitis-C virus NS5b, the protein kinase, the protein farnesyltransferase (PFT), human leukocyte elastase, and others (Figure 7.1.1.1b).[5] They also appear to be an essential precursor for the synthesis of sultams, a class of (benzo)fused cyclic sulfonamides via various routes like, hydrogenation, annulation, nucleophilic addition, and Michael addition reactions, among others, and also in an enantioselective fashion.[6] The most popular example of this class of compounds is 1,2-benzisothiazoline 1,1-dioxide or saccharin, commonly used as an artificial sweetener with a food energy value of almost nil.[7] Functionalized benzosultams are also medicinally important heterocyclic scaffolds and found to have diverse therapeutic applications with a borad range of biological activities including anti-HIV, antiallergic (CRTh2 antagonists), anticancer (kinase and γ-secretase inhibitor), antibacterial, anti-diabetic and aldose reductase inhibitory properties, among others (Figure 7.1.1.1b).[8] In addition to their biological efficacy, benzosultams are enriched with vast synthetic utility in terms of being common synthons for the synthesis of complex molecules as well as chiral auxiliaries in asymmetric synthesis.[9]

7.1.2. Strategies For Transition Metal-Catalyzed C–H Arylation

These fundamental importances of the biaryl motif have encouraged the organic chemistry fraternity to build them among the C–C bond formation protocols. In this realm, as discussed in Chapter 1, Section 1.1, several transition metal-catalyzed homocoupling and cross-coupling reactions, *viz.* Ullmann reaction (symmetrical biaryls), and Suzuki-Miyaura, Stille, Negishi, Corriu-Kumada, Hiyama coupling, etc. (unsymmetrical biaryls) have been extensively employed.[10] These strategies use organohalides (I, Br, Cl) or organotriflates (OTf) to couple with organometallic reagents (B, Sn, Zn, Mg, Si, etc.) to furnish biaryl compounds. Also, Grignard reagents have been utilized for their generation in an unsymmetrical manner.[11]

Although these traditional approaches provide high yields and selectivity, but they still suffer from a number of drawbacks including pre-functionalization/pre-activation of both substrates and coupling partners thereby increasing the overall number of steps due to its installation which may show regioselectivity issues and also generates a lot of toxic waste from the use of activating agents and their disposal. To overcome these shortcomings, chemists all over the world in tandem with pharmaceutical industries have looked upon C–H activation as one of the most wanted routes to synthesize these kinds of compounds in a more environmentally benign, atom and step-economic and cost-effective manner.[12]

In this context, over the last two decades, transition metal-catalyzed direct arylation of activated as well as unactivated C–H bonds has come to the forefront for the installation of aryl motifs in diverse molecules.[13] In this way, chemists have been able to build C(sp^3)–aryl, C(sp)–aryl, and more commonly C(sp^2)–aryl bonds easily from readily available chemical feedstocks taking advantage of the ubiquitous nature of C–H bonds. Directing groups have also been explored in this regime for the site-selective arylation of different compounds. Direct C–H arylation has seen a range of arylating sources used in a judicious manner. These include aryl halides, arylboronic acids, aryldiazonium salts, diaryliodonium triflate salts, aryltrifluoroborate salts, simple arenes and heteroarenes, among others.

As discussed above, over the years, Hiyama cross-coupling has been recognized as one of the most robust techniques for C–C bond formation and introducing aryl moieties in organic molecules. The use of organosilicon reagents provides a plethora of synthetic advantages over the commonly used conventional aryl sources like organoboranes, other organometallic nucleophiles, and others in terms of low toxicity, environmental benignity, ready availability, high stability, easy handling, cost effectiveness, controllable reactivity, ease of introduction into substrates, wide scope and excellent functional group compatibility.[10c,14] Despite the supremacy of organosilicon reagents over its counterparts, their use in direct C–H arylation reactions has been less investigated owing to its relatively lower nucleophilicity.

In recent years, a handful of reports have appeared on transition metal-catalyzed C–H arylation using arylsiloxanes as organosilicon-based aryl source limited to Pd,[15] Rh,[16] Ru,[17] Ni,[18] and Co[19] catalysis only. Some of these notable contributions are depicted in Scheme 7.1.2.1. In 2007, Shi group developed the first palladium-catalyzed amide-directed *ortho* C–H arylation of acetanilides using trialkoxyarylsilanes as arylating agent (Scheme 7.1.2.1a).[15a] Two years later, Loh and co-workers extended the concept to cyclic enamides to produce aryl substituted

enamide derivatives in good yields (Scheme 7.1.2.1b).[15b] In 2010, Zhang *et al.* achieved a Pd-catalyzed cross-coupling between indoles and arylsiloxanes through C–H functionalization reaction under mild reaction conditions in an acidic medium (Scheme 7.1.2.1c).[15c] Following year, Sun group reported *ortho* arylation of 2-arylpyridines with arylsiloxanes using a catalytic system of $Pd(OAc)_2$/AgF/BQ (Scheme 7.1.2.1d).[15d] In 2015, Yu and co-workers demonstrated for the first time a Pd-catalyzed β-C(sp^3)–H arylation of carboxylic acid derivatives with arylsilanes which required a quinoline-based ligand (Scheme 7.1.2.1e).[15h] Wang *et al.* described a C7-arylation protocol of indolines utilizing the weakly directing keto-carbonyl DG, which could be conveniently transformed to C7-arylated indoles under palladium catalysis (Scheme 7.1.2.1f).[15i]

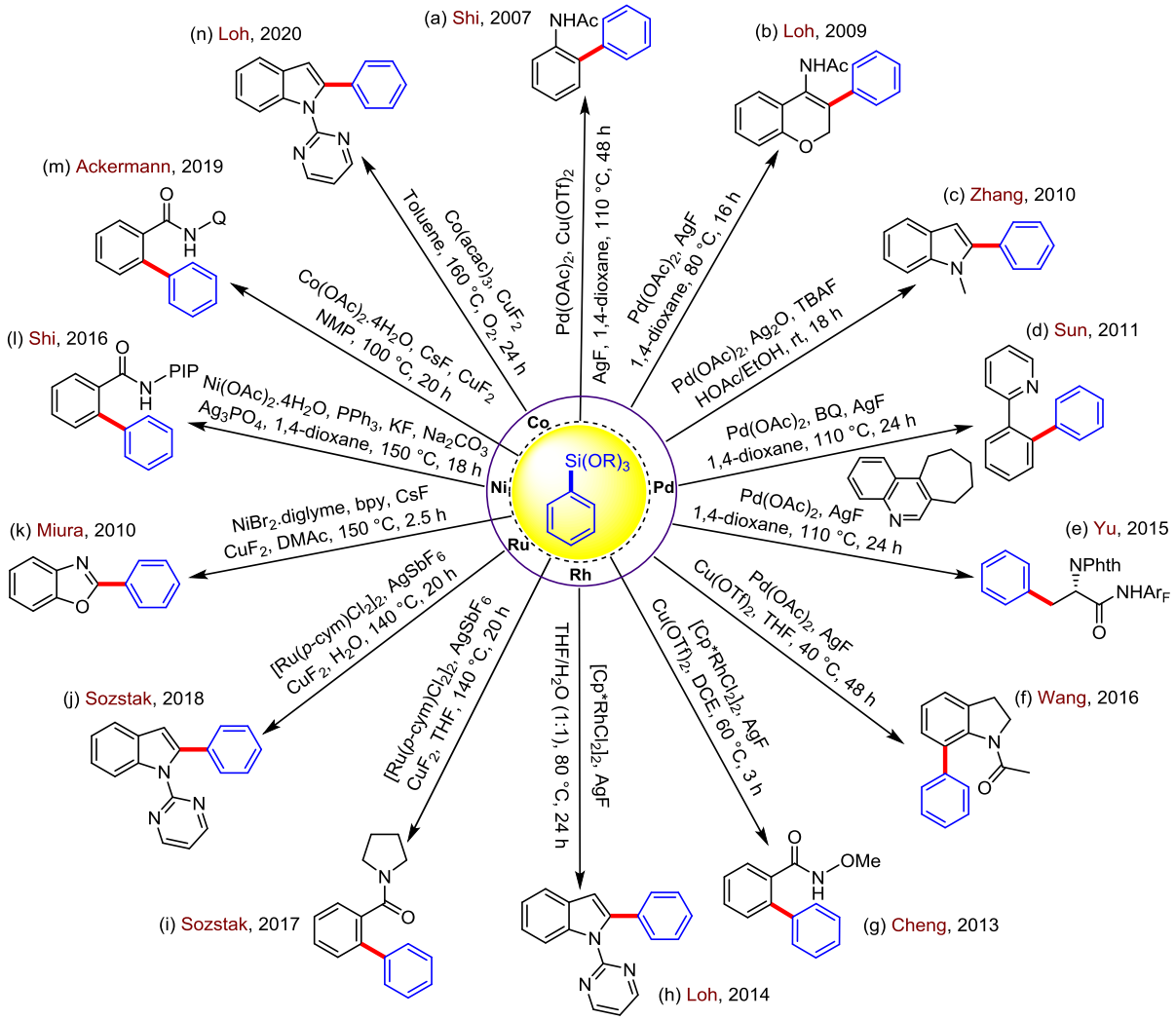

Scheme 7.1.2.1. Transition metal-catalyzed direct C–H arylation using arylsiloxanes.

Moving to rhodium catalysis, in 2013, Cheng *et al.* developed a one-pot strategy to furnish substituted phenanthridinones from *N*-methoxybenzamides and arylsiloxanes via dual

C–H/N–H bond activation employing Rh catalysis (Scheme 7.1.2.1g).[16a] Next year, Loh and co-workers devised a Rh(III)-catalyzed direct and regioselective arylation of (hetero)arenes with organosilanes in aqueous media (Scheme 7.1.2.1h).[16b] Ruthenium catalysis employing organosilanes was first reported by Szostak in 2017, when they showcased an oxidative cross-coupling between challenging weakly coordinating cyclic and *N*,*N*-dialkyl benzamides with arylsiloxanes as aryl source (Scheme 7.1.2.1i).[17a] The same group described a Ru(II)-catalyzed C2-selective arylation of indoles with arylsilanes in water/aqueous media as a sustainable solvent in C–H functionalization (Scheme 7.1.2.1j).[17c]

Apart from noble metals, earth abundant first-row transition metal catalysis has also been employed for direct C–H arylation reactions with organosilicon sources. In 2010, Miura and co-workers delineated a Ni-catalyzed Hiyama-type cross-coupling for the direct arylation activated C–H bonds of heteroarenes with organosilanes leading to π-extended heterocycles (Scheme 7.1.2.1k).[18a] In 2016, Shi *et al.* reported a Ni(II)-catalyzed *ortho* arylation of bidentate PIP-directed (hetero)arylamides with arylsiloxanes featuring a broad substrate scope with good functional group tolerability (Scheme 7.1.2.1l).[18b] Recently, cobalt catalysis has entered the picture, when Ackermann group demonstrated an unprecedented Co-catalyzed Hiyama-type C–H arylation of 8-aminquinoline tethered benzamides with organosiloxanes (Scheme 7.1.2.1m).[19a] Challenging sp^3 C–H arylation could also be performed using biomass-derived GVL as solvent. In 2020, Loh and co-workers reported a C2-arylation of indoles with diverse (hetereo)arylsilanes employing cobalt catalysis making use of copper(II) fluoride as a bifunctional silane activator and catalyst re-oxidant (Scheme 7.1.2.1n).[19b]

Although chelation assisted C–H arylation has made tremendous grounds in recent years, these established protocols suffer from some major drawbacks, *viz.* need for higher temperatures, prolonged reaction time, and the requirement of strongly coordinating groups in most cases. These stumbling blocks were recently minimized of late by employing iridium catalysis.[20] Chang group, for the first time, devised a new methodology for Ir-catalyzed direct C–H arylation of diverse directing arenes with arylsiloxanes as a nucleophilic aryl donor under mild reaction conditions featuring a wide scope synthesizing value-added molecules in good yields (Scheme 7.1.2.2).[20a] They have performed a number of mechanistic experiments to have a thorough understanding of the reaction pathway.

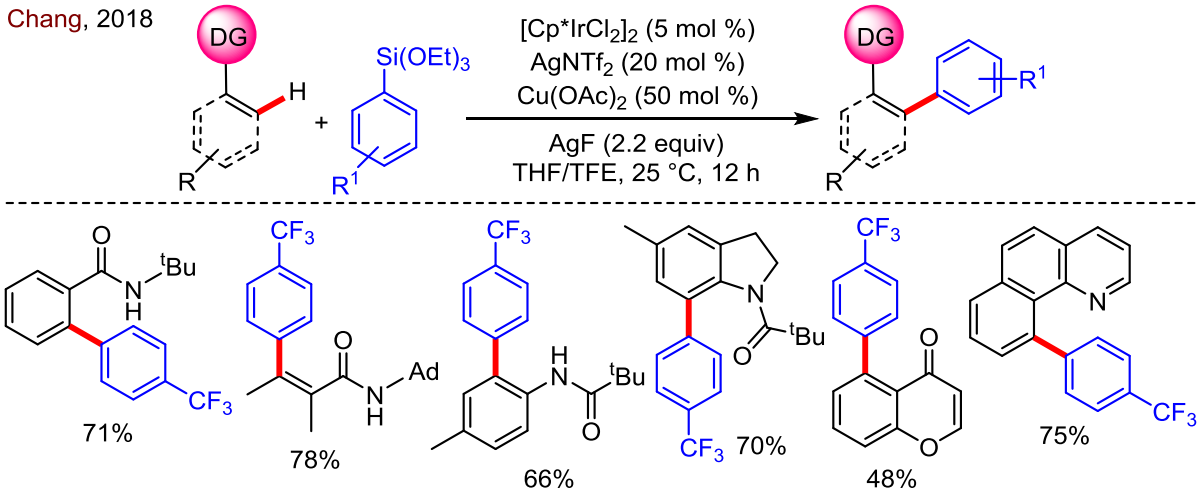

Scheme 7.1.2.2. Iridium-catalyzed C–H arylation with arylsiloxanes.

7.1.3. Cyclic *N*-Sulfonyl Ketimines as Directing Group in C–H Activation

Cyclic *N*-sulfonyl ketimines are a unique class of ketimines with a plethora of biological as well as synthetic utilities in organic chemistry as discussed in Section 7.1.1. They are used in various important transformations, but their application as a directing group in transition metal-catalyzed C–H activation has been largely limited and only a handful number of reports have surfaced for their direct C–H functionalization.[21] One of the primary reasons for the dearth of interest in them can be attributed to the weakly coordinating nature of the iminyl nitrogen atom due to the presence of neighbouring sulfonyl group. Some of these notable works are depicted in Scheme 7.1.3.1 and discussed below.

In 2013, Nishimura group first reported a [3+2]-annulation via C–H functionalization between cyclic *N*-sulfonyl ketimines and 1,3-dienes under Ir(I) catalysis (Scheme 7.1.3.1a).[21a] This methodology gives access to aminoindane derivatives in high yields and with good regio- and diastereoselectivity. Dong and co-workers disclosed a Rh(III)-catalyzed Grignard-type [3+2]-spiroannulation of cyclic ketimines with internal alkynes to synthesize challenging spirocyclic sultams (Scheme 7.1.3.1b).[21b] In 2014, Wei *et al.* achieved *ortho* olefination of cyclic *N*-sulfonyl ketimines with a range of alkenes employing rhodium catalysis (Scheme 7.1.3.1c).[21c] Concurrently, Dong group devised a Rh-catalyzed tandem three-component cyclization reaction of imines, alkynes and aldehydes furnishing polycyclic skeletons with high stereo- and regioselectivity (Scheme 7.1.3.1d).[21e] Following year, Wei and co-workers described a Rh(III)-catalyzed *ortho* C–H allylation of *N*-sulfonyl ketimines with allyl carbonates via an olefin insertion/β-oxygen elimination reaction steps sequence (Scheme 7.1.3.1e).[21f] Jeganmohan *et*

al. delineated a direct amidation protocol using organic sulfonyl azides under ruthenium-catalyzed oxidative conditions (Scheme 7.1.3.1f).[21k] Wei group developed a Cp*Rh(III)-catalyzed approach to spirocyclic sultams and heterobiaryls through cross-dehydrogenative coupling of *N*-sulfonylimines and thiophenes or furans (Scheme 7.1.3.1g).[21h]

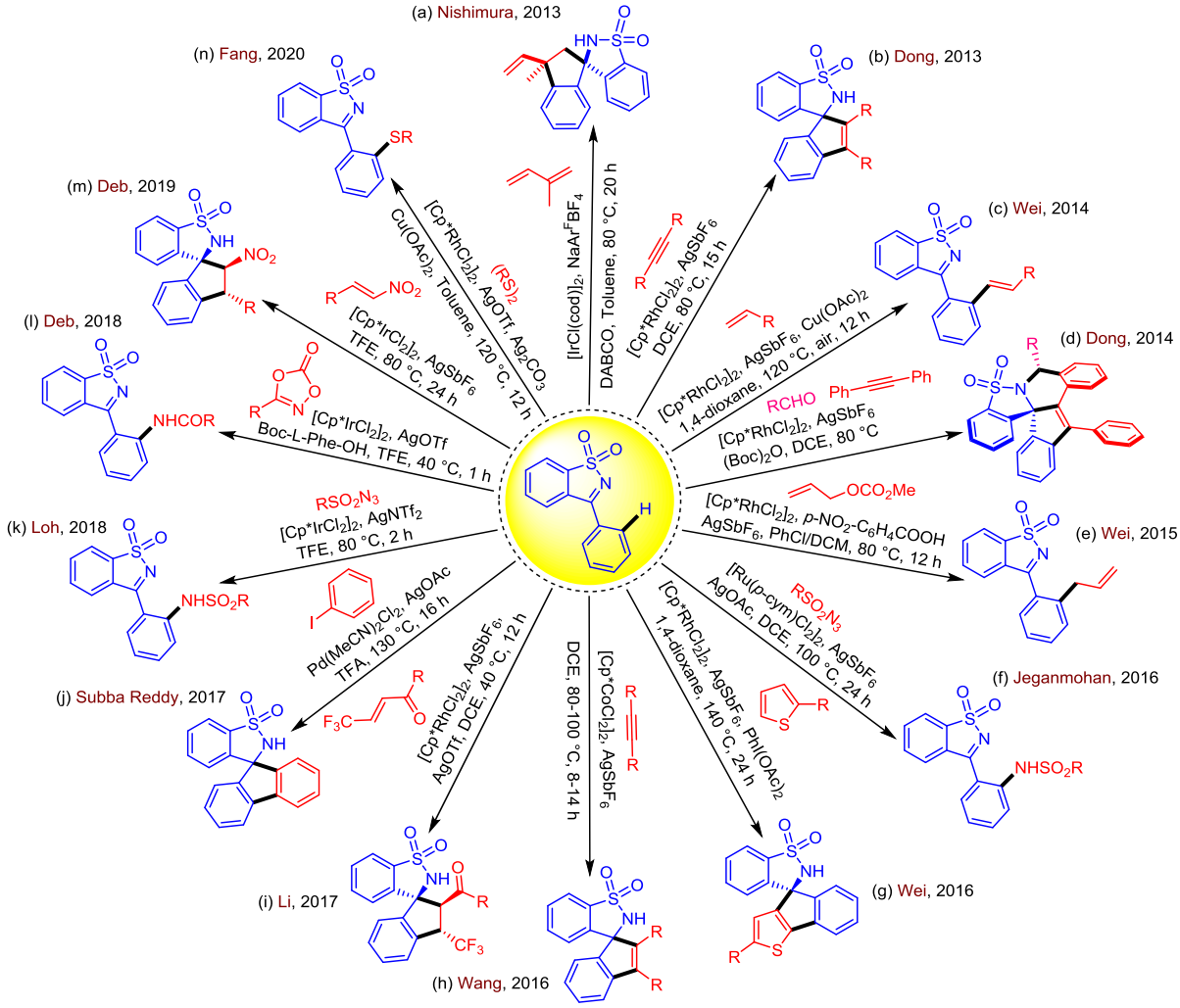

Scheme 7.1.3.1. Cyclic *N*-sulfonyl ketimine as DG in C–H functionalizations.

Wang group employed Cp*Co(III) catalysis for cascade [3+2]-spiroannulation between cyclic *N*-sulfonyl ketimines and alkynes to produce an array of spiro-indenyl benzosultams (Scheme 7.1.3.1h).[21j] In 2017, Li *et al.* realized a redox-neutral diastereodivergent [3+2]-spiroannulation of *N*-sulfonyl ketimines with activated alkenes under Rh-catalyzed mild reaction conditions (Scheme 7.1.3.1i).[21l] Subba Reddy and co-workers developed a strategy for making spirofluorenyl benzosultams from sulfonyl ketimines and aryl iodides via a Pd-catalyzed spiroannulation reaction (Scheme 7.1.3.1j).[21m] In 2018, Loh group reported an iridium-catalyzed direct amidation of cyclic *N*-sulfonyl ketimines with a series of organic azides as

C–N bond forming reagents accompanying high chemo- and regioselectivity (Scheme 7.1.3.1k).[21n] During the same time, Deb *et al.* realized an Ir(III)-catalyzed mild amidation protocol of cyclic ketimines with dioxazolones as a robust amidating agent accelerated by the presence of mono protected-L-amino acid (Scheme 7.1.3.1l).[21o] Next year, they described a [3+2]-annulation of cyclic *N*-sulfonyl ketimines with nitroalkenes under iridium-catalyzed redox-neutral conditions delivering spirocycles with three consecutive stereogenic centers (Scheme 7.1.3.1m).[21r] In 2020, Fan group revealed a Rh(III)-catalyzed *ortho* C–H thiolation of cyclic *N*-sulfonyl ketimines using disulfides as sulfur source (Scheme 7.1.3.1n).[21s]

In between, Cramer group successfully employed cyclic *N*-sulfonyl ketimines in an enantioselective [3+2]-spirocyclization with alkynes using Cp^x-Rh(III) catalyst containing atropchiral cyclopentadienyl ligand in combination with carboxylic acid additive giving chiral spirocyclic indenyl sultams in high yields and enantiomeric ratios (Scheme 7.1.3.2).[21i]

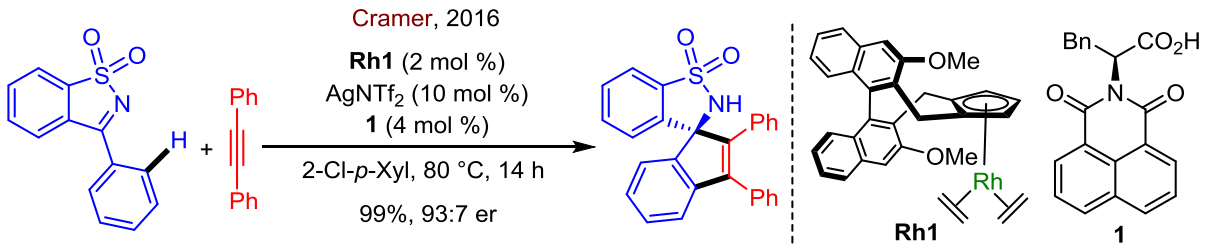

Scheme 7.1.3.2. Cyclic *N*-sulfonyl ketimine as DG in enantioselective C–H functionalization.

7.2. Objective

From literature, it is evident that biaryl moieties are prevalent in several bioactive scaffolds. So, a methodology involving direct C–C bond formation for biaryl synthesis is highly solicitated in today's world. As discussed above, several groups have designed unique strategies for direct C–H arylation of various heterocycles using the help of DG aided transition metal-catalyzed C–H activation. Cyclic *N*-sulfonyl ketimine motifs are present in a broad spectrum of biologically active compounds and have served as an efficient directing group for C–H transformations but due to its weak directing nature, reports of its direct functionalization are scarce. On the other hand, aryl siloxanes as an aryl group source prove to be advantageous over contemporary sources like aryl halides, aryl triflates, aryl boronic acids, etc. owing to its low toxicity and easy availability. Transition metals like Pd, Rh, Ru, Ni and Co catalysts in combination with aryl siloxanes have been used for C–H arylation techniques, but with some limitations like longer reaction times, harsh conditions and use of strongly coordinating

directing groups. Only one report on Ir catalysis has emerged by Chang group. To the best of our attention, synthesis of biaryl scaffolds containing cyclic *N*-sulfonyl ketimines remain unexplored. Persistent with our research interest in transition metal-catalyzed C–H functionalization, we hypothesized that this objective could be achieved under Ir catalysis. In this context, we disclosed an unprecedented Ir(III)-catalyzed *ortho* arylation reaction involving cyclic *N*-sulfonyl ketimines and relatively less explored aryl siloxanes (Scheme 7.2.1).

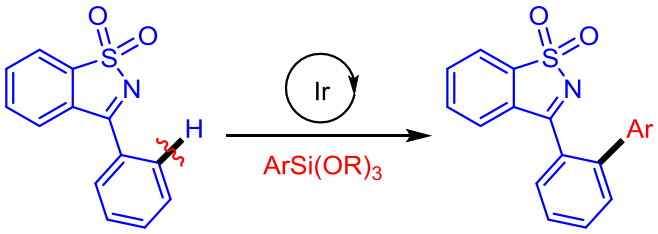

Scheme 7.2.1. Objective of this work: iridium-catalyzed sp^2 C–H arylation of cyclic *N*-sulfonyl ketimines.

7.3. Results and Discussion

7.3.1. Optimization Studies

We started off our venture subjecting the representative substrate 3-phenylbenzo[*d*]isothiazole-1,1-dioxide (**1a**) to react with the arylating reagent trimethoxyphenylsilane (**2a**) (1.1 equiv) in presence of $[Cp^*IrCl_2]_2$ (5 mol %) catalyst, $AgSbF_6$ (20 mol %) halide scavenger, $Cu(OAc)_2$ (50 mol %) co-oxidant and AgF (2.2 equiv) as both the fluoride source as well as an oxidant in TFE (0.1 M) solvent at room temperature (approx. 30 °C) for 1 h under nitrogen atmosphere (Table 7.3.1.1, entry 1). To our delight, we obtained the desired *ortho* arylated compound 3-([1,1'-biphenyl]-2-yl)benzo[*d*]isothiazole 1,1-dioxide (**3aa**) as an inseparable mixture of mono- and bis-arylated products in 72% combined yield with excellent mono selectivity. First, screening of different silver additives was performed (Table 7.3.1.1, entries 2-5). It showed similar yields of the reaction (62-83%) with good to excellent selectivities except for AgOTs which gave poor selectivity (Table 7.3.1.1, entry 5). Among them, $AgNTf_2$ provided the maximum yield of 83% with high selectivity (<25:1) (Table 7.3.1.1, entry 3). Next in line was the optimization of solvents of both polar/non-polar and protic/aprotic nature, but changing them had a detrimental effect on the yield of the product (Table 7.3.1.1, entries 6-14). HFIP gave a reduced yield with high selectivity (Table 7.3.1.1, entry 10), DCE and DCM also produced diminished yields along with average selectivity (Table 7.3.1.1, entries 6-7), whereas other solvents like Toluene, THF, 1,4-dioxane, MeCN, DMA, mixture solvent of THF/TFE (1:1) did not furnish the arylated product **3aa** (Table 7.3.1.1, entries 8-9, 11-14).

Table 7.3.1.1. Optimization of reaction conditions[a]

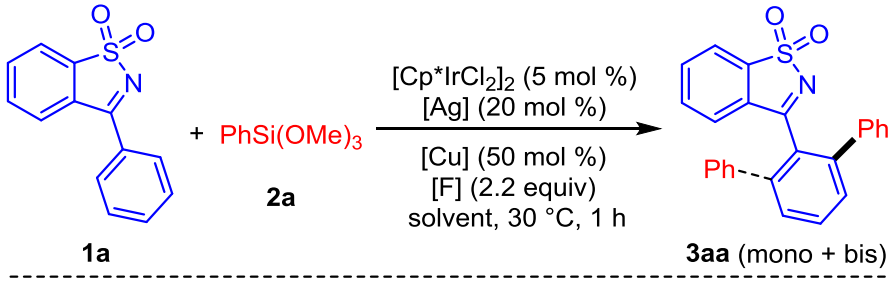

entry	[Ag]	[Cu]	[F]	solvent (0.1 M)	yield (%) of **3aa**[b] (mono:bis)
1	$AgSbF_6$	$Cu(OAc)_2$	AgF	TFE	72 (>25:1)
2	AgOTf	$Cu(OAc)_2$	AgF	TFE	62 (>25:1)
3	**$AgNTf_2$**	**$Cu(OAc)_2$**	**AgF**	**TFE**	**83 (20:1)**
4	$AgBF_4$	$Cu(OAc)_2$	AgF	TFE	79 (>25:1)
5	AgOTs	$Cu(OAc)_2$	AgF	TFE	63 (1:1)
6	$AgNTf_2$	$Cu(OAc)_2$	AgF	DCE	53 (4:1)
7	$AgNTf_2$	$Cu(OAc)_2$	AgF	DCM	31 (3:1)
8	$AgNTf_2$	$Cu(OAc)_2$	AgF	Toluene	nr
9	$AgNTf_2$	$Cu(OAc)_2$	AgF	THF	nr
10	$AgNTf_2$	$Cu(OAc)_2$	AgF	HFIP	69 (>25:1)
11	$AgNTf_2$	$Cu(OAc)_2$	AgF	1,4-dioxane	nr
12	$AgNTf_2$	$Cu(OAc)_2$	AgF	MeCN	nr
13	$AgNTf_2$	$Cu(OAc)_2$	AgF	DMA	nr
14	$AgNTf_2$	$Cu(OAc)_2$	AgF	THF:TFE (1:1)	nr
15	$AgNTf_2$	$Cu(OAc)_2$	CuF_2	TFE	nr
16	$AgNTf_2$	$Cu(OAc)_2$	TBAF	TFE	nr
17	$AgNTf_2$	$Cu(OAc)_2$	TBAF:AgF (1:1)	TFE	nr
18	$AgNTf_2$	$Cu(OTf)_2$	AgF	TFE	nr
19	$AgNTf_2$	$CuBr_2$	AgF	TFE	nr
20	$AgNTf_2$	$CuCl_2$	AgF	TFE	18 (1:1)
21	$AgNTf_2$	CuO	AgF	TFE	nr
22[c]	$AgNTf_2$	$Cu(OAc)_2$	AgF	TFE	22 (1:1)
23[d]	$AgNTf_2$	-	AgF	TFE	63 (>25:1)
24[e]	$AgNTf_2$	$Cu(OAc)_2$	AgF	TFE	nr
25[f]	$AgNTf_2$	$Cu(OAc)_2$	AgF	TFE	65 (21:1)
26[g]	$AgNTf_2$	$Cu(OAc)_2$	AgF	TFE	nr
27	-	$Cu(OAc)_2$	AgF	TFE	49 (2:1)
28	$AgNTf_2$	-	AgF	TFE	29 (2:1)
29	$AgNTf_2$	$Cu(OAc)_2$	-	TFE	nr
30[h]	$AgNTf_2$	$Cu(OAc)_2$	AgF	TFE	nr

[a]Reaction Conditions: Unless otherwise mentioned, **1a** (0.1 mmol), **2a** (1.1 equiv), $[Cp^*IrCl_2]_2$ (5 mol %), additive/[Ag] (20 mol %), co-oxidant/[Cu] (50 mol %) and fluoride source/[F] (2.2 equiv) in solvent (0.1 M) at room temp. (approx. 30 °C) under N_2 for 1 h. [b]All yields refer to combined isolated yield of mono and bis-arylated products. The ratio of mono and bis products was determined by ^1H NMR. [c]$Cu(OAc)_2$ (2.0 equiv). [d]O_2 used in place of $Cu(OAc)_2$. [e]AgF (1.1 equiv). [f]$[Cp^*IrCl_2]_2$ (3 mol %). [g]without $[Cp^*IrCl_2]_2$. [h]$IrCl_3$ in place of $[Cp^*IrCl_2]_2$. nr = no reaction.

Testing other external fluoride sources which could also act as an oxidant proved unfruitful, since the reaction did not undergo upon changing the fluoride source from AgF to CuF_2 or TBAF or a 1:1 TBAF/AgF mixture (Table 7.3.1.1, entries 15-17). Further screening of various copper salts (Table 7.3.1.1, entry 18-21), *viz.* $Cu(OTf)_2$, $CuBr_2$, CuO as co-oxidants or additives resulted in no reaction at all except for $CuCl_2$ which gave a paltry yield with the formation of a higher amount of bis-product (Table 7.3.1.1, entry 20). Elevating the loading of $Cu(OAc)_2$ proved disadvantageous from both the aspects of yield and selectivity (Table 7.3.1.1, entry 22). Employing a greener co-oxidant like molecular oxygen generated the arylated product in a decreased 63% yield with very good selectivity (Table 7.3.1.1, entry 23). Again, lowering the loading of AgF did not deliver the corresponding product (Table 7.3.1.1, entry 24). Decreasing the loading of the catalyst to 3 mol % led to a fall in the yield of the reaction to 65% continuing the good selectivity (Table 7.3.1.1, entry 25).

Control experiments showed that omitting $[Cp^*IrCl_2]_2$, formation of **3aa** was not observed (Table 7.3.1.1, entry 26). Again in absence of $AgNTf_2$ and $Cu(OAc)_2$, the product was formed in diminished yields accompanying poor selectivity (Table 7.3.1.1, entry 27-28); when AgF was not used, the formation of arylated product was not observed (Table 7.3.1.1, entry 29). These observations emphasized the importance of the additives required in the present protocol. Alternatively, when other Ir(III) salt like $IrCl_3$ was employed as a catalyst, it did not furnish any product (Table 7.3.1.1, entry 30). Entry 3 thus emerged as the optimized condition for the current arylation protocol.

7.3.2. Scope of the Reaction

A series of cyclic *N*-sulfonyl ketimines **1** and **4** were prepared following literature procedures, discussed in the experimental section.

Five-membered cyclic *N*-sulfonyl ketimines (**1a-1p**) were prepared following the literature procedure by reacting benzo[*d*]isothiazol-3(2*H*)-one 1,1-dioxide with aryl magnesium bromides in THF at room temperature followed by quenching with solid NH_4Cl (Table 7.3.2.1).

Table 7.3.2.1. List of 5-membered cyclic *N*-sulfonyl ketimine substrates prepared

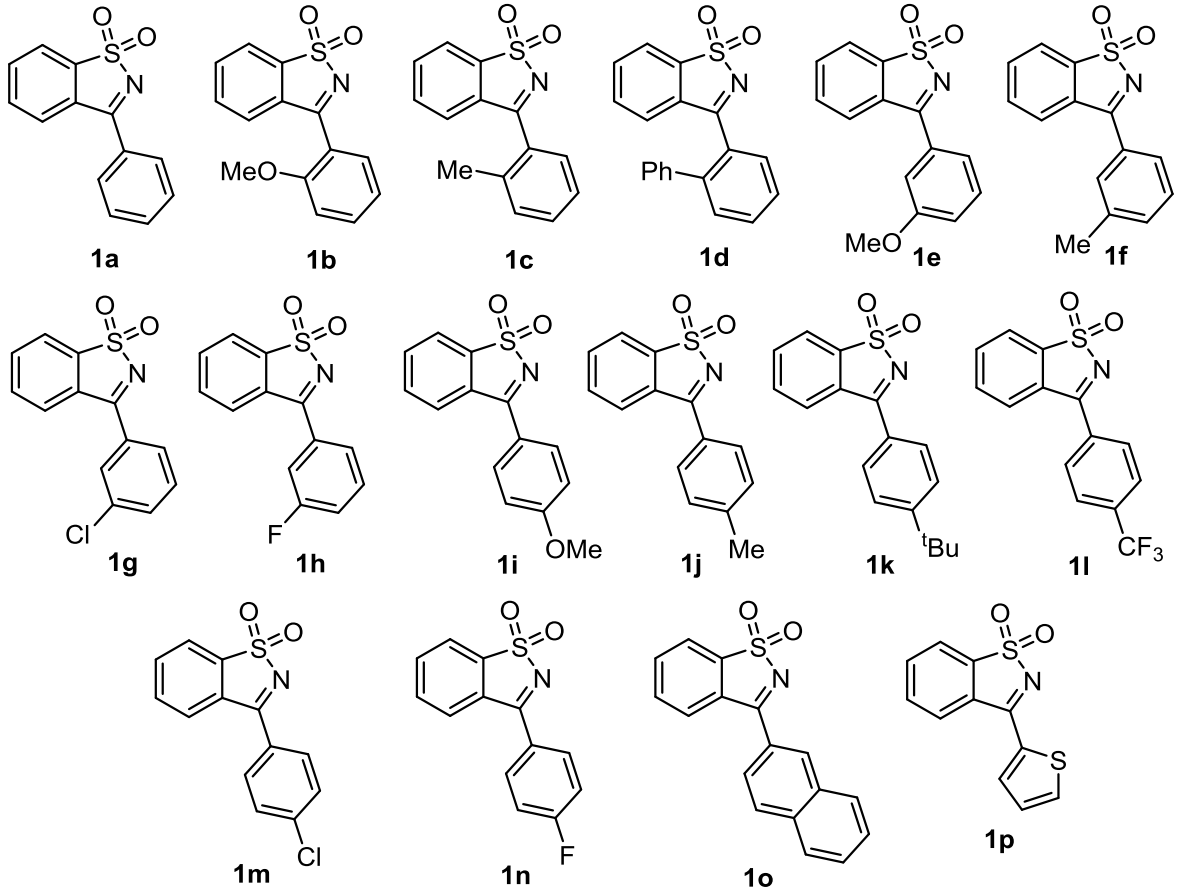

Six-membered cyclic *N*-sulfonyl ketimines (**4a**-**4f**) were prepared following the literature procedure using 2-hydroxybenzophenones (Table 7.3.2.2).

Table 7.3.2.2. List of 6-membered cyclic *N*-sulfonyl ketimine substrates prepared

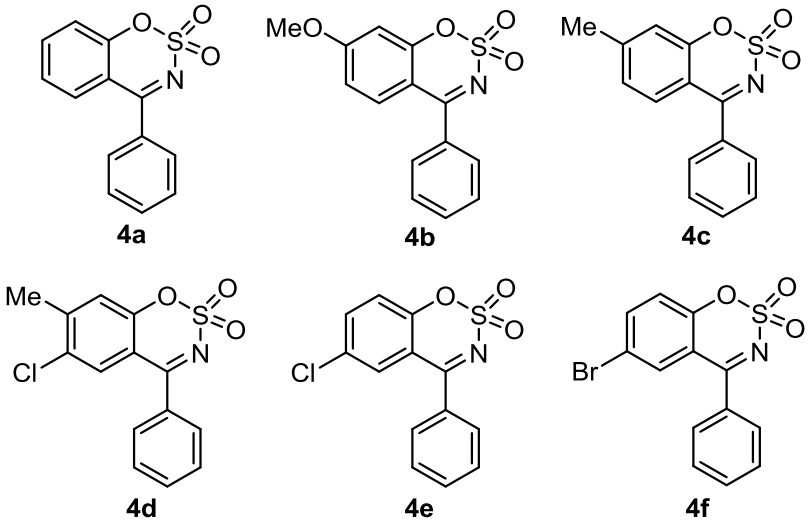

After the preparation of substituted cyclic ketimines (**1** and **4**), they were subjected to the arylation reaction with various arylsiloxanes (**2**) under the standard reaction conditions to check the generality and limitations of the reaction (Table 7.3.2.3, 7.3.2.4). First, the five-membered cyclic *N*-sulfonyl ketimines (**1**) were tested (Table 7.3.2.3). The parent substrate **1a** gave the corresponding *ortho* arylated product **3aa** on reaction with trimethoxyphenylsilane (**2a**) in 83% yield with 5:1 mono:bis ratio in 0.2 mmol scale. Electron-donating substituents (Me, OMe, Ph) at the *ortho* position of the aryl ring gave moderate to good yields (**3ba**-**3da**; 60-82%) with no scope for bis-arylation. Shifting to *meta* position, a methoxy and fluoro group gave their products **3ea** (77%) and **3ha** (73%) respectively in good yields with only slight amounts of the bis-product; other electron-donating (methyl) and withdrawing (chloro) substituents at this position produced good to excellent yields (**3fa**, **3ga**) with no formation of the bis-product. At the *para* position, when a methoxy group was placed, it yielded the mono-arylated product **3ia** exclusively in 70% yield. Other electron-donating substituents (methyl, tert-butyl) at this position gave the desired products (**3ja**, **3ka**) in good to excellent yields with only a trace amount of bis-product in each case. Electron-withdrawing groups (trifluoromethyl, chloro, fluoro) at the same position yielded good amounts of their respective products (**3la**-**3na**) accompanying trace amounts of bis-product. Bulky substituent like a naphthyl group delivered the mono-arylated product **3oa** exclusively in excellent 84% yield. Pleasingly, a heterocyclic variant like thiophene containing substrate (**1p**) was also well tolerated giving a very good yield of **3pa** in 80% yield with exclusive mono selectivity.

Till now the parent siloxane **2a** was screened. Now, the scope was extended to other arylsiloxanes containing different substituents (**2b**-**2e**). Among them, the electron-donating aryl (*para* methyl and methoxy substituted), thienyl and naphthyl siloxanes worked well giving good to excellent yields of the arylated products (**3bb**-**3be**; 65-84%). When (4-methoxyphenyl)trimethoxysilane (**2b**) was used as coupling partner with several *meta*-substituted *N*-sulfonyl ketimines (**1d**-**1g**), moderate to excellent yield of products were obtained (**3db**-**3gb**), where formation of trace amount of bis-products were observed in case of electron-deficient ketimines (**1f**, **1g**). There was a reversal in the observation when the same siloxane was made to react with *para*-substituted sulfonyl ketimines (**1h**-**1m**). Electron-donating groups at the *para* position furnished moderate to good yields of mono-arylated products with minor amounts of the bis-product (**3hb**-**3jb**), whereas electron-withdrawing groups gave the mono-arylated product exclusively (**3kb**-**3mb**) in moderate to good yields. With **2b** as arylating reagent, sterically encumbered naphthyl group containing substrate

produced an excellent yield of **3nb** (88%), and similarly also one carrying a heterocyclic thiophene variant (**3ob**, 82%), all of them with exclusive mono selectivity.

Table 7.3.2.3. Scope of arylation of substituted *N*-sulfonyl ketimines **1**[a]

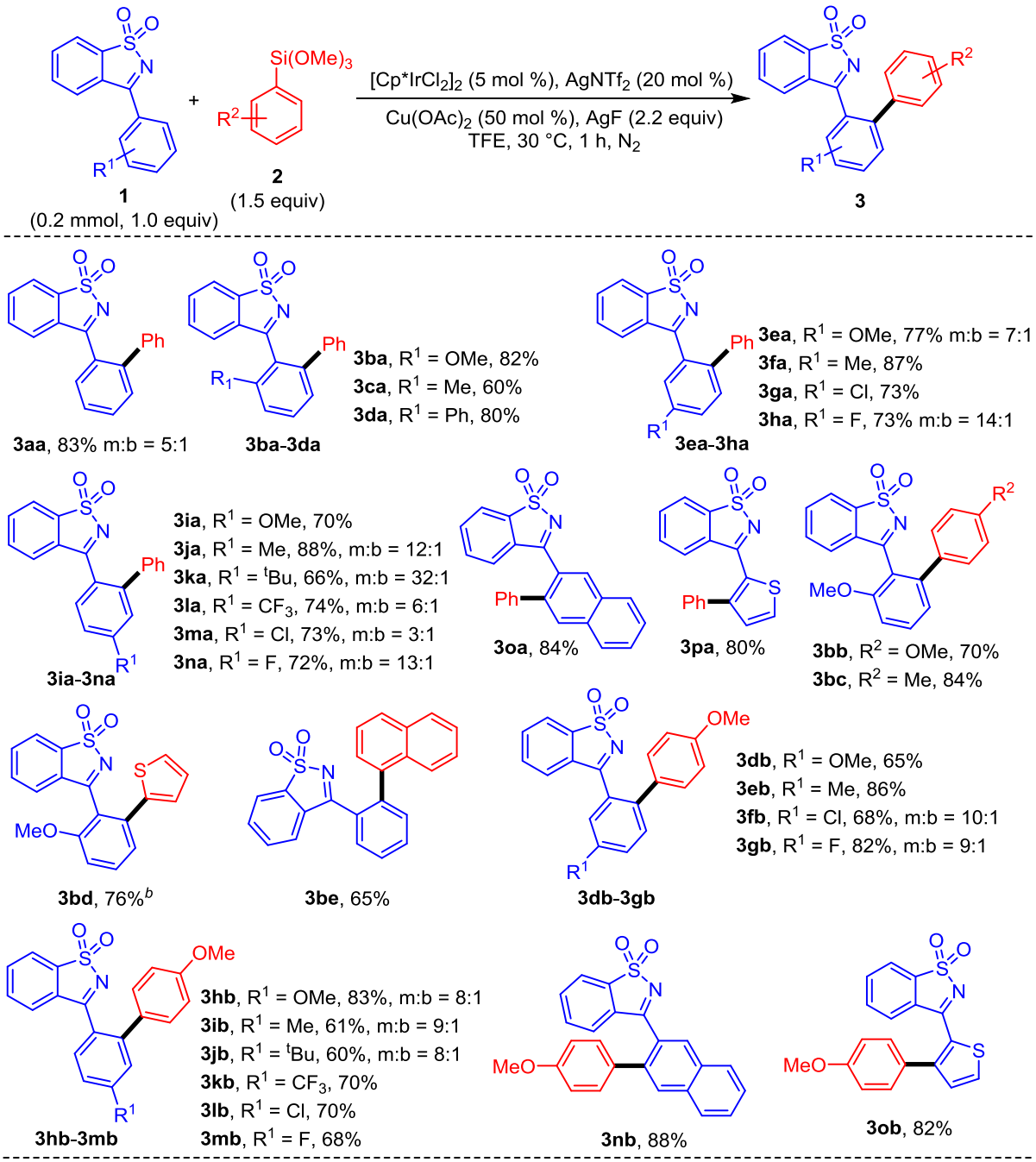

[a]All yields reported are of isolated products. The expression m:b depicts the ratio of mono and bis-arylated products determined from ^{1}H NMR. [b]triethoxy-2-thienylsilane was used.

Encouraged by these findings, we extended this methodology to another class of six-membered cyclic *N*-sulfonyl ketimines **4** with diverse arylsiloxanes **2** (Table 7.3.2.4). The substrate 4-phenylbenzo[*e*][1,2,3]oxathiazine 2,2-dioxide (**4a**) provided an excellent yield of 95% of its

respective arylated product 4-([1,1'-biphenyl]-2-yl)benzo[*e*][1,2,3]oxathiazine 2,2-dioxide (**5aa**) with absolute mono selectivity under standard reaction conditions. Varying electron-donating and withdrawing substituents at the 6 and 7 position of the ketimine **4** had minimal effect on the yield of their arylated products (**5ba**-**5fa**) with electron-withdrawing Cl and Br functional groups giving slight amounts of bis-arylated products (**5ea**, **5fa**). Electron-rich arylsiloxanes (*para* methoxy and methyl substituted) gave higher yields of the products (**5ab**-**5ac**) along with lower amounts of bis arylation.

Table 7.3.2.4. Scope of arylation of substituted *N*-sulfonyl ketimines **4**[a]

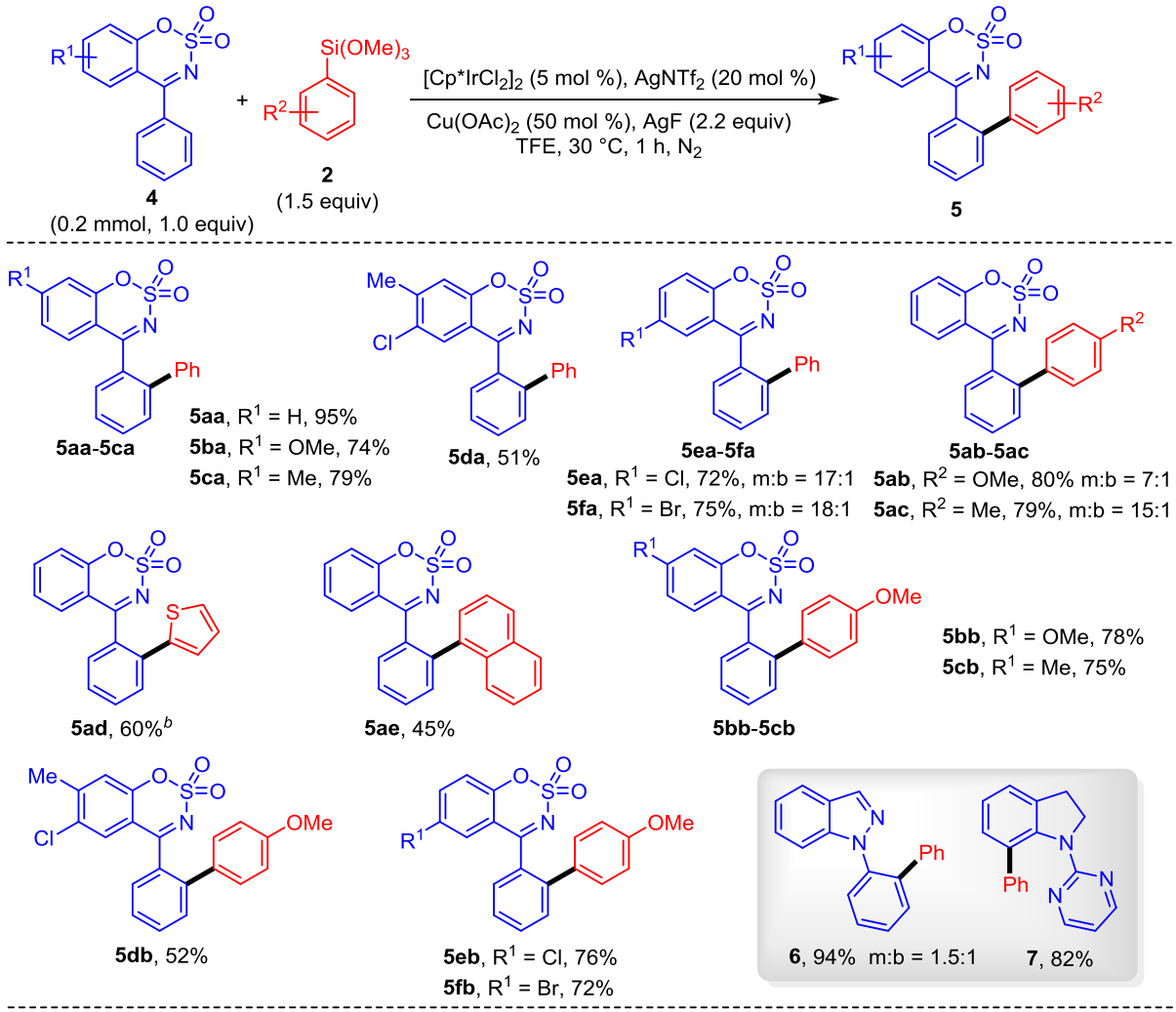

[a]All yields reported are of isolated products. The expression m:b depicts the ratio of mono and bis arylated products determined from ^{1}H NMR. [b]triethoxy-2-thienylsilane was used.

Heterocycle-based thiophene and sterically hindered naphthyl siloxanes provided the products (**5ad**-**5ae**) in moderate yields presumably due to electronic and steric effects respectively. Use of (4-methoxyphenyl)trimethoxysilane (**2b**) as the arylating partner with various ketimines did

not cause much variation in the yield of the corresponding products (**5bb**-**5fb**). Mono-arylated products were formed solely in all the cases. To diversify the strategy and check the versatility of this reaction, other nitrogen-directing heterocycles like 1-phenyl indazole and 1-(pyrimidin-2-yl)indoline were employed under the standard conditions with **2a**. Delightfully, the arylated products **6** (94% yield) although with poor selectivity (mono:bis 1.5:1) and product **7** (82% yield) with exclusive mono selectivity were formed respectively.

To check whether the present arylation protocol could be performed under Pd and Ni-catalyzed C–H arylation conditions, the arylation reaction of **1a** with **2a** was performed employing Pd and Ni catalysis following the literature reports (Scheme 7.3.2.1).[15a,d,18b] However, the formation of **3aa** was not observed in any of the cases which therefore strengthened the superiority of this iridium-catalyzed arylation strategy.

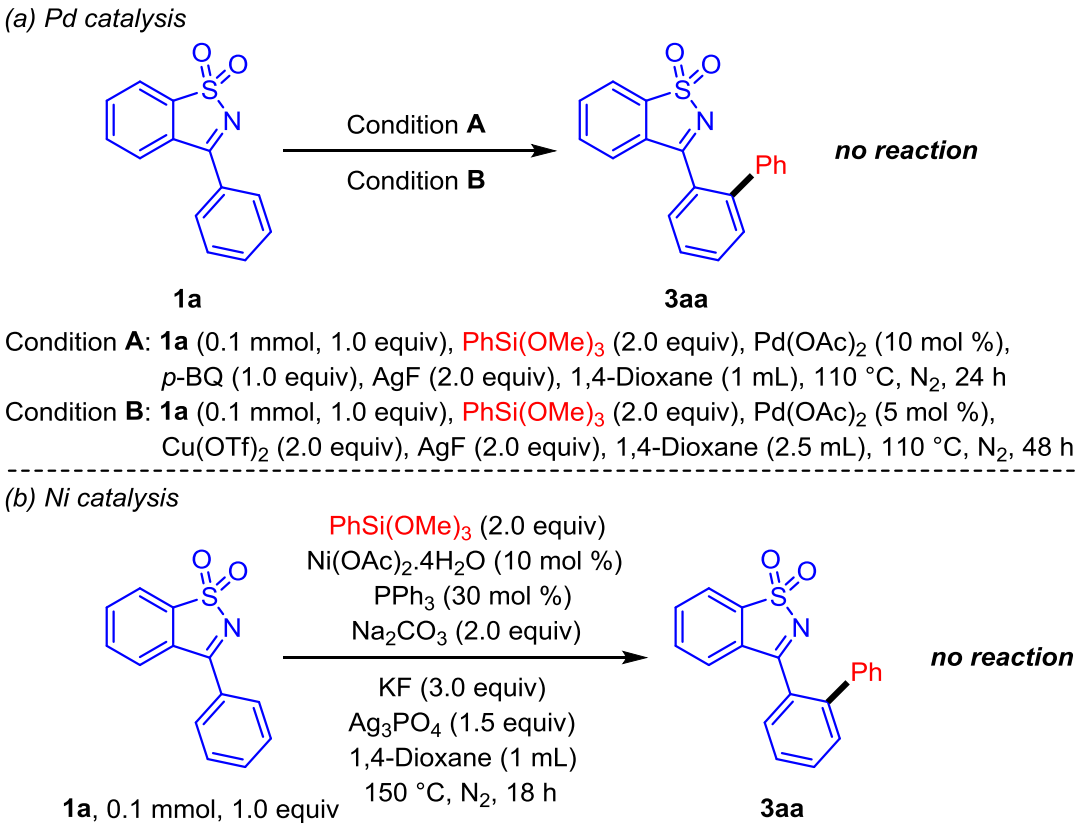

Scheme 7.3.2.1. C–H arylation reaction under Pd and Ni catalysis.

All the arylated products (**3** and **5**) were duly characterised by ^{1}H, ^{13}C NMR and HRMS. Single crystal X-ray analysis of **3ca** and **5ab** further confirmed their structures (Figure 7.3.2.1).

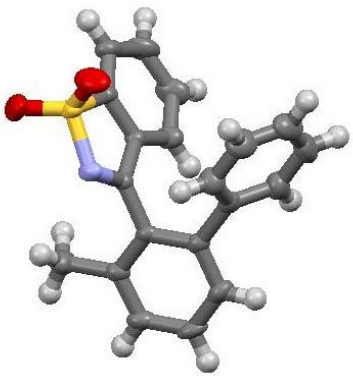

3ca
CCDC No. 1891261

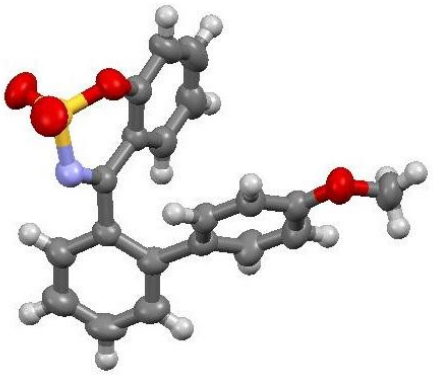

5ab
CCDC No. 1891262

Figure 7.3.2.1. X-ray crystal structures of **3ca** and **5ab** (ellipsoid contour at 50% probability level).

A few arylsiloxane derivatives which did not fare well under the standard reaction conditions and failed to deliver the desired product are represented in Figure 7.3.2.2. Electron-withdrawing group at the *para* position of the siloxane as in (4-chlorophenyl)trimethoxysilane hindered the reaction and formation of **S3a** was not observed, possibly because of electronic reasons. When aliphatic siloxanes like trimethoxy(propyl)silane and trimethoxy(3, 3, 3-trifluoropropyl)silane were employed in place of aromatic siloxanes, they did not provide the corresponding desired alkylated products **S3b** and **S3c** under the standard conditions. This could be again due to electronic reasons which implied the importance of the aryl moiety in the arylsiloxane reagent.

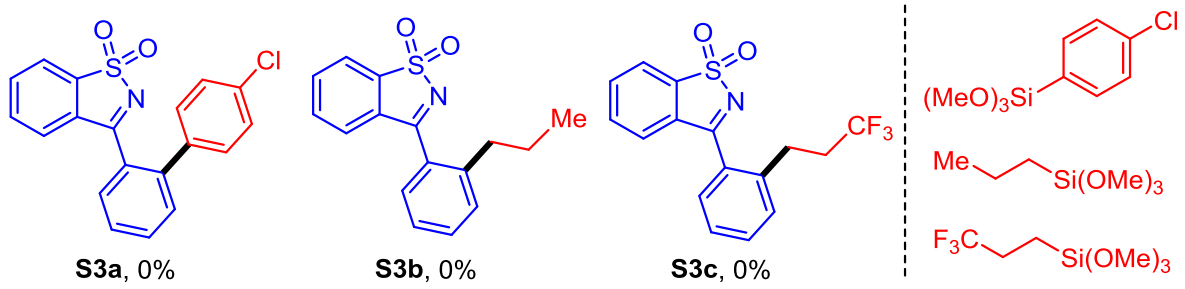

S3a, 0% **S3b**, 0% **S3c**, 0%

Figure 7.3.2.2. List of failed aryl and alkylsiloxanes.

Other monodentate and bidentate *N*-directing substrates bearing pyridine and pyrimidine based directing groups were screened under the optimized reaction conditions (Figure 7.3.2.3). 9-(pyrimidin-2-yl)-9*H*-carbazole gave its arylated product **I** in a poor 17% yield with exclusive mono selectivity. 2-phenylpyridine furnished entirely bis-arylated product **II** in a low 23% yield. But, bidentate system like *N*-(naphthalen-1-yl)picolinamide did not deliver its

corresponding arylated product **III** emphasizing the fact that bidentate directing groups were unable to react under the present reaction conditions.

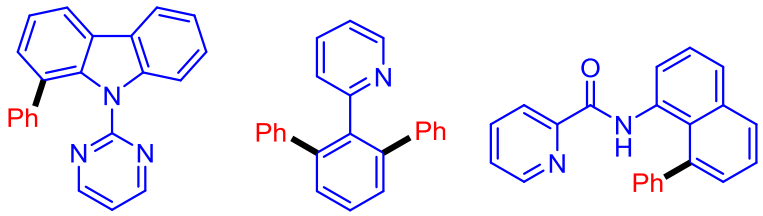

I, 17% **II**, 23% **III**, 0%

Figure 7.3.2.3. List of other DG attached substrates.

7.3.3. Gram-Scale Reaction and Synthetic Transformation of the Product

To showcase the practicality of this catalytic process and extend the synthetic utility of the methodology, a gram-scale reaction was conducted using 1.0 g of **1a** with trimethoxy(phenyl)silane (**2a**) under standard conditions. The arylated product **3aa** was obtained in a splendid 80% yield (1.05 g) similar to millimolar scale (Scheme 7.3.3.1).

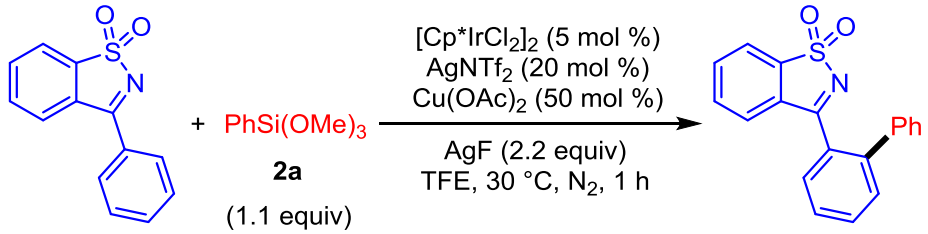

1a
1.0 g, 4.1 mmol

3aa
1.05 g, 80%

Scheme 7.3.3.1. Gram-scale reaction.

Also, to decorate the parent arylated product **3aa**, it was successfully transformed into a new class of fused oxaziridine system 3-([1,1'-biphenyl]-2-yl)benzo[*d*]isothiazole 1,1-dioxide (**8**) in 82% yield via an epoxidation reaction using *m*-CPBA as oxidizing agent (Scheme 7.3.3.2). Single-crystal X-ray analysis of **8** confirmed its structure (Figure 7.3.3.1).

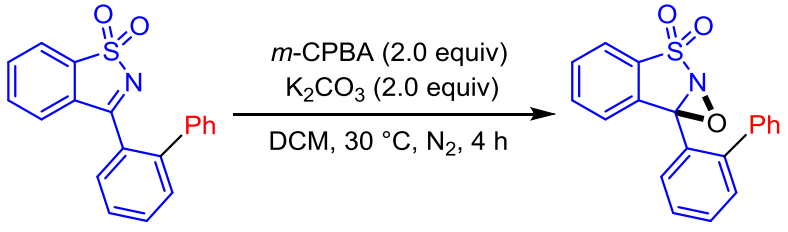

3aa **8**, 82%

Scheme 7.3.3.2. Epoxidation of the arylated product.

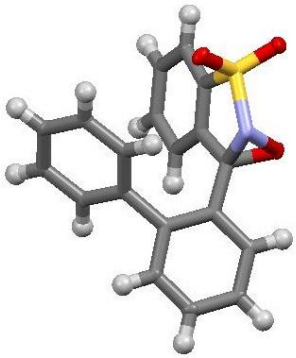

CCDC No. 2014574

Figure 7.3.3.1. X-ray crystal structure of **8** (ellipsoid contour at 50% probability level).

7.3.4. Mechanistic Experiments and Plausible Mechanism

In order to gain insights into the reaction mechanism and understand the catalytic cycle of the current arylation reaction, several kinetic experiments were performed.

First, H/D exchange experiment was set up with the parent deuterated cyclic *N*-sulfonyl ketimine substrate **1a**-d_5 (Scheme 7.3.4.1). When **1a**-d_5 was made to react under the standard conditions in absence of $PhSi(OMe)_3$ (**2a**), rapid deuterium-proton exchange was observed in the recovered starting material **1a**-d_n (Scheme 7.3.4.1a). ^1H NMR study showed 80% H-incorporation in **1a**-d_n (Figure 7.3.4.1). The result suggested that the C–H bond cleavage step may be reversible in nature.

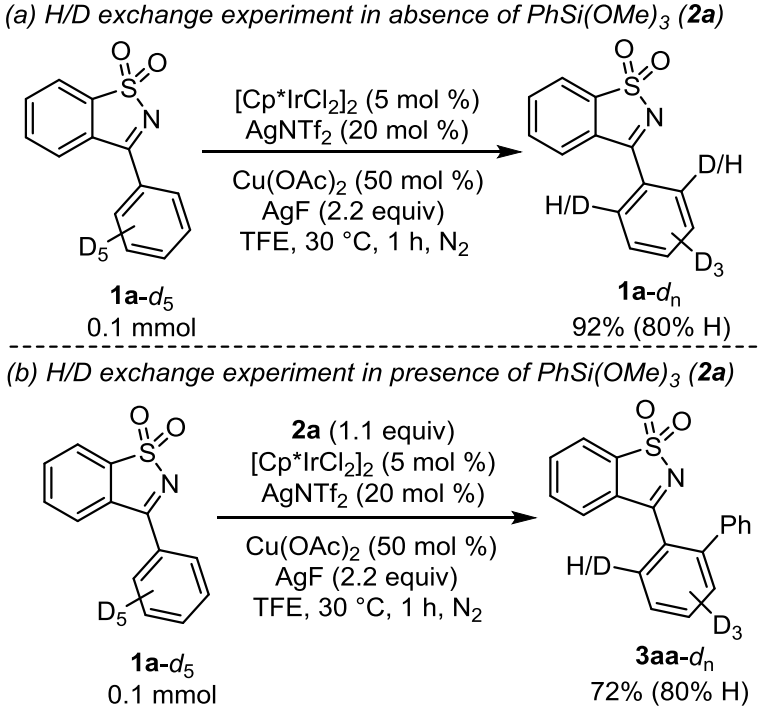

Scheme 7.3.4.1. H/D exchange experiments with **1a**-d_5.

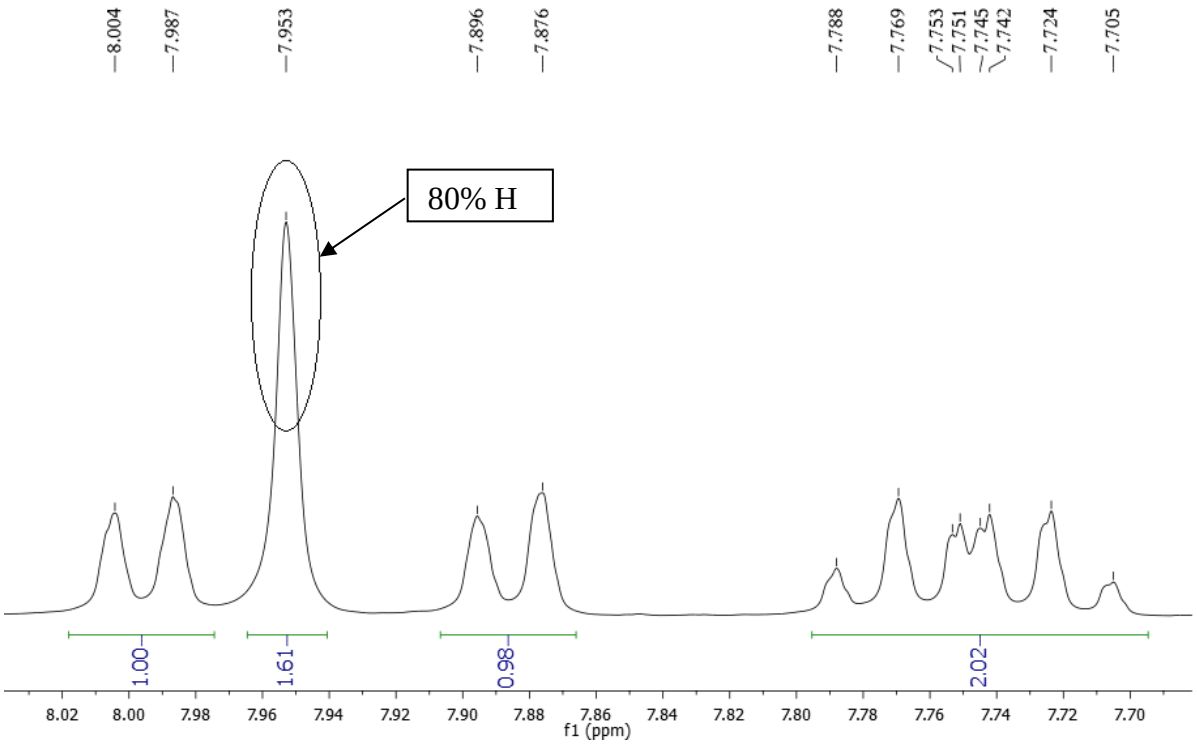

Figure 7.3.4.1. ^{1}H NMR spectrum of **1a**-d_n after H/D exchange experiment (in absence of **2a**).

Again, When **1a**-d_5 was put under the standard conditions in presence of $PhSi(OMe)_3$ (**2a**), quantitatively a similar deuterium-proton exchange was observed in the arylated product **3a**-d_n (Scheme 7.3.4.1b). ^{1}H NMR study showed 80% H-incorporation in **3aa**-d_n (Figure 7.3.4.2). This result went hand-in-hand with the previous outcome and clearly suggested that the C–H bond cleavage step of the present reaction is reversible in nature.

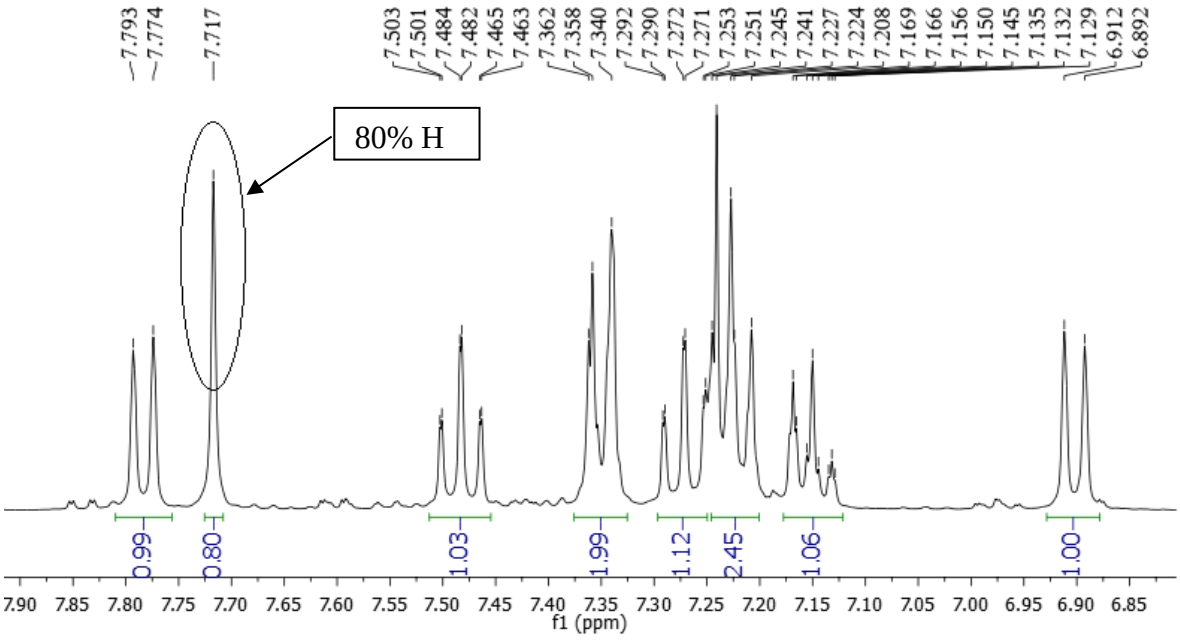

Figure 7.3.4.2. ^{1}H NMR spectrum of **3aa**-d_n after H/D exchange experiment (presence of **2a**).

A set of parallel reactions between **1a** and **1a**-d_5 were performed separately in different reaction vessels under the standard condition for shorter reaction time (Scheme 7.3.4.2) and the ratio of **3aa** and **3aa**-d_4 was determined by ^{1}H NMR spectroscopy (Figure 7.3.4.3). Primary kinetic isotopic effect (KIE) was found to be $\boldsymbol{k_H/k_D}$ = (0.67/0.33) = 2.0.

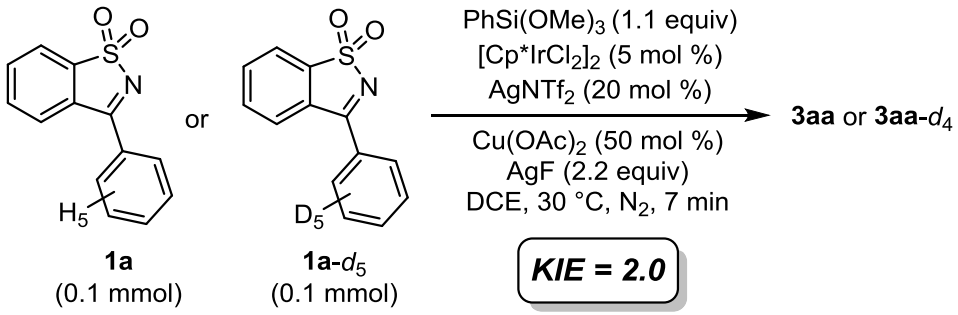

Scheme 7.3.4.2. Parallel experiment between **1a** and **1a**-d_5.

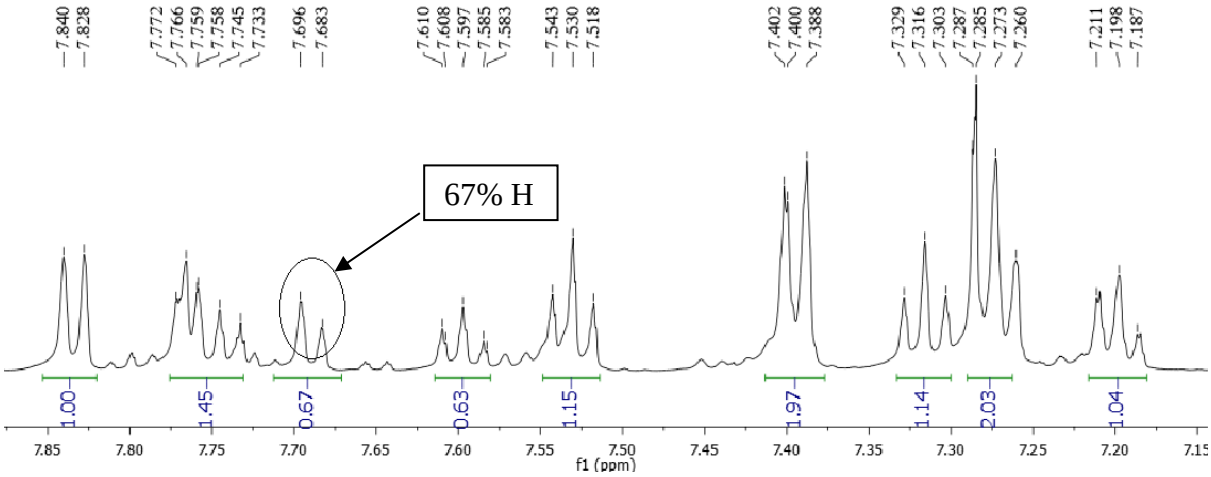

Figure 7.3.4.3. ^{1}H NMR spectrum for parallel experiment between **1a** and **1a**-d_5.

A mixture of **1a** and **1a**-d_5 was subjected to standard condition in a same reaction vessel for shorter reaction time (Scheme 7.3.4.3) and the ratio of **3aa** and **3aa**-d_4 was determined by ^{1}H NMR spectroscopy (Figure 7.3.4.4). Primary kinetic isotopic effect (KIE) was found to be $\boldsymbol{k_H/k_D}$ = (0.73/0.27) = 2.7.

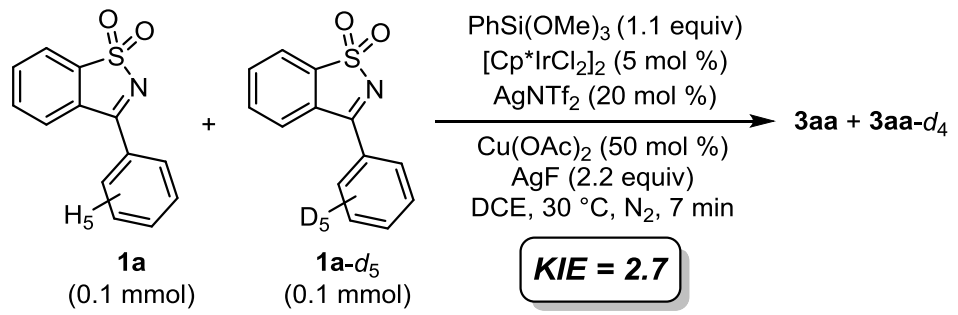

Scheme 7.3.4.3. Competitive experiment between **1a** and **1a**-d_5.

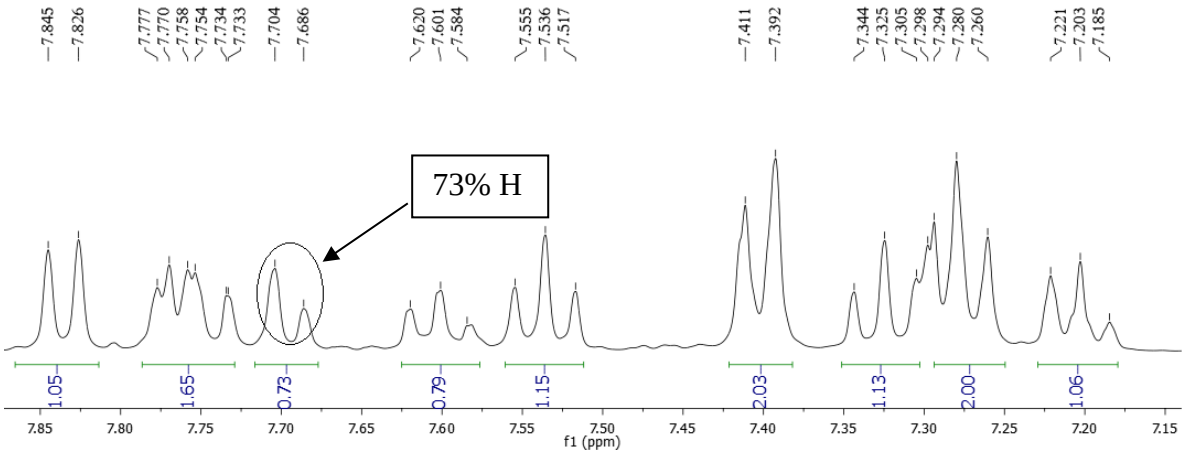

Figure 7.3.4.4. ^{1}H NMR spectrum for competitive experiment between **1a** and **1a**-d_5.

High kinetic isotope effect (KIE) values of 2.0 and 2.7 in the intermolecular parallel and competitive experiments respectively between **1ao** and **1ao**-d_5 implied that the *ortho* C−H bond cleavage of the cyclic *N*-sulfonyl ketimines **1** may be involved in the rate determining step of the reaction under the present reaction conditions.

Based on the above experimental evidences and preceding literature reports,[20] a plausible catalytic cycle is outlined in Scheme 7.3.4.4. Firstly, the $[Cp^*IrCl_2]_2$ dimer may in situ generate a cationic and more reactive monomeric species **A** by reacting with Ag(I) species and $Cu(OAc)_2$. This species undergoes chelation with the sulfonyl imine *N*-atom of **1a** and a reversible C−H activation occurs leading to the iridacycle **B**. Next, this cyclometallated Ir(III) species may participate in a transmetalation reaction with a copper- or silver-phenyl species, possibly generated in situ from the reaction of $PhSi(OMe)_3$ (**2a**) with copper or silver additive, to produce another iridacycle complex intermediate **C**. Thereafter, this intermediate may now produce the high valent intermediate **D** on oxidation by Ag(I) which may finally complete the catalytic cycle by oxidatively induced reductive elimination pathway giving the desired *ortho*-arylated product **3aa** and also regenerates the catalytically active Ir(III) species **B**. However, as an alternative route, another pathway that proceeds via the production of Ir(V) species **E** by one-electron oxidation of species **D** and then subsequent reductive elimination from species **E** may give the product **3aa** and regenerate the active species **B** which can be cannot be completely ignored either.

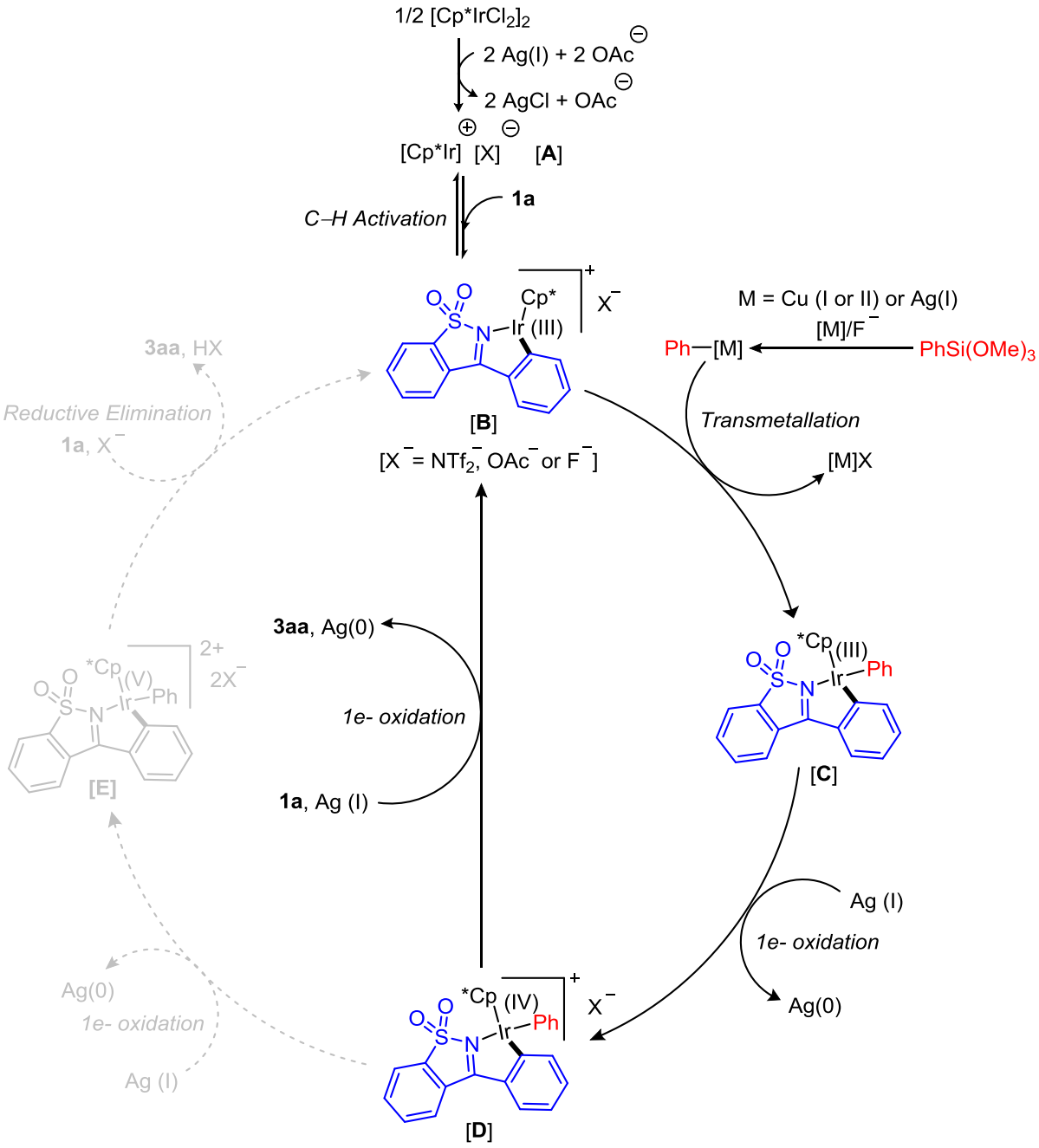

Scheme 7.3.4.4. Plausible reaction mechanism.

7.4. Summary

In summary, we have developed a practical and efficient iridium-catalyzed direct *ortho* arylation of cyclic *N*-sulfonyl ketimines using arylsiloxanes as an environmentally benign aryl source under operationally simple and mild reaction conditions. The methodology utilizes the weak coordinating nature of *N*-sulfonyl ketimines as well as sluggish reactivity of arylsilanes that give rise to structurally important novel biaryl scaffolds, fundamental in organic synthesis with potential biological implications. A broad substrate scope with a good tolerance for a wide

array of functional groups, scalability to gram scale, and the swift reaction in very less time are the prime features of this reaction. A series of kinetic experiments were conducted to gain an understanding of the mechanism of the reaction, which indicated that a reversible C−H bond cleavage step may be involved in the rate-determining step of the reaction. Further transformation of the arylated product was conducted to showcase the synthetic utility of the protocol.

7.5. Experimental Section

7.5.1. General Information

All the information is same as that provided in Section 2.5.1 of Chapter 2 unless otherwise mentioned. The CIF files were submitted to CCDC (1891261, 1891262, and 2014574) and can be obtained at https://summary.ccdc.cam.ac.uk/structure-summary-form.

7.5.2. General Procedure for the Preparation of Starting Materials

All the cyclic *N*-sulfonyl ketimines (**1a**−**1p**)[6e] and (**4a**−**4f**)[6b] were prepared following literature methods (Scheme 7.5.2.1, 7.5.2.2).

To a solution of benzo[*d*]isothiazol-3(2*H*)-one 1,1-dioxide (saccharin) (1.0 equiv) in THF (1.0 M) was slowly added ArMgBr (1.0 M in THF, 2.0 equiv) at 0 °C, and the resulting mixture was stirred at room temperature for 16 h. Solid NH_4Cl was added at 0 °C, and the reaction mixture was then stirred at room temperature for 30 min. The mixture was passed through a short column of alumina with ethyl acetate as eluent. The solvent was removed on a rotary evaporator and the solid residue was recrystallized from hot absolute ethanol and chloroform to give **1** (Scheme 7.5.2.1).

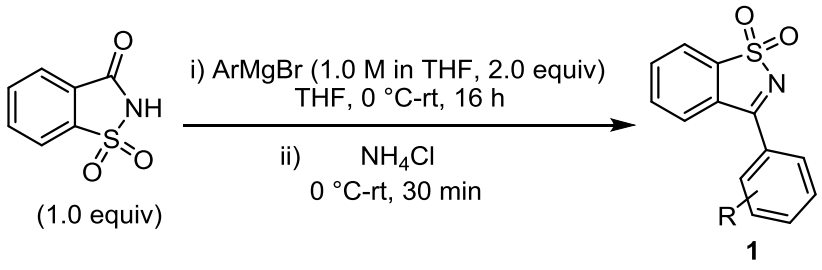

Scheme 7.5.2.1. Preparation of cyclic *N*-sulfonyl ketimines **1**.

Formic acid (2.0 equiv) was added dropwise to neat chlorosulfonyl isocyanate (2.0 equiv) at 0 °C with rapid stirring. Vigorous gas evolution was observed during the addition process. The resulting viscous suspension was stirred at room temperature until gas evolution ceased (1-2 h). To the resulting sulfamoyl chloride ($ClSO_2NH_2$) was added 2′-hydroxyacetophenone (1.0

equiv). After the mixture was cooled to 0 °C, DMA (0.7 M) was slowly added. The mixture was stirred for 10 min at room temperature, followed by addition of sodium hydride (1.2 equiv) in portions. After stirring again for 30 min, another batch of sodium hydride (1.2 equiv) was added in portions again. After stirring for 1 h at room temperature, the reaction mixture was allowed to stir for 12 h at 50 °C. The reaction was quenched by adding water and the aqueous layer was extracted with ethyl acetate. The combined organic layers were washed with brine, and concentrated under vacuo. Purification by silica gel column chromatography afforded the desired imines **4** (Scheme 7.5.2.2).

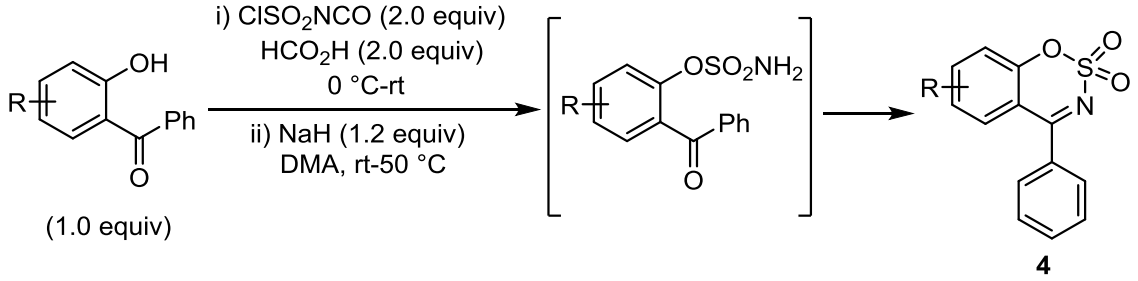

Scheme 7.5.2.2. Preparation of cyclic *N*-sulfonyl ketimines **4**.

7.5.3. General Procedure for Arylation

(0.2 mmol scale):

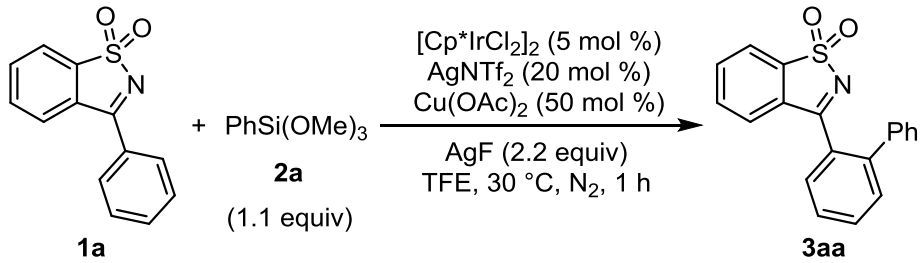

An oven-dried 10 mL Schlenk tube was charged with 3-phenylbenzo[*d*]isothiazole 1,1-dioxide (**1a**) (48.7 mg, 0.2 mmol), trimethoxy(phenyl)silane (**2a**) (41 µL, 0.22 mmol), silver (bistrifluoromethanesulfonyl)imide (15.5 mg, 20 mol %), copper acetate (18.1 mg, 50 mol %), silver fluoride (55.8 mg, 2.2 equiv) and catalyst $[Cp^*IrCl_2]_2$ (8.0 mg, 5 mol %). The tube was evacuated and backfilled with nitrogen and to it was added TFE (2.0 mL, 0.1 M) under nitrogen atmosphere. The reaction mixture was degassed and backfilled with nitrogen 3 times. It was then closed with teflon-lined cap and kept at 30 °C while stirring for 1 h. After completion of the reaction, the reaction mixture was filtered through a short pad of celite, the solvent was removed under reduced pressure and the crude reaction mixture was directly purified through

column chromatography on silica gel using petroleum ether/ethyl acetate as eluent to obtain 3-([1,1'-biphenyl]-2-yl)benzo[d]isothiazole 1,1-dioxide (**3aa**) (53.0 mg, 83% yield).

(gram-scale):

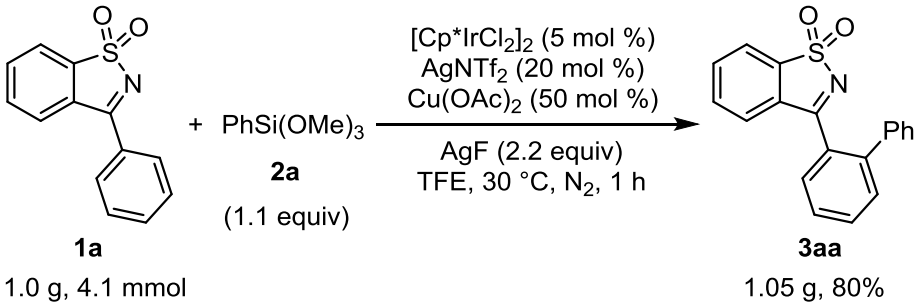

An oven-dried 100 mL two-neck round bottom flask was charged with 3-phenylbenzo[*d*]isothiazole-1,1-dioxide (**1a**) (1.0 g, 4.1 mmol), trimethoxy(phenyl)silane (**2a**) (0.84 mL, 4.5 mmol), silver (bistrifluoromethanesulfonyl)imide (318.9 mg, 20 mol %), copper acetate (372.3 mg, 50 mol %), silver fluoride (1.14 g, 2.2 equiv) and catalyst $[Cp^*IrCl_2]_2$ (163.3 mg, 5 mol %). The flask was evacuated and backfilled with nitrogen and to it was added TFE (41 mL, 0.1 M) under nitrogen atmosphere. The reaction mixture was degassed and backfilled with nitrogen 3 times. It was then closed with a stopper and kept at 30 ^oC while stirring for 1 h. After completion of the reaction, the reaction mixture was filtered through a short pad of celite, the solvent was removed under reduced pressure and the crude reaction mixture was directly purified through column chromatography on silica gel using petroleum ether/ethyl acetate as eluent to obtain 3-([1,1'-biphenyl]-2-yl)benzo[d]isothiazole 1,1-dioxide (**3aa**) (1.05 g, 80% yield).

Cases where the mono and bis-arylated products were obtained as an inseparable mixture, the ratio of mono and bis-products was determined by ^1H NMR. The characterization data for all the mono-arylated products are given below. Compounds **3ma, 5ea, 5fa, 5ab, 5ac** were recrystallized from EtOH to get mono-arylated product exclusively.

7.5.4. Characterization Data for the Arylated Products

3-([1,1'-biphenyl]-2-yl)benzo[*d*]isothiazole 1,1-dioxide (3aa):

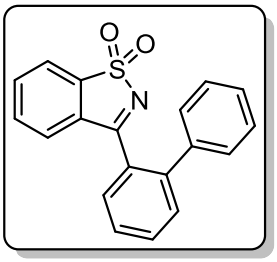

Combined Yield 83% (55 mg); **mono**:**bis** 5:1; colourless solid; $\mathbf{R_f}$ 0.5 (petroleum ether/ethyl acetate = 7:3); **eluent composition** petroleum ether/ethyl acetate = 7:3; **mp** 130-132 ^{o}C; **^{1}H NMR** (400 MHz, $CDCl_3$) δ 6.92 (d, *J* = 7.6 Hz, 1H), 7.15-7.19 (m, 1H), 7.22-7.25 (comp, 2H), 7.29 (dd, *J* = 7.8 Hz, 2.2 Hz, 1H), 7.37 (app d, *J* = 8.0 Hz, 2H), 7.50 (td, *J* = 7.6 Hz, 2.0 Hz, 1H), 7.55-7.59 (m, 1H), 7.65-7.67 (m, 1H), 7.70-7.74 (comp, 2H), 7.80 (d, *J* = 7.2 Hz, 1H); **^{13}C NMR** (100 MHz, $CDCl_3$) δ 122.3, 126.5, 128.1, 128.4, 129.0, 129.2, 129.8, 130.1, 130.6, 131.0, 132.3, 132.9, 133.1, 139.6, 139.7, 141.5, 174.4; **HRMS** (ESI, m/z) calcd for $C_{19}H_{13}NO_2S$ $[M+H]^+$ 320.0745, found 320.0737.

3-(3-methoxy-[1,1'-biphenyl]-2-yl)benzo[*d*]isothiazole 1,1-dioxide (3ba):

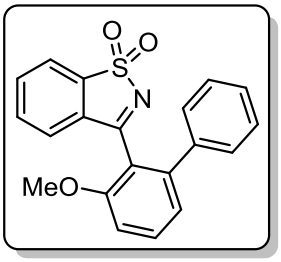

Yield 82% (57 mg); colourless solid; $\mathbf{R_f}$ 0.6 (petroleum ether/ethyl acetate = 7:3); **eluent composition** petroleum ether/ethyl acetate = 7:3; **mp** 112-114 ^{o}C; **^{1}H NMR** (400 MHz, $CDCl_3$) δ 3.81 (s, 3H), 7.07 (d, *J* = 8.4 Hz, 1H), 7.16 (d, *J* = 7.8 Hz, 2H), 7.18-7.26 (comp, 5H), 7.49 (t, *J* = 7.6 Hz, 1H), 7.57-7.61 (comp, 2H), 7.82 (d, *J* = 7.6 Hz, 1H); **^{13}C NMR** (100 MHz, $CDCl_3$) δ 56.3, 110.3, 118.4, 122.3, 122.8, 125.9, 128.1, 128.6, 129.1, 132.3, 132.4, 133.0, 133.5, 139.1, 139.4, 143.3, 157.8, 172.0; **HRMS** (ESI, m/z) calcd for $C_{20}H_{15}NO_3S$ $[M+H]^+$ 350.0851, found 350.0851.

3-(3-methyl-[1,1'-biphenyl]-2-yl)benzo[*d*]isothiazole 1,1-dioxide (3ca):

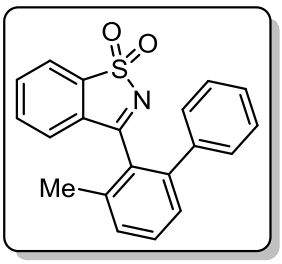

Yield 60% (40 mg); colourless solid; $\mathbf{R_f}$ 0.6 (petroleum ether/ethyl acetate = 7:3); **eluent composition** petroleum ether/ethyl acetate = 7:3; **mp** 150-152 ^{o}C (crystallization from $CDCl_3$ and hexane); **^{1}H NMR** (400 MHz, $CDCl_3$) δ 2.39 (s, 3H), 6.91 (d, *J* = 7.6 Hz, 1H), 7.10-7.13 (m, 1H), 7.20 (t, *J* = 7.4 Hz, 2H), 7.32-7.43 (comp, 5H), 7.50-7.56 (comp, 2H), 7.79 (d, *J* = 7.6 Hz, 1H); **^{13}C NMR** (100 MHz, $CDCl_3$) δ 20.1, 122.3 (x 2), 126.0, 127.9, 128.1, 128.6, 128.7, 129.3, 130.2, 130.9, 131.5, 133.1, 133.3, 137.3, 139.5, 139.8, 141.3; **HRMS** (ESI, m/z) calcd for $C_{20}H_{15}NO_2S$ $[M+H]^+$ 334.0902, found 334.0886.

Crystal data and structure refinement for 3ca, CCDC No. 1891261

Empirical formula	$C_{20}H_{15}NO_2S$
Formula weight	333.39
Temperature/K	273.15
Crystal system	Monoclinic
Space group	$P2_1/c$
a/Å	7.4364(5)
b/Å	26.4068(16)
c/Å	8.4485(5)
α/°	90
β/°	94.973(2)
γ/°	90
Volume/Å^3	1652.80(18)
Z	4
ρ_{calc}g/cm^3	1.340
μ/mm^{-1}	0.207
F(000)	696.0
Crystal size/mm^3	0.74 × 0.52 × 0.41
Radiation	Mo Kα (λ = 0.71073)
2Θ range for data collection/°	5.08 to 49.998
Index ranges	$-8 \le h \le 8$, $-31 \le k \le 31$, $-10 \le l \le 10$
Reflections collected	19836
Independent reflections	2892 [R_{int} = 0.0318, R_{sigma} = 0.0167]
Data/restraints/parameters	2892/0/218
Goodness-of-fit on F^2	1.086
Final R indexes [I>=2σ (I)]	R_1 = 0.0461, wR_2 = 0.1078
Final R indexes [all data]	R_1 = 0.0477, wR_2 = 0.1089
Largest diff. peak/hole / e Å^{-3}	0.36/-0.50

3-([1,1':3',1''-terphenyl]-2'-yl)benzo[*d*]isothiazole 1,1-dioxide (3da):

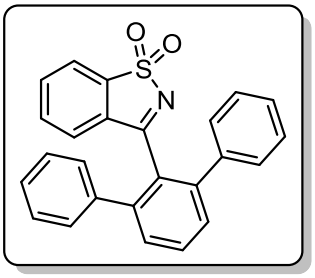

Yield 80% (63 mg); colourless solid; **R_f** 0.5 (petroleum ether/ethyl acetate = 7:3); **eluent composition** petroleum ether/ethyl acetate = 7:3; **mp** 180-182 °C; **^{1}H NMR** (600 MHz, $CDCl_3$) δ 7.00 (d, *J* = 7.8 Hz, 1H), 7.19-7.22 (comp, 2H), 7.24 (app d, *J* = 7.8 Hz, 3H), 7.26-7.28 (comp, 5H), 7.35 (t, *J* = 7.5 Hz, 1H), 7.47 (t, *J* = 7.5 Hz, 1H), 7.58 (d, *J* = 7.8 Hz, 2H), 7.69-7.73 (comp, 2H); **^{13}C NMR** (150 MHz, $CDCl_3$) δ 122.3, 125.7, 128.1, 128.3, 128.6, 129.2, 129.7, 130.9, 132.2, 132.8, 133.2, 139.4, 139.5, 142.3, 173.6; **HRMS** (ESI, m/z) calcd for $C_{25}H_{17}NO_2S$ $[M+H]^+$ 396.1058; found 396.1057.

3-(4-methoxy-[1,1'-biphenyl]-2-yl)benzo[*d*]isothiazole 1,1-dioxide (3ea):

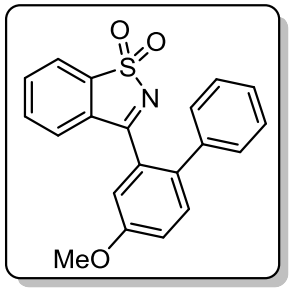

Combined Yield 77% (55 mg); **mono**:**bis** 7:1; colourless solid; $\mathbf{R_f}$ 0.6 (petroleum ether/ethyl acetate = 7:3); **eluent composition** petroleum ether/ethyl acetate = 7:3; **^{1}H NMR** (400 MHz, $CDCl_3$) δ 3.94 (s, 3H), 6.95 (d, *J* = 8.0 Hz, 1H), 7.13-7.17 (m, 1H) 7.23 (d, *J* = 7.6 Hz, 2H), 7.28-7.30 (comp, 2H), 7.32-7.36 (comp, 3H), 7.52 (t, *J* = 7.6 Hz, 1H), 7.60 (d, *J* = 8.0 Hz, 1H), 7.82 (d, *J* = 7.6 Hz, 1H); **^{13}C NMR** (100 MHz, $CDCl_3$) δ 55.9, 114.3, 119.0, 122.3, 126.6, 127.9, 128.9, 129.2, 130.7, 130.9, 131.9, 132.9, 133.0, 133.9, 139.5, 139.7, 159.4, 174.3; **HRMS**(ESI, m/z) calcd for $C_{20}H_{15}NO_3S$ $[M+H]^+$ 350.0851, found 350.0852.

3-(4-methyl-[1,1'-biphenyl]-2 yl)benzo[*d*]isothiazole 1,1-dioxide (3fa):

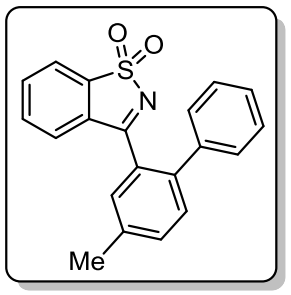

Yield 87% (58 mg); colourless solid; $\mathbf{R_f}$ 0.5 (petroleum ether/ethyl acetate = 7:3); **eluent composition** petroleum ether/ethyl acetate = 7:3; **mp** 110-112 °C; **^{1}H NMR** (400 MHz, $CDCl_3$) δ 2.48 (s, 3H), 6.90 (d, *J* = 8.0 Hz, 1H), 7.12-7.17 (m, 1H), 7.23 (t, *J* = 7.6 Hz, 2H), 7.27 (td, *J* = 7.6 Hz, 0.8 Hz, 1H), 7.34-7.36 (comp, 2H), 7.49 (td, *J* = 7.9 Hz, 0.7 Hz, 1H), 7.52-7.56 (comp, 3H), 7.80 (d, *J* = 7.6 Hz, 1H); **^{13}C NMR** (100 MHz, $CDCl_3$) δ 21.1, 122.3, 126.6, 128.1, 129.0, 129.2, 129.7, 130.5, 130.6, 131.1, 132.8, 133.0, 133.1, 138.3, 138.7, 139.7, 139.8, 174.6; **HRMS** (ESI, m/z) calcd for $C_{20}H_{15}NO_2S$ $[M+Na]^+$ 356.0721, found 356.0720.

3-(4-chloro-[1,1'-biphenyl]-2-yl)benzo[*d*]isothiazole 1,1-dioxide (3ga):

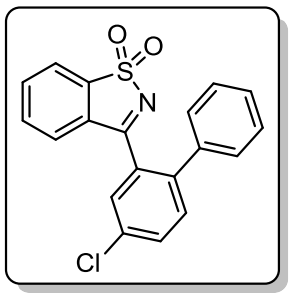

Yield 73% (52 mg); colourless solid; $\mathbf{R_f}$ 0.4 (petroleum ether/ethyl acetate = 7:3); **eluent composition** petroleum ether/ethyl acetate = 7:3; **mp** 120-122 °C; **^{1}H NMR** (400 MHz, $CDCl_3$) δ 6.89 (d, *J* = 7.6 Hz, 1H), 7.18 (app t, *J* = 7.2 Hz, 1H), 7.23 (app s, 1H), 7.25 (app s, 1H), 7.29-7.34 (comp, 3H), 7.52 (app t, *J* = 7.4 Hz, 1H), 7.60 (d, *J* = 8.0 Hz, 1H), 7.68 (dd, *J* = 8.4 Hz, 2.0 Hz, 1H), 7.73 (m, 1H), 7.81 (d, *J* = 7.2 Hz, 1H); **^{13}C NMR** (100 MHz, $CDCl_3$) δ 122.5, 126.3, 128.7, 129.1, 129.9, 130.5, 131.2, 131.9, 132.3, 133.2, 134.4, 136.7, 138.6, 138.6, 139.7, 140.0, 173.0; **HRMS** (ESI, m/z) calcd for $C_{19}H_{12}ClNO_2S$ $[M+H]^+$ 354.0356; found 354.0346.

3-(4-fluoro-[1,1'-biphenyl]-2-yl)benzo[*d*]isothiazole 1,1-dioxide (3ha):

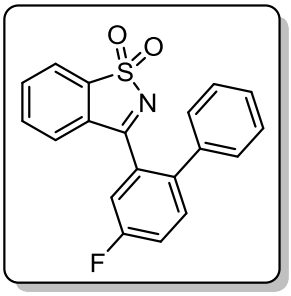

Combined Yield 73% (50 mg); **mono**:**bis** 14:1; colourless solid; **R$_f$** 0.4 (petroleum ether/ethyl acetate = 7:3); **eluent composition** petroleum ether/ethyl acetate = 7:3; **^{1}H NMR** (600 MHz, $CDCl_3$) δ 6.99 (d, *J* = 7.8 Hz, 1H), 7.18 (app t, *J* = 7.5 Hz, 1H), 7.25 (app t, *J* = 7.5 Hz, 2H), 7.34 (dd, *J* = 7.2 Hz, 0.9 Hz, 1H), 7.36 (app s, 1H), 7.37 (app s, 1H), 7.45 (td, *J* = 8.1 Hz, 1.2 Hz, 1H), 7.51-7.56 (comp, 3H), 7.79 (d, *J* = 7.2 Hz, 1H); **^{13}C NMR** (150 MHz, $CDCl_3$) δ 119.6 (d, $^2J_{F–C}$ = 23.1 Hz), 122.4, 125.6 (d, $^4J_{F–C}$ = 3.6 Hz), 126.3, 128.7, 128.9, 129.0 (d, $^3J_{F–C}$ = 6.75 Hz), 129.2 (d, $^3J_{F–C}$ = 6.6 Hz), 130.0, 130.0, 130.5, 130.5 (d, $^2J_{F–C}$ = 20.8 Hz), 132.6, 133.1, 133.1, 139.6, 159.7 (d, $^1J_{F–C}$ = 247.9 Hz), 172.9 (d, *J* = 3.0 Hz); **HRMS** (ESI, m/z) calcd for $C_{19}H_{12}FNO_2S$ $[M+H]^+$ 338.0651, found 338.0650.

3-(5-methoxy-[1,1'-biphenyl]-2-yl)benzo[*d*]isothiazole 1,1-dioxide (3ia):

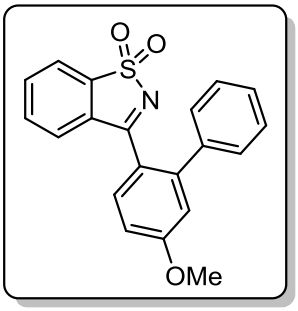

Yield 70% (49 mg); colourless solid; **R$_f$** 0.6 (petroleum ether/ethyl acetate = 7:3); **eluent composition** petroleum ether/ethyl acetate = 7:3; **mp** 88-90 ºC; **^{1}H NMR** (400 MHz, $CDCl_3$) δ 3.99 (s, 3H), 6.96 (d, *J* = 7.6 Hz, 1H), 7.11 (dd, *J* = 8.6 Hz, 2.6 Hz, 1H), 7.18 (d, *J* = 2.4 Hz, 1H), 7.22 (d, *J* = 7.2 Hz, 1H), 7.28 (s, 1H), 7.29-7.32 (comp, 2H), 7.40 (d, *J* = 7.2 Hz, 2H), 7.51 (t, *J* = 7.6 Hz, 1H), 7.76 (d, *J* = 8.4 Hz, 1H), 7.82 (d, *J* = 7.6 Hz, 1H); **^{13}C NMR** (100 MHz, $CDCl_3$) δ 55.9, 113.6, 116.3, 122.2 (x 2), 122.4, 126.6, 128.5, 129.0, 129.2, 131.4, 132.4, 132.6, 132.8, 139.9, 143.7, 162.8, 173.8; **HRMS** (ESI, m/z) calcd for $C_{20}H_{15}NO_3S$ $[M+H]^+$ 350.0851, found 350.0840.

3-(5-methyl-[1,1'-biphenyl]-2-yl)benzo[*d*]isothiazole 1,1-dioxide (3ja):

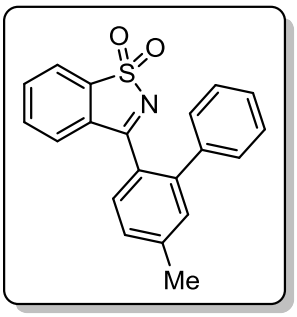

Combined Yield 88% (59 mg); **mono**:**bis** 12:1; colourless solid; **R$_f$** 0.5 (petroleum ether/ethyl acetate = 7:3); **eluent composition** petroleum ether/ethyl acetate = 7:3; **^{1}H NMR** (400 MHz, $CDCl_3$) δ 2.56 (s, 3H), 6.95 (d, *J* = 7.6 Hz, 1H), 7.16-7.20 (m,1H), 7.24 (app s, 1H), 7.28 (m, 1H), 7.31 (dd, *J* = 7.6 Hz, 0.8 Hz, 1H), 7.37 (app s, 1H), 7.39 (app s, 1H), 7.41-7.42 (m, 1H), 7.49 (app s, 1H), 7.52 (d, *J* = 7.6 Hz, 1H), 7.67 (d, *J* = 7.6 Hz, 1H), 7.81 (d, *J* = 6.8 Hz, 1H); **^{13}C NMR** (100 MHz, $CDCl_3$) δ 21.8, 122.2, 126.6, 127.1, 128.3, 128.9, 128.9, 129.2, 130.3, 131.2, 131.4, 132.7, 132.9, 139.8, 139.9, 141.6, 142.9, 174.3; **HRMS** (ESI, m/z) calcd for $C_{20}H_{15}NO_2S$ $[M+H]^+$ 334.0902, found 334.0904.

3-(5-(tert-butyl)-4'-methoxy-[1,1'-biphenyl]-2yl)benzo[*d*] isothiazole 1,1-dioxide (3ka):

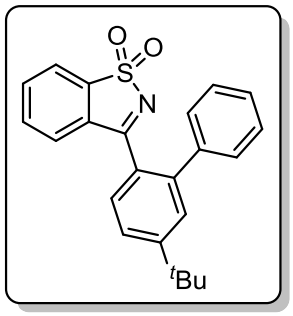

Combined Yield 66% (50 mg); **mono**:**bis** 32:1; colourless solid; **R_f** 0.6 (petroleum ether/ethyl acetate = 7:3); **eluent composition** petroleum ether/ethyl acetate = 7:3; **mp** 160-162 ^oC; **^{1}H NMR** (400 MHz, $CDCl_3$) δ 1.44 (s, 9H), 6.97 (d, *J* = 8.0 Hz, 1H), 7.14-7.19 (m, 1H), 7.24 (d, *J* = 8.0 Hz, 1H), 7.26-7.27 (m, 1H), 7.28 (app t, *J* = 7.2 Hz, 1H), 7.36-7.39 (comp, 2H), 7.49 (td, *J* = 7.4 Hz, 0.8 Hz, 1H), 7.59 (dd, *J* = 8.2 Hz, 1.8 Hz, 1H), 7.65 (d, *J* = 2.0 Hz, 1H), 7.69 (d, *J* = 8.4 Hz, 1H), 7.80 (d, *J* = 7.6 Hz, 1H); **^{13}C NMR** (100 MHz, $CDCl_3$) δ 31.4, 35.4, 122.2, 125.3, 126.7, 127.1, 127.8, 128.2, 128.9, 129.3, 130.1, 131.2, 132.8, 132.9, 139.8, 140.4, 141.4, 156.1, 174.3; **HRMS** (ESI, m/z) calcd for $C_{23}H_{21}NO_2S$ $[M+H]^+$ 376.1371, found 376.1373.

3-(5-(trifluoromethyl)-[1,1'-biphenyl]-2-yl)benzo[*d*]isothiazole1,1-dioxide (3la):

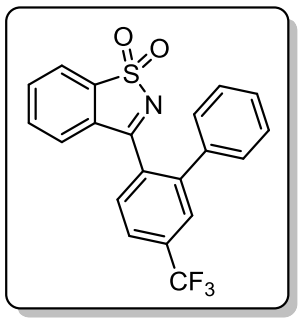

Combined Yield 74% (58 mg); **mono**:**bis** 6:1; colourless solid; **R_f** 0.3 (petroleum ether/ethyl acetate = 7:3); **eluent composition** petroleum ether/ethyl acetate = 7:3; **^{1}H NMR** (600 MHz, $CDCl_3$) δ 6.90 (d, *J* = 7.8 Hz, 1H), 7.22 (app t, *J* = 7.5 Hz, 1H), 7.27-7.30 (comp, 2H), 7.33 (app t, *J* = 7.8 Hz, 1H), 7.38-7.40 (comp, 2H), 7.54 (app t, *J* = 7.5 Hz, 1H), 7.82-7.84 (comp, 2H), 7.86 (d, *J* = 7.8 Hz, 1H), 7.92 (app s, 1H); **^{13}C NMR** (150 MHz, $CDCl_3$) δ 122.6, 124.9 (q, *J* = 3.5 Hz), 126.1, 127.4 (q, *J* = 3.5 Hz), 128.8, 128.9, 129.2, 129.3, 130.4, 130.7, 133.2, 133.3, 133.3, 134.1 (q, *J* = 32.8 Hz), 139.0 (q, *J* = 207.5 Hz), 142.4, 173.1; **HRMS** (ESI, m/z) calcd for $C_{20}H_{12}F_3NO_2S$ $[M+H]^+$ 388.0619, found 388.0618.

3-(5-chloro-[1,1'-biphenyl]-2-yl)benzo[*d*]isothiazole 1,1-dioxide (3ma):

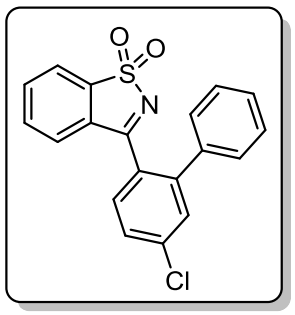

Combined Yield 73% (54 mg); **mono**:**bis** 3:1; colourless solid; **R_f** 0.4 (petroleum ether/ethyl acetate = 7:3); **eluent composition** petroleum ether/ethyl acetate = 7:3; **mp** 98-100 ^oC; **^{1}H NMR** (600 MHz, $CDCl_3$) δ 6.89 (d, *J* = 7.8 Hz, 1H), 7.19-7.22 (m, 1H), 7.25-7.27 (comp, 2H), 7.30 (td, *J* = 7.5 Hz, 0.8 Hz, 1H), 7.35-7.36 (comp, 2H), 7.52 (td, *J* = 7.5 Hz, 0.8 Hz, 1H), 7.56 (dd, *J* = 8.1 Hz, 2.1 Hz, 1H), 7.66 (d, *J* = 1.8 Hz, 1H), 7.69 (d, *J* = 7.8 Hz, 1H), 7.81 (d, *J* = 7.8 Hz, 1H); **^{13}C NMR** (150 MHz, $CDCl_3$) δ 122.5, 126.3, 128.3, 128.4, 129.0, 129.1, 129.2, 130.7, 130.7, 131.6,

133.1, 133.1, 138.5, 138.5, 139.7, 143.2, 173.3; **HRMS** (ESI, m/z) calcd for $C_{19}H_{12}ClNO_2S$ $[M+H]^+$ 354.0356, found 354.0358.

3-(5-fluoro-[1,1'-biphenyl]-2-yl)benzo[d]isothiazole 1,1-dioxide (3na):

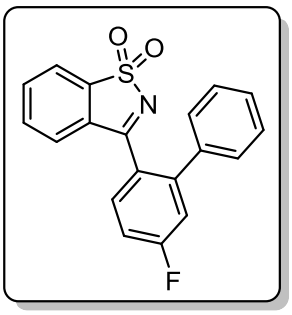

Yield 45% (42.6 mg); colorless solid; **R_f** 0.30 (pet ether/ethyl acetate = 9:1); **eluent composition** petroleum ether/ethyl acetate = 19:1; **mp** 136-138 °C; **^{1}H NMR** (400 MHz, $CDCl_3$) δ 10.05 (br s, 1H), 9.02 (dd, *J* = 7.2 Hz, 1.6 Hz, 1H), 8.77 (dd, *J* = 4.0 Hz, 1.6 Hz, 1H), 8.20 (dd, *J* = 8.4 Hz, 1.6 Hz, 1H), 7.72-7.70 (comp, 2H), 7.64 (app t, *J* = 8.0 Hz, 1H), 7.60-7.57 (comp, 2H), 7.49-7.45 (comp, 3H), 7.30 (d, *J* = 7.6 Hz, 1H), 2.33 (s, 3H), 0.32 (s, 9H); **^{13}C NMR** (100 MHz, $CDCl_3$) δ 170.0, 148.4, 145.4, 144.5, 142.2, 138.6, 137.3, 136.6, 134.5, 132.5, 131.5, 129.8, 129.7 (x 2), 129.1 (q, *J* = 41.0 Hz), 128.2, 127.7, 127.1 (q, *J* = 282.0 Hz), 125.3 (q, *J* = 4.0 Hz), 122.3, 121.9, 117.1, 17.5, 0.0; **HRMS** (ESI, m/z) calcd for $C_{27}H_{25}F_3N_2OSi$ $[M + H]^+$ 479.1766, found 479.1768.

3-(3-phenylnaphthalen-2-yl)benzo[*d*]isothiazole 1,1-dioxide (3oa):

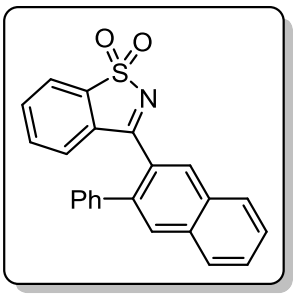

Yield 84% (62 mg); colourless solid; **R_f** 0.6 (petroleum ether/ethyl acetate = 7:3); **eluent composition** petroleum ether/ethyl acetate = 7:3; **mp** 122-124 °C; **^{1}H NMR** (400 MHz, $CDCl_3$) δ 6.98 (d, *J* = 7.6 Hz, 1H), 7.19 (app t, *J* = 7.4 Hz, 1H), 7.28-7.33 (comp, 3H), 7.47 (d, *J* = 7.6 Hz, 2H), 7.51 (app t, *J* = 7.6 Hz, 1H), 7.61 (td, *J* = 7.5 Hz, 0.9 Hz, 1H), 7.68 (td, *J* = 7.5 Hz, 0.9 Hz, 1H), 7.82 (d, *J* = 7.6 Hz, 1H), 7.99 (d, *J* = 8.4 Hz, 2H), 8.10 (s, 1H), 8.30 (s, 1H); **^{13}C NMR** (100 MHz, $CDCl_3$) δ 122.3, 126.7, 127.5, 128.2, 128.2 (x 2), 128.8, 128.9, 129.0, 129.3, 129.9, 131.0, 131.3, 132.0, 132.9, 133.1, 134.9, 137.6, 139.7, 139.9, 174.2; **HRMS** (ESI, m/z) calcd for $C_{23}H_{15}NO_2S$ $[M+H]^+$ 370.0902, found 370.0893.

3-(3-phenylthiophen-2-yl)benzo[*d*]isothiazole 1,1-dioxide (3pa):

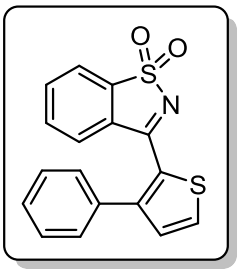

Yield 80% (52 mg); colourless solid; **R_f** 0.5 (petroleum ether/ethyl acetate = 7:3); **eluent composition** petroleum ether/ethyl acetate = 7:3; **mp** 114-116 °C; **^{1}H NMR** (400 MHz, $CDCl_3$) δ 6.93 (d, *J* = 8.0 Hz, 1H), 7.23 (td, *J* = 7.8 Hz, 0.8 Hz, 1H), 7.28-7.31 (comp, 3H), 7.35-7.38 (comp, 2H), 7.39 (d, *J* = 5.2 Hz, 1H), 7.54 (td, *J* = 7.6 Hz, 0.8 Hz, 1H), 7.76 (d, *J* = 5.2 Hz, 1H), 7.86 (d, *J* = 7.2 Hz, 1H); **^{13}C NMR** (100 MHz, $CDCl_3$) δ 122.5, 127.4, 127.7,

129.0, 129.2, 129.4, 130.2, 131.3, 132.3, 132.9, 133.0, 135.5, 140.7, 147.8, 166.6; **HRMS** (ESI, m/z) calcd for $C_{17}H_{11}NO_2S_2$ $[M+H]^+$ 326.0310, found 326.0309.

3-(3,4'-dimethoxy-[1,1'-biphenyl]-2-yl)benzo[*d*]isothiazole1,1-dioxide (3bb):

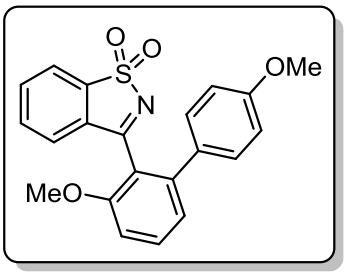

Yield 70% (53 mg); colourless solid; **R_f** 0.6 (petroleum ether/ethyl acetate = 7:3); **eluent composition** petroleum ether/ethyl acetate = 7:3; **mp** 120-122 ^oC; **^{1}H NMR** (400 MHz, $CDCl_3$) δ 3.70 (s, 3H), 3.80 (s, 3H), 6.74-6.77 (comp, 2H), 7.03 (d, *J* = 8.0 Hz, 1H), 7.10 (d, *J* = 7.6 Hz, 1H), 7.13 (dd, *J* = 8.0 Hz, 0.4 Hz, 1H), 7.18-7.22 (comp, 2H), 7.46 (td, *J* = 7.6, 0.8 Hz, 1H), 7.55 (d,*J* = 8.0 Hz, 1H), 7.58-7.60 (m, 1H), 7.83 (d, *J* = 7.6 Hz, 1H); **^{13}C NMR** (100 MHz, $CDCl_3$) δ 55.4, 56.3, 110.0, 114.1, 118.3, 122.3, 122.8, 125.9, 130.4, 131.5, 132.2, 132.5, 132.9, 133.5, 139.5, 142.9, 157.8, 159.5, 172.1; **HRMS** (ESI, m/z) calcd for $C_{21}H_{17}NO_4S$ $[M+H]^+$ 380.0957, found 380.0959.

3-(3-methoxy-4'-methyl-[1,1'-biphenyl]-2-yl)benzo[*d*]isothiazole 1,1-dioxide (3bc):

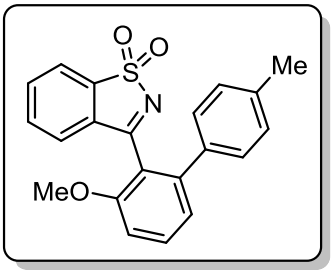

Yield 84% (61 mg); colourless solid; **R_f** 0.6 (petroleum ether/ethyl acetate = 7:3); **eluent composition** petroleum ether/ethyl acetate = 7:3; **mp** 162-164 ^oC; **^{1}H NMR** (400 MHz, $CDCl_3$) δ 2.24 (s, 3H), 3.80 (s, 3H), 7.02-7.06 (comp, 3H), 7.14-7.16 (comp, 4H), 7.48 (app t, *J* = 7.6 Hz, 1H), 7.55-7.60 (comp, 2H), 7.83 (d, *J* = 7.6 Hz, 1H); **^{13}C NMR** (100 MHz, $CDCl_3$) δ 21.2. 56.3, 110.1, 118.3, 122.3, 122.9, 125.9, 129.0, 129.4, 132.2, 132.5, 132.9, 133.5, 136.2, 137.9, 139.5, 143.3, 157.8, 172.1; **HRMS** (ESI, m/z) calcd for $C_{21}H_{17}NO_3S$ $[M+H]^+$ 364.1007, found 364.0997.

3-(2-methoxy-6-(thiophen-2-yl)phenyl)benzo[*d*]isothiazole1,1-dioxide (3bd):

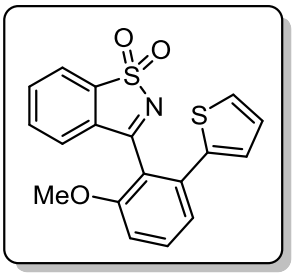

Yield 76% (54 mg); colourless solid; **R_f** 0.4 (petroleum ether/ethyl acetate = 7:3); **eluent composition** petroleum ether/ethyl acetate = 7:3; **mp** 88-90 ^oC; **^{1}H NMR** (400 MHz, $CDCl_3$) δ 3.78 (s, 3H), 6.84 (dd, *J* = 4.8 Hz, 3.6 Hz, 1H), 6.96 (dd, *J* = 3.6 Hz, 0.8 Hz, 1H), 7.03 (d, *J* = 8.4 Hz, 1H), 7.11 (d, *J* = 7.6 Hz, 1H), 7.17 (dd, *J* = 5.0 Hz, 0.6 Hz, 1H), 7.24-7.25 (m, 1H), 7.48 (app t, *J* = 7.6 Hz, 1H), 7.54 (app t, *J* = 8.0 Hz, 1H), 7.60 (app t, *J* = 7.4 Hz, 1H), 7.85 (d, *J* = 7.6 Hz, 1H); **^{13}C NMR** (100 MHz, $CDCl_3$) δ 56.4, 110.8, 118.1, 122.4, 122.8, 125.4, 127.0, 128.0, 128.2, 132.3, 132.3, 133.1, 133.7, 135.4, 139.4, 140.2, 157.9, 171.8; **HRMS** (ESI, m/z) calcd for $C_{18}H_{13}NO_3S_2$ $[M+H]^+$ 356.0415, found 356.0406.

3-(2-(naphthalen-1-yl)phenyl)benzo[*d*]isothiazole1,1-dioxide (3be):

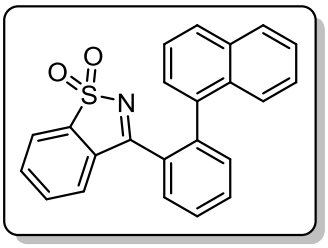

Yield 65% (48 mg); colourless solid; **R_f** 0.4 (petroleum ether/ethyl acetate = 7:3); **eluent composition** petroleum ether/ethyl acetate = 7:3; **mp** 152-154 ^oC; **^{1}H NMR** (400 MHz, $CDCl_3$) δ 7.00-7.06 (comp, 2H), 7.31 (app t, *J* = 7.4 Hz, 1H), 7.34-7.39 (comp, 2H), 7.44-7.50 (comp, 2H), 7.63-7.68 (comp, 3H), 7.73-7.79 (comp, 3H), 7.82 (d, *J* = 7.6 Hz, 1H), 7.94 (d, *J* = 7.6 Hz, 1H); **^{13}C NMR** (100 MHz, $CDCl_3$) δ 122.2, 125.2, 125.4, 125.6, 126.2, 127.0, 128.3, 128.7, 129.0, 129.1, 130.0, 130.8, 131.4, 131.4, 131.6, 132.4, 132.6, 132.9, 133.8, 136.8, 139.4, 139.9, 173.7; **HRMS** (ESI, m/z) calcd for $C_{23}H_{15}NO_2S$ $[M+H]^+$ 370.0902, found 370.0888.

3-(4,4'-dimethoxy-[1,1'-biphenyl]-2-yl)benzo[*d*]isothiazole 1,1-dioxide (3db):

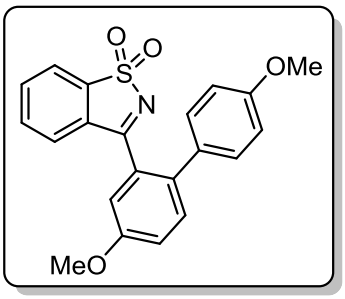

Yield 65% (49 mg); colourless solid; **R_f** 0.7 (petroleum ether/ethyl acetate = 7:3); **eluent composition** petroleum ether/ethyl acetate = 7:3; **mp** 140-142 ^oC; **^{1}H NMR** (400 MHz, $CDCl_3$) δ 3.68 (s, 3H), 3.90 (s, 3H), 6.73-6.76 (comp, 2H), 6.91 (d, *J* = 7.6 Hz, 1H), 7.20-7.25 (comp, 4H), 7.30 (d, *J* = 7.6 Hz, 1H), 7.49 (dd, *J* = 7.6 Hz, 0.4 Hz, 1H), 7.53 (d, *J* = 8.4 Hz, 1H), 7.81 (d, *J* = 7.6 Hz, 1H); **^{13}C NMR** (100 MHz, $CDCl_3$) δ 55.4, 55.9, 114.1, 114.4, 119.2, 122.3, 126.7, 130.3, 130.5, 131.0, 131.8. 132.0, 132.9, 133.1, 133.7, 139.7, 159.1, 159.5, 174.5; **HRMS** (ESI, m/z) calcd for $C_{21}H_{17}NO_4S$ $[M+H]^+$ 380.0957, found 380.0946.

3-(4'-methoxy-4-methyl-[1,1'-biphenyl]-2-yl)benzo[*d*]isothiazole1,1-dioxide (3eb):

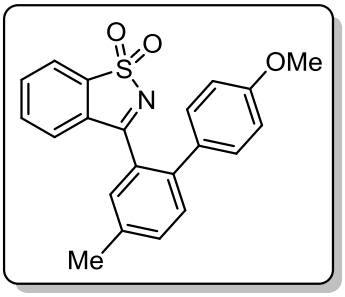

Yield 86% (63 mg); colourless solid; **R_f** 0.6 (petroleum ether/ethyl acetate = 7:3); **eluent composition** petroleum ether/ethyl acetate = 7:3; **mp** 126-128 ^oC; **^{1}H NMR** (400 MHz, $CDCl_3$) δ 2.46 (s, 3H), 3.68, (s, 3H), 6.74-6.77 (comp, 2H), 6.89 (d, *J* = 8.0 Hz, 1H), 7.25-7.26 (m, 1H), 7.26-7.27 (m, 1H), 7.29 (dd, *J* = 7.6 Hz, 0.8 Hz, 1H), 7.47-7.51 (comp, 3H), 7.53 (m, 1H), 7.80 (dd, *J* = 7.6 Hz, 0.4 Hz, 1H); **^{13}C NMR** (100 MHz, $CDCl_3$) δ 21.1, 55.4, 114.4, 122.2, 126.7, 129.5, 130.3 (x 2), 130.5, 131.1, 132.2, 132.8, 133.1, 133.1, 137.8, 138.3, 139.7, 159.6, 174.8; **HRMS** (ESI, m/z) calcd for $C_{21}H_{17}NO_3S$ $[M+H]^+$ 364.1007, found 364.0995.

3-(4-chloro-4'-methoxy-[1,1'-biphenyl]-2yl)benzo[*d*]isothiazole1,1-dioxide (3fb):

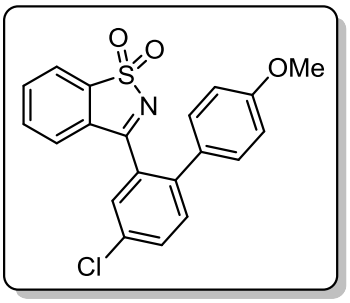

Combined Yield 68% (54 mg); **mono**:**bis** 10:1; colourless solid; **R$_f$** 0.5 (petroleum ether/ethyl acetate = 7:3); **eluent composition** petroleum ether/ethyl acetate = 7:3; **^{1}H NMR** (400 MHz, $CDCl_3$) δ 3.71 (s, 3H), 6.77-6.80 (comp, 2H), 6.89 (d, *J* = 7.6 Hz, 1H), 7.28 (d, *J* = 2.0 Hz, 1H), 7.33 (td, *J* = 8.0 Hz, 0.9 Hz, 1H), 7.53 (dd, *J* = 7.6 Hz, 0.8 Hz, 1H), 7.56-7.60 (comp, 2H), 7.66 (dd, *J* = 8.4 Hz, 2.4 Hz, 1H), 7.72 (d, *J* = 2.0 Hz, 1H), 7.83 (d, *J* = 7.6 Hz, 1H); **^{13}C NMR** (100 MHz, $CDCl_3$) δ 55.4, 114.6, 122.5, 126.4, 129.8, 130.3, 130.6, 130.9, 131.0, 131.7, 132.2, 133.1, 133.2, 133.9, 139.6, 139.7, 160.1, 173.2; **HRMS** (ESI, m/z) calcd for $C_{20}H_{14}ClNO_3S$ $[M+H]^+$ 384.0461, found 384.0448.

3-(4-fluoro-4'-methoxy-[1,1'-biphenyl]-2-yl)benzo[*d*]isothiazole 1,1-dioxide (3gb):

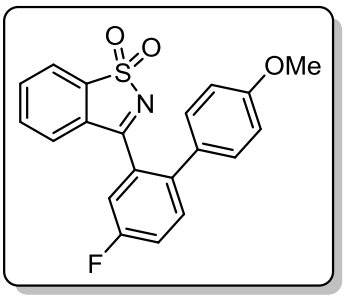

Combined Yield 82% (62 mg); **mono**:**bis** 9:1; colourless solid; **R$_f$** 0.5 (petroleum ether/ethyl acetate = 7:3); **eluent composition** petroleum ether/ethyl acetate = 7:3; **^{1}H NMR** (600 MHz, $CDCl_3$) δ 3.69 (s, 3H), 6.78 (d, *J* = 9.0 Hz, 2H), 6.96 (d, *J* = 8.0 Hz, 1H), 7.30 (dd, *J* = 8.7 Hz, 1.5 Hz, 2H), 7.34 (td, *J* = 7.6 Hz, 0.8 Hz, 1H), 7.41-7.45 (m, 1H), 7.50-7.52 (comp, 2H), 7.53 (dd, *J* = 7.5 Hz, 0.9 Hz, 1H), 7.80 (d, *J* = 7.8 Hz, 1H); **^{13}C NMR** (150 MHz, $CDCl_3$) δ 55.4, 114.2, 119.5 (d, $^2J_{F–C}$ = 23.2 Hz), 122.4, 124.8, 125.6 (d, $^3J_{F–C}$ = 3.6 Hz), 126.4, 128.6 (d, $^2J_{F–C}$ = 16.9 Hz), 129.5 (d, $^3J_{F–C}$ = 8.7 Hz), 130.6, 131.7, 131.8, 132.4 (d, $^4J_{F–C}$ = 3.1 Hz), 133.1, 133.2, 139.6, 159.8 (d, $^1J_{F–C}$ = 247.0 Hz), 160.0, 173.2; **HRMS** (ESI, m/z) calcd for $C_{20}H_{15}FNO_3S$ $[M+H]^+$ 368.0757, found 368.0756.

3-(4',5-dimethoxy-[1,1'-biphenyl]-2-yl)benzo[*d*]isothiazole 1,1-dioxide (3hb):

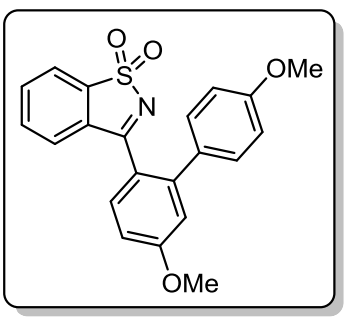

Combined Yield 83% (65 mg); **mono**:**bis** 8:1; colourless solid; **R$_f$** 0.6 (petroleum ether/ethyl acetate = 7:3); **eluent composition** petroleum ether/ethyl acetate = 7:3; **^{1}H NMR** (400 MHz, $CDCl_3$) δ 3.69 (s, 3H), 3.94 (s, 3H), 6.75-6.79 (comp, 2H), 6.90 (d, *J* = 8.0 Hz, 1H), 7.03 (dd, *J* = 8.6 Hz, 2.6 Hz, 1H), 7.10 (d, *J* = 2.4 Hz, 1H), 7.26-7.30 (comp, 3H), 7.48 (td, *J* = 7.5 Hz, 0.7 Hz, 1H), 7.70 (d, *J* = 8.8 Hz, 1H), 7.79 (d, *J* = 7.6 Hz, 1H); **^{13}C NMR** (100 MHz, $CDCl_3$) δ 55.4, 55.8, 113.2, 114.1, 114.5, 115.9, 122.2, 122.3, 126.8, 130.4, 131.4, 132.4, 132.6, 132.9, 139.9, 143.4,

160.0, 162.8, 174.0; **HRMS** (ESI, m/z) calcd for $C_{21}H_{17}NO_4S$ $[M+H]^+$ 380.0957, found 380.0948.

3-(4'-methoxy-5-methyl-[1,1'-biphenyl]-2-yl)benzo[*d*]isothiazole 1,1-dioxide (3ib):

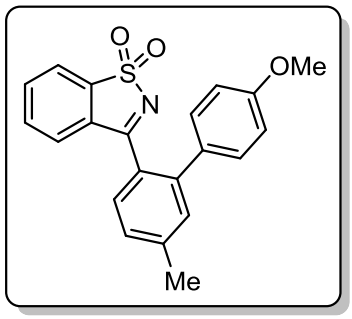

Combined Yield 61% (46 mg); **mono**:**bis** 9:1; colourless solid; **R$_f$** 0.7 (petroleum ether/ethyl acetate = 7:3); **eluent composition** petroleum ether/ethyl acetate = 7:3; **^{1}H NMR** (600 MHz, $CDCl_3$) δ 2.52 (s, 3H), 3.69 (s, 3H), 6.76 (d, *J* = 9.0 Hz, 2H), 6.90 (d, *J* = 7.8 Hz, 1H), 7.27-7.29 (comp, 3H), 7.33 (d, *J* = 7.8 Hz, 1H), 7.43 (app s, 1H), 7.49 (app t, *J* = 7.5, 1H), 7.62 (d, *J* = 7.8 Hz, 1H), 7.80 (d, *J* = 7.8 Hz, 1H); **^{13}C NMR** (150 MHz, $CDCl_3$) δ 21.8, 55.4, 114.4, 122.2, 126.7, 127.0, 128.4, 130.3, 130.4, 131.1, 131.3, 132.4, 132.7, 133.0, 139.8, 141.2, 142.9, 159.7, 174.6; **HRMS** (ESI, m/z) calcd for $C_{21}H_{17}NO_3S$ $[M+H]^+$ 364.1007, found 364.0993.

3-(5-(tert-butyl)-4'-methoxy-[1,1'-biphenyl]-2-yl)benzo[*d*]isothiazole 1,1-dioxide (3jb):

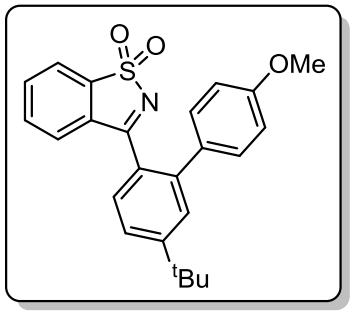

Combined Yield 60% (50 mg); **mono**:**bis** 8:1; colourless solid; **R$_f$** 0.7 (petroleum ether/ethyl acetate = 7:3); **eluent composition** petroleum ether/ethyl acetate = 7:3; **^{1}H NMR** (400 MHz, $CDCl_3$) δ 1.40 (s, 9H), 3.68 (s, 3H), 6.74-6.78 (comp, 2H), 6.92 (d, *J* = 7.6 Hz, 1H), 7.24-7.25 (m, 1H), 7.26-7.28 (comp, 2H), 7.47 (td, *J* = 7.4 Hz, 0.7 Hz, 1H), 7.52 (dd, *J* = 8.2 Hz, 1.8 Hz, 1H), 7.58 (d, *J* = 2.0 Hz, 1H), 7.64 (d, *J* = 8.4 Hz, 1H), 7.78 (d, *J* = 7.6 Hz, 1H); **^{13}C NMR** (100 MHz, $CDCl_3$) δ 31.4, 35.4, 55.4, 114.4, 122.2, 124.9, 126.8, 127.0, 127.6, 130.1, 130.5, 131.3, 132.7, 132.9, 133.0, 139.8, 141.0, 156.0, 159.8, 174.6; **HRMS** (ESI, m/z) calcd for $C_{24}H_{23}NO_3S$ $[M+H]^+$ 406.1477, found 406.1468.

3-(4'-methoxy-5-(trifluoromethyl)-[1,1'-biphenyl]-2yl)benzo[*d*] isothiazole1,1-dioxide (3kb):

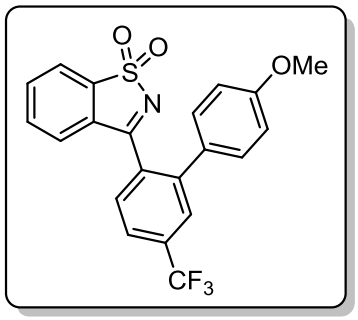

Yield 70% (58 mg); colourless solid; **R$_f$** 0.5 (petroleum ether/ethyl acetate = 7:3); **eluent composition** petroleum ether/ethyl acetate = 7:3; **mp** 102-104 ^{o}C; **^{1}H NMR** (400 MHz, $CDCl_3$) δ 3.71(s, 3H), 6.78-6.82 (comp, 2H), 6.87 (d, *J* = 8.0 Hz, 1H), 7.30-7.32 (comp, 2H), 7.34 (dd, *J* = 7.6 Hz, 0.8 Hz, 1H), 7.55 (td, *J* = 7.4 Hz, 0.5 Hz, 1H), 7.78 (dd, *J* = 8.0 Hz, 1.2 Hz, 1H), 7.83-7.85 (comp, 2H), 7.87 (app s, 1H); **^{13}C NMR** (100 MHz, $CDCl_3$) δ 55.5, 114.8,

122.6, 124.3 (q, *J* = 3.6 Hz), 126.2, 127.2 (q, *J* = 3.6 Hz), 130.5, 130.7, 130.7, 132.9, 133.3, 133.4, 134.1 (q, *J* = 32.4 Hz), 139.7, 140.9 (q, *J* = 227.7 Hz), 142.0, 160.4, 173.4; **HRMS** (ESI, m/z) calcd for $C_{21}H_{14}F_3NO_3S$ $[M+H]^+$ 418.0725, found 418.0714.

3-(5-chloro-4'-methoxy-[1,1'-biphenyl]-2-yl)benzo[*d*]isothiazole 1,1-dioxide (3lb):

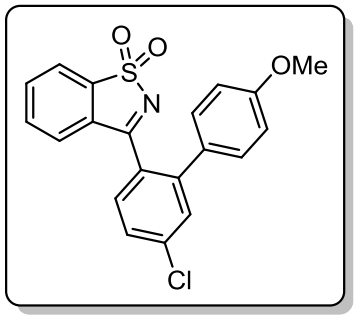

Yield 70% (54 mg); colourless solid; **R_f** 0.5 (petroleum ether/ethyl acetate = 7:3); **eluent composition** petroleum ether/ethyl acetate = 7:3; **mp** 136-138 °C; **^{1}H NMR** (400 MHz, $CDCl_3$) δ 3.68 (s, 3H), 6.73-6.77 (comp, 2H), 6.84 (d, *J* = 7.6 Hz, 1H), 7.23-7.25 (comp, 2H), 7.29 (dd, *J* = 7.6 Hz, 0.8 Hz, 1H), 7.46-7.52 (comp, 2H), 7.59 (d, *J* = 2.0 Hz, 1H), 7.64 (d, *J* = 8.4 Hz, 1H), 7.79 (d, *J* = 7.6 Hz, 1H); **^{13}C NMR** (100 MHz, $CDCl_3$) δ 55.5, 114.6 , 122.4, 126.4, 127.9, 128.1, 130.4 (x 2), 130.8, 130.9, 131.6, 133.0, 133.2, 138.4, 139.8, 142.9, 160.2, 173.6; **HRMS** (ESI, m/z) calcd for $C_{20}H_{14}ClNO_3S$ $[M+H]^+$ 384.0461, found 384.0448.

3-(5-fluoro-4'-methoxy-[1,1'-biphenyl]-2-yl)benzo[*d*]isothiazole1,1-dioxide (3mb):

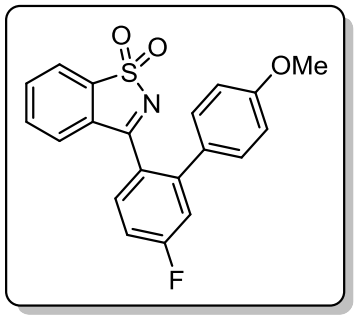

Yield 68% (50 mg); colourless solid; **R_f** 0.5 (petroleum ether/ethyl acetate = 7:3); **eluent composition** petroleum ether/ethyl acetate = 7:3; **mp** 120-122 °C; **^{1}H NMR** (400 MHz, $CDCl_3$) δ 3.67 (s, 3H), 6.73-6.77 (comp, 2H), 6.85 (d, *J* = 8.0 Hz, 1H), 7.20 (td, *J* = 8.2 Hz, 2.7 Hz, 1H), 7.24-7.26 (comp, 2H), 7.28-7.31 (comp, 2H), 7.49 (td, *J* = 7.6 Hz, 0.8 Hz, 1H), 7.70 (dd, *J* = 8.8 Hz, 5.6 Hz, 1H), 7.79 (d, *J* = 7.6 Hz, 1H); **^{13}C NMR** (100 MHz, $CDCl_3$) δ 55.4, 114.6, 115.0 (d, $^2J_{F-C}$ = 21.9 Hz), 117.3 (d, $^2J_{F-C}$ = 22.1 Hz), 122.4, 125.8 (d, $^4J_{F-C}$ = 2.6 Hz), 126.5, 130.3, 130.9, 131.1, 132.6 (d, $^3J_{F-C}$ = 9.3 Hz), 133.0, 133.1, 139.8, 144.0 (d, $^3J_{F-C}$ = 8.6 Hz), 160.2, 164.9 (d, $^1J_{F-C}$ = 252.1 Hz), 173.6; **HRMS** (ESI, m/z) calcd for $C_{20}H_{14}FNO_3S$ $[M+H]^+$ 368.0757, found 368.0763.

3-(3-(4-methoxyphenyl)naphthalen-2-yl)benzo[*d*]isothiazole 1,1-dioxide (3nb):

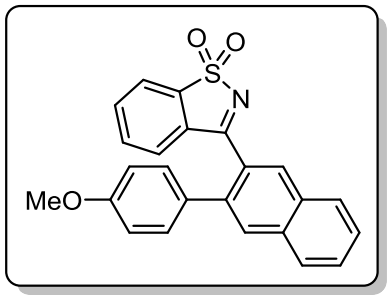

Yield 88% (70 mg); colourless solid; **R_f** 0.6 (petroleum ether/ethyl acetate = 7:3); **eluent composition** petroleum ether/ethyl acetate = 7:3; **mp** 80-82 °C; **^{1}H NMR** (400 MHz, $CDCl_3$) δ 3.71 (s, 3H), 6.81 (d, *J* = 8.8 Hz, 2H), 6.95 (d, *J* = 7.6 Hz, 1H), 7.31 (app t, *J* = 7.6 Hz, 1H), 7.38-7.40 (comp, 2H), 7.52 (app t, *J* = 7.6 Hz, 1H), 7.59 (app t, *J* = 7.6 Hz, 1H),

7.65 (app t, *J* = 7.6 Hz, 1H), 7.82 (d, *J* = 7.6 Hz, 1H), 7.97 (d, *J* = 8.0 Hz, 2H), 8.04 (s, 1H), 8.27 (s, 1H); **^{13}C NMR** (100 MHz, $CDCl_3$) δ 55.4, 114.5, 122.2, 126.8, 127.3, 128.1, 128.3, 128.8, 128.8, 129.4, 130.4, 130.9, 131.3, 131.8, 132.4, 132.9, 133.1, 135.0, 137.2, 139.7, 159.6, 174.4; **HRMS** (ESI, m/z) calcd for $C_{24}H_{17}NO_3S$ $[M+H]^+$ 400.1007, found 400.1008.

3-(3-(4-methoxyphenyl)thiophen-2-yl)benzo[*d*]isothiazole1,1dioxide (3ob):

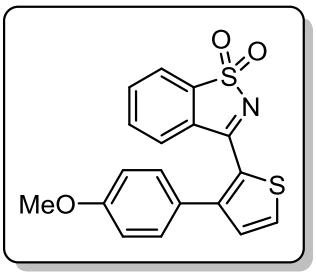

Yield 82% (58 mg); colourless solid; **R_f** 0.4 (petroleum ether/ethyl acetate = 7:3); **eluent composition** petroleum ether/ethyl acetate = 7:3; **mp** 136-138 °C; **^{1}H NMR** (400 MHz, $CDCl_3$) δ 3.76 (s, 3H), 6.80-6.84 (comp, 2H), 6.96 (d, *J* = 7.6 Hz, 1H), 7.25 (dd, *J* = 7.6 Hz, 0.8 Hz, 1H), 7.27-7.30 (comp, 2H), 7.34 (d, *J* = 4.8 Hz, 1H), 7.55 (td, *J* = 7.5 Hz, 0.92 Hz, 1H), 7.73 (d, *J* = 4.8 Hz, 1H), 7.86 (d, *J* = 7.6 Hz, 1H); **^{13}C NMR** (100 MHz, $CDCl_3$) δ 55.5, 114.6, 122.4, 126.8, 127.5, 128.0, 130.3, 130.7, 131.2, 132.2, 133.0, 133.0, 140.7, 147.6, 160.3, 166.7; **HRMS** (ESI, m/z) calcd for $C_{18}H_{13}NO_3S_2$ $[M+H]^+$ 356.0415, found 356.0414.

4-([1,1'-biphenyl]-2-yl)benzo[*e*][1,2,3]oxathiazine 2,2-dioxide (5aa):

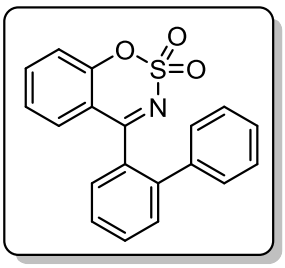

Yield 95% (64 mg); colourless solid; **R_f** 0.5 (petroleum ether/ethyl acetate = 7:3); **eluent composition** petroleum ether/ethyl acetate = 7:3; **mp** 78-80 °C; **^{1}H NMR** (400 MHz, $CDCl_3$) δ 6.97-7.01 (m, 1H), 7.10 (dd, *J* = 8.0 Hz, 1.6 Hz, 1H), 7.12-7.15 (comp, 2H), 7.20 (app t, *J* = 7.4 Hz, 2H), 7.23-7.25 (comp, 2H), 7.46 (td, *J* = 7.8 Hz, 1.5 Hz, 1H), 7.54-7.58 (comp, 2H), 7.67-7.72 (comp, 2H); **^{13}C NMR** (100 MHz, $CDCl_3$) δ 117.1, 118.7, 125.4, 127.9, 128.0, 128.7, 129.1, 130.4, 130.5, 131.2, 132.1, 133.3, 136.7, 139.5, 142.2, 153.8, 178.7; **HRMS** (ESI, m/z) calcd for $C_{19}H_{13}NO_3S$ $[M+Na]^+$ 358.0514, found 358.0518.

4-([1,1'-biphenyl]-2-yl)-7-methoxybenzo[*e*][1,2,3]oxathiazine2,2-dioxide (5ba):

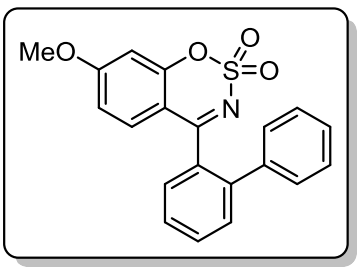

Yield 74% (54 mg); colourless solid; **R_f** 0.7 (petroleum ether/ethyl acetate = 7:3); **eluent composition** petroleum ether/ethyl acetate = 7:3; **mp** 56-58 °C; **^{1}H NMR** (400 MHz, $CDCl_3$) δ 3.84 (s, 3H), 6.53 (dd, *J* = 9.0 Hz, 2.6 Hz, 1H), 6.63 (d, *J* = 2.4 Hz, 1H), 7.05 (d, *J* = 8.8 Hz, 1H), 7.18-7.22 (m, 1H), 7.24-7.26 (m, 1H), 7.27-7.31 (comp, 3H), 7.56 (td, *J* = 6.6 Hz, 1.2 Hz, 1H), 7.59 (d, *J* = 4.8 Hz, 1H), 7.64-7.66 (m, 1H), 7.70 (td, *J* = 7.6 Hz, 1.5 Hz, 1H); **^{13}C NMR** (100 MHz, $CDCl_3$) δ 56.3, 102.8, 110.5, 112.9, 127.8, 127.9, 128.7, 129.0, 130.2, 130.5, 131.8, 132.9, 133.5,

139.5, 141.9, 156.3, 166.3, 177.8; **HRMS** (ESI, m/z) calcd for $C_{20}H_{15}NO_4S$ $[M+H]^+$ 366.0800, found 366.0840.

4-([1,1'-biphenyl]-2-yl)-7-methylbenzo[*e*][1,2,3]oxathiazine2,2-dioxide (5ca):

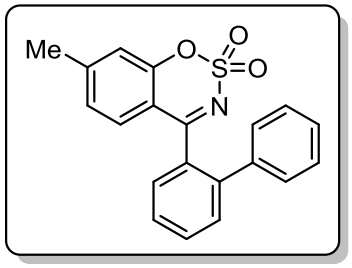

Yield 79% (55 mg); colourless solid; $\mathbf{R_f}$ 0.6 (petroleum ether/ethyl acetate = 7:3); **eluent composition** petroleum ether/ethyl acetate = 7:3; **mp** 154-156 ^oC; **^{1}H NMR** (400 MHz, $CDCl_3$) δ 2.33 (s, 3H), 6.79 (d, *J* = 8.0 Hz, 1H), 6.95 (app s, 1H), 6.98 (d, *J* = 8.0 Hz, 1H), 7.15 (t, *J* = 7.0 Hz, 1H), 7.21 (app t, *J* = 7.4 Hz, 2H), 7.25 (d, *J* = 7.2 Hz, 2H), 7.52-7.57 (comp, 2H), 7.63-7.69 (comp, 2H); **^{13}C NMR** (100 MHz, $CDCl_3$) δ 22.2, 114.8, 118.9, 126.4, 127.8, 127.9, 128.7, 129.1, 130.3, 130.5, 131.0, 131.9, 133.4, 139.6, 142.1, 149.2, 153.9, 178.4; **HRMS** (ESI, m/z) calcd for $C_{20}H_{15}NO_3S$ $[M+Na]^+$ 372.0670, found 372.0662.

4-([1,1'-biphenyl]-2-yl)-6-chloro-7methylbenzo[*e*][1,2,3] oxathiazine2,2-dioxide (5da):

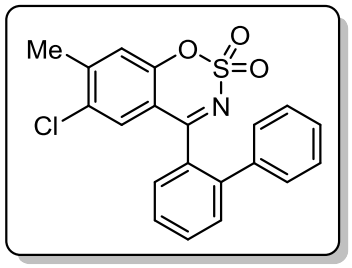

Yield 51% (39 mg); colourless solid; $\mathbf{R_f}$ 0.6 (petroleum ether/ethyl acetate = 7:3); **eluent composition** petroleum ether/ethyl acetate = 7:3; **mp** 160-162 ^oC; **^{1}H NMR** (400 MHz, $CDCl_3$) δ 2.33 (s, 3H), 7.00 (d, *J* = 8.0 Hz, 2H), 7.15-7.17 (m, 1H), 7.23-7.24 (comp, 4H), 7.58-7.72 (comp, 4H); **^{13}C NMR** (100 MHz, $CDCl_3$) δ 21.1, 115.7, 120.6, 128.1, 128.1, 128.8, 129.0, 130.6, 130.6, 130.9, 131.0, 132.4, 132.8, 139.6, 142.3, 146.5, 151.9, 177.5; **HRMS** (ESI, m/z) calcd for $C_{20}H_{15}ClNO_3S$ $[M+Na]^+$ 384.0461, found 384.0481.

4-([1,1'-biphenyl]-2-yl)-6-chlorobenzo[*e*][1,2,3]oxathiazine 2,2-dioxide (5ea):

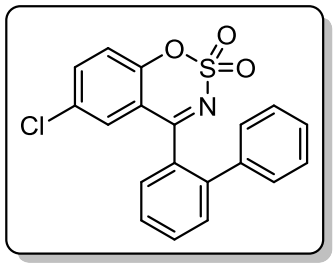

Combined Yield 72% (54 mg); **mono**:**bis** 17:1; colourless solid; $\mathbf{R_f}$ 0.4 (petroleum ether/ethyl acetate = 7:3); **eluent composition** petroleum ether/ethyl acetate = 7:3; **mp** 144-146 ^oC; **^{1}H NMR** (400 MHz, $CDCl_3$) δ 6.99 (d, *J* = 2.4 Hz, 1H), 7.07 (d, *J* = 8.4 Hz, 1H), 7.12-7.17 (m, 1H), 7.22-7.23 (comp, 4H), 7.36 (dd, *J* = 8.8 Hz, 2.4Hz, 1H), 7.60 (app t, *J* = 7.4 Hz, 2H), 7.72-7.75 (comp, 2H); **^{13}C NMR** (100 MHz, $CDCl_3$) δ 117.7, 120.1, 128.2, 128.3, 128.7, 128.9, 129.0, 130.6, 130.6, 130.7, 132.6, 132.7, 136.2, 139.6, 142.4, 152.0, 177.7; **HRMS** (ESI, m/z) calcd for $C_{19}H_{12}ClNO_3S$ $[M+H]^+$ 370.0305, found 370.0292.

4-([1,1'-biphenyl]-2-yl)-6-bromobenzo[*e*][1,2,3]oxathiazine 2,2-dioxide (5fa):

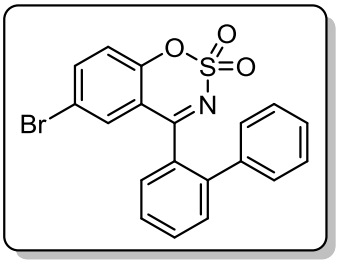

Combined Yield 75% (62 mg); **mono**:**bis** 18:1; colourless solid; **R_f** 0.5 (petroleum ether/ethyl acetate = 7:3); **eluent composition** petroleum ether/ethyl acetate = 7:3; **mp** 120-122 °C; **^{1}H NMR** (400 MHz, $CDCl_3$) δ 7.00 (d, *J* = 8.8 Hz, 1H), 7.13-7.17 (comp, 2H), 7.22-7.26 (comp, 4H), 7.50 (dd, *J* = 8.8 Hz, 2.0 Hz, 1H), 7.58-7.62 (comp, 2H), 7.72-7.76 (comp, 2H); **^{13}C NMR** (100 MHz, $CDCl_3$) δ 118.0, 118.0, 120.3, 128.2, 128.3, 128.9, 129.0, 130.6, 130.8, 132.7, 132.7, 133.6, 139.0, 139.6, 142.4, 152.5, 177.6; **HRMS** (ESI, m/z) calcd for $C_{19}H_{12}BrNO_3S$ $[M+H]^+$ 413.9800, found 413.9820.

4-(4'-methoxy-[1,1'-biphenyl]-2-yl)benzo[*e*][1,2,3]oxathiazine 2,2-dioxide (5ab):

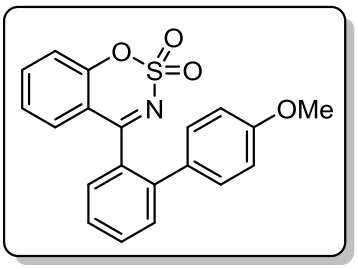

Combined Yield 80% (60 mg); **mono**:**bis** 7:1; colourless solid; **R_f** 0.7 (petroleum ether/ethyl acetate = 7:3); **eluent composition** petroleum ether/ethyl acetate = 7:3; **mp** 98-100 °C (crystallization from $CDCl_3$ and hexane); **^{1}H NMR** (400 MHz, $CDCl_3$) δ 3.70 (s, 3H), 6.71-6.75 (comp, 2H), 6.99 (td, *J* = 7.6 Hz, 0.93 Hz, 1H), 7.07 (dd, *J* = 8.0 Hz, 1.6 Hz, 1H), 7.13-7.18 (comp, 3H), 7.45-7.49 (m, 1H), 7.50-7.54 (comp, 2H), 7.64-7.69 (comp, 2H); **^{13}C NMR** (100 MHz, $CDCl_3$) δ 55.4, 114.2, 116.9, 118.7, 125.4, 127.5, 130.2, 130.3, 130.4, 131.2, 132.0 (x 2), 133.1, 136.7, 141.7, 153.8, 159.4, 179.0; **HRMS** (ESI, m/z) calcd for $C_{20}H_{15}NO_4S$ $[M+H]^+$ 366.0800, found 366.0811.

Crystal data and structure refinement for 5ab, CCDC No. 1891262

Empirical formula	$C_{20}H_{15}NO_4S$
Formula weight	365.39
Temperature/K	298
Crystal system	Monoclinic
Space group	$P2_1/n$
a/Å	8.107(7)
b/Å	11.495(9)
c/Å	19.194(16)
α/°	90
β/°	93.585(10)
γ/°	90
Volume/Å^3	1785(3)
Z	4
ρ_{calc}g/cm^3	1.359
μ/mm^{-1}	0.206
F(000)	760.0
Crystal size/mm^3	0.6 × 0.2 × 0.2

Radiation	Mo Kα (λ = 0.71073)
2Θ range for data collection/°	4.132 to 52.708
Index ranges	$-10 \leq h \leq 9$, $-14 \leq k \leq 14$, $-23 \leq l \leq 22$
Reflections collected	22553
Independent reflections	3549 [R_{int} = 0.1755, R_{sigma} = 0.1126]
Data/restraints/parameters	3549/0/236
Goodness-of-fit on F^2	0.966
Final R indexes [I>=2σ (I)]	R_1 = 0.0956, wR_2 = 0.2265
Final R indexes [all data]	R_1 = 0.1832, wR_2 = 0.3164
Largest diff. peak/hole / e $Å^{-3}$	0.61/-0.94

4-(4'-methyl-[1,1'-biphenyl]-2-yl)benzo[*e*][1,2,3]oxathiazine 2,2-dioxide (5ac):

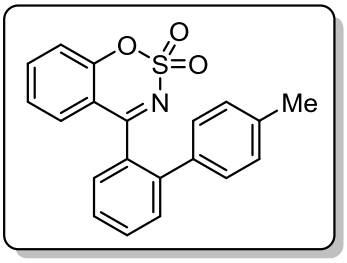

Combined Yield 79% (56 mg); **mono**:**bis** 15:1; colourless solid; **R_f** 0.6 (petroleum ether/ethyl acetate = 7:3); **eluent composition** petroleum ether/ethyl acetate = 7:3; **mp** 100-124 °C; **^{1}H NMR** (400 MHz, $CDCl_3$) δ 2.21 (s, 3H), 6.97-7.01 (comp, 3H), 7.09 (dd, *J* = 8.0 Hz, 1.6 Hz, 1H), 7.13-7.15 (comp, 3H), 7.47 (td, *J* = 7.8 Hz, 1.6 Hz, 1H), 7.51-7.56 (comp, 2H), 7.63-7.69 (comp, 2H); **^{13}C NMR** (100 MHz, $CDCl_3$) δ 21.1, 117.0, 118.6, 125.4, 127.6, 128.9, 129.4, 130.2, 130.5, 131.2, 132.0, 133.1, 136.6, 136.6, 137.8, 142.0, 153.7, 178.9; **HRMS** (ESI, m/z) calcd for $C_{20}H_{15}NO_3S$ $[M+Na]^+$ 372.0670, found 372.0671.

4-(2-(thiophen-2-yl)phenyl)benzo[*e*][1,2,3]oxathiazine 2,2-dioxide (5ad):

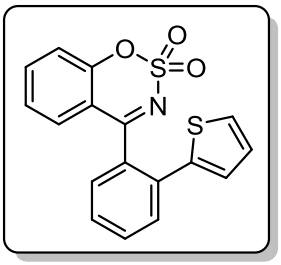

Yield 60% (41 mg); colourless solid; **R_f** 0.4 (petroleum ether/ethyl acetate = 7:3); **eluent composition** petroleum ether/ethyl acetate = 7:3; **mp** 128-130 °C; **^{1}H NMR** (400 MHz, $CDCl_3$) δ 6.81 (dd, *J* = 4.8 Hz, 3.6 Hz, 1H), 6.89 (dd, *J* = 3.6 Hz, 1.2 Hz, 1H), 7.05 (td, *J* = 7.6 Hz, 0.8 Hz, 1H), 7.11 (dd, *J* = 7.8 Hz, 1.8 Hz, 1H), 7.16 (dd, *J* = 5.0 Hz, 1.0 Hz, 1H), 7.20 (dd, *J* = 8.4 Hz, 0.8 Hz, 1H), 7.50-7.56 (comp, 2H), 7.63-7.66 (comp, 3H); **^{13}C NMR** (100 MHz, $CDCl_3$) δ 117.0, 118.8, 125.6, 127.3, 128.1, 128.1, 128.3, 130.2, 130.5, 130.6, 132.0, 133.2, 134.4, 136.8, 141.0, 153.8, 178.3; **HRMS** (ESI, m/z) calcd for $C_{17}H_{11}NO_3S_2$ $[M+H]^+$ 342.0259, found 342.0293.

4-(2-(naphthalen-1-yl)phenyl)benzo[e][1,2,3]oxathiazine 2,2-dioxide (5ae):

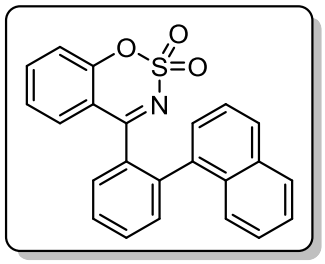

Yield 45% (35 mg); colourless solid; **R_f** 0.5 (petroleum ether/ethyl acetate = 7:3); **eluent composition** petroleum ether/ethyl acetate = 7:3; **mp** 102-104 ^oC; **^{1}H NMR** (400 MHz, $CDCl_3$) δ 6.91 (d, *J* = 8.0 Hz, 1H), 7.13 (d, *J* = 6.8 Hz, 1H), 7.24-7.40 (comp, 4H), 7.42-7.48 (comp, 2H), 7.60 (d, *J* = 7.6 Hz, 1H), 7.66-7.68 (comp, 2H), 7.71-7.74 (m, 1H), 7.75-7.77 (m, 1H), 7.80-7.82 (comp, 2H); **^{13}C NMR** (100 MHz, $CDCl_3$) δ 116.8, 118.2, 119.6, 124.6, 125.0, 125.8, 126.2, 126.7, 128.3 (x 2), 128.5, 128.7 (x 2), 129.0, 130.4, 130.7, 131.3, 132.1, 133.6, 134.9, 136.2, 153.1, 178.4; **HRMS** (ESI, m/z) calcd for $C_{23}H_{15}NO_3S$ $[M+H]^+$ 386.0851, found 386.0883.

7-methoxy-4-(4'-methoxy-[1,1'-biphenyl]-2-yl)benzo[*e*][1,2,3]oxathiazine 2,2-dioxide (5bb):

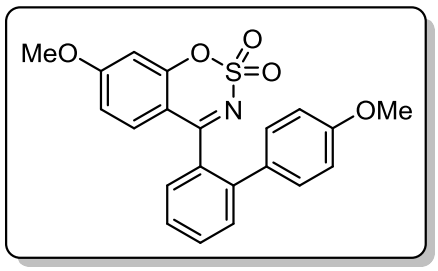

Yield 78% (62 mg); colourless solid; **R_f** 0.7 (petroleum ether/ethyl acetate = 7:3); **eluent composition** petroleum ether/ethyl acetate = 7:3; **mp** 94-96 ^oC; **^{1}H NMR** (400 MHz, $CDCl_3$) δ 3.72 (s, 3H), 3.81 (s, 3H), 6.49 (dd, *J* = 8.8 Hz, 2.4 Hz, 1H), 6.60 (d, *J* = 2.4Hz, 1H), 6.74-6.78 (comp, 2H), 6.98 (d, *J* = 9.2 Hz, 1H), 7.18-7.21 (comp, 2H), 7.47-7.52 (comp, 2H), 7.58 (dd, *J* = 7.8 Hz, 1 Hz, 1H), 7.63 (td, *J* = 7.5 Hz, 1.2 Hz, 1H); **^{13}C NMR** (100 MHz, $CDCl_3$) δ 55.4, 56.3, 102.8, 110.4, 112.9, 114.2, 127.4, 130.2, 130.2, 130.3, 131.7, 132.0, 132.9, 133.3, 141.4, 156.3, 159.4, 166.3, 178.1; **HRMS** (ESI, m/z) calcd for $C_{21}H_{17}NO_5S$ $[M+Na]^+$ 418.0725, found 418.0739.

4-(4'-methoxy-[1,1'-biphenyl]-2-yl)-7-methylbenzo[*e*] [1,2,3]oxathiazine2,2-dioxide (5cb):

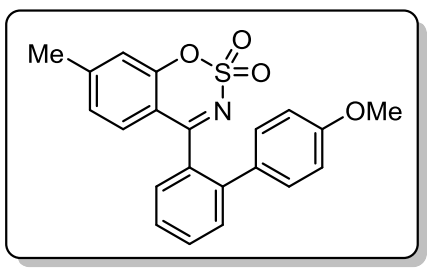

Yield 75% (55 mg); colourless solid; **R_f** 0.7 (petroleum ether/ethyl acetate = 7:3); **eluent composition** petroleum ether/ethyl acetate = 7:3; **mp** 108-110 ^oC; **^{1}H NMR** (400 MHz, $CDCl_3$) δ 2.34 (s, 3H), 3.72 (s, 3H), 6.73-6.76 (comp, 2H), 6.79 (dd, *J* = 8.0 Hz, 0.8 Hz, 1H), 6.94-6.96 (comp, 2H), 7.16-7.20 (comp, 2H), 7.48-7.53 (comp, 2H), 7.60-7.67 (comp, 2H); **^{13}C NMR** (100 MHz, $CDCl_3$) δ 22.2, 55.4, 114.3, 114.7, 119.0, 126.4, 127.4, 130.2 (x 2), 130.4, 131.0,

131.8, 132.1, 133.2, 141.6, 149.1, 154.0, 159.4, 178.7; **HRMS** (ESI, m/z) calcd for $C_{21}H_{17}NO_4S$ $[M+Na]^+$ 402.0775, found 402.0776.

6-chloro-4-(4'-methoxy-[1,1'-biphenyl]-2-yl)-7-methylbenzo[e][1,2,3]oxathiazine-2,2-dioxide (5db):

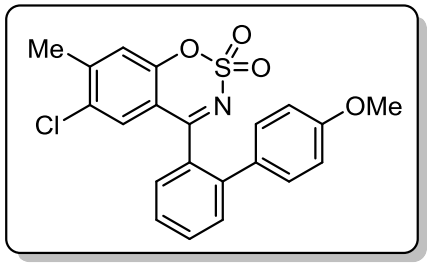

Yield 52% (45 mg); colourless solid; $\mathbf{R_f}$ 0.6 (petroleum ether/ethyl acetate = 7:3); **eluent composition** petroleum ether/ethyl acetate = 7:3; **mp** 122-124 ^oC; **^{1}H NMR** (400 MHz, $CDCl_3$) δ 2.34 (s, 3H), 3.72 (s, 3H), 6.76 (d, *J* = 8.4 Hz, 2H), 6.97 (s, 1H), 7.03 (s, 1H), 7.16 (d, *J* = 8.4 Hz, 2H), 7.52-7.56 (comp, 2H), 7.65-7.70 (comp, 2H); **^{13}C NMR** (100 MHz, $CDCl_3$) δ 21.1, 55.5, 114.4, 115.6, 120.7, 127.7, 130.2, 130.5 (x 2), 130.9, 131.0, 132.1, 132.4, 132.7, 141.8, 146.4, 152.0, 159.5, 177.7; **HRMS** (ESI, m/z) calcd for $C_{21}H_{17}ClNO_4S$ $[M+H]^+$ 414.0567, found 414.0601.

6-chloro-4-(4'-methoxy-[1,1'-biphenyl]-2-yl)benzo[*e*] [1,2,3]oxathiazine 2,2-dioxide (5eb):

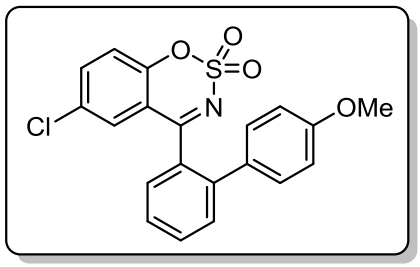

Yield 76% (61 mg); colourless solid; $\mathbf{R_f}$ 0.4 (petroleum ether/ethyl acetate = 7:3); **eluent composition** petroleum ether/ethyl acetate = 7:3; **mp** 118-120 ^oC; **^{1}H NMR** (400 MHz, $CDCl_3$) δ 3.71 (s, 3H), 6.75-6.78 (comp, 2H), 6.97 (d, *J* = 2.4 Hz, 1H), 7.09 (d, *J* = 8.8 Hz, 1H), 7.14-7.17 (comp, 2H), 7.38 (dd, *J* = 8.8 Hz, 2.4 Hz, 1H), 7.54-7.58 (comp, 2H), 7.69-7.73 (comp, 2H); **^{13}C NMR** (100 MHz, $CDCl_3$) δ 55.5, 114.4, 117.6, 120.1, 127.8, 130.2 , 130.5, 130.6, 130.6, 130.7, 132.0, 132.5, 132.6, 136.2, 141.9, 152.1, 159.5, 177.9; **HRMS** (ESI, m/z) calcd for $C_{20}H_{14}ClNO_4S$ $[M+H]^+$ 400.0410, found 400.0434.

6-bromo-4-(4'-methoxy-[1,1'-biphenyl]-2-yl)benzo[*e*] [1,2,3]oxathiazine 2,2-dioxide (5fb):

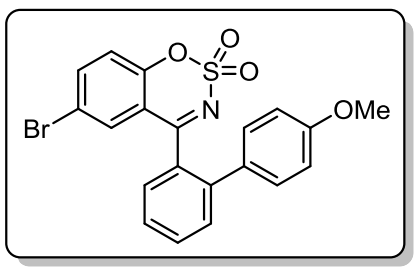

Yield 72% (64 mg); colourless solid; $\mathbf{R_f}$ 0.5 (petroleum ether/ethyl acetate = 7:3); **eluent composition** petroleum ether/ethyl acetate = 7:3; **mp** 120-124 ^oC; **^{1}H NMR** (400 MHz, $CDCl_3$) δ 3.72 (s, 3H), 6.75-6.78 (comp, 2H), 7.02 (d, *J* = 8.4 Hz, 1H), 7.11-7.16 (comp, 3H), 7.50-7.56 (comp, 3H), 7.71-7.75 (comp, 2H); **^{13}C NMR** (100 MHz, $CDCl_3$) δ 55.5, 114.4, 117.9, 118.0, 120.3,

127.8, 130.2, 130.5, 130.7, 132.1, 132.5, 132.6, 133.6, 139.0, 142.0, 152.6, 159.6, 177.8; **HRMS** (ESI, m/z) calcd for $C_{20}H_{14}BrNO_4S$ $[M+H]^+$ 443.9905, found 443.9901.

1-([1,1'-biphenyl]-2-yl)-1*H*-indazole (6):[22]

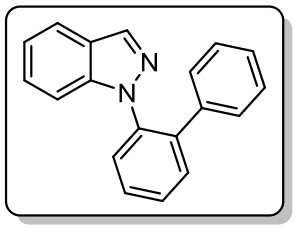

Combined Yield 94% (28 mg, 0.1 mmol scale); **mono**:**bis** 1.5:1; colourless oil; $\mathbf{R_f}$ 0.4 (petroleum ether/ethyl acetate = 19:1); **eluent composition** petroleum ether/ethyl acetate = 19:1; **^{1}H NMR** (400 MHz, $CDCl_3$) δ 7.01-7.02 (m, 1H), 7.07-7.08 (comp, 3H), 7.09-7.11 (comp, 3H), 7.14-7.18 (m, 1H), 7.56-7.58 (comp, 3H), 7.61 (dd, *J* = 8.0 Hz, 1.6 Hz, 1H), 7.67-7.69 (m, 1H), 8.11 (d, *J* = 0.8 Hz, 1H). The ^{1}H NMR data correspond with that reported in the literature.

7-phenyl-1-(pyrimidin-2-yl)indoline (7):[23]

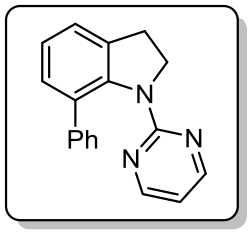

Yield 82% (45 mg); colourless oil; $\mathbf{R_f}$ 0.2 (petroleum ether/ethyl acetate = 9:1); **eluent composition** petroleum ether/ethyl acetate = 9:1; **^{1}H NMR** (400 MHz, $CDCl_3$) δ 3.19 (t, *J* = 8.0 Hz, 2H), 4.47 (t, *J* = 8.0 Hz, 2H), 6.38 (t, *J* = 4.8 Hz, 1H), 7.08-7.11 (m, 1H), 7.12-7.18 (comp, 3H), 7.24 (dd, *J* = 7.6 Hz, 1.2 Hz, 1H), 7.28 (dd, *J* = 8.0 Hz, 0.8 Hz, 1H), 7.32-7.35 (comp, 2H), 7.96 (d, *J* = 4.8 Hz, 2H). The ^{1}H NMR data correspond with that reported in the literature.

7.5.5. Synthetic Transformation of the Arylated Product 3aa

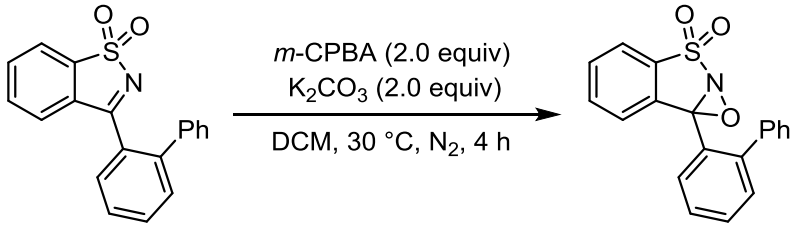

3aa **8**, 82%

In an oven-dried 10 mL round bottomed flask, **3aa** (64 mg, 0.2 mmol, 1.0 equiv) was taken and to it *m*-CPBA (69 mg, 0.4 mmol, 2.0 equiv), K_2CO_3 (55 mg, 0.4 mmol, 2.0 equiv) and DCM (10 mL) were added. The reaction mixture was degassed and backfilled with nitrogen. It was then closed with a stopper and kept at 30 ℃ while stirring for 4 h. After completion of reaction (checked by TLC), the reaction mixture was quenched with saturated NH_4Cl solution and then it was extracted with ethyl acetate. The combined organic layers were given brine wash and concentrated under vacuo. The crude reaction mixture was subjected to column

chromatography using ethyl acetate/petroleum ether as eluent to give 7b-([1,1'-biphenyl]-2-yl)-7b*H*-benzo[*d*][1,2]oxazireno[2,3-*b*]isothiazole 3,3-dioxide (**8**) in 82% yield.

Yield 82% (55 mg); colourless solid; **R_f** 0.5 (pet ether/ethyl acetate = 4:1); **eluent composition** petroleum ether/ethyl acetate = 4:1; **mp** 88-90 ºC (crystallization from $CHCl_3$); **^{1}H NMR** (400 MHz, $CDCl_3$) δ 7.04 (d, *J* = 7.6 Hz, 1H), 7.08 (d, *J* = 7.6 Hz, 1H), 7.18 (app t, *J* = 7.6 Hz, 2H), 7.29 (dd, *J* = 8.0 Hz, 0.8 Hz , 2H), 7.34 (td, *J* = 8.0 Hz, 0.8 Hz, 1H), 7.44 (td, *J* = 8.0 Hz, 0.8 Hz, 1H), 7.49 (dd, *J* = 7.6 Hz, 1.2 Hz, 1H), 7.52-7.56 (comp, 2H), 7.65 (td, *J* = 7.6 Hz, 1.2 Hz, 1H), 7.72 (dd, *J* = 7.6 Hz, 1.2 Hz, 1H); **^{13}C NMR** (100 MHz $CDCl_3$) δ 85.8, 123.3, 126.5, 127.2, 127.8, 128.0, 128.7, 128.8, 129.4, 131.0, 131.4, 132.0, 133.0, 133.2, 135.4, 139.4, 142.8; **HRMS** (EI, m/z) calcd for $C_{19}H_{13}NO_3S$ [M^+] 335.0616, found 335.0608.

Crystal data and structure refinement for 8, CCDC No. 2014574

Empirical formula	$C_{19}H_{13}NO_3S$
Formula weight	335.36
Temperature/K	100.0
Crystal system	monoclinic
Space group	$P2_1/n$
a/Å	9.9907(2)
b/Å	8.1808(2)
c/Å	19.0908(5)
α/°	90
β/°	90.2160(10)
γ/°	90
Volume/Å^3	1560.32(6)
Z	4
ρ_{calc}g/cm^3	1.428
μ/mm^{-1}	1.992
F(000)	696.0
Crystal size/mm^3	0.35 × 0.25 × 0.18
Radiation	Cu Kα (λ = 1.54184)
2Θ range for data collection/°	10.008 to 130.144
Index ranges	$-11 \le h \le 11$, $-9 \le k \le 9$, $-22 \le l \le 22$
Reflections collected	19662
Independent reflections	2642 [R_{int} = 0.0914, R_{sigma} = 0.0507]
Data/restraints/parameters	2642/0/218
Goodness-of-fit on F^2	1.226
Final R indexes [I>=2σ (I)]	R_1 = 0.0589, wR_2 = 0.1253
Final R indexes [all data]	R_1 = 0.0622, wR_2 = 0.1269
Largest diff. peak/hole / e Å^{-3}	0.43/-0.40

7.5.6. Mechanistic Experiments

(a) Procedure for H/D exchange experiment: (in absence of arylsiloxane)

An oven-dried 10 mL Schlenk tube was charged with **1a**-d_5 (24.3 mg, 0.1 mmol), silver (bistrifluoromethanesulfonyl)imide (7.7 mg, 20 mol %), copper acetate (9.0 mg, 50 mol %), silver fluoride (27.9 mg, 2.2 equiv) and catalyst $[Cp^*IrCl_2]_2$ (4.0 mg, 5 mol %). The tube was evacuated and backfilled with nitrogen and to it was added anhydrous TFE (1.0 mL, 0.1 M) under nitrogen atmosphere. The reaction mixture was degassed and backfilled with nitrogen 3 times. It was then closed with teflon-lined cap and kept at 30℃ while stirring for 1 h. After completion of the reaction, the reaction mixture was filtered through a short pad of celite, the solvent was removed under reduced pressure and the crude reaction mixture was directly purified through column chromatography on silica gel using petroleum ether/ethyl acetate (7:3) as eluent to recover the starting material **1a**-d_n (92%). The proton incorporation (80%) was determined by ^{1}H NMR spectroscopy.

(b) Procedure for H/D exchange experiment: (in presence of arylsiloxane)

An oven-dried 10 mL Schlenk tube was charged with **1a**-d_5 (24.3 mg, 0.1 mmol), trimethoxyphenylsilane (20.5 µL, 1.1 equiv), silver (bistrifluoromethanesulfonyl)imide (15.5 mg, 20 mol %), copper acetate (18.1 mg, 50 mol %), silver fluoride (55.8 mg, 2.2 equiv) and catalyst $[Cp^*IrCl_2]_2$ (8.0 mg, 5 mol %). The tube was evacuated and backfilled with nitrogen and to it was added anhydrous TFE (1.0 mL, 0.1 M) under nitrogen atmosphere. The reaction mixture was degassed and backfilled with nitrogen 3 times. It was then closed with teflon-lined cap and kept at 30℃ while stirring for 1 h. After completion of the reaction, the reaction mixture was filtered through a short pad of celite, the solvent was removed under reduced pressure and the crude reaction mixture was directly purified through column chromatography on silica gel using petroleum ether/ethyl acetate (7:3) as eluent yielding the product **3aa**-d_n (72%). The proton incorporation (80%) was determined by ^{1}H NMR spectroscopy.

(c) Procedure for parallel experiment between 1a and 1a-d_5:

Two separate oven-dried 10 mL Schlenk tubes were charged with **1a** (24.3 mg, 0.1 mmol) and **1a**-d_5 (24.8 mg, 0.1 mmol). To each were added trimethoxyphenylsilane (20.5 µL, 1.1 equiv), silver (bistrifluoromethanesulfonyl) imide (15.5 mg, 20 mol %), copper acetate (18.1 mg, 50 mol %), silver fluoride (55.8 mg, 2.2 equiv) and catalyst $[Cp^*IrCl_2]_2$ (8.0 mg, 5 mol %). The tubes were evacuated and backfilled with nitrogen and to it was added anhydrous DCE (1.0 mL, 0.1 M) under nitrogen atmosphere. The reaction mixtures were degassed and backfilled

with nitrogen 3 times and kept for stirring at 30℃. After 7 min, the reactions were quickly quenched by adding ethyl acetate keeping in an ice bath. The reaction mixtures were filtered through a short pad of celite, both the reaction mixtures were combined and concentrated under vacuo. The crude reaction mixture was directly purified by column chromatography on silica gel using petroleum ether/ ethyl acetate (7:3) as eluent. The ratio of **3aa** and **3aa**-d_4 was determined by ^{1}H NMR spectroscopy. Primary kinetic isotopic effect (KIE) was found to be $\boldsymbol{k_H/k_D}$ = 0.67/0.33 = 2.0.

(d) Procedure for competitive experiment between 1a and 1a-d_5:

An oven-dried 10 mL Schlenk tube was charged with **1a** (24.3 mg, 0.1 mmol), **1a**-d_5 (49.6 mg, 0.1 mmol), trimethoxyphenylsilane (41µL, 1.1 equiv), silver (bistrifluoromethanesulfonyl) imide (15.5 mg, 20 mol %), copper acetate (18.1 mg, 50 mol %), silver fluoride (55.8 mg, 2.2 equiv) and catalyst $[Cp^*IrCl_2]_2$ (8.0 mg, 5 mol %). The tube was evacuated and backfilled with nitrogen and to it was added anhydrous DCE (2.0 mL, 0.1 M) under nitrogen atmosphere. The reaction mixture was degassed and backfilled with nitrogen 3 times and kept for stirring at 30℃. After 7 min, the reaction was quickly quenched by adding ethyl acetate keeping in an ice bath. The reaction mixture was filtered through a short pad of celite and concentrated under vacuo. The crude reaction mixture was directly purified by column chromatography on silica gel using petroleum ether/ethyl acetate (7:3) as eluent. The ratio of **3aa** and **3aa**-d_4 was determined by ^{1}H NMR spectroscopy. Primary kinetic isotopic effect (KIE) was found to be $\boldsymbol{k_H/k_D}$ = 0.73/0.27 = 2.7.

7.6. ^{1}H and ^{13}C NMR Spectra of Representative Compounds

^{1}H NMR of **1a** (400 MHz, $CDCl_3$):

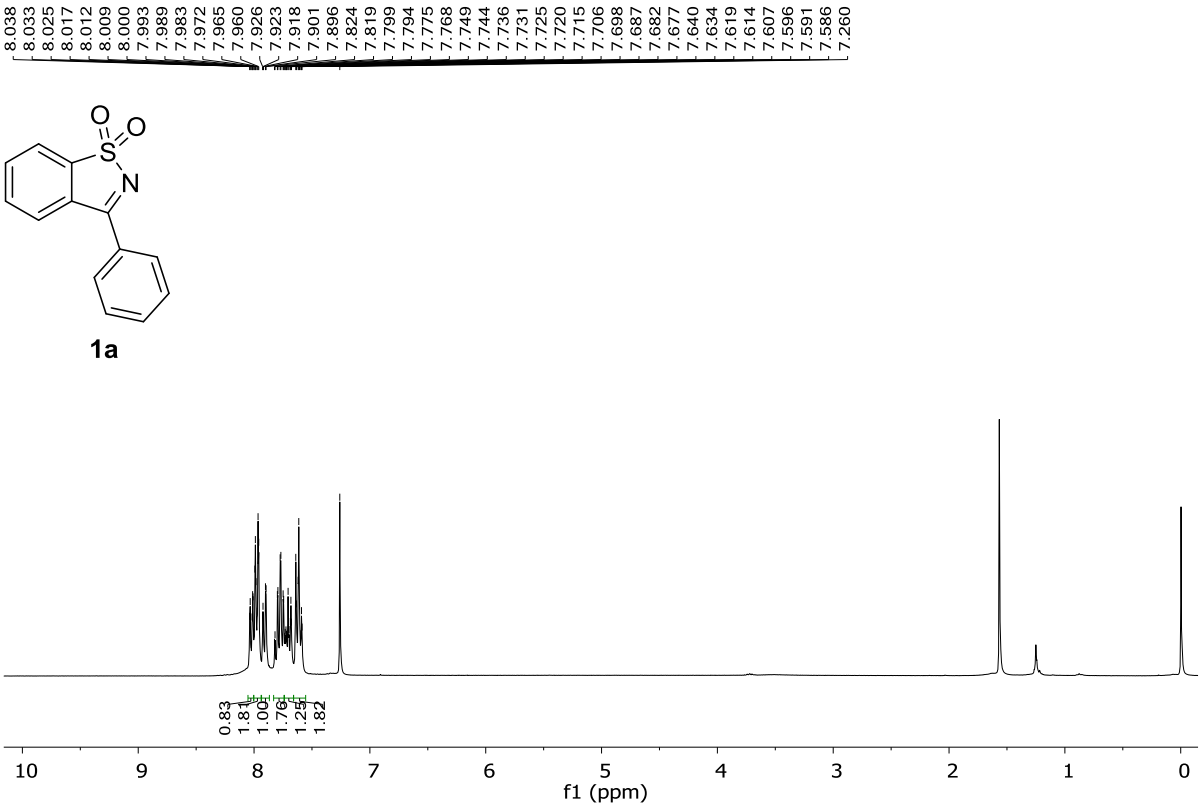

^{1}H NMR of **4a** (400 MHz, $CDCl_3$):

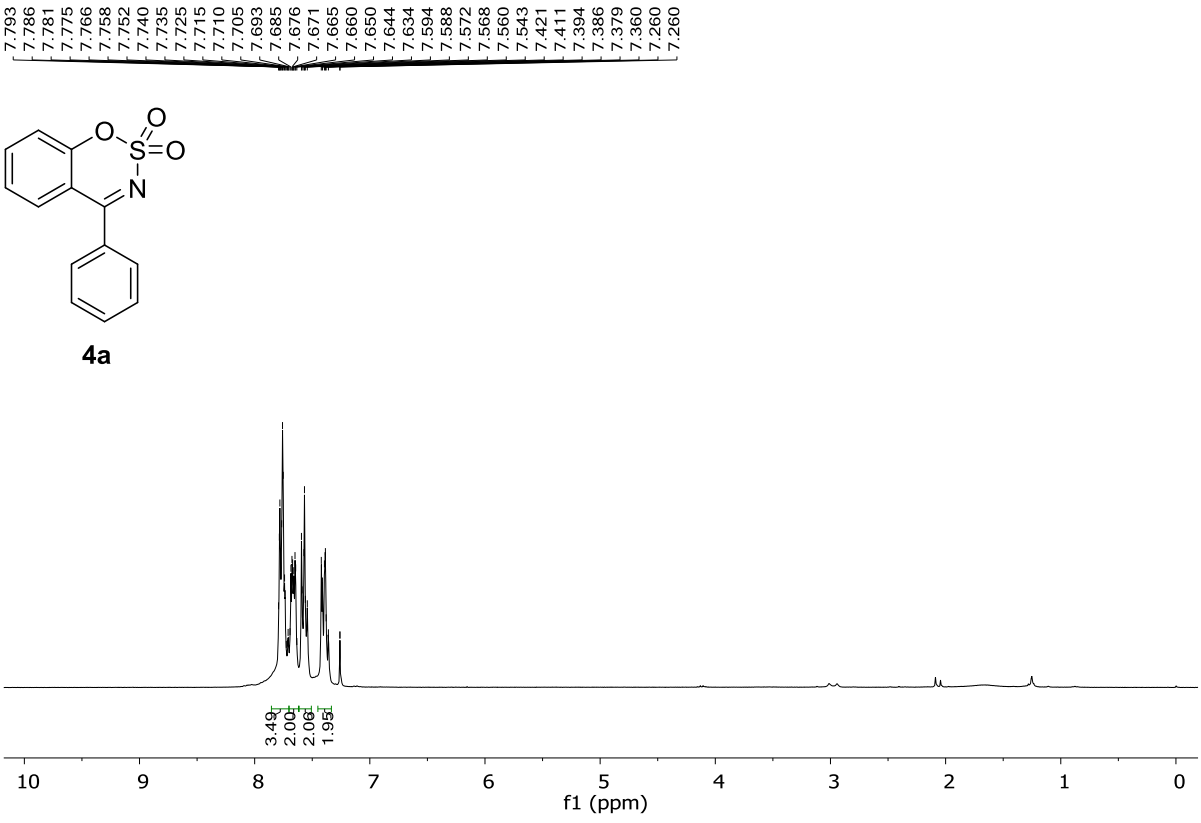

^{1}H NMR of **3aa** (400 MHz, $CDCl_3$):

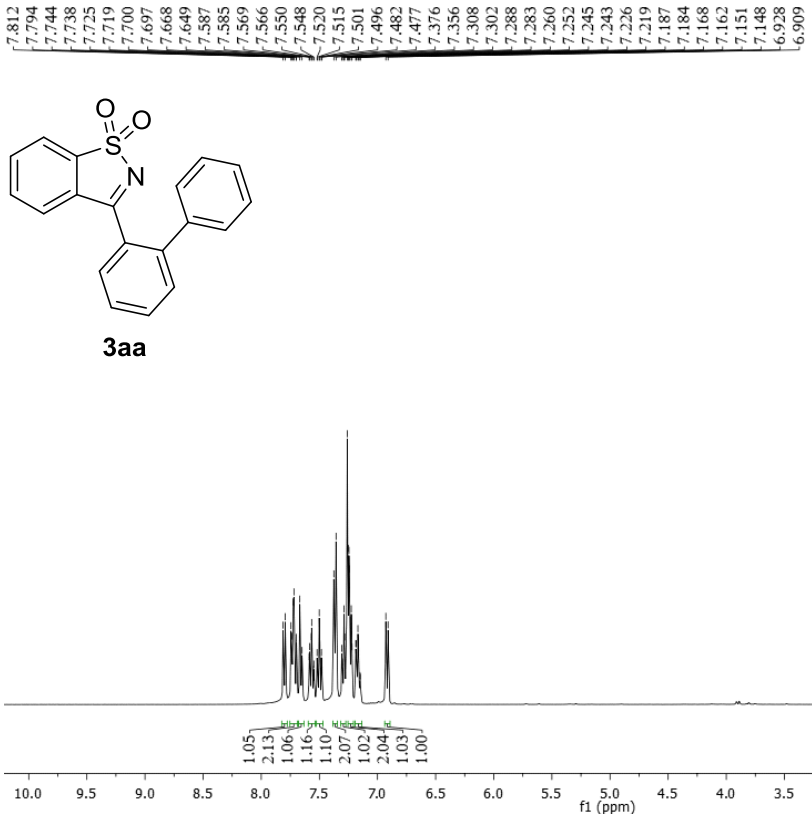

^{13}C NMR of **3aa** (100 MHz, $CDCl_3$):

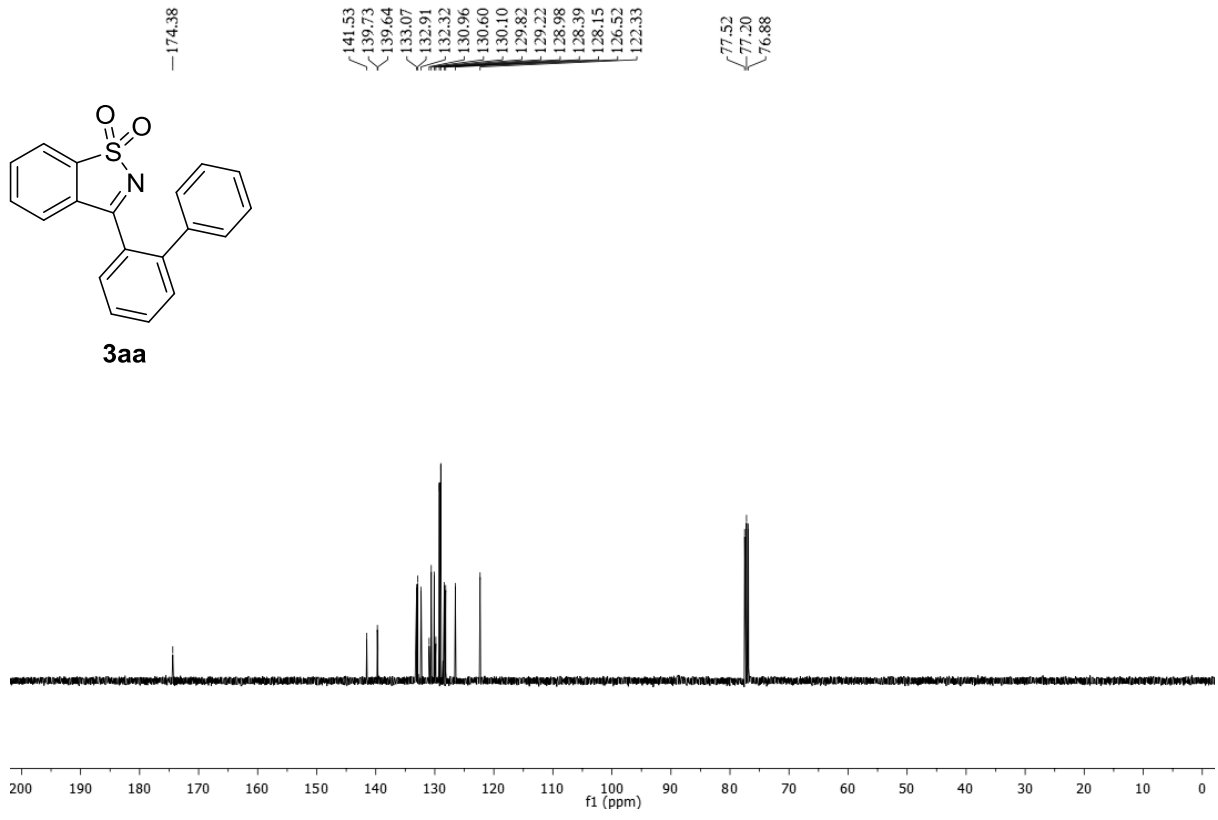

^{1}H NMR of **3ca** (400 MHz, $CDCl_3$):

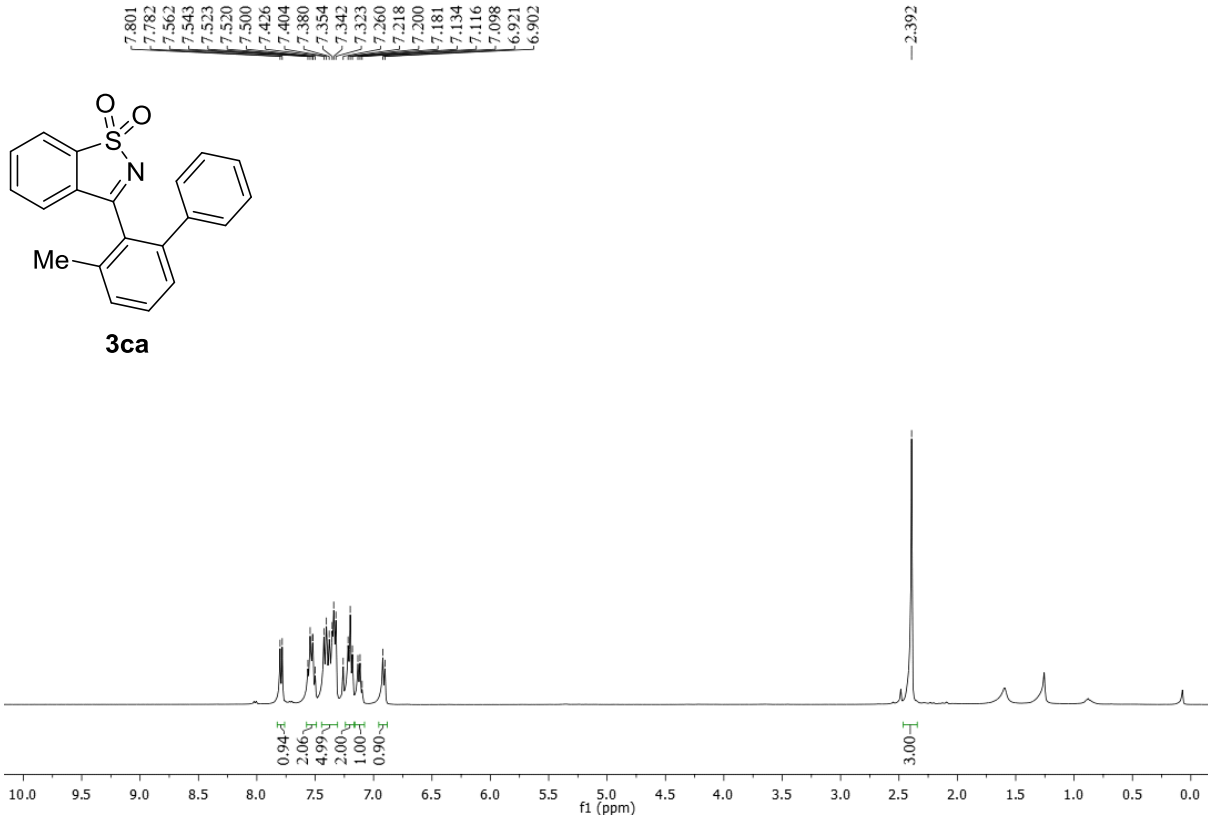

^{13}C NMR of **3ca** (100 MHz, $CDCl_3$):

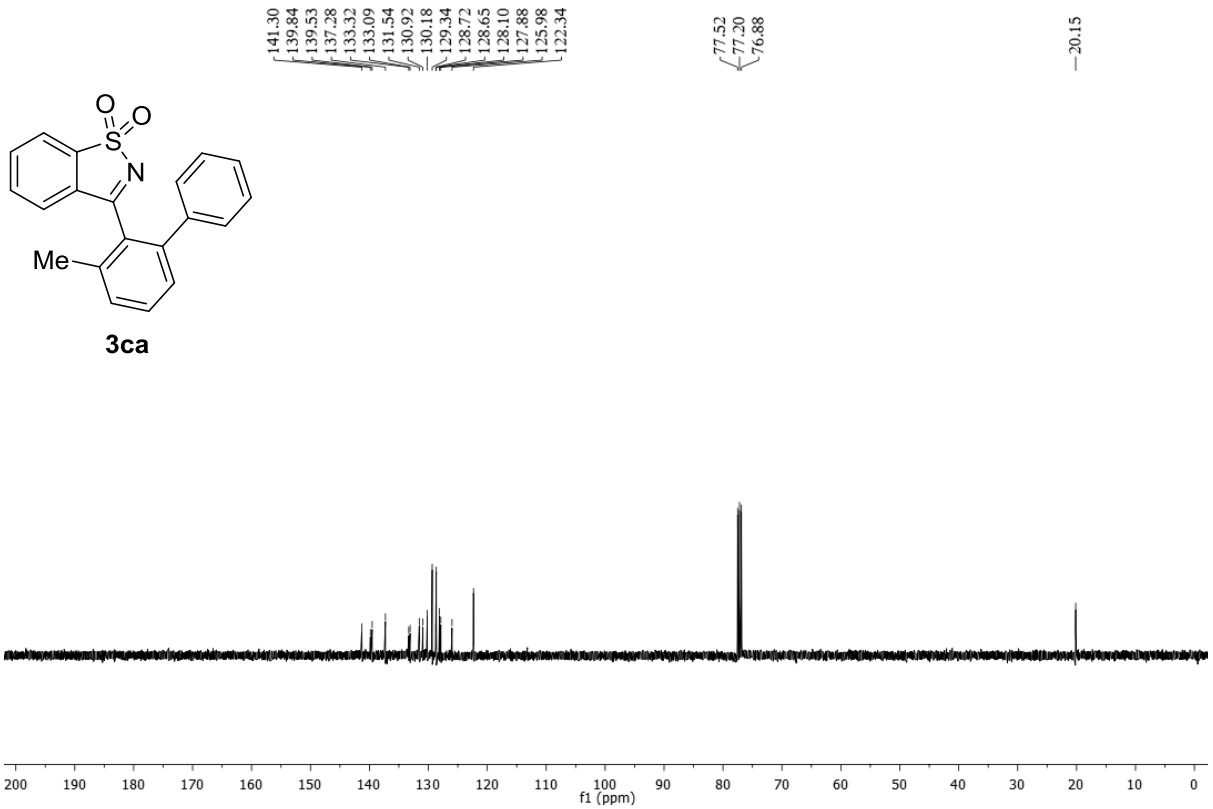

^{1}H NMR of **3da** (600 MHz, $CDCl_3$):

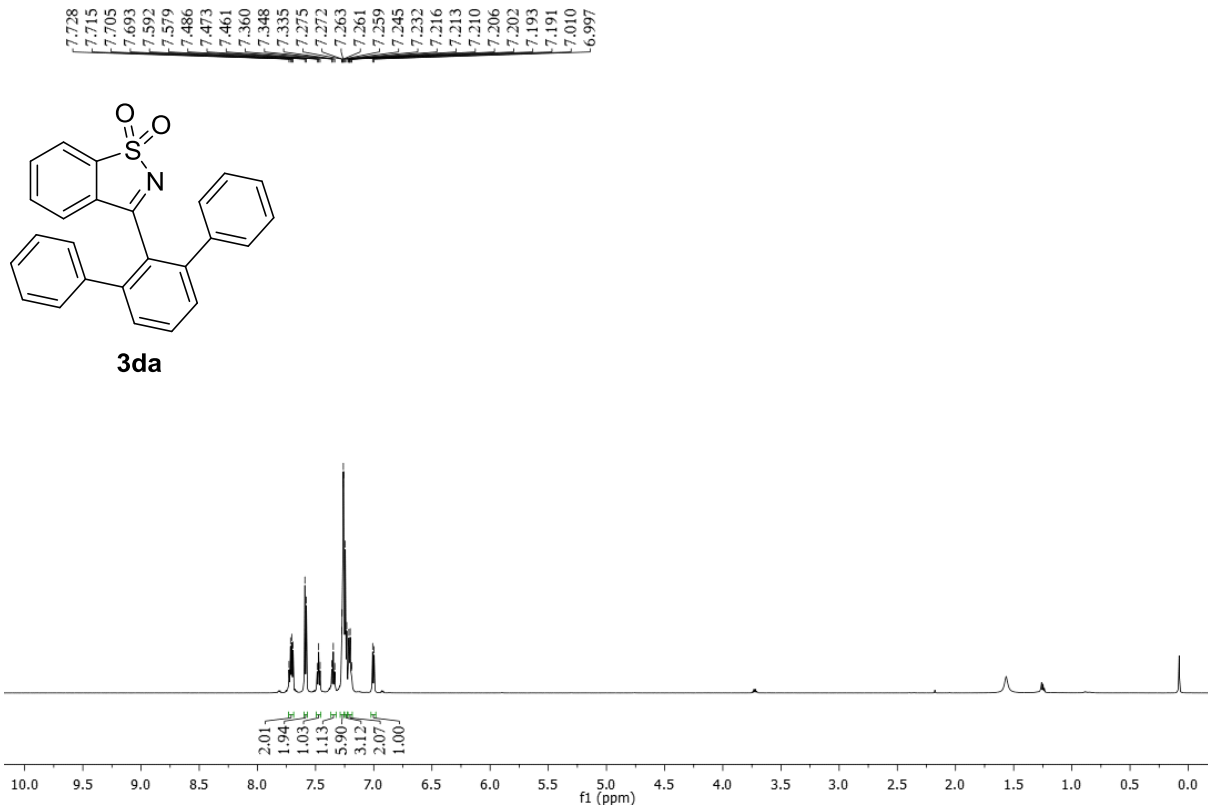

^{13}C NMR of **3da** (150 MHz, $CDCl_3$):

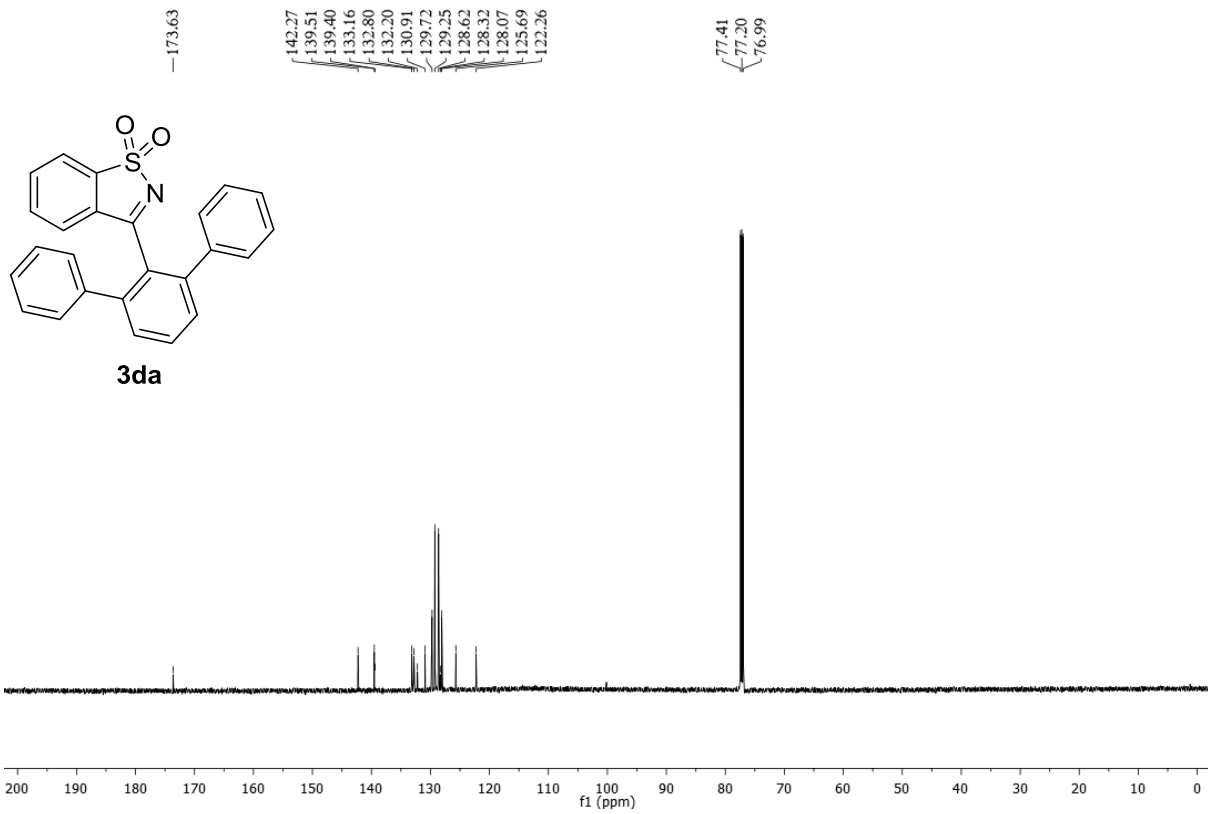

^{1}H NMR of **3ea** (400 MHz, $CDCl_3$):

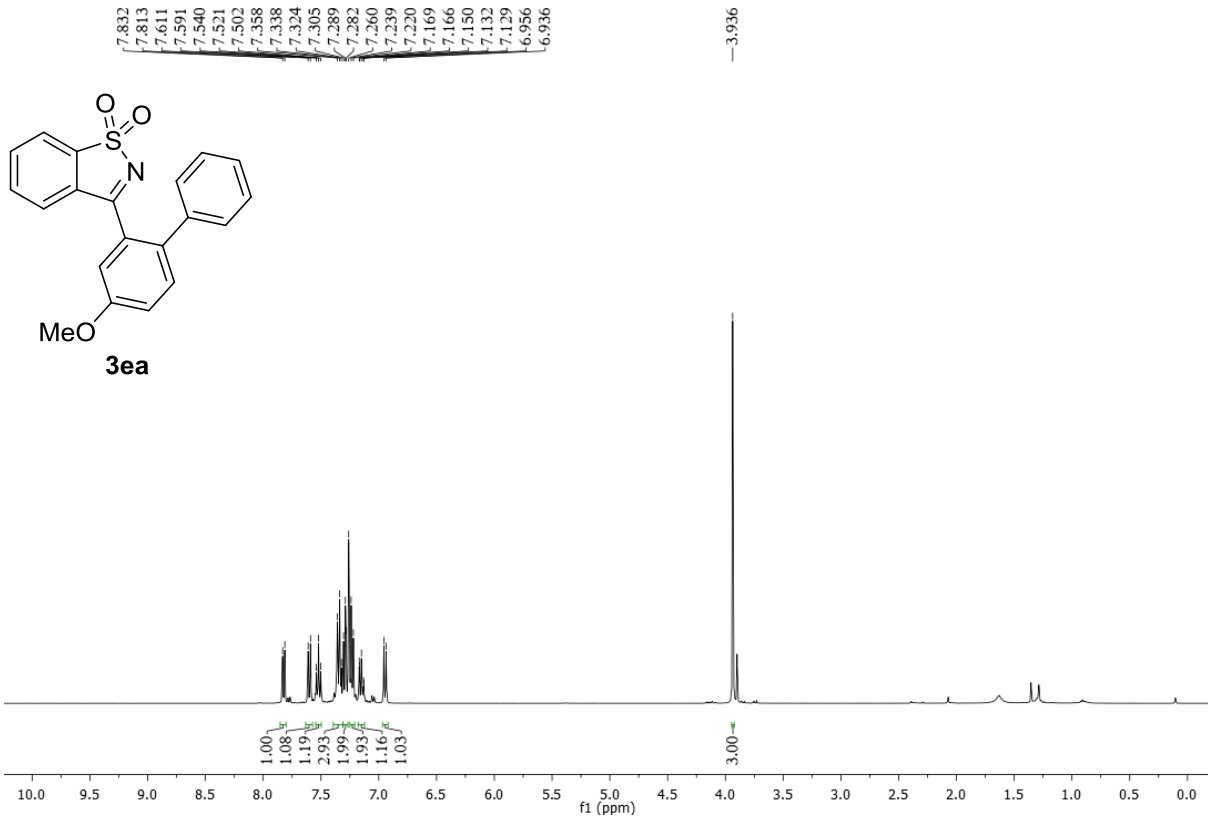

^{13}C NMR of **3ea** (100 MHz, $CDCl_3$):

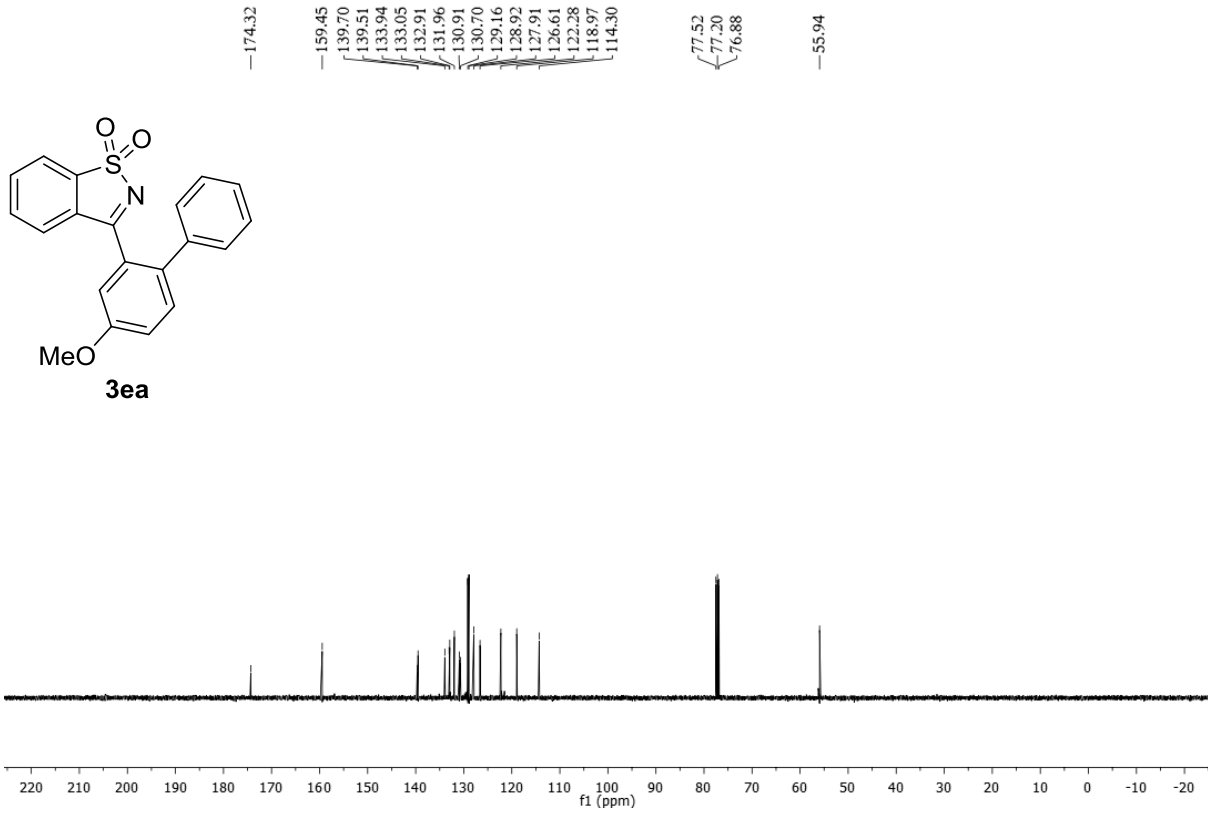

^{1}H NMR of **3ha** (600 MHz, $CDCl_3$):

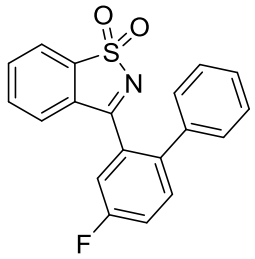

3ha

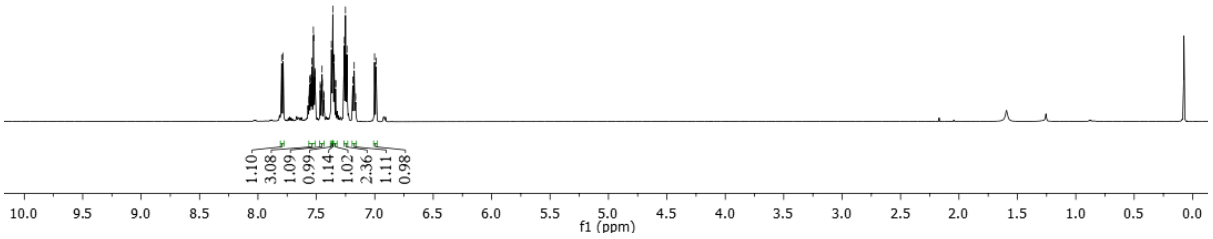

^{13}C NMR of **3ha** (150 MHz, $CDCl_3$):

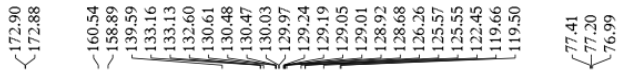

3ha

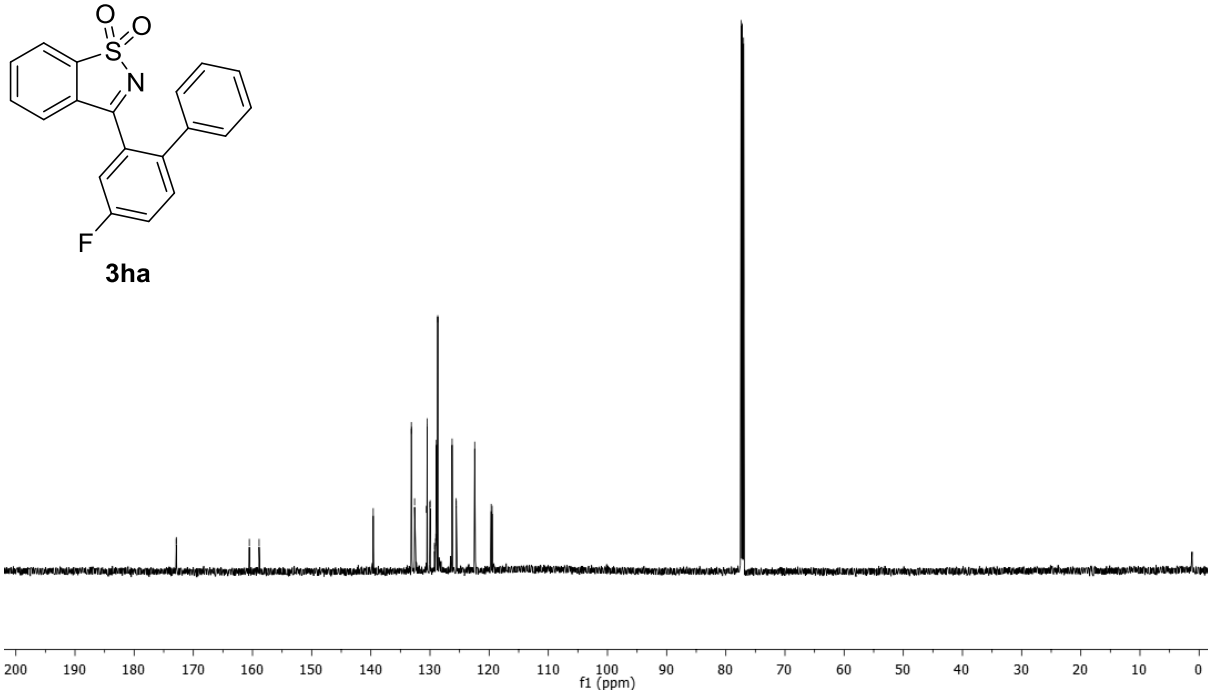

^{1}H NMR of **3ka** (400 MHz, $CDCl_3$):

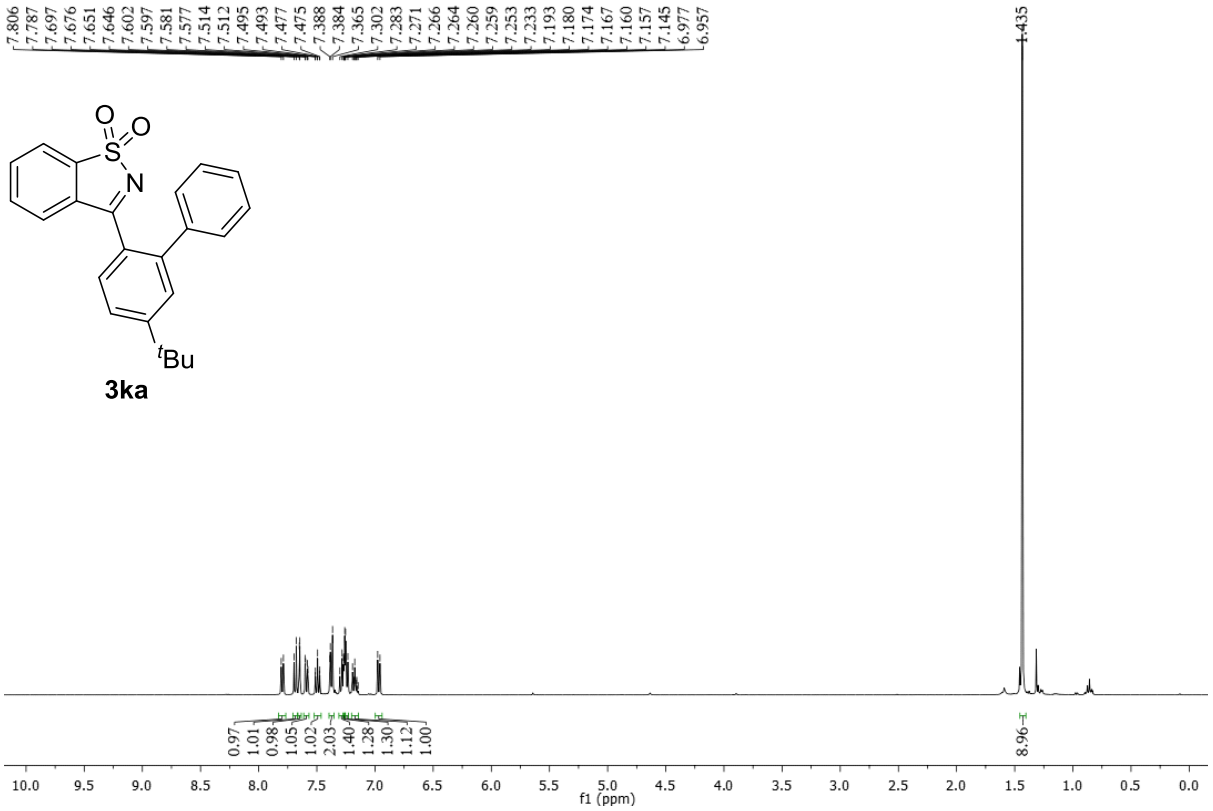

^{13}C NMR of **3ka** (100 MHz, $CDCl_3$):

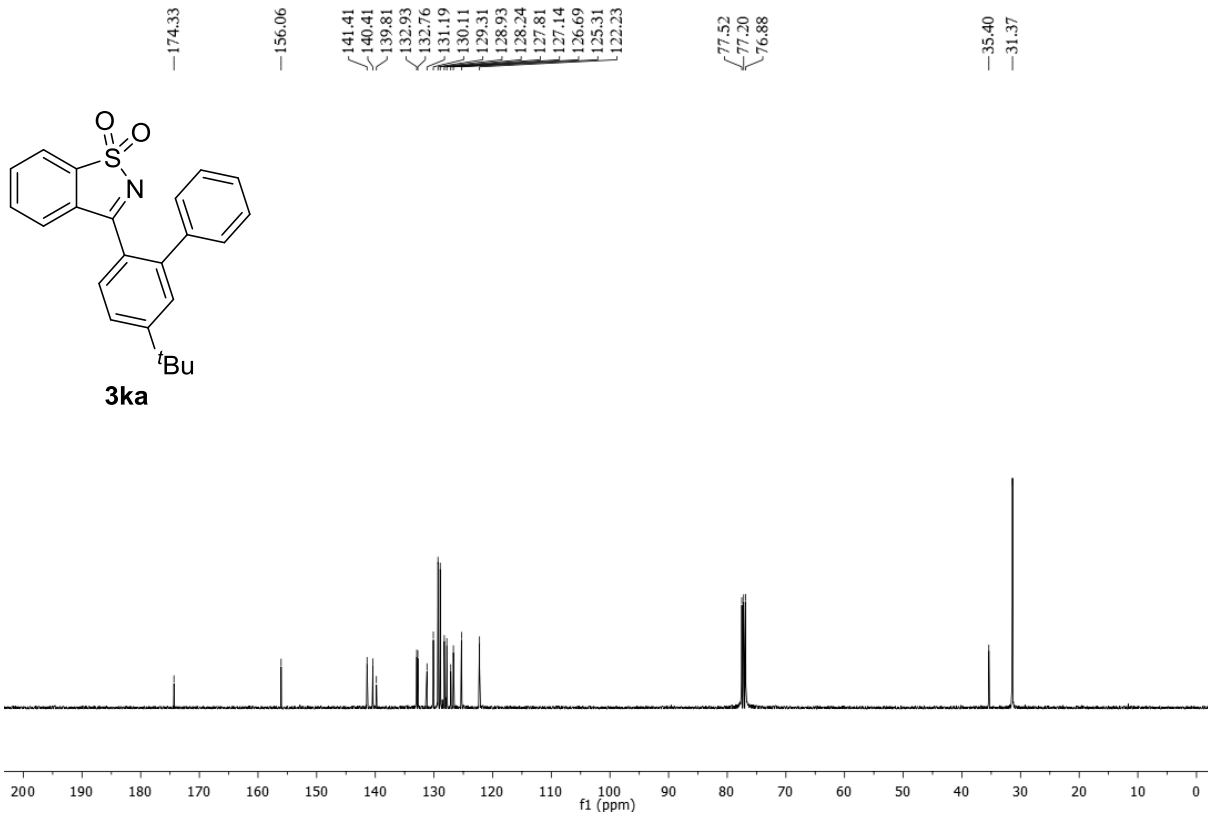

^{1}H NMR of **3ma** (600 MHz, $CDCl_3$):

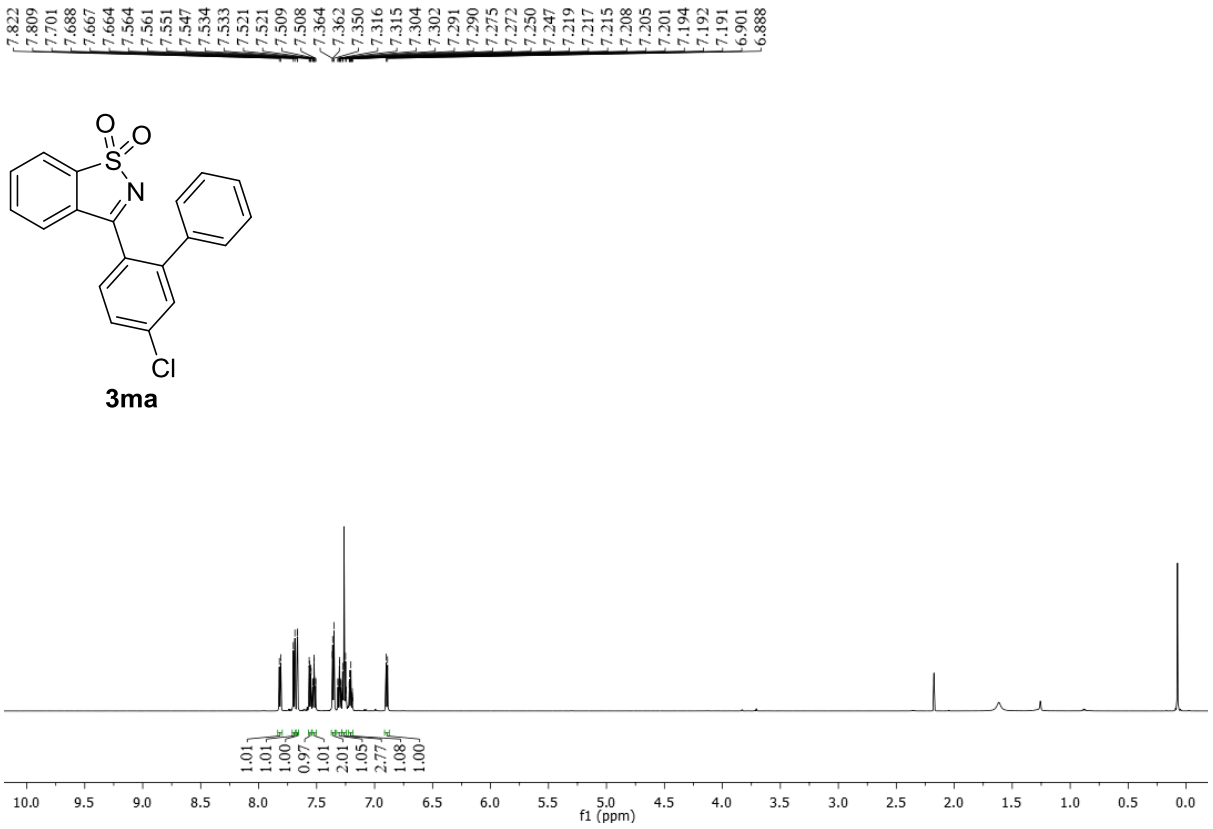

^{13}C NMR of **3ma** (150 MHz, $CDCl_3$):

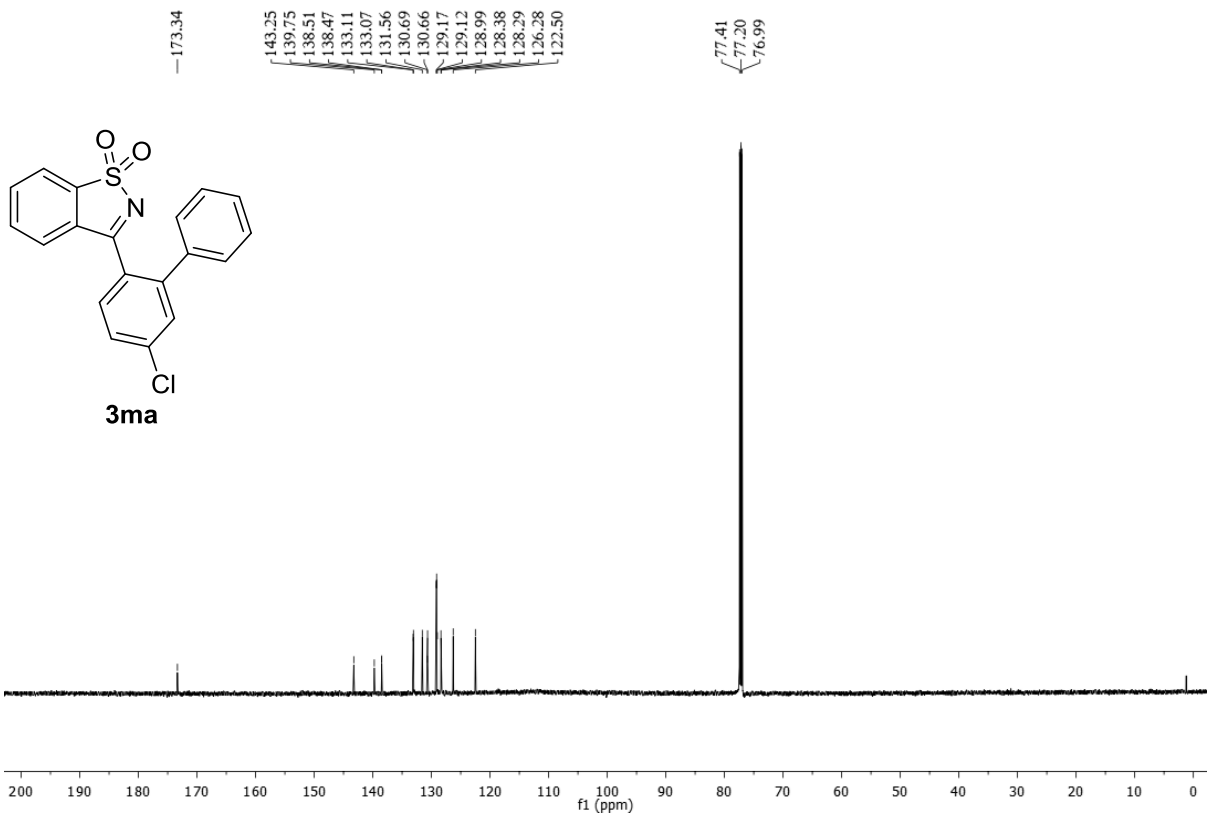

^{1}H NMR of **3oa** (400 MHz, $CDCl_3$):

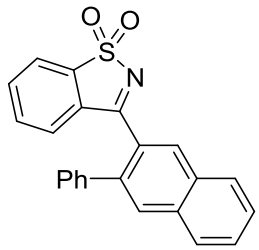

3oa

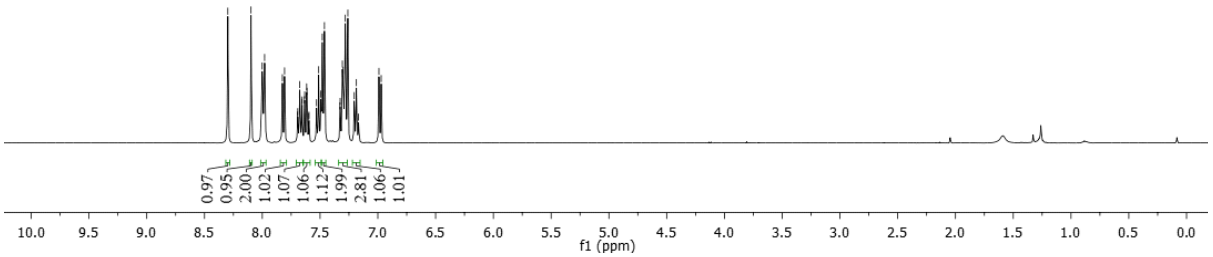

^{13}C NMR of **3oa** (100 MHz, $CDCl_3$):

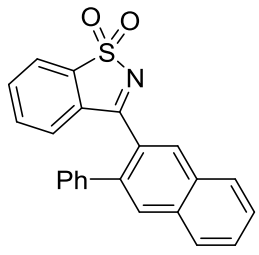

3oa

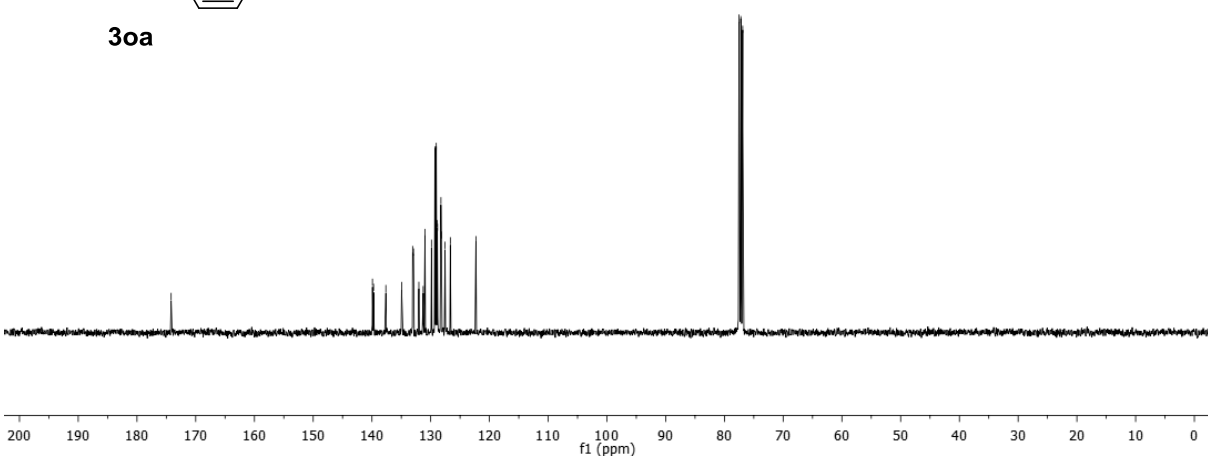

^{1}H NMR of **3bc** (400 MHz, $CDCl_3$):

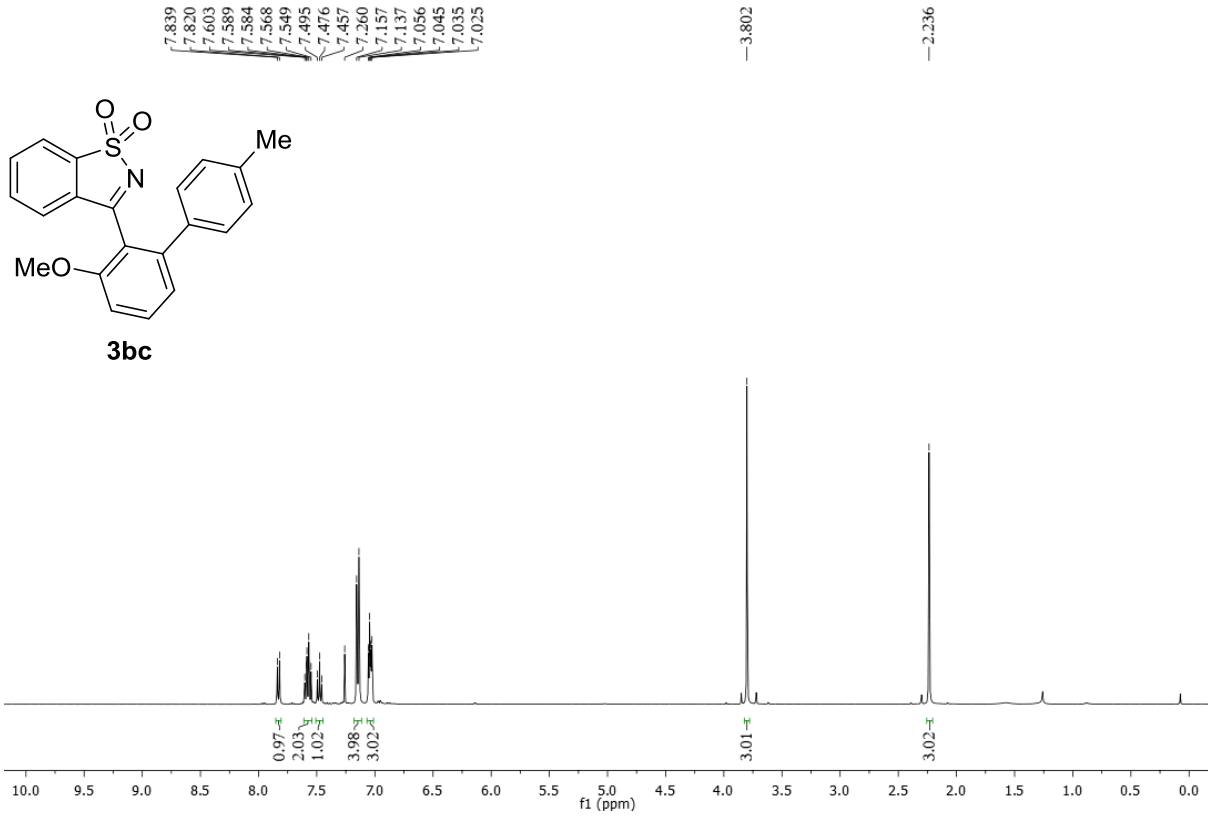

3bc

^{13}C NMR of **3bc** (100 MHz, $CDCl_3$):

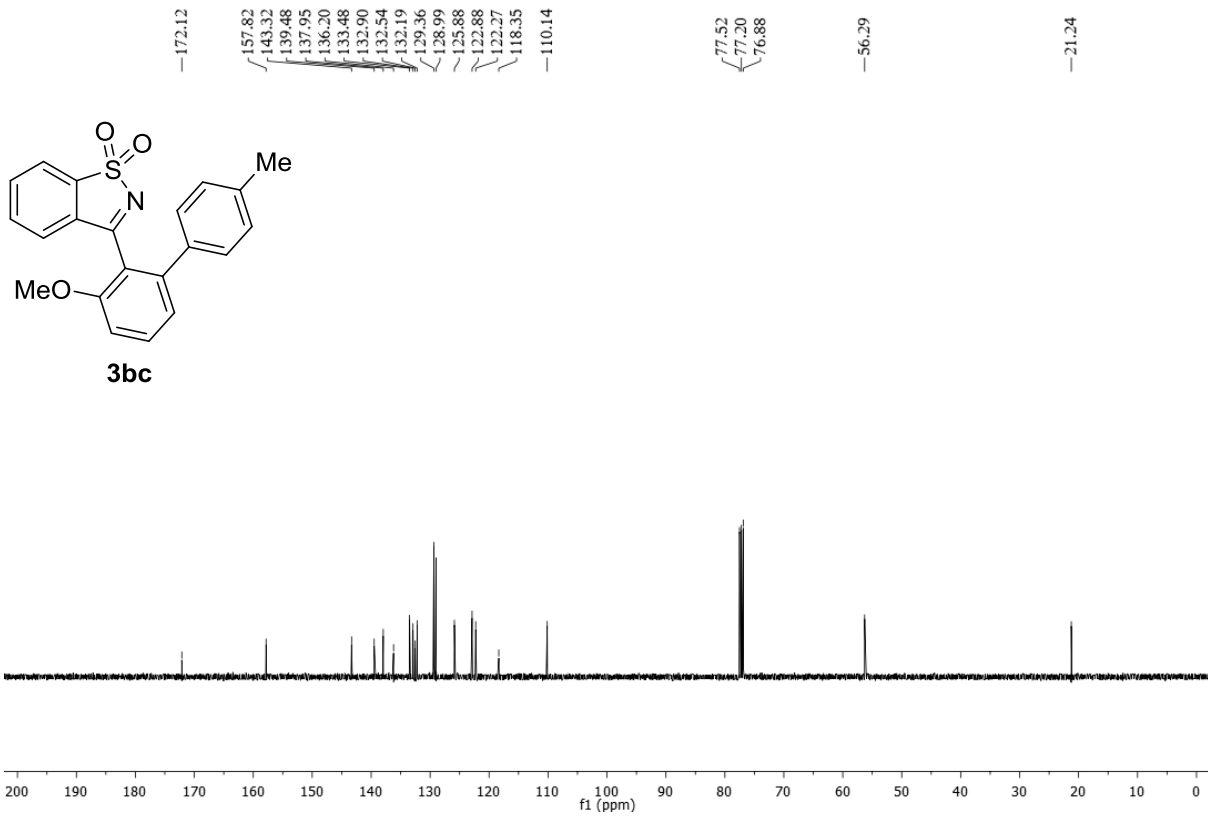

3bc

^{1}H NMR of **3bd** (400 MHz, $CDCl_3$):

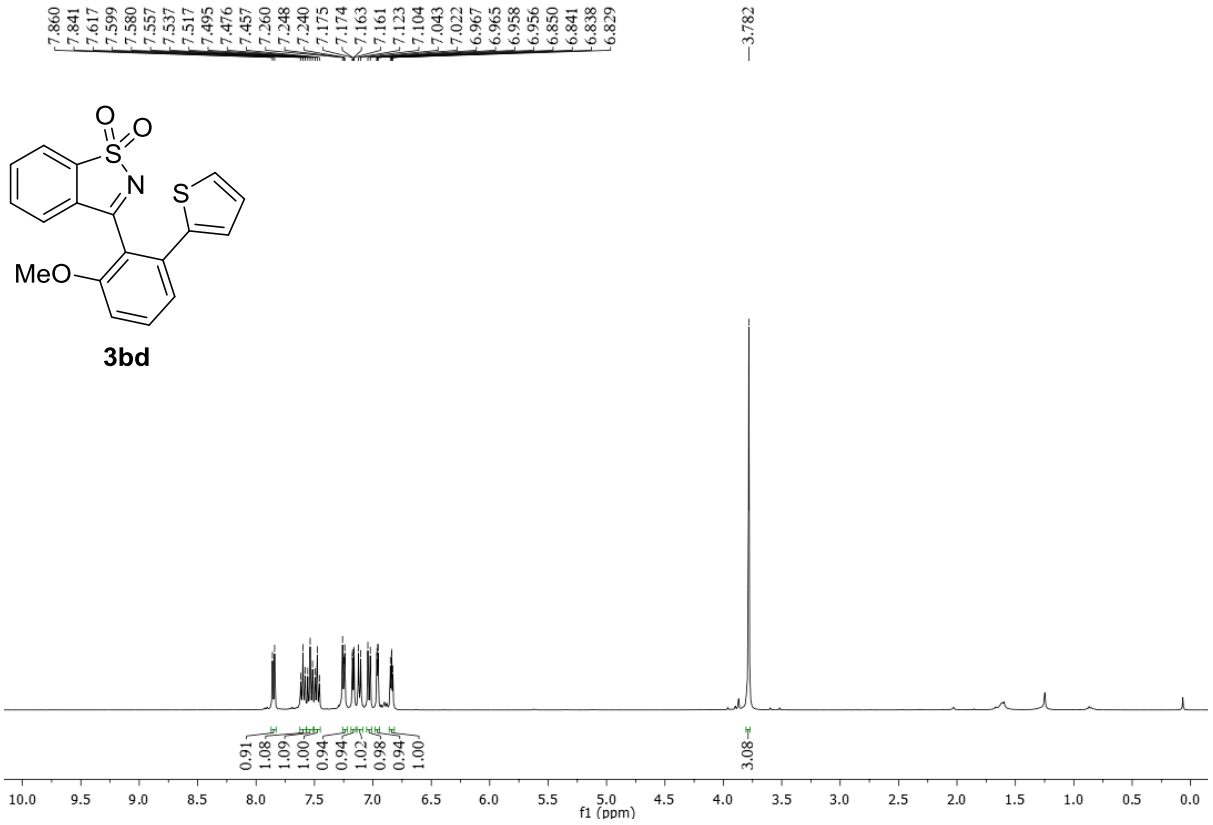

^{13}C NMR of **3bd** (100 MHz, $CDCl_3$):

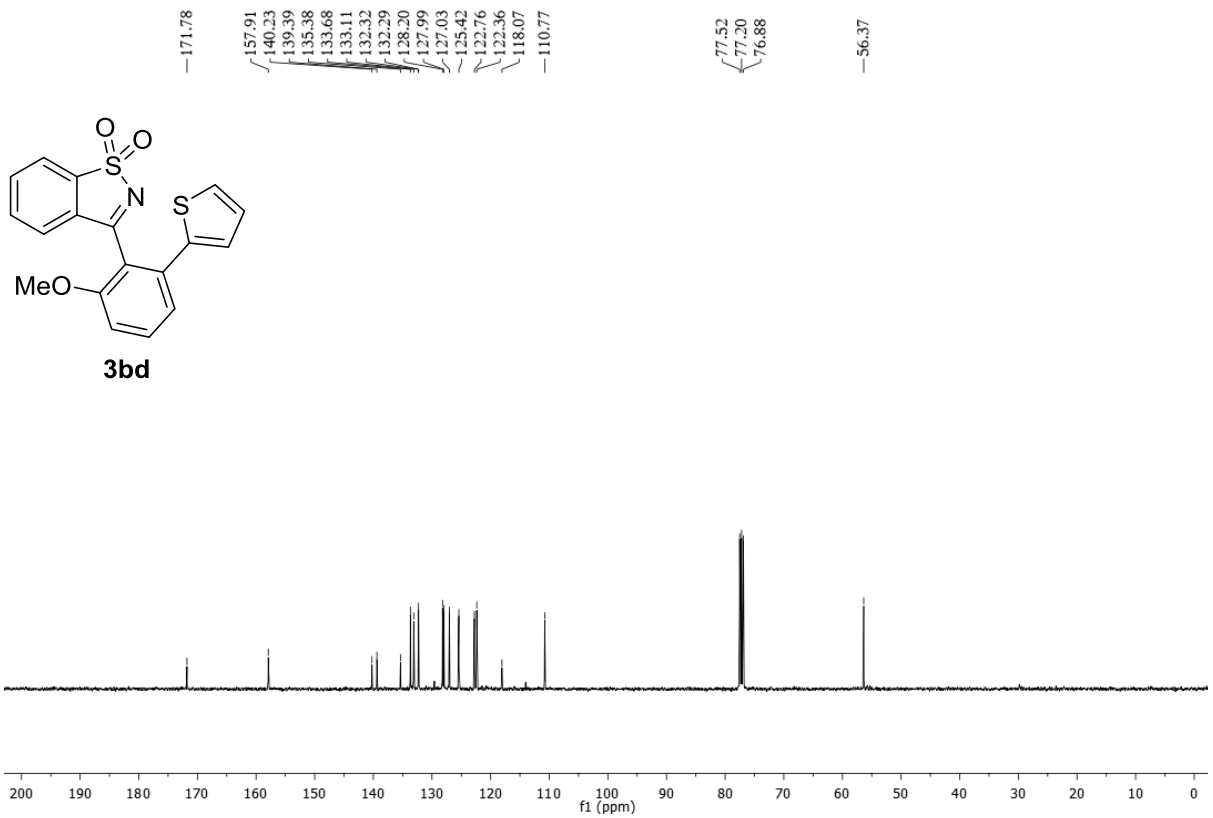

^{1}H NMR of **3be** (400 MHz, $CDCl_3$):

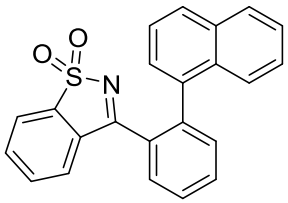

3be

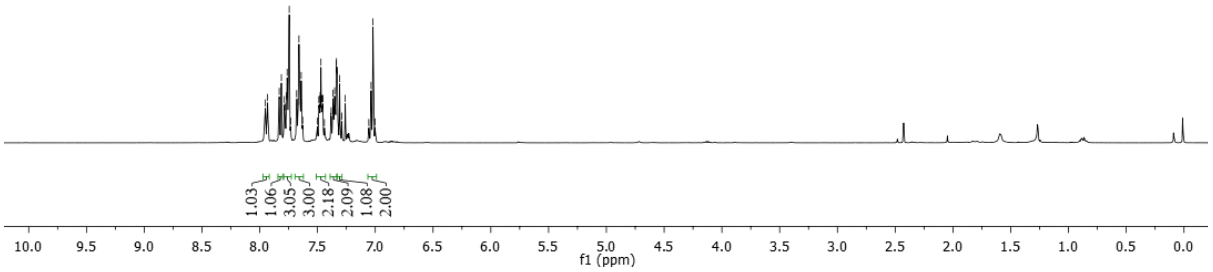

^{13}C NMR of **3be** (100 MHz, $CDCl_3$):

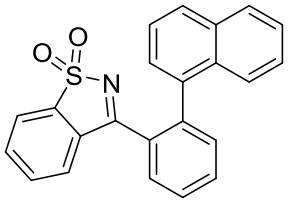

3be

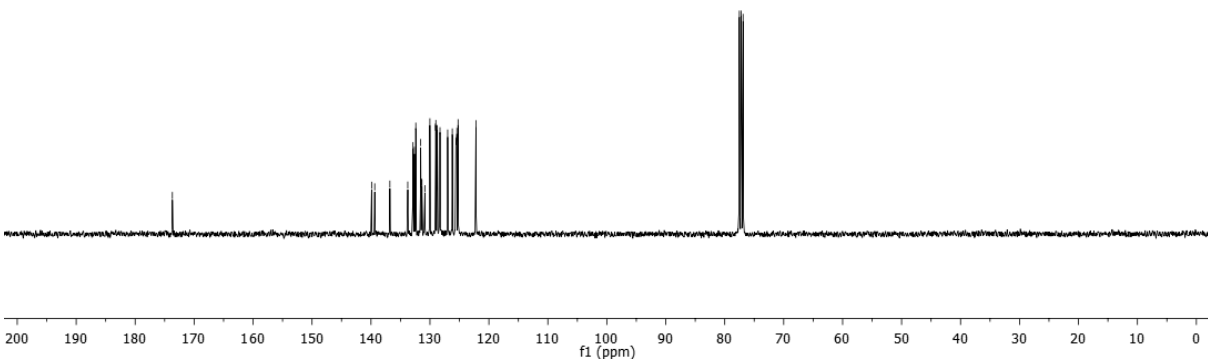

^{1}H NMR of **3fb** (400 MHz, $CDCl_3$):

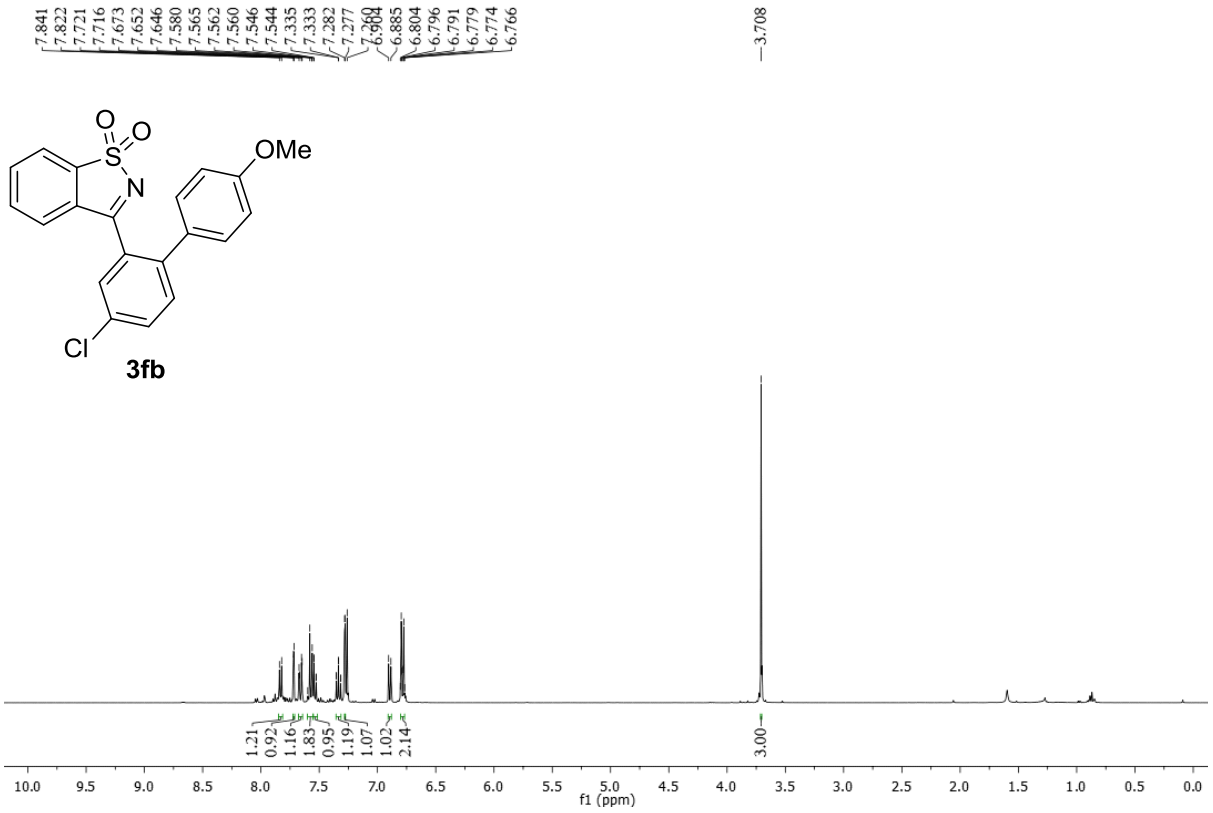

^{13}C NMR of **3fb** (100MHz, $CDCl_3$):

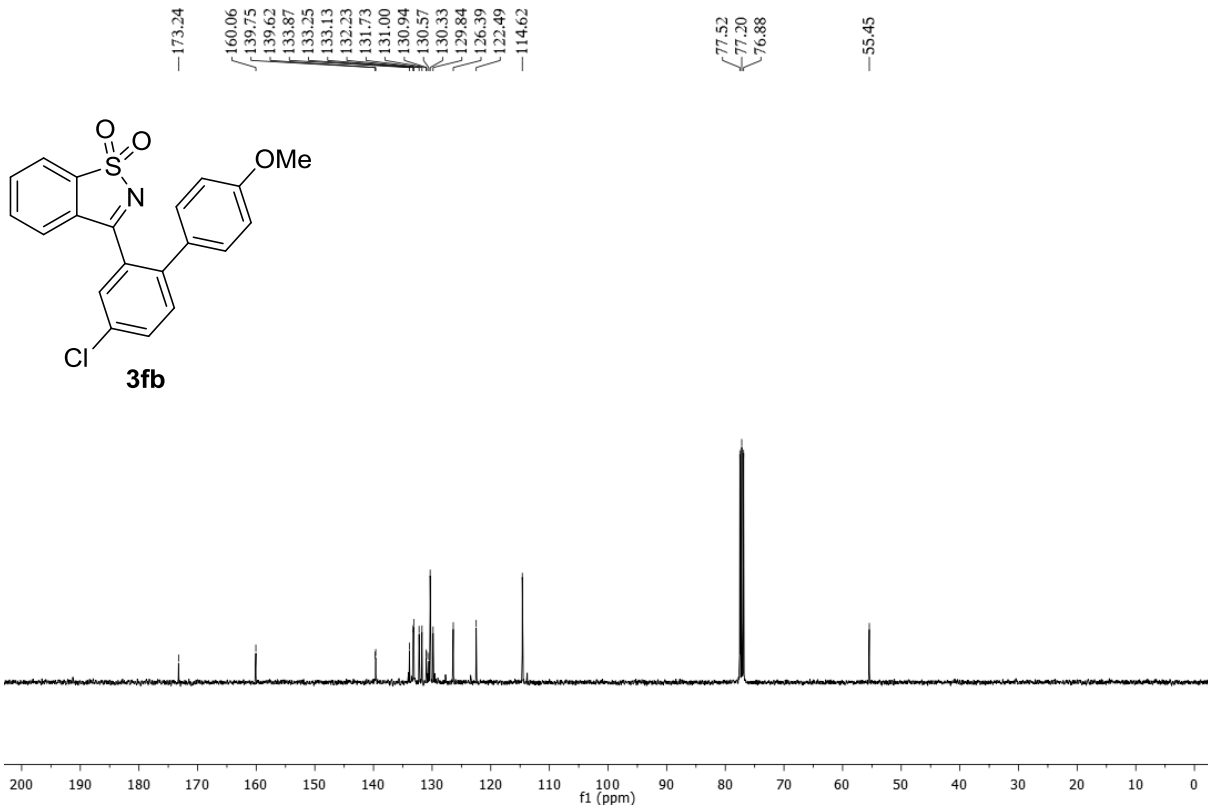

^{1}H NMR of **3kb** (400 MHz, $CDCl_3$):

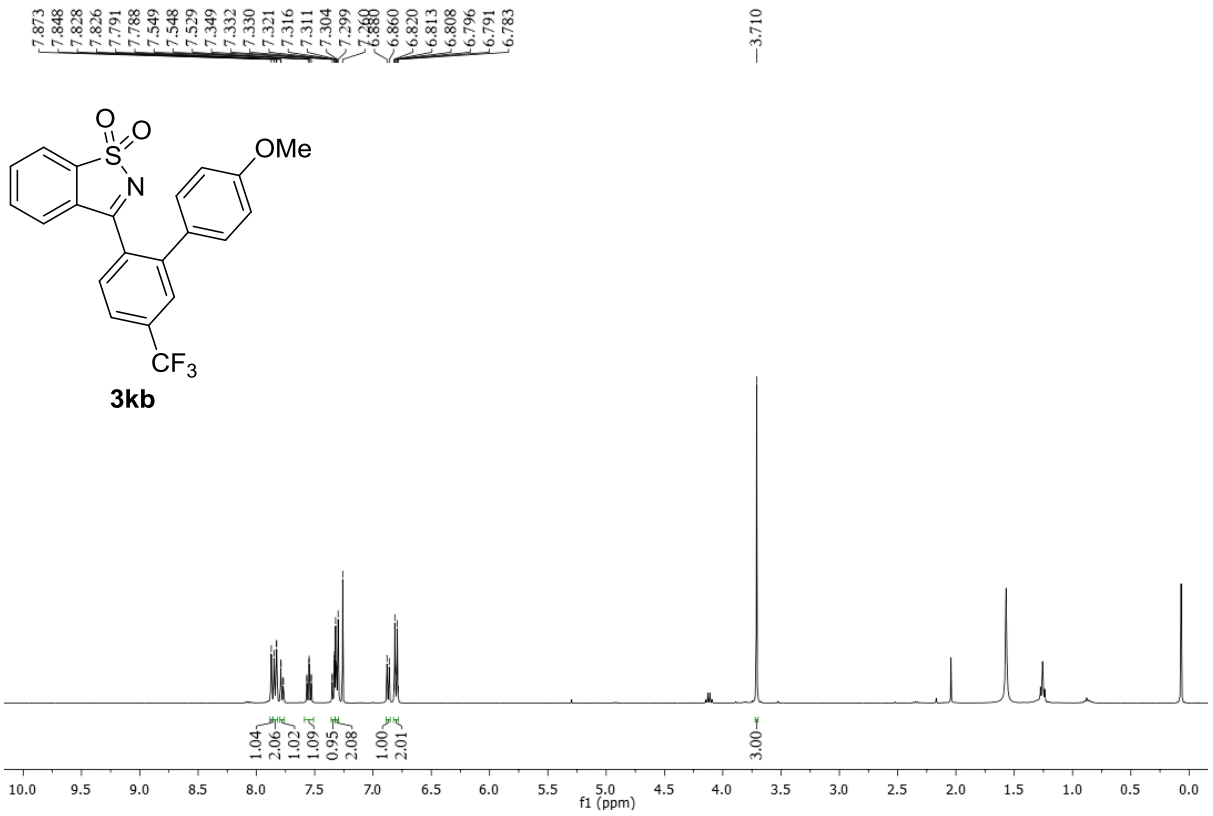

^{13}C NMR of **3kb** (100 MHz, $CDCl_3$):

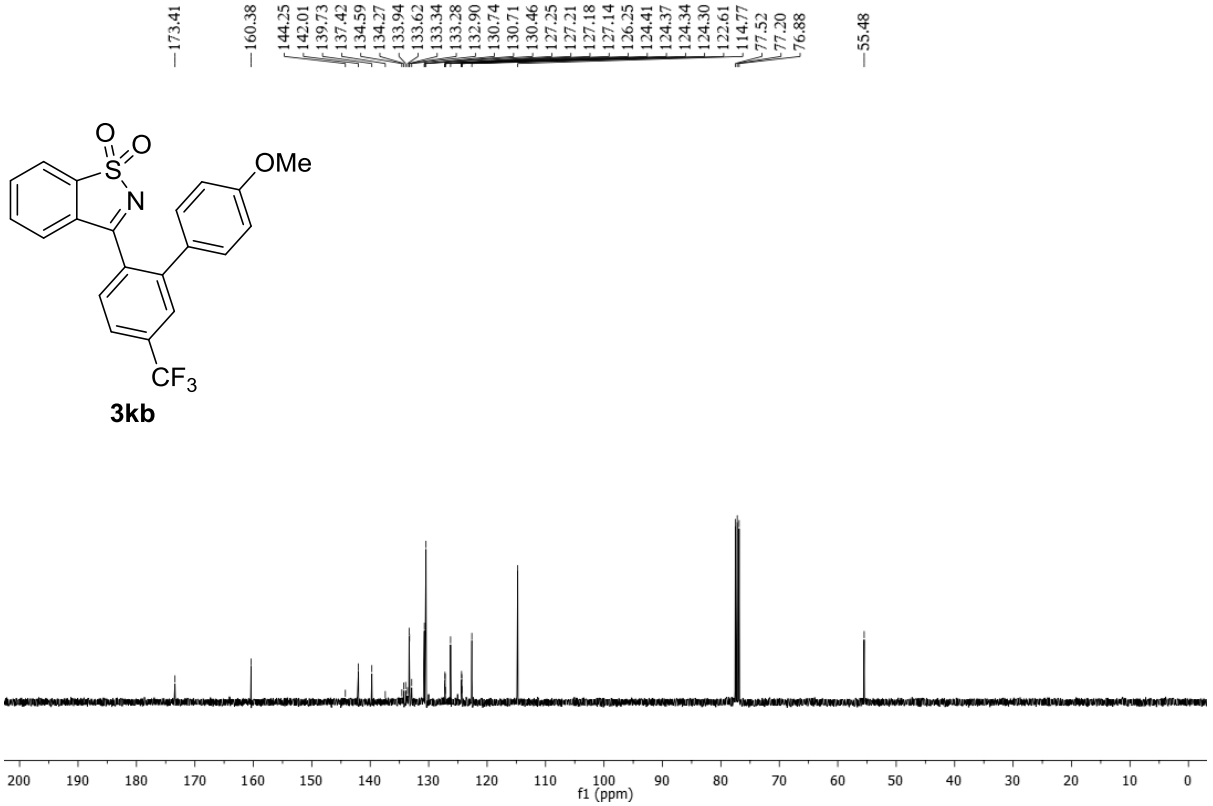

^{1}H NMR of **3ob** (400 MHz, $CDCl_3$):

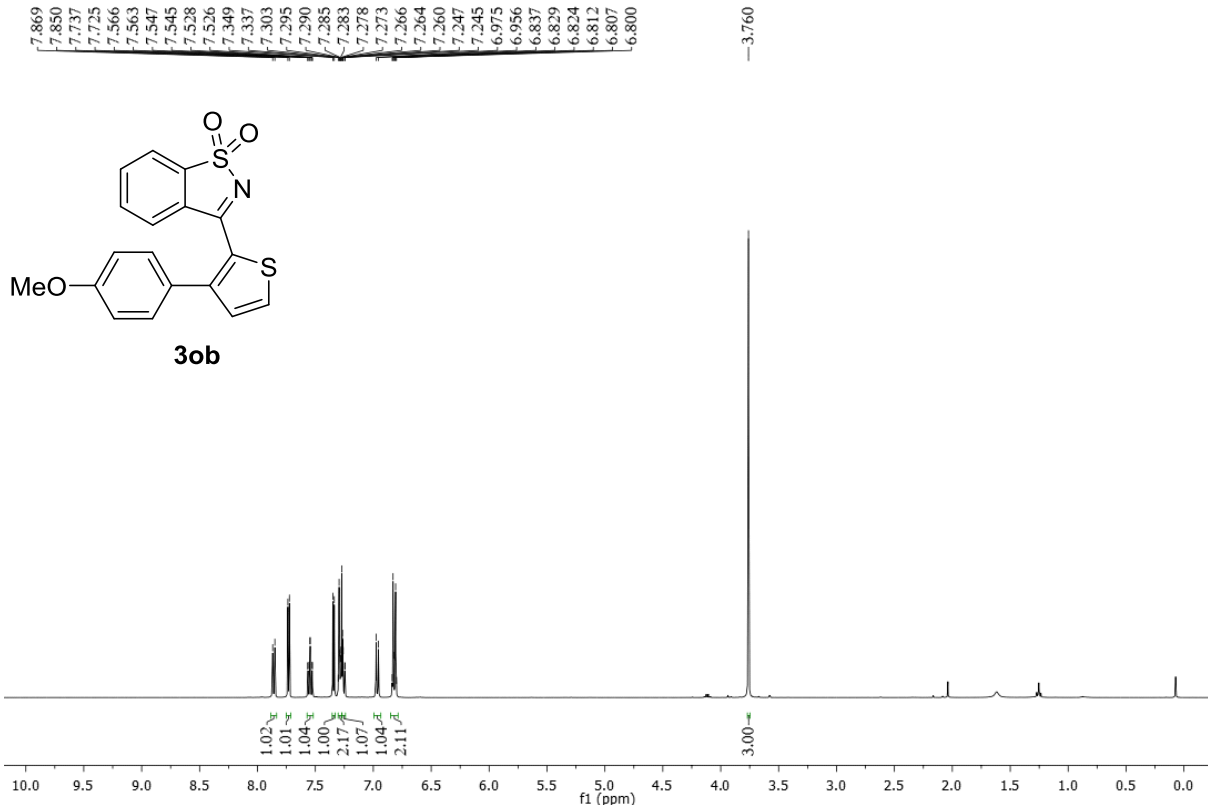

3ob

^{13}C NMR of **3ob** (100 MHz, $CDCl_3$):

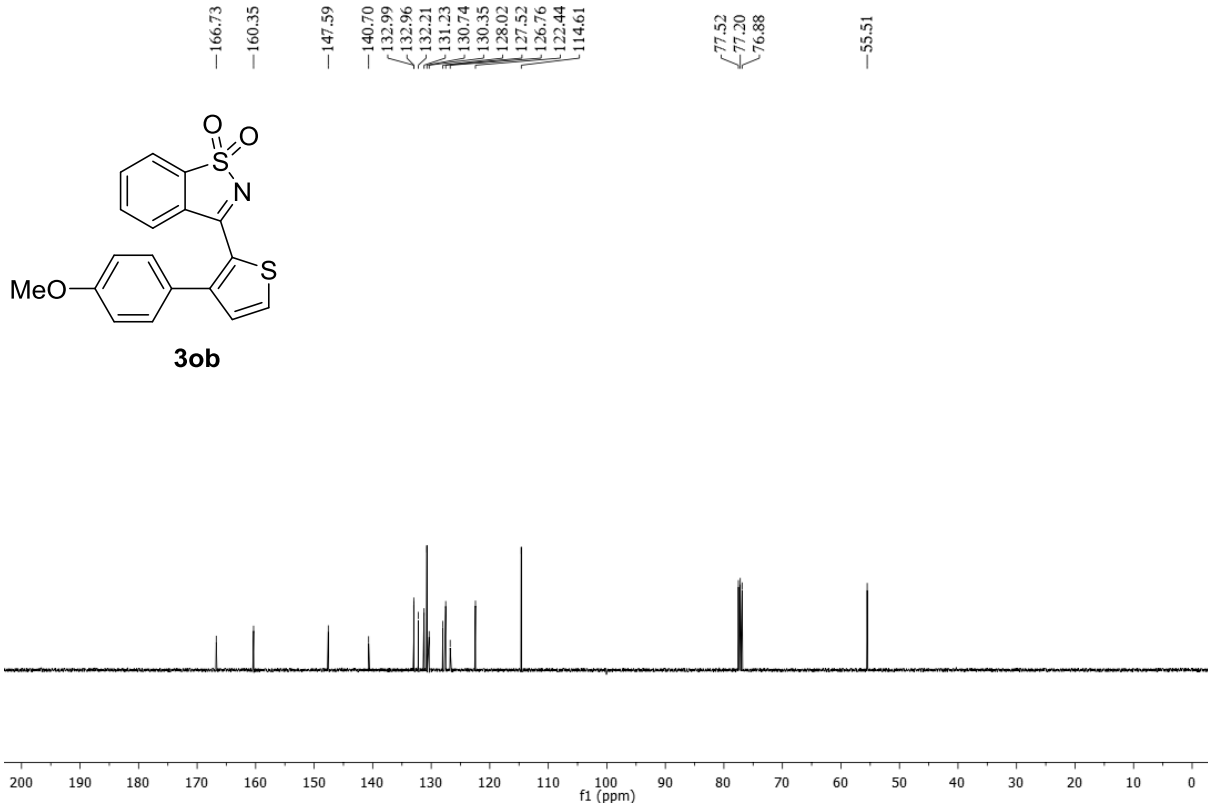

3ob

^{1}H NMR of **5aa** (400 MHz, $CDCl_3$):

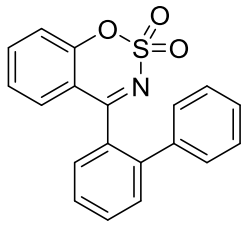

5aa

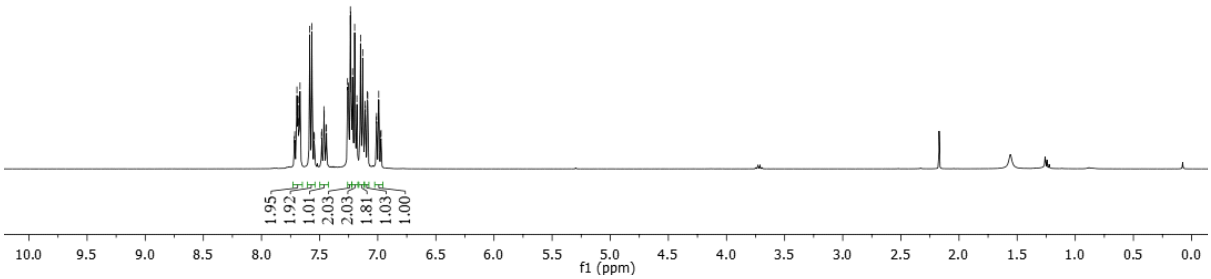

^{13}C NMR of **5aa** (100 MHz, $CDCl_3$):

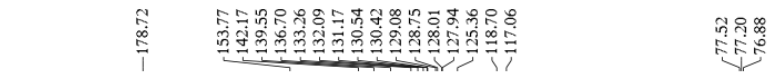

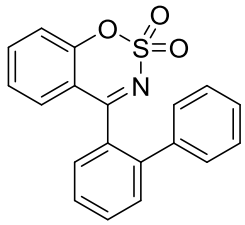

5aa

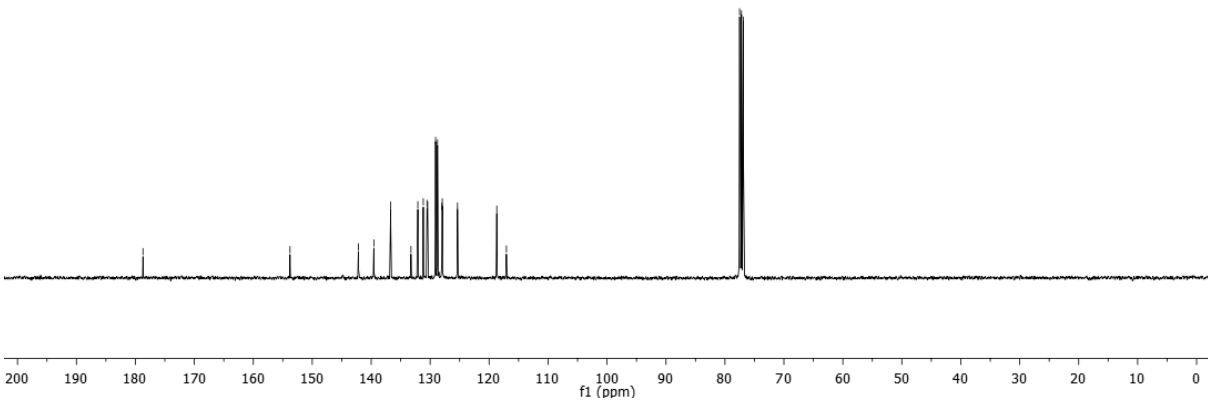

^{1}H NMR of **5ba** (400 MHz, $CDCl_3$):

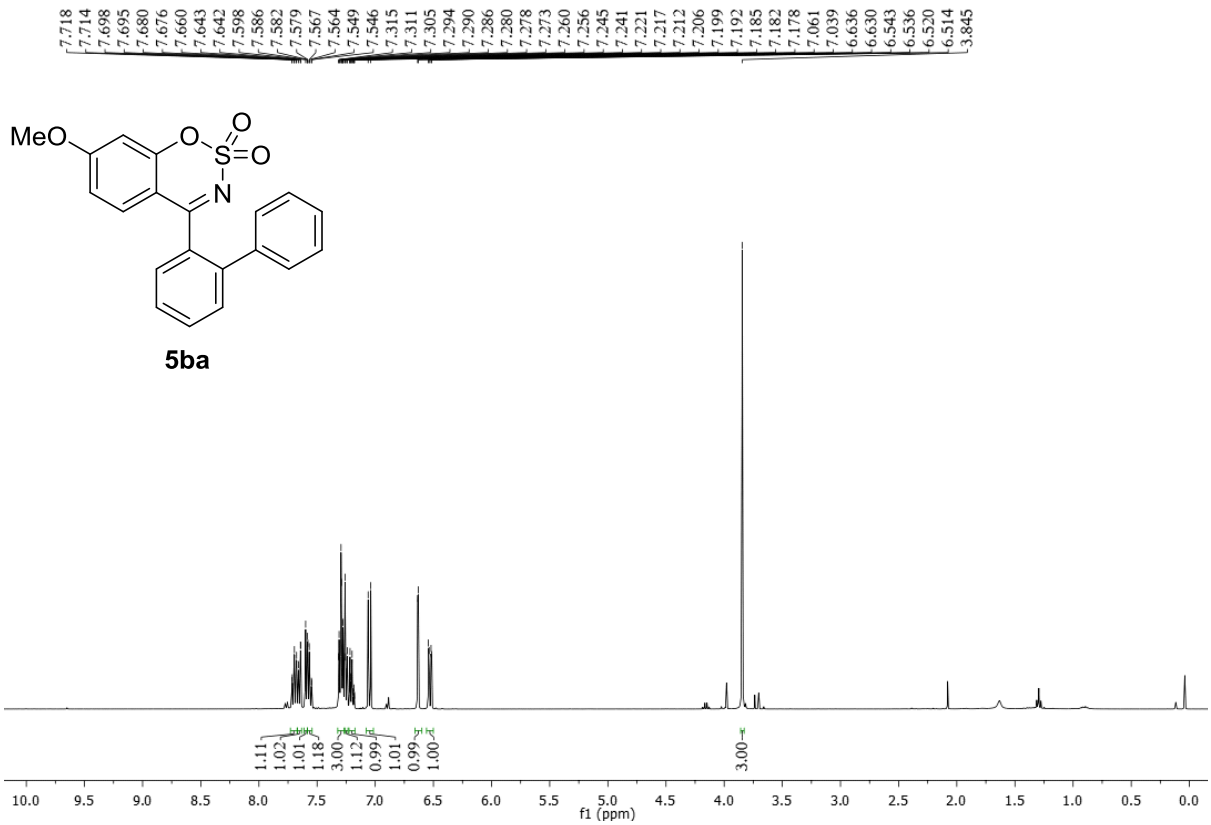

5ba

^{13}C NMR of **5ba** (100 MHz, $CDCl_3$):

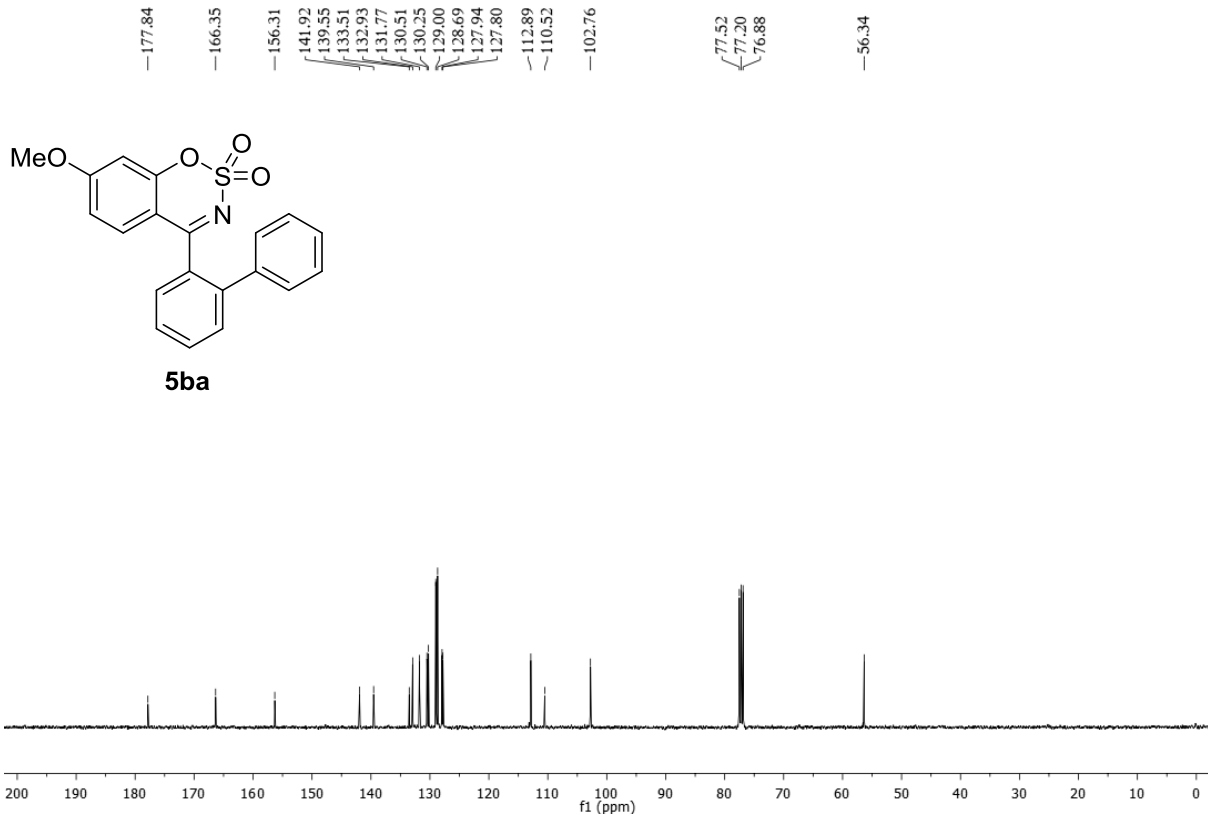

5ba

^{1}H NMR of **5da** (400 MHz, $CDCl_3$):

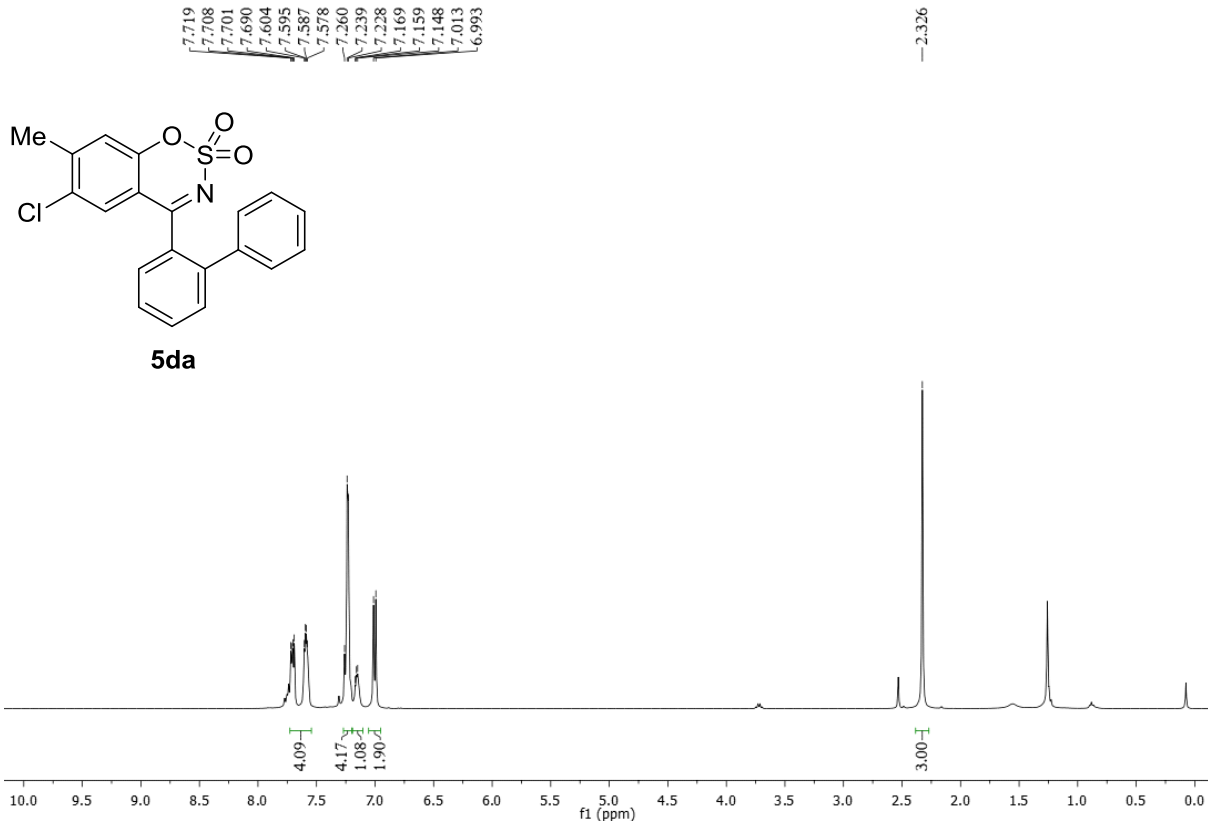

^{13}C NMR of **5da** (100 MHz, $CDCl_3$):

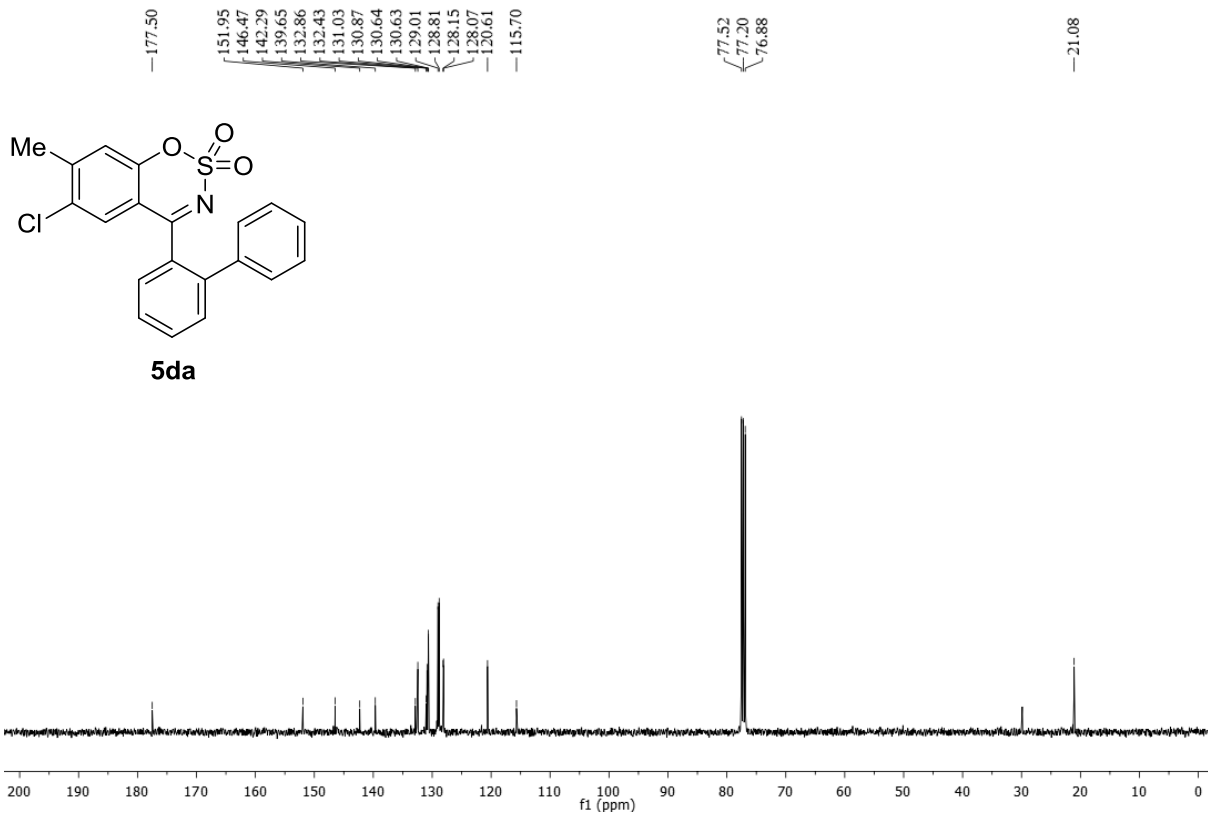

^{1}H NMR of **5fa** (400 MHz, $CDCl_3$):

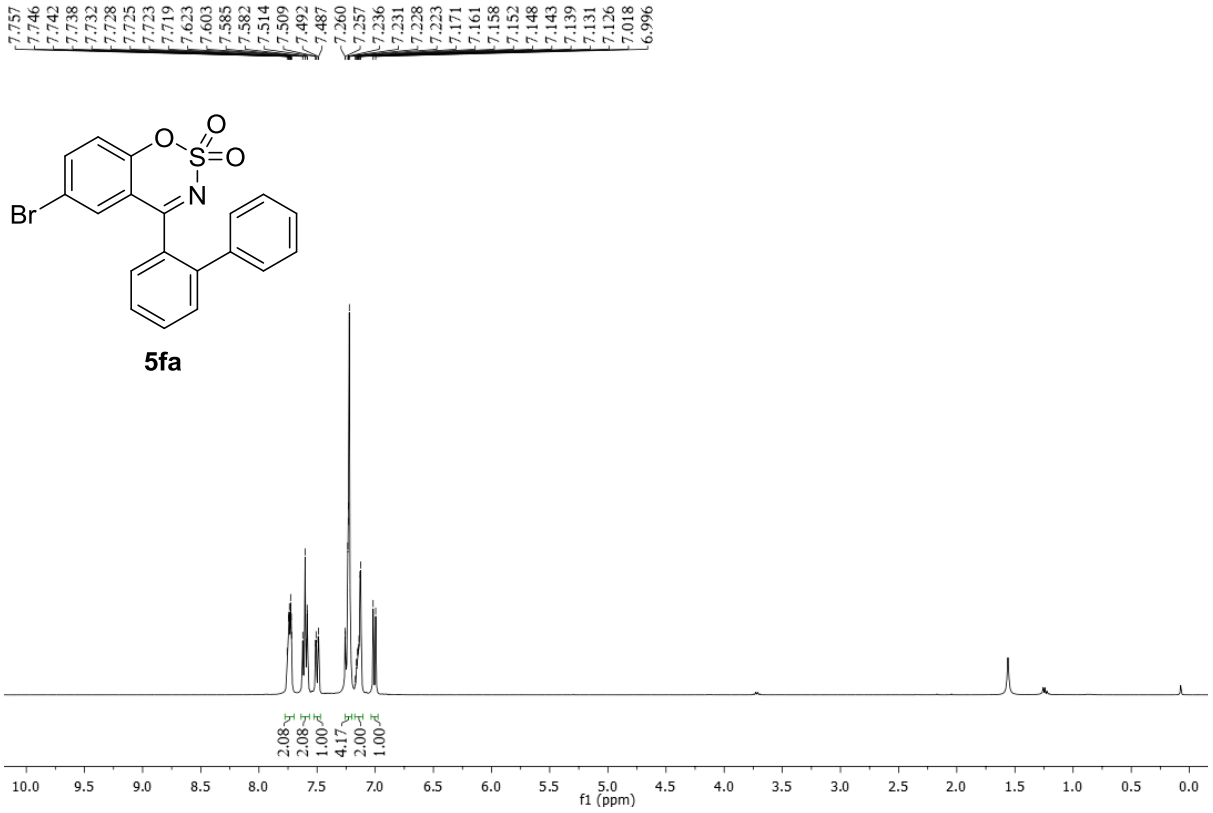

^{13}C NMR of **5fa** (100 MHz, $CDCl_3$):

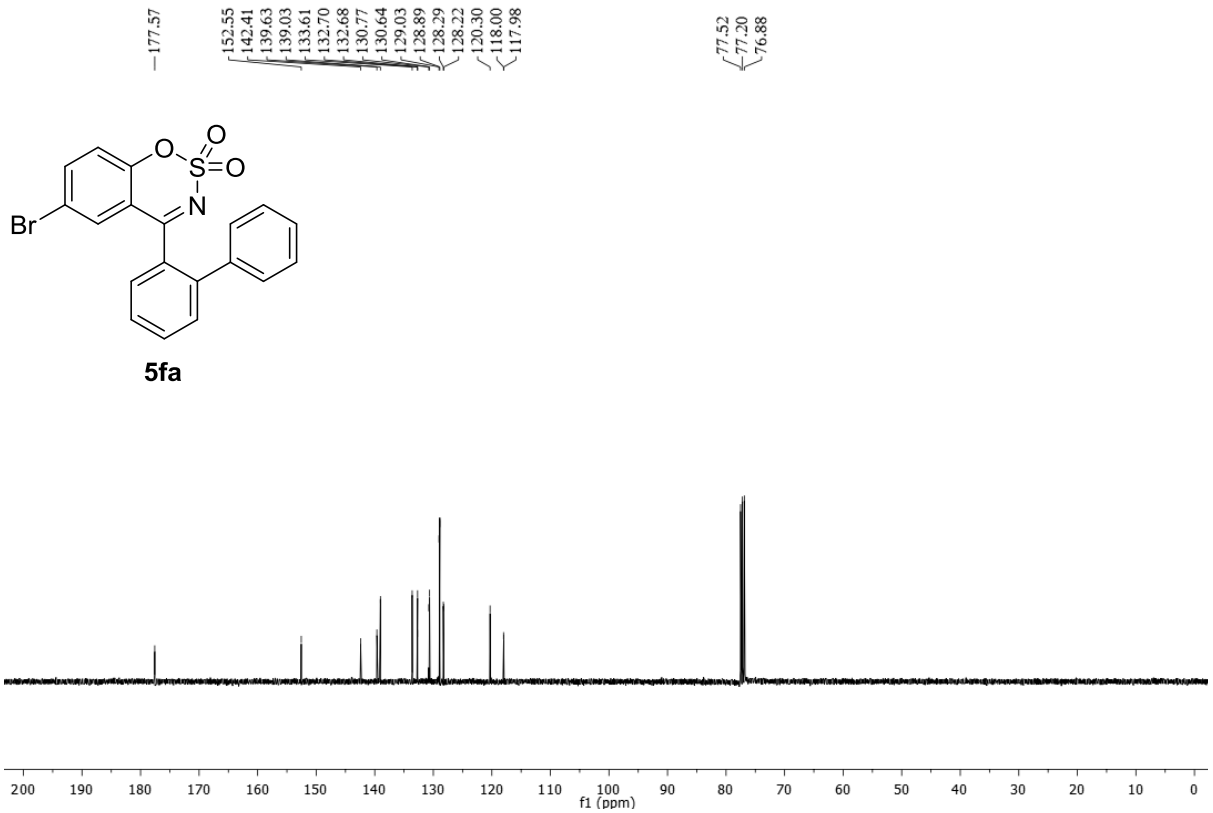

^{1}H NMR of **5ab** (400 MHz, $CDCl_3$):

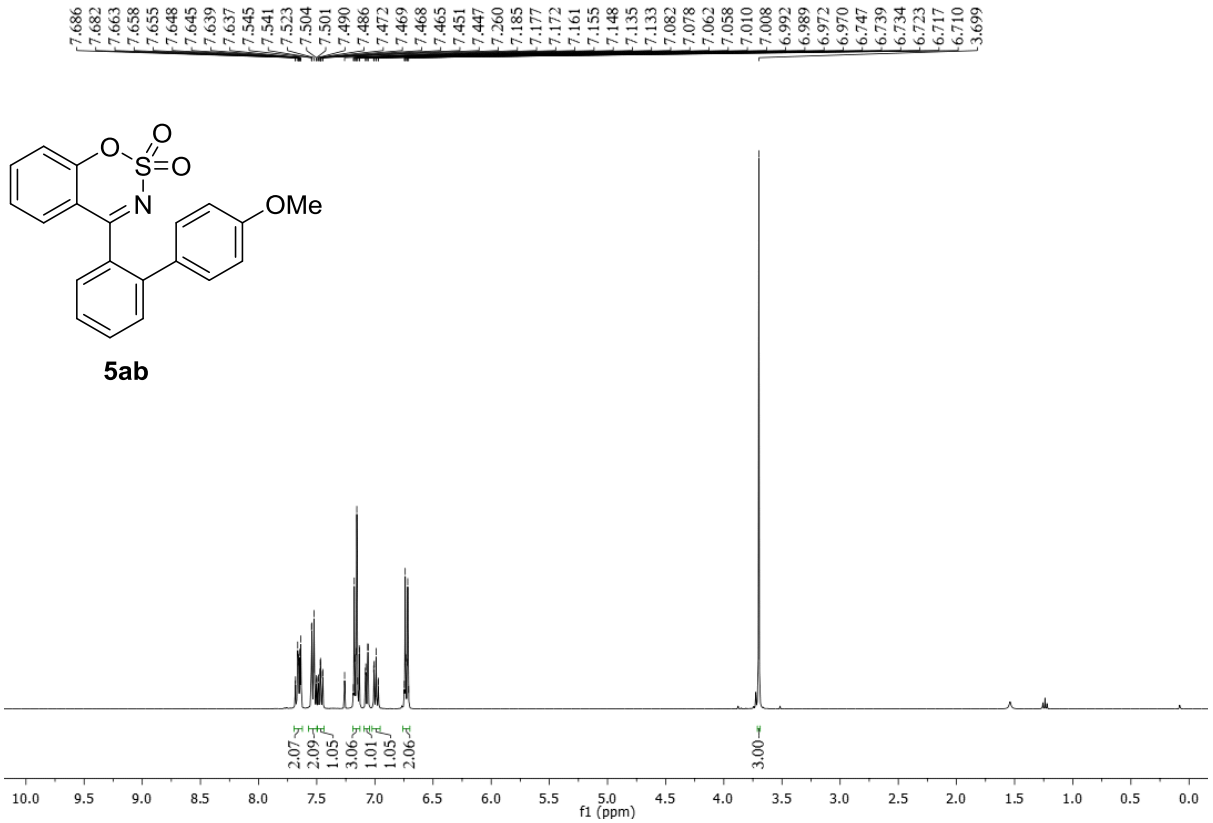

^{13}C NMR of **5ab** (100 MHz, $CDCl_3$):

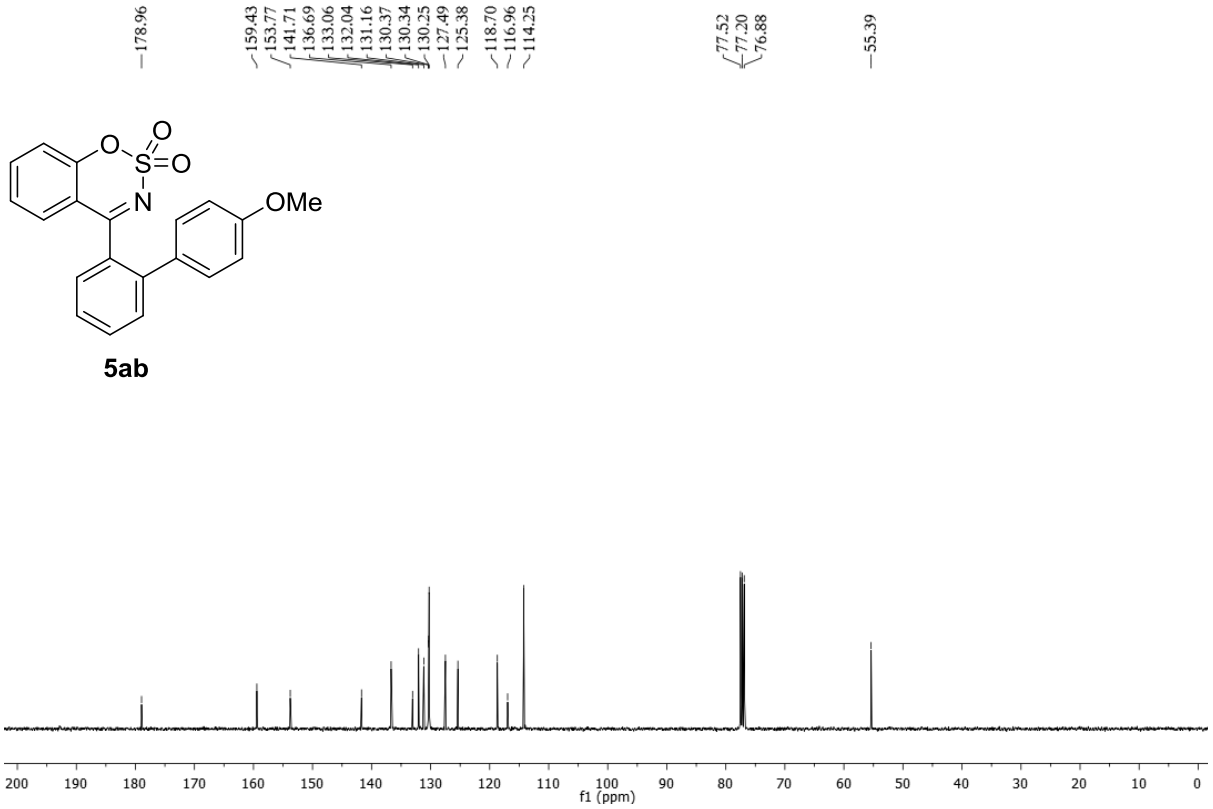

^{1}H NMR of **5cb** (400 MHz, $CDCl_3$):

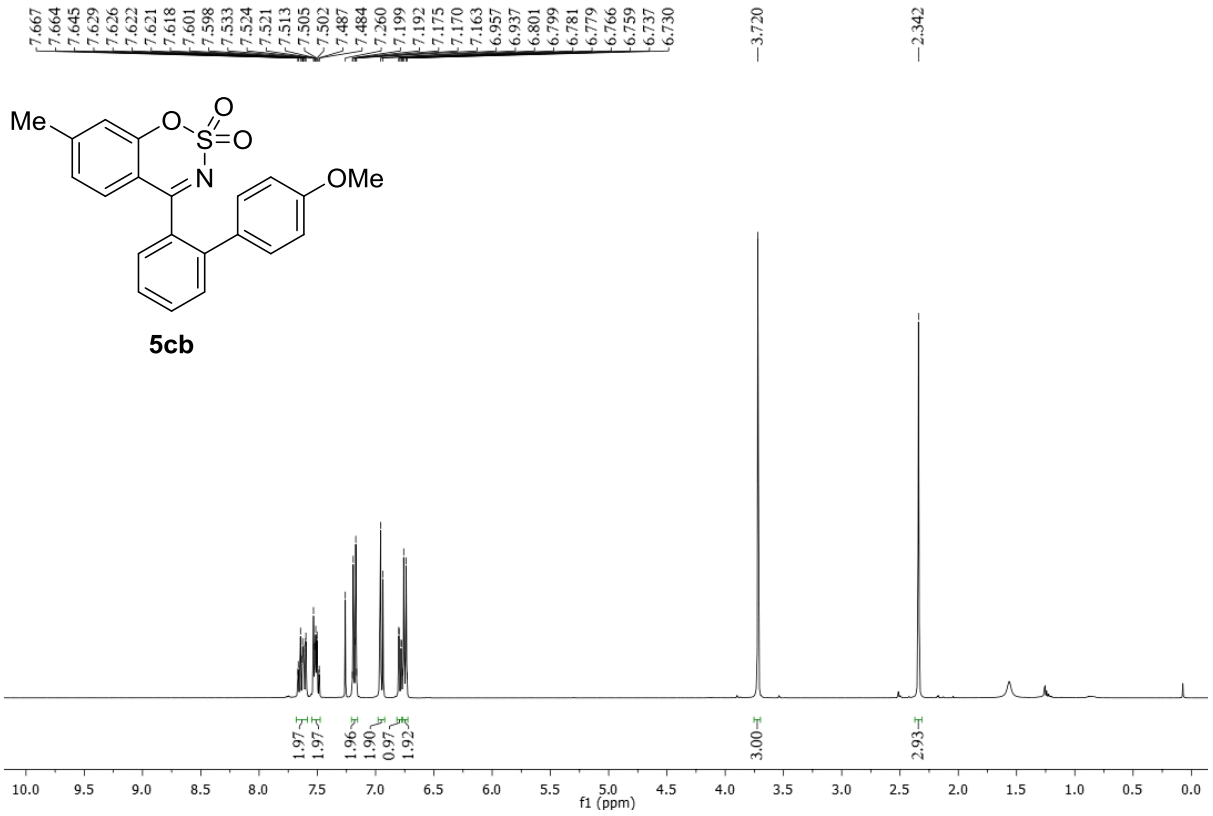

^{13}C NMR of **5cb** (100 MHz, $CDCl_3$):

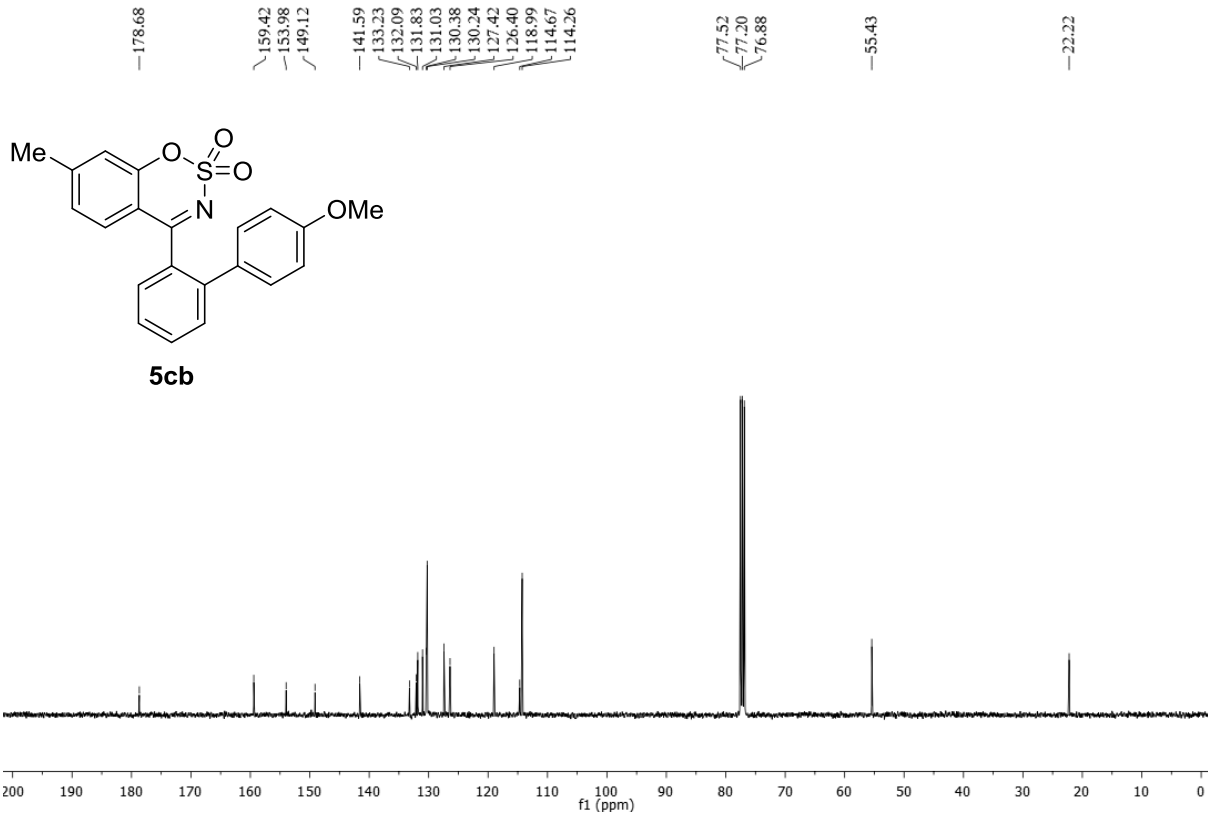

^{1}H NMR of **5eb** (400 MHz, $CDCl_3$):

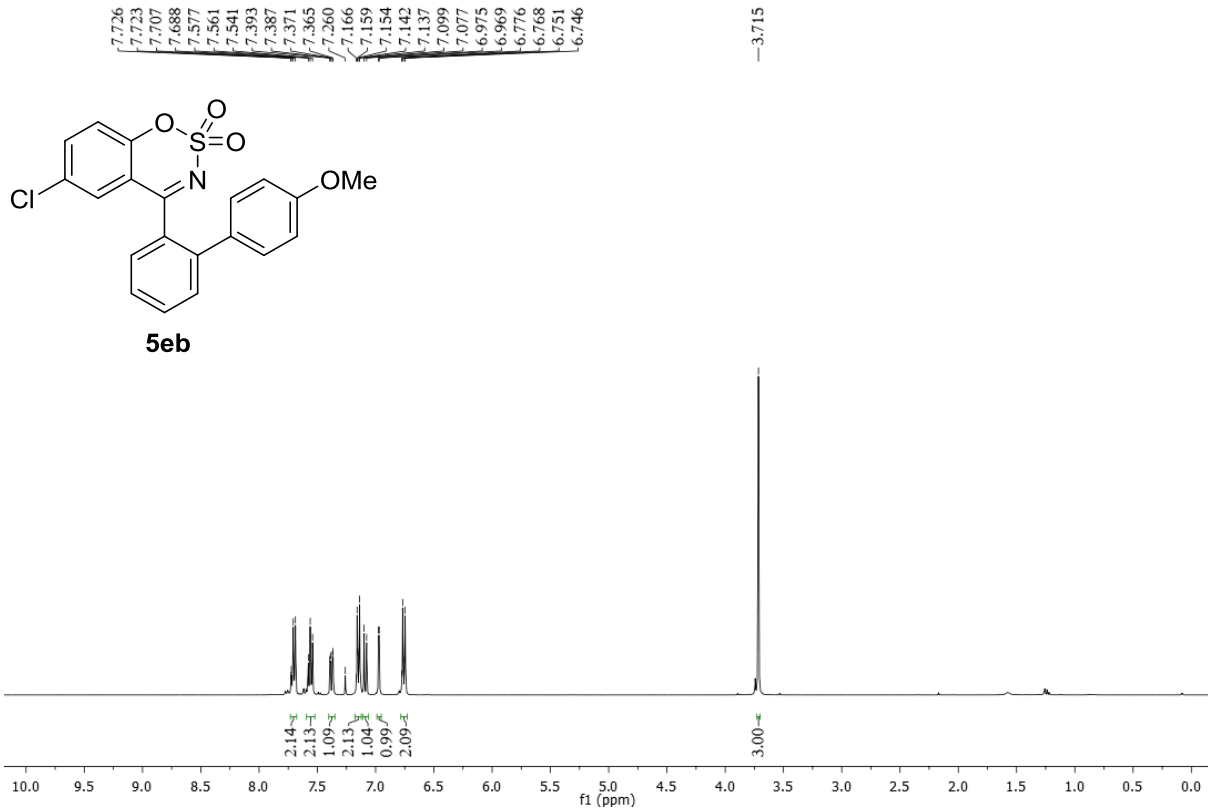

^{13}C NMR of **5eb** (100 MHz, $CDCl_3$):

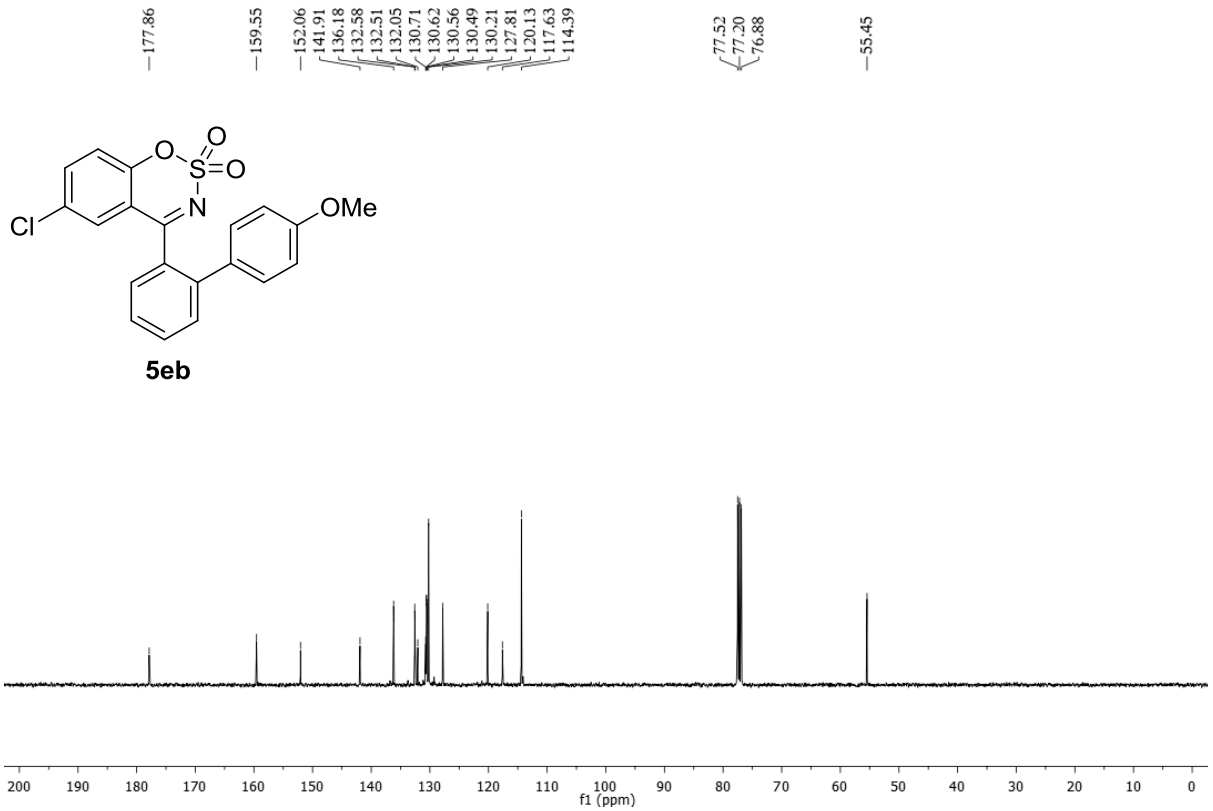

^{1}H NMR of **6** (400 MHz, $CDCl_3$):

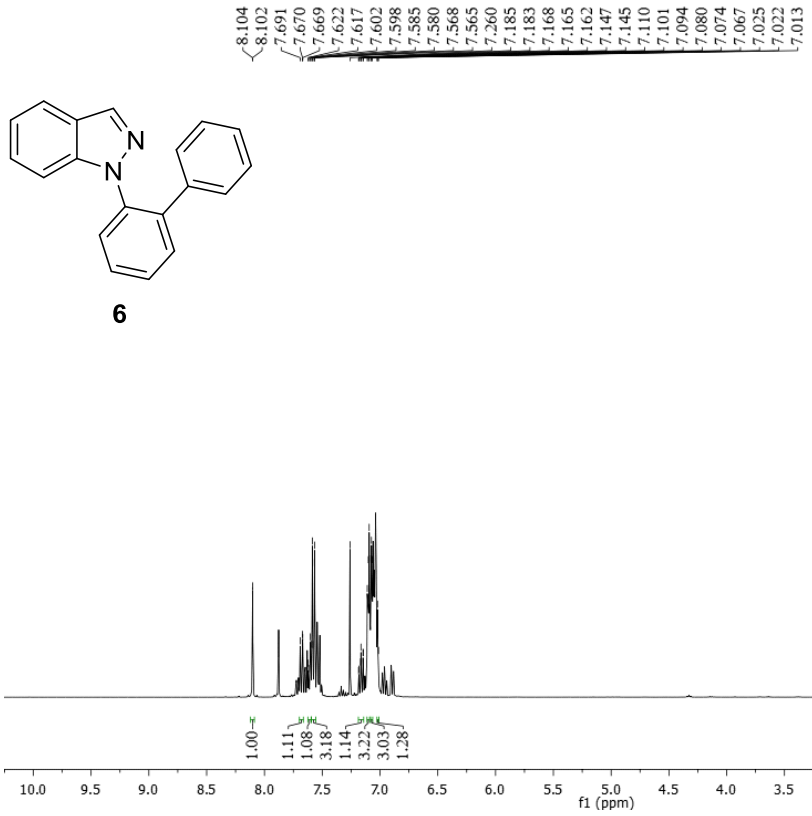

^{1}H NMR of **7** (400 MHz, $CDCl_3$):

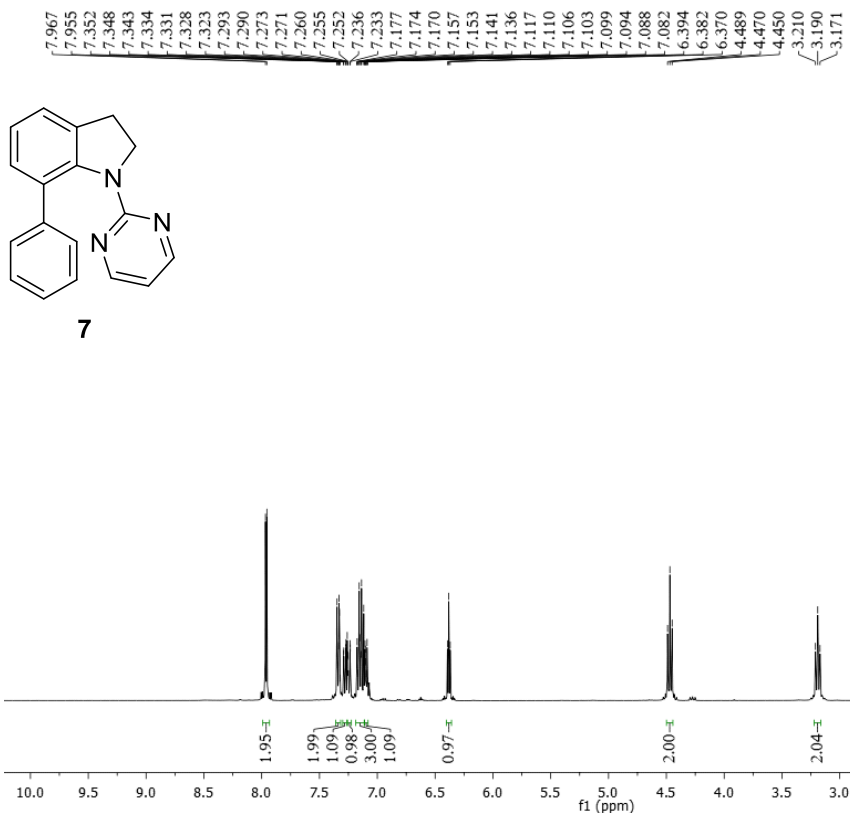

^{1}H NMR of **8** (400 MHz, $CDCl_3$):

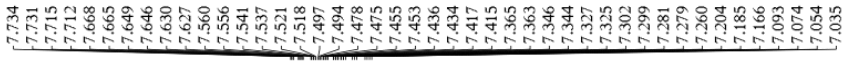

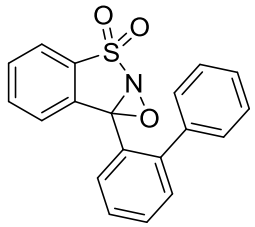

8

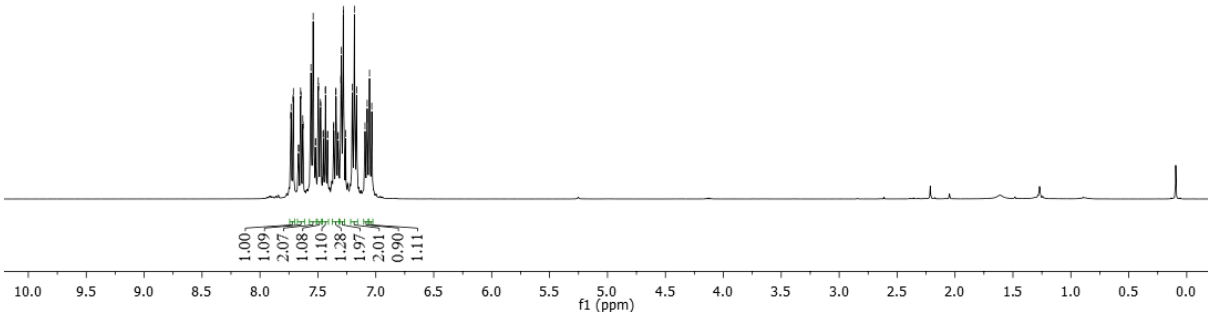

^{13}C NMR of **8** (100 MHz, $CDCl_3$):

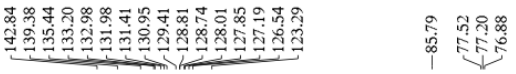

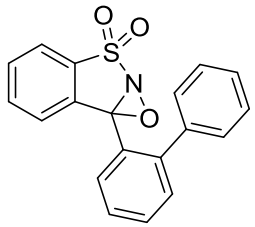

8

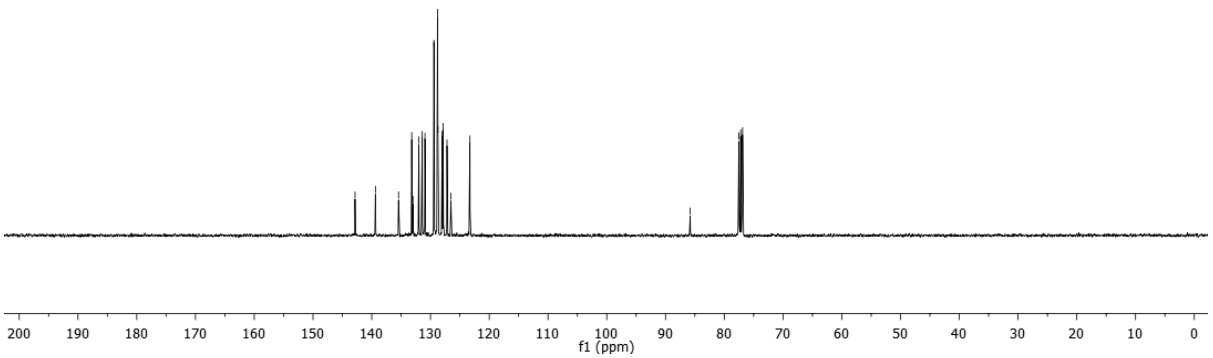

7.7. References

1. For selected reviews and examples, see: (a) Duncia, J. V.; Carini, D. J.; Chiu, A. T.; Johnson, A. L.; Price, W. A.; Wong, P. C.; Wexler, R. R.; Timmermans, P. B. M. W. M. *Med. Res. Rev.* **1992**, *12*, 149. (b) McCarthy, P. A. *Med. Res. Rev.* **1993**, *13*, 139. (c) Horton, D. A.; Bourne, G. T.; Smythe, M. L. *Chem. Rev.* **2003**, *103*, 893. (d) Henry, K. J.; Wasicak, J.; Tasker, A. S.; Cohen, J.; Ewing, P.; Mitten, M.; Larsen, J. J.; Kalvin, D. M.; Swenson, R.; Ng, S.-C.; Saeed, B.; Cherian, S.; Sham, H.; Rosenberg, S. H. *J. Med. Chem.* **1999**, *42*, 4844. (e) Augeri, D. J.; Janowick, D.; Kalvin, D.; Sullivan, G.; Larsen, J.; Dickman, D.; Ding, H.; Cohen, J.; Lee, J.; Warner, R.; Kovar, P.; Cherian, S.; Saeed, B.; Zhang, H.; Tahir, S.; Ng, S.-C.; Sham, H.; Rosenberg, S. H. *Bioorg. Med. Chem. Lett.* **1999**, *9*, 1069.
2. Hajduk, P. J.; Bures, M.; Praestgaard, J.; Fesik, S. W. *J. Med. Chem.* **2000**, *43*, 3443.
3. For selected reviews and examples, see: (a) Noyori, R.; Takaya, H. *Acc. Chem. Res.* **1990**, *23*, 345. (b) Gray, G. W. *Liq. Cryst.* **1998**, *24*, 5. (c) Bringmann, G.; Menche, D.; Bezabih, M.; Abegaz, B. M.; Kaminsky, R. *Planta Med.* **1999**, *65*, 757. (d) Matheron, M. E.; Porchas, M. *Plant Dis.* **2004**, *88*, 665. (e) Nagamani, C.; Guo, J.; Thayumanavan, S. *J. Polym. Sci., Part A: Polym. Chem.* **2012**, *50*, 1187. (f) Yuan, S.; Chang, J.; Yu, B. *Top Curr. Chem.* **2020**, *378*, 23.
4. For selected examples, see: (a) Iwanejko, J.; Wojaczyńska, E. *Org. Biomol. Chem.* **2018**, *16*, 7296. (b) Weinreb, S. M. *Top. Curr. Chem.* **1997**, *190*, 131. (c) Freitag, D.; Metz, P. *Tetrahedron* **2006**, *62*, 1799. (d) Zhong, D.; Wu, D.; Zhang, Y.; Lu, Z.; Usman, M.; Liu, W.; Lu, X.; Liu, W.-B. *Org. Lett.* **2019**, *21*, 5808.
5. For selected examples, see: (a) Clerici, F.; Gelmi, M. L.; Yokoyama, K.; Pocar, D.; Van Voorhis, W. C.; Buckner, F. S.; Gelb, M. H. *Bioorg. Med. Chem. Lett.* **2002**, *12*, 2217. (b) Hendricks, R. T.; Spencer, S. R.; Blake, J. F.; Fell, J. B.; Fischer, J. P.; Stengel, P. J.; Leveque, V. J. P.; LePogam, S.; Rajyaguru, S.; Najera, I.; Josey, J. A.; Swallow, S. *Bioorg. Med. Chem. Lett.* **2009**, *19*, 410. (c) Elsayed, M. S. A.; El-Araby, M. E.; Serya, R. A. T.; El-Khatib, A. H.; Linscheid, M. W.; Abouzid, K. A. M. *Eur. J. Med. Chem.* **2013**, *61*, 122.
6. For selected examples, see: (a) Zimmermann, S.; Akbarzadeh, M.; Otte, F.; Strohmann, C.; Sankar, M. G.; Ziegler, S.; Pahl, A.; Sievers, S.; Kumar, K. *Chem. Eur. J.* **2019**, *25*, 15498. (b) Wang, Y.-Q.; Yu, C.-B.; Wang, D.-W.; Wang, X.-B.; Zhou, Y.-G. *Org. Lett.* **2008**, *10*, 2071. (c) Yu, C.-B.; Wang, D.-W.; Zhou, Y.-G. *J. Org. Chem.* **2009**, *74*, 5633.

(d) Kravina, A. G.; Mahatthananchai, J.; Bode, J. W. *Angew. Chem. Int. Ed.* **2012**, *51*, 9433. (e) Nishimura, T.; Noishiki, A.; Chit Tsui, G.; Hayashi, T. *J. Am. Chem. Soc.* **2012**, *134*, 5056. (f) Yang, G.; Zhang, W. *Angew. Chem. Int. Ed.* **2013**, *52*, 7540. (g) An, Q.; Li, J.; Shen, J.; Butt, N.; Liu, D.; Liu, Y.; Zhang, W. *Chem. Commun.* **2015**, *51*, 885. (h) Liu, R.-R.; Wang, D.-J.; Wu, L.; Xiang, B.; Zhang, G.-Q.; Gao, J.-R.; Jia, Y.-X. *ACS Catal.* **2015**, *5*, 6524. (i) Jiang, T.; Wang, Z.; Xu, M.-H. *Org. Lett.* **2015**, *17*, 528. (j) Ling, Z.; Singh, S.; Xie, F.; Wu, L.; Zhang, W. *Chem. Commun.* **2017**, *53*, 5364.

7. Chattopadhyay, S.; Raychaudhuri, U.; Chakraborty, R. *J. Food Sci. Technol.* **2014**, *51*, 611.
8. For selected examples, see: (a) Wrobel, J.; Dietrich, A.; Woolson, S. A.; Millen, J.; McCaleb, M.; Harrison, M. C.; Hohman, T. C.; Sredy, J.; Sullivan, D. *J. Med. Chem.* **1992**, *35*, 4613. (b) Pineiro, J. L. C.; Collins, I. J.; Harrison, T., Patent US20050143369 A1, June 30, 2005. (c) Tumey, L. N.; Robarge, M. J.; Gleason, E.; Song, J.; Murphy, S. M.; Ekema, G.; Doucette, C.; Hanniford, D.; Palmer, M.; Pawlowski, G.; Danzig, J.; Loftus, M.; Hunady, K.; Sherf, B.; Mays, R. W.; Stricker-Krongrad, A.; Brunden, K. R.; Bennani, Y. L.; Harrington, J. J. *Bioorg. Med. Chem. Lett.* **2010**, *20*, 3287. (d) Azevedo, C. M. G.; Watterson, K. R.; Wargent, E. T.; Hansen, S. V. F.; Hudson, B. D.; Kępczyńska, M. A.; Dunlop, J.; Shimpukade, B.; Christiansen, E.; Milligan, G.; Stocker, C. J.; Ulven, T. *J. Med. Chem.* **2016**, *59*, 8868.
9. For selected reviews and examples, see: (a) Liu, Z.; Takeuchi, Y. J. H. *Heterocycles* **2002**, *56*, 693. (b) Debnath, S.; Mondal, S. *Eur. J. Org. Chem.* **2018**, *2018*, 933. (c) Ahn, K. H.; Kim, S.-K.; Ham, C. *Tetrahedron Lett.* **1998**, *39*, 6321. (d) Ahn, K. H.; Baek, H.-H.; Lee, S. J.; Cho, C.-W. *J. Org. Chem.* **2000**, *65*, 7690. (e) Kumaraswamy, G.; Padmaja, M.; Markondaiah, B.; Jena, N.; Sridhar, B.; Kiran, M. U. *J. Org. Chem.* **2006**, *71*, 337.
10. (a) Stanforth, S. P. *Tetrahedron* **1998**, *54*, 263. (b) Hassan, J.; Sévignon, M.; Gozzi, C.; Schulz, E.; Lemaire, M. *Chem. Rev.* **2002**, *102*, 1359. (c) Denmark, S. E.; Sweis, R. F. *Acc. Chem. Res.* **2002**, *35*, 835. (d) Anastasia, L.; Negishi, E. *Handbook of organopalladium chemistry for organic synthesis*, Wiley, New York, 2002, pp 311–334.
11. Bumagin, N. A.; Luzikova, E. V. *J. Organomet. Chem.* **1997**, *532*, 271.
12. Constable, D. J. C.; Dunn, P. J.; Hayler, J. D.; Humphrey, G. R.; Leazer, J. J. L.; Linderman, R. J.; Lorenz, K.; Manley, J.; Pearlman, B. A.; Wells, A.; Zaks, A.; Zhang, T. Y. *Green Chem.* **2007**, *9*, 411.
13. For selected reviews, see: (a) Macklin, T.; Snieckus, V. *Handbook of C–H Transformations: Applications in Organic Synthesis*, Volumes 1-2 edited by Gerald

Dyker (Bochum University, Germany). Wiley-VCH Verlag GmbH & Co. KGaA: Weinheim, 2005. (b) Alberico, D.; Scott, M. E.; Lautens, M. *Chem. Rev.* **2007**, *107*, 174. (c) Tetsuya, S.; Masahiro, M. *Chem. Lett.* **2007**, *36*, 200. (d) Seregin, I. V.; Gevorgyan, V. *Chem. Soc. Rev.* **2007**, *36*, 1173. (e) Li, B.-J.; Yang, S.-D.; Shi, Z.-J. *Synlett* **2008**, *2008*, 949. (f) McGlacken, G. P.; Bateman, L. M. *Chem. Soc. Rev.* **2009**, *38*, 2447. (g) Ackermann, L.; Vicente, R.; Kapdi, A. R. *Angew. Chem. Int. Ed.* **2009**, *48*, 9792. (h) Daugulis, O.; Do, H.-Q.; Shabashov, D. *Acc. Chem. Res.* **2009**, *42*, 1074. (i) Chen, X.; Engle, K. M.; Wang, D.-H.; Yu, J.-Q. *Angew. Chem. Int. Ed.* **2009**, *48*, 5094. (j) Lyons, T. W.; Sanford, M. S. *Chem. Rev.* **2010**, *110*, 1147. (k) Colby, D. A.; Bergman, R. G.; Ellman, J. A. *Chem. Rev.* **2010**, *110*, 624. (l) Lei, A.; Liu, W.; Liu, C.; Chen, M. *Dalton Trans.* **2010**, *39*, 10352. (m) Ashenhurst, J. A. *Chem. Soc. Rev.* **2010**, *39*, 540. (n) Bellina, F.; Rossi, R. *Chem. Rev.* **2010**, *110*, 1082. (o) Liu, C.; Zhang, H.; Shi, W.; Lei, A. *Chem. Rev.* **2011**, *111*, 1780. (p) Zhao, D.; You, J.; Hu, C. *Chem. Eur. J.* **2011**, *17*, 5466. (q) Yeung, C. S.; Dong, V. M. *Chem. Rev.* **2011**, *111*, 1215. (r) Cho, S. H.; Kim, J. Y.; Kwak, J.; Chang, S. *Chem. Soc. Rev.* **2011**, *40*, 5068. (s) Yamaguchi, J.; Yamaguchi, A. D.; Itami, K. *Angew. Chem. Int. Ed.* **2012**, *51*, 8960. (t) Yamaguchi, J.; Muto, K.; Itami, K. *Eur. J. Org. Chem.* **2013**, *2013*, 19. (u) Rossi, R.; Bellina, F.; Lessi, M.; Manzini, C. *Adv. Syn. Catal.* **2014**, *356*, 17. (v) Giri, R.; Thapa, S.; Kafle, A. *Adv. Syn. Catal.* **2014**, *356*, 1395. (w) Liu, C.; Yuan, J.; Gao, M.; Tang, S.; Li, W.; Shi, R.; Lei, A. *Chem. Rev.* **2015**, *115*, 12138. (x) Yang, Y.; Lan, J.; You, J. *Chem. Rev.* **2017**, *117*, 8787. (y) Yang, Y.; Shi, Z. *Chem. Commun.* **2018**, *54*, 1676.

14. (a) Hiyama, T.; Hatanaka, Y. *Pure Appl. Chem.* **1994**, *66*, 1471. (b) Hiyama, T.; Shirakawa, E. *Top. Curr. Chem.* **2002**, *219*, 61. (c) Denmark, S. E.; Regens, C. S. *Acc. Chem. Res.* **2008**, *41*, 1486. (d) Denmark, S. E.; Liu, J. H.-C. *Angew. Chem. Int. Ed.* **2010**, *49*, 2978. (e) Nakao, Y.; Hiyama, T. *Chem. Soc. Rev.* **2011**, *40*, 4893. (f) Soriano-Ursúa, M. A.; Farfán-García, E. D.; López-Cabrera, Y.; Querejeta, E.; Trujillo-Ferrara, J. G. *Neurotoxicology* **2014**, *40*, 8. (g) Hansen, M. M.; Jolly, R. A.; Linder, R. J. *Org. Process Res. Dev.* **2015**, *19*, 1507. (h) Denmark, S. E.; Ambrosi, A. *Org. Process Res. Dev.* **2015**, *19*, 982. (i) Luo Haiqing, Z. Z., Liu Haidong, Liu Huijin *Youji Huaxue* **2015**, *35*, 802. (j) Farfán-García, E. D.; Pérez-Rodríguez, M.; Espinosa-García, C.; Castillo-Mendieta, N. T.; Maldonado-Castro, M.; Querejeta, E.; Trujillo-Ferrara, J. G.; Soriano-Ursúa, M. A. *Toxicol. Appl. Pharmacol.* **2016**, *307*, 130.

15. (a) Yang, S.; Li, B.; Wan, X.; Shi, Z. *J. Am. Chem. Soc.* **2007**, *129*, 6066. (b) Zhou, H.; Xu, Y.-H.; Chung, W.-J.; Loh, T.-P. *Angew. Chem. Int. Ed.* **2009**, *48*, 5355. (c) Liang,

Z.; Yao, B.; Zhang, Y. *Org. Lett.* **2010**, *12*, 3185. (d) Li, W.; Yin, Z.; Jiang, X.; Sun, P. *J. Org. Chem.* **2011**, *76*, 8543. (e) Han, W.; Mayer, P.; Ofial, A. R. *Chem. Eur. J.* **2011**, *17*, 6904. (f) Bi, L.; Georg, G. I. *Org. Lett.* **2011**, *13*, 5413. (g) Fan, H.; Shang, Y.; Su, W. *Eur. J. Org. Chem.* **2014**, *2014*, 3323. (h) He, J.; Takise, R.; Fu, H.; Yu, J.-Q. *J. Am. Chem. Soc.* **2015**, *137*, 4618. (i) Luo, H.; Liu, H.; Zhang, Z.; Xiao, Y.; Wang, S.; Luo, X.; Wang, K. *RSC Adv.* **2016**, *6*, 39292.

16. (a) Senthilkumar, N.; Parthasarathy, K.; Gandeepan, P.; Cheng, C.-H. *Chem. Asian J.* **2013**, *8*, 2175. (b) Lu, M.-Z.; Lu, P.; Xu, Y.-H.; Loh, T.-P. *Org. Lett.* **2014**, *16*, 2614. (c) Ghaderi, A.; Iwasaki, T.; Kambe, N. *Asian J. Org. Chem.* **2019**, *8*, 1344. (d) Luo, H.; Xie, Q.; Sun, K.; Deng, J.; Xu, L.; Wang, K.; Luo, X. *RSC Adv.* **2019**, *9*, 18191.
17. (a) Nareddy, P.; Jordan, F.; Szostak, M. *Chem. Sci.* **2017**, *8*, 3204. (b) Nareddy, P.; Jordan, F.; Szostak, M. *Org. Biomol. Chem.* **2017**, *15*, 4783. (c) Nareddy, P.; Jordan, F.; Szostak, M. *Org. Lett.* **2018**, *20*, 341.
18. (a) Hachiya, H.; Hirano, K.; Satoh, T.; Miura, M. *Angew. Chem. Int. Ed.* **2010**, *49*, 2202. (b) Zhao, S.; Liu, B.; Zhan, B.-B.; Zhang, W.-D.; Shi, B.-F. *Org. Lett.* **2016**, *18*, 4586.
19. (a) Bu, Q.; Gońka, E.; Kuciński, K.; Ackermann, L. *Chem. Eur. J.* **2019**, *25*, 2213. (b) Lu, M.-Z.; Ding, X.; Shao, C.; Hu, Z.; Luo, H.; Zhi, S.; Hu, H.; Kan, Y.; Loh, T.-P. *Org. Lett.* **2020**, *22*, 2663.
20. (a) Shin, K.; Park, Y.; Baik, M.-H.; Chang, S. *Nat. Chem.* **2018**, *10*, 218. (b) Kim, J.; Shin, K.; Jin, S.; Kim, D.; Chang, S. *J. Am. Chem. Soc.* **2019**, *141*, 4137.
21. For representative examples of cyclic *N*-sulfonyl ketimines as DG, see: (a) Nishimura, T.; Ebe, Y.; Hayashi, T. *J. Am. Chem. Soc.* **2013**, *135*, 2092. (b) Dong, L.; Qu, C.-H.; Huang, J.-R.; Zhang, W.; Zhang, Q.-R.; Deng, J.-G. *Chem. Eur. J.* **2013**, *19*, 16537. (c) Wang, N.-J.; Mei, S.-T.; Shuai, L.; Yuan, Y.; Wei, Y. *Org. Lett.* **2014**, *16*, 3040. (d) Zhang, Q.-R.; Huang, J.-R.; Zhang, W.; Dong, L. *Org. Lett.* **2014**, *16*, 1684. (e) Huang, J.-R.; Song, Q.; Zhu, Y.-Q.; Qin, L.; Qian, Z.-Y.; Dong, L. *Chem. Eur. J.* **2014**, *20*, 16882. (f) Mei, S.-T.; Jiang, K.; Wang, N.-J.; Shuai, L.; Yuan, Y.; Wei, Y. *Eur. J. Org. Chem.* **2015**, *2015*, 6135. (g) Mei, S.-T.; Wang, N.-J.; Ouyang, Q.; Wei, Y. *Chem. Commun.* **2015**, *51*, 2980. (h) Mei, S.-T.; Liang, H.-W.; Teng, B.; Wang, N.-J.; Shuai, L.; Yuan, Y.; Chen, Y.-C.; Wei, Y. *Org. Lett.* **2016**, *18*, 1088. (i) Pham, M. V.; Cramer, N. *Chem. Eur. J.* **2016**, *22*, 2270. (j) Liu, H.; Li, J.; Xiong, M.; Jiang, J.; Wang, J. *J. Org. Chem.* **2016**, *81*, 6093. (k) Manoharan, R.; Jeganmohan, M. *Eur. J. Org. Chem.* **2016**, *2016*, 4013. (l) Liu, B.; Hu, P.; Zhang, Y.; Li, Y.; Bai, D.; Li, X. *Org. Lett.* **2017**, *19*, 5402. (m) Reddy, K. N.; Rao, M. V. K.; Sridhar, B.; Reddy, B. V. S. *Eur. J. Org. Chem.*

2017, *2017*, 4085. (n) Maraswami, M.; Chen, G.; Loh, T.-P. *Adv. Syn. Catal.* **2018**, *360*, 416. (o) Mishra, A.; Mukherjee, U.; Vats, T. K.; Deb, I. *J. Org. Chem.* **2018**, *83*, 3756. (p) Reddy, K. N.; Rao, M. V. K.; Sridhar, B.; Reddy, B. V. S. *Org. Biomol. Chem.* **2018**, *16*, 2522. (q) Reddy, K. N.; Krishna Rao, M. V.; Sridhar, B.; Reddy, B. V. S. *ChemistrySelect* **2018**, *3*, 5062. (r) Mishra, A.; Mukherjee, U.; Sarkar, W.; Meduri, S. L.; Bhowmik, A.; Deb, I. *Org. Lett.* **2019**, *21*, 2056. (s) Shi, G.; Khan, R.; Zhang, X.; Yang, Y.; Zhan, Y.; Li, J.; Luo, Y.; Fan, B. *Asian J. Org. Chem.* **2020**, *9*, 788.

22. Moselage, M.; Li, J.; Kramm, F.; Ackermann, L. *Angew. Chem. Int. Ed.* **2017**, *56*, 5341.
23. De, P. B.; Pradhan, S.; Banerjee, S.; Punniyamurthy, T. *Chem. Commun.* **2018**, *54*, 2494.

List of Publications

Publications Included in this Thesis

1) *"Copper-Catalyzed Direct sp^2 C–H Silylation of Arylamides Using Disilanes"*. **Sarkar, W.***; Mishra, A.; Bhowmik, A.; Deb, I.* *Org. Lett.* **2021**, *21*, 4521-4526. (*As corresponding author) [Selected as journal cover page]

2) *"Iridium-Catalyzed Direct C–H Arylation of Cyclic N-Sulfonyl Ketimines with Arylsiloxanes at Ambient Temperature"*. **Sarkar, W.**†; Bhowmik, A.†; Das, S.; Balaram Sulekha, A.; Mishra, A.; Deb, I.* *Org. Biomol. Chem.* **2020**, *18*, 7074-7078. (†Contributed equally) [Selected as journal cover page]

3) *"Copper-Mediated Direct and Selective C–H Thiolation of Quinazolinones"*. **Sarkar, W.**†; Mishra, A.†; Bhowmik, A.; Deb, I.* *Asian J. Org. Chem.* **2019**, *8*, 819-822. (†Contributed equally)

4) *"Cobalt-Catalyzed Directed sp^2 C–H Acetoxylation of Arenes Employing $Mn(OAc)_3{\cdot}2H_2O$ as Acetoxy Source"*. **Sarkar, W.**; Bhowmik, A.; Mishra, A.; Vats, T. K.; Deb, I.* *Adv. Synth. Catal.* **2018**, *360*, 3228-3232.

5) *"Regio- and Diastereoselective [3+2]-Spiroannulation of Benzoxazines with Chalcones: A Rh(III)-Catalyzed Redox-Neutral Approach to α-Aroyl Spiro-Indanamines"*. **Sarkar, W.**; Mishra, A.; Deb, I.* (*Manuscript submitted*)

Other Co-authored Publications

6) *"Rhodium-Catalyzed C–H Functionalization to Construct Annulated Molecules"*. *In Handbook of CH Functionalization (CHF), Maiti, D., Ed.; Wiley-VCH: Weinheim, 2022.* Mahato, S.; **Sarkar, W.**; Naskar, K.; Deb, I.* (**Book Chapter**) (*In Print*)

7) *"A Radical-Radical Cross-Coupling Reaction of Xanthene with Sulfonyl Hydrazides: Facile Access to Xanthen-9-sulfone Derivatives"*. Das, S.; Roy, S.; Bhowmik, A.; **Sarkar, W.**; Mondal, I.; Mishra, A.; Saha, S. J.; Karmakar, S.; Mishra, A.; Deb, I.* *Chem Commun.* **2022**, *58*, 2902-2905.

8) *"Straightforward Access to Anthrone Functionalized Benzylic Amines via Organocatalytic 1,2-Addition of Anthrones to Imines at Ambient Temperature"*. Das, S.; Bhowmik, A.; **Sarkar, W.**; Mishra, A.; Deb, I.* *J. Org. Chem.* **2021**, *86*, 4131-4142.

9) *"Diastereoselective Spirocyclization via Intramolecular C(sp^3)–H Bond Functionalization Triggered by Sequential [1,5]- Hydride Shift/Cyclization Process: Approach to Spiro-*

tetrahydroquinolines". Bhowmik, A.; Das, S.; **Sarkar, W.**; Saidalvi, K. M.; Mishra, A.; Roy, A.; Deb, I.* *Adv. Synth. Catal.* **2021**, *363*, 826-832.

10) *"Diastereoselective Spirocyclization of Benzoxazines with Nitroalkenes via Rhodium-Catalyzed C–H Functionalization/Annulation Cascade under Mild Conditions"*. Mishra, A.; Bhowmik, A.; Samanta, S.; **Sarkar, W.**; Das, S.; Deb, I.* *Org. Lett.* **2020**, *22*, 1340-1344.

11) *"Diastereoselective Spirocyclization of Cyclic N-Sulfonyl Ketimines with Nitroalkenes via Iridium-Catalyzed Redox-Neutral Cascade Reaction"*. Mishra, A.; Mukherjee, U.; **Sarkar, W.**; Meduri, S. L.; Bhowmik, A.; Deb, I.* *Org. Lett.* **2019**, *21*, 2056-2059. [Selected as journal cover page]

Papers Presented in Conferences

1) *"Synthesis of Functionalized Heterocycles via Copper and Rhodium-Catalyzed C–H Activation"*. **Writhabrata Sarkar**. **ORAL** presentation in ***XVII NOST Conference for Research Scholars (JNOST 2022)*** at Hotel Le Meridien, Hyderabad organized by the School of Chemistry, University of Hyderabad.

2) *"First-Row Transition Metal-Catalyzed C–O and C–Si Bond Formation via Directing Group Aided C–H Activation"*. **Writhabrata Sarkar** and Indubhusan Deb.* **POSTER** (online) presentation in ***27th CRSI National Symposium in Chemistry 2021 (Hybrid mode)*** organized by IISER-Kolkata, West Bengal.
DOI: https://doi.org/10.26226/morressier.6144c24d87a68d83cb5d42cf

3) *"C–O and C–S bond formation using cheap and readily available 1st row transition metal catalysis via directing group aided C–H activation"*. **Writhabrata Sarkar** and Indubhusan Deb.* **POSTER** presentation in ***International Conference on Chemistry for Human Development (ICCHD-2020)*** at Heritage Institute of Technology, Kolkata.

Reprints of the First Page of the Published Papers

ChemComm

ROYAL SOCIETY OF CHEMISTRY

COMMUNICATION

View Article Online
View Journal | View Issue

Published on 02 February 2022. Downloaded by Indian Institute of Chemical Biology on 2/24/2022 1:41:07 PM.

Check for updates

Cite this: *Chem. Commun.*, 2022, **58**, 2902

Received 20th December 2021,
Accepted 31st January 2022

DOI: 10.1039/d1cc07143b

rsc.li/chemcomm

A radical–radical cross-coupling reaction of xanthene with sulfonyl hydrazides: facile access to xanthen-9-sulfone derivatives†

Sumit Das,‡[ab] Shantonu Roy,‡[a] Arup Bhowmik,[a] Writhabrata Sarkar,[a] Imtiaj Mondal,[a] Aniket Mishra,[a] Shubhra Jyoti Saha,[a] Sudip Karmakar[a] and Indubhusan Deb *[a]

A straightforward strategy for direct incorporation of sulfonyl units into a xanthene moiety for accessing xanthen-9-sulfone derivatives in good to excellent yields has been established *via* metal-free radical–radical cross-coupling reaction of xanthenes and sulfonyl hydrazides. Using easily accessible starting materials, this methodology proceeds efficiently with a high degree of functional group compatibility and with a wide scope of both xanthenes and sulfonyl hydrazides under operationally simple reaction conditions. Mechanistic investigations revealed that sulfonyl radicals could be generated from sulfonyl hydrazides in the presence of TBHP under an oxygen atmosphere.

Cross-coupling processes which involve a C–H functionalization step are well-known as straightforward and quick methods for carbon–carbon (C–C) and carbon–heteroatom (C–X) bond formation in an environmentally friendly, sustainable, and highly atom-efficient manner avoiding the use of halides, pseudohalides, and organometallic reagents.[1] In this context, carbon–heteroatom bond formation,[2] specifically C–H sulfonylation reaction has recently gained much attention for the synthesis of functionalized sulfones.[3] In particular, the sulfonyl radical has been used as an important reactive intermediate for the synthesis of various sulfone derivatives. There are extensive reports where the *in situ* generated sulfonyl radicals from various precursors undergo sulfonylation reaction with unsaturated hydrocarbons such as alkenes, alkynes and (hetero) arenes.[4–10] For example, in the presence of radical initiators and/or under photocatalytic conditions, sulfonyl halides,[5] cyanides,[6] azides,[7a] selenides,[7a,b] sodium sulfinates[8] and sulfonyl hydrazides[9,10] produce the corresponding sulfonyl radicals and react with different substrates. Despite the substantial development in sulfonylation reactions *via* a reactive sulfonyl radical intermediate generated *in situ* from sulfonyl hydrazides, their use in metal-free C(sp^3)–H sulfonylation remains underexplored. Sulfones, particularly aryl–alkyl sulfones, are well-known for their wide range of applications in pharmaceuticals, agrochemicals and materials science.[11,12] On the other hand, xanthene and its derivatives are widely reported as biologically active scaffolds present in various pharmaceuticals and imaging agents such as acrotrione, fluorescein, *etc.* (ESI,† Fig. S1).[13] For the synthesis of 9-substituted xanthenes, C(sp^3)–H functionalization with various nucleophiles has gained considerable attention. In this context, Klussmann and co-workers delineated an aerobic oxidative C–C bond formation approach to modify the 9-position of xanthene using sulfonic acid as the catalyst in the presence of molecular oxygen (Scheme 1a).[14] Subsequently, direct activation of the benzylic C(sp^3)–H bond of xanthenes to construct C–C, C–P and C–N bonds was independently reported by Jiao, Perica15 Loh, Zhang, Osuka,[16] Chen,[17] Zeng, and Li[18] (Scheme 1a–d). However, to the best of our knowledge, C(sp^3)–H sulfonylation at the 9-position of xanthenes *via* a radical–radical cross-coupling reaction using sulfonyl hydrazides remains unexplored. Continuing with our research interest in benzylic C(sp^3)–H functionalization, herein, for the first time we unveiled a straightforward radical–radical cross-coupling reaction between xanthenes and sulfonyl hydrazides for the synthesis of xanthen-9-sulfone derivatives using TBHP under an oxygen atmosphere (Scheme 1e).

In our initial study, xanthene **1a** and *p*-toluenesulfonyl hydrazide **2a** were selected to optimize the reaction conditions using different solvent combinations and oxidants (Table 1 and ESI,† Table S1). When the reaction was performed in THF using TBHP (1.5 equiv.) in the open air, the reaction yielded the corresponding sulfonylated product **3a** in 85% yield (Table 1,

[a] *Organic and Medicinal Chemistry Division, CSIR-Indian Institute of Chemical Biology, 4-Raja S. C. Mullick Road, Jadavpur, Kolkata 700032, India. E-mail: indubhusandeb@iicb.res.in, indubhusandeb@gmail.com*
[b] *Academy of Scientific and Innovative Research (AcSIR), Ghaziabad, Uttar Pradesh 201002, India*

† Electronic supplementary information (ESI) available: Experimental procedures, characterization data, ^{1}H and ^{13}C NMR spectra of all new compounds (PDF) and single crystal X-ray diffraction data for compound **3a** (CIF). CCDC 2118371. For ESI and crystallographic data in CIF or other electronic format see DOI: 10.1039/d1cc07143b

‡ SD and SR contributed equally.

This journal is © The Royal Society of Chemistry 2022

OL | Organic Letters

pubs.acs.org/OrgLett Letter

Copper-Catalyzed Direct sp^2 C−H Silylation of Arylamides Using Disilanes

Writhabrata Sarkar,* Aniket Mishra, Arup Bhowmik, and Indubhusan Deb*

Cite This: *Org. Lett.* 2021, 23, 4521−4526 Read Online

ACCESS | Metrics & More | Article Recommendations | Supporting Information

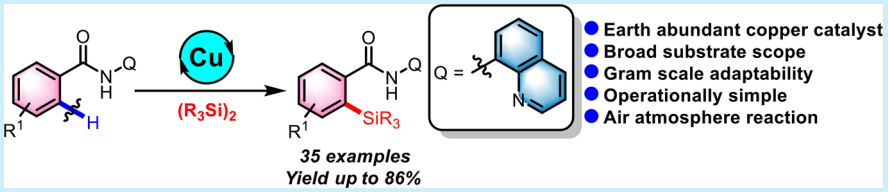

ABSTRACT: A copper-catalyzed method for direct intermolecular *ortho*-silylation of benzamides has been developed that affords organosilane products in moderate to high yields. The key features include: (i) use of commercially available disilanes as a silicon source with 8-aminoquinoline as a bidentate directing group, (ii) use of earth-abundant first-row transition metal, (iii) operationally simple conditions without the need of an inert atmosphere, and (iv) tolerance of a wide range of functional groups. The practicality and effectiveness of this method have been demonstrated by a gram-scale experiment. This strategy, therefore, constitutes a convenient way of constructing C−Si bonds useful for synthetic organic chemistry.

Downloaded via CSIR-INDIAN INST CHEMICAL BIOLOGY on February 14, 2022 at 06:56:47 (UTC).
See https://pubs.acs.org/sharingguidelines for options on how to legitimately share published articles.

The C−Si bond possesses unique physical, chemical, and bioactive properties, and the development of methods for its formation is therefore indispensable in synthetic organic chemistry. The organosilicon compounds are valuable building blocks and have numerous applications in organic chemistry.[1] Besides, these have found potential uses in the fields of material science, polymer chemistry,[2] and pharmaceutical industries[3]—a growing number of reports in medicinal chemistry deal with the incorporation of silicon groups in diverse drug candidates.[4] In consequence, significant efforts have been made in recent years for the strategic installation of silyl groups into organic frameworks. Among these, the synthesis of organosilanes through transition-metal-catalyzed direct C−H bond functionalizations, as compared to traditional approaches of silylation reactions[5] and transition-metal-free techniques,[6] has emerged as the most sought-after protocol from the viewpoints of atom economy and high efficiency.[7−12] The high abundance, low cost, and environmentally benign nature of silicon have in addition allowed the development of catalytic silylation methods via C−H bond activation. In the past decades, several advances have been made in this field for the silylation of C(sp^2)−H as well as C(sp^3)−H variants using Ru,[7] Rh,[8] Ir,[9] Sc,[10] and Pt[11] as transition metal catalysts (Scheme 1a).

Kuninobu and Kanai reported the first Pd-catalyzed silylation of carboxamides with disilanes as silicon sources, applying a directing group strategy (Scheme 1b).[12a] Following this pioneering work, Zhang and Shi's groups developed elegant procedures for the silylation of aliphatic β-C(sp^3)−H bonds,[12c,d] which were then impressively extended to distal γ-C(sp^3)−H silylation by Maiti and co-workers.[12e] Maiti and Liu have made splendid breakthroughs in both regioselective *meta* and *para* C−H silylation techniques with the help of intricately designed directing templates suitable for C−H bond activation.[12g,h] In 2019, Yang et al. developed another approach for *meta* C−H silylation to access silicon-containing 1,1′-biaryl-2-acetamides employing palladium catalysis.[12i]

Scheme 1. Transition-Metal-Catalyzed C−H Silylation

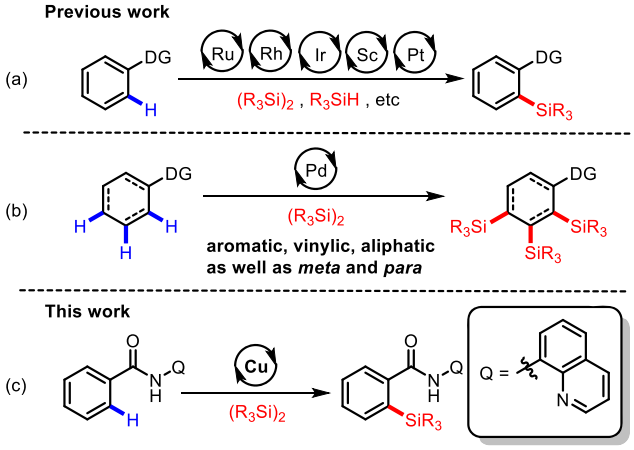

Received: April 1, 2021
Published: May 13, 2021

© 2021 American Chemical Society

https://doi.org/10.1021/acs.orglett.1c01129
Org. Lett. 2021, 23, 4521−4526

Copper-Catalyzed Direct sp^2 C–H Silylation of Arylamides Using Disilanes (Selected as journal cover page)

JOC The Journal of Organic Chemistry

pubs.acs.org/joc Article

Straightforward Access to Anthrone Functionalized Benzylic Amines via Organocatalytic 1,2-Addition of Anthrones to Imines at Ambient Temperature

Sumit Das, Arup Bhowmik, Writhabrata Sarkar, Aniket Mishra, and Indubhusan Deb*

Cite This: J. Org. Chem. 2021, 86, 4131−4142 Read Online

ACCESS | Metrics & More | Article Recommendations | Supporting Information

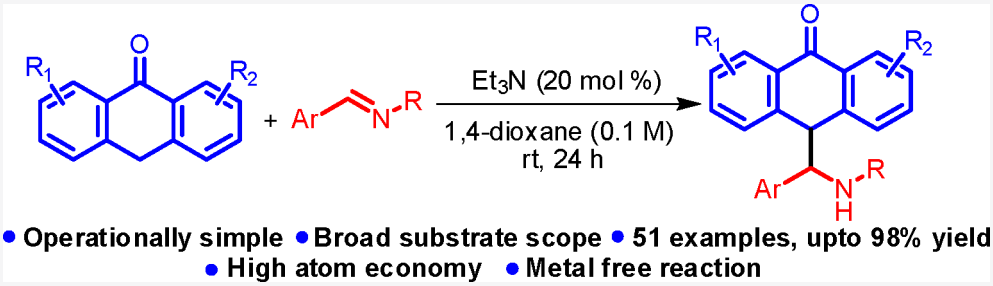

ABSTRACT: Activation of anthrone via benzylic deprotonation in the presence of triethylamine paves the way for the 1,2-addition reaction with imines to provide the desired functionalized anthrones in good to excellent yields under mild and operationally simple reaction conditions with a broad range of substrate scopes without using any external additives or toxic stoichiometric reagents.

INTRODUCTION

Anthrone and its reduced or oxidized forms are present in many pharmaceuticals, dyes, and optoelectronic materials.[1−4] It is also an imperative framework of many natural products and restorative drugs such as variecolortide (I, II), cassialoin (III), and knipholone (IV) (Figure 1).[5,6] A number of its

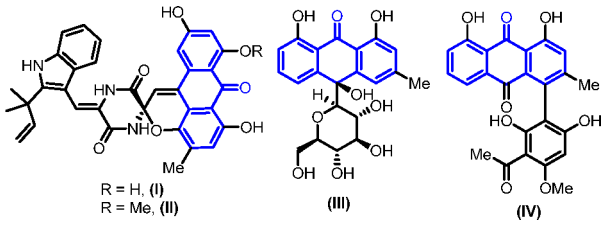

Figure 1. Representative bioactive molecules containing anthrone scaffolds.

derivatives have shown substantial clinical potency like antimicrobial, diuretic, antipsoriatic, telomerase inhibitory activities and selective antitumor activity[7] (Figure 1).

Anthrone can be converted into its nucleophilic enolate under basic conditions or as a diene for Diels−Alder reactions under suitable conditions.[8] Various methodologies have been developed by different groups for the synthesis of functionalized anthrone derivatives employing nonasymmetric or asymmetric 1,4-addition and Diels−Alder reactions with different dienophiles under various catalytic conditions.[9,10] Sporadic examples of 1,2-addition of anthrone to iminium are known in the literature. In this context, Kitamura et al. reported the coupling reactions of 2-hydroxyindoline with anthrone in the presence of $BF_3{\cdot}Et_2O$ (Scheme 1a).[11] Later on, White's group developed a two-step methodology for the controlled oxidation of proline, catalyzed by Fe(PDP) followed by 1,2-addition of anthrone (Scheme 1b).[12] However, 1,2-addition of anthrone to imine as a coupling partner remains unknown to date (Scheme 1c).

N-Sulfonyl imine has been used as a reaction partner in various nucleophilic addition reactions,[13] radical reactions,[13a] and hetero Diels−Alder reactions.[14] *N*-Sulfonyl amide derivatives serve as an important class of structural motifs prevalent in numerous drugs such as thromboxane receptor antagonists,[15a] inhibitors of *Mycobacterium tuberculosis*,[15b] and antitrypanosomal agents.[15c] Taking account of the importance of anthrone and *N*-sulfonylamides and in continuation of our ongoing interests toward the synthesis of densely functionalized molecules,[16] herein for the first time we wish to report a triethylamine-catalyzed direct 1,2-addition of anthrone to *N*-sulfonylaldimines under mild reaction conditions toward the synthesis of benzyl amine functionalized anthrone (Scheme 1c).

Received: December 16, 2020
Published: February 23, 2021

Downloaded via CSIR-INDIAN INST CHEMICAL BIOLOGY on February 14, 2022 at 07:10:51 (UTC).
See https://pubs.acs.org/sharingguidelines for options on how to legitimately share published articles.

ACS Publications © 2021 American Chemical Society

https://dx.doi.org/10.1021/acs.joc.0c02959
J. Org. Chem. 2021, 86, 4131−4142

DOI: 10.1002/adsc.202001011
Advanced Synthesis & Catalysis

Diastereoselective Spirocyclization via Intramolecular C(sp^3)–H Bond Functionalization Triggered by Sequential [1,5]-Hydride Shift/Cyclization Process: Approach to Spiro-tetrahydroquinolines

Arup Bhowmik,[a] Sumit Das,[a, b] Writhabrata Sarkar,[a] K. M. Saidalavi,[a] Aniket Mishra,[a] Anupama Roy,[a] and Indubhusan Deb[a,*]

[a] Organic and Medicinal Chemistry Division, Indian Institute of Chemical Biology, 4-Raja S. C. Mullick Road, Jadavpur, Kolkata 700032, India
E-mail: indubhusandeb@iicb.res.in; indubhusandeb@gmail.com
[b] Academy of Scientific and Innovative Research (AcSIR). Kamla Nehru Nagar, 201002, Ghaziabad, India

Manuscript received: August 24, 2020; Revised manuscript received: November 11, 2020; Version of record online: December 8, 2020

Supporting information for this article is available on the WWW under https://doi.org/10.1002/adsc.202001011

Abstract: A direct synthesis of spiro[5.5]and [5.4]-tetrahydroquinolines has been developed through C(sp^3)–H bond functionalization triggered by sequential [1,5]- hydride shift /cyclization sequence using *ortho* amino benzaldehydes and active methylene compounds such as 2-coumaranone, 4-hydroxycoumarin, 3-coumaranone, and 3-isochromanone. This protocol provides a Lewis acid catalyst-free straight forward one-pot reaction in cases of 2-coumaranone and 4-hydroxycoumarin, Lewis acid-catalyzed stepwise reaction for 3-coumaranone and 3-isochromanone to access a wide range of spiro-heterocycles in excellent to good yields and diastereoselectivity.

Keywords: [1,5]-hydride shift reaction; Lewis acid catalyst; Spirocycles; tetrahydroisoquinoline; 2-coumaranone; 3-isochromanone.

Introduction

Coumaranone containing scaffolds have drawn much attention since aeons due to their presence in many biologically relevant molecules such as naturally occurring isoaurones(**I**),[1] isoaurostatin[2] marginalin[3] pterocarposide[4] radulifolin-B,[5] Commiphoranes (**III**),[6] aurones[7] and spirocyclic Griseofulvin analogues (**IV**)[8] an orally active antimycotic drug (Figure 1).

Various spirocyclic 2-coumaranones (**II**), benzofuran-3-one (**V**), 3-isochromanone (**VI**)[8b,d–e] derivatives, and isoaurones, aurones are well known pharmaceutically important compounds and natural products to exhibit excellent activity against different biological targets.[9–10] There has been enormous progress in the area of spirocyclic chemistry,[11] however the development of a highly stereoselective and atom-economic method for the construction of spirocyclic scaffold containing 2-coumaranones fused with *N*-heterocycles has hardly been explored.[12] Moreover, the presence of tetrahydroisoquinoline (THIQ) moiety, a powerful building block has given another dimension to construct a variety of bioactive molecules.[13] Recently,

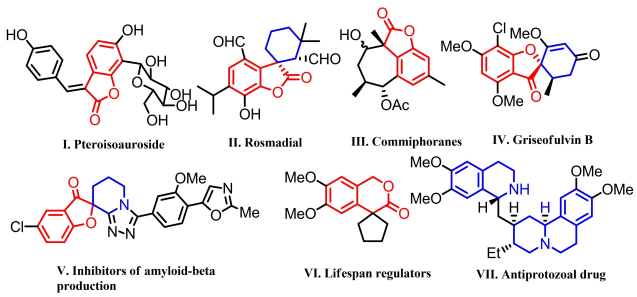

Figure 1. Representative example of relevant bioactive molecules.

© 2020 Wiley-VCH GmbH

Organic & Biomolecular Chemistry

ROYAL SOCIETY OF CHEMISTRY

COMMUNICATION

View Article Online
View Journal | View Issue

Published on 14 July 2020. Downloaded by Indian Institute of Chemical Biology on 2/14/2022 6:56:40 AM.

Check for updates

Cite this: *Org. Biomol. Chem.*, 2020, **18**, 7074

Received 12th June 2020,
Accepted 13th July 2020

DOI: 10.1039/d0ob01212b

rsc.li/obc

Iridium-catalyzed direct C–H arylation of cyclic *N*-sulfonyl ketimines with arylsiloxanes at ambient temperature†

Writhabrata Sarkar, ‡[a] Arup Bhowmik,‡[a] Sumit Das,[a,b] Aiswarya Balaram Sulekha,[a] Aniket Mishra *[a] and Indubhusan Deb *[a]

An iridium-catalyzed *ortho*-selective C–H arylation of cyclic *N*-sulfonyl ketimines has been achieved with environmentally benign aryl siloxanes. The reaction is highly efficient and proceeds at ambient temperature which is the key feature of the methodology considering the weak coordination nature of the substrate as well as the sluggish reactivity of siloxanes. A wide array of pharmaceutically relevant novel biaryls has been synthesized under operationally simple conditions.

Among the C–C bond formation protocols, arylation has been a major preoccupation of organic chemists as most of the biaryl compounds are found as substructures of many bioactive scaffolds.[1] The Hiyama cross-coupling is considered as one of the most robust techniques for incorporating an aryl unit in an organic molecule. The use of an organosilicon reagent is particularly advantageous over more frequently used organoboranes in terms of broad substrate scope, low toxicity and easier accessibility.[2] Unlike traditional cross-coupling reactions, the direct C–H arylation strategies preclude the prefunctionalization of substrates and hence are preferred over the former.[3]

A diverse array of reagents like halides/pseudohalides and metalloarenes (Ar–M, M = B, Mg) has been widely explored for such reactions or arylations.[3o] Despite the significant advantages of organosilicon reagents over their counterparts, the direct C–H arylation employing them has been less studied owing to their low nucleophilicity.[2a–c,3o] Therefore, a handful of reports have appeared in recent years limited to Pd,[4] Rh,[5] Ru[6] and Ni[7] catalysis only. Although directing group assisted C–H arylation strategies have witnessed tremendous progress in the last few decades, the established protocols still suffer from major drawbacks in terms of longer reaction time, high temperature and strongly coordinating directing groups. Very recently, Chang *et al.* described an iridium-catalyzed C–H arylation of directing arenes under mild conditions using aryl siloxanes and to the best of our knowledge, it is the only report for iridium-catalyzed C–H arylation by exploiting aryl siloxanes.[8a]

On the other hand, the functionalized cyclic *N*-sulfonyl ketimine motif is widely present in various biologically active compounds including potential inhibitors against hepatitis-C virus NS5b,[9a,b] the protein farnesyltransferase,[9c] *etc*. They also appear to be the essential precursors for the synthesis of benzosultams, a medicinally important scaffold with a wide range of biological activities including anti-HIV, anti-diabetic and aldose reductase inhibitory properties (Fig. 1).[10] However, a limited number of reports can be obtained in the literature for the direct C–H functionalization of cyclic *N*-sulfonyl ketimines.[11] Very recently, our group has achieved an iridium-catalyzed mild C–H amidation[12a] and an iridium-catalyzed diastereoselective spirocyclization with nitroolefins of cyclic *N*-sulfonyl ketimines.[12b] Herein, we disclose an unprecedented Ir(III) catalyzed *ortho*-selective arylation strategy involving the relatively less explored aryl siloxanes and weakly directing cyclic *N*-sulfonyl ketimines.

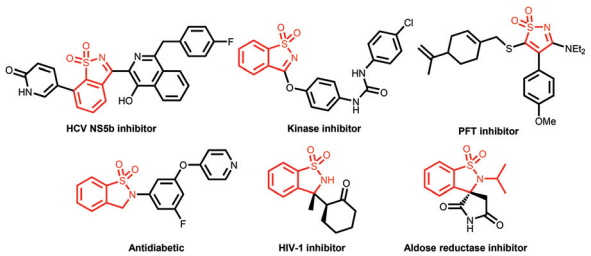

Fig. 1 Representative bioactive molecules containing sulfonyl ketimine/amide scaffolds.

[a]*Organic & Medicinal Chemistry Division, CSIR-Indian Institute of Chemical Biology, 4-Raja S. C. Mullick Road, Jadavpur, Kolkata 700032, India. E-mail: indubhusandeb@iicb.res.in, indubhusandeb@gmail.com, aniket01mishra@gmail.com; Fax: (+91)-33-24735197; Tel: (+91)-33-24995938*
[b]*Academy of Scientific and Innovative Research (AcSIR), India*

†Electronic supplementary information (ESI) available: Experimental details and characterization data for new compounds. CCDC 1891261, 1891262 and 2014574. For ESI and crystallographic data in CIF or other electronic format see DOI: 10.1039/d0ob01212b

‡These authors contributed equally.

This journal is © The Royal Society of Chemistry 2020

Iridium-Catalyzed Direct C–H Arylation of Cyclic *N*-Sulfonyl Ketimines with Arylsiloxanes at Ambient Temperature
(Selected as journal cover page)

Volume 18
Number 36
28 September 2020
Pages 6969-7226

Organic & Biomolecular Chemistry

rsc.li/obc

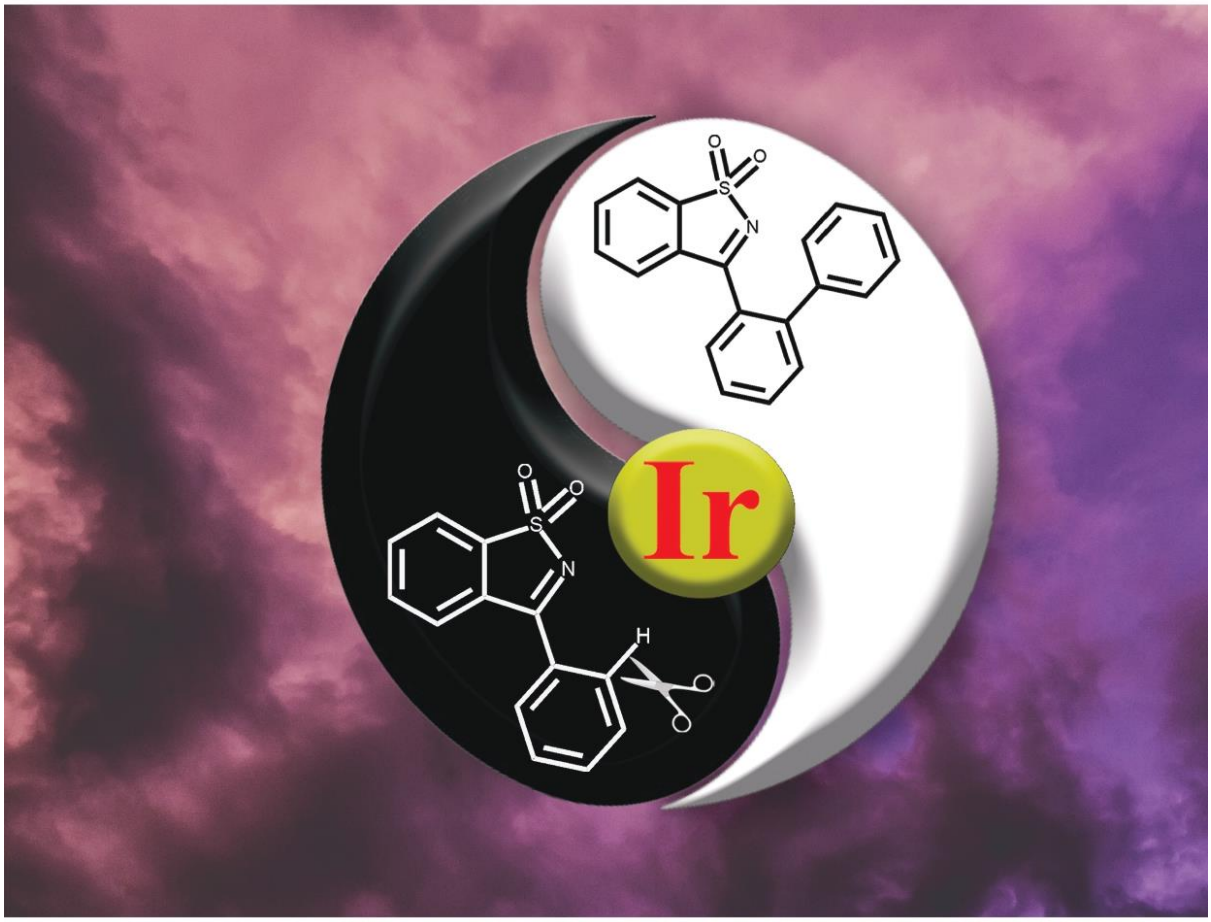

ISSN 1477-0520

ROYAL SOCIETY OF CHEMISTRY

COMMUNICATION
Aniket Mishra, Indubhusan Deb *et al.*
Iridium-catalyzed direct C–H arylation of cyclic *N*-sulfonyl ketimines with arylsiloxanes at ambient temperature

OL | Organic Letters

pubs.acs.org/OrgLett Letter

Diastereoselective Spirocyclization of Benzoxazines with Nitroalkenes via Rhodium-Catalyzed C−H Functionalization/Annulation Cascade under Mild Conditions

Aniket Mishra, Arup Bhowmik, Siddhartha Samanta, Writhabrata Sarkar, Sumit Das, and Indubhusan Deb*

Cite This: *Org. Lett.* 2020, 22, 1340−1344 Read Online

ACCESS | Metrics & More | Article Recommendations | Supporting Information

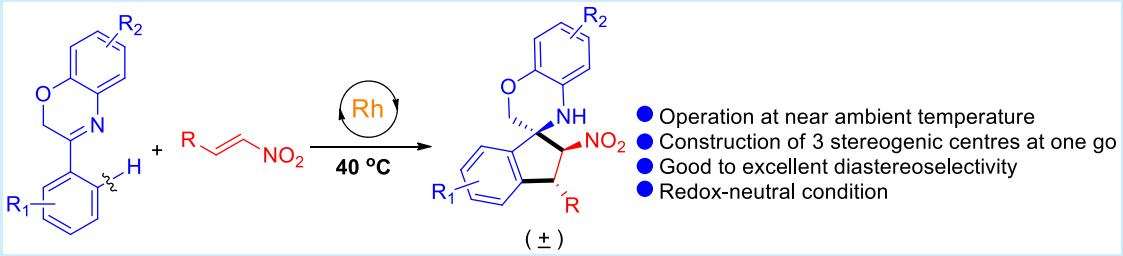

ABSTRACT: A Rh(III)-catalyzed [3 + 2] annulation of benzoxazines with nitroolefins that proceeds via redox-neutral C−H functionalization has been demonstrated, leading to the novel class of spirocycles in a single step. The construction of three continuous stereogenic centers has been achieved starting from easily accessible achiral substrates in an atom-efficient manner under mild reaction conditions. A broad range of pharmaceutically relevant nitro substituted spirocyclic 2,3-dihydro-1,4-benzoxazine derivatives has been synthesized in good to excellent yields with high diastereoselectivity.

A wide array of biologically active small molecules comprising of 2,3-dihydro-1,4-benzoxazine core has been identified with diverse biological activities such as antithrombotic, antihyperlipidemic, calcium antagonism, anti-arrythmic, etc. (Figure 1). Levofloxacin and ofloxacin are among the commercially available antibiotics, and obscurinervidine is a naturally occurring alkaloid containing this structural unit.[1] The most straightforward and practical approach for the synthesis of this type of molecules involves the reduction of 2*H*-1,4-benzoxazines,[2] but a conceivably more interesting approach capable of delivering new structural types would be to exploit the iminyl nitrogen capable of acting as a robust DG for transition-metal-catalyzed C−H functionalization chemistry. However, despite the remarkable development in the field in recent years, the benzoxazines have hardly been utilized in this area.[3n]

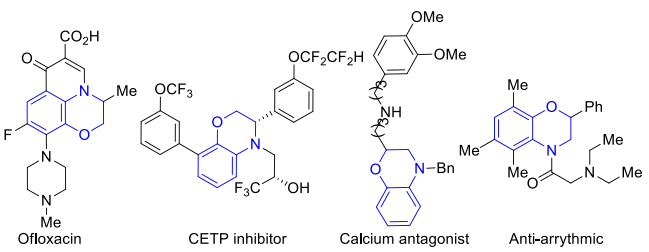

Figure 1. Representative bioactive 2,3-dihydro-1,4-benzoxazines.

Recently, C−H functionalization and subsequent [3 + 2] annulation guided by the imine functionality have been shown to have tremendous potential for the synthesis of interesting structural backbones.[3] But many established protocols still suffer from major issues like the requirement of using activated ketimines containing electron-withdrawing acyl, sulfonyl or phosphoryl groups, extensive dependence on some common partners such as alkynes, allenes, isocyanates, maleimides, or acrylates, high reaction temperature, etc. We noted that nitroalkenes, which have served as a versatile partner in various synthetic protocols,[4] have rarely been explored in transition-metal-catalyzed C−H functionalization reactions presumably due to their high affinity toward metal centers, which leads to catalyst poisoning. Though Ellman et al. demonstrated in 2017 that nitroolefins can be subjected to amide-directed C−H alkylation using rhodium catalysts, only a sporadic number of applications have appeared since.[5] Very recently, our group has reported a unique iridium-catalyzed diastereoselective spiroan-

Received: December 27, 2019
Published: January 30, 2020

Downloaded via CSIR-INDIAN INST CHEMICAL BIOLOGY on February 14, 2022 at 07:06:48 (UTC).
See https://pubs.acs.org/sharingguidelines for options on how to legitimately share published articles.

© 2020 American Chemical Society

https://dx.doi.org/10.1021/acs.orglett.9b04652
Org. Lett. 2020, 22, 1340−1344

ACES Asian Chemical Editorial Society

DOI: 10.1002/ajoc.201900199

ASIAN JOURNAL OF ORGANIC CHEMISTRY Communication

Copper-Mediated Direct and Selective C–H Thiolation of Quinazolinones

Writhabrata Sarkar[+], Aniket Mishra[+], Arup Bhowmik, and Indubhusan Deb*[a]

Abstract: Direct thiolation of quinazolinones by selective cleavage of a relatively inert C–H bond, mediated by earth-abundant copper and guided by a pyridine or pyrimidine moiety, has been achieved under operationally simple conditions. The devised protocol does not require any toxic or reactive reagents and provides direct access to a broad spectrum of pharmaceutically relevant thioquinazolinones.

Quinazolinone is one of the most privileged scaffolds with a vast range of bio-activities and prevalent in several pharmaceutical molecules and drug candidates. 4-Quinazolinone derivatives, such as the sedatives methaqualone, afloqualone, piriqualone, diproqualone and cloroqualone, the antimalarial febrifugine, and the diuretic metolazone are among commercially available marketed drugs (Figure 1).[1] On the other hand, thioethers constitute a unique class of structural element present in several drugs, such as nelfinavir, albendazole, cimetidine, and tiodazosin. Additionally, organothioethers are common building blocks in organic synthesis and also highly useful as fluorescent probes.[2] Recently, quinazolinone tethered thioethers having anti-cancer, antiplatelet and anti-inflammatory activities have been reported (Figure 1),[3] underlining the immense importance of developing syntheses of thioquinazolinones.

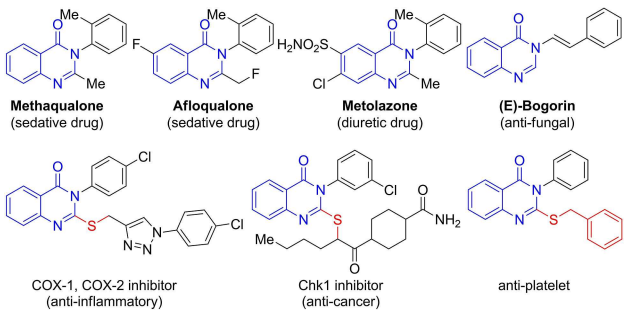

Figure 1. Representative related bioactive molecules.

Most of the practiced methods to synthesize thioquinazolinones (Scheme 1a) suffer from drawbacks such as the use of toxic starting materials, electronically biased substrates, or highly reactive reagents; additionally, these have low atom and step economy, offer low yields or demand harsh reaction conditions, calling for newer and more efficient approaches.[4]

In this context, we became interested in harnessing the power of transition metal promoted direct C–H activation strategy, which has witnessed enormous growth during the last two decades accomplishing various challenging synthetic tasks through shorter routes and exploiting readily available starting materials. Both expensive Pd, Rh, Ru as well as earth abundant Cu, Co, Ni etc. have emerged as highly utilized transition metals for direct sulfenylation reactions.[5]

Such elegant synthetic approaches are mainly based on pyridine,[6] amide,[7] oxime,[8] acid,[9] pyrimidine,[10] 7-azaindole[11] and diverse bidentate auxiliaries.[12] But to our knowledge, quinazolinone substrates have hardly been explored through C–H activation strategy except for a few reports available in literature where they themselves have been used as a directing group[13] and directly functionalized.[14]

We set out to explore the possibility of developing an alternate and more practical method for the synthesis of thioquinazolinones employing C–H activation strategy, continuing our persistent efforts towards the development of sustainable metal catalyzed C–H activation[15] and in particular C–H sulfenylation.[11] Herein, we report a copper promoted direct sulfenylation of 4-quinazolinones using easily affordable disulfides (Scheme 1b).

We commenced the study with the model substrate 3-(pyridin-2-yl)quinazolin-4(3H)-one (**1a**) and 1.0 equiv. of diphenyl disulfide (**2a**) as the thiolating reagent in presence of 2.0 equiv. of $CuCl_2$ in DMSO at 140 °C for 24 h under N_2

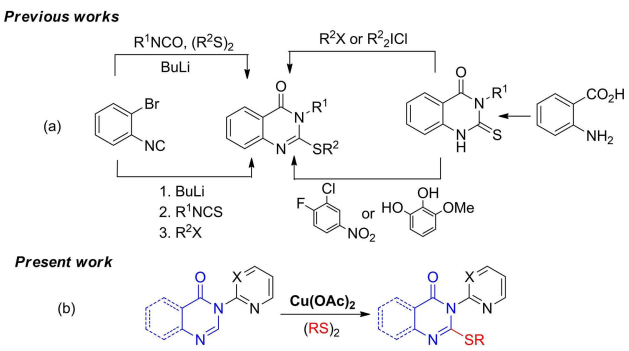

Scheme 1. Synthetic routes towards thioquinazolinones.

[a] *W. Sarkar,[+] A. Mishra,[+] A. Bhowmik, Dr. I. Deb*
Organic& Medicinal Chemistry Division
CSIR-Indian Institute of Chemical Biology
4-Raja S. C. Mullick Road, Jadavpur
Kolkata 700032, India
Phone: (+91)-33-24995938
Fax (+91)-33-24735197
E-mail: indubhusandeb@iicb.res.in
indubhusandeb@gmail.com
[+] *WS and AM contributed equally.*

Supporting information for this article is available on the WWW under https://doi.org/10.1002/ajoc.201900199

© 2019 Wiley-VCH Verlag GmbH & Co. KGaA, Weinheim

OL | Organic Letters

Letter

Cite This: Org. Lett. 2019, 21, 2056−2059

pubs.acs.org/OrgLett

Diastereoselective Spirocyclization of Cyclic *N*-Sulfonyl Ketimines with Nitroalkenes via Iridium-Catalyzed Redox-Neutral Cascade Reaction

Aniket Mishra, Upasana Mukherjee, Writhabrata Sarkar, Sudha Lahari Meduri, Arup Bhowmik, and Indubhusan Deb*

Organic and Medicinal Chemistry Division, CSIR-Indian Institute of Chemical Biology, 4-Raja S. C. Mullick Road, Jadavpur, Kolkata 700032, India

Supporting Information

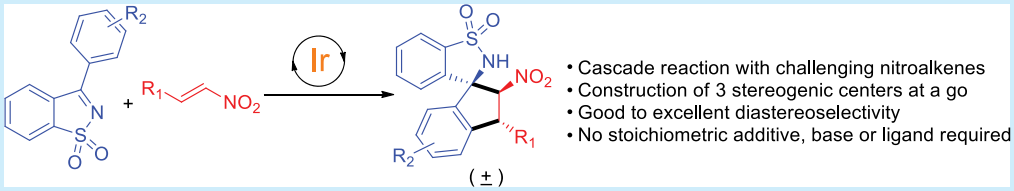

ABSTRACT: An Ir(III)-catalyzed [3 + 2] annulation of weakly coordinating *N*-sulfonyl ketimines with challenging *α*, *β*-unsaturated nitro olefins has been achieved via redox-neutral C−H functionalization in the presence of a catalytic amount of silver hexafluoroantimonate. The generation of three consecutive stereogenic centers in a single step via direct C−H functionalization is the prime feature of this methodology. A wide array of pharmaceutically relevant nitro-substituted spirocyclic benzosultams was synthesized with good to excellent diastereoselectivity as well as in high yield starting from easily accessible substrates.

Nitro olefins are versatile synthons employed in synthetic organic chemistry as Michael acceptors as well as dienophiles in Diels−Alder reactions, and the nitro group can be easily transformed into various useful functional groups;[1] however, nitro olefins have hardly been explored in the field of transition-metal-catalyzed C−H functionalizations presumably due to the strong affinity of them toward transition metals leading to catalyst deactivation. A major breakthrough was achieved by Ellman's group very recently when they reported the first rhodium-catalyzed addition of inert C−H bond to *α*,*β*-unsaturated nitroalkenes via amide assistance.[2a] Since then, few reports have emerged limited to rhodium catalysis only.[2b,c] Therefore, there is ample scope for further exploration of nitroalkenes in transition-metal-catalyzed C−H functionalization processes.

On the other hand, the directing-group-assisted C−H functionalization followed by annulation has recently emerged as a robust tool for the generation of molecular complexity.[3] In this context, [3 + 2] annulations have attracted the interest of organic chemists; however, only alkynes, allenes, acrylates, and maleimides are among the extensively used partners.[4] Various imine derivatives have served as ideal substrates for this type of transformation. Cyclic benzosultams are among medicinally privileged heterocycles[5] and spirocyclic benzosultams have been identified as potent antidiabatic[5a] and anticancer[5b] agents (Figure 1). Cyclic *N*-sulfonyl ketimines[6] could be a good choice as substrates for synthesizing them via C−H functionalization followed by annulation. However, the presence of the sulfonyl group makes the nitrogen weakly coordinating. As a result, these

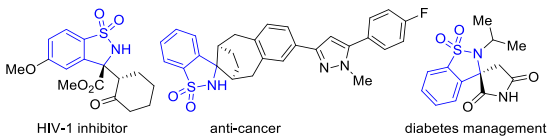

Figure 1. Representative bioactive benzosultams.

substrates have been less studied in such annulation reactions, and generation of more than one stereogenic center employing cyclic *N*-sulfonyl ketimines is particularly rare. In 2013, Nishimura reported Ir(I)-catalyzed [3 + 2] annulations between cyclic *N*-sulfonyl ketimines and 1,3-dienes via direct C−H functionalization for the first time.[7a] Since then, a few groups have reported annulation reactions employing alkynes, heterocycles, aryl halides, isocyanates, and CF_3-substituted enones under Rh(III), Co(III), and Pd(II) catalysis.[7] Recently, we have developed a mild and efficient Ir(III)-catalyzed C−H amidation of *N*-sulfonyl ketimines.[6g] In continuation of our interest in transition-metal-catalyzed C−H functionalization reactions,[8] herein we wish to report an Ir(III)-catalyzed diastereoselective spiroannulation of *N*-sulfonyl ketimines and *α*,*β*-unsaturated nitro olefins under a redox-neutral process.

We initiated the study by taking the representative substrate 3-phenylbenzo[*d*]isothiazole 1,1-dioxide (**1a**, 0.1 mmol) with (*E*)-(2-nitrovinyl)benzene as the *α*,*β*-unsaturated nitroalkene

Received: January 23, 2019
Published: February 21, 2019

Downloaded via CSIR-INDIAN INST CHEMICAL BIOLOGY on February 14, 2022 at 07:06:07 (UTC).
See https://pubs.acs.org/sharingguidelines for options on how to legitimately share published articles.

© 2019 American Chemical Society

DOI: 10.1021/acs.orglett.9b00295
Org. Lett. 2019, 21, 2056−2059

Diastereoselective Spirocyclization of Cyclic *N*-Sulfonyl Ketimines with Nitroalkenes via Iridium-Catalyzed Redox-Neutral Cascade Reaction (Selected as journal cover page)

Check for updates

COMMUNICATIONS DOI: 10.1002/adsc.201800398

Advanced Synthesis & Catalysis

Cobalt-Catalyzed Directed sp^2 C–H Acetoxylation of Arenes Employing $Mn(OAc)_3 \cdot 2H_2O$ as Acetoxy Source

Writhabrata Sarkar,[a] Arup Bhowmik,[+a] Aniket Mishra,[+a] Tripta Kumari Vats,[a] and Indubhusan Deb[a,*]

[a] Organic & Medicinal Chemistry Division, CSIR-Indian Institute of Chemical Biology, 4-Raja S.C. Mullick Road, Jadavpur, Kolkata 700032, India.
Phone: (+91)-33-24995938
Fax (+91)-33-24735197
E-mail: indubhusandeb@iicb.res.in; indubhusandeb@gmail.com

[+] AB and AM contributed equally.

Received: March 27, 2018; Revised: June 7, 2018; Published online: July 11, 2018

Supporting information for this article is available on the WWW under https://doi.org/10.1002/adsc.201800398

Abstract: A cobalt-catalyzed sp^2 C–H acetoxylation of amides having 8-aminoquinoline as a directing group has been achieved using manganese (III) acetate both as an oxidant and an acetoxy source. Operational simplicity, broad range of functional group tolerance, use of an earth abundant first row transition metal, and, most importantly, exploitation of an unprecedented acetoxy source are the key features. The method is scalable and does not require any additive. The mechanism of the reaction has been established by conducting a series of experiments.

Keywords: Cobalt; C–H bond activation; 8-aminoquinoline; manganese(III) acetate; acetoxylation

The acetoxy group acts as a functional group modifier while imparting polar nature to a molecule. It is ubiquitous in a plethora of pro-drugs, natural products, antimicrobial agents, and herbicidal materials.[1] Newer methods of regiospecifically introducing this group in organic molecules continues therefore to be of relevance. In this regard, metal based protocols depending on a suitable directing group have emerged as useful propositions for direct and regioselective acetoxylation of relatively inert C–H bonds in atom and step economic manner. Most of these methods rely on palladium,[2] ruthenium[3] and rhodium[4] catalysis. Apart from their expensive nature, the catalysts also suffer from their low earth abundance as well as bio-incompatibility. Though a handful of stoichiometric or sub-stoichiometric copper-mediated acetoxylation methods have also been reported[5] in the literature (Scheme 1, eq 1), an efficient catalytic method relying on the cheaper and earth-abundant first row transition metal catalysts in place of the expensive second row ones continues to be highly solicited in organic synthesis.

Very recently, several transformations have been reported in synthetic organic chemistry which rely on C–H activation using cobalt catalysts in different oxidation states.[6] Inspired by the pioneering research reported by Yoshikai using low valent cobalt and by Kanai using high valent Co(III), various methodologies have been designed by different research groups.[7,8] The major problems associated with these methods are the use of highly reactive Grignard reagents or expensive Cp* ligands. As an advancement, Daugulis *et al.* demonstrated 8-aminoquinoline[10] directed oxidative alkyne annulations[9a] using easily affordable cobalt salts in the presence of stoichiometric amounts of an oxidant. Most of the seminal works in this field concentrate on direct

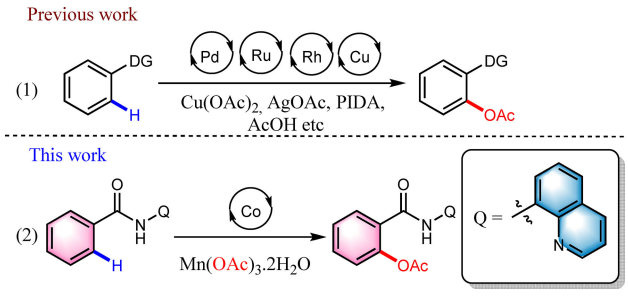

Scheme 1. Transition metal catalyzed C–H acetoxylation.

© 2018 Wiley-VCH Verlag GmbH & Co. KGaA, Weinheim